FEB - FRESENIUS ENVIRONMENTAL BULLETIN
Founded jointly by F. Korte and F. Coulston
Production by PSP - Vimy Str. 1e, 85354 Freising, Germany in
cooperation with PRT-Parlar Research & Technology
Vimy Str 1e, 85354 Freising

Printed in Germany-ISSN 1018-4619

Fresenius Environmental Bulletin is abstracted/indexed in:
Biology & Environmental Sciences, BIOSIS, CAB International, Cambridge Scientific abstracts, Chemical Abstracts, Current Awareness, Current Contents/Agriculture, CSA Civil Engineering Abstracts, CSA Mechanical & Transportation Engineering, IBIDS database, Information Ventures, NISC, Research Alert, Science Citation Index (SCI), Scisearch, Selected Water Resources Abstracts

CONTENTS

ORIGINAL PAPERS

© by PSP Volume 27 – No. 7/2018 pages 4589-4597 Fresenius Environmental Bulletin

DISTRIBUTION OF CHIRONOMIDAE (DIPTERA-INSECTA) OF HIGH-ALTITUDE LAKES IN THE EASTERN BLACK SEA REGION OF TURKEY

Ayse Tasdemir*, Mustafa Rusen Ustaoglu, Hasan Musa Sari

Ege University, Faculty of Fisheries, Department of Hydrobiology, 35100-Bornova, Izmir

ABSTRACT

Six samplings were carried out during July and August 2005–2007 in order to determine the Chironomidae fauna of high-altitude lakes at the Eastern Black Sea region. All the investigated lakes are located at altitudes between 2530 and 3370 m a.s.l, except Uzungöl (1100 m). Hereby, some measured environmental factors accompanied with Chironomidae fauna of 59 lakes are presented for the first time. As a result of the study, a total of 35 identified chironomid represent new records for the region.

KEYWORDS:
Chironomidae, Eastern Black Sea Range, Turkey, glacial lakes.

INTRODUCTION

Remote mountain lakes, hardly accessible, with little human activity in their catchment area, are considered as least disturbed freshwater ecosystems in Europe [1]. Although situated far from local sources of pollution, these lakes are threatened by deposition of atmospheric pollutants (acidity and toxic air pollutants) and by climate changes. The high mountain lakes are sensitive to these threats because of their poor buffering capacities of soil and rocks in the watershed to neutralize acidic deposition [2].

The Chironomidae is the freshwater insect family which comprises the highest number of species, both in lentic and lotic habitats [3]. They are well known indicators of trophic condition in lakes, of organic pollution in run-ning waters and are considered an interesting biogeographic material as well [4].

Despite their importance and abundance at high altitude, chironomid communities in mountain lakes in the Alps were neither extensively nor intensively studied until the 20th century. Notwithstanding the rich literature produced in early 20th century, no papers dealing with chironomids of mountain lakes in the Alps above the treeline were written [5].

A few studies are available on the Chironomidae fauna of the glacial and tectonic lakes on the mountains of high altitude in Turkey [6-10].

Aditionally, in Turkey, Gültutan and Kazancı [11] reported 20 species of Chironomidae through their research at high-elevated lakes of Eastern Black sea region.

This preliminary study is as pioneering research in determining the Chironomidae communities in the glacial lakes of Turkey.

The aim of this study is to examine the composition of Chironomidae fauna of the high mountain lakes of Eastern Black sea Region, Turkey.

MATERIALS AND METHODS

In order to study the Chironomidae fauna of 59 mountain-lakes in the Eastern Black sea region, six excursions were conducted in 2005-2007. Due to the high altitude, most of the sites are completely covered by snow and/or ice during 8-9 months of the year and open only in warm months, i.e. July and August.

In-vivo measured environmental variables are temperature (T), pH, dissolved oxygen (DO), electrical conductivity (EC) and salinity (S) and turbidity were measured in sito by using a WTW pH-meter (model 330), a WTW oxygen-meter (model 330) and an YSI 30 model SCT-meter and a Secchi disc. Other variables (PO_4^{-3}-P, NO_2^- -N, NO_3^- -N, NH_4^- -N, Chl-a) measured in-vitro following the standard methods of APHA [12].

The samples were taken by an Ekman - Birge grab (15 x 15cm) or by a hand-net with 180 µm mesh size. After that, collected samples were sieved through a 500 µm mesh size sieves and fixed in 4% formaldehyde solution in the field. Later on, samples washed under tap waters in-vitro to sort the chironomids. Sorted specimens were preserved in 70% alcohol until identification. Identification of larvae was done under stereomicroscope after preparing permanent slide with Euparal. We mostly used Hirvenoja [13], Wiederholm [14], [3] Klink and Moller Pillot [15] for identical and taxonomical means.

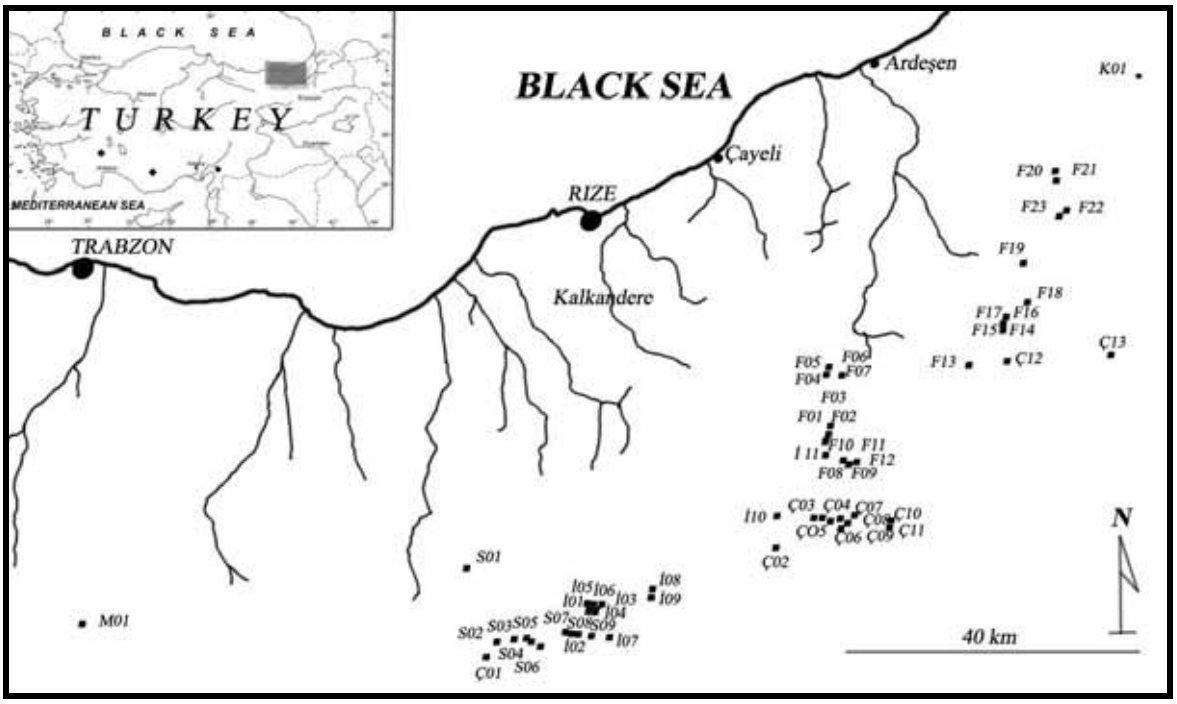

FIGURE 1
Ploted sampling stations and 6 drainage basins. Abbreviations: (Ç = Çoruh River Basin, F = Fırtına Stream Basin, İ = İyidere Basin, K = Kabisra Stream Basin, S = Solaklı Stream Basin, M = Maçka Stream Basin)

TABLE 1
Information of investigated localities and sampling dates. St= Station; other abbreviations are given on Figure 1.

St. No	Sampling Dates	Lakes	Basins	Alti-tude(m)	Coordinates	Area (ha)	Maxi-mum-depth(m)	Substratum
1	30.07.2007	Göloba	Ç01	2540	40º 30′ 36″ N 40º 19′ 12″ E	0,79	3,00	muddy
2	19.08.2005	Dağbaşı	Ç02	2710	40º 37′ 02″ N 40º 46′ 47″ E	2,63	2,90	hard, gravel
3	04.08.2006	Batıaksu	Ç03	3050	40 39 13 N 40 50 39 E	2,55	7,50	sandy, stony
4	04.08.2006	Kuzeyaksu	Ç04	3070	40 39 19 N 40 50 57 E	1,36	3,00	sandy, stony
5	04.08.2006	Doğuaksu	Ç05	3120	40 39 09 N 40 51 06 E	1,44	20,00	sandy, stony, rocky
6	26.07.2007	Ovit-Ortagöl	Ç06	2960	40 38 51 N 40 52 09 E	2,21	10,00	stony, muddy, sandy
7	19.08.2005	Üstgöl	Ç07	3030	40 38 51 N 40 52 54 E	3,28	4,40	hard, gravel
8	06.07.2005 19.08.2005	Adalıgöl	Ç08	3020	40 38 43 N 40 53 10 E	8,90	8,10	hard, gravel
9	06.07.2005 19.08.2005	Ortagöl	Ç09	3010	40 38 53 N 40 53 18 E	0,86	4,10	hard, gravel
10	30.07.2006	Büyükgöl	Ç10	2670	40 56 13 N 41 12 02 E	4,11	0,96	stony, sandy
11	19.08.2005	Altgöl	Ç11	2950	40 38 53 N 40 53 40 E	2,01	2,80	hard, gravel
12	23.08.2006	Deniz	Ç12	3370	40 49 07 N 41 09 39 E	8,38	49,00	rocky, silty, stony
13	24.08.2006	Kartal	Ç13	2940	40 50 20 N 41 18 04 E	1,63	2,80	rocky
14	24.08.2006	Devise	Ç14	2935	40 50 22 N 41 18 12 E	0,11	1,00	silty, stony
15	22.08.2005	Keçi	F01	3070	40 44 25 N 40 51 50 E	1,79	12,30	gravel, stony
16	22.08.2005	Çermeş Karagöl	F02	2990	40 44 37 N 40 52 04 E	4,60	32,70	gravel, stony
17	09.07.2005 22.08.2005	Çermeş	F03	2780	40 44 58 N 40 52 09 E	4,77	6,20	gravel, stony
18	25.08.2007	Kayakaynak	F04	3080	40 49 17 N 40 52 43 E	1,02	1,00	stony, muddy
19	25.08.2007	Büyük Balıklı	F05	2990	40 49 28 N 40 52 51 E	6,92	11,00	muddy,stony
20	01.08.2006	Sırpal	F06	2940	40 49 21 N 40 53 40 E	0,95	0,70	sandy-muddy - hard

St. No	Sampling Dates	Lakes	Basins	Alti-tude(m)	Coordinates	Area (ha)	Maxi-mum-depth(m)	Substratum
21	01.08.2006	Çahberik	F07	2810	40 49 17 N 40 54 09 E	1,00	0,50	sandy-muddy
22	08.07.2005 21.08.2005	Atmeydan	F08	2910	40 43 11 N 40 54 01 E	3,24	3,70	sandy-muddy
23	08.07.2005 21.08.2005	Kumlugöl	F09	2860	40 43 22 N 40 54 17 E	0,49	0,80	sandy-muddy
24	08.07.2005 21.08.2005	İncegöl	F10	2915	40 43 06 N 40 54 23 E	0,86	3,00	sandy-muddy
25	21.08.2005	Büyük Kapılı	F11	3000	40 43 00 N 40 54 54 E	6,07	3,70	hard, macrophyta
26	21.08.2005	Altkapılı	F12	3000	40 43 11 N 40 54 57 E	1,45	8,50	sandy-muddy
27	31.07.2006	Kıblekaya	F13	2870	40 49 24 N 41 06 06 E	0,56	3,20	sandy-muddy
28	11.07.2005 24.08.2005	Büyükdeniz	F14	2900	40 52 09 N 41 09 42 E	5,83	15,10	muddy, stony
29	24.08.2005	Meterez	F15	2990	40 51 49 N 41 09 45 E	1,86	0,50	stony, sandy
30	11.07.2005 24.08.2005	İsimsizgöl	F16	2890	40 52 28 N 41 09 46 E	0,55	3,10	muddy, stony
31	24.08.2005	Karadeniz	F17	2770	40 52 42 N 41 10 03 E	2,30	11,50	stony
32	29.07.2006	Ceymakcur	F18	2650	40 53 44 N 41 11 30 E	0,33	1,50	stony
33	06.07.2005 19.08.2005	Büyükgöl	F19	2980	40 38 45 N 40 53 36 E	2,43	10,20	hard, gravel
34	22.08.2007	Tobamızga	F20	2620	41 02 19 N 41 15 37 E	0,75	3,50	sandy-muddy
35	22.08.2007	Küçük Tobamızga	F21	2630	41 02 08 N 41 15 39 E	0,14	1,00	sandy-muddy
36	23.08.2007	Büyük Çiftegöl	F22	2600	40 59 24 N 41 15 41 E	2,27	6,50	sandy-muddy, rocky
37	23.08.2007	Küçük Çiftegöl	F23	2550	40 59 36 N 41 15 49 E	1,11	6,00	sandy-muddy, rocky
38	20.08.2006	Dipsizgöl	İ01	2670	40 33 28 N 40 28 25 E	0,93	2,00	gravel, stone, muddy
39	25.07.2007	Koyun	İ02	3010	40 31 34 N 40 28 58 E	1,68	10,0	rocky, stony,
40	20.08.2006	Küçükhatalan	İ03	2800	40 33 16 N 40 29 22 E	0,24	0,80	silty, muddy, stony,
41	20.08.2006	Hatalan	İ04	2810	40 33 11 N 40 29 24 E	0,61	4,00	silty, muddy, stony,
42	20.08.2006	Küçüksivri	İ05	2710	40 33 36 N 40 29 50 E	0,10	1,00	rocky, silty
43	20.08.2006	Sivrinin	İ06	2700	40 33 39 N 40 29 52 E	0,42	1,50	rocky, silty
44	02.08.2006	Akçaağıl	İ07	2940	40 31 19 N 40 30 40 E	0,59	2,50	sandy-muddy- gravel, stony
45	21.08.2006	Katreç	İ08	2700	40 34 06 N 40 34 51 E	1,73	6,50	rocky, silty
46	21.08.2006	Küçükkatreç	İ09	2690	40 34 13 N 40 34 58 E	0,03	1,00	rocky, silty
47	03.08.2006	Çitrik	İ10	2850	40 39 31 N 40 46 59 E	2,80	14,00	sandy-muddy-gravel-stony
48	03.04.2006	Salar	İ11	2820	40 43 28 N 40 52 09 E	3,20	2,50	sandy-muddy- gravel-stony
49	25.08.2006	Arhavi Karagöl	K01	2660	41 09 28 N 41 24 19 E	7,17	9,00	rocky, silty
50	26.08.2007	Çakır	M01	2530	40 34 34 N 39 41 26 E	5,46	10,00	sandy-muddy, rocky, gravel, a plenty of macro-phyta
51	26.08.2006	Uzungöl	S01	1100	40 37 14 N 40 17 44 E	8,50	6,90	muddy
52	30.07.2007	Kırklarcami	S02	2740	40 31 46 N 40 20 06 E	0,36	4,10	muddy, rocky
53	29.07.2007	Multat Karagöl	S03	2800	40 31 30 N 40 21 46 E	4,70	24,90	muddy
54	27.07.2007	Balık	S04	2570	40 31 54 N 40 23 01 E	4,26	4,50	muddy
55	27.07.2007	Aygır	S05	2710	40 31 39 N 40 23 28 E	4,08	13,00	muddy, sandy, stony
56	29.07.2007	Sarıçiçek	S06	2880	40 31 15 N 40 24 21 E	1,46	5,20	muddy
57	28.07.2007	Büyükyayla Karagöl	S07	2930	40 31 41 N 40 27 03 E	2,13	16,50	muddy
58	28.07.2007	Pirömer	S08	2870	40 32 00 N 40 27 09 E	1,32	16,50	muddy
59	28.07.2007	Buz	S09	3040	40 31 58 N 40 27 36 E	1,98	13,80	muddy

Specimens and mounted materials are being kept in the collection of the authors in Bentological Museum of Fisheries Faculty, University of Ege, İzmir.

Study area. The Pontic mountain range (Eastern Black sea coast) is one of the three major glacier regions of Turkey. Its highest peak is Kaçkar Mountain with 3937 m a.s.l. The mountains are partially glaciated, alpine in character, with steep rocky peaks and numerous mountain lakes.

The locations of the 59 lakes studied as well the characteristics of the sampling sites are shown in Figure 1 and Table 1. All the studied lakes (Table 1) are located above the timber line in a range of altitude from 2530 to 3370 m a.s.l. (except Lake Uzungöl with 1100 m a.s.l.). Surface area of 59 lakes are between 0.03-8.9 ha, while depths from 0.5 to 49 m [16]. They remain frozen from October or November until May or June.

TABLE 2
Minimum and maximum values of the enviromental variables.

Variables	Min	Max
Secchi depth (cm)	50.00	1100.00
Temperature (°C)	2.50	21.00
pH	6.75	9.71
DO (mg L^{-1})	5.30	10.10
EC (µS 25 °C cm^{-1})	12.00	121.80
d°H	0.80	3.40
NO_2^- N (µg L^{-1})	0.00	5.21
NO_3^- N (µg L^{-1})	0.00	105.00
NH_4^- N (µg L^{-1})	0.00	106.90
PO_4^{-3}P (µg L^{-1})	0.00	10.95
Chlorophylll-a (µg L^{-1})	0.00	2.32

TABLE 3
List of species collected from the area during this study.

Tanypodinae	Stations
Ablabesmyia (A) longistyla	51
Apsectrotanypus sp.	36,49,55
Arctopelopia sp.	9
Brundiniella sp.	8
Conchapelopia sp.	53
Macropelopia nebulosa	1,13,14,17,22,33,40,42,43,46,47,49,50,51,53,54,57,59
Macropelopia notata	25
Procladius(Holotanypus)sp	1,2,4,6,8,9,11,17,18,20,21,23,26,28,30,31,34,38,41,43,51,53,57,58
PRODIAMESINAE	
Prodiamesa olivacea	37,51
DIAMESINAE	
Pseudodiamesa (P.) arctica	1,4,5,6,12,17,20,27,32,37,40,42,43,45,46,47,48,50,52,57
Pothastia gaedii	17
ORTHOCLADIINAE	
Corynoneura scutellata	42,43
Cricotopus sp.	1, 19,38,43,54
Cricotopus (I.) trifasciatus	6,13, 39,53
Eukiefferiella sp.	9,55
Metriocnemus sp.	43
Paratrichocladius rufiventris	8
Psectrocladius (A.) platypus	58
Psectrocladius (P.) barbimanus	53,58
Psectrocladius (P.) limbatellus	6,18,51,57,58,59
Psectrocladius (P.) sordidellus	1,3,4,6,13,20,27,42,48,53,56,58
CHIRONOMINAE	
Chironomini	
Chironomus (C.) anthracinus	1,8,9,10,22,25,26,28,30,34,35,51
Chironomus (C.) plumosus	51
Chironomus (C.) tentans	28
Cladopelma goetghebueri	8,9,11
Einfeldia pagana	28
Microtendipes pedellus	9,51
Tanytarsini	
Cladotanytarsus mancus	23,47
Microspectra sp.	3,17,21,28,33,36,37,44,47,48, 49,50,51,52,57,59
Microspectra notescens	10,51,52,57,59
Paratanytarsus austriacus	52,57,58,59
Paratanytarsus dissimilis	57,58,59
Paratanytarsus lauterborni	17,19,2340,43,48
Rheotanytarsus sp.	17,46,52,58
Tanytarsus sp	2,3,4,5,6,8,9,11,18,20,21,24,26,27,29,31,32,33,36,40,41,42,43, 45,47,48,51,53,55,56,57,58,59

RESULTS

Minimum and maximum values of the environmental variables of studied lakes are shown in the Table 2. According to the ammonium, nitrite, nitrate nitrogen levels and total phosphorus level, all of the studied lakes can be classified as 1st class. Similarly, the quality classes of the lakes were changed between I-III according to levels of dissolved oxygen. When the Total Nitrogen (TN) and Total Phosphourus (TP) are taking into consideration, all the lakes show oligotrophic character. Chlorophyll-a concentration of the lakes were generally low and this character also support the above mentioned results [17].

A total of 35 recorded species belong to 5 subfamilies (Tanypodinae, Prodiamesinae, Diamesinae, Orthocladiinae and Chrironominae) of family Chironomidae. Among them subfamilies Chirinominae and Orthocladiinae with 14 and 10 recorded taxa respectively are the two dominant subfamilies in this area.

According to Table 3, the most frequent species is *Tanytarsus* sp. belongs to tribe Tanytarsini that occurred from 33 out of 59 lakes. After that, *Procladius* (*Holotanypus*) sp., *Pseudodiamesa (Pachydiamesa*) *arctica, Micropsectra* sp., and *Psectrocladius* (*P*) *sordidellus* with 24, 20, 16 and 12 occurrence are at the second, third, fourth and fifth rate of frequency respectively.

From the richness point view of catchments related to distribution of Chironomidae, the richest catchment is Solakli Rivers' catchment with 22 taxa. The catchments of Çoruh River (19 taxa), Fırtına River (16 taxa) and İyidere (14 taxa) stand in the next rates. These are followed by Kabisra River and Maçka River's catchments each with 3 taxa.

From quantitative aspects, Fırtına River catchment with 9978 no/m^2, Çoruh River's catchment with 4679 no/m^2 and finally İyidere catchment with 3919 no/m^2 are in the first, second and third rates respectively (Figure 2).

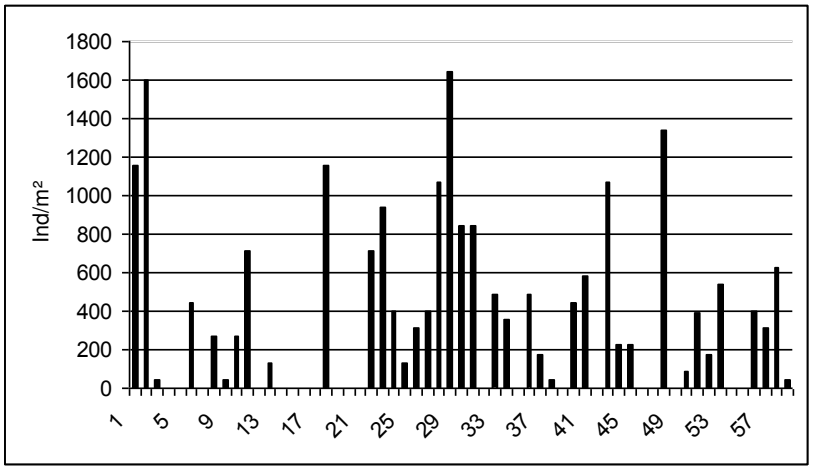

FIGURE 2
Classification of lakes based on obtained quantitative results. (Ind./m^2)

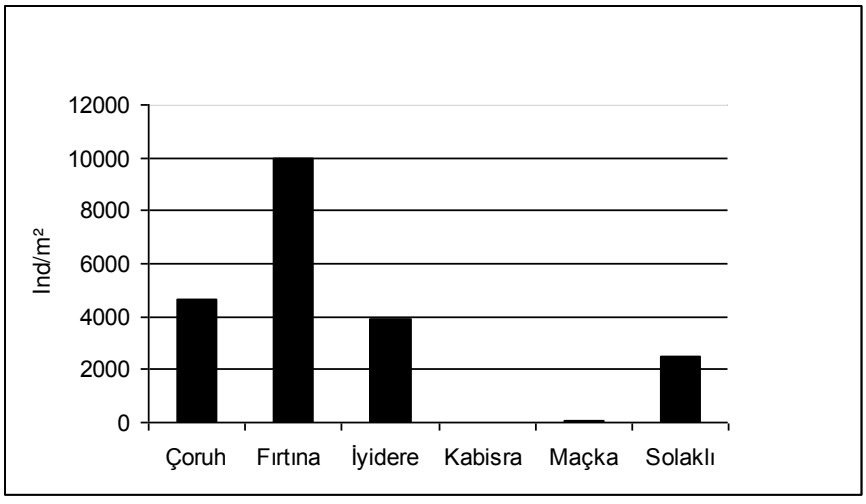

FIGURE 3
Classification of basins based on obtained quantitative results. (Ind./m^2)

In this study area, according to the biodiversity of Chironomidae populations, the richest lake with 10 species is Uzungöl (St 51). Demirkapı Lake (St 57) and Pirömer Lake (St 58) follow Uzungöl by 9 taxa. These lakes are followed by Sivrinin Lake (St 43) with 8 species and finally Ortagöl (St 6), Adalıgöl (Ç08), Ortagöl (Ç09), Çermeş Lake (F03), Büyükdeniz Lake (F14) and Multat Karagöl (S03) each with 6 taxa.

According to the recorded individuals' number, Meterez Lake (St 29) with 1647 no/m^2, Dağbaşı Lake (St 2) with 1603 no/m^2, Salar Lake (St 48) with 1336 no/m^2 and Kayakaynak Lake (St 18) with 1158 no/m^2 are the richest stations respectively.

DISCUSSION

High mountain glacial lakes represent a very special environment for aquatic organisms. These biotops characterized by their low average annual temperature, oligotrophic features and the minor antropogenic impacts [18].

In high elevation mountainous regions, macroinvertebrates have adapted to unique and often extreme environmental conditions. Seasons of macroinvertebrate development are often short and the food resources reduced and irregular. Dispersal and distribution of high mountain macroinvertebrates are complicated by topographic and physiographic barriers, and the scarcity of appropriate habitats [19].

The variation in the diversity and density of macrozoobenthos with water depth has been studied in many lakes and a fall in both parameters has been frequently observed, even in high mountain lakes [20]. The abundance of chironomid larvae usually does not reach very high values in high mountain lakes mainly due to the low productivity of these lakes [18].

They are well known indicators of trophic condition in lakes, of organic pollution in running waters and are considered an interesting biogeographic material as well (4). This is also illustrated in Vorderer Finstertaler Sea, Austria at 2237 m a.s.l.(21). Similarly, the chironomid assemblages of alpine Tatra lakes are characterized by lower species richness and total absence of taxa of tribe Chironomini [22].

Our study shows some similarities with the above mentioned studies in terms of low species richness.

Catalan et al. [23] recorded 4 genera of subfamily Tanypodinae (Ablabesmyia, Macropelopia, Procladius, Zavrelimyia), 3 genera of subfamily Orthocladiinae (Corynoneura, Heterotrissocladius, Psectrocladius) moreover, 3 genera of subfamily Chironominae (Micropsectra, Paratanytarsus, Tanytarsus) during their conducted researche at high-elevated lakes of Pyrenees Mountain (82 lakes). These genera and obtained via present reseach show an obviouse similarity.

Tanytarsini is the most encountered tribus in our study due to record of *Tanytarsus* sp. from 33 stations and *Micropsectra* sp. from 16 stations. This situation is appropriate according to explanation above and as an addittion the lakes we examined have secondary oligotrophic features in terms of recorded species of chironomid. Minor chlorophyll-levels determined in the lakes confirm their oligotrophic beeings. Furthermore, Bryce and Hobart [24] stated that subfamily Tanytarsini (*Tanytarsus, Micropsectra*) and sometimes species of subfamily Diamesinae are common dwellers of moderat oligotrophic lakes.

Mousavi [25] pinpointed that species of subfamilies Diamesinae and Prodiamesinae are the indicator of high pH in vast and deep lakes. Moreover, species of subfamily Orthocladiinae inhabit relatively small lakes with low pH and electrical conductivity. The same author also introduces members of subfamily Tanytarsini as biological indicators of high-pH lakes.

Although Tanytarsini was reported as the typical subfamily of oligotrophic lakes by Mousavi [25] *Tanytarsus* belonging to this tribus, is an eurytopic and a cosmopolitan genus that is observed in almost all limnetic habitats. In addition, it has some marine and even terrestrial types. They are observed within high-altitude mountain lakes with oligotrophic characteristics. We recorded the species of this genus from 33 lakes in altitude range of 1100–3120 m, 6.95–9.71 of pH, 2.5–20.9 °C, 14.6–108.0 $\mu S_{25°C}$ of electrical conductivity. In studies of Boggero et al. [5] conducted in 89 lakes at Alps, optimum altitude, pH and electrical conductivity for species of genus Tanytarsus determined 1882 m, 7.39 and 117.6 $\mu S_{25°C}$ respectively.

Genus *Micropsectra* belonging to Tanytarsini tribus is observed in temporary and warm waters of various habitats. Particularly, it is frequently observed in muddy and floppy bottoms of streams and in mesotrophic-oligotrophic lakes. Many species belonging to this genus have cold stenotherm feature. In our study *Micropsectra* sp. reported from 16 stations (Table 3), is observed between 1100-3050 m of altitude, 6.90-8.82 pH, 3.0-19.7 °C temperature, 24.7-108.0 $\mu S_{25°C}$ electrical conductivity. Boggero et al. [5] determined optimum altitude, pH and electrical conductivity for species belonging to the genus *Micropsectra* 2402 m, 6.91 and 111.4 $\mu S_{25°C}$ respectively.

The genus *Paratanytarsus*, belonging to the same tribus, is a eurytophic and mostly occurred genus. 3 taxa of this genus have been identified during our study and these species have been observed between 2700-3040 m of altitude, 7.14–9.71 of pH, 2.5–20.9 °C of temperature and 18.6–79.0 $\mu S_{25°C}$ of electrical conductivity. Species of the

genus *Paratanytarsus* preffer 2066 m of altitude, 7.40 pH and 89.4 $\mu S_{25°C}$ electrical conductivity [5]. Also the results of research on chironomids of 81 Boreal lakes by Mousavi [25] showed that dispersion of species of genus *Paratanytarsus* in lakes shows a negative correlation with depth. In the present study the most part of species of this genus were recorded from littoral zone of lakes and a very little part of them were caught from deep parts (16.5 m).

Chironomids of Genus *Pseudodiamesa* belonging to Diamesinae subfamily prefer cold-water habitats [26]. Larvae of this genus are usually occupied lakes and streams of cold regions of Holarctic and oriental regions. Larvae of genus *Pseudodiamesa* feed on detritus, small chironomids and other small aquatic invertebrates. Species belonging to this genus show high adaptability to environmental conditions (Milner et al. 2001) [27]. Among them *P. arctica* is the characteristic species of high mountain lakes. This species has been recorded from habitats in 2000-3000 m altitude. They can compose colony in cold habitats in periglacial regions at low altitudes (345-230 meters) [28]. This species has already been reported from the European Alps [4], [5], Tatras [22], [29], Pyrenees [30], Arctic and subarctic regions of Scandinavian, Iceland so far.

We reported *Pseudodiamesa (P.) arctica* and *Pothastia gaedii* from subfamily Diamesinae in the present study.

P. arctica is the third most frequent species in this study and reported from 20 lakes (Table 3). This species were recorded from habitats with 2530-3370 m altitude, 6.95-8.12 of pH, 6.3-21.0 ºC of temperature and 14.6- 58.8 $\mu S_{25°C}$ of electrical conductivity. According to Boggero *et al*. [5] optimum altitude, pH, temperature and electrical conductivity of members of genus *Psedodiamesa* are 2364 m, 7.67 and 79.7 $\mu S_{25°C}$ respectively.

Pothastia gaedii another species of the same subfamily was encountered only from Çermeş Lake.

Orthocladiinae is the dominant chironomid subfamily of arctic zone; however, decline on diversity of its species is obvious as they get closed to temperate zones. Deep lakes and shallow waters in arctic region have their own characteristic faunas [21]. Genus *Psectrocladius* is one genus belong to this subfamily that its species (*P. sordidellus* and *P. limbatellus*) are characteristic species of oligotrophic and cold lakes. Members of this genus are mostly reported from cold north lakes of Europe, i.e. Tatras of Slovenia. In this research *P. sordidellus*, recorded from 12 stations, 2540-3070 m of altitude range, 7.22-8.12 pH, 12.4-21.0 ºC of temperature range and 25.4-77.5 $\mu S_{25°C}$ of electrical conductivity. Another cognate species of later species is *P. limbatellus* was recorded from 6 stations with 1100- 3040 m of altitude, 7.31-7.82 pH, 13.3-18.3 ºC of temperature intervale and 23.8-108.0 $\mu S_{25°C}$ electrical conductivity. Oprtimum altitude, pH and electrical conductivity determined for species of genus *Psectrocladius* are 1905 m, 7.66 and 7.66 $\mu S_{25°C}$ respectively [5].

A large number of larvae of the species belonging to the genus *Procladius* (*Holotanypus*) sp. and subfamily Tanypodinae prefer muddy substrates with slow flowing water, especially in pools or small lakes. Species of this genus are widely distributed all over the world in various zoogeographical zones [14].

Species of genus *Procladius* prefer habitats with 2051 m altitude, 6.87 pH and 50.8 $\mu S_{25°C}$ electrical conductivity.

During this study *Procladius* (*Holotanypus*) sp., one of the dominant species in our study area with 24 occurrence from 1100- 3080 m altitude, 6.96-9.82 pH, 2.5-21.0 ºC temperature and 12-108 $\mu S_{25°C}$ electrical conductivity.

Optimum altitude for species of genus Chironomus was calculated about 1455 m. Additionally they prefer 8.48 pH and 106.1 $\mu S_{25°C}$ of electrical conductivity of water [5].

Chironomus (*C.*) *anthracinus* is a species belong to Chironomini tribus, that during present study it was encountered from 12 stations. Habitats occupied by this species were in 1100- 3020 m of altitude, pH range of water were measured 6.75-9.82, water temperature were 2.5-21.0 ºC and electrical conductivity were measured between 13.5-108.0 $\mu S_{25°C}$.

Based on measured environmental variables and also biological features obtained during this study from all the 59 lakes, these habitats could be classified in the first class of water quality. Because of the importance of high-altitude lakes, monitoring and protection of these biyotops is an essential item that should be considered. For instance, governments can remove or at least limite the contaminant activities such as agriculture, livestocks etc. around these lakes. Even though some lakes of study area are under protection (Kaçkar Mountains National Park, the Uzungöl Nature Park and Uzungöl Special Environmental Protection Area and Altindere Valley National Park), others are at risk due to tourism, farming and illegal fishing activities. Moreover, eventhough Uzungöl is an under protection area, currently is impacted by intensive residential and tourism.

ACKNOWLEDGEMENTS

We would like to thank Dr. Süleyman Balik, Dr. Murat Özbek, Dr. Cem Aygen, Dr. Ali İlhan, Dr. Esat T. Topkara and Mesut Kaptan for their valuable scientific and technical supports. We also appreciate The Scientific and Technical Research Council of Turkey (TUBITAK) for supporting the

project (grant number: 104/Y/ 183), which these results are a part of that.

REFERENCES

[1] Galas, J. (2004) Invertebrate communities of high mountain lakes (Polish Tatra Mts.). Teka Komisji Ochrony i Kształtowania Środowiska Przyrodniczego. 1, 57-63.

[2] Mosello, R. (1986) Effect of acid deposition on subalpine and alpine lakes in NW Italy. Memorie dell' Istito Italiano di Idroboilogia. 44, 117-146.

[3] Cranston, P.S. (1982) A Key to the Larvae of the British Orthocladiinae (Chironomidae). Ambleside. Freshwater Biol Assoc Sci Publ. 45, 152p.

[4] Rossaro, B., Boggero, A., Lencioni, V. and Marziali, L. (2009) Benthic macroinvertebrates as indicators in lakes. Atti XIX Congr. SiTE 15-18/9/2009 Bolzano. 107-114.

[5] Boggero, A., Füreder, L., Lencioni, V., Simcic, T., Thaler, B., Ferrarese, U., Lotter, A.F. and Ettinger, R. (2006) Littoral chironomid communities of Alpine lakes in relation to enviromental factors. Hydrobiologia. 562, 145-165.

[6] Taşdemir, A., Yıldız, S., Topkara, E.T., Özbek, M., Balık, S. and Ustaoğlu, M.R. (2004) Yayla Gölü'nün (Buldan-Denizli) Bentik Faunası. Türk Sucul Yaşam Dergisi. 2, 182-190.

[7] Taşdemir, A., Ustaoğlu, M.R. and Balık, S. (2011) Contribution to the Knowledge on the Distribution of Chironomidae and Chaoboridae (Diptera: Insecta) Species of Lakes on Taurus Mountain Range (Turkey). Journal of the Entomological Research Society. 13, 15-25.

[8] Toksöz, A. and Ustaoğlu, M.R. (2005) Gölcük Gölü'nün (Bozdağ, Ödemiş) Profundal Makrobentik Faunası Üzerine Araştırmalar. Ege Üniversitesi Su Ürünleri Dergisi. 22, 173-175.

[9] Ustaoğlu, M.R., Balık, S., Sarı, H.M., Özdemir Mis D., Aygen, C., Özbek, M., İlhan, A., Taşdemir, A., Yıldız, S. and Topkara, E.T. (2008) Uludağ (Bursa)'daki Buzul Gölleri ve Akarsularında Faunal bir Çalışma. Ege Üniversitesi Su Ürünleri Dergisi. 25, 295-299.

[10] Yıldız, S., Taşdemir, A., Özbek, M., Balık, S. and Ustaoğlu, M.R. (2005) Macrobenthic invertebrate fauna of Lake Eğrigöl (Gündoğmuş-Antalya). Turkish Journal of Zoology. 29, 275-282.

[11] Gültutan, Y. and Kazancı, N. (2009) A research on Chironomidae (Diptera) Fauna of Eastern Region and water quality relationship. Review of Hydrobiology. 2, 57-79.

[12] APHA (1989) Standard Methods for the Examination of Water and Waste Water. American Water Works Association and Water Pollution Control Federation. American Public Health Association, Washington D.C.

[13] Hirvenoja, M. (1973) Revision der Gattung Cricotopus von der Wulp und ihrer Verwandten (Diptera, Chironomidae). Annales Zoologici Fennici. 10, 1-363.

[14] Wiederholm, T. (1983) Chironomidae of the Holarctic region. Keys and diagnoses. Part I. Larvae. Entomologica Scandinavica. 19, 1-457.

[15] Klink, A.G. and Moller Pillot, H.K.M. (2003) Chironomidae larvae. Key to the Higher Taxa and Species of the Lowlands of Northwestern Europe. World Biodiversity Database, CD-ROM Series. Expert Center for Taxonomic Identification, University of Amsterdam.

[16] Sarı, H.M., Ustaoğlu, M.R., İlhan, A. and Özbek, M. (2015) Morphometrical features of the lakes on Kaçkar and Soğanlı Mountains (Turkey). Ege Journal of Fisheries and Aquatic Sciences. 32, 31-36.

[17] Aygen, C., Özdemir Mis, D. and Ustaoğlu, M.R. (2012) Discovering the hidden biodiversity of Crustacea (Branchiopoda Maxillopoda and Ostracoda) assemblages in the high mountain lakes of kaçkar mountains (Turkey). Journal of Animal and Veterinary Advances. 11, 67-73.

[18] Tátosová, J. and Stuchlik, E. (2006) Seasonal dynamics of chironomids in the profundal zone of a mountain lake (Ladove pleso, the Tatra Mountains, Slovakia). Biologia (Bratisl). 18, 203-212.

[19] Mani, M.S. (1968) Ecology and Biogeography of High Altitude Insects. Dr. W. Junk N. V. Publishers, The Hague. 55, 501-502.

[20] Rieradevall, M., Bonada, N. and Prat, N. (1999) Substrate and depth preferences of macroinvertebrates along a transect in a Pyrenean high mountain lake (Lake Redó, NE Spain). Limnetica. 17, 127-134.

[21] Armitage, P., Cranston, P.S. and Pinder, L.C.V. (1995) The Chironomidae. The biology and ecology of non-biting midges. Chapman and Hall, London, UK, 572p.

[22] Bitušík, P., Svitok, M., Kološta, P. and Hubková, M. (2006) Classification of the Tatra Mountain lakes (Slovakia) using chironomids (Diptera, Chironomidae). Biologia (Bratisl). 61, 191-201.

[23] Catalan, J., Camarero, L., Felip, M., Pla, S., Ventura, M., Buchaca, T., Bartumeus, F., de Mendoza, G., Miró, A., Casamayor, E.O., Medina-Sánchez, J. M., Bacardit, M., Altuna, M., Bartrons, M. and de Quijano, D.D. (2006) High mountain lakes: extreme habitats and witnesses of environmental changes. Limnetica. 25, 551-584.

[24] Bryce, D. and Hobart, A. (1972) The biology and identification of the larvae of the Chirono-

midae (Diptera). Entomologist's Gazette. 23, 175-218.

[25] Mousavi, S.K. (2002) Boreal chironomid communities and their relation to environmental factors – the impact of lake depth, size and acidity. Boreal Environment Research. 7, 63-75.

[26] Serra-Tosia, B. (1976) Chironomides des Alpes: Le genre Pseudodiamesa (Diptera, Chironomidae). Travaux Scientifiques du Parc National de la Vanoise. 7, 117-138.

[27] Milner, A.M., Brittain, J.E., Castella, E., Petts, G.E. (2001) Trends of macroinvertebrate community structure in glacier-fed rivers in relation to environmental conditions: asynthesis. Freshwater Biololgy. 46, 1833–1847.

[28] Ilyashuk, B.P., Ilyashuk, E.A., Makarchenko, E.A. and Heiri, O. (2010) Midges of the genus Pseudodiamesa Goetghebuer (Diptera, Chironomidae): current knowledge and palaeoecological perspective. Journal of Paleolimnology. 44, 667–676.

[29] Krno, I., Šporka, F., Štefková, E., Tirjaková, E., Bitušík, P., Bulánková, E., Lukáš, J., Illéšová, D., Derka, T., Tomajka, J. and Černý, J. (2006) Ecological study of a high-mountain stream ecosystem (Hincov potok, High Tatra Mountains, Slovakia). Acta Societatis Zoologicae Bohemicae. 69, 299–316.

[30] Rieradevall, M., Jiménez, M. and Prat, N. (1998) The zoobenthos of six remote high mountain lakes in Spain and Portugal. Verhandlungen des Internationalen Verein Limnologie. 26, 2132-2136.

Received: **01.11.2017**
Accepted: **26.04.2018**

CORRESPONDING AUTHOR

Ayse Tasdemir
Ege University,
Faculty of Fisheries,
Department of Hydrobiology,
35100-Bornova – Izmir

e-mail: ayse.tasdemir@ege.edu.tr

© by PSP Volume 27 – No. 7/2018 pages 4598-4605 Fresenius Environmental Bulletin

Mn(II)-ACTIVATED PERSULFATE FOR OXIDATIVE DEGRADATION OF DDT

Zhiqi Wei[1], Ting Gao[1], Jizeng Wang[4], Hui Liu[2,3], Chengshuai Liu[1], Jushu Zhu[1], Jianmin Zhou[2,*], Manjia Chen[1]

[1]Guangdong Key Laboratory of Agricultural Environment Pollution Integrated Control, Guangdong Institute of Eco-Environmental and Soil Sciences, Guangzhou 510650, China
[2]South China Institute of Environmental Sciences, Ministry of Environmental Protection, Guangzhou 510655, China
[3]Qianjiang Environmental Protection Bureau of Hubei Province, Qianjiang 433199, China
[4]College of Environmental Science and Engineering, Zhongkai University of Agricultural and Engineering, Guangzhou 510225, China

ABSTRACT

The process of in situ chemical oxidation (ISCO) by persulfate ($S_2O_8^{2-}$) can be accelerated by metal ion activation, so as to more effectively degrade the subsurface pollutants owing to the enhancement of sulfate radicals ($SO_4^{\bullet -}$) generation. Mn^{2+} is a natural soil metal ion usually exists together with organic pollutants in contaminated soils and groundwater. In this study, the oxidative degradation of DDT by Mn^{2+} activated persulfate at different reaction conditions was systematically studied. The results showed that Mn^{2+} is a more stable activator for persulfate oxidation than other reported metal ions (e.g. Fe^{2+} reported in many papers previously). The activation of persulfate by Mn^{2+} ions gave DDT a long lasting and efficient degradation effect and a high mineralization rate. With fixed DDT and persulfate concentrations, higher Mn^{2+} concentrations would give DDT higher degradation rates, and higher temperature accelerated DDT degradation with Mn^{2+} activation. The pH conditions also posed a significant effect on DDT degradation by Mn^{2+} activated persulfate, and acidic conditions were found to be more favorable for DDT degradation. The results obtained in this study may give a promising indication and new technology with persulfate for in situ remediating soils and groundwater that contaminated by organo-chlorine pesticides.

KEYWORDS:
ISCO, Manganese ion, Persulfate activation, Degradation, Organo-chlorine pesticides, pH, Temperature

INTRODUCTION

Organo-chlorine pesticides are among the most popular and commonly used pesticides worldwide, and are primarily employed for control of plant disease, annual grasses, and broadleaf weeds in farmland. As expected, the comprehensive use of these pesticides has resulted in serious non-point contamination, and organo-chlorine pesticides have been widely detected in groundwater and soils. For example, metolachlor is among the top five most frequently detected pesticides in groundwater in the United States [1-8]. Organo-chlorine pesticides have been reported to be of moderate to high chronic toxicity to aquatic vertebrates and invertebrates, and of high toxicity to aquatic plants and some green algae [2, 3]. Most organo-chlorine pesticides have been demonstrated to be carcinogenic in several studies [4]. Therefore, the development of strategies aiming to remove organo-chlorine pesticides from contaminated groundwater and remediate the contaminated soil sites is a timely and important task

Although organo-chlorine pesticides may be subject to natural attenuation and biotransformation in water and soils, such processes are often very slow particularly under nutrient-limited conditions, such as in subsurface soils or groundwater [9-11]. Hydrolysis is a main and natural decomposition process of organo-chlorine pesticides in soils and groundwater [11], and several nucleophilic sulfur compounds, such as bisulfide [12], polysulfide [12], dithionite [13], thiosulfate [14], and bisulfate [2], have been studied to increase the hydrolysis rates of chloroacetanilides. However, the toxicity threat still exists owing to the considerable amounts of intermediates generated through weak degradation, and some of them may be even more toxic than their parent compounds [15]. Similar shortcomings may also exist in organo-chlorine remediation technologies relying on iron-bearing clay minerals, iron oxides, or organic matters for reduction processes in anaerobic soils and groundwater [13-16]. Therefore, it is necessary to explore more effective chloroacetanilide decomposition technology under oxygen-depleted condition for soil and groundwater remediation.

In past 20 years, in situ chemical oxidation (ISCO) has become a promising remediation technology for soils and groundwater contaminated with organic pollutants, and it was usually performed by injecting chemical oxidants, such as hydrogen peroxide, permanganate, ozone, or persulfate [17]. Among those available oxidants, per-

sulfate is the newest and least-studied one, but it has received increasing attention for being an alternative oxidant for soil and groundwater remediation in ISCO [18, 19]. Besides the high oxidative potential (E^0 = 2.01 V), persulfate is moderately stable in the subsurface and can provide the transport potential from the point of injection to target pollutants in low permeability region.

Persulfate is usually activated by heat [20], UV light [21], alkaline [22], Ultrasound [23], transition metals [24], or soil minerals [25, 26] to form sulfate radical ($SO_4^{\bullet -}$), which even has a greater oxidative potential (E^0= 2.6 V) than persulfate. In soils and groundwater, the resulting sulfate radicals are free to react with a wide range of contaminants, and this can further generate other reactive species, such as the hydroxyl radical (OH•), peroxymonosulfate (HSO_5^-), and hydrogen peroxide (H_2O_2) [25]. Subsequent reactions involving OH• and H_2O_2 can yield molecular oxygen [27] which is also critical for the destruction of organic pollutants in soils and groundwater.

However, exploring a feasible activation method for ISCO is a major challenge and the primary limitation is the insufficient knowledge of the reaction pathways of activated persulfate at subsurface environment [22]. UV light, heat, ultrasound, and alkaline may not be appropriate activation methods for ISCO because of the application limitation and the disturbance of soil composition [19]. As part of the soil constitutes, some transition metals in earth minerals, such as pyrite, birnessite, and goethite, may be efficient and appropriate for persulfate activation at subsurface environment [26]. However, extreme conditions, such as strong acid or base, may sometimes be needed for effective degradation of target pollutants, and, furthermore, some of these solids may decrease the utilization efficiency of sulfate radicals [28]. Metal ions, especially ferrous, have been proven to be an efficient persulfate activator, and can be easily injected for ISCO in soils and groundwater [19]. The same as ferrous, Mn^{2+} also is a natural produced in soil and groundwater, in which significant amounts of Mn^{2+}can be produced adsorbed on mineral surface through anaerobic reduction of manganese minerals [29], and in contaminated soils and groundwater, Mn^{2+}may usually exists together with the pollutants [30]. To our knowledge, however, little work was carried out to investigate the persulfate activation by manganese ions for degrading organo-chlorine pesticides.

Therefore, this study attempts to (1) determine the persulfate activating efficiency by manganese ions for DDT degradation; (2) evaluate the influence of reaction conditions (temperature and pH) on DDT degradation by persulfate activated by manganese ions. DDT (1,1,1-trichloro-2,2-bis(4-chlorophenyl) ethane) was selected as the studied organo-chlorinated pesticide because it has been widely used in farmland [31] and DDT contamination of soil and groundwater remains a widespread environmental concern although it has been banned as an insecticide in many countries for over 40 years [32]. DDT is of highly persistent and stable in environment, and it has been classified as priority pollutants by United States Environmental Protection Agency due to its toxicity, long biological half-time, and high lipophilicity [33].

MATERIALS AND METHODS

Chemicals. Sodium persulfate ($Na_2S_2O_8$, 98+% purity) was obtained from Sigma-Aldrich (St. Louis, MO, USA). DDT (100% purity) was obtained from Accustandard (USA). Ascorbic acid (> 99%) was obtained from Guangzhou Chemical Industry Co. Ltd (Guangzhou, China). All other chemicals were in analytical grade and purchased from BDH Chemicals (Poole, UK). Eighteen MΩ water obtained from a Milli-Q water purification system was used to prepare the reaction solutions and the mobile phase for high performance liquid chromatography (HPLC) analysis. All chemicals were used without further purification.

Experimental procedures. Stock solution of DDT (50 mg/L) was prepared with methanol (HPLC grade) and stored at -18 ºC. Prior to experiment, DDT solution was diluted to the designated concentration of 10 mg/L by double distilled water (DDW), and the sodium persulfate solution (20 mM) was also prepared by DDW. The reaction pH was kept constant by the phosphate buffer solution, together by adjusting with 0.1 M NaOH or 0.1 M HCl, if necessary. All reactions were conducted in 40 mL sealed polypropylene copolymer (PPCO) test tubes in triplicate. Reaction solutions were first prepared by adding $MnCl_{2(aq)}$ with DDT solution into the phosphate buffer solution. The reaction was then initiated by adding the persulfate into the prepared reaction solution in PPCO tubes which were subsequently shaken in a 150-rpm orbital shaker (LMS Cooled Incubators, Wolf Laboratories Limited, York, UK) at constant temperature. At designated sampling time, a 4-mL sample was collected from each tube and immediately passed through a 0.22-μm hydrophilic PTFE filter (Millipore, MA, USA) for the compositional analysis. The samples of ecological toxicity test were collected (40 mL) with 10 h reaction time and were immediately added with 1.0 mL ascorbic acid (1.0 M) to quench further oxidative reaction. All experiments were carried out in two replicates with the mean values of their results reported.

Analytical methods. The DDT concentration in aqueous solution was determined using a gas

chromatograph (Thermo Fisher Trace) equipped with a Thermo Fisher DSQ mass selective detector and Trace RT-5MS silica fused capillary column (Thermo Fisher Scientific, USA, 30 m × 0.25 mm i.d., 0.25-μm film thickness). The injector temperature was 200 °C and the flow rate of helium was 1.0 mL/min. The column temperature was set at 100 °C for 2 min and increased at a rate of 15 °C to 600 °C, and then switched to a rate of 5 °C/min. The temperature was finally increased to 270 °C and maintained isothermally for 10 min. The ion used for quantification of DDT was *m/z* of 235. The concentrations of total organic carbon (TOC) were determined by a total organic analyzer (TOC-V CPH, Shimadzu, Japan). Sodium persulfate concentration was determined by the iodometric method [34], and the concentrations of generated sulfate ions were determined by a Dionex ICS-90 IC (Sunnyvale, CA, USA), with a mobile phase of 1.0 mM $NaHCO_3$-8.0 mM Na_2CO_3 aqueous solution at a flow rate of 1.0 mL/min.

RESULTS AND DISCUSSION

DDT degradation by Mn^{2+} activated persulfate. By using 5 mg/L as the initial DDT concentration, Fig. 1 shows the results of oxidative degradation of DDT and the removal of TOC by persulfate activated with manganese ions at 25 °C. Without Mn^{2+} in the solution, DDT underwent a steady but much slow degradation process due to the low-concentration sulfate radicals generated by the self-decomposition of persulfate and the removal results were 9.6% for initial DDT and 2.1% for TOC at reaction time of 72 hours. When manganese ions were introduced into the reaction system, the DDT degradation with Mn^{2+} activated persulfate exhibits a steady and efficient degradation process throughout the reaction period, with 72.4% and 36.7% of the initial DDT removed and mineralized in 72 hours, respectively.

The activation of persulfate by manganese ions was found to be successful and the degradation of DDT was effectively enhanced (Fig. 1). Furthermore, the corresponding resulted SO_4^{2-} reaction product in Fig. 2 may also indicate an activation process that Mn^{2+} activates persulfate to form sulfate radicals and sulfate ion.

$$Mn^{2+} + S_2O_8^{2-} \rightarrow Mn^{3+} + SO_4^{-\cdot} + SO_4^{2-} \quad (1)$$

The Mn^{2+}can be oxidized to become Mn^{3+} although with a lower reaction rate and higher energy barrier to overcome [24]. However, Mn^{2+} is thus more stable and the generated sulfate radicals were mainly consumed by DDT oxidation. Another potential mechanism of the enhanced DDT oxidation may be due to the generation of Mn^{3+} which is unstable and may act as an oxidant for DDT degradation. The recurred Mn^{2+}ion in such process is also capable to activate another persulfate, and this may explain the well-maintained DDT degradation efficiency throughout the entire reaction period. At the end of reaction period (72h), both the DDT and TOC removals were found higher with the experiment activated by Mn^{2+} ions. In addition, we observed the lower consumption of persulfate with Mn^{2+}activation, indicating the high efficient use of persulfate for the oxidation and mineralization of DDT.

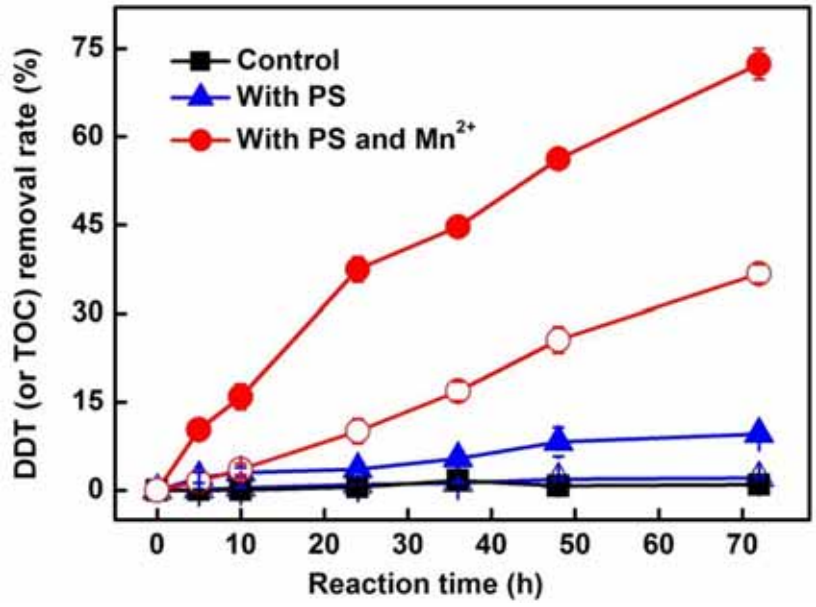

FIGURE 1

Oxidative degradation of 5 mg/LDDT by 5.0 mM persulfate (PS) at pH 4 and 25 °C. The concentration of activation manganese ions was 2.5 mM, if used. Solid symbol represents DDT removal; open symbol is for

TOC removal. Values for data points represent the mean of duplicate reactions; error bars not visible are smaller than symbols

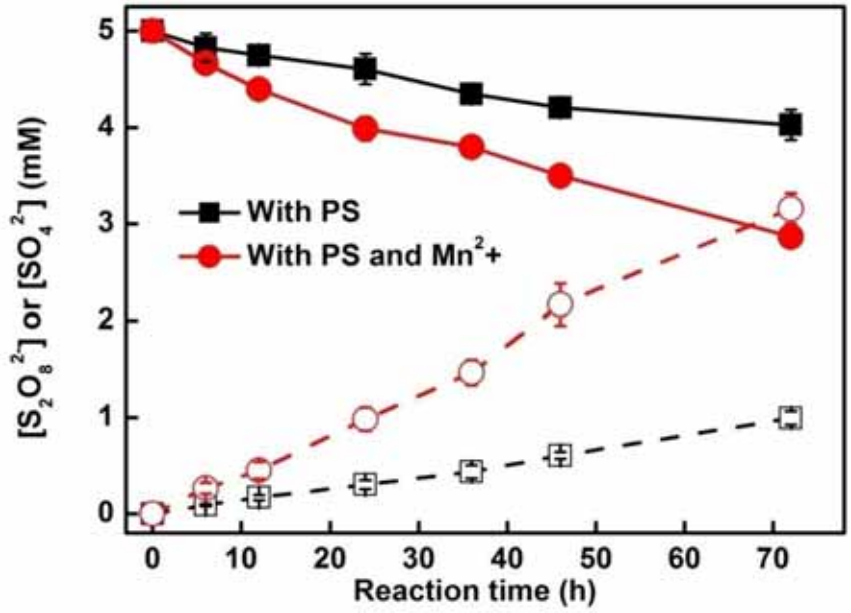

FIGURE 2

Concentrations of persulfate (solid line with solid symbols) and sulfate ions (dash dot line with open symbols) in the system during the DDT degradation processes portrayed in Fig. 1. Values for data points represent the mean of duplicate reactions; error bars not visible are smaller than symbols

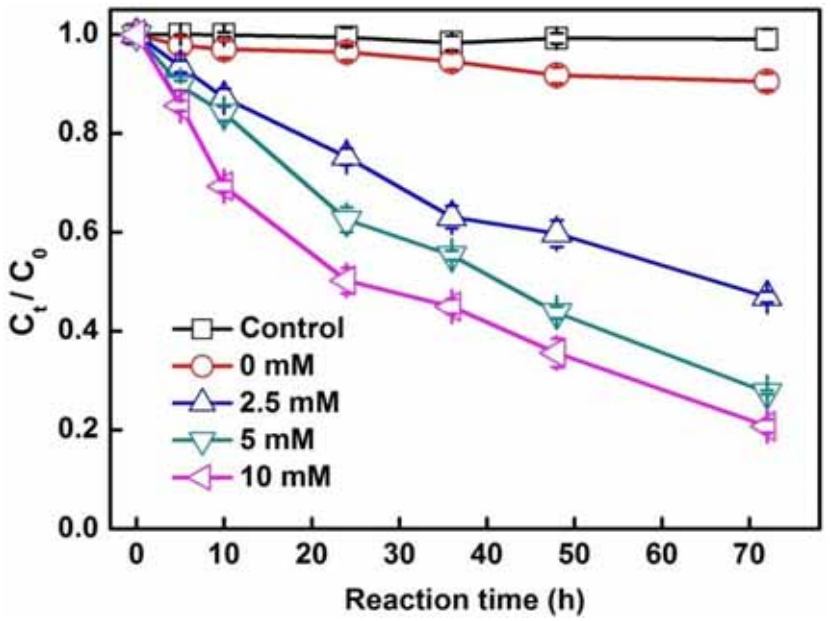

FIGURE 3

Degradation of DDT by persulfate oxidation activated by different concentrations of Mn^{2+} ions under pH 4.0 and 25°C. The initial concentration of DDT is 5 mg/L, and the persulfate is of 5.0 mM. Values for data points represent the mean of duplicate reactions; error bars not visible are smaller than symbols

Effects of different Mn^{2+} concentrations. With 5.0 mM persulfate at 25 °C, different concentrations of Mn^{2+} were added separately to investigate their effect for DDT degradation (Fig. 3). As discussed in previous section, the persulfate activation by Mn^{2+} generally shows a continuous degradation process throughout the reaction period. Higher Mn^{2+} concentration was also found to facilitate the degradation rate, and when Mn^{2+} concentrations were 2.5, 5.0, and 10 mM, the removal of DDT after 72 days was around 53.1%, 72.4%, and 79.2%, respectively. According to equation (1), 5.0 mM persulfate can be activated by 5.0 mM of Mn^{2+} ions. This proposed activation process can also be

confirmed by observing the limited effect of increasing the DDT degradation by Mn^{2+} ion concentration higher than this stoichiometric restriction, such as in 10 mM (Fig. 3).

Temperature effect on DDT degradation. Fig. 4 demonstrates the results of DDT degradation at 25°C and 45 °C through the persulfate activation by 2.5 mM Mn^{2+} ions. Without manganese ions activator, the DDT degradation rate at 45 °C was significantly increased when comparing to that at 25 °C and achieved a 79.2% removal of DDT in 72 h. Heat is another important and efficient method to activate persulfate [20], and as a result the DDT degradation was enhanced in the experiment. Activating persulfate by Mn^{2+} ions at elevated temperatures was found to be more beneficial for the DDT degradation. The enhanced effect shows an increase with the progress of reaction time, and the result has further achieved a complete DDT degradation (100% removal) in 48 h at 45 °C. In such system, both Mn^{2+} and heat may activate persulfate to generate more $SO_4^{-}\cdot$ radicals for the DDT degradation. Since the generated $SO_4^{-}\cdot$ is not consumed by Mn^{2+}, much higher DDT degradation rate can be obtained at higher temperatures. A potential mechanism may also arise from the acceleration of metal activation rate for persulfate due to the increase of reaction temperature. Persulfate may be more ready to be decomposed at higher reaction temperature, and Mn^{2+} ions can thus more efficiently activate persulfate to generate $SO_4^{-}\cdot$ radicals for DDT degradation. The overall effect for DDT removal was found to be 21.4%, 39.4%, 65.9%, 79.5%, and 100% by Mn^{2+} activation at 45 °C for reaction time of 5, 10, 24, 36, and 48 h, respectively. Such result is clearly a significant enhancement, comparing to the corresponding 10.3%, 15.9%, 37.4%, 44.7%, and 56.2% removals obtained at the 25 °C experiment (Fig. 4).

Effect of solution pH. The reaction pH commonly plays an important role in the degradation of organic pollutants in ISCO process. We investigated the degradation behavior of DDT by 5.0 mM persulfate activated with 2.5 mM Mn^{2+}ions under acidic (pH 4), neutral (pH 7), and alkaline (pH 10) conditions at 25 °C (Fig. 5). In general, the rate of DDT degradation decreases with the increase of pH, due to the more favorable sulfate radical generation under acidic condition. However, different persulfate activation mechanisms may dominate under different pH environments. For example, the metal ion activation mechanism may be responsible for sulfate radical generation under acidic condition and lead to the degradation of DDT. Under neutral or even alkaline condition, levels when the reaction pH is increased to neutral and even alkaline levels, the strong hydrolysis of Mn^{2+}ions may significantly interfere the persulfate activation by free aqua metal ions [24]. Therefore, at high pH the base-activated persulfate may be mainly responsible for the generation of sulfate radicals for DDT degradation. The base activation mechanism has been confirmed by Furman et al. as follows [22]:

$$2S_2O_8^{2-} + 2H_2O \rightarrow SO_4^{-}\cdot + 3SO_4^{2-} + O_2^{-}\cdot + 4H^+ \quad (2)$$

Furthermore, under highly alkaline condition, sulfate radicals can also react with hydroxyl anions to generate hydroxyl radicals (OH·) which have lower oxidation potential than that of sulfate radicals:

$$SO_4^{-}\cdot + OH^- \rightarrow + SO_4^{2-} + OH\cdot \quad (3)$$

As a result, the very low DDT degradation rates were observed in the experiments of pH=10.

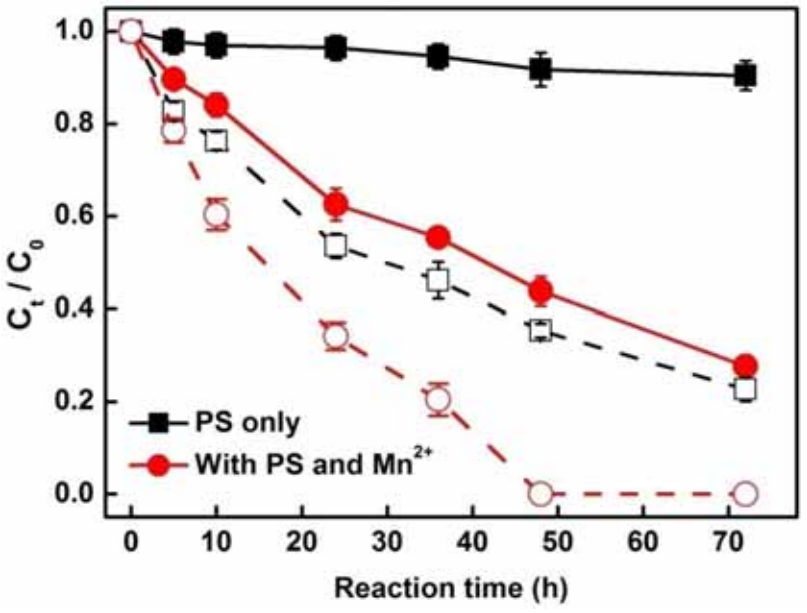

FIGURE 4

Degradation of DDT 5 mg/L by persulfate (5 mM) (PS) oxidation activated by Mn^{2+} (2.5 mM) at 25 °C (solid line with solid symbols) and 45 °C (dash dot line with open symbols) reaction temperature under pH

4.0. Values for data points represent the mean of duplicate reactions; error bars not visible are smaller than symbols

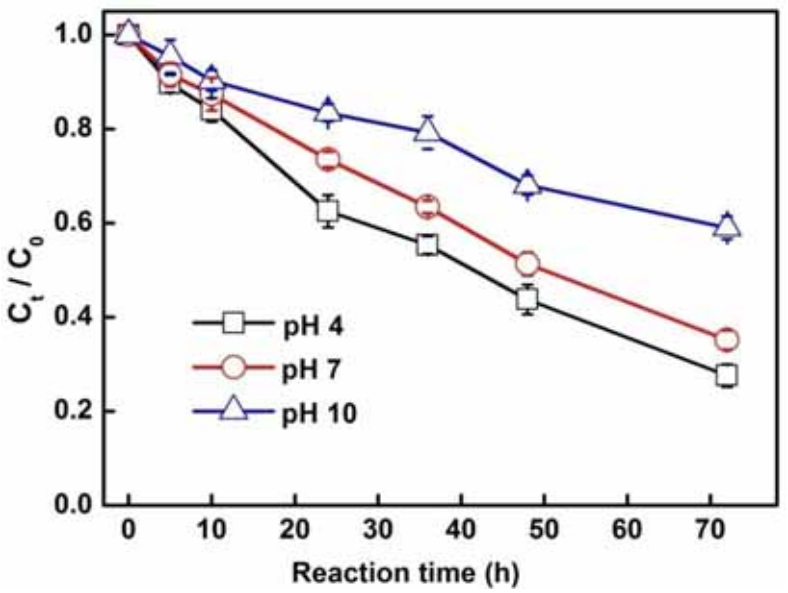

FIGURE 5

Degradation of DDT (5 mg/L) under different pH conditions by 2.5 mMMn^{2+} activated persulfate at 25 °C. The persulfate concentration was 5 mM and the pH was controlled by phosphate buffer solution. Values for data points represent the mean of duplicate reactions; error bars not visible are smaller than symbols

CONCLUSIONS

In this study, Mn^{2+} ions were used to activate persulfate for DDT degradation. Compared to Fe^{2+} activated persulfate oxidation for pollutants degradation, that have been widely reported previously, Mn^{2+} activation persulfate was proven to lead to a more steady and efficient process for oxidative degradation of DDT. Based on the same DDT and persulfate concentrations, the rate of DDT degradation increased when the higher Mn^{2+} concentration was used for persulfate activation. Higher temperatures generally can enhance the degradation rate, since the activation of persulfate may be achieved by both heat and metal ions. The further testing under different pH values showed the preference of acidic environment in DDT degradation, with the design of activating persulfate by Mn^{2+} ions in the treatment process.

ACKNOWLEDGEMENTS

This word was funded by the Special Fund for Agro-Scientific Research in the Public Interest of China (201503107), the National Key R & D Program of China (2017YFD0800700), the Construction Project of Modern Agricultural Science and Technology Innovation Alliance of Guangdong Province, China (2016LM2149), the Science and Technology Planning Project of Guangdong Province, China (2016B020242006, 2016TX03Z086 and 2016A020209005), and the Science and Technology Planning Project of Guangzhou, China (201704020200).

REFERENCES

[1] Kolpin, D.W., Barbash, J.E. and Gilliom, R.J. (2000) Pesticides in ground water of the United States, 1992-1996. Ground Water. 38, 858-863.

[2] Bian, H., Chen, J., Cai, X., Liu, P., Wang, Y., Huang, L., Qiao, X. and Hao, C. (2009) Dechlorination of chloroacetanilide herbicides by plant growth regulator sodium bisulfite. Water Res. 43, 3566-3574.

[3] Samtani, J.B., Masiunas, J.B. and Appleby, J.E. (2010) White oak and northern red oak leaf in leaf injury from exposure to chloroacetanilide herbicides. Hortsci. 45, 696-700.

[4] Oosterhuis, B., Vukman, K., Vági, E., Glavinas, H., Jablonkai, I. and Krajcsi, P. (2008) Specific interactions of chloroacetanilide herbicides with human ABC transporter proteins. Toxicol. 248, 45-51.

[5] Hatzianestis I., Sklivagou E. and Georgakopoulou E. (2001) Hydrocarbons, pesticides and PCBs in sediments from Thermaikos Gulf. Fresen. Environ. Bull. 10, 63-68.

[6] Semeena S. and Lammel G. (2003) Effects of various scenarios of entry of DDT and gamma-HCH on the global environmental fate as predicted by a multicompartment chemistry-transport model. Fresen. Environ. Bull. 12, 925-939.

[7] Dünnbier U., Heberer T. and Reilich C. (1997) Occurrence of bis (chlorophenyl) acetic acid(DDA) in surface and ground water in Berlin. Fresen. Environ. Bull. 6, 753-759.
[8] Milun, V. and Zvonarić, T. (2008) Monitoring of chlorinated pesticides and PCBs in the eastern Adriatic coastal waters using mussels Mytilusgalloprovincialis as indicator. Fresen. Environ. Bull. 17, 1891-1900.
[9] Krause, A., Hancock, W.G., Minard, R.D., Freyer, A.J., Honeycutt, R.C., LeBaron, H.M., Paulson, D.L., Liu, S. and Bollag, J.M. (1985) Microbial transformation of the herbicide metolachlor by a soil actinomycete. J. Agric. Food Chem. 33, 584-589.
[10] Potter, T.L. and Carpenter, T.L. (1995) Occurrence of alachlor environmental degradation products in groundwater. Environ. Sci. Technol. 29, 1557−1563.
[11] Carlson, D.L., Than, K.D. and Roberts, A.L. (2006) Acid- and base-catalyzed hydrolysis of chloroacetamide herbicides. J. Agric. Food Chem. 54, 4740-4755.
[12] Loch, A.R., Lippa, K.A., Carlson, D.L., Chin, Y.P., Traina, S.J. and Roberts, A.L. (2002) Nucleophilic aliphatic substitution reactions of DDT, alachlor, and metolachlor with bisulfide (HS^-) and polysulfide (S_n^{2-}). Environ. Sci. Technol. 36, 4065-4073.
[13] Boparai, H.K., Shea, P.J., Comfort, S.D. and Snow, D.D. (2006) Dechlorinating chloroacetanilide herbicides by dithionite-treated aquifer sediment and surface soil. Environ. Sci. Technol. 40, 3043-3049.
[14] Cai, X., Sheng, G. and Liu, W. (2007) Degradation and detoxification of acetochlor in soils treated by organic and thiosulfate amendments. Chemosphere. 66, 286-292.
[15] Kocsis, Z., Marcsek, Z.L., Jakab, M.G., Szende, B. and Tompa, A. (2005) Chemopreventive properties of trans-resveratrol against the cytotoxicity of chloroacetanilide herbicides in vitro. Int. J. Hyg. Environ. Health. 208, 211-218.
[16] Chen, M.J., Cao, F., Li, F.B., Liu, C.S., Tong, H., Wu, W.J. and Hu, M. (2010) Anaerobic transformation of DDT related to iron(III) reduction and microbial community structure in paddy soils. J. Agric. Food Chem. 118, 13-26.
[17] Seol, Y., Zhang, H. and Schwartz, F.W. (2003) A review of in situ chemical oxidation and heterogeneity. Environ. Eng. Geosci. 9, 37-49.
[18] Watts, R.J. and Teel, A.L. (2006) Treatment of contaminated soils and groundwater using ISCO. Pract. Period, Hazard. Toxic Radioact. Waste Manage. 10, 2-9.
[19] Tsitonaki, A., Petri, B., Crimi, M., Mosbaek, H., Siegrist, R.L. and Bjerg, P.L. (2010) In situ chemical oxidation of contaminated soil and groundwater using persulfate: A review. Crit. Rev. Environ. Sci. Technol. 40, 55-91.
[20] Liu, C.S., Higgins, C.P., Wang, F. and Shih, K. (2012) Effect of temperature on oxidative transformation of perfluorooctanoic acid (PFOA) by persulfate activation in water. Sep. Purif. Technol. 91, 46-51.
[21] Monteagudo, J.M., Duran, A., Gonzalez, R. and Exposito, A.J. (2015) In situ chemical oxidation of carbamazepine solutions using persulfate simultaneously activated by heat energy, UV light, Fe^{2+} ions, and H_2O_2. Appl. Catal. 176, 120-129.
[22] Furman, O.S., Teel, A.L. and Watts, R.J. (2010) Mechanism of base activation of persulfate. Environ. Sci. Technol. 44, 6423-6428.
[23] Li, B. and Zhu, J. (2016) Simultaneous degradation of 1,1,1-trichloroethane and solvent stabilizer 1,4-dioxane by a sono-activated persulfate process. Chem. Eng. J. 284, 750-763.
[24] Liu, C., Shih, K., Sun, C.X. and Wang, F. (2012) Oxidative degradation of DDT by ferrous and copper ion activated persulfate. Sci. Total Environ. 416, 507-512.
[25] Liang, C., Guo, Y., Chien, Y. and Wu, Y. (2010) Oxidative degradation of MTBE by pyrite-activated persulfate: Proposed reaction kinetics. J. Contam. Hydrol. 49, 8858-8864.
[26] Usman, M., Faure, P., Ruby, C. and Hanna, K. (2012) Application of magnetite-activated persulfate oxidation for the degradation of PAHs in contaminated soils. Chemosphere. 87, 234-240.
[27] Kolthoff, I.M. and Miller, I.K. (1951) The chemistry of persulfate. I. The kinetics and mechanism of the decomposition of the persulfate ion in aqueous medium. J. Am. Chem. Soc. 73, 3055-3059.
[28] Costanza, J., Otano, G., Callaghan, J. and Pennell, K.D. (2010) PCE oxidation by sodium persulfate in the presence of solids. Environ. Sci. Technol. 44, 9445-9450.
[29] Duckworth, O.W. and Sposito, G. (2005) Siderophore-manganese(III)-interactions II. Manganite dissolution promoted by desferrioxamine. Environ. Sci. Technol. 39, 6045-6051.
[30] Oren, O., Garvieli, I., Burg, A., Guttman, J. and Lazar, B. (2007) Manganese mobilization and enrichment during soil aquifer treatment (SAT) of effluents, the Dan Region Sewage Reclamation Project (Shafdan), Israel. Environ. Sci. Technol. 41, 766-772.
[31] Huang, T., Li, X.Y., Tian, G.G., Yang, X.M., Wang, L., Zhao, Y., Ma, J.M. and Gao, H. (2013) Gridded inventories of historical usage for selected pesticides in Gansu Province, China. Environ. Sci. Pollut. Res. 20, 7167-7174.

[32] Zhang, H. and Shan, B.Q. (2014) Historical distribution of DDT residues in pond sediments in an intensive agricultural watershed in the Yangtze-Huaihe region, China. J. Soil Sediment. 14, 980-990.
[33] Kirman, C.R., Aylward, L.L., Hays, S.M., Krishnan, K. and Nong, A. (2011) Biomonitoring equivalents for DDT/DDE. Regul. Toxicol. Pharm. 60, 172-180.
[34] Kolthoff, I.M. and Stenger, V.A. (1947) Volumetric analysis, acid-base, precipitation and complex reactions, Second revised edition. Titration Methods, Vol. II. Interscience Publishers, Inc., New York.

Received: **26.04.2016**
Accepted: **01.02.2017**

CORRESPONDING AUTHOR

Jianmin Zhou
South China Institute of Environmental Sciences, Ministry of Environmental Protection, Guangzhou 510655, China

e-mail: zhoujianmin@scies.org

© by PSP Volume 27 – No. 7/2018 pages 4606-4614 Fresenius Environmental Bulletin

MOLECULAR AND MORPHOLOGICAL IDENTIFICATION AND DISTRIBUTION OF *CYSTOSEIRA* C. AGARDH, 1820 SPECIES IN NORTHERN MEDITERRANEAN COASTS OF TURKEY

Inci Tuney-Kizilkaya*, Atakan Sukatar

Ege University, Faculty of Science, Department of Biology, Hydrobiology Section, 35100 Bornova, Izmir, Turkey

ABSTRACT

The brown algae species, *Cystoseira* spp., forms an important habitat for many marine species. Changes in ecological conditions as salinity, seawater temperature and other factors such as urbanization, costal development, domestic and chemical pollutions effect the distribution and existence of these species. To protect and maintain their existence it is needed to identify and monitor *Cystoseira* spp. accurately. For this reason the distribution of the *Cystoseira* species in Northern Aegean Turkish Coasts were compared with previous data. The species were identified by both morphologically and phylogenetically. 35 *Cystoseira* samples were collected from 20 stations. Morphological features were used to identify 29 samples out of 35. From these species 10 of them gave appropriate results with sequence analysis.

The genus *Cystoseira* has been identified as a potential indicator of water quality in Mediterranean waters, and our preliminary results suggest that *Cystoseira* species may also be good bioindicators for ecological conditions.

KEYWORDS:
ITS, PCR, phylogenetics, Fucales

INTRODUCTION

One of the important constituents of Mediterranean rocky reef coastline is *Cystoseira* (Fucales) species. There are 41 taxa of *Cystoseira* species (species and infra species level) reported from Mediterranean Sea [1]. *Cystoseira* forms complex communities providing an important habitat for numerous epiphytic species and shelter for many other marine organisms from shallow waters to 100 m depth [2]. It harbours a high biodiversity as well as nursery for juvenile fish and invertebrates [2-6]. *Cystoseira* assemblages provide high primary production and food for other organisms. Also they form an important habitat for sheltering and protection.

Urbanization and other anthropogenic pressures such as overfishing, eutrification, maritime traffic and habitat lost cause shifts on Mediterranean rocky reef systems. Especially *Cystoseira* canopies shift to erect or turf algae or barren habitats [4, 7, 8] thus all marine ecocystem composition changes. Other impacts on *Cystoseria* habitats are over-grazing by sea urchins and invasive fish species such as *Siganus luridus* and *S. rivulatus* [9].

Having antifungal and antibacterial compounds make *Cystoseira* species special for pharmachetical industries [10-12, 5, 13, 14]. Thus harvesting and trampling of *Cystoseira* becomes a destructive practice.

In Mediterranean Sea, especially for warm-water Lessepsian species, tropical and subtropical organisms have competitive advantage considering to local organisms [15]. Proliferation of *Caulerpa* species through Mediterranean coast is a good example of this phenomenon. In addition, climate change causes changes on spatial distribution of marine species. It is known that *Cystoseira* assemblages shift to turf-forming algae habitats. Invasive herbivorous fish species such as *Coris julis*, *S. luridus*, *S. rivulatus* and sea urchins known to lead shift *Cystoseira* complexes to barren rocks [3, 15].

Cystoseira is characterized by highly differentiated basal and apical regions and the presence of air-vesicles. Old thallus have an elongated main axis, and in time the primary laterals become proportionally elongated. Their lower parts are strongly flattened into 'foliar expansions' or basal leaves. Fertile regions are called receptacles and located at the tips of the branches above the aerocyst [16]. Up to 34 morphologically distinct variants of *Cystoseira spp.* have been previously recognized in the coastal regions of Turkey, however, definitive taxonomic identification can be difficult because there is widespread cryptic inter- and intraspecific morphological variability within the genus.

This study aims to compare the past and present state of dispersion of the *Cystoseira* genus in North Aegean Sea. As known there is a systematic confusion about the taxonomy of species within the *Cystoseira* because the hybridization ratio between the species is high. Also the morphological structure of

this alga changes according to its life stage, sex and ecological conditions. As a result greater diversity is predicted for morphological results than molecular results. Thus the second aim of this study is to identify *Cystoseira* species by morphological and molecular methods.

MATERIALS AND METHODS

Sample collection and morphological identification. *Cystoseira* species were collected from the stations at the coast of Northern Aegean Sea, according to previous studies [17-20]. Samples were collected from the rocky, upper infralittoral zone of the North Aegean Sea along a 500 km section of the western coast of Turkey. Samples were collected from 20 stations (Figure 1) in this region, influenced by colder, fresher Black Sea waters at northern stations and warm, salty Mediterranean Sea waters at southern stations. All stations seawater temperatures were measured with a multi parameter probe (WP600 Series Meters, Oakton).

A total of 35 *Cystoseira* thalli were collected for identification. Morphological identification was conducted according to blade branching patterns, base and thallus structure, absence/presence of tophules, absence/presence of aerocysts and structure of the apex (Figure 2). Identified samples were submitted to Ege University Botanical Garden & Herbarium Research and Application Center.

DNA isolation and PCR analysis. *Cystoseira* samples were transferred to laboratory and was cleaned with distilled water and the epiphytes were removed under stereoscope. Before DNA extraction tissues were grind in liquid nitrogen by mortar and pestle. Total DNA was extracted from thalli using modified CTAB protocol of Doyle and Doyle [21] and Tuney and Sukatar [22]. Isolated DNA was analysed and quantified on a 0.8% agarose gel and with spectrophometer.

25 µl PCR mix contained 1 U Taq polymerase (DNAZyme Taq DNA polymerase, Finnzyme), 1× reaction buffer (Finnzyme), 0.2 mM dNTP mix (Finnzyme), 0.2 µM forward and reverse primers (Alpha DNA and IONTEK), 50-100 ng DNA and ultrapure water (HyClone). PCR conditions for used primer pairs were started with initial denaturation step at 95°C for 30 seconds was followed by 40 cycles of DNA denaturation at of 95 °C for 1 min, primer annealing at 47°C for 75 s, and DNA strand extension at 72°C for the 75 s and a final extension step at 72°C for 5 min. The PCR products were analyzed by 1% agarose gel electrophoresis in Tris-Boric acid-EDTA (TBE) buffer×1, at 5V/cm and stained with EtBr and visualized under UV illumination.

The gene sequence of *C. osmundacea* from NCBI was used to design primers (ITSF-ITSR) with PerlPrimer programme [23]. The other primer sequences were used for amplification according to Harvey and Goff [24] (CysF5- CysF4SAR, FrbcL-RrbcS ve Alg26SF- Alg26SR) and White et al. [25] (ITS1-ITS4). The sequence and melting temperatures of the primers are given in Table 1.

Sequence and Phylogenetic Analysis. Sequence analysis of the PCR amplicons was performed with the universal primers. ITS gene sequences of samples were aligned with reference sequences retrieved from GenBank using the ClustalW program version 4.0 in MEGA 5. Aligned data set was used for creating phylogenetic trees with MEGA 5 software [26]. Neighbor Joining (NJ) and Maximum Likelihood (ML) algorithms were used for inferring the phylogenetic relationships.

FIGURE 1
Sampling stations; 1- Sazlıca 2- Foça , 3- Aliağa 4- Şakran, 5- Çandarlı, 6- Dikili Bademli Köyü, 7- Dikili Liman, 8- Pelitköy, 9- Güvercinada, 10- Altınoluk, 11- Küçükyalı, 12- Asos, 13- Lapseki, 14- Kepez, 15- Dardanos, 16- Güzelyalı, 17- Troya National Park, 18- Gelibolu, 19- Seferihisar, 20-Kuşadası-Davutlar

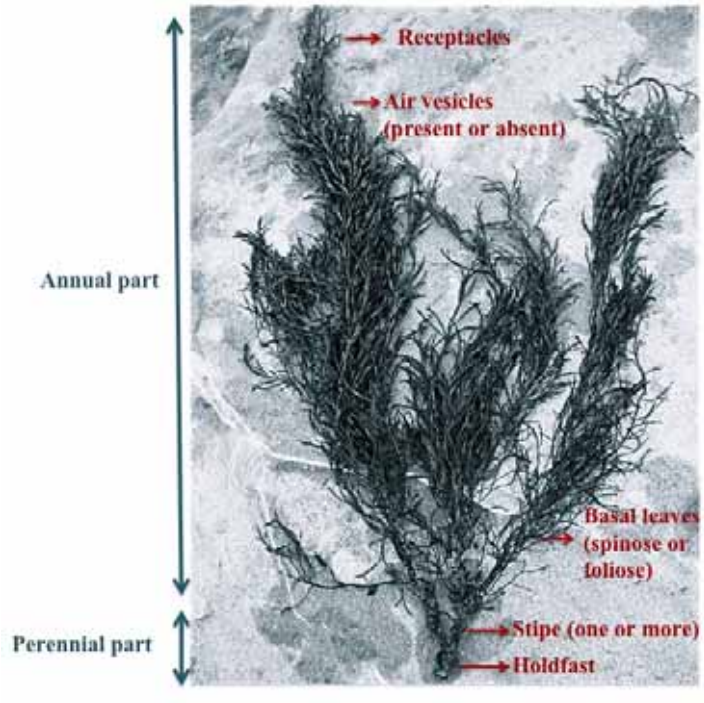

FIGURE 2
Morphological features of *Cystoseira* sp.

TABLE 1
Primers used for PCR analysis and their melting temperatures.

Primer #	Name	Sequence	M_T (ºC)
F1	ITSF	5'- CGA TTG AAT GTT TCG GTG AA-3'	M_T: 56.3
R1	ITSR	5'- AGA CAT CCG TCG CTG AAA GT-3'	M_T: 60.4
F2	CysF5	5'- CGC ACC TAC CGA TTG AAT TGT-3'	M_T: 57.9
R2	CysF4SAR	5'- CTC TAG CCT TGG GTG GAC TC-3'	M_T: 61.4
F3	Alg26SF	5' AGA GCT CGT GAT GAG AAC CC-3'	M_T: 59.4
R3	Alg26SR	5'- GCT CAC ACT CAA ACC TCG AC-3'	M_T: 59.4
F4	FrbcL	5'-ATTGTGGTCAAATGCATCAAC -3'	MT: 58.0
R4	RrbcS	5'-ATCATCTGTCCATTCTACACT -3'	MT: 58.0
F5	ITS1	5'-TCC GTA GGT GAA CCT GCG G -3'	MT: 62.0
R5	ITS4	5'-TCC TCC GCT TAT TGA TAT GC -3'	MT: 58.0

TABLE 2
Morphologically identified species, collection sites and herbarium accession numbers of phylogenetically analysed samples.

Species	Collection site	Coordinates	Herbarium accession #
C. crinita	Foca	38º 44' 202'' N 26º 52' 486'' E	EU42024
C. barbata	Sakran	38º 52' 005'' N 27º 03' 596'' E	EU42025
C. humilis	Dikili	39º 02' 363'' N 26º 48' 773'' E	EU42027
C. foeniculata	Dikili	39º 02' 363'' N 26º 48' 773'' E	EU42029
C. crinita	Pelitkoy	39º 27' 337'' N 26º 51' 282'' E	EU42031
C. corniculata	Pelitkoy	39º 27' 337'' N 26º 51' 282'' E	EU42032
C. mediterranea	Guvercinada	39° 21' 31.2" N 26° 37' 54.54"E	EU42033
Cystoseira sp.	Asos	39° 32' 24.06"N 26° 34' 39.72"E	EU42037
C. humilis	Dardanos	40° 4' 19.08" N 26° 21' 30.96"E	EU42040
C. recegovicii	Kusadasi	46° 44' 34.2" N 27° 50' 25.2"E	EU42044

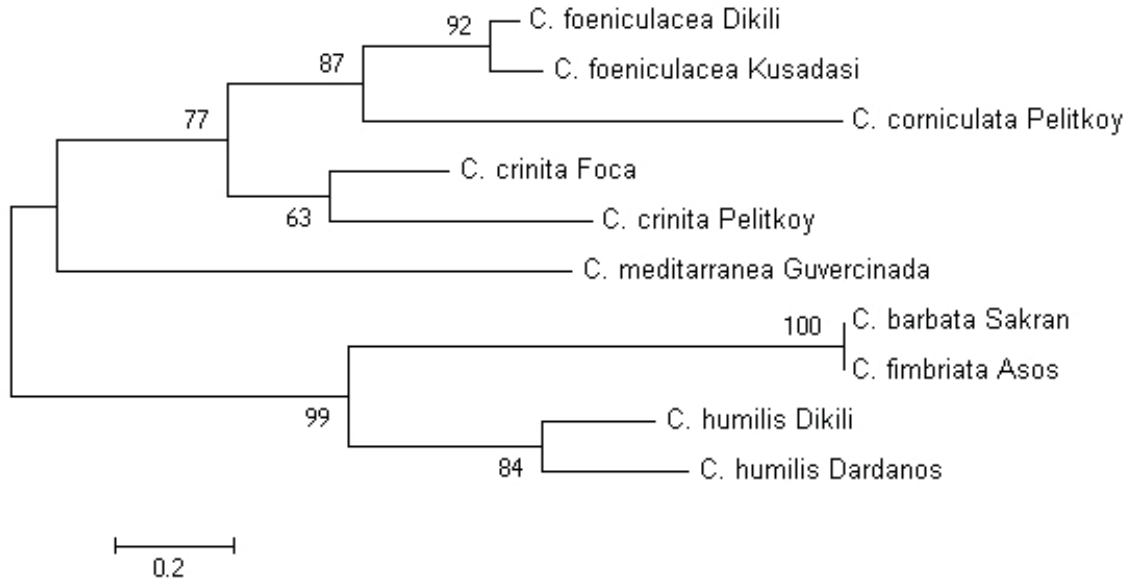

FIGURE 3
ML tree of *Cystoseira* species, collected from Turkish Aegean Coasts, based on the ITS gene constructed by Tamura-Nei method with 100 bootstrap.

Sequenced ITS regions of the samples and the sequences of *C. setchellii*, *C. neglecta* and *C. osmundacea* from GenBank were used to investigate the relationship with sampled species (Figure 4).

RESULTS

29 of the 35 samples were identified morphologically. Within 29 samples there were 10 different species identified as; *C. crinita* Duby (6 samples), *C. compressa* (Esper) Gerloff & Nizamuddin (2 samples), *C. barbata* (Stackhouse) C. Agardh (7 samples), *C. humilis* Schousboe ex Kützing (3 samples), *C. foeniculacea* (Linnaeus) Greville (3 sample), *C. corniculata* (Turner) Zanardini (2 samples), *C. mediterranea* Sauvageau (1 sample), *C. fimbriata* Bory de Saint-Vincent (1 sample), *C. barbatula* Kützing emend. Cormaci, G. Furnari & Giaccone (3 samples), *C. stricta* (Montagne) Sauvageau (1 sample), *C. ercegovicii* Giaccone (2 samples).

A Pearson correlation was also used to determine whether a relationship between the thallus length and the seawater temperature was evident. As for thallus length, no correlation between the seawater temperature was found; $r = -0.03$, $n = 31$, and $p = 0.431$ ($p > 0.05$).

9 of the 35 samples did not result with any PCR products with any of the primers. 6 of them gave results with FrbcL-RrbcS primers; 10 of them gave results with ITSF-ITSR primers; 20 of them gave results with ITS1-ITS4 primers and 15 of them gave results with Alg26SF-Alg26SR primer pairs. Only 10 of the samples amplified with ITS1-ITS4 primers gave results with sequence analysis thus only these sequences were used for phylogenetic analysis (Table 2).

Sequences of 10 samples were used for phylogenetic analysis. ML, NJ and MP methods were used for tree construction, all trees gave similar results thus only ML is shown in Figure 3.

DISCUSSION

Genus *Cystoseira* is one of the main algae species on the rocky substratum of Mediterranean Sea from the shallow coastal areas to over 100 m depth. Because it is a canopy forming algae, it provides important habitats for variety of different species. *Cystosiera* species are dominant elements of benthic vegetation [27] and known as climax of algal succession [28]. They are very sensitive to stress factors originated from recreational activities, such as anchoring, pollution, increased seawater temperatures etc. Because of its sensitivity, their existence is suggested as water quality indicator (EU, 94/C22/06) [29, 30]. Also *Cystoseira* species are listed on the Annex-II in Barcelona Convention (1995) [31] as threatened or endangered species [32]. According to European Water Framework regulations and Habitat Directive NATURA 2000 (92/43/EEC) [33], *Cystoseira* species were suggested to be used as an indicator of determination of costal water quality (2000/60/EC). Thus it is important to have historical data of these algal assemblages and monitoring the diversity of *Cystoseira* species to setup data for future studies.

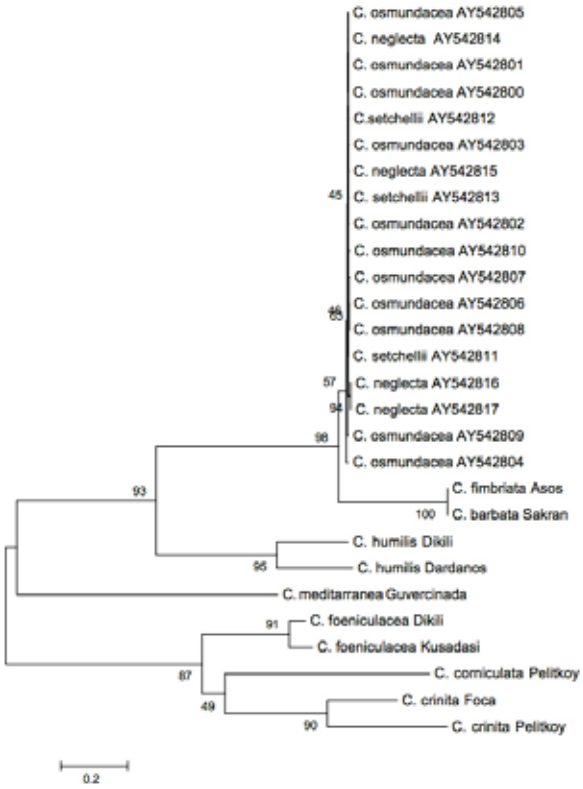

FIGURE 4
ML tree of *Cystoseira* species, collected in this study and from Genbank data, based on the ITS gene constracted by Tamura-Nei method with 100 bootstrap.

There are several studies conducted in Turkish coasts on *Cystoseira* species. Güner and Aysel [34, 17], defined *C. barbata, C. compressa*, *C. ercegovicii*, *C. ericoides* and *C. mediterranea* at coasts of Marmara Sea. After that study Aysel [35] and Aysel et al. [36], described 23 *Cystoseira* taxa all along Turkish Coasts; *C. barbata* f. *aurantia*, *C. adriatica C. barbata* f. *barbata, C. compressa, C. corniculata var. corniculata, C. corniculata var. laxior* Ercegovic*, C. corniculata, C. crinita* f. *bosforica, C. crinita* f. *crinita*, *C. crinita, C. crinitophylla, C. dubia, C. elegans, C. ercegovicii f. ercegovicii, C. ercegovicii f. tenviramosa, C. funki, C. humilis, C. mediterranea var. mediterranea, C. schiffneri, C. spinosa var. spinosa, C. spinosa var. squarrosa, C. stricta var. amentacea* and *C. stricta var. spicata*. In a similar study Dural [37], descibed *C. adriatica* in Ayvalık, Gulf of Izmir and Bodrum; *C. barbata* in Gulf of Izmir; *C. compressa* in Gumuldur, Fethiye and Marmaris; *C. corniculata* in Gulf of Izmir, Çeşmealtı, Mordogan, Gumuldur, Gokova and Bodrum; *C. crinita* in Gulf of Izmir; *C. elegans* in Fethiye, Bodrum and Gulf of Izmir; *C. ercegovicii* in Ayvalık, Dikili, Gumuldur, Urla and Gulf of Izmir; *C. mediterranea* in Marmaris, Çeşmealtı and Gulf of Izmir; *C. spinosa* and *C. crinita* in Gulf of Izmir. Sukatar [38] identified *C. compressa*, *C. crinita* and *C. ercegovicii* in Kusadasi. Kocatas et al. [39] described *C. crinita*, *C. corniculata* and *C. schiffneri* from Dikili; *C. compressa* from Sakran and *C. crinita* from Foca. Parlakay et al. [40] defined 8 *Cystoseira* species in South Aegean Coasts of Turkey; *C. amentacea* var. *stricta* Montagne, *C. barbata* (Stackhouse) C. Agardh, *C. compressa* (Esper) Gerloff *et* Nizamuddin, *C. corniculata* (Turner) Zardarini, *C.crinita* Duby, *C. elegans, C. meditarrenea* Sauvageau, *C. schiffneri* G. Hamel. Taskin et al [19] decribed 23 *Cystoseira* taxa in the checklist of Turkish macroalgae; *Cystoseira amentacea* (C. Agardh) Bory, *C. amentacea* var. s*tricta* Montagne, *C. amentacea* var. *spicata* (Ercegovic) Giaccone, *C. barbata* (Stackhouse) C. Agardh forma *barbata, C. barbata* f. *repens* Zinova *et* Kalugina, *C. compressa* (Esper) Gerloff *et* Nizamuddin, *C. corniculata* (Turner) Zanardini, *C. crinita* Duby, *C. crinita* f. *bosphorica* (Sauvageau) Zinova *et* Kalugina, *C. crinitophylla* Ercegovic, *C. dubia* Valiante, *C. elegans* Sauvageau, *C. foeniculacea* (L.) Greville, *C. foeniculacea* f. *latimarosa* (Ercegovic) Garreb, Barcelo, Ribera and Lluch, *C. foeniculacea* forma *tenuiramosa* G. Garreta, Barcelo, Ribera and Lluch, *C. funkii* Schiffner *ex* Gerloff *et* Nizamuddin, *C. humulis* Schousboe ex Kützing, *C. mediterranea* Sauvageau, *C. mediterranea* var. *valiantei* Sauvageau, *C. sauvageauana* G. Hamel, *C. spinosa* Sauvageau, *C. squarrosa* De Notaris, *C. tamariscifolia* (Hudson) Papenfuss syn: *C. ericoides* (L.) C. Agardh, *C. zosteroides* (C. Agardh).

The sampling stations were selected according to previous studies' stations for an accurate comparison. In this study 12 different species of *Cystoseira*; *C. crinita* Duby, *C. compressa* (Esper) Gerloff & Nizamuddin, *C. barbata* (Stackhouse) C. Agardh, *C. humilis* Schousboe ex Kützing, *C. foeniculacea* (Linnaeus) Greville, *C. corniculata* (Turner) Zanardini, *C. mediterranea* Sauvageau, *C. fimbriata* Bory de Saint-Vincent, *C. barbatula* Kützing emend. Cormaci, G. Furnari & Giaccone, *C. stricta* (Montagne) Sauvageau and *C. ercegovicii* Giaccone were identified from Nothern Aegean Sea Coasts of Turkey. When the results were compared with previous studies, Kocatas et al. [39] found *C. corniculata*, *C. crinita* and *C. schiffneri* and Dural identified *C. ercegovicii* (former name of *C. foeniculacea*) in Dikili while this study identified *C. humilis* and *C. foeniculacea.*

There wasn't any *Cystoseira* species in Ayvalık while in 1990 Dural [37] identified *C. ercegovicii*. Kocatas et al. [39], found *C. compressa* in Sakran and *C. crinita* in Foca while in this study *C. barbata* and *C. compressa* were found, respectively. For Kusadası station only *C. foeniculacea* was identified while Dural [37] identified *C. compressa*, *C. crinita* and *C. ercegovicii*. The reasons for missing species in same stations after approx 10 years might be the result of increasing water temperatures, human activities and costal development.

Guner et al. [41] and Taskin et al. [1] prepared an identification key for *Cystoseira* species. For all those check-list and identification key studies, still it is not clear to identify *Cystoseira* species morphologically. Morphological features may change according to ecological conditions, life cycle stages and several other factors. Thus there are too many characteristics to be considered during identification of this genus. Because of this it is more useful and accurate to identify species by molecular techniques as well as morphological identification. Ribosomal Internal Transcript Spacer (ITS) and rbcL (RUBISCO) regions are generally used for this purpose in algal studies [42-55, 24]. In his study we used 5 different primer pairs to amplify ITS and rbcL regions of sampled *Cystoseira* species. Within the 35 samples 9 of them did not give any PCR products. And only 10 of them gave acceptable results with sequence analysis with ITS1 and ITS4 primer pair. The reason of this failure in PCR and sequence analysis may be the result of high contents of secondary metabolites of genus *Cystoseira*. In brown seaweeds phlorotannins (polyphenolics) are the most common secondary metabolites. They reduce fouling and attacks by pathogenic organisms, deter feeding by fishes, urchins, gastropods and crustacean herbivores and act as UV-light absorbing compounds and chelators of metal ions. The presence of secondary metabolites, such as polyphenols inhibit DNA polymerase enzyme action during PCR analysis. Besides, they inhibit PCR analysis by their tendency to form complexes with nucleic acids. Most of the samples were collected in warmer months that *Cystoseira* species predicted to have high polyphenolic compounds to avoid UV-damages that may result the PCR failure.

According to statistical results there was no relation between thallus size and temperature. But there might be a relationship between water temperature and distribution of the species. *C. barbata* and *C. crinita* distributed in all water temperature ranges whereas *C. stricta* exist only in cooler waters (below 15ºC). The species *C. barbatula, C. fimbriata, C. humilis, C. mediterranea, C. compressa, C. corniculata* and *C. foeniculacea* seems to distrubute more in temperate waters (above 20ºC). As mentioned in Otero et al.'s report, until today the surface temperatures have risen by 1ºC and it is expected to rise by 2.5ºC on average in next hundred years in Mediterranean [15]. Also the salinity increased by 0.05 ppt in intermediate and deep layers in 20th century and the surface water salinity is expected to increase 0.5 ppt by 2100. These highly expected scenarios would lead spatial shifts on distribution of marine species. Piron et al. [56] and Poloniato et al. [57] revealed the regression of Adriatic endemic seaweed *Fucus virsoides* and appearance of *Cystoseira* spp., *Cymodosea nodosa* and invasive herbivore fish *C. julis*, *S. luridus* in Miramare Marine Protected Area, Italy. As in this study *Cystosira* spp. seems to shift their disturbance towards northern parts and also the disturbance of the herbivores those feed on them also shifts with them. To be ensure with this phenomenon, monitoring studies encouraged by authorities throughout Mediterranean coasts. We believe that our findings on disturbance of *Cystoseira* species along Northern Aegean coasts will contribute to this data.

There is a systematic confusion about the taxonomy of the species within the *Cystoseira* because the hybridization ratio between the species is high. And the structure of this alga changes according to its life stage, sex and ecological conditions as mentioned before. Because of these greater diversity is predicted from morphological results than molecular results. The sequences recovered fell into three distinct ITS1 clades. Morphologically defined as *C. barbata* and *C. fimbriata* samples were formed a clade with 100 bootstrap value even if their morphological features are different. While *C. fimbriata* has caespitose axis, *C. barbata* has single axis. Although *C. fimbriata*'s apex is spinose, *C. barabata* has smooth apex. In Figure 4, these two samples are in the same clade with *C. neglecta, C. osmundacea* and *C. setchellii* conversely other Turkish *Cystoseira* species. Two *C. humilis* samples collected from two different stations apperared in the same clade in both trees as expected. *C. crinita* and *C. compressa* are in the same sub-clade with a low bootstrap value (35) (Figure 3). Both these species have caestipose axis and lack of tophules. They both have aerocysts and

common in the Mediterranean Sea. Only morphological characteristics different between these two is their apex structure. *C. compressa* has smooth apex while *C. crinita* has prominent apex with spines. *C. mediterranea* which is the only sample with single axis while they have caespitose, forms a seperate clade in Figure 4. *C. foeniculacea* species from Dikili and Kusadası formed a clade as expected.

The phylogenetic results in this study, pointed out the lack of molecular based identification studies in Turkey on *Cystoseira* species. Without enough molecular data it is not convenient to compare the results with other *Cystoseira* species. There is a clear need for further studies to increase the number of available sequences of genetic markers for different species of *Cystoseira* genus. It is believed that establishing large-scale sequence databases will help to identify species easily and accurately. As a future study it is planned to work on phylogenetically important regions (rbcL, 26S rRNA, etc.) for all samples and determined which region will be convenient for revealing phylogenetic relationship between *Cystoseira* species.

ACKNOWLEDGEMENTS

This study was funded by Ege University, Faculty of Science, Scientific Research Project # 2007/FEN/025.

We thank to our colleague Elizabeth Grace ERONAT for language editing.

REFERENCES

[1] Taskin, E., Jahn, R., Öztürk, M., Furnari, G., Cormaci, M. (2012) The Mediterranean Cystoseira (with photographs). 1st ed. Celar Bayar University Publisher, Manisa.

[2] Devescovi, M. (2015) Effects of bottom topography and anthropogenic pressure on northern Adriatic Cystoseira spp. (Phaeophyceae, Fucales). Aquatic Botany. 121, 26-32.

[3] Thibaut, T., Blanfune, A., Markovic, L., Verlaque, M., Boudouresque, C.F., Perret-Boudouresque, M., Macic, V., Bottin, L. (2014) Unexpected abundance and long-term relative stability of the brown alga Cystoseira amentacea, hitherto regarded as a threatened species, in the north-western Mediterranean Sea. Marine Pollution Bulletin. 89, 305-323.

[4] Cheminée, A., Sala, E., Pastor, J., Bodilis, P., Thiriet, P., Mangialajo, L., Cottalorda, J.M., Francour, P. (2013) Nursery value of Cystoseira forests for Mediterranean rocky reef fishes. Journal of Experimental Marine Biology and Ecololgy. 442, 70–79.

[5] Ballesteros, E., Martín, D., Uriz, M.J. (1992) Biological activity of extracts from some Mediterranean macrophytes. Botanica Marina. 35, 481–485.

[6] Hoffmann, L., Renard, R., Demoulin, V. (1992) Phenology, growth and biomass of Cystoseira balearica in Calvi (Corsica). Marine Ecology Progress Series. 80, 249–254.

[7] Bonaviri, C., Vega Fernández, T., Fanelli, G., Badalamenti, F., Gianguzza, P. (2011) Leading role of the sea urchin Arbacia lixula in maintaining the barren state in southwestern Mediterranean. Marine Biology. 158(11), 2505–2513.

[8] Hereu, B. (2004) The role of trophic interactions between fishes, sea urchins and algae in the northwest Mediterranean rocky infralittoral. PhD thesis. Universitat de Barcelona. 237p.

[9] Mineur, F., Arenas, F., Asis, J., Davies A.J., Engelen, A.H., Fernandes, F., Malta E., Thibaut, T., Nguyen, T.V., Vaz-Pinto, F., Vranken, S., Serrao E.A., De Clerk, O. (2015) European seaweeds under pressure: Consequences for communities and ecosystem functioning. Journal of Sea Research. 98, 91-108.

[10] Calvo, M.A., Cabañes, F.J., Abarca, L. (1986) Antifungal activity of some Mediterranean algae. Mycopathologia. 93(1), 61–63.

[11] Bernard, P., Pesando, D. (1989) Antibacterial and antifungal activity of extracts from the rhizomes of the Mediterranean seagrass Posidonia *oceanica*. Bot Mar. 32, 85–88.

[12] Uriz, M.J., Martín, D., Turon, X. (1991) An approach to the ecological significance of chemically mediated bioactivity in Mediterranean benthic communities. Marine Ecology Progress Series. 70, 175–188.

[13] Salvador, N., Gómez, A., Lavelli, L. (2007) Antimicrobial activity of Iberian macroalgae. Scientia Marina. 71(1), 101–113.

[14] Llolet, J. (2010) Human health benefits supplied by Mediterranean marine biodiversity. Marine Pollution Bulletin. 60, 1640–1646.

[15] Otero, M., Garrabou, J., Vargas, M. (2013) Mediterranean Marine Protected Areas and climate change: A guide to regional monitoring and adaptation opportunities. IUCN. Malaga, Spain, 1-52.

[16] Kim, S. (2015) Handbook of Marine Biotechnology. 1st ed. Springer-Verlag Press. Berlin, Heidelberg.

[17] Güner, H., Aysel, V., Sukatar, A., Öztürk, M. (1984) Check-List of Izmir Bay Marine Algae: II. Phaeophyceae, Chlorophyceae and Cyanophyceae. Ege University Faculty Science Journal Series B. 7(1), 57-65.

[18] Öztürk, M. (1985) Distribution and Taxonomy of Phaeophyta (Brown algae) species on Aegean and Mediterranean Cosats of Turkey (Türkiye'nin Ege ve Akdeniz Kıyılarındaki Phaeophyta (Kahverengi Algler) Üyelerinin Yayılımı ve Taksonomisi). MSc Thesis. Ege University, Science Faculty. Izmir.

[19] Taşkın, E., Öztürk, M., Kurt, O., Öztürk, M. (2008a) The check-list of the marine flora of Turkey. 1st ed. Ecem Kırtasiye. Manisa.

[20] Taşkın, E. (2008b) The Marine Brown Algae of the east Aegean Sea and Dardanelles. II. Ectocarpaceae, Chordariaceae and Scytosiphonaceae. Cryptogamie Algologie. 29(2), 173- 186.

[21] Doyle, J.J., Doyle, J.L. (1987) A rapid DNA isolation procedure for small quantities of fresh leaf tissue. Phytochemistry Bulletin. 19, 11–1.

[22] Tuney, I., Sukatar, A. (2010) DNA Extraction Protocol from Brown Algae. Biological Diversity and Conservation. 3, 51-55.

[23] Marshall, O.J. (2004) PerlPrimer: cross-platform, graphical primer design for standard, bisulphite and real-time PCR. Bioinformatics. 20(15), 2471-2472.

[24] Harvey, J.B.J., Goff, L.J. (2006) A reassessment of species boundaries in Cystoseira and Halidrys (Phaeophyceae, Fucales) along the North American West Coast. Journal of Phycology. 42, 707-720.

[25] White, T.J., Bruns, T., Lee, S., Taylor, J.W. **(**1990) PCR Protocols: A guide to Methods and Applications. Academic Press Inc. New York, 315-322.

[26] Tamura, K., Peterson, D., Peterson, N. (2011) MEGA5: Molecular Evolutionary Genetics Analysis using Maximum Likelihood, Evolutionary Distance, and Maximum Parsimony Methods. Molecular Biology and Evolution. 28, 2731-2739.

[27] Soltan, D., Verlaque, M., Boudouresque, CF., Francour, P. (2001) Changes in macroalgal communities in the vicinity of a Mediterranean seawage out- fall after the setting up of a treatment plant. Marine Pollution Bulletin. 42, 59-70.

[28] Peres, J.M., Picard, J. (1964) Nouveau manuel de bionomie benthique de la mer Mediterrane. Recueil des Travaux de la Stations Marine d'Endoume. 31(47), 1-137.

[29] Panayotidis, P., Feretopoulou, J., Montesanto, B. (1999) Benthic vegetation as an ecological quality descriptor in an Eastern Mediterranean coastal area (Kalloni Bay, Aegean Sea, Greece). Estuarine Coastal and Shelf Science. 48, 205–214.

[30] Panayotidis, P., Siakavara, A., Orfanidis, S., Haritonidis, S. (2001) Identification and description of habitat types at sites of interest for conservation. Study 5: Marine habitats. Final Technical Report. Athens.

[31] Barcelona Convention (1995) Convention for the Protection of the Marine Environment and the Coastal Region of the Mediterranean. Website http://www.unep.ch/regionalseas/regions/med/ t_barcel.htm (25.03.2015).

[32] Macic, V. (2013) Some characteristics of the *Cystoseira* (Phaeophyceae) assemblages in the intertidal fringe on the coast of Montenegro. Natura Montenegrina Podgorica. 12(2), 325-333.

[33] EU Water Frame Directive 2000/60/EU. Website http://eur-lex.europa.eu/LexUriServ/LexUriServ.do?uri=CELEX:32000L0060:en:NOT (25.03.2015).

[34] Güner, H., Aysel, V. (1978) Ege ve Marmara Denizi'nin Üst İnfra-littoralinde Bulunan Bazı Alg Topluluklarının Kalitatif ve Kantitatif Değerlendirilmesi. TBAG-174, Izmir.

[35] Aysel, V. (1988) Akdeniz Alg Florası. Ege University, Faculty of Science, İzmir.

[36] Aysel, V., Sukatar, A., Dural, B., Erduğan, H. (2000) Türkiye'nin Karadeniz Kıyıları Deniz Florası. TBAG-1325, İzmir.

[37] Dural, B. (1990) Eski Foça-Çeşme Arasında Yayılış Gösteren Alglerin Taksonomisi ve Ekolojisi. Ege University, Izmir.

[38] Sukatar, A., Aysel, V., Güner, H. (1992) Güney Ege Bölgesi'ndeki Cystoseira ercegovicii Giaccone Topluluğunun Kalitatif ve Kantitatif Değerlendirilmesi. XI. Ulusal Biyoloji Kongresi. Elazığ, 199-206.

[39] Kocatas, A., Katagan, T., Sezgin, M., Kirkim, F., Kocak, C. (2003) Crustacean Diversity Among the Cystoseira Facies of the Aegean Coast of Turkey. Turkish Journal of Zoology. 28, 309-316.

[40] Parlakay, A., Sukatar, A., Şenkardeşler, A. (2005) Marine Flora Between South Çeşme and Cape Teke (Izmir, Aegean Sea, Turkey), Ege University Journal of Fisheries and Aquatic Science. 22, 187-194s.

[41] Güner, H. (1981) *Cystoseira* Agardh 1821 Cinsinin Ayrımında Yeni Bir Yöntem. E.Ü. Fen Fak. Dergisi. Seri B.(Suppl.), 273-279.

[42] Polanco, C., Gonzalez, A.I., Fuente, A., Dover, G.A. (1998) Multigene family of ribosomal DNA in *Drosophila melanogaster* reveals contrasting patterns of homogenization for IGS and ITS spacer regions: a possible mechanism to resolve this paradox. Genetics. 149, 243–256.

[43] Serrao, E.A., Alice, L.A., Brawley, S.H. (1999) Evolution of the Fucaceae (Phaeophyceae) Inferred from nrDNA-ITS. Journal of Phycology. 35, 382-394.

[44] Zuccarello, G.C., West, J.A., Kamiya, M., King, R.J. (1999) A Rapid Method to Score Plastid Haplotypes in Red Seaweeds and Its Use in Determining parental Inheritance of Plastids in the Mangrove Red Alga *Bostrychia* (Ceramiales). Hydrobiologia. 401, 207-214.

[45] Stiger, V., Horiguchi, T., Yoshida, T., Coleman, A.W., Masuda, M. (2003) Phylogenetic Relationships of *Sargassum* (Sargassaceae, Phaeophyceae) with Reference to a Taxonomic Revision of the Section *Phyllocystae* based on ITS-2 nrDNA sequences. Phycological Research. 48, 251-260.

[46] Tan, I.H., Druehl, L.D. (1994) A Molecular analysis of *Analipus* and *Ralfsia* (Phaeophyceae) Suggests the Order Ectocarpales is Polyphyletic. Journal of Phycology. 30, 721-729.

[47] Peters, A.F., Ramiez, M.E. (2001) Molecular Phylogeny of Small Brown Algae, with Special Reference to the Systematic Position of *Caepidium antarticum* (Adenocystaceae, Ectocarpales). Cryptogamie. 22(2), 187-200.

[48] Yoon, H.S., Lee, J.Y., Boo, S.M., Bhattacharya, D. (2001) Phylogeny of Alariaceae, Laminariaceae and Lessoniaceae (Phaeophyceae) Based on Plastid-Encoded RuBisCo Spacer and Nuclear-Encoded ITS Sequence Comparisons. Molecular Phylogenetics and Evolution. 21(2), 231-243.

[49] Santos, R.S., Taylor, D.J., Kinzie, R.A., Hidaka, M., Sakai, K., Coffroth, M.A. (2002) Molecular Phylogeny of Symbiotic Dinoflagellates inferred from Partial Chloroplast LSU (23S) rDNA Sequences. Molecular Phylogenetics and Evolution. 23, 97-111.

[50] Blomster, J., Maggs, A.C., Stanhope, M.J. (1998) Molecular and morphological analysis of *Enteromorpha intestinalis* and *E. compressa* (chlorophyta) in the British Isles. Journal of Phycology. 34, 219-340.

[51] Coleman, A.W., Suarez, A., Goff, L.J. (1994) Molecular Delination of Species and Syngens in Volvocalean Green algae (Chlorophyta), Journal of Phycology. 30, 80-90.

[52] Coleman, A.W., Mai, J.C. (1997) Ribosomal DNA ITS-1 and ITS-2 sequence comparisons as tool for predicting genetic relatedness. Journal of Molecular Evolution. 45, 168-177.

[53] Bakker, F.T., Stam, E.T., Olsen, J.L. (1995) Global Phylogeography in the Cosmopolitan Species *Cladophora vagabunda* (Chlorophyta) Based on Nuclear rDNA ITS Sequences. European Journal of Phycology. 30, 197-208.

[54] Yotsukura, N., Denboh, T., Horiguchi, T., Coleman, W.A., Ichimura, T. (1999) Little Divergence in rDNA ITS-1 and ITS-2 Sequences among non-digitate Species of Laminaria from Hokkaido, Japan. Phycological Research. 47, 71-80.

[55] Meusnier, I., Olsen, J.L., Stam, W.T., Destombe, C., Valero, M. (2001) Phylogenetis Analysis of *Caulerpa taxifolia* and of its Associated Bacterial Microflora Provide Clues to the origin of Mediterranean Introduction. Molecular Ecology. 10, 931-946.

[56] Piron, M., Balasso, E., Poloniato, D., Odorico, R. (2007) First record of *Coris julis* in the Miramare Nature Reserve. Annales Series Historia Naturalis. 17(2), 165-170.

[57] Poloniato, D., Ciriaco, S., Odorico, R., Dulcic, J., Livej, L. (2010) First record of the dusky spinefoot *Siganus luridus* (Rüppell, 1828) in the Adriatic Sea. Annales Series Historia Naturalis. 20(2), 161-166.

Received: **22.06.2016**
Accepted: **25.03.2018**

CORRESPONDING AUTHOR

Inci Tuney-Kizilkaya
Ege University,
Faculty of Science,
Department of Biology,
35100 Bornova, Izmir – Turkey

e-mail: inci.tuney@ege.edu.tr

© by PSP Volume 27 – No. 7/2018 pages 4615-4623 Fresenius Environmental Bulletin

CONCENTRATION AND SIZE DISTRIBUTION PROPERTIES OF ATMOSPHERIC AEROSOL PARTICLES DURING SUMMER AND AUTUMN IN YINCHUAN, CHINA

Jiandong Mao*, Jiangfeng Shao

School of Electrical and Information Engineering, Beifang University of Nationalities, Yinchuan, 750021, China

ABSTRACT

Using information acquired by an aerodynamic particle sizer deployed in Yinchuan (China), this study investigated the physical and chemical properties of aerosols and provided basic data for the analysis of their climatic and environmental effects. The evolutions of the concentration and size distribution of atmospheric aerosol particles were measured during summer and early autumn, and the mass concentrations, mass size distributions, and PM2.5 concentrations were studied using cluster analysis. In addition, meteorological data were obtained to determine the relationship between size distribution and weather. The following conclusions were obtained. (1) The size distribution and concentration of aerosols changed considerably and their variations wee related closely to weather conditions. (2) The averaged number size distribution was unimodal with a peak in the accumulation mode. The averaged area size distribution was bimodal with peaks in both the accumulation and the coarse modes. The averaged mass size distribution was trimodal with peaks in the accumulation and coarse modes. The maximum peaks of the three types of size distribution were all located in the accumulation mode. (3) In Yinchuan, the mass size distribution could be divided into six categories during summer and early autumn. Cluster A was found to occur during periods following rain, clusters B and C occurred mainly on continuously sunny days, and clusters D–F appeared on cloudy and windless or continuously overcast days. The research results improve the understanding of the distribution characteristics, evolution, and factors affecting the size distributions of atmospheric aerosol particles in the Yinchuan area.

KEYWORDS:
Atmospheric aerosol, Concentration, Size distribution, Cluster analysis, PM2.5, Yinchuan area

INTRODUCTION

Many observations and studies have shown that aerosols, as substances that affect the urban environment, have considerable impact on climate, the environment, and human health [1-5]. The concentration and size distribution of aerosols are important physical parameters that define aerosol characterization. Thus, research on such characteristics has considerable importance regarding the study of the nature, sources, and effects of aerosols on climate, the environment, and human health.

Since the 1970s, many scientists have observed and analyzed the physical parameters of the concentration, size distribution, and influencing factors of aerosols under different environmental conditions [6-13]. Such research has also been undertaken in China; however, most studies have concentrated on the eastern region and the coastal cities of China. For example, Zhao et al. [14] observed aerosol size distribution and its temporal evolutionary process during a seriously polluted winter in the Beijing area. Huang et al. [15] studied the properties of aerosol number concentration and size distribution during winter in Hefei. Chen et al. [16] obtained aerosol concentrations and size distributions during winter in Huangshan. In Northwest China, similar observations were also performed in Lanzhou by Zhao et al. [17] who observed and studied the size distribution properties of atmospheric aerosol particles during summer and autumn. In the Yinchuan area, which is a main transportation pathway and a source area of sand dust in Northwest China, Sang et al. [18] observed and analyzed the short-term diurnal variation of aerosol particles. However, because of instrumentation limitations, the very short observation period, and minimal classification of particle sizes, they were unable to define explicitly the characteristics of aerosol concentration, size distribution, and variation in the Yinchuan area.

MATERIALS AND METHODS

The Aerodynamic Particle Sizer® 3321 (APS™ spectrometer) developed by TSI Inc. (U.S.A.) can provide real-time aerodynamic measurements of particle size distributions and concentrations of aerosols with diameters >0.37 μm. The instrument divides the particle diameter range from

0.5 to 20.0 μm into 52 files using a logarithmic scale, and it can measure the particle concentration from 0.001 to 10^4 cm^{-3}. The APS™-3321 uses a dual laser beam aerodynamic particle sizing method to measure the aerosol particle sizes [15, 19-23]. In the measurement process, the aerosol particles are restricted to the central accelerated airflow by sheath flow, and two orthogonal focused beams simultaneously pass vertically through the particles. In accordance with light-scattering principles, the instrument can calculate the time of flight of each particle, from which the particle speed can be determined. The flight speed of an aerosol particle is related closely to its aerodynamic diameter [24]. Depending on the different inertia of the aerosol particles, the APS™-3321 can obtain the velocity distribution of the aerosol particles (i.e., smaller particles have higher speeds and larger particles have smaller speeds). Polystyrene rubber balls are used to calibrate the APS™-3321 instrument [25], based on which the relationship between flight speed and particle size can be determined and thus, the aerodynamic diameters of sampled particles can be ascertained.

The sampling point used in this study was positioned at a height of 20 m at No. 17 Teaching Building at Beifang University of Nationalities (38°29'N, 106°06'E) in Xixia District, Yinchuan, China, well away from any serious pollution sources. During the entire observation period, uninterrupted sampling was conducted at 5-min intervals daily from 20:00 to 22:00. Therefore, the measured data can be considered to reflect the general situation of the Yinchuan area.

The number concentration of atmospheric aerosol particles refers to the number of all aerosol particles within a certain size range in a unit volume of atmosphere [26]. As mentioned above, the APS™-3321 is suitable for measuring particles with diameters of 0.5–20.0 μm. Considering that aerosol particles with diameters <2.5 μm have the greatest extinction effect, this diameter was selected as the cutoff point, i.e., particles with diameters <2.5 and >2.5 μm were defined as accumulation mode and coarse mode particles (or fine and coarse particles), respectively.

RESULTS AND DISCUSSION

Evolution of aerosol number concentration and size distribution. Table 1 lists the number concentrations of atmospheric aerosol particles during the entire observation period. It was found that fine particles were predominant in summer and early autumn, accounting for 96.7%–99.9% of the total number of particles (average: 98.9%). The main sources of fine particles are secondary aerosols that originate primarily from the emissions of various combustion processes and automobile exhausts; however, a small fraction is derived from native soil particles [15, 27].

TABLE 1
Number concentrations of atmospheric aerosol particles during entire observation period

Date	Sampling time	Weather	Maximum number concentration	Minimum number concentration	Averaged number concentration	Averaged Number concentration of accumulation mode	Averaged number concentration of coarse mode
2013.08.23	20:00-22:00	Overcast day	3400	2050	2517.2	2492.43	24.77
2013.08.24	20:00-22:00	Cloudy	6630	1760	4106	4073.48	32.52
2013.08.25	20:00-22:00	Cloudy	2740	1860	2318.95	2280.43	11.64
2013.08.26	20:00-22:00	Rain	9670	6090	7623.75	7611.84	11.91
2013.08.28	20:00-22:00	Sunny day	543.5	229.4	335.63	324.55	11.08
2013.08.29	20:00-22:00	Sunny day	802.1	421.5	596.87	586.75	10.12
2013.08.30	20:00-22:00	Sunny day	3110	558.2	1650.65	1634.73	15.92
2013.08.31	20:00-22:00	Cloudy	1410	873.9	1135.38	1119.25	16.13
2013.09.02	20:00-22:00	Sunny day	4820	2170	3021.2	3011.46	9.74
2013.09.03	20:00-22:00	Rain	5940	2260	3636.19	3625.38	10.81
2013.09.04	20:00-22:00	Cloudy	1780	1060	1358	1338.2	19.80
2013.09.05	20:00-22:00	Sunny day	4860	1910	3187.92	3133.03	26.35
2013.09.06	20:00-22:00	Sunny day	3330	1190	2194.8	2165.12	29.68
2013.09.09	20:00-22:00	Cloudy	5040	2020	3350	3318.15	31.85
2013.09.10	20:00-22:00	Sunny day	3910	1510	2712	2694.87	17.13
2013.09.11	20:00-22:00	Sunny	1510	676.5	1096.33	1078.64	17.69
2013.09.12	20:00-22:00	Sunny day	4600	1740	2382.8	2334.26	48.54
2013.09.14	20:00-22:00	Cloudy	3540	2050	2498	2457.82	40.18
2013.09.15	20:00-22:00	Cloudy	1690	1080	1340.8	1310.81	9.58
2013.09.17	20:00-22:00	Overcast day	10500	1010	5546	5527.65	18.35
2013.09.18	20:00-22:00	Overcast day	4470	3100	3542.4	3495.97	46.43
2013.09.19	20:00-22:00	Cloudy	6480	2130	4430.8	4400.68	30.12
2013.09.20	20:00-22:00	Cloudy	3030	1600	2302.8	2272.04	30.76
2013.09.21	20:00-22:00	Sunny day	4780	2330	3336	3312.11	23.89
2013.09.23	20:00-22:00	Overcast day	2530	1580	1890.91	1858.39	32.52

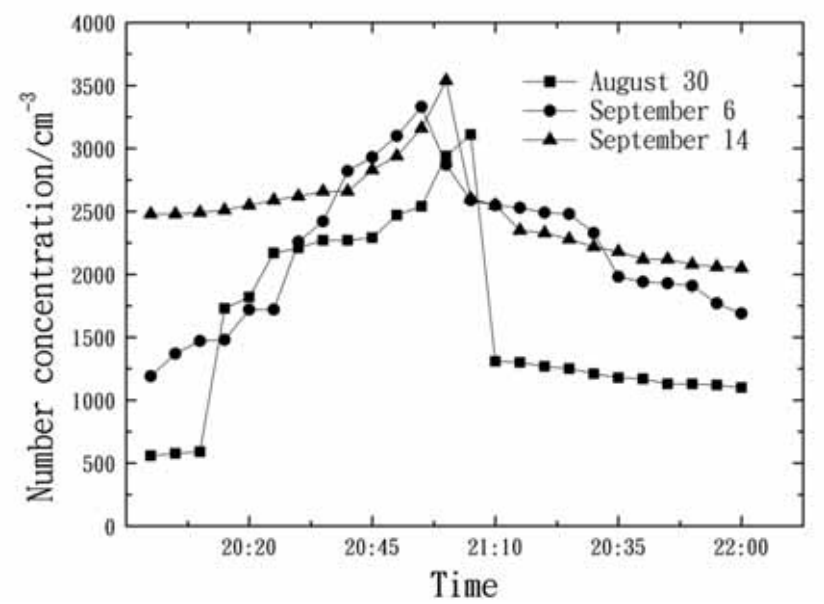

FIGURE 1
Variation of aerosol number concentration on three days in the Yinchuan area

On the daily basis, the range of aerosol number concentrations was large with the maximum value 3–10 times bigger than the minimum value. The monthly variation in the range of aerosol number concentrations was also large with the lowest average value of 335.63 cm^{-3} and the highest average value of 7623.75 cm^{-3}. The number concentration was found related closely to weather conditions. The aerosol number concentration on overcast days was found larger than on sunny day; on overcast days, the maximum, minimum, and average number concentrations were 10500, 1010, and 5546 cm^{-3}, respectively. However, following a period of rain, the aerosol number concentration was very low, i.e., the maximum value of 543.5 cm^{-3} was lower than the minimum value under general weather conditions and the minimum value was only 229.4 cm^{-3} (average: 225.63 cm^{-3}). This constitutes strong evidence that precipitation can be effective in scavenging atmospheric aerosols.

Figure 1 shows the variations of aerosol number concentration during the evening on three days in summer and autumn in Yinchuan. It can be seen that the variation of aerosol number concentration on each of the three days shows a regular single-peak structure, and that the maximum values occur between 20:50 and 21:10, i.e., soon after sunset. This is because the ground temperature starts to decrease in the early evening before sunset, while the upper air tends to cool more slowly; thus, convection is very weak. Such atmospheric conditions cause the aerosol particles produced by various human outdoor activities and rush-hour traffic to accumulate gradually. However, after about 21:00, human activities start to decrease and traffic pressure is alleviated, especially large temperature difference between day and night in Yinchuan make the air convection enhance and air exchange promote, and these factors result in the rapid decrease of aerosol concentration.

Usually, aerosol particle size distributions can be characterized by three types of distribution: number, surface area, and mass size. As the number distribution of smaller particles is usually large, it can reflect the characteristics of small particles well. However, because the content of large particles (diameters: >2.5 μm) is generally very low, it is difficult to reflect their distribution characteristics based on a number distribution; therefore, the surface area and mass size distributions are used to describe the characteristics of large particles [15].

Figure 2 shows the averaged number, surface area, and mass distributions of aerosol particles during the entire observation period. It can be seen that the number distribution is unimodal with a peak centered at 0.7 μm in the accumulation mode. The surface area distribution is bimodal, with the first peak at 0.7 μm in the accumulation mode and the second peak centered at 3.1 μm in the coarse mode. The mass distribution is trimodal with peaks located at 0.7, 3.8, and 7.8 μm; the first peak is in the accumulation mode, while the second and third peaks are in the coarse mode. In all three types of distribution, the maximum peaks are located in the accumulation mode. These three types of distribution during summer and autumn in the Yinchuan area are not only different from other cities in eastern China, e.g., Jinan, Guangzhou, and Beijing [28-30], but they differ from Lanzhou, which similar to the Yinchuan area is located within a semiarid region. In the Lanzhou area, the averaged mass distribution was found to exhibit a bimodal distribution, in which the first and second peaks were located at diameters of 0.67–0.72 and 4.7–5.1 μm, respectively, and the maximum value was always in the coarse mode [17, 26, 31-36].

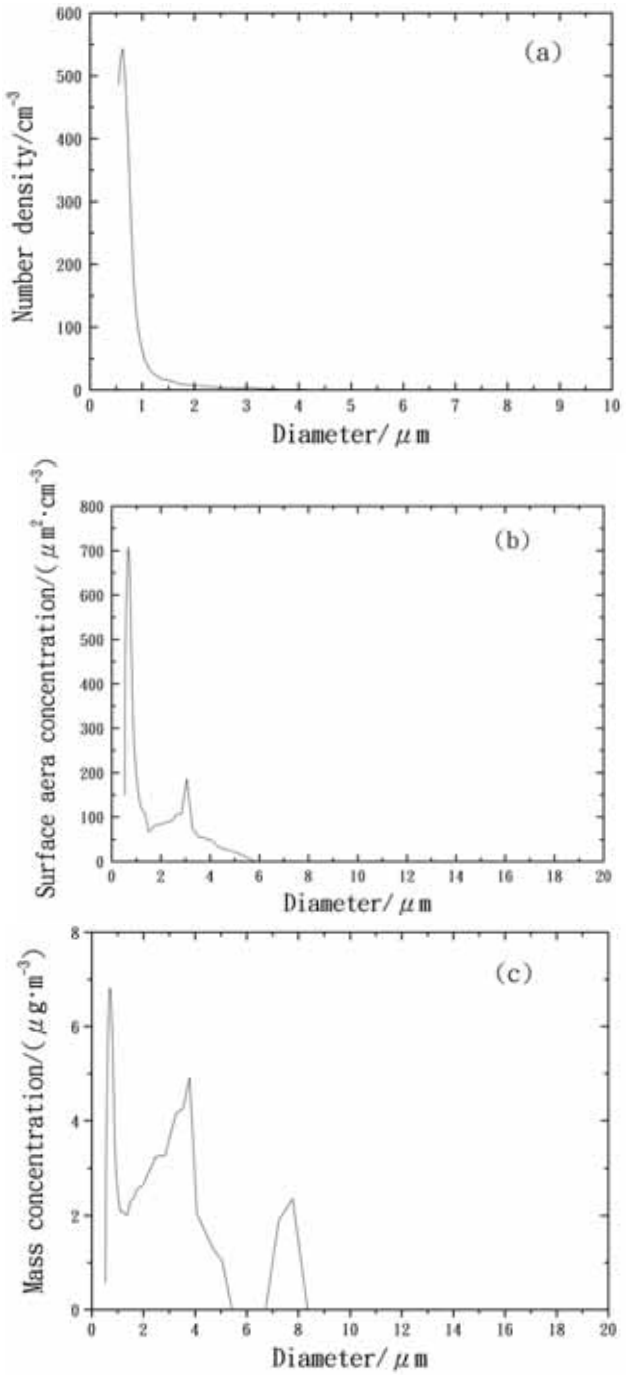

FIGURE 2
Averaged (a) number, (b) surface area, and (c) mass distributions of aerosol particles in the Yinchuan area

Cluster analysis of mass concentrations and size distributions. As a cluster analysis technique, the K-means method can be used to divide the mass distribution of aerosol particles into several categories. In applying the method, *K* objects are first chosen at random from *N* data objects as initial cluster centers. Then, each of the remaining objects is assigned to a cluster based on object–cluster similarity. Finally, by calculating the average value of all the objects of each new class, the new cluster center of each new class is obtained [36]. The steps of the above process are repeated until the mean square starts error to converge.

Using the K-means cluster method, the mass distribution data during the entire observation period of this study were analyzed and six representative classes obtained. Figure 3 shows the mass distributions for clusters A–F, and Table 2 lists the occurrence frequency of each class and the corresponding averaged mass concentration. Table 2 also shows the averaged PM2.5 value (selected as a standard for describing air quality in China) and the corresponding weather conditions, e.g., averaged temperature, wind speed, and relatively humidity.

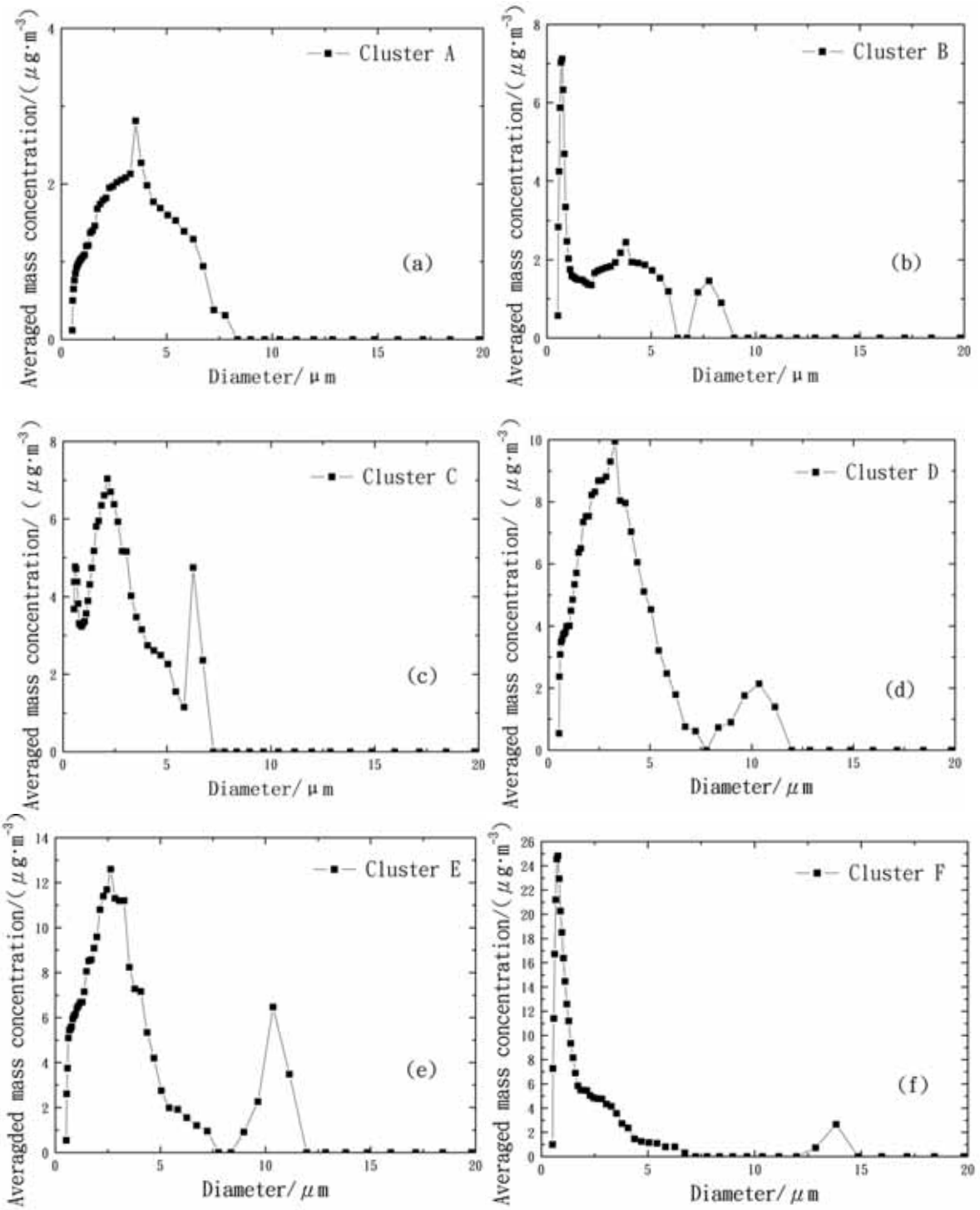

FIGURE 3
(a)–(f) Mass distributions for clusters A–F, respectively.

TABLE 2
Occurrence frequencies of clusters A–F, and the corresponding mean mass concentrations and PM2.5 values

		Cluster A	Cluster B	Cluster C	Cluster D	Cluster E	Cluster F
Frequency of occurrence %		22.5	24.8	21.8	16.7	9.4	4.8
averaged mass con-	0.5-2.5μm	27.6	60	99	137.4	188	280
centrations (μg/m^3)	2.5-20μm	19.4	40	59	70.6	67	37
	0.5-20μm	47	100	158	208	255	317
Averaged temperature/℃		21	20	19	19	18	19
Averaged wind speed/m/s		4.4	3.3	2.9	2.1	1.5	0.9
Averaged relative humidity/%		45	48	49	53	57	64

As can be seen in Fig. 3(a), cluster A has an obvious unimodal distribution; the averaged peak is from 3.05 to 3.79 μm, its frequency of occurrence is 22.5%, and the averaged concentration of coarse particles accounts for 41.3% of the total. Moreover, the averaged mass concentration of PM2.5 is 27.6 μg m^{-3}. Therefore, according to the air quality index classification of China, cluster A belongs to the "excellent" level, which is highly suitable for normal human activities. Cluster A was found to appear mainly on sunny days following periods of rain in late August, and it accounted for 33.1% of all samples in August.

In Fig. 3(b) and 3(c), clusters B and C, respectively, show obvious trimodal distributions. For cluster B, the main peak is from 0.6–0.7 μm in the accumulation mode. The second peak is from 3.0–3.5 μm and the minimum peak is from 7.23–8.35 μm; both of which are in the coarse mode. Cluster B accounts for 24.8% of all samples and in the class, the coarse particles account for 40%. Cluster B was found to occur mainly in early September. After several sunny days, dry and hot weather conditions, which are not conducive to the deposition of particles, tend to lead to the increase of atmospheric aerosols. Thus, cluster B was found related closely to hot and dry weather. For cluster C, the main peak is from 2.29–2.64 μm in the coarse mode, the second peak is from 0.58–0.72 μm in the accumulation mode, and the minimum peak is from 6.73–7.77 μm in the coarse mode. Cluster C accounts for 21.8% of all samples, and the coarse particles account for 37.3% in the class. Cluster C was found to disappear mainly during calm and cloudy weather because such conditions are unfavorable for convection and aerosol diffusion. The PM2.5 values of clusters B and C are 60 and 99 μg m^{-3}, respectively; thus, both belong to the "good" level that is considered not to harm public health.

In Fig. 3(d)–(f), it can be seen that clusters D–F, respectively, all show bimodal distributions. The main peaks of clusters D and E are from 3.05–3.52 and 2.45–2.84 μm, respectively, and both belong to the coarse mode. The second peaks of clusters D and E are from 11.14–12.86 μm and they also belong to the coarse mode. The main peak of cluster F is from 0.67–0.77 μm in the accumulation mode, and the second peak is from 8.35–9.65 μm in the coarse mode. Cluster D accounts for 16.7% of all samples, in which the coarse particles account for 33.9%. Cluster D was found to occur mainly in calm and cloudy weather in mid-September. Cluster E accounts for 9.4% of all samples, and in this class, the coarse particles account for 26.3%. Cluster F accounts for 4.8% of all samples and the coarse particles account for 11.7%. Clusters E and F were found to occur mainly during overcast weather after continuously cloudy days. During overcast weather in the evening in summer and early autumn, convection is very weak and it is not favorable for the diffusion of aerosol particles produced by human activities and automobile exhausts. Thus, these factors can lead to a rapid increase in PM2.5 concentration.

For clusters D and E, the PM2.5 values are 137.4 and 158 μg m^{-3}, respectively, which belong to "slight" and "moderate" levels of pollution, both of which represent slight hazards to public health. During such weather conditions, vulnerable members of the population should limit their outdoor activity. For cluster F, the PM2.5 value reaches 280 μg m^{-3}, which is classified as "moderate" pollution that could do serious harm to human health. During such weather, even healthy people could experience discomfort.

The analysis above identifies that all clusters occur under different weather conditions. From cluster A–F, the PM2.5 value increases gradually; therefore, during summer and early autumn evenings, weather conditions have considerable influence on air quality in the Yinchuan area.

As can be seen in Table 2, both the PM2.5 value and the mass concentration are related closely to weather conditions. The PM2.5 value has a negative relation with wind speed, i.e., higher wind speeds mean lower PM2.5 concentrations. This is an effective illustration of how wind can decrease PM2.5 concentrations. PM2.5 has a positive relation with relative humidity, i.e., higher relative humidity is associated with higher PM2.5 concentrations. For example, for cluster F, the reasons for the high PM2.5 value are the low wind speed and the high relative humidity.

The proportion of accumulation mode particles in the total mass concentrations was found to have a positive relation with PM2.5, whereas a negative relation was found between the proportion of coarse mode particles in the total mass concentrations and PM2.5.

The proportion of accumulation mode particles in the total mass concentrations was found to have a negative relation with wind speed. Conversely, the proportion of coarse mode particles in the total mass concentrations showed a positive relation with wind speed. The proportion of accumulation mode particles in the total mass concentrations showed a positive relation with relative humidity, whereas the proportion of coarse mode particles exhibited a negative relation with relative humidity.

According to the air quality standard of China, the PM2.5 value of "excellent" air quality is 75 μg m^{-3}. The samples in this study with aerosol concentrations <75 μg m^{-3} account for 47.3% of all samples, and they are concentrated mainly in clusters A and B (Table 2). Based on examination of the air quality ranking of key cities in China, the compliance rates of the Yinchuan area in August and September 2013 were listed as Nos. 11 and 15, respectively, of 76 cities in China. The compliance rates

of these two months are much higher than some northwestern cities, e.g., Xi'an and Lanzhou but lower than Haikou (ranked No. 1), which is a very clear city on the island of Hainan in the South China Sea.

CONCLUSIONS

This study used an APS™-3321 to acquire continuous observations of the concentrations and size distributions of atmospheric aerosols from August 23 to September 23, 2013, in the Yinchuan area (China). The mass concentrations, mass size distributions, and PM2.5 concentrations were investigated using cluster analysis. In addition, meteorological data were obtained to determine the relationship between size distribution and weather. The following conclusions were derived.

(1) Aerosol number concentrations showed significant daily and monthly variations during the observational period; the daily variations exhibited a regular single-peak structure. The monthly variations were found related to weather conditions, e.g., aerosol concentrations on cloudy days were higher than on sunny days. Because precipitation has an important role in atmospheric cleansing, the number concentration of aerosols was found very low following a period of rain.

(2) Fine particles were found dominant during the entire observation period, and their number concentration accounted for 98.8% of all particles. The number distribution was unimodal with a peak in the accumulation mode. The surface area distribution was bimodal with peaks in both the accumulation and the coarse modes, and the maximum peak was in the accumulation mode. The mass distribution was trimodal with peaks in the accumulation and coarse modes; the maximum peak was found in the accumulation mode.

(3) The mass distribution of aerosol particles during the entire observational period could be divided into six categories. The mass distribution and concentration were found related closely to weather conditions. Cluster A occurred on the day following a period of rain, whereas clusters B and C occurred mainly on continuously sunny days and cloudy days, respectively. Clusters D–F occurred mainly on windless cloudy days and during overcast weather after continuously cloudy days. Through analysis and comparison of the PM2.5 concentrations, clusters A and B were found to reflect the "excellent" level of the air quality standard of China. During the entire observational period, the excellent weather rate reached 47.3% and the good weather rate was more than 69.1%, i.e., higher than other cities in Northwest China.

Although the experimental results obtained in this study provide insight into the distribution characteristics, evolution, and factors affecting the size distributions of atmospheric aerosol particles in the Yinchuan area, quarterly and annual variations of aerosol concentrations and size distributions should be observed and analyzed to derive conclusions that have greater value.

ACKNOWLEDGEMENTS

This work was supported by the National Natural Science Foundation of China (NSFC) (Nos. 61565001, 61765001, and 61168004), Leading Talents of Scientific and Technological Innovation of Ningxia, Plan for Leading Talents of the State Ethnic Affairs Commission of the People's Republic of China, Key Scientific Research Project of Beifang University of Nationalities (No. 2015KJ02), and Scientific Research Project of Beifang University of Nationalities (No. 2016GQR07). We thank James Buxton MSc from Liwen Bianji, Edanz Group China (www.liwenbianji.cn./ac), for editing the English text of this manuscript.

REFERENCES

[1] Chiaral, M.C. (1997) Atmospheric aerosol optical properties: a database of radiative characteristics for different components and classes. App. Opt. 36(30), 8031-8041.

[2] Jacobson, M.Z. (2001) Strong radioactive heating due to the mixing-state of black carbonization morphemic aerosols. Nature. 409(6821), 695-697.

[3] Hinz, K.P., Trimborn, A., Weingartner, E., Henning, S., Baltensperger, U., Spengler, B. (2005) Aerosol single particle composition at the jungfraujoch. Aerosol Science. 36(1), 123-145.

[4] Kaufman, Y.J., Tanre, D., Boueher, O. (2002) A satellite view of aerosols in the climate system. Nature. 419(6903), 215-223.

[5] Sokolik, I.N., Winker, D.M., Bergametti, G., Gillette, D.A., Carmichael, G., Kaufman, Y.J., Gomes, L., Schuetz, L., Penner, J.E. (2001) Introduction to section: outstanding problems in quantifying the radiative impacts of mineral dust. Journal of Geophysical research. 106(D16), 18015-18027.

[6] Morawska, L., Thomas, S., Jamriska, M., Johnson, G. (1999) The modality of particle size distributions of environmental aerosols. Atmosphere Environment. 33(27), 4401-4411.

[7] Tunved, P., Strom, J., Hansson, H. C. (2004) An investigation of processes controlling the evolution of the boundary layer aerosol size distribution properties at the Swedish background station Aspvreten. Atmosphere Chemistry and physics. 4(11/12), 2581-2592.

[8] Ketzel, M., Wahlin P., Kristensson A., Swietlicki, E., Berkowicz, R., Nielsen, O. and Palmgren, F. (2004) Particle size distribution and particle mass measurements at urban, near-city and rural level in the Copenhagen area and Southern Sweden. Atmosphere Chemistry and Physics. 4(1), 281-292.

[9] Kim J.Y., Jung C.H., Choi B.C., Oh, S.N., Brechtel, F.J., Yoon, S.-C., Kim, S.W. (2007) Number size distribution of atmospheric aerosols during ACE-Asia dust and precipitation events. Atmosphere Environment. 41(23), 4841-4855.

[10] Kalivitis, N., Birmili, W., Stock, M., Wehner, B., Massling, A., Wiedensohler, A., Gerasopoulos, E., Mihalopoulos N. (2008) Particle size distributions in the Eastern Mediterranean troposphere. Atmosphere Chemistry and Physics. 8(22), 6729-6738.

[11] Buonanno, G., Lall, A.A., Stabile, L. (2009) Temporal size distribution and concentration of particles near a major highway. Atmosphere Environment. 43(5), 1100-1105.

[12] Nicolás, J., Yubero, E., Galindo, N., Giménez, J., Castañer, R., Carratalá, A., Crespo, J., and Pastor, C. (2009) Characterization of events by aerosol mass size distributions. Journal of Environment Monitoring. 11, 394-399.

[13] Wang, L., Morawska, L., Jayaratne, E.R., Mengersen, K., Heuff, D. (2011) Characteristics of airborne particles and the factors affecting them at bus stations. Atmosphere Environment. 45(3), 611-620.

[14] Zhao, D., Tang, D., Zhou, Z., Ma, L., Wang, Y. (1988) The aerodynamics size distribution of atmospheric aerosol in winter in Beijing. Scientia Atmospherica Scinica. 12(2), 170-179.

[15] Huang, H., Huang, Y., Rao, R. (2006) Observational study on the concentration and size distribution of atmospheric aerosol over the Hefei area. Infrared and Laser Engineering. 35(1), 391-395.

[16] Chen, J., Jiang, N., Xia Z., Wang, X. (1991) Characteristics of the concentration and spectrum size distribution of atmospheric aerosol at MT. Huangshan. Journal of Nanjing institute of Meteorology. 14(3), 354-358

[17] Zhao, S., Yu, Y., Chen, J., Liu, N., He, J. (2012) Size Distribution Properties of Atmospheric Aerosol Particles During Summer and Autumn in Lanzhou. Environment and Science. 33(3), 687-693.

[18] Sang, J., Yang, Y. (2003) Characteristics of aerosol particle size distribution during summer in Yinchuan City, Ningxia Province. Journal of Desert Research. 23(3), 328-330.

[19] Wilson, J.C., Liu, B.Y.H. (1980) Aerodynamic particle size measurement by laser-doppler velocimetry. Journal of Aerosol Science. 11(2), 139-150.

[20] Thomas, M.P., David, L. (2003) Concentration measurement and counting efficiency of the aerodynamic particle sizer 3321. Journal of Aerosol Science. 34(5), 627-634.

[21] Prather, K.A., Nordmeyer, T., Salt K. (1994) Real-time characterization of individual aerosol particles using time-of-flight mass spectrometry. Analytical Chemistry. 66(9), 1403-1407.

[22] Gard, E., Mayer, J.E., Morrical, B.D., Dienes, T., Fergenson, D.P. and Prather K.A. (1997) Real-time analysis of individual atmospheric aerosol particles: design and performance of a portable ATOFMS. Analytical Chemistry. 69(20), 4083-4091.

[23] Salt, K., Noble C.A. and Prather, K.A. (1996) Aerodynamic particle sizing versus light scattering intensity measurement as methods for Real-time particle sizing coupled with time-of-flight mass spectrometry. Analytical Chemistry. 68(1), 230-234.

[24] Dahneke, B. (1980) Sampling and analysis of suspended particles and vapors by continuum source particle beams. In: Engel, A. (eds.) Emission Control from Stationary Power Sources, AIChE. Symp. Ser. 201(76), AIChE, New York, 134-143.

[25] Park, D., Kim, Y., Park, C.W., Huang, J., Kim, Y. (2009) New bio-aerosol collector using a micromachined virtual impactor. Journal of Aerosol Science. 40(5), 415-422.

[26] Wang, S., Feng, X., Zeng, X., Ma, Y., Shang, K. (2009) A study on variations of concentrations of particulate matter with different sizes in Lanzhou China. Atmosphere Environment. 43(17), 2823-2828.

[27] Almeida, D., Schutz, L. (1983) Number, mass and volume distribution of mineral aerosol and soils of the Sahara. Journal of Applied Meteorology. 22(2), 233-243.

[28] Gao, J., Wang, J., Cheng, S., Yang, L., Wang, W., Wang, T. (2007) Studies on characteristics of size distribution and formation mechanism of fine particle matters in summer of Ji'nan. Journal of the Graduate School of the Chinese Academy of Sciences. 24(5), 680-687.

[29] Zhang, T., Tao, J., Wang, B., Zhang, R. (2010) Research on size distribution of particles and its impact on visibility in urban Guangzhou during spring. Journal of the Graduate School of the Chinese Academy of Sciences. 27(3), 331-337.
[30] Hu, M., Liu, S., Wu, Z., Zhang, J., Zhao, Y. (2006) Effect of high temperature, high humidity and rain Process on particle size distributions in the summer of Beijing. Environment and Science. 27(11), 2293-2298.
[31] Wang, X., Xi, X., Guo, Z., Liu, Z., Chen X. (2006) Analysis of the sand-stormy weather in Lanzhou during the spring of 2002. Journal of Lanzhou University. 42(3), 44-47.
[32] Liu, J., Chen, C. (2003) A comprehensive study of the characteristics of atmospheric aerosol in winter in Lanzhou City. Journal of Lanzhou University. 39(4), 104-108.
[33] Yu, Y., Xia, D., Chen, L., Liu, N., Chen, J., Gao, Y. (2010) Analysis of Particulate Pollution Characteristics and Its Causes in Lanzhou, Northwest China. Environmental and Science. 31(1), 22-28.
[34] Wang, Z., Zhang, W., Shi, J., Huang, J., Chen, Y., Bi, J., Zhang B. (2010) The size distribution and concentration of atmospheric aerosol particles in semiarid zone. Journal of Desert Research. 30(5), 1186-1193.
[35] Xu, X., Wang, X., Huang, J. (2011) The observational size distribution of dusty aerosol in Lanzhou. Plateau Meteorology. 30(1), 208-216.
[36] Zhang, C., Zhou, W. (1995) Atmospheric Aerosol Tutorial. Meteorology Publishing House, Beijing.

Received: **10.08.2016**
Accepted: **21.04.2018**

CORRESPONDING AUTHOR

Jiandong Mao
School of Electrical and Information Engineering
Beifang University of Nationalities
Yinchuan, 750021 Ningxia – P.R. China

e-mail: mao_jiandong@163.com

© by PSP Volume 27 – No. 7/2018 pages 4624-4630 Fresenius Environmental Bulletin

USE OF GIS TO EVALUATE CLOSED-END FURROW IRRIGATION

Ehsan Dayer[1], Ebrahim Pazira[2,*], Heydar Ali Kashkuli[3], Hossein Sedghi[1]

[1]Department of Water Sciences and Engineering, Science and Research Branch, Islamic Azad University, Tehran, Iran
[2]Department of Soil Science, Science and Research Branch, Islamic Azad University, Tehran, Iran
[3]Department of Water Sciences and Engineering, Ahvaz Branch, Islamic Azad University, Ahvaz, Iran

ABSTRACT

Irrigation water management has a key role in increasing food grain production with less water. It also helps meet the ever increasing demand for other water uses. To assess the efficiency of furrow irrigation, a 4 ha plot (87 furrows). cultivated with sugarcane was selected in Khuzestan Province, Iran Then, the inflow, outflow runoff, soil moisture before irrigation, depth of root development, and depth of water infiltration were measured. These measurements were then used to calculate the water use efficiency, uniformity coefficient, and distribution uniformity for the selected plot. The Geographical Information System, in ArcView, was used to analyze the irrigation efficiency levels for the closed-end furrow method. Irrigation efficiency for the closed-end furrow method ranged from 0.1982–0.7179 with a weighted mean of 45.78 and the coefficient of uniformity for the closed-end furrow method ranged between 84.04 and 99.376 with a weighted mean of 69.78%. These results suggest that GIS is a versatile tool that can be used to produce results in the form of a map and will improve the irrigation management decision making process.

KEYWORDS:
Furrow Irrigation, Water Use Efficiency, Spatial Analysis

INTRODUCTION

In the near future, irrigated agriculture will need to produce two-thirds of the increase in food products required by a large population increase [1]. In Iran, 92% of the total water is used for agricultural irrigation and 6% for public services. The ecological impacts of irrigation relate to the changes in the quantity and quality of soil and water as a result of irrigation and the effects on natural and social conditions in river basins that are downstream of irrigation schemes. The impacts stem from the altered hydrological conditions caused by the installation and operation of an irrigation scheme.

Irrigation water management has a key role in increasing food grain production with less water. It also helps meet the ever increasing demand for other water uses. Traditionally, sugarcane has always been considered to have large water requirements. Where there is no water, sugarcane cannot be planted. Very often, the lack of a reliable water supply can lead to destruction of the entire standing crop or generate heavy crop losses. The heavy water requirement for sugarcane growing is one of the major factors that affect attempts to extend sugar cane growing into new areas.

Ucak and Bagdatli stated that there was a significant linear relationship ($p < 0.01$) between plant water consumption (ETa) values and seed yields [2]. In particular, it has been shown that water application efficiencies on high infiltration soils in the sugar industry are generally low (average ~30%) while on low infiltration soils it is generally high (typically > 60%). However, furrow irrigation efficiency has also been shown to be closely related to irrigation design and management practices, with large variations between sites and throughout the season being attributed to management and environmental differences.

Water use efficiency (WUE) affects water distribution, surface runoff, and deep percolation from the root zone. There have been previous studies on the effects of irrigation systems on soil biological properties, such as microbial biomass and soil enzymes [3]. Zou et al. discussed the impacts of irrigation schedule on soybean biomass, yield, WUE, and irrigation water use efficiency (IWUE) in the black soil region of northeast China [4]. In one study, the water productivity and fiber quality parameters of deficit irrigated cotton cultivars in a semi-arid environment were investigated. According to this study, the most suitable irrigation program for increased cotton yield in a region without irrigation water restrictions was treatment (IL-100) where water was fully applied to the Carmen cotton variety [5]. In contrast, traditional surface irrigation resulted in a considerable wastage of water through runoff and deep percolation below the root zone and this could result in a number of undesirable hazards, such as leaching of available nutrients, water stagnation, limited soil aeration, and weed infestation. All of these negative effects lead to a decline in yield. A study on a cotton field in Australia evaluated irrigation application efficiency to be 48% on average [6].

Furrow irrigation is widely used. However, it requires a large primary investment and a uniform distribution. Furthermore, irrigation efficiency never exceeds 60%–70% and its average is 50%–55%. Furrow irrigation WUE is influenced by factors such as furrow geometric parameters (length, slope, and cross-section), the flow value, age of plants, and the texture and structure of the soil [7]. Furrow irrigation efficiency has also been shown to be closely related to irrigation design and management practices, and large variations between sites and throughout the season have been attributed to management and environmental differences [8, 9, 10]. However, application efficiencies for individual irrigation events range from 14% to 90% [11]. Kanber et al. compared the surge and continuous furrow method for cotton grown on the Harran Plain [12]. In this study, WUE for the surge method was 64%–73% and the average uniformity distribution (efficiency) was between 69% and 89%. The continuous furrow method produced WUEs of between 46% and 60% and average uniformity distributions that were between 83% and 88%. In Turkish sweet potato fields, the IWUE and WUE ranged from 36.8 to 65.7 kg ha^{-1} mm^{-1} and from 33.2 to 75.9 kg ha^{-1} mm^{-1}, respectively [13]. More efficient furrow irrigation methods than conventional or continuous-flow irrigation have been developed to promote water savings in agriculture. This was the reason why the cutback and surge methods were created. To achieve high efficiency and uniform irrigation using unpressurized gravity water application methods, all parts of an irrigated field should receive water for near equal lengths of time, with a minimum of water lost to runoff or deep percolation below the root zone [10].

Most of the data related to irrigation management is complex, spatially distributed, and temporal in nature. The integration of the irrigation data and its use in irrigation planning and management has led to the introduction of Geographic Information Systems (GIS) and other technologies [14, 15, and 16]. The extrapolation of site-level WUE estimates from flux sites to regional or global scales remains a challenge [18]. GIS is an effective tool for exploring, storing, managing, and displaying spatial data and can be used to improve decision making and management functions that are central to the planning and management of any irrigation scheme. Therefore, the objective of this study was to use GIS to evaluate the WUE, the deep percolation level, the runoff ratio, and the distribution uniformity in a sugarcane field in Khuzestan Province, Iran.

MATERIALS AND METHODS

Study area and field measurements. This study was conducted in a 4 ha (87 furrows) area of an experimental field cultivated with sugarcane in Khuzestan Province, Iran. Furrow irrigation using closed-end methods was evaluated, and residual water for use in downstream irrigation was analyzed.

Soil physical properties. The tissue type was determined by taking hydrometer readings and soil texture compound samples from various depths between 0 and 100 cm. The overall soil texture type was silt loam. Bulk density *(bp)* was measured by sampling the soil using metal rings of a certain volume. A hole was drilled to a depth of 1.5 m and a width of 1 m and four samples from the 0–25, 25–50, 50–75, and 75–100 cm soil layers were prepared. These samples were then transferred to the laboratory where they were dried in an oven at 105°C. The *bp* of the soil was calculated from the modified equation:

Equation 1: $$bp = Ws / Vs$$

Where *Ws* is dry weight of the soil and *Vs* is the soil volume (Table 1).

Soil moisture surveys. Before each irrigation event, the soil moisture for each sampling station and spatial data, such as descriptive information for the second layer input, was collected. Before, irrigation, the sugar cane root activities in the 0–100 cm soil layer were measured along with the average soil moisture in the 0–25, 25–50, 50–75, and 75–100 cm soil layers. In each evaluation, 140 samples were taken before irrigation and sent to the laboratory for soil moisture determination. Each sample was weighed and placed in an oven at 105°C for 24 h. Then the dried samples were weighed and soil moisture content was calculated from the following equation. The results are shown in Table 1.

Equation 2: **Soil moisture** =

$$\frac{weight\ of\ wet\ soil - weight\ of\ dried\ soil}{weight\ of\ dried\ soil}$$

The differences between the moisture content before and after irrigation, and *bp* at each rooting depth were used to determine the net irrigation depth (*In*):

Equation 3 : $$In = pb * MAD * D_{rz} (Ø_{fc} - Ø)$$

where *In* is "input" (cm), $Ø_{fc}$ is the moisture weight at soil field capacity (decimal), $Ø$ is the moisture weight before irrigation (decimal), D_{rz} is the rooting depth (cm), *MAD* is the permissible moisture depletion (0.65, as recommended by the Food and Agriculture Organization of the United Nations), and *bp* is bulk density (mg cm^{-3}). The aim of all irrigation systems is to raise soil moisture content to the desired amount. Therefore, a field trial was used to determine soil gravimetric moisture content in the study area at field capacity. The surface of part of the tested furrows (length 1.5–2 m) was covered with black plastic and consecutive samples were taken every 12 h after irrigation to determine the moisture

TABLE 1
Initial soil moistures of the sampling stations before irrigation and their physical characteristics

Station number	X	Y	Weighted moisture before irrigation (closed-end)	Soil bulk density (g cm^{-3}).	moisture FC%
1	257015	3426992	20.65	1.6	25.45
2	256975	3426992	19.5	1.6	25.45
3	256935	3426992	19.85	1.6	25.45
4	256895	3426992	19.8	1.6	25.45
5	256855	3426992	20.175	1.6	25.45
6	257015	3426952	20.67	1.6	25.45
7	256975	3426952	21.6	1.6	25.45
8	256935	3426952	19.7	1.6	25.45
9	256895	3426952	20.32	1.6	25.45
10	256855	3426952	21.25	1.6	25.45
11	257015	3426912	20.3	1.6	25.45
12	256975	3426912	19.8	1.6	25.45
13	256935	3426912	22.05	1.6	25.45
14	256895	3426912	23.2	1.6	25.45
15	256855	3426912	23.07	1.6	25.45
16	257015	3426872	19.55	1.6	25.45
17	256975	3426872	20.82	1.6	25.45
18	256935	3426872	22.1	1.6	25.45
19	256895	3426872	20.97	1.6	25.45
20	256855	3426872	18.75	1.6	25.45
21	257015	3426832	20.67	1.6	25.45
22	256975	3426832	21.6	1.6	25.45
23	256935	3426832	19.7	1.6	25.45
24	256895	3426832	20.32	1.6	25.45
25	256855	3426832	21.25	1.6	25.45
26	257015	3426792	20.3	1.6	25.45
27	256975	3426792	19.8	1.6	25.45
28	256935	3426792	220.5	1.6	25.45
29	256895	3426792	23.2	1.6	25.45
30	256855	3426792	23.07	1.6	25.45
31	257015	3426752	19.55	1.6	25.45
32	256975	3426752	20.82	1.6	25.45
33	256935	3426752	22.1	1.6	25.45
34	256895	3426752	20.97	1.6	25.45
35	256855	3426752	18.75	1.6	25.45

content of the covered part until it became constant. The mean gravimetric moisture percentage at field capacity for the study area was 25.45%.

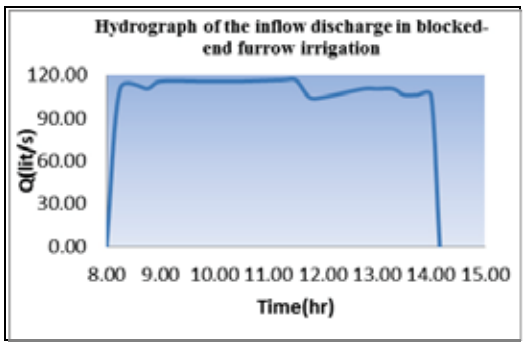

FIGURE 1
Hydrograph of the inflow discharge during closed-end furrow irrigation

Irrigation operation. The irrigation operation was applied using the hydroflume irrigation system. Water was supplied through a 38 cm diameter polyethylene pipe with outlet valves (5.1 cm in diameter) for each furrow. The volume of water from the outlet ports delivered to each furrow in each replicate was recorded. The inlet flow from the mouth of the hydroflume pipe was recorded at different times. An inlet flow hydrograph was constructed using time (h) and water flow (L/s) (Figure 1).

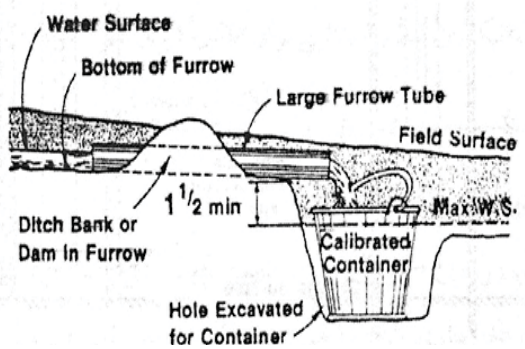

FIGURE 2
Method used to obtain the water flow at the closed-end of the furrow

Following this operation, the inlet flows to the furrow and the runoff outlet at the end of the furrow were measured using the volumetric method and a hydrograph was drawn (Figure 2). Furthermore,

three samples for water quality analysis were taken from the input water and tail water during the experiment. These were taken at the beginning, middle, and end of the experiment. A Wilcox chart, was then used to classify the inlet water and tail water.

Assessment indicators. The collected data was used to derive assessment indicators, such as irrigation efficiency (Equation 4), the deep percolation ratio (DPR) (Equation 5), the coefficient of uniformity (CU) (Equation 6), and the distribution uniformity (DU) (Equation 7).

Equation 4: $\mathbf{Ea} = \frac{In}{Ig}$

Where *Ea* is irrigation efficiency, *In* is the net irrigation depth, and *Ig* is the gross irrigation depth

Equation 5: $\mathbf{DPR} = \frac{(Ig - In)}{Ig}$

Equation 6: $\mathbf{CU} = \mathbf{100\text{-}[1} - \frac{\text{sum of absolute differences between observed values and the mean}}{\text{sum of percolation values in all of the points}}$]

Equation 7: $\mathbf{DU = 100 - 1.59(100 - CU)}$

Assessment by ArcView. As the areas under irrigation are generally small, the results of the models used to assess furrow irrigation systems have always been viewed with skepticism and the assessment indicators have not always been accurate. However, ArcGIS spatial analysis and GIS can create, query, map, and analyze cell-based raster data; perform integrated raster/vector analysis; derive new information from existing data; query information across multiple data layers; and fully integrate cell-based raster data with traditional vector data sources.

The 87 furrows in the field (160 m in width and 240 m in length), covering ~ 4 ha, were selected to evaluate open and closed-end furrow irrigation systems. Then, the study area was surveyed and the map was designed using AutoCAD software and, finally an output DXF file was imported as the first layer in the ArcView software for further examination.

In this study, 40×40 networks were designed, 35 points inside the study area were marked, and the geographical coordinates of each point were determined using Garmin GPS equipment. These points were prepared as a spatial layer by Microsoft Excel using UTM coordinates and a DBF file.

RESULTS AND DISCUSSION

The results for zoning moisture distribution before irrigation are shown in Figure 3. The maximum moisture distribution area for the closed-end furrow method ranged between 20.156 and 20.962 with a weighted mean of 20.99%. The reason for the increased moisture enhancement by the closed-end furrow method is that the duration of water accumulation in the furrows was longer than for the open system. Soil moisture before irrigation greatly affects infiltration: the greater soil moisture before irrigation, the lower the infiltration, whereas water infiltration increases when soil moisture is low. This point was very clearly observed in this study.

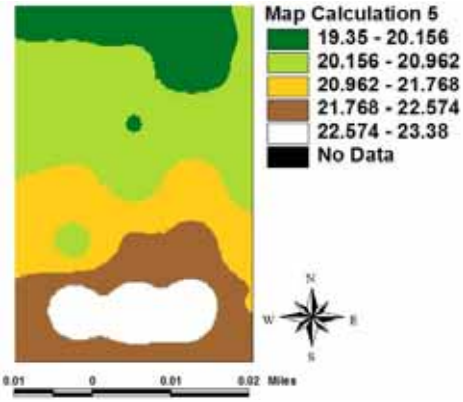

FIGURE 3
Moisture distribution for closed-end furrows

Zoning net irrigation depth. Figure 4 shows the net irrigation depth before irrigation for the closed-end method. The results suggest that at 100 cm depth, the soil deficient moisture level prior to irrigation was 2.77 centimeters for the closed-end furrow method.

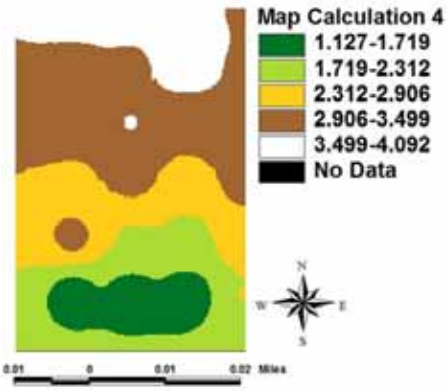

FIGURE 4
Distribution of net irrigation depth in closed-end furrows

Zoning irrigation application efficiency. The gross irrigation depths were determined from the input water flow. Then Arc view and GIS were used to divide the net irrigation depths (Equation 3) before irrigation. This allowed the irrigation application efficiency to be calculated.

Figure 5 shows a white area at the start of the furrow, and the yellow and green areas represent the irrigation efficiencies with ranges of 0.7179–0.544, 0.544–0.371, and 0.371–0.1982, respectively, which cover about 42.46, 32.72, and 24.81% of the total study area, respectively. Figure 5 also shows that the

irrigation efficiency for the closed-end furrow method ranged between 0.1982–0.7179 with a weighted mean of 45.78%.

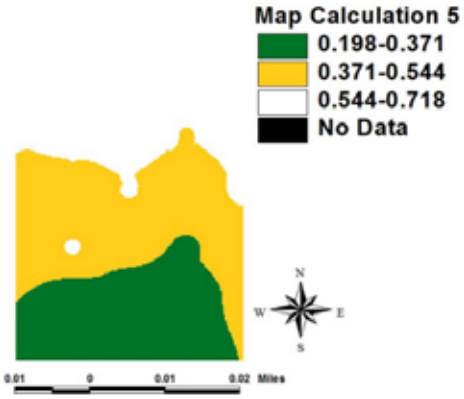

FIGURE 5
Irrigation efficiency distribution in closed-end furrows

Zoning DPR. The net irrigation requirements (*In*) and the gross irrigation requirements (*Ig*) were used to calculate the deep percolation values. The DPR was determined using Equation 5 and repeated macro scripting in ArcView. Figure 6 shows green, yellow, and white areas, which have DPR ranges of 0.282–0.456, 0.456–0.629, and 0.629–0.8018, respectively. These areas cover ~ 42.46%, 32.72%, and 24.81% of the total study area, respectively. Figure 6 shows that the DPRs for the closed-end furrow method ranged between 28.21 and 80.18 with a weighted mean of 54.23%. Raine and Baker reported that WUE decreased when depth losses increased, but reducing depth losses usually led to higher WUE [9].

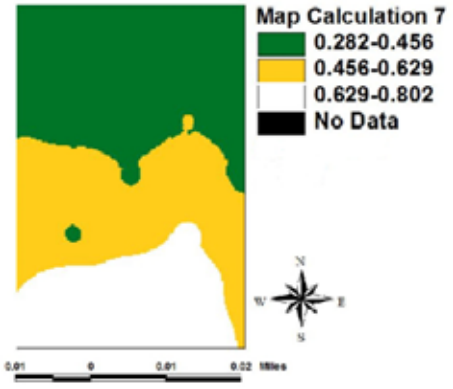

FIGURE 6
Deep percolation in closed-end furrows

Zoning coefficient of uniformity. Deep percolation values at every point in the experiment were calculated using *In* and *Ig*, and then Equation 6 was obtained by repeated macro scripting in the ArcView GIS environment to determine the coefficient of uniformity. Figure 7 shows deep green, light green, yellow, brown, and white areas. Their coefficients of uniformity ranges were 47.7615–56.0688, 56.07–65.4485, 65.4498–74.8274, 74.8274–83.2079, and 83.2089–92.5708, respectively, and they covered ~ 1.88%, 23.1%, 38.16%, 31.28%, and 5.56% of the total study area, respectively. Figure 8 shows that the coefficient of uniformity for the closed-end furrow method ranged between 84.04 and 99.376 with a weighted mean of 69.78%.

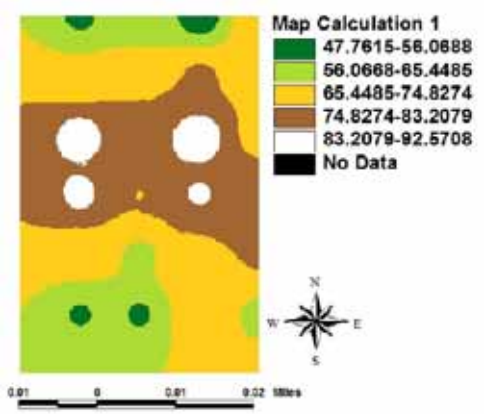

FIGURE 7
Distribution of uniformity in closed-end furrows

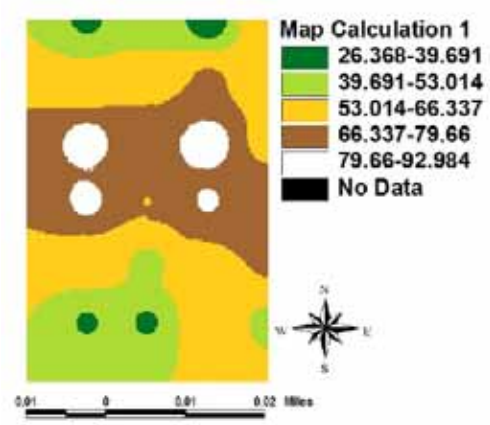

FIGURE 8
Distribution of uniformity coefficients in closed-end furrows

Zoning distribution uniformity. The distribution uniformity was derived from Equation 7, which was obtained by calculating the coefficients of uniformity in the previous section and repeated macro scripting using the ArcView GIS software.

In Figure 8, the dark green, light green, yellow, brown, and white areas have distribution uniformity ranges of 26.3681–39.6854, 39.6854–53.0131, 53.0131–66.3355, 66.3355–79.6598, and 79.6598–92.9836, respectively. They cover ~1.89%, 23.1%, 38.16%, 31.27%, and 5.57% of the total study area, respectively. Figure 8 shows that the distribution uniformity of the closed-end furrow method ranged between 26.3681 and 92.9836 with a weighted mean of 62.85%. Kanber et al. compared the surge and

continuous furrow methods for cotton on the Harran plain [12]. Their results showed that the WUE for the surge method was between 64% and 73% and the average uniformity distribution (efficiency) was between 69% and 89%. The WUE for the continuous furrow method was between 46% and 60% and the uniformity distribution was between 83% and 88%.

CONCLUSION

The closed-end furrow surface irrigation moisture before irrigation was between 23.38 and 19.35, and the weighted average was 20.99%. The reason for the increased moisture enhancement after using the closed-end furrow method is that the water accumulation duration in the furrows was longer than it was for the open-ended furrows. Soil moisture before irrigation greatly affects water infiltration and net irrigation. The net irrigation depth for the closed system was between 1.126 and 4.092, and the weighted average was 2.77%. The closed-end furrow irrigation efficiency ranged between 0.1982 and 0.7172 with a weighted average of 45.78%. Around 55% of the closed-end area had an efficiency >37%. The uniformity coefficient was between 84.04 and 99.376 and the weighted average was 69.78%. Furthermore, 98% of the total study area had a uniformity coefficient above 56%. The results show that the land use efficiency was acceptable. The constant flow rates in the furrows showed that improperly sloped furrows and closed-end furrows led to low efficiencies. However, furrow irrigation performance is affected by a range of factors, including the inflow discharge, soil infiltration characteristics, field length, required application volume, cutoff time, surface roughness, and field slope [17 and 18]. Geographical information system analysis (GIS), data were organized in a set of layers and detailed attributes were attached to each data element in this study. Remote sensing and GIS data collection and analysis capabilities are now viewed as efficient and effective tools for irrigation water management. The ability of GIS to analyze the information across space and time can help manage dynamic systems, such as irrigation systems.

REFERENCES

[1] English, M.J., Solomon, K.H. and Hoffman, G.J.A. (2002) Paradigm shift in irrigation management. Journal of Irrigation and Drainage Engineering of ASCE. 128, 267-277.

[2] Ucak A.B. and Bagdatli, M.C. (2017) Effects of deficit irrigation treatments on seed yeald, oil ration and water use efficiency of sunflower (*Helianthus annuus L.*) Fresen. Environ. Bull. 26, 2983-2991.

[3] Kocyigit, R. and Genc, G. (2017) Impact of drip and furrow irrigations on some soil enzyme activates during tomato growing season in a semi-arid ecosystem. Fresen. Environ. Bull. 26, 1047-1051.

[4] Zou, W., Lu, X., Han, X. (2017) Effect of irrigation regime on soybean biomass, yield, water use efficiency in a semi-arid and semi-humid region in northeast China. Fresen. Environ. Bull. 26, 1865- 1875.

[5] Akcay, S. and Dagdelen, N. (2017) Water productivity and fiber quality parameters of deficit irrigated cotton cultivars in a semi-arid environment. Fresen. Environ. Bull. 26, 6500-6507.

[6] Smith, R.J., Raine, S.R. and Minkevich, J. (2005) Irrigation application efficiency and deep drainage potential under surface Irrigated Cotton. Agricultural Water Management. 71, 117-130.

[7] Fatemi, M., Shokrolahy, A. and Shiravi, M.H. (1998) The effect of integrated land agriculture on irrigation efficiency in Dez irrigation network. The seventh seminar on Iranian National Committee on Irrigation and Drainage (In Persian).

[8] Humbert, R.P. (1968) The Growing of Sugar Cane. Elsevier Publishing Company. Amsterdam, 311-358.

[9] Raine, S.R. and Bakker, D.M. (1996) Increased Productivity through better design and management of irrigated cane fields Increased. Sugar research and development corporation. Project number-BS90S.

[10] Lieb, B. and Ley, T.W. (2003) Drought Advisory: Surface Irrigation Systems, Washington State University Cooperative Extension, WA, USA.

[11] Raine, S.R. and Walker W.R. (2004) A design and management to improve Surface Irrigation efficiency. Trans of the ASAE. 10(3), 19-23.

[12] Kanber, R., Koksal, H., Onder, S., Kapur, S. and Sahan, S. (2001) Comparison of surge and continuous furrow method for cotton in the Harran plain. Agricultural Water Management. 47, 119-135.

[13] Onder, D., Onder, S., Caliskan M.E., Caliskan, S. (2015) Influence of different irrigation methods and irrigation levels on water use efficiency, yield, and yield attributes of sweet potatoes. Fresen. Environ. Bull. 24, 3398- 3403.

[14] Su, M.D. and Wen, T.H. (2001) Spatial decision system for irrigation demand planning. In: Phelps, D., Sehlke, G. (Eds.) Bridging the GAP meeting the Worlds Water and Environmental Challenges. Proceedings of the World Water and Environmental Resources Congress, 20-24 May 2001, Orlando, FL. ASCE, EWRI, P.11.

[15] Bioggio, M.R. and Ding, Y. (2001) An integrated regional watershed model. In: Phelps, D., Sehlke, G., (Eds.) Bridging the Gap Meeting the World's Water and Environmental Resources Challenges. Proceedings of the World Water and Environmental Resources Congress, 20– 24 May 2001, Orlando, FL. American Society of Civil Engineers, ASCE, EWRI, p. 10. CD ROM publication.
[16] Kjelds, J. and Storm, B. (2001) Integrated water resources modeling water use and water quality simulation. In: Phelps, D., Sehlke, G., (Eds.) Bridging the Gap Meeting the Worlds Water and Environmental Resources Challenges, Proceedings of the World Water and Environmental Resources Congress, 20–24 May 2001, Orlando, FL. American Society of Civil Engineers, ASCE, EWRI, p. 10. CDROM publication.
[17] Pereira, L. (1999) Higher performance through combined improvements in irrigation methods and scheduling: a discussion. Agric. Water Manage. 40, 153-169.
[18] Eldeiry, A., Garcia, L.A., El-Zaher, A.S., and Kiwan, M.E. (2005) Furrow irrigation system design for clay soils in arid regions. Appl. Eng. Agric. 21, 411-420.

Received: **29.05.2017**
Accepted: **30.04.2018**

CORRESPONDING AUTHOR

Ebrahim Pazira
Department of Soil Science,
Science and Research Branch,
Islamic Azad University,
Tehran – Iran

e-mail: ebrahimpazira@gmail.com

© by PSP Volume 27 – No. 7/2018 pages 4631-4636 Fresenius Environmental Bulletin

THE STUDY OF SMART GROWTH OF SALT LAKE CITY AND NOTTINGHAM CITY USING THE ENTROPY METHOD TO EXPLORE THE SOCIAL, ENVIRONMENT AND ECONOMIC CHANGES

Mei Liu, Shengshu Yang, Kexin Zhang, Jingjing Li, Heying Liu, Yingjie Dai*

Northeast Agricultural University, School of Resources Environment, 59 Mucai Str., Xiangfang District, 150030 Harbin, China

ABSTRACT

In order to slow down the rapid rate of the world urbanization, America is the first proposed the "smart growth" strategy as well as the ten smart growth principles. In order to curb the spread of the city, and establish a sustainable city which is economically prosperous, socially equitable, and environmentally sustainable. This article combines the ten principles with the 3E index into consideration, adopting the three most important indicators-environmental, social, and economic indicators to establish the index system for evaluating the sustainability of the city.

In this article we choose two middle-sized cities from two different continents, the Salt Lake City in the United States and the Nottingham in the UK. According to the index system model, we evaluate the current growth plan. We use the entropy evaluation method to calculate the weight of each indicator. The factors weight of Salt Lake City is 0.508; 0.351; 0.141 in society, environment and economy respectively. The factors weight of Nottingham, England is 0.486; 0.337; 0.177 in society, environment and economy respectively. And the introduction of sustainable coefficients and coordination coefficients is to assess whether the city is smart growth. It turns out that, after 2013, the coordination coefficient of the two cities are gradually reduced, going to the unsustainable development. Based on the intelligent growth evaluation index system, and using the improved urban plan. The unary linear regression is used to predict the data from 2046 to 2050, while the entropy method is used to evaluate the future development of the two cities. The result shows that the two cities are sustainable cities which conform to the principles of the smart growth.

KEYWORDS:
Smart growth, Entropy method, Sustainable Development

INTRODUCTION

With the development of economy, the world is rapidly moving towards urbanization. It is projected that by 2050, 66 percent of the world's population will be urban [1]. As the urban land is constantly expanding, unrestricted and low density growth mode of urban areas has brought a series of problems, such as long-term consumption of land, the increase of municipal infrastructure investment, the increase of the traffic pressure, inferior planning of utilization of land and the mismatching of the population spatial distribution and jobs, also with some social problems [2]. This phenomenon of urbanization is known as "City Spreading". The phenomenon causes the urban environment rapidly worsened and urban green space reduced, leading to the decrease of the quality of living environment directly. Secondly, there are Isolation and diversity of live in various urban communities, which contributes to the social class differentiation and it is not conducive to social stability. In addition, the city financial shortage leads to the main investment reduced and it is not conducive to the construction of high-tech zone.

For this problem, the American planning association put forward ten principles of smart growth [3], respectively, from the land use, community construction, environmental planning and other aspects of urban development requirements. The goal of "Smart growth" is to plan a compact community through considering transportation and land use, giving fully play to the effectiveness of the existing infrastructure and providing a variety of traffic and housing choices in an effort to control the spread of the city, at the same time , the city development will be integrated into the overall regional ecological system and the coordinated development of man and society, creating a sustainable city which is economically prosperous, socially equitable, and environmentally sustainable [4].

If we could combine the ten principles of smart growth to define an index system for measuring urban smart growth rate, we can analyze whether the current growth plan is in line with the city smart growth. If not, we can formulate an urban

smart growth planning of the city through the index evaluation system in order to realize the sustainable development, which has important significance to achieve the rational development of the cities of the 21st century world.

In order to define a rational evaluation index system of smart growth success rate, first of all, combined with the above principles and objectives to select the evaluation index. The ultimate success of smart growth is urban sustainable development. Based on the principles of scientific, feasibility, hierarchy, dynamism, and typicality of the index system, we set smart growth success rate evaluation index system from the urban space expansion related factors and the ten principles of smart growth, to evaluate the relevant cities' smart growth is good or bad from environment, society and economy [5].

MATERIALS AND METHODS

Index selection and interpretation. When we establish the index system, we first determine the target layer which is used to evaluate the success rate of the urban smart growth. Then we determine the domain layer which reflects the sustainability of urban development from environment, social and economy. The index layer is based on the domain layer to select some more specific indicators to reflect the sustainability of their own domain layer. Finally, we combine with the principle of smart growth to determine the variable layer with 23 indicators. According to the indexes we choose, we establish the evaluation index system of urban intelligent growth success rate, which is the evaluation index system of urban sustainable development index system (see Table 1).

The construction of the model. To ensure the integrity of the research problem, we select two mid-sized cities with a population of about 100,000 to 500,000 in two different continents. Considering a number of factors, we chose Salt Lake City in the United States and Nottingham, England in UK as our study areas. With the economic and social development, urbanization accelerated, Salt Lake City is facing air pollution and many other issues, the city's smart growth is particularly necessary. With the rapid economic, social development and the acceleration of urbanization in Nottingham, England, the problem of many people and less land are troubling the government of Nottingham, England. Therefore, it is reasonable to choose these two cities for research.

The data used in this paper include the population, personal income and land area of the two cities from 2010 to 2014. When it is designed, the data availability and simplification are considered, most of the indicator data can be found from the statistical department. In the case of a missing indicator, it is replaced by an average of two years.

TABLE 1
Evaluation index system of urban smart growth

Target layer	Domain layer	Index layer	Variable layer
The degree of smart growth	Resources and environment	Land resources	The cultivated land resource at the end of year (thousands of hectares)
			The green coverage rate of the built up area (%)
			The residential area (square meters)
		Environmental pollution control	The hazard-free treatment rate of domestic garbage (%)
			The domestic sewage treatment rate (%)
			The standard rate of the industrial sewage discharged (%)
			The SO_2 emissions of every ten thousand dollars of industrial output value (kilogram/ten thousand dollars)[a]
			The area with the standard noise exposure (square kilometers)
	Society	Population index	The proportion of non-agricultural population (%)
			The natural population growth rate (%)
			The population density (people /square kilometer)
			The net migration rate (%)
		Urban traffic	The number of car owned by per ten thousand people (cars/ten thousand people)
			The number of non-operational car (thousands of cars)
			The length of the road (kilometer)
			The per capita road area (square meters)
			The built up area (square kilometers)[b]
		Construction land	The proportion of construction land of the total area of the city (%)
			The completed real estate development area (million square meters)
	Economy	Economic aggregate	The per capita GDP (dollars per person)
			The GDP growth rate (%)
		Economic development	The proportion of tertiary industry output value in the GDP (%)
			The investment in cities and towns (hundred million dollars)

Note: **a**. The SO_2 emissions of every ten thousand dollars of industrial output value: This index is used to describe the emissions of the industrial waste water within the city, the general use of industrial emissions of sulfur dioxide emissions and the ratio of industrial output value to that. The index value is higher, the environmental pollution is more serious.
b. The built up area: It refers to the various types of land requisitioned in the urban administrative area and the non-agricultural production and construction land actually constructed. It is used to reflect the actual extent of urban space development generally.

After finishing the data collecting, all the data need standardized treatment. Because each group of data units and indicators of positive and negative orientation are different, if untreated, we cannot make reasonable comparison and analysis between the data. The larger the index is, the more beneficial to the development of the system. On the contrary, we use negative indicators method for data processing. The computation formulas (1) and (2) are as follows:

Positive indicator:

$$Z_{ij} = \frac{x_{ij} - \min\left(x_j\right)}{\max\left(x_j\right) - \min\left(x_j\right)} \quad (1)$$

Negative indicator:

$$Z_{ij} = \frac{\max\left(x_j\right) - x_{ij}}{\max\left(x_j\right) - \min\left(x_j\right)} \quad (2)$$

Max (x_j), $\min(x_j)$ are the maximum and minimum values of the j evaluation index of the i sample, respectively, and x_{ij} is the value of the j-th evaluation index of the i-th sample.

There are many ways to calculate Weight Value which generally were divided into two types: subjective weighting method, such as analytic hierarchy process, Delphi method; objective weighting method, such as the entropy method. Because a lot of quantitative data are used in this paper, the entropy method to calculate weight is more objective and reliable. Based on the principle of establishing index system, the environmental, social and economic indicators are decomposed and summarized: from land resources and environmental pollution control to reflect the change of urban land use patterns and the quality of environmental protection; the population index, transportation, construction land are used to describe the city's construction and development; the total economic volume, the level of economic development are used to measure the level of national economic development. In this study, a total of 7 categories of 23 variable layer indicators were selected, and the weights were calculated by entropy method after normalizing the data. Formula (3) to (5) shows below:

Information entropy:

$$e_j = -1/\ln n \cdot \sum_{i=1}^{m} Z_{ij} \cdot \ln Z_{ij} \quad (3)$$

Information utility value:

$$d_j = 1 - e_j \quad (4)$$

Index Weight:

$$W_j = d_j / \sum_{j=1}^{n} d_j \quad (5)$$

e_j is the entropy of indicators, n is the number of indicators, m is the number of years evaluated, Z_{ij} is the index value after standardization, d_j is the information utility value and W_j is the weight of the i-th index.

$e_j - 1$ is considered as information utility value, therefore, the greater the information entropy is, the smaller the utility value of the index information and the index weight are and vice versa.

The evaluation method we use is mainly to analyze the sustainability of urban space to evaluate whether the current urban planning is in line with the principle of smart growth. If sustainability is stronger, the closer the current plan is to smart growth, the more successful the plan is and vice versa.

Each subsystem index. According to the index system of three subsystems (environment, society and economy), the sustainability of urban space is divided into three aspects to evaluate.

The formula (6) used to calculate the evaluation values of the three indices of environment, society and economy is:

$$F_{ki} = \sum_{j=1}^{p} W_j \cdot Z_{ij} \quad (6)$$

F_{ki} is the corresponding index of the i-th sample. The domain of this study includes three aspects, so it is equal to 1, 2, 3. It represents the environmental, social and economic development respectively. p is the number of indicators included in each index.

The sustainability coefficient of urban space. The index weight determined by the entropy method indicates the relative change rate of the index in the index system [7], while the relative levels of the indicators are shown by the sample standardized matrix, the cumulative result of the two together to get the final evaluation value [8], then reflect indicator development level and the relative speed of the combination, which called sustainable coefficient. The evaluation system has the hierarchical structure characteristic, the sustainable coefficient of the urban space can be calculated by the comprehensive weighting method.

The formula (7) is:

$$S_i = \sum_{k=1}^{3} W_k \cdot F_{ki} \quad (7)$$

S is the comprehensive evaluation value of the i-th sample.

The coordination coefficient of urban space. Urban sustainable development mainly refers to the coordinated development of environment, society and economy [9]. We evaluates urban sustainable development mainly from the coordination coefficient of environmental, social and economic indicators. The formula (8) is:

$$C_i = 1 - D_i / \overline{F_i} \quad (8)$$

C_i is the cooperation index, D_i is the standard deviation of the environmental, social and economic indices of sample i and $\overline{F_i}$ is the average of the environmental, social and economic indices of sample i.

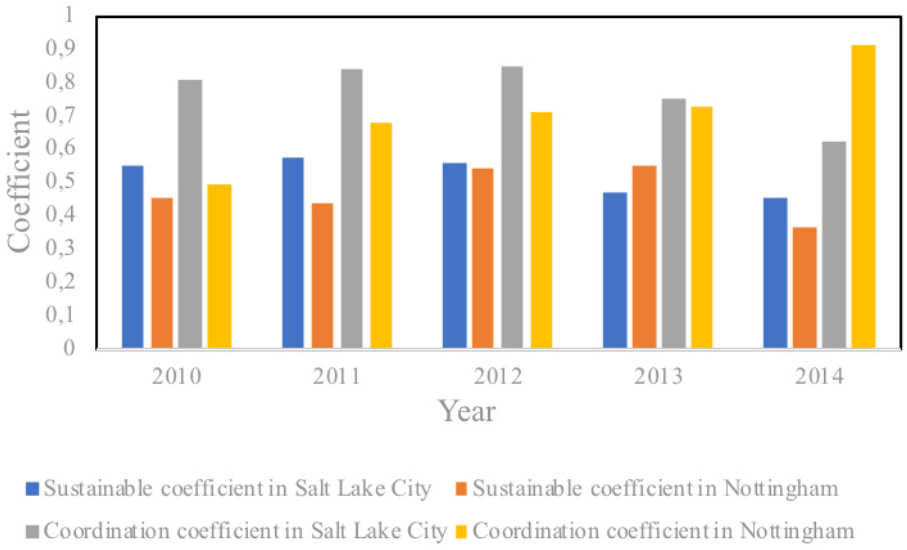

FIGURE 1
Sustainable and coordination coefficient statistical figure from 2010 to 2014

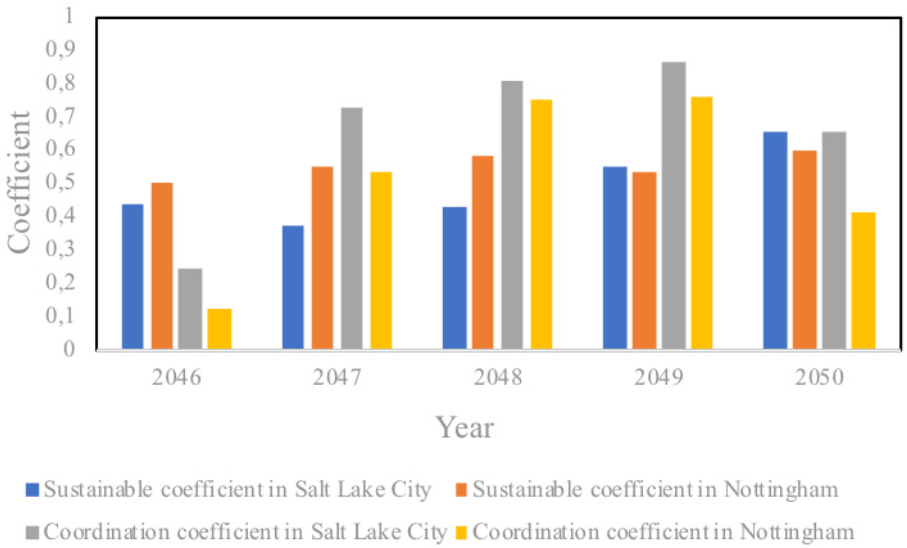

FIGURE 2
Sustainable and coordination coefficient statistical figure from 2046 to 2050

RESULTS AND DISCUSSION

We can see that the weights of environment, society and economy respectively are 0.351, 0.508, 0.141; 0.337, 0.486, 0.177 in Salt Lake City and Nottingham, England in the intelligent growth evaluation index system. Thus, the environmental and social impact on the effect of intelligent growth accounted for a large proportion [10]. Economic impact is less. Then the sustainability coefficient and the coordination coefficient were calculated from 2010 to 2014. At last, we get the evaluation results. The corresponding trend is shown in Fig 1.

The results show that the two cities are gradually moving towards unsustainable development after 2013. Both urban co-ordination coefficients are declining rapidly. The weight of the cultivated land resource at the end of years the largest, which indicates that the environmental impact caused by population growth is much larger than the carrying capacity of land. It indicates that the efficiency of the land use pattern of the two cities is not high.

It is the necessary way for the sustainable development of Salt Lake City and Nottingham, England to be adopted to optimize the method and formulate the optimization plan of urban smart growth. For the Salt Lake City, we must first enhance the main city function, the main city of the old city as the focus of the transformation, and adjusting the land function, as the future development of high-end service industry in the Salt Lake City. To solve this problem, we propose to improve

the land use efficiency by strengthening the vertical composite utilization of urban land, and give the land use zoning map of Nottingham, England City space. Second, the reuse and re-development of inefficient industrial land.

Through the optimized urban planning based on the principle of intelligent growth, the forecast values of 2046 -2050 are obtained.

The results show that the use of intelligent growth evaluation system after the optimization of urban planning, the Salt Lake City and Nottingham, England Sustainability Index continues to rise by 2049 and the index of coordination increases year after year after using the optimized urban planning coupled with a smart growth assessment system, demonstrating that the two cities are in the smart Growth and achieve Economically Prosperous, Socially Equitable, and Environmentally Sustainable. At the same time, we also find that both the urban sustainability index and the coordination index decline in 2050. Although the two cities sustainable development index and coordination index has declined, but also maintained at a high level, we think the rapid population growth has a great impact on smart Growth, which is not conducive to sustainable development.

CONCLUSIONS AND PROSPECTS

It can be seen from the weighting results of this work, whether it is Nottingham, England or Salt Lake City, the social factors have the greatest impact on the evaluation index system of smart growth effect. Therefore, in the future urban planning and development, should be from the population, transportation and land planning point of view, select the optimal program to reduce the phenomenon of urban sprawl. "Smart growth" can provide a new interpretation perspective for "sustainable development". The idea of "smart growth" was put forward after the concept of sustainable development. Therefore, the vast majority of "smart growth" principles are in line with the principles of sustainable development, and "smart growth" is the inevitable stage of sustainable development, sustainable development is its ultimate goal.

We get the weight of each index by calculating the dates and then calculate the total weight of the three subsystems (environment, society and economy) in the index system to assess the sustainability of urban space. This model's adaptability is strong and it can be applied to evaluate various types of city to judge whether the tested city is in line with the smart growth. But the indicators of index system are selected according to the feasibility principle and data are from statistical year book. Although the data obtained from these resources are relatively accurate, there are still some indicators which can better reflect the sustainability of urban space are not being selected because of the difficulty of obtaining them, so the index system is one-sided. In order to make index system more suitable for evaluating the sustainability of urban space, we should collect and combine some suggestions from experts when establishing our system. So we should combine with some experts' suggestions to make the establishment of the index system better service for evaluating the sustainability of urban space.

ACKNOWLEDGEMENTS

This work was supported by Program of Student Innovation Practice Training (SIPT) of Northeast Agricultural University in 2018.

REFERENCES

[1] United Nations, (2014) World Urbanization Prospects. https://esa.un.org/unpd/wup/.
[2] Ma, Q., Xu, X.C. (2004) Strategy of "smart growth" and urban spatial expansion in China. City Planning Review. 151, 16-22
[3] EPA (2011) Smart Growth: A guide to developing and implementing greenhouse gas reductions programs. http://www.sustainablecitiesinstitute.org/Documents/SCI/Report_Guide/Guide_EPA_SmartGrowthGHGReduction_2011.pdf.
[4] EPA (2016) This is Smart Growth. https://www.epa.gov/smartgrowth/smart-growth-publication.
[5] Wang Y.M. (2008) Evaluation of Sustainable Development. Beijing. China Standard Press.
[6] Zhang, W.M. (2004) Evaluation model of urban sustainable development based on entropy method. Journal of Xiamen University. 162, 109-115
[7] Tang X.L. (2009) "Smart growth" research summary. Urban Problems. 169, 98-102
[8] Zhu L. (2008) Evolutional analysis of social, environmental and economic development of Guangzhou (1978—2003) by using entropy theory. Ecology and Environment. 17, 411-415
[9] Sun, C.J. (2006) Qingdao city sustainable development evaluation index system design and application. Master' dissertation. Qingdao University.
[10] Wang Z.H. (2000) "Smart and progressive" concept and its discussion. Planning Research. 3, 33-35

Received: **05.07.2017**
Accepted: **09.04.2018**

CORRESPONDING AUTHOR

Yingjie Dai
Northeast Agricultural University,
School of Resources Environment,
No. 600 Changjiang Road,
Xiangfang District,
150030 Harbin – China

e-mail: dai5188@hotmail.com

© by PSP Volume 27 – No. 7/2018 pages 4637-4647 Fresenius Environmental Bulletin

INTEGRATED HYDROLOGIC AND QUALITY MODEL FOR ZARQA RIVER BASIN IN JORDAN

Abbas Al-Omari[1,*], Jawad Al-Bakri[2], Muna Hindiyeh[3], Zain Al-Houri[4], Ibrahim Farhan[5], Fida' Jibril[6]

[1]Water, Energy and Environment Center, The University of Jordan, Amman, Jordan
[2]College of Agriculture, the University of Jordan, Amman, Jordan
[3]School of Natural Resources Engineering and Management, German Jordanian University, Madaba, Jordan
[4]Texas A&M University, College Station, TX, USA
[5]Department of Geography, the University of Jordan, Amman, Jordan
[6] Royal Scientific Society, Amman, Jordan

ABSTRACT

An integrated hydrologic and quality model for Zarqa River basin has been developed based on the Water Evaluation and Planning system. For hydrological modeling, the Soil Conservation Service Curve Number method was integrated into the Water Evaluation And Planning system using its expression builder. Climatological, hydrologic, stream flow, water quality data, and soil maps were collected. Land use maps were generated in GIS format for the basin. The results of the hydrologic model showed good agreement between measured and modeled Zarqa River flow after calibration. However, during peak flood significant differences between measured and simulated flows were observed which is attributed to several reason such as inaccuracies in measurements during peak flow and inaccuracies in the estimated curve number. The results also showed good agreement between measured and simulated river quality parameters, namely: temperature and COD. However, discrepancies were also observed at peak flows.

KEYWORDS:
Hydrologic modeling, integrated modeling, Water Evaluation and Planning (WEAP) system, water quality modeling, Zarqa River basin.

INTRODUCTION

Zarqa River basin (ZRB) is the most heavily populated and industrialized basin in Jordan. It hosts about 60% of Jordan's population and includes the two largest cities in Jordan namely; Amman and Zarqa [1]. In addition, about 85 % of the industries in Jordan are located in ZRB [2]. Zarqa River is used for restricted irrigation upstream of King Talal Dam (KTD) and for unrestricted irrigation in the Jordan Valley after mixing with fresh water from King Abdulla Canal (KAC). Zarqa River used to be Perennial River. However, due to the heavy over abstraction of the ground water to satisfy the increasing domestic demand in the basin as a result of the high population growth [3], the springs that used to feed the river stopped flowing which caused the river to flow during winter storms only.

Besides the diminishing river flow, the river water quality has deteriorated tragically over the past three decades due to the following reasons: the disposal of inefficiently treated wastewater from As Samra Wastewater Treatment Plant (WWTP) to the river, the disposal of untreated industrial wastewater by many industries that exist along the river, overflow of Ein Ghazal and west Zarqa wastewater pumping stations which are adjacent to the river, leaks from sewer lines that pass through the river course, seepage from septic tanks as well as from the leachate of Al Russiefa solid waste disposal site and agricultural runoff, and return flow from farms at the river banks [4, 5]. In a complicated environment of diminishing river flow in addition to the different sources of pollution, point and non-point that dynamically vary over time and space, the development of an integrated tool that can help understand the interaction between the basin hydrology and the river water quality to support the current management practices and rehabilitation efforts of the river is a necessity. This research is a first step in this direction.

Worldwide models have been developed and implemented to predict the behavior and response of river basins to certain hydrologic changes and pollution events, examples are [6-17].

Due to the importance of Zarqa River as a primary irrigation water resource in the basin and in the Jordan Valley downstream, in addition to its environmental value, many attempts were made to study the river basin from different perspectives: rainfall runoff modeling, water resources management, identification of pollution sources to the river, impact of the river water quality on the soil, and climate change impact on the river flow [18-26].

Rahbeh [18] modeled rainfall runoff relationship of the ZRB to determine management options of KTD by applying the Linear Decision Rule (LDR). Al Abed et al. [19] modeled river flow by implementing the Spatial Water Budget Model

(SWBM) and the HEC-HMS/HEC-Geo HMS. Al Abed and Al Sharif [25] developed a Hydrologic model for Zarqa River using the Hydrologic Simulation Program-Fortran (HSPF). Al-Afayfeh et al. [21] developed a water resources management system for ZRB. Demand and supply balance model was implemented for this purpose. However, water quality of the river was not modeled. Grabow et al. [22] performed a planning activity at the Jordan Ministry of Water and Irrigation which took into consideration sources and demands in the basin. Water quality and other non-conventional water resources were considered. However, this planning activity did not result in a calibrated and verified model that can be used for water resources management at the basin level from an integrated perspective. Al-Omari et al. [1] developed a Water Management Support System (WMSS) for ZRB basin based on the Water Evaluation and Planning (WEAP) system. The developed WMSS considered all sources and demands as well as the socioeconomic status of the basin. However, Zarqa River flow and groundwater modeling were not integrated into the developed WMSS. Rather, they were modeled separately using Watershed Management System (WMS) and ModFlow. The developed WMSS became the basis for an integrated model that integrates surface and groundwater modeling in addition to water allocation in one tool based on WEAP which was customized to meet the needs of the Jordan Ministry of Water and Irrigation Al-Omari and Huber [27]. However the hydrologic modeling in WEAP was simple, in addition, water quality of Zarqa River was not modeled.

Abderahman and Abu Rukah [20] investigated heavy metals distribution within the soil in the upper course of ZRB. It was found that the soils contained different concentrations of Pb, Ni, Cu, Cr, and Zn that changes with the distance from the WWTP as well as with the depth. Additional efforts by different researchers and consulting firms have been made to identify sources of pollution to the River. B & E Engineers in association with the Arabic International Center for Environmental Health (AICEH) [2] studied sources of pollution to Zarqa River along its path from Wadi Abdoun to the Jordan valley in the context of the ZRB wastewater and solid waste treatment project. Al Wer [4] analyzed and evaluated the current environmental status of the river by identifying point and non-point sources of pollution to the river. In addition, mitigation measures to improve the river water quality were proposed. The International Union for the Conservation of Nature (IUCN) in the context of the capacity building for the rehabilitation of Zarqa River project [5] identified sources of pollution to Zarqa River along its path as well. It can be concluded that, despite the extensive efforts made to date to identify sources of pollution to the river, no effort has been made to quantify nor to model them. In addition, no attempt to date has been made to integrate both hydrologic and quality modeling in one tool. The ultimate objective of this paper is the development of an integrated model that combines hydrologic and water quality simulations into one tool for ZRB. Rainfall runoff and two quality parameters, namely: Chemical Oxygen Demand (COD) and temperature are modeled.

METHODOLOGY

The study area. ZRB lies in the northern part of Jordan with a total area of 4,586 km^2. About 4,074 km^2 of which is in Jordan and 512 km^2 is in Syria [28]. The basin extends from the Syrian city of Salkhad in Jebal al-Arab at an elevation of 1460 m to south of Amman and then westward to the Jordan Valley at an elevation of about -350 m. Zarqa River starts at Wadi Abdoun area in Amman where the main feeder to the river, Ras El Ein spring, is located. It then passes through Russeifa and Zarqa where it joins Wadi Dhulail a short distance after Sukhna village and then continues to KTD upstream of the Jordan Valley. The average annual rainfall in the western part of the basin is about 400 mm while it rarely exceeds 150 mm in the eastern part [23]. The main cities located within the basin are the capital Amman, Zarqa, Jarash, part of Mafraq and part of Balqa. The basin is shown in Figure 1.

The WEAP model. The WEAP model developed by the Stockholm Environmental Institute [29] is an integrated water resources management tool that integrates biophysical, socioeconomic and policy variables in addressing water resources management at the basin level. The hydrologic modeling tool in WEAP employs water balance at the basin level by considering all the elements of the hydrologic cycle, i.e. precipitation, interception, evapotranspiration, and infiltration to estimate runoff. Inflows to and outflows from a water course are also considered. Excess rainfall is divided between infiltration and runoff based on user input fractions. The quality part of the model considers pollution generation form point and nonpoint sources as well as pollution generation from demand sites. The fate of pollutant in a water course is determined by user defined processes such as mixing and decay. Temperature is modeled in WEAP based on a built in model that considers mixing of different streams of different temperatures, heat gain from net solar short-wave radiation and atmospheric long wave radiation in addition to heat losses due to conduction, convection and evaporation. Furthermore, the expression builder tool in WEAP enables the user to model processes that are not built in it which makes it a powerful modeling tool.

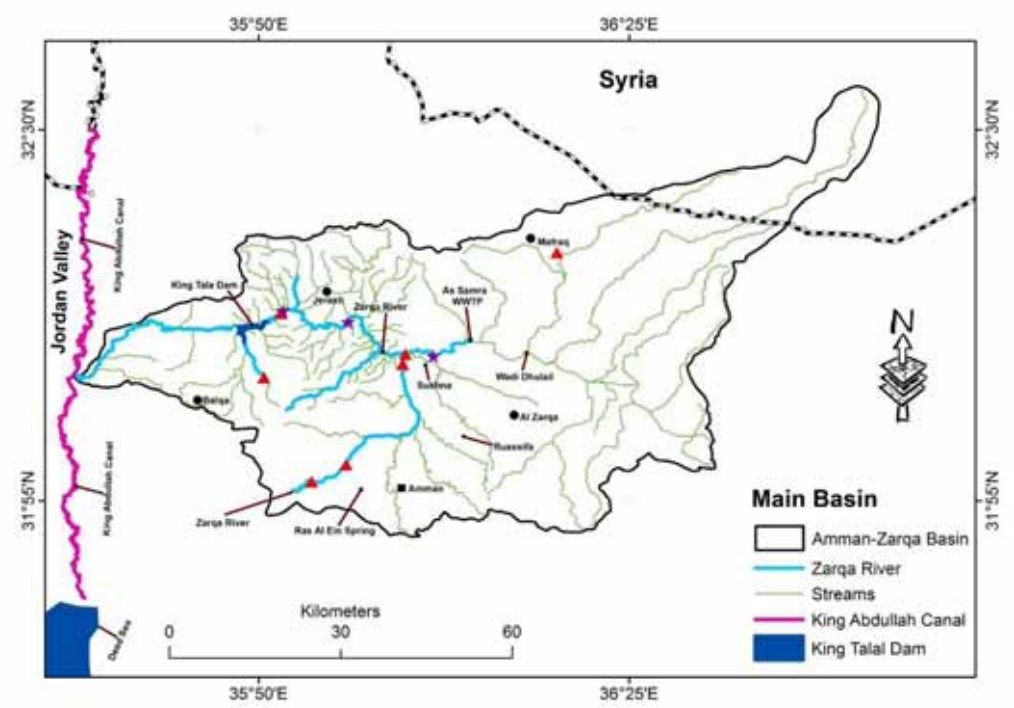

FIGURE 1
Study area

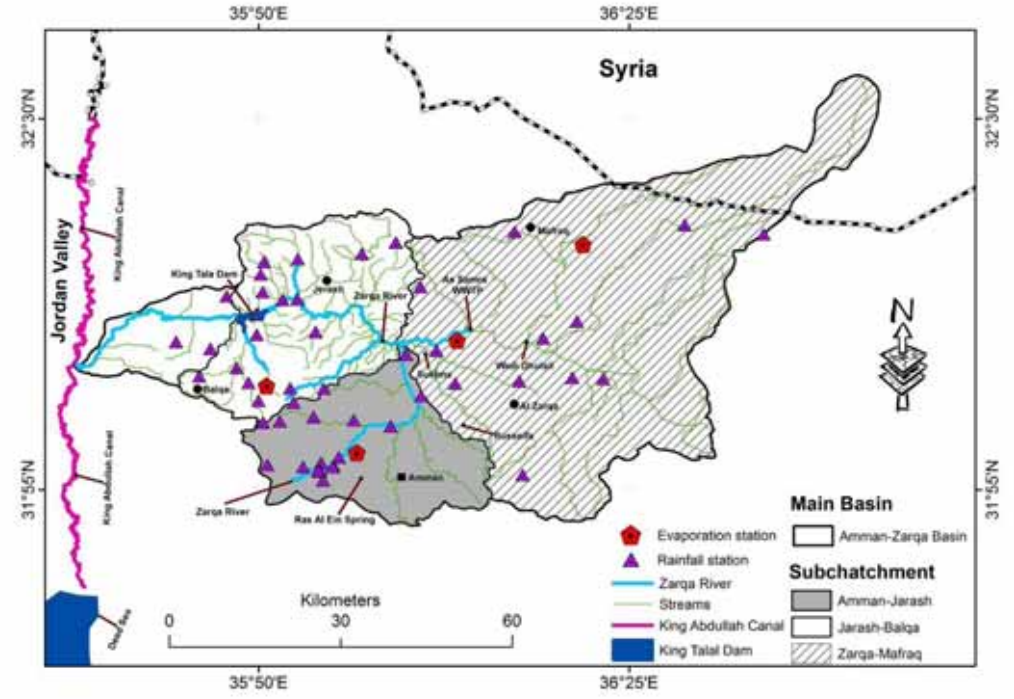

FIGURE 2
Hydrologic features of ZRB

Delineation of the sub-catchments in the basin. Delineation of the hydrologic features of the ZRB was carried out using remote sensing data and GIS tools. A Digital Elevation Model (DEM) with 30 m resolution was used for delineating the stream network and the main subcatchments of ZRB. The DEM, originally derived from the data of Advanced Space borne Thermal Emission and Reflection Radiometer (ASTER) [30], was processed in GIS to fill sinks and to derive layers of flow directions and accumulation. The stream network (Figure 1) was derived from the flow accumulation layer and was then modified using topographic maps with scales of 1:50000. The maps were also used to correct positional shifts of stream and subcatchments.

Data Collection and Processing. Rainfall data. ZRB includes fifty nine rainfall gauging stations distributed over the basin. It was found that twenty nine of these gauging stations contain almost continuous rainfall record from 1980 until 2010 (Figure 2).

Average monthly rainfall for each sub-catchment for the period between 1980 and 2010 was determined by the Thiessen Polygon which was prepared by GIS.

Evaporation. ZRB contains six evaporation stations (Figure 2). Data from four of these evaporation stations were used in the developed model. One station in Amman subcatchment, one station in Jarsh_Balqa subcatchment and two stations in Zarqa_Mafraq subcatchment. Missing data were estimated by statistical correlation between the stations. Pan A coefficient was estimated according to the FAO Irrigation and Drainage paper no. 56 [31].

Stream flow data. ZRB contains six stream flow gauging stations (Figure 3). The gauging station located near Jarash Bridge, which is the farthest downstream, was used for hydrologic model calibration as it includes good record from Jan. 1980 till Sep. 2010.

Water quality data. Data needed for river water quality modeling includes length of each river reach, flow stage, width, and velocity relationship, weather data i.e. air temperature, humidity, wind speed, cloudiness fraction and upstream water temperature and latitude. Reach lengths were obtained from the shape files. Flow stage, width and velocity were measured at four sections along the river between July 2012 and January 2014. Weather data were obtained from the Department of Meteorology for the period between 2000 and 2013.

The most comprehensive real time water quality monitoring system for Zarqa River is that operated by the Environment Monitoring And Research Central Unit (EMARCU) of the Royal Scientific Society. The system consists of thirteen fully automated telemetry monitoring stations distributed along Zarqa River, KAC, Yarmouk River and Jordan River. The parameters monitored are COD, temperature, turbidity, Total Nitrogen (TN), Total Phosphorus (TP), Electrical Conductivity (EC) and pH. Real time water quality data at monitoring stations 9 and 10 between January 2005 and Sep. 2010 were used for calibrating and verifying the results of the water quality model. The locations of these monitoring stations are shown in Figure 3.

Estimation of the hydrologic parameters. Runoff and infiltration fractions. Hydrologic modeling in WEAP is based on the hydrologic cycle. Runoff and infiltration are calculated based on user input fractions. Runoff and infiltration user input fractions were calculated based on the Soil Conservation Service Curve Number (SCS-CN) method as follows:

$$S = \frac{1000 - 10\,CN}{CN} \tag{1}$$

Where S is potential maximum retention or infiltration and CN is curve number [32],

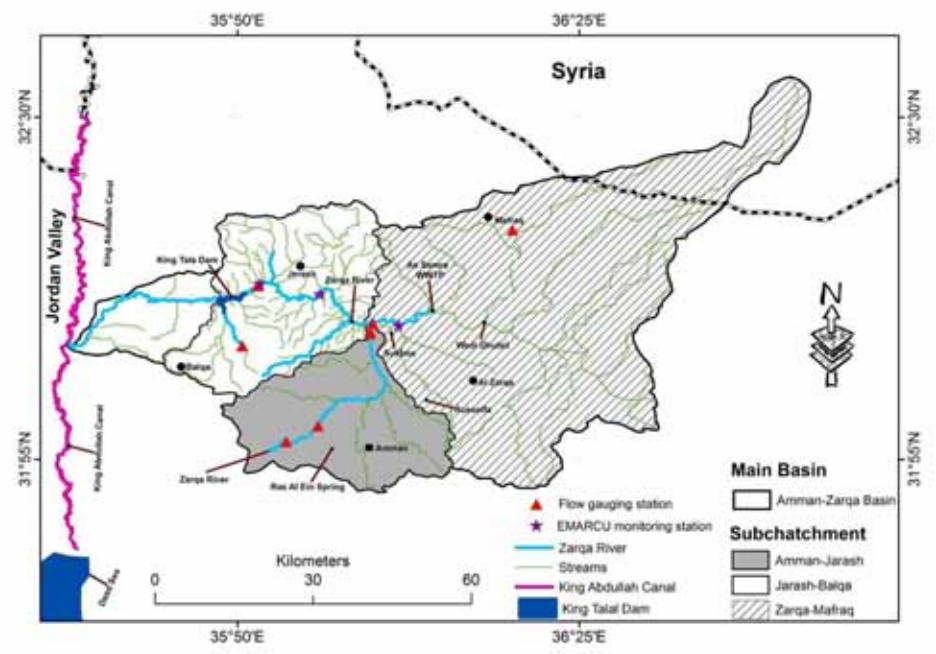

FIGURE 3
Stream flow gauging stations and EMARCU monitoring stations

$$Q = \frac{(P - I_a)^2}{P + S - I_a} \quad (2)$$

Where Q is direct runoff in inches and P is precipitation in inches [32], and I_a is initial abstraction which is assumed equal to 0.20 S.

S is calculated by equation 1 based on the curve number and then runoff is calculated by equation 2. Runoff fraction is then calculated by equation 3.

$$Runoff\ fraction = (\frac{Q}{P}) \times 100 \quad (3)$$

$$Infilt.\ fraction = 100 - runoff\ fraction \quad (4)$$

Runoff and infiltration are then calculated by WEAP based on these fractions and the hydrologic balance for the basin. Equations 1 to 4 are incorporated into WEAP by the use of the WEAP expression builder.

Estimation of the curve number. Land use mapping. The soil map shown in Figure 4 which was produced by the Ministry of Agriculture [33] according to the USDA classification system [34] was used for estimating the CN for the three subcatchments in the basin. The map includes 30 soil units, each composed of an association of different soils, known as great groups. The scale of the soil map is 1:250,000. The characteristics of each soil unit were obtained from the USDA-SSS monograph and the hardcopy atlas of the soil map. An attribute of soil texture was appended to the map so that hydrologic soil groups can be identified based on soil physical properties that correspond to different infiltration rates [35]. Slight modifications were made to the soil units in the eastern part of the study area where soil crusting can reduce infiltration rate and subsequently increase runoff. The modifications were based on field observations while preparing the soil map [33]. The Hydrologic Soil Groups (HSG) for the three subcatchment are shown in Figure 5.

The land use/cover (LUC) map, on the other hand, was prepared by digital classification of medium resolution images of Landsat ETM+ [36]. The class of urban areas was modified and updated using visual interpretation of Google Earth images. Land use/cover of the Syrian part of ZRB was obtained from a previous work that used supervised classification of Landsat ETM+ to obtain the different categories of land use/cover. In order to assign the CNs for the different polygons (parcels) of land use/cover (Figure 6), it was necessary to decode the land use/cover map into the SCS codes and according to the hydrological soil group [35].

Soil and land use/cover maps were intersected. The output from this intersection was a map of land use/cover polygons with codes of hydrologic soil group (Figure 6). Following this step, the CNs were joined to the attribute table of the map (land use/cover-hydrologic soil group, LUC-HSG) resulted from the intersection. The sub-catchments map was then used to clip the LUC-HSG map for each of the three subcatchments. The attribute table of each map was exported in dbf format and was then opened in Excel spreadsheets. The weighted average CN for each subcatchment was calculated based on the area which are 78, 86 and 84 for Jarash-Balqa, Zarqa-Mafraq and Amman sub-catchments, respectively.

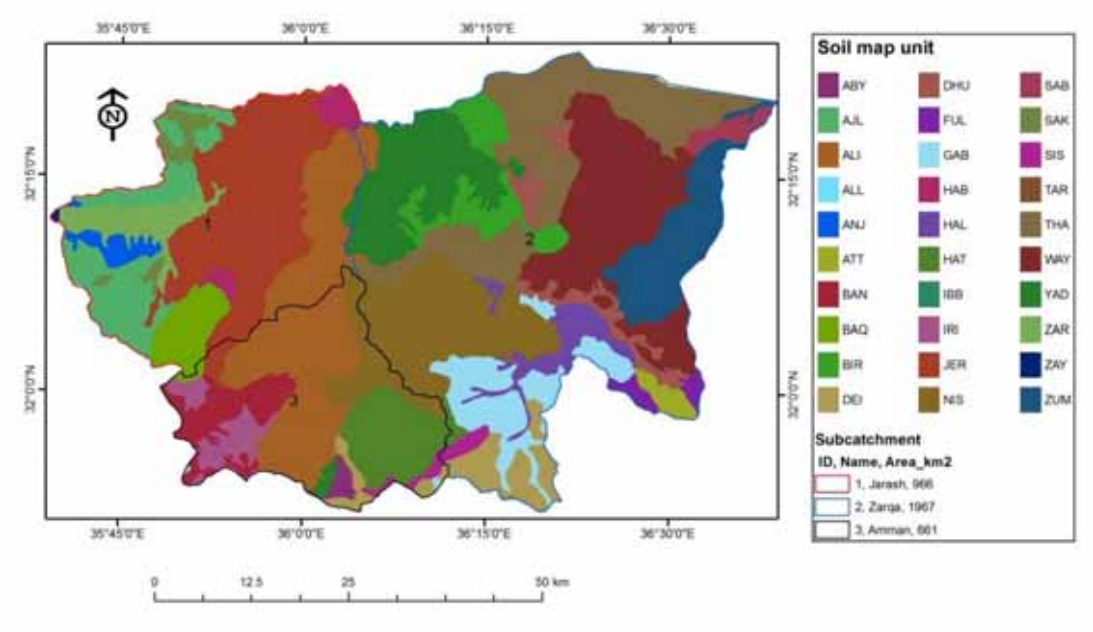

FIGURE 4
Zarqa River watershed soil map (MoA 1993) [33]

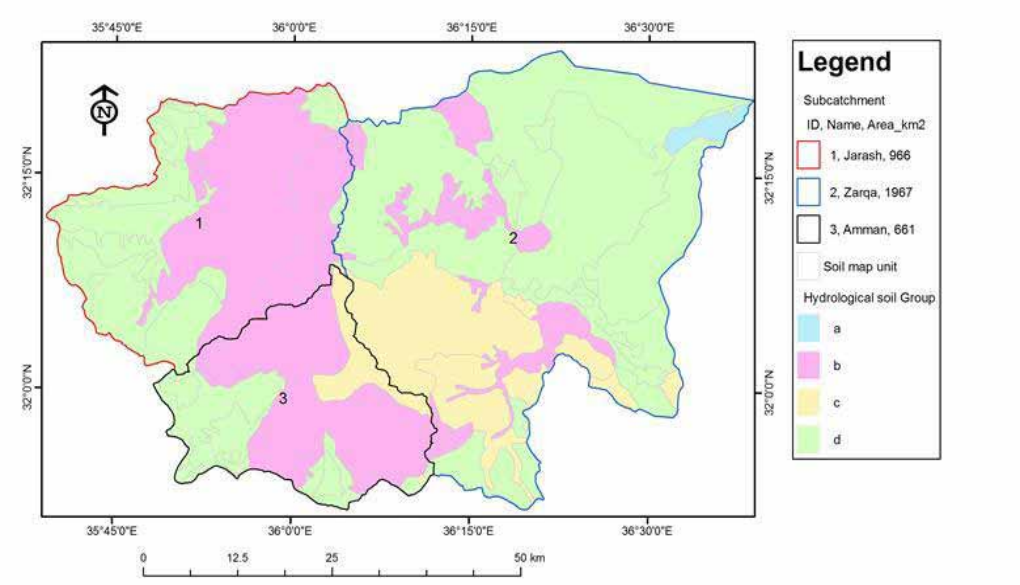

FIGURE 5
Map of the Hydrologic soil group of the main sub-catchments of the basin

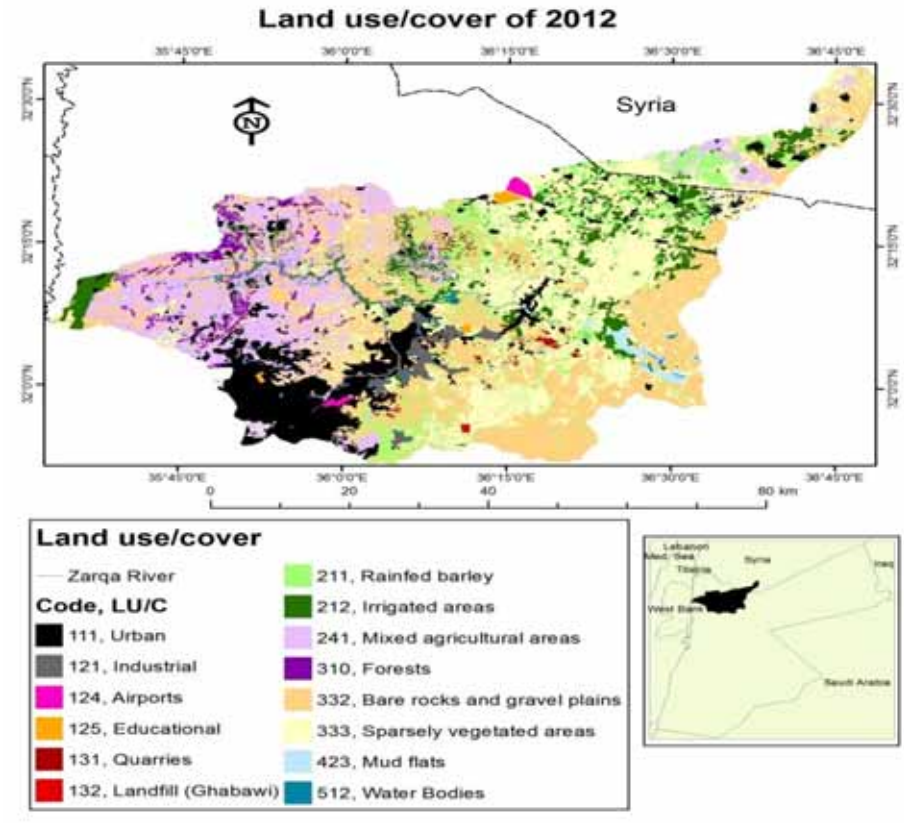

FIGURE 6
Land use/cover map of the ZRB

Water quality modeling. Chemical Oxygen Demand was modeled by assuming first order decay and complete mixing of the different tributaries to the river [29]. The upstream COD concentration was input for Zarqa River as well as for all tributaries to the river. The COD first decay coefficient was also input for all Zarqa River reaches and all tributaries to the river.

Zarqa River temperature was modeled by a built in model in WEAP which considers mixing of inflows from all tributaries to the river, and gains of heat from net solar short-wave radiation and atmospheric long-wave radiation, and losses of heat due to conduction, convection and evaporation. The upstream temperature was input for Zarqa River as well as for all the tributaries to the river [29].

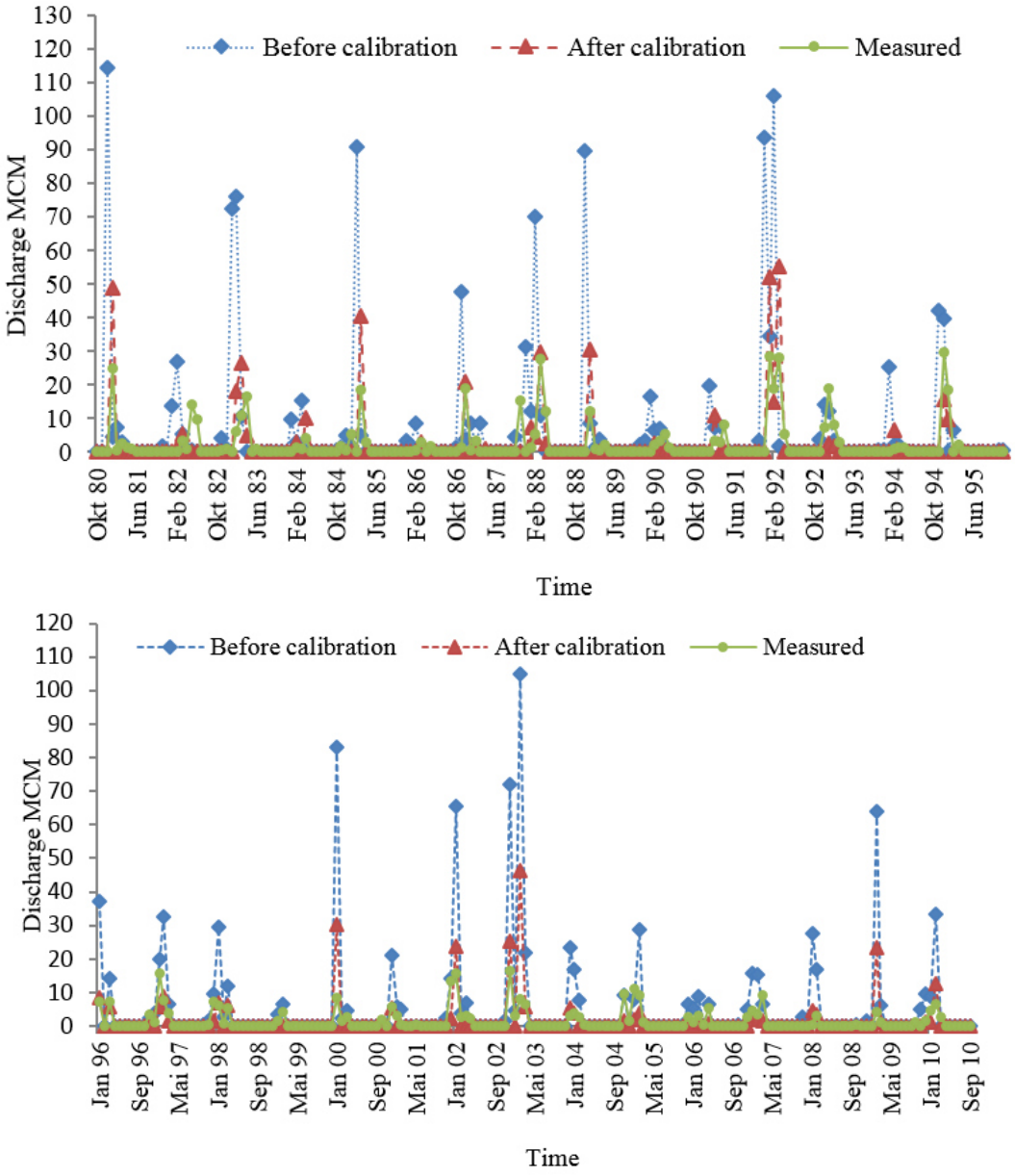

FIGURE 7
WEAP modeled versus measured Zarqa River flow at Jarash Bridge for the period 1980-2010

Model Calibration. The results of the hydrologic model are sensitive to the initial storage fraction (0.2) and to the curve number. The initial abstraction fraction of 0.2 was used for the three subcatchements and the curve number was estimated as explained in the previous section. To minimize the difference between WEAP modeled and measured river flows, the initial abstraction proportion was adjusted to 0.3 for Amman and Balqa subcatchments. Amman subcatchement is an urban area which means that interception by building roofs is expected to be high while Jarash and Balqa areas are agricultural areas that include large forest and planted areas which means that interception by trees is expected to be high. The curve numbers of the different subcatchments were also adjusted iteratively to reduce the difference between WEAP modeled and measured Zarqa River flow at Jarash Bridge gauging station.

The COD first order decay rate coefficient was adjusted iteratively to improve the agreement between modeled and measured COD concentrations. However, in WEAP it is not possible to adjust the first order decay rate coefficient over time.

RESULTS AND DISCUSSION

River discharge. Figure 7 shows that the difference between measured and WEAP modeled flows has been considerably reduced by calibration. However, some significant differences still exist during months of high rainfall. Similar conclusions

were reached by using other models. Al Abed and Al Sharif [24] who used the Hydrologic Simulation Program-Fortran (HSPF) to model Zarqa River flow found out that the model did not simulate the peak runoffs very well for most of the years. The significant differences between measured and modeled Zarqa River flows during months of high rainfall is attributed to: the lack of long record of flow measurements for the different wadis within the subcatchments which made it not possible to calibrate each subcatchment independently; inaccuracies associated with estimating the curve number for the different subcatchments, limitations associated with the SCS-CN method, namely: Its sensitivity to the estimated curve number, the absence of clear guidance on how to vary antecedent moisture content, the method's varying accuracy for different biomes, the absence of explicit provision for spatial scale effects, and the fixing of the initial abstraction at 0.20, which does not consider geologic and climatic conditions [32]. Another reason that has probably added to the discrepancy between modeled and measured flows is the accuracy level of the input maps, i.e. soil and land use/cover maps. The soil map of the basin is a reconnaissance map with a scale of 1:250 000. The large scale of the map is expected to have impacted the accuracy of the estimated curve numbers of the subcatchments and consequently the modeled runoff. Also, the land use/cover classes derived from digital classification could have variable accuracy for the different categories of agricultural classes [37]. In addition, no verified information on land use/cover map of the Syrian part was available. These limitations could reduce the accuracy of modeling, as errors could propagate during the map intersection. The use of more accurate maps is expected to improve the rainfall runoff modeling results.

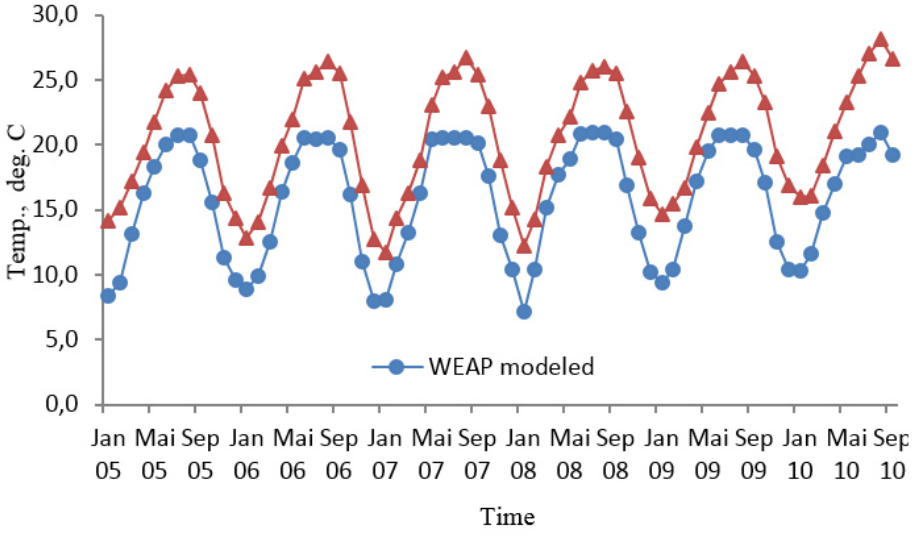

Monitoring station 9

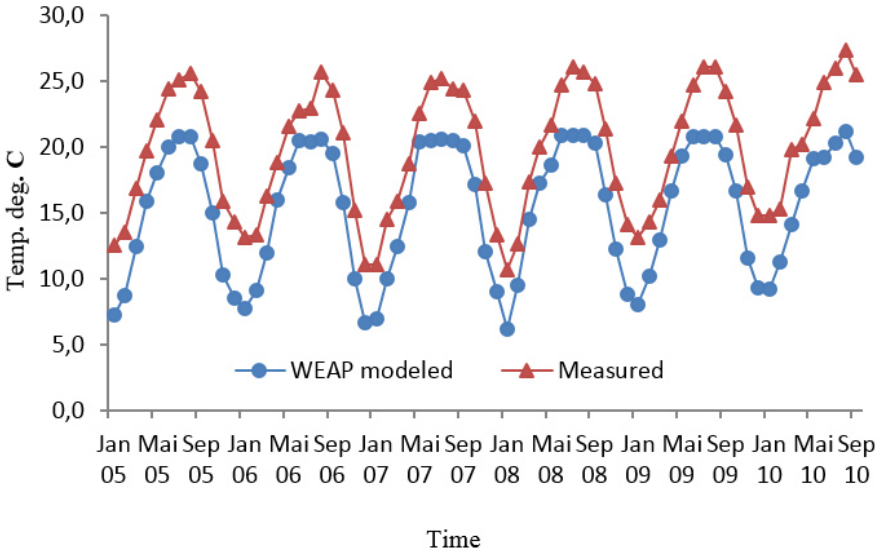

Monitoring station 10

FIGURE 8
WEAP modeled versus measured ZR temperature at monitoring stations 9 & 10

Temperature. Figure 8 show reasonable agreement between WEAP modeled and measured temperatures at monitoring stations 9 and 10. It is important to note that part of the discrepancy in the quality parameters is due to discrepancies in river discharge as all quality parameters are strong functions in river discharge. The high observed difference in January between modeled and measured temperatures at both monitoring stations is due to the fact that modeled river flow is significantly higher than the measured flow during January for all the years.

Chemical oxygen demand. Figure 9 shows good agreement between WEAP modeled and measured COD at some instances and poor at others at both monitoring stations. Reasons advanced for the difference between modeled and measured COD values are inaccuracy in the input first order decay rate coefficient taking into consideration that, in WEAP, it is not possible to let the first order decay rate coefficient vary over time. The peaks in the measured COD concentrations at both monitoring stations that are not associated with a drop in the modeled COD are most likely attributed to accidental illegal disposal of untreated sewage to the river [4, 5, 38]. However, the high measured COD concentrations that correspond to a drop in the modeled COD during January of 2006 and 2007 for example are apparently due to agricultural runoff, while the drop in the modeled COD is apparently due to dilution effect as a result of high modeled flow.

As for the other quality parameters, inaccuracies in the modeled river discharge are responsible for part of the discrepancy between measured and modeled COD. The noted decrease in the measured COD of the river after the year 2007 is due to the upgrade of As Samra WWTP which discharges its treated effluent to the river.

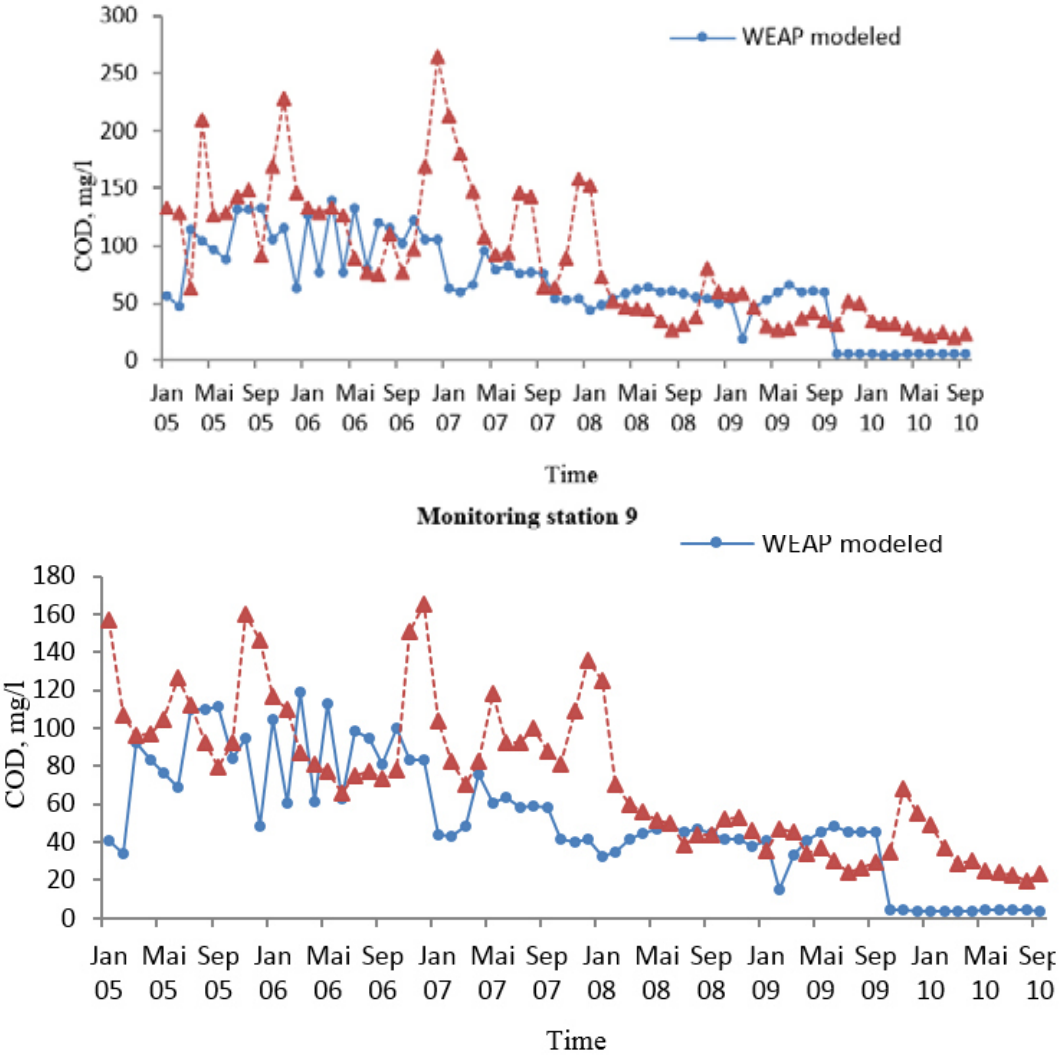

FIGURE 9
WEAP modeled versus measured Chemical Oxygen Demand at monitoring stations 9 & 10 before calibration

CONCLUSION

A model that integrates hydrologic and quality modeling of ZRB has been developed. The Water Evaluation and Planning (WEAP) model was used for this purpose. The results showed reasonable agreement between measured and simulated river flows at low flow values, while considerable differences were observed at peak flows. For the two quality parameters modeled, the results showed good agreement between simulated and measured values. However, some discrepancies were observed between modeled and measured values at peak flows. The developed model is the first attempt to model Zarqa River water quality which can serve as a management tool for the river.

ACKNOWLEDGEMENTS

The authors would like to express their gratitude to the Scientific Research Support Fund in Jordan for funding this research (grant number 2010\07\01\ه).

REFERENCES

[1] Al-Omari, A., Al-Quraan, S., Al-Salihi, A., Abdulla, F. (2009) A water management support system for Amman Zarqa Basin in Jordan. Water Resources Management. 23, 3165–3189.

[2] B & E Engineers and the Arabic International Center for Environmental Health (AICEH) (2008) Zarqa River Basin Wastewater and Solid Waste Treatment Projects. Project document, submitted to Ministry of Environment of the Hashemite Kingdom of Jordan, Amman, Jordan.

[3] Al-Bakri, J., Duqqah, M., Brewer, T. (2013) Application of remote sensing and GIS for modeling and assessment of land use/cover change in Amman/Jordan. Journal of Geographic Information System. 5(5), 509-519.

[4] Al Wer, I. (2009) The Zarqa River Rehabilitation and Sustainable Management. Master's Thesis. Royal Institute of Technology (KTH). Stockholm, Sweden.

[5] International Union for the Conservation of Nature (IUCN) (2009) Rapid Rural Appraisal for Zarqa River basin. Project document.

[6] Chapra, S., Runkel, R. (1999) Modeling impact of storage zones on stream dissolved oxygen. Journal of Environmental Engineering. 125(5), 415-419.

[7] Manson, J., Wallis, S. (1999) Conservative semi-Lagrangian algorithm for pollutant transport in rivers. Journal of Environmental Engineering. 125(5), 486-489.

[8] Thackston, E., Murr, A. (1999) CSO control project modifications based on water quality studies. Journal of Environmental Engineering. 125(10), 979-987.

[9] Zhang, W., Wang, Y., Peng, H., Li, Y., Tang, J., Wu, K. (2010) A coupled water quantity–quality model for water allocation analysis. Water Resources Management. 24, 485–511.

[10] Sudheer, C., Anand, N., Panigrahi, B., Mathur, S. (2013) Streamflow forecasting by SVM with quantum behaved particle swarm optimization. Neurocomputing. 101(4), 18–23.

[11] Manshadi, H., Niksokhan, M., Ardestani, M. (2015) A quantity-quality model for inter-basin water transfer system using game theoretic and virtual water approaches. Water Resources Management. 29(13), 4573-4588.

[12] Viancelli, A., Deuner, C.W., Rigo, M., Padilha, J., Marchesi, J.A., Fongaro, G. (2015) Microbiological quality and genotoxic potential of surface water located above the Guarani aquifer. Environ Earth Sciences. 74(7), 5517-5523.

[13] Evers, M. (2016) Integrative river basin management: challenges and methodologies within the German planning system. Environmental Earth Sciences. 75, 1085.

[14] Keshtegar, B., Allawi, M., Afan, H., El-Shafie, A. (2016) Optimized river stream-flow forecasting model utilizing high-order response surface method. Water Resources Management. 30(11), 3899–3914.

[15] Wu, L., Li, P., Ma, X.Y. (2016) Estimating non-point source pollution load using four modified export coefficient models in a large easily eroded watershed of the loess hilly–gully region, China. Environmental Earth Sciences. 75, 1056.

[16] Yan, R., Gao, J., Li, L. (2016) Streamflow response to future climate and land use changes in Xinjiang basin, China. Environmental Earth Sciences. 75, 1108.

[17] Yang, T., Wang, Q., Su, L., Wu, L., Zhao, G., Liu, Y., Zhang, P. (2016) An approximately semi-analytical model for describing surface runoff of rainwater over sloped land. Water Resources Management. 30(11), 3935-3948.

[18] Rahbeh, M. (1996) Rainfall-Runoff relationships for Zarqa River. Master's Thesis. University of Jordan, Amman, Jordan.

[19] Al-Abed, N., Abdulla, F., Abu Khyarah, A. (2005) GIS-hydrological models for managing water resources in the Zarqa River basin. Environmental Geology. 47, 405–411.

[20] Abderahman, N., Abu Rukah, Y. (2006) An assessment study of heavy metal distribution within soil in upper course of Zarqa River basin/Jordan. Environmental Geology. 49, 1116–1124.

[21] Al-Afayfeh, N., Al-bakri, J., Naber, S., Shammout, M. (2006) Optimization for sustainable water resources management. Environmental Software and Services. GMBH Austria.
[22] Grabow, L., McCornick, P. (2007) Planning for water allocation and water quality using a spreadsheet based model. Journal of Water Resources Planning and Management. 133(6), 560–564.
[23] Abdulla, F., Al-Omari, A. (2008) Impact of climate change on the monthly runoff of a semi-arid catchment: Case study Zarqa River Basin (Jordan). Journal of Applied Biological Sciences. 2(1), 43-50.
[24] Abdulla, F., Eshtawi, T., Assaf, H. (2009) Assessment of the impact of potential climate change on the water balance of semi-arid watershed. Water Resources Management. 23, 2051-2068.
[25] Al-Abed, N., Al-Sharif, M. (2008) Hydrological modeling of Zarqa River basin–Jordan using the hydrological simulation program—FORTRAN (HSPF) model. Water Resources Management. 22, 1203–1220.
[26] Hammouri, N. (2009) Assessment of climate change impacts of water resources in Jordan. International Conference and Exhibition on Green Energy & Sustainability for Arid Regions & Mediterranean Countries. Amman-Jordan, Nov. 10-12, 2009.
[27] Al-Omari, A., Huber, M. (2010) The Red Sea Dead Sea project: a solution to the water crisis in Jordan. Proceedings of the International Sustainable Water and Wastewater Management Symposium (USAYS). Konya, Turkey 26-28, 10, 2010.
[28] Associates in Rural Development Inc. (ARD) (2001) The water resource policy support activity. A report submitted to the Ministry of Water and Irrigation, Amman, Jordan.
[29] Stockholm Environment Institute (SEI) (2012) WEAP: User Guide for WEAP21. Tellus Institute, Boston, USA.
[30] Advanced Spaceborne Thermal Emission and Reflection Radiometer (ASTER) web site. http://asterweb.jpl.nasa.gov/.
[31] Allen, R., Pereira, L., Raes, D., Smith, M. (2006) Crop Evapotranspiration, (Guidelines for Computing Crop Water Requirements). Irrigation and Drainage Paper No. 56, FAO, Rome, Italy.
[32] Mishra, S., Singh, V. (1999) Another look at SCS-CN method. Journal of Hydrologic Engineering. 4(3), 257-264.
[33] Ministry of Agriculture, Jordan (MoA) (1993) The Soils of Jordan: Level 1 (Reconnaissance Survey). Report of the National Soil Map and Land Use Project, Volume 1, Ministry of Agriculture, Amman.
[34] USDA-SSS (United States Department of Agriculture, Soil Survey Staff) (1990) Keys to Soil Taxonomy. 4thed. SMSS, Technical monograph 19, Blacksburg, Virginia.
[35] Viessman, W., Lewis, G. (2011) Introduction to Hydrology. 5th ed. Upper Saddle River, N.J.: Pearson Education. ISBN 0-673-99337-X.
[36] Ababsa (2013) Atlas of Jordan, http://books.openedition.org/ifpo/4560.
[37] Al-Tamimi, S., Al-Bakri, J. (2005) Comparison between supervised and unsupervised classifications for mapping land use/cover in Ajloun area. Jordan Journal of Agricultural Sciences. 1(1), 73-83.
[38] Al-Omari, A., Al-Houri, Z., Al-Weshah, R. (2013) Impact of the As Samra wastewater treatment plant upgrade on the water quality (COD, electrical conductivity, TP, TN) of the Zarqa River. Water Science and Technology. 67(7), 1455-1464.

Received: **25.07.2017**
Accepted: **24.01.2018**

CORRESPONDING AUTHOR

Abbas Al-Omari
Water, Energy and Environment Center,
The University of Jordan,
Amman – Jordan

e-mail: abbas.alomari@ymail.com

Zain Al-Houri is visiting scholar at Texas A&M University, College Station.

© by PSP Volume 27 – No. 7/2018 pages 4648-4657 Fresenius Environmental Bulletin

HIGH EFFICIENT PRETREATMENT ON CORN STRAW AND SALIX PSAMMOPHILA AND ETHANOL FERMENTATION BY CONSOLIDATED BIOPROCESSING

Xiaoyan Zhang[1], Jianguo Liu[2], Yuying Du[1], Yali Shi[1], Mingda Zhu[1], Zhanying Liu[1,3,*], Yongli Li[1], Jianhua Hu[1]

[1]School of Chemical Engineering, Inner Mongolia University of Technology, Hohhot, Inner Mongolia 010051, China
[2]Department of Environmental Engineering, Inner Mongolia University of Technology, Inner Mongolia 010051, China
[3]Institute of Coal Conversion & Cyclic Economy, Inner Mongolia University of Technology, Hohhot, Inner Mongolia 010051, China

ABSTRACT

Many mass-cultivated plants are not efficiently utilized to their potential because of their complex recalcitrant structures. In this study, three kinds of ionic liquid(IL), [BMIM]Cl, [EMIM]Ac and [BPy][HSO4], were used to pretreat corn straw and Salix psammophila to improve their degradation ratio, and then produce ethanol by consolidated bioprocessing (CBP). FT-IR， SEM and XRD were used to analyze the change in performance of pretreated corn straw and S. psammophila. The results showed that pretreated corn straw and S. psammophila were more amorphous, and the structure of lignocellulosic biomass had been disrupted. The degradation ratio of cellulose and hemicellulose in corn straw were increased by 24.3% and 10.8% respectively through [EMIM]Ac pretreatment. The degradation ratio of cellulose and hemicellulose of S. psammophila pretreated by [BMIM]Cl had increased by 28.4% and 15.4% respectively. The crystallinity indexes of native and [Emim]Ac-pretreated corn straw were 49.0% and 31.1% respectively. The crystallinity indexes of native and [Bmim]Cl-pretreated S. psammophila were 37.4% and 22.3% respectively. Untreated and pretreated corn straw and S. psammophila were fermented to produce ethanol by CBP. The results showed the ethanol production from pretreated corn straw and S. psammophila were increased by 32% and 19% respectively. The recovery rates of [Emin]Ac, [Bmim]Cl and [Bhy][HSO4] reached 85%, 80% and 78% respectively. These results suggest that ionic liquid is an effective and low-cost pretreatment method. A higher ethanol titer was produced by *Clostridium thermocellum* comparing with untreated corn straw and S. psammophila with CBP.

KEYWORDS:
Corn straw, S. psammophila, ionic liquid (IL), ethanol, recovery rates

INTRODUCTION

Depletion of fossil energy and a continuous increase in greenhouse gas levels in the atmosphere have led to interest in the development of renewable and sustainable energy [1]. Lignocellulosic material is a natural and renewable feedstock for biofuel production. However, its three main components, cellulose, hemicellulose and lignin, and their rigid structure inhibit the biological conversion [2]. Especially, the most significant block to the use of the sugar in cellulose and hemicellulose is the recalcitrance of lignocellulose to depolymerization [3]. It is very difficult to dissolve lignocellulose in water and most common organic solvents because of the compact hydrogen bonding and van der Waals interactions [4]. These interactions lead to cellulose's notorious resistance to hydrolysis. Many methods, including biological, physical, chemical and physicochemical processes, have been investigated for the ability to break down lignocellulose efficiently [5].

Ionic liquid is a type of environmentally friendly molten salt, most of which have the virtue of excellent solvency, low melting point, nonvolatility and designability [6]. Rogers et al. first reported [C_4mim]Cl could dissolve cellulose efficiently [7]. The dissolution of cellulose in [C_4mim][Cl] is attributed to disruption of hydrogen bond within or between molecular chains, and coordination of chloride ions to the hydroxyl groups of cellulose. Interest in using IL as biomass solvents has so far been centred on the dissolution and processing of pure cellulose [8]. Swotloskid et al. studied the properties of cellulose dissolution in 1-butyl-3-methylimidazolium chloride ([Bmim]Cl) [9]. Swotloskid found that [Bmim]Cl had a similar mechanism to [C_4mim][Cl] when acting on cellulose. Singh et al. showed that 1-ethyl-3-methylimidazolium acetate ([Emim]Ac) was an effective solvent to solubilize the plant cell wall at a mild temperature, and subsequent cellulose precipitation and regeneration via addition of water as

antisolvent could reject lignin in the solution significantly based on the imaging techniques [10]. Shoda et al. studied the solubility of pyridine IL, 1-buthyl-3-methylpyridinium chloride ([Bmpy][Cl]), on bagasse and eucalyptus. [Bmpy][Cl] showed better performance than [Emim]Ac [11]. ([BPy][HSO_4]) has not been reported for the pretreatment of lignocellulose.

At present study, there are four kinds of bioprocessing for producing bioethanol from lignocellulosic biomass. They are separate hydrolysis and fermentation (SHF), simultaneous saccharification and fermentation (SSF), simultaneous saccharification and cofermentation (SSCF), and consolidated bioprocessing (CBP). Large amounts of expensive commercial cellulases are needed in SSF, SSCF and SHF, which increases the cost [12]. CBP, also called direct microbial conversion, featuring cellulase production, cellulose hydrolysis, and fermentation in one step, is widely recognized as the attractive strategy for converting cellulosic biomass to high value-added products because of a significant lower cost [13].

Agricultural wastes are a relatively cheap source of biomass. A large number of corn straw is produced every year as an agriculture waste. S. psammophila is a kind of desert shrub. Due to its particular biological characteristics, the stems of S. psammophila need to be cut once every 3 to 5 years to avoid its death, thus producing a large amount of residual matter. In this study, [BPy][HSO_4], [Bmim]Cl and [Emim]Ac, due to their good cellulose solubility, were selected to pretreat corn straw and S. psammophila, and then the two kinds of pretreated lignocellulosic biomass were fermented by CBP to produce ethanol.

MATERIALS AND METHODS

Material. Mature corn straw was obtained from local village near Hohhot (China). The variety of the corn straw is Xian fen 555. S. psammophila was obtained from Kubuqi desert (China). The main compositions of corn straw and S. psammophila are summarized in Table 1. Corn straw and S. psammophila were air dried, and then pulverized by using a grinder and sieved through a 40 meshes sieve before pretreatment. *Clostridium thermocellum* ATCC 27405 used in this study was a gift from Professor Lee Lynd in Dartmouth. It is a strain often used for ethanol production from biomass by consolidated bioprocessing. Pretreated corn straw or S. psammophila was used to replace microcrystalline cellulose as carbon source in MTC medium which prepared by combining six sterile solutions under a nitrogen atmosphere, as described in Kridelbaugh et al. [14].

Synthesis of ionic liquids. ILs, [BPy]HSO_4, [Bmim]Cl and [Emim]Ac, were synthesized and purified according to the literature [15-17].

Pretreatment. A 96 % ionic liquid (IL) solution was prepared by combining 200 mg of corn straw and S. psammophila with 4.8 g IL in a 100 mL serum bottle. The serum bottles containing the samples were stirred (150 rpm) and heated in an oil bath at 110 ℃ for 90 min [18]. After 90 min of incubation, the reaction mixtures were cooled down to 60 ℃ and then 50 mL ethanol as an anti solvent was added to precipitate and regenerate the dissolved cellulose. Next, the precipitated material was filtered through filtering paper using a Buchner funnel under a reduced pressure and washed with deionized water to ensure that excess IL had been removed. At last, the precipitates were dried at 60 ℃ for 48 h.

Recovery of ionic liquid. The supernatant filtered was destained for 12 h with 80 g/mL active carbon. Ethanol was removed in vacuo using a rotary evaporator at 50 ℃ for 2 h [19]. The resulting residue was dried under vacuum at room temperature for 16 h. The recovered IL was measured gravimetrically.

TABLE 1
Basic components of corn straw and S. psammophila

Fiber material type	Cellulose	Hemicellulose	Lignin	Ash
Corn straw	34.84%±0.40%±1.41%[cB]	12.35%±0.2%	10.12%±3.5%	6.6%±1.5%
S. psammophila	38.37%±3.59%	11.35%±0.85%	24.48%±6.7%	1.6%±1.2%

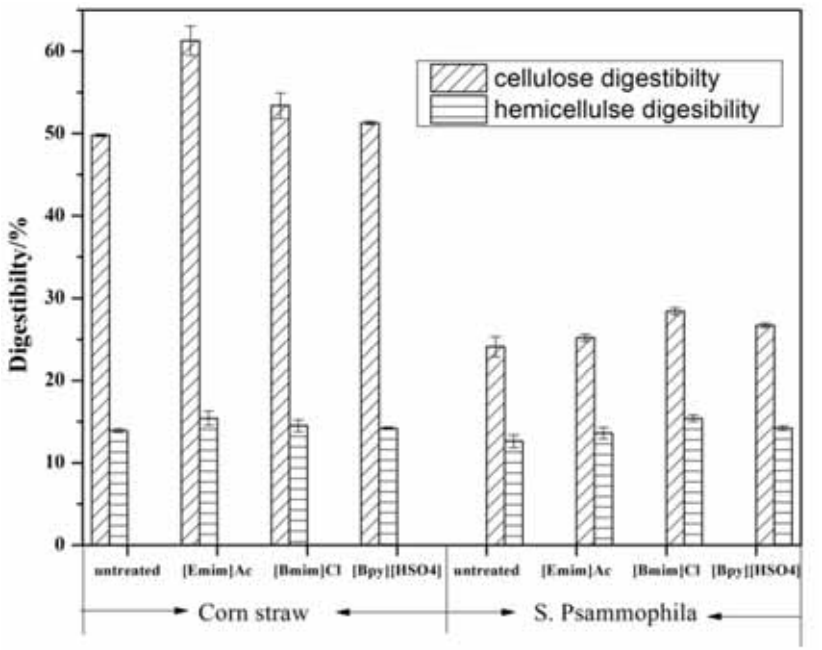

FIGURE 1
Effect of different ILs on cellulose and hemicellulose digestibility of Corn straw and S. psammophila.

XRD analysis. The X-ray powder diffraction pattern of the original and regenerated cellulose preparations was measured using an 8-Adrance instrument with a Cu Kα radiation source at 40 kV and 40 mA. Samples were scanned from 2θ= 5–50° at a speed of 2°/min. The cellulose crystallinity index (CrI) of non-pretreated and pretreated samples was measured by equation 1.

$$CRI = \frac{I_{002} - I_{am}}{I_{002}} \times 100 \qquad (1)$$

Here I_{002} is the scattered intensity of cellulose I at about 2θ = 22.5°, and I_{am} is the peak for the amorphous portion assessed as the minimum intensity between the main and the secondary peaks at 2θ = 18.5°

SEM analysis. SEM was used to investigate the microstructure and the surface morphology of corn straw and S. psammophila. Samples were embedded in paraffin wax and air-dried overnight. Transverse sections were cut using a rotary microtome. Thicker sections were coated with gold/palladium using an ion sputter coater and observed with a SN-3400 electron microscope operated at 20 kV.

FT-IR analysis. Fourier Transform Infrared (FTIR) spectroscopic analysis of untreated and pretreated residue was carried out to detect changes in functional groups. FTIR spectrum was recorded between 4000 and 400 cm^{-1} using a spectrometer with detector at 4 cm^{-1} resolution and 25 scans per sample. Discs were prepared by mixing 3 mg of dried sample with 300 mg of KBr in an agate mortar. The resulting mixture was pressed at 10 MPa for 3 min.

RESULTS AND DISCUSSION

Cellulose and hemicellulose digestibility. The effects of three ILs, [BMIM]Cl, [EMIM]Ac and[BPy][HSO_4], on the dissolution of corn straw and S. psammophila were investigated. Cellulose and hemicellulose digestibility for untreated and pretreated corn straw and S. psammophila under the same fermentation condition was shown in Fig.1. After pretreatment with three different ILs, cellulose and hemicellulose digestibility of S. psammophila and corn straw were improved. [EMIM]Ac had the best effect in three ILs on the pretreatment of corn straw. Compared with untreated corn straw, the degradation ratio of cellulose was increased 24.3%, and the degradation ratio of hemicellulose was increased 10.8% after [EMIM]Ac pretreatment. S. psammophila pretreated by [BMIM]Cl had cellulose and hemicellulose digestibility of 28.4% and 15.4% respectively, which are higher than the other two ILs. In the study of Trinh LTP et al., [Bmim]Cl was used to pretreat softwood at 120 ℃ for 300 min, and cellulose degradation ratio of 51% was achieved [20]. Their result was consistent with the present study.

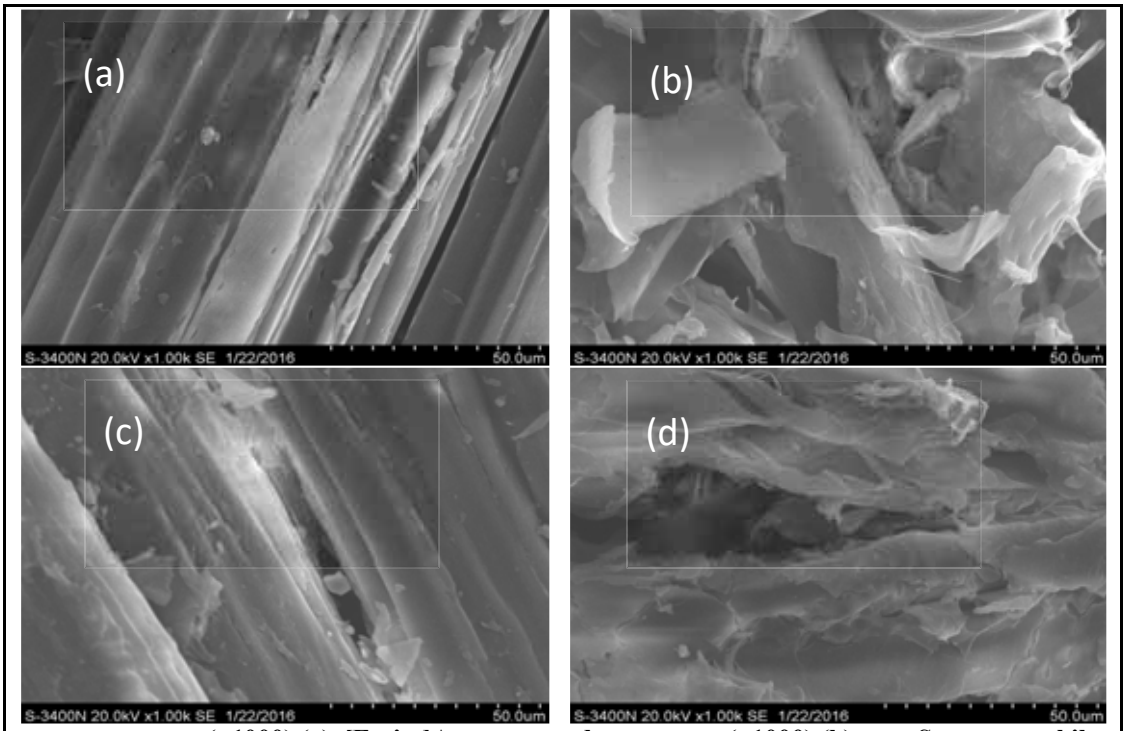

raw corn straw (×1000) (a), [Emim]Ac-pretreated corn straw (×1000) (b), raw S. psammophila (×1000) (c), [Bmim]Cl -pretreated S. psammophila (×1000) (d)

FIGURE 2 SEM images of corn straw and S. psammophila

Characterization of pretreated lignocellulose. SEM, XRD and FTIR data revealed difference between the native and pretreated samples. Morphological changes of native and pretreated samples were examined by SEM to evaluate structural modification of the surface. The lignocellulosic biomass with the highest degradation ratio was selected to observe the surface structure. The result was shown in Fig. 2. SEM images of untreated and pretreated corn straw and S. psammophila were taken at ×1000 magnification.

The structure of untreated corn straw (Fig. 2 a-c) was compact, rigid and ordered. The surface of corn straw became swollen and loose and the original fibrous structure has been distorted after pretreatment by [Emim]Ac (Fig. 2 d-f). The same phenomenon was also investigated on the S. psammophila. The distorted structure and increase in surface area of the pretreated biomass led to an improvement in hydrolysis efficiency.

The research showed that alkyl imidazolo ionic liquid had a strong effect on cellulose. In 2002, Swatloski discovered that cellulose can be directly dissolved by 1-butyl-3-methyl imidazole chloride ([Bmin]Cl) [7]. Zhai et al. found that [BMIM]Cl was able to dissolve cellulose in wood pulp, wheat straw and Pennisetum sinese Roxb [21].

The FTIR spectra of lignocellulosic biomass was influenced by the spectra of its three main biopolymers, cellulose, hemicelluloses and lignin [22]. The FTIR spectra of corn straw and S. psammophila with and without IL pretreatment was presented in Fig.3. Difference was detected in the absorption spectra, i.e. absorbance and shapes of the band and their locations. The most representative band is summarized. The absorption of O-H stretching vibration shifted from 3004 cm^{-1} of the original biomass to 3256 cm^{-1} of the pretreated biomass, which indicated that the content of the free hydroxyl group increased in the regenerated cellulose [23]. The peak at 2897 cm^{-1} was due to the C-H stretching in CH_2 and CH_3 groups, which was affected by changes of crystallinity. The characteristic lignin band at 1600 cm^{-1} was found to be absent in pretreated samples, indicating the depolymerization of the guaiacyl aromatic ring of lignin during pretreatment [24]. The absorption band at 1427 cm^{-1} of the original cellulose was attributed to crystallized cellulose I and amorphous cellulose [25]. The band widening at 1318 cm^{-1} can be ascribed to CH_2 wagging vibrations in cellulose. A similar observation was reported by Raveendran Sindhu et al. [26].

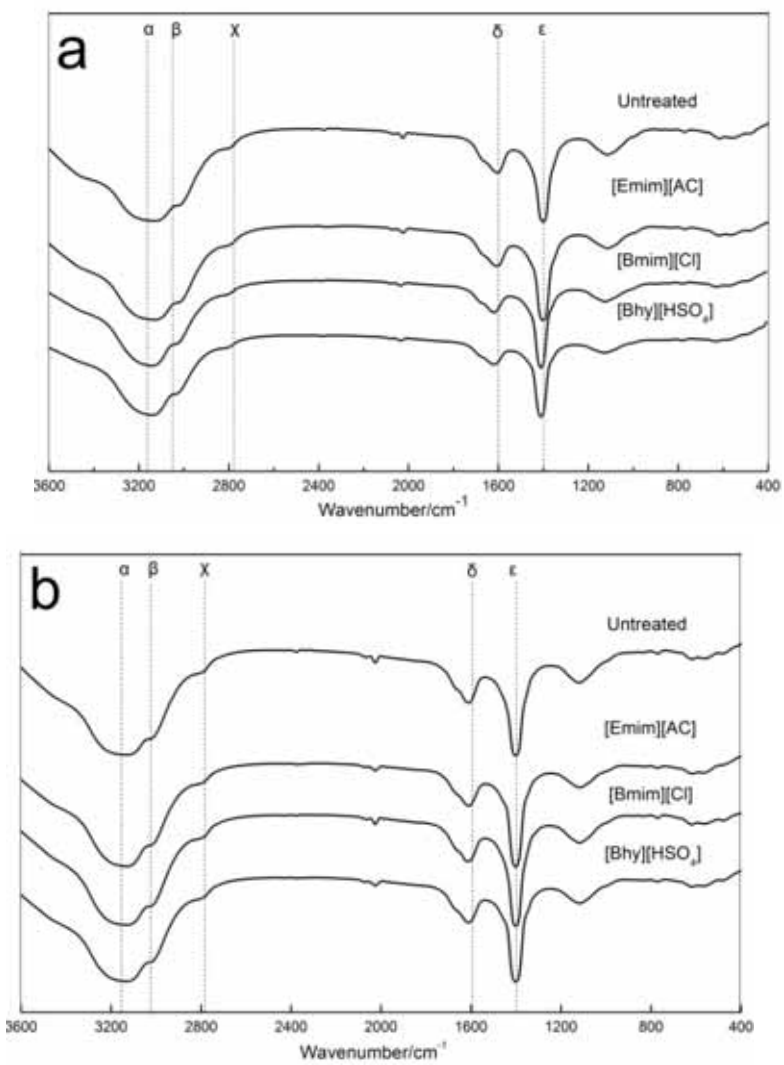

FIGURE 3
Infrared spectra of corn straw (a) and S. psammophila (b) treated by different ionic liquids
FT-IR spectral bands (cm^{-1}): α(3156); β(3004); χ(2879); δ(1600); ε(1427).

The powder XRD values of untreated and treated corn straw and S. psammophila was presented in Fig. 4. There were three broad peaks at 15.1°, 22.1°and 35.0° for untreated corn straw and S. psammophila, which was consistent with known values in the cellulose I lattice structure [27]. XRD has been used to determine the crystallinity index by assessing the relative contributions of crystalline fractions to the overall scattering pattern for a long time[28]. The crystallinity indexes of native and [Emim]Ac-pretreated corn straw were 49.0% and 31.1% respectively. Kosan et al. used ionic liquid 3-ethyl-1-methyl imidazole acetate ([EMIM]Ac) to treat cellulose and discovered that cellulose was dissolved by ionic liquid directly[29]. The crystallinity indexes of native and [Bmim]Cl-pretreated S. psammophila were 37.4% and 22.3% respectively. The lower crystallinity index revealed that a large amount of amorphous cellulose was present in the regenerated cellulose. High-crystalline cellulose had great resistance against enzymatic saccharification and hindered the action of microorganisms as a result of the strong hydrogen-bond networks [30].

Effect of ionic liquid pretreatment on ethanol production. The pretreatment of lignocellulose is a critical step in the production of fuel ethanol by lignocellulosic biomass. Ethanol production from untreated and pretreated corn straw and S. psammophila was shown in Fig. 5. The ethanol production from untreated corn straw and S. psammophila were 0.19 g/L and 0.12 g/L respectively. In contrast, the ethanol production from corn straw and S. psammophila were increased after ionic liquid pretreatment. The ethanol production for [EMIM]Ac-pretreated corn straw was increased by 32%. With [BMIM]Cl-pretreated S. psammophila, ethanol production increased by 19%.

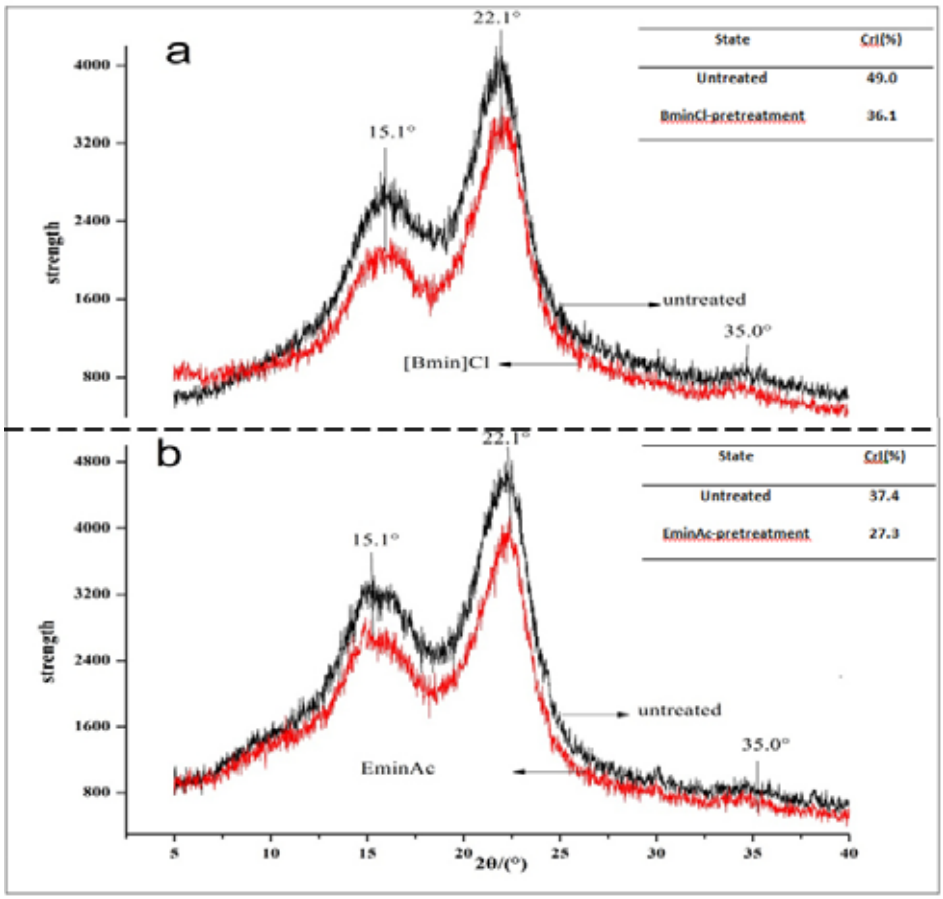

FIGURE 4
X- ray diffraction pattern and CrI of pretreated and unpretreated S. psammophila (a) and Corn straw (b).

TABLE 2
Ethanol production by *C.thermocellum* under different pretreatment methods

strain	Pretreatment method	ethanol yield(g/L)	material	Reference
Clostridium thermocellum ATCC 27405	Dilute sulfuric Acid (190℃, 60s)	0.2	Switchgrass	[36]
Clostridium thermocellum ATCC 27405	dilute sulfuric acid (190℃, 60s)	0.3	Populus	[36]
Clostridium thermocellum ATCC 27405	dilute sulfuric acid (121℃, 1h)	0.8(0.6)	rice straw	[30]
Clostridium thermocellum ATCC 27405	steam exploded (560psi,250 ℃, 20s)	0.73	aspen wood	[28]
Clostridiurn thermocellum ATCC 31924	steam exploded (560 psi, 250 ℃, 20s)	0.41	wheat straw	[29]

Ethanol production by *C.thermocellum* with lignocellulosic biomass by different pretreatment methods was listed in Table2. In the study of Saddler JN et al. [31, 32], ethanol production from aspen wood and wheat straw by ammonia explosion pretreatment was higher than those in the present study. However, ammonia explosion pretreatment requires high energy consumption and equipment requirements. IL-pretreatment requires temperatures of only 110℃. In the study of Hua Z et al., ethanol production from rice straw pretreated by dilute sulfuric acid increased 25%, which was lower than [EMIM]Ac-pretreated corn straw in this study [33]. In addition, dilute sulfuric acid pretreatment method also led to an environmental pollution. Therefore, the ionic liquid pretreatment method described in the present study can be considered as an effective pretreatment method for corn straw and S. psammophila.

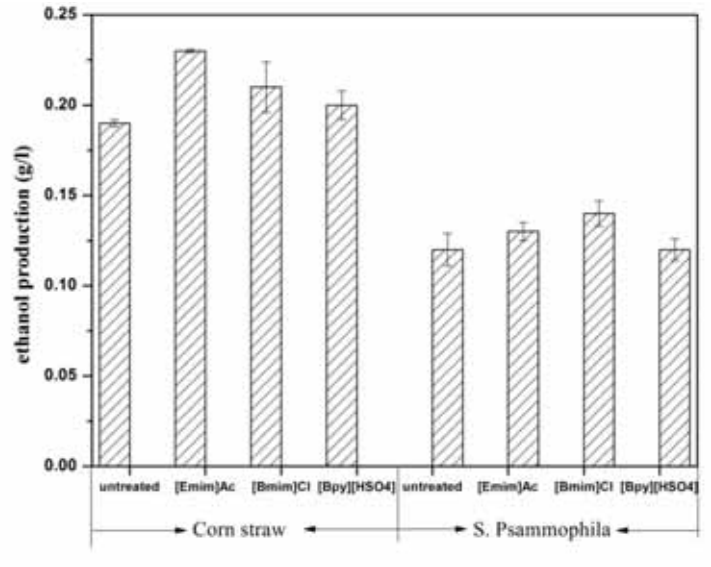

FIGURE 5
Effect of different ionic liquid pretreatment on ethanol production from corn Straw and S. psammophila

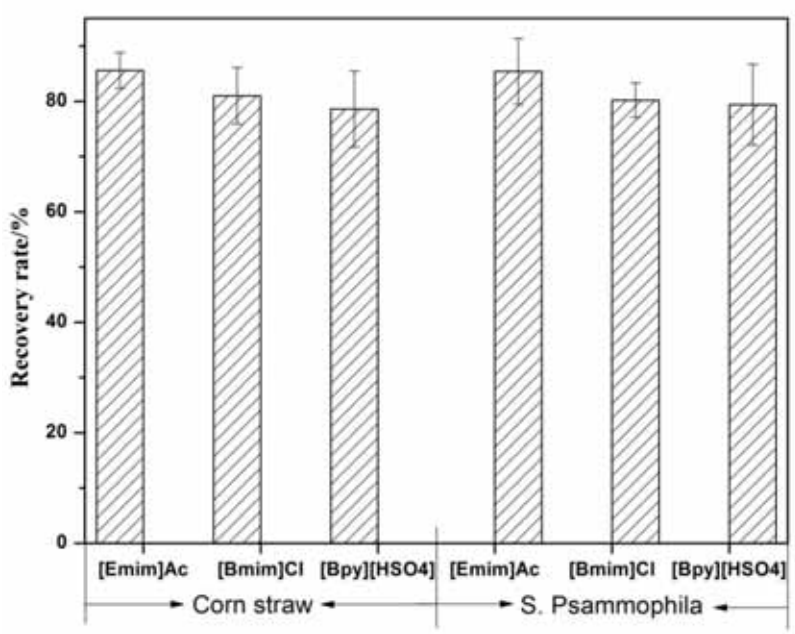

FIGURE 6
Recovery rate of three kinds of ionic liquids.

Characterization of recycled [EMIM][DEP]. To demonstrate potential cost efficiencies, IL was recycled after pretreatment of S. psammophila and corn straw. The recovery percentage of three ionic liquids was shown in Fig. 5. The recovery rate of [Emin]Ac, [Bmim]Cl, and [Bhy][HSO_4] reached 85%, 80%, and 78% respectively. A low recovery percentage of [EMIM][DEP], 75%, was obtained by Li et al. [34]. In the research of Liu et al., 1-Methyl-3-allylimidazolium chloride ([Amim]Cl) was recovered and the recovery rates were 82% and 79% for the first time and the second time respectively [35]. As a result, it is evident that IL has strong potential for efficient recycling, and thus the cost will be cut [36].

Pretreatment methods such as acid, dilute alkali, steam explosion and ammonia explosion have some disadvantages, for example environmental pollution, high energy consumption, and special equipment requirements [37, 38]. Ionic liquids as a type of environmentally friendly molten salt and green solvent has some advantages in the application of pretreatment. The pretreatment cost can be reduced by high recovery rates of ionic liquid. These efficiencies urge the further industrialization of ionic liquid pretreatment method.

ACKNOWLEDGEMENTS

This work was supported by the National Natural Science Foundation of China (NSFC) (Grant No. 61361016); Program for Young Talents of Science and Technology in the Universities of the Inner Mongolia Autonomous Region; West Light Foundation of The Chinese Academy of Sciences talent cultivation plan; Research Fund for the Doctoral Program of Higher Education of China (RFDP) (2013151412000); Foundation of Talent Development of Inner Mongolia and The "Prairie talent" project of Inner Mongolia (CYYC20130034).

REFERENCES

[1] Song, Z., Sun, X., Yang, G., Yan, Z., Yuan, Y., Li, D., Li, X., Liu, X. (2014) Effect of NaOH pretreatment on methane yield of corn straw at different temperatures by anaerobic digestion. CIESC Journal.

[2] Vancov, T., Alston, A.S., Brown, T., Mcintosh, S. (2012) Use of ionic liquids in converting lignocellulosic material to biofuels. Renewable Energy. 45(3), 1-6.

[3] Groff, D., George, A., Sun, N., Sathitsuksanoh, N., Bokinsky, G., Simmons, B.A., Holmes B.M., Keasling, J.D. (2013) Acid enhanced ionic liquid pretreatment of biomass. Green Chemistry. 15(5), 1264.

[4] Hermanutz, F., Gähr, F., Uerdingen, E., Meister, F., Kosan, B. (2008) New Developments in Dissolving and Processing of Cellulose in Ionic Liquids. Macromolecular Symposia. 262(1), 23-27.

[5] Taherzadeh, M.J., Karimi, K. (2008) Pretreatment of Lignocellulosic Wastes to Improve Ethanol and Biogas Production: A Review. International Journal of Molecular Sciences. 9(9), 1621-1651.

[6] Brandt, A., Erickson, J.K., Hallett, J.P., Murphy, R.J., Potthast, A., Ray, M.J., Rosenau, T., Schrems, M., Welton, T. (2012) Soaking of pine wood chips with ionic liquids for reduced energy input during grinding. Green Chemistry. 14(4), 1079-1085.

[7] Swatloski, R.P., Spear, S.K., And Holbrey, J.D., Rogers, R.D. (2002) Dissolution of Cellose with Ionic Liquids. Journal of the American Chemical Society. 124(18), 4974-4975.

[8] Mokudai, H., Fukaya, Y., Nakamura, N., Ohno, H. (2012) Synthesis of Ionic Liquids as Solvents for Poly(3-Hydroxybutyrate) under Mild Condition. Electrochemical Society.

[9] Swatloski, R.P., Spear, S.K., Holbrey, J.D., Rogers, R.D. (2002) Dissolution of cellulose [correction of cellose] with ionic liquids. Journal of the American Chemical Society. 124(18), 4974-4975.

[10] Singh, S., Simmons, B.A., Vogel, K.P. (2009) Visualization of biomass solubilization and cellulose regeneration during ionic liquid pretreatment of switchgrass. Biotechnology & Bioengineering. 104(1), 68.

[11] Shoda, Y., Nakamoto, A., Goto, M., Tokuhara, W., Noritake, Y., Katahira, S., Ishida, N., Nakashima, K., Ogino, C., Kamiya, N. (2012) Short time ionic liquids pretreatment on lignocellulosic biomass to enhance enzymatic saccharification. Bioresource Technology. 103(1), 446-452.

[12] Cao, G.L., Zhao, L., Wang, A.J., Wang, Z.Y., Ren, N.Q. (2014) Single-step bioconversion of lignocellulose to hydrogen using novel moderately thermophilic bacteria. Biotechnology for Biofuels. 7(1), 82.

[13] Balusu, R., Paduru, R.R., Kuravi, S.K., Seenayya, G., Reddy, G. (2005) Optimization of critical medium components using response surface methodology for ethanol production from cellulosic biomass by Clostridium thermocellum SS19. Process Biochemistry. 40(9), 3025-3030.

[14] Kridelbaugh, D.M., Nelson, J., Engle, N.L., Tschaplinski, T.J., Graham, D.E. (2013) Nitrogen and sulfur requirements for Clostridium thermocellum and Caldicellulosiruptor bescii on cellulosic substrates in minimal nutrient media. Bioresource Technology. 130(130C), 125-135.

[15] Du, Y.Y., Tian, F.L., Zhao, W.Z. (2006) [BPy]HSO_4 Acidic Ionic Liquid as a Novel, Efficient and Environmentally Benign Catalyst for Synthesis of 1,5-Benzodiazepines under Mild Conditions. Synthetic Communications. 36, 1661-1669.

[16] Huddleston, J.G., Visser, A.E., Reichert, W.M., Willauer, H.D., Broker, G.A., Rogers, R.D. (2001) Characterization and comparison of hydrophilic and hydrophobic room temperature ionic liquids incorporating the imidazolium cation. Green Chem. 3, 156-164.

[17] Zhu, H.X., Li, J.S., Xu, R., Yang, S.Y. (2012) An environmental friendly approach for the synthesis of the ionic liquid 1-ethyl-3-methylimidazolium acetate and its dissolubility to 1, 3, 5-triamino-2, 4, 6-trinitrobenzene. Journal of Molecular Liquids. 165, 173-176.

[18] Mood, S.H., Golfeshan, A.H., Tabatabaei, M., Abbasalizadeh, S., Ardjmand, M. (2013) Comparison of different ionic liquids pretreatment for barley straw enzymatic saccharification. Biotech. 3(5), 399-406.

[19] Ninomiya, K., Inoue, K., Aomori, Y., Ohnishi, A., Ogino, C., Shimizu, N., Takahashi, K. (2015) Characterization of fractionated biomass component and recovered ionic liquid during repeated process of cholinium ionic liquid-assisted pretreatment and fractionation. Chemical Engineering Journal. 259, 323-329.
[20] Trinh, L.T.P., Lee, Y.J., Lee, J.W., Lee, H.J. (2015) Characterization of ionic liquid pretreatment andthe bioconversion of pretreated mixed softwood biomass. Biomass & Bioenergy. 81, 1-8.
[21] Zhai, W., Chen, H.Z., Ma, R.Y. (2007) Structural characteristics of cellulose after dissolution and regeneration from the ionic liquid [bmim]Cl. Journal of Beijing University of Chemical Technology. 34(2), 138-141.
[22] Adel, A.M., El–Wahab, Z.H.A., Ibrahim, A.A., Al ‐ Shemy, M.T. (2010) Characterization of microcrystalline cellulose prepared from lignocellulosic materials. Part I. Acid catalyzed hydrolysis. Bioresource Technology. 101(12), 4446-4455.
[23] Zhang, Y.H.P., Lynd, L.R. (2004) Toward an aggregated understanding of enzymatic hydrolysis of cellulose: Noncomplexed cellulase systems. Biotechnology & Bioengineering. 88(7), 797-824.
[24] Pandey, A.K., Negi, S. (2015) Impact of surfactant assisted acid and alkali pretreatment on lignocellulosic structure of pine foliage and optimization of its saccharification parameters using response surface methodology. Bioresource Technology. 192, 115-125.
[25] Bian, J., Peng, F., Peng, X.P., Xiao, X., Peng, P., Xu, F., Sun, R.C. (2014) Effect of [Emim]Ac pretreatment on the structure and enzymatic hydrolysis of sugarcane bagasse cellulose. Carbohydr. Polym. 100, 211-217.
[26] Sindhu, R., Kuttiraja, M., Binod, P., Sukumaran, R.K., Pandey, A. (2014) Physicochemical characterization of alkali pretreated sugarcane tops and optimization of enzymatic saccharification using response surface methodology. Renewable Energy. 62, 362-368.
[27] Cruz, A.G., Scullin, C., Mu, C., Cheng, G., Stavila, V., Varanasi, P., Xu, D., Mentel, J., Chuang Y.D., Simmons B.A. (2012) Impact of high biomass loading on ionic liquid pretreatment. Biotechnology for Biofuels. 6(1), 1-10.
[28] Kim, T.H., Kim, J.S., Sunwoo, C., Lee, Y.Y. (2003) Pretreatment of corn stover by aqueous ammonia. Bioresource Technology. 90(1), 39-47.
[29] Kosan, B., Michels, C., Meister, F. (2008) Dissolution and forming of cellulose with ionic liquids. Cellulose. 15(1), 59-66.
[30] Sannigrahi, P., Miller, S.J., Ragauskas, A.J. (2010) Effects of organosolv pretreatment and enzymatic hydrolysis on cellulose structure and crystallinity in Loblolly pine. Carbohydrate Research. 345(7), 965-970.
[31] Saddler, J.N., Chan, K.H. (1982) Optimization of Clostridium thermocellum growth on cellulose and pretreated wood substrates. Applied Microbiology and Biotechnology. 16(2), 99-104.
[32] Saddler, J.N., Chan, M.K.H. (1984) Conversion of pretreated lignocellulosic substrates to ethanol by Clostridium thermocellum in mono- amd co-culture with Clostridium thermosaccharolyticum and Clostridium thermohydrosulphuricum. Canadian Journal of Microbiology. 30(2), 212-220.
[33] Hua, Z., Wang, Y.J., Fan, L., Chai, L.N., Shao, L.M., He, P.J. (2015) Effects of dilute acid pretreatment on physicochemical characteristics and consolidated bioprocessing of rice straw. Waste and Biomass Valorization. 6(2), 217-223.
[34] Li, Q., He, Y.C., Xian, M., Jun, G., Xu, X., Yang, J.M., Li, L.Z. (2009) Improving enzymatic hydrolysis of wheat straw using ionic liquid 1-ethyl-3-methyl imidazolium diethyl phosphate pretreatment. Bioresource Technology. 100(14), 3570-3575.
[35] Liu., Jianfeia., Cao, B., Yang, Y., Li, M., Xing, H., Jianmin. (2012) Saccharification of the Pretreated Corn Stover by Microwave Assisted DMSO/AmimCl Co-solvents. Acta Chimica Sinica -Chinese Edition. 70(18), 1950-1956.
[36] Tan, S.S.Y., Macfarlane, D.R., Upfal, J., Edye, L.A., Doherty, W.O.S., Patti, A.F., Pringle, J.M., Scott, J.L. (2009) Extraction of lignin from lignocellulose at atmospheric pressure using alkylbenzenesulfonate ionic liquid. Green Chemistry. 11(3), 339-345.
[37] Ye, S., Cheng, J. (2002) Hydrolysis of Lignocellulosic Materials for Ethanol Production: A Review. Bioresource Technology. 83(1), 1-11.
[38] Taherzadeh, M.J., Karimi, K. (2008) Pretreatment of Lignocellulosic Wastes to Improve Ethanol and Biogas Production: A Review. International Journal of Molecular Sciences. 9(9), 1621-1651.
[39] Wilson, C.M., Miguel, Rodriguez, J., Johnson, C.M., Martin, S.L., Chu, T.M., Wolfinger, R.D., Hauser, L.J., Land, M.L., Klingeman, D.M., Syed, M.H. (2013) Global transcriptome analysis of Clostridium thermocellum ATCC 27405 during growth on dilute acid pretreated Populus and switchgrass. Biotechnology for Biofuels. 6(1), 1-18.

Received: **07.08.2017**
Accepted: **15.04.2018**

CORRESPONDING AUTHOR

Zhanying Liu
School of Chemical Engineering,
Inner Mongolia University of Technology,
Hohhot, Inner Mongolia 010051 – China

e-mail: zyliu1979@163.com

© by PSP Volume 27 – No. 7/2018 pages 4658-4667 Fresenius Environmental Bulletin

ARTIFICIAL NEURAL NETWORK COMBINED WITH IMPERIALIST COMPETITIVE ALGORITHM FOR DETERMINATION OF RIVER SEDIMENTS

Mehdi Nikoo[1], Seyyed Abdonnabi Razavi[2], Marijana Hadzima-Nyarko[3,*]

[1]Young Researchers and Elite Club, Ahvaz Branch, Islamic Azad University, Ahvaz, Iran
[2]Department of Civil Engineering, Abadan Branch, Islamic Azad University, Abadan, Iran
[3]Faculty of Civil Engineering, University of J.J. Strossmayer, Vladimira Preloga 3, 31000, Osijek, Croatia

ABSTRACT

Estimation of sediment volume transported by a river has become an important water engineering issue. Due to the lack of exact and detailed information on the parameters affecting the non-linear nature of sedimentation process including spatial and temporal variances, a comprehensive sedimentation model cannot be formulated. The new evolving technique of utilizing artificial neural networks, which is based on an optimization algorithm, has found vast applications in different scientific fields, especially in water and river engineering. The Imperialist Competitive Algorithm (ICA) is based on random populations and the idea of the human's socio-political evolution. In this algorithm, a number of imperialist countries and their colonies search for a generalized optimization method for finding optimizing solutions. This research is based on the Feed Forward Artificial Neural Network (FF-ANN) model and attempts to predict and determine sedimentation in rivers. One of the elements used as a new method is employment of ICA for finding the optimized values within ANNs, which is also used for predicting river sedimentations of Karoon River in Ahvaz, Iran. For this purpose, discharge, month of year, height, and density coefficient are the input parameters, and sedimentation estimation is the output value. To determine accuracy of the FF-ICA model, it was compared with genetic and particle swarm group algorithms. This comparison was carried out in three stages of investigation, training, and testing. The results state that the ANN with its weights optimized within ICA, when compared with Genetic Algorithm (GA) and Particle Swarm Optimization (PSO) Algorithm, has greater flexibility and accuracy in predicting river sedimentation.

KEYWORDS:
Imperialist Competitive Algorithm (ICA), Artificial Neural Network (ANN), Sedimentation, Karoon River, Genetic Algorithm (GA), PSO Algorithm

INTRODUCTION

Determining the exact volume of sediments carried by rivers has great importance in many water management projects. Up to now, many numerical models, which are based on the theory of nonequilibrium sediment transport, have been provided for predicting river sedimentation and are widely used in the pre-design phase for engineering projects. However, the biggest disadvantage is that the simulated results of classic numerical model usually disagree with the measurements, what may be attributed to the imperfection of the model structure and the difficulty in parameter calibration [1]. According to Fang et al. [1], to improve the numerical model accuracy, there are three approaches which can be employed: (1) data assimilation method, which originates from weather prediction; (2) building up coupled numerical models, in which the flow, sediment transport and morphological evolution processes are strongly coupled with one another and (3) to use a series of optimal methods, such as artificial intelligence and neural networks (e.g. [2], [3], [4]).

Considering the nonlinear behavior of hydraulic parameters make us to find some more progressive alternatives instead of the older classic methods such as rating curve models which do not have the required accuracy [5]. Recent research has shown that Artificial Neural Network Models can be used as a black-box method in modeling hydraulic parameters. Yitian and Gu [6] modeled river flow and sedimentations in river systems with artificial neural networks. For this purpose, ANN model based on an existing river was developed to predict river flow and sedimentations. Results indicated that artificial neural networks are powerful tools for real-time prediction of this occurrence in a complex river system. Alp and Cigizoglu [7] considered the meteorological data within Artificial Neural Models to predict river sedimentations. They used feed-forward back-propagation (FFBP) method and radial basis functions (RBF) to model the suspended load of sediments in the Catchment River. Dogan et al. [8] used artificial neural networks to predict the total sediment load. Their aim was to create an effective model regarding sediment load, greater slopes, and the size of the load

particles. Results illustrated that the developed neural network determined greater accuracy than the Acaroglu equation and Graf model. Kisi [9] predicted river sedimentations using Fuzzy models. Results showed that fuzzy models could predict the river sediment loads with a very high accuracy. Yand et al. [10] used effective parameters on neural network for sediment determination. They also used four parameters of average flow velocity, water surface slopes, average flow depth, and median particle diameter for sediment determination. Results showed that the ANN model with minimum input parameters is a reliable method for predicting the total sediment. Melesee et al. [11] predicted the suspended sedimentation load of rivers using MLP network. The input parameters in that research were discharge, previous day's discharge, rainfall, and the output was river sedimentation. They also used nonlinear regression and time series models. Results indicated that artificial neural networks have suitable accuracy in predicting the level of river sedimentations. Rajaee [12] used combination of wavelets and artificial neural networks to determine river sedimentation. They evaluated the model using multi linear regression and rating curve. The results showed that in comparison with the other two models, the combinational Wavelet Artificial Neural Network (WANN) model provides better results in predicting the suspended river loads. Ramezani et al. [13] determined sediment on Maron River using both artificial neural network and social-based algorithm. They used social-based algorithm to optimize the artificial neural network weights due to determination of sediment on Idenak, Tang Takab, Cham Nezam and Jookang stations. Likewise, the input data were length, discharge, and height of every station, and the output was sediment. They illustrated that artificial neural network combined by social-based algorithm is more flexible and able to determine the sediment on Maron river.

Different methods for solving optimization problems have been introduced. Some of them are repetitive methods, which are gradient based and find the optimized cost function value. Although they have great speed, one of their weakness in concentrating on local optimizations [14]. The main aim of this study is to use the Imperialist Competitive Algorithm for optimizing weights within Artificial Neural Networks as a new optimizing algorithm for predicting river sedimentation. The advantages of this system include: (1) Introducing the new fundamental idea of use of Imperialist Competitive Algorithm as the first optimizing algorithm based on a socio-political process; (2) The ability equal to or even higher than different optimization algorithms in facing different optimization issues and (3) Suitable speed in finding solutions.

In this article, Karoon river sedimentation prediction has been carried out using Feed Forward Artificial Neural Network. Existing data from Ahvaz station were employed in a suitable model of Artificial Neural Networks. For this purpose, discharge, month of year, height and density coefficient are the input parameters, and sedimentation estimation is the output. For evaluation of accuracy of the FF-ICA model, it was compared with the genetic algorithm and PSO algorithm. This research was carried out in three stages of training, testing and prediction.

INTRODUCING IMPERIALIST COMPETITIVE ALGORITHM AND ARTIFICIAL NEURAL NETWORKS

Imperialist Competitive Algorithm. Imperialist Competitive Algorithm (ICA) is an evolutionary empirical method that addresses the optimization process in different fields. This algorithm is formed by making a mathematical model of socio-political evolution to provide a mathematical algorithm for optimization solutions. For practical purposes, it falls within the same category as the evolutionary optimization algorithms, such as Genetic Algorithms (GA), Particle Swarm Optimization (PSO), Ant Colony Optimization (ACO), and Simulated Annealing (SA) algorithms. Like all algorithms in this category, ICA also forms a group initial probable solution. These early solutions in ICA are also known as "country". ICA within a special process develops these early solutions (countries) and advances them to an optimization point until it reaches state. The foundations of this algorithm are unification, competitive colonization, and revolution [14]. Consider this as mimicking the processes of socio-economic and political evolution in countries. Based on these processes, they created a mathematical algorithm to solve complex optimization problems. In fact, this method presents a repetitive process of gradual improvements -looked at in terms of countries- so to provide a final optimized solution. ICA starts with a random number of societies, each called a country. The numbers of the best elements amongst these are considered as imperialist countries and the rest as colonies. The imperialists depending on their influence try to within a certain process, pull the colonies toward themselves. The power of each empire depends on two elements. One is the imperialist as the central node, and the other its colonies. This dependency has mathematically been considered as the power of the empire, as the power of the imperialist country, plus an average percentage of power of the colonies [14]. Within the formation of the early empires, imperialistic competition between them starts. Any imperialist, which cannot act successfully in colonial competition and add to its power (or at least cannot stop reduction of its power) will be eliminated from the imperialist competition scene. Therefore, survival of any empire depends on absorbing other empires' colonies, and their addition to its circle of power. Thus, in Imperialist competitions,

power of greater empires will gradually increase, and the weaker empires will gradually diminish until they reach to the point of extinction. In order to increase the power of empires it is needed to develop their colonies.

Absorption Policy. Colony Movements toward Imperialist. Policy of uniformity (absorption) with the aim of analyzing the culture & social structure of the colonies was placed in the culture of the central government. As stated earlier, imperial countries in order to progress their influence, started to develop these countries (by creation of universities, transport systems etc.) (i.e. advancing the colonies' infrastructure). In this policy, the colony on the line connecting the colony to the imperialist moves X units toward the imperialist, and reaches a new point. X is a random number with uniform distribution (or any other suitable). If the distance between the colony and the imperialist is shown by d, the amount or parameter d is shown in Equation (1) [14]:

$$x \sim U(0,ß*d), \quad (1)$$

where ß is a number greater than 1 and close to 2. A suitable choice can be ß =2. Coefficient ß≥1 causes the colony while moving towards the imperialist can get close to it in different aspects. In addition, during this movement, a small angular diversion with uniform divergence occurs, which is added to the movement path. A graphical representation of absorption policy in ICA is presented in the two dimensional plane in Fig. 1a [14].

Colony and Imperialist Position Exchange. During movement of the colonies toward the imperialist, it is possible that some colonies will reach a better position than the imperialist will (they reach some points in the cost function, which may cost less than the imperialist may). Under this condition, the colony and the imperialist exchange position, and the algorithm with a new position for the imperialist country. This time, this new imperialist country carries out a new unification policy. New positioning of the colony is shown in Fig. 1b [14].

Introducing Artificial Neural Networks. ANNs have become one of the most active research areas in recent years, which have attracted the attention of scientists in many fields. Neural networks are data processing systems consisting of a large number of simple, highly interconnected processing elements (artificial neurons) in an architecture inspired by the structure of the central cortex of the brain. It has the ability to learn from experiences and information in order to improve its performance and to adapt itself to changes in the environment [15]. Recent research in the field of ANNs has shown that it has great potentials in solving all complex engineering problems. Although ANNs cannot be compared with natural neutral systems, they have features that make them capable of carrying out certain tasks such as differentiating models or where there is need for learning linear or nonlinear mapping. Among the features and capabilities of neural network models is the ability to learn, adapt to the existing data, the ability to develop, apply to similar conditions, parallel processing of entries to a system, and consequently higher speeds of processing and high error tolerance etc. to name but a few [16].

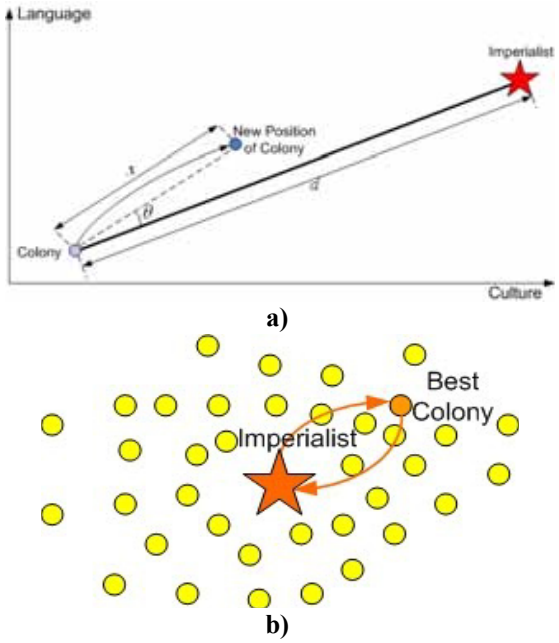

FIGURE 1
a) Carrying out the absorption policy in Imperialist Competitive Algorithm, b) Exchanging positions between imperialist and the colony [14]

Typically, an ANN divides the available data into a training set and a test set: performance of the training- set-calibrated ANN model is verified using the test subset. The early stopping method, however, requires one more subset between the training and the test sets, called the validation set. The typical ANN approach monitors the training error only during the training procedure, but the early stopping method monitors the validation error as well as the training error. The training procedure is terminated when the mean-square error (MSE) of the validation set reaches its minimum. If the ANN is trained further, then it begins to overfit and the mean-square error begins increasing from its minimum.

ANNs are parallel mass data processors that resemble the human brain neural network. The principals of an ANN are: (1) Processing occurs in singular units known as nodes; (2) Signals between the nodes are transmitted via link lines, (3) The given weight to each link line represents its line link power and (4) Each node normally has activating functions and conversion for determining output signals based on input data to the system [16].

Structure of the ANN is introduced in terms of model node connections, method of weight determination, and activity function. The normal structure of an ANN consists of input output layers and hidden inner layer(s) (Fig. 2).

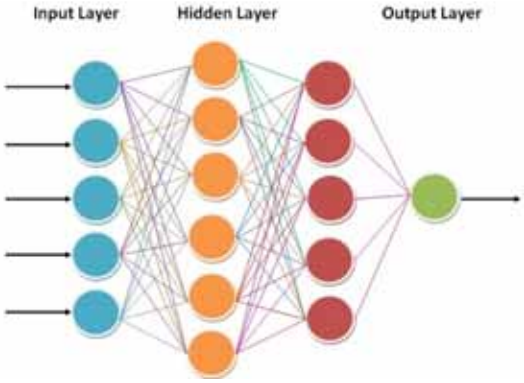

FIGURE 2
Feed Forward ANN or 5-6-5-1 hidden layers

The input layer can be explained as gathering data and transferring it into the system. The output layer is for presenting the predicted outputs by the network. The middle or hidden layer(s) that consist of practicing the nodes have the task of processing the input data. The number of hidden layer(s) and number of nodes in each layer are found via trial and error or using the optimization algorithms. The nodes in each pair of contagious layers are wholly connected to each other. Inputs to each layer could consist of input or output parameters of other nodes. Each node has a transfer function. Inputs are vector spaces in form of X (x_1, x_2, x_3, …, x_n). Every input is weighted and connected to a processing node. Consequently, a collection of weights in the form of W (w_1, w_2, w_3,…, w_n) are linked to the relevant node. "w" shows the link weight from the node on the previous layer to the present layer's node. The output of the node is termed y and is calculated using Equation (2):

$$y = f\left(x.w - b\right) \qquad (2)$$

where y is node output, f is the function, x is input data, w is weight vector, and b is bias, which process the outputs of the node [16].

METHODS

Data and Normalization Methods. The area under study is one covered by the Karoon River Ahvaz Station which is shown in Fig. 3. The Karoon River is the largest river in Iran which makes it to be the only partially navigable river in that country. In other words, with 950 kilometers of route and tributaries, it is the longest river and has the largest volume of water of rivers, which flows only within Iran's boarders. Drinking water of many populated areas including the city of Ahvaz is provided by this river [17], [18].

Monthly data form synopsis stations from 1968 to 2009 was considered. Ahvaz station is located at 39°, 44", 48' longitude and 44°, 20", 31' latitude. Monthly data on parameters including month of the year, discharge, gauge, and sediment density coefficient at Ahvaz station are presented in the Table 1.

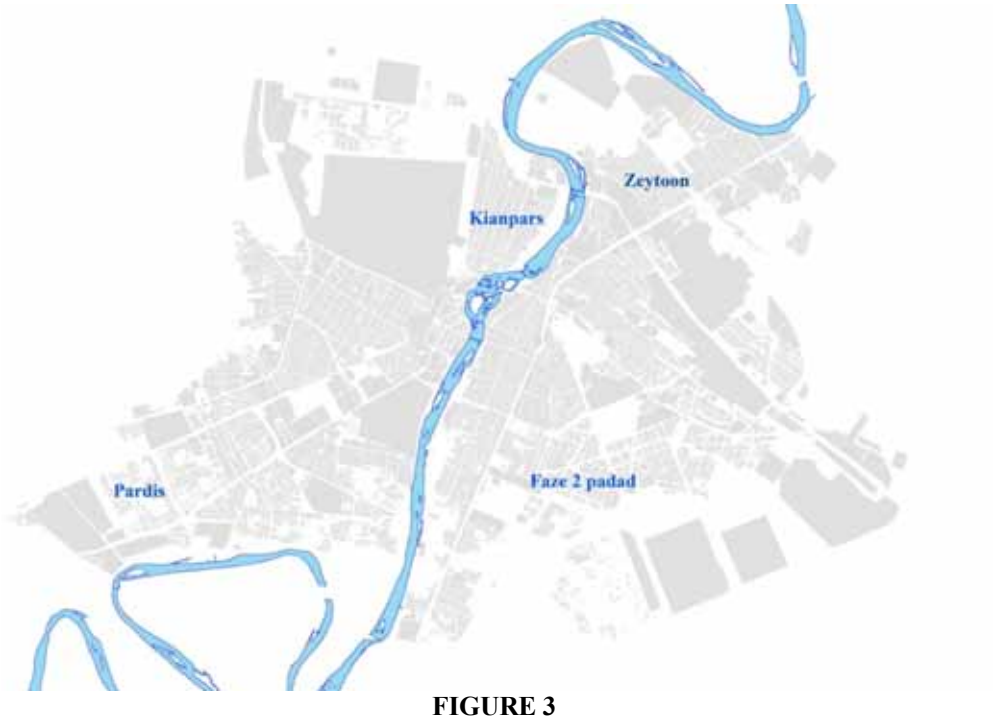

FIGURE 3
Ahvaz station area in Karoon river

TABLE 1
The number of models used along the river

No.	River	Station	Year	Number of used models
1			1968-1971	90
2			1972-1981	169
3	Karoon	Iran-Ahvaz	1982-1991	127
4			1992-2001	133
5			2002-2012	104
		Total		623

TABLE 2
Statistical characteristics of Karoon river parameters at Ahvaz station

No.	Parameter type	Parameter name	Minimum value	Maximum value	Average	Divergence
1	Input	Discharge	8.61	4387	691.23	691.23
2	Input	Height	15	566	175.19	175.19
3	Input	Month	1	12	6.78	6.78
4	Input	Density Coefficient	11	12832.7	626.98	626.98
5	Output	Sediment	99.185	1880000	77137.07	77137.07

TABLE 3
Optimized structure Feed Forward model with features of ICA

		Neural network's features					Utilized initialization parameters in ICA		
No.	Models' name	Number of input	Number of output	Number of hidden layer	Number of nodes in hidden layer	Transfer function	Number of country	Number of imperialist	Number of decade
1	50GEN_2IN	2	1	1	4	tansig	300	20	50
2	50GEN_3IN	3	1	2	4_3	tribas	200	25	50
3	50GEN_4IN	4	1	1	8	satlins	400	40	50
4	50GEN_5IN	5	1	3	4_4_3	satlins	300	30	50
5	100GEN_2IN	2	1	1	4	satlins	300	30	100
6	100GEN_3IN	3	1	1	7	tansig	400	40	100
7	100GEN_4IN	4	1	2	5_4	tansig	500	50	100
8	100GEN_5IN	5	1	2	7_4	satlins	450	45	100
9	150GEN_2IN	2	1	1	5	poslin	400	20	150
10	150GEN_3IN	3	1	1	6	hardlims	250	25	150
11	150GEN_4IN	4	1	1	9	purelin	450	45	150
12	150GEN_5IN	5	1	2	5_5	satlins	400	400	150
13	200GEN_2IN	2	1	1	4	tribas	600	60	200
14	200GEN_3IN	3	1	1	6	satlins	250	25	200
15	200GEN_4IN	4	1	3	3_3_3	poslin	450	45	200
16	200GEN_5IN	5	1	1	11	tribas	600	300	200
17	250GEN_2IN	2	1	1	5	logsig	500	50	250
18	250GEN_3IN	3	1	2	4_3	radbas	250	25	250
19	250GEN_4IN	4	1	1	9	purelin	300	30	250
20	250GEN_5IN	5	1	2	6_5	tansig	500	50	250

Actual statistical data is also presented in Table 2.

Ahvaz station currently has measuring equipment: height and gauge equipment, measuring flume and online sediment measuring system. In order to obtain accurate results, numerical parametric entry data must be normalized for placing in the ANN model. For this purpose, Equation (3) was used:

$$xN = (x - MinX) / (MaxX - MinX) * 2 - 1 \quad (3)$$

where xN is the normalized entry data, x the entry data, MinX the minimum value of all of the data and MaxX the maximum value of all of the data.

The output parameter is found according to Equation (4):

$$yN = (y - MinY) / (MaxY - MinY) * 2 - 1 \quad (4)$$

where yN is the normalized sediment data, y is the sediment data, Min Y is minimum of all presented sediment data, and MaxY is the maximum value of all presented data. Therefore, all normalized data fall within the [-1, +1] range.

Research Process. The ANN used in this research was Feed Forward. The inputs were discharge, previous day's discharge, gauge, month of

the year, and sediment density, and the output is sediment volume. This network is shown in Fig. 2. From 623 data models, 80% (503) were used for training and 20% (125) for testing the network. Equation (5) was used for determining the number of hidden nodes experimental [19]:

$$N_H \leq 2N_I + 1 \quad (5)$$

where N_H is the maximum number of nodes in the hidden layer(s) and N_I is the number of entered data.

Considering that the number of entered data is five, the maximum nodes in the hidden layer(s) is 11 (i.e. $(N_H \leq 11)$). Competitive Imperialist Algorithm was used for optimizing the weight of each of the artificial neural models. Table (3) presents the optimized structure of each model together with features of the ICA. Tables (4) and (5) show the results of training and testing with optimization of each structure from Table (3). In order to determine each model's performance and finding the best result, MSEtest and MSEtrain of each model is compared with the other models. Considering the gained results Feed Forward model with its weights optimized through Imperialist Competitive Algorithm, and with the 1-5-6-5 structure, having specification of 500 countries, 50 empires, and 250 optimization repeats, provides the best results among the considered models.

TABLE 4
Results from Feed Forward models with features of ICA in testing and training

No.	Model	Best fitting line in training phase		Best fitting line in testing phase		Results in MATLAB		
		Equation	R^2	Equation	R^2	MSE train	MSE test	Best Cost
1	50GEN_2IN	y = 0.4018x - 0.2518	0.3727	y = 0.3974x - 0.2639	0.2995	0.1198	0.1197	0.1198
2	50GEN_3IN	y = 0.005x + 0.0048	0.0981	y = 0.0042x + 0.0044	0.0252	0.9019	0.8959	0.9019
3	50GEN_4IN	y = 0.549x - 0.379	0.3033	y = 0.6026x - 0.3575	0.3216	0.0551	0.0425	0.0551
4	50GEN_5IN	y = 0.1287x - 0.0512	0.2393	y = 0.1691x - 0.0155	0.2599	0.6047	0.596	0.6047
5	100GEN_2IN	y = 0.5683x - 0.1899	0.3403	y = 0.5295x - 0.2423	0.2519	0.0866	0.0889	0.0866
6	100GEN_3IN	y = 0.5621x - 0.2331	0.3659	y = 0.5732x - 0.2392	0.3102	0.0883	0.0859	0.0883
7	100GEN_4IN	y = 0.4041x - 0.5228	0.4293	y = 0.3375x - 0.58	0.2661	0.0493	0.0535	0.0493
8	100GEN_5IN	y = 0.7321x - 0.2593	0.6706	y = 0.476x - 0.4996	0.3767	0.0293	0.0479	0.0293
9	150GEN_2IN	y = 0.0231x + 0.0223	0.1657	y = 0.0293x + 0.0288	0.1396	0.9017	0.8961	0.9017
10	150GEN_3IN	y = 0.3284x - 0.6757	0.1483	y = 0.1984x - 0.7898	0.0429	0.0982	0.1125	0.0982
11	150GEN_4IN	y = 0.5531x - 0.3228	0.2135	y = 0.7998x - 0.1144	0.3967	0.1199	0.0778	0.1199
12	150GEN_5IN	y = 0.6825x - 0.303	0.6629	y = 0.473x - 0.4949	0.4441	0.0295	0.0411	0.0295
13	200GEN_2IN	y = 0.0324x + 0.0314	0.2447	y = 0.0521x + 0.0538	0.056	0.9016	0.9011	0.9016
14	200GEN_3IN	y = 0.5609x - 0.3377	0.3071	y = 0.5526x - 0.3708	0.2671	0.0569	0.0483	0.0569
15	200GEN_4IN	y = 0.0103x + 0.7791	0.0048	y = 0.0539x + 0.816	0.1557	3.1136	3.1240	3.1136
16	200GEN_5IN	y = 0.1657x + 0.1568	0.4162	y = 0.1312x + 0.1238	0.271	0.8981	0.8947	0.8981
17	250GEN_2IN	y = 0.0356x + 0.076	0.3178	y = 0.0419x + 0.0814	0.2901	0.9771	0.9727	0.9771
18	250GEN_3IN	y = 0.0098x + 0.0128	0.219	y = 0.0109x + 0.0139	0.181	0.8849	0.8743	0.8849
19	250GEN_4IN	y = 0.493x - 0.3398	0.229	y = 0.6992x - 0.168	0.385	0.1051	0.0734	0.1051
20	250GEN_5IN	y = 0.823x - 0.1484	0.8698	y = 0.768x - 0.199	0.894	0.0267	0.0350	0.0267

TABLE 5
Statistical results of optimized ANNs through ICA

No.	Model	MAE		RMSE		MARE		RMSD	
		train	test	train	test	train	test	train	test
1	50GEN_2IN	0.334	0.323	0.132	0.127	-0.476	-0.397	0.566	0.556
2	50GEN_3IN	0.921	0.915	0.879	0.867	-0.284	-0.152	0.952	0.951
3	50GEN_4IN	0.129	0.104	0.076	0.066	-0.091	0.094	0.247	0.213
4	50GEN_5IN	0.759	0.752	0.595	0.581	-4.211	-3.953	0.865	0.863
5	100GEN_2IN	0.250	0.236	0.107	0.107	-0.401	-0.346	0.459	0.443
6	100GEN_3IN	0.214	0.200	0.087	0.085	-0.177	-0.184	0.430	0.413
7	100GEN_4IN	0.101	0.108	0.048	0.054	-0.203	0.032	0.260	0.272
8	100GEN_5IN	0.058	0.075	0.029	0.047	-0.118	-0.047	0.169	0.182
9	150GEN_2IN	0.921	0.915	0.878	0.867	-0.098	-0.061	0.952	0.951
10	150GEN_3IN	0.109	0.124	0.097	0.114	-0.077	-0.075	0.206	0.216
11	150GEN_4IN	0.200	0.158	0.119	0.076	-2.629	-0.202	0.369	0.326
12	150GEN_5IN	0.056	0.066	0.029	0.040	-0.071	-0.017	0.167	0.176
13	200GEN_2IN	0.921	0.920	0.878	0.875	-0.223	-0.170	0.952	0.954
14	200GEN_3IN	0.134	0.116	0.079	0.075	-0.375	0.357	0.254	0.224
15	200GEN_4IN	1.662	1.659	2.844	2.818	2.164	2.169	1.281	1.282
16	200GEN_5IN	0.914	0.911	0.873	0.864	13.312	13.456	0.945	0.947
17	250GEN_2IN	0.961	0.955	0.954	0.941	24.460	24.760	0.973	0.972
18	250GEN_3IN	0.925	0.918	0.885	0.872	291.004	288.035	0.954	0.952
19	250GEN_4IN	0.194	0.158	0.104	0.072	3.013	-0.676	0.370	0.333
20	250GEN_5IN	0.046	0.044	0.011	0.009	-0.017	-0.088	0.183	0.182

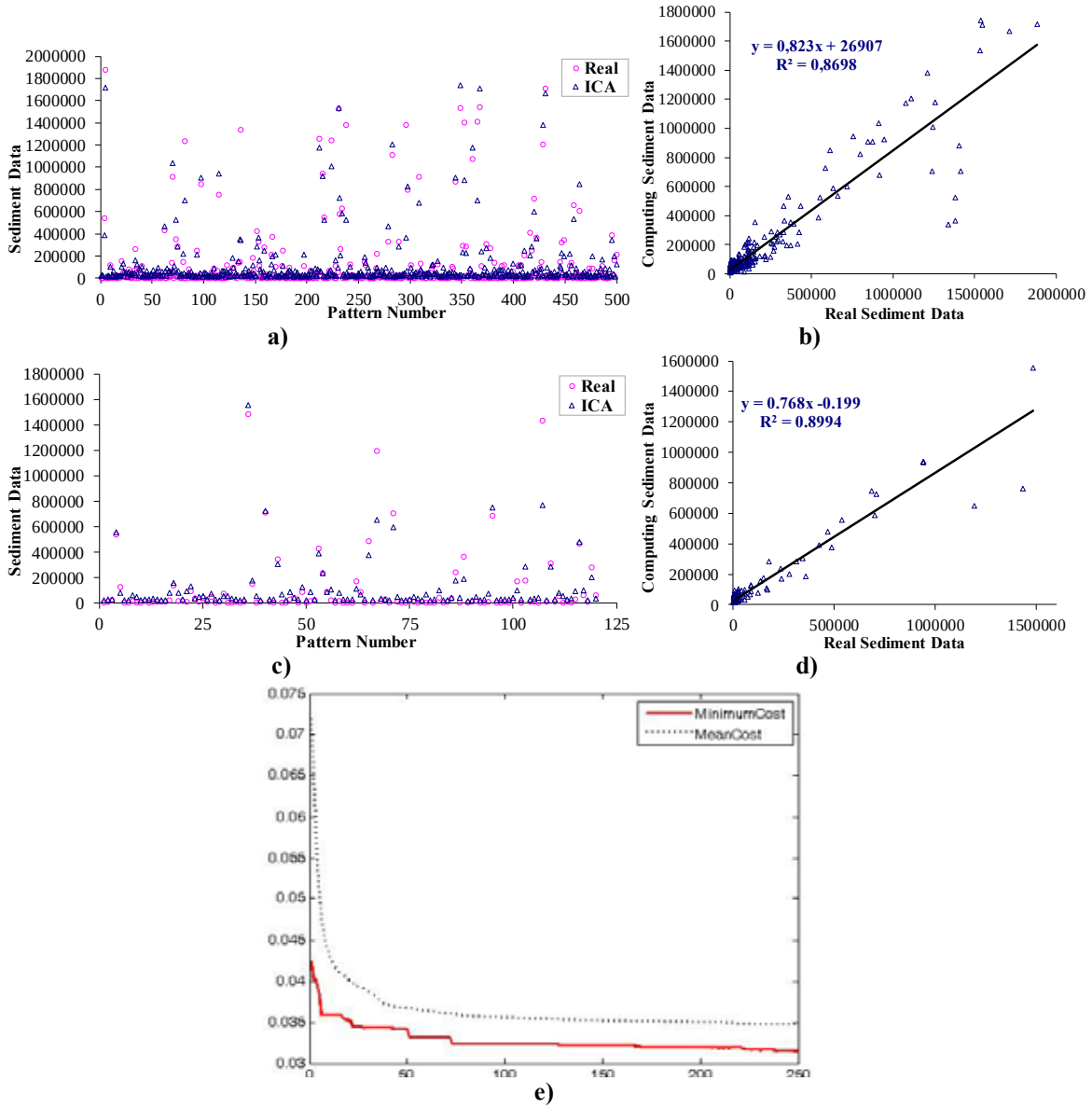

FIGURE 4

a) Determining sedimentation by combined FF and ICA models in training stage, b) Sedimentation comparison in combined FF and ICA models in training stage according to collected data, c) Determining sedimentation by combined FF and ICA models in testing stage, d) Sedimentation comparison in combined FF and ICA models in testing stage according to collected data, e) Cost diagram for 250 repetition on FF-ICA-20 model as the best model

The R^2 coefficient which ranges from 0 to 1 provides a measure of how well observed outcomes are replicated by the model, as the proportion of total variation of outcomes explained by the model. The best model is the one which demonstrates a higher value of R^2. As presented in Table 4, in Model No. 20, R^2 is the coefficient for sedimentation parameter. For training and testing, these values were 0.8698 and 0.894, respectively. For the straight-line slope, this parameter is 0.823 and 0.768, respectively, which states the degree of accuracy of the sedimentation modeling. From Table 5, MAE, RMSE, MARE and RMSD coefficients in the two stages of training and testing of the Artificial Neural Network with structure of 5-6-5-1 and specification of 500 countries, 50 empires, and 250 optimization repeats provide the least value, which indicates the lower error of this model. Therefore, the FF model labeled 250GEN_5IN presented higher accuracy than its other similar models. The results of the FF model with specification of 5-6-5-1 structure with 500 countries, 50 empires, and 250 repeats in relation with other models used are provided in Fig. 4a) to 4d). In addition, the minimum cost and mean cost diagrams are presented as the best models in Fig. 4e). From this diagram, minimum cost and mean cost coefficients are found as 0.0347 and 0.0315, respectively.

TABLE 6
Introducing GA, PSO and ICA algorithm parameters

GA		PSO		ICA	
Population	150	Maximum of Swarm	200	Countries	500
Mutation Rate	15	Cognition Coefficient	2		
Crossover Rate	50	Social Coefficient	2	Empires	50
Generation	250	Maximum of Generation	250	Generation	250

TABLE 7
Results of different algorithms in the two stages of training and testing

No	Model	Best fitting line in training phase		Best fitting line in testing phase	
		Equation	R^2	Equation	R^2
1	250GEN_5IN	y = 0.823x - 0.1484	0.8698	y = 0.768x - 0.199	0.894
2	GA	y = 0.5618x - 0.3865	0.5861	y = 0.7502x - 0.1948	0.7048
3	PSO	y = 0.6376x - 0.3221	0.642	y = 0.7425x - 0.2118	0.7044

TABLE 8
Optimized ANN statistical data with different algorithms in the two stages of training and testing

No.	Model	MAE		RMSE		MARE		RMSD	
		train	test	train	test	train	test	train	test
1	250GEN_5IN	0.046	0.044	0.011	0.009	-0.017	-0.088	0.183	0.182
2	GA	0.072	0.072	0.035	0.024	-0.017	-0.058	0.224	0.229
3	PSO	0.055	0.059	0.030	0.024	-0.003	-0.040	0.194	0.203

Evaluation of the Model. To evaluate the optimized FF model using ICA, it was compared to Genetic Algorithm and PSG. Their features are presented in Table 6. In addition, FF ANN model with 5-6-5-1 structure with Tansig excitation function was used for the three algorithms.

Table 7 shows coefficients of the three studied models for the given training data, R^2 testing coefficients and the slope of the straight line.

Table 7 shows sedimentation results from the three models. Table 8 also shows the statistical data. Figs. 5 a) and b) make a comparison between calculated and observed data by the three models in the training stage. In addition, the cost diagram for the three models is shown in Fig. 5 c).

Using the given equations of fitted lines over calculated and observed values in each model, and coefficient of determination in Table 7, and the collected statistical data in Table 8, it is shown that the optimized ANN by ICA has a greater accuracy over the Genetic and PSO algorithms. Due to sediment predictions in the three models in Fig. 5a - b, it is clear that the optimized ANN by ICA has greater accuracy over the other two models. The cost diagram is presented in Fig. 5c.

CONCLUSION

Results of this study show that the suggested method (i.e. use of ANNs and ICA for finding optimization point for these functions) is successful. In addition, different practical problems resolved via this algorithm show that the suggested optimization strategy can be used successfully alongside other methods of optimization such as genetic algorithm and particles swarm group in solving river engineering problems. Comparison of the results obtained by this algorithm with other popular optimization methods also indicates provision of better results. Optimization of imperialistic competitive algorithm can be used as a powerful tool in optimizing weights within artificial neural networks.

Comparison of the results from training and testing of different artificial neural networks optimized by imperialistic competitive algorithm with the structure 5-6-5-1 with Tan sigmoid transfer function and specifications of 500 countries, 50 empires and 250 repeats has better ability and greater accuracy in sediment prediction.

In the best artificial neural network optimized by imperialistic competitive algorithm, for predicting sedimentation coefficient R^2 in training and testing stages, these were 0.894 and 0.8698, respectively. The straight-line slope for this parameter is 0.768 and 0.823, respectively, which states the degree of accuracy of sedimentation modeling. The statistical coefficients MAE, RMSE, MARE and RMSD were less than the other models. This indicates lesser error of this model. For evaluating the optimized ANN by ICA, the ICA was compared with GA and PSO algorithm. Results showed that the optimized ANN by ICA has greater accuracy and flexibility over the other two algorithms.

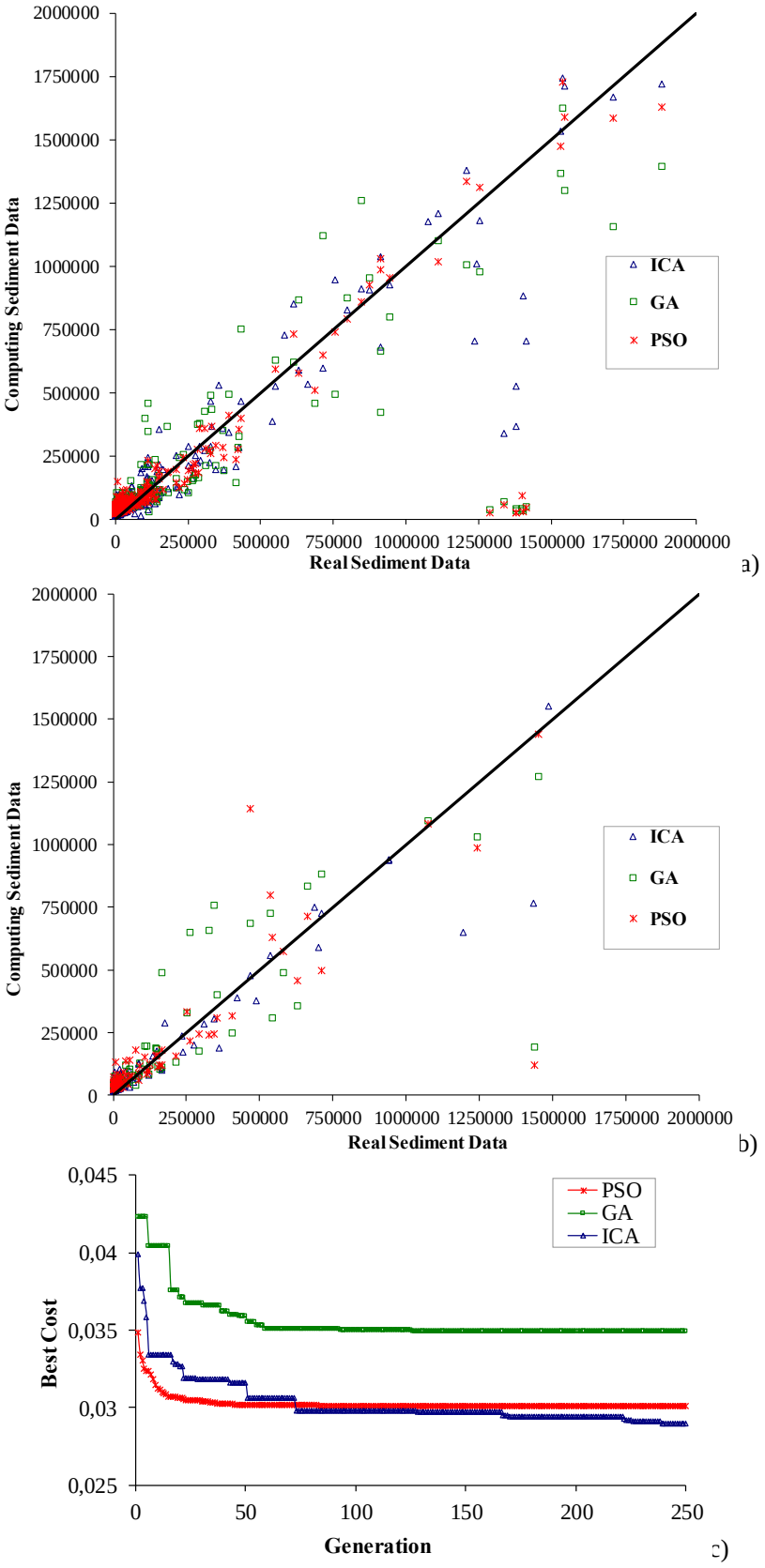

FIGURE 5
Comparison of estimated and observed sedimentation by ICA, GA and PSO algorithms in: a) training stage, b) testing stage, c) cost diagram for 250 repeats for FF-PSO, FF-GA and FF-ICA

REFERENCES

[1] Fang, H.W., Lai, R.X., Lin, B.L., Xu, X.Y., Zhang, F.X. and Zhang, Y.F. (2016) Variational-Based Data Assimilation to Simulate Sediment Concentration in the Lower Yellow River, China. Journal of Hydrological Engineering. 21(5), 04016010-1– 04016010-11.

[2] Hadzima-Nyarko, M., Rabi, A. and Šperac, M. (2014) Implementation of Artificial Neural Networks in Modeling the Water-Air Temperature Relationship of the River Drava. Water Resources Management. 28, 1379–1394.

[3] Santos C.A.G. and da Silva, G.B.L. (2014) Daily streamflow forecasting using a wavelet transform and artificial neural network hybrid models. Hydrological Sciences Journal. 59(2), 312–324.

[4] Rabi, A., Hadzima-Nyarko, M. and Šperac, M. (2015) Modelling river temperature from air temperature: case of the River Drava (Croatia). Hydrological Sciences Journal. 60(9), 1490-1507.

[5] Fathian, H., Nikoo, M. and Nikoo, M. (2011) River Flood Routing Using Evolutionary Artificial Neural Networks. Water Engineering. 3(5), 13–23.

[6] Yitian, L. and Gu, R.R. (2003) Modeling Flow and Sediment Transport in a River System Using an Artificial Neural Network. Environ Manage. 31(1), 0122–0134.

[7] Alp, M. and Cigizoglu, H. (2007) Suspended sediment load simulation by two artificial neural network methods using hydrometeorological data. Environmental Modelling & Software. 22(1), 2–13.

[8] Doğan, E., Yüksel, İ. and Kişi, Ö. (2007) Estimation of total sediment load concentration obtained by experimental study using artificial neural networks. Environmental Fluid Mechanics. 7(4), 271–288.

[9] Kisi, Ö. (2008) Constructing neural network sediment estimation models using a data-driven algorithm. Mathematics and Computers in Simulation. 79(1), 94–03.

[10] Yang, C.T., Marsooli, R. and Aalami, M.T. (2009) Evaluation of total load sediment transport formulas using ANN. International Journal of Sediment Research. 24(3), 274–286.

[11] Melesse, A., Ahmad, S., McClain, M., Wang, X. and Lim, Y. (2011) Suspended sediment load prediction of river systems: An artificial neural network approach. Agricultural Water Management. 98(5), 855–866.

[12] Rajaee, T. (2011) Wavelet and ANN combination model for prediction of daily suspended sediment load in rivers. Science of the Total Environment. 409(15), 2917–2928.

[13] Ramezani, F., Nikoo, M. and Nikoo, M. (2014) Artificial neural network weights optimization based on social-based algorithm to realize sediment over the river. Soft Computing. 19, 375–387.

[14] Atashpaz-Gargari, E. and Lucas, C. (2007) Imperialist competitive algorithm: An algorithm for optimization inspired by imperialistic competition. In: Proceedings of the IEEE Congress on Evolutionary Computation. Singapore. 4661 – 4667.

[15] Nikoo, M., Ramezani, F., Hadzima-Nyarko, M., Nyarko, E.K. and Nikoo, M. (2016) Flood-routing modeling with neural network optimized by social-based algorithm. Natural Hazards. 82, 1–24.

[16] Galushkin, A.I. (2007) Neural Networks Theory. Springer Berlin Heidelberg, Berlin.

[17] Afkhami, M., Shariat, M., Jaafarzadeh, N., Ghadiri, H. and Nabizadeh, R. (2007) Regional water quality management for the Karun–Dez River basin, Iran. Water and Environment Journal. 21, 192–199.

[18] Afshar, A., Mariño, M.A., Saadatpour, M. and Afshar, A. (2011) Fuzzy TOPSIS Multi-Criteria Decision Analysis Applied to Karun Reservoirs System. Water Resources Management. 5(2), 545–563.

[19] Bowden, G.J., Dandy, G.C. and Maier, H.R. (2005) Input determination for neural network models in water resources applications. Part 1-background and methodology. Journal of Hydrology. 301, 75–92.

Received: **17.08.2017**
Accepted: **31.01.2018**

CORRESPONDING AUTHOR

Marijana Hadzima-Nyarko
Faculty of Civil Engineering,
University of J.J. Strossmayer,
Vladimira Preloga 3,
31000 Osijek – Croatia

e-mail: mhadzima@gfos.hr

© by PSP Volume 27 – No. 7/2018 pages 4668-4673 Fresenius Environmental Bulletin

ASSESSMENT OF RELATIONSHIP BETWEEN FRUIT CHARACTERISTICS OF ALMOND SELECTIONS FROM AYDIN REGION USING CANONICAL CORRELATION ANALYSIS METHOD

Ersin Gulsoy[1,*], Mikdat Simsek[2], Mehmet Kazim Kara[3], Fikri Balta[4]

[1]Igdir University, Faculty of Agriculture, Department of Horticulture, Igdir, Turkey
[2]Dicle University, Faculty of Agriculture, Department of Horticulture, Diyarbakir, Turkey
[3]Igdir University, Agricultural Faculty, Biometry and Genetic of Animal Husbandry, Igdir, Turkey
[4]Ordu University, Faculty of Agriculture, Department of Horticulture, Ordu, Turkey

ABSTRACT

Selection of promising genotypes possessing superior yield and quality traits among the rich almond seedling population in Turkey is necessary for increasing the contribution of these genotypes to the Turkish economy through propagation. It is also important to consider the relationship between yield and quality traits when making this selection. The aim of this study was to determine the relationship between two sets of variables created considering characteristics of fruit and kernel of almond by using the canonical correlation analysis method, which is one of the multivariable analysis methods. In this method, the relationship between two canonical variables and the major variables of the same set was examined. It was concluded that the increase in fruit weight (FWe) and fruit thickness (FT) led to a significant decrease in kernel weight (KWe) and kernel ratio (KR).

KEYWORDS:
Almond, fruit and kernel traits, canonical correlation

INTRODUCTION

Cultivated almond, which is classified in the subgenus Amygdalus from the genus Prunus of the family Rosaceae in the order Rosales, has a wide distribution area in the world. The subgenus Amygdalus includes about 40 cultivars of almond, and 12 of them are grown in Turkey [1- 4]. Almond is one of the popular fruits being increased in both production and consumption owing to the fact that human health and beneficial all over the word [5, 6]. Furthermore, sweet almond fruit is used in the food industry and almond oil obtained from bitter almond used in the chemistry industry [7-9]. In addition, almond is one of the important fruits recommended and be consumed in the human diet, due to its contents of fatty acids, protein, dietary fiber, polyphenols, vitamins C and E and many minerals [10-13]. In this context, the almond kernels have been used to prevent important diseases of the heart and autoimmune system, rheumatoid arthritis, and cancer in recent years [9, 14].

Almond is cultivated in every region from east to west and from north to south in Turkey, however, cultivation is mostly centered in Aegean, Mediterranean, and Marmara regions [15-17]. According to 2014 data, Turkey is ranked as the world's 6th almond-producing country [18].

Although Turkey has a rich genetic resource pool of almond, production, mainly obtained from seedling trees, causes to have several problems in terms of both cultivation and marketing [19].

For solution of such problems, transition to modern cultivation has recently been started by grafting standard almond cultivars onto clonal rootstocks [20, 21]. However, since almond has been directly cultivated from the seed in Turkey for thousands of years, an extremely wide and diverse almond population of seed origin has occurred in different localities of Turkey. A large number of promising almond genotypes with respect to quality and yield characteristics have also been identified by several selection studies conducted on this rich population [22-24]. The issue mostly addressed in selection studies is to obtain individuals with high yield and quality [4]. In this context, it is considerably important to know the relationship between yield and quality traits in order to get the expected benefit from selection studies [25]. A correct approach is to put emphasis on generally more than one traits and examine these traits one by one, as seen in in numerous scientific studies. However, addressing and evaluating these traits together via appropriate analysis methods may enable the researcher to have more information [26]. Canonical correlation is one of these methods. The relationship between two sets of variables, consisting of numerous variables in each, can only be investigated by canonical correlation analysis method [27- 31]. In the present study, it was aimed to identify the relationship between some fruit

and kernel traits of almond by using canonical analysis method in almond genotypes selected from the Aydın region.

MATERIALS AND METHODS

Material. Material used in the study consisted of 307 almond genotypes. A total of 10 parameters including 5 fruit traits (fruit weight, fruit length, fruit width, fruit thickness, shell thickness) and 5 kernel traits (kernel weight, kernel length, kernel width, kernel thickness, kernel ratio) were investigated. Five of them was grouped as X while the remaining 5 was grouped as Y.

Method. When it comes to comparing different treatment groups, it is known that evaluating them together will provide additional information to researcher. In case that both dependent and independent variables are more than one, canonical correlation, based on determination of the linear relationship between canonical variables (X and Y) consisting of linear components of variables that are found in these two sets of variables, is used to identify the relationship between both sets of variables [32, 33].

In case that numbers of variables (p, q) of variable sets are q≥p, the correlation between these can be calculated via linear combinations of variables in these two sets. Correlation coefficients calculated in this way are called as canonical correlation and the new variables consisting of linear combinations of variables are called as canonical variables.

Canonical variables and canonical correlations between them are calculated independently [34-36]. (When a variable set of X is presented as X' [X_1, X_2,.....X_p] and a variable set of Y is presented as Y' [Y_1,Y_2,.....Y_q], the correlation between U= a′X linear combination calculated from the variable set of X and V=b′Y linear combination calculated from the variable set of Y can be calculated. Hereunder, the canonical correlation between U (the canonical variable) and V (the canonical variable) is calculated as follows;

r_{UV}= a′S_{12}b

The test method suggested by Bartlett [37] determines whether the correlation between two variables is significant or not [38]. The statistics of χ^2 (Chi-square) is calculated as follows;

χ^2= -[n-0.5 (v_1+v_2 + 1)]x log(λ).

In this equation, n is the number of observations, v_1 is the number of variables in the first set, v_2 is the number of variables in the second set. Lambda (λ) is calculated as follows;

λ= (1-R^2_{k1}) (1-R^2_{k2})…….(1-R^2_{kp}). χ^2 statistics calculated from here is compared to table value of χ^2 with (p x q) degrees of freedom. By this way, the number of significant canonical correlation coefficients are calculated.

RESULTS AND DISCUSSION

Table 1 shows descriptive statistics of the traits addressed in the present study and Table 2 shows the correlation coefficients of these traits. When Table 2 was examined, it was observed that there was a significant negative correlation between kernel ratio (KR) and fruit weight (FWe), fruit length (FL), fruit width (FW), shell thickness (ST), fruit thickness (FT), and kernel width (KW). Likewise, a significant negative correlation was also determined between kernel thickness (KT), fruit length (FL), and shell thickness (ST).

Other correlations were generally found to be positively significant. However, no correlation was determined between kernel ratio (KR) and kernel weight (KWe), and between kernel thickness (KT) and fruit weight (Few), and fruit width (FW).

TABLE 1
Descriptive statistics for the studied traits

	Variables	Mean	SEM	Std	Min.	Max.
X variable set	FWe (g)	4.71	0.07	1.31	1.89	9.82
	FL (mm)	32.30	0.24	4.17	21.27	50.68
	FW (mm)	22.09	0.14	2.53	15.55	31.99
	ST (mm)	3.28	0.04	0.63	1.86	5.47
	FT (mm)	15.17	0.09	1.59	11.15	19.99
Y variable set	KWe (g)	0.98	0.01	0.21	0.50	1.88
	KL (mm)	22.60	0.17	2.89	13.30	30.37
	KW (mm)	12.90	0.09	1.61	8.18	17.99
	KT (mm)	6.43	0.04	0.74	3.31	9.39
	KR (%)	21.47	0.25	4.37	10.02	47.31

FWe: Fruit Weight, FL: Fruit Length, FW: Fruit Width, ST: Shell Thickness, FT: Fruit Thickness, KWe: Kernel Weight,
KL: Kernel Length, KW: Kernel Width, KT: Kernel Thickness, , KR: Kernel Ration. SEM: standard error of the differences between means.

TABLE 2
Pearson correlation coefficients in two sets

	FWe	FL	FW	ST	FT	KWe	KL	KW	KT	KR
FWe	1									
FL	0.679**	1								
FW	0.883**	0.554**	1							
ST	0.800**	0.371**	0.727**	1						
FT	0.735**	0.253**	0.711**	0.792**	1					
KWe	0.706**	0.574**	0.658*	0.337**	0.592**	1				
KL	0.589**	0.798**	0.450**	0.214**	0.191**	0.701**	1			
KW	0.705**	0.404**	0.785**	0.505**	0.564**	0.744**	0.546**	1		
KT	-0.052	-0.172**	-0.108	-0.208**	0.255**	0.424**	0.133*	0.205**	1	
KR	-0.593**	-0.316**	-0.500**	-0.724**	-0.361**	0.097	-0.056	-0.181**	0.520**	1

FWe: Fruit Weight, FL: Fruit Length, FW: ST: Shell Thickness Fruit Width, FT: Fruit Thickness, KWe: Kernel Weight, KL: Kernel Length, KW: Kernel Width, KT: Kernel Thickness, KR: Kernel Ration *p<0.05 **p<0.01

TABLE 3
Canonical correlation coefficients

Canonical variable	Canonical correlation	P value	Wilk's Lambda
U_1V_1	0.974	0.0001	0.7744
U_2V_2	0.851	0.0001	0.8863
U_3V_3	0.8257	0.0001	0.9780
U_4V_4	0.5803	0.0001	0.9997
U_5V_5	0.0820	0.1550	1.000

TABLE 4
Standardized canonical coefficients and canonical loadings for X variable set

		X variable set				
		FWe	FL	FW	ST	FT
Standardized canonical coefficients	U_1	0.825	0.1193	0.1435	0.0161	-0.0723
Canonical loadings	U_1	0.6313	0.0286	0.0567	0.0256	-0.0455

FWe: Fruit Weight, FL: Fruit Length, ST: Shell Thickness, FW: Fruit Width, FT: Fruit Thickness

TABLE 5
Standardized canonical coefficients and canonical loadings for Y variable set

		Y variable set				
		KWe	KL	KW	KT	KR
Standardized canonical coefficients	V_1	0.7384	0.0926	0.0501	-0.1334	-0.5875
Canonical loadings	V_1	3.5171	0.0321	0.0310	-0.1795	-0.1345

KWe: Kernel Weight, KL: Kernel Length, KW: Kernel Width, KT: Kernel Thickness, KR: Kernel Ration

The numbers of variables in both sets of variables were not equal in the study (p=5, q=5). Table 3 shows 5 pairs of canonical variables and 5 canonical correlations, significance degrees and Wilk Lambda values of these correlations. As is seen in Table 3, the first four canonical correlation coefficients were high at extremely significant level (p< 0.001). Table 4 and Table 5 shows canonic coefficients which were standardized according the first canonic variable pair by considering the first highest canonic correlation.

Occurrence of canonical variables in a set of variables is written considering the coefficients indicating the impact ratios (contributions) of the original variables in that set to the equations of canonical variables U_1 and V_1 as follows;

U_1= 0.825 FWe+0.119 FL+ 0.1435 FW+ 0.016ST-0.072 FT

V_1 = 0.738KWe+ 0.093 KL-0.05 KW-0.133 KT-0.588KR

While impact ratio (contribution) of fruit weight (FWe) was substantially high (0.83) in occurrence of canonical variable U_1, the contribution of fruit length (FL) was 0.119 and the contribution of fruit width (FW) was relatively high. The contribution of shell thickness (ST) was 0.016, which was considerably low. The contribution of fruit length (FL) was -0.072, which was relatively low in the negative direction.

In occurrence of V_1 canonical variable, while the contribution of kernel weight (KWe) was high

(0.738), the contribution of kernel width (KW) was relatively low (0.093). Here, the contribution of kernel ratio (KR) was quite high in the negative direction (0.588). In other words, this variable was effective on occurrence of V_1 canonical variable. The contribution of kernel thickness (KT) was negative but low (-0.133). The contribution of kernel width (KW) was negative and very low (-0.05).

When we looked at canonical loadings between variables in the variable set of X and their canonic variables (U_1) in Table 4, fruit weight (FWe) variable was observed to have the maximum value of loading (0.631). Fruit length (FL) (0.0286), fruit width (FW) (0.0567), and shell thickness (ST) (0.0256) were found to be quite low. According to standardized coefficients, while the loading of fruit weight (FWe), which had the highest coefficient of 0.825, the loading of fruit length (FL) was 0.119, which was also relatively high. The loading of fruit thickness was negative and observed as -0.0455. In variable set of Y, the highest canonical loading value (3.5171) was observed in kernel weight (KWe). Values of kernel length (KL) (0.032) and kernel width (KW) (0.031) were fairly low. Loadings for Kernel thickness (KT) and kernel ratio variables were found to be negative but relatively high as -0.179 and -0.134, respectively. According to standardized coefficients, the variable with the highest coefficient was kernel weight (KWe). However, kernel ratio (KR) and kernel thickness (KT) carrying very low canonical loadings had a negative effect on standardized canonical coefficients.

In a study considering fruit and kernel traits in walnut, the correlations between canonical variables in all of X and Y variables (except for ST) were positive and very high [25]. On the other hand, in the present study, the increase in fruit weight (FWe) and fruit thickness (FT) of almond substantially caused a decrease in kernel weight (KWe) and kernel ratio (KR).

CONCLUSION

Selection constitutes the basis of plant breeding and it is based on the process of selecting expedient superior individuals from within a genetically-variable plant population. At the first step of selection, it is quite important to select individuals with high yield and quality. When selection succeeds, a population that is phenotypically and genotypically different from the initial population is obtained.

Thanks to canonical analysis method which is used to identify the relationship between two sets of variables including a multiple number of variables in each one, it is possible to address and evaluate several traits examined on selection studies. Therefore, researchers can also utilize multivariate analysis as well as univarite analysis. In addition, researchers should be encouraged to use canonical analysis more since this method enables the researchers to obtain more information when compared to univarite analysis method.

In the present study, it was aimed to identify the relationship between fruit traits which are considered to be important for almond breeding by using canonical analysis. Analysis results revealed that as fruit weight, length, width and thickness of almonds increased, kernel ratio decreased; kernel ratio decreased with increasing kernel width as well. The present study is expected to be beneficial for researchers studying on almond breeding and selection fields.

ACKNOWLEDGEMENTS

This study was produced by Ersin Gulsoy's PhD thesis.

REFERENCES

[1] Gülcan, R. (1976) Seçilmiş badem tipleri üzerinde fizyolojik ve morfolojik araştırmalar. Ege Üniv. Zir. Fak. Yay. No:310, Bornova, İzmir, 72p.
[2] Özbek, S. (1977) Genel meyvecilik. Ç.Ü. Ziraat Fak. Yayınları No:111 DK: 6, Adana, 386p.
[3] Socias i Company, R. and Felipe, A.J. (1992) Almond: a diverse germplasm. Hort Science. 27(7), 718.
[4] Şimşek, M., Çömlekçioğlu, S. and Osmanoğlu, A. (2010) Çüngüş ilçesinde doğal olarak yetişen bademlerin seleksiyonu üzerinde bir araştırma. Harran Üniversitesi Ziraat Fakültesi Dergisi. 14(1), 37-44.
[5] Chen, C.Y., Milbury, P.E., Lapsley, K. and Blumberg, J.B. (2005) Flavonoids from almond skins are bioavailable and act synergistically with vitamins C and E to enhance hamster and human LDL resistance to oxidation. Journal of Nutrition. 135(6), 1366-1373.
[6] Oguz, H.I., Erdogan, O., and Bagdatli, M.C. (2017) Effect of Different Applications on Rooting of Cutting of Some Almond Rootstocks (Prunus dulcis L.). Fresen. Environ. Bull. 26, 2609-2614.
[7] Davis, A.P. and Iwahasi K.C. (2001) Whole almonds almond fractions reduce aberrant crypt foci in a rat model of colon carcinogenesis. Cancer Lett. 165, 27-33.
[8] Piscopo A., Romeo F.V., Petrovicova, B. and Poiana M. (2010) Effect of the harvest time on kernel quality of several almond varieties (Prunus dulcis Mill). Scientia Horticulturae. 125, 41-46.

[9] Şimşek, M. and Kızmaz, V. (2017) Determination of Chemical and Mineral Compositions of Promising Almond (*Prunus amygdalus* L.) Genotypes from Beyazsu (Mardin) Region. International Journal of Agriculture and Wildlife Science (IJAWS). 3(1), 6-11.

[10] McManus, K., Antinoro, L. and Sacks, F. (2001) A randomized controlled trial of a moderate-fat, low-energy diet compared with a low fat, low-energy diet for weight loss in overweight adults. Int Journal of Obesity and Related Metabolic Disorders. 25, 1503 –1511.

[11] Fraser, G.E., Bennett, H.W., Jaceldo, K.B and Sabate, J. (2002) Effect on body weight of a free 76 kilojoule (320 calorie) daily supplement of almonds for six months. J American College of Nutrition. 21, 275–283.

[12] Jaceldo-Siegl, K., Sabate, J., Rajaram, S. and Fraser, G.E. (2004) Long-term almond supplementation without advice on food replacement induces favourable nutrient modifications to the habitual diets of free-living individuals. British Journal of Nutrition. 92, 533–540.

[13] Mandalari, G., Tomaino, A., Arcoraci, T., Martorana, M., Lo Turco, V., Cacciola, F., Rich, G.T., Bisignano, C., Saija, A., Dugo, P., Cross, M.L., Parker, K., Waldron W. and Wickham, M.S.J. (2010) Characterization of polyphenols, lipids and dietary fibre from almond skins (Amygdalus communis L.). Journal of Food Composition and Analysis. 23, 166–174.

[14] Jenkins, D.J.A., Kendall, C.W.C., Marchie, A., Parker, T.L., Connelly, P.W., Qian, W., Haight, J.S., Faulkner, D., Vidgen, E., Lapsley, K.G. and Spiller, G.A. (2002) Dose response of almonds on coronary heart disease risk factors-blood lipids, oxidized LDL, Lp (a), homocysteine and pulmonary nitric oxide: a randomized controlled cross-over trial. Circulation. 106, 1327-1332.

[15] Kester, D.E. and Asay, R. (1975) Almonds. In: Janick, J. and Moore, J.N. (Eds.) Advances in fruit breeding. Purdue Univ. Press. Lafayette, Indiana, 387-419.

[16] Aslantas, R. (1993) Erzincan'ın Kemaliye ilçesinde doğal olarak yetişen bademlerin (*Amygdalus communis L.*) seleksiyon yoluyla ıslahı üzerinde bir araştırma. Master's thesis, unpublished. Atatürk Üniv. Fen Bilimleri Enstitüsü, Bahçe Bitkileri Anabilim Dalı, Erzurum.

[17] Küden, A.B. (1998) Crop situation and production of almonds r&d production and economics of nut crops. Advanced Course. Adana.

[18] FAO (2017) Agriculture statistics database. www.fao.org. Accessed Date: 20.02.2017.

[19] Beyhan, Ö. and Simsek, M. (2007) Kahramanmaraş merkez ilçe bademlerinin (*Prunus Amygdalus L*) seleksiyon yoluyla ıslahı üzerinde bir araştırma. Bahçe. 36(1-2), 11-18.

[20] Balta, M.F. (2002) Elazığ merkez ve Ağın ilçesi bademlerinin (*Prunus amygdalus L*.) seleksiyon yoluyla ıslahı üzerinde araştırmalar. PhD thesis, unpublished. Y.Y.Ü. Fen Bilimleri Enstitüsü Bahçe Bitkileri Anabilim Dalı, Van.

[21] Yıldırım, A.N. (2007) Isparta yöresi bademlerinin *(P. Amygdalus L.)* seleksiyonu. PhD thesis, unpublished. Adnan Menderes Üniversitesi Fen Bilimleri Enstitüsü, Bahçe Bitkileri Anabilim Dalı, Aydın.

[22] Şimşek, M. and Küden, A.B. (2007) Şanlıurfa'nın Hilvan ilçesinin bahçecik köyünde doğal olarak yetişen bademlerin *(Prunus amygdalus L)* seleksiyon yoluyla ıslahı üzerinde bir araştırma. Ç.Ü. Ziraat Fakültesi Dergisi. 22(1), 125-132.

[23] Şimşek, M. and Yılmaz, K.U. (2010) Diyarbakır'ın Silvan ilçesinde doğal olarak yetişen badem (*Prunus amygdalus L.)* tiplerinin seleksiyonu. Alatarım. 9(1), 22-30.

[24] Gülsoy, E., Ertürk, Y.E., and Şimşek, M. (2016) Türkiye lokal badem *(Prunus amygdalus L.)* seleksiyon çalışmaları. Yüzüncü Yıl Üniversitesi Tarım Bilimleri Dergisi. 26(1), 126-134.

[25] Sakar, E., Ünver, H., Keskin, S., and Sakar, Z.M. (2016) The investigation of relationships between some fruit and kernel traits with canonical correlation analysis in Ankara region walnuts. Erwerbs-Obstbau. 58(1), 19-23. 71.

[26] Keskin, S. and Ozsoy, A.N. (2004) Canonical correlation analysis and its an application. J Agric Sci. 10(1), 67–71

[27] Kettenring, J.R. (1971) Canonical analysis of several sets of variables. Biometrika. 58, 433-451.

[28] Gürbüz, F. (1989) Değişken takımları arasındaki ilişkilerin kanonik korelasyon yöntemi ile araştırılması. Ankara Üniversitesi, Ziraat Fakültesi, Yayın No: 1162, Ankara, 55p.

[29] Borowick, K., Zbierska, J., and Jusik, S. (2011) Canonical Correspondence Analysis (Cca) As A Tool for Interpretation of Bioindicator Plant Response to Ambient Air Pollution. Fresen. Environ. Bull. 20, 2264-2270.

[30] Yurtseven, I. (2012) Determination of Hydrologicalhydrochemical Parameters and Macroinvertebrate Variability in Forested Watersheds by Canonical Correlation Analysis. Fresen. Environ. Bull. 21, 2230-2238.

[31] Yuce, A.M., Yeken, T. and Kebapci, U. (2016) Marine Algae - Environment Parameters by Canonical Correspondence Analysis (Marmara Sea - Turkey). Fresen. Environ. Bull. 25, 2585-2593.

[32] Darlington, R., Weinberg, S.L. and Walberg H.J. (1973) Canonical variate analysis and related techniques. Review of Educational Research. 43(4), 433-454.

[33] Timm, N.H. (2002) Applied multivariate analysis. Springer-Verlag Inc. New York. 693p.

[34] Kendall, M.G. (1980) Multivariate analysis. Charles Griffin Company Ltd. London, 210p.
[35] Tabachnick, B. and Fidell, L.S. (2001) Using multivariate statistics. A Pearson Education Company. Needham Heights, USA, 966p.
[36] Johnson, R.A. and Wichern, D.W. (2002) Applied multivariate statistical analysis. Charles Griffin & Company Ltd. London, 210p.
[37] Bartlett, M.S. (1941) The statistical significance of canonical correlations. Biometrica. 32, 29–38.
[38] Thompson, B. (1985) Canonical correlation analysis. Sage Publication Ltd. London, 69p.

Received: **27.08.2017**
Accepted: **04.05.2018**

CORRESPONDING AUTHOR

Ersin Gulsoy
Faculty of Agriculture,
Department of Horticulture
University of Igdir,
76000, Igdir – Turkey

e-mail: ersin.gulsoy@igdir.edu.tr

© by PSP Volume 27 – No. 7/2018 pages 4674-4678 Fresenius Environmental Bulletin

IDENTIFICATION OF VOLATILE COMPOUNDS AND ANTIMICROBIAL ACTIVITIES OF *MUSCARI NEGLECTUM* GROWING IN TURKEY

Esra Eroglu-Ozkan[1,*], Serpil Demirci-Kayiran[2], Gizem Gulsoy-Toplan[1], Emel Mataraci-Kara[3], Mine Kurkcuoglu[4]

[1]Istanbul University, Faculty of Pharmacy, Department of Pharmacognosy, 34116, Beyazit, Istanbul, Turkey
[2]Cukurova University, Faculty of Pharmacy, Department of Pharmaceutical Botany, Balcali, 01330, Adana, Turkey
[3]Istanbul University, Faculty of Pharmacy, Department of Pharmaceutical Microbiology, 34116, Beyazit, Istanbul, Turkey
[4]Anadolu University, Faculty of Pharmacy, Department of Pharmacognosy, 26470, Eskisehir, Turkey

ABSTRACT

The absolute essential oils obtained from the bulbs and the aerial parts of *M. neglectum* collected from Kahramanmaraş (Turkey) were analysed by GC-FID and GC-MS. In GC-MS analyses, 17 components comprising 100% of the essential oil of the bulbs and 17 components comprising 97.1% of the essential oil of the aerial parts. Major constituents of the absolute essential oil of the bulbs were found to be ethyl palmitate (18.7%), ethyl linoleate (16.3%), palmitic acid (15.2%) and linoleic acid (10.8%). The aerial parts oil mainly contents palmitic acid (28.5%), oleic acid (10.9%), linoleic acid (22.6%) and linolenic acid (11.4%). The absolute essential oils were analyzed by using microdilution assay for antimicrobial activity against three Gram-positive, four Gram-negative bacteria and one of fungus. The oils obtained from bulbs and aerial parts possessed activity against *Staphylococcus epidermidis* with MIC values of 625 and 1250 μg/mL, respectively. The bulbs oil showed antibacterial activity against *Enterococcus faecalis* and *Escherichia coli* with 156.2 μg/mL and 625 μg/mL MIC values. The bulbs oil exhibited antifungal activity against *Candida albicans* with 312.5 μg/mL MIC value. This is the first report on the chemical composition and antimicrobial activity of the essential oils obtained from *M. neglectum* growing in Turkey.

KEYWORDS:
Hyacinthaceae, Muscari neglectum, volatile compounds, GC-MS, antimicrobial activity, Turkey.

INTRODUCTION

The genus *Muscari* Mill. (Hyacinthaceae) has a wide distribution in Mediterranean basin as far as Caucasus, temperate Europe, North Africa, South West Asia [1, 2]. In Turkey, it is represented by 37 species, 25 of which are endemic [3, 4]. *Muscari* species are known as "sümbül, arap sümbülü, morbaş, misk soğanı, horozibiği, karga pabucu, dağ soğanı" in Turkey [5]. Among them, *Muscari neglectum* Guss. ex Ten. has been used in traditional medicine as antirheumatic, stomachic, diuretic, expectorant and antiverruca [6]. The fruits of *M. neglectum* have been used for curing of rheumatism disease [7, 8]. The leaves, flowers and flower buds are edible as raw, boiled, grilled or pickled. It has also been used as food for humans and animals, dye, toys, ornamental plants in parks and gardens [9]. The bulbs of *M. neglectum* have pectoral stimulatory effects, anti-inflammatory, anti-allergic and aphrodisiac effects [10]. The blue flower buds and bulbs of *M. neglectum* are edible especially in Mediterranean region. *Muscari* bulbs tastes like mixed bitter onion and garlic, while the flowers have a sweet taste. The flowers and flower buds can be pickled in vinegar [11].

The chemical composition of the *M. neglectum* is composed of anthocyanins, flavonoids, homoisoflavanones, spirocyclic nortriterpenoid glycosides, polyhydroxylated pyrrolizidine alkaloids and essential oil [12].

The aim of the study was to investigate the volatile compounds and antimicrobial activity of *Muscari neglectum*. The absolute essential oils obtained from the bulbs and aerial parts of *M. neglectum* were analyzed by GC-FID and GC-MS. The antimicrobial activities of the oils against several bacteria and one of fungus were evaluated by using microdilution assay.

This is the first report on the chemical composition and antimicrobial activity of the essential oils obtained from *M. neglectum* growing in Turkey.

MATERIALS AND METHODS

Plant Material. The aerial parts and bulbs of *Muscari neglectum* were collected from Kahramanmaraş in April, 2015 and dried at room temperature under shade. Specimens were identified and vouchers were deposited in the Herbarium of Istanbul University, Faculty of Pharmacy (ISTE) under code number of ISTE 100115.

Preparation of Extracts. The absolute essential oil extracts were prepared by maceration of small pieces of the plant material with n-hexane (95%) for 48 hours. The extracts filtered through a Whatman paper, then evaporated off the solvent in vacuum by rotary evaporator to yield light yellow oil and dried over by adding anhydrous Na_2SO_4. In absolute essential oil extracts was dissolved in minimum volume of absolute alcohol to remove the natural waxes present in the essential oil. It was kept at 14°C for 48 hours and then it was filtered through a filter paper. Alcohol was removed by distillation and traces of alcohol were removed by passing nitrogen gas through [13].

GC and GC-MS Conditions. The absolute essential oil extracts were analyzed by Gas Chromatography (GC) and Gas Chromatography-Mass Spectrometry (GC-MS) using a Agilent GC-MSD system (Mass Selective Dedector-MSD).

GC-MS analysis. The GC-MS analysis was carried out with an Agilent 5975 GC-MSD system (Agilent, USA; SEM Ltd., Istanbul, Turkey). Innowax FSC column (60m x 0.25mm, 0.25μm film thickness) was used with helium as carrier gas (0.8 mL/min.). GC oven temperature was kept at 60°C for 10 min and programmed to 220°C at a rate of 4°C/min, and kept constant at 220°C for 10 min and then programmed to 240°C at a rate of 1°C/min and then kept constant at 240°C for 20 min. Split ratio was adjusted 40:1. The injector temperature was at 250°C. The interphase temperature was at 280°C. MS were taken at 70 eV. Mass range was from m/z 35 to 450.

GC analysis. GC analyses were performed using an Agilent 6890N GC system. FID temperature was set to 300°C and the same operational conditions were applied to a triplicate of the same column used in GC–MS analyses. Simultaneous auto injection was done to obtain equivalent retention times. Relative percentages of the separated compounds were calculated from integration of the peak areas in the GC-FID chromatograms.

Identification of Compounds. The components of the absolute essential oil extracts of *M. neglectum* were identified by comparison of their mass spectra with those in the Baser Library of Essential Oil Constituents, Adams Library, MassFinder Library, Wiley GC/MS Library and confirmed by comparison of their retention indices [14-16]. These identifications were accomplished by comparison of retention times with authentic samples or by comparison of their relative retention index (RRI) to a series of n-alkanes. Alkanes were used as reference points in the calculation of relative retention indices (RRI) [17]. Relative percentage amounts of the separated compounds were calculated from FID chromatograms.

Antimicrobial Activity. In vitro antibacterial activities of extracts against *Staphylococcus aureus* ATCC 29213, *Staphylococcus epidermidis* ATCC 12228, *Enterococcus faecalis* 29212, *Pseudomonas aeruginosa* ATCC 27853, *Escherichia coli* ATCC 25922, *Klebsiella pneumonia*e ATCC 4352, *Proteus mirabilis* ATCC 14153 and antifungal activities against *Candida albicans* ATCC 10231 were investigated. Minimum inhibitory concentrations (MICs) of extracts were determined by microbroth dilution technique as described by the Clinical and Laboratory Standards Institute [18-20]. Mueller-Hinton broth for bacteria and RPMI-1640 medium for yeast strain were used as the test medium. Serial twofold dilutions ranging from 5000 mg/L to 4.8 mg/L were prepared in medium. The inoculum was prepared using a 4–6h broth culture of each bacteria type and 24h culture of yeast strains adjusted to a turbidity equivalent to 0.5 McFarland standard, diluted in broth media to give a final concentration of 5×10^5 cfu/ml for bacteria and 5×10^3 cfu/mL for yeast in the test tray.The trays were covered and placed into plastic bags to prevent evaporation.The trays containing Mueller-Hinton broth were incubated at 35°C for 18–20h while the trays containing RPMI-1640 medium were incubated at 35°C for 46–50h.The MIC was defined as the lowest concentration of extracts giving complete inhibition of visible growth. As control, antimicrobial effects of the extracts were investigated against test microorganisms. According to values of the controls, the results were evaluated.

RESULTS

The chemical compositions of the *M. neglectum* oils were identified by GC–MS and the study results are given in Table 1 and 2. In the oil obtained from the bulbs and the aerial parts, 17 compounds were identified representing 100% and 17 compounds were identified representing 97.1% of the volatile compounds, respectively. The main compounds were found to be ethyl palmitate (18.7%), ethyl linoleate (16.3%), palmitic acid (15.2%) and linoleic acid (10.8%) for the bulbs and palmitic acid (28.5%), oleic acid (10.9%), linoleic acid (22.6%) and linolenic acid (11.4%) for the aerial parts.

According to literature survey, two phytochemical studies are found about *M. neglectum* which grows in Iran [9, 13].

Nasrabadi et al. investigated the chemical composition of the essential oil obtained from the aerial parts of *M. neglectum* collected from Iran. It was reported that 32 bioactive phytochemical compounds were identified representing 79.7%. The oil was characterized by bis (2-ethylhexyl) phthalate

(18.6%), tributylethylstannane (10.1%), bis (chlorophenyl) sulphone (8.7%), gibberellin (4.9%), 1, 6, 10-dodecatrien- 3-ol, 3, 7, 11-trimethyl (3.3%) [13]. The differences between our results and these results can be attributed to the growing geographical area, the seasonal changes in temperature and humidity.

Antimicrobial assay results of *M. neglectum* oils are given in Table 3. The results revealed that the oils have exhibited moderate activity against Gram-positive bacteria. The oils possessed activity against *S.epidermidis* with MIC values of between 625 and 1250 μg/mL. The bulb oil showed good antibacterial activity against *E. faecalis* with 156.2 μg/mL MIC value. The bulb oil also has antibacterial

TABLE 1
The components of the absolute essential oil extracts of *M. neglectum* bulbs

Compounds	RRI	%	ID
Ethyl tetradecanoate	2057	0.3	Ms
Heneicosane	2100	3.4	s, Ms
Methyl hexadecanoate	2228	0.7	Ms
Ethyl hexadecanoate	2260	**18.7**	Ms
Tricosane*	2300	5.8	s, Ms
Ethyl heptadecanoate	2361	Tr	Ms
Ethyl octadecanoate	2467	1.7	Ms
Ethyl oleate	2493	3.0	Ms
Pentacosane	2500	2.4	Ms
Ethyl linoleate	2538	**16.3**	Ms
Ethyl linolenate	2613	1.6	Ms
Ethyl eicosanoate	2670	3.7	Ms
Heptacosane	2700	2.1	Ms
Ethyl docosanoate	2872	7.6	Ms
Hexadecanoic acid	2921	**15.2**	Ms
Squalene	3059	3.8	s, Ms
Linoleic acid	3292	**10.8**	s, Ms
Number of compounds		**17**	
Total %		**97.1**	

RRI; Relative retention indices calculated against n-alkanes. %; calculated from the FID chromatogram. tr; Trace (<0.1 %) *Impure. ID; s, Identification based on comparison with co-injected with standards; Ms. Tentatively identified using Wiley, Adams and MassFinder mass spectra libraries and published RRI.

TABLE 2
The components of the absolute essential oil extracts of *M. neglectum* aerial parts

Compounds	RRI	%	ID
Neophytadiene isomer I	1933	0.3	Ms
Hexahydrofarnesyl acetone	2135	0.4	s, Ms
Methyl hexadecanoate	2228	0.6	Ms
Ethyl hexadecanoate	2260	7.2	Ms
Ethyl octadecanoate	2467	0.7	Ms
Ethyl oleate	2493	1.4	Ms
Methyl linoleate	2509	1.1	Ms
Ethyl linoleate	2538	5.2	Ms
Methyl linolenate	2583	0.6	Ms
Ethyl linolenate	2613	4.3	Ms
Phytol	2622	1.4	Ms
Heptacosane	2700	1.7	Ms
Hexadecanoic acid	2921	**28.5**	Ms
Stearic acid	3151	1.7	Ms
Oleic acid	3200	**10.9**	Ms
Linoleic acid	3292	**22.6**	s, Ms
Linolenic acid	3300	**11.4**	s, Ms
Number of compounds		**17**	
Total %		**100.0**	

RRI; Relative retention indices calculated against n-alkanes. %; calculated from the FID chromatogram.
ID; s, Identification based on comparison with co-injected with standards; Ms. Tentatively identified using Wiley, Adams and MassFinder mass spectra libraries and published RRI.

TABLE 3
Antimicrobial activity of essential oils from bulbs and aerial parts of *M. neglectum*

Microorganisms		Source	MIC values (µg/mL)	
			Bulbs essential oil	Aerial parts essential oil
Gram-positive	*Staphylococcus aureus*	ATCC 29213	Na	Na
	Staphylococcus epidermidis	ATCC 12228	625	1250
	Enterococcus faecalis	ATCC 29212	156.2	312.5
Gram-negative	*Pseudomonas aeruginosa*	ATCC 27853	Na	Na
	Escherichia coli	ATCC 25922	625	Na
	Klebsiella pneumoniae	ATCC 4352	Na	Na
	Proteus mirabilis	ATCC 14153	Na	Na
Fungus	*Candida albicans*	ATCC 10231	312.5	Na

Na: Non active

activity against *E. coli* with 625 µg/mL MIC value. The test-culture of *P.aeruginosa*, *P. mirabilis* and *K. pneumoniae* appeared not to be susceptible to tested oils. Evaluation of the antifungal activity of the bulb oil showed that moderate activity with MIC 312.5 µg/mL for *C. albicans*. The results also reveal that the oils have both antibacterial and antifungal activities.

The results are compared with previous study by Mahboubi and Taghizadeh who investigated the antimicrobial activity of the ethanol extract of aerial parts of *M. neglectum* growing in Iran. Their results showed that the MIC values of the extract were 56 µg/ml for *Shigella flexneri*, 56 µg/ml for *Aspergillus niger*, 87.11 µg/ml for *E. coli*, 224 µg/ml for *S. aureus* and 37.3 µg/ml for *C. albicans* [9]. According to the results, the oil and the ethanol extract of the aerial parts of *M. neglectum* have antibacterial activity against Gram-positive and Gram-negative microorganisms with different MIC values.

As a conclusion, ethyl palmitate, ethyl linoleate, palmitic acid and linoleic acid were determined as major component in essential oil obtained from the bulbs of *M. neglectum* as well as palmitic acid, oleic acid, linoleic acid and linolenic acid in the aerial parts essential oil. We also reported that the oils have antibacterial and antifungal activities. This is the first report on the chemical composition and antimicrobial activity of the essential oils obtained from *M. neglectum* growing in Turkey.

REFERENCES

[1] Speta, F. (1998) Hyacinthaceae. In: Kubitzki, K. (Ed.) The families and genera of vascular plants, Monocotyledons. Springer-Verlag, Heidelberg, 261-285.

[2] Jafari, A., Maassoumi, A.A., Farsi, M. (2008) Karyological study on Bellevalia and Muscari (Liliaceae) species of Iran. Asian Journal of Plant Sciences. 7(1), 50-59.

[3] Demirci, S., Özhatay, N., Koçyiğit, M. (2013) Muscari erdalii (Asparagaceae, Scilloideae), a new species from Southern Turkey. Phytotaxa. 154(1), 38-46.

[4] Yildirim, H. (2016) Muscari elmasii sp. nova (Asparagaceae): a new species from western Anatolia, Turkey. Turkish Journal of Botany. 40, 380-387.

[5] Baytop, T. (1999) Therapy with Medicinal Plants in Turkey, Past and Present. Nobel Tip Press, Istanbul, 372.

[6] Kayıran, S.D., Özkan, E.E. (2017) The ethnobotanical uses of Hyacinthaceae species growing in Turkey and a review of pharmacological activities. Indian Journal of Traditional Knowledge. 16(2), 243-250.

[7] Erol, M., Tuzlacı, E. (1995) Eğirdir (Isparta) yöresinin geleneksel halk ilacı olarak kullanılan bitkileri. XI. BİHAT, 22-24.

[8] Ugurlu, E., Secmen, O. (2008) Medicinal plants popularly used in the villages of Yunt Mountain (Manisa-Turkey). Fitoterapia. 79, 126-131.

[9] Mahboubi, M., Taghizadeh, M. (2016) The antimicrobial and antioxidant activity of Muscari neglectum flower ethanol extract. Herba Polonica. 62, 39-48.

[10] Usher, G. (1974) A dictionary of plants used by man. Constable and Company Ltd. London.

[11] Lim, T. (2014) Muscari neglectum, Edible medicinal and non-medicinal plants. Springer, Dordrecht. 122-125.

[12] Mulholland, D.A., Schwikkard, S.L., Crouch, N.R. (2013) The chemistry and biological activity of the Hyacinthaceae. Natural product reports. 30, 1165-1210.

[13] Nasrabadi, M., Halimi, M., Nadaf, M. (2013) Phytochemical Screeningand Chemical Composition of Extract of Muscari neglectum. Middle-East Journal of Scientific Research. 14, 566-569.

[14] Adams, R.P. (2007) Identification of essential oil components by gas chromatography/mass spectrometry. Allured Publishing Corporation. USA.

[15] Hochmuth, D.H. (2008) MassFinder-4. Hochmuth Scientific Consulting, Hamburg, Germany.

[16] McLafferty, F.W.S. (1989) The Wiley/NBS registry of mass spectral data. Wiley. New York.

[17] Curvers, J., Rijks, J., Cramers, C., Knauss, K., Larson, P. (1985) Temperature programmed retention indices: Calculation from isothermal data. Part 1: Theory. Journal of Separation Science. 8, 607-610.
[18] (CLSI), C.a.L.S.I., (1997) M27-A2, Reference Method for Broth Dilution Antifungal Susceptibility Testing of Yeasts; Approved Standard. CLSI: Wayne, PA, USA.
[19] (CLSI), C.a.L.S.I., (2006) Approved Standard M7-A7, Methods for Dilution Antimicrobial Susceptibility Tests for Bacteria That Grow Aerobically. CLSI: Wayne, PA, USA.
[20] (CLSI), C.a.L.S.I., (2010) 7th Informational Supplement; M100-S20, Performance Standards for Antimicrobial Susceptibility Testing. CLSI: Wayne, PA, USA.

Received: **05.09.2017**
Accepted: **29.04.2018**

CORRESPONDING AUTHOR

Esra Eroglu-Ozkan
Istanbul University
Faculty of Pharmacy,
Department of Pharmacognosy,
34116, Fatih, Istanbul – Turkey

e-mail: esraeroglu@gmail.com

© by PSP Volume 27 – No. 7/2018 pages 4679-4688 Fresenius Environmental Bulletin

USE OF CITRUS SINENSIS LEAVES AS A BIOADSORBENT FOR REMOVAL OF CONGO RED DYE FROM AQUEOUS SOLUTION

Muhammad Imran Khan[1,*], Shagufta Zafar[2], Abdul Rehman Buzdar[3], Muhammad Farooq Azhar[4], Warda Hassan[5], Abida Aziz[6]

[1]CAS Key Laboratory of Soft Matter Chemistry, Lab of Functional Membranes, School of Chemistry and Material Science, University of Science and Technology of China, Hefei, Anhui 23006, P.R China
[2]Department of Chemistry, The Govt Sadiq College Women University, Bahawalpur, Pakistan
[3]Department of CS&E, HITEC University, Taxila Cantt 47050, Pakistan
[4]Department of Forestry and Range Management Bahauddin Zakariya University, Multan, Pakistan
[5]Department of Chemistry, The Women University of Multan, Multan, Pakistan
[6]Department of Botany, The Women University of Multan, Multan, Pakistan

ABSTRACT

The removal of Congo Red (CR) from aqueous solution by leaves powder of Citrus Sinensis (CS) was investigated at room temperature. The effect of parameters such as contact time, amount of adsorbent, initial dye concentration and ionic strength on the removel of dye was studied. The kinetic models namely pseudo-first-order and pseudo-second were employed to describe the adsorption kinetics. The results show that adsorption data fitted-well to the pseudo-second-order kinetic model. The experimental data were revealed by Langmuir, Freundlich, Temkin and Dubinin-Redushkevich (D-R) isotherms models. The results indicates that the adsorption of CR onto leave powder of CS followed the Freundlich isotherm. The value of mean free energy (E) shows that adsorption of CR onto CS leaves powder was physical adsorption. Thermodynamic parameters such as change in Gibb's (ΔG^o) free energy, enthalpy (ΔH^o) and entropy (ΔS^o) were measured. The positive value of enthalpy (ΔH^o) indicates the endothermic nature of adsorption process whereas the nagative value of Gibb's free (ΔG^o) energy shows the feasibility and spontaniety of adsorption process.

KEYWORDS:
Adsorption, Congo Red, Citrus sinesis, Freundlich isotherm, Pseudo-second-order model, Endothermic

INTRODUCTION

Synthetic dyes are mostly employed for textile dyeing, leather dyeing, color photography, paper printing and as additives in petroleum product [1]. Reactive dyes are the most common dyes used because of their importance, such as bright colors, excellent color fastness and ease of application [2, 3]. They have different chemical structures. It depends on substituted aromatic and heterocyclic groups. A large number of reactive dyes are azo compounds that are linked by an azo groups [4]. Many reactive dyes are toxic to some organisms and they cause direct destruction of creature in water [5]. In addition, since reactive dyes are highly soluble in water, their removal from effluent is difficult by conventional physicochemical and biological treatment methods [6, 7]. Conventional treatment methods for the removal of dyes in wastewater include physical, chemical and biological process such as adsorption [8], coagulation [9], oxidation [10], reduction [11], filteration [12], and biological treatment [13]. Adsorption and biological treatment are two important methods available for wastewater treatment. The biological treatment is difficult to start up and control [14] and intermediate product (aromatic amines) formed during anaerobic reduction of azo dyes are known to be potential carcinogens [15]. Adsorption on the other hand, should be a favourable procedure due to economic feasibility, simlicity of design, should a favourable procedure due to economic feasibility, simplicity of design, recycling of adsorbent and nonextence of harmful residues. The adsorption capacity depends on several factors such as nature of adsorbent, the nature of adsorbate and the solution condition [16]. Generally, the commercial activated carbon is indeed effective for color removal but the high cost of activated carbon has restricted its widespread use. Therefore, searching a low-cost and effective adsorbents should be of considerable significance for practical application of adsorption [17]. Researcher have shown the use of materials like walnut husk [18], composites [19], biochars from crop residues [20], natural clinoptilolite [21], sesame hull [22], biomass of penicillium YWO1 [23], natural zealite [24], cross-linked succinyl chitosan [25], modified bentonite [26], modified attapulgite [27], clay material [28-30], activated carbon [31], dehydrated beet pulp carbon [32], polyurethane foam [33], etc as adsorbent for removal of dyes from wastewater. In

this contex, agriculture by-products have shown its potential as a low-cost adsorbent and they are usually being modified chemically in order to enhance their adsorption capacty toward dye [34].

However, There are some adsorbents which do not have good adsorption capacities for anionic dyes because most have anionic or hydrophobic surfaces. Hence, there is a need to search for more effective adsorbents [35].

In this article, anionic dye Congo Red was used as typical pollutant and citrus sinensis (CS) leaves powder was used as adsorbent for removal of Congo Red (CR) dye from aqueous solution. The effect of various parameters such as contact time, amount of adsorbent, effect of initial concentration, effect of ionic strength and effect of temperature on removal of dye were also investigated. The adsorption kinetics, isotherms and thermodynamics for CR dye on CS leaves powder was also analyzed.

EXPERIMENTAL

Adsorbent. The orange (citrus sinensis) is a commonly grown tree in the world. The united state has higher production of orange in the world. Sweat oil is a by-product of the juice industry. It is utilized as a drink, flavouring of food and for its fragrance in perfumes. Sweat orange oil has 90 % d-Limestone, a solvent used in many household chemicals such as to condition wooden furniture and along with other CS oils in grease removal and as a hand cleaning agent [36].

Adsorbate. Congo Red (Sodium salt of benzdinediazobis-1-nephthylamine-4-sulphonic acid) is a benzidine-based azo dye and it was used as a adsorbate in this study. The molecular formula of CR is $C_{32}H_{22}N_6Na_2O_6S_2$ and its molecular stucture is shown in Fig.1. Congo Red (CR) mainly occurs in the effluents discharged from textile, paper, printing, leather industries, etc. [37] and during dyeing operation; about 15% of it ends up in wastewaters [38]. All of the reagents were of analytical grade and deionized water was used throughout the experiments.

Adsorption. Batch adsorption of Congo Red (CR) dye from aqueous solution was carried out by using citrus sinensis (CS) leaves powder as a adsorbents at temperature 298 K. For these experiments, calculated amounts of adsorbents were added into measured volume of dye solution into 100 ml flasks. The bottles were shaked at constant speed of 120 rpm. Once the equilibrium was reached, the concentration of CR was determined by SP-50 spectrophotometer (Gallen Camp UK) at its maximum wavelength of 490 nm. The CR adsorption on CS at time t, was calculated by equation 1.

$$q_t = \frac{C_o - C_t}{W} \times V \quad (1)$$

Where C_o and C_t are the concentration of CR at initial state and at time t respectively. Similarly V and W are volume of CR aqueous solution and weight of adsorbent respectively.

RESULTS AND DISCUSSION

Effect of Contact Time. The effect of contact time on the percentage removal of CR from aqueous solution was studied keeping the concentration of adsorbate (25 mg/L), amount of adsorbent, shaking speed (120 rmp) and temperature (298K) constant. The results are shown in Fig. 2. It has been observed that percentage removal of CR dye increases with increasing contact time and attains saturation in 35 minutes. This shows that adsorption process reached to equilibrium whitin 35 minutes and further experiments were carried out at this optimum contact time. The results indicate that rate of dye removal was rapid in the start because of the increased in number of available empty sites on the surface of adsorbent for adsorption of dye during the initial stage. Similar results have been previously reported in the literature for dye removal [39].

Effect of amount of adsorbent. The effect of amount of adsorbent is essential to invetigate the maximum adsorption with small possible quantity of adsorbent. The influence of amount of adsorbent on the removal of CR from aqueous solution was invetigated keeping the other parameters namely contact time, initial dye concentration, shaking speed and temperature constant. It is clear that percentage removal of CR dye increases with increasing amount of adsorbent as shown in Fig. 3. The removal CR increased from 25.76-76.23 % with increasing the amount of adsorbent from 0.1-1 g because number of vacant sites available inceases with increasing the amount of adsorbent. Similarl results have been previously reported in the literature [40]. However, further increment in the adsorbent dosage did not give any significant changes in the percentage removal and this could be due to the saturation of binding sites [41].

Effect of initial dye concentration. The initial dye concentration has significant effect on the removal of dye from aqueous solution. The infuence of intial dye concentration on removal of CR was studied keeping the other factor such as contact time, amount of adsorbent, shaking speed and temperature constant. The effect of initial dye concentration from 2.5-25 mg/L on CR removal using CS leaves powder was studied and results are shown in Fig. 4. The initial dye concentration gives the useful driving fource to overcome the resistance of mass transfer

from the aqueous phase to the solid phase [42]. It increase the interaction between CR and leaves powder of CS. Hence, an increase in initial concontration increases the adsorption capability of CS leaves powder for CR dye. But the percentage removal of CR was found to be decreased with concentration as shown in Fig. 4.

Effect of Temperatures. The effect of temperature on the removal of CR dye from aqueous solution by using CS leaves powder was studied and results are shown in Fig. 5. The percentage removal of CR was increased with increasing temperature indicating the endothermic nature of adsorption process. It may be due to higher mobility of the molecules at higher temperatures and a greater availability of molecules with enough energy to intract with active site on the surface. Moreover, the increasing temperature resulted in swelling of the internal structure of CS leaves powder which help to facilitate the movement of large dye molecules [43].

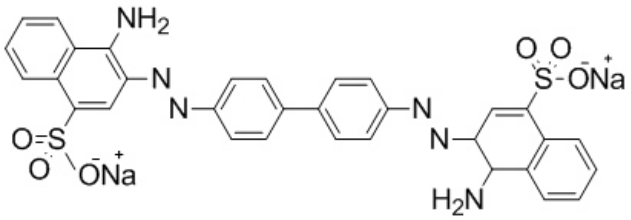

FIGURE 1
Chemical structure of Congo Red (CR) dye.

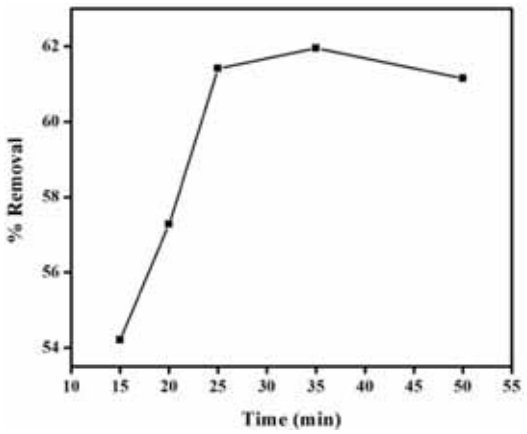

FIGURE 2
Effect of contact time on the removal of CR by CS leaves powder.

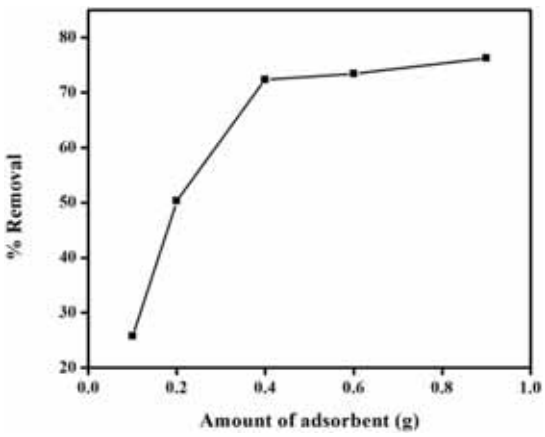

FIGURE 3
Effect of amount of adsorbent on the removal of Congo red from aqueous solution.

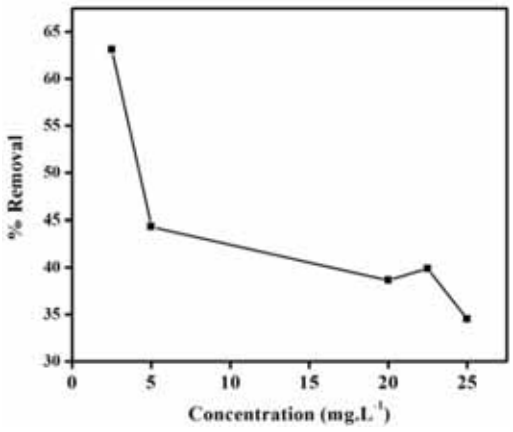

FIGURE 4
Effect of initial dye concentration on the removal of Congo red by CS leaves powder.

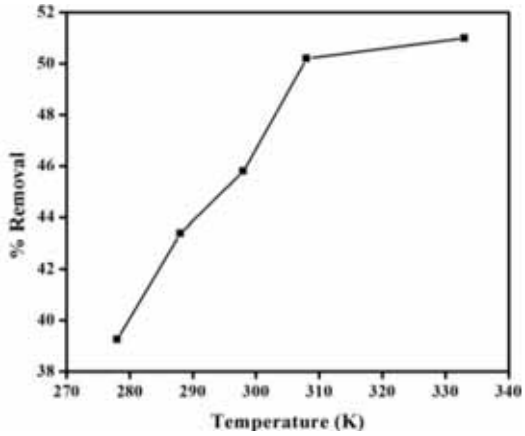

FIGURE 5
Effect of temperature on the removal of Congo red by CS leaves powder.

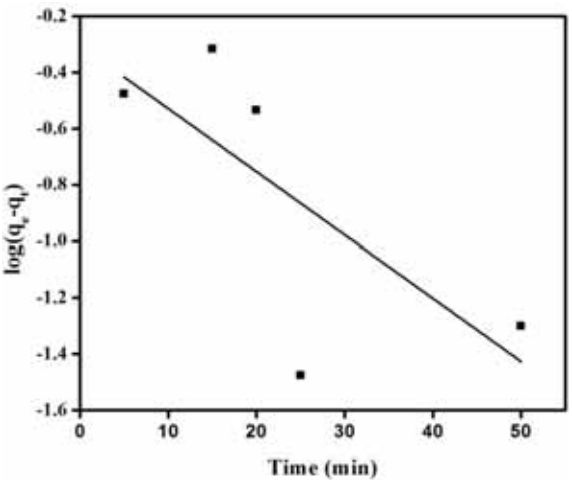

FIGURE 6
Pseudo-first-order kinetics for adsorption of Congo Red onto CS leaves powder.

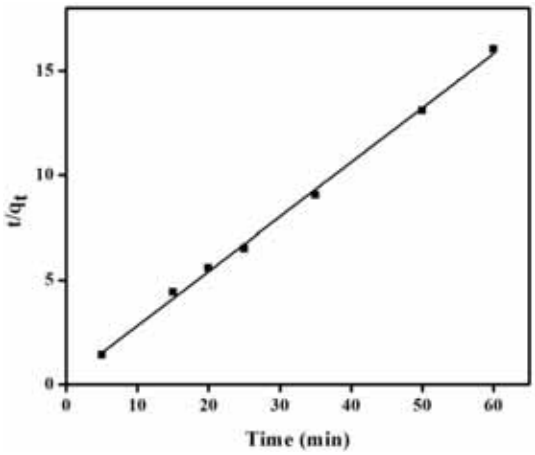

FIGURE 7
Pseudo-second-order kinetics for adsorption of Congo Red onto CS leaves Powder.

TABLE 1
Pseudo-first-order and pseudo-second-order rate constants.

Pseudo-first order				Pseudo-second-order		
$q_{e(exp)}$	$q_{e\ (cal)}$	k_1	R^2	q_e	k_2	R^2
3.87	0.50	0.022	0.346	3.84	0.318	0.997

(q_e : mg/g; k_1: (/min); k_2: g/mg.min)

ADSORPTION KINETICS

The kinetics of CR removal by CS leaves powder was investigated to calculate the rate of dye uptake from aqueous solution which controls the system of dye adsorption. The kinetic models namely pseudo-first-order and pseudo-second-order were fitted to experimental data better to find out the potential rate-controlling steps of the CR adsorption kinetics.

Pseudo-first-order model. The linearized form of the Lagergren Pseudo-first-order rate equation is given by [44]

$$log(q_e - q_t) = \log q_e - \frac{K_1 t}{2.303} \quad (2)$$

Where q_e and q_t is the amount of adsorbate adsorbed at equilibrium and time t repectively and k_1 (/min) is the rate constant of pseudo-first-order adsorption model. The plot of log(q_e-q_t) verses t for pseudo-first-order model is shown in Fig.6. The values of of q_e and k_1 were calculated from slope and intercept of Fig. 6 and given in Table 1. It has been observed that calculated value of q_e does not agree with experimental one as shown Table 1. Moreover, the value of correlation coefficient (R^2) was lower (0.346) for pseudo-first-order model. These parameters shows that adsorption of CR onto leaves powder of CS does not follow pseudo-first order kinetic model.

Pseudo-second-order model. The linearized form of pseudo-second kinetic model is expressed as [45]:

$$t / q_t = \frac{1}{k_2 q_e^2} + \frac{t}{q_e} \quad (3)$$

where k_2 (g/mg.min) is the rate constant of pseudo-second-order model. The plot of t verses t/qt for pseudo-first-order model is shown in Fig. 7. The values of q_e and k_2 are calculated from slope and intercept of Fig. 7 and given in Table 1. The value of correlation coefficient (R^2>0.99) is close to unity for pseudo-second-order model. In addition to this, the calculated value of adsorption capacity ($q_{e,\ cal}$) is in good agreement with experimental one ($q_{e,\ exp}$). This indicates that adsorption of CR dye onto leaves powder of CS followed pseudo-second-order kinetic model.

ADSORPTION ISOTHERMS

The adsorption isotherm shows the distribution of molecules between solid and liquid phases at equilibrium state. The analysis of isotherm data by fitting the data to different isotherm models is an important step in finding the most suitable model that can be used to describe the adsorption process [46]. There are several isotherm model to describe the isotherm data. In the present study, Langmuir, Freundlich, Temkin and Dubinin-Redushkevich (D-

R) isotherm models are employed to analyze the experimental results. The Langmuir model depends upon the maximum adsorption coincides to the saturated monolayer of liquid (adsorbate) molecules on the solid (adsorbent) surface. The linearized form of Langmuir model is given as follows [47].

$$\frac{C_e}{q_e} = \frac{1}{bq_m} + \frac{C_e}{q_m} \quad (4)$$

where b is Langmuir constant (L/mg) and q_m is Langmuir monolayes adsorption capacity ($mg.g^{-1}$), C_e is supernatant concentration at equilibrium state of the system (mg/L), and q_e is the amount of dye adsorbed at equilibrium state of system (mg/g). The plot of C_e verses C_e/q_e for Langmuir model is shown in Fig. 8. The values of q_m and b are calculated from slope and intercept of Fig. 8 and given in Table 2. The value of correlation coefficient (R^2) was 0.729 for CR adsorption on to leaves powder of CS. Moreover, the value of calculated q_m (5.88 mg/g) is in close to the experimental value (4.31 mg/g). Thus, the Langmuir model describe (poorly fitted) the adsorption of CR dye onto CS leaves powder.

The essential characteristics of Langmuir isotherm can be expressed in term of dimensionless constant separation factor R_L that is give by [48].

$$R_L = \frac{1}{1 + bC_o} \quad (5)$$

The value of R_L shows the shape of the isotherm to be either unfavourable (R_L>1), linear (R_L=1), favourable (0<R_L>0), or irreversible (R_L=0) [49]. The values of R_L for adsorption of CR onto leaves powder of CS lies in the range (0.18-0.68) which are in between 0 and 1, therefore verifying the favourable adsorption process. Moreover, the low R_L values impied that the interaction of dyes molecules with leaves powder of CS might be relatively strong [50].

The widely used Freundlich model is an empirical relation used to explain the heterogeneous system. The Freundlich isotherm model is expressed as [51].

$$\log q_e = \log K_f + \frac{1}{n}\log C_e \quad (6)$$

where K_f and n are Freundlich constant. The values of n and K_f are calculated from slope and intercept of Fig. 9 and given in Table 2. The value of correlation coefficient (R^2) is 0.947 indicating that adsorption data fitted well to the Freundlich model. The value of Freundlich contant n decides the favourability of adsorption process. For favourable adsorption process, the value n should be less than 1 and greater than 10. The value of n for CR adsorption onto CS leaves powder was greater than 1 and less than 10 indicating the favourable adsorption process.

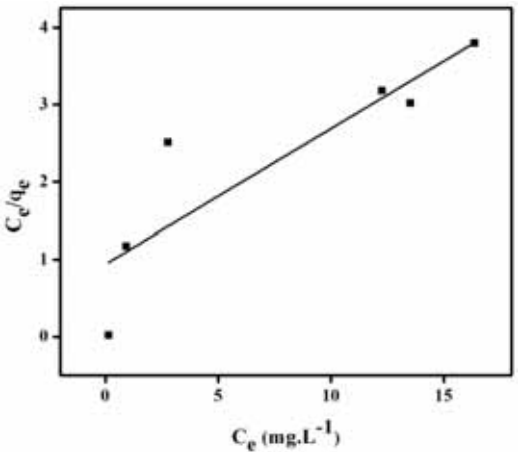

FIGURE 8
Langmuir adsorption isotherm for adsorption of Congo Red onto CS leaves powder.

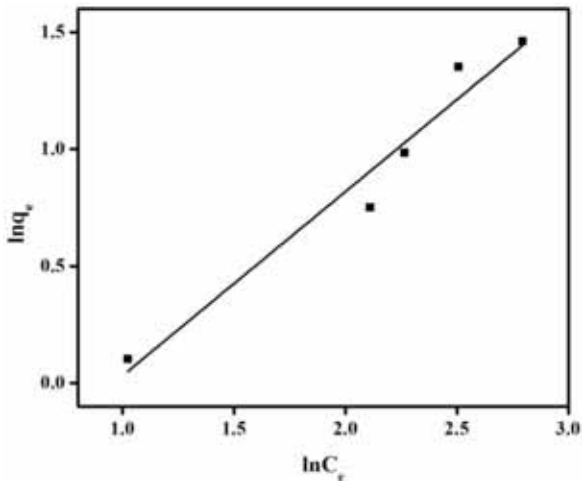

FIGURE 9
Freundlich adsorption isotherm for adsorption of Congo Red onto CS leaves powder.

TABLE 2
Langmuir and Freundlich isotherm parameters for CR adsorption onto CS.

Langmuir isotherm			Freundlich isotherm		
q_m	b	R^2	n_F	K_f	R^2
5.88	0.182	0.729	1.28	0.470	0.947

(q_m: mg/g; q_m: mg/g)

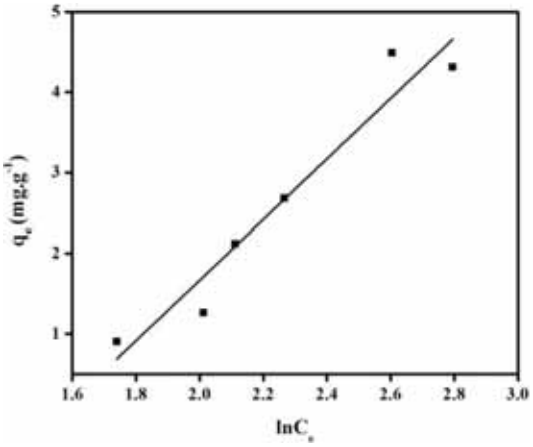

FIGURE 10
Temkin adsorption isotherm for adsorption of Congo Red onto CS leaves powder.

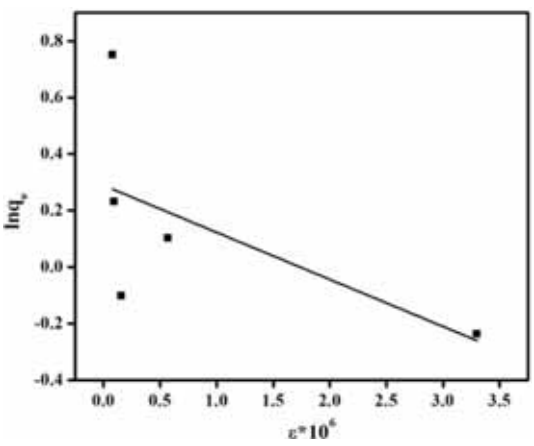

FIGURE 11
Dubinin- Redushkevich (D-R) adsorption isotherm for adsorption of Congo Red onto CS leaves powder.

TABLE 3
Tempkin and D-R isotherm parameters for CR adsorption onto CS.

Tempkin isotherm			D-R isotherm			
B_T	A_T	R^2	q_m	β	E	R^2
658.94	0.21	0.928	1.33	0.167	1.73	0.153

(b_T: J/mol; A_T: L/mg; q_m= mg/g; β= mol^2/Kg^2; E: KJ/mol)

The Tempkin isotherm assumes that the heat of adsorption of all the molecules decrease linearly with the coverage of the molecules due to the adsorbate-adsorbate repulsion and the adsorption of adsorbate is uniformly distributed and that the fall in the heat of adsorption is linear rather than logarithmic [52]. It is expressed as

$$q_e = B_T \ln A_T + B_T \ln C_e \quad (7)$$

where B_T=RT/b_T, T is absolute temperature (K) and R is gas constant (8.31 J/mol.K). The constant b_T is related to the heat of adsorption and A_T is equilibrium binding constant coinciding to the maximum binding energy. The plot of q_e verses lnC_e for Temkin model is shown in Fig. 10. The values of B_T and A_T are determined from slope and intercept of Fig. 10 and are given in Table 3. The value of correltaion coefficient (R^2) was 0.9267 lower than the Freundlich model indicating the adsorption data was not fitted to the Temkin model.

The Dubinin-Redushkevich (D-R) model is expressed as

$$\ln q_e = \ln q_m - \beta\varepsilon^2 \quad (8)$$

where β (mol^2.KJ^{-2}) is constant related to the adsorption energy and ε is the polanyi potential can be calculated using following relation

$$\varepsilon = RT \ln(1 + \frac{1}{C_e}) \quad (9)$$

where R is gas constan (8.31 KJ.mol^{-1}) and T is absolute temperature (K). The mean free energy E (KJ/mol) can be calculated by following relation

$$E = \frac{1}{\sqrt{2\beta}} \quad (10)$$

The plot of lnq_e verses ε^2 for D-R model is shown in Fig. 11. The values of β and q_m were calculated from slope and intercept of Fig. 11 and given in Table 3. The mean adsorption energy (E) in the D-R isotherm can act as a ruler to distinguish chemical and physical adsorption [53]. The value of mean free energy (E) for CR adsorption onto CS leaves powder is 1.73 KJ.mol^{-1}. It shows that adsorption of CR onto CS leave powder is physiosorption.

ADSORPTION THERMODYNAMICS

Thermodynamic parameters indicate the feasibility and spontaneous nature of adsorption process. The parameters such as change in Gibb's free energy (ΔG^o), enthalpy (ΔH^o) and entropy (ΔS^o) were calculated by following relations

$$\ln Kc = \frac{\Delta S^o}{R} - \frac{\Delta H^o}{RT} \quad (11)$$

TABLE 4
Thermodynamic parameters for adsorption of CR onto CS.

		ΔG (KJ/mol)			
ΔH (KJ/mol)	ΔS (J/mol)	278K	288K	298K	308K
10.14	32.84	-9.11	-9.44	-.9.77	-10.10

$$K_c = \frac{C_a}{C_e} \quad (12)$$

$$\Delta G^o = \Delta H^o - T\Delta S^o \quad (13)$$

where K_c, C_a, C_e, R, T are the the equilibrium constant, amount of dye (mol/L) adsorbed on the adsorbent per litre (L) of the solution at equilibrium, equilibrium concentration (mol/L) of dye in solution, gas contant (8.31 J/mol.K) and absolute temperature (K) respectively. Similarly ΔG^o, ΔH^o and ΔS^o are the change in Gibb's free energy (KJ/mol), enthalpy (KJ/mol) and entropy (J/mol.K) respectively. The graphical representation of $\ln K_c$ verses 1/T is shown in Fig. 12. The values of adsorption enthalpy (ΔH^o) and entropy (ΔS^o) were calculated from slope and intercept of Fig. 12 and are given in Table 4. The values of Gibb's free energy (ΔG^o) were (-9.11, -9.44, -9.77 and -10.10 KJ.mol^{-1}) at all temperatures 278K, 288K, 298K and 308K repectively. The negative values of Gibb's free energy (ΔG^o) indicate the feasibility and spontaneous nature of adsorption process. The positive value of enthalpy (ΔH^o) suggests that the adsorption process is endothermic in nature. Similarly the positive value of entropy (ΔS^o) showed increased randomness at the adsorbate-adsorbent interface during the adsorption process of CR onto leaves powder of CS.

CONCLUSIONS

This manuscript shows that the leaves powder of citrus sinensin (CS) is efficient for removal Congo Red (CR) from aqueous solution. The removal CR from aqueous is largly dependent on parameters such as contact time, amount of adsorbent, initial dye concentration and temperature. The removal of (CR) dye increases with increasing contact time and temperature but decreased with initial dye concentration. The ionic strength has adverse effect on the removal of (CR) dye from aqueous solution. The adsorption kinetics study indicates that adsorption of CR onto leaves powder of CS follows the pseudo-second-order kinetics. The experimental data was analyzed by various isothermal models such as Langmuir, Freundlich, Temkin and Dubinin-Redushkevich (D-R) model but the experimental data fitted well to the Freundlich model. Thermodynamic study reveals that the adsorption of CR onto leaves powder of CS are endothermic and spontaneous. The present study shows that the leaves powder of citrus sinensis (CS) could be employed as an efficient adsorbent for removal of CR dye from aqueous solution.

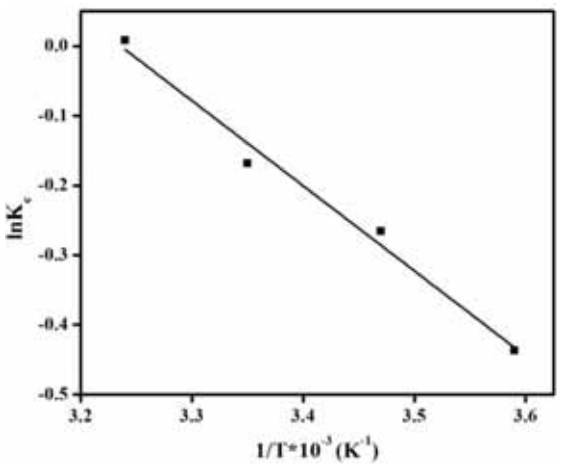

FIGURE 12
Plot of $\ln k_c$ verses 1/T for Congo Red dye onto CS leaves powder.

ACKNOWLEDGEMENTS

The authors are highly thankful to CAS-TWAS President's fellowship for PhD programs for financial support.

REFERENCES

[1] Radha, K.V., Regupathi, I., Arunagiri, A., Murugesan, T. (2005) Decolorization studies of synthetic dyes using phanerochaete chrysosporium and their kinetics. Process Biochemistry. 40, 3337-45.
[2] Yang, X.Y., Al-Duri, B. (2001) Applicationof branched pore diffusion model in the adsorption of reactive dyes on activated carbons. Chemical Engineering Journal. 83, 15-23.
[3] O'Mahony, T., Guibal, E., Tobin, J.M. (2002) Reactive dye biosorption by Rhizopus arrhizus biomass. Enzyme Microbial Technology. 31, 456-63.
[4] Raymound, E.K., Dunald, F. (1984) Encyclopedia of chemical technology. New York: Wiley.

[5] Papic, S., Koprivanac, N., Bozic, A.L., Metal, A. (2004) Removal of some reactive dyes from synthetic wastewater by combined Al(III) coagulation/carbon adsorption process. Dyes & Pigments. 62, 291-298.
[6] Chern, J.M., Huan, S.N. (1998) Study of nonlinear wave propagation theory: 1. Dye adsorption by activated carbon. Industrial & Engineering Chemistry Research. 37, 253-7.
[7] Ozacar, M., Sengil, I.A. (2003) Adsorption of reactive dyes on calcined alunite from aqueous solutions. Journal of Hazardous Material. B98, 211-24.
[8] Maheria, K.C., Chudasama, U.V. (2007) Sorptive removal of dyes using titanium phosphate. Industrial & Engineering Chemistry Research. 46, 6852-6857.
[9] Shi, B., Li, G., Wang, D., Feng, C., Tang, H. (2007) Removal of direct dyes by coagulation: the performance of performed polymeric aluminum species. Journal of Hazardous Materials. 143, 567-574.
[10] Emmert III, F.L., Thomas, J., Hon, B., Gengenbach, A.J. (2008) Metalloporphyrin catalyzed oxidation of methyl yellow and related azo compounds. Inorganica Chimica Acta. 361, 2243-2251.
[11] Shu, H.-Y., Chang, M.-C., Yu, H.-H., Chen, W.-H. (2007) Reduction of an azo dye Acid Black 24 solution using synthesized nanoscale zerovalent iron particles. Journal of Colloid and Interface Science. 314, 89-97.
[12] Caper, G., Yetis, U., Yilmaz, L. (2006) Membrane based strategies for the pre-treatment of acid bath wastewaters. Journal of Hazardous Materials. 135, 423-430.
[13] Georgiou, D., Aivasidis, A. (2006) Decoloration of textile wastewater by means of a fluidized-bed loop reactor and immobilized anaerobic bacteria. Journal of Hazardous Material. 135, 372-377.
[14] Rakhshaee, R. (2011) Rule of FeO nano-particles and biopolymer structures in kinds of the connected pairs to remove Acid yellow 17 from aqueous solution: Simultaneous removal of dye in two paths and by four mechanisms. Journal of hazardous Material. 197, 144-152.
[15] Forgacs, E., Cserhati,T., Oros,G. (2004) Removal of synthetic dyes from wastewaters: a review. Environmental International. 20, 953-971.
[16] Mohammad, N.I., Ahmad, Z.A., Ahmad, M.A., Ahmad N., sulaiman, S.K. (2011) Optimization of process variables for malachite green dye removal usin rubber seed coat based activated carbon. International Journal of Engineering &Technology IJET-IJENS. 11, 10-12.
[17] Bi, B., Xu, L., Xu, B., Liu, X. (2011) Heteropoly blue-intercalated layeded double hydroxides for cationic dye removal from aqueous media. Applied Clay Science. 54, 241-247.
[18] Celekli, A., Birecikligil, S.S., Geyik, F., Bozkurt, H. (2012) Prediction of removal efficiency of Lanaset Red G on walnut husk using artificial neural network model. Bioresource Technology. 103, 64-70.
[19] Zhu, H.Y., Jiang, R., Fu, Y.Q., Jiang, J.H., Xiao, L., Zeng, G.M. (2011) Prepararion, characterization and dye adsorption properties of c-Fe2O3/SiO2/chitosan composite. Applied Surface Science. 258, 1337-1344.
[20] Xu, R., Xiao, S., Yuan, J., Zhao, A. (2011) Adsorption of methyl violet from aqueous solutions by the biochars derived from crop residues. Bioresource Technology. 102, 10293-10298.
[21] Farias, T., De Menorval, L.C., Zajac, J., Rivera, A. (2011) Benzalkonium chloride and sulfamethoxazole adsorption onto natural clinoptilolite: effect of time, ionic strength, pH and temperature. Journal of Colloid & Interface Science. 363, 465-475.
[22] Yang, F., Wang, Y., Ma, L., Wu, Y., Kerr. P.G., Yang, L. (2011) Basic dye adsorption onto an agro-based waste material-Sesame hull (Sesame indicum L.). Bioresource Technology. 102, 10280-10285.
[23] Yang, Y., Jin, D., Wang, G., Liu, D., Jia, X., Zhao, Y. (2011) Biosorption of Acid Blue 25 by unmodified and CPC-modified biomass of Penicillium YWO1: kinetic study, equilibrium isotherm and FTIR analysis. Colloids & surfaces B: Biointerfaces. 88, 521-526.
[24] Akgul, M., Karabakan, A.K. (2011) Promoted dye adsorption performance over desilicated natural zeolite. Microporous Mesoporous Materials. 145, 157-164.
[25] Huang, X.Y., Bu, H.B., Jiang, G.B. Zeng, M.H. (2011) Cross-linked succinyl chitosan as an adsorbent for the removal of Methylene Blue from aqueous solution. International Journal of Biological Macromolecules. 49, 643-651.
[26] Kan, T., Jiang, X., Zhou, L., Yang, M., Duan, M., Liu, P., Jiang, X. (2011) Removal of methyl orange from aqueous solutions using a bentonite modified with a new Gemini surfactant. Applied Clay Science. 54, 184-187.
[27] Xue, A., Zhou, S., Zhao, Y., Lu, X., Han, P. (2011) Effective NH2-grafting on attapulgite surfaces for adsorption of reactive dyes. Journal of Hazardous Material. 194, 7-14.
[28] Elass, K., Laachach, A., Alaoui, A., Azzi, M. (2011) Removal of methyl violet from aqueous solution using a steven site-rich clay from Morocco. Applied Clay Science. 54, 90-96.

[29] Lv, G., Li, Z., Jiang,W.T., Chang, P.H., Jeanc, J.S., Lin, K.H. (2011) Mechanism of acridine orange removal from water by low charge swelling clays. Chemical Engineering Journal. 174, 603-611.
[30] Chen, H., Zhao, J., Zhong, A., Jin, Y. (2011) Removal capacity and adsorption mechanism of heat-treated palygorskite clay for methylene blue. Chemical Engineering Journal. 174, 143-150.
[31] Ghaedi, M., Hossainian, H., Montazerozohori, M., Shokrollahi, A., Shojaipour, F., Soylak, M., Purkait, M.K. (2011) A novel acron based adsorbent for the removal of brilliant green. Desalination. 281, 226-233.
[32] Dursun, A.Y., Tepe, O. (2011) Removal of Chemazol Reactive Red 195 from aqueous solution by dehydrated beet pulp carbon. Journal of Hazardous Material. 194, 303-311.
[33] De Jesus, J., Neta, D.S., Moreira, G. C., Da Silva, C.J., Reis, C., Reis, E.L. (2011) Use of polyurethane foams for the removal of the Direct Red 80 and Reactive Blue 21 dyes in aqueous medium. Desalination. 281, 55-60.
[34] Wong, S.Y., Tan, Y.P., Abdullah, A.H., Ong, S.T. (2009) Removal of basic Blue 3 and reactive orange 16 by adsorption onto quartenized sugar cane bagasse. The Malaysian Journal of Analytical Science. 13, 185-193.
[35] Sudipta, C., Lee, D.S., Lee, M.W,. Woo, S.H. (2009) Enhanced adsorption of congo red from aqueous solutions by chitosan hydrogel beads impregnated with cetyl trimethyl ammonium bromide. Bioresource Technology. 100, 2803-2809.
[36] Tsuda, H., Ohshima, Y., Nomoto. H. (2004) Cancer prevention by natural compounds. Drug metabolism and pharmacokinetics. 19, 245.
[37] Han, R., Ding, D., Xu, Y., Zou, W., Wang, Y., Li, Y., Zou, L. (2008) Use of rice husk for adsorption for adsorption of congo red from aqueous solution in column mode. Bioresource Technology. 99, 2938-2946.
[38] Sudipta, C., Min, W., Lee S., Wooa, H. (2010) Adsorption of congo red by chitosan hydrogel beads impregnated with carbon nanotubes. Bioresource Technology. 101, 1800-1806.
[39] Chanzu, H.A., Onyari, J.M., Shiundu, P.M. (2012) Biosorption of malachite green from aqueous solution onto poly lactide/spent brewery grains films: Kinetics and equilibrium studies. Journal of Polymer Environment. 20, 665-672.
[40] Hu, Z., Chen, H., Ji, F., Yuan, S. (2010) Removal of Congo Red from aqueous solution by cattail root. Journal of Hazardous Material. 173, 192-297.
[41] Mohan, S., Gandhimathi, R. (2009) Removal of heavy metal ions from municipal solid waste leachate using coal fly ash as an adsorbent. Journal of Hazardous Material. 169, 351-359.
[42] Zhang, J., Zhou, Q., Ou, L. (2012) Kinetic, Isothermal and thermodynamis Study of the adsorption of Methyl Orange from Aqueous Solution by Chitosan/Alumina composite. Journal of Chemical Engineering Data. 57, 412-419.
[43] Asfour H.M., Fadali, O.A., Naseer, M.M., EI Geundi, M.S. (1985) Equilibrium studies on adsorption of basic dyes on hardwood. Journal of Chemical Technology & Biotechnology. 35, 21-27.
[44] Ho, Y.S. (1995) Adsorption of heavy metals from waste streams by peat. Ph.D. Thesis. University of Birmingham, Birmingham, U.K.
[45] Ho, Y.S. (2006) Second-order kinetic model for the sorption of cadmium onto tree fern: A comparison of linear and non-linear methods. Water Research. 40, 119-125
[46] Royer, B., Cardoso, N.F., Lima, E.C., Vaghetti, J.C.P., Simon, N.M., Calvete, T., Veses, R.C. (2009) Applications of Brazilian pine-fruit shell in natural and carbonized form as adsorbent to removal of methylene blue from aqueous solutions: Kinetics and equilibrium study. Journal of Hazardous Material. 164, 1213-1222.
[47] Langmuir, I. (1916) The constitution and fundamental properties of solids and liquids. Journal of Amercan Chemical Society. 38, 2221-2295.
[48] Weber, T.W., Chakravorti, R.K. (1974) Pore and solid diffusion models for fixed-bed adsorbents. AlChE Journal. 20, 228-238.
[49] McKay, G. (1982) Adsorption of dyestuffs from aqueous solution with activated carbon. I. Equilibrium and batch contact time studies. Journal of Chemical Technology & Biotechnology. 32, 759-772
[50] Xiong, L., Yang, Y., Mai, J., Sun, W., Zhang, C., Wei, D., Chen, Q., Ni, J. (2010) Adsorption behaviour of methylene blue onto titanate nanotubes. Chemical Engineering Journal. 156, 313-320.
[51] Freundlich, H.M.F. (1906) Uber dye adsorption in Losungen. Z. Phys. Chem. 57, 385-470.
[52] Chen, S.H., Yue, Q.Y., Gao, B.Y., Li, Q., Xu, X. (2011) Removal of Cr(VI) from aqueous solution using modified corn stalks characteristic, equilibrium, kinetics and thermodynamic study. Chemical Engineering Journal. 168, 909-917.
[53] Hu, B.J., Luo, H.J., Chen, H., Dong, T.T. (2011) Adsorption of chromate and para-nitrochlorobenzene on inorganic-organic montmorillonite. Applied Clay Science. 51, 198-201.

Received: **07.09.2017**
Accepted: **10.04.2018**

CORRESPONDING AUTHOR

Muhammad Imran Khan
CAS Key Laboratory of Soft Matter Chemistry,
Lab of Functional Membranes,
School of Chemistry and Material Science,
University of Science and Technology of China,
Hefei, Anhui 23006 – P.R. China

e-mail: raoimranishaq@gmail.com

© by PSP Volume 27 – No. 7/2018 pages 4689-4698 Fresenius Environmental Bulletin

ANALYSES OF THE DISTRIBUTION AND CHARACTERIZATION OF RHIZOSPHERE MICROORGANISMS OF *ZIZIPHUS JUJUBA* L. IN THE TARIM BASIN

Yipeng Guo, Yue Yang, Jiangui Li*, Jing Li, Shengliang Liu, Shuliang Zhu, Xianhui Qi

Institute of Forestry, Xinjiang Agricultural University, Urumqi 830000, Xinjiang, China

ABSTRACT

A growing body of evidence has suggested that microbial fertilizers can be used in organic agriculture to increase yield and improve the quality of jujube. In the Tarim Basin, soil samples were collected from main production regions which planted different varieties of jujube for 4 and 8 years. Our aim was to provide useful information to develop a special microbial fertilizer that is available for jujube. We identified four types of rhizosphere microorganisms, including growth-promoting bacteria, fungi, and actinomycetes. Comparative analyses were performed on soil microbes, the results of which indicated that the largest amount of bacteria, fungi, and actinomycetes existed in Tourfan Prefecture. The 4-year-old "Junzao" jujube had a higher number of soil microbe populations than the 8-year-old jujube. For growth-promoting bacteria, *Bacillus toyonensi* BCT-711 (P7) and *Bacillus subtilis subsp. subtilis str.* 168 (P3) showed stronger phosphate-solubilizing ability than other bacteria. K-releasing bacteria, especially *Bacillus megaterium*, *Enterobacter aerogene,* and *Pseudomonas syringae,* accounted for the greatest percentage of whole growth-promoting bacteria. *Acinetobacter* spp., *Pseudomonas* spp., *Enterobacter* spp., and *Bacillus* spp., as nitrogen-fixing bacteria, were related to nitrogen release and accumulation.

KEYWORDS:
Jujube, Tarim Basin, growth-promoting bacteria, fungus, actinomycetes

INTRODUCTION

The Tarim Basin is the largest and least explored inland basin in China [1]. Because most of the area is covered by the Takla Makan Desert, the climate of the Tarim Basin is a typical temperate continental climate. Under continuous drought conditions, the climate of this region tends to be hyper-arid. Scarce precipitation and intense evaporation caused by a shortage of water resources has seriously limited the development of agriculture in the area. Jujube (*Ziziphus jujuba* L.), as one of the most important economic crops, is widely grown in the Tarim Basin because jujube has a strong tolerance for and adaptability to drought stress [2-4].

Jujube is usually used as a human food with different productions. Therefore, it is necessary that red dates are produced without applying chemical fertilizers and pesticides. In addition, there is a serious phenomenon involving the application of chemical fertilizer during growth and development of jujube fruits, especially the improper use of N, P, and K fertilizers [5-6]. With the constant expansion of the jujube cultivation regions, the chemical fertilizers resulting in over-fertilization of soils and pollution of the aquatic and atmospheric environments have become an important issue that needs to be addressed. Microbial fertilizers raise soil fertility significantly, thus increasing the content of organic matter and the quantity of microorganisms, and improve useful soil microbial density [7-9]. Moreover, microbial fertilizers promote the production of a variety of physiologically-active substances that stimulate and regulate plant growth under abiotic stress conditions [10]. Therefore, microbial fertilizers have been applied to organic agriculture to increase yield and improve the quality of economic crops, such as tomatoes, wheat, and tobacco [11-13]. Above all, to develop a special microbial fertilizer used for jujube has vital practical significance and value.

Few studies have investigated the rhizosphere microbial populations from soils in which different red jujube varieties were planted during various growth ages in the Tarim Basin. In the current study we identified three types of rhizosphere microorganisms, including bacteria, fungi, and actinomycetes. Comparative analyses were performed on these microbes which indicated that the largest amount of bacteria, fungi, and actinomycetes was observed in the Tourfan Prefecture and the 4-year-old "Junzao" maintained a greater number of the soil microbe populations than the 8-year-old red dates. K-releasing bacteria accounted for the greatest percentage of whole growth-promoting bacteria. Additionally, *Bacillus* spp, *Pseudomonas* spp., *Enterobacter* spp., and *Acinetobacter* spp. were shown to be important

components of the growth-promoting bacteria of red dates.

MATERIALS AND METHODS

Study sites and soil samples. The experimental sites were selected in the red dates production regions in Tarim Basin, including the Kashi (38°11′N 77°16′ E), Hotan (37°07′ N 79°56′ E), Aksu (38°29 ′N 40°47′ E), Bayingolin Mongolia Autonomous (42°18′ N 86° 02′ E), and Tourfan Prefectures (42°51′N 89 29′ E). The experimental sites were situated on flat slopes, with sandy soil and lower groundwater levels (1% organic content; pH 7.4-8.3). Soil salinity content ranged from 0.1%-0.2% at a depth of 0-50 cm. The annual average sunshine was up to 2,996 h and the annual average temperature was $\geq$ 10°C; the effectively accumulated temperature was 3802-4388°C. Minimum cardinal (-15°C) and extremely minimum (-21°C) temperatures were observed in the experimental area. Soil samples were collected from the rhizosphere soils of two red date varieties ("Junzao" and "Huizao") at a depth of 10-20 cm in the experimental fields. Greater than or equal to five soil samples were collected at each of the study sites. The rhizosphere soil samples were collected from jujube tree roots, then divided into two groups and put into aseptic bags. One-half of the samples were applied to determine the water ratio and nutrient component with methods as described below, and the remaining samples were used to study the biomass of the soil by microbe analysis. The soil organic matter [14], soil available phosphate [15], soil available potassium (K) [16], and soil alkali hydrolyzable nitrogen (N) content [17] were calculated with the formulae, respectively. The pH values of the soils were determined using a pH measuring apparatus (Tenovo International Co., Matthaus, Germany). Significance analysis was performed using one-way ANOVA (version 19; SPSS, Inc., Chicago, IL, USA). LSD values were calculated when specific parameters changed significantly ($P<0.05$ or $P<0.01$).

Isolation and identification of rhizosphere microorganisms. The changes in rhizosphere microbial populations of soils with respect to two "Junzao" and "Huizao" varieties at different sampling sites were determined. Fungi and actinomycetes of soil samples were isolated using Martin substratum and Gauze's Medium No. 1. Nitrogen-fixing bacteria, inorganic P-releasing bacteria, organophosphate-degradation bacteria, and K-releasing bacteria were separated by Ashby nitrogen-free culture medium, NBRI-BPB medium), PVK medium and potassium bacteria selective medium. Under aseptic conditions, approximately 50 g per sample was dissolved with sterile water to acquire a 10^{-1} bacterial liquid. The microorganisms were fully dispersed by vibrating at 170 rpm/min for 30 min 28°C. One milliliter of bacterial liquid was added to 9 ml of sterile water to produce a 10^{-2} bacterial liquid, then 10^{-3}, 10^{-4}, and 10^{-5} solutions were similarly obtained and cultured for 4 days under constant temperature.

To isolate different bacteria from samples, 100 µl of the bacterial solution was placed centrally on a Baird-Parker plate, then the spreader was used to evenly smear the diluted samples on the plate. Similarly, different concentrations of diluted liquid were carefully applied to the isolation medium with different gradients. The bacteria were isolated by diluted liquids (10^{-4}, 10^{-5}, and 10^{-6}), then cultured at 37°C for 3 days. Isolation of fungi was performed using 3 prepared diluted liquids (10^{-2}, 10^{-3}, and 10^{-4}) at 25°C for 7 days. Similarly, the isolated actinomycetes were obtained through application to different diluted liquids (10^{-3}, 10^{-4}, and 10^{-5}) at 28°C for 1-3 days. Nitrogen-fixing bacteria were cultured using 10^{-4} and 10^{-5} diluted liquids at 37°C for 7 days. Similarly, single colonies of inorganic phosphorus-dissolving bacteria, organophosphate-degrading bacteria, and K-releasing bacteria were selected and transferred to the corresponding media, then the number of colonies with opacity and transparency were recorded.

Sequence analysis of 16S rDNA and phylogenetic tree analysis. Total genomic DNA was extracted using a DNA extraction kit (Tiangen Biochemical Technology Co., Ltd., Beijing, China). Those samples with an OD_{260}:OD_{280} ratio within the range of 1.8-2.0 were qualified for PCR amplification by NanoDrop ND-2000 (Thermo Fisher Scientific, Wilmington, DE, USA). These genomic DNA were then amplified by PCR with oligonucleotide primers designed by the Shanghai Health Bioengineering Technology Co., Ltd. (Shanghai, China). Three independent biological replicates of each sample and three technical replicates of each biological replicate were used in the RT-PCR using the ABI7500 Fast Real-Time PCR System (Applied Bio-Systems, USA) with a 96-well block. The forward primer (27 F) sequence was 5'-AGAGTTTGATCATGGCTCAG-3' and the reverse primer (1492 R) sequence was 5'-GGTTACCTTACGACTT-3'. PCR amplifications were performed in 50 uL-total volume reactions containing 5 µL of 10X buffer, 1.0 µL × 10 mmol·L^{-1} dNTPs, 10 mmol·L^{-1} templates, 2U TaqDNA polymerase, 2× uL bacterial genome DNA, and 1 uL of each primer. The reaction conditions were 3 min at 94°C, followed by 30 cycles at 72°C for 10 min and 72°C for 1 min. PCR products were identified by sequencing, and finally the PCR product was purified by a gel extraction kit to prepare for sequencing. Sequence data were aligned and compared with available standard sequences of

bacterial lineage in the National Center for Biotechnology Information GenBank database using BLAST search software and the species of the bacteria was identified according to Blast results. Using CLUSTALX 1.83 and MEGA 5.0 software, a phylogenetic tree was constructed using the neighbor joining method from distance matrices (bootstrap value=1000).

RESULTS

Distribution and quantity changes of rhizosphere microbes in different planting regions. To observe the distribution of rhizosphere microorganisms under different rhizosphere soil conditions, a total of three types of soil microbes were separated from some of the samples that were collected from five study sites, which were bacteria (nitrogen-fixing, inorganic phosphorus-dissolving, organophosphate-degrading, and K-releasing bacteria), fungi, and actinomycetes. The results showed that rhizosphere soil has a significant effect on microbial activity, such as bacteria, fungi, and actinomycetes (Figure 1). Akesu Prefecture had the most abundance of bacteria (4.28×10^6 cfu/g), followed by the Kashgar (3.63×10^6 cfu/g), Hotan (3.35×10^6 cfu/g), and Korla Prefectures (2.60×10^6 cfu/g)，whereas the least amount of bacteria and fungi were observed in Tourfan Prefecture （1.40×10^6 cfu/g). Similarly, the Akesu and Tourfan Prefectures had the highest (6.75×10^4cfu/g) and lowest number (2.00×10^4 cfu/g) of fungi in the sample, respectively. The amount of actinomycetes was significantly increased to 8.03×106 cfu/g in the Korla Prefecture, but were dramatically decreased in the Aksu, Kashgar, and Hotan Prefectures, and reached the lowest number in the Turpan Prefecture. The results revealed that rhizosphere soil of the Aksu Prefecture was conducive to the growth of bacteria, fungi, and actinomycetes when compared with other regions, especially in the Tourfan Prefecture. For growth-promoting bacteria, a large number of inorganic P-releasing and K-releasing bacteria was detected from samples of experimental regions, which accounted for greater than one-half of the total number of growth-promoting bacteria in Kashgar, Korla, and Tourfan Prefectures **(**Figure 2). A large number of K-releasing bacteria was found in the samples of Kashgar and Hotan Prefectures and was significantly higher than the Tourfan Prefecture. Soil condition had no significant effect on activity of nitrogen-fixing bacteria.

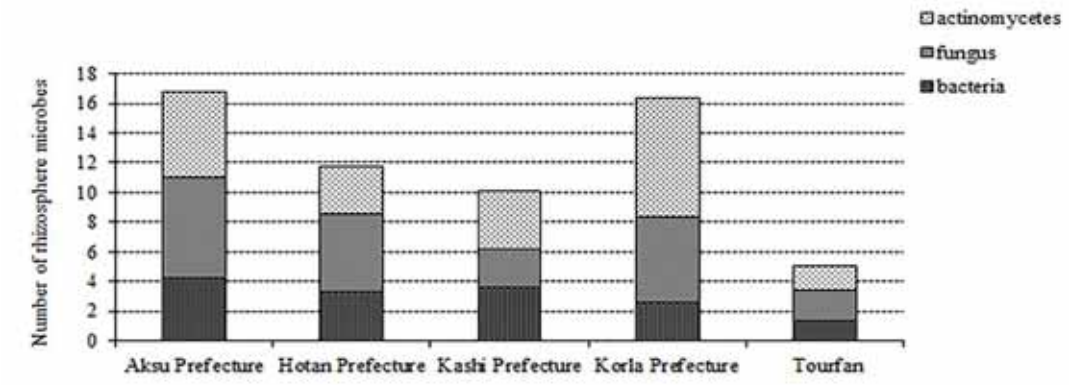

FIGURE 1
Changes in the number of bacteria, fungi, and actinomycetes from red jujube in the different planting areas.

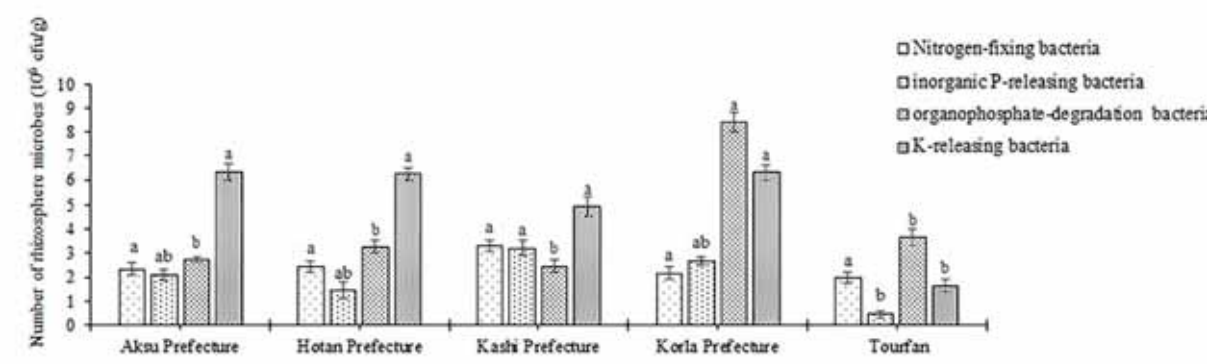

FIGURE 2
Changes in the population of growth-promoting bacteria in the five experimental sites.

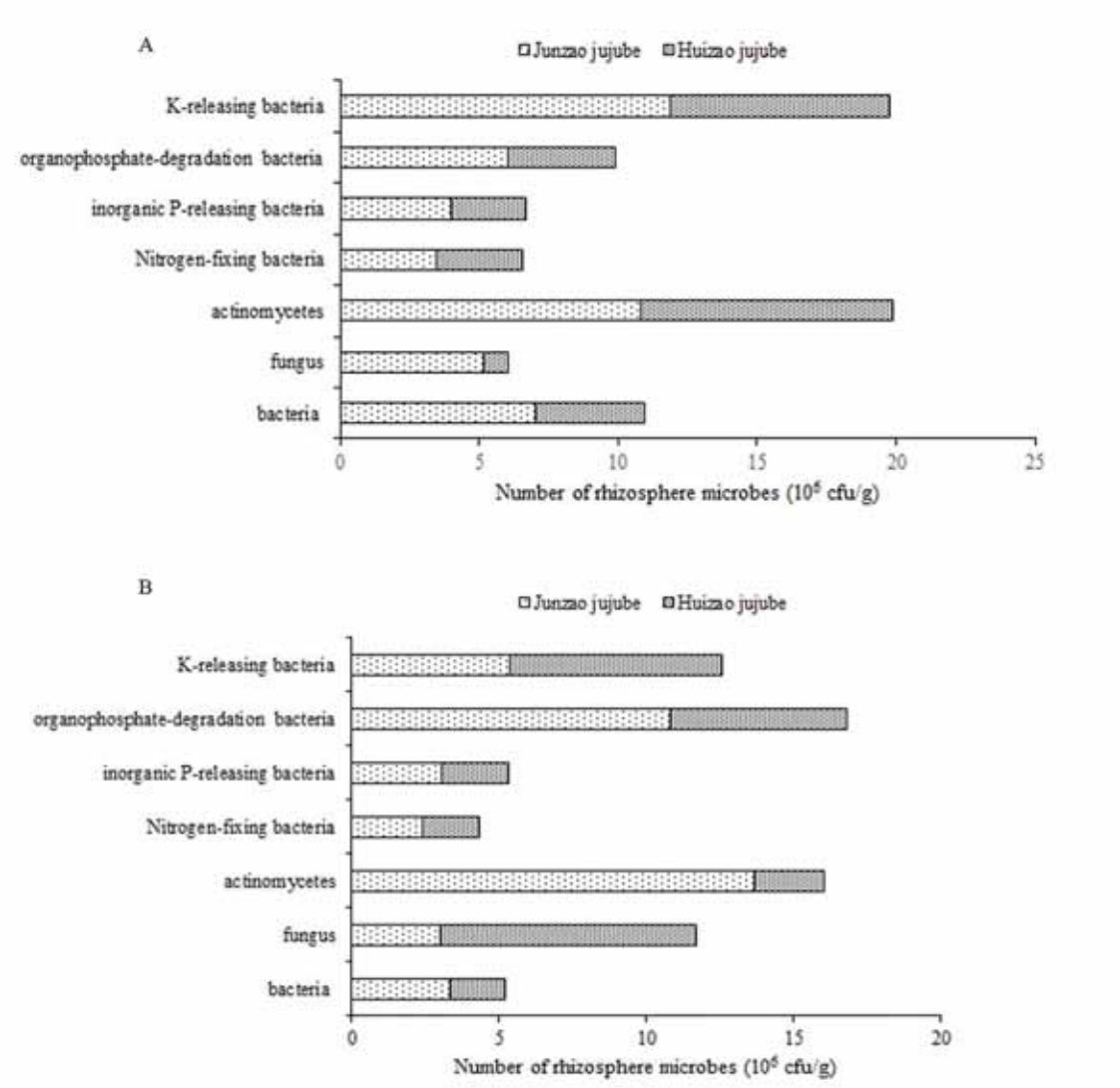

FIGURE 3
The difference in rhizosphere microbe number of two red jujube varieties ("Junzao" and "Huizao") in the Aksu (A) and Korla Prefectures (B).

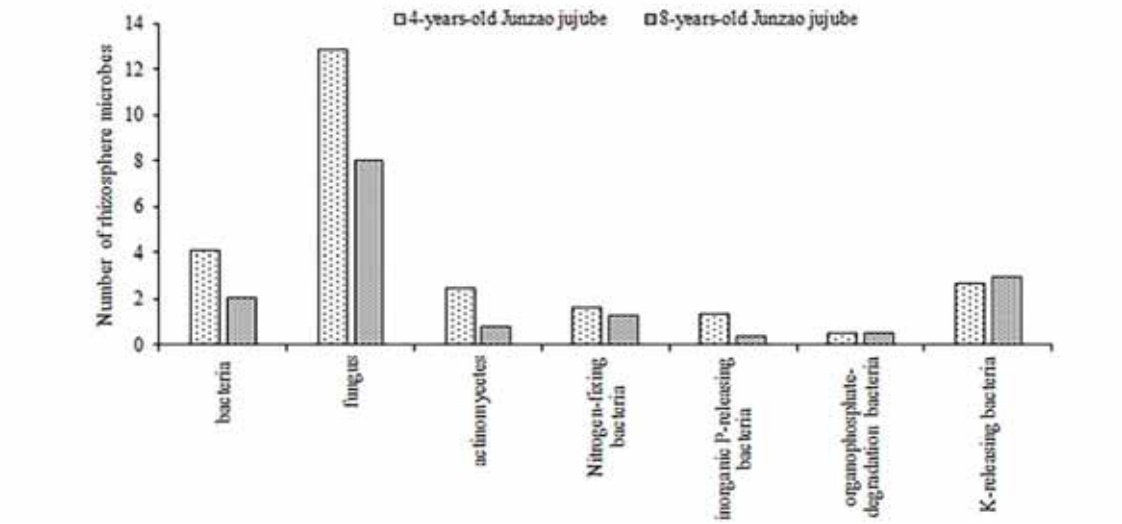

FIGURE 4
The number of rhizosphere microbes in 4- and 8-year-old "Junzao" jujube.

TABLE 1
Sequence alignment results of P-releasing bacteria, K-releasing bacteria and in red dates

Strain No.	Description	Identify	Accession No.
P1	*Agrobacterium sp*. H13-3 chromosome linear, complete sequence	99%	NC_015508.1
P2	*Enterobacter aerogenes* KCTC 2190 chromosome, complete genome	98%	NC_015663.1
P3	*Bacillus subtilis subsp*. subtilis str. 168 chromosome, complete genome	99%	NC_000964.3
P4	*Bacillus cereus* ATCC 14579 chromosome, complete genome	99%	NC_004722.1
P5	*Acinetobacter oleivorans* DR1 chromosome, complete genome	96%	NC_014259.1
P6	*Bacillus toyonensis* BCT-7112, complete genome	99%	NC_022781.1
P7	*Bacillus toyonensi* BCT-7112, complete genome	99%	NC_022781.1
P8	*Acinetobacter oleivorans* DR1 chromosome, complete genome	97%	NC_014259.1
P9	*Pseudomonas chlororaphis* O6 chromosome, whole genome shotgun sequence	99%	NZ_CM001490.1
P10	*Pseudomonas syringae pv*. phaseolicola 1448A chromosome, complete genome	99%	NC_005773.3
P11	*Acinetobacter oleivorans* DR1 chromosome, complete genome	97%	NC_014259.1
P12	*Acinetobacter oleivorans* DR1 chromosome, complete genome	96%	NC_014259.1
P13	*Acinetobacter oleivorans* DR1 chromosome, complete genome	99%	NC_014259.1
P14	*Pseudomonas putida* KT2440 chromosome, complete genome	99%	NC_002947.3
P15	*Acinetobacter oleivorans* DR1 chromosome, complete genome	98%	NC_014259.1
P16	Enterobacter aerogenes KCTC 2190 chromosome, complete genome	98%	NC_015663.1
P17	*Pseudomonas fluorescens* Pf0-1 chromosome, complete genome	99%	NC_007492.2
P18	*Enterobacter aerogenes* KCTC 2190 chromosome, complete genome	99%	NC_015663.1
P19	*Enterobacter aerogenes* KCTC 2190 chromosome, complete genome	98%	NC_015663.1
P20	*Lysinibacillus sphaericus* C3-41 chromosome, complete genome	94%	NC_010382.1
K1	*Bacillus subtilis subsp* . subtilis str. 168 chromosome, complete genome	99%	NC_000964.3
K2	*Enterobacter aerogenes* KCTC 2190 chromosome, complete genome	98%	NC_015663.1
K3	*Pseudomonas fluorescens* Pf0-1 chromosome, complete genome	99%	NC_007492.2
K4	*Pseudomonas fluorescens* Pf0-1 chromosome, complete genome	99%	NC_007492.2
K5	*Enterobacter aerogenes* KCTC 2190 chromosome, complete genome	98%	NC_015663.1
K7	*Bacillus megaterium* DSM 319 chromosome, complete genome	99%	NC_014103.1
K8	*Bacillus megaterium* DSM 319 chromosome, complete genome	99%	NC_014103.1
K9	*Bacillus megaterium* DSM 319 chromosome, complete genome	99%	NC_014103.1
K10	*Bacillus sp* . 1NLA3E, complete genome	96%	NC_021171.1
K11	*Bacillus megaterium* DSM 319 chromosome, complete genome	99%	NC_014103.1
K12	*Bacillus megaterium* DSM 319 chromosome, complete genome	99%	NC_014103.1
K13	*Bacillus megaterium* DSM 319 chromosome, complete genome	99%	NC_014103.1
K14	*Bacillus megaterium* DSM 319 chromosome, complete genome	99%	NC_014103.1
K15	*Bacillus megaterium* DSM 319 chromosome, complete genome	99%	NC_014103.1
K16	*Bacillus megaterium* DSM 319 chromosome, complete genome	99%	NC_014103.1
K17	*Acinetobacter oleivorans* DR1 chromosome, complete genome	99%	NC_014259.1
K18	*Bacillus megaterium* DSM 319 chromosome, complete genome	99%	NC_014103.1
K19	*Acinetobacter oleivorans* DR1 chromosome, complete genome	99%	NC_014259.1
K20	*Enterobacter aerogenes* KCTC 2190 chromosome, complete genome	98%	NC_015663.1
K21	*Bacillus megaterium* DSM 319 chromosome, complete genome	99%	NC_014103.1
K22	*Bacillus megaterium* DSM 319 chromosome, complete genome	99%	NC_014103.1
K23	*Pseudomonas syringae pv*. phaseolicola 1448A chromosome, complete genome	99%	NC_005773.3
K24	*Bacillus megaterium* DSM 319 chromosome, complete genome	99%	NC_014103.1
K25	*Acinetobacter oleivorans* DR1 chromosome, complete genome	99%	NC_014259.1
K26	*Pseudomonas syringae pv*. phaseolicola 1448A chromosome, complete genome	99%	NC_005773.3
j2	*Bacillus megaterium* DSM 319 chromosome, complete genome	99%	NC_014103.1
j3	*Bacillus megaterium* DSM 319 chromosome, complete genome	99%	NC_014103.1
j4	*Bacillus pumilus* SAFR-032 chromosome, complete genome	99%	NC_009848.1
j5	*Acinetobacter oleivorans* DR1 chromosome, complete genome	98%	NC_014259.1
j6	*Bacillus megaterium DSM* 319 chromosome, complete genome	99%	NC_014103.1
j8	*Pseudomonas syringae pv*. phaseolicola 1448A chromosome, complete genome	99%	NC_005773.3
j9	*Acinetobacter oleivorans* DR1 chromosome, complete genome	99%	NC_014259.1

Comparative analysis of the changes in population of rhizosphere microbes associated with red jujube varieties and growth ages. To investigate the difference in soil microbes between the two red jujube varieties ("Junzao" and "Huizao"), rhizosphere soil samples were taken for testing the distribution of bacteria, fungi, and actinomycetes in the Aksu and Korla Prefectures (Figure 3). The number of rhizosphere soil microbes of "Junzao" were dramatically greater than "Huizao" in the two regions, while the opposite result was observed with respect to K-releasing bacteria. The 4- and 8-year-old "Junzao" were used for studying the changes in the amount of bacteria, fungi, and actinomycetes (Figure 4). Compared with jujube growth for 8 years, the 4-year-old "Junzao" maintained a higher number of bacteria and fungi. In contrast, as the number of years of cropping increased, the number of growth-promoting bacteria in the rihzosphere showed an increasing trend, with the exception of organophosphate-degrading bacteria.

Identification of growth-promoting bacteria in different rhizosphere soils using 16S rRNA sequencing. To study the species and amount of growth-promoting bacteria populations in red jujube, 16S rDNA sequence analysis was used to identify inorganic P-releasing, K-releasing, and nitrogen-fixing bacteria (Table 1). According to the results of

Blast NCBI and GeneBank, the major types of P-releasing bacteria found were *Agrobacterium* spp.*, Enterobacter aerogenes, Bacillus subtilis subsp., Bacillus cereus, Acinetobacter oleivorans, Bacillus toyonensis, Pseudomonas* spp.*,* and *Lysinibacillus sphaericu*. The highest number of P-releasing bacteria was *Enterobacter aerogenes*, *Acinetobacter oleivorans,* and *Bacillus toyonensi*. Three K-releasing bacteria (*Bacillus megaterium*, *Enterobacter aerogen*e, and *Pseudomonas syringae)* were observed, which might play significant roles in the soil microbial community changes for red dates. Similarly, *Bacillus megaterium Acinetobacter* spp., and *Pseudomonas* spp., as two types of important nitrogen-fixing bacteria were identified in the various soil samples (Table 1).

Based on the results of sequence alignment, 20 strains of different P-releasing bacteria were grouped into 4 categories. The first category included 5 P-releasing bacteria (P_5, P_8, P_{11}, P_{12}, P_{13}, and P_{15}) with 99% genetic similarity to *Acinetobacter* spp. (C25JX177 713.1) and *Acinetobacter* spp. *S3* (MAC.013HM063 913.1). The second group contained *Bacillus cereus* ATCC 14579 (P_4), *Bacillus toyonensis* BCT-7112 (P_7), and *Lysinibacillus sphaericus* C3-41 (P_{20}); among the bacteria, the similarity coefficient between *Bacillus toyonensi* BCT-7112 (P_7) and *Bacillus* spp. WP09-2 (KF719 307.1) was 0.99. Four types of *Pseudomonas* spp., including *Pseudomonas chlororaphis* O6 (P_9), *Pseudomonas syringae pv. phaseolicola* 1448A (P_{10}), *Pseudomonas putida* KT2440 (P_{14}), and *Pseudomonas fluorescens* Pf0-1 (P_{17}), were classified into 1 category, which showed 96%–97% similarity and was highly homologous with the closest known species, *Pseudomonas* spp. 5 060 （KC236 637.1）in GenBank. In addition, *Agrobacterium* spp. H13-3 (P_1) and *Bacillus subtilis subsp. subtilis str.* 168 (P_3) had high genetic similarity with *Rhizobium* spp. XGL136 (JQ041 733.1) and *Bacillus subtilis* strain F111 (HQ647 257.1), respectively (Figure 5A).

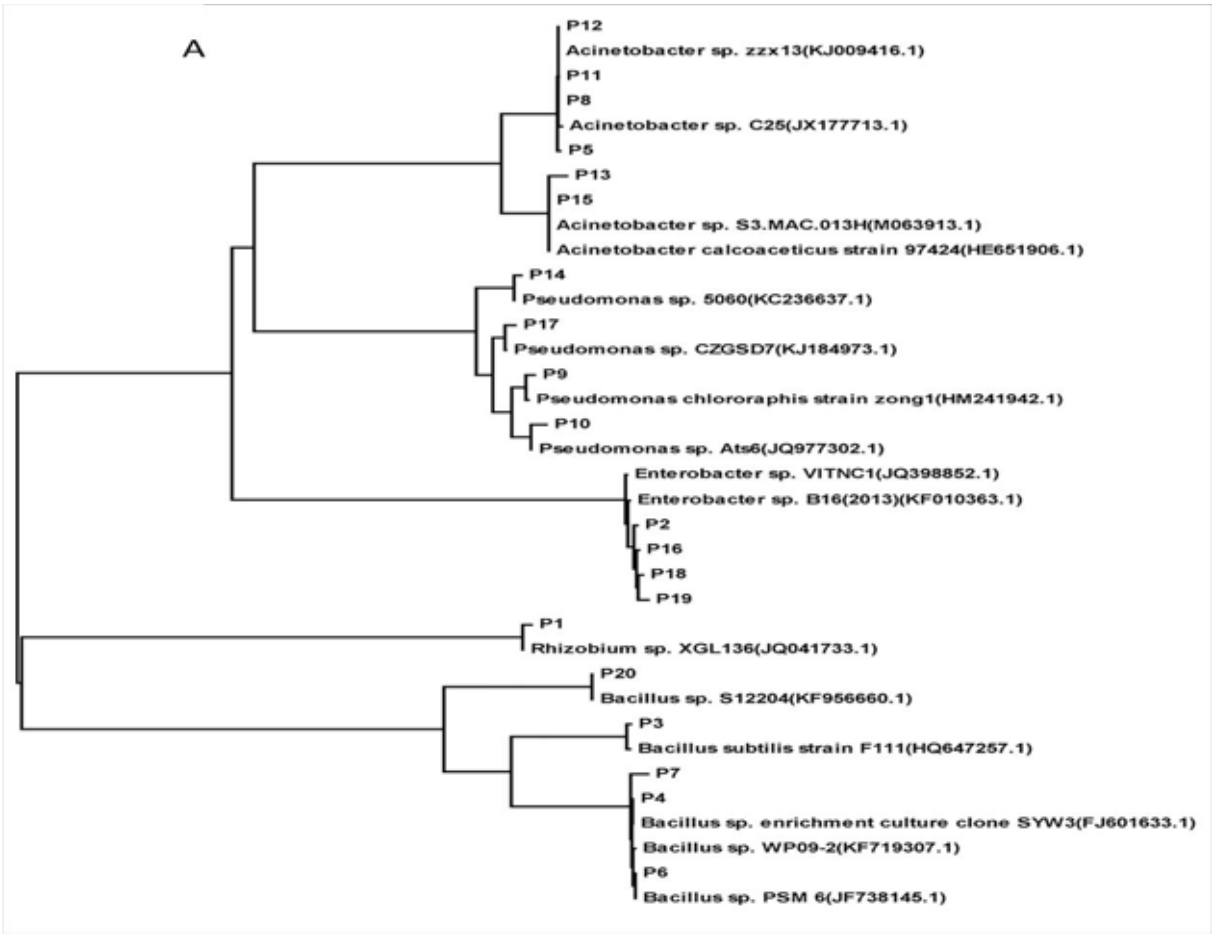

FIGURE 5A
Phylogenetic tree showing the relationship of jujube P-releasing bacteria based on 16 S rDNA sequence.

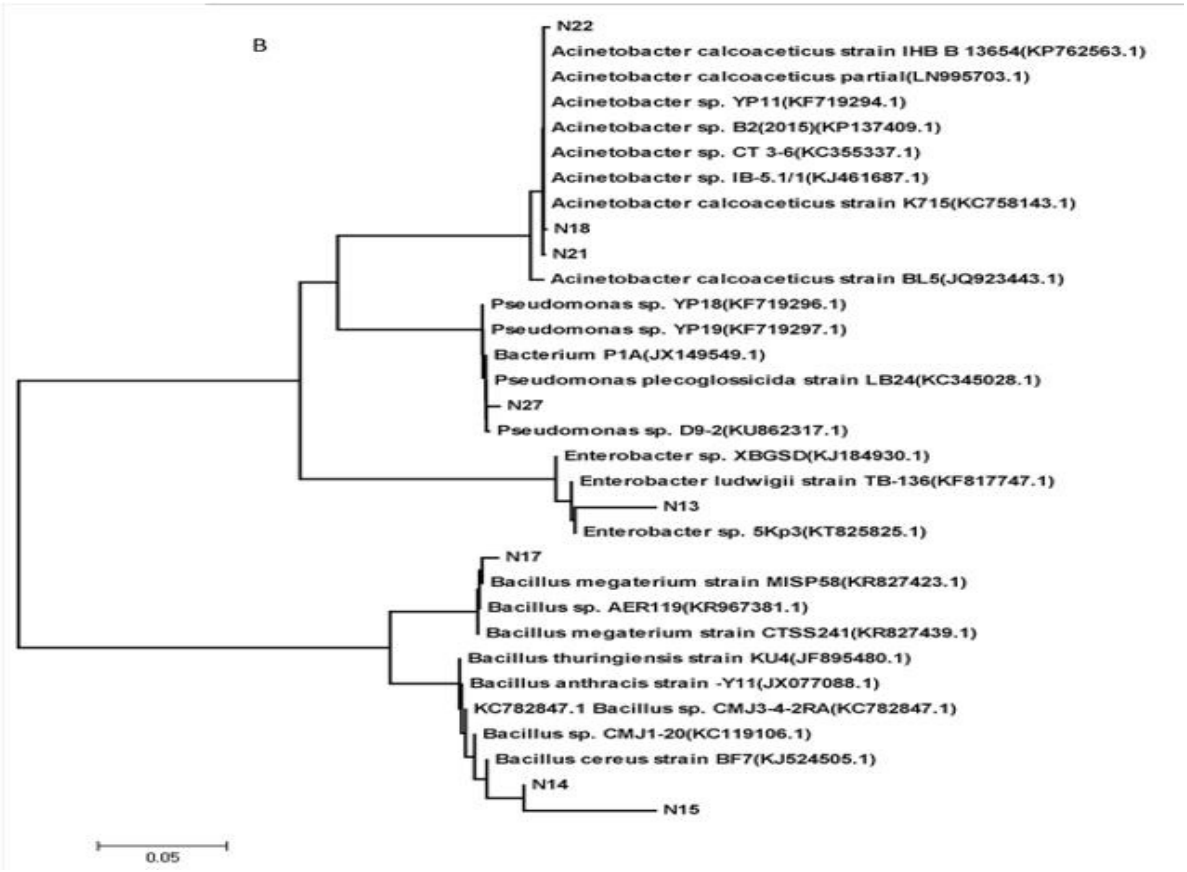

FIGURE 5B
Phylogenetic tree showing the relationship of jujube K-releasing bacteria based on 16 S rDNA sequence.

For K-releasing bacteria, 24 sequenced strains were divided into 4 groups. *Bacillus subtilis subsp. subtilis str.* 168 (K_1), *Bacillus megaterium DSM 319* (K_7, K_8, and K_9), *Bacillus* spp. 1NLA3E (K_{10}), *Bacillus megaterium* DSM 319 (K_{11}, K_{13}, K_{14}, K_{15}, K_{16}, K_{21}, K_{22}, and K_{24}) and *Acinetobacter oleivorans DR1* (K_{18}) were classified as the first group (Figure 5B); the highest similarity was calculated between K_1 and *Bacillus subtilis* strain F111 (HQ647257.1). Similar results were observed between K_{10} and *Bacillus* spp. G08 (JQ977012.1), Moreover, other K-releasing bacteria had 99% homology with *Bacillus megaterium* strain KUDC1720 (KC414700.1) and Bacillus spp. CMJ1-21(KC119107.1). The second group was *Pseudomonas fluorescens* Pf0-1(K_3 and K_4) and *Pseudomonas syringae pv. phaseolicola* 1448A (K_{23} and K_{26}). High genetic similarities existed between *Pseudomonas fluorescens* Pf0-1(K3 and K4) and *Pseudomonas* spp. FSBSA9 (KJ185013.1). The results from K23, K26, *Pseudomonas frederiksbergensis* strain B27 (JN377673.1), and *Pseudomonas* spp. RT2 (JF778675.1) were consistent. Furthermore, high genetic similarity among *Enterobacter aerogenes* KCTC 2190 (K2, K5, and K20) and *Enterobacter ludwigii* strain AR-165 (KF843728.1) revealed that they have a close genetic distance and are distributed on the same branch. K17, K19, and K25 were grouped as 1 category belonging to *Acinetobacter* spp.; *Acinetobacter oleivorans* DR1 (K17 and K19) showed genetic homology with *Acinetobacter* spp. 3. MAC.013 (HM063913.1; approximately 0.99), and K25 were closely relate to *Acinetobacter* spp. YP11 (KF719294.1).

Eight strains of nitrogen-fixing bacteria were divided into different categories, as shown in Figure 5C. The three types of nitrogen-fixing bacteria, *Acinetobacter* spp. mkj-33 (N18), *Acinetobacter calcoaceticus* (N21), and *Acinetobacter* spp. YP11 (N22), were highly correlated genetically with different *Acinetobacter baumannii* spp., including *Acinetobacter* spp. YP11 (KF719294.1), *Acinetobacter calcoaceticus* strain R-53748 (LN995703.1), and Acinetobacter spp. 2 (2015 [KP137409.1]). *Pseudomonas* spp. LZJ-9 (N27) and *Enterobacter* spp. XBGSD (N15) showed > 95% genetic similarities with *Pseudomonas* spp. D9-2(KU862317.1) and *Enterobacter* spp. 5Kp3 (KT825825.1), respectively. The remaining nitrogen-fixing bacteria (N14, N15, and N17) were grouped as an independent cluster, which have a homologous relationship between *Bacillus thuringiensis* strain KU4 (N14 and N15) and *Bacillus* spp. HH07 (KC857472.1). Similarly, *Bacillus megaterium* strain CTSS241 (N17) was related to *Bacillus* spp. AER119 (KR967381.1) and *Bacillus megaterium* strain MISP58 (KR827423.1).

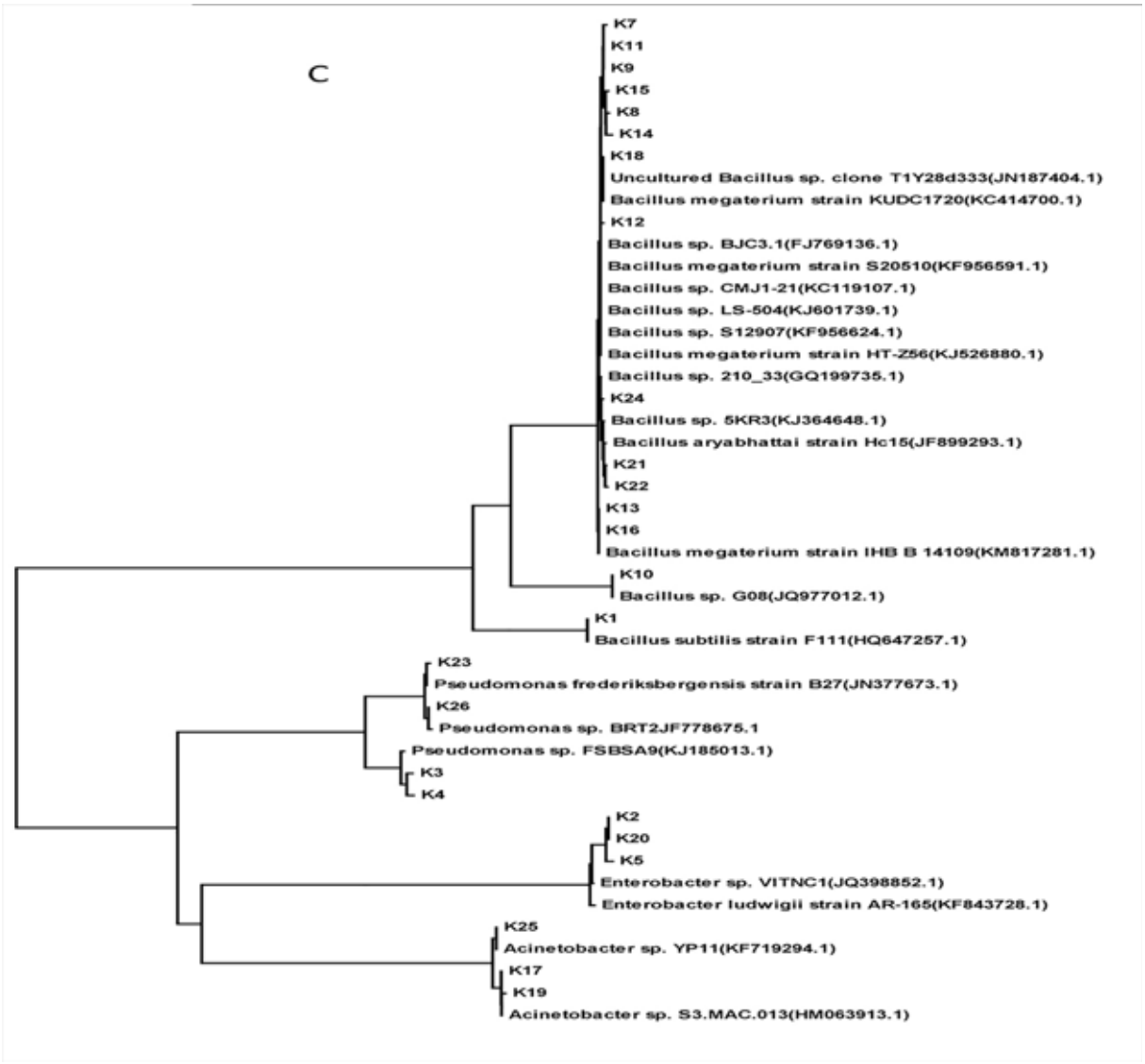

FIGURE 5C
Phylogenetic tree showing the relationship of jujube nitrogen-fixing bacteria (C) based on 16 S rDNA sequence.

DISCUSSION

Soil microbes are participated in a range of processes that essential for the transformation of soil N, P, and K, and are thus an integral part of the soil nutrient cycle and the decomposition of organic matter [18-19]. The quantity of bacteria, fungi, and actinomycetes is often one of the important indices that reflects the activity of soil microbes [20-21]. Bacteria and fungi play vital roles in soil ecosystems by regulating decomposition activity [22-23]. Actinomycetes play an important role in the decomposition and degradation of organic matter associations with woody plants [24]. Plant growth-promoting bacteria (PGPB) are soil and rhizosphere bacteria that can benefit plant growth by different mechanisms [25]. The ability of a few soil microorganisms to convert insoluble forms of phosphorus and potassium to accessible forms is an important trait in plant growth-promoting bacteria for increasing plant yields [26].

The distribution of soil microbes has extremely remarkable differences in the various regions that lead to different moisture properties, soil particle size, salinity, and pH [27]. For example, topsoil samples have a higher number of phosphate-solubilizing microbes than subsoil [28]. In the current study, the least amount of microbes, such as bacteria and fungi, were found in the Tourfan Prefecture when compared with other study sites. However, a large number of soil microbes was identified in the Aksu Prefecture. Indeed, the sum of bacteria and actinomycetes was almost 10 times greater than the number of fungi. There is little information concerning the distribution characteristics of the rhizosphere microbe population in "Junzao" and "Huizao," which are two of the important varieties of red dates. According to the results of our research, the amount of soil microbes in the "Junzao" jujube was higher than the number of rhizosphere microbes in the "Huizao" jujube. The diversity of the fungi in the rhizosphere

soil collected by the 3-year old jujube was greater than the 8-year-old jujube tree [29]. Our results are also evidence to support this finding. Compared with jujube growth for 8 years, the 4-year-old "Junzao" maintained a higher number of fungi. The quality of growth-promoting bacteria showed opposite results in this study, perhaps because growth-promoting bacteria are severely influenced by environmental factors, such as soil types [30].

Plant growth-promoting bacteria are vital and can convert nutritionally-important elements from an unavailable to available form through biological processes [31]. In this study, several types of growth-promoting bacteria were identified, such as *Bacillus* spp., *Acinetobacter* spp., *Pseudomonas* spp., and *Staphylococcus* spp. The results are consistent with a previous study involving phosphate-solubilizing bacteria [32]. Research has shown that *Bacillus* spp. and *Pseudomona*s spp. have a strong ability to convert insoluble forms of phosphorus to an accessible form [33-34]. In our study, *Bacillus toyonensi* BCT-711 (P_7) and *Bacillus subtilis subsp*. *subtilis str.* 168 (P_3) belonging to the family *Bacillus* sp., had stronger phosphate-solubilizing ability than other bacteria.

ACKNOWLEDGEMENTS

Financial support from the Key Research and Development Program of Xinjiang, Techniques Research and Integration on Quality Improvement and Simplified Cultivation of Red Jujube in Xinjiang, (Project 1, 2017B01002-1) and The Natural Science Foundation of China, Operating Mechanism of Soil and Fertilizar Factors on the Formation of cAMP in Fruit of Jujube (cv.gray jujube) in Xinjiang (Project, 31360194).

REFERENCES

[1] Li, D.S., Liang, D.G., Jia, C.Z. and Wang, G. (1996) Hydrocarbon accumulations in the Tarim basin, China. AAPG bulletin. 80, 1587-1603.

[2] Lyrene, P.M. and Crocker, R.E. (1994) The Chinese jujube. [Fact Sheet HS-50]. University of Florida Cooperative Extension Service, Gainesville. 2 and 8.

[3] Abrol, D.P. (2015) Subtropical Fruits. In: Abrol, D.P. (ed.) Pollination Biology. Springer International Publishing. Switzerland. Vol: 1, 347-397.

[4] Li, X., Feng, G., Sharratt, B. and Zheng, Z. (2015) Aerodynamic properties of agricultural and natural surfaces in northwestern Tarim Basin. Agricultural and Forest Meteorology. 204, 37-45.

[5] Nayak, P., Patel, D., Ramakrishnan, B., Mishra, A.K. and Samantaray, R.N. (2009) Long-term application effects of chemical fertilizer and compost on soil carbon under intensive rice–rice cultivation. Nutrient cycling in agroecosystems. 83, 259-269.

[6] Oliveira, R.S., Ma, Y., Rocha, I., Carvalho, M.F., Vosátka, M. and Freitas, H. (2016) Arbuscular mycorrhizal fungi are an alternative to the application of chemical fertilizer in the production of the medicinal and aromatic plant Coriandrum sativum L. Journal of Toxicology and Environmental Health. Part A. 79, 320-328.

[7] Bulluck, L.R., Brosius, M., Evanylo, G.K. and Ristaino, J.B. (2002) Organic and synthetic fertility amendments influence soil microbial, physical and chemical properties on organic and conventional farms. Applied Soil Ecology. 19, 147-160.

[8] He, Y.H., Wu, Z.H., Tu, L., Han, Y.J., Zhang, G.L. and Li, C. (2015) Encapsulation and characterization of slow-release microbial fertilizer from the composites of bentonite and alginate. Applied Clay Science. 109, 68-75.

[9] Liu, L., Hu, H., Tian, Y., Chen, N., Quan, J. and Liu, H. (2015) Chemical characteristics, sources and health impacts of urban ambient pm2.5 in wuhan during the Chinese spring festival pollution episode. Fresen. Environ. Bull. 24, 3853-3864.

[10] Magalhães, P.O., Lopes, A.M., Mazzola, P.G., Rangel-Yagui, C., Penna, T.C. and Pessoa, A. (2007) Methods of endotoxin removal from biological preparations: a review. J Pharm Pharm Sci. 10, 388-404.

[11] Xia, Z.Y., Li, Y.H. and Yang, S.J. (2002) Effects of microbial fertilizer on flue-cured tobacco on field. Chinese Tobacco Science. 3, 009.

[12] Tu, C., Jean, B.R. and Hu, S. (2006) Soil microbial biomass and activity in organic tomato farming systems: Effects of organic inputs and straw mulching. Soil Biology and Biochemistry. 38, 247-255.

[13] Dozet, G., Cvijanovic, G., Djukic, V., Cvijanovic, D. and Kostadinovic, L. (2014) Effect of microbial fertilizer on soybean yield in organic and conventional production. Turkish Journal of Agricultural and Natural Sciences. 6, 1333-1339.

[14] Walkley, A. (1947) A critical examination of a rapid method for determining organic carbon in soils-Effect of variations in digestion conditions and of inorganic soil constituents. Soil Science. 63, 251-264.

[15] Heinonen, J.K. and Lahti, R.J. (1981) A new and convenient colorimetric determination of inorganic orthophosphate and its application to the assay of inorganic pyrophosphatase. Analytical biochemistry. 113, 313-317.

[16] Isaac, R.A. and Kerber, J.D. (1971) Atomic absorption and flame photometry: Techniques and uses in soil, plant, and water analysis. In: Walsh, L.M. (ed.) Instrumental methods for analysis of soils and plant tissue. Soil Society of America. Madison, WI, 17-37.
[17] Emmrich, M. (1999) Kinetics of the alkaline hydrolysis of 2, 4, 6-trinitrotoluene in aqueous solution and highly contaminated soils. Environmental science & technology. 33, 3802-3805.
[18] Chen, Y.P., Rekha, P.D., Arun, A.B., Shen, F.T., Lai, W.A. and Young, C.C. (2006) Phosphate solubilizing bacteria from subtropical soil and their tricalcium phosphate solubilizing abilities. Applied soil ecology. 34, 33-41.
[19] Hou, S., Xin, M., Wang, L., Jiang, H., Li, N., Wang, Z. (2014) The effects of erosion on the microbial populations and enzyme activity in black soil of northeastern China. Acta Ecologica Sinica. 34, 295-301.
[20] Page, A.L. (1982) Methods of soil analysis. Part 2. Chemical and microbiological properties. American Society of Agronomy, Soil Science Society of America. Madison, WI.
[21] Subramanian, K.S., Muniraj, I. and Uthandi, S. (2016) Role of Actinomycete-Mediated Nanosystem in Agriculture. In: Plant Growth Promoting Actinobacteria. Springer: Singapore 233-247.
[22] Altieri, M.A. (1999) The ecological role of biodiversity in agroecosystems. Agriculture, Ecosystems & Environment. 74, 19-31.
[23] Schimel, J.P ., Schaeffer, S.M . (2012) Microbial control over carbon cycling in soil. 3, 348.
[24] McVeigh, H.P., Munro, J. and Embley, T.M. (1996) Molecular evidence for the presence of novel actinomycete lineages in a temperate forest soil. Journal of industrial microbiology. 17, 197-204.
[25] Glick, B.R., Karaturovic, D.M. and Newell, P.C. (1995) A novel procedure for Rapid Isolation of plant growth promoting pseudomonas. Can. J. Microbiol. 41, 533-536.
[26] Sivasakthi, S., Usharani, G. and Saranraj, P. (2014) Biocontrol potentiality of plant growth promoting bacteria (PGPR)-Pseudomonas fluorescens and Bacillus subtilis: A review. African Journal of Agricultural Research. 9, 1265-1277.
[27] Yergeau, E., Bokhorst, S., Huiskes, A.H., Boschker, H.T., Aerts, R., Kowalchuk, G.A. (2007) Size and structure of bacterial, fungal and nematode communities along an Antarctic environmental gradient. FEMS microbiology ecology. 59, 436-451.
[28] Yang, S.S., Fan, H.Y., Yang, C.K. and Lin, I.C. (2003) Microbial population of spruce soil in Tatachia mountain of Taiwan. Chemosphere. 52, 1489-1498.
[29] Liu, P., Wang, X.H., Li, J.G., Qin, W., Xiao, C.Z., Zhao, X. Jiang, H.X, Sui, J.K, Sa, R.B, Wang, W.Y. and Liu, X.L. (2015) Pyrosequencing reveals fungal communities in the rhizosphere of Xinjiang jujube. BioMed research international. 2015, 8p.
[30] Egamberdiyeva, D. (2007) The effect of plant growth promoting bacteria on growth and nutrient uptake of maize in two different soils. Applied Soil Ecology. 36, 184-189.
[31] Vessey, J.K. (2003) Plant growth promoting rhizobacteria as biofertilizers. Plant and soil. 255, 571-586.
[32] Rivas, R., Peix, A., Mateos, P.F., Trujillo, M.E., Martínez-Molina, E. and Velázquez, E. (2007) Biodiversity of populations of phosphate solubilizing rhizobia that nodulates chickpea in different Spanish soils. In: First international meeting on microbial phosphate solubilization. Springer: Netherlands, 23-33.
[33] Rodríguez, H. and Fraga, R. (1999) Phosphate solubilizing bacteria and their role in plant growth promotion. Biotechnology advances. 17, 319-339.
[34] Othman, F., Heydari, M., Ahmadizadeh, M., Nozari, H. and Sadeghian M.S. (2017) Investigating the effectiveness of seasonalization based on statistical parameters in normalizing, modeling and forecasting inflow time series. Fresen. Environ. Bull. 26, 590-597.

Received: **18.09.2017**
Accepted: **08.01.2018**

CORRESPONDING AUTHOR

Jiangui Li
Institute of Forestry,
Xinjiang Agricultural University,
Urumqi 830000, Xinjiang – China

e-mail: jiangui_li@126.com

© by PSP Volume 27 – No. 7/2018 pages 4699-4706 Fresenius Environmental Bulletin

THE COMPARISON OF AGRICULTURAL AND TECHNOLOGICAL PROPERTIES OF SOME CORN (*ZEA MAYS* L.) VARIETIES AS THE MAIN AND SECOND CROP

Aydin Alp[1,*], Serif Kahraman[2]

[1]Dicle University, Faculty of Agriculture, Department of Field Crops, Diyarbakir, Turkey
[2]GAP International Agricultural Research and Educational Center, Diyarbakir, Turkey

ABSTRACT

No doubt, investigating the possibility of cultivating maize in two different periods without a decline in yield and quality of the maize will contribute to the cultivation of maize in the region. In this study, the agricultural and technological properties of grain maize varieties grown as main and second crop were investigated. The study was conducted in the research and application field of GAP International Agricultural Research and Educational Center between 2014-2015 as three replicates in Randomized Blocks Trial Design. Different 15 grain maize varieties that were compatible with the Southeastern Anatolia Region climatic conditions which had different vegetation periods and which were provided from different seed institutes were used as the material in the study.

In terms of two year average values in the main and second cropping periods; significant differences according to 1 % among the maize varieties in silking periods (82.4-64.9 day), first ear height (99.4-102.6 cm), stem thickness (21.9-23.50 mm), ear length (21.0-21.4 cm), ear thickness (46.58-48.97 mm), number of ear per plant (1.032-1.039 number), kernel/ear (% 85.58-81.32), moisture (% 15.64-25.17). It was determined that a plant grain yield was 188.59 g in main cropping, 176.3 g in second cropping. In terms of unit area grain yield, the average of maize varieties was found significantly different according to 5%; the average unit area yield was determined as 138.88 kg/ha in main cropping and 126.60 kg/ha in second cropping.

As a conclusion, it was determined that, PR31D24, Sy Radioso, Suertoda, 72May80, P.31G98, Katone and Sy Lucroso varieties had superior values in the main crop, and Katone, PR31D24 and Kerbanis varieties had superior values in the second crop in Diyarbakır climatic conditions in terms of yield and technological properties.

KEYWORDS:
Maize, Main Crop, Second Crop, Yield, Quality, Technological Properties

INTRODUCTION

Maize is used as nutrient and feed for humans and animals, and as raw material in the production of alcohol, oil, semolina, glue, bioethanol, starch-based sugar [1, 2].

Feed industry is the most important usage area of maize with a rate of 70%. It is estimated that 950 thousand tons of maize are used in starch industry mainly in the production of Starch-Based Sugar (SBS) [3]. Another field in which maize is used in food industry is the maize oil production. In direct consumption, it has also been reported in recent years that the use of maize flour is also common especially in the Black Sea Region; however, it has also been reported that the use of it is decreasing [4].

Maize ranks the first in the world cereal production with 184-million-hectare sowing area, 1.016 million tons production and 552 kg/da average yield [5]. Important changes were observed in Turkey in maize production as of 2000. The maize production was 2.300 thousand tons in 2000 in Turkey, and the average yield was 4160 kg/ha; and grain maize production was 5.950.000 tons in 2014, and the average yield was 9070 kg/ha. In 69,2 % (455.500 ha) of the cultivation areas in Turkey, main crop; and in 30,8 % (203.100 ha) second crop maize cultivation was performed. 72,3% (4.301.000 tons) of the total maize production are obtained from main crop, 27.7% (1.649.000 tons) are obtained from second crop maize cultivation. The yield per hectare is 949 kg in main crop, and around 815 kg in the second crop maize cultivation [6].

The maize production is around 1.544.000 tons in Southeastern Anatolia Region. 26 % of the production in Turkey is covered by the Southeastern Anatolia Region. In Southeastern Anatolia Region, 76 % (1.178.000 tons) of the total production is covered by the second crop, 24 % (366.000 tons) is covered by the first crop maize cultivation. While the first crop maize yield is around 104,9 kg/ha in this region, it is 83,4 kg/ha in the second crop. The grain maize cultivation area in Diyarbakır was 19.971 hectares in 2014, and the production was 229.201 tons. The average yield

was 114,8 kg/ha. Nearly 92 % of the grain maize planting areas in Diyarbakır constitutes the main crop, 8% constitutes the second crop. In Şanlıurfa, 96 % of the cultivation areas is used for second crop, and 4 % is used for main crop; and in Mardin, 99 % of the cultivation areas is used for second crop, 1% is used for main crop maize cultivation [6].

Increasing irrigation facilities has caused that the second crop production increased in Southeastern Anatolia, and the intense production in Çukurova was transferred to this region. As of 2013, this development has caused that 1.3 million tons of the total 1.9 million tons second crop maize production in Turkey was performed in Southeastern Anatolia. On the other hand, the second crop maize planting is not performed in the whole of the region, but in Şanlıurfa and Mardin in an intense manner. The total second crop maize production amount of these two cities is 1.2 million tons. In addition, nearly all of the total maize production in both cities consists of second crop maize cultivation. Mostly, maize is planted after wheat and may be included in crop alternation with lentil and cotton in the region [7].

In Diyarbakır, Batman, Adıyaman and Siirt, mostly main crop cultivation is performed. In these cities, the reasons of the second crop maize cultivation being low is the high harvest moisture and low yield in harvest. The detection of high yield and quality corn varieties, which do not have high grain moisture problem at harvest is important. For this reason, increases in the yield may be achieved by selecting proper varieties in the second crop maize planting especially after lentil and chickpea [8].

In this study, the aim was to determine the high-yield grain maize varieties that are suitable for the conditions of Diyarbakır, that cover the demands of the producers and consumers in terms of yield and quality, which will be planted as main crop and second crop. It was also aimed to determine the factors that affected the grain yield and some quality parameters in different growth periods and recommend to the farmers in the region. It is foreseen that this study will contribute to the socio-economic development and increase the regional agricultural production volume. Another aim of the study was to investigate the possibility of obtaining crop in the same field more than once a year since the climatic conditions of the area are suitable for this. It is predicted that by selecting proper varieties for proper times, the losses in the yield that stem from negative conditions like high temperature stress will decrease.

MATERIALS AND METHODS

The present study was conducted to determine quality and high-yield grain maize varieties that are suitable for the climatic conditions of Diyarbakır and that cover the demands of the producers and consumers to be cultivated as a main and second crop. Fifteen (15) grain maize varieties (Ada 95.16, Ada 334, Sakarya, Sy Radioso, Sy Lucroso, 72May80, PR31D24, P34N24, P.31G98, Suerto, Breaker, As 71, 71may69, Kerbanis and Katone) were used as the material in the study. These varieties were recommended by different seed companies for Diyarbakır Region and had different vegetation periods.

The study area was located on the 37º30’ and 38º43’ Northern Latitudes, and 40º37’ and 41º20’ Eastern Longitudes, and the altitude above the sea level was nearly 570 m. The soil samples were taken and analyzed from 0-30 cm depth from Diyarbakır GAP International Agricultural Research and Education Center Management, where the study was conducted, and had red-brown, loamy structure, lightly alkali (pH 7.75 and 7.92), slightly limy (2.83 % CaCO3), slightly salty (0.071%), poor in terms of phosphor content (0.56 kg/da), and the organic substance content was extremely low (1.00 %).

The whole of the precipitation in Diyarbakır where the field trials were performed is mostly observed between September and June. In summer, there is almost no precipitation, and the relative humidity in the air is extremely low. According to the Regional Management of Meteorology in Diyarbakır records for 2014-2015 vegetation period, the average temperature values varied between 12.4 and 31.7°C, average maximum temperature 18.4-40.0°C, monthly total precipitation 0.0 and 84.2 mm, and average relative humidity 21.3% and 69.6% between April and October. The annual total temperature for 2015 in the period from the planting and harvest was 3883°C in main crop, and 3947°C in the second crop period.

The trial planting in the main crop cultivation was performed in the fallow field by hand on 15.04.2014 in the first year, on 20.04.2015 in the second year in the same field; and the second crop planting was performed on 13.06.2014 in the first year, and on 15.06.2015 in the second year after the lentil harvest, and the irrigation was made by Sprinkler Irrigation System after the planting. The trial was established according to Randomized Blocks Design in 3 repetitions.

The trials were made in a way that would form a 4-row structure with 5 m parcel length, 70 cm between the rows, and 20 cm over each row. The seeds were sown in a way that there would be 7142 seeds in each decare.

The irrigation was performed with Sprinkler System until the middlebreaking, and after this process, the furrow method was used when the plants needed water. The last irrigation was on August 8, 2014 in the first year in the main crop,

and on August 17, 2015 in the second year. In the second crop, the last irrigation was on September 8, 2014, and on September 2015 in the second year. The irrigation was performed for 10 times (in total) in the main crop, and for 8 times (in total) in the first year, and 9 times (in total) in the second year. The harvests in the main crop were made on September 16, 2014 in the first year; and on September 17, 2015 in the second year. The harvests in the second crop were made on November 12, 2014 in the first year; and on November 12, 2015 in the second year.

The same amount of manure was used in the main and second crop trials. 25 kg/da pure nitrogen (N) and 10 kg/da pure (P) phosphor were used as manure, and 10 kg/da of the nitrogen manure and the whole of the phosphorous manure were given before the planting as 20-20-0 composed manure, and the remaining 15 kg pure nitrogen was given when the plants were 50-60 cm.

Ear Silking Period (days), First Ear Height (cm), Stem Thickness (mm), Lodging (pcs/parcel), Ear Length (cm), Ear Thickness (mm), Ear Number per Plant (pcs/plant), Kernel/Ear Rate (%), Single Plant Yield (g/plant), Grain Moisture Rate (%), Leaf Erection (Leaf Erection value were scored according to the characters scale 1-3 in UPOV-International Union For The Protection of New Varieties of Plants document), Unit Area Grain Yield (kg/ha), Ear Closure (1-5), Leaf Curling Rate (Open Leaves: 1, Slight Curving: 2, leaves slightly in the form of "V" 3, leaves are about to close completely: 4, leaves are curved like onion: 5) were used in assessments.

The data obtained as a result of the research were analyzed in the JUMP Statistical Package Program, and the AOF Test was applied to determine the differences between the average values and were calculated as Variation Coefficient (VC) as percentages.

RESULTS AND DISCUSSION

When the two year average values of the varieties obtained in this study are analyzed it is seen that the longest Ear Silking Period in ADA 334 variety 84.5 days and the lowest time was in P34N24 variety with 79.7 days in the main crop production. In the second crop production, when the average values for both years are analyzed in terms of Ear Silking Period, it is seen that the longest Ear Silking Period is in ADA 334 variety with 67.5 days and the lowest value is in P34N24 variety with 60.5 days (Table 1).

Ear silks generally appear 2-3 days after the tasseling. In this trial, the average tasseling period was 61.3 days, the ear silking period average was 64.9 days. In the pollination period, the temperature that reaches beyond 34°C and affects the pollination in a negative way together with low relative humidity, which cause reductions in the yield. In this study, more frequent irrigation was performed during pollination period and the humidity in the study area was kept high [9, 10, 11, 12].

The First Ear Height was the highest in ADA 95.16 variety as main crop with 125.1 cm; and the lowest in 71May69 variety with 79.8 cm. In the second crop production, the highest First Ear Height was determined in ADA 95.16 variety with 128.1 cm and the lowest First Ear Height was determined in 71May69 variety with 78.0 cm (Table 1).

TABLE 1
Ear silking period (days), First ear height (cm), Stem thickness (mm) and Lodging (%) values and groups according to LSD test

	Ear Silking Period (Days)		First Ear Height (cm)		Stem Thickness (mm)		Lodging (%)	
Varieties	**Main Crop**	**Second Crop**	**Main Crop**	**Second Crop**	**Main Crop**	**Second Crop**	**Main Crop**	**Second Crop**
PR31D24	82.0 B-D	65.2 CD	96.5 E-G	101.1 C	22.6 A-C	24.53 A	0.00	0,33
Sy Radioso	80.3 DE	63.2 EF	87.5 HI	81.2 FG	21.3 C-E	23.37 A-D	0.00	2.00
Suerto	82.8 A-C	66.8 AB	102.7 DE	112.8 B	23.3 AB	23.92 AB	0.00	15.33
72May80	81.5 C-E	64.2 DE	96.1 FG	97.0 CD	21.5 C-E	23.45 A-D	0.00	1.67
P.31G98	84.2 A	66.0 BC	109.8 BC	110.8 B	21.4 C-E	23.63 A-C	0.00	2.67
Katone	83.2 A-C	64.8 CD	93.2 GH	96.1 CD	20.6 E	21.80 E	0.00	0.00
Sy Lucroso	83.3 A-C	64.8 CD	96.8 E-G	90.0 DE	21.8 C-E	23.47 A-D	0.00	0.67
Kerbanis	79.8 E	62.5 F	87.1 HI	98.8 C	18.9 F	22.55 B-E	0.00	0.67
AS 71	83.5 AB	65.7 BC	114.9 B	116.3 B	23.5 A	24.87 A	0.00	2.67
Breaker	83.8 AB	66.8 AB	108.4 CD	112.8 B	22.7A-C	24.33 A	0.00	4.67
71May69	83.5 AB	64.8 CD	79.8 J	78.0 G	21.2 DE	22.00 DE	0.00	0.00
Ada 334	84.5 A	67.5 A	109.6 BC	116.6 B	22.0 B-D	23.73 A-C	0.00	8.67
P34N24	79.7 E	60.5 G	83.3 IJ	87.8 EF	20.7 DE	22.33 C-E	0.00	1.00
Sakarya	80.2 DE	64.2 DE	99.8 EF	112.0 B	23.1 AB	24.83 A	7.33	14.00
Ada 95.16	84.0 A	66.8 AB	125.1 A	128.1 A	23.7 A	23.62 A-C	0.00	6.33
Average	82.4	64.9	99.4	102.6	21.9	23.50	0.488	4.045
LSD Year	0.74	N.S.	N.S.	3.27	0.89	0.48		
LSD Variety	1.91	1.42	1.91	8.12	1.37	1.50		
LSD Year*Var	N.S.	N.S.	N.S.	N.S.	1.94	N.S.		
CV (%)	2.01	1.89	5.55	6.84	5.45	5.53		

*The differences between the averages indicated by the same letter does not significant according to 0.05 level

In terms of Stem Thickness, it was observed that the highest value was detected in ADA 95.16 variety as main crop with 23.7 mm; and the lowest Stem Thickness value was detected in Kerbanis variety with 18.9 mm. The highest Stem Thickness value in the second crop production was determined in AS 71 variety with 24.87 mm; and the lowest Stem Thickness value was determined in Katone variety with 21.80 mm (Table 1).

In the main crop plots, no lodging was observed in 2014. It was only observed in Sakarya variety (average 7.33 %) in 2015. In the second crop plots, no lodging was observed in 2014. The highest lodging values in 2015 was determined in Suerto variety 15.33 %, and in Sakarya variety 14 %. Lodging was observed in some varieties because of the severe wind, rain and hail in October 2015 (Table 1).

The highest Ear Length in the main crop production was determined in the ADA 334 variety (23,1 cm) and the lowest Ear Length value was determined in Kerbanis variety (18,8 cm), in the second crop production, the highest Ear Length was determined in P.31G98 variety (22,77 cm) and the lowest Ear Length was determined in Kerbanis variety (18,83 cm). The highest ear thickness as the main crop was determined in Sy Lucroso variety (48,55 mm) and the lowest ear thickness was determined in ADA 334 variety (43,92 mm); and in the second crop production, the highest ear thickness was determined in Kerbanis variety (52,38 mm) and the lowest ear thickness was determined in P34N24 variety (45,68 mm).

In the main crop production, the Ear Number per Plant was varied between 0,975 pieces (71May69 variety) and 1,071 pieces (P34N24 variety); in the second crop production, it varied between 0,957 pieces (Sakarya variety) and 1,112 pieces (P.31G98 variety). In the main crop production, the highest Grain Weight and Ear Weight Rate was determined in PR31D24 variety with 88,00 %, in Kerbanis variety with 87,90 % and in P.31G98 variety with 87,13 %; and the lowest kernel/ear rate was determined in Sy Lucroso variety with 83,63%. In the second crop production, the highest kernel/ear rate was determined in Kerbanis variety with 84,03% and the lowest kernel/ear rate was determined in Sakarya variety with 79,14% (Table 2).

In the main crop production, the highest single plant yield was determined in PR31D24 variety with 212,72 g; and the lowest single plant yield was determined in P34N24 variety with 176,52 g. In the second crop production, the highest single plant yield was determined in Katone variety with 206,1 g; and the lowest single plant yield was determined in Breaker variety with 148,6 g. As the distance between plants increases, a decrease is observed in the single plant yield (Table 3).

When the biannual average values of the varieties as main crop were analyzed in terms of grain moisture in harvest, it was observed that the highest grain moisture was determined in Ada 95.16 variety with 16,75 % and in Sakarya variety with 16,70 %; and the lowest Grain Moisture was determined in P.31G98 variety with 13,16%. P.31G98 variety was the second one with the longest Ear Silking Period, and the lowest grain moisture in harvest in this variety shows that this loses moisture with a greater rate after maturation. In the second crop varieties, the highest Grain Moisture was determined in Ada 334 variety with 28,15 %; and the lowest Grain Moisture was determined in Kerbanis variety with 21,80 %. It was

TABLE 2
Ear length (cm), Ear thickness (mm), Ear number per plant (pieces/plant) and Kernel/ear rate (%) values and groups according to LSD test

	Ear Length (cm)		Ear Thickness (mm)		Ear No per Plant (pcs/plant)		Kernel/Ear Rate (%)	
Varieties	**Main Crop**	**Second Crop**	**Main Crop**	**Second Crop**	**Main Crop**	**Second Crop**	**Main Crop**	**Second Crop**
PR31D24	20.5 D-F	21.35 BC	47.83 A	50.60 B	1.054 A-D	1.069 A-C	88.00 A	83.10 AB
Sy Radioso	21.8 BC	20.78 C	47.43 AB	49.85 BC	1.051 A-E	1.019 CD	84.86 B-D	80.84 D-G
Suerto	20.3 EF	21.60 BC	48.35 A	49.48 B-D	1.025 C-F	1.033 B-D	84.93 BC	80.93 D-F
72May80	21.8 BC	22.17 AB	45.07 CD	46.92 F-H	1.061 A-C	1.047 B-D	85.84 B	81.11 C-F
P.31G98	21.1 C-E	22.77 A	44.17 D	47.57 E-G	1.067 AB	1.112 A	87.13 A	82.13 B-E
Katone	22.0 B	22.25 AB	47.32 AB	50.43 B	1.032 B-F	0.994 DE	84.84 B-D	82.54 A-C
Sy Lucroso	20.9 DE	21.42 BC	48.55 A	50.37 B	1.036 A-F	1.042 B-D	83.63 D	79.32 GH
Kerbanis	18.8 G	18.83 D	48.47 A	52.38 A	1.009 FG	1.043 B-D	87.90 A	84.03 A
AS 71	21.1 C-E	21.70 BC	45.30 CD	47.17 FG	1.015 D-F	1.057 A-C	85.46 B	80.57 E-H
Breaker	19.8 F	21.12 C	48.42 A	48.10 D-F	1.016 D-F	1.033 B-D	85.43 B	79.61 F-H
71May69	21.3 B-D	21.05 C	47.92 A	50.42 B	0.975 G	1.010 C-E	85.39 B	80.57 E-H
Ada 334	23.1 A	21.72 BC	43.92 D	46.55 GH	1.013 E-G	1.020 CD	85.83 B	82.13 B-E
P34N24	20.6 D-F	21.37 BC	44.03 D	45.68 H	1.071 A	1.086 AB	85.46 B	81.54 B-E
Sakarya	20.6 D-F	22.25 AB	46.17 BC	50.30 B	1.010 FG	0.957 E	83.73 CD	79.14 H
Ada 95.16	21.1 C-E	20.78 C	45.72 C	48.75 C-E	1.050 A-E	1.064 A-C	85.19 B	82.24 B-D
Average	21.0	21.41	46.58	48.97	1.032	1.039	85.58	81.32
LSD Year	N.S.	0.76.	N.S.	N.S.	0.027	Ö.D	0.71	N.S.
LSD Variety	0.88	0.98	1.42	1.45	0.038	0.058	1.28	1.58
LSD Year*Var	1.25	N.S.	N.S.	N.S.	N.S.	N.S.	1.81	2.24
CV (%)	3.65	3.95	2.64	2.55	3.25	4.90	1.29	1.68

*The differences between the averages indicated by the same letter does not significant according to 0.05 level

determined that in order to preserve kernels for longer durations, the moisture must be below 14 %. The kernels with high moisture are stored after their moisture rates are decreased below 14 % in maize drying units. The difference between grain moisture in harvest may vary according to the varieties used, the number of the varieties, vegetation duration of the verities, environmental factors, and to the time of sowing and harvest and to the applications in these periods (Table 3).

The Leaf Erection scale values of the varieties as main crop varied between 1 and 3. In terms of Leaf Erection values, it was observed that AS 71, Katone, Sy Radıoso, Breaker, Kerbanis, Suerto and Sy Lucroso varieties formed erected leaf structures in both years (Table 3). Increasing Leaf Erection is important in terms of its positive effects on the efficiency of using the light, and casting less shadow on the nearby plant. Frequent sowing is recommended in erected leaf varieties [13]. It was observed that the Leaf Erection scale values of the varieties as second crop changed between 1 and 3. In terms of Leaf Erection values, it was determined that 71May69, AS 71, Sy Radıoso and Breaker varieties formed leaves in erected position in both years. In flat and wider leaves, shadow is cast on the soil by the leaves and therefore the vaporization occurs less in the soil [8].

In this study, when the two-year data of unit area grain yield in the main crop varieties are analyzed it is seen that the highest grain yield was determined in PR31D24 variety with 158,02 kg/ha; and the lowest grain yield was determined in Ada 95.16 variety with 127,87 kg/ha. In the second crop production, the highest grain yield was determined in Katone variety with 150,23 kg/ha, and the lowest grain yield was determined in Breaker variety with 108,22 kg/ha; and the average values in both years in the main crop were calculated as 138,88 kg/ha and in the second crop as 126,60 kg/ha (Table 4).

The Ear Closure values of the varieties were assessed according to "1: Closed; 5: Open" Scale, and in the main crop, the varieties changed in 1 and 2 scale values. In the main crop, AS 71, Katone and PR31D24 varieties had the best values in both years. In the second crop, the Ear Closure Scale Values of the varieties changed between 1-3. It was observed that AS 71, 72May80, Breaker and P34N24 varieties had a medium-level view, and the other varieties had good values (Table 4).

The leaf curling rate was assessed according to "1: Open Leaves; 5:Fully-curved Leaf" Scale; and in the main crop, the curling rate in the leaves varied between 3 and 4. It was observed that P34N24, PR31D24, 71May69, P.31G98 and Kerbanis varieties had higher scale value in both years. In the second crop, the curling rate in the Leaves varied between 2-5 scale values. In terms of curling rate in the leaves, it was observed that P34N24 and PR31D24 varieties had higher curling rate in the leaves, and the curling in the leaves was more in 2015 than in 2014 (Table 4).

Increasing curling in the leaves has an effect that reduces the water loss in the plant during a drought stress [14]. Decreases were observed at a statistically significant level in the transpiration rate parallel to the severity of the drought and curling in the leaf; and the speed of photosynthesis decreased at a significant level as the severity of the drought increased and as the curling level of the leaves increased [15]. It was reported in the literature that one of the survival mechanisms for plants under drought stress was the rolling of the leaves, and the lucky plants that had this mechanism could survive for longer durations [16, 17].

TABLE 3
A plant yield (g), Grain moisture rate (%) and Leaf erection (1-3 Scale) values and groups according to LSD test

	A Plant Yield (g)		Grain Moisture Rate (%)		Leaf Erection (1-3 Scale)	
Varieties	**Main Crop**	**Second Crop**	**Main Crop**	**Second Crop**	**Main Crop**	**Second Crop**
PR31D24	212.72	192.1 AB	14.32 C-E	25.58 B-E	1.5	2.5
Sy Radioso	199.24	181.0 BC	15.83 AB	25.48 B-E	1	1
Suerto	197.99	181.3 BC	16.55 AB	26.58 A-D	1	1.5
72May80	197.48	171.8 BC	16.49 AB	23.87 E-G	2.5	2.5
P.31G98	194.85	172.9 BC	13.16 E	26.82 A-C	2	2
Katone	193.48	206.1 A	16.39 AB	24.23 D-F	1	2
Sy Lucroso	193.89	171.0 BC	16.34 AB	25.83 A-E	1	1.5
Kerbanis	181.26	186.6 A-C	14.14 DE	21.80 G	1	1.5
AS 71	185.80	178.7 BC	15.43 BC	23.68 E-G	1	1
Breaker	179.97	148.6 D	15.79 AB	25.08 C-E	1	1
71May69	179.20	165.3 CD	16.03 AB	25.32 B-E	1.5	1
Ada 334	178.22	167.9 CD	16.34 AB	28.15 A	2.5	2.5
P34N24	176.52	173.1 BC	14.36 CD	22.32 FG	2.5	2.5
Sakarya	179.95	170.6 C	16.70 A	25.28 B-E	2	2
Ada 95.16	178.21	178.2 BC	16.75 A	27.53 AB	2	2
Average	188.59	176.3	15.64	25.17	1.566	1.766
LSD Year	N.S.	N.S.	0.28	N.S.		
LSD Variety	N.S.	21.36	1.19	2.39		
LSD year*Var	N.S.	N.S.	1.68	N.S.		
CV (%)	10.84	10.47	6.59	8.20		

*The differences between the averages indicated by the same letter does not significant according to 0.05 level

TABLE 4
Unit Area Grain Yield (kg/ha), Ear Closure (1-5 Scale) and Leaf Curling Rate (1-5 Scale) values and groups according to LSD test

	Unit Area Grain Yield (kg/ha)		Ear Closure (1-5 Scale)		Leaf Curling Rate (1-5 Scale)	
Varieties	**Main Crop**	**Second Crop**	**Main Crop**	**Second Crop**	**Main Crop**	**Second Crop**
PR31D24	158.02 A	140.26 AB	1	2	4	4.5
Sy Radioso	148.01 AB	131.25 B-D	2	1.5	3.5	3.5
Suerto	147.93 AB	131.24 B-D	1.5	2	3	3
72May80	146.71 AB	123.28 C-E	2	2.5	3	3
P.31G98	144.75 A-C	125.48 B-D	2	2	4	4
Katone	143.63 A-D	150.23 A	1	2	3	3
Sy Lucroso	142.65 A-D	125.05 B-D	1.5	2	3.5	3.5
Kerbanis	135.57 B-D	133.01 BC	2	2	4	3.5
AS 71	133.58 B-D	125.07 B-D	1	3	3.5	3.5
Breaker	132.37 B-D	108.22 E	1.5	3	3	3.5
71May69	132.19 B-D	116.52 DE	1.5	2	4	3.5
Ada 334	131.53 B-D	121.53 C-E	2	2	3	3.5
P34N24	129.88 CD	125.96 B-D	2	3	4	4.5
Sakarya	128.57 CD	116.60 DE	1.5	2	3	3
Ada 95.16	127.87 D	125.25 B-D	2	2	3	3.5
Average	138.88	126.60	1.63	2.20	3.43	3.53
LSD Year	N.S.	N.S.				
LSD Variety	167.7	153.84				
LSD Year*Var	N.S.	N.S.				
CV (%)	10.39	9.42				

*The differences between the averages indicated by the same letter does not significant according to 0.05 level

TABLE 5
Comparison of Average of two years datas of main product and second product

	Main Crop			Second Crop		
Features	**The Lowest**	**The Highest**	**Overall Average**	**The Lowest**	**The Highest**	**Overall Average**
Ear Silking Period	79.7	84.5	82.4	60.5	67.5	64.9
First Ear Height	79.8	125.1	99.4	78.0	128.1	102.6
Stem Thickness	18.9	23.7	21.9	21.8	24.9	23.5
Lodging	0.00	7.33	0.48	0.00	14.00	4.04
Ear Length	18.8	23.1	21.0	18.8	22.8	21.4
Ear Thickness	43.9	48.6	46.6	45.7	52.4	49.0
Ear Number per Plant	0.98	1.07	1.03	0.96	1.11	1.04
Kernel/Ear Rate	83.6	88.0	85.6	79.1	84.0	81.3
A Plant Yield	176.5	212.7	188.6	148.6	206.1	176.3
Grain Moisture Rate	13.2	16.8	15.6	21.8	28.2	25.2
Leaf Erection	1	2.5	1.56	1	2.5	1.76
Unit Area Grain Yield	127.87	158.02	138.88	108.22	150.23	126.60
Ear Closure	1	2	1.63	1.5	3	2.20
Leaf Curling Rate	3	4	3.43	3	4.5	3.53

TABLE 6
Determination of bilateral relations between grain characteristics and other characteristics studied

	Main Crop	Second Crop
Features	**Correlation coefficient**	**Correlation Coefficient**
Ear Silking Period	-0.1839	-0.1791
First Ear Height	0.0346	0.0493
Stem Thickness	0.1384	-0.1029
Lodging	-	-
Ear Length	0.247*	0.2171*
Ear Thickness	0.4329**	0.4799**
Ear Number per Plant	0.3076**	0.2071*
Kernel/Ear Rate	0.4043**	0.5522**
A Plant Yield	0.965**	0.972**
Grain Moisture Rate	-0.0977	0.0283
Leaf Erection	-0.0693	0.0682
Ear Closure	0.028	-0.1392
Leaf Curling Rate	0.0801	-0.131

** significant according to 0.01, * significant according to 0.05

When the general average values are considered in terms of the main and second crops, it is observed in Table 5 that Ear Silking Period, Kernel/Ear Rate, Single Plant Yield, Unit Area Grain Yield values were higher in the main crop; and First Ear Height, Stem Thickness, Lodging, Ear Length, Ear Thickness, Ear Number per Plant, Grain Moisture in Harvest, Leaf Erection, Ear Closure and Curling Rate in the Leaves were lower when compared with the second crop (Table 5).

A Correlation Analysis was applied to determine the relation between the grain yield and all the other parameters handled in the study and it was determined that there were positive and significant relations between Grain Yield and Ear Length, Ear Thickness, Ear Number per Plant, Kernel/Ear Rate, Single Plant Yield in the main and second crop production (Table 6).

In the present study, the highest grain yield as the main crop was determined in PR31D24 variety 158,02 kg/ha, Sy Radıoso variety 148,01 kg/ha, Suerto variety 147,93 kg/ha, respectively; and the average value as the main crop was 138,88 kg/ha. It was observed that the PR31D24 variety had the highest values in terms of ear thickness, ear number, kernel/ear rate, single plant yield, grain moisture in harvest, lodging, ear closure, curling rate in the leaves and grain yield [14].

It was observed that the highest grain moisture in the main crop corn cultivation was in Ada 95.16 variety with a rate of 16,75 %; and the lowest grain moisture was in P.31G98 with a rate of 13,16 %; and the average in the study was 15,64 %. The P.31G98 variety having the lowest moisture in the harvest shows that it loses its moisture in a fast manner after maturation. No moisture problem was observed in any of the varieties used as the main crop.

The highest grain yield in the second crop production was determined in Katone, as 150,23 kg/ha; in PR31D24, as 140,26 kg/ha; in Kerbanis, as 130,31 kg/ha, respectively. The average value of second crop was determined as 126,60 kg/ha. In terms of grain yield, it was determined that the highest values were detected in Katone, PR31D24 and Kerbanis varieties, respectively. These varieties are recommended to the farmers in our city. The moisture rates of these varieties were determined as 24,23 % in Katone; and as 25,58 % in PR31D24; and as 21,80 % in Kerbanis.

It was determined that PR31D24 and Katone varieties came to the forefront both in main and second crop production, do not pose any problems in pollination due to high temperatures, and has superior properties in terms of yield and some other characteristics.

ACKNOWLEDGEMENTS

This work was supported by a grant from Dicle University Research Funding (DUBAP; Project No. 14-ZF-133).

REFERENCES

[1] Akarken, N., Tas, T. (2014) Determination of Leaf Chlorophyll Densities of Some Corn Lines. International Mesopotamia Agriculture Congress. 22-25 September, Diyarbakır, 953.

[2] Cirilo, A.G. and Andrade, F.H. (1994) Sowing Date and Maize Productivity. II. Kernel Number Determination. Crop Science. 34(4), 1044 - 1046.

[3] Anonymous, 2014. Turkey Sugar Factories Corporation 2014 Annual Report. Retrieved from http://www.turkseker.gov.tr/ FaaliyetRapor/Seker_Fabrikalari_Faaliyet_Raporu_2014.pdf

[4] TMO, 2014. General Directorate of Turkish Grain Board. 2014 Year Cereal Sector Report. Retrieved from http://www.tmo.gov.tr/ Upload/Document/raporlar/2014hububatsektorraporu.pdf

[5] FAO, 2013. Food and Agriculture Organization (FAO) Food Outlook. Retrieved August 12, 2014 from http://www.fao.org/docrep/ 016/ al993e/al993e00.pdf

[6] TUIK, 2014. Turkish Statistical Institute. Agricultural Statistics (Crop Production Statistics, Crop Products Balance Sheets). Retrived from http://www.tuik.gov.tr/PreTablo.do?alt_id=1001

[7] Anonymous (2015) Ministry of Food, Agriculture and Livestock, Agricultural Economy and Policy development institute, Status and Forecast: Maize 2014/2015.

[8] Ritchie, S.W., Hanway, J.J. (1984) How a corn plant develops. Iowa State University, Coop. Ext. Serv. Spec. Rep. 48, Ames, Iowa, USA.

[9] Celep, H. (2006) The Influence of Previous Plant and Different Nitrogen Doses on Some Characters of Corn Plant. Graduate Thesis. Kahramanmaras Sutcu Imam University, Institute of Natural and Applied Science, Field Crops Department, Kahramanmaras.

[10] Sari, O. (2009) Determination of Yield and Yield Components of Some Hybrid Corn Varieties in the Second Product in Manisa Conditions. Master Thesis. Adnan Menderes University, Graduate School of Natural and Applied Sciences, Department of Field Crops, Aydin.

[11] Coskun, Y., Coskun, A., Kosar, I. (2013) Yield Performance of Some Horse Maize Varieties in Semi-Arid Climate Conditions. National KOP Regional Development Symposium, 14-16 November, Konya.

[12] Idikut, L., Kara, S.N. (2013) Determination of some yield components and grain starch ratios of second crop corn varieties KSU. Journal of Natural Sciences. 16(1), 8-15.

[13] Begg, J.E. (1980) Morphological Adaptation of Leaves to Water Stress. In: Turner, N.C., Kramer, P.J. (eds.) Adaptation of Plants to Water and High Temperature Stress. Wiley and Sons. New York. 33-42.
[14] Matthews, R.B., Azam-Ali, S.N., Peacock, J.M. (1990) Response of Four Sorghum Lines to Mid-Season Drought: II. Leaf Characteristics. Field Crop Res. 25, 297-308.
[15] Sağlam, A. (2011) Investigation of Photosynthetic Changes During Leaf Curl in Maize Varieties in Arid Condition. PhD Thesis. Karadeniz Technical University, Institute of Science, Department of Biology, Trabzon.
[16] Kadıoglu, A. (2012) Biotic and Abiotic Stres Reactions in Plants: Leaf Curl. 21st National Biology Congress. 03–07 September 2012, Ege University, İzmir, 47.
[17] Saglam, A., Demiralay, M., Kadioğlu, A., Terzive, R. (2012) Leaf Curling Protect Photosynthesis and Efficacy in Maize Varieties (Zea mays, Poaceae) in Drought Conditions. 21st National Biology Congress. 03-07 September 2012, Ege University, İzmir, 96.

Received: **22.09.2017**
Accepted: **28.04.2018**

CORRESPONDING AUTHOR

Aydin Alp
Dicle University,
Faculty of Agriculture,
Department of Field Crops,
Diyarbakır – Turkey

e-mail: aydinalp21@hotmail.com

© by PSP Volume 27 – No. 7/2018 pages 4707-4714 Fresenius Environmental Bulletin

IMPROVEMENT IN ELECTROKINETIC REMEDIATION OF LEAD-CONTAMINATED SOILS WITH SINGLE-PASS SOIL WASHING AND APPROACHING ANODES

Zongping Cai[1,2], Xiaojie Zheng[1], Shuiyu Sun[1,2,*], Wenxiang Wang[1], Lihong Yuan[1], Chan Jiang[1]

[1]Key Laboratory of Heavy Metal Pollution Control and Resources Comprehensive Utilization of Guangdong Polytechnic of Environmental Protection Engineering, Guangdong Engineering and Technology Research Center of Solid Waste Resource Recovery and Heavy Metal Pollution Control, Guangdong Polytechnic of Environmental Protection Engineering, Foshan 528216, China
[2]School of Environmental Science and Engineering, School of Chemical Engineering and Light Industry, Guangdong University of Technology, Guangzhou 510006, China

ABSTRACT

The soils contaminated by Pb near a mine tailing were remedied via an improved electrokinetical method utilizing single-pass soil washing and approaching anodes (AAs). The variations of the removal efficiency and the soil pH as a function of the treatment time were determined. The maximum Pb removal efficiency was found to be as high as 63.1% under a voltage gradient of 1 V/cm for 48 hours; in contrast to 31.5% when the electrokinetic remediation with AAs without soil washing was employed. After single-pass soil washing, the rate of water content of soil increased to more than 80%, which is very suitable for electrokinetic remediation, at the same time, more ions were desorbed from the soil particles. The mechanism of Pb electromigration behavior in soils during an enhanced EK method is described as the elution in an electrokinetically driven chromatogram.

KEYWORDS:
Electrokinetic remediation, single-pass soil washing, approaching anodes (AAs), Pb contamination, soil remediation.

INTRODUCTION

Soil contaminated by heavy metals, becomes more and more serious in the recent years in many areas across the world [1-4]. Pb is a common contaminant in the soil near lead acid battery factories. Accumulated Pb in soil poses threats to human health by contaminating crops and groundwater [5, 6].

Over the past few decades, electrokinetic (EK) remediation has been demonstrated to be one of the most effective methods for in situ or ex situ soil decontamination. Numerous EK remediation investigations have shown success in degrading soil contaminants and removing heavy metals [7-9].

In the EK remediation process, electrode reactions take place on the surface to generate protons (H^+) and hydroxyl (OH^-) at anode and cathode, respectively. The concentration of these ions near the electrodes creates an acid front that moves from anode to cathode and a basic front that moves the other way [10, 11]. At the same time, the generation of OH^- ions at the cathode leads to the precipitation of the heavy metals called the "focusing effect" [12]. This is the main barrier to electrokinetic remediation of heavy metal contaminated soils [13].

Many studies have been performed with the aim to control the soil pH and enhance the capability of electrokinetic remediation for heavy metal removal. Measures include adding strong complexing agents, such as EDTA (Ethylene Diamine Tetraacetic Acid) into soil [14] and using ion exchange membranes (IEM) to control the pH and zeta potential [15]. These modified techniques are complicated and the use of additional chemicals or devices results in secondary contamination [16, 17]. To enhance the electrokinetic remediation of heavy metals-contaminated soil, the distribution and mobility of H^+ ions and heavy metals in soils were investigated in this study.

Usually, the EK process is operated with one fixed anode (FA). An enhanced EK method with approaching anodes (AAs) and single-pass soil washing using distilled water without chemicals is believed to strengthen the remediation effect. For the rate of water content of soil increased to more than 80% after single-pass soil washing, which is very suitable for electrokinetic remediation, at the same time, more ions were desorbed from the soil particles After single-pass soil washing. Compared with other remediation methods, we speculate that if the area of the "focusing effect" can be migrated towards the cathode in a step-by-step manner, more Pb would be precipitated in a narrow area and extracted from the contaminated soil. Therefore, to determine EK and soil washing parameters suitable for the soil contaminated by Pb near a mine tailing, local soils were picked up and examined with the approaching anode

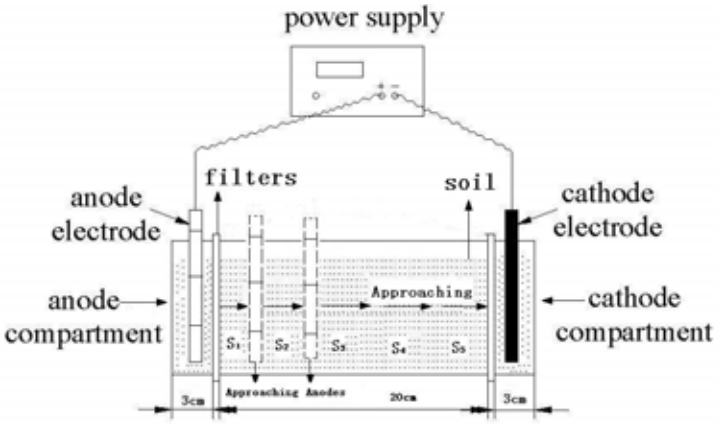

(a)

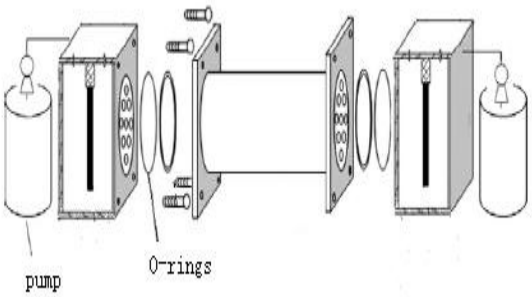

(b)

FIGURE 1
Schematic diagram of the electrokinetic laboratory apparatus with approaching anodes (AAs) technique ((a) experimental set-up and (b) detailed components of chambers and soil cell, unit: cm).

and single-pass soil washing method. A combined technology is proposed.

MATERIALS AND METHODS

Soil preparation. Soil samples were collected near a mine tailing in Shaoguan, China. To simulate the contamination process, $PbSO_4$ was dissolved with a little distilled water and added into the collected soils. They were kept in container for about 6 months outside room simulating natural polluting courses. Then they were air-dried and mildly ground to pass through a 60-mesh sieve, homogenized and stored for subsequent analysis.

The measured concentration of Pb was 661.3 mg/kg for the soil samples and the moisture content was approximately 9.1%. The initial soil pH was 7.63. For each electrokinetic test, approximately 1000 g of dry soil sample was loaded into the electrokinetic cell. Distilled water was used as the electrolysis solution and single-pass soil washing.

Electrokinetic cell. EK remediation experiments were carried out in a rectangular translucent plexiglas test cell with the following dimensions: length = 26.0 cm, width = 10.0cm, and height = 10.0 cm, as depicted in Fig. 1. The soil was filled into the cell up to a length of 20 cm. A constant voltage of 20 V (1 V cm^{-1}) was applied with a DC power source. The filter paper and an O-ring were used between the electrode chambers and the soil cell to avoid any possible leakage. Graphite was used for both anode and cathode and was inserted into each electrode chamber and connected with DC power. To provide an uniform electric current, the whole soil cross-section was covered with graphite electrode with a surface area of 54 cm^2 (3×9×2 cm). The thickness of the soil was 2 cm in anode compartment or cathode compartment. Electrode chambers were filled with distilled water, which was cycled by pumps to avoid concentration gradients within the compartments.

Experimental apparatus of soil washing. The single-pass experimental apparatus of soil washing is made using plastic bottle, as depicted in Fig. 2, which is cylinder-shaped, with the following dimensions: diameter = 7.0 cm, and height = 18.0 cm, a 250-mesh gauze is placed at the bottom of the apparatus of soil washing.

Methodology. The soil sample was divided into five sections within the cell, named S1–S5 moving from anode to cathode. EK remediation with AAs was operated in the same apparatus with the

same intensity of electric field, except that five graphite electrodes were inserted as AAs in the treated soil. AAs were placed at distance of 3 cm, 6 cm, 9 cm,12 cm, and 15 cm from anode. They were sequentially switched on at 5 h,10 h, 15 h, 25 h and 36 h after the EK process started, and at the same time, the solution was refilled.

The single-pass soil washing and electrokinetic remediation with AAs was carried out with soil washing first, the washing electrolysis is distilled water, the optimum washing residence time is 24h and the optimum water to soil ratio (mass ratio) is 0.5:1. After single-pass soil washing, the soil was remedied by electrokinetic remediation with AAs.

Analysis was carried out in the same way with EK remediation. Soil pH was measured in the five different sections by a pH meter (soil/water = 1/2.5), the pH and Cu concentration were measured after the remediation at different sections S1-S5 respectively.

For total Pb analysis, 0.2 g samples, in duplicate, were digested with HNO_3-HF-$HClO_4$ in 25 ml Teflon beakers for soil clearing up. An inductively coupled plasma-optical emission spectroscopy (ICP-OES, Agilent) was used to determine the concentration of total Pb. The pH and Pb concentration were measured for two samples from each section, and two standard soil samples (i.e., soil with a controlled concentration of heavy metals) were analyzed for quality control. The EK remediation experiments were repeated three times.

RESULTS AND DISCUSSION

Soil characteristics. Major physico-chemical characterizations of the experimented soil with respect to the soil pH, texture, organic carbon, cation exchange capacity, zero point charge(ZPC) and metallic contaminant content are tabulated in Table 1. The soil was composed of a number of minerals where $3MgO4SiO_2H_2O$ dominates and accounts for 58.5% in weight. The tested soil of the coastal plain showed a sandy texture, which can be attributed to the silt loam according to the USDA classification system. The soil was slightly alkaline, a typical feature in Southern China.

The charge characteristic of the clay minerals in the soil is that most of the experimented soils carry negative charges on the surface, and the negative charges increase with the pH value, indicating that the negative charge is variable. The positive charge was very low in the experimented soil [18]. Other metallic contaminant content in the sample has been provided in Table 1, other than Pb, Zn 6.1 mg/Kg, Cu 12.4 mg/Kg. Other metallic contaminant is low than the limit of determination, which is 5ug/L. The point of zero charge (ZPC) of the experimented soil, determined by potentiometric titration, is around 3.0-3.5. The ZPC of the soil can be a better indicator to evaluate the surface chemical property of the soil, which is the pH when the charge of grain surface is zero. It is necessary to keep the pH in soils to be low enough when most heavy metals are to be removed by EK remediation. With AAs method, the distance between anodes and the cathode is gradually shortened, migration distances of H^+ ions decrease. Therefore, ZPC indicates the efficiency of AAs remediation process. The low cation exchange capacity (about 15.3 $cmol.kg^{-1}$, due to low organic matter and clay contents) suggests that the Pb ions are not highly absorbed onto the soil particles, which is propitious to the migration of Pb ions in the soil [19].

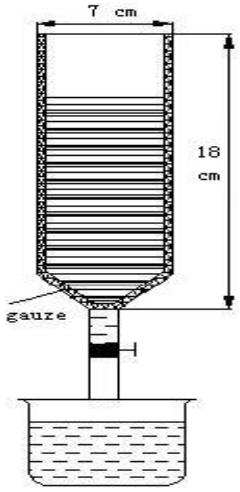

FIGURE 2
Experimental apparatus of single-pass soil washing (unit: cm).

TABLE 1
Composition and properties of the experimental soil specimen.

Property	Value
Texture (%)	
Sand	19.3
Slit	62.4
Clay	18.3
Minerals (%)	
Chlorite	58.5
Mica	12.0
Smectite	4.4
Kaolinite	3.6
Pinguite	2.7
Feldspar	15.1
Picrite	3.7
Initial pH	7.6
Cation exchange capacity ($cmol{\cdot}kg^{-1}$)	15.3
Total organic carbon ($g{\cdot}kg^{-1}$)	10.9
Moisture content (m%)	9.1
conductivity ($us{\cdot}cm^{-1}$)	167.0
zero point charge(ZPC)	3.0-3.5
Zn (mg/Kg)	6.1
Pb (mg/Kg)	661.3
Cu (mg/Kg)	12.4

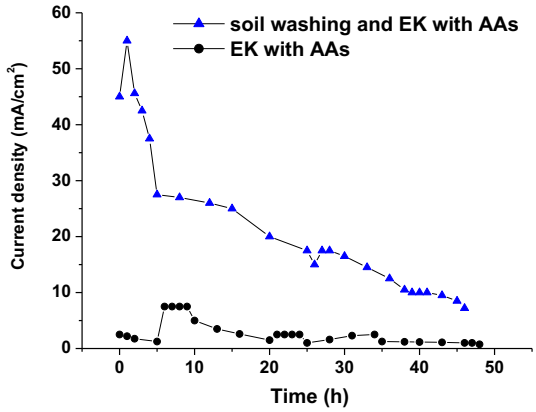

FIGURE 3
Variations of electric current intensity profile for EK remediation using AAs with soil washing and without soil washing.

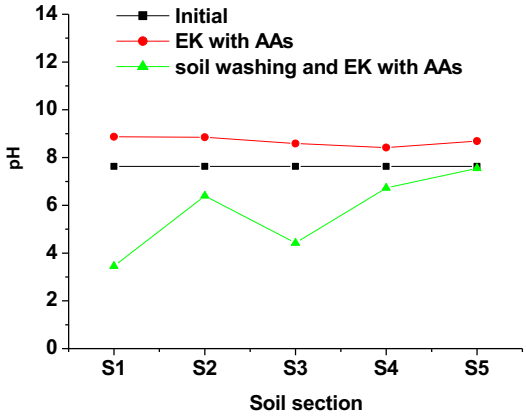

FIGURE 4
Soil pH profile for the EK remediation using AAs with soil washing and without soil washing.

Current changes during the experiments. The electric current is an indicator of the amount of ion electro-migration. The changes in the electric current during the treatments are shown in Fig. 3. During the single-pass soil washing and EK remediation with AAs treatment, higher current density passed through the system than what was observed during the EK remediation with AAs, and the current intensity fluctuated. The current density of the single-pass soil washing and EK remediation with AAs started from 45.0 mA/cm^2 and increased to the maximum value of 55.0 mA/cm^2. The maximum value for the EK remediation with AAs treatment was only 7.5 mA/cm^2, indicating the accelerated charge transport. Upon reaching the maximum value, the current density for the single-pass soil washing and EK remediation with AAs began to decrease until it increased again to 17.5 mA/cm^2 after 27 hours because the precipitates re-dissolve and thus provide more ions for current transport. Finally, the current density decreased and reached a value of 7.2 mA/cm^2 for 48 hours. The decay in current intensity was due to the combination of the OH^- and H^+ ions yielding H_2O thereby removing ions that transport charges to the electrode chambers. In addition, the resistance in the interface between electrodes and electrolyte might increase due to the concentration polarization and water dissociation [20]. Ions with positive or negative charges move to both ends of the electric cell, as in electrodialysis, and result in the drop of ionic strength in soils and the current.

In the single-pass soil washing and EK remediation with AAs, after washing, the rate of water content of soil increased to more than 80%, which is very suitable for electrokinetic remediation, at the same time, more ions were desorbed from the soil particles. Therefore, the soil washing and EK remediation with AAs method could maintain more mobile ions in the system and higher current changes. This phenomenon partially explained the possible mechanism of enhanced Pb and removal in the single-pass soil washing and EK remediation with AAs tests.

pH variation. Low pH in soil is necessary when most heavy metals are to be removed by means of EK remediation [21]. Fig. 4 shows the pH variations in the soil profiles during single-pass soil washing and EK remediation with AAs, only EK remediation with AAs. The soil pH was 7.63 before remediation. The pH of the soil close to the anode was 3.45 after soil washing and EK remediation with AAs. This is significantly lower than that of other soil parts. It can be seen that the pH values in the soil bed drop evidently faster with soil washing and EK remediation with AAs than without soil washing. During the soil washing and EK remediation with AAs, the rate of water content of soil increased, H+ ions can approach the cathode sooner.

Redox potential variation. Redox potential greatly influences chemical association of Pb on soil particles. High redox potential near the anode indicates highly oxidizing conditions, while low redox potential near the cathode indicates reducing conditions. Redox potentials in the soil bed before and after EK remediation are depicted in Fig.5. Before remediation treatment, the redox potential of the soils is 18.5 V. After soil washing and EK remediation with AAs, redox potentials in treated soils increase linearly from 18.57 V to 19.35 V along sites from the anode to the cathode. This is due to the electric potential of DC (Direct Current) and its redox reactions at electrodes. In reductive environments, almost all particulate Lead is complexed by insoluble organic matter or bonded to sulfide minerals. In contrast, Pb tends to be set off from soil particulates in oxidative environments because of the effect mechanisms of

redox potential on heavy metals [22, 23]. After soil washing and EK remediation with AAs, redox potentials are higher near the cathode than after EK remediation with AAs without soil washing. Therefore, Lead migration capability is enhanced in soil washing and EK remediation with AAs.

Total Pb concentration variation. The changes of total Pb concentration in the soil bed during EK remediation are displayed in Fig. 6 and Fig. 7, where C/C_o represents the ratio between Pb concentrations after and before remediation. Before the treatment the concentration of Pb was 661.3 mg/kg and Pb is removed from sections near the cathode and accumulated near the anode. After 48 hours, the average concentration of Pb for S_1 to S_5 region is 244.1 mg/kg using soil washing and EK remediation with AAs, compared to 453.2 mg/kg using EK with AAs without soil washing. Consequently, 63.1% of total Pb was removed using soil washing and EK remediation with AAs. This is in stark contrast with the 31.5% of total Pb removed via EK with AAs without soil washing. Therefore, the removal efficiency was enhanced and it shows great improvement of electro-migration velocity. The removal velocity of Pb concentration is the largest near the cathode as shown by the increase in slope of the graph. During the soil washing and EK process with AAs, soil turns to be in a more waterish and acidic condition, in which Pb exists in a free form. It can be presumed that the removal efficacy increased as more Pb ions desorbed from the soil particles as a consequence of pH decline.

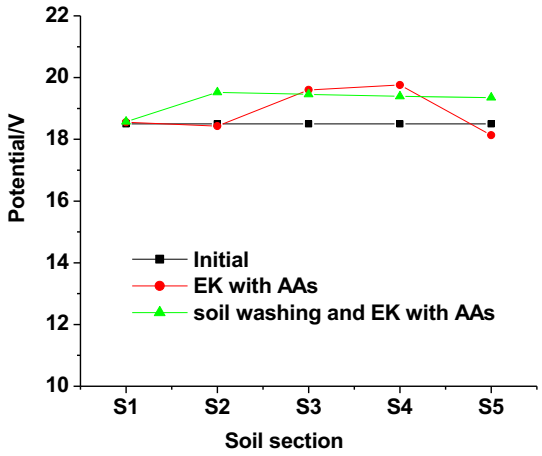

FIGURE 5
Variations of redox potential in the soil profiles using AAs with soil washing and without soil washing.

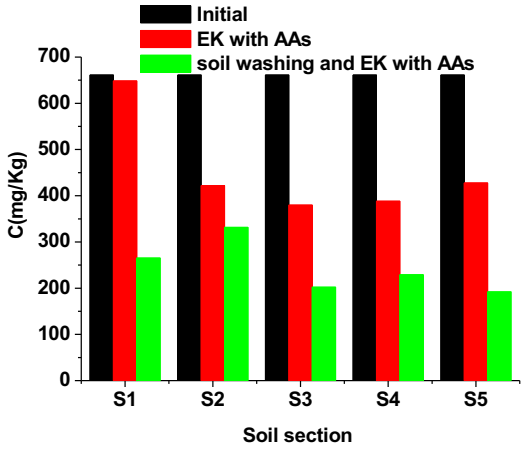

FIGURE 6
Pb^{2+}concentration in soil after EK remediation using AAs with soil washing and without soil washing.

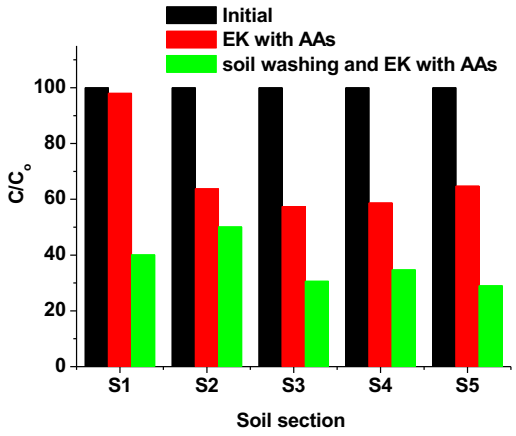

FIGURE 7
Pb^{2+} distribution in soil after EK remediation using AAs with soil washing and without soil washing. (C/C_o is represented for the proportion of Pb concentration after remediation and before remediation.)

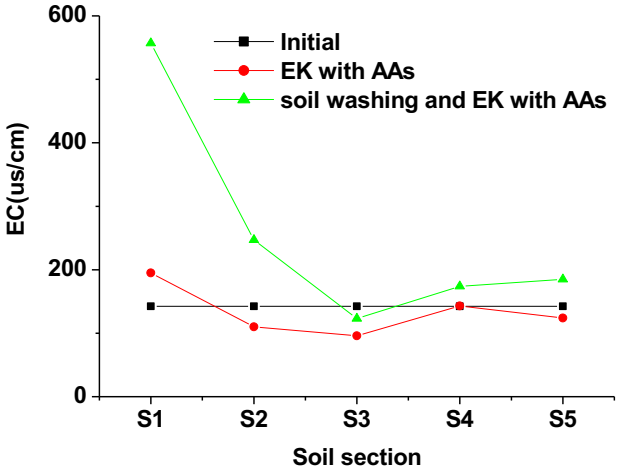

FIGURE 8
Comparison of conductance of remnant Pb^{2+} for EK remediation using AAs with soil washing and without soil washing.

Electrical conductivity. The results of the electrical conductivity (EC) characterization are presented in Fig. 8. The EC profile of the conventional electrokinetic remediation with AAs without soil washing after 48 h treatment was in the shape of a bowl. The EC was higher for S_1 and S_5 regions near the electrode chambers, and lower in S_2 to S_4 regions. This trend was observed because there were more H^+ species near the anode and more OH^- and Pb ions near the cathode [24]. The EC for soil washing and EK remediation with AAs was similar. The EC was higher for S_1 and S_5 regions, and higher for region S_4 because the precipitates re-dissolved due to higher concentration of Pb ions. Compared to the EC of electrokinetic remediation with AAs without soil washing, the EC of the soil washing and electrokinetic remediation with AAs was higher due to the increase of H^+ ion formation at the anodes as well as increased Pb ion desorption from the particles. Therefore, the EC for EK remediation with AAs coincided with the pH and Pb distribution profiles of Fig. 4 and 6.

Mechanism. The pH values and redox potentials in treated soils vary linearly after soil washing and EK remediation with AAs. Its mechanism lies in that OH^- ions are confined in the cathode compartment. Consequently, acidic fronts steadily move towards the cathode. Thereafter, H^+ ions have to react with negative groups in the soil solution and on soil particles when moving forward. The chemical reaction behavior of H^+ ions in soils during soil washing and EK remediation with AAs process is similar to that in an electrokinetically driven chromatogram [25]. After soil washing and EK remediation with AAs, the soil is waterish and the distance between the anodes and the cathode is gradually shortened. Thus the soil pH was lowered and Pb precipitated and re-dissolved before migrating towards the cathode. H^+ ions that were produced at the anode and continuously supplied into the treated soil are similar to a mobile phase. Soil particles react as a stationary phase. When the mobile phase pH decreases, heavy metals with positive charge will accelerate electromigration towards cathode like elution. Many types of reactions occur during the remediation, including desorption, ion exchange, decomplexation, dissolution, destruction of the active sites on the soil surface, and diffusion from the inner sites of the crystal lattices. However, the most important aspect in electrochemical soil remediation is soil pH [14]. Often it is an acidic front, which is developing in the soil from the anode towards the cathode during remediation, used for mobilizing many heavy metals. When met with an acidic front, non-charged Pb fractions can be ion-exchanged by hydrogen ions according to the following equation.

$$PPb + 2H^+ = PH_2 + Pb^{2+} \qquad \text{Eq. (1)}$$

The lower the soil pH becomes, the greater the positive charge Pb fractions. Pb with net positive charges will expedite to electro-migrate towards the cathode. Linear model pH may be the main mechanism that can account for the linear Pb removal velocity in soil washing and EK remediation with AAs process. Low pH aids the release of heavy metals from the soil particles and reinforces the electroremediation effect [22], especially near the anode. This result illustrates why single-pass soil washing and EK with AAs may be an effective treatment approach.

CONCLUSIONS

The application of electrokinetic remediation with approaching anodes (AAs) for 48 hours led to a Pb removal efficiency of about 31.5% from the soil near a mine tailing in Shaoguan city of Guangdong province in China. An enhanced EK method with single-pass soil washing and approaching anodes (AAs) improved the efficiency to 63.1%. The improvement was attributed to an increased water electrolysis and production of H^+ ions at the implemented anodes via water electrolysis and a greater desorption of Pb ions from the soil particles. For after washing, the rate of water content of soil increased to more than 80%, which is very suitable for electrokinetic remediation. Additionally, oxygen produced at the anodes changes the redox potential in the soil and results in Pb reorganization from oxidizable and stable forms to more dissoluble ones. More Pb can be thus removed from the soil than the EK treatment does. The electric migration rate of Pb is enhanced, showing a very high applicability of the combined technology to the remediation of Pb contaminated soil with improved performances and low costs.

ACKNOWLEDGEMENTS

This work was financially supported from the National Natural Science Foundation of Guangdong Province (No.2015A030308008), 2017 innovation team of Guangdong regular college (2017 GKCX TD004), Higher Vocational Education Brand Specialty Construction project of Guangdong Province (No.2016gzpp036), Shaoguan City Science and Technology Special Project (No. 2017sgtyfz102), Foshan City Science and Technology Innovation Project (No. 2017 AB 003952，No. 2017AG10072, 2016 AG100522, 2016AG100482), and Principal Fund Matching Project (No.K6823180119 12).

REFERENCES

[1] Cai, Z.P., Zheng, X.J., Sun, S.Y., Lin, W.X. and Yuan. L.H. (2017) Assessing effect of electrode material on the efficiency of Lead removal from soil by an electrokinetic remediation process. Fresen. Environ. Bull. 26, 4238-4243.

[2] Zulfiqar, W., Iqbal, M. and Butt, M. (2017) Pb^{2+} ions mobility perturbation by iron particles during electrokinetic remediation of contaminated soil. Chemosphere. 169, 257-261.

[3] Han, P., Li, C, Feng, X.Y., Ma, Z.H., Lu, A.X., Pan, L.G. and Wang, J.H. (2014) Impact of wastewater irrigation on the distribution of heavy metals in agricultural soils: A case study in Fangshan, Beijing. Fresen. Environ. Bull. 23, 1662-1667.

[4] Yang, J., Yu, K. and Liu, C. (2017) Chromium immobilization in soil using quaternary ammonium cations modified montmorillonite: Characterization and mechanism. J. Hazard. Mater. 321, 73-80.

[5] Shahid, M., Pinelli, E. and Dumata, C. (2012) Review of Pb availability and toxicity to plants in relation with metal speciation; role of synthetic and natural organic ligands. J. Hazard. Mater. 219, 1-12.

[6] Zhang, J., Wang, L.H., Yang, J.C., Liu, H. and Dai, J.L. (2015) Health risk to residents and stimulation to inherent bacteria of various heavy metals in soil. Sci Total Environ. 508(1), 29−36.

[7] Sun, T.R. and Ottosen, L.M. (2012) Effects of pulse current on energy consumption and removal of heavy metals during electrodialytic soil remediation. Electrochim. Acta. 86, 28-35.

[8] Page, M.M. and Page, C.L. (2002) Electroremediation of contaminated soils. J. Environ. Eng. 128, 208-219.

[9] Huang, J.Y., Liao, W.P., Lai, S.M. and Yang, R. (2013) Use of Hydraulic Pressure –Improved Electrokinetic Technique to Enhance the Efficiencies of the Remediation of PCP-Contaminated Soil. J. Environ. Eng. 139(9), 1213-1221.

[10] Méndez, E., Pérez, M., Romero, O, Beltrán, E.D., Castro, S., Corona, J.L., Corona, A., Cuevas, M.C. and Bustos, E. (2012) Effects of electrode material on the efficiency of hydrocarbon removal by an electrokinetic remediation process. Electrochim. Acta. 86, 148-156.

[11] Li, D., Xiong, Z., Li, S.C., Zhang, L.Y. and Wang, S.S. (2012) Near-anode focusing phenomenon caused by the high anolyte concentration in the electrokinetic remediation of chromium(VI) –contaminated soil. J. Hazard. Mater. 229, 282-291.

[12] Probstein, R.F. and Hicks, R.E. (1993) Removal of contaminants from soils by electric fields. Science. 260, 498-503.

[13] Lu, P., Feng, Q.Y., Meng, Q.J. and Yuan, T. (2012) Electrokinetic remediation of chromium and cadmium-contaminated soil from abandoned industrial site. Sep. Purif. Techno. l98, 216-220.

[14] Ottosen, L.M., Pedersen, A.J., Ribeiro, A.B. and Hansen, H.K. (2005) Case study on the strategy and application of enhancement solutions to improve remediation of soils contaminated with Cu, Pb and Zn by means of electrodialysis. Eng. Geol. 77, 317-329.

[15] Amrate, S., Akretche, D.E., Innocent, C. and Seta, P. (2006) Use of cation-exchange membranes for simultaneous recovery of lead and EDTA during electrokinetic extraction. Desalination. 193, 405-410.

[16] Rojo, A. and Cubillos, L. (2009) Electrodialytic remediation of copper mine tailings using bipolar electrodes. J. Hazard. Mater. 168, 1177-1183.

[17] Hansen, H.K., Rojo, A. and Ottosen, L.M. (2007) Electrokinetic remediation of copper mine tailings: Implementing bipolar electrodes. Electrochim. Acta. 52, 3355-3359.
[18] Zhang, X.H., Zhang, G.L. and Yang, J.L. (2014) Dynamic Change of Point of Zero Charge Along a Typical Soil Chronosequence in Tropical Hainan Island and Its Implications for Pedogenesis. Soils. 46(2), 347-351.
[19] Rajić, L., Božo, D. and Dalmacija, M. (2012) Enhancing electrokinetic lead removal from sediment: Utilizing the moving anode technique and increasing the cathode compartment length. Electrochim. Acta. 86(30), 36-40.
[20] Shrestha, R., Fischer, R. and Rahner, D. (2003) Behavior of cadmium, lead and zinc at the sediment–water interface by electrochemically initiated processes. Colloid. Surf. A. 222, 261-271.
[21] Zhou, D.M., Deng, C.F., Cang, L., and Alshawabkeh, A.N. (2005) Electrokinetic remediation of a Cu-Zn contaminated red soil by controlling the voltage and conditioning catholyte pH. Chemosphere. 61, 519-527.
[22] Cao, X.D., Chen, Y., Wang, X.R., and Deng, X.H. (2001) Effects of redox potential and pH value on the release of rare earth elements from soil. Chemosphere. 44, 655-659.
[23] Kamon, M., Zhang, H.Y. and Katsumi, T. (2002) Redox effects on heavy metal attenuation in landfill clay liner. Soils and Foundations. 42, 115-118.
[24] Gunvor, M.K., Lisbeth, M.O. and Arne, V. (2009) Electrodialytic remediation of harbour sediment in suspension-Evaluation of effects induced by changes in stirring velocity and current density on heavy metal removal and pH. J. Hazard. Mater. 169, 685-690.
[25] Xu, W.S. and Regnier, F.E. (1999) Electrokinetically-driven cation-exchange chromategraphy of proteins and its comparison with pressure-driven high-performance liquid chromatography. J. Chromatogr. A. 853, 243-256.

Received: **04.10.2017**
Accepted: **23.03.2018**

CORRESPONDING AUTHOR

Shuiyu Sun
Key Laboratory of Heavy Metal Pollution Control and Resources Comprehensive Utilization of Guangdong Polytechnic of Environmental Protection Engineering,
Guangdong Engineering and Technology Research Center of Solid Waste Resource Recovery and Heavy Metal Pollution Control,
Guangdong Polytechnic of Environmental Protection Engineering,
Foshan 528216 – China

e-mail: sysun@gdut.edu.cn

© by PSP Volume 27 – No. 7/2018 pages 4715-4724 Fresenius Environmental Bulletin

COMPARISON OF REDOX-POTENTIAL CALCULATED AND MEASURED TO CALCULATE THE SPECIATION OF ARSENIC AND SELENIUM: A CASE STUDY

Ruiiln Wang[1,2], Xinyu Wang[1,3,4,*], Zeming Shi[1,4], Shijun Ni[1,4], Jie Dai[5]

[1]Geochemistry Department of Chengdu University of Technology& Sichuan Province Key Laboratory of Nuclear Techniques in Geosciences, Chengdu, 610059, China
[2]College of Materials and Chemistry& Chemical Engineering, Chengdu University of Technology, Chengdu, 610059, China
[3]State Key Laboratory of Geological Processes and Mineral Resources, China University of Geosciences, Wuhan, Hubei, 430074, China
[4]Department of Geochemistry, University of Bristol, BS8 1RJ, United Kingdom
[5]Key Laboratory of Sedimentary Basin and Oil and Gas Resources, Ministry of Land and Resources& Chengdu Center of Geological Survey, China Geological Survey, Chengdu 610081, China

ABSTRACT

To discuss the availability of thermodynamic modeling to qualitatively identify the arsenic and selenium species in river water, the Mianyuan River in southwest of China was studied as a case. Redox potential (Eh) calculated from the redox couple NO_3^- /NO_2^- were much higher than Eh measured in Mianyuan River. Eh calculated by the redox couple NO_3^- /NO_2^- and Eh measured were both considered. In this river, $HAsO_4^{2-}$ was the only dominated specie of arsenic in water regardless of the Eh measured or Eh calculated was adopted. $HSeO_3^-$ in water was dominated if Eh measured was used, while SeO_4^{2-} became dominated if Eh calculated was adopted. Authors more inclined to believe the result according to Eh calculated. This case study suggests that the method of thermodynamic modeling to qualitatively reveal the major specie was more suitable to arsenic than selenium because selenium speciation distribution was more sensitive to the redox potential which was difficult to obtain.

KEYWORDS:
Arsenic speciation, selenium speciation, river water, Eh-pH diagrams

INTRODUCTION

An excess of arsenic in aqueous environment will be harmful to organisms [1-5]. Arsenic can occur in four oxidation states, arsenate (+Ⅴ), arsenite (+Ⅲ), elemental arsenic (0), and arsine (-Ⅲ). And the speciation distribution of arsenic in solution can be affected by its physical chemistry conditions. The toxicity and mobility of arsenic in water is related to its speciation [6]. Generally, inorganic arsenite (+Ⅲ) is more toxic than arsenate (+Ⅴ). Therefore, acknowledging the speciation of arsenic in water is important to predict the bioavailability and mobility of arsenic in groundwater [7] and river [8, 9]. Selenium is another kind of non-metal trace elements in environment. Low content of Se is beneficial to organisms, while high content of selenium plays a reverse role [10]. Toxicity of selenium is also related to its speciation in water [10, 11]. Recently, selenium has become an emerging global metalloid contaminant second only to mercury [11, 12]. Their studies suggest a need to consider selenium speciation not only total selenium in water [10-12]. Selenium can occur in four oxidation states: selenate (+Ⅵ), selenite (+Ⅳ), elemental selenium (0), and selenide (-Ⅱ). Generally, inorganic selenite (+Ⅳ) is more toxic than selnate (+Ⅵ) [12].

Arsenic speciation in water can be measured using high performance liquid chromatography inductively coupled plasma mass spectrometry (HPLC-ICP-MS) [8, 12]. Selenium speciation in water can be determined using hydride generation atomic fluorescence spectrometry (HF-AFS) [11]. Arsenic and selenium were both oxyanions with similar mobility. Therefore, the speciation of arsenic and selenium in natural water usually need to be simultaneously considered. These methods were accurate but costly and time consuming. Nowadays, there is an increasing need to qualitative identify the speciation of arsenic and selenium in natural water before accurate determination, especially for environmental protection departments. In these situations, the tool of Eh-pH diagram is useful. In fact, the redox potential (Eh) and hydrogen ion activity (pH) are the most important factors controlling the speciation of arsenic and selenium [9, 15]. Although the tool of Eh-pH diagram is convenient to acknowledge speciation of arsenic and selenium, a meaningful Eh value in water is usually difficult to obtain. The internal disequilibrium among redox couples in natural water widely exists [16, 17]. Alternative method is taking the Eh measured and Eh calculated from Nernst equation together into consideration [17]. Therefore, our aim

is to present a case study to discuss the availability of thermodynamic modeling to qualitatively acknowledge the speciation of arsenic and selenium in a river located in southwest of China.

MATERIALS AND METHODS

Study area. Mianyuan River originates from the north of the Jiudingshan Mountains, and flows through the cities of Mianzhu and Deyang, respectively. The map of study area was drawn in Figure 1. The city of Deyang is an important industrial city of China, which has a population of 3.9 millions. The Mianyuan River is the major living water of Deyang City (Site 12 in Figure 1). River length of is about 133.6 km and catchment area is about 1212 km^2 [4]. Its average annual runoff is 690 million cubic meters. Phosphate mining (sites 2 and 4 in Figure 1), industry (sites from 9 to 11 in Figure 1) and agriculture regions (sites from 13 to 16 in Figure 1) are located along the riverbank. This river was affected by Wenchun Earthquake at 2008, and formed two dammed lakes (sites 3 and 7 in Figure 1) in upstream.

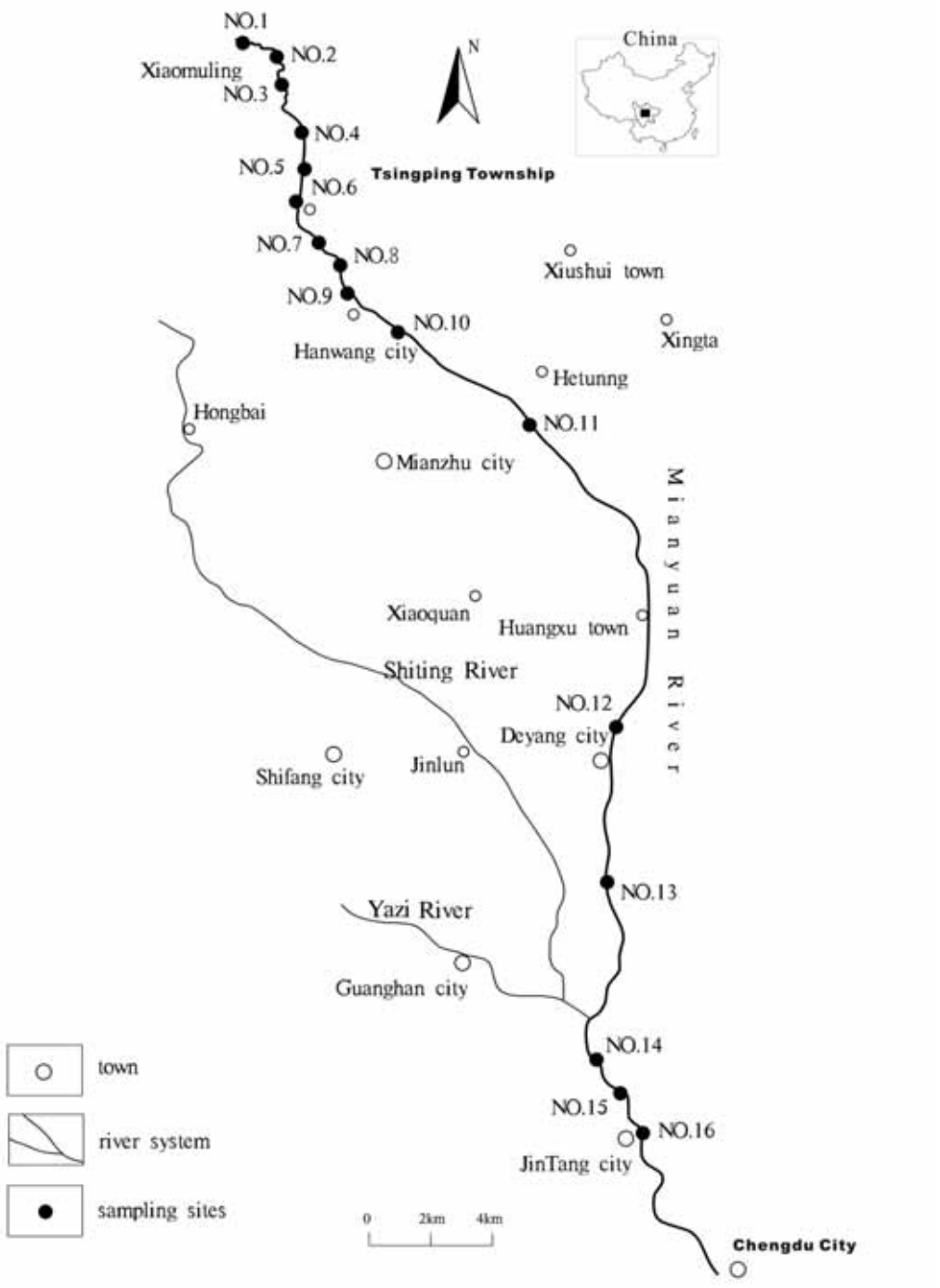

FIGURE 1
Location of the Mianyuan River in Sichuan Province of China [4]

TABLE 1
Parameters and concerned elements in river water [4]

Sampling sites	pH	Eh (mea) mV	Eh (cal) mV	Eh(cal)-Eh(mea) mV	T °C	K^+ mg/l	Na^+ mg/l	Ca^{2+} mg/l	Mg^{2+} mg/l	HCO_3^- mg/l	SO_4^{2-} mg/l	NO_3^- mg/l	NO_2^- mg/l	Cl^- mg/l	Fe ug/l	As ug/l	Se ug/l
Upstream																	
1	7.2	143	516	373	0	0.78	2.26	40.5	21.1	151	61	2.55	<0.01	0.73	25	0.58	0.25
2	7.6	293	493	200	2	4.03	3.44	54.7	20.6	150	104	2.75	<0.01	2.13	23	0.23	0.58
3	8.3	240	455	215	2	2.40	3.13	57.6	21.8	148	117	2.72	<0.01	1.32	397	0.31	0.86
4	7.4	173	434	261	4	3.73	3.69	58.8	22.0	139	114	0.00	<0.01	2.30	29	0.35	0.40
5	8.3	70	448	378	3	1.31	3.96	58.9	22.2	157	113	1.70	<0.01	1.49	30	0.22	0.61
6	7.5	136	499	363	3	3.32	1.86	80.4	71.8	205	316	3.16	<0.01	3.13	57	1.26	1.72
Downstream																	
7	8.6	155	423	268	5	1.82	4.20	58.9	22.2	162	110	1.12	<0.01	1.86	63	0.58	0.63
8	8.2	166	463	297	6	3.61	4.97	112.1	23.8	127	274	5.51	<0.01	2.66	240	0.30	1.47
9	8.3	212	444	232	8	1.44	4.43	75.2	27.5	172	166	2.15	<0.01	1.68	223	0.35	0.64
10	8.1	-40	450	490	12	1.97	6.02	64.8	22.8	171	122	2.37	<0.01	2.70	97	0.79	0.42
11	8.3	185	452	267	4	2.96	8.09	71.8	25.6	150	158	2.85	<0.01	14.9	39	1.54	1.45
12	8.1	84	469	385	6	3.61	41.3	68.5	27.5	212	80	5.84	<0.01	86.0	39	1.45	0.43
13	8.2	75	465	390	7	4.00	23.2	81.1	28.7	243	123	7.46	<0.01	26.2	281	2.20	0.52
14	10.4	120	273	153	13	5.91	9.07	58.6	18.1	115	135	3.54	0.59	7.85	32	0.93	0.46
15	10.2	194	343	149	15	4.82	21.2	49.7	14.9	172	56	9.31	<0.01	21.4	29	3.59	0.29
16	8.4	136	398	262	10	5.04	9.21	58.4	18.2	103	140	8.12	0.80	7.76	63	0.94	0.46

Sampling. Sixteen river water samples were collected at April 20, 2012. All materials used were cleaned by Milli-Q water before the collection of water samples. Parameters of pH, temperature, Eh were in situ analyzed. Temperature was determined using thermometer. Values of pH and Eh were measured using the instrument of YSI-100 (Ecosense, U.S.A) which has the uncertainties of pH at 0.01 and Eh at 1 mV. Its working principles included: (1) activity of H^+ is detected by a glass sensing bulb and different activities of H^+ can create a potential which will be calculated versus the stable potential of the reference electrode; (2) Eh is obtained with oxidative reductive potential(ORP) using Ag/AgCl reference electrode**.** Temperature, pH and Eh were included in Table 1. In addition, some parameters in Table 1 have been published [4].

Three same water samples were collected at each site after filtered by 0.45 μm polycarbonate filters [8]. Copy added with 1 ml diluted HCl (1:1) was used to measure concentrations of metals. Acid free copy was used to measure the concentrations of anions. Another acid free copy was used as parallel sample in analysis to decrease the error in sampling [4]. The water samples were transported and restored in a refrigerator at about 5 °C. All water samples were analyzed in the next 3 days following sampling.

Analysis. Chemical analysis was performed in laboratory at temperature from 22 to 25°C and humidity about 85 %. Cations of K, Na, Ca, Fe, Mg and Al were measured using inductively coupled plasma atomic emission spectrometry (ICP-AES). The recovery was from 97.2 % to 102 %. The concentrations of SO_4^{2-}, NO_3^- and NO_2^- and Cl^- were measured using ion chromatography (IC). The recovery was from 96.5 % to 105.1 %. The concentrations of As and Se were measured using hydride generation atomic absorption spectroscopy (HGAAS). The method detection limit (MDL) of As was 0.02 μg/l. Its recovery was 105 %. The method detection limit (MDL) of Se was 0.03 μg/l. Its recovery was 110 %.

Thermodynamic modeling. The thermodynamic modeling code PHREEQC [18, 19] was adopted. The potential (Eh) - hydrogen ion activity (pH) diagrams of (a) arsenic/ sodium chloride/ water system (As-NaCl-H_2O system with chemical composition: concentration of total arsenic: 1×10^{-5} mol/kg, concentration of sodium chloride (NaCl): 1×10^{-3} mol/kg) and selenium/ sodium chloride/ water

system (Se-NaCl-H_2O system with chemical composition: concentration of total selenium: 1×10^{-5} mol/kg, concentration of sodium chloride (NaCl): 1×10^{-3} mol/kg at temperature: 25 °C and atmosphere pressure: 1.013×10^5 Pa were drawn using the PHREEPLOT [19]. The Eh-pH diagrams of these systems were presented (FIGURE 2, 3, 4 and 5). The MINTEQA database was used [20]. Equilibrium constants of some reactions were updated and presented (Table 2). The speciation of arsenic and selenium in the Mianyuan River at each site were calculated using the code PHREEQC which will automatically fix the equilibrium constant of reactions concerned corresponding to different temperatures according to the standard value at 25℃ using the van't Hoff equation.

TABLE 2
Equilibrium constants of reactions about soluble species and solids of arsenic and selenium at 25℃, 1 bar

Reaction	Log K
Arsenic	
$H_3AsO_3^0 = H_2AsO_3^- + H^+$	-9.17 [21]
$H_2AsO_3^- = HAsO_3^{2-} + H^+$	-14.10 [21]]
$HAsO_3^{2-} = AsO_3^{3-} + H^+$	-15.00 [21]
$H_3AsO_3^0 = HAsO_3^{2-} + 2H^+$	-23.27 [21]
$H_3AsO_3^0 = AsO_3^{3-} + 3H^+$	-38.27 [21]
$3H_3AsO_3^0+6HS^-+5H^+=As_3S_4(HS)_2^-+9H_2O$	72.23 [21]
$H_3AsO_3^0+2HS^-+H^+=AsS(OH)(HS)^-+H_2O$	18.008 [21]
$H_3AsO_4^0 = H_2AsO_4^- + H^+$	-2.3 [21]
$H_3AsO_4^0 = HAsO_4^{2-} + 2H^+$	-9.29 [21]
$H_3AsO_4^0 = AsO_4^{3-} + 3H^+$	-21.08 [21]
$H_3AsO_4^0 + 2H^+ + 2e^- = H_3AsO_3^0 + H_2O$	19.35 [21]
$Fe^{3+} + H_3AsO_4^0 = FeAsO_4^0 + 3H^+$	-6.97 [22]
$Fe^{3+} + H_3AsO_4^0 = FeHAsO_4^+ + 2H^+$	0.59 [22]
$Fe^{3+} + H_3AsO_4^0 = FeH_2AsO_4^{2+} + H^+$	1.88 [22]
$Fe^{3+} + H_3AsO_3^0 = FeH_2AsO_3^{2+} + H^+$	-1.98 [22]
$Fe^{2+} + H_3AsO_4^0 = FeH_2AsO_4^+ + H^+$	0.41 [22]
$Fe^{2+} + H_3AsO_4^0 = FeHAsO_4^0 + 2H^+$	-5.99 [22]
$Fe^{2+} + H_3AsO_4^0 = FeAsO_4^- + 3H^+$	-13.53 [22]
$AsO_4^{3-} + Al^{3+} = AlAsO_4^0$	18.9 [23]
$HAsO_4^{2-} + Al^{3+} = AlHAsO_4^+$	6.45 [23]
$H_2AsO_4^- + Al^{3+} = AlH_2AsO_4^{2+}$	4.04 [23]
$AsO_4^{3-} + Mg^{2+} = MgAsO_4^-$	6.34 [23]
$HAsO_4^{2-} + Mg^{2+} = MgHAsO_4^0$	2.86 [23]
$H_2AsO_4^- + Mg^{2+} = MgH_2AsO_4^+$	1.52 [23]
$HAsO_4^{2-} + Ca^{2+} = CaHASO_4^0$	2.69 [23]
$H_2AsO_4^- + Ca^{2+} = CaH_2AsO_4^+$	1.06 [23]
Selenium	
$SeO_4^{2-} + H^+ = HSeO_4^-$	1.80 [24]
$HSeO_4^- + H^+ = H_2SeO_4^0$	-2.01 [24]
$SeO_4^{2-} + Ca^{2+} = CaSeO_4^0$	2.00 [24]
$SeO_4^{2-} + 2Na^+ = Na_2SeO_4^0$	0.02 [25]
$HSeO_4^- + Na^+ = NaHSeO_4^0$	0.01 [25]
$SeO_4^{2-} + Mg^{2+} = MgSeO_4^0$	2.2 [26]
$SeO_3^{2-} + H^+ = HSeO_3^-$	8.54 [23]
Arsenic solids	
$As(\alpha, cr) + 3H_2O=H_3AsO_3^0 + 3H^+ + 3e^-$	-12.525 [21]
$As_2O_5(cr)+3H2O = 2H_3AsO_4^0$	8.26 [21]
$FeAsO_4{:}2H_2O$ (scorodite) = $Fe^{3+} + AsO_4^{3-} + 2H_2O$	-26.08 [27]
$FeAsO_4{:}2H_2O$ (am) = $Fe^{3+} + AsO_4^{3-} + 2H_2O$	-23.29 [27]
As_2O_3(arsenolite) + $3H_2O = 2H_3AsO_3^0$	-1.38 [21]
As_2O_3(claudetite) + $3H_2O = 2H_3AsO_3^0$	-1.34 [21]
As_2S_3(orpiment) + $6H_2O = 2H_3AsO_3^0 + 3HS^- + 3H^+$	-46.3 [21]
As_2S_3(am) + $6H_2O = 2H_3AsO_3^0 + 3H_2S$	-23.9 [21]
AsS(realgar) + $3H_2O =H_3AsO_3^0 + HS^- + 2H^+ + e^-$	-20.11 [21]
AsS(β, realgar) + $3H_2O = H_3AsO_3^0 + HS^- + 2H^+ + e^-$	-20.05 [21]
FeAsS(arsenopyrite)+ $3H_2O=H_2AsO_3^- + Fe^{2+} + HS^- + 3H^+ + 3e^-$	-34.799 [21]
Selenium solids	
$Se(hex) + H^+ + 2e^- = HSe^-$	-7.6963 [20]
$Se(A) + H^+ + 2e^- = HSe^-$	-7.1099 [20]
$FeSe + H^+ = HSe^- + Fe^{2+}$	-7.1466 [20]
$SeO_2 + H_2O = HSeO_3^- + H^+$	0.1246 [20]
$SeO_3 + H_2O = SeO_4^{2-} + 2H^+$	21.044 [20]
$CaSeO_4{:}2H_2O = Ca^{2+} + SeO_4^{2-} + 2H_2O$	-2.9473 [20]
$Fe_2(SeO_3)_3{:}2H_2O + 3H^+ = 3HSeO_3^- + 2Fe^{3+} + 2H_2O$	-20.6262 [20]
$MgSeO_3{:}6H_2O + H^+ = HSeO_3^- + Mg^{2+} + 6H_2O$	4.0314 [20]

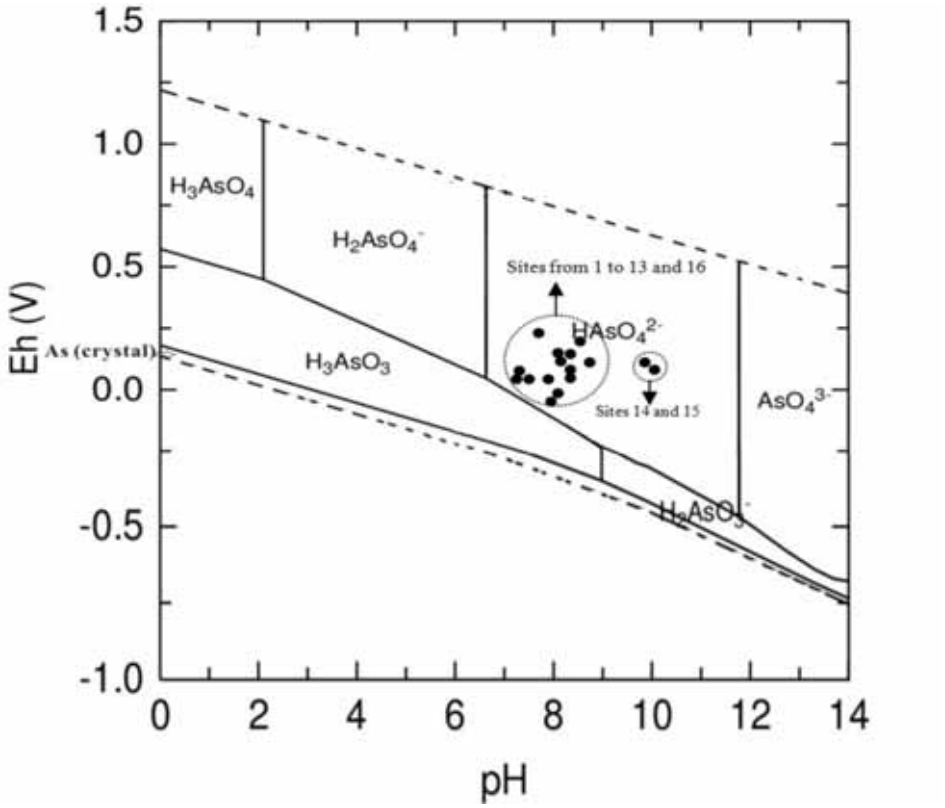

FIGURE 2
Potential (Eh) - hydrogen ion activity (pH) diagrams of arsenic/ sodium chloride/ water (As-NaCl-H_2O) system using Eh measured.

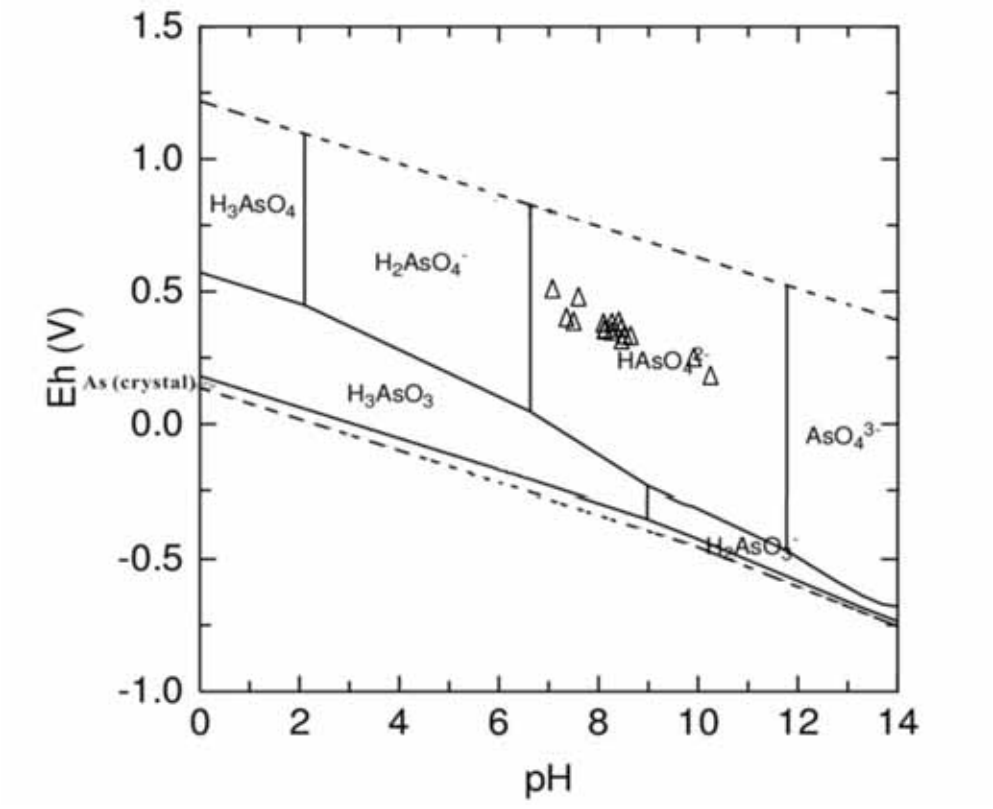

FIGURE 3
Potential (Eh) - hydrogen ion activity (pH) diagrams of arsenic/ sodium chloride/ water (As-NaCl-H_2O) system using Eh calculated.

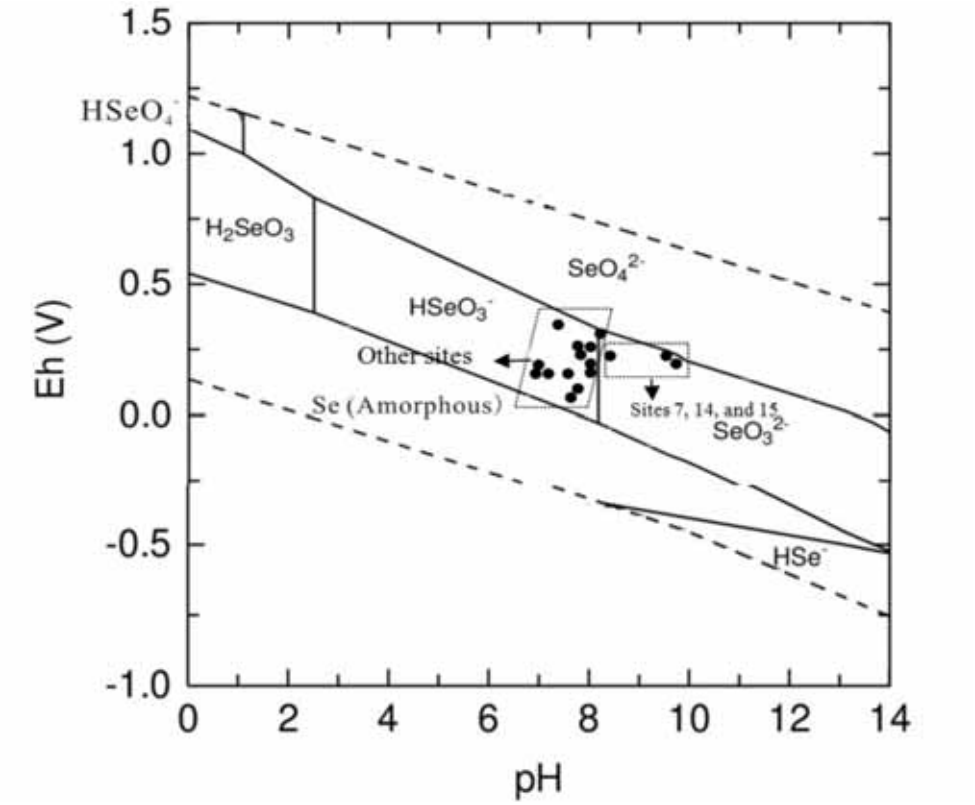

FIGURE 4
Potential (Eh) - hydrogen ion activity (pH) diagrams of selenium/ sodium chloride/ water (Se-NaCl-H_2O) system using Eh measured.

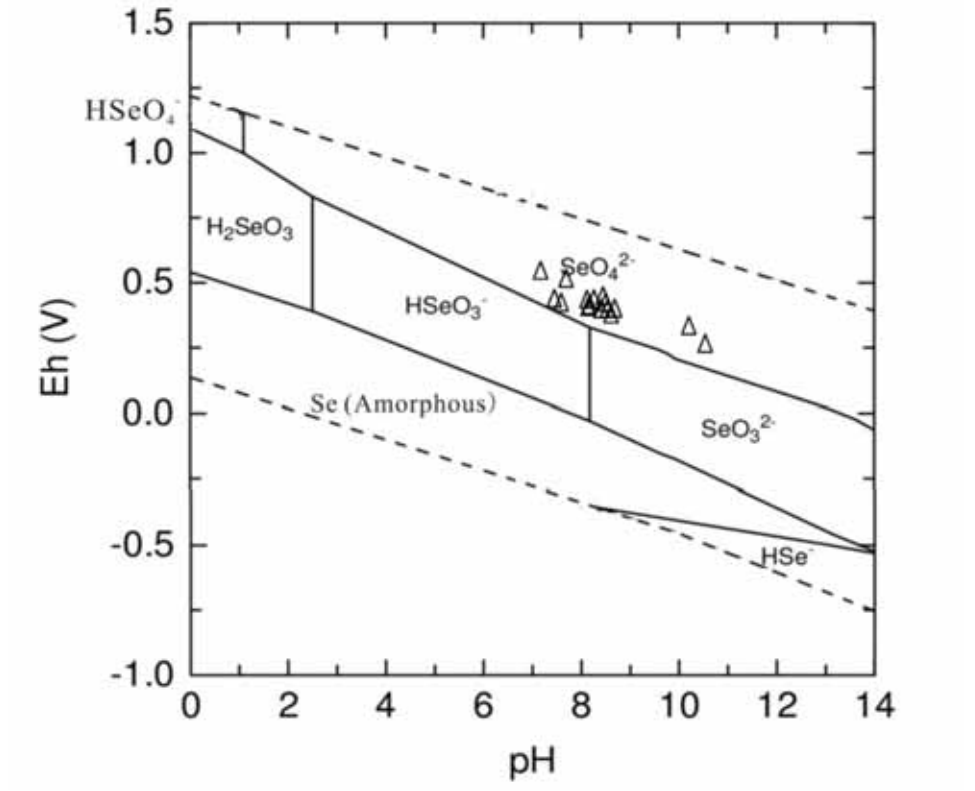

FIGURE 5
Potential (Eh) - hydrogen ion activity (pH) diagrams of selenium/ sodium chloride/ water (Se-NaCl-H_2O) system using Eh calculated.

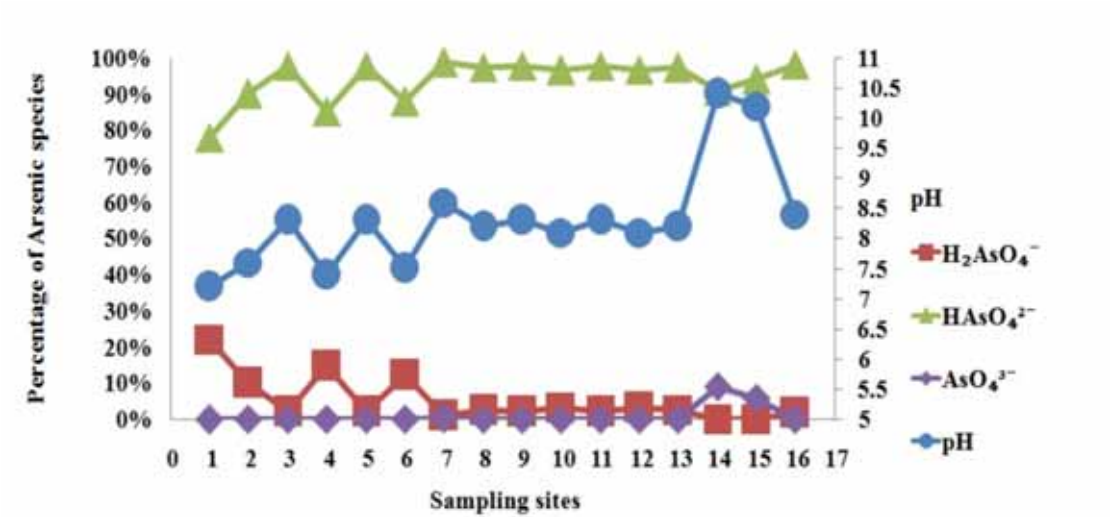

FIGURE 6
Speciation distributions of arsenic in river water at all sites using Eh calculated.

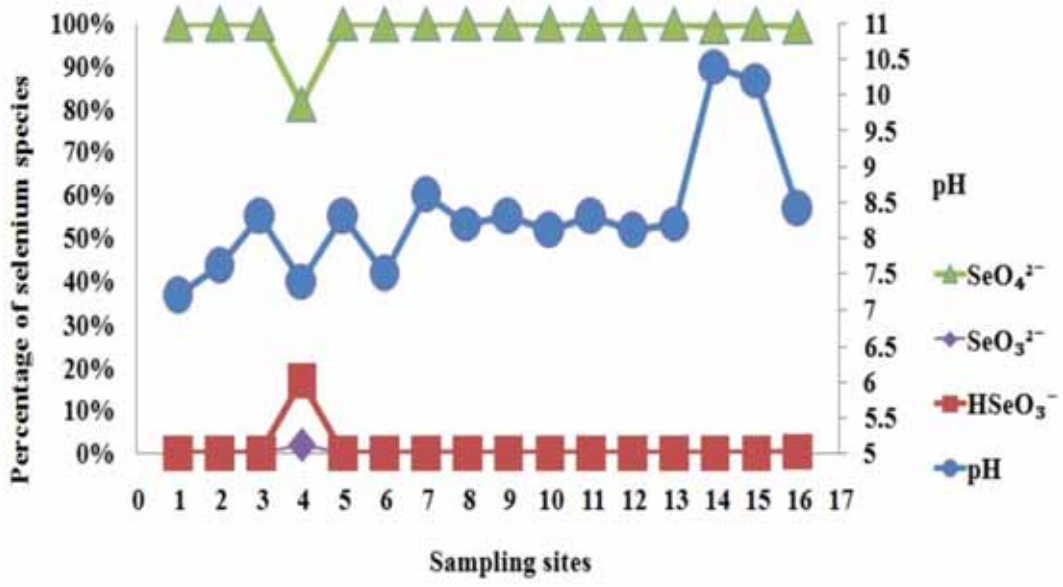

FIGURE 7
Speciation distributions of selenium (b) in river water at all sites using Eh calculated.

RESULTS AND DISCUSSION

Validity of pH and Eh in situ measured. Generally, pH and Eh are critical factors in affecting the distribution of arsenic and selenium speciation. The reliability of pH measured in field work can be assumed only if user's operation is correct and the instrument works well. Unfortunately, the availability of Eh to reflect the true state of oxidative and reductive potential is limited, because of the lack of internal equilibrium. As Lindberg and Runnells noted "*…The potential observed in natural waters are usually mixed potentials which are impossible to relate to a single dominate redox couple in solution…*" [16]. Eh measurement is still useful as an indicator of redox state of solution, but it would be better to use the concentrations of redox couples of interest to give a meaningful Eh value by application of Nernst equation [16].

Eh measured vs Eh calculated of Mianyuan River. Eh value measured in river water varies from - 40 mV to 293 mV, with the mean about 146 mV ± 53%. And pH measured in water varies from 7.2 to 10.4, with the mean of 8.31 ± 10%. Concentration of Fe in most sites was too low to serve as a decisive redox element (Table 1). We did not measure the Fe(Ⅱ) and Fe(Ⅲ) of all water. The theoretical Eh of NO_3^-/NO_2^- couple at equal molar ion at pH = 7 and 25 ℃ equals to 431 mV [17.], which is comparatively closing to the Eh measured (Table 1). In addition, the redox couple NO_3^- and NO_2^- can be measured together using the same instrument of ion chromatography. The *Nernst* equation (equation 1) was adopted

to calculate Eh. All water had enough amounts NO_3^- to be measured. However, there were only two sites having NO_2^- above the detection limit 0.01 mg/l (Table 1). The concentration NO_3^- in Mianyuan River was higher than NO_2^- about three orders of magnitude (Table 1). Equation 1 can be transformed to equation 2. And Eh value increased with the decrease of NO_2^- (equation 2). In fact, the coefficient "-0.0296" before the term "log[NO_2^-]" is quite small. Even if the concentration of NO_2^- at 0.01 mg/l decreased 100 times to 0.0001 mg/l, Eh would improve only 55 mV than the initial value when other conditions kept constant. In this situation, lower concentration of NO_2^- than 0.01 mg/l had little effect on the Eh calculated. Therefore, we set that 0.01 mg/l of NO_2^- was adopted in calculation of Eh for water having NO_2^- lower than detection limit.

$$Eh(V) = 0.845 + 0.0296\log\frac{[NO_3^-][H^+]^2}{[NO_2^-]} \quad \text{(Equation 1)}$$

$$= 0.845 + 0.0296\log[NO_3^-] + 0.592\log[H^+] - 0.0296\log[NO_2^-] \quad \text{(Equation 2)}$$

Eh (cal) calculated at all sites were higher than Eh (mea) measured. The difference between Eh (cal) and Eh (mea) ranged from 149 to 490 mV with the mean of 293 mV. It suggested the existence of internal disequilibrium among redox elements in river water. Eh (cal) at sites of 14 and 15 with alkaline pH were more closing to the Eh (mea) than other sites (Table 1).

Eh-pH diagrams of As -NaCl-H_2O and Se-NaCl-H_2O systems. Eh-pH diagram was constructed to show the dominate species' areas of arsenic and selenium. To improve the accuracy of speciation calculation, the latest and updated thermodynamic parameters of arsenic and selenium were included. Those authors [20-27] have critically reviewed the internal consistency of these parameters. The Eh-pH diagrams of As-H_2O system have been reported in literatures [27, 28]. Figure 2 and Figure 3 were similar to the Eh-pH diagram of As-H_2O in study [27], because most of the equilibrium constants had same sources. Eh-pH diagram of arsenic (1.0×10^{-5} M) included: arsenate (H_3AsO_4, $HAsO_4^{2-}$, $H_2AsO_4^-$, AsO_4^{3-}), arsenite (H_3AsO_3, $H_2AsO_3^-$), and natural crystal arsenic solid (FIGURE 2 and 3). Eh-pH diagrams of Se-H_2O systems have been drawn in studies [28, 29-31]. The difference between Figure 2, 3 and other diagrams [28, 29-31] was resulted by the difference of equilibrium constant sources. The Eh-pH diagram of Se in water included regions of selenate ($HSeO_4^-$, SeO_4^{2-}), selenite (H_2SeO_3, $HSeO_3^-$, SeO_3^{2-}), and natural amorphous selenium solid (Figure 4 and 5). Factor pH plays a key role in controlling the speciation of arsenic and selenium if redox potential keeps stable. In oxidative aqueous environment, H_3AsO_3 mainly exists in water when pH < 2, $H_2AsO_3^{2-}$ mainly exists when 2 < pH < 6.5, $HAsO_3^{2-}$ mainly exists when 6.5 < pH < 11.8, and AsO_3^{3-} mainly exists when pH >11.8 (Figure 2 and 3). Similarly, in oxidative aqueous environment, H_2SeO_3 mainly exists when pH < 2.5, $HSeO_3^-$ mainly exists when 2.5 < pH < 8.3, and SeO_3^{2-} mainly exists when pH > 8.3 (Figure 4 and 5).

Qualitative prediction of arsenic and selenium speciation in Mianyuan River. Water samples at all sites were projected on Figure 2, 3, 4 and 5 according to the pH and Eh (measured and calculated). According to Eh measured, arsenic in the Mianyuan River existed as the less toxic arsenate (+V) (FIGURE 2). In addition, the dominate arsenate (+V) specie in the Mianyuan River was $HAsO_4^{2-}$. In spite of Eh calculated was higher than Eh measured, the result using Eh calculated to predict arsenic speciation was same to Eh measured (Figure 2 and 3). However, the distribution of selenite specie in the river was more complicated. Most water samples were located at the area of $HSeO_3^-$ when Eh measured was used (Figure 4). Only were the water at sites 7 (dammed lake), 14 and 15 (farmland) located at the area of SeO_3^{2-} (Figure 4). However, the dominate specie became SeO_4^{2-} if Eh calculated was adopted (Figure 5), suggesting that selenium was more sensitive to the redox potential than arsenic.

Calculation of percentages of arsenic and selenium species using PHREEQC. Eh-pH diagrams cannot directly give the percentage of each species in water. Therefore, we used PHREEQC to calculate the percentages of arsenic and selenium species in water according to Eh calculated (Figure 6 and 7). The percentage of $HAsO_4^{2-}$ in water accounted for 78 % to 99 %. $H_2AsO_4^-$, and AsO_4^{3-} accounted for tiny. The distribution of arsenic speciation in Mianyuan River was mainly controlled by pH in water. Another study has revealed that the increasing of pH at sites 14 and 15 was related with the using of phosphate fertilizer [4]. Although the reaction equilibrium constants among As, S, and Fe in Table 1 were considered, the concentrations of S, and Fe in water were too low to affect the arsenic speciation.

Specie SeO_4^- was obviously dominated at all sites, with the percentage ranging from 81 % to 99 %. Selenium speciation distribution in Mianyuan River was more affected by Eh than pH (Figure 4 and 5), which is related with the broad pH and narrow Eh of SeO_4^- predominance determine.

CONCLUSIONS

Redox potential (Eh) calculated from the redox couple NO_3^-/NO_2^- were much higher than Eh measured in Mianyuan River. In this river, $HAsO_4^{2-}$ was the only dominated specie of arsenic in water regardless of Eh measured or Eh calculated was adopted. $HSeO_3^-$ in river water was dominated if Eh measured was used, while SeO_4^{2-} became dominated if Eh calculated was adopted. Authors more inclined to believe the result according to the Eh calculated. Therefore, SeO_4^{2-} was the main selenium specie in Mianyuan River. This case study suggests that the method of thermodynamic modeling was more suitable to qualitatively reveal the major species of arsenic than selenium because selenium speciation distribution was more sensitive to the redox potential which was difficult to obtain.

ACKNOWLEDGEMENTS

Special project of China in environmental non-profit industry research (201509024), The National Nature Science Foundation of China (41373120) financially supported this research and State Key Laboratory of Geological Processes and Mineral Resources (GPMR201707) supported this research. Key Project of Natural Sciences of the Department of Sichuan Provincial Education (15ZA0077, 16ZA0098, 17TD0002). We also appreciate the support from China Scholarship Council (CSC, No. 2016080515059).

REFERENCES

[1] Ng, J.C. (2005) Environmental contamination of arsenic and its toxicological impact on humans. Environ. Chem. 2(3), 146-160.

[2] Wang, X., Shi, Z., Ni, S. Xu, W., Wang R. (2017) Geochemical factors affecting chronological reconstruction of a historical arsenic pollution accident in Lake Qionghai, Southwest of China. Aquat. Ecosyst. Health & Management. 20(4), 457-464.

[3] Wang, X., Shi, Z., Shi, Y., Ni, S., Wang, R., Xu, W., Xu, J. (2018) Distribution of potentially toxic elements in sediment of the Anning River near the REE and V-Ti magnetite mines in the Panxi Rift, SW China. J.Geochem. Explor. 184, 110-118.

[4] Wang, X., Ni, S., Shi, Z. (2014) Uranium distribution in the sediment of the Mianyuan River near a phosphate mining region in China and the related uranium speciation in water. Chem. Erde-Geochem. 74(4), 661-669.

[5] Shi, Z., Wang, X., Ni, S. (2015) Metal Contamination in sediment of one of the upper reaches of the Yangtze River: Mianyuan River in Longmenshan Region, Southwest of China. Soil. Sediment. Contam. 24(4), 368-385.

[6] Leermakers, M., Baeyens, W., De Gieter, M., Smedts, B., Meert, C., De Bisschop, H., Morabito, R., Quevauviller, P. (2006) Toxic arsenic compounds in environmental samples: Speciation and validation. Trac-Trend Anal. Chem. 25(1), 1-10.

[7] McArthur, J., Ravenscroft, P., Safiulla, S., Thirlwall, M. (2001) Arsenic in groundwater: testing pollution mechanisms for sedimentary aquifers in Bangladesh. Water. Resour. Res. 37 (1), 109-117.

[8] Sanchez-Rodas, D., Luis Gomez-Ariza, J., Giraldez, I., Velasco, A., Morales, E. (2005) Arsenic speciation in river and estuarine waters from southwest Spain. Sci. Total Environ. 345(1-3), 207-17

[9] Baeyens, W., de Brauwere, A., Brion, N., De Gieter, M., Leermakers, M. (2007) Arsenic speciation in the River Zenne, Belgium. Sci. Total Environ. 384 (1-3), 409-19.

[10] Han, D., Li, X., Xiong, S., Tu, S., Chen, Z., Li, J., Xie, Z. (2013) Selenium uptake, speciation and stressed response of Nicotiana tabacum L. Environ. Exp. Bot. 95, 6-14.

[11] Zhang, H., Feng, X., Larssen, T. (2014) Selenium speciation, distribution, and transport in a river catchment affected by mercury mining and smelting in Wanshan, China. Appl. Geochem. 40, 1-10.

[12] Hu, X., Wang, F., Hanson, M.L. (2009) Selenium concentration, speciation and behavior in surface waters of the Canadian prairies. Sci. Total. Environ. 407(22), 5869-5876.

[13] Ilgen, A.G., Rychagov, S.N., Trainor, T.P. (2011) Arsenic speciation and transport associated with the release of spent geothermal fluids in Mutnovsky field (Kamchatka, Russia). Chem. Geo. 288(3-4), 115-132

[14] Schmeisser, E., Goessler, W., Kienzl, N., Francesconi, K.A. (2004) Volatile analytes formed from arsenosugars: determination by HPLC-HG-ICPMS and implications for arsenic speciation analyses. Anal. Chem. 76(2), 418-423.

[15] Masscheleyn, P.H., Delaune, R.D., Patrick Jr, W.H. (1990) Transformations of selenium as affected by sediment oxidation-reduction potential and pH. Environ. Sci. Technol. 24(1), 91-96.

[16] Lindberg, R.D., Runnells, D.D. (1984) Ground water redox reactions: an analysis of equilibrium state applied to Eh measurement sand geochemical modeling. Science. 225, 925-927.

[17] Langmuir, D. (1997) Aqueous environmental geochemistry. Prentice-Hall, Inc.
[18] Parkhurst, D.L., Appelo, C. (1999) User's guide to PHREEQC (Version 2): A computer program for speciation, batch-reaction, one-dimensional transport, and inverse geochemical calculations. U.S. Geological Survey. U.S.A. 326.
[19] Kinniburgh, D.G., Cooper. D.M. (2004) Predominance and mineral stability diagrams revisited. Environ. Sci. Technol. 38(13), 3641-3648.
[20] Allison, J.D., Brown, D.S., Kevin, J. (1991) MINTEQA2/PRODEFA2, a geochemical assessment model for environmental systems: Version 3.0 user's manual. Environmental Research Laboratory, Office of Research and Development, U. S. Environmental Protection Agency Athens, U.S.A.
[21] Nordstrom, D.K., Archer, D.G. (2003) Arsenic thermodynamic data and environmental geochemistry. In: Welch, A.H., Stollenwerk, K.G. (Eds.) The Arsenic in Groundwater. Kluwer Academic Publishers: Boston. 1-25.
[22] Marini, L., Accornero, M. (2007) Prediction of the thermodynamic properties of metal–arsenate and metal–arsenite aqueous complexes to high temperatures and pressures and some geological consequences. Environ. Geol. 52(7), 1343-1363.
[23] Whiting, K.S. (1992) The thermodynamics and geochemistry of arsenic with application to subsurface waters at the Sharon Steel Superfund site at Midvale, Utah. Press: Colorado School of Mines, U.S.A. 440p.
[24] Seby, F., Potin-Gautier, M., Giffaut, E., Borge, G., Donard, O.A (2001) Critical review of thermodynamic data for selenium species at 25 °C. Chem. Geol. 171(3), 173-194.
[25] Elrashidi, M., Adriano, D., Workman, S., Lindsay, W. (1987) Chemical Equilibria of Selenium in Soils: A Theoretical Development1. Soil Sci. 144(2), 141-152.
[26] Parker, D.R., Tice, K.R., Thomason, D.N. (1997) Effects of ion pairing with calcium and magnesium on selenate availability to higher plants. Environ. Toxicol Chem. 16(3), 565-571.
[27] Lu, P., Zhu, C. (2010) Arsenic Eh–pH diagrams at 25°C and 1 bar. Environ. Earth Sci. 62(8), 1673-1683.
[28] Pourbaix, M. (1966) Atlas of electrochemical equilibria. Press: National Association of Corrosion Engineers, U.S.A. 644p.
[29] Takeno, N. (2005) Atlas of Eh-pH diagrams. Press: Geological survey of Japan, Japan. 419p.
[30] Howard III, H. (1977) Geochemistry of selenium: formation of ferroselite and selenium behavior in the vicinity of oxidizing sulfide and uranium deposits. Geochim. Cosmochim. Ac. 41(11), 1665-1678.
[31] Neal, R.H., Sposito, G. (1989) Selenate adsorption on alluvial soils. Soil Sci. Soc. Am. J. 53(1), 70-74.

Received: **09.10.2017**
Accepted: **10.04.2018**

CORRESPONDING AUTHOR

Xinyu Wang
Geochemistry Department of Chengdu University of Technology& Sichuan Province
Key Laboratory of Nuclear Techniques in Geosciences,
Chengdu, 610059 – China

e-mail: wangxinyucdut@gmail.com

© by PSP Volume 27 – No. 7/2018 pages 4725-4733 Fresenius Environmental Bulletin

IMPROVING ENERGY USE EFFICIENCY OF CORN PRODUCTION BY USING DATA ENVELOPMENT ANALYSIS (A NON-PARAMETRIC APPROACH)

Adnan Abbas[1], Minli Yang[1,2,*], Khurram Yousaf[3], Muhammad Ahmad[4], Ehsan Elahi[5], Tahir Iqbal[6]

[1]College of Engineering, China Agricultural University, Beijing 100083, China
[2]China Research Center for Agricultural Mechanization Development, China Agricultural University, Beijing 100083, China
[3]College of Engineering, Nanjing Agricultural University, Nanjing 210031, China
[4]Department of Structure and Environmental Engineering, University of Agriculture, Faisalabad 38040, Pakistan
[5]School of Business, Nanjing University of Information Science and Technology, Nanjing Shi, Pukou Qu, 210044, China
[6]School of Renewable Energy, North China Electric Power University, Beijing 102206, China

ABSTRACT

Modern farming technologies and researches are used to enhance the crop productivity in the developed countries that are too specific to be implemented directly in developing countries due to variations in soil properties, farmers knowledge, available farm powers and local plant nutrients. Therefore, this study was performed in the agriculture rich country Pakistan that have similar land properties with most of the top agriculture dependent countries (India, Sri Lanka). Energy use pattern of corn production was studied and the degrees of technical efficiency of farmers were analyzed using Data Envelopment Analysis (DEA) technique (non-parametric). Based on the outcomes of the DEA analysis, the inefficient energy inputs were identified and further explored with core objective of significant reduction of excess valuable resources. Randomly, 200 corn growers were interviewed to collect information on profound questionnaire (utilized labor, seed, fertilizers, farmyard manure (FYM), chemicals, agricultural machinery, diesel fuel and water for irrigation and corn yield) with major attention to include all possible energy inputs-outputs. Our results suggested that the total energy of 37361.62 MJ/ha was consumed for corn production, with an average technical efficiency of 83% under constant returns to scale assumptions. The major energy input belongs to fertilizer that if applied and managed according to our optimized value (30969.47 MJ/ha) could save 17.11% resources that will ultimately add equal amount in corn-yield. The findings of the study suggest a vibrant utilization and outreach of extension services to disseminate the knowledge about optimum utilization of inputs to save the extra utilization of energy at farm level which we believe can rapidly increase the economy of all developing countries.

KEYWORDS:
Energy input-output, energy saving target, optimum requirement, technical efficiency, data envelopment analysis, agricultural production

INTRODUCTION

High demands of sustainable economy growth have been directing old-agriculture strategies to the modern agriculture farming which is indeed more stable and précised in developed nations. In contrast, the agriculture dependent counties like Pakistan, India, Sri Lanka etc. are far away from the modern agriculture due to lack of some region-based studies, low interactions of farmers-community and inefficient utilization of valuable resources. Farmers in Pakistan are following old practices without proper knowledge of agriculture and usually they misuse of resource such as over or underutilize farm inputs on the field. Ultimately, it reduces the efficiency, profit and on the same loss of energy [1]. An efficient use of energy resources and improving energy use efficiency is a possible pathway for reducing the environmental footprints of energy inputs in food production, and so, providing sustainable agricultural production, since it brings financial savings, fossil resources preservation and air pollution reduction [2, 3, 4, 5].

The application of parametric and non-parametric approaches could be explored in more efficient and cost-effective way so that minimum energy inputs can produce high corn yields. For example: Ogunniyi and Ajao [6] evaluated efficiency for food crop production in Nigeria by parametric technique of Stochastic Frontier Production Function (SFPF), and non-parametric technique of Data Envelopment Analysis (DEA). Nassiri and Singh [7] measured the efficiency of paddy farms using the Cobb-Douglas frontier function. In other study, Moreira-Lopez and Bravo- Ureta [8] applied a meta-regression analysis for efficient measurement of livestock farms in England and Spain.

DEA is a non-parametric technique of frontier estimation that determines both the relative efficiency of a number of decision making units (DMUs) and targets for their improvement [9]. DEA allows the decision makers to simultaneously consider multiple inputs and outputs, where efficiency of each

DMU is compared to that of an ideal operating unit rather than to the average performance. The decision makers can differentiate efficient and inefficient DMUs and address the sources and amount of inefficiency for each of the inefficient ones [10, 11]. DEA has many advantages that big advantage of DEA is, it does not need any prior assumptions on the underlying functional relationships between inputs and outputs [12].

Due to the many advantages of DEA, there are a large number of its applications for evaluating the performances of DMUs in different sectors, such as production, economy, energy, etc. in the agricultural, some of them been mentioned the following. Khoshnevisan et al. [13] applied DEA approach to determine the efficiency scores of strawberry productions with regard to input parameters of human labor, diesel, seed, farmyard manure, fertilizers, machinery, etc. energy inputs and the strawberry yield as the output parameter. Elhami et al. [14] and Nabavi-Pelesaraei et al. [15, 16] improved the energy requirement for crop production by using data envelopment analysis DEA method and determined the effect of energy optimization on GHG emissions for orange and watermelon production.

Energy optimization is a lucrative industry and low cost for the national economy. It will widely promote employment, create energy security and reduce environmental pollution. Several studies were found in literature for energy consumption and its optimization in various ways. Such as lack of equipment, prohibit excessive use of pesticides and fertilizers, the use of renewable fuels to replace fossil fuels, manage consumption of inputs, increasing the efficiency of combustion systems, etc. [17-22]. Considering the importance of energy efficiency in agriculture production systems, there was no study on improving energy efficiency with application of DEA in corn production. This study is aimed to fill this gap. Therefore, this research is to specify the energy use pattern in corn production, analyze the energy efficiency and determines the optimum energy requirement for corn production farms in selected cities of Pakistan.

MATERIALS AND METHODS

Four districts (Figure 1) of the main corn producing province (Punjab) of Pakistan were chosen. Data was collected from corn growing farmers of the said districts in the production year (2015-16), by using face to face questionnaire method. Fifty farmers from each district (a total of 200 farmers) were interviewed for quantitative information of inputs used in field practices such as (1)- field preparation, (2)- seeding, (3)- fertilization, (4)- irrigation, (5)- plant protection, (6)- harvesting (cobs picking), (7)- post harvesting (cutting of corn stalks and residue) and threshing, and output gained. The questionnaire was pretested on 20 farmers for any error, however, these farmers were not included in the final survey.

Energy calculation. A standard procedure was used to convert each agricultural inputs and output into energy equivalents. The energy associated with all inputs-output except machinery was estimated directly by multiplying their equivalences shown in Table 1, however, machine energy was calculated as given below in equation 1 [23].

$$E_M = \frac{W \times E_q \times t}{T} \qquad (1)$$

Where, E_M is machine energy in MJ/ha, E_q is the energy equivalent for machinery (Table 1), W is the machine weight in kg, t is the machine used time per unit area (hr./ha), T is the machine's economic life (hr.)

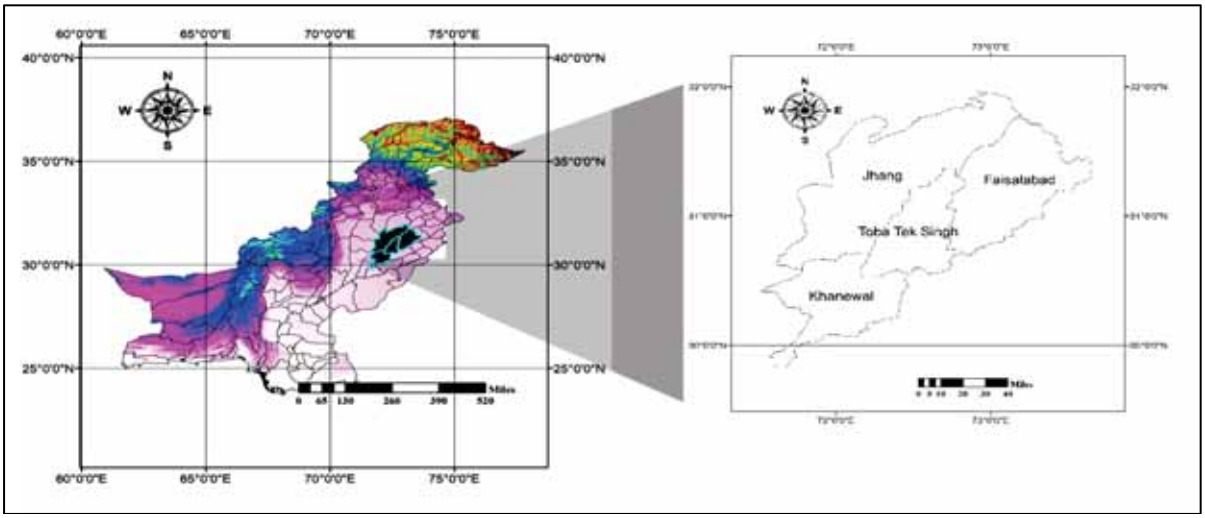

FIGURE 1
Site selection for the whole course of the study (the zoom-in represents the target districts, where corn is considered major crop after wheat)

TABLE 1
Energy equivalents

Input-output (unit)	Energy equivalent (MJ per unit)	References
1. Inputs		
1. Labor (hr.)	1.96	[37]
2. Seed (kg)		
Corn	14.7	[24]
3. Fertilizer (kg)		
Nitrogen (N)	78.1	[37]
Phosphate (P_2O_5)	17.4	[37]
Potassium (K_2O)	13.7	[37]
4. Machinery (hr.)	62.7	[37]
5. Chemicals (Kg)		
Insecticides	199	[37]
Herbicide/Weedicide	238	[37]
Fungicides	92	[37]
6. Diesel fuel (L)	47.8	[37]
7. Water (m^3 ha^{-1})	1.02	[37]
2. Output (kg)		
8. Corn Yield	14.7	[24]

Data regarding energy inputs and output equivalents were entered in excel and SPSS 16 spread sheets, the indices of energy consumption including energy efficiency, energy productivity, specific energy and net energy gain were assessed using the following Eqs. [24].

$$EU_{\eta} = \frac{EO}{EI} \quad (2)$$

$$E_{spec.} = \frac{EI}{Y} \quad (3)$$

$$E_{prod.} = \frac{Y}{EI} \quad (4)$$

$$E_{ng} = EO - EI \quad (5)$$

DEA, a non-parametric approach. DEA is a method to estimate non-parametric efficiency frontiers of multi-product and multi-input systems. DEA involves the use of linear programming to build a non-parametric surface over the data; thus, efficiency measures are calculated relative to this surface or frontier [20]. Some scientist for instance, Charnes, Cooper and Rhodes (CCR) [25] utilized the optimization technique of mathematical programming to generalize single-output/input efficiency measure presented by Farrell [26] to multiple-output/multiple-input instance. The reduction of the multiple-output/multiple-input situation for each DMU to a single virtual output and a single virtual input ratio is key features of the CCR ratio model. This ratio prepares an efficiency measure for a DMU, that is a function of multipliers. The aim is to find the largest sum of weighted outputs of DMUk, while keeping the sum of its weighted inputs at the unit value (or least sum of weighted inputs of DMUk, while keeping the sum of its weighted outputs at the unit value), as a result the ratio of the weighted output to the weighted input for any DMU to be less than one. The CCR model is also called as the CRS model, and identifies inefficient DMUs with considering of their scale size. This is a simple presentation of a basic DEA model. It is possible to create and estimate models that provide input-oriented or output-oriented projections. An input-oriented model attempts to maximize the proportional decrease in input variables while remaining within the envelopment space. On the other hand, an output-oriented model maximizes the proportional increase in the output variables while remaining within the envelopment space.

$$\eta = \frac{w_{so}}{w_{si}} \quad (6)$$

Where η is efficiency, w_{so} weighted sum of outputs, w_{si} weighted some of inputs. Consider $s_1, s_2 \ldots\ldots\ldots$ are weights given to output $n(n = 1, 2 \ldots\ldots\ldots N)$, $O_1^{j*}, O_2^{j*} \ldots\ldots\ldots O_N^{j*}$ are the amount of output $n(n = 1, 2 \ldots\ldots\ldots N)$, of DMU j^*, $r_1, r_2 \ldots\ldots\ldots$ are the weight given to input $m(m = 1, 2 \ldots\ldots\ldots M)$, $I_1^{j*}, I_2^{j*} \ldots\ldots\ldots I_M^{j*}$ are the amount of input $m(m = 1, 2 \ldots\ldots\ldots M)$, to DMU j^*, and j^* is the considered DMU. So, standard form equation 6 is given below,

$$\eta = \frac{s_1 O_1^{J*} + s_2 O_2^{J*} + \ldots\ldots\ldots + s_N O_N^{J*}}{r_1 I_1^{J*} + r_2 I_2^{J*} + \ldots\ldots\ldots + r_M I_M^{J*}} \quad (7)$$

In the analysis of efficient and inefficient DMUs, the energy saving target ratio (ESTR) was used to specify the inefficiency level of energy usage for the DMUs under consideration. The formula is as below [27]:

$$\text{ESTR}_j = \frac{Energy\ saving\ target_j}{Actual\ energy\ input_j} \quad (8)$$

Where energy saving target is the total reducing amount of energy inputs that could be saved without reducing the output level and j represents jth DMU. The minimal value of energy saving target is zero, so the values of ESTRj will be between zero and 1. A higher ESTR values implies higher energy use inefficiency, and thus, a higher energy saving amount [27].

RESULTS AND DISCUSSIONS

Energy used and energy gained in corn production. Published and valuable literature suggested that effective utilization of farm energy can maximize the earnings of middle and low-income farmers, therefore energy utilization (Figure 2) and optimization was performed during course of this study. Unlikely to energy used for all inputs, the chemical fertilizer has a biggest share (17807.57 MJ/ ha) among all inputs. Many studies have confirmed that synthetic fertilizers are the main consumers in crop production [28]. Similarly, irrigation water and diesel fuel are at the second and third position respectively for the energy used. Excessive use of chemical fertilizers energy input in agriculture may create serious environmental consequences such as nitrogen loading in the environment, poor water quality [29, 30, 31], carbon emissions and contamination of the food chain [32]. On the other hand, the energy used for the labor in corn production is higher than energy used for the machinery because corn is a labor-intensive crop. It is deemed that mostly labor used during planting, irrigation and at harvesting time. To decrease the labor requirement, these processes must be mechanized [1]. Also, diesel fuel was mainly utilized for operating tractors and shellers in the farms. Nowadays more than three third of farmers in Pakistan use tractors for different field activities [33, 34, 35].

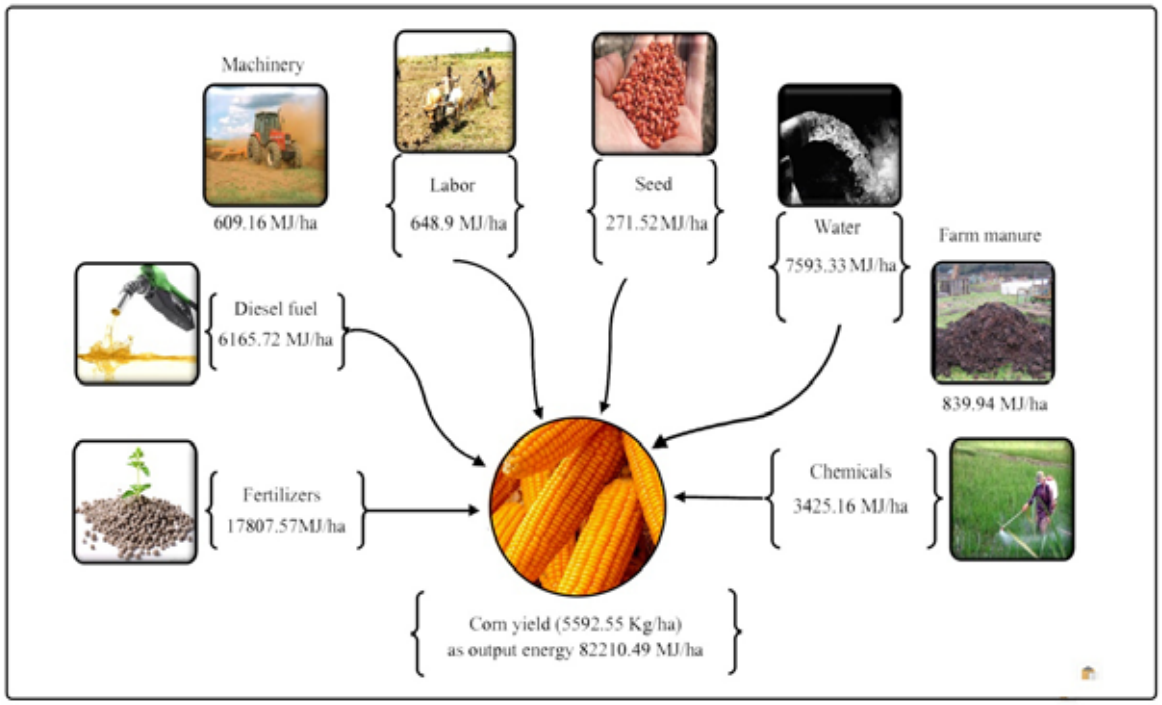

FIGURE 2
Energy being applied during the production of corn in Pakistan

TABLE 2
Input-output energy ratio in corn production

Items	Unit	Actual Quantity	Optimum Quantity	Difference
Energy use efficiency	N/A	2.20	2.65	20.64 (%)
Specific energy	MJ Kg^{-1}	6.68	5.54	-17.11 (%)
Energy productivity	Kg MJ^{-1}	0.15	0.18	20.64 (%)
Net energy gain	MJ ha^{-1}	44848.84	51240.99	14.25 (%)

Furthermore, energy use efficiency indices for corn crop were calculated and presented in Table 2. The energy use efficiency is 2.20, technically the inefficiency may be caused due to mismanagement of resources [36], if we compare it with optimum energy efficiency, our results depicted that inputs have been misutilized and found unproductive in the study area. From the specific ratio, we found that for the production of one-kilogram corn 6.68 MJ energy is required, while the value of energy productivity is reported that 0.15 kilogram of corn is produced from one MJ of inputs. If we compare our results with case of Iran [24] it can be seen that energy utilization efficiency and specific energy were higher in Iran than Pakistan while the energy productivity **i**s almost at the same level. The net energy gain has also not touched to the frontier line because of the misutilization of inputs. Perhaps, approach of Pakistani farmers towards precision agriculture is not well defined that they could better utilize all the necessary inputs for the crops production.

Sustainability and technical efficiency by means of data envelopment analysis (DEA). To study the trend of energy utilizing efficiency in target districts, data envelopment analysis has been employed. The most popular input oriented CCR model as mentioned earlier, is adopted for the estimation of technical efficiency. For input data base of CCR model, labor, seed, fertilizer, farmyard manure, chemicals, agriculture machinery, diesel fuel and irrigation water were considered as input and yield as output. Several authors studied the energy use efficiency in crop production by using different levels of inputs and yield as output in data envelopment analysis [18, 19, 24]. More specifically, DEA approach was used to compute the relative efficiency of corn growers in four districts of the study area, namely Jhang, khanewal, Faisalabad and Toba Tek Singh followed by DMU1, DMU2, DMU3 and DMU4 respectively. Technical efficiency of considered DMUs with their respective ranking based on CCR results were presented in Figure 3. According the depicted results DMU3 (Faisalabad) and DMU1 (Jhang) were found the efficient and most inefficient DMUs. In more specific interpretation, the farmers of Faisalabad exhibit the higher level of technical efficiency than others because they might have surplus usage of inputs or deficit in corn yield as compared to Faisalabad.

Results have shown an uneven trend of technical efficiency in the studied area, implies that farmers are not applying appropetiate production techniques in suitable time and optimum quantity. The optimum energy requirement and saving energy of various farm inputs for corn production based on the results of CCR model are given in Table 3.

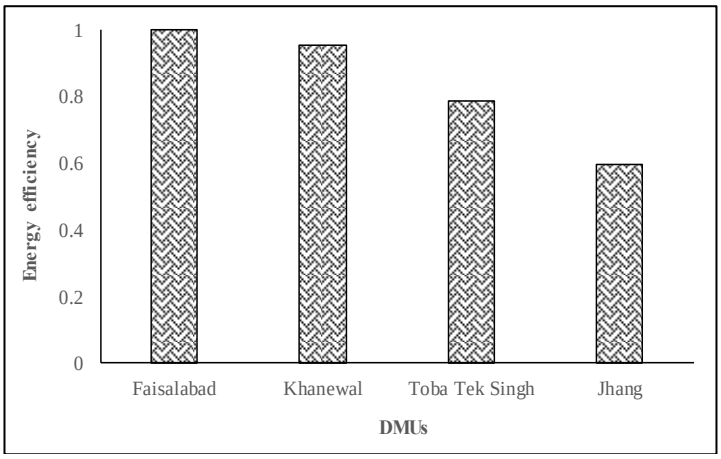

FIGURE 3
Energy efficiency of the selected districts with leading difference (Faisalabad has highest efficient although all regions are categorized on same fertility level)

TABLE 3
The energy saving target for the corn production

Inputs	Optimum energy requirements (MJ/ha)	Energy saving target	ESTR (%)
Labor	534.10	114.81	17.69
Seed	226.98	44.54	16.40
Fertilizer	14760.24	3047.33	17.11
FYM	681.46	158.49	18.87
Chemicals	2786.57	638.89	18.65
Machine	504.85	104.30	17.12
Diesel fuel	5141.40	1024.32	16.61
Water	6333.87	1259.47	16.59
Total	30969.47	6392.15	17.11

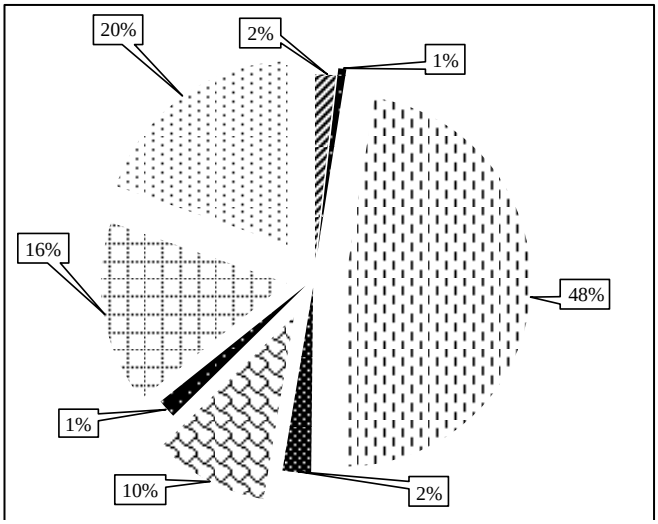

FIGURE 4
The proposed share of input energy that if properly saved can play a vital role in the maximization of the Corn-Yield (the 48% amount of fertilizers can be reduced)

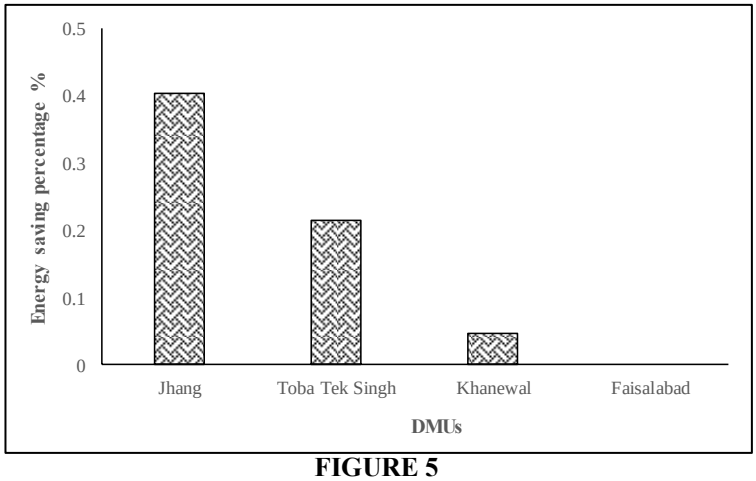

FIGURE 5
Energy saving potential for each DMU

The results revealed that the total optimum energy required for corn production was 30969.47 MJ/ha. Also the percentage of total saving energy in optimum requirement over total actual use of energy was calculated as 17.11%, indicating that by following the recommendations resulted from this study, on an average, about 6392.15 MJ/ha of total input energy could be saved. As mentioned, in the agricultural production, a farmer has more control over inputs rather than output levels. The shares of the various resources from total input energy saving are presented in Figure 4. Results revealed that the highest contribution to the total saving energy was 48% for fertilizer followed by water and diesel fuel. The shares of seed, human labor, machinery and biocides energy inputs were relatively low, indicating that they have been used in the right proportions by almost all the farmers. Chauhan et al. [20] reported that the contribution of fertilizer and diesel fuel energy inputs from total saving energy in paddy production were 33% and 24%, respectively. Mousavi-Avval et al. [19] reported that the contribution of electricity and seed energy inputs by 78.1% and 0.05% from total energy saving in soybean production was the highest and lowest.

From the distribution of inputs used in corn production, a handsome amount of energy could be saved by optimum use of inputs. So the goal of sustainability could be achieved by optimum use of inputs. We also determined the estimated potential of resource savings in each district as compared to Faisalabad. For example, efficiency score of DMU1 (Jhang) was 60 %, that means same level of output can be achieved with 60% of the resources if the DMU is performing on frontier. This implies that by raising the performance of DMU1 to highest level, a total of 40% of resources could be saved. Similarly, there is a potential of resource savings i.e 5% and 21% respectively, if DMU2 and DMU4 were performed on frontier. The possible resource saving potential in considered districts have been demonstrated in Figure 5.

CONCLUSION AND POLICY RECOMMENDATIONS

Advance farming is urgently required to overcome the increasing food scarecity in the developing countries. Input-output energy analysis for crops is an cost-effective approach towards an efficient utilization of available resources that can increase efficiency and sustainability of old-agriculture. However, in the developing countries such as Pakistan, mismanagement of inputs lead to the loss of high fraction of corn-yield. To identify, the possible energy loss, we applied the energy balance at corn farms and data was analyzed by DEA that provided us optimum requirement and energy saving target. The energy consumed for the inputs in production of corn crops is 37361.62 MJ/ha with an average corn yield of 5592.548 kg/ha. Among all selected districts for the study area, Faisalabad is the most efficient district which is working at frontier line in case of corn crop, while average technical efficiency of corn growers was 83 %. The DEA approach found an improper and inefficient trend of energy use in corn production, due to excessive consumption of energy inputs (mainly fertilizer, diesel fuel and water) in considered areas. Moreover, we also found a potential for energy improvement in corn crop with optimum value of input energy 30969.47 MJ/ha and overall 17.11% resources could be saved in the study area if farmers operate at their efficient level.

ACKNOWLEDGEMENTS

This study is part of PhD dissertation. We are thankful to China Scholarship council (CSC-reference number 2014GXZA87.) for providing PhD scholarship funding.

REFERENCES

[1] Abbas, A., Minli, Y., Elahi, E., Yousaf, K., Ahmad, R. and Iqbal, T. (2017) Quantification of mechanization index and its impact on crop productivity and socioeconomic factors. International agricultural engineering Journal. 26(3), 49-54.

[2] Mousavi-Avval, S.H., Rafiee, S., Jafari, A. and Mohammadi, A. (2011) Improving energy use efficiency of canola production using data envelopment analysis (DEA) approach. Energy. 36, 2765-2772.

[3] Abbas, A., Yang, M., Ahmad, R., Yousaf, K. and Iqbal, T. (2017) Energy use efficiency in wheat production, a case study of Punjab Pakistan. Fresen. Environ. Bull. 26, 6773-6779.

[4] Hosseinzadeh-Bandbafha, H., Safarzadeh, D., Ahmadi, E., Nabavi-Pelesaraei, A. and Hosseinzadeh-Bandbafha, E. (2017) Applying data envelopment analysis to evaluation of energy efficiency and decreasing of greenhouse gas emissions of fattening farms. Energy. 120, 652-662.

[5] Taner, A., Arisoy, Z.R., Kaya, Y., Gultekin, I. and Partigoc, F. (2015) The effects of various tillage systems on grain yield, quality parameters and energy indices in winter wheat production under the rainfed conditions. Fresen. Environ. Bull. 24, 1463-1473.

[6] Ogunniyi, L.T. and Ajao, A.O. (2011) Measuring the technical efficiency of maize production using parametric and non-parametric methods in Oyo state, Nigeria. Journal of Environmental Issues and Agriculture in Developing Countries. 3(3), 113-122.

[7] Nassiri, S.M. and Singh, S. (2009) Study on energy use efficiency for paddy crop using data envelopment analysis (DEA) technique. Applied Energy. 86(7), 1320-1325.

[8] Moreira-Lopez, V.H. and Bravo-Ureta B.E. (2009) A study of dairy farm technical efficiency using meta-regression: an international perspective. Chil J Agric Res. 69, 214-223.

[9] Malana, N.M. and Malano H.M. (2006) Benchmarking productive efficiency of selected wheat areas in Pakistan and India using data envelopment analysis. Irrig. and Drain. 55(4), 383-394.

[10] Angulo-Meza, L. and Lins, M.P. (2001) Review of methods for increasing discrimination in data envelopment analysis. Annals of operation research. 116(1-4), 225-242.

[11] Zhang, X., Huang, G.H., Lin, Q. and Yu, H. (2009) Petroleum-contaminated groundwater remediation systems design: a data envelopment analysis based approach. Expert systems with applications. 36(3), 5666-5672.

[12] Seiford, L.M. and Thrall, R.M. (1990) Recent developments in DEA: the mathematical programming approach to frontier analysis. Journal of Econometrics. 46(1), 7-38.

[13] Khoshnevisan, B., Shariati, H.M., Rafiee, S. and Mousazadeh, H. (2014) Comparison of energy consumption and GHG emissions of open field and greenhouse strawberry production. Renewable and sustainable energy reviews. 29, 316-324.

[14] Elhami, B., Akram, A. and Khanali, M. (2016) Optimization of energy consumption and environmental impacts of chickpea production using data envelopment analysis (DEA) and multi objective genetic algorithm (MOGA) approaches. Information processing in agriculture. 3(3), 190-205.

[15] Nabavi-Pelesaraei, A., Abdi, R., Rafiee, S. and Mobtaker, H. G. (2014) Optimization of energy required and greenhouse gas emissions analysis for orange producers using data envelopment analysis approach. Journal of cleaner production. 65, 311-317.

[16] Nabavi-Pelesaraei, A., Abdi, R., Rafiee, S. and Bagheri, I. (2016) Determination of efficient and inefficient units for watermelon production-a case study: Guilan province of Iran. Journal of the Saudi Society of Agricultural Sciences. 15(2), 162-170.

[17] Nabavi-Pelesaraei, A., Kouchaki-Penchah, H. and Amid, S. (2014) Modeling and optimization of CO_2 emissions for tangerine production using artificial neural networks and data envelopment analysis. International Journal of Biosciences. 4(7), 148-158.

[18] Mohammadi, A., Rafiee, S., Mohtasebi, S.S., Mousavi-Avval, S.H. and Rafiee, H. (2011) Energy efficiency improvement and input cost saving in kiwifruit production using Data Envelopment Analysis approach. Renewable Energy. 36(9), 2573-2579.

[19] Mousavi-Avval, S.H., Rafiee, S., Jafari, A. and Mohammadi, A. (2011) Optimization of energy consumption for soybean production using Data Envelopment Analysis (DEA) approach. Applied Energy. 88(11), 3765–3772.

[20] Chauhan, N.S., Mohapatra, P.K. and Pandey, K.P. (2006) Improving energy productivity in paddy production through bench marking an application of data envelopment analysis. Energy conversion and management. 47(9), 1063-1085.

[21] Baran, M.F., Polat, R. and Gokdogan, O. (2016) Comparison of energy use efficiency of different tillage methods on the secondary crop sunflower production. Fresen. Environ. Bull. 25, 4937-4943.

[22] Marakoglu, T. and Carman, K. (2017) A comparative study on energy efficiency of wheat production under different tillage practices in middle Anatolia of Turkey. Fresen. Environ. Bull. 26, 3163-3169.

[23] Kitani, O. (1990) CIGR Handbook of Agricultural Engineering. Vol: V energy and biomass engineering. Chapter 1 Natural Energy and Biomass. Part 1.3 biomass resources. 330p.

[24] Banaeian, N. and Zangeneh, M. (2011) Study on energy efficiency in corn production of Iran. Energy. 36, 5394–5402.

[25] Charnes, A., Cooper, W.W. and Rhodes, E. (1979) Measuring the efficiency of decision making units. European journal of operational research. 3(4), 339.

[26] Farrell, M.J. (1957) The measurement of productive efficiency. Journal of the royal statistical society. Series A. 120(3), 253-290.

[27] Hu, J.L. and Kao, C.H. (2007) Efficient energy-saving targets for APEC economies. Energy Policy. 35(1),373-382.

[28] Elahi, E., Abid, M., Zhang, L., ul Haq, S., Sahito, J.G.M. (2018) Agricultural advisory and financial services; farm level access, outreach and impact in a mixed cropping district of Punjab, Pakistan. Land Use Policy. 71, 249-260.

[29] Elahi, E., Abid, M., Zhang, H., Weijun, C. and Hasson, S.U. (2018) Domestic water buffaloes: access to surface water, disease prevalence and associated economic losses. Preventive Veterinary Medicine. 154(1), 102-112.

[30] Elahi, E., Zhang, L., Abid, M., Javed, M.T., Xinru, H. (2017) Direct and indirect effects of wastewater use and herd environment on the occurrence of animal diseases and animal health in Pakistan. Environmental Science and Pollution Research. 24(7), 241-14.

[31] Elahi, E., Abid, M., Zhang, L., Alugongo, G.M., (2017) The use of wastewater in livestock production and its socioeconomic and welfare implications. Environmental Science and Pollution Research. 24(21), 17255-17266.

[32] Khan, S., Khan, M.A., Hanjra, M.A. and Mu, J. (2009) Pathways to reduce the environmental footprints of water and energy inputs in food production. Food Policy. 34(2), 141-149.

[33] Rehman, T. ur., Khan, M.U., Tayyab, M., Akram, M.W. and Faheem, M. (2016) Current status and overview of farm mechanization in Pakistan – A review. Agricultural Engineering International: CIGR Journal Eng Int: CIGR Journal. 18(2), 83–93.

[34] Iqbal, M.A., Iqbal, A., Afzal, S., Akbar, N., Abbas, R.N. and Khan, H.Z. (2015) In Pakistan, Agricultural Mechanization Status and Future Prospects. American-Eurasian J. Agric. & Environ. Sci. 15(1), 122–128.

[35] Abbas, A., Yang, M., Yousaf, K., Khan K.A., Iqbal, T. and Hassan S.G. (2018) Comparative analysis of energy use efficiency in food grain production systems of Pakistan. Fresen. Environ. Bull. 27, 1053-1059.

[36] Padilla-Fernandez, M.D. and Nuthall, P.L. (2009) Technical Efficiency in the Production of Sugar Cane in Central Negros Area, Philippines: An Application of Data Envelopment Analysis. Journal of the International Society for Southeast Asian Agricultural Sciences. 15(1), 77–90.

[37] Nabavi-Pelesaraei, A., Hosseinzadeh Bandbafha, H., Qasemi-Kordkheili, P., Kouchaki-penchah, H. and Riahi-Dorcheh, F. (2016) Applying optimization techniques to improve of energy efficiency and GHG (greenhouse gas) emissions of wheat production. Energy. 103, 672-678.

Received: **16.10.2017**
Accepted: **31.01.2018**

CORRESPONDING AUTHOR

Minli Yang
College of Engineering,
China Agricultural University,
Beijing 100083 – China

e-mail: qyang@cau.edu.cn

© by PSP Volume 27 – No. 7/2018 pages 4734-4742 Fresenius Environmental Bulletin

SELECTIVE CULTIVATION OF TWO STRAINS OF *ACIDITHIOBACILLUS THIOOXIDANS* AND BIO-OXIDATION OF ELEMENTAL SULFUR

Qiyong Yang[1,3,4,*], Wenfeng Yang[2,4], Qiong Zhu[4], Qingfang Zhang[2], Mei Tang[4]

[1]Poyang Lake Eco-economy Research Center, Jiujiang University, Jiujiang Jiangxi, 332005, China
[2]College of Petrochemical Engineering, Lanzhou University of Technology, Lanzhou Gansu, 730050, China
[3]Jiujiang Key Laboratory of basin management and ecological protection, Jiujiang University, Jiujiang Jiangxi, 332005, China
[4]College of Chemistry and Environmental Engineering, Jiujiang University, Jiujiang Jiangxi, 332005, China

ABSTRACT

Bioleaching with *Acidithiobacillus* species is an environment-friendly and economical technology to remove heavy metals from sludge. Two strains of acidophilic sulfur-oxidizing bacterium were isolated from the secondary activated sludge of sewage treatment plants. According to the colonial morphology, SEM image of strains, physiological-biochemical properties and 16S rRNA gene sequence analysis, the two strains were identified as *Acidithiobacillus thiooxidans* JJU-1 and JJU-4. The gene sequence of JJu-1 was deposited into the GenBank database under the following Accession No. KM101109. The microfiltration membrane experiment confirmed that *Acidithiobacillus thiooxidans* must be in direct physical contact with the sulfur particle before sulfur-oxidation could take place. The experiment results indicated that the two strains were efficient in acid production. Especially, the strain JJU-1 was superior to JJU-4 in sulfur-oxidation and JJU-1 can grow at extreme acid environments (at a pH of 0.7 or below). The pH of strain JJU-1 declined from 3.03 to 1.2 on the 8th day at optimum conditions (pH=2.5-3.5, *T*= 28-30℃, sulfur size < 75 μm), and dropped from 3.1 to 0.8 in the presence of surfactant agent Tween-60 of 0.8 $g \cdot L^{-1}$. Therefore, *Acidithiobacillus thiooxidans* JJU-1 could be widely used in sewage sludge bioleaching for removal of heavy metals.

KEYWORDS:
Acidithiobacillus thiooxidans, sulfur-oxidation, elemental sulfur, 16S rRNA; isolation

INTRODUCTION

With the widely development of urbanization process and wastewater treatment, a large amount of sewage sludge has constantly increased. According to the report, up to June of 2015, there were 3802 municipal sewage treatment plants in China and about 161 million tons of sewage per day was treated [1]. It can be estimated about 44 million tons of wet sewage sludge (80% moisture content) per year was generated by municipal sewage treatment plants in China. The treatments and disposals of sewage sludge have been regarded as important environmental issue. There are several disadvantages hindering the utilization of sludge, such as high concentration of heavy metals.

Bioleaching with *Acidithiobacillus* species is an environment-friendly and economical technology to remove heavy metals from sludge [2, 3, 4]. The mechanism takes place under aerobic conditions, and the bacterial activity either leads to the production of sulfuric acid, resulting in the acidification of the sediments and extraction of heavy metals adsorbed on sediment particles (indirect mechanism), or to the direct solubilization of metal sulfides by enzymatic oxidation stages (direct mechanism) [5, 6, 7].

The major microorganisms in sludge bioleaching are *Acidithiobacillus spp.*, such as *Acidithiobacillus ferrooxidans and Acidithiobacillus thiooxidans* [7, 8, 9]. *Acidithiobacillus thiooxidans* was first described in 1921 by Waksman and Joffe [10] and since then lots of studies have been carried out due to its participation in bioleaching processes. It found out the enzyme and mechanisms of sulfur oxidation by *Acidithiobacillus thiooxidans* [11]. In order to obtain additional insights about the bioleaching characteristics of the bacterium, several draft genome sequence corresponding to *Acidithiobacillus thiooxidans* had been released and published [12, 13, 14].

The biological oxidation of sulfur by *Acidithiobacillus thiooxidans* is the committed step of bioleaching of heavy metal from sludge. The microorganisms play important roles in maintaining acidic conditions by producing sulfuric acid. The exposure of *Acidithiobacillus thiooxidans* to heavy metals had resulted in greater rate of acid production [15]. Particularly, *Acidithiobacillus thiooxidans* can grow at extreme acid environments (at a pH of 0.5 or below) [15]. However, the natural bacterial strains isolated from environment are still lack of acid producing capacity [16, 17, 18]. Therefore, some measures were employed to improve the sulphur-oxidation in the presence of *Acidithiobacillus thiooxidans.* Pith

Otero et al. [19] added a surfactant agent (Tween 80) to a medium containing sulphur and a culture of *Thiobacillus thiooxidans,* which resulted in the increasing of the sulphur oxidation rate and sulphuric acid production. Microwave and ultraviolet induction breeding were also adopted to further improve the acid production of *Acidithiobacillus thiooxidans* [17].

In this work, two strains of acidophilic sulfur-oxidizing bacterium were isolated and cultivated to investigate their characteristics of acid production. It is expected to find a method for improving the effect of its acid production in the bioleaching process.

MATERIALS AND METHODS

Sewage sludge sampling. Strain JJU-1 was isolated from the secondary activated sludge of Jiujiang University Sewage Treatment Plant (Jiangxi Province, China). The treatment plant receives mostly domestic wastewater and the daily total wastewater was about 2000 tons. Strain JJU-4 was isolated from the secondary activated sludge of Jiujiang Industrial Park Wastewater Treatment Plant (Jiangxi Province, China). The daily total wastewater was 23 thousand tons and the CAST technology was applied. The sewage sludge was incubated at 4℃ in a refrigerator before utilization.

Culture media. Waksman solid medium and Waksman liquid medium were used for isolation and enrichment of the sulfur-oxidizing microorganisms. The Waksman solid medium contained 2.0g of $(NH_4)_2SO_4$, 0.1g of KCl, 0.33g of $K_2HPO_4 \cdot 3H_2O$, 0.25g of $MgSO_4 \cdot 7H_2O$, 0.01g of $Ca(NO_3)_2 \cdot 4H_2O$ and 10 g of agar in 1000 ml of distilled water. The initial pH of the medium was adjusted to 3.0-3.5 before it was autoclaved at 105 ℃ for 30 minutes. The Waksman liquid medium contained 0.20 g of $(NH_4)_2SO_4$, 3.93 g of $K_2HPO_4 \cdot 3H_2O$, 0.50g of $MgSO_4 \cdot 7H_2O$ and 0.19g of $CaCl_2$ in 1000 ml of distilled water. In addition, 1g elemental sulfur was used as energy source for *Acidithiobacillus thiooxidans*. The pH of basal salt solution was adjusted to 3.5-4.0 before it was autoclaved at 105 ℃ for 30 min.

Isolation and morphology observation. The incubation of sulfur-oxidizing bacteria was performed according to the technique of Jain and Tyagi [20] with some modifications. Strain JJU-1 and JJU-4 were first enriched with Waksman liquid medium at 28℃ before isolation respectively. The isolation process of JJU-1 and JJU-4 were just the same. Ten milliliter of sludge mixture was added to a flask containing 90 ml of Waksman liquid medium. The flask was then incubated at 28℃ in a gyratory shaker at 180 rpm. When the pH of medium dropped to below 2.0, 5 ml of the acidified culture medium was added to another flask containing 95 ml of Waksman liquid medium. After the above procedures were repeated thrice, spread plate method was adopted to isolate and purify these isolates onto Waksman solid medium. The colonies grown on solid medium were picked and enriched with Waksman liquid medium at 28℃ and 180 rpm after they were about one millimeter in size. After the multiple of isolation and purification, the strain JJU-1 and JJU-4 were isolated and designated. These isolates were stored at 4℃ for future bioleaching experiments.

The morphology of bacteria was observed by scanning electron microscope (SEM).

Amplification, sequencing and phylogenetic analysis of 16SrRNA genes. The strain of JJU-1 DNA was extracted by the Ezup column of bacterial genomic DNA Extraction Kit (SK8255 biology engineering Limited by Share Ltd, Shanghai). Then, the 16SrRNA genes of JJU-1 was amplified by PCR using forward primer (F27):5'-AGTTTGATCMTGGCTCAG-3' and reverse primer (R1492):5'-GGTTACCTTGTTACGACTT-3'.
Each 25μl reaction mixture contained 1μL dNTP (2.5 $mmol \cdot l^{-1}$), 2.5μl 10X buffer, 0.5μl of sample DNA, 0.2μl Taq DNA polymerase, 0.5μl of each primer (10uM), 1μl $MgCl_2$ (25 $mmol \cdot l^{-1}$), and added distilled water to 25μl. Amplification was carried out with a program consisting of an initial denaturation at 94℃ for 4 minutes, 30sycles of 94℃ for 45 seconds, 55℃ for 45 seconds, and 72℃ for 1 minute, a final elongation cycle at 72℃ for 10 minutes, and then stopped the reaction at 4℃. The resulting PCR product was purified by agar extration kits and was sequenced by biology engineering Limited by Share Ltd, Shanghai.

Physiological characterization. Optimal growth conditions. The incubation was performed at different temperatures and initial pH to obtain the optimal growth conditions of JJU-1and JJU-4, from 20 ℃ to 45 ℃ and values ranging from 1.0 to 7.0. During the process, the OD_{600} value of the medium was periodically measured.

Utilization of energy sources and nitrogen sources. To determine what energy source JJU-1and JJU-4 utilizes, the Waksman liquid medium was supplemented with one of these energy source (in grams per liter): sulfur (10) and ammonium sulphate (2); sodium thiosulfate (10) and ammonium sulphate (2); peptone (1) and ammonium sulphate (2); glucose (1) and ammonium sulphate (2); ferrous sulfate (44.7) and ammonium sulphate (2). All cultures were incubated at 28℃ for 7 days, and the initial pH of medium was adjusted to about 3. During the process, the OD_{600} values and pH values of the medium were periodically measured.

To determine what nitrogen sources JJU-1and JJU-4 utilizes, the strains grew in Waksman liquid medium which the ammonium sulphate was replaced

with ammonium carbonate, potassium nitrate and peptone as nitrogen source respectively, and elemental sulfur was used as energy source. Specifically, Waksman liquid medium was supplemented with one of these energy source (in grams per liter): sulfur (10) and ammonium carbonate (1); sulfur (10) and Potassium nitrate (1); sulfur (10) and peptone (5). All cultures were incubated at 28℃ for 7days, and the initial pH of medium was adjusted to about 3.0. During the process, the OD_{600} values and pH values of the medium were periodically determined.

Sulfur-oxidation experiments. Effect of the size of sulfur particle on sulfur-oxidation. The sulfur particles less than or equal to 75 μm were used as energy source to determine sulfur-oxidation of JJU-1 and JJU-4 in the experiment. Three grams of elemental sulfur was added to a flask containing 350 ml of Waksman liquid medium and pH of medium was adjusted to about 4.0. After sterilized and cooled, 10 ml of the bacterium solution of JJU-1and JJU-4 was added to flasks respectively. Finally, the flasks were incubated at 28℃ in a gyratory shaker at 180 rpm. The pH of the medium was periodically monitored during this process.

Effect of surfactant agent on sulfur-oxidation. To research the effect of surfactant agent on sulfur-oxidation, the strains of JJU-1 and JJU-4 incubated at the optimum condition with sulfur particles less than or equal to 75 μm as energy source. Surfactant agent Tween-60 was added to a flask containing 350 ml of Waksman liquid medium. The concentration of Tween-60 was optimally 0.8 $g \cdot l^{-1}$ and then pH of medium was adjusted to about 4. The following process was as mentioned above.

RESULTS AND DISCUSSION

Morphological characterization. The sulfur particles floated on the liquid surface during the early incubation of JJU-1 and JJU-4, then gradually dispersed and dipped into the bottom of the bottle. The medium gradually became turbid. The pH value of medium of JJU-1was declined sharply to about 1.5 after 5 days. In contrast, it took 7 days for JJU-4. According to the SEM images (Figure 1 and 2), Strain JJU-1and JJU-4 were motile, gram negative, rod-shaped. Strain JJU-1 is 1-3 μm × 0.3 μm in size and JJU-4 is 0.5-1 μm × 0.5 μm in size. The colonies of JJU-1 and JJU-4 are rounding, moist, raised and yellowy with a regular edge.

Physiological and biochemical characterization. Optimal growth conditions. The two strains grew at temperatures ranging from 20 ℃ to 45 ℃ and initial pH values ranging from 1.0 to 7.0 for 7 days. According to Figure 3, the optimal temperature of the two strains was between 28℃ and 30 ℃. Similarly, the optimal pH of the two strains was between 2.5 and 3.5 (Figure 4). However, the experiment results indicated that the sulfur-oxidation of JJU-1 was superior to JJU-4.

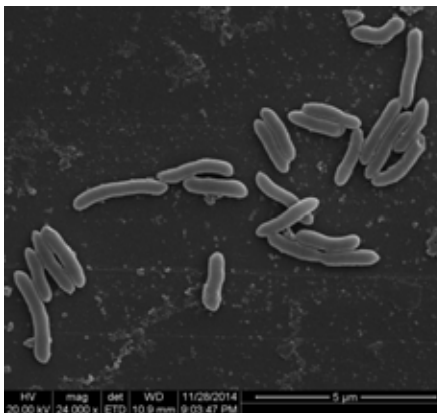

FIGURE 1
SEM image of strain JJU-1

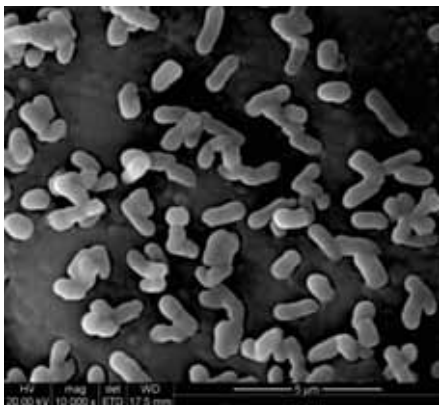

FIGURE 2
SEM image of strain JJU-4

Growth curve. The growth curves are shown in Figure 5. The pH of strain JJU-1 dropped from 3.4 to 0.7 on the 7th day, while pH of strain JJU-4 dived from 3.9 to 1.6. The two strains showed efficient in sulfur-oxidation in comparison with the *Acidithiobacillus thiooxidans* isolated by Wang et al. [21], which took 17 days for the decreasing of pH from 3.3 to 1.0. Wen et al. [18] reported that *Acidithiobacillus thiooxidans* isolated from sewage sludge significantly decreased the pH from 5.30 to 1.07 after a leaching period of 15 days. Particularly, JJU-1 can grow at extreme acid environments (at a pH of 0.7) just as previous study [15]. The OD_{600} values of strain JJU-1 were greater than that of strain JJU-4. The pH downtrend of two strains indicated that the acid production of strain JJU-1 was much better than strain JJU-4.

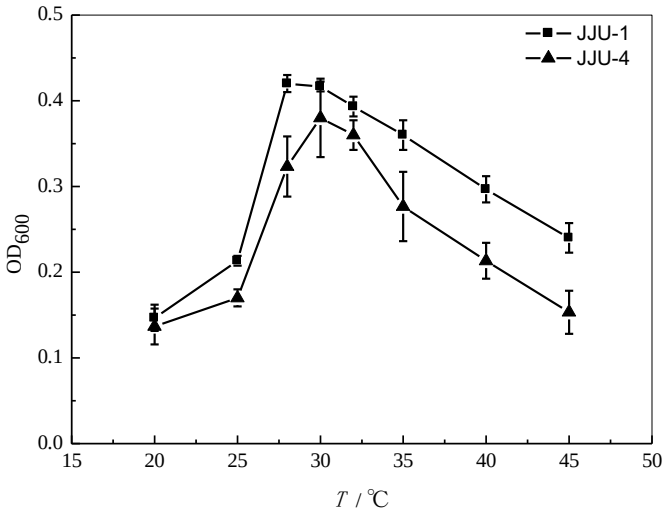

FIGURE 3
Effect of temperature on growth of strain JJU-1 and JJU-4（initial pH=3.0，t=7d)

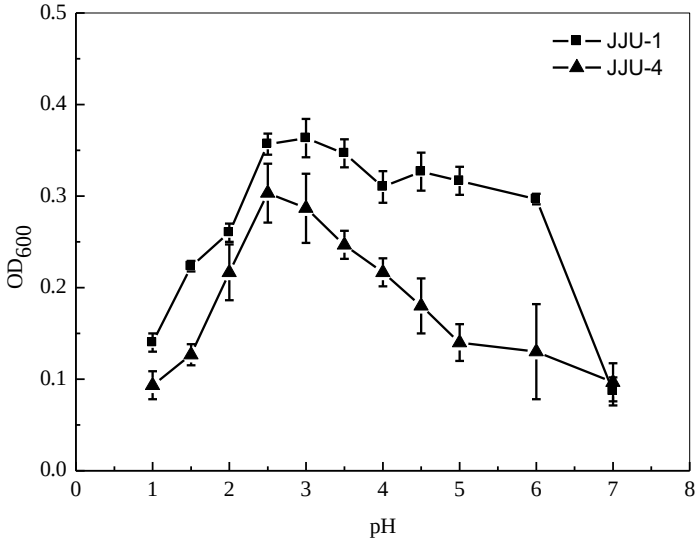

FIGURE 4
Effect of initial pH on growth of strain JJU-1 and JJU-4（*T*= 28℃，*t*=7d）

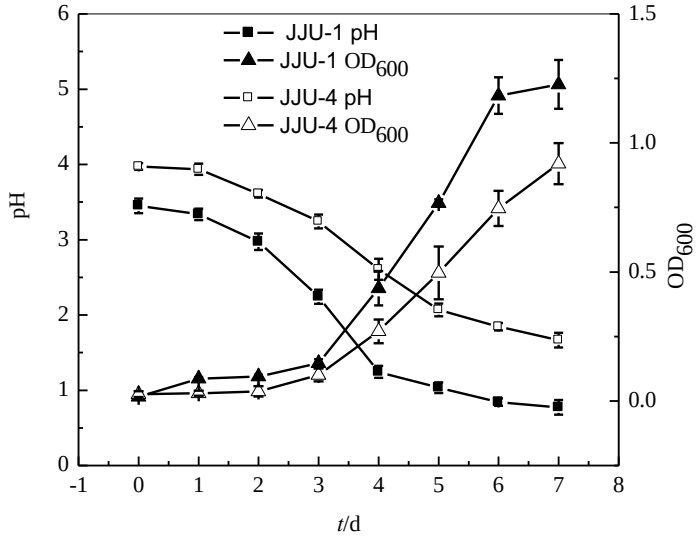

FIGURE 5
Growth curves of strain JJU-1 and JJU-4（initial pH=3.0，*T*= 28℃）

TABLE 1
The utilization of energy sources

Energy sources (in grams per liter)	Nitrogen sources (in grams per liter)	JJU-1	JJU-4
sulfur（10）	ammonium sulphate（2）	+	+
sodium thiosulfate（10）	ammonium sulphate（2）	+	+
peptone（1）	ammonium sulphate（2）	-	-
glucose（1）	ammonium sulphate（2）	-	-
ferrous sulfate（44.7）	ammonium sulphate（2）	-	-
sulfur（10）	ammonium carbonate（1）	+	+
sulfur（10）	potassium nitrate（1）	+	+
sulfur（10）	peptone（5）	+	+

Nont"+" means growth, "-" means no growth

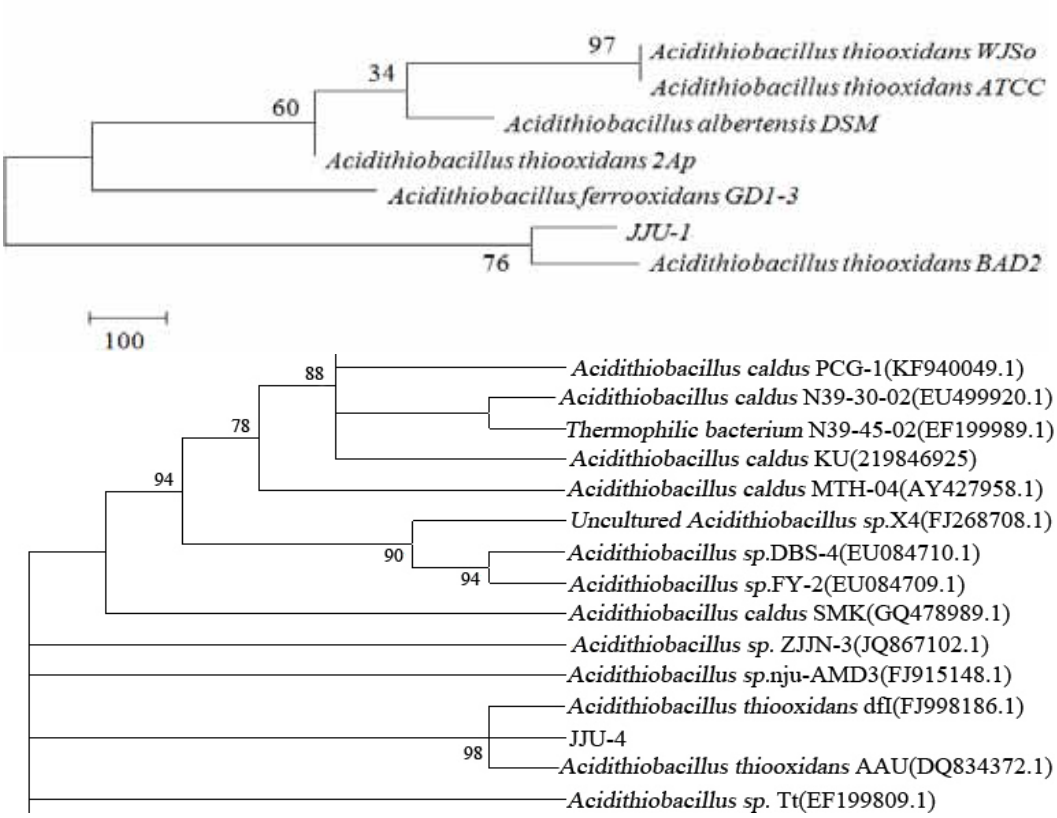

FIGURE 6
Phylogenetic dendrogram of JJU-1 and JJU-4

Utilization of energy sources. As shown in Table 1, the strains of JJU-1 and JJU-4 grew autotrophically by using elemental sulfur and sodium thiosulfate as sole energy source. However, Growth did not occur in media containing any of these energy sources (i.e. peptone, glucose and ferrous sulfate) as sole energy sources. It indicated that strains were not identified as *Acidithiobacillus ferrooxidans,* which could use ferrous sulfate as sole energy source.

When the two strains incubated with ammonium carbonate, potassium nitrate and peptone as nitrogen source respectively, the pH of the media decreased and the OD_{600} values of media increased. The results indicated that the two strains grew rapidly with inorganic nitrogen as nitrogen sources, whereas slowly with organic nitrogen as nitrogen sources.

The preliminary conclusion could be achieved that the two strains were identified as *Acidithiobacillus thiooxidans* according to [22]. The following will be further carried on 16S rRNA gene sequence analysis.

16S rRNA gene sequence analysis and identification. The 16S rRNA gene sequence of two strains JJU-1 and JJU-4 were successfully amplified by PCR, with the expected fragment sizes of 1422 bp and 1387 bp, respectively. After sequencing the PCR product, the newly identified sequence of JJU-1 was deposited into the GenBank database under the following Accession No. KM101109. A BLAST search against the GenBank or NCBI databases showed that the 16S rDNA sequence of strain JJU-1 and JJU-4

all showed 99% similarity with *Acidithiobacillus thiooxidans.* The phylogenetic tree was constructed by the neighbor-joining (NJ) method using the MEGA 4 software. According to this phylogenetic analysis, strain JJU-1 was shown to be the closest to the *Acidithiobacillus thiooxidans* BAD2, while strain JJU-4 clustered with *Acidithiobacillus thiooxidans AAU* and *Acidithiobacillus thiooxidans dfI* (Figure 6).

Sulfur-oxidation of Acidithiobacillus thiooxidans. Effect of the size of sulfur on sulfur-oxidation. It was confirmed that *Acidithiobacillus thiooxidans* must be in direct physical contact with the sulfur particle before sulfur-oxidation occurs, and the size of sulfur particle has an effect on the sulfate formation [23]. According to the prior research, the sulfur particles passing through 180 μm yielded lower rates of sulfate formation than these of size below 180μm [24]. Therefore, the sulfur particles less than or equal to 75 μm were used as sole energy source to determine sulfur-oxidation of JJU-1 and JJU-4 in the experiment. The oxidation curves are shown in Figure 7. The pH of strain JJU-1 declined from 3.03 to 1.2 on the eighth day, while dropped to 1.5 for JJU-4. It demonstrated that the sulfur-oxidation of JJU-1 was superior to JJU-4.

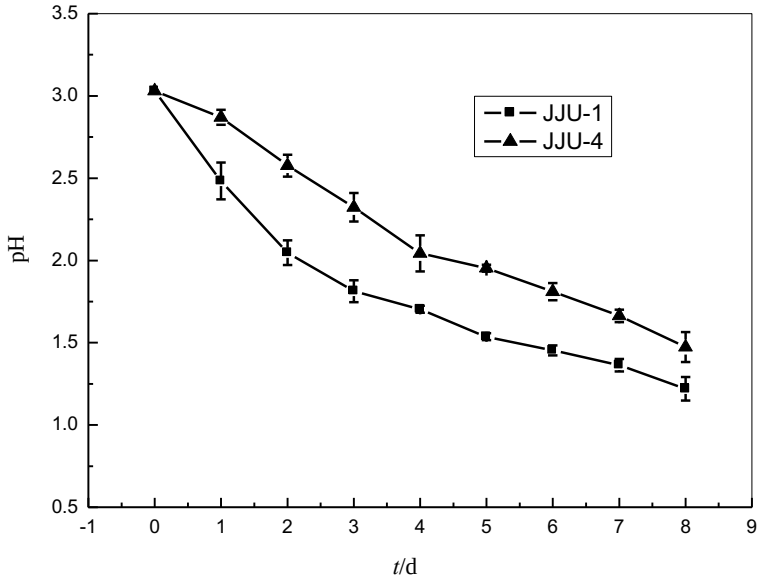

FIGURE 7
Effect of the size of sulfur on sulfur-oxidation of JJU-1 and JJU-4

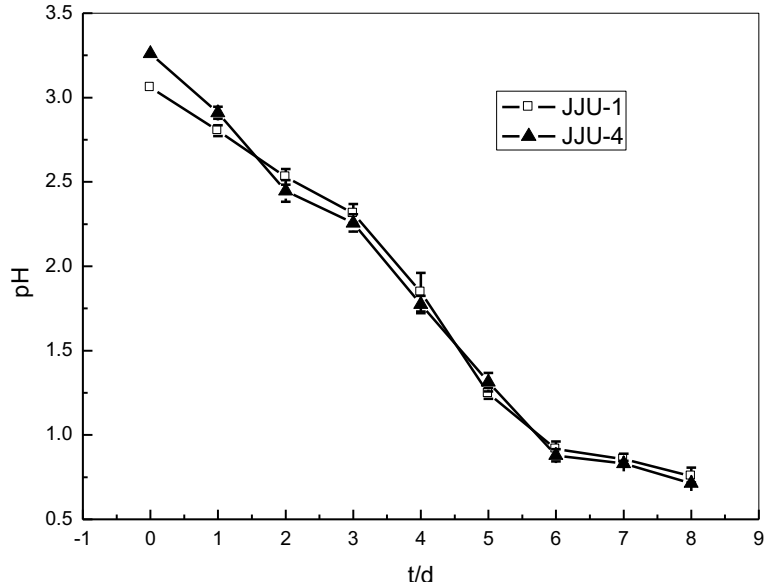

FIGURE 8
Effect of surfactant agent Tween-60 on sulfur-oxidation of JJU-1 and JJU-4

Effect of surfactant agent Tween-60 on sulfur-oxidation. With surface tension of the medium is changed, the sulfur-oxidation rates will be increased [23]. The conclusion demonstrated that 10^{-2} $g \cdot L^{-1}$ surfactant agent Tween-80 could greatly promote the growth of *Acidithiobacillus ferrooxidans* [25]. When the concentration of Tween-60 was up to 0.8 $g \cdot L^{-1}$, it was beneficial to the sulfur-oxidation of *Acidithiobacillus thiooxidans* [24]. In order to determine sulfur-oxidation of JJU-1 and JJU-4, the optimal concentration of Tween-60 (i.e. 0.8 $g \cdot L^{-1}$) was utilized in the experiment. The sulfur-oxidation curves of JJU-1 and JJU-4 were shown in Figure 8. The pH of strain JJU-1 declined from 3.1 to 0.8 on the eighth day. It was interesting that the pH of strain JJU-4 decreased from 3.3 to 0.7 on the eighth day, which indicated that the sulfur-oxidation rates of strain JJU-4 was close to strain JJU-1 in the presence of surfactant agent. However, it was not inconsistent with above conclusion. The results demonstrated that the surfactant agent Tween-60 had greater effect on strain JJU-4 than JJU-1 due to the size of JJU-4 was smaller than JJU-1.

Analysis of the mechanism of sulfur-oxidation. Some hypotheses assumed that insoluble elemental sulfur should be soluble and then diffuse into the interior of the cell before the occurrence of sulfur-oxidation by *Acidithiobacillus thiooxidans*. In previous experiments [24], some measures were adopted to accelerate the sulfur-oxidation, such as increasing the dosage of sulfur, reducing the size of sulfur and adding the surfactant agent. All these methods increased the direct contact space between bacteria and sulfur particles. Accordingly, it would be inferred that direct contact was a precondition for sulfur-oxidation.

In order to certify the conclusion, three gram elemental sulfur was wrapped and sealed by a piece of flat microfiltration membrane with less than or equal to 0.1 μm micropore, and then added to 300 ml of Waksman liquid medium with 10 ml bacteria suspension. The flask was incubated at 28℃ in a gyratory shaker at 180 rpm. The control experiment was carried on without flat microfiltration membrane at the same conditions.

After 10 days, the pH values of medium which elemental sulfur was wrapped and sealed by flat microfiltration membrane approximately maintained at around 3.0, whereas the pH values of control experiment dropped to about 1.0. In the experiment, the elemental sulfur particles were insulated from bacteria by membrane to avoid the direct contact between bacteria and sulfur particle. The sulfur particles were observed by scanning election microscope, respectively. As shown in Figure 9, the surface of sulfur particles, wrapped by flat membrane, were smooth and hardly eroded, whereas the sulfur particles of control experiment were seriously eroded. It was confirmed that *Acidithiobacillus thiooxidans* must be in direct contact with sulfur particles before sulfur-oxidation can take place.

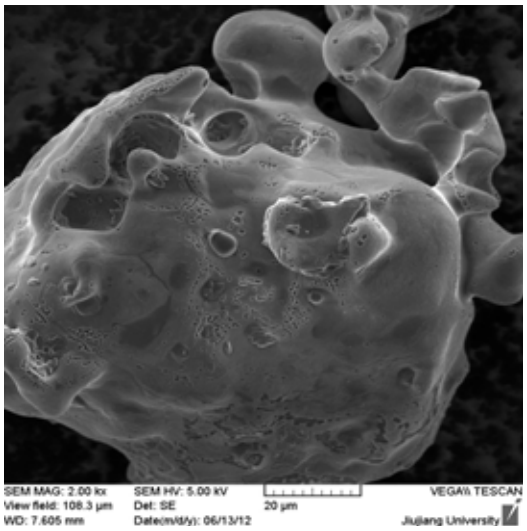

(a)

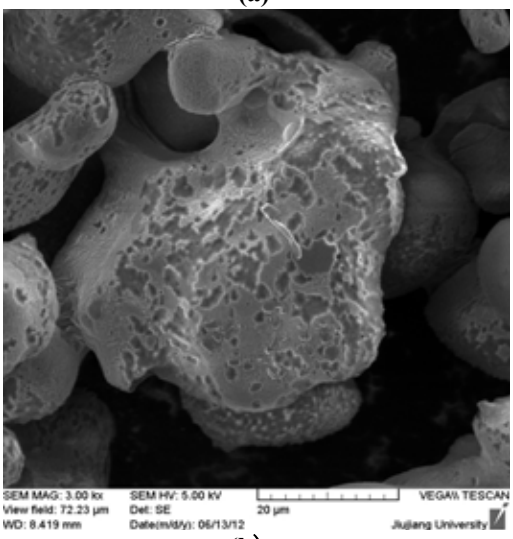

(b)

FIGURE 9

SEM images of surface characteristics of elemental sulfur (a: elemental sulfur was wrapped and sealed by flat microfiltration membrane, b: elemental sulfur was in direct contact with *Acidithiobacillus thiooxidans*)

CONCLUSION

Two strains of JJU-1 and JJU-4 were isolated and characterized. The optimal temperature for growth was between 28℃ and 30 ℃ and the optimal initial pH was between 2.5 and 3.5. The strains grew autotrophically by using elemental sulfur as sole energy source, but not ferrous sulfate. The two strains grew rapidly with inorganic nitrogen as nitrogen sources, whereas slowly with organic nitrogen as nitrogen sources. It should be noted that the sulfur-oxidation of JJU-1 was superior to JJU-4.

According to the morphological, biochemical

and physiological characterizations and 16S rRNA gene sequence analysis (more than 99% 16S rRNA sequence similarity), the two strains were identified as *Acidithiobacillus thiooxidans*. The gene sequence of strain JJu-1 was deposited into the GenBank database under the following Accession No. KM101109.

When JJU-1 and JJU-4 used the optimum size of sulfur (less than or equal to 75 μm) as energy source at the optimal growth conditions, the rate of sulfur oxidization by JJU-1 was much better than JJU-4. However, the sulfur-oxidation rates of strain JJU-4 was close to strain JJU-1 in the presence of surfactant agent Tween-60, which had greater effect on JJU-4 than JJU-1 due to the size of JJU-4 was smaller than JJU-1.

The strain JJU-1 has shown efficient in sulfur-oxidation and can grow at extreme acid environments (at a pH of 0.7 or below). The pH of strain JJU-1 declined from 3.03 to 1.2 on the 8th day at optimum conditions (pH=2.5-3.5, T= 28-30℃, sulfur size < 75 μm). In the presence of surfactant agent Tween-60 of 0.8 $g \cdot L^{-1}$, the pH of strain JJU-1 declined from 3.1 to 0.8 on the 8th day. Therefore, JJU-1 could be widely used in sewage sludge bioleaching for removal of heavy metals or bioleaching of sulphide minerals.

The flat microfiltration membrane experiment confirmed that direct contact was a precondition for sulfur-oxidation of *Acidithiobacillus thiooxidans*. Therefore, it is beneficial to find out some measures to accelerate the sulfur-oxidation. In the follow-up study, there is a need to investigate the effects of different anions and cations, osmotic pressure and extracellular polymeric substances on the sulfur-oxidation.

ACKNOWLEDGEMENTS

This work was supported by the National Natural Science Foundation of China (21367014), Natural Science Foundation of Jiangxi Province, China (20151BAB203026), External Science and Technology Cooperation Program of Jiangxi Province, China (20132BDH80008) and Science and Technology Program of Education Department of Jiangxi Province, China (GJJ14732).

REFERENCES

[1] Wang, S., Chen, X.G., Chen, Y., Yang, Q.Q., Li, J. (2015) Recent advances on deep dewatering of sludge in wastewater treatment plant. Environmental Science & Technology. 38(12Q), 186-190. (in Chinese).

[2] Zhang, P.Y., Zhu, Y., Zhang, G.M., Zou, S., Zeng, G.M., Wu, Z. (2009) Sewage sludge bioleaching by indigenous sulfur-oxidizing bacteria: Effects of ratio of substrate dosage to solid content. Bioresource Techn. 100(3), 1394-1398.

[3] Kumar, K., Suthar, S., Dastidar, M.G., Sreekrishnan, T.R. (2014) Bioleaching of heavy metals from textile sludge by indigenous sulfur-and-iron-oxidizing microorganisms using elemental sulfur and ferrous sulfate as energy sources: A comparative study. Geomicrobiol. 31(10), 847-854.

[4] Marchenko, A.M., Pshinko, G.N., Demchenko, V.Ya., Goncharuk, V.V. (2016) Bioleaching of heavy metals from wastewater sludge by ferrous iron oxidizing bacteria. Water Chem. Techn. 38(1), 51-55.

[5] Seidel, H., Ondruschka, J., Morgenstern, P., Stottmeister, U. (1998) Bioleaching of heavy metals from contaminated aquatic sediments using indigenous sulfur-oxidizing bacteria: a feasibility study. Water Sci. Technol. 37, 387-394.

[6] Akinci, G., Guven, D.E.（2011）Bioleaching of heavy metals contaminated sediment by pure and mixed cultures of *Acidithiobacillus spp.* Desalination. 26, 221-226.

[7] Vera, M., Schippers, A., Sand, W. (2013) Progress in bioleaching: fundamentals and mechanisms of bacterial metal sulfide oxidation - part A. Appl. Microbiol. Biot. 97, 7529-7541.

[8] Wang, Y.D., Li, G.Y., Liu, Y.L., Ding, D.X. (2007) Isolation, purification and cultivation of a new strain of *Thiobacillus thiooxidans.* Journal of University of South China (Science and Technology). 21(7), 1-3. (in Chinese).

[9] Zheng, G.Y., Wang, Z.Y., Wang, D.Z., Zhou, L.X. (2016) Enhancement of sludge dewaterability by sequential inoculation of filamentous fungus *Mucor circinelloides* ZG-3 and *Acidithiobacillus ferrooxidans* LX5. Chem. Eng. J. 284, 216-223.

[10] Waksman, S.A., Joffe, J.S. (1921) Acid production by a new sulfur-oxidizing bacterium. Science. 53, 216.

[11] Suzuki, I., Chan, C.W., Takeuchi, T.L. (1992) Oxidation of elemental sulfur to sulfite by *Thiobacillus Thiooxidans* cells. App. Environ. Microb. 58(11), 3767-3769.

[12] Valdes, J., Ossandon, F., Quatrini, R., Dopson, M., Holmes, D.S. (2011) Draft genome sequence of the extremely acidophilic biomining bacterium *Acidithiobacillus thiooxidans* ATCC 19377 provides insights into the evolution of the *Acidithiobacillus genus*. J. Bacteriol. 193, 7003e4.

[13] Dante, T., Maria, P.C, Mauricio, L., Alex, D.G., Marko, B., Roberto, A.B, Pilar, P., González, M., Alejandro, M. (2014) A new genome of Acidithiobacillus thiooxidans provides insights into adaptation to a bioleaching environment. Res. Microbiol. 165(9), 743-752.

[14] Yin, H., Zhang, X., Liang, Y., Xiao, Y., Niu, J., Liu, X. (2014) Draft genome sequence of the extremophile *Acidithiobacillus thiooxidans* A01, isolated from the wastewater of a coal dump. Genome Announc. 2, e00222e14.

[15] Jang, H.C., Valix, M. (2017) Overcoming the bacteriostatic effects of heavy metals on Acidithiobacillus thiooxidans for direct bioleaching of saprolitic Ni laterite ores. Hydrometallurgy. 168, 21-25.

[16] Huang, F.Y., Wang, S.M., Zhou, L.X. (2006) Optimum growth condition of *Acidithiobacillus thiooxidans* TS6 and its resistance to heavy metals. Acta Scientiae Circumstantiae. 26(8), 1290-1294. (in Chinese).

[17] Peng, H.Q., Zhao, Y.H. (2009) Study on improving the acid-producing capacity of *Acidithiobacillus thiooxidans.* Metal Mine. 395(5), 143-245. (in Chinese).

[18] Wen, Y.M., Wang, Q.P., Lin, H.Y., Chen, Z.L. (2009) Bioleaching of heavy metal from sewage sludge by isolated *Thiobacillus thiooxidan.* Environmental Pollution & Control. 31(7), 52-55 (in Chinese).

[19] Otero, A.P, Curutchet, G., Donati, E., Tedesco, P. (1995) Action of *Thiobacillus thiooxidans* on sulphur in the presence of a surfactant agent and its application in the indirect dissolution of phosphorus. Process biochem. 30(8), 747-750.

[20] Jain, D.K., Tyagi, R.D. (1992) Leaching of heavy metals from anaerobic sewage sludge by sulfur-oxidizing bacteria. Enzyme Microb. Tech. 14, 376-383.

[21] Wang, Y.S., Pan, Z.Y., Lang, J.M., Xu, J.M., Zheng, Y.G. (2007) Bioleaching of chromium from tannery sludge by indigenous *Acidithiobacillus thiooxidans.* J. Hazard. Mater. 147, 319-324.

[22] Buchanan, R.E., Gibbons, N.E. (1974) Bergey's Manual of Determinative Bacteriology (8th Edition). Philadelphia: Williams & Wilkins.

[23] Vogler, K.G., Umbreit, W.W. (1941) The necessity for direct contact in sulfur oxidation by *Thiobacillus Thiooxidans*. Soil Sci. 51(5), 331-338.

[24] Yang, Q.Y., Qiu, X.W., Cheng, P.F., Li, Y., Han, J.F., Jiang, S., Shan, Y.Y., Sun, C. (2015) Isolation, identification of an *Acidithiobacillus Thiooxidan* strain and its characteristic of acid production. Ecology and Environmental Sciences. 24(8), 1366-1374. (in Chinese).

[25] Peng, A.A., Liu, H.C., Nie, Z.Y., Xia, J.L. (2012) Effect of surfactant Tween-80 on sulfur oxidation and expression of sulfur metabolism relevant genes of *Acidithiobacillus ferrooxidans*. Transactions of Nonferrous Metals Society of China. 22, 3147-3155.

Received: **24.10.2017**
Accepted: **26.04.2018**

CORRESPONDING AUTHOR

Qiyong Yang
Poyang Lake Eco-economy Research Center, Jiujiang University,
Jiujiang Jiangxi, 332005 – China

e-mail: yqy46901@163.com

© by PSP Volume 27 – No. 7/2018 pages 4743-4750 Fresenius Environmental Bulletin

COLONIZATION OF FRESH WATER LEECH *ERPOBDELLA OCTOCULATA* LINNAEUS, 1758 (ANNELIDA: HIRUDINIDA) IN DIFFERENT HABITATS IN TUNCA RIVER, EDIRNE

Nurcan Ozkan*

Trakya University, Education Faculty, Department of Science Education, Edirne, Turkey

ABSTRACT

In this study, it was aimed to investigate the colonization of *Erpobdella octoculata* Linnaeus, 1758 fauna in Tunca River (Edirne) at 3 stations and 5 different leaf packages. In this respect, 5 sampling were performed and some water parameters were recorded in June - October 2012. The distribution of *Erpobdella octoculata* belonging to Erpobdellidae family according to leaf package types, months and stations were given. In addition, this species was recorded for the first time in Tunca River of Trakya region.

KEYWORDS:
Erpobdella octoculata, colony structures, Tunca River, Edirne, Trakya

INTRODUCTION

Leeches involve over 15000 species in Annelida group. The majority of these species are ectoparasites and are blood-sucking animals. More than 650 of these species are found in the Hirudinea class. These class members involve sea, freshwater and land leeches [1]. Not all leeches are blood-suckers. Some species are fed on invertebrates, individuals from other Annelida classes, snails and insect larvae. Blood-suckers live as ectoparasites in vertebrate animals such as fish, frogs, turtles, snails and shellfish [2]. Although almost every group of vertebrates is a host, fish are the most attacked group [3-4].

Most leeches that are hermaphrodite live for about a year. The leeches that come out of the eggs in the spring, then they mature in the year following. Life deviations depend on the eating habits and the living environment. Although some leeches are in the sea, most aquatic species live in freshwater, such as the pool, lake, and the edge of lightly flowing streams, which are found in shallow plants. Even if the leeches are spread all over the world (from the pole oceans to the water resources in the desert) they are found in more temperate lake and pool waters. Reproduction structures are important character for defining families, genus, and species.

Erpobdellid leeches are macrophagous predators of aquatic invertebrates [5], whose ancestors abandoned their blood-feeding habits [6-7]. The species in this group have been studied both as a study of invertebrate species interactions [8-9] and as an indicator species for freshwater toxicology has been studied as a model for a long time [10-12].

Erpobdella octoculata is one of the most common species of leech in freshwaters [13]. Typical habitat examples are city park ponds, as well as lowland lakes, streams and rivers [14- 15]. Many leeches have significant adverse effect on freshwater culture and animal health [16].

Such high concentrations may be present at the levels of streams contaminated by organic matter. (Up to 900 individuals / m^2) [17]. It has been shown that *E. octoculata* mainly feeds on chironomid larvae (up to 80% of the diet) followed by oligochaeta and other invertebrates [18].

The leeches forming the research theme constitute a group of benthic invertebrates both ecologically and economically important [19]. The first studies about the subject of our country scientists were initiated by Geldiay [20], in which the macro and micro fauna of Çubuk Dam and Emir Lake were investigated and *Hirudo medicinalis* species was reported. Geldiay and Tareen [21] studied the benthic fauna of Gölcük Lake and reported species *Helobdella stagnalis*, *Piscicola geometra*, *Hirudo medicinalis*, *E. octoculata* and *E. testacea.*

Then, the type of work carried out was determined species *Hirudo medicinalis* L., 1758, *H. verbana* Carena, 1820, *Helobdella stagnalis* (L., 1758), *Piscicola geometra* (L. 1761), *Erpobdella octoculata* Linnaeus, 1758, *Dina vignai* (Minelli, 1978), *D. lineata* (O.F. Müller, 1774), *Haementaria costata* (F. Mller, 1846), *Batracobdella euxina* Neubert & Nesemann, 1995, *Hemiclepsis marginata* (O.F. Müller, 1774), *Glossosiphonia complanata* (L., 1758), *Haemopis sanguisuga* L., 1758, *Trocheta bykowskii* Gedroyc, 1913 and *Theromyzon tessulatum* (O. F. Müller, 1774).

This study aims to investigate the colonization of *E. octoculata* strain which is distributed in some stations in the Tunca River and to contribute to the uncovering of our country biodiversity in this context.

MATERIALS AND METHODS

Five samplings were carried out between June and October in 2012 in order to determine the colonization of *E. octoculata* fauna at 3 stations in Tunca River in Trakya Region (Figure 1).

First of all, the foliage of the trees and the growth of the leaves were expected until May. Then *Juglans regia* L. (walnut), *Morus alba* L. (mulberry), *Ulmus leavis* Pall. (elm) leaves were collected because of the widespread presence around the river. In addition, *Buxus* sp. (artificial boxwood) and *Platanus orientalis* L. (dried plane leaf) poured from plane trees in the autumn of the previous year were collected. Then, 5 kg of potato bags were filled separately from each kind of leaves and these packages were ordered each month to receive a total of 5 potato bags from each of the leaves. Leaf packets were connected to each other by durable wires and marked with different colored plastic numbers. When the leaves began to get decay in the coming months, it was guaranteed to be able to distinguish which leaf in which number. For each station, 25 leaf packets were prepared to collect a total of 5 leaf packs, one from each different leaf pack each month, and placed on the ground of the river. In order to prevent drifting with the water current, the floors were fixed with thick iron and connected to the land by ropes (Figure 3). Within the following 5 months, a total of 5 leaf packets, one from each different leaf package, were collected from the sampling stations once a month. Leaves were filtered by mixing with a large amount of water in the bucket and washing the eyes in different sieves (Hole Range - 0,600µ, 300µ and 1,18mm). By collecting with the help of pens, the first fixations were made with 4% formaldehyde solution. For the determination of some small-sized species, Olympus WMZ model stereo-microscope was used.

Determination of taxon type determined according to Sawyer [4], Neubert and Nesemann [22], Elliott and Mann [23] and Koperski et al. [24].

The physico-chemical properties of the water samples from sampling stations and some parameters were measured in the laboratory. These were; water temperature, pH, electrical conductivity, dissolved oxygen, total hardness and the amount of suspended solids.

RESULTS AND DISCUSSION

Classis: Clitellata
Ordo: Arhynchobdellida
Familia: Erpobdellidae
Genus: *Erpobdella*
Species: *Erpobdella octoculata* (L., 1758)

Registrations from Turkey. Gölcük Lake, İzmir [21]; Gümüldür Stream, İzmir [25]; some rivers in the North Aegean Region [26]; some lakes in Western Black Sea Region [19].

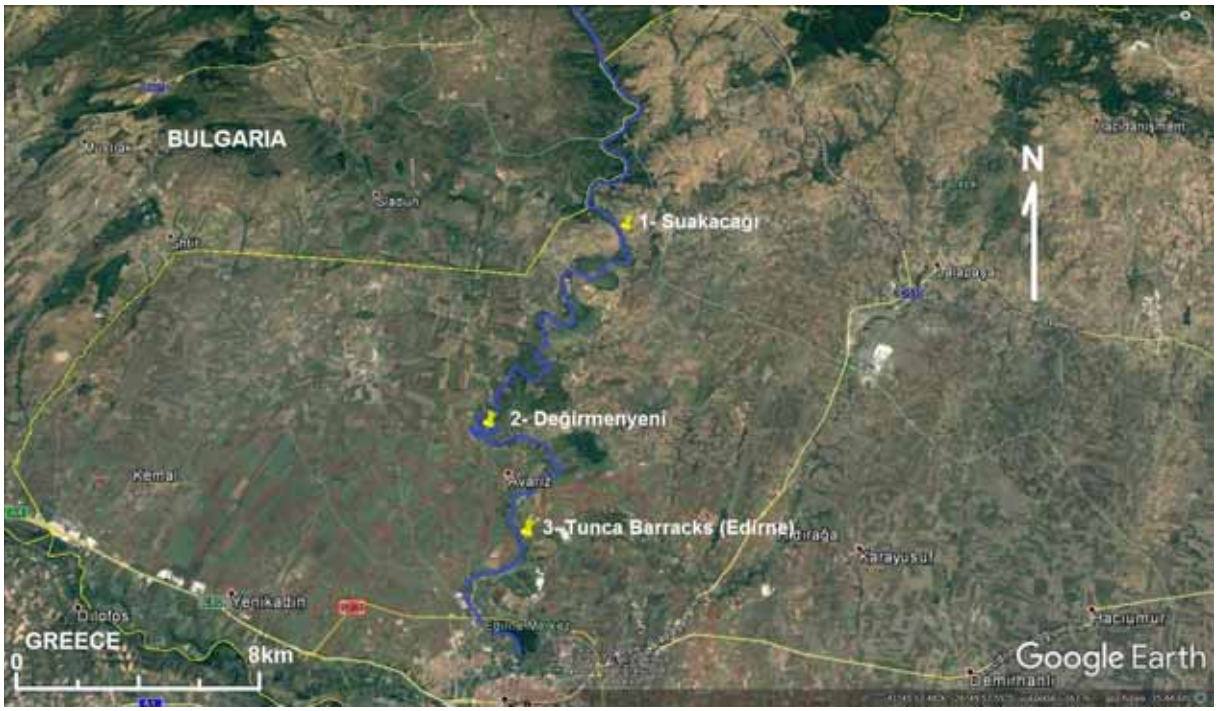

FIGURE 1
Tunca River sampling stations: 1. Suakacağı village (465409.00 D, 4632519.00 K, 47m); 2. Değirmenyeni village (461067.00 D, 4623425.00 K, 40 m); 3. Trakya University Tunca Barracks (462965.63 D, 4619414.88 K, 37m)

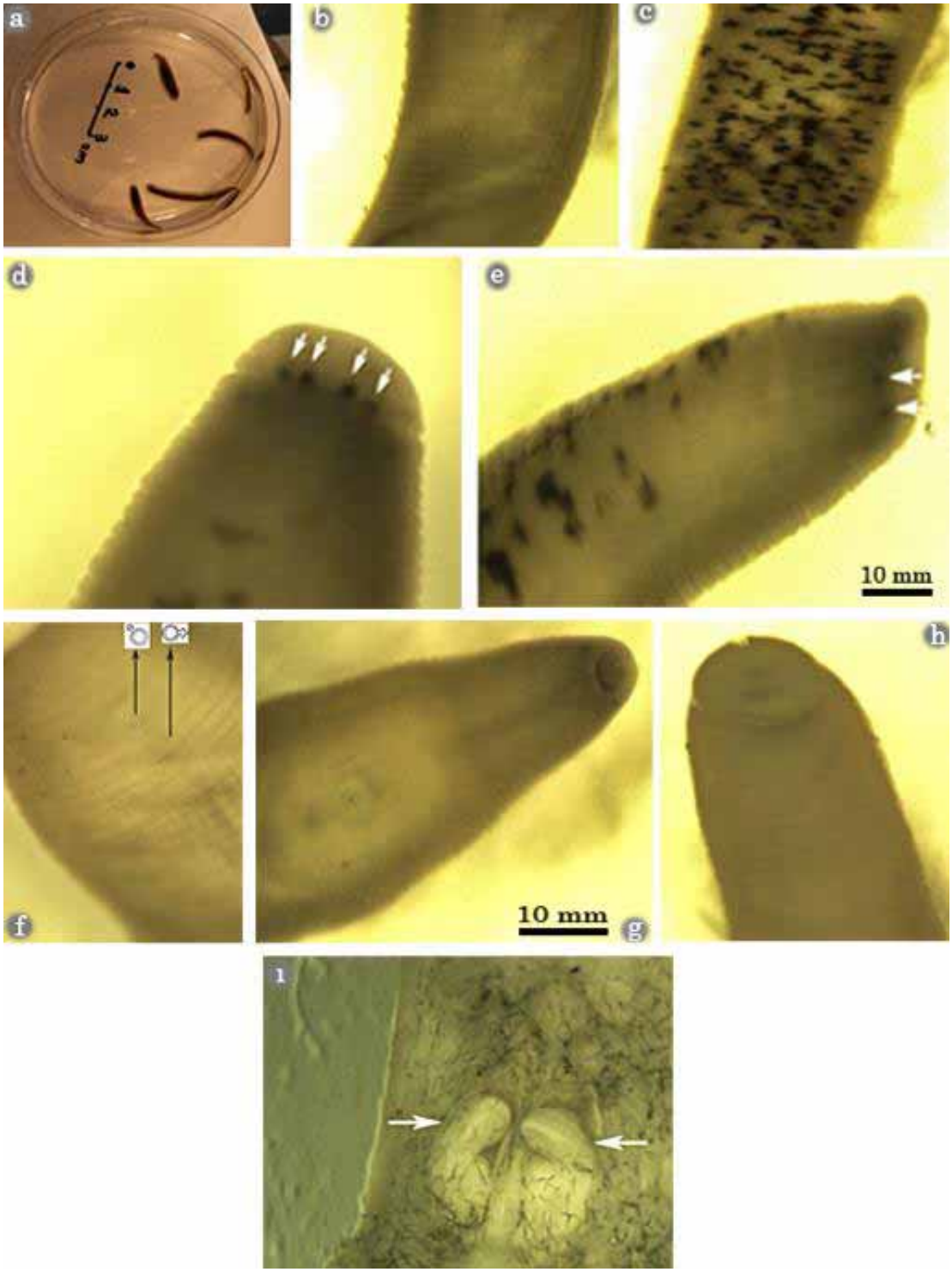

FIGURE 2
***Erpobdella octoculata* (L., 1758) a) General dimensions of the body; b) The ringing structure of the classical Erpobdella genus; c) Dorsal colour pattern; d) Labial eye pairs; e) Right buccal eye pair; f) Male and female genital cavities; g) Anterior pull; h) Posterior pull; i) Atrium's dorsal view and horns**

Description. The length is relatively large leeches, which can be up to 3-7cm (Figure 2a). They have a segment structure with 5 rings. The width of the rings is similar and no false ringing occurs (Figure 2b). The anterior part of the body is conical and the front sucker is small. The clitellar and postklitellar part of the body carries sharp side crests. The tail sucker is smaller than the maximum body width. Living individuals are ranging from greenish yellow to brownish red. Individuals stored in the stores are

light gray. The ventral part is usually pigments. In some populations, there may be 2 light-colored strips in the ventral part (Figure 2c).

They have 4 pairs of eyes. Two pairs of these are labial (Fig. 2d) and two pairs are buccal (Fig. 2e). There are usually 2.5 rings between genital gaps (sometimes 3-3.5). The male genital gap is considerably larger than the female genital gap (Figure 2f). Anterior pull is small (Figure 2g). The posterior pull is smaller than the maximum body width (Figure 2h). The atrium is as flat and wide as the height, horns never sharply separate from the atrium (Figure 2i). It has a wide distribution.

The Tunca River aquatic fauna is rich. This can be attributed to the fact that the ground of the river has different substrates, the continuous flow of water, and sometimes it is rich in shallow and vegetation for the reason that it draws too much water especially for the rice in the spring. There are no other species of leeches except the tide that is working in the river, and it belongs to the only species *E. octoculata.*

The values obtained from the physico-chemical measurements made in the study area are given in Table 1.

According to Bray-Curtis similarity index, September and October (96%), September and August (95%) are the most similar in terms of some physicochemical measurement values in Tunca River. The least similar months are June and July (80%), but this is quite high. When the stations are compared in terms of similarity, the most similar stations are 3 and 2, then 1 and 3, and last 1 and 2 (Figure 3).

The level of dissolved oxygen was found to be low during the months outside June due to the decrease in water level and the warming of the water due to the desiccation of the air and watering for irrigation. The rate of dissolved oxygen was found to be high due to the fact that the water level was high in the river in June. Excess water shortage due to excessive water withdrawal for paddy fields in July could be considered as a reason for the high rate of suspended solids.

Consequently, irrigation, sewage system, variable flow rate, temperature, etc. affect the quality of water in Tunca. The structure of benthic macrofauna in the river changes with effects of environmental variables.

CONCLUSION

In general, all species of leech that live as ectoparasites on a living thing need similar ecological conditions. First, they prefer places where aquatic plants are abundant so they can approach the nutrient without distinction. In such environments there are more places to hide (leaves under the leaves and plants) and the target living will provide more propagation as it will feed on abundant vegetation habitats. Because these living things usually find nutrients easier where plants are more abundant.

Only *E. octoculata* (L., 1758) belonging to the Erpobdellidae family was found in the study area. *E. octoculata* are leeches known as stone leeches. They usually live in slow-flowing lotic habitats and often under the stones [23, 25]. This species, which is distributed in the Palaearctic region, does not have records from Japan and North Africa, but it is also considered to be distributed in these regions [23]. There is also evidence that the distribution of *E. octoculata* is also distributed in bitter water up to 5 ‰ [19].

In this study, 3 puppies' total 22 individuals, *E. octoculata*, were identified in Tunca River. The species is found in the leaf packs rather than the natural environment. It preferred more artificial boxing than leaf packs. It lives by hiding in the environment and uses invertebrates living in the environment as nutrients. Because artificial boxwood are abundant in other groups (especially Chironomidae and Oligochaeta). It was never found in walnut and mulberry leaf packs. The disappearance of the mulberry leaf in a short time is likely to have a negative impact on hiding and hunting. The antihelmintic effect of walnut leaf may have kept it away from this leaf (Figure 4).

TABLE 1
Some physicochemical parameter values according to stations in Tunca River

	June			July			August			September			October		
Parameters	1	2	3	1	2	3	1	2	3	1	2	3	1	2	3
Water Temperature (°C)	27	27	28	28	29	29	29	28	28	27	26	26	23	23	22
pH	7,61	7,53	7,85	8,67	8,17	8,17	8,22	8,17	8,27	8,67	8,17	8,17	7,73	7,77	8,08
Electrical conductivity (µS/cm)	583	622	621	616	709	666	596	690	646	626	685	693	677	710	716
Dissolved Oxygen (mg/lt)	11,31	10,15	10,31	4,8	2,5	3,8	3,8	2,9	3,7	4,86	3,97	4,89	7,12	8,01	6,4
Total hardness (FS^O)	24,4	25	25,4	24.4	25	25,4	24,4	25	25,4	24,4	25	25,4	24,4	25	25,4
Suspended solid (mg/lt)	3,2	3,3	3	269	215	303	75	63	86	29	28	33	13	20	18

(1, 2 and 3 localities)

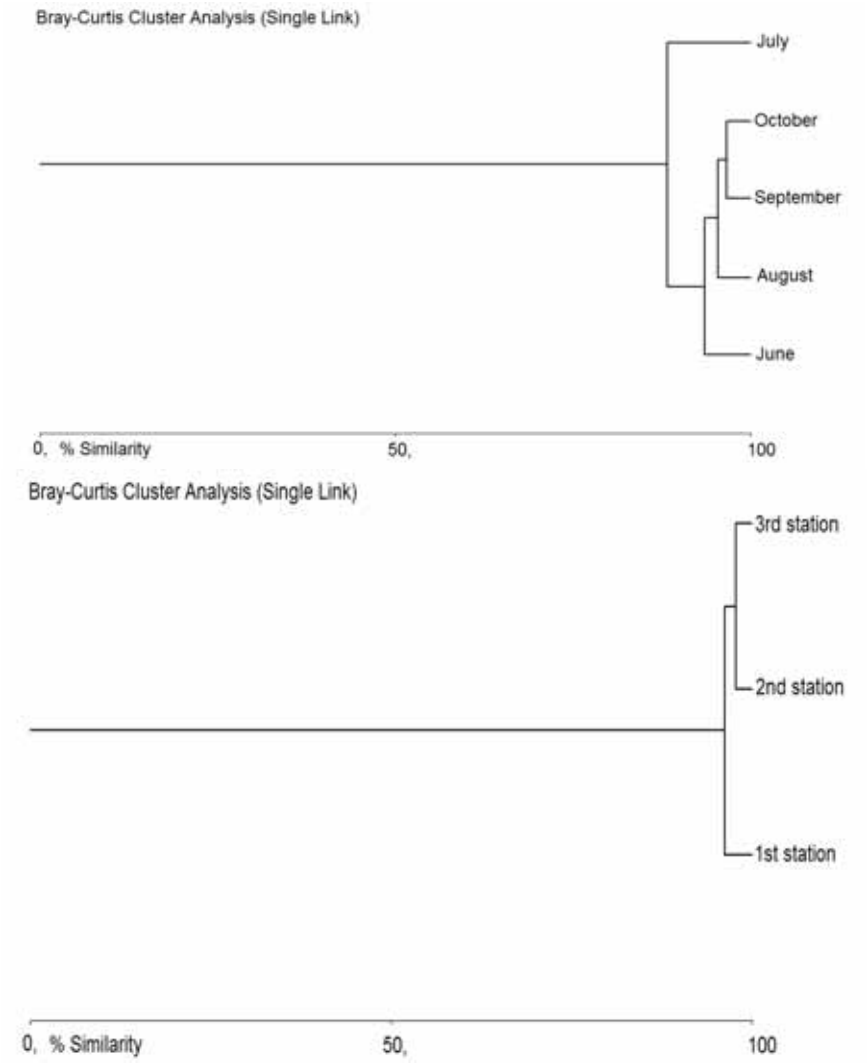

FIGURE 3
The dendrogram of similarity of stations and months in Tunca River in respect of benthic macroinvertebrates (single linkage, Bray-Curtis, log base 10)

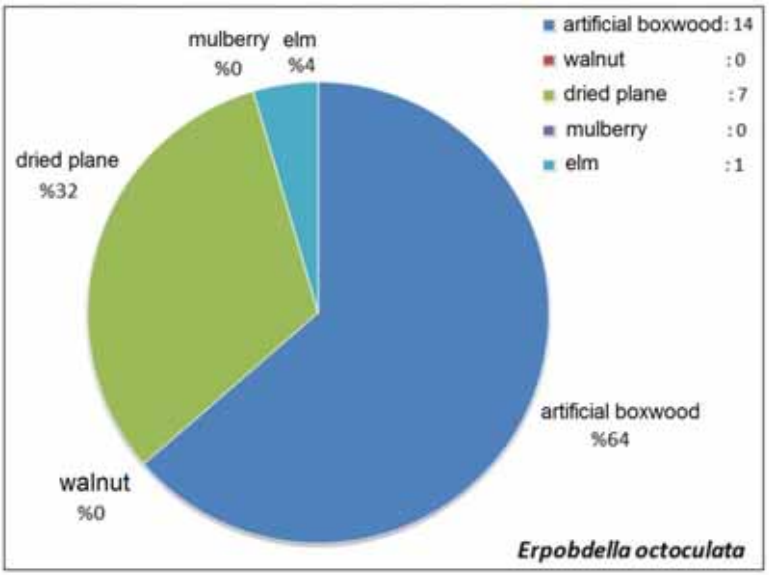

FIGURE 4
Number and percentage of individuals in leaf package varieties of *Erpobdella octoculata*

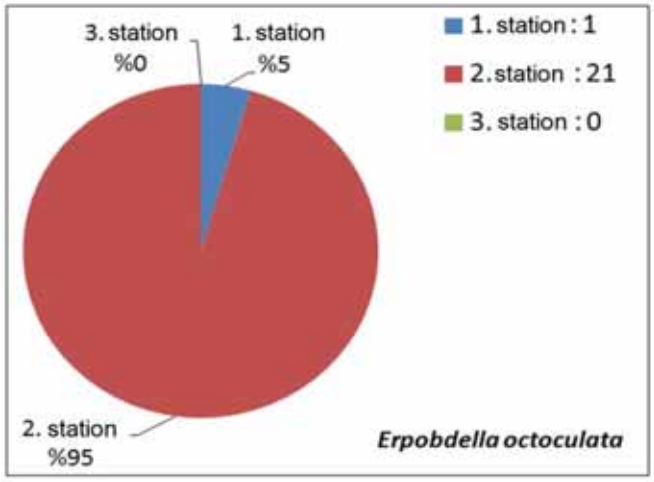

FIGURE 5
Number and percentage of individuals according to *Erpobdella octoculata* strain stations

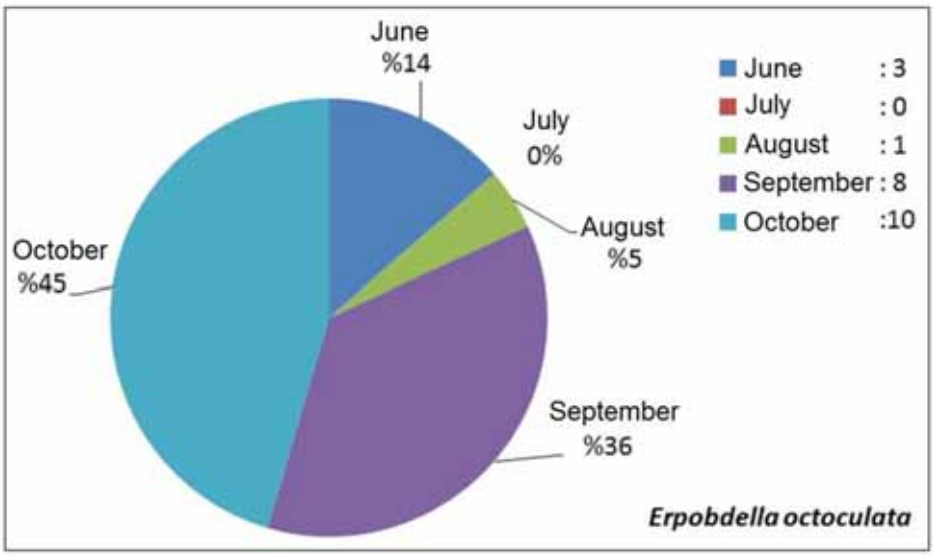

FIGURE 6
Individual number and percentage of *Erpobdella octoculata* strain relative to the month

When we look at the distribution of *E. octoculata* according to stations, it is understood from figure 4 that it is intensively located at the 2nd station. 3. never found in the station. Station 2 is richest in terms of plant variety and quantity, and station 3 is the least. For this reason, the number of individuals in the 2nd station is intense (Figure 5).

As shown in Figure 6, it is observed that the highest number of individuals in the stream is in September and October, when the amount of water in the river is generally minimum. It may be that the number of leeches individuals is higher because the drifting of organisms that occur at high water currents does not occur when the amount of water decreases, providing more nutrients.

As a result, *E. octoculata* prefers natural vegetation more intensively at stations and months when water flow rate decreases. Camur-Elipek et al. [27] did not diagnose at the species level, even though the leech was found at a low density in the study of benthos in Tunca River. The mentioned species have not been found in the literature before in the Tunca River and they are recorded for the first time for stations that have been identified.

ACKNOWLEDGEMENTS

This study is supported by Trakya University Scientific Research Project TUBAP 2011/130. This work was presented as a poster presentation in the XIII. Congress of Ecology and Environment with International Participation held in Edirne, Turkey on September 12-15, 2017 and its summary were published.

The author thanks to Dr. Mustafa Ceylan in Süleyman Demirel University (Directorate of Fisheries Research Institute) for his kind helps in identification of the material and shaping.

REFERENCES

[1] Barnes, R.D. (1974) Invertebrate zoology. Philadelphia-Washington: W.B. Saunders Company, 316p.
[2] Kaestner A. (1967) Invertebrate zoology. Interscience Publishers. A Division of John Wiley and Sons, New York, London, Sydney, 597p.
[3] Sağlam, N. (1998) *Hirudo medicinalis* (L., 1758) ile Gökkuşağı alabalığı (*Oncorhynchus mykiss*) arasındaki ilişkinin deneysel incelenmesi. 111. Su Ürünleri Sempozyumu, 10-12 Juin. Erzurum, 559-63.
[4] Sawyer, R.T. (1986) Leech biology and behavior. Vol: 2. Clarendon Press, Oxford, 1065p.
[5] Toman, M.J. and Dall, P.C. (1997) The diet of *Erpobdella octoculata* (Hirudinea: Erpobdellidae) in two Danish lowland streams. Archiv für Hydrobiologie. 140, 549–563.
[6] Siddall, M.E. and Burreson, E.M. (1998) Phylogeny of leeches (Hirudinea) based on mitochondrial cytochrome *c* oxidase subunit I. Molecular Phylogenetics and Evolution. 9, 156–162.
[7] Apakupakul, K., Siddall, M.E. and Burreson, E.M. (1999) Higher level relationships of leeches (Annelida: Clitellata: Euhirudinea) based on morphology and gene sequences. Molecular Phylogenetics and Evolution. 12, 350–359.
[8] Anholt, B. (1986) Prey selection by the predatory leech *Nephelopsis obscura* in relation to three alternative models of foraging. Canadian Journal of Zoology. 64, 649–655.
[9] Zerbst-Boroffka, I. (1999) Osmotic adaptation of the endemic fauna to the ancient freshwater Lake Baikal. Naturwissenschaften. 86, 330–333.
[10] Wicklum, D. and Davies, R.W. (1996) The effects of chronic cadmium stress on energy acquisition and allocation in a freshwater benthic invertebrate predator. Aquatic Toxicology (Amsterdam). 35, 237–252.
[11] Wicklum, D., Smith, D.E.C. and Davies, R.W. (1997) Mortality preference, avoidance, and activity of a predatory leech exposed to cadmium. Archives of Environmental Contamination and Toxicology. 32, 178–183.
[12] Zaranko, D.T., Griffiths, R.W. and Kaushik, N.K. (1997) Biomagnification of polychlorinated biphenyls through a riverine food web. Environmental Toxicology and Chemistry. 16, 1463–1471.
[13] Yang, T. (1996) Fauna Sinica, Annelida: Hirudinea. Science Press, Beijing, China, 117-129.
[14] Koperski, P. (2006) Relative importance of factors determining diversity and composition of freshwater leech assemblages (Hirudinea; Clitellata): A meta-analysis. Archiv für Hydrobiologie. 166, 325-341.
[15] Mann, K.H. (1953) The life history of *Erpobdella octoculata* (Linnaeus, 1758). The Journal of Animal Ecology. 22, 199-207.
[16] Ikizceli, I., Avsarogullari, L., Sözüer, E., Yürümez Y. and Akdur, O. (2005) Bleeding due to a medicinal leech bite. Emergency Medicine Journal. 22, 458-460.
[17] Schönborn, W. (1985) Die ökologische Rolle von *Erpobdella octoculata* (L.) (Hirudinea: Erpobdellidae) in einem abwasserbelasteten Fluß. – Zoological Journal Systematics. 112, 477–494.
[18] Kutschera, U. (2003) The feeding strategies of the leech *Erpobdella octoculata* (L.): A laboratory study. International Review of Hydrobiology. 88, 1. 94 – 101.
[19] Özbek, M. and Sarı, H.M. (2007) Batı Karadeniz Bölgesi'ndeki bazı göllerin Hirudinae (Annelida) faunası. Ege Üniversitesi Su Ürünleri Dergisi. 24(1-2), 83-88.
[20] Geldiay, R. (1949) Çubuk Barajı ve Emir Gölünün makro ve mikro faunasının mukayeseli incelenmesi. Ankara Üniversitesi Fen Fakültesi Mecmuası. 2, 106.
[21] Geldiay, R. and Tareen, I.U. (1972) Bottom fauna of Gölcük Lake. 1. Population study of chironomids, *Chaoborus* and oligochaeta. Ege Üniversitesi Fen. Fakültesi. İlmi Raporlar Serisi. No: 137, 15p.
[22] Neubert, E. and Nesemann, H. (1999) Annelida, Clitellata. Branchiobdellida, Acanthobdellea, Hirudinea. In: Schwoerbel, J. and Zwick, P. (Eds.) Süßwasserfauna von Mitteleuropa 6/2. Spektrum Akademischer Verlag, Heidelberg, 189p.
[23] Elliott, J.M. and Mann, K.H. (1979) A key to the British freshwater leeches with notes on their life cycles and ecology. Freshwater Biological Association Scientific Publications. No. 40, 72p.
[24] Koperski, P., Milanowski, R. and Krzyk, A. (2011) Searching for cryptic species in *Erpobdella octoculata* (L.) (Hirudinea: Clitellata): discordance between the results of genetic analysis and cross-breeding experiments. Contributions to Zoology. 80(1), 85-94.
[25] Ustaoğlu, M.R., Balık, S., Sarı, H.M. and Özbek, M. (1998) Tahtalı baraj havzasının (Gümüldür - İzmir) Hirudinea faunası. Ege Üniversitesi Su Ürünleri Dergisi. 15(1-2), 111-116.

[26] Ustaoğlu, M.R., Balık, S., Özbek, M. and Sarı, H.M. (2003) The Freshwater leeches (Annelida-Hirudinea) of the Gediz catchment area (Izmir region). Zoology in the Middle East. 29, 118-120.
[27] Camur-Elipek, B., Arslan, N., Kirgiz, T. and Oterler, B. (2006) Benthic macrofauna in Tunca River (Turkey) and their relationships with environmental variables. Acta Hydrochimica Et. Hydrobiologica. 34, 360 – 366.

Received: **02.11.2017**
Accepted: **15.04.2018**

CORRESPONDING AUTHOR

Nurcan Ozkan
Trakya University,
Education Faculty,
Department of Science Education,
Edirne – Turkey

e-mail: nurcanozkan@hotmail.com

© by PSP Volume 27 – No. 7/2018 pages 4751-4758 Fresenius Environmental Bulletin

A NEW RADIO-THERANOSTIC AGENT CANDIDATE: SYNTHESIS AND ANALYSIS OF (ADH-1)c-EDTA CONJUGATE

Burcu Ucar[1,2,*], Tayfun Acar[1], Pelin Pelit-Arayici[1,4], Mehmet Onur Demirkol[2,3], Zeynep Mustafaeva[1]

[1]Yildiz Technical University, Chemical and Metallurgical Engineering Faculty, Bioengineering Department, Istanbul, Turkey
[2]VKF American Hospital, Department of Nuclear Medicine and Molecular Imaging, Istanbul, Turkey
[3]Koc University, School of Medicine, Department of Nuclear Medicine and Molecular Imaging, Istanbul, Turkey
[4]Uskudar University, Vocational School of Health Services, Department of Medical Laboratory Techniques, Istanbul, Turkey

ABSTRACT

The aim of this article are to synthesis, conjugate and characterize of (ADH-1)c (cell adhesion molecule) cyclic peptide sequence c(N-Ac-CHAVC-NH_2) of N-CAD (N-cadherin) antagonist from a novel family of cyclic peptide antagonists. (ADH-1)c specifically targets and blocks N-cadherin, which can cause tumor vasculature disruption, inhibition of tumor cell growth, induction of tumor cell and endothelial cell apoptosis. (ADH-1)c is a cyclic pentapeptide vascular-disrupting agent with antineoplastic and antiangiogenic interactions. In peptide synthesis, microwave irradiation-assisted solid phase peptide synthesizer system with fluorenylmethyloxycarbonyl chemistry has been used to complete peptide sequences with high yields and smaller amount of racemization. i→i+5 macrocyclization was performed with ammonium acetate (5% w/v) following linear peptide synthesis. Conjugates of the cyclic peptide were synthesized with the EDTA chelator by application of water-soluble carbodiimide procedure. A wide range of HPLC (High Performance Liquid Chromatography) conditions for the purification of the peptides were examined by using an acetonitrile-based solvent system with CH_2O_2 as the ion pairing agent which has provided efficient purification. The purified peptide was characterized by liquid chromatography-electrospray ionization-mass spectrometry (LC-ESI-MS). The formation mechanism, physicochemical properties and electrical charges of the synthesized conjugate was characterized by Fluorescence Spectrophotometer, Zetasizer and LC-ESI-MS.

KEYWORDS:
Solid phase peptide synthesis, macrocyclization, conjugation, N-cadherin, (ADH-1)c, cancer

INTRODUCTION

Peptides are normally taken into account as poor drug candidates because of their low oral bioavailability and propensity which rapidly metabolized. Production of synthetic therapeutic peptides has become applicable with recent development of SPPS (solid-phase peptide synthesis) has invented by Merrifield [1]. The basic SPPS strategies are sequential synthesis, convergent synthesis and chemical ligation. Sequential synthesis involves the step by step extension of amino acids. Convergent synthesis is generally a convenient way to synthesize peptides that contain greater than fifty amino acids in sequence [2]. CL (Chemical Ligation) helps to overcome the shortcomings of SPPS to synthesize peptides that are more than 50 amino acid residues [3, 4]. N-cadherin monomers exist in many different grades within the surface of the cell's plasma membrane and at intercellular adhesive contacts, where they function as homophilic CAMs (Cell Adhesion Molecules) [5-7]. The monomers have to interact with in the plane of the plasma membrane to form stable intercellular adhesive junctions which as shown at Figure 1 demonstrating the site of *cis* and *trans* interactions. These -*cis* and -*trans* interactions are centred round the CAR (cell adhesion recognition) sequence HAV (His-Ala-Val), which is found towards the end of the EC1 (first extracellular) subdomain of N-cadherin [5-8]. The His (Histidin) and Val (Valin) residues collocate with *cis* interactions, whereas the Ala (Alanine) residue facilitates *trans* interactions [5-7]. Three types of antagonists are based upon the CAR sequence HAV: non-peptidyl peptidomimetics, synthetic linear peptides and synthetic cyclic peptides [9]. Non-peptidyl peptidomimetics of (ADH-1)c have also been identified. Unlike peptides, which are rapidly degraded by gastrointestinal enzymes, such small molecule inhibitors might be suitable for oral administration [10, 11]. Synthetic linear peptides which containing the HAV motif were the first peptides, have been shown as capable of inhibiting N-cadherin-dependent processes [12-14]. Synthetic cyclic peptides, harbouring the HAV motif, were subsequently shown to act as

N-cadherin antagonists [15]. The most studied cyclic peptide is N-Ac-CHAVC-NH_2 (designated (ADH-1)c) [11]. This cyclic peptide is capable of disrupting a wide variety of N-cadherin-mediated processes like the linear peptide. Even more important, inhibiting effect of (ADH-1)c to angiogenesis has been shown [16]. (ADH-1)c does not affect the normal vascular system however might be cause of apoptosis of multiple myeloma [17], neuroblastoma [18] and pancreatic [19] cancer cells. Furthermore, (ADH-1)c in combination with a chemotherapeutic drug have shown commitment in the cancer therapies [20].

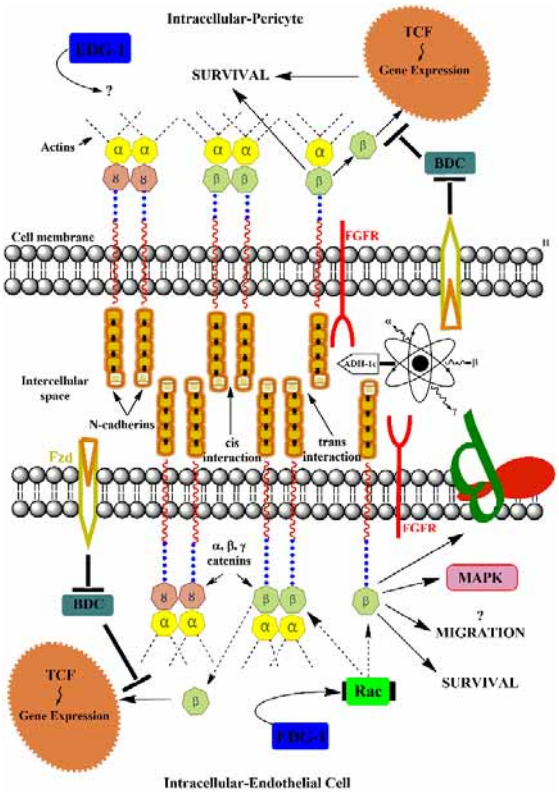

FIGURE 1
Cadherin domain structure and N-cadherin-mediated cell-cell junctions. (ADH-1)c may function as signaling molecules to disrupt cadherin based cell-cell adhesion. The homologous repeats (C1-C5) are bridged by calcium ions (Ca^{2+}). The cytoplasmic domain binds to p120-catenin and alfa catenin binds to beta catenin to link the cadherin complex to the actins

In this study, N-cadherin antagonist (ADH-1)c peptide which can be used as a targeted radionuclide therapy agent for diagnosis and therapy at different types of solid tumor types was synthesized and characterized and for the first time (ADH-1)c peptide was conjugated with EDTA chelator and characterized with spectroscopic and chromatographic methods.

EXPERIMENTAL

Materials. All chemicals used in this study were obtained from commercial sources. Fmoc-Cys(Trt)-Rink Amide MBHA Resin (100-200 mesh, subst.: 0.49 meq/g) was purchased from Ligand Biotechnology Ltd. Fmoc-Cys(Trt)-OH, Fmoc-His(Trt)-OH, Fmoc-Ala-OH, Fmoc-Val-OH, 1H-Benzotriazolium-1-[bis(dimethylamino)methylene]5-chloro hexafluorophosphate (1-),3-oxide (HCTU), 1-Hydroxybenzotriazole hydrate (HOBt.H_2O) were purchased from Fluka. N,Ndimethylformamide (DMF), N-Methyl-2-pyrrolidone (NMP), N,N-Diisopropylethylamine (DIPEA), Trifluoroacetic acid (TFA), Acetic anhydride, Piperidine, Dichloromethane (DCM), HPLC grade Acetonitrile, Diethyl ether, Thioanisole, 1,2-Ethanedithiol (EDT) Triisopropylsilane (TIS), 1-ethyl-3- (3-dimethylaminopropyl) carbodiimide hydrochloride (EDC) and Ethylenediaminetetraacetic acid (EDTA) were ordered from Sigma-Aldrich (St. Louis, MO). Other chemicals were obtained from Merck (Darmstad, Germany). Ultra-pure water was obtained from Millipore Milli-Q system.

Methods. Synthesis Procedure. Linear ADH-1 was synthesized with N-terminal acetylation (Ac-Cys-His-Ala-Val-Cys-$CONH_2$) using Fmoc chemistry on a CEM Liberty Automated Microwave Peptide Synthesizer. Firstly, resin beads (200 mg, 0.1 mmol) were transferred to the 30 mL standard glass reaction vessel after swelling in DMF for three hours (25mL). Microwave energy used for the deprotection step was 55 W to maximum 45 °C for 2 min and it was 25 W to maximum 75 °C for 3 min for the coupling step. Respectively, HCTU/HOBT (0.5 M in DMF) and DIEA/NMP (2 M in DMF) solutions which used as activator and activator bases were added to fmoc protected aminoacides which dissolved in DMF on the microwave coupling step. The deprotection and coupling procedures were repeated for all amino acids in the linear ADH-1 sequence. After the coupling four amino acid residues, resin-bound peptide was treated with a solution of acetic anhydride for acetylation of N-terminus of the peptide sequence. After the acetylation the resin was cleaned by washing with three times in DMF and five times in DCM respectively for preparation of the cleavage process. Then, cleavage of the peptide from the resin beads and removing the side-chain protecting groups was simultaneously performed with the TFA/TIS/EDT/H2O (92.5/2.5/2.5/2.5) cocktail solution. Crude peptide was precipitated with cold diethyl ether (-20 °C) after the vacuum evaporation of TFA cocktail (Heidolph Laborota 4010). The obtained peptide was lyophilized to a white powder [21-24].

Macrocyclization Procedure. The choice of ring closure method in peptide macrocyclization

plays a key role in cyclization. Macrocyclization through disulfide bond formation is a typical side chain cyclization method. In this method, a disulfide bridge was formed between two cysteine aminoacids. Linear ADH-1 peptide product was diluted to 1 mM with ammonium acetate (5% w/v) and pH adjusted to 7.0 with ammonium hydroxide (25% w/v) for disulfide bond formation under nitrogen atmosphere [25]. During the cyclization process, 25 µL sample was taken from reaction medium in at the end of 1st and 24th hours and injected to an analytical column (Teknokroma Tracer Exel 120 ODS-A 5 µm in the dimensions of 20 cm length and 2.1 mm inlet diameter) for monitoring the disulfide oxidation of the linear peptid. After the process was completed, the cyclic peptide was purified and lyophilized.

Conjugation Procedure. Conjugates of the (ADH-1)c peptide, one of the N-cadherin antagonists, were synthesized with the EDTA chelator by the water-soluble carbodiimide procedure in the presence of EDC crosslinker. The amount of the EDTA required for the n_{ADHpep} / n_{EDTA} = 1 ratio was calculated and stock solution of the EDTA was prepared. The pH of the EDTA (0.510 mg) was reduced to 5 and constant amount of EDC was added for activation one of four -COOH groups of the EDTA and then stirred for 2 hours. The peptide solution at a constant concentration was added to the activated EDTA and mixture was stirred overnight at 4 °C and then the pH raised to 7.4. The formation mechanism, physicochemical properties and electrical charges of the synthesized conjugates were characterized by Fluorescence Spectrophotometer, Zetasizer and LC-ESI-MS [26].

Analytical Procedure. LC-MS Conditions. Molecular weight of the peptide was confirmed by using LC-UV-PDA (photo-diode array) at 210 and 280 nm and LC-MS (Shimadzu 2010 EV) with using Electro Spray Ionization (ESI) probe. Teknokroma Tracer Exel 120 ODS-A 5 µm in the dimensions of 20 cm length and 2.1 mm inlet diameter was used. Eluent A (water, 0.1% (v/v) formic acid) and eluent B (acetonitrile, 0.1% (v/v) formic acid) gradient elution was programmed as follows: 0-5 min, 20% B; 5-15 min, 20-40% B; 15-25 min, 40-80% B; 25-30 min, 80-20% B at a flow rate of 0.2 mL/min. Higher and narrower peaks were achieved through adding formic acid to the mobile phase as ion pairing agent for better resolution than without using formic acid. Proteins and peptides are usually analyzed under positive ionisation mode, that's why analysis were carried out under the acidic conditions. [22, 23, 27]. Nitrogen was used as nebulizer gas, with a flow rate of 1,5 $Lmin^{-1}$. The mass spectra were acquired from 200 to 1000 m/z with a scan speed of 2000 m/z per s.

Purification Conditions. Purity analysis was performed by using analytical reversed phase (RP)-HPLC (Shimadzu) equipped with Shim-pack PRC-ODS HPLC column (20 mm x 25 cm) and UV-PDA detector at 210 and 280 nm. Eluent A (water, 0.1% (v/v) formic acid) and eluent B (acetonitrile, 0.1% (v/v) formic acid) gradient elution was programmed as follows: 0-5 min, 20% B; 5-15 min, 20-40% B; 15-25 min, 40-80% B; 25-30 min, 80-20% B at a flow rate of 14 mL/min [22].

Fluorescence Spectroscopy Conditions. Fluorescence emission spectra of chelator and peptide-chelator conjugates were obtained through QM-4/2003 Quanta Master Steady State Spectrofluorometer (Photon Technology International, Canada). Analysis were run in quanta counting mode with a slit gap of 3 nm for excitation and emission monochromators. Excitation was performed in 280 nm. and spectra were measured between 290-450 nm's.

Zeta-Sizer Conditions. Particle size, polydispersity index and zeta potential of the conjugates were determined by dynamic light scattering (DLS) technique (Malvern Zetasizer, ZS, Malvern, UK). Measurements were done in triplicate, at 25 °C, using 0.8872 cP viscosity and 1.330 refractive index for the solutions, dielectric constant 79; f(ka) 1.50 (Smoluchowski). Before the measurements, all samples were diluted with ultra-pure water (Millipore).

RESULTS AND DISCUSSION

In this research, we have studied the SPPS of the small cyclic N-cadherin antagonist (N-Ac-CHAVC-$CONH_2$) with Fmoc chemistry. We have focused on the cyclization procedure and chromatographic characterization of the peptide. Furthermore, conjugation and characterization of the peptide with EDTA were also studied.

In this study the (ADH-1)c cyclic peptide analogue was prepared from its linear peptide counterpart by using Fmoc based SPPS method with HCTU/HOBt.H_2O as the coupling agents. The cyclization process was based on the procedure described by Dubey et al. [25]. i→i+5 cyclization was performed with ammonium acetate (5% w/v) after synthesis, cleavage and characterization of the linear ADH-1 peptide sequence were done. Moleculer weight of linear and cyclic peptides were confirmed by mass spectrometry analysis. LC-UV chromatogram, LC-MS TIC (total ion chromatogram) and MS spectrum of linear ADH-1 peptide was illustrated on Figure 2A, 2B and 3 respectively. An ion, which is in the analysis medium binds to the peptide. As a result of this occasion peptide molecules convert into more hydrofobic structure. Therefore, a small peak seems to the next of high peak at Figure 2A. The molecular weight of peptide was calculated using m/z

values of these ions. The m/z values representing the molecular ions of $[M+H^+]^+$=575; $[M+2H^+]^{2+}$=287; $[M+2(H_2O+H^+)+H^+]^+$=613; $[M+28(CO)]^{2+}$=314 $[M+2(H_2O+H)^+ +H^+]^{2+}$=306,5 that is understood from the Figure 3. M stands for the molecular mass of the linear ADH-1 peptide. Molecular ion was observed at m/z 575, which indicated that H^+ atoms are attached to the peptide molecules (calculated mass from the empirical formula: m/z 572,71 Da). m/z=314 was assumed that the formyl group of formic acid that used as ion pairing agents in LC-MS is attached to the peptide molecules. At this stage, leaving a hydrogen atom from the amine group of peptide. m/z 306,5 was indicated that two molecule hydronium ion binds to the peptide molecules.

Selection of the ring closure site plays a key role in peptide macrocyclization. A poor choice for closing the ring causes slow reaction rates, low yields, and undesired side reactions including racemization at the C-terminus residue or dimerization [28]. The side chain cyclization approaches (head-to-side chain and side chain-to-side) typically include macrocyclization via the formation of a disulfide bridge. LC-UV chromatogram of (ADH-1)c cyclic peptide and LC-UV chromatogram of (ADH-1)c cyclic peptide at 1st and 24th hours comparetively were given on the Figure 4A and 4B. It is understood from Figure 4B that the disulfide oxidation was highly completed in 24 hours and cyclic structure was obtained.

TIC and MS spectrum of (ADH-1)c cyclic peptide were represented at Figure 4C and 5. Disulfide linkage was determined within LS-ESI-MS. The obtained molecular ion peaks $[M+H^+]^+$=573, $[M+2(H_2O+H^+)+H^+]^+$=611, $[M+2(H_2O+H^+)+2H^+]^{2+}$=306 confirmed the theoretical molecular weight (570,69 Da). The m/z 573 ion represents the monoisotopic peak and m/z 306 ion represents the double charged state of the intramolecular disulfide-linked peptide.

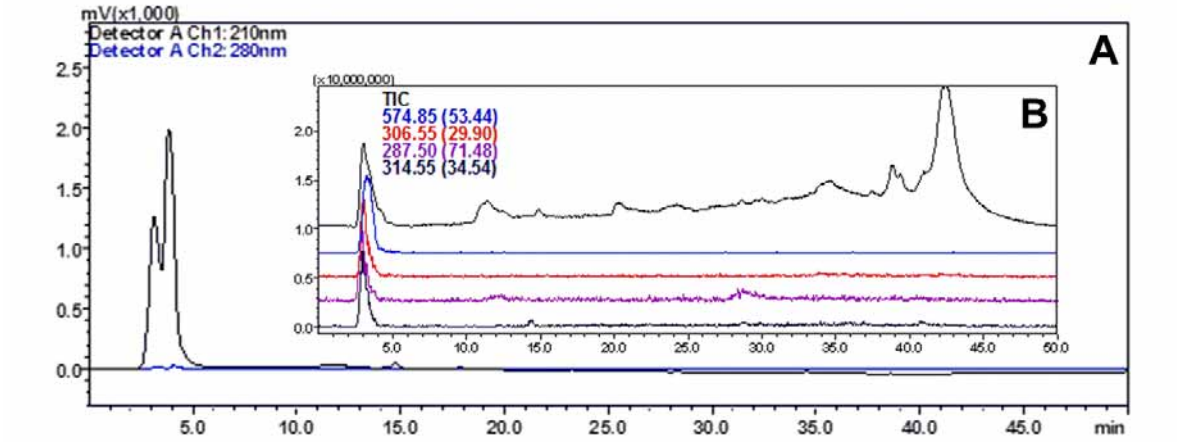

FIGURE 2

LC-UV-PDA chromatogram (A) and LC-MS total ion chromatogram (TIC) (B) of linear ADH-1 peptide sequence sample. Chromatographic conditions in experimental

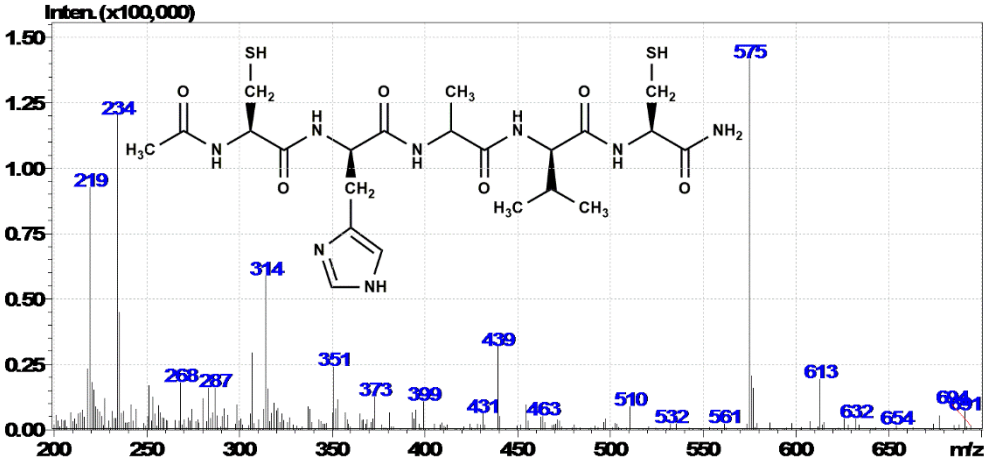

FIGURE 3

LC-MS spectra of linear ADH-1 sample. Chromatographic conditions in experimental

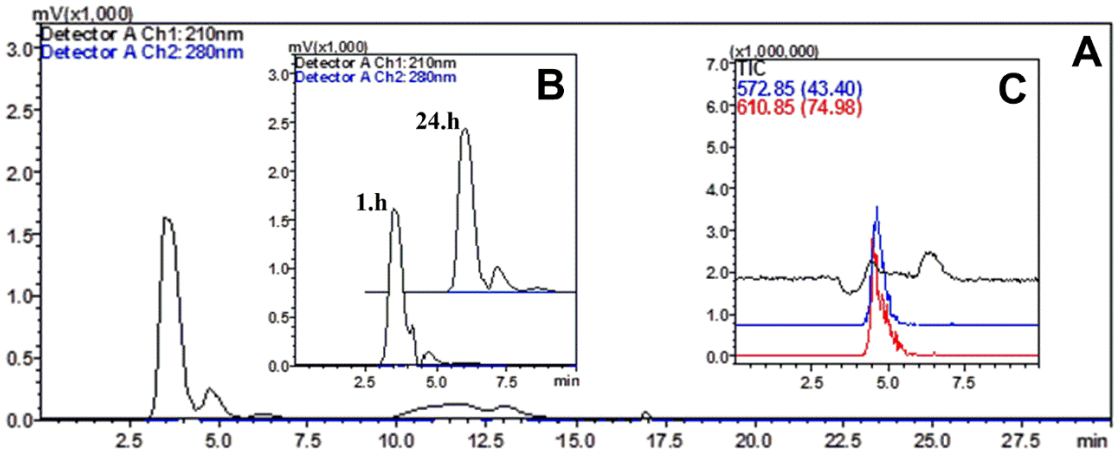

FIGURE 4

LC-UV-PDA chromatogram of (ADH-1)c cyclic peptide (A), LC-UV-PDA chromatogram of ADH-1c cyclic peptide at 1st and 24th hour comparetively B), LC-MS total ion chromatogram (TIC) of (ADH-1)c sample (C). Chromatographic conditions in experimental

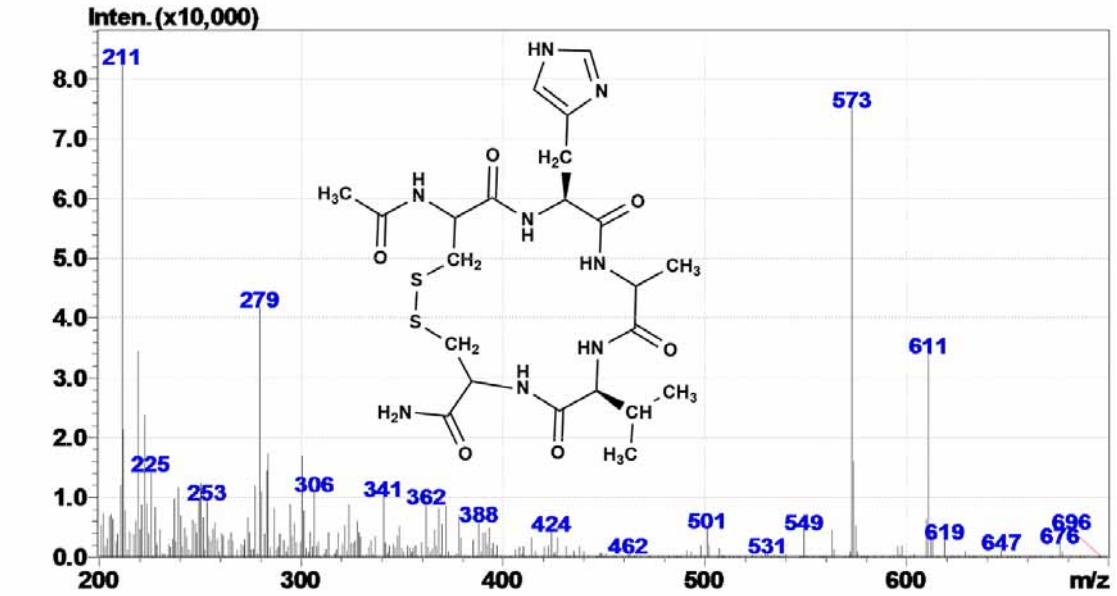

FIGURE 5

LC-MS spectra of (ADH-1)c sample. Chromatographic conditions in experimental

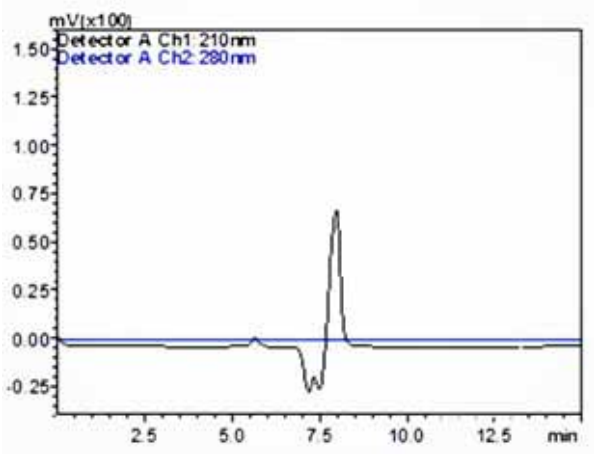

FIGURE 6

LC-UV choromatogram of purified (ADH-1)c cyclic peptide

The obtained cyclic crude peptide was separated to fractions with preparative reversed-phase (RP)-HPLC. Collected fractions in prep. HPLC were analyzed by mass, and crude peptide was purified to give a white powder of (ADH-1)c. LC-UV chromatogram of purified peptide was illustrated in Figure 6.

Figure 7 shows the product ion spectra of the EDTA-(ADH-1)c conjugate. Peak at m/z 867 was proved formation of conjugate and at 849 without water ([(ADH-1)c]-EDTA - [H_2O]) have supported this result. Fragmentation products of the conjugate were also observed at m/z 294 and 572.

Since the conjugation may cause changes in the fluorescence spectrum, whereby the conjugate and chelators in this assay were characterized by the maximum emission and wavelength at the maximum fluorescence intensity. Typical fluorescence spectrum of the EDTA chelator and synthesized EDTA-(ADH-1)c conjugate at pH 7 at $n_{Peptide}$ / n_{EDTA} = 1 is shown in Figure 8. After cross-linking between the amine groups of the (ADH-1)c peptide molecule and the carboxyl groups of the anionic EDTA chelator, the fluorescence intensity of the synthesized conjugates were increased. A maximum of 8 nm red shift from 339 nm to 347 nm was observed.

The zeta potential values of the synthesized $n_{peptide}$ / n_{EDTA} = 1 bioconjugate are given in the Table 1. The zeta potentials of the conjugate and EDTA chelator were found to be -61.3 mV and -42 mV, respectively. When the zeta potential of the conjugate synthesized at $n_{peptide}$ / n_{EDTA} = 1 ratio is examined, it is seen that the potential value of zeta decreases with conjugation. Whether or not forming of the conjugate have been carried out was proved from the difference between average molecular size of the conjugate and chelating agent. The increase in the size of the peptide-bound conjugate relative to the free chelator indicates that the conjugate has got larger and consequently the conjugate was formed [29, 30]. The analysis results are given in Table 1.

In this work, synthesis, analysis and conjugation of (ADH-1)c cyclic peptide were studied. The synthesis of this peptide, the conjugation with a chelator and its characterization are the main parts of a novel theranostic design.

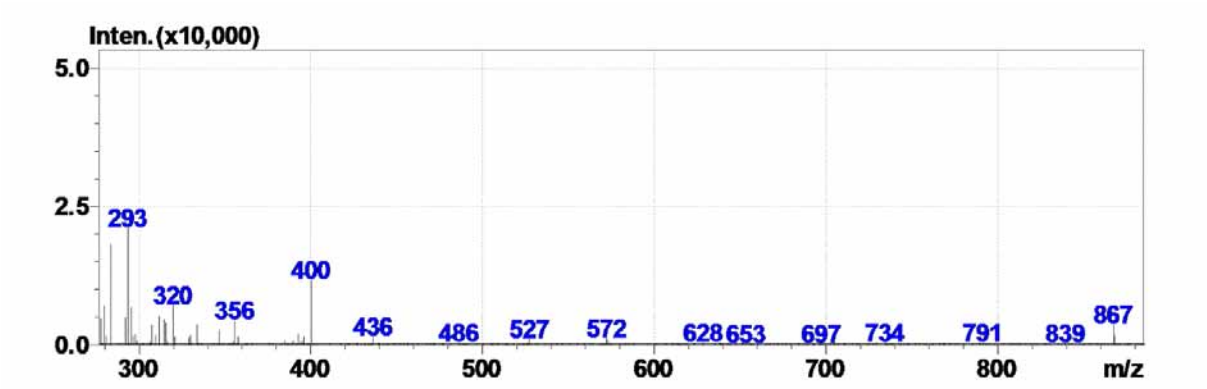

FIGURE 7
LC-MS spectra of EDTA-(ADH-1)c sample. Chromatographic conditions in experimental

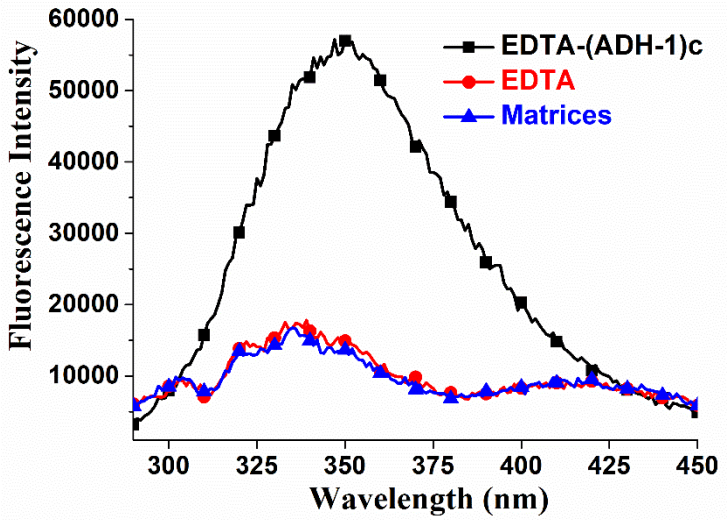

Figure 8 Fluorescence spectrum of EDTA-(ADH-1)c conjugates

TABLE 1
Z-Average and Zeta potential values of EDTA-(ADH-1)c conjugate

	Z-Average (nm)	Zeta potential (mV)
EDTA-(ADH-1)c Conjugate	327,8 ± 29,07	-61,3 ± 1,78
EDTA (DMSO + PBS)	214,5 ± 10,95	-42 ± 1,89
DMSO + PBS	115,4 ± 12,17	-13,2 ± 1,53

CONCLUSIONS

We performed the synthesis of the targeting peptide molecule, the conjugation with the chelating agent, and characterization studies.

High purity peptide synthesis was carried out with microwave supported SPPS method. As considering complicacy of ionization of small and cyclic molecules, our (ADH-1)c's LC-ESI-MS results might enrich literature. In addition to LC-ESI-MS results, both increasing zeta average molecular size of the conjugate and changing of zeta potential of the conjugate and also occurring stoke shift in fluorescence spectrum of conjugate was supported the conjugate forming.

These studies are the key steps in the synthesis of a radiopharmaceutical agent that can be applied as a theranostic agent in Nuclear Medicine and Molecular Imaging Departments [31]. The present study can provide a radioactive metal-labeled N-cadherin antagonist which is obtained by binding a radioactive metallic element such as gallium-68, lutetium-177 to the (ADH-1)c conjugate. The radioactive metal-labeled cyclic (ADH-1)c molecule which contains cancer therapeutic agent (ADH-1)c as an active ingredient is highly accumulated in cancer tissue and exhibits high cancer tissue-shrinking effect [32]. Therefore, by use of the cancer therapeutic agent, theranostic application can be effectively performed without causing adverse side effects. Also, by use of the cancer diagnostic agent, the efficacy of the cancer therapeutic agent can be predicted, and the therapeutic effect thereof can be confirmed. Tomographic and scintigraphic kinetic studies using animal experiments are needed to assess the effects of this antagonist on tumors and their vasculature. These new indications can be imaged in the near future in patients.

ACKNOWLEDGEMENTS

The authors many thank for deceased Prof. Dr. Mamed Mustafaev Akdeste who was the Constitutive Head of the Bioengineering Department of Yildiz Technical University.

Conflicts of Interest. Burcu Ucar, Tayfun Acar, Pelin Pelit Arayici, Mehmet Onur Demirkol, Zeynep Mustafaeva declare that they have no conflict of interest.

REFERENCES

[1] Merrifield, R.B. (1963) Solid phase peptide synthesis. I. The synthesis of a tetrapeptide. Journal of the American Chemical Society. 85(14), 2149.
[2] Guzmán, F., Barberis, S., Illanes, A. (2007) Peptide synthesis: chemical or enzymatic. Electronic Journal of Biotechnology. 10(2), 279.
[3] Dawson, P.E., Kent, S.B. (2000) Synthesis of native proteins by chemical ligation. Annual review of biochemistry. 69(1), 923.
[4] Muir, T.W., Dawson, P.E., Kent, S.B. (1997) Protein synthesis by chemical ligation of unprotected peptides in aqueous solution. Methods in enzymology. 289, 266.
[5] Brasch, J., Harrison, O.J., Honig, B., Shapiro, L. (2012) Thinking outside the cell: how cadherins drive adhesion. Trends in cell biology. 22(6), 299.
[6] Bunse, S., Garg, S., Junek, S., Vogel, D., Ansari, N., Stelzer, E.H., Schuman, E. (2013) Role of N-cadherin cis and trans interfaces in the dynamics of adherens junctions in living cells. PLoS One. 8(12), e81517.
[7] Harrison, O.J., Jin, X., Hong, S., Bahna, F., Ahlsen, G., Brasch, J., Wu, Y., Vendome, J., Felsovalyi, K., Hampton, C.M. (2011) The extracellular architecture of adherens junctions revealed by crystal structures of type I cadherins. Structure. 19(2), 244.
[8] Hatta, K., Nose, A., Nagafuchi, A., Takeichi, M. (1988) Cloning and expression of cDNA encoding a neural calcium-dependent cell adhesion molecule: its identity in the cadherin gene family. J. Cell Biol. 106(3), 873.
[9] Blaschuk, O.W. (2012) Discovery and development of N-cadherin antagonists. Cell and tissue research. 348(2), 309.
[10] Gour, B.J., Blaschuk, O.W., Ali, A., Ni, F., Chen, Z., Michaud, S.D., Wang, S., Hu, Z., (2007) Peptidomimetic modulators of cell adhesion. Google Patents, US7268115B2.
[11] Blaschuk, O.W., Devemy, E. (2009) Cadherins as novel targets for anti-cancer therapy. European journal of pharmacology. 625(1), 195.
[12] Wilby, M.J., Muir, E.M., Fok-Seang, J., Gour, B.J., Blaschuk, O.W., Fawcett, J.W. (1999) N-Cadherin inhibits Schwann cell migration on astrocytes. Molecular and Cellular Neuroscience. 14(1), 66.

[13] Mege, R., Goudou, D., Diaz, C., Nicolet, M., Garcia, L., Geraud, G., Rieger, F. (1992) N-cadherin and N-CAM in myoblast fusion: compared localisation and effect of blockade by peptides and antibodies. Journal of Cell Science. 103(4), 897.
[14] Blaschuk, O.W., Sullivan, R., David, S., Pouliot, Y. (1990) Identification of a cadherin cell adhesion recognition sequence. Developmental biology. 139(1), 227.
[15] Blaschuk, O.W., Gour, B.J. (2001) Compounds and methods for modulating cell adhesion. Google Patents, US6169071B1.
[16] Blaschuk, O.W., Gour, B.J., Farookhi, R., Ali, A. (2003) Compounds and methods for modulating endothelial cell adhesion. Google Patents, WO2001077146A2.
[17] Blaschuk, O.W. (2015) N-cadherin antagonists as oncology therapeutics. Phil. Trans. R. Soc. B. 370(1661), 20140039.
[18] Lammens, T., Swerts, K., Derycke, L., De Craemer, A., De Brouwer, S., De Preter, K., Van Roy, N., Vandesompele, J., Speleman, F., Philippe, J. (2012) N-cadherin in neuroblastoma disease: expression and clinical significance. PLoS One. 7(2), e31206.
[19] Shintani, Y., Fukumoto, Y., Chaika, N., Grandgenett, P.M., Hollingsworth, M.A., Wheelock, M.J., Johnson, K.R. (2008) ADH-1 suppresses N-cadherin-dependent pancreatic cancer progression. International journal of cancer. 122(1), 71.
[20] Beasley, G.M., McMahon, N., Sanders, G., Augustine, C.K., Selim, M.A., Peterson, B., Norris, R., Peters, W.P., Ross, M.I., Tyler, D.S. (2009) A phase 1 study of systemic ADH-1 in combination with melphalan via isolated limb infusion in patients with locally advanced in-transit malignant melanoma. Cancer. 115(20), 4766.
[21] Palasek, S.A., Cox, Z.J., Collins, J.M. (2007) Limiting racemization and aspartimide formation in microwave-enhanced Fmoc solid phase peptide synthesis. Journal of Peptide Science. 13(3), 143.
[22] Ozdemir, Z.O., Topuzogulları, M., Karabulut, E., Akdeste, Z.M. (2009) Characterization and Purification of Viral Peptides Synthesized with Microwave Assisted Solid Phase Method. International Journal of Natural & Engineering Sciences. 3(2), 45.
[23] Ozdemir, Z.O., Karahan, M., Karabulut, E., Mustafaeva, Z. (2010) Characterization of Foot-and-Mouth Disease Virus's Viral Peptides with LC-ESI-MS. Journal of the Chemical Society of Pakistan. 32(4), 531.
[24] Mäde, V., Els-Heindl, S., Beck-Sickinger, A.G. (2014) Automated solid-phase peptide synthesis to obtain therapeutic peptides. Beilstein journal of organic chemistry. 10(1), 1197.
[25] Dubey, N., Varshney, R., Shukla, J., Ganeshpurkar, A., Hazari, P.P., Bandopadhaya, G.P., Mishra, A.K., Trivedi, P. (2012) Synthesis and evaluation of biodegradable PCL/PEG nanoparticles for neuroendocrine tumor targeted delivery of somatostatin analog. Drug delivery. 19(3), 132.
[26] Arayici, P.P., Acar, T., Maharramov, A.M., Karahan, M., Mustafaeva, Z.A. (2017) Synthesis and Characterization of Bioconjugates of Antigenic Rabies Virus Peptide Epitope with Polyacrylic Acid. Fresen. Environ. Bull. 26, 2753-2759.
[27] Niessen, W.M. (2006) Liquid chromatography-mass spectrometry. Third Edition, CRC Press, Taylor & Francis Group, Boca Raton.
[28] Jiang, S., Li, Z., Ding, K., Roller, P.P. (2008) Recent progress of synthetic studies to peptide and peptidomimetic cyclization. Current Organic Chemistry. 12(17), 1502.
[29] Kizilbey, K., Mansuroglu, B., Derman, S., Battal, Y.B., Akdeste, Z.M. (2009) Conjugation of BSA Protein and VP/AA Copolymers. International Journal of Natural & Engineering Sciences. 3(2), 36-40.
[30] Filenko, A., Demchenko, M., Mustafaeva, Z., Osada, Y., Mustafaev, M. (2001) Fluorescence study of Cu2+-induced interaction between albumin and anionic polyelectrolytes. Biomacromolecules. 2(1), 270.
[31] Velikyan, I. (2014) Prospective of 68Ga-radiopharmaceutical development. Theranostics. 4(1), 47.
[32] Farahani, E., Patra, H.K., Jangamreddy, J.R., Rashedi, I., Kawalec, M., Rao Pariti, R.K., Batakis, P., Wiechec, E. (2014) Cell adhesion molecules and their relation to (cancer) cell stemness. Carcinogenesis. 35(4), 747.

Received: **17.11.2017**
Accepted: **29.04.2018**

CORRESPONDING AUTHOR

Burcu Ucar
Yildiz Technical University,
Chemical and Metallurgical Engineering Faculty,
Bioengineering Department,
Istanbul – Turkey

e-mail: burcuu@amerikanhastanesi.org

© by PSP Volume 27 – No. 7/2018 pages 4759-4768 Fresenius Environmental Bulletin

EFFECT OF SEED PRIMING ON YIELD AND YIELD COMPONENTS OF SORGHUM HYBRIDS (*SORGHUM BICOLOR* L. MOENCH. X *SORGHUM SUDANENSE* STAPH.)

Negar Ebrahim Pour Mokhtari[1,*], Hasan Yavuz Emeklier[2]

[1]Islahiye Vocational School, Organic Farming Department, Gaziantep University, Gaziantep, Turkey
[2]Department of Field Crops, Ankara University, Ankara, Turkey

ABSTRACT

The present study was carried out at two locations over the experimental fields of Field Crops Department of Ankara University Agricultural Faculty and Eskişehir Transitional Zone Agricultural Research Institute. Two different hybrid sorghum cultivars (Sugar Grazer II and Digestivo) were used as the experimental material. Putrescine, jasmonic acid, kinetin, KNO_3, salicylic acid and control treatments were applied to selected genotypes. The lowest number of days (the earliest) to 50% emergence (9.75 days) was obtained from KNO_3-primed aged Sugar Grazer II seeds at Eskişehir location. The greatest panicle seed yield per plant (78.21 g) was obtained from KNO_3-primed unaged Digestivo seeds at Eskişehir location. The greatest seed yield per decare (694.91 kg/da) was obtained from salicylic acid-primed aged Sugar Grazer II seeds at Eskişehir location. The greatest protein ratio (15.07%) was obtained from KNO_3-primed unaged Digestivo seeds at Ankara location. Priming with salicylic acid, KNO_3 and jasmonic acid yielded the best outcomes for quality traits of sorghum hybrids.

KEYWORDS:
Accelerated aging, priming, quality, seed, sorghum, yield.

INTRODUCTION

Sorghum is the fifth most important cereal crop that used cereals in human and animal nutrition. It ability to grow in hot, dry environments, resistance to drought, and also can survive under water logged conditions. Currently, the consequences for global warming and the consequent climate change forecast have increased aridity levels and in frequency of extreme events of water shortage in different parts of the globe. Limited access to clean water supplies globally and the increasing food demands due to an ever-increasing world population further exacerbate the droughts. In Turkey Central Anatolia, East Anatolia, Southeastern Anatolia and Transition Zone also have a terrestrial climate of high temperature and low rainfall during summer and early autumn. [11, 45]. Early season water shortages influence the germination and stand establishment because of the reduced water uptake throughout the imbibition phase of germination [39, 47, 50]. Priming treatments involves the soaking of seeds in osmotica of low water potential to regulate the amount of water supplied to the seed. Priming ensures that some of the metabolic processes required for the germination to occur without the actual germination taking place. Primed seeds, usually pass the imbibition stages and lag stage of germination and are ready for germination [19]. A few processes take place at the time of priming at cellular level, such as the activation of cell cycle [18] and utilization of storage proteins [22]. Priming of aged-seeds gradually restores the primary germination ability and it also reduces the lipid peroxidation levels [4]. Priming usually includes the soaking of seeds in osmotica of low water latency such as salicylic acid. Priming usually improves crop yields substantially [31], impedes ethylene bio-synthesis and it increases the chlorophyll content [27]. Polyamines (PAs), plant phenolic substances of pervasive nature, play different roles in plant metabolism that include cell division, differentiation and proliferation, DNA, cell death, protein synthesis and gene expression [13, 29]. Xu et al. [52] reported that tobacco (*Nicotiana tabacum* L.) seed priming with putrescine improved the germination percentage, germination index, seedling length and dry weight of the seed. Cytokinins can also be used as a priming agent. In a previous study, it was reported that cytokinins at 10 or 100 mg L^{-1} considerably increased the rate of germination of the pigeon pea seeds as compared to the unprimed seeds [44]. Methyl jasmonate (MeJA) and its free acid jasmonic acid (JA) are known to affect many features of plant growth, including seed sprouting and seedling growth [16], tuber formation, tendril coiling, leaf senescence, stomata opening, fruit ripening, root growth, fertility. MeJA also plays fundamental roles in plant defense re-

sponses against insect harms and microbial pathogens attacks that impact plant growth and development [51]. Numerous reports show that MeJA inhibited germination of seeds in angiosperms, such as *Amarantus caudatus* [35, 8], sunflower [14], tobacco [41] and cocklebur [38]. One of the consequences of germination inhibition is the decrease in the growth of the root [14, 46]. Salicylic acid is (SA) an endogenous growth regulator of phenolic nature. SA treatments are accompanied by a temporary increase in the H_2O_2 levels. The seed treatments using H_2O_2 has an easing effect on the oxidative damage that is caused by the salt stress in wheat plants. It seems possible that SA may apply its protective effect partly through the briefly increased H_2O_2 levels. Kattimani et al. [32] indicated that primed seeds accompanied with nitrate solutions produced energetic seedlings, more dry matter accumulation and an increase in the root length as compared to unprimed seeds. Sorghum seeds generally lose their biological characteristics in a short time. Such a case then influence plant genetic characteristics and storage conditions. Sorghum seeds generally have 1000-seed weights of between 12-40 g and they need quite well-prepared seed beds for production. Therefore, when the sowing was not made in mellowed soils in a shallow fashion, germination and emergence rates will be quite low. On the other hand, since seed vigor is lost rapidly, sorghum seeds should be preserved under quite well conditions. Therefore, some priming chemicals are used to improve the seed vigor. This study was conducted under field conditions at Ankara and Eskişehir locations to investigate the effects of different priming chemicals on aged and unaged seeds of two hybrid sorghum cultivars (Sugar Grazer II and Digestivo).

MATERIALS AND METHODS

Experiments were conducted under field conditions of two different locations (Ankara and Eskişehir). Aged and unaged seeds of sorghum hybrid (*Sorghum bicolor* L. Moench. X *Sorghum sudanense* Staph.) Sugar Grazer II cultivar and hybrid silage sorghum Digestivo cultivar were used as the plant material of the study. Five different chemicals (8 mg/L putrescine, 2 mg/L jasmonic acid, 100 mg/L kinetin, 50 mg/L KNO_3 and 4.5 mg/L salicylic acid) were used for priming treatments. A control treatment without priming was also included into the experiments. Seeds of each cultivar and treatment were soaked into these solutions. Sugar Grazer II seeds were kept in solutions for 8 hours and Digestivo seeds for 6 hours. Following the priming duration, seeds were washed through distilled water, dried in petri dishes at room temperature for 24 hours and made ready for sowing.

Accelerated Aging Test. For aging, seeds were placed in plastic boxes and supplemented with distilled water to provide high relative humidity. Seeds were placed in a single layer over the wire section of the box as not to touch each other. Aging boxes were placed in zip lock bags to prevent moisture loss and they were aged in an oven previously heated to 42°C at 100% relative humidity and dark for 24 hours. Following the aging procedure, aged seeds were placed in jars, closed with stretch film and kept in a fridge at 5°C for 24 hours to have the seed moisture balanced [20]. Experiments were conducted in four replications at both locations. Experimental results were subjected to variance analyses with Jump statistical software in accordance with Randomized Blocks Factorial Experimental Design. Significant differences were tested with F test and means were grouped with Duncan test.

TABLE 1
Long term and experimental year climate data for experimental locations

	Ankara						Eskişehir					
	Precipitation (kg/m^2)		Mean temperature (ºC)		Relative humidity (%)		Precipitation (kg/m^2)		Mean temperature (ºC)		Relative humidity (%)	
Months	**L.T.A. 1970-2010	2011	**L.T.A. 1970-2010	2011	**L.T.A. 1970-2010	2011	**L.T.A. 1970-2010	2011	**L.t.A. 1970-2010	2011	**L.T.A. 1970-2010	2011
March	36.7	**57.5**	6.2	**5.8**	63.4	**68.1**	36.8	**20.0**	5.1	**3.7**	84.7	**88.0**
April	50.0	**50.1**	11.3	**9.8**	59.8	**66.9**	43.4	**56.9**	10.2	**7.2**	81.8	**91.0**
May	50.3	**73.1**	16.1	**15.0**	56.9	**64.6**	44.4	**145.8**	15.1	**12.3**	75.6	**88.3**
June	50.3	**44.4**	20.2	**19.3**	52.0	**58.6**	31.0	**9.4**	19.1	**16.6**	74.3	**84.6**
July	15.5	**10.7**	23.6	**25.0**	46.0	**47.5**	13.2	**8.5**	21.7	**21.9**	69.9	**70.8**
August	12.0	**20.8**	23.3	**23.4**	45.8	**48.4**	8.7	**0**	21.4	**20.0**	66.6	**72.2**
September	17.5	**0.6**	18.7	**19.9**	49.8	**45.4**	14.5	**2.1**	17.2	**17.4**	76.4	**68.5**
October	33.2	**62.4**	13.0	**11.0**	60.9	**67.7**	30.6	**57.9**	12.0	**8.5**	76.8	**83.6**

*Turkish State Meteorological Service, **L.T.A.: Long Term Average

TABLE 2
Soil characterizes of experimental locations

Parameter	Ankara	Eskişehir
Depth (cm)	0-30	0-30
Soil reaction (pH)	8.20	7.54
Lime (%)	9.92	8.0
Organic matter (%)	1.24	1.77
Available phosphorus (P_2O_5) mg kg^{-1}	12.2	27.8
Available potassium (K_2O) mg kg^{-1}	430	493
Texture	Clay loam	Sandy clay

TABLE 3
Effects of cultivar x seed aging x priming interactions on number of days to 50% emergence, number of plants per square meter and plant height (cm) of sorghum cultivars grown under field conditions of Ankara and Eskişehir

Cultivar	Seed aging	Priming	Number of days to 50% emergence		Number of plants per m^2		Plant height (cm)	
			Ankara	Eskişehir	Ankara	Eskişehir	Ankara	Eskişehir
Sugar Graze II	Aged	Putrescine	18.75 jk*	14.50ns	12.50 g*	20.50 b*	221.1 d*	242.7de*
		Jasmonic acid	17.75 l	14.50	13.50 f	15.50 jk	216.1 ef	248.5 cd
		Kinetin	20.00 gh	16.25	17.00 d	19.00 cd	222.5 cd	242.0 e
		KNO_3	15.75 m	9.75	16.00 e	20.50 b	222.4 cd	225.5 g
		Salicylic acid	18.50 k	15.25	20.00 b	20.50 b	226.6 bc	255.2 ab
		Control	23.50 d	19.25	12.50 g	15.00 k	166.3 j	190.4 kl
	Unaged	Putrescine	18.25 kl	12.75	14.00 f	18.50 de	235.9 a	241.5 e
		Jasmonic acid	17.75 l	12.25	14.00 f	20.50 b	227.3 b	257.9 a
		Kinetin	20.50 g	17.50	12.50 g	19.50 c	235.7 a	250.3 bc
		KNO_3	14.75 n	10.50	22.00 a	20.50 b	219.9 de	239.9 ef
		Salicylic acid	19.25 ij	14.50	18.00 c	18.00 ef	215.0 f	237.0 ef
		Control	26.25 b	20.25	12.50 g	15.50 jk	181.9 h	186.4 l
Digestivo	Aged	Putrescine	21.25 f	20.75	19.50 b	15.00 k	189.7 g	196.8 jk
		Jasmonic acid	22.25 e	22.75	20.00 b	16.50 hi	173.8 I	216.7 h
		Kinetin	24.25 c	24.00	10.00 I	17.50 fg	166.1 j	186.8 l
		KNO_3	19.75 hi	19.25	14.00 f	11.00 m	167.2 j	215.6 h
		Salicylic acid	20.25 gh	16.00	18.00 c	17.00 gh	170.6 ij	208.5 I
		Control	27.00 a	26.25	11.50 h	12.00 l	154.4 k	161.4 n
	Unaged	Putrescine	21.75 ef	20.75	19.50 b	15.50 jk	172.6 i	234.2 f
		Jasmonic acid	19.25 ij	16.50	19.50 b	21.50 a	174.8 I	202.9 ij
		Kinetin	24.75 c	22.00	14.00 f	12.00 l	182.8 h	201.7 j
		KNO_3	21.50 f	18.75	16.00 e	16.00 ij	174.2 I	192.8 kl
		Salicylic acid	16.25 m	13.75	18.00 c	17.00 gh	190.5 g	221.2 gh
		Control	26.25 b	23.25	14.00 f	12.00 l	156.3 k	169.4 m

*) significant at $p<0.05$ and **) significant at $p<0.01$ ns: non-significant

RESULTS AND DISCUSSION

Number of days to 50% emergence. As it can be seen from Table 3, The effects of seed priming treatments on number of days to 50% emergence of two different sorghum hybrids were found to be significant at Ankara location ($p<0.05$) and insignificant at Eskişehir location. On the other hand, effects of priming treatments on number of plants per square meter of two different sorghum hybrids were found to be significant at both locations (Ankara – Eskişehir) ($p<0.05$). In Ankara location, the lowest number of days to 50% emergence (27.00 days) was obtained from control treatment of aged Digestivo seeds and the greatest value (14.75 days) was obtained from KNO_3-primed unaged Sugar Graze II seeds (Table 3). In Eskişehir location, number of days to 50% emergence of seed primed sorghum hybrids varied between 9.75 - 24.00 days. Present findings on number of days to emergence of KNO_3-primed seeds comply with the results of İlbi and Eser [30] reported for number of days to emergence of onion seeds was similar with the finding of Madakadze *et al.* [37] reported for millet seeds and with the findings of Büyükçıngıl [10]. Present finding for KNO3 primed seeds reported for sorghum seed. Preset finding for Jasmnic acid primed seeds comply with the finding of Tiryaki et al [49] reported for sorghum seeds.

Number of plants per square meter. The effects of seed priming treatments on number of plants per square meter of two different sorghum hybrids were found to be significant at both locations ($p<0.05$) (Table 3). In Ankara location, the greatest number of plants per square meter (22.00) was obtained from KNO_3-primed unaged Sugar Graze II seeds and the lowest value (10.00) was obtained from Kinetin-primed aged Digestivo seeds. In Eskişehir location, the greatest number of plants per square meter (21.50) was obtained from Jasmonic acid-primed unaged Digestivo seeds and the lowest value (11.00) was obtained from KNO_3-primed aged Digestivo seeds. Present findings on

number of plants per square meter of putrescine-primed seeds comply with the findings of Tekin and Bozcuk [48]

Plant height (cm). The effects of seed priming treatments on plant height (cm) of two different sorghum hybrids were found to be significant at both locations (Ankara and Eskişehir) ($p<0.05$) (Table 3). In Ankara location, plant heights varied between 154.9 – 235.9 cm (Table 3) with the greatest value from putrescine-primed aged Sugar Grazer II seeds and the lowest value from the control treatment of unaged Digestivo seeds. The putrescine-primed aged Sugar Grazer II seeds and kinetin-primed aged Sugar Grazer II seeds had statistically similar plant heights. In Eskişehir location, plant heights varied between 161.4 and 257.9 cm. The greatest plant height was obtained from jasmonic acid-primed aged Sugar Grazer II seeds and they were followed by salicylic acid-primed unaged Sugar Grazer II seeds which were placed in the same statistical group. The lowest value was obtained from the control treatment of unaged Digestivo seeds. Putrescine exists in all living organism and plays significant roles in formation and development of metabolites and cells [21]. Present findings on plant heights were similar with the ones reported by Flores et al. [21] indicating increasing number of cells and cell sizes with priming treatments. Benkova et al. [6] indicated that putrescine had significant effects on vegetative growth and development, especially on cell growth. Creelman and Mullet [15, 16] reported that jasmonic acid stimulated plant growth and ripening, improved fertility of pollens and increased protein ratios of the seeds. Senaranta et al. [43] pointed out the roles of salicylic acid in cell reproduction, plant growth and photosynthesis. Present finding comply with all those earlier reports. Effects of spray salicylic acid treatments on plant height were also reported by Datta and Nanda [17] for millet, by Gutierrez-Coranado et al. [24] for soybean and by Kaydan and Yağmur [34] for lentils and wheat. Researchers reported similar findings with the present ones. Bray [9] also reported increasing plant heights with KNO_3-priming. According to Bray [9], KNO_3 treatments improved seed performance and thus resulted in greater plant heights.

Shoot diameter (mm). The effects of seed priming treatments on shoot diameter of two different sorghum hybrids were found to be significant at Ankara and Eskişehir locations ($p<0.05$) (Table 4). In Ankara location, shoot diameters varied between 15.00 – 22.38 mm with the greatest value from kinetin-primed unaged Digestivo seeds and the lowest value from the control treatment of aged Sugar Grazer II seeds. With regard to lowest shoot diameter, control treatment of aged and unaged Sugar Grazer II seeds had statistically similar results. In Eskişehir location, shoot diameters varied between 17.15 - 26.42 mm with the greatest value from

TABLE 4
Effects of cultivar x seed aging x priming interactions on shoot diameter (mm), plant weight (g/plant) and number of days to 50% flowring of sorghum cultivars grown under field conditions of Ankara and Eskişehir

Cultivar	Seed aging	Priming	Shoot diameter (mm)		Plant weight (g/plant)		Number of days to 50% flowring	
			Ankara	Eskişehir	Ankara	Eskişehir	Ankara	Eskişehir
Sugar Graze II	Aged	Putrescine	17.60 kl*	21.36ef*	341.1 h**	375.4 i*	83.00 f*	83.50 f*
		Jasmonic acid	19.07 gh	19.78 I	308.5 j	389.2 h	81.25 g	81.00 g
		Kinetin	16.72 mn	20.03 hi	368.4 efg	341.4 k	90.00 abc	84.25 ef
		KNO_3	16.90 m	18.31 k	382.7def	513.2 c	73.75 j	85.50 de
		Salicylic acid	16.51 n	21.13 fg	545.9 a	350.5 jk	81.25 g	78.50 h
		Control	15.93 o	17.73 lm	229.6 m	280.2 m	89.75 bc	90.00 a
	Unaged	Putrescine	16.55 n	17.53 m	367.6fg	352.2 j	85.00 e	75.50 I
		Jasmonic acid	17.82 k	20.79 g	396.5 d	563.7 b	82.00 fg	84.75 de
		Kinetin	17.58 kl	18.02 kl	426.9 b	475.4 d	90.00 abc	85.50 de
		KNO_3	16.46 n	19.01 j	360.2 g	450.2 e	78.25i	86.00 cd
		Salicylic acid	18.89 h	21.60 e	434.3 b	407.3 g	83.00 f	83.25 f
		Control	15.88 o	17.15 n	245.4 l	289.2m	89.00 cd	90.00 a
Digestivo	Aged	Putrescine	21.36 b	18.35 k	381.0 ef	352.3 j	89.00 cd	88.00 b
		Jasmonic acid	19.89 e	20.27 h	324.2 i	355.2 j	80.00 h	88.00 b
		Kinetin	22.38 a	24.97 b	545.9a	456.4 e	90.75 ab	91.00 a
		KNO_3	19.29 fg	26.42 a	377.4 ef	596.6 a	88.00 d	91.00 a
		Salicylic acid	18.09 j	22.27 d	331.8 hi	436.8 f	78.00i	85.50 de
		Control	17.39 l	17.73 lm	212.7 n	311.1 l	88.00 d	87.25 bc
	Unaged	Putrescine	20.73 c	22.52 d	383.6de	371.3 i	82.00 fg	88.00 b
		Jasmonic acid	20.34 d	18.11 kl	374.6 efg	377.8 i	86.00 e	87.00 bc
		Kinetin	21.53 b	24.97 b	437.3 b	477.7 d	89.00 cd	86.00 cd
		KNO_3	18.52 i	19.23 j	346.1 h	411.8 g	89.75 bc	87.00 bc
		Salicylic acid	19.41 f	20.28 h	412.8 c	388.6 h	79.00 hi	85.50 de
		Control	18.19 j	17.84 lm	281.5 k	288.5m	91.00 a	87.50 b

*: significant at $p<0.05$, **: significant at $p<0.01$, ns: non-significant

KNO_3-primed unaged Digestivo seeds and the lowest value from the control treatment of aged Sugar Grazer II seeds. Benkova et al. [6] indicated that cytokinins had significant effects on vegetative growth and development, especially on cell growth. Complying with the present findings, Hadinezhad et al. [25] reported increasing sapling diameters in chestnut oak (*Quereus castaneifolia*) with KNO_3-priming.

Plant weight (g/plant). As it can be seen from Table 4, The effects of seed priming treatments on plant weights (g/plant) of two different sorghum hybrids were found to be significant at Ankara ($p<0.01$) and Eskişehir ($p<0.05$) locations. In Ankara location, plant weights varied between 212.7 - 545.9 g/plant with the greatest value from kinetin-primed unaged Digestivo seeds and the lowest value from the control treatment of unaged Digestivo seeds. In Eskişehir location, plant weights varied between 280.2 -596.6 g/plant with the greatest value from KNO_3-primed unaged Digestivo seeds and the lowest value from the control treatment of unaged Sugar Graze II seeds (Table 4). Complying with the present findings, Bernier et al. [7], Chang et al. [12] and Benkova et al. [6] also reported increasing plant weights with kinetin treatments. Benkova et al. [6] indicated that cytokinins played significant roles in plant vegetative growth-development and especially on cell growth. According to Bernier et al. [7] and Chang et al. [12], cytokinins play significant roles in leaf formation, flowering and flower development. Bray [9] reported increasing plant weights with KNO_3 treatments since KNO_3 improved seed vigor and thus had positive effects on plant weights.

Number of days to 50% flowering (days). The effects of seed priming treatments on number of days to 50% flowering of two different sorghum hybrids were found to be significant at both locations (Ankara and Eskişehir) ($p<0.05$) (Table 4). In Ankara location, number of days to 50% flowering varied between 73.75 - 91.00 days. The greatest value was obtained from the control treatment of aged Digestivo seeds and they were flowed by kinetin-primed unaged Digestivo seeds, kinetin-primed aged and unaged Sugar Grazer II seeds which all were placed in the same statistical group. The lowest value was obtained from KNO_3-primed unaged Sugar Grazer II seeds. In Eskişehir location, number of days to 50% flowering varied between 75.50 - 91.00 days. The greatest value was obtained from KNO_3-primed unaged Digestivo seeds and they were followed by kinetin-primed unaged Digestivo seeds and the control treatment of aged and unaged Sugar Graze II seeds which all were placed in the same statistical group. The lowest value was obtained from putrescine-primed aged Sugar Grazer II seeds. Present findings about the effects of putrescine treatments on number of days to flowering comply with the findings of Bais et al. [5] for chicory (*Cichorium intybus* L.) seeds.

TABLE 5
Effects of cultivar x seed aging x priming interactions on panicle seed yield per plant (g/plant) unit area seed yield (kg/da) and seed harvest moisture (%) of sorghum cultivars grown under field conditions of Ankara and Eskişehir

Cultivar	Seed aging	Priming	Panicle seed yield per plant (g/plant)		Unit area seed yield (kg/da)		Seed harvest moisture (%)	
			Ankara	Eskişehir	Ankara	Eskişehir	Ankara	Eskişehir
Sugar Graze II	Aged	Putrescine	31.44 g*	67.16 c*	338.6 g**	590.8 e**	13.44^{ns}	14.66 ij**
		Jasmonic acid	27.67 hij	59.89 e	302.6 ij	598.0 de	13.10	15.70 efg
		Kinetin	25.07 k	57.21 fg	231.0 n	556.4 f	13.19	13.90 lm
		KNO_3	27.40 ij	71.25 b	271.1lm	610.5 d	14.40	16.74 b
		Salicylic acid	46.02 e	53.88 h	499.1 b	546.7 f	13.07	15.53 fg
		Control	22.51 l	36.72 m	215.3 o	414.7 l	15.01	16.14 cd
	Unaged	Putrescine	28.43 hi	65.30 cd	262.4 m	629.1 c	14.94	15.67 fg
		Jasmonic acid	29.34 h	51.19 ij	293.7 jk	470.7 ıj	14.01	16.90 b
		Kinetin	24.81 k	53.19 hi	218.0no	498.0 gh	14.44	16.31 c
		KNO_3	26.13 jk	51.31 ij	267.9lm	508.9 g	14.20	14.01 lm
		Salicylic acid	32.30 g	70.20 b	322.8 h	694.4 a	13.54	14.87 hi
		Control	22.87 l	43.61 l	200.1 p	447.0 k	15.41	17.60 a
Digestivo	Aged	Putrescine	56.72 b	49.74 j	407.1 d	486.0 hı	11.70	13.76 m
		Jasmonic acid	54.10 c	50.86 j	320.3 h	471.6 ıj	11.59	14.92 hi
		Kinetin	63.09 a	66.16 c	268.7lm	438.6 k	12.26	15.02 h
		KNO_3	57.69 b	78.21 a	555.5a	503.7 gh	12.47	14.20 kl
		Salicylic acid	51.04 d	76.40 a	398.8 d	668.9 b	13.08	14.47 jk
		Control	40.30 f	46.54 k	232.0 n	396.2 m	13.54	16.04 cde
	Unaged	Putrescine	58.38 b	58.82 ef	451.5c	447.4 k	11.95	13.26 n
		Jasmonic acid	50.90 d	55.14 gh	344.0 fg	375.0 n	11.40	13.31 n
		Kinetin	54.00 c	66.84 c	308.8 hi	510.0 g	14.06	11.82 o
		KNO_3	58.44 b	63.60 d	356.0 f	466.1 j	13.37	14.37 jk
		Salicylic acid	51.83 d	53.28 hi	380.3 e	456.9 jk	12.55	15.46 g
		Control	41.47 f	46.29 k	279.9 kl	375.0 n	14.93	15.88 def

*: significant at $p<0.05$, **: significant at $p<0.01$, ns: non-significant

Panicle seed yield per plant (g/plant). The effects of seed priming treatments on panicle seed yield per plant (g/plant) of two different sorghum hybrids were found to be significant at both Ankara and Eskişehir locations ($p<0.05$) (Table 5). In Ankara location, panicle seed yields per plant varied between 22.51 - 63.09 g with the greatest value from kinetin-primed unaged Digestivo seeds and the lowest value from the control treatment of unaged Sugar Grazer II seeds and they were followed by the control treatment of aged Sugar Grazer II seeds which were placed in the same statistical group. In Eskişehir location, panicle seed yields per plant varied between 36.72 - 78.21 g. The greatest value was obtained from KNO_3-primed unaged Digestivo seeds, they were followed by salicylic acid-primed unaged Digestivo seeds which were placed into the same statistical group and the lowest value was obtained from the control treatment of unaged Sugar Grazer II seeds. Present findings about the effects of kinetin priming were similar with the findings of Angrish et al. [2], Kaya et al. [33], Ashraf and Foolad [3] and Pakmehr [40]. Current findings about the effects of KNO_3 treatments on yields comply with the findings of Hajikhani et al. [26] and Hussain [28] reported for sunflower.

Unit area seed yield (kg/da). As it can be seen from Table 5, priming treatments had significant effects on unit area seed yields (kg/da) at both Ankara and Eskişehir locations ($p<0.01$). In Ankara location, unit area seed yields varied between 200.1-555.5 kg/da with the greatest value from KNO_3-primed unaged Digestivo seeds and the lowest value from the control treatment of aged Sugar Grazer II seeds. In Eskişehir location, unit area seed yields varied between 375.00 - 694.4 kg/da with the greatest value from salicylic acid-primed aged Sugar Grazer II seeds and the lowest value from the control treatment of aged Digestivo seeds. Present findings about the effects of salicylic acid priming on seed yield were similar with the findings of Ahmad et al. [1] Raza et al. [42] and Senaranta *et al*. [43]. Klessig and Malamy [36] and Creelman and Mullet [15] indicated that jasmonic acid and salicylic acid stimulated growth reactions in plant tissues, thus increases plant growth and development and facilitated cation exchange under stress conditions. Present findings about KNO_3 treatments were similar with the results of Ghasemi-Golezani et al. [23], but different from the findings of Hajikhani et al. [26]. Such differences were mostly because of genotypes and ecological conditions.

Seed harvest moisture (%). The effects of seed priming treatments on seed harvest moisture of two different sorghum hybrids were found to be significant at Eskişehir location ($p<0.01$) (Table 5), but insignificant at Ankara location. In Eskişehir location, harvest moisture of the seeds varied between 11.82 - 17.60% with the greatest value from the control treatment of aged Sugar Grazer II seeds and the lowest value from kinetin-primed aged Digestivo seeds. In Ankara location, harvest moisture of the seeds varied between 11.40 - 15.41%. Bernier et al. [7] and Chang et al. [12] reported

TABLE 6
Effects of cultivar x seed aging x priming interactions on thousand seed weight (g), hectoliter weight (kg/hL) and protein ratio (%) of sorghum cultivars grown under field conditions of Ankara and Eskişehir

Cultivar	Seed aging	Priming	Thousand seedweight (g)		Hectoliter weight (kg/hL)		Protein ratio (%)	
			Ankara	Eskişehir	Ankara	Eskişehir	Ankara	Eskişehir
Sugar Graze II	Aged	Putrescine	15.40 mn*	14.91 i*	68.49 kl*	64.76 c*	12.32 k**	9.840 g*
		Jasmonic acid	15.66 lm	14.19 l	70.14 hi	61.71 k	11.87 m	10.91 c
		Kinetin	15.69 lm	15.50 g	71.82 ef	66.45 h	11.54 n	10.49 ef
		KNO_3	15.46 mn	14.57 k	69.13 jk	67.40 ef	12.33 k	9.460 hi
		Salicylic acid	16.79 I	14.80 ijk	71.21 fg	64.46 j	12.94 hi	9.570 h
		Control	15.13 n	15.01 hi	67.57 m	67.58 e	11.02 o	9.140 j
	Unaged	Putrescine	15.77 klm	14.89 ij	72.75 cd	67.19 efgh	12.10 l	10.37 f
		Jasmonic acid	15.65 lm	14.78 ijk	69.07 jk	67.34 efg	12.78 ij	9.490 h
		Kinetin	16.17 jk	14.59 jk	63.53 n	64.64 j	11.46 n	8.250 l
		KNO_3	16.30 j	14.58 k	67.81 lm	61.49 k	12.45 k	8.660 k
		Salicylic acid	15.93 jkl	14.76 ijk	71.30 fg	65.56 i	12.73 j	10.96 c
		Control	16.21 jk	15.89 f	70.68 gh	60.26 l	11.11 o	8.110 l
Digestivo	Aged	Putrescine	22.29 d	18.21 c	76.05 a	67.26 efg	12.14 l	9.650 h
		Jasmonic acid	23.12 c	18.75 b	73.15 c	72.11 b	13.83 d	10.54 def
		Kinetin	21.58 e	17.54 d	74.83 b	66.64 fgh	13.21 f	12.10 a
		KNO_3	22.50 d	18.06 c	75.21 b	74.24 a	15.07 a	9.530 h
		Salicylic acid	22.08 d	20.57 a	76.10 a	71.94 b	13.18 fg	10.72 d
		Control	23.15 c	15.28 gh	72.21 de	70.01 d	11.98 lm	9.280 ij
	Unaged	Putrescine	20.44 g	18.04 c	72.76 cd	66.56 gh	13.77 d	11.88 b
		Jasmonic acid	20.96 f	16.68 e	74.84 b	71.04 c	13.53 e	10.54 def
		Kinetin	24.36 b	18.21 c	73.09 c	70.33 d	14.77 b	10.72 d
		KNO_3	19.44 h	18.90 b	68.83 k	73.82 a	14.45 c	10.56 def
		Salicylic acid	24.99 a	18.04 c	71.96 ef	69.96 d	13.33 f	10.66 de
		Control	24.66 ab	17.74 d	69.70 ij	71.46 bc	13.02 gh	10.50 ef

*: significant at $p<0.05$, **: significant at $p<0.01$, ns: non-significant

significant roles of kinetin hormone in flowering and flower development and consequently on seed formation. Early formed seeds usually ripen early, thus have lower moisture levels at harvest.

Thousand seed weight (g). As it can be seen from Table 6, the effects of seed priming treatments on thousand seed weights were found to be significant at both locations (Ankara-Eskişehir) ($p<0.05$). In Ankara location, thousand seed weights varied between 15.13 - 24.99 g. The greatest value was obtained from salicylic acid-primed aged Digestivo seeds, they were followed by the control treatment of aged Digestivo seeds which were placed in the same statistical group and lowest value was obtained from the control treatment of unaged Sugar Graze II seeds. In Eskişehir location, thousand seed weights varied between 14.19 - 20.57 g with the greatest value from salicylic acid-primed unaged Digestivo seeds and the lowest value from jasmonic acid-primed unaged Sugar Graze II seeds. Present findings about the effects of salicylic acid treatments on thousand seed weights were similar with the findings of Kaydan and Yağmur [34] reported for lentils and wheat seeds, but different from the findings of Pakmehr reported for cowpea.

Hectoliter weight (kg/hL). The effects of seed priming treatments on hectoliter weights of two different sorghum hybrids were found to be significant at both locations (Ankara-Eskişehir) ($p<0.05$) (Table 6). In Ankara location, hectoliter weights varied between 63.53 - 76.10 kg. The greatest value was obtained from salicylic acid-primed unaged Digestivo seeds, they were followed by putrescine primed unaged Digestivo seeds which were placed in the same statistical group and the lowest value was obtained from kinetin-primed aged Sugar Grazer II seeds. In Eskişehir location, hectoliter weights vary between 60.26 - 74.24 kg. The greatest value was obtained from KNO_3-primed unaged Digestivo seeds, they were followed by KNO_3 primed aged Digestivo seeds and the lowest value was obtained from the control treatment of aged Sugar Grazer II seeds. Present findings about the effects of salicylic acid treatments on hectoliter weights were similar with the findings of Ahmad et al. [1], Raza et al. [42] and Senaranta et al. [43]. Current findings about the effects of KNO_3 treatments on hectoliter weights also comply with the findings of Hajikhani et al. [26] and Hussain [28].

Protein ratio (%). As it can be seen from Table 6, seed priming treatments had significant effects on protein ratios of two different sorghum hybrids at Ankara location ($p<0.01$) and Eskişehir location ($p<0.05$) (Table 6). In Ankara location, protein ratios varied between 11.2 - 15.07% with the greatest value from KNO_3-primed unaged Digestivo seeds and the lowest value from the control treatment of unaged Sugar Grazer II seeds. They were followed by the control treatment and aged Sugar Grazer II seeds which were placed into the same statistical group. In Eskişehir location, protein ratios varied between 8.11 - 12.10% with the greatest value from kinetin-primed unaged Digestivo seeds and the lowest value from the control treatment of aged Sugar Grazer II seeds. They were followed by the control treatment of unaged Sugar Grazer II seeds which were placed into the same statistical group. The greatest crude protein ratios of both cultivars were obtained from Ankara location since Ankara had higher temperatures and precipitations and lower relative humidity values than Eskişehir. Crude protein ratios generally increase at hot temperatures and sandy soils. Present findings about the effects of KNO_3 treatments on protein ratios were different from the findings of Hussain et al. [28] reported for sunflower. Cytokinins play significant roles in plant vegetative growth and development. When the plants get into vegetative period early, leaf area index values increase, then such an increase allows plants to get more sunshine and to have higher photosynthesis rates and consequently have higher protein ratios.

Considering the entire findings, it was concluded that reactions of priming agents were different in aged and unaged seeds. Salicylic acid, jasmonic acid and KNO_3 priming treatments yielded positive and successful outcomes. It was concluded based on current findings that priming treatments may result in different outcomes based on the cultivars and locations. Results may be positive in some locations and negative in some others. In seed industry, priming with different chemicals can successfully be used to stimulate-activate seed vigor.

REFERENCES

[1] Ahmad, A., Haque, I. and Aziz, O. (1995) Physiomorphological changes in triticale improved by pyridoxine applied through grain soaking. Acta Agron. Hung. 43, 211-221.

[2] Angrish, R., Kumar, B. and Datta, K.S. (2001) Effect of gibberellic acid and kinetin on nitrogencontent and nitrate reductase activity in wheat under saline condition. Indian Journal of Plant Physiology. 6, 172-177.

[3] Ashraf, M. and Foolad, M.R. (2005) Pre-Sowing Seed Treatment- A Shotgun Approach to Improve Germination, Plant Growth and Crop Yield Under Saline and Non-Saline Conditions. Advances in Agronomy. 88, 225-270.

[4] Bailly, C., Benamar, A., Corbineau, F.and Côme, D. (1998) Free radical scavenging as affected by accelerated ageing and subsequent priming in sunflower seeds. Physiol Plant. 104, 646-652.
[5] Bais, H.P., Sudha, G.S. and Ravshankar, G.A. (2000) Putrescine and silver nitrate influences shoot multiplication, in vitro flowering and endogenous titers of polyamines in *Cichorium intybus* L. cv. Luchnow local. J. Plant Growth Regul. 19, 238-248.
[6] Benkova, E., Michniewicz, M., Sauer, M., Teichmann, T., Seifertova, D., Jurgens, G. and Friml, J. (2003) Local, efflux-dependent auxin gradients as a common module for plant organ formation. Cell. 115, 591–602.
[7] Bernier, G., Havelange, A., Houssa, C., Petitjean, A. and Lejeune, P. (1993) Physiological signals that induce flowering. The Plant Cell. 5, 1147–1155.
[8] Bialecka, B. and Kepczynski, J. (2003) Regulation of α-amylase activity in *Amaranthus caudatus* seeds by methyl jasmonate, gibberellin A3, benzyladenine and ethylene. Journal of Plant Growth Regulation. 39, 51-56.
[9] Bray, C.M. (1995) Biochemical Processes during the Osmopriming of Seeds. In: Kigel, J., Galili, G. (ed.) Seed Development and Germination. Marcel Dekker, New York, 767-789.
[10] Büyükçıngıl, Y. (2007) Priming uygulamas Sorgum [Sorghum bicolor (L.) Moench] tohumlarının düşük sıcaklıkdaki çimlenme ve çıkış performansı üzerine etkileri. KSÜ Fen Bilimleri Enstitüsü Tarla Bitkileri Anabilim Dalı. Master Thesis. 56p.
[11] Budak, F. and Kizil Aydemir, S. (2017) Determination and comparison of yield and yield components of sorghum (*Sorghum bicolor* L.), sudan grasses (*Sorghum sudanense* L.), sorghum sudangrass hybrids (*Sorghum bicolor* x *Sorghum bicolor* var. sudanense) and corn (*Zea mays* L.) varieties grown as a second crop on western transition zone after hungarian vetch (*Vicia pannonica* crantz). Fresen. Environ. Bull. 26, 5153-5162.
[12] Chang, P.L., Sauer, M.V. and Brown, S. (1999) Y chromosome micro deletions of different types in interval 6 of Yq11. Hum. Genetics, 102, in a father and his four infertile sons. Hum. Reprod. 14, 2689–94.
[13] Childs, A., Mehta, D. and Gerner, E. (2003) Polyamine-dependent gene expression. Cell Mol. Life Sci. 60, 1394-1406.
[14] Corbineau, F., Rudnicki, R.M. and Come, D. (1988) The effects of methyl jasmonate on sunflower (*Helianthus annuus* L.) seed germination and seedling development. Plant Growth Regul. 7, 157-169.
[15] Creelman, R.A. and Mullet, J.E. (1995) Jasmonic acid distribution and action in plants: Regulation during development and response to biotic and abiotic stress. Proc. Natl. Acad. Sci. 92, 4114-4119.
[16] Creelman, R.A. and Mullet, J.E. (1997) Biosynthesis and action of jasmonates in plants. Ann. Rev. Plant Physiol. 48, 355-381.
[17] Datta, K.S. and Nanda, K.K. (1985) Effect of some phenolic compounds and gibberellic acid on growth and development of cheena millet (*Panicum miliaceum* L.) Indian J. Plant Physiol. 28, 298-302.
[18] De Castro, R.D., van-Lammeren, A.A.M., Groot, S.P.C., Bino, R.J. and Hilhorst, H.W.M. (2000) Cell division and subsequent radicle protrusion in tomato seeds are inhibited by osmotic stress but DNA synthesis and formation of microtubular cytoskeleton are not. Plant Physiol. 122, 327-335.
[19] Eisvand, H.R. (2008) Effects of Some phytohormones on physiological quality improvement of tall wheatgrass (*Agropyron elongatum*) aged seeds under drought stress. Ph.D. Thesis. University of Tehran.
[20] Ekşi, C. (2010) Hızlandırılmış kontrollü bozulma tohum gücü testinin pırasa ve soğan tohum partilerinde depo ömrünün tahmininde kullanılması. Master Thesis. Ankara Üniversitesi, Fen Bilimleri Enstitüsü, Bahçe Bitkileri Anabilim Dalı, Ankara.
[21] Flores, H.E., Protacio, C.M. and Signs, M.W. (1989) Primary and secondary metabolism of polyamines in plants. Rec Adv Phytochem. 23, 329-393.
[22] Gallardo, K., Job, C., Groot, S.P.C., Puype, M., Demol, H., Vandekerckhove, J., Job, D. (2001) Proteomic analysis of Arabidopsis seed germination and priming. Plant Physiol. 126, 835–848.
[23] Ghassemi-Golezani, K., Jabbarpour, S., Zehtab-Salmasi, S. and Mohammadi, A. (2010) Response of winter rapeseed (*Brassica napus* L.) cultivars to salt priming of seeds. African Journal Agric. 5, 1089-1094.
[24] Gutierrez-Coronado, M.A., Trejo-Lopez, C. and Larque- Saavedra, A. (1998) Effect of salicylic acid on the growth of roots and shoots in soybean. Plant Physiol Biochem. 36, 563–565.
[25] Hadinezhad, P., Payamenur, V., Mohamadi, J. and Ghaderifar, F. (2013) The effect of priming on seed germination and seedling growth in *Quereus castaneifolia*. Seed Science and Technology. 41(1), 121-124.
[26] Hajikhani, S., Habibi, H., Shekari, F. and Fotoukian, M.H. (2011) The Effect of Seed Priming on Grain Yield and its Components of Spotted Bean Cultivars under Water Deficit Stress. Iranian Journal of Field Crop Science. 42(1), 191-197.

[27] Hamid, M., Ashraf, M.Y., Rehman, K.U. and Arshad, M. (2008) Influence of salicylic acid seed priming on growth and some biochemical attributes on wheat growth under saline conditions. Pak. J. Bot. 40(1), 361-367.
[28] Hussain, M., Farooq, M., Basra, S.M.A and Ahmad, N. (2006) Influence of seed priming techniques on the seedling establishment, yield and quality of hybrid sunflower. Int. J. Agric. Biol. 8, 14-18.
[29] Igarashi, K. and Kashiwagi, K. (2000) Polyamines: mysterious modulators of cellular functions. Biochem. Bioph. Res. Co. 271, 559-564.
[30] İlbi, H. and Eser, B. (2004) Tohum uygulamalarının soğan tohumlarında yaşlanmaya etkileri. E. Ü. Ziraat Fakültesi Dergisi. 41(1), 39-49.
[31] Iqbal, M. and Ashraf, M. (2006) Wheat seed priming in relation to salt tolerance: growth, yield and levels of free salicylic acid and polyamines. Ann. Bot. Fenn. 43, 250-259.
[32] Kattimani, K.N., Reddy, Y.N. and Rajeswar Rao, B. (1999) Effect of pre-sowing seed treatment on germination, seedling emergence, seedling vigoure and root yield of Ashwagandha (*Withania somnifera* Daunal.). Seed Science Technology. 27, 483-488.
[33] Kaya, M.D., Bayramin, S. and Kaya, G. (2015) The effect of planting geometry and seed priming on sunflower yield under rain-fed conditions. Fresen. Environ. Bull. 24, 4095–4101.
[34] Kaydan, D. and Yağmur, M. (2006) Farklı salisilik asit dozları ve uygulama şekillerinin buğday (*Triticum aestivum* L.) ve mercimekte (*Lens culinaris* Medik) verim ve verim öğeleri üzerine etkileri. Tarım Bilimleri Dergisi. Ankara Üni. Ziraat Fakültesi. 12(3), 285-293.
[35] Kepczynski, J. and Bialecka, B. (1994) Stimulatory effect of ethephon, ACC, gibberellin A3 and A4+7 on germination of methyl jasmonate inhibited *Amaranthus caudatus* L. seeds. Plant Growth Regulation. 14, 211-216.
[36] Klessig, D.F. and Malamy, J. (1994) The salicylic acid signal in plants. Plant Mol. Biol. 26, 1439-1458.
[37] Madakadze, I.C., Prithiviraj, B., Madakadze, R.M., Stewart, K., Peterson, P., Coulman, B.E. and Smith, D.L. (2000) Effect of preplant seed conditioning treatment on the germination of switch grass (*Panicum virgatum* L.). Seed Sci. and Technol. 28, 403-411.
[38] Nojavan-Asghari, M. and Ishizava, K. (1998) Inhibitory effects of methyl jasmonate on the germination and ethylene production in cocklebur seeds. J. Plant Growth Regul. 17, 13-18.
[39] Okçu, G., Kaya, M.D. and Atak, M. (2005) Effects of salt and drought stresses on germination and seedling growth of pea (*Pisum sativum* L.). Turk. J. Agric. For. 29, 237–242
[40] Pakmehr, A. (2009) Effect of priming by salicylic acid on morphological and physiological traits of cowpea (*Vigna unguiculata* L.) under water deficit. MSc. Thesis. Faculty of Agriculture, Zanjan University. Iran.
[41] Preston, C.A., Betts, H. and Baldwin, I.T. (2002) Methyl jasmonate as an allelopathic agent: sagebrush inhibits germination of a neighboring tobacco, *Nicotiana attenuata*. J. Chem. Ecol. 28, 2343 2369.
[42] Raza, S.H., Shafiq, F., Chaudhary, M. and Khan, I. (2013) Seed invigoration with water, ascorbic and salicylic acid stimulates development and biochemical characters of okra (*Ablemoschus esculentus*) under normal and saline conditions. Int. J. Agric. Biol. 15, 486-492.
[43] Senaranta, T., Teuchela, D., Bumm, E. and Dixon, K. (2000) Acetyl salicylic acid physiological parameters. Journal of Plant Science. 139, 223-232.
[44] Sneideris, L.C., Gavassı, M.A., Campos, M.L., D'amicodamião, V. and Carvalho RF. (2015) Effects of hormonal priming on seed germination of pigeon pea under cadmium stress. An Acad Bras Cienc. 87, 1847-1852.
[45] Somerville, C. and Briscoe, J. (2001) Genetic engineering and water. Science. 292, 217
[46] Staswick P.E., Su, W. and Howell, S.H. (1992) Methyl jasmonate inhibition of root growth and induction of a leaf protein are decreased in an Arabidopsis thaliana mutant. Proc Natl Acad Sci USA. 89, 6837-6840.
[47] Taiz, L. and Zeiger, E. (2010) Plant Physiology. 5th edition. Sinauer Associates Inc Publishers, Sunderland, M.A., USA.
[48] Tekin, F. and Bozcuk, S. (1998) Effects of Salt and Exogenous Putrescine on Seed Germination and Early Seedling Growth of *Helianthus annuus* L. var. Santafe. Turkish Journal of Biology. 22(3), 331-340.
[49] Tiryaki, I., Korkmaz, A., Ozbay, N. and Nas, M. N. (2005) Effect of Priming Supplemented with Plant Growth Regulators on Sorghum (*Sorghum bicolor* L. Moench) Seed Germination and Seedling Emergence at Low Temperature. Türkiye VI. Tarla Bitkileri Kongresi, Antalya.
[50] Wang, X., Xing, W., Hong Wu, S. and Hua Liu, G. (2009) Allelopathic Effects of Seed. Extracts of Four Wetland Species on Seed Germination and Seedling Growth of *Brassica rapa* spp. *pekinensis*, *Oryza rufipogon* and *Monochoria korsakowii*. Fresen. Environ. Bull. 18, 1832-1838.
[51] Wasternack, C. (2007) Jasmonates, an update on biosynthesis, signal transduction and action in plant stress response, growth and development. Annals of Botany. 100, 681– 697.

[52] Xu, S., Hu, J., Li, Y., Ma, W., Zheng, Y. and Zhu, S. (2011) Chilling tolerance in *Nicotiana tabacum* induced by seed priming with putrescine. Plant Growth Regul. 63, 279-290.

Received: **18.11.2017**
Accepted: **20.04.2018**

CORRESPONDING AUTHOR

Negar Ebrahim Pour Mokhtari
University of Gaziantep,
Islahiye Vocational School,
Department of Organic Farming
Gaziantep – Turkey

e-mail: n_mokhtary@yahoo.com

© by PSP Volume 27 – No. 7/2018 pages 4769-4776 Fresenius Environmental Bulletin

OPTIMIZATION OF GAS DIFFUSION ELECTRODE FOR TREATMENT OF DIMETHYL PHTHALATE USING RESPONSE SURFACE METHODOLOGY

Wenzhao Jiang[1], Jianwei Guo[1,*], Zhitao Wu[1], Wang Yi [2], Liu Hong [2]

[1]School of Chemical Engineering & Light Industry, Guangdong University of Technology, Guangzhou 510006, China
[2]School of Chemistry and Chemical Engineering, Sun Yat-sen University, Guangzhou 510275, China

ABSTRACT

XC-72 Carbon/PTFE gas diffusion electrode was prepared and characterized by Field Emission Scanning Electron Microscope (FESEM). This gas diffusion electrode has been applied to remove dimethyl phthalate (DMP). Based on response surface methodology (RSM), central composite design (CCD) was used to study the effect of several operating parameters – Fe^{2+} concentration, the initial pH and cathodic potential on the DMP removal efficiencies. According to the experimental results, the RSM model was derived and the response surface plots were given. The optimal condition for removal of DMP is 0.49mM of c(Fe^{2+}), -0.55V of cathodic potential and initial pH=3. The actual degradation ratio of DMP could reach 90% under that condition. Apart from the discussing of the relative mechanism, the recyclability of XC-72 Carbon/PTFE gas diffusion electrode was also evaluated.

KEYWORDS:
Electro-Fenton, XC-72 Carbon/PTFE gas diffusion electrode, dimethyl phthalate (DMP), response surface methodology (RSM), optimal condition

INTRODUCTION

As one of typical indispensable additive of plastics, dimethyl phthalate (DMP) has been widely used [1, 2]. The total consumption of DMP is about 6 million tons in the world each year [3]. However, overdose and metabolites of DMP may result in damage of human's endocrine systems [4, 5]. The threat of DMP has brought a great concern to academia and public.

Usage of the advanced oxidation processes (AOPs) is a promising way for organic pollutant degradation [6]. Among AOPs, the electro-Fenton (EF) process is an effective method to combine hydroxyl radicals ($OH^{\bullet}$) produced in the Fenton reaction with electrochemistry [7]. In classical EF process (Fig. 1), reaction mechanism for the formation of $OH^{\bullet}$ can be described as follows:

$$Fe^{2+} + H_2O_2 \rightarrow Fe^{3+} + HO\bullet + OH^- \quad (1)$$

Fe^{3+} can be reduced to Fe^{2+} via Eqs. (2) and (3).

$$Fe^{3+} + H_2O_2 \rightarrow Fe^{2+} + HO\bullet_2 + H^+ \quad (2)$$

$$Fe^{3+} + HO\bullet_2 \rightarrow Fe^{2+} + O_2 + H^+ \quad (3)$$

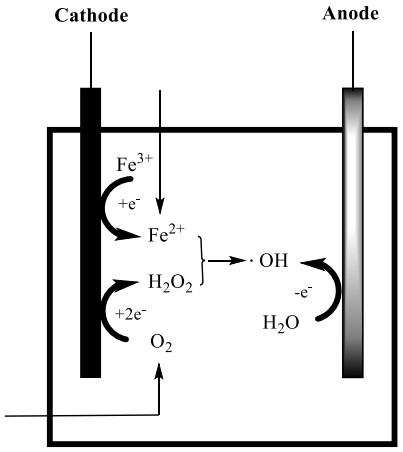

FIGURE 1
Schematic representation of EF process

However, the limitations of EF applications is the low concentration of H_2O_2 which produced by O_2 dissolved in the solution ($O_2 + 2e^- + 2H^+ \rightarrow H_2O_2$). Therefore, gas diffusion cathode (GDC) has been used to accelerate oxygen diffusion and enhance the availability of H_2O_2 [8]. Carbon and PTEF-based GDC has been applied to remove refractory organics from solutions in the EF process [9]. Response surface methodology (RSM) has been applied to model and optimize several wastewater treatment processes including adsorption [10, 11], Fenton's oxidation [12] and photocatalytic decolorization processes [13]. In this study, the RSM was used to study the influence of experimental parameters (Fe^{2+} concentration, initial pH and cathodic potential) on the degradation efficiency of DMP by EF process. The degradation efficiency was selected as the response for optimiza-

tion and the functional relationship between the response and the most significant independent variables (factors) was established by means of experimental design. All the parameters are simultaneously applied in order to calculate their relative effect.

MATERIALS AND METHODS

Chemicals. Dimethyl phthalate (DMP), was chosen as the model compound and used without further purification. Analytical grade sulfuric acid, anhydrous sodium sulfate, sodium hydroxide and ethanol polytetrafluoroethylene (PTFE) solution and XC-72 carbon were obtained from Aladdin Industrial Corporation, Shanghai, China.

Preparation of XC-72 Carbon/PTFE Gas Diffusion Electrode. Appropriate amounts of XC-72 Carbon (0.1 g), PTFE (0.42 g), distilled water (60 ml) and ethanol were mixed in an ultrasonic bath for 10 min to create a highly dispersed mixture. The resulting mixture was heated at 80 ℃ until it resembled an ointment in appearance. The ointment was bonded to 50% PTFE-loaded carbon papers and sintered at 350 ℃ for 30 min under inert conditions (N_2). The resulting plate was then cut to obtain operational plates XC-72 Carbon–PTFE plates of 25 mm diameter and about 0.6 mm thickness.

Experimental procedure. Fig. 2 shows the schematic illustration of the experimental set-up. The experiments were conducted at room temperature in an open glass cell of 1L capacity and performed at constant current. O_2 was fed onto the anode surface at a flow rate of 400 mL min^{-1}. The degradation ratio of DMP was measured at 120 minutes after the processes started.

Analytical methods. The pH of solution was measured by Mettler-Toledo FE20 pH meter (Mettler-Toledo Instruments Co., Ltd., Shanghai). DMP was quantified by high performance liquid chromatography (LC-20AT/SPD-M20, SHIMADZU, Japan). The column temperature was maintained at 30℃, and keeping the sample loop volume at 20 μL. The concentration of DMP was determined by HPLC with the detection wavelength of 276 nm, which is the maximum adsorption of DMP. A mixture of acetonitrile and water at a ratio of 50:50 (v/v) at a flow rate of 1.0 mL • min^{-1} was used as the mobile phase. Before taking HLCP test, the sample removed from reactor was quenched with HLCP-grade methanol to prevent further degradation.

The selection of actual values of variable levels for central composite design (CCD). The performance of photo-Fenton process is closely related to the Fe^{2+} concentration, cathodic potential, and pH of the experimental solution. A series of experiments were carried out at different Fe^{2+} concentration from 0.2 to 0.6mM while the initial pH from 1 to 5, cathodic potential were kept at -1.5V and -0.5 V, respectively. As shown in Fig. 3a, with the increasing concentration of Fe^{2+}, the degradation ratio of DMP ascends to a constant value. Hence, 0.2mM and 0.6mM of Fe^{2+} were chosen as the low and high level, respectively. As shown in Fig. 3b, the degradation ratio of DMP increases initially and then decreases with the increasing values of the pH [14]. Thus, 2.0 and 4.0 were chosen as the low and high level of pH, respectively. Keeping the initial pH=3.0 and the concentration of Fe^{2+} at 0.4 mM, experiments were proceeded with cathodic potential from -1.5 to -0.2.V. According to Fig. 3c, the degradation ratio of DMP rises at first, and then falls with the increasing cathodic potential.

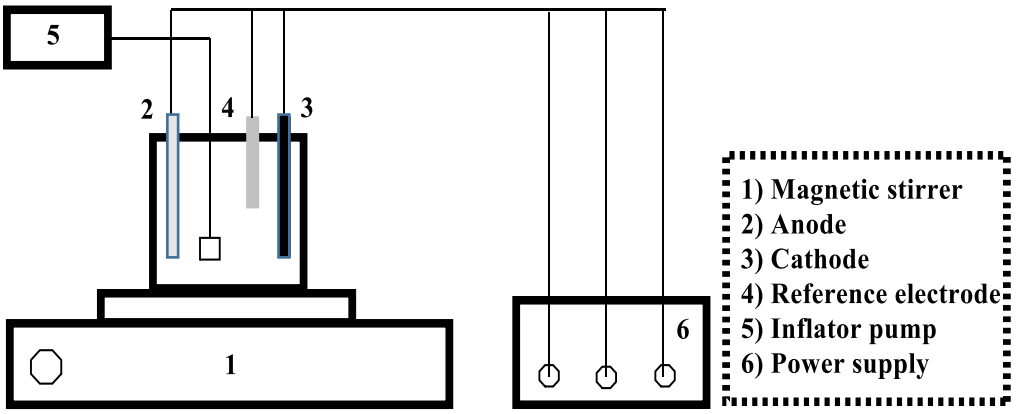

FIGURE 2
Schematic illustration of the experimental set-up.

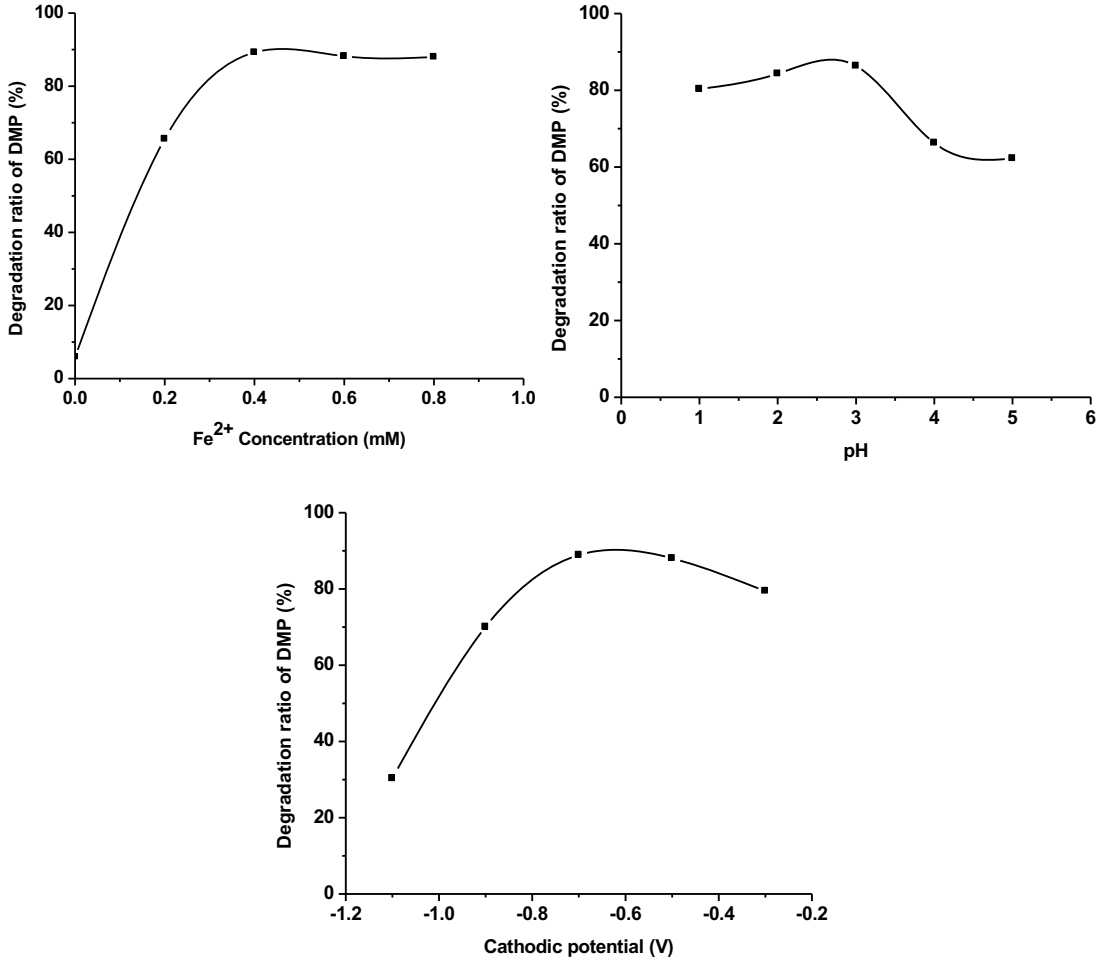

FIGURE 3
(a) Effect of Fe^{2+} concentration on the degradation of DMP; (b) Effect of initial pH on the degradation of DMP; (c) Effect of cathodic potential on the degradation of DMP.

TABLE 1
Levels of the independent variables for central composite design.

Variable	Symbol	Coded levels				
		-1.68	-1	0	1	1.68
Fe^{2+}concentraton	x_1	0.06	0.2	0.4	0.6	0.74
initial pH	x_2	1.32	2	3	4	4.68
Cathodic potential	x_3	-1.04	-0.9	-0.7	-0.5	-0.36

For passage from coded variable level to natural variable level, the following equations were used:
$X_1=(x_1-0.4)/0.2$; $X_2=(x_2-3)$; $X_3=(x_3+0.7)/0.2$,x_i refer to the actual values, X_i refer to the coded values

Central composite design (CCD). In order to investigate the effect of the three independent variables, namely, Fe^{2+} concentration (χ_1), initial pH (χ_2) and cathodic potential (χ_3) on the degradation of DMP, the following second-order polynomial response equation was used to correlate the dependent and independent variables:

$$Y=a_0+a_1X_1+a_2X_2+a_3X_3+a_{11}X_1^2+a_{22}X_2^2+a_{33}X_3^2+a_{12}X_1X_2+a_{13}X_1X_3+a_{23}X_2X_3$$

where Y is a response variable of the degradation ratio of DMP. a_i are regression coefficients for linear effects, a_{ii} the regression coefficients for squared effects, a_{ik} the regression coefficients for interaction effects, and xi are coded experimental levels of the variables.

The actual values of variable levels were selected based on the results provided above. The experimental ranges and the levels of the independent variables for DMP removal are given in Table 1. A total number of twenty experiments was employed for response surface modeling. The experimental results and predicted values for DMP removal efficiencies are presented in Table 2. The "Design expert" software (version 8.0) was used for regression analysis.

TABLE 2
The detail of experimental response and design of CCD with coded values.

No.	Variable levels/ coded values			Residual ratio/% (Y)	
	Fe^{2+} concentration (X_1)	initial pH (X_2)	Cathodic potential (X_3)	Observed	Predicted
1	-1	-1	-1	82.33	79.46
2	1	-1	-1	71.94	71.13
3	-1	1	-1	72.17	74.51
4	1	1	-1	61.95	68.76
5	-1	-1	1	32.24	27.72
6	1	-1	1	21.88	21.84
7	-1	1	1	92	95.1
8	1	1	1	86.65	91.81
9	-1.68	0	0	82.15	84.42
10	1.68	0	0	80.15	74.64
11	0	-1.68	0	21.85	27.86
12	0	1.68	0	91.78	82.53
13	0	0	-1.68	82.17	80.02
14	0	0	1.68	56.98	55.89
15	0	0	0	87.1	88.5
16	0	0	0	91.49	88.5
17	0	0	0	81.23	88.5
18	0	0	0	89	88.5
19	0	0	0	90.6	88.5
20	0	0	0	91	88.5

TABLE 3
ANOVA for response surface reduced quadratic model.

Source	F-value	Prob-F	
model	30.1	<0.0001	Significant
Lack of Fit	3.76	0.0863	Not Significant

RESULTS AND DISCUSSION

Characterization of XC-72 Carbon/PTFE Gas Diffusion Electrode. In Fig. 4, the morphology of XC-72 Carbon/PTFE Gas Diffusion Electrode was determined by scanning electron microscopy (SEM, JSM-6330F, Japan electron optics laboratory CO., LTD).

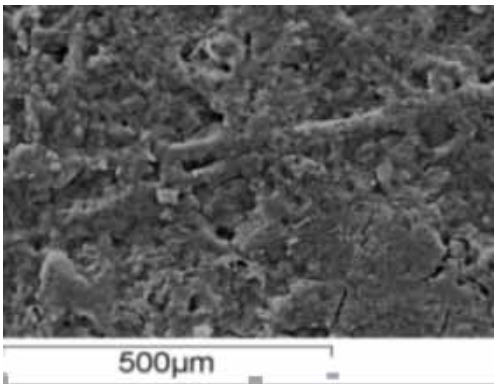

FIGURE 4
SEM of XC-72 Carbon/PTFE Gas Diffusion Electrode.

Model evaluation according to analysis of variance (ANOVA) and data analysis. Based on these results, an empirical relationship between the response and independent variables was attained and expressed by the following second-order polynomial equation:

$$Y=88.5-2.91X_1+16.25X_2-7.17X_3+0.65X_1X_2+0.61X_1X_3+18.09X_2X_3-3.17X_{12}-11.77X_{22}-7.26X_{32}$$

The relative contribution of the three variables to the degradation ratio of DMP (y) was directly measured by the respective coefficient in the fitted model. As indicated in Table 3, analysis of variance (ANOVA) of this model was given. The model "F-value" of 30.1 implies the model is significant. Values of "Prob-F" less than 0.0500 indicate model terms are significant. Values greater than 0.1000 indicate the model terms are not significant. The value of "Prob-F" in this model is far less than 0.0001 (<0.0001), implying the terms in this model are significant. The "Lack of Fit F-value" of 3.76 implies the "Lack of Fit" is not significant relative to the pure error. There is a 8.63% chance that a "Lack of Fit F-value" of that large could occur due to noise.

According to Table 4, the value of "R-Squared" and "Adj R-Squared" are 0.9644 and 0.9324, respectively, which indicate that the quadratic model have a satisfactory adjustment with experimental data.

The "C.V." (coefficient of variance) is used to measure the reproducibility of the model. In general, a model can be considered reasonably reproducible if the value of "C.V." is not bigger than 10% [15]. "Adeq Precision" measures the signal to noise ratio. A ratio greater than 4 is desirable. The ratio of 17.39 indicates an adequate signal. This model can be used to navigate the design space. The value of "Std. Dev." (5.96) and "Press" (2240.88) also illustrate that the quadratic model is reliable.

TABLE 4
Statistic summary of this quadratic model.

Variable of model	Values
R-Squared	0.9644
Adj. R-Squared	0.9324
Std. Dev	5.96
C.V. (Coefficient of variance) / %	8.13
Adeq. precision	17.39
Press	2240.88

In addition to regression coefficient, the adequacy of the models was also evaluated by the residuals (difference between the observed and the predicted response value). the Normal probability plot (Fig. 5a), internally studentized residuals versus predicted value plot (Fig. 5b) and predicted values of degradation ratio vs. experimental points plot (Fig. 5c) were given. According to Fig. 4a, the linear shape plot indicates that the residuals follow a normal distribution and there is no need for transformation of response. The random scatter of residues suggests that the variance of original observation is constant for all values of the response, as shown in Fig. 5b. In Figure 5c, all points are distributing relatively near to the regression, indicating that the predicted values of degradation ratio are in good agreement with the experimental ones. Results confirm that the experimental values are in good agreement with the predicted values.

Response surface for electro-Fenton treatment of DMP. The response surface of the model-predicted responses, while one variable kept at constant and the others varying within the experimental ranges, were obtained by the "Design expert" software (version 8.0) and utilized to assess the interactive relationships between the process variables and treatment outputs for electro-Fenton treatment of DMP. As can be seen from Fig. 6, the highest degradation efficiency (>93%) occurred when Fe^{2+} concentration was kept at about 0.5mM. The degradation efficiency decreased with an increasing Fe^{2+} concentration. The initial pH and cathodic potential have a influence on the degradation efficiency.

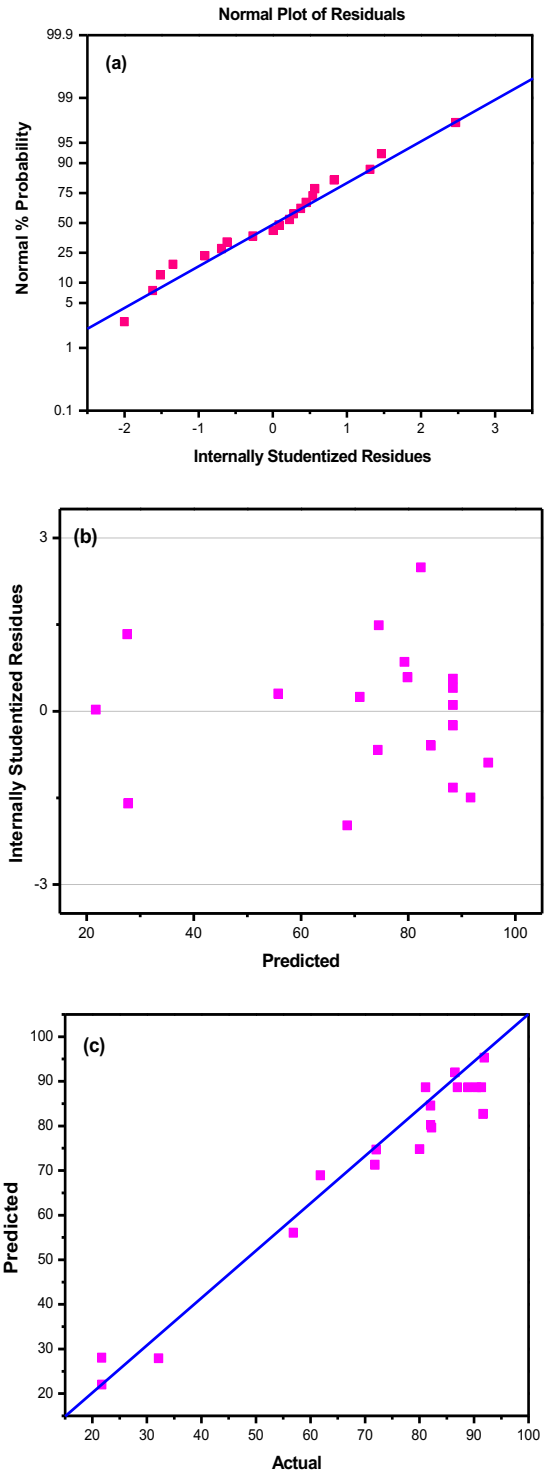

FIGURE 5
(a) Normal % probability vs. internally studentized residuals for the degradation of DMP; (b) internally studentized residuals vs. predicted value plot; (c) Predicted vs. actual plot for degradation efficiency.

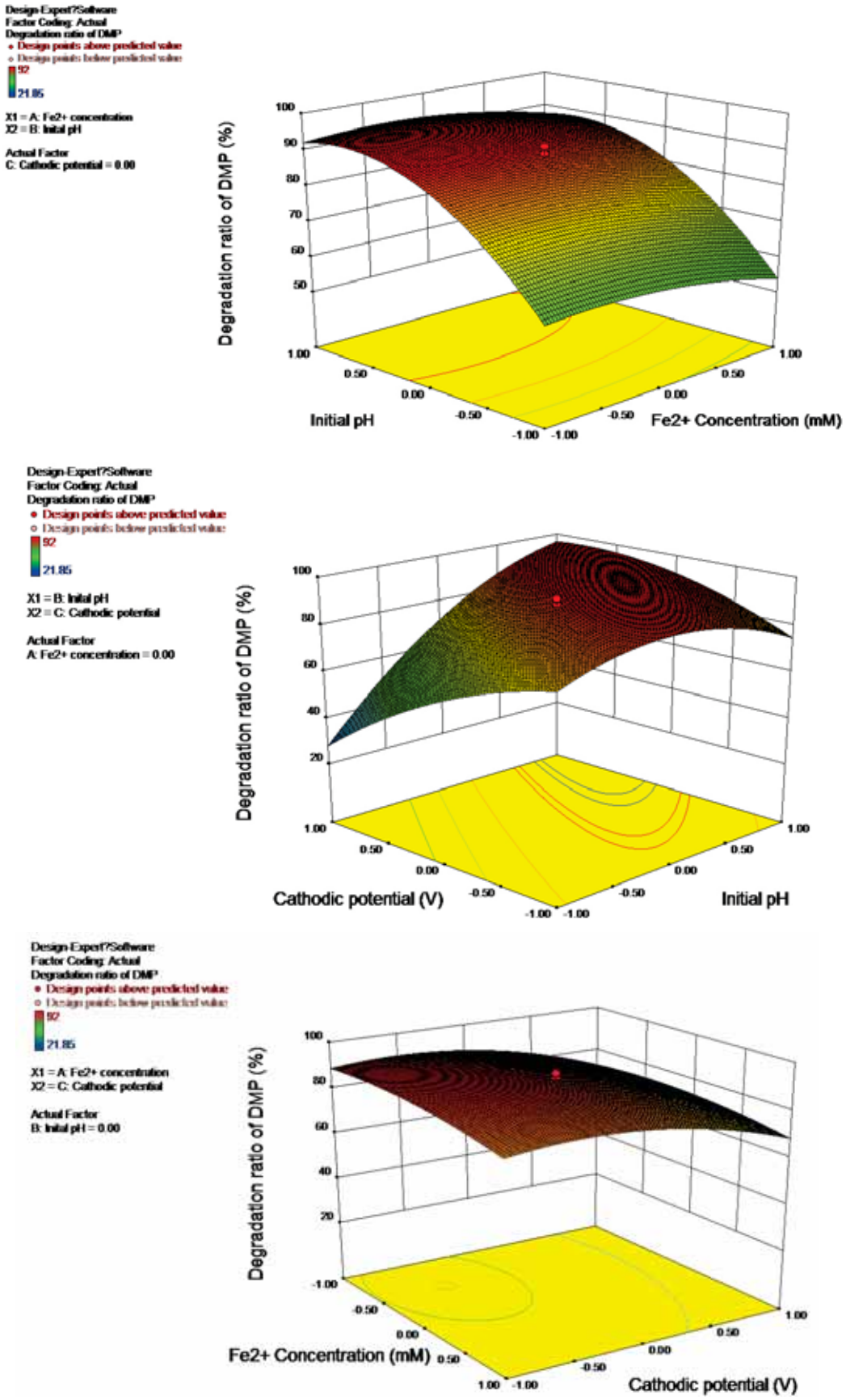

FIGURE 6
The dependence of DMP removal on (a) initial pH and Fe^{2+} concentration; (b) initial pH and cathodic potential; (c) Fe^{2+} concentration and potential

Optimization of DMP degradation. The desired goal in term of decolorization efficiency was defined as "maximize" to achieve highest treatment performance. The optimum values of the process variables for the maximum DMP efficiency are shown in Table 5. As is shown in Fig. 7, degradation ratio of DMP decreased to 40% with reused after 5 times reused.

TABLE 5
Optimum operating conditions of the process variables for complete decolorization efficiency.

Variables	Optimum value
Fe^{2+} concentration (mM)	0.49
initial pH	3
cathodic potential (v)	-0.55

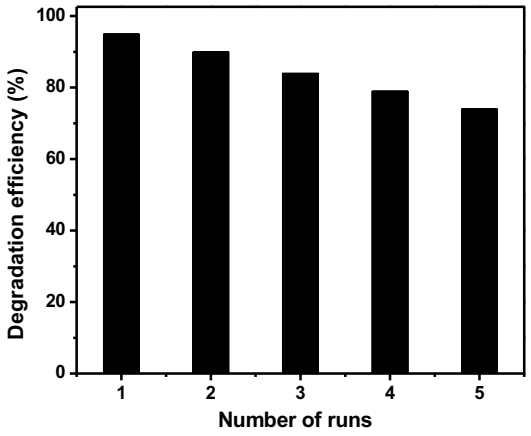

FIGURE 7
Bar charts of the degradation ratio of DMP vs. used times.

CONCLUSIONS

The experimental design methodology was used to study the influence of experimental parameters (Fe^{2+} concentration, initial pH and cathodic potential) on the degradation efficiency of DMP by electro-Fenton. Based on the experimental results, an empirical relationship between the response and independent variables was attained and expressed by the second-order polynomial equation. ANOVA showed a high coefficient of determination value (R^2=0.9644), thus, ensuring a satisfactory adjustment of the second-order regression model with the experimental data. The optimal condition for treatment of DMP was determined. Keeping initial pH=3, the concentration of Fe^{2+} at 0.49mM, the cathodic potential at -0.55V, degradation ratio of DMP could reach to the maximum. With high recyclability, Vulcan XC-72 carbon gas diffusion electrode could be reused for over 5 times.

ACKNOWLEDGEMENTS

This work was supported by the Natural Science Foundation of China (21077136, 50978260) and the Fundamental Research Funds for the Central Universities of China.

REFERENCES

[1] Yuan, B.L., Li, X.Z., Graham, N. (2008) Aqueous oxidation of dimethyl phthalate in a Fe(VI)-TiO2-UV reaction system. Water Research. 42(6-7), 1413-1420.
[2] Yuan, B.L., Li, X.Z., Graham, N. (2008) Reaction pathways of dimethyl phthalate degradation in TiO2-UV-O-2 and TiO2-UV-Fe(VI) systems. Chemosphere. 72(2), 197-204.
[3] Julinova, M. and Slavik, R. (2012) Removal of phthalates from aqueous solution by different adsorbents: A short review. Journal of Environmental Management. 94(1), 13-24.
[4] Heudorf, U., Mersch-Sundermann, V. and Angerer, J. (2007) Phthalates: Toxicology and exposure. International Journal of Hygiene and Environmental Health. 210(5), 623-634.
[5] Jurewicz, J. and Hanke, W. (2011) Exposure to Phthalates: Reproductive Outcome and Children Health. a review of epidemiological studies. Internal Journal of Occupational Medicine and Environmental Health. 24(2), 115-141.
[6] Vilhunen, S. and Sillanpää, M. (2010) Recent developments in photochemical and chemical AOPs in water treatment: a mini-review. Reviews in Environmental Science and Biotechnology. 9(4), 323-330.
[7] Ren, G., Zhou, M., Liu, M. (2016) A novel vertical-flow electro-Fenton reactor for organic wastewater treatment. Chemical Engineering Journal. 298, 55-67.
[8] Luo, H., Li, C., Wu, C. and Dong, X. (2015) In situ electrosynthesis of hydrogen peroxide with an improved gas diffusion cathode by rolling carbon black and PTFE5. Rsc Advances. 5(80), 65227-65235.
[9] Luo, H., Li, C., Wu, C., Zheng, W. and Dong, X. (2015) Electrochemical degradation of phenol by in situ electro-generated and electro-activated hydrogen peroxide using an improved gas diffusion cathode. Electrochimica Acta. 186, 486-493.
[10] Annadurai, G., Juang, R.S., Lee, D.J. (2002) Factorial design analysis for adsorption of dye on activated carbon beads incorporated with calcium alginate. Advances in Environmental Research. 6, 191-198.

[11] Mohapatra, H., Gupta, R. (2005) Concurrent sorption of Zn(II), Cu(II) and Co(II) by Oscillatoria angustissima as a function of pH in binary and ternary metal solutions. Bioresource Technology. 96(12), 1387-1398.
[12] Ahmadi, M., Vahabzadeh, F., Bonakdarpour, B., Mofarrah, E., Mehranian, M. (2005) Application of the central composite design and response surface methodology to the advanced treatment of olive oil processing wastewater using Fenton's peroxidation. Journal of Hazardous Materials. 123(1-3), 187-195.
[13] Liu, H.L., Chiou, Y.R. (2005) Optimal decolorization efficiency of Reactive Red 239 by UV/TiO2 photocatalytic process coupled with response surface methodology. Chemical Engineering Journal. 112, 173-179.
[14] Sun, Y., Pignatello, J.J. (1993) Photochemical reactions involved in the total mineralization of 2,4-D by iron(3+)/hydrogen peroxide/UV. Environmental Science and Technology. 27(2), 304-310.
[15] Beg, Q.K., Sahai, V. and Gupta, R. (2003) Statistical media optimization and alkaline protease production from Bacillus mojavensis in a bioreactor. Process Biochemistry. 39(2), 203-209.

Received: **20.11.2017**
Accepted: **05.03.2018**

CORRESPONDING AUTHOR

Jianwei Guo
School of Chemical Engineering & Light Industry,
Guangdong University of Technology,
Guangzhou 510006 – China

e-mail: guojw@gdut.edu.cn

© by PSP Volume 27 – No. 7/2018 pages 4777-4781 Fresenius Environmental Bulletin

ENHANCING 37.5% EFFICIENCY IN REMOVING COD FROM PURIFIED TEREPHTHALIC ACID (PTA) WASTEWATER VIA THE MICROBIAL ACTIVATION TECHNIQUE BASED ON THE CONVENTIONAL AOO METHOD

Jingmei Yuan, Zhanping Gao, Hui Cao*

China Electric Environmental Protection Co., Ltd., Nanjing 211102, P.R. China

ABSTRACT

We report the pilot test by using the microbial activation technique at the second stage of the original contact oxidation tank on the basis of the conventional AOO method in treating PTA wastewater. It is proven that the COD in the effluent drops from 80 to 50 mg L^{-1}, which is about 37.5% enhancement in efficiency. Three cases with the inflow of 0.5, 1.0, and 2.0 $m^3 h^{-1}$ were investigated. Our test indicates that the COD of effluent that is less than 50 mg L^{-1} can be guaranteed when the volume load of COD is less than 0.4 kg m^{-3} d^{-1}. The mechanism of the microbial activation technique is discussed. Porous activated powders provide the large amount of surface for the growth of microbial agents, while the nutrient activated liquid greatly enhances the microbial activity in the local porous environment, facilitating the total oxidation of pollutant molecules in PTA wastewater.

KEYWORDS:
PTA, wastewater treatment, activated powder, activated liquid, COD, removal efficiency

INTRODUCTION

Purified terephthalic acid (PTA) has been widely used as an important raw material in petrochemical industry [1-3]. Generally, in PTA wastewater five aromatic compounds including 4-carboxybenzaldehyde, benzoic acid, p-toluic acid, phthalic acid, and acetic acidcontribute about 75% to the total chemical oxygen demand (COD), invoking serious environmental problems [4].

So far, many techniques such as anaerobic and aerobic biological treatment [5-7], advanced oxidation processes (AOP) [8], supercritical wateroxidation [9], ultrasound enhanced ozonation [10], electrocoagulation [11, 12], coagulation- flocculation [13], adsorption [14], membrane separation [15] and photocatalysis [16] have been used for the treatment of PTA wastewater. Among these methods, biodegradation technology has been widely studied and used with lower costs and considerable efficiencies.

In a petrochemical plant, PTA wastewater treated with the conventional AOO method cannot meet the new requirement for discharge. The existing treatment technique comprises of pretreatment, anaerobic, first-stage contact oxidation, intermediate sedimentation, second-stage contact oxidation, and the final sedimentation. With this PTA treatment technique, the COD in the outlet of the second-stage oxidation tank is about 80 mg L^{-1}.

In this work, we report the pilot test by using the microbial activation technique at the second stage of the original contact oxidation tank. The COD in the effluent reaches the level of lower than 50 mg L^{-1}, enhancing about 37.5% efficiency in removing COD from PTA wastewater.

METHODS

The pilot test flow block is shown in Figure 1. The outlet of the intermediate sedimentation is lifted to the tester, the outlet of which is discharged into the existing second-stage contact oxidation tank.

Test Equipments and Analytical Instruments. Test equipment includes lift pump, integrated biochemical pool, water collection tank, efflux pump, aeration fan, activated liquid dosing device, and activated powder dosing device. Detailed parameters refer to drawing (microbial activation technique test flow diagram).

Potassium dichromate titration includes 500 ml all-glass reflux unit, electric stove, 25 mL acid burette, and 500 ml conical flask.

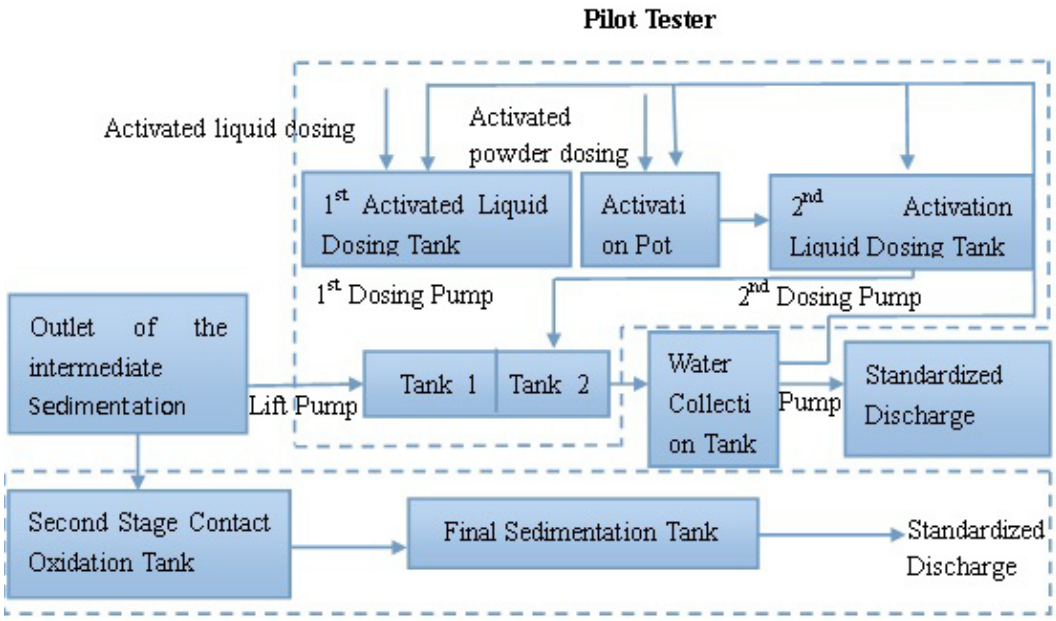

FIGURE 1
The scheme of pilot test flow block.

Other equipment includes the online COD instrument, PH instrument, thermometer, and flowmeter.

Agentia and materials. Relevant agentia includes Potassium dichromate standard solution, Ferroin indicator solution, ammonium ferrous sulfate standard solution, mercury sulfate, and digestive juice.

Test Procedure. Pre-test Preparation. Whether the positions of the inlet and outlet and the ways of water distribution and collection meet the requirement of the process design must be checked and verified.

Before formal working, aeration detection must be carried out. In detail, 1/4 to 1/3 capacity of the draught fan is delivered to the aeration pipe of microbial chemical pool, and check the quality of connection between all nodes located at the pipe, guaranteeing that there is no leakage anywhere.

Check all the places and their methods for fastening, guaranteeing the reliability.

Check the installation of aeration pipes and aerators, guaranteeing that they are located at the same horizontal plane with the error less than 1mm.

In the first operation, water level must be about 0.5 m higher than the aeration pipes and aerators, then start the draught fan to check whether the aeration pipes and aerators can work well. The system works perfectly when the air volume is large, the bubble is fine, and the tumbling is even.

Microbe culture. In activation pot. Add 350 g activated powders and 3.5 g activated liquid in 350 L activation pot with full water. The culture finishes after continuous aeration for 72 hours (the diffusion velocity of the bubble emerging from water is 15 ~ 30 cm s^{-1}).

In tank 1. Start the agitator with 10 m^3 water in tank 1 and add 3 kg activated powders (300 mg L^{-1}) and 100 g activated liquid (10 mg L^{-1}) in it. After 72 hours, another 3 kg activated powders are added and begin to fill water with the inflow of 5 m^3 d^{-1}. At the same time the activated liquid are added with the concentration of 5 mg L^{-1} corresponding to the inflow. When tank 2 is full the agitator is started.

In tank 2. The effective volume of tank 2 is about 16.5 m^3. And the dissolved oxygen is controlled by air inflow of aeration with the concentration of 2~3 mg L^{-1} detected in 2 hours. Then 6 kg activated powders (about 1000 mg L^{-1}) and 60 kg activated liquid (about 10 mg L^{-1}) are added into tank 1 and aerates for 48 hours. Afterwards, the inflow is set as 0.5 m^3 h and the activated liquid (10 mg L^{-1}) is added from the inlet of tank 1. At the same time, the microbe cultured in the activation pot is also added evenly with the dosage of 1/3 volume of the activation pot per day (it is suggested that the microbe is first diluted in another pot and added with a dosing pump). 1/3 volume water, 110 g activated powders, and 1.1 g activated liquid are supplemented in the activation pot.

At the initial stage, the inner recycle is performed. The effluent discharges when the COD stabilizes. The inflow maintains at the level of 0.5 m^3h^{-1} until the COD in effluent meets the design value. Then, the inflow is adjusted to 1.0 m^3 h^{-1} and

performs the same procedure. The test finishes when the inflow reaches 2.0 m^3 h^{-1} and COD in effluent meets the design value.

RESULTS AND DISCUSSION

Twenty eight days after the microbe culturing, the inflow, the quality of inflow and effluent, the dosage, and the actual volume load are recorded corresponding to different inflow of 0.5, 1.0, and 2.0m^3 h^{-1} respectively.

When the inflow is 0.5 m^3 h^{-1}, the dosage of activated powders and liquid and the online COD in the inflow and effluent are shown in Figure 2. The dosage of activated powders and liquid is fixed at the level of 10 mg L^{-1} and 20 mg L^{-1}. It can be seen that the COD in the effluent locates between 39 and 49 mg L^{-1} when the COD in inflow is between 226 and 363 mg L^{-1}. Although the COD in the inflow fluctuates in a large scale, the COD in the effluent distributes in a very narrow region. This indicates that the system has an efficient impact resistance.

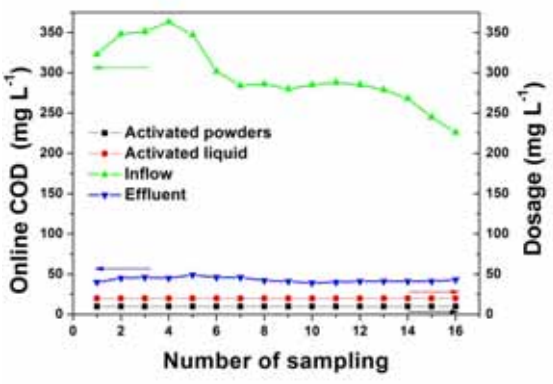

FIGURE 2
Dosage of activated powders and liquid and the online COD in the inflow and effluent when the inflow in 0.5 m^3 h^{-1}.

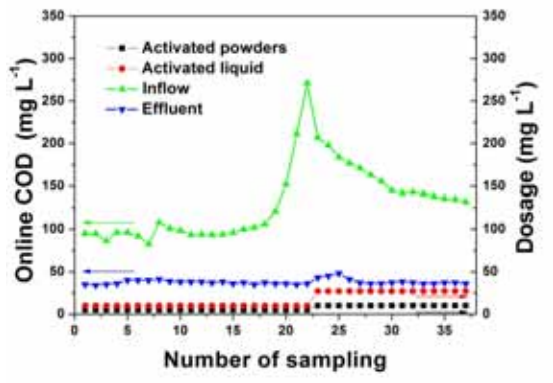

FIGURE 3
Dosage of activated powders and liquid and the online COD in the inflow and effluent when the inflow in 1.0 m^3 h^{-1}.

Figure 3 shows the case of the inflow of 1.0 m^3/h. The COD in effluent increases slightly when the COD in the inflow increases dramatically but with an apparent delay. However, the COD in the effluent remains to be lower than 50 mg L^{-1}. The COD in effluent returns smoothly to the equilibrium value of about 37 mg L^{-1} when the COD in inflow drops down. At the highest value of COD in inflow we increase the dosage of activated powders from 5 to 10 mg L^{-1} and that of activated liquid from 10 to 27 mg L^{-1}. But this change in dosage of activated powders and liquid seems to be of no effect on reducing the COD in effluent.

Figure 4 shows the case of the inflow of 2.0 m^3 h^{-1}. The dosage of activated powders and liquid are 10 mg L^{-1} and 27 mg L^{-1} respectively. When the COD in inflow is between 124 and 134 mg L^{-1}, the COD in effluent is no more than 50 mg L^{-1}.

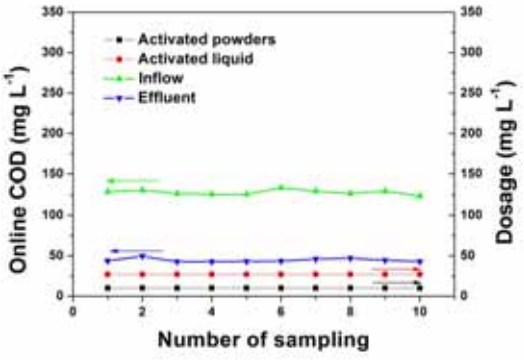

FIGURE 4
Dosage of activated powders and liquid and the online COD in the inflow and effluent when the inflow in 2.0 m^3 h^{-1}.

When the volume load is lower than 0.4 kg m^{-3} d^{-1}, the COD is lower than 50 mg L^{-1}. Compared to the conventional AOO method the COD removal efficiency by using the microbial activation technique has an enhancement of 37.5%.

Mechanism of improving the removal efficiency of COD in PTA wastewater. In the early anaerobic biological treatment, macromolecular or insoluble organic materials have been decomposed into small organic molecules, which are in favor of the growth of filamentous bacteria in the next aerobic biological treatment. However, the overgrowth of filamentous bacteria can cause the serious sludge bulking. One effective method in controlling the filamentous sludge bulking is to take the bio-contact oxidation technique, which effectively reduces the overgrowth of the free-floating filamentous bacteria in the tank [17].

In our microbial activation technique, activated powders are the porous materials similar to the activated carbon, providing great amount of surface for the growth of filamentous bacteria. Moreover, the porous activated powders can effectively adsorb

small organic molecules. Thus, the porous activated powders provide the local bacteria- and pollutant-rich environment at the same time, which can greatly enhance the oxidation efficiency.

To maintain the the local rapid oxidation process, it is necessary to provide nutrients for the continuous growth of microbial agents. In our research, it is found that the mole ratio of C: N: P = 100: 5: 1 in the activated liquid can effectively enhance the microbial activity, facilitating the total oxidation reaction of the small pollutant molecules.

CONCLUSIONS

Firstly, when the COD of inflow is less than 363 mg L^{-1}, the COD of effluent is less than 50 mg L^{-1}. The efficiency in removing COD rises about 37.5%, compared with the old existing system. Secondly, the COD of effluent does not decrease apparently when the concentration of activated powders and liquid increases. Thirdly, when the inflow is 2 m^3 h^{-1} and its COD is between 100 and 200 mg L^{-1}, the COD of effluent is the lowest with the value between 37 and 40 mg L^{-1}.

Therefore, there is no influence on the COD of effluent when dosage doubles. When the COD of inflow fluctuates between 83 and 363 mg L^{-1}, the final COD of effluent drops to less than 50 mg L^{-1}. Our test indicates that the COD of effluent that is less than 50 mg L^{-1} can be guaranteed when the volume load of COD is less than 0.4 kg m^{-3} d^{-1}.

Apart from the porous activated powders that provide the large amount of surface for the growth of microbial agents, appropriate mole ratio of nutrient elements of Carbon, Nitrogen, and Phosphorus (100: 5: 1) is important for the enhancement of microbial activity in PTA wastewater.

ACKNOWLEDGEMENTS

We gratefully acknowledge the financial support by the National Natural Science Foundation of China (Grant No 21473092).

REFERENCES

[1] Daramola, M.O., Aransiola, E.F., Adeogun, A.G. (2011) Comparative study of thermophilic and mesophilic anaerobic treatment of purified terephthalic acid (PTA) wastewater. Nat. Sci. 3(5), 371-378.

[2] Lee, Y.S., Han, G.B. (2016) Application of sequential expanded granular sludge bed reactors for biodegradation of acetate, benzoate, terephtalate and p-toluate in purified terephtalic acid production wastewater. Environ. Technol. 37(9), 1141-1150.

[3] Ma, K.L., Wang, K., Ren, Y.H., Chu, Z.R., Zhang, J. (2017) Role of temperature on microbial community profiles in an anaerobic bioreactor for treating PTA wastewater. Chem. Eng. J. 308, 256-263.

[4] Dükkanci, M., Gündüz, G., Ezdesir, A., Aykac**,** H. (2016) Application of several advanced oxidation processes for the destruction of organics in effluents of PTA production. Anadolu Univ. J. of Sci. and Technology – A – Appl. Sci. and Eng. 17(2), 233-249.

[5] Pophali, G.R., Khan, R., Dhodapkar, R.S., Nandy, T., Devotta, S. (2007) Anaerobic-aerobic treatment of purified terephthalic acid (PTA) effluent; a techno-economic alternative to two-stage aerobic process. J. Environ. Manage. 85(4), 1024-1033.

[6] Joung, J.Y., Lee, H.W., Choi, H., Lee, MW., Park, J.M. (2009) Influences of organic loading disturbances on the performance of anaerobic filter process to treat purified terephthalic acid wastewater. Bioresour. Technol. 100(8), 2457-61.

[7] Chen, Y., Zhao, J., Li, K., Xie, S. (2016) A novel fast mass transfer anaerobic inner loop fluidized bed biofilm reactor for PTA waste-water treatment. Water Sci. Technol. 74(5), 1088.

[8] Brillas, E., Cabot, P.L., Rodríguez, R.M., Arias, C., Garrido, J.A., Oliver, R. (2004) Degradation of the herbicide 2,4-DP by catalyzed ozonation using the O 3 /Fe 2+ /UVA system. Appl. Catal. B. 51(2), 117-127.

[9] Park, T.J., Lim, J.S., Lee, Y.W., Kim, S.H. (2003) Catalytic supercritical water oxidation of wastewater from terephthalic acid manufacturing process. J. Supercrit. Fluids. 26(3), 201-213.

[10] Rong, F., Liu, J., Qiu, Y., Wu, W. (2011) Study on the treatment of PTA productive wastewater using ultrasound enhanced ozonation. Third International Conference on Measuring Technology and Mechatronics Automation. IEEE Computer Society. 586-588.

[11] Garg, K.K., Prasad, B. (2016) Treatment of multicomponent aqueous solution of purified terephthalic acid wastewater by electrocoagulation process: Optimization of process and analysis of sludge. J. Chin. Inst. Chem. Eng. 60, 383-393.

[12] Garg, K.K., Prasad, B., Srivastava, V.C. (2014) Comparative study of industrial and laboratory prepared purified terephthalic acid (PTA) waste water with electro-coagulation process. Sep. Purif. Technol. 128(19), 80-88.

[13] Karthik, M., Dafale, N., Pathe, P., Nandy, T. (2008) Biodegradability enhancement of purified terephthalic acid wastewater by coagulation-flocculation process as pretreatment. J. Hazard. Mater. 154(1–3), 721-730.
[14] Khachane, P.K., Heesink, A.B.M., Versteeg, G.F., Pangarkar., V.G. (2003) Adsorptive Separation and Recovery of Organic Compounds from Purified Terephthalic Acid Plant Effluent. Sep. Sci. Technol. 38(1), 93-111.
[15] Memon, N.A., Ahmedb, N., Ismaila, S., Jalbania, N., Asghara, U., Ayazb, T., Beguma, R. (2016) Removal of COD in Purified Terephthalic Acid (PTA) Effluent with Coagulation, Aqueous Oxidation and High Porosity Membrane. Pak. J. Sci. Ind. Res. A: Phys. Sci. 59(3), 151-156.
[16] Chen, Y., Wan, H., Han, M., Guan, G. (2009) Photocatalytic Degradation of Organic Pollutants in Purified Terephthalic Acid Wastewater with Activated Carbon Supported Titanium Dioxide. International Conference on Energy and Environment Technology. IEEE Computer Society. 658-661.
[17] Li, G., Shen, L.X. (1995) Pure terephthalic acid wastewater treatment. China Biogas. 13(4), 1-6.

Received: **21.11.2017**
Accepted: **29.04.2018**

CORRESPONDING AUTHOR

Hui Cao
China Electric Environmental Protection Co., Ltd., Nanjing 211102 – P.R. China

e-mail: yccaoh@hotmail.com

© by PSP Volume 27 – No. 7/2018 pages 4782-4788 Fresenius Environmental Bulletin

SPATIAL VARIABILITY IN WATER QUALITY AND RELATIONSHIPS WITH LAND USE IN A COAL-MINING SUBSIDENCE AREA OF CHINA

Li Xiang[1,2], Liugen Zheng[1], Hua Cheng[1,*]

[1]School of Resource and Environment Engineering, Anhui University, Hefei 230601, The People's Republic of China
[2]Department of Environment and Energy Engineering, Anhui Jianzhu University, 230601, Hefei, The People's Republic of China

ABSTRACT

The heavy metal and nutrient contents of surface water were determined in an area affected by coal mining-related subsidence. Samples were collected from sites (n = 42) in the Huainan region of China, and the sources of pollution were also investigated. The concentrations of several pairs of metals were correlated (P-As, Cu-Ni, and Fe-Mn), indicating that they originated from same source. This was substantiated by analysis of spatial distribution, which found that two pairs of metals (Cu-Ni and Fe-Mn) had similar distributions. Principal component analysis indicated that three components explained 70% of the total variance in water quality, being N, P-As, and Cd-Pb. The Water Quality Integrative Pollution Index and the land use type of each sampling site were obtained, and correlations between them were observed.

KEYWORDS:
Coal mine, metal pollution, land use, Huainan, subsidence

INTRODUCTION

The Huainan mining area has one of the thirteen largest coal reserves in China and is its sixth-largest electricity producer. It is rich in good quality coal and has a large capacity for production [1]. While mining has undoubtedly brought wealth and employment, it has simultaneously caused extensive environmental degradation and disruption to society's traditional values [2]. The environmental challenges include damage to hydrological systems, mining waste disposal, and air pollution [3]. Additionally, the excavation of coal seams has caused extensive land subsidence. Where subsidence has exceeded the depth of the water table, groundwater has inundated the land and formed perennial waterlogged zones [4].

Coal mining processes are also regarded as the main anthropogenic source of heavy metals. Heavy metals in coal or coal gangue can be released by many processes, including weathering, washing, leaching, and combustion. Besides metals, nutrients (nitrogen and phosphorous) are also carried into subsident land by rainfall runoff [5, 6]. Eutrophication within these waters is the most important environmental issue in this region [7].

Over the last few decades, trace metal mobility and partitioning in the soils and sediments of coal mining areas has received intense attention because of the potentially great hazards it poses to the ecosphere and to humans [8-14]. However, in spite of prolific mining activities, little information is available from Huainan on trace metal pollution and its fate in surface waters. Until now, there has been limited recognition of the pollution of water bodies caused by subsidence. The objectives of the present work were to (1) assess water quality in terms of several standards; (2) evaluate the spatial distribution of heavy metals across the sampling area; (3) explore trace element sources by multivariate statistics; and (4) determine the relationship between water quality and land use types. The results will be useful for improving water management practices.

MATERIALS AND METHODS

Sampling and Analysis. The study area encompasses the city of Huainan and extends to the city of Fuyan in western Anhui Province. From west to east, the area spans longitudes 116°14'38.19" to 116°53'05.67" E, while from south to north it spans latitudes 32°36'10.49" to 32°51'59.42" N. The study was conducted during December in 2016. Samples from 42 sites were used to assess water quality in subsidence areas of Huainan, Anhui Province (Figure 1).

The total phosphorous (TP), total nitrogen (TN), and ammonia nitrogen (NH_3-N) contents of the water samples were determined by following Chinese standard methods [15, 16]. Water TP was analyzed by the ammonium molybdenum ascorbic acid method, with water samples digested using mixed,

concentrated, nitric and perchloric acids. The concentrations of TN in water samples were analyzed using the UV spectrophotometric method after pretreatment by alkaline potassium persulfate oxidation. The NH_3-N concentrations were measured by Nessler's reagent spectrophotometry method. Dissolved trace heavy metals were measured by inductively-coupled plasma-atomic emission spectrometry (ICP-AES, Perkin Elmer). To ensure quality control, each batch of samples was assessed with detection standard reference material and spiked samples. All analyses were conducted in triplicate to increase the robustness of the results.

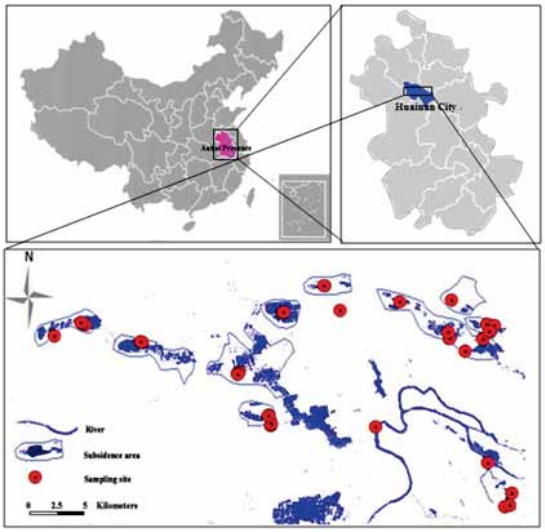

FIGURE 1
Map of the study area and sampling sites

Statistics Methods. Principal component analysis (PCA) was employed to explore the possible sources of trace elements. This involved reducing the dataset's dimensions to exclude less influential factors and was conducted as described in [17]. A Pearson correlation coefficient matrix was constructed with the investigated elements to assess the extent of the inter-metallic relations. All data analysis was conducted using SPSS 16.0 software**.**

Water Quality Integrative Pollution Index (WQI). Water quality was assessed according to the water quality integrative pollution index, which is an indicator of comprehensive water quality Before calculating the WQI, the dataset was first standardized to avoid the numerical ranges of the original variables by *z*-scale transformation, as follows [18]:

$$Z_{ij} = \frac{x_{ij} - \overline{x_j}}{S_j} \; i = 1, 2, \ldots, \; n; j = 1, 2, \ldots, \; n \quad \ldots \text{Eq. (1)}$$

where, Z_{ij} stands for the normalized value of the j^{th} indicator at the i^{th} sampling site, the subscripts of x_{ij} represent the original value of the j^{th} indicator at the i^{th} sampling site, and $\overline{x_j}$ is average of the j^{th} indicator. Subscripts *i* and *j* are natural numbers. Three principal components were extracted with excellent cumulative in the present work. A principal component index (F_n) was calculated as:

$$F_{n\ (n=1,2,3)} = \sum C \times Z \times x_{ij} \ldots\ldots \text{Eq. (2)}$$

where F_n is the index of the principal component ranging from 1 to 3, and *C* is the component value from the component matrix. Then, the WQI value for each sampling site was calculated as F_n multiplied by the initial eigenvalues of each component [19]. Land use pattern analysis was performed via GIS spatial analysis technology using ArcGIS 10.1 for Desktop software. The buffer circle areas were set at radii of 1 and 5 km [20]. All contour maps of elemental and WQI distributions were drawn using Surface 10 software.

TABLE 1
Parameter characteristics of physicochemical and trace metals from 42 samples, and water quality standards for drinking water and surface water (μg/L)

	T (°C)	pH	TP	TN	NH_3-N	Cr	Mn	Fe	Ni	Cu	Zn	As	Cd	Hg	Pb
Mean	9.1	8.2	263.357	2027.12	961.205	14.373	33.427	382.193	10.392	10.289	103.257	3.503	0.039	0.623	1.592
SD	1.1	0.294	363.446	1055.514	535.583	22.914	33.687	259.06	24.808	27.029	201.934	3.783	0.018	0.764	0.703
Max	12.6	8.91	1470	4520	2676	103.323	155.665	1074.405	114.313	124.488	878.89	17.523	0.085	2.97	3.915
Min	7.1	7.44	26	735	250	5.71	9.507	155.498	0.98	2.193	10.39	0.593	0.013	0.11	0.84
Range	5.5	1.47	1444	3785	2426	97.613	146.158	918.908	113.333	122.295	868.5	16.93	0.073	2.86	3.075

[a.] Chinese drinking water standards.
[b.] Chinese surface water standards.

RESULTS AND DISCUSSION

Water Chemistry. Surface water was sampled at 42 subsidence sites. Descriptive statistics of its physical and physicochemical characteristics and its elemental concentrations are presented in Table 1. The concentrations of trace elements in the samples were low but detectable at all locations.

Of note are the concentrations of toxic metals found in the water bodies surrounding the mining area. The levels of Cr ranged from 5.71—103.323 μg/L with a mean ± SD of 14.373 ± 22.914. The large SD reflects the uneven distribution of Cr concentrations, with high levels detected at certain sites such as ZJ-01 (116º30′08.34" E, 32º45′46.97"N). As values varied from 0.593 to 17.523 μg/L with "mean ± SD" of "3.503 ± 3.783" μg/L, Cd mean concentration was 0.039 μg/L with SD of 0.018 μg/L. A minority of the samples (4 samples located near the Xinji area; 116º32′51.94"E, 32º41′58.71"N) were found to have Hg concentrations above the permissible limit (1μg/L) for drinking water (according to the GB 5749-2006 standard). The mean concentrations of trace elements Pb, Hg, and Cr were 21.20, 1.8, and 14.35 μg/L in the Datong mining subsidence area, and were 45.8, 2.1, and 14.9 μg/L in the Xie'er mining subsidence pool, respectively [21].

It is noteworthy that pH values ranged from 7.1—12.6 (mean ± SD = 9.102 ± 1.131) indicating that all samples were slightly alkaline. However, they were within the permissible range for all categories of the Chinese surface water quality standard GB 3838-2002. In general, the results suggest there is a higher rate of metal release into the sediment-water system at lower pH than at higher pH [22]. However, the association between pH and Zn and Cd metal concentrations was much weaker. Hence, acidification has not resulted in increased concentrations of Zn and Cd occurring in rivers [23].

Correlation Coefficient Analysis. A Pearson correlation analysis was used to provide some information on the relationships between trace metals and their common sources and pathways. [24] Results showed strong and statistically significant ($p < 0.05$) correlations between concentrations of As-P (r = 0.834), Cu-Ni (r = 0.984), and Pb-Cd (r = 0.686). This suggests that these elements originate from common or similar sources [25]. Also, significant but relatively moderate correlations were found between N-Mn (r = 0.41), Fe-Mn (r = 0.524), and Fe-Pb (r = 0.377), suggesting that the sources of these metals are linked to some extent (Table 2). The values of TN were the sum of NO_3-N, nitrite-nitrogen (NO_2-N), NH_3-N and organically-bonded nitrogen concentrations. This could explain the strong correlations between TN and NH_3-N concentrations (r = 0.733, $p < 0.01$).

Spatial Variability of Trace Elements. Based on their total mean concentrations, the elements were categorized into two grades divided by a 10.0 μg/L threshold. The more abundant elements were Fe, Mn and Zn (> 10.0 μg/L), while As, Cd, Hg and Pb were less abundant. Figure 2 illustrates the variation in heavy metal concentrations and their distribution across the sampling sites. The distributions of Ni and Cu were extremely similar. Meanwhile, Fe had three areas of high concentration and had a similar distribution to that of Mn, which was most concentrated at 32.7°0'0" N, 116.7°0'0" E. Based on the spatial distribution of 10 heavy metal elements, we conclude

TABLE 2
Correlation matrix of trace elements and physicochemical parameters.

	TP	TN	NH4	Cr	Mn	Fe	Ni	Cu	Zn	As	Cd	Hg	Pb
TP	1												
TN	0.389*	1											
NH4	0.149	0.733**	1										
Cr	-0.109	-0.285	-0.224	1									
Mn	0.197	0.410**	0.395**	-0.116	1								
Fe	0.025	0.084	0.182	0.347*	0.524**	1							
Ni	-0.086	-0.188	-0.193	0.006	-0.076	0.007	1						
Cu	-0.088	-0.19	-0.184	-0.003	-0.052	0.013	0.984**	1					
Zn	-0.117	0.001	0.004	-0.051	0.033	0.014	0.13	0.074	1				
As	0.834**	0.292	-0.024	0.003	0.049	0.107	-0.043	-0.06	-0.07	1			
Cd	0.096	0.076	-0.153	-0.119	0.032	0.141	0.266	0.223	0.321*	0.219	1		
Hg	0.091	0.136	0.213	-0.085	-0.065	0.01	-0.044	-0.083	-0.166	0.019	0.08	1	
Pb	0.176	0.391*	0.082	-0.131	0.188	0.377*	0.147	0.132	0.168	0.283	0.686**	0.013	1

*. Correlation is significant at the 0.05 level (2-tailed).

**. Correlation is significant at the 0.01 level (2-tailed).

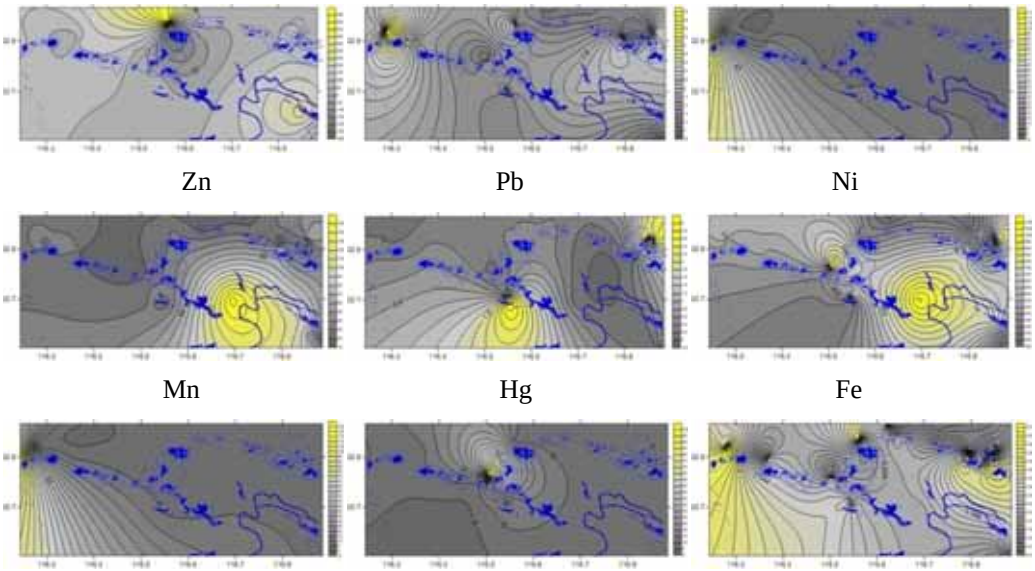

FIGURE 2
Distribution of elemental concentrations across the sampling area (μg/L).

TABLE 3
Total Variance Explained

Initial Eigenvalues			Extraction Sums of Squared Loadings			Rotation Sums of Squared Loadings		
Total	% of Variance	Cumula-tive %	Total	% of Variance	Cumula-tive %	Total	% of Variance	Cumulative %
2.601	32.514	32.514	2.601	32.514	32.514	1.965	24.564	24.564
1.66	20.749	53.263	1.66	20.749	53.263	1.936	24.205	48.769
1.383	17.289	70.552	1.383	17.289	70.552	1.743	21.783	70.552
0.95	11.878	82.431						
0.842	10.52	92.951						
0.265	3.317	96.268						
0.165	2.059	98.327						
0.134	1.673	100						

that Ni, Cu and Cd concentrations were higher in the surface water of Fuyang city than in Huainan. There were higher concentrations of Mn, Fe and Cr in subsidence areas of Huainan than in Fuyang.

Multivariate Statistical Analysis. The number of significant factors and the percentage of variance explained by each were calculated (Table 3). The first three PCs explained about 70.55 % of the total variance, with eigenvalues > 1.3. Only PCs with eigenvalues > 1.3 were considered crucial. Because the initial eigenvalue of the third PC was 1.383, the initial eigenvalue of the fourth PC decreased dramatically to 0.95. Thus, the first three PCs were used for further analysis. The first PC, with 35.51 % of the total data variance, had a strong positive loading of nitrogen in the forms of TN and NH_3-N, indicating that there was a strong interrelationship between them. The second PC, responsible for 22.749 % of the total variance, had strong positive loadings of TP (0.942) and As (0.946). The third PC accounted for 19.289% of the total variance, with strong loadings of Cd (0.927) and Pb (0.871). The communalities of the variances with high values (0.137—0.929) indicates that the extracted factors fit well except for elements Cr (0.31) and Hg (0.137).

Relationship between WQI and Land Use Type. The influence of land use on the water quality of streams is scale-dependent and varies temporally and spatially [26]. As mentioned in the Liu (2016), construction land was the main source of pollution of the Taihu Lake basin. To the best of our knowledge, there was no research on the effect of coal mining subsidence on surface water quality. The magnitude of nutrient losses from agriculture to ground and surface water has been demonstrated [27, 28]. In particular, N and P losses can negatively affect the quality of soils, ground water, surface water and the atmosphere, thus affecting the functioning of ecosystems and the earth as a whole [29].

We obtained the WQI for all surface water samples obtained from subsidence sites. The *F* values

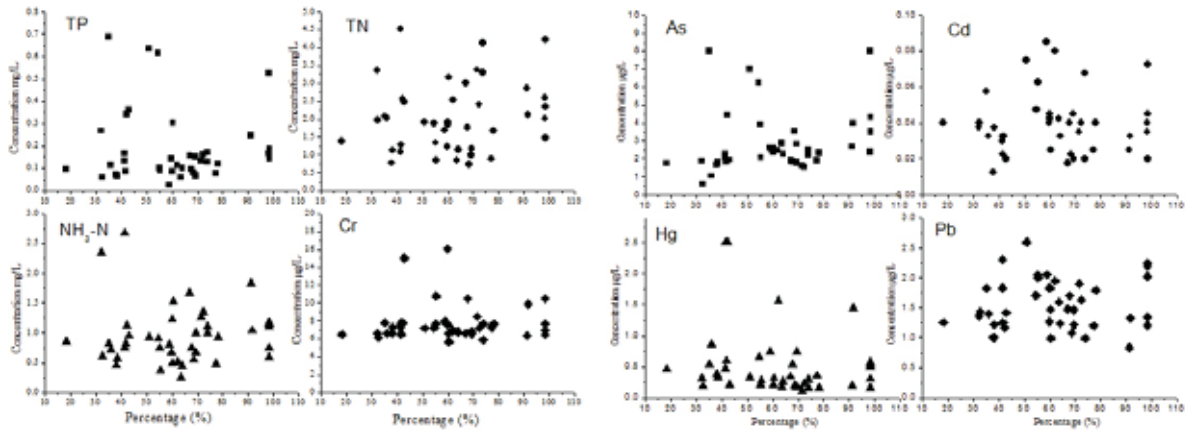

FIGURE 3
The percentage of water and agricultural area (1 km) to all land uses type versus elemental concentrations.

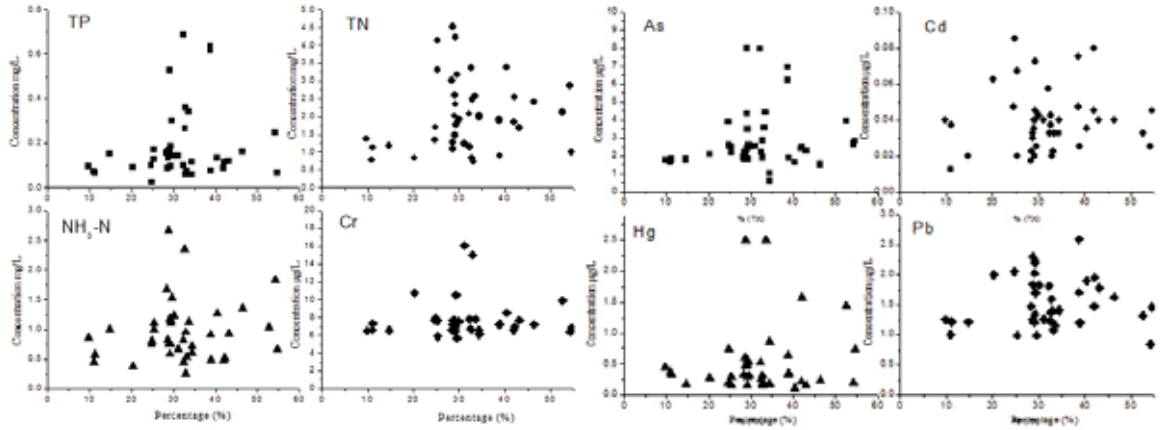

FIGURE 4
The percentage of water and agricultural area (5 km) to all land uses type versus elements concentrations.

ranged from 0.0273 to 9.8756, indicating that water quality varies substantially. The spatial distribution of the WQI indicates that surface water in the Fuyang coal mining subsidence area was polluted to some extent. This phenomenon could be explained by recent excavation activities which may have caused liquor from coal gangue to leach into surface water.

We also gave consideration to the relationship between land use type, and nutrient and toxic heavy metal concentrations (Figs. 3 and 4). The concentrations of N and P clearly varied with land use type, with a positive relation with agriculture field to some extent. However, metal concentrations had no relation with land use and appeared to be randomly distributed. Previous findings have consistently reported close relationships between urban land use and water quality [30]. Agricultural land use has shown a significant positive correlation with chemical oxygen demand (COD_{cr}), indicating that agriculture is one of the primary causes of water quality deterioration [31]. Hosen et al. (2014) reported that increasing the impervious coverage of catchment areas was associated with decreasing amounts of dissolved organic matter (DOM) in streams[32].

CONCLUSION

The subsidence area of Huainan is extensively used as a water source for irrigation, washing, livestock, and the domestic needs of rural inhabitants. In particular, subsidence areas have been used as fishery water body, which is the main pathway of water pollution. The results of the present study demonstrate that nutrients are moderately abundant in water, while heavy metals are less abundant, except for Fe (> 300 μg/L), Mn (> 30 μg/L), and Ni (> 10 μg/L). We also found that correlated elements (P-As, Cu-Ni, and Fe-Mn), could be derived from the same source from the pedosphere. The distribution of trace elements in the water body indicates that the main

heavy metal pollutants varied according to the sampling site. The relationship between WQI and land use type revealed that water quality was affected by the land type of water and agriculture directly. The percentage of the land use type of water and agricultural land was positively correlated with the concentrations of N and P, rather than those of heavy metals. The results also suggest that the integration of water quality chemistry and GIS technology is useful as a new method for assessing pollution sources and aquatic toxicity.

ACKNOWLEDGEMENTS

The work was financially supported by the Major Projects of the National Social Science Foundation (No. Y06061764), the Project Financed by the International Science & Technology Cooperation Plan of Anhui Province (No. 1704e1002225).

REFERENCES

[1] Fang, T., Liu, G., Zhou, C., Lu, L. (2015) Lead in soil and agricultural products in the Huainan Coal Mining Area, Anhui, China: levels, distribution, and health implications. Environ Monit Assess. 187(3), 152.

[2] Shahbaz, M., Farhani, S., Ozturk, I. (2015) Do coal consumption and industrial development increase environmental degradation in China and India? Environ Sci Pollut Res Int. 22(5), 3895-907.

[3] Xu, J., Lv, C., Zhang, M., Yao, L., Zeng, Z. (2015) Equilibrium strategy-based optimization method for the coal-water conflict: A perspective from China. J Environ Manage. 160, 312-23.

[4] Zhang, Y., Feng, Q., Meng, Q., Lu, P., Meng, L. (2012) Distribution and bioavailability of metals in subsidence land in a coal mine China. Bull Environ Contam Toxicol. 89(6), 1225-30.

[5] Tripathi, N., Singh, R.S., Singh, J.S. (2009) Impact of post-mining subsidence on nitrogen transformation in southern tropical dry deciduous forest, India. Environ Res. 109(3), 258-266.

[6] Qu, X.J., Yi, Q.T., Hu, Y.B., Yan, J.P., Yu, H.J., Dong, X.L. (2013) Nutrient spatiotemporal distribution and eutrophication process in subsidence waters of Huainan and Huaibei mining areas, China. Ying Yong Sheng Tai Xue Bao. 24(11), 3249-58.

[7] Yi, Q., Xie, K., Sun, P., Kim, Y. (2014) Characterization of phosphorus in the sedimentary environments of inundated agricultural soils around the Huainan Coal Mines, Anhui, China. Sci Total Environ. 472, 538-49.

[8] Zhang, S.Z., Liu, G.J., Sun, R.Y., Wu, D. (2016) Health risk assessment of heavy metals in groundwater of coal mining area: A case study in Dingji coal mine, Huainan coalfield, China. Hum Ecol Risk Assess. 22(7), 1469-1479.

[9] You, M., Huang, Y.E., Lu, J., Li, C.P. (2016) Fractionation characterizations and environmental implications of heavy metal in soil from coal mine in Huainan, China. Environ Earth Sci. 75(1).

[10] Niu, S.P., Gao, L.M., Zhao, J.J. (2015) Distribution and Risk Assessment of Heavy Metals in the Xinzhuangzi Reclamation Soil from the Huainan Coal Mining Area, China. Hum Ecol Risk Assess. 21(4), 900-912.

[11] Wang, X.M., Chu, Z.X., Zha, F.G., Liu, S.M., Liu, G.J., Dong, Z.B. (2015) Determination of Heavy Metals in Water and Tissues of Crucian Carp (Carassius auratus Gibelio) Collected from Subsidence Pools in Huainan Coal Fields (China). Anal Lett. 48(5), 861-877.

[12] You, M., Huang, Y.E., Lu, J., Li, C.P. (2015) Characterization of Heavy Metals in Soil Near Coal Mines and a Power Plant in Huainan, China. Anal Lett. 48(4), 726-737.

[13] Fang, T., Liu, G.J., Zhou, C.C., Lu, L.L. (2015) Lead in soil and agricultural products in the Huainan Coal Mining Area, Anhui, China: levels, distribution, and health implications. Environ Monit Assess. 187(3), 152.

[14] Fang, T., Liu, G.J., Zhou, C.C., Yuan, Z.J., Lam, P.K.S. (2014) Distribution and assessment of Pb in the supergene environment of the Huainan Coal Mining Area, Anhui, China. Environ Monit Assess. 186(8), 4753-4765.

[15] Ministry of environmental protection, P.C. 1990 Water Quality-determination of Total Nitrogen-alkaline Potassium Persulfate Digestion-UV Spectrophotometric Method (GB 11894-89) of China.

[16] Ministry of environmental protection, P.C. 2009 Water Quality-determination of Total Phosphorus-ammonium Molybdate Spectrophotometric Method (GB 11893-89) of China..

[17] Beebe, R.K., Pell, R.J., Seasholtz, M.B. (1998) Chemometrics:A Practical Guide. New York: John Wiley & Sons.

[18] Chen, K.P., Jiao, J.J., Huang, J.M., Huang, R.Q. (2007) Multivariate statistical evaluation of trace elements in groundwater in a coastal area in Shenzhen, China. Environ Pollut. 147(3), 771-780.

[19] Liu, X., Ying, X., Ji, Y.P., Ren, Y.P. (2015) An assessment of water quality in the Yellow River estuary and its adjacent waters based on principal component analysis. China Environ Sci. 35(10), 3187-3192.

[20] Tonne, C., Melly, S., Mittleman, M., Coull, B., Goldberg, R., Schwartz, J. (2007) A case-control analysis of exposure to traffic and acute myocar-dial infarction. Environ Health Persp. 115(1), 53-57.
[21] Yao, E.Q., Gui, H.R. (2008) Four trace elements contents of water environment of mining subsidence in the Huainan diggings, China. Environ Monit Assess. 146(1-3), 203-10.
[22] Gomez, N., Ouyang, J., Nguyen, M.D., Vinson, A.R., Lin, A.A., Yuk, I.H. (2010) Effect of temperature, pH, dissolved oxygen, and hydrolysate on the formation of triple light chain antibodies in cell culture. Biotechnol Prog. 26(5), 1438-45.
[23] Johansson, K., Bringmark, E., Lindevall, L., Wilander, A. (1995) Effects of acidification on the concentrations of heavy metals in running waters in Sweden. Water Air Soil Poll. 85(2), 779-784.
[24] Klake, R.K., Nartey, V.K., Doamekpor L.K., Edor K.A. (2012) Correlation between Heavy Metals in Fish and sediment in Sakumo and Kpeshie Lagoons, Ghana. J Environ Prot. 3. 1070-1077.
[25] Krishna, A., Satyanarayanan, M., Govil, P. (2009) Assessment of heavy metal pollution in water using multivariate statistical techniques in an industrial area: A case study from Patancheru, Medak District, Andhra Pradesh, India. J Hazard Mater. 167(1-3), 366-373.
[26] Buck, O., Niyogi, D., Townsend, C. (2004) Scale-dependence of land use effects on water quality of streams in agricultural catchments. Environ Pollut. 130(2), 287-299.
[27] Novotny, V. (1999) Diffuse pollution from agriculture - A worldwide outlook. Water Sci Technol. 39(3), 1-13.
[28] Pretty, J.N., Mason, C.F., Nedwell, D.B., Hine, R.E., Leaf, S., Dils, R. (2003) Environmental costs of freshwater eutrophication in England and Wales. Environ Sci Technol. 37(2), 201-8.
[29] Freibauer, A. (2003) Regionalised inventory of biogenic greenhouse gas emissions from European agriculture. Eur J Agron. 19(2), 135-160.
[30] Lee, S., Hwang, S., Lee, S., Hwang, H., Sung, H. (2009) Landscape ecological approach to the relationships of land use patterns in watersheds to water quality characteristics. Landscape Urban Plan. 92(2), 80-89.
[31] White, M., Greer, K. (2006) The effects of watershed urbanization on the stream hydrology and riparian vegetation of Los Penasquitos Creek, California. Landscape Urban Plan. 74(2), 125-138.
[32] Hosen, J.D., McDonough, O.T., Febria, C.M., Palmer, M.A. (2014) Dissolved organic matter quality and bioavailability changes across an urbanization gradient in headwater streams. Environ Sci Technol. 48(14), 7817-24.

Received: **04.12.2017**
Accepted: **15.04.2018**

CORRESPONDING AUTHOR

Hua Cheng
School of Resource and Environment Engineering,
Anhui University,
Hefei 230601 – P.R. China

e-mail: hcheng916@126.com

© by PSP Volume 27 – No. 7/2018 pages 4789-4796 Fresenius Environmental Bulletin

PHYSIOLOGICAL CHARACTERISTICS OF TWO PASTURES ON DIFFERENT COPPER POLLUTED PURPLE SOILS

Wenbin Li[1,*], Haixia He[1], Hongyan Deng[1], Le Kang[1], Run Qiu[1], Dengqin Yang[1], Qian Zhuang[1], Zhaofu Meng[2,3], Yunxiang Li[1,4]

[1]College of Environmental Science and Engineering, China West Normal University, Nanchong, Sichuan 637009, China
[2]Department of Natural Resource and Environment, Northwest A&F University, Yangling 712100, China
[3]Key Laboratory of Plant Nutrition and Agri-Environment in Northwest China, Ministry of Agriculture, Yangling 712100, China
[4]Ministry of Education Key Laboratory of Southwest China Wildlife Resources Conservation, China West Normal University, Nanchong, Sichuan 637002, China

ABSTRACT

In this study, six kinds of Cu^{2+} polluted soils were prepared by adding different concentrations of Cu^{2+} in typical purple soil, the physiological characteristics such as germination rate, plant height, above-ground biomass and underground biomass of two pastures on the six Cu^{2+} polluted samples were determined by indoor potted experiments, and the correlation among the various physiological indicators were analyzed. The results indicated: (1) Low concentration of Cu^{2+} could promote seed germination of the two pastures, when the concentration of Cu^{2+} exceeded 20 mg/L, seed germination of *sorghum sudanense* was suppressed, but under 100 mg/L Cu^{2+}, seed germination of *ryegrass* was further promoted. The growth rate (plant height) of the *ryegrass* was slightly higher than that of *sorghum sudanense*, but the concentration of Cu^{2+} had little effect on the height of two herbage plants. (2) The above-ground biomass of two pastures was inhibited in the first 15-days when the Cu^{2+} concentration in excess of 20 mg/L, but *ryegrass* was greatly inhibited under the same conditions. When the Cu^{2+} concentration was 50~200 mg/L (*sorghum sudanense*), the fresh weight and dry weight of the *sorghum sudanense* (above-ground biomass) in 30-day were gradually decreased compared to 20 mg/L, while the above-ground biomass of *ryegrass* increased with the increase of Cu^{2+} concentration. (3) The root of two herbage plants could reach a maximum of both the fresh weight and dry weight at 20 mg/L Cu^{2+} treatment, but the root weight decreased with different degrees when Cu^{2+} concentration in exceed of 20 mg/L, and the root weight reduction of *ryegrass* was greater than *sorghum sudanense* at the same conditions. (4) The correlation among the plant height, the above-ground biomass and the underground biomass of the *sorghum sudanense* was positive, while the correlation between the above-ground and underground physiological indexes of *ryegrass* was lower.

KEYWORDS:
Cu^{2+} pollution, purple soil, pastures, physiological characteristics

INTRODUCTION

Copper is an essential trace element for plant growth, but it is also a kind of heavy metal element which is polluting the environment [1]. When Cu^{2+} enters the soil environment, it is difficult to biodegrade, and it is harmful to human health when people absorb Cu^{2+} through breath, hand or mouth touching and other ways [2]. Furthermore, Cu^{2+} can also enter the surface water and groundwater through leaching and runoff, and result in potential hazards for water environment [3]. In recent years, with the rapid development of industrial technology, "three wastes" emissions seriously increased, leading to soil environment contaminated by heavy metals, copper has become one of the dominating element in soil heavy metal pollution [4], copper pollution treatment work has become a difficult and hotspot of research [5].

At present, the physical, chemical and biological repair methods were mainly used in the soil remediation for reducing the heavy metal migration and the biological validity, so as to restore the original nature and function of soil [6-7]. In recent years, phytoremediation as a green remediation technology has attracted much attention. it was through cultivating plants in contaminated soil, and using the accumulation effect of heavy metals by normal plants to fix the soil, it was a new repair method by dealing with the final harvest of plants which has enriched heavy metals [3]. Furthermore, as a potential application method for bioremediation, phytoremediation had the advantages such as low cost, less environmental disturbance, no secondary pollution, environmental friendly, large area implements, purify and beautify the environment [8-10]. Researches showed that low concentrations of copper pollution conditions could not only improve the seed germination rate of plants, but also promote the growth of plant

[11-12], when copper ions in the soil (Cu^{2+}) exceeded a certain load could seriously affect the growth of crops and vegetation [13-15]. Study on Hu et al. [16] showed that 5 μmol/L copper was toxic to maize (*Zea mays Linn. Sp.*) seedlings, the growth of roots and shoots was inhibited obviously, and with the increase of Cu^{2+} concentration, the growth inhibition was more obvious. When Yuan et al. [17] studied the effects of heavy metal copper on the plant height of *pakchoi* (*Brassica chinensis var chinensis*), it was found that low concentration of copper (< 25 mg/kg) could promote the growth of *pakchoi*, and the high concentration of copper (> 25 mg/kg) could inhibit the growth of *pakchoi*. The previous researches on copper ion pollution of plants had made provisionality progress. if a plant with strong growth ability and short growth cycle can be used for copper ion adsorption, and a bioremediation research for typical copper polluted soil can be carried out, it will promote the sustainable development of regional agriculture, but necessary research is relatively defective.

Sorghum sudanense and *ryegrass* are two grass species adapted to climatic conditions in Sichuan province. They are also a soil and water conservation plants with extensive ecological plasticity. Studies on the cultivation techniques of these two plants in saline alkali environment, the breeding of resistant varieties and the mechanism of resistance had extensive implemented [18-20], but researches about heavy metal pollution in ecological environment was not deep enough. This study was based on the typical purple copper contaminated soil, and potted experiment on the growth ability of the two grass species was implemented, changes of physiological indexes of *sorghum sudanense* and *ryegrass* in different concentration of copper contaminated soil were evaluated to provide a theoretical reference for the remediation study of copper contaminated soil.

MATERIALS AND METHODS

Experimental materials. Potted soil was collected from the typical purple soil in the experimental field of China West Normal University. After multi-point sampling, the soil samples were mixed evenly, dried and crushed, and their physical and chemical properties were determined after screening, as shown in Table 1. The tested pastures were *sorghum sudanense* and *ryegrass*, and the seed was provided by Yayi flowers Taobao shop. The concentration of copper pollution in the experimental treatment was counted by Cu^{2+}, prepared with $CuSO_4 \cdot 5H_2O$. This analytical reagent was purchased from Xilong Chemical reagent Co., Ltd.

Experimental design. The impurities, insects and low-maturity seeds were discarded, and 180 full seeds of two pastures was selected respectively. The seeds were soaked by potassium permanganate solution (1%) for 15 min, and cleaned with deionized water 3 times, dehydrated by the filter paper. In pot experiment, the polluted concentration of Cu^{2+} were set at 0 (CK), 20, 50, 100, 150 mg/L and 200 mg/L, and two replicates per treatment. Plastic pots with diameter of 18 cm, height of 11 cm were used in the pot experiment, then 6 pots were filled with 1 kg of purple soil respectively. Followed by adding different concentrations of 250 mL Cu^{2+} solution, after Cu^{2+} solution penetrated the soil, 30 seeds with the same kind of pasture were evenly seeded under the soil surface of each pot with 1~2 cm, and watered 100 mL per week after germination (4 times in total). The germination rate and plant height were measured at the growth stage, and the above-ground and underground biomass of pasture were measured after harvest.

TABLE 1
Basic properties of the tested soil

Soil layer (cm)	pH value	CEC (mmol/kg)	TOC content (g/kg)	Cu^{2+} content (mg/kg)
0~30	8.08	288.46	16.66	18.60

Experimental methods. At the beginning of the experiment, the germination of *sorghum sudanense* and *ryegrass* were observed daily, and the germination number of seeds was recorded every 12 h during germination. When the number of germination was no longer changed in the consecutive 3 d, it was thought to be complete and statistical germination rate. The formula of germination rate is: germination rate = (seed germination number / total number of seed tested) × 100%. The average plant height of *sorghum sudanense* and *ryegrass* seedlings were measured 1 times every 3 days after germination, a total of 10 times.

After 15 d of growth, the pastures were harvested half, and the other half were harvested after 30 d of growth. The plants were divided into above-ground parts (stems and leaves) and underground parts (roots) during harvest. Firstly, the dust and dirt in plant samples should be cleaned by tap water, and then rinsed with deionized water 2~3 times, filtered the water and weighed the each part separately. After weighing, the samples were put into the bag and dried to constant weight, and then weighed the dry weight of the above-ground parts and underground parts.

Data processing. EXCEL and SPSS16.0 statistical analysis software were used to process the experimental data.

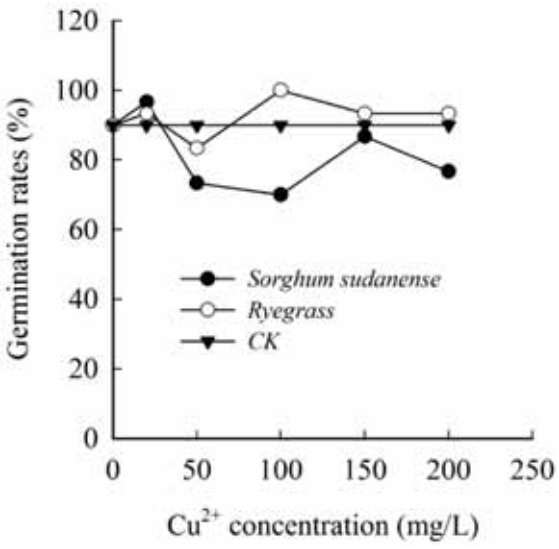

FIGURE 1
Effect of Cu^{2+} concentration on germination rate of two pastures

RESULTS AND DISCUSSION

Effects on germination rate of copper contaminated soil. Figure 1 showed that the germination rate of *sorghum sudanense* and *ryegrass* were all higher than that of untreated (CK) under the condition of low concentration (20 mg/L) of Cu^{2+} pollution, and the increment were 6.67% (*Sorghum sudanense*) and 3.33% (*Ryegrass*) respectively. For *sorghum sudanense*, high concentration (20~200 mg/L) of Cu^{2+} had significant inhibitory effect on the germination; With the increase of Cu^{2+} concentration, the germination rate decreased in varying degrees comparing with CK, and the lowest germination rate was 70% (100 mg/L), decreased by 20% compared with CK; While in 100~200 mg/L under the treatment of Cu^{2+} had different effect on *ryegrass* germination, the highest germination rate could enhance 10% compared with CK.

The germination rates of two pastures under different Cu^{2+} treatments were all more than 70%. The germination rates of two kinds of pasture were the same (90%) at CK treatment, with the increase of Cu^{2+} concentration, the germination rates of *sorghum sudanense* and *ryegrass* seeds increased at first and then decreased, and the highest germination rate of the two groups appeared in 20 mg/L (*sorghum sudanense*) and 100 mg/L (*ryegrass*) treatments respectively. Low concentration of Cu^{2+} promoted the germination of *sorghum sudanense* and *ryegrass* seeds, high concentrations of copper had inhibitory effect on the germination. Gao et al. [21] also found lower Cu^{2+} concentration (< 10 mg/L) could promote the seed germination and seedling growth of *sorghum sudanense.*

Effects on plant height of copper polluted soil. Figure 2 showed that after the germination of *sorghum sudanense* (after 3 d), the plant height gradually increased with the increasing growth time. In the first 6 d (3~9 d) after germination, the plant growth rate was higher, the average daily growth height was 1.63 cm, and the maximum was 1.88 cm/d. At 9~30 d, plant height increased slowly, the total growth was 2.7 cm. For *ryegrass*, the average daily growth height in the first 6 d was 1.88 cm, the maximum was 2 cm/d, and 9~30 d increased by 3 cm. In general, the growth rate of *ryegrass* plant height was slightly higher than that of *sorghum sudanense*, indicating that *ryegrass* had stronger adaptability to copper contaminated soil. For different Cu^{2+} concentration treatments, the length of the first 9 d of the 20 mg/L treatment was better, but the overall difference was not significant. It indicated that the Cu^{2+} concentration had little effect on the plant height of the two pastures.

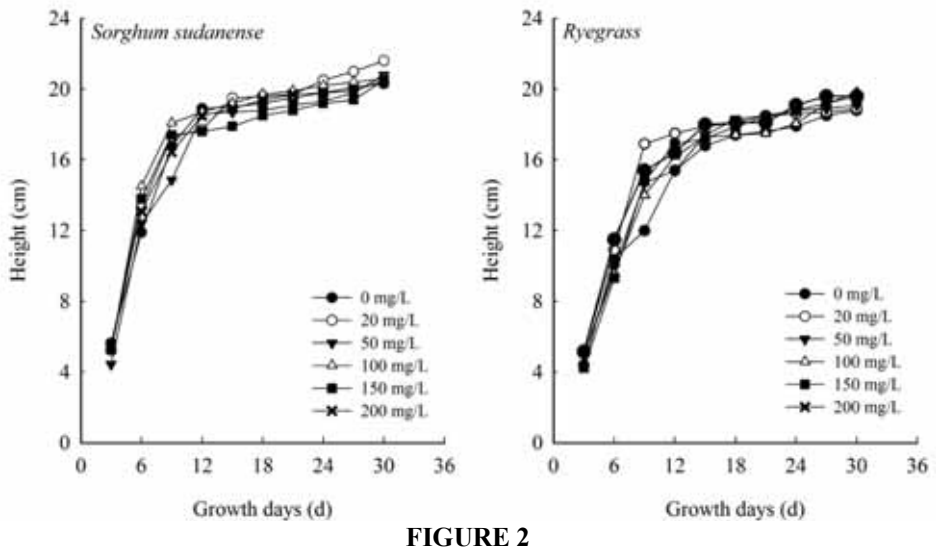

FIGURE 2
The average plant height of *sorghum sudanense (Piper) Stapf* and *Lolium perenne L*

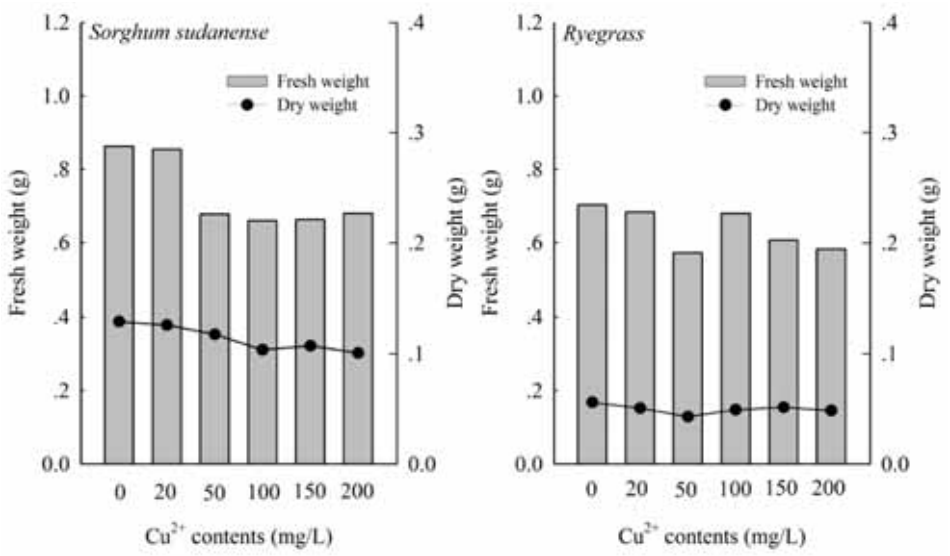

FIGURE 3
Above-ground fresh and dry weight of *sorghum sudanense* and *ryegrass* (15 days harvest)

Effects on the above-ground fresh and dry weight. The fresh weight and dry weight of *sorghum sudanense* and *ryegrass* growing for 15 days (Figure 3) could be found that with the increase of Cu^{2+} concentration, the above-ground fresh weight and dry weight of the two pastures were all reduced in different degrees compared with CK (0 mg/L). The fresh weight and dry weight for *Sorghum sudanense* in the treatment of CK were 0.8632 g and 0.1292 g respectively, and it showed 0.7029 g and 0.0559 g of *ryegrass* under CK treatment. *Sorghum sudanense*'s biomass of above-ground parts was bigger than that of *ryegrass*. The minimum values of fresh weight and dry weight presented at the Cu^{2+} treatment of 100 mg/L (*sorghum sudanense*) and 50 mg/L (*ryegrass*). For the different Cu^{2+} treatments, 0 mg/L and 20 mg/L treatments were adapted to plant growth of the two pastures. Low concentration of Cu^{2+} promoted plant growth, when the concentration of Cu^{2+} was more than 20 mg/L, the growth of plants would be inhibited. The results was consistent with the germination results of the two pastures. The fresh weight and dry weight of the two pastures showed a corresponding relationship, but the fresh weight / dry weight of *ryegrass* was 1.88 times larger than that of *sorghum sudanense*.

For the 30 days growing biomass of pasture (Figure 4), fresh weight and dry weight were 0.9320 g and 0.1110 g of *sorghum sudanense* under CK. At the concentration of Cu^{2+} was 20 mg/L, fresh weight and dry weight was the largest, and showed 1.29 and 1.2 times higher than that of CK respectively. When the treatment concentration of Cu^{2+} was 50~200 mg/L (*sorghum sudanense*), the fresh weight and dry weight decreased gradually compared with 20 mg/L, and the decrease range was 0.1742~0.4050 g (fresh weight) and 0.0346~0.0355 g (dry weight) respectively. For the upper part of *ryegrass*, 30 days of fresh weight and dry weight basically increased with the increase of Cu^{2+} concentration, the above-ground fresh weight and dry weight of Cu^{2+} at 20~200 mg/L increased by 0.0288~0.2047 g and 0.0032~0.0258 g, respectively, comparing with CK. The biomass in 30 days of the two pastures was affected by the copper ions showed the opposite results. The variation trend of 30 days biomass for *sorghum sudanense* showed the same to 15 days biomass, fresh weight and dry weight was the largest at 20 mg/L. But for *ryegrass*, the 30 day biomass was the highest when the Cu^{2+} concentration of 200 mg/L, indicating that the accumulation and adaptability of Cu in the *ryegrass* increased rapidly after 15 days of growth [22].

Effects on the underground fresh weight and dry weight in different copper polluted soil. In Figure 5, the underground (roots) fresh weight and dry weight of *sorghum sudanense* and *ryegrass* fluctuated with the increase of Cu^{2+} concentration. Root fresh weight and dry weight were 0.0962 g and 0.0179 g of *Sorghum sudanense* under CK, at the concentration of Cu^{2+} was 20 mg/L, the fresh weight and dry weight of roots reached the maximum, were 1.56 and 1.53 times higher than that of CK. When the Cu^{2+} concentration in 50~200 mg/L, the root fresh weight and dry weight decreased to different extent comparing with 20 mg/L, and reduced in the range of 0.0108~0.0260 g (fresh weight) and 0.0003~0.0059 g (dry weight). For *ryegrass*, the root fresh weight and dry weight were the greatest under 20 mg/L Cu^{2+} treatment, presenting 0.0877 g (fresh weight) and 0.0144 g (dry weight) respectively, while the minimum values appeared at Cu^{2+} concentration of 50 mg/L (fresh weight) and CK (dry weight) treatment respectively. The root fresh weight and dry weight of two pastures decreased by 0.0008~0.0391 g (*ryegrass*) and 0.0006~0.0061 g

(*Sorghum sudanense*) at Cu^{2+} concentration of 50~200 mg/L compared with 20 mg/L, and the reduction of *ryegrass* was greater under the same conditions. For the different concentration of Cu^{2+} treatment, root fresh weight and dry weight of two kinds of pasture all showed a corresponding relationship, but the root fresh weight and dry weight of *sorghum sudanense* was significantly higher than that of *ryegrass*, indicating that the adaptability of *sorghum sudanense* roots to purple soil polluted by Cu^{2+} was stronger. The two pastures was grown well under the treatment of Cu^{2+} in 20~200 mg/L, indicating that the high concentration of Cu^{2+} promoted the root growth of two kinds of pasture.

Correlation analysis among physiological indices of *sorghum sudanense* and *ryegrass*. Table 2 showed a closely positive correlation between different physiological index of *sorghum sudanense*. The plant height and root fresh weight, root dry weight were highly correlated (very significant). The above ground fresh weight on the 15 day and the above ground dry weight on the 15 day, the above ground dry weight on the 30 day, also the fresh weight and dry weight on the 30 day had a moderate positive correlation. At the same time, root fresh weight and root dry weight also showed significantly positive correlation, and the rest treatments showed low correlation or no correlation. Under the condition of copper ion pollution, some plant height and biomass of *sorghum sudanense* were positively correlated with the underground biomass, indicating that *sorghum sudanense* could adapt to different concentrations of Cu^{2+} pollution.

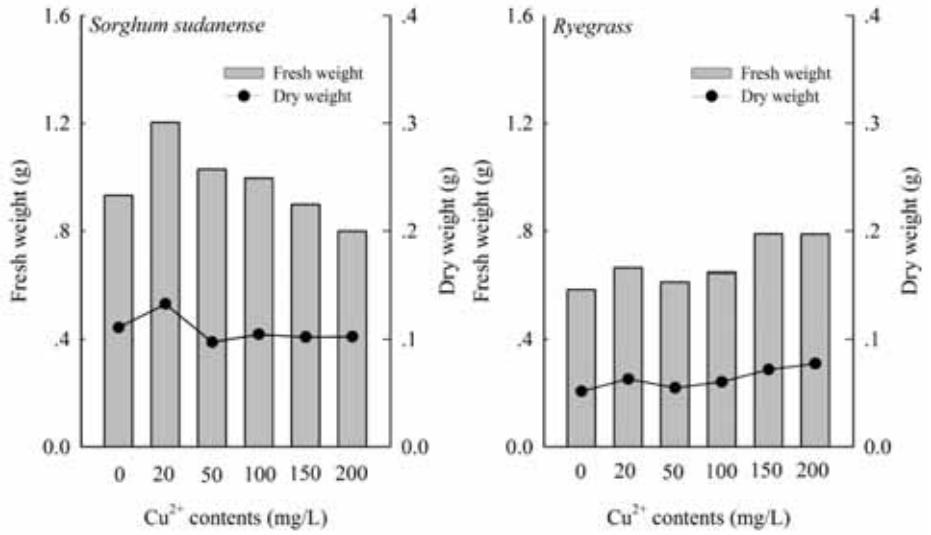

FIGURE 4
Above-ground fresh and dry weight of *sorghum sudanense* and *ryegrass* (30 days harvest)

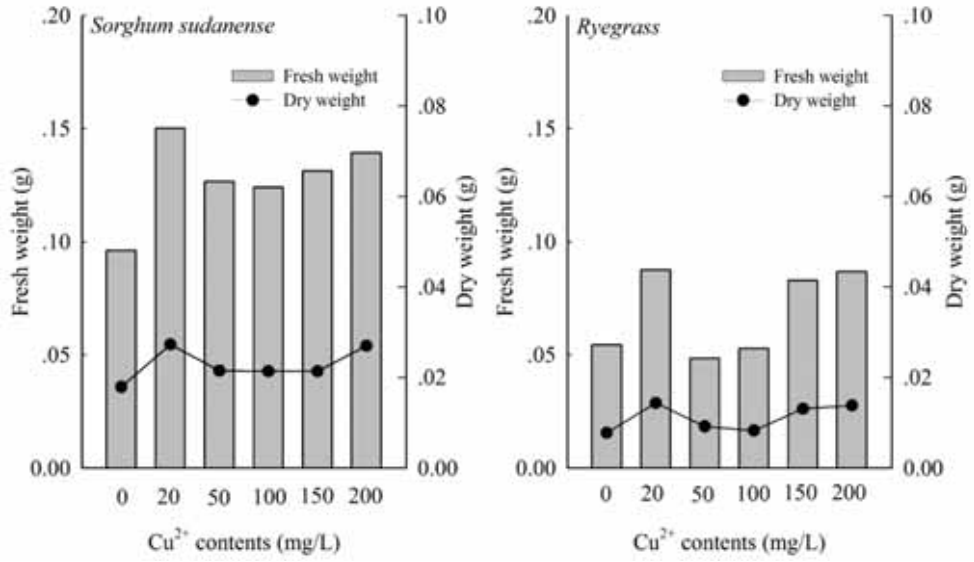

FIGURE 5
Underground fresh and dry weight of *sorghum sudanense* and *ryegrass* (30 days harvest)

TABLE 2
Correlation analysis of physiological indexes of *sorghum sudanense*

Correlation coefficients	Plant height (cm)	Above ground fresh weight on 15 days (g)	Above ground fresh weight on 30 days (g)	Above ground dry weight on 15 days (g)	Above ground dry weight on 30 days (g)	Root fresh weight (g)	Root dry weight (g)
Plant height (cm)	1	0.0346	0.0277	0.1093	0.0860*	0.9345**	0.9319**
Above ground fresh weight on 15 days (g)		1	0.2317	0.7758	0.6277	0.0472	0.0006
Above ground fresh weight on 30 days (g)			1	0.3641	0.5210	0.1023	0.0398
Above ground dry weight on 15 days (g)				1	0.3533	0.1025	0.0653
Above ground dry weight on 30 days (g)					1	0.1190	0.1856
Root fresh weight (g)						1	0.8334*
Root dry weight (g)							1

Note: ** or * indicates that the correlation coefficient is significant at p=0.01 or p=0.05 level (r=0.9172 or r=0.8114 when the degree of freedom f=4 and the level of significance p=0.01 or p=0.05), the same below.

TABLE 3
Correlation analysis of physiological indexes of *ryegrass*

Correlation coefficients	Plant height (cm)	Above ground fresh weight on 15 days (g)	Above ground fresh weight on 30 days (g)	Above ground dry weight on 15 days (g)	Above ground dry weight on 30 days (g)	Root fresh weight (g)	Root dry weight (g)
Plant height (cm)	1	0.4781	0.0126	0.0978	0.0011	0.0265	0.0049
Above ground fresh weight on 15 days (g)		1	0.2849	0.5308	0.2425	0.0262	0.1004
Above ground fresh weight on 30 days (g)			1	0.002	0.9543**	0.6109	0.5689
Above ground dry weight on 15 days (g)				1	0.1776	0.0366	0.0007
Above ground dry weight on 30 days (g)					1	0.6659	0.5201
Root fresh weight (g)						1	0.9329**
Root dry weight (g)							1

Table 3 showed that the plant height of *ryegrass* was low correlated with the above ground fresh weight on 15 d. The above ground fresh weight on 15 d and the dry weight on the 15 day, also the above ground dry weight on 30 d and the root fresh weight, the dry weight of the root were all moderately correlated. The above ground fresh weight on 30 d was significantly correlated with the dry weight on 30 d, and was moderately correlated with root fresh weight and root dry weight. Root fresh weight was highly correlated with root dry weight, and the rest treatments showed low correlation or no correlation. It could be seen that under the influence of copper ions, the correlation between the the upper part and the underground part of the *ryegrass* was not high, which indicated that the growth of the *ryegrass* affected by the pollution of copper ion was more than that of *sorghum sudanense.*

CONCLUSION

(1) Under 20 mg/L Cu^{2+} pollution, the increment of germination rates on the two pastures were 6.67% (*sorghum sudanense*) and 3.33% (*ryegrass*) than that of CK. High concentration (20~200 mg/L) Cu^{2+} had obvious inhibitory effect on the germination of *sorghum sudanense*, and 100~200 mg/L Cu^{2+} treatment promoted the germination of *ryegrass* in some degree. The plant height growth rate of *ryegrass* was slightly higher than that of *sorghum sudanense*, and the Cu^{2+} pollution had little effect on the plant height of two pastures.

(2) Under 0~20 mg/L Cu^{2+} treatment, the above-ground biomass of the pasture was larger, and the growth rate of the plant was inhibited when the concentration of Cu^{2+} was more than 20 mg/L, the above-ground biomass of *sorghum sudanense* on 15 days was larger than that of *ryegrass* under the same conditions. when the concentration of Cu^{2+} was 20

mg/L, the above-ground biomass of *sorghum sudanense* were the highest on 30 days. When the concentration of Cu^{2+} was 50~200 mg/L (*sorghum sudanense*), the fresh weight and dry weight of *sorghum sudanense* gradually decreased compared to 20 mg/L of Cu^{2+}. The above-ground fresh weight and dry weight of *ryegrass* (30 days) kept increasing with the increase of Cu^{2+} concentration.

(3) When the concentration of Cu^{2+} was 20 mg/L, root fresh weight and dry weight of two pastures were the highest, but in the 50~200 mg/L, it decreased in different degree compared with that of 20 mg/L. In addition, *ryegrass* decreased more greatly under the same conditions.

(4) The plant height and above-ground biomass had a high positive correlation with below ground biomass of *Sorghum sudanense*, the correlation between above-ground and below ground parts of *ryegrass* biomass was not high.

ACKNOWLEDGEMENTS

The authors wish to acknowledge and thank the financial assistance from the scientific research fundation of Sichuan science and technology agency (2018JY0224), the scientific research fundation of the education department of Sichuan province (18ZB0576) and the doctor initial funding of China west normal university (17E057).

Conflict of Interests. The authors declare that they have no conflict of interest.

REFERENCES

[1] Wang, X.L., Gao, Z., Huang, Y.Z., Liu, T., Yu, F. (2014) Effects of copper stress on three kinds of herbaceous plants growth and heavy metal accumulation. Asian Journal of Ecotoxicology. 9(4), 699-706.

[2] Lanphearb, P., Roghmannk, J. (1997) Pathways of lead exposure in urban children. Environmental Research. 74, 67-73.

[3] Zhang, J.Y. (2013) Research on different materials adopted in copper contaminated soil remediation. Nanjing Agricultural University, Nanjing.

[4] Jin, Y., Fu, Q.L., Zheng, J., Kang, W., Liu, Y.H., Hu, H.Q. (2012) Research status on phytoremediation of copper contaminated soil with hyperaccumulator. Journal of Agricultural Science and Technology. 14(4), 93-100.

[5] Huang, Y.Z., Hao, X.W., Lei, M., Tie, B.Q. (2013) The remediation technology and remediation practice of heavy metals-contaminated soil. Journal of Agro-Environment Science. 32(3), 409-417.

[6] Wei, S.H., Zhou, Q.X., Liu, R. (2005) Utilization of weed resources in remediation of soil contaminated by heavy metals. Journal of Natural Resources. 20(3), 432-440.

[7] Xu, L., Zhou, J., Cui, H.B., Tao, M.J., Liang, J.N. (2014) Research progress in remediation and its effect evaluation of heavy metal contaminated soil. Chinese Agricultural Science Bulletin. 20(30), 161-167.

[8] Yang, X.E., Feng, Y., He, Z.L., Stoffella, P.J. (2005) Molecular mechanisms of heavy metal hyperaccumulation and phytoremediation. Journal of Trace Elements in Medicine and Biology. 18(4), 339-353.

[9] Cuningham, S.D., Qw, D.W. (1996) Promise and prospects of phytoremediation. Plant Physiol. 110(3), 715-719.

[10] Barceló, J., Poschenrieder, C. (2011) Hyperaccumulation of trace elements: from uptake and tolerance mechanisms to litter decomposition; selenium as an example. Plant and Soil. 341(1-2), 31-37.

[11] Xiong, J.L., Yu, Q.Y. (2013) Effects of copper stress on germination of oat seeds. Anhui Agricultural Science Bulletin. 19(21), 15-16.

[12] Liu, C.Y. (2012) Effects of single and combined pollution of Cu and Cd on the growth of *Brassica napus* L. Anhui Normal University, Anhui.

[13] Fu, Z., Xiao, R.L., Shen, W.M., Zhou, C.Y., Qu, Y.H., Wan, H.W., Zhai, J., Hou, P. (2016) Remote sensing monitoring and analysis of heavy metal pollution on vegetation in typical mining area: a case study of Dexing copper mine in Jiangxi. Environment and Sustainable Development. 41(06), 66-68.

[14] Chu, L., Jin, S., Wu, X.F., Liu, D.Y. (2006) Effects of Cu pollution on *Medicago lupulina* L. seedlings growth and active oxygen metabolism. Chinese Journal of Ecology. 25(12), 1481-1485.

[15] Li, X., Han, X.L., Guo, L.P. (2012) Effects of soil copper stress on growth and artemisinin Artemisia. China Journal of Chinese Materia Medica. 37(11), 1553-1557.

[16] Hu, Z.B., Chen, Y.H., Wang, G.P., Shen, Z.G. (2006) Effects of copper stress on growth, chlorophyll fluorescence parameters and antioxidant enzyme activities of *Zea mays* seedlings. Chinese Bulletin of Botany. 23(2), 129-137.

[17] Yuan, X., Li, Y.M., Zhang, X.C. (2008) Effect of copper addition on the growth and the activities of protective enzymes in leaves of brassica chinensis. Journal of Agro-Environment Science. 27(2), 467-471.

[18] Pan, J., Wang, L.Y., Xiao, H., Cheng, W.J., Yang, Y. (2015) Dynamic changes of soil nutrients of salt-tolerant herbaceous plants in coastal saline soil. Chinese Agricultural Science Bulletin. 31(18), 168-172.

[19] Lin, W.J., Xiao, T.F., Ao, Z.Q., Xing, J., Ma, H.C., Hu, T.X. (2007) Limiting factors of waste land revegetation in indigenous zine smelting areas of western Guizhou. Chinese Journal of Applied Ecology. 18(3), 631-635.
[20] Liu, J.X., Wan, G.X., Jia, H.Y., Li, D.B. (2012) The difference in response to NaCl and Na-HCO_3 with ryegrass seedlings light stress. Journal of Desert Research. 32(5), 1342-1348.
[21] Gao, Z., Wang, X.L., Liu, T.Y., Wang, B.Q., Yu, F.X. (2013) Effects of heavy metals copper pollution on seed germination and seddlings growth of *sorghum sudanense* (piper) stapf. Chinese Agricultural Science Bulletin. 29(25), 199-204.
[22] Chen, S.J. (2000) Effects of organic substances on plant growth in copper contaminated soil. Soil and Environmental Science. 9(3), 183-185.

Received: **06.12.2017**
Accepted: **05.05.2018**

CORRESPONDING AUTHOR

Wenbin Li
College of Environmental Science and Engineering,
China West Normal University,
No.1, Shida Road,
Shunqing District, Nanchong,
Sichuan province, 637009 – P.R. China

e-mail: lwb062@163.com

© by PSP Volume 27 – No. 7/2018 pages 4797-4801 Fresenius Environmental Bulletin

FREQUENCY OF VENOUS THROMBOSIS RELATED DNA POLYMORPHISMS IN A HEALTHY TURKISH POPULATION

Sule Menziletoglu-Yildiz[1,2,*], Derya Kocamaz[1], Fildaus Nyrahabimana[1], Yusuf Gozet[3], Birol Guvenc[1,4,5]

[1]The Blood Bank Center of Balcali Hospital, Cukurova University, Adana, Turkey
[2]Vocational School of Health Services, Cukurova University, Adana, Turkey
[3]Department of Medicine, Cukurova University, Adana, Turkey
[4]Hemapheresis, Stem Cell and Cryopreservation Unit, Balcali Hospital, Cukurova University, Adana, Turkey
[5]Department of Internal Medicine, Division of Hematology, Balcali Hospital, Cukurova University, Adana, Turkey

ABSTRACT

Environmental and genetic factors play important role for the development of venous thromboembolic diseases. This study investigated the prevalence coagulation factor V Leiden (FVL) and factor II G20210A (FII) in a sample (N=96) of the Turkish population depending on age and weight. Participants were stratified into two age groups: 20-39 years, 40-59 years and their body mass index: normal (<24.9), obese (>25). The heterozygous FII genotype was identified in 2 (8.33%) of normal donors in 20-30 years while it was found in 1 (4.16%) of obese donors in 40-59 years. The mutant homozygous FVL genotype was found in 1 (4.16%) of obese donors in 20-30 years. The distribution of allele and genotype frequencies of FVL and FII polymorphisms did not differ significantly between normal and obese groups. Also, the frequencies of carriage rates of FVL and FII polymorphisms in 20-39 and 40-59 years were similar. In our study, observed FII allelic frequencies are higher than other healthy populations whereas the prevalence of factor V Leiden gene polymorphism was found to be consistent. Knowledge of the prevalence of these coagulation factor variations in a given population may contribute to the design of effective preventive measures against venous thrombosis.

KEYWORDS:
Factor II, Factor V Leiden, Healthy Population, Polymorphism, Venous thrombosis

INTRODUCTION

Obesity is a serious health and social problem that leads to haemostatic system and thrombosis-related diseases. Unfortunately, the number of obese adults have increased significantly over the last 25 years across all racial/ethnic and age groups [1]. Aging is very complex and multifactorial process that progresses to the gradual deterioration in normal function and leads to degenerative diseases and death [2]. Previous studies have shown that aging is one of the strongest and most prevalent risk factor for venous thrombosis [3]. But, venous thromboembolism is a multicausal disease as consequence of environmental and genetic risk factors [4]. Factor V Leiden (FVL) G1691A and factor II G20210A are the most common inherited factors for thrombosis. Single nucleotide substitution G1691A in factor V gene leads to an amino acid substitution, therefore, active protein C can't neutralize activated factor Va which acts as a cofactor in the conversion prothrombin to thrombin [5]. Based on venous thrombosis patients' data, it has been suggested that heterozygous FVL carriers have 7 fold higher risk of deep venous thrombosis [6]. Factor II G2021A is the second most common mutation after Factor V Leiden mutation. This mutation is associated with the increase of plasma prothrombin quantity and resulting from the substitution of guanidine adenine at the 20210 locus in the untranslated 3' region of the FII gene [7]. Studies reported that heterozygous FII carriers have 3 fold higher risk of deep venous thrombosis.

Most of the genetic factors are associated with venous thrombosis in selected patient groups, but the relationship between genetic and environmental risk factors still is not fully understood in healthy population. Therefore, in this study, we investigated FII G20210A and Factor V Leiden genes related to venous thrombosis diseases in a healthy Turkish population for different age and weight and compared the frequencies of these coagulation factor variations with other populations.

MATERIALS AND METHODS

Experimental design. This prospective study was carried out in the Regional Blood Center of Cukurova University. The study's protocol was approved by the Human Subject Ethics Committee of the Cukurova University (2016, 24) and was conducted in accordance with Helsinki Declaration. Peripheral blood was collected in disodium EDTA

from 96 male Caucasian healthy blood donors living in Cukurova Region. Participants were stratified into two age groups: 20-39 years, 40-59 years and their body mass index: normal (<24.9), obese (>25).

Molecular Assays. Genomic DNA was isolated from buffy coat using Qiagen DNA extraction kit. The Factor II G20210A and Factor V Leiden genotypes were determined by Real Time PCR (Roche, Cobas Z 480) using commercial kits from TIB, MOLBIOL, LightMix (CN: 40-0593-64, 40-0594-64).

Data analysis. The differences in genotype were analysed statistically using Fischer's exact test. The associations between allele frequencies in all groups were evaluated by computing the odds ratios (OR) and their confidence intervals using Hardy-Weinberg equilibrium. P<0.05 was considered statistically as significant.

RESULTS AND DISCUSSION

All donors of obese in 20-39 age group and normal in 40-59 age group were found to have homozygous for FII G20210A while 2 (8.33%) of normal donors in 20-39 age group and 1 (4.16%) of obese donors in 40-59 age group were found to have heterozygous (TABLE 1-2). Cardiovascular diseases represented by 30% of global deaths in 2008 and still remain the most important cause of morbidity and mortality in worldwide. In the studies conducted, it was observed that more than 80% of cardiovascular disease-related deaths occurred in low- and middle-income countries, and the incidence was similar in males and females. The polymorphisms in coagulation factors are among the unchangeable risk factors of cardiovascular diseases [8]. Previous studies with healthy populations in different regions reported that, the prevalence of factor II G20210A was 0.6-2.4% in North Europe, 1.1-4.0% in South Europe, 0.7-2.5% in North America, 0.0-3.7% in Africa, 1.3-2.0% in Hispanic, 0.0-1.8% in West Asia, 6.8% in Chilean native, 0.0% in East Asia and 0.0% in Indians of Malesia [9-20]. In this study, results showed that the prevalence of heterozygous prothrombin factor II G20210A genotype was higher than other populations but it was not related to the age and body mass index (p=0.361 between normal and obese donors in 20-39 years, p=1 between normal and obese donors in 40-59 years). Higher prevalence of heterozygous may be due to differences in the genetic background due to heavy/fatty dietary habits and environmental factors as well as the constant migration status.

TABLE 1
Genotype frequencies of FII G20210A gene in normal and obese donors of two age groups

Genotype	Age Groups			
	20-39 (n/%)		40-59 (n/%)	
	Normal Donors	Obese Donors	Normal Donors	Obese Donors
GG	22 (91.66%)	24 (100%)	24 (100%)	23 (95.83%)
GA	2 (8.33%)	-	-	1 (4.16%)
AA	-	-	-	-

TABLE 2
Allele frequencies in peripheral blood FII G20210A gene in normal and obese donors of two age groups

Allele	Age Groups			
	20-39 (n/%)		40-59 (n/%)	
	Normal Donors	Obese Donors	Normal Donors	Obese Donors
G	46 (95.83%)	48 (100%)	46 (95.83%)	46 (95.83%)
A	2 (4.16%)	-	2 (4.16%)	2 (4.16%)
Odds Ratio	*0.191*		*0.416*	

TABLE 3
Genotype frequencies of FVL G1691A gene in normal and obese donors of two age groups

Genotype	Age Groups			
	20-39 (n/%)		40-59 (n/%)	
	Normal Donors	Obese Donors	Normal Donors	Obese Donors
GG	22 (91.66%)	23 (95.83%)	22 (91.66%)	22 (91.66%)
GA	2 (8.33%)	-	2 (8.33%)	2 (8.33%)
AA	-	1 (4.16%)	-	-

TABLE 4
Allele frequencies in peripheral blood FVL G1691A gene in normal and obese donors of two age groups

	Age Groups			
	20-39 (n/%)		40-59 (n/%)	
Allele	Normal Donors	Obese Donors	Normal Donors	Obese Donors
G	46 (95.83%)	46 (95.83%)	46 (95.83%)	46 (95.83%)
A	2 (4.16%)	2 (4.16%)	2 (4.16%)	2 (4.16%)
Odds Ratio	*1.0*		*1.0*	

The most common genetic defect of venous thrombosis is Factor V Leiden G1691A polymorphism. In this study, the heterozygous and mutant homozygous FVL genotypes were identified in 2 (8.33%) of normal and 1 (4.16%) of obese donors in the 20-39 age group. In 40-59 age group, the heterozygous FVL were found in 2 (8.33%) of normal and 2 (8.33%) of obese donors (TABLE 3-4). The prevalence of heterozygous FVL G1691 in the Aegean region of Turkey was declared as 7.3% in healthy population [21]. The prevalence of the FVL carriers in different regions were reported to be 1.1-7.3% in North Europe, 0.6-5.1% in Central Europe, 0.9-4.0% in South Europe, 2.7-3.0% in North America, 1.0-10.2% in Africa, 0.4-1.4% in Hispanic and 2.1- 3.8, 2.7% in Australia, 5.5% in Chilean residents, 1.9% in Northern India and 5.5% in South India [22-31]. In our study, the prevalence of heterozygous FVL was found to be consistent with the reported studies. However, it is understood that is not depending on age and body mass index (p=0.244 between normal and obese donors in 20-39 years, p=1 between normal and obese donors in 40-59 years). Factor V Leiden mutation is estimated to have occurred in the vicinity of Anatolia approximately 15.000 to 30.000 years ago [33]. This explains the geographic distribution of this polymorphism on the general population and the high prevalence rate in our region.

CONCLUSION

In this study, the prevalence of factor II G20210A was higher than other healthy populations, whereas the prevalence of FVL was found consistent. The genetic structure of the Turkish population is complicated by the demographic history and the reason for its location in Central Asia, Europe and the Middle East. There are differences between the genetic of Turkish and European populations, which contribute to the explanation of the health problems and the pharmacogenetic differences observed in Turkish populations living in Europe. Also, comprehensive knowledge about the lifestyle and eating habits of the Turkish population will strengthen understanding of the relationship between environmental and genetic risk factor of cardiovascular diseases. A comparison of genotype frequencies among healthy populations at different age groups is a useful strategy for evaluating polymorphisms associated with vascular diseases. In addition, having knowledge of the prevalence of these coagulation factor variations in a given population may contribute to the design of effective preventive measures against venous thrombosis.

ACKNOWLEDGEMENTS

This study was supported by Cukurova University (BAP-TSA 2016-6194), Adana, Turkey.

REFERENCES

[1] Wang, H., Dwyer-Lindrgen, L., Lofgren, K.T, Rajaratnam, J.K., Marcus, J.R., Levin-Rector, A., Levitz, C.E., Lopez, A.D., Murray, C.J. (2010) Age-Spesific and Sex –Specific Mortality in 187 Countries, 1970-2010: A Systematic Analysis for the Global Burden of Disease Study 2010. Lancet. 380, 2071-2094.

[2] Grody, W.W., Griffin, J.H., Taylor, A.K., Korf, B.R., Heit, J.A. (2001) American College of Medical Genetics Consensus Statement on Factor V Leiden Mutation Testing. Genet Med. 3, 139-148.

[3] Engbers, M.J., van Hyckama Vlieg, A., Rosendaal, F.R. (2010) Venous Thrombosis in the Elderly: Incidence, Risk Factors and Risk Groups. J Thromb Haemost. 8, 2105-2112.

[4] Chalal, N., Demmouche, A., Cherif Touil, S. (2015) Frequency of Factor II G20210A and Factor V Leiden Mutations in Algerian Patients with Venous Thromboembolism. J Blood Disord Transfus. 6, 247.

[5] Frikha, R., Abdelmoula, N.B., Rebai, T. (2012) A Duplex PCR-RFLP Assay for Simultaneous Detection of FV Leiden and Prothrombin G20210A Mutations in Women with Recurrent Miscarriage. J Exp Clin Med. 4, 194-196.

[6] Arsov, T., Miladinova, D., Spiroski M. (2006) Factor V Leiden is associated with Higher Risk of Deep Venous Thrombosis of Large Blood Vessels. Crot Med. 47, 433-439.

[7] Poort, S.R., Rosendaal, F.R., Reitsma, P.H., Bertina, R.M. (1996) Common Genetic Variation in the 3'-untraslated Region of the Protrombin Gene is associated with Elevated Plasma Prothrombin Levels and an Increase in Venous Thrombosis. Blood. 88, 3698-3703.

[8] Wu, A.H.B., Tsongalis, G.J. (2001) Correlation of Polymorphisms to Coagulation and Biochemical Risk Factors for Cardiovascular Diseases. Am J Cardiol. 87, 1361-1366.

[9] Rosendaal, F.R., Doggen, C.J., Zivelin, A., Arruda, V.R., Aiach, M., Siscovick, D.S., Hillarp, A., Watzke, H.H., Bernardi, F., Cumming, A.M., Preston, F.E., Reitsma, P.H. (1998) Geographic Distribution of the 20210 G to A Prothrombin Variant. Thromb Haemost. 79, 706-708.

[10] Souto, J.C., Coll, I., Llobet, D., del Río, E., Oliver, A., Mateo, J., Borrell, M., Fontcuberta, J. (1998) The Protrombin 20210A Allele is the Most Prevalent Genetic Risk Factor for Venous Thromboembolism in the Spanish Population. Thromb Haemost. 80, 366-369.

[11] Lu, Y., Zhao, Y., Liu, G., Wang, X., Liu, Z., Chen, B., Hui, R. (2002) Factor V Gene G1691A Mutation, Prothrombin Gene G20210A Mutation, and MTHFR Gene C677T Mutation are not Risk Factors for Pulmonary Thromboembolism in Chinese population. Thromb Res. 106, 7-12.

[12] Dowling, N.F., Austin, H., Dilley, A., Whitsett, C., Evatt, B.L., Hooper, W.C. (2003) The Epidemiology of Venous Thromboembolism in Caucasians and African-Americans: The GATE Study. J Thromb Haemost. 1, 80-87.

[13] Almawi, W.Y., Keleshian, S.H., Borgi, L., Fawaz, N.A., Abboud, N., Mtiraoui, N., Mahjoub, T. (2005) Varied Prevalance of Factor V G1691A (Leiden) and Prothrombin G20210A Single Nucleotide Polymorphisms among Arabs. J Thromb Thrombolysis. 20, 163-168.

[14] Ameen, G., Irani-Hakime, N., Fawaz, N.A., Mahjoub, T., Almawi, W.Y. (2005) An Arab Selective Gradient in the Distribution of Factor V G1691A (Leiden), Prothrombin G20210A, and Methylenetetrahydrofolate reductase (MTHFR) C6777T. J Thromb Haemost. 3, 2126-2127.

[15] Mazoyer, E., Ripoll, L., Gueguen, R., Tiret, L., Collet, J.P., dit Sollier, C.B., Roussi, J., Drouet, L. (2009) Prevalance of Factor V Leiden and Prothrombin G20210A Mutation in a Large French Population Selected for Nonthrombotic History: Geographical and Age Distribution. Blood Coagul Fibrinolysis. 20, 503–510.

[16] Abdullah, W.Z., Subashini, K., Ghazali, S., Yusoff, N.M. (2010) Factor V Leiden and Prothrombin G20210A Mutations among Healthy Indians in Malaysia. Lab Medicine. 41, 284-287.

[17] Jadaon, M.M. (2011) Epidemiology of Prothrombin G20210A Mutation in the Mediterranean Region. Mediterr J Hematol Infect Dis. 3, e2011054.

[18] Stur, E., Silveira, A.N., Selvatici, L.S., Alves, L.N., de Vargas Wolfgramm, E., Tovar, T.T., De Nadai Sartori, M.P., de Paula, F., Louro, I.D. (2012) Polymorphism Analysis of MTHFR, Factor II and Factor V Genes in the Pomeranian Population of Espirito Santo, Brazil. Genet Test Mol Biomarkers. 16, 219-222.

[19] Frere, C., Saut, N., Boukef, M.K., Zili, M., Toumi, N.E. (2003) Factor V Leiden G1691A and Prothrombin G20210A Mutations are Common in Tunisia. J Thromb Haemost. 1, 2451-2452.

[20] Roco, A., Ouiñones, L.A., Sepúlveda, P., Donoso, H., Lapostol, C., Alarcón, R., Torres, M.E., Véliz, P.C., Acuña, G., Wilke, O., Acevedo, C. (2015) Prevalence of Seven Cardiovascular-related Genetic Polymorphisms in a Chilean Mestizo Healthy Population. Acta Cardiol. 70, 528-535.

[21] Kabukcu, S., Keskin, N., Keskin, A., Atalay, E. (2007) The Frequency of Factor V Leiden and Concomitance of Factor V Leiden with Prothrombin G20210A Mutation and Methylene tetrahydofolate Reductase C677T Gene Mutation in Healthy Population of Denizli, Aegean Region of Turkey. Clin App Thromb Hemost. 13, 166-171.

[22] Rees, D.C. (1996) The Population Genetics of Factor V Leiden (Arg506Gln). Br J Haematol. 95, 579-586.

[23] Ridker, P.M., Miletich, J.P., Hennekens, C.H., Buring, J.E. (1997) Ethnic Distribution of Factor V Leiden in 4047 Men and Women. Implications for Venous Thromboembolism Screening. JAMA. 277, 1305-1307.

[24] Larsen, T.B., Lassen, J.F., Brandslund, I., Byriel, L., Petersen, G.B., Nørgaard Pedersen, B. (1998) The Arg506Gln Mutation (FV Leiden) among a Cohort of 4188 Unselected Danish Newborns. Thromb Res. 89, 211-215.

[25] Majluf-Cruz, A., Moreno-Hernández, M., Ruiz-de-Chávez-Ochoa, A., Monroy-García, R., Majluf-Cruz, K., Guardado-Mendoza, R., Molina-Avila, I., Isordia-Salas, I., Corona-de la Peña, N., Vargas-Vorackova, F., Vela-Ojeda, L., García-Chávez, J. (2008) Activated Protein C Resistance and Factor V Leiden in Mexico. Clin Appl Thromb Hemost. 14, 428-437.

[26] Said, J.M., Brennecke, S.P., Moses, E.K., Walker, S.P., Monagle, P.T., Campbell, J., Byrant, V.J., Borg, A.J., Higgins, J.R. (2008) The Prevalence of Inherited Thrombophilic Polymorphisms in an Asymptomatic Australian Antenatal Population. Aust N Z J Obstet Gynaecol. 48, 536-541.

[27] Sottilotta, G., Mammi, C., Furló, G., Oriana, V., Latella, C., Trapani Lombardo, V. (2009) High Incidence of Factor V Leiden and Prothrombin G20210A in Healthy Southern Italians. Clin Appl Thromb Hemost. 15, 356- 359.
[28] Pasquier, E., Bohec, C., Mottier, D., Jaffuel, S., Mercier, B., Férec, C., Collet, M., De Saint Martin, L. (2009) Inherited Thrombophilias and Unexplained Pregnancy Loss: An Incident Case-Control Study. J Thromb Haemost. 7, 306-311.
[29] Eroglu, A., Sertkaya, D., Akar, N. (2012) The Role of Factor V Leiden in Adult Patients with Venous Thromboembolism: A Meta-Analysis of Published Studies from Turkey. Clin App Thromb Hemost. 18, 40-44.
[30] Hadhri, S., Rejab, M.B., Guedria, H., Ifa, L., Chatti, N., Skouri, H. (2012) Factor V Leiden, Prothrombin 20210G>A, MTHFR 677C>T and 1298A>C, and Homocysteinemia in Tunisian Blood Donors. J Clin Lab Anal. 26, 167-173.
[31] Farajzadeh, M., Bargahi, N., Zonouzi, A.P., Farajzadeh, D., Pouladi, N. (2014) Polymorphisms in Thrombophilic Genes are associated with Deep Venous Thromboembolism in an Iranian population. Meta Gene. 2, 505-513.
[32] Alkan, C., Kavak, P., Somel, M., Gokcumen, O., Ugurlu, S., Saygı, C. Dal, E., Bugra, K., Gungor, T., Sahinalp, S.C., Ozoren, N., Bekpen, C. (2014) Whole Genome Sequencing of Turkish Genomes Reveals Function Private Alleles and Impact of Genetic Interactions with Europe, Asia and Africa. BMJ Genomics. 15, 963.
[33] Karaca, S., Erge, S., Cesuroglu, T., Polimanti, R. (2015) Nutritional Habits, Lifestyle, and Genetic Predisposition in Cardiovascular and Metabolic Traits in Turkish Population. Nutrition. 32, 693-701.

Received: **07.12.2017**
Accepted: **28.04.2018**

CORRESPONDING AUTHOR

Sule Menziletoglu-Yildiz
The Blood Bank Center of Balcali Hospital,
Cukurova University,
Adana – Turkey

e-mail: smenziletogluyildiz@gmail.com

© by PSP Volume 27 – No. 7/2018 pages 4802-4812 Fresenius Environmental Bulletin

ADSORPTION MECHANISM OF ALKALI–EARTH METAL IONS FROM AQUEOUS SOLUTIONS BY USING HYDRATED FERRIC OXIDE–LOADEDCHINESE KULUMUTI TEA RESIDUE

Ziyuan Gao[1], Yutao Wang[2,3], Binbin Xu[1], Siming Zhu[1,2,3,*]

[1]School of Food Science and Technology, South China University of Technology, Guangzhou 510641, P.R. China
[2]College of Life and Geographic Sciences, Kashgar University, Kashgar 844000, P.R. China
[3]The Key Laboratory of Ecology and Biological Resources in Yark and Oasis at Colleges & Universities under the Department of Education of Xinjiang Uygur Autonomous Region, Kashgar University, Kashgar 844000, P.R. China

ABSTRACT

Hymenoleana nana is a traditional tea and medicinal herb in China. In this study, hydrated ferric oxide was successfully impregnated into *H. nana* tea residue by precipitation, and its properties of Ca^{2+} and Mg^{2+} removal from aqueous solutions were investigated. Batch experiments were conducted to assess the factors affecting adsorption of Ca^{2+} and Mg^{2+}, including contact time, initial pH, temperature, and initial concentration of metal ions. Adsorption equilibrium and kinetic models were also fitted. Results indicated that the modified tea residue exhibits the maximum adsorption capacity for Ca^{2+} or Mg^{2+} under the conditions of pH 6.0 and 40ºC, and the highest metal uptakes ofCa^{2+} and Mg^{2+} per gram dry matter were 16.39 and 13.16 mg/g, respectively. Sorption process reached equilibrium after a contact time of 60 min. In addition, the adsorption behavior of Ca^{2+} and Mg^{2+} by the modified tea residue fitted the Langmuir isotherm model well, and the pseudo–second–order kinetic model can be used to describe adsorption. The *H. nana* tea residue, which is of low commercial value and easily obtained, can be used after modification as an efficient Ca^{2+} and Mg^{2+} adsorbent for softening hard water in Xinjiang.

KEYWORDS:
Hydrated ferric oxide, modified tea residue of kulumuti, adsorption, alkali–earth metal ions, isotherms and kinetics

INTRODUCTION

Hard water with high Ca^{2+} and Mg^{2+} content presents several problems human health and industrial production and causes massive economic losses to industries [1]. High hardness of water can result in clogged pipes owing to scale precipitation and reduced the heat transfer efficiency in industries [2]. Scale deposition increases energy consumption and maintenance costs and even result in production interruption or plant shutdown [3]. Hard water not only affects industrial production but also exerts a harmful effect on human health. Long–term drinking of hard water can easily cause a variety of lithiasis. Steeping the tea in hard water changes the color and flavor of original tea and reduces the quality of tea drinks.

Numerous treatment processes, such as membrane filtration [4], ion exchange [5, 6], adsorption on activated carbon [7–10], and chemical precipitations [11], are currently used for the removal of metal ions from aqueous solutions. These methods display good scavenging effect but are not cost–effective solutions. Owing to the high cost of activated charcoal, numerous publications have recently focused on the removal of metal ions from aqueous solutions by using adsorption techniques with environmentally friendly and low–cost biomass materials. Most of the investigated sorbent materials are obtained from natural biomass, such as the leaves [12], rice hulls [13], soils [14], zeolite [15], fungi [16, 17], and algae [18–20]. However, most of these raw materials show unsatisfactory sorption capacity toward metal ions. Thus, reasonable structure modification is expected to enhance metal sorption capacity. For example, Altundogan et al. reported that copper is removed from aqueous solution by sugar beet pulp modified by sodium hydroxide and citric acid [21]. Wong et al. studied the removal of lead and copper by tartaric acid treated rice husk [22]. Guo et al. used chemically modified maize straw to investigate its adsorption characteristic for cadmium [23]. Multiple studies have shown that chemical modification positively affects the adsorption capacity of raw materials toward metal ions.

Hymenoleana nana is commonly grown in the northwest region of China, such as Xinjiang Province. However, the tea herb with many bioactivities remains undeveloped, since it grows at an altitude of 4000 to 4500 meters. Water hardness (1027 mg/L) in Xinjiang Province is much higher than permitted level of 450 mg/L in China. This finding is beneficial to the health of local people. A wandering herdsman

can resist altitude sickness and the harm of hard water by using the local tea herb. In fact, tea leaves mainly comprise insoluble cell wall, such as cellulose, hemicelluloses, and lignin [24]. Moreover, tea residue usually contains a large number of carboxyl groups, amino groups, and other functional groups, as demonstrated by its infrared (IR) spectrum. In other words, tea residue exhibits good potential as a metal or heavy metal adsorbent. Recently, several researchers have reported the application of tea residue as metal scavengers for the removal of chromium [25], copper [26], lead [27], nickel [28]. Moreover, research has shown that hydrated ferric oxide is capable of efficiently adsorbing heavy metal ions [29-32]. With the aim of softening hard water in the northwest region of China by using local tea residue as a simple water–softening method for local herdsmen or nomads, this work attempted to modify Kulumuti (*H. nana*) tea residue by hydrated ferric oxide and use the modified residue as a new sorbent.

In our study, tea residue from Kulumuti was selected as raw material, and iron (III) chloride was impregnated by precipitation to obtain a new sorbent. Meanwhile, the potential of tea residue in removing calcium and magnesium from aqueous solutions was researched. Batch experiments were conducted to evaluate the influence of solution pH, contact time, temperature, and initial concentration of metal ions on adsorption. In addition, isotherm experiments and kinetics of batch adsorption were discussed. The possible binding mechanism of the modified tea residue was also preliminarily discussed using Fourier transform infrared (FTIR) spectroscopy. The research can provide a reference to healthy tea drinking method in the northwest of China by using local tea leaf or residue to soften ground water or well water because water with high hardness is common in northwest China. This work can also provide a method for adsorbing alkali metal–earth ions for environmental pollution mitigation using local tea residue. Moreover, Xinjiang is the largest cotton–producing province in China and is rich in mineral resources, causing abundant textile and heavy metal wastewater. Therefore, pollution is worsening in this area. Thus, our work can also be a reference to control the organic or inorganic pollution matters in waste water using the Kulumuti tea residue. So, our work is significant on accelerating ecological development.

MATERIALS AND METHODS

Preparation of the adsorbent. The dried aerial parts of whole plants of Kulumuti (nickname in Xinjiang) or *H. nana* were collected from Tashikurgan, Xinjiang Province, China in October 2016 and identified by Prof. *Ping Sheng* from the Xinjiang Medical University. Prior to the experiments, colored components and other soluble matters were removed from tea plants by washing and soaking with boiling water. This procedure was repeated until the resulting water was colorless. Cleaned tea residue was then dried in an oven for 24h at 50°C, grounded with a blender, and sieved to obtain particles with the diameter of 150 μm to 500 μm. Fifty grams of tea residue was mixed with 1L of 0.15M$FeCl_3$ solution in a 2L beaker. The mixture was agitated at 200 rpm for 24h at room temperature. Treated tea residue was poured onto a decompress filter and rinsed with distilled water to remove excess $FeCl_3$ solution. The product was dried at 50ºC until constant weight and designated HNF. HNF was mixed with a solution containing 5% NaCl and 0.2M NaOH at a ratio of 1.0g of material to 20 mL of solution. The mixture was shaken at 200rpm for 24h at room temperature. Subsequently, modified tea residue was placedona on gauze and washed by deionized water to remove excess base. This procedure was repeated until no pH variation in wash water was observed. We dried the final product in an oven at 50ºC until constant weight and named it as HN–HFO. The final product was stored for all the experiments.

Adsorbate solution preparation containing Ca^{2+} and Mg^{2+}. The adsorbate solution was prepared by dissolving analytical grade anhydrous calcium chloride and anhydrous magnesium chloride in pure water to obtain the required concentration. The initial pH value of the solution was adjusted to 6.0.

Batch adsorption experiments. Batch adsorption experiments involved equilibrating 1 g of HN–HFO with 100 mL of aqueous solution at a given concentration in a beaker. The removal rate was negligible after 60 min of preliminary experiments. Therefore, a contact time of 60 min was used for batch tests. The effect of contact time (5–90 min), initial concentration of metal ions (200–1200 mg/L), pH (3–8), and quantity of the HN–HFO (0.5–3.0 g) on single uptake was also studied. For pH values (3–8) adjustments, 0.1M HCl and 0.1M NaOH solutions were used.

Adsorption kinetics and isotherm experiments. For obtaining the kinetic curves, the mixture solution was shaken on a digital display mixer at a speed of 200 min^{-1}, and 5 mL of the solution was sampled at various time intervals. For isotherm experiments, a known weight of HN–HFO (1.0 g) was equilibrated with 100 mL of metal ion solution of known concentration ranging from 100 mg/L to 1000 mg/L in a flask.

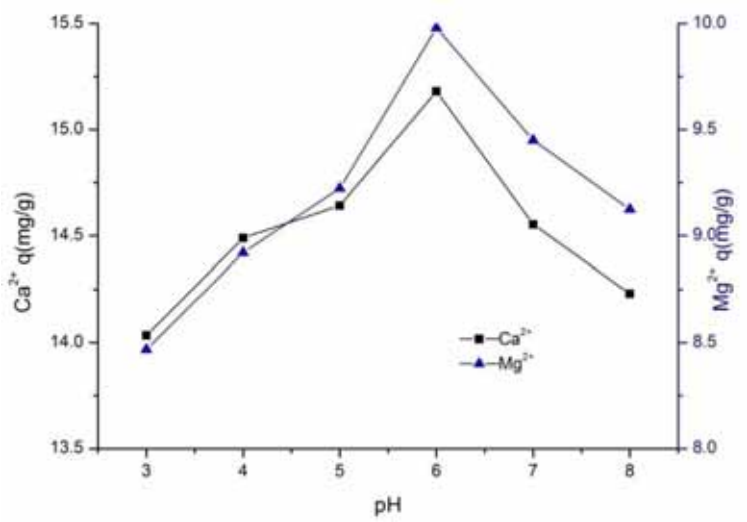

FIGURE 1
Effect of pH on the adsorption of $Ca^{2+}$and $Mg^{2+}$by HN–HFO: 0.5 or 1g of HN–HFO mixed with 100mL Ca^{2+} or Mg^{2+} solution respectively at 40ºC.

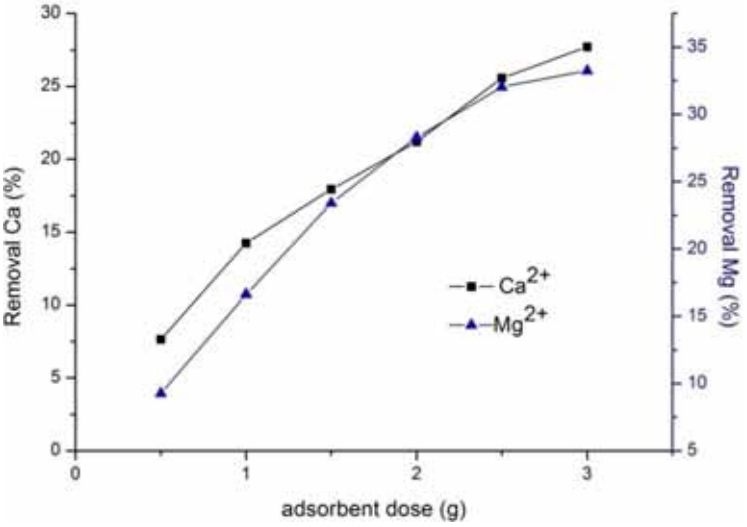

FIGURE2
Effect of adsorbent dose on the adsorption of Ca^{2+}or Mg^{2+}on HN–HFO:100mL of Ca^{2+} solution and Mg^{2+} solution respectively at 40ºC and pH=6.

RESULTS AND DISCUSSION

Effect of solution Ph. As reported by numerous studies, pH plays an important role in the sorption uptake of metals by biomasses. Figure 1 shows the adsorption capacity of Ca^{2+} or Mg^{2+} per gram of HN–HFO(q) within the pH value range of 3–8. The HN–HFO adsorbent showed the maximum adsorption capacity at pH 6.0 for Ca^{2+}or Mg^{2+}. The adsorption capacity of Ca^{2+} or Mg^{2+}wasthelowest at pH<4 and increased with increasing pH value from pH4 to pH 6. This phenomenon may be ascribed to the variation in interchangeable ions binding with the function groups of the HN–HFO matrix, such as H^+ ions. The concentration and surface charge of the adsorbent may also affect adsorption capacity under different pH values. At low pH values, adsorbent exhibited low adsorption capacity because of the competition between H^+ ions and cations in the solution. Owing to high negative charge on the adsorbent surface at elevated pH values, the adsorbents displayed strong attraction toward cations. The cations in solution can form complexes and precipitate with OH^- ultimately with further increase in pH value [33, 34]. Numerous biomass materials, such as orange peel [35] and coconut shell [36], present analogical results. Thus, the optimum pH for adsorption of Ca^{2+} and Mg^{2+} was graphically determined at pH 6.0.

Effect of adsorbent dose. The effect of adsorbent dose on the adsorption of Ca^{2+} and Mg^{2+} on HN–HFO was studied, and the results are shown in

Figure2. The removal percentage of metal ions increased with increasing adsorbent dose in 100mLof adsorbate solution from 0.5 g to 3.0 g. The number of adsorption sites increased by further increase in the weight of adsorbent dose, leading to a high removal percentage of metal ions. Meanwhile, the adsorption capacity of metal ions adsorbed per gram of adsorbent decreased, whereas the adsorbent dose increased (Figure 3). This phenomenon may be ascribed to the decrease in metal ion concentration to a low value at high adsorbent dose, and the adsorption sites did not become saturated for adsorbing metal ions. This condition resulted in low "*q*" values when the system reached equilibrium [37].

Effect of initial metal ions concentration. Figure 4shows the influence of initial metal ion concentration on adsorption capacity. The adsorption capacity per gram of HN–HFO for Ca^{2+} or Mg^{2+} increases with initial concentration. The adsorption capacities of per gram of HN–HFO on $Ca^{2+}$and Mg^{2+} reached a maximum value at a concentrations of 1000 mg/L for Ca^{2+} and 600 mg/L for Mg^{2+}. However, the adsorption capacity of HN–HFO decreased with the increase in metal ion concentration. This result indicated a limitation of the adsorption process.

Adsorption isotherms. Ambient temperature is a significant influencing factor for sorption. The effect of temperature on the removal of $Ca^{2+}$and Mg^{2+} by HN–HFO was studied. Isothermal adsorption experiments were performed at 303, 313, and 323 K. Experimental data were fitted to the Langmuir [38] and Freundlich [39] models and used to describe adsorption equilibrium. Table 1 shows the linear forms of isotherms.

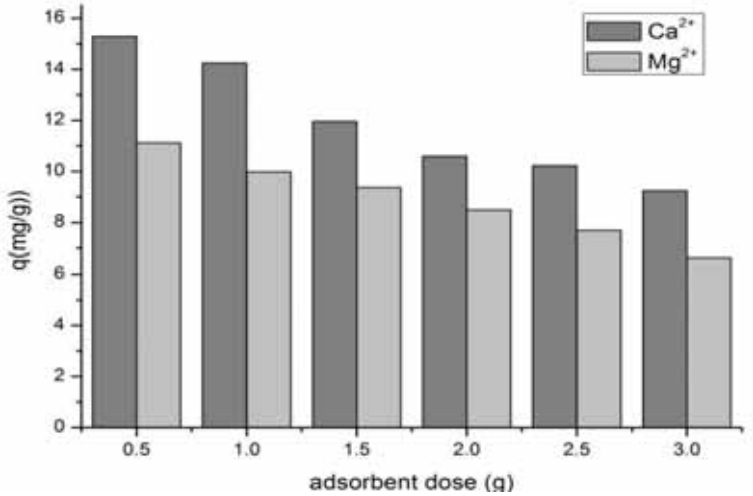

FIGURE 3
Comparison of adsorption capacities of theCa^{2+}or Mg^{2+} on HN–HFO:100mLof solution at 40ºC and pH=6.

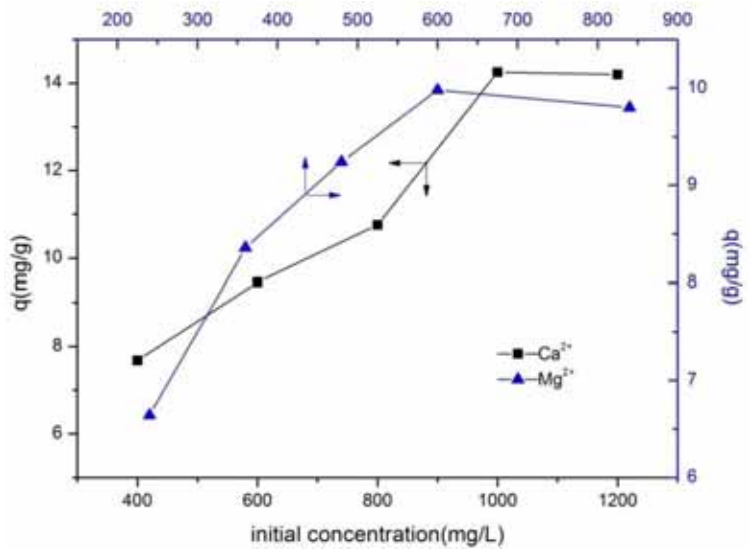

FIGURE 4
Effect of the initial concentration of Ca^{2+} or Mg^{2+}onthe adsorption capacity of HN–HFO:1 g of HN–HFO mixed with 100mL Ca^{2+} and Mg^{2+} solution respectively at 40ºCand pH=6.

TABLE 1
The Linear Forms of the Langmuir and Freundlich isotherms

Isotherms name	Langmuir	Freundlich
Equation	$q_e = q_m k_L c_e / (1 + k_L c_e)$	$q_e = K_F c_e^{1/n}$
Linear form	$c_e/q_e = 1/k_L q_m + c_e/q_m$	$\ln q_e = \ln K_F + 1/n \ln c_e$
q_e	Amount of solute adsorbed by per gram of adsorbent at equilibrium state	
q_m	Amount of solute adsorbed by per gram of adsorbent when all corresponding sites are covered	
c_e	Residual solute concentration in liquid phase at equilibrium state	
K_F andn	Constants related to the Freundlich adsorption capacity and the adsorption intensity respectively	
k_L	Constant of the Langmuir isotherm	

TABLE 2
The parameters of the Langmuir and Freundlich isotherms

Metals	Temp(K)	Langmuir			Freundlich		
		q_m (mg/g)	K_L (L/mg)	R^2	K_f ($mg^{1-n}L^n/g$)	1/n	R^2
Ca^{2+}	303K	15.87	0.0260	0.994	1.257	0.499	0.971
	313K	16.39	0.0277	0.999	1.507	0.466	0.990
	323K	16.12	0.0273	0.998	1.423	0.477	0.983
Mg^{2+}	303K	12.66	0.0574	0.994	1.639	0.454	0.988
	313K	13.16	0.0624	0.998	1.857	0.430	0.982
	323K	12.82	0.0619	0.998	1.766	0.444	0.981

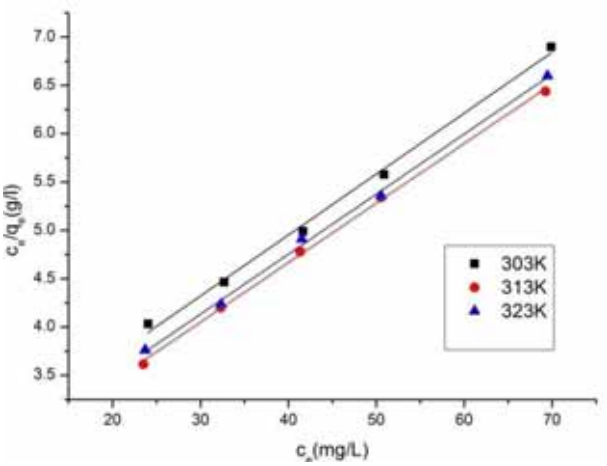

FIGURE 5(a)
Adsorption isotherms of Ca^{2+} according to the Langmuir model (1g of HN–HFO mixed with 100mL adsorbate solution at pH6.0)

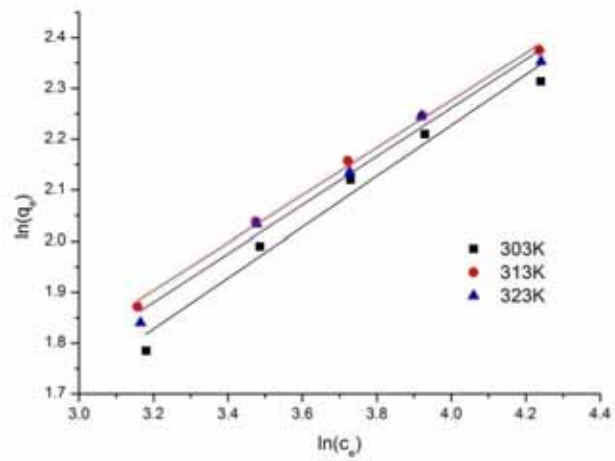

FIGURE 5(b)
Adsorption isotherms of Ca^{2+} according to the Freundlich model (1 g of HN–HFO mixed with 100mL adsorbate solution at pH6.0)

Adsorption isotherms ofCa^{2+} and Mg^{2+} on HN–HFO are shown in Figures 5 and 6. The relative parameters of the Langmuir and Freundlich models are summarized in Table 2. The higher R^2 value suggests that experimental data were fitted the Langmuir model better than the Freundlich model [40]. Values of1/n for Ca^{2+}or $Mg^{2+}$are in the range of0–1, indicating favorable adsorption[41]. HN–HFO shows higher adsorption capacity for Ca^{2+}compared with Mg^{2+}. The maximum adsorption capacity q_m for $Ca^{2+}$and Mg^{2+} by HN–HFO were 16.39 and 13.16 mg/g at 313K, respectively.

Numerous researchers have investigated other natural biomasses as low-cost biosorbents to remove metal ions. The sorption capacities for Ca^{2+} and Mg^{2+} by HN–HFO and other materials are listed and compared in Table3. In general, *H. nana* or Kulumuti is a superior adsorbent than other natural bioadsorbent materials because the modified HN–HFO tea residue exhibits higher adsorption capacity.

TABLE 3
Reported adsorption capacities for several natural materials

Adsorbent	q_{max} (mg/g)		Reference
	Ca^{2+}	Mg^{2+}	
Natural zeolitic tuff	––	2.5	[42]
Rice husk activated carbon	15.14	6.90	[43]
Kraft fiber	0.426	––	[44]
Sugar cane bagasse modified with tartaric acids	14.72	–	[45]
Chemically modified cellulose	15.6	13.5	[46]
Hymenoleana nana	1.3	1.1	this paper
HN–HFO	16.39	13.16	this paper

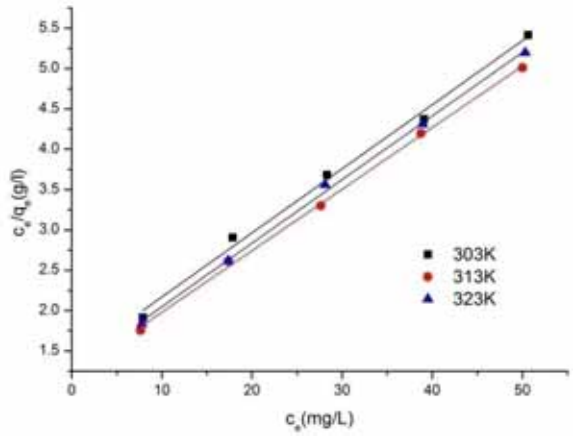

FIGURE 6(a)
Adsorption isotherms of Mg^{2+} according to the Langmuir model
(1g of HN–HFO mixed with 100mL adsorbate solution at pH6.0)

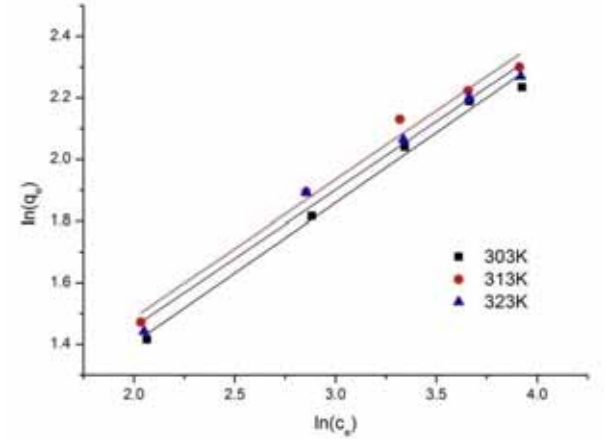

FIGURE 6(b)
Adsorption isotherms of Mg^{2+}according to the Freundlich model
(1 g of HN–HFO mixed with 100mL adsorbate solution at pH 6.0)

TABLE 4
Second order kinetic parameters for the adsorption of $Ca^{2+}$and $Mg^{2+}$by HN–HFO

Metal	Initial solution concentration (mg/L)	Initial adsorption rate h ((mg/g)/min)	Rate constant k_2((mg/g)/min)	Experimental adsorption capacity q_{exp}(mg/g)	Predicted adsorption capacity q_{pre} (mg/g)	R^2
Ca^{2+}	1000	1.968	0.0073	14.25	16.39	0.995
Ca^{2+}	800	1.366	0.0087	10.76	12.5	0.997
Mg^{2+}	600	1.005	0.0074	9.98	11.63	0.995
Mg^{2+}	480	0.993	0.0077	9.24	11.36	0.999

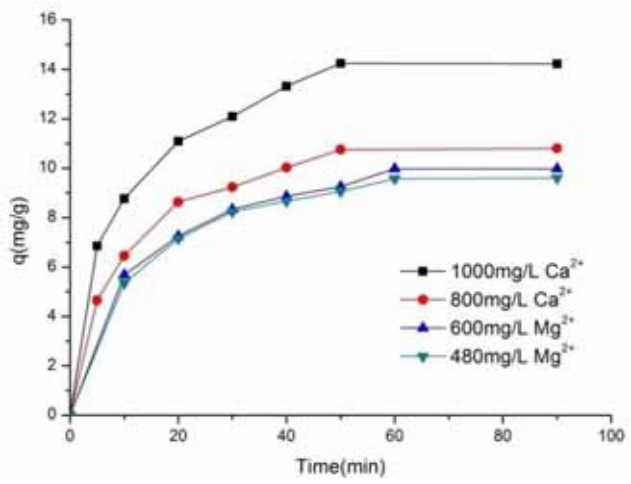

FIGURE 7
Adsorption of $Ca^{2+}$and $Mg^{2+}$by HN–HFO over time (1g of HN–HFO mixed with 100mL of solution at 40ºCand pH6.0)

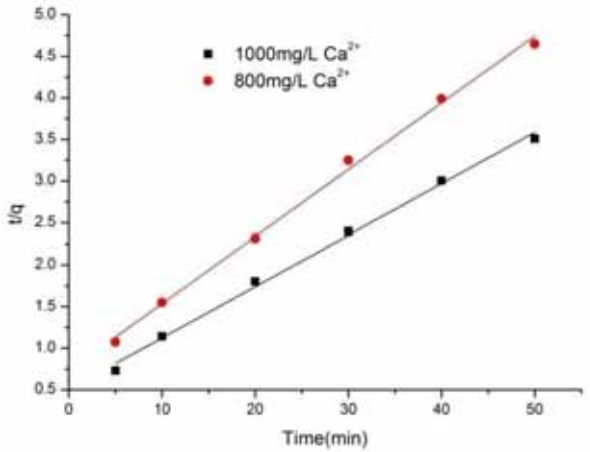

FIGURE 8
Pseudo–second order model for the removal of Ca^{2+} by HN–HFO mixed with 100mL of solution at 40ºC and pH 6.0

Adsorption kinetics. Figure 7 shows that the equilibrium ofCa^{2+} and Mg^{2+}adsorptionwas reached at 60 min. The uptake of Ca^{2+} and Mg^{2+}increasedrapidly in the first 10 min and then increased slowly until the system reaches equilibrium.

Adsorption kinetics describes the uptake rate of the adsorbate and its residence time. The results first showed a rapid increase in adsorption capacity for each ion on HN–HFO, followed by a slow increase. Initially, the driving force was high owing to the concentration difference between the solid–liquid interface and the solution, leading to a high adsorption rate[47]. The adsorption rate decreased owing to a slow diffusion of adsorbate into HN–HFO. In this study, the first-order model and the second-order model were fitted to experimental data and to describe the dynamic adsorption. The Lagergren pseudo-first-order model [48] is illustrated in Eqs. (1) and (2)

$$d_q/d_t = K_1 (q_e - q_t) \quad (1)$$

$$\ln(q_e - q_t) = \ln q_e - K_1 t \quad (2)$$

The pseudo-second order model [49] can be expressed in Eqs.(3) and (4)

$$d_q/d_t = K_2 (q_e - q_t)^2 \quad (3)$$

$$t/q_t = 1/K_2 q_e^2 + t/q_e \quad (4)$$

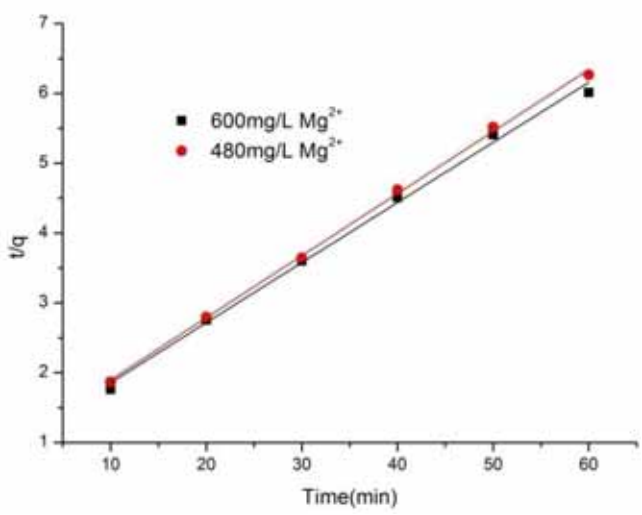

FIGURE 9
Pseudo–second order model for the removal of Mg^{2+} by HN–HFO mixed with 100mL of solution at 40°C and pH 6.0

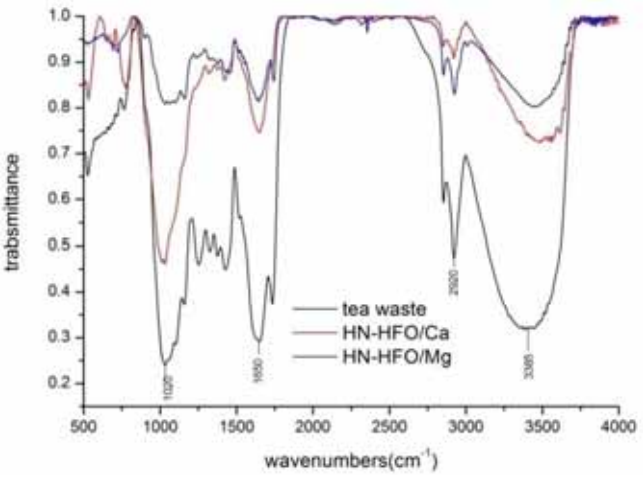

FIGURE 10
FT–IR spectra of tea residue and HN–HFO loaded with different metal ions

In Eqs. (1)–(4), q_t and q_e are the amount of metal ions adsorbed per gram of adsorbent (mg/g) at any time t and at the equilibrium time, respectively, andk_1 and k_2 are the adsorption rate constants. The initial adsorption rate (h (mg/g/min)) is equal tok_1q_e and $k_2q_e^2$ for two models.

Figures 8 and 9 show that the experimental data fitted the pseudo-second order model better than the pseudo-first order model according to the squared correlation coefficient R^2. The kinetic parameters of the pseudo-second order model are calculated and presented in Table 4. The initial adsorption rate increased with the initial Ca^{2+} or Mg^{2+}concentration, and the rate constant (k_2) decreased with increasing initial metal Ca^{2+} or Mg^{2+}concentration. The calculated q values (16.39 and 12.5 mg/g for Ca^{2+} and 11.63 and 11.36 mg/g for Mg^{2+}) also approached experimental data (14.25 and 10.76 mg/g for Ca^{2+} and 9.98 and 9.24 mg/g for Mg^{2+}) [50]. For the exchange mechanism or driving force, this finding may be due to the concentration difference between the metal ion concentration in the solution and that on the solid–liquid interface. Thus, high initial adsorbate concentration indicates high initial adsorption rate for selected adsorbate[51]. The adsorption of Ca^{2+} or Mg^{2+} may be partially ascribed to the exchange of alkali-earth metal ions with Na^+ or H^+. In addition, physical adsorption may also partially be dedicated to the adsorption of Ca^{2+} or Mg^{2+} by HN–HFO.

Infrared spectra analysis. The functional groups responsible for adsorbing Ca^{2+}or Mg^{2+} were determined by FTIR analysis. The IR spectra of tea residue HN–HFO loaded with Ca^{2+} or Mg^{2+} is shown in Figure 10. The IR spectrum of the tea residue showed an intense band at 3385cm^{-1}, indicating the presence of the hydroxyl groups on the adsorbent surface. The adsorption peak at 2920$cm^{-1}$was associated with C–H stretching vibration. Moreover, the strong peak at 1020$cm^{-1}$was in accordance with the

vibration of the C–O group of carboxylic acids. In addition, spectral peaks observed at 1650 cm^{-1}corresponded to the stretching vibrations of the carbonyl portion of the amide function groups [52]. After adsorption of metal ions, these bands shifted slightly, suggesting that the reactive groups participated in adsorption reaction. In a word, metal ions, such as Ca^{2+} or Mg^{2+} in solution, were bound to HN–HFO and occupied the possible adsorption sites. Tea residue was loaded with ferric oxide through ionic exchange or complexation reaction before use and was thus responsible for Ca^{2+}or Mg^{2+} adsorption. However, the adsorption capacity of unmodified tea residue was not comparable with that of HN–HFO. This condition indicated that the structural modification of Kulumuti tea residue is important for the adsorption of Ca^{2+} or Mg^{2+} by HN–HFO.

CONCLUSION

In this study, HN–HFO was successfully prepared by impregnating ferric chloride into tea residue. Practical tests for the removal of Ca^{2+} or Mg^{2+} in aqueous solution by HN–HFO show that HN–HFO possesses good adsorption potential. The maximum adsorption capacities for $Ca^{2+}$and Mg^{2+} per gram of HN–HFO were 16.39 and 13.16 mg/g at pH 6.0 and 40℃. This finding indicated that HN–HFO possesses a strong capability for removing Ca^{2+} or Mg^{2+}. The results also showed that the adsorption capacity was influenced by adsorbent dose and initial adsorbate concentrations in the solution. The adsorption kinetics followed the pseudo–second–order model better than the pseudo–first–order model. The adsorption equilibrium was reached at 60 min of contact time. In addition, experimental data fitted the Langmuir isotherm model better than the Freundlich isotherm. Furthermore, the adsorption of Ca^{2+} or Mg^{2+} can be characterized as complexation and exchanging reactions with hydrated ferric oxide-loaded tea residue, that is, HN–HFO. Compared with unmodified tea residue, HN–HFO exhibited improved adsorptive capacity for Ca^{2+} or Mg^{2+}. The results further demonstrated that HN–HFO exhibits greater potential, such as Ca^{2+} or Mg^{2+} removal from hard water, compared with other modified natural biosorbents indicated in this study. Considering that *H. nana* is a widely available material in the northwest region of China, further studies, such as those on the removal of harmful heavy metal ions by modified tea residue from industrial wastewater, the recycled use of HN–HFO, or the adsorption and desorption cycles for removing cations by HN–HFO, should be carried out and given considerable attention

ACKNOWLEDGEMENTS

The authors thank the financial support received from the National Natural Science Foundation of China (NSFC) foundation (U1203183), the Science and Technology Innovation team's construction Foundation in Xinjiang Uygur Autonomous Region (2014751002) and the Science and Technology Planning Project of Guangdong Province, China (2014A020209019 and 2015A020210039)

Competing interests. All the authors declare that there are no competing interests.

REFERENCES

[1] Ketrane, R., Saidani, B., Gil, O., Leleyter, L., Baraud, F. (2009) Efficiency of five scale inhibitors on calcium carbonate precipitation from hard water: Effect of temperature and concentration. Desalination. 249(3), 1397–1404.

[2] Shakkthivel, P., Sathiyamoorthi, R., Vasudevan, T. (2004) Development of acrylonitrile copolymers for scale control in cooling water systems. Desalination. 164(2), 111–123.

[3] Gill, J.S. (1999) A novel inhibitor for scale control in water desalination. Desalination. 124(1–3), 43–50.

[4] Fu, F.L., Wang, Q. (2011) Removal of heavy metal ions from wastewaters: A review. Journal of Environmental Management. 92(3), 407–418.

[5] Yu, Z.H., Qi, T., Qu, J.K., Wang, L., Chu, J.L. (2009) Removal of Ca(II) and Mg(II) from potassium chromate solution on Amberlite IRC 748 synthetic resin by ion exchange. Journal of Hazardous Materials. 167(1–3), 406–412.

[6] Dabrowski, A., Hubicki, Z., Podkościelny, P., Robens, E. (2004) Selective removal of the heavy metal ions from waters and industrial wastewaters by ion–exchange method. Chemosphere. 56(2), 91–106.

[7] Ahn, C.K., Donghee, P., Woo, S.H., Park, J.M. (2009) Removal of cationic heavy metal from aqueous solution by activated carbon impregnated with anionic surfactants. Journal of Hazardous Materials. 164(2–3), 1130–1136.

[8] Qadeer, R. (2005) Kinetics Study of Lead ion Adsorption on Active Carbon. Turkish journal of chemistry. 29(1), 95–99.

[9] Gaikwad, R.W. (2004) Removal of Cd(II) from aqueous solution by activated charcoal derived from coconut shell. Electronic Journal of Environmental Agricultural and Food Chemistry. 3(4), 702–709.

[10] Pesavento, M., Profumo, A., Alberti, G., Conti, F. (2003) Adsorption of lead(II) and copper(II) on activated carbon by complexation with surface functional groups. Analytica Chimica Acta. 480(1), 171–180.
[11] Karidakis, T., Agatzini–Leonardou, S., Neou–Syngouna, P. (2005) Removal of magnesium from nickel laterite leach liquors by chemical precipitation using calcium hydroxide and the potential use of the precipitate as a filler material. Hydrometallurgy. 76(1–2), 105–114.
[12] Boudrahem, F., Aissani–Benissad, F., Soualah, A. (2011) Adsorption of Lead(II) from Aqueous Solution by Using Leaves of Date Trees As an Adsorbent. Journal of Chemical & Engineering Data. 56(5), 1804–1812.
[13] Jeon, C. (2011) Removal of copper ion using rice hulls. Journal of Industrial and Engineering Chemistry. 17(3), 517–520.
[14] Diatta, J.B., Grzebisz, W. (2009) Copper in selected soils and their capacity for regulating its solution concentrations. Fresen. Environ. Bull. 18, 1950–1956.
[15] Wang, Y.F., Wang, H.M., Yao, Y.Y., Zhu, M. (2016) Synthesis of zeolites from a low-grade Chinese natural clinoptilolite for adsorption of CO_2. Fresen. Environ. Bull. 25, 3606–3611.
[16] Saäy, Y. (2001) Biosorption of heavy metals by fungal biomass and modeling of fungal biosorption: a review. Separation and Purification Methods. 30(1), 1–48.
[17] Dhankhar, R., Hooda, A. (2011) Fungal biosorption – an alternative to meet the challenges of heavy metal pollution in aqueous solutions. Environmental Technology. 32(5–6), 467–493.
[18] Liu, Y.H., Cao, Q.L., Luo, F., Chen, J. (2009) Biosorption of Cd^{2+}, Cu^{2+}, Ni^{2+} and Zn^{2+} ions from aqueous solutions by pretreated biomass of brown algae. Journal of Hazardous Materials. 163(2–3), 931–938.
[19] Ahmady–Asbchin, S., Andres, Y., Gerente, C., Le, C.P. (2009) Natural seaweed waste as sorbent for heavy metal removal from solution. Environmental Technology. 30(7), 755–762.
[20] Davis, T.A., Volesky, B., Mucci, A. (2003) A review of the biochemistry of heavy metal biosorption by brown algae. Water Research. 37(18), 4311–4330.
[21] Altundogan, H.S., Arslan, N.E., Tumen, F. (2007) Copper removal from aqueous solutions by sugar beet pulp treated by NaOH and citric acid. Journal of Hazardous Materials. 149(2), 432–439.
[22] Wong, K.K., Lee, C.K., Low, K.S., Haron, M.J. (2003) Removal of Cu and Pb by tartaric acid modified rice husk from aqueous solutions. Chemosphere. 50(1), 23–28.
[23] Guo, H., Zhang, S.F., Kou, Z.N., Zhai, S.R., Ma, W., Yang, Y. (2015) Removal of cadmium(II) from aqueous solutions by chemically modified maize straw. Carbohydrate Polymers. 115(115), 177–185.
[24] Cay, S., Uyanik, A., Ozasik, A. (2004) Single and binary component adsorption of copper(II) and cadmium(II) from aqueous solutions using tea–industry waste. Separation and Purification Technology. 38(3), 273–280.
[25] Malkoc, E., Nuhoglu, Y. (2006) Fixed bed studies for the sorption of chromium(VI) onto tea factory waste. Chemical Engineering Science. 61(13), 4363–4372.
[26] Djati, U.H., Hunter, K. A. (2006) Adsorption of Divalent Copper, Zinc, Cadmium and Lead Ions from Aqueous Solution by Waste Tea and Coffee Adsorbents. Environmental Technology. 27(1), 25–32.
[27] Wan, S.L., Ma, Z.Z., Xue, Y., Ma, M.H., Xu, S.Y., Qian, L.P., Zhang, Q.R. (2014) Sorption of Lead(II), Cadmium(II), and Copper(II) Ions from Aqueous Solutions Using Tea Waste. Industrial and Engineering Chemistry Research. 53(9), 3629–3635.
[28] Malkoc, E., Nuhoglu, Y. (2005) Investigations of nickel(II) removal from aqueous solutions using tea factory waste. Journal of Hazardous Materials. 127(1–3), 120–128.
[29] Kuo, S. (1986) Concurrent Sorption of Phosphate and Zinc, Cadmium, or Calcium by a Hydrous Ferric Oxide1. Soil Science Society of America Journal. 50(6), 1412–1419.
[30] Boukhalfa, C. (2010) Sulfate removal from aqueous solutions by hydrous iron oxide in the presence of heavy metals and competitive anions: Macroscopic and spectroscopic analyses. Desalination. 250(1), 428–432.
[31] Liu, W.F., Zhang, J., Zhang, C.L., Wang, Y.F., Li, Y. (2010) Adsorptive removal of Cr(VI) by Fe–modified activated carbon prepared from Trapanatans husk. Chemical Engineering Journal. 162(2), 677–684.
[32] Eren, E., Gumus, H., Ozbay, N. (2010) Equilibrium and thermodynamic studies of Cu(II) removal by iron oxide modified sepiolite. Desalination. 262(1), 43–49.
[33] Yang, X.P., Cui, X.N. (2013) Adsorption characteristics of Pb(II) on alkali treated tea residue. Water Resources and Industry. 3(2), 1–10.
[34] Adak, A., Bandyopadhyay, M., Pal, A. (2005) Removal of crystal violet dye from wastewater by surfactant–modified alumina. Separation and Purification Technology. 44(2), 139–144.
[35] Dhakal, R.P., Ghimire, K.N., Inoue, K. (2005) Adsorptive separation of heavy metals from an aquatic environment using orange waste. Hydrometallurgy. 79(3–4), 182–190.

[36] Amuda, O.S., Giwa, A.A., Bello, I.A. (2007) Removal of heavy metal from industrial wastewater using modified activated coconut shell carbon. Biochemical Engineering Journal. 36(2), 174–181.
[37] Li, Y.H., Xia, B., Zhao, Q.S., Liu, F.Q., Zhang, P., Du, Q.J., Wang, D.C., Li, D., Wang, Z.H., Xia, Y.Z. (2011) Removal of copper ions from aqueous solution by calcium alginate immobilized kaolin. Journal of Environmental Sciences. 23(3), 404–411.
[38] Langmuir, I. (1916) Constitution and fundamental properties of solids and liquids. Journal of the American Chemical Society. 38, 2221–2295.
[39] Parida, K.M., Sahu, B.B., Das, D.P. (2004) A comparative study on textural characterization: cation–exchange and sorption properties of crystalline α–zirconium(IV), tin(IV), and titanium(IV) phosphates. Journal of Colloid and Interface Science. 270(2), 436–445.
[40] Okoye, A.I., Ejikeme, P.M., Onukwuli, O.D. (2010) Lead removal from wastewater using fluted pumpkin seed shell activated carbon: adsorption modeling and kinetics. International Journal of Environmental Science and Technology. 7(4), 793–800.
[41] Huang, Q., Zhu, S.M., Zeng, D., Yu, S.J. (2016) Kinetic and thermodynamic study of the adsorption of calcium onto sugar beet pulp. Sugar Industry. 141(9), 565–570.
[42] Tomić, S., Rajić, N., Hrenović, J., Povrenović, D. (2012) Removal of Mg from spring water using natural clinoptilolite. Clay Minerals. 47(1), 81–92.
[43] Rostamian, R., Heidarpour, M., Mousavi, S.F., Afyuni, M. (2014) Removal of Calcium and Magnesium by Activated Carbons Produced from Agricultural Wastes. Advances in Environmental Biology. 8(12), 202–208.
[44] Duong, T.D., Hoang, M., Nguyen, K.L. (2005) Sorption of Na^{+}, Ca^{2+} ions from aqueous solution onto unbleached kraft fibers–kinetics and equilibrium studies. Journal of Colloid and Interface Science. 287(2), 438–443.
[45] Soliman, E.M., Ahmed, S.A., Fadl, A.A. (2011) Removal of calcium ions from aqueous solutions by sugar cane bagasse modified with carboxylic acids using microwave–assisted solvent–free synthesis. Desalination. 278(1), 18–25.
[46] Karnitz Júnior, O., Gurgel, L.V.A., Gil, L.F. (2010) Removal of Ca(II) and Mg(II) from aqueous single metal solutions by mercerized cellulose and mercerized sugarcane bagasse grafted with EDTA dianhydride (EDTAD). Carbohydrate Polymers. 79(1), 184–191.
[47] Liu, X., Zhang, L.F. (2015) Removal of phosphate anions using the modified chitosan beads: Adsorption kinetic, isotherm and mechanism studies. Powder Technology. 277, 112–119.
[48] Agrawal, A., Sahu, K.K. (2006) Kinetic and isotherm studies of cadmium adsorption on manganese nodule residue. Journal of Hazardous Materials. 137(2), 915–924.
[49] Chen, C.L., Li, X.L., Zhao, D.L., Tan, X.L., Wang, X.K. (2007) Adsorption kinetic, thermodynamic and desorption studies of Th(IV) on oxidized multi–wall carbon nanotubes. Colloids and Surfaces A Physicochemical and Engineering Aspects. 302(1–3), 449–454.
[50] Yang, F.C., Sun, S.Q., Chen, X.Q., Chang, Y., Zha, F., Lei, Z.Q. (2016) Mg–Al layered double hydroxides modified clay adsorbents for efficient removal of Pb^{2+}, Cu^{2+} and Ni^{2+} from water. Applied Clay Science. 123, 134–140.
[51] Amarasinghe, B.M.W.P.K., Williams, R.A. (2007) Tea waste as a low cost adsorbent for the removal of Cu and Pb from wastewater. Chemical Engineering Journal. 132(1), 299–309.
[52] Liu, J.M., Ou, Z.W., Mo, J.C., Wu, H., Zhao, Y.L. (2016) Immobilization of chromium using low-calcium fly ash with the "absorption-abruption-curing" method. Fresen. Environ. Bull. 25, 6012–6019.

Received: **08.12.2017**
Accepted: **26.04.2018**

CORRESPONDING AUTHOR

Siming Zhu
School of Food Science and Engineering,
South China University of Technology,
381 Wushan Road, Tianhe District,
Guangzhou 510640 – P.R. China

e–mail: lfsmzhu@scut.edu.cn

© by PSP Volume 27 – No. 7/2018 pages 4813-4821 Fresenius Environmental Bulletin

EXAMINATION OF THE WOODY PLANT DIVERSITY IN THE BESKAYALAR AND BALLIKAYALAR NATURAL PARKS WITHIN THE SCOPE OF FLORA TOURISM

Murat Zencirkiran[1,*], Elvan Ender[1], Esma Eraslan[2], Sena Cetiner[2], Aysegul Gorur[2], Duygu Tanriverdi-O[2], Betul Humeyra Celik[2], Burcu Muduk[2]

[1]University of Uludag, Faculty of Agriculture, Department of Landscape Architecture, Gorukle Campus, Nilufer, Bursa, Turkey
[2]University of Uludag, Institute of Natural Sciences, Landscape Architecture, Gorukle Campus, Nilufer, Bursa, Turkey

ABSTRACT

Turkey has a rather important place for flora or botanic tourism with its plant diversity resources and there has been a substantial rise in the number of activities realized within this scope in recent years. Within this scope, it is extremely important to elaborate on these resource areas included within the geography of our country for flora tourism activities and reveal their potentials in terms of sustainability. In this study, the Beskayalar and Ballıkayalar Natural Parks included within the protected area system of our country were examined and their woody plant potentials tried to be revealed within the scope of the flora tourism values. The obtained results indicated that both natural parks were satisfactorily good for the flora or botanic tourism activities thanks to the presence of woody taxon, but there was more taxon diversity in the Beskayalar natural park.

KEYWORDS:
Species diversity, ecotourism, Kocaeli, botanic tourism.

INTRODUCTION

In parallel to the rapid change taking place in the world, the understanding of tourism changes, too. Tourism activities having been performed on the basis of the triple of sea, sand and sun for many years have differed in recent years in a way to cover nature protection-based tourism activities. People have started to prefer quieter places in quieter periods to mass tourism and this has developed such tourism phenomena as ecotourism, responsible tourism, green and nature tourism.

Ecotourism features prominently among the various alternative forms of tourism being debated [1]. Ecotourism, one of the phenomena making use of environmental values as the most important resource, taking shape as an alternative in the tourism sector and identifying with the concepts of nature-based and sustainability [2, 3], is defined as environmentally responsible, enlightening travel and visitation to relatively undisturbed natural areas in order to enjoy and appreciate nature (and any accompanying cultural features both past and present) that promotes conservation, has low visitor impact, and provides for beneficially active socio-economic involvement of local populations [4]. According to this definition, ecotourism can involve both cultural and environmental tourism and, in addition, benefits to the local population should be an integral part of the activity [5].

Ecotourism is divided into such sub-activity areas as trekking, photo safari, mounted nature walks, agriculture and farm-based tourism, bike or tableland tourism, mountain climbing and flora or botanic tourism [6]. The flora or botanic tourism included within these activity areas appears to have become a type of tourism covering activities which many people perform or at least want to perform at least a few times a year in recent years. Flora or botanic tourism covers all the activities of daytrips, nature walks and knowing the nature starting with picnics, examining plants and adding a sample plant taken from the nature to living spaces [6].

Turkey geography is very rich in terms of biological (vegetation, wild life, ecosystem, habitat, etc.) and physical natural resources (geographical position, geology, mineralogy, paleontology, etc.) and aesthetic resources [7] and it is an important source for especially rich bio-diversity, flora or botanic tourism activities [8]. This opportunity gives to the country prestigious place between the three continents [9]. In Turkey, most of the places having biological, physical and aesthetic resource values are included within the system of "protected areas" and this system includes 11 different structures, namely national park, nature protection area, natural park, natural monument, wild life improvement area, protection forest, natural site, special environmental protection area, ramsar area, biosphere reserve, world heritage area [10].

Of these structures, Natural Parks are the areas having such important functions as the protection, management, development and restoration of great landscapes as well as the development of the recreation opportunities of countries by achieving the

maintainable uses of natural resources and especially the promotion of tourism development in areas which are weak in terms of structure and also they provide opportunities for many activities such as environmental education, special activities for children and young people, recreation, physical exercise, coming together with nature and landscape and exploring cultures [11, 12].

Natural Parks defined as the "nature parts which have vegetation and wild life characteristics and are appropriate for people to have a rest and enjoy themselves within the view integrity" are one of the 11 structures included within the system of protected areas in our country. Nature-based tourism and recreation, including in protected areas, is increasing worldwide [13] and in Turkey. One of the most important places in term of nature-based tourism is nature parks in Turkey. Because of their natural resource values, natural parks are very important places for the flora and botanic tourisms as well as they are areas where biological riches are taken under protection [14]. On the other hand, these types of protected areas play an important role in the monitoring of global change and in longitudinal ecological studies [15].

As of July 2015, in Turkey, there are 203 natural parks declared on an area of 969.574,2 decares. As of area, 3,55 % of the natural parks in Turkey are located within the city borders of Kocaeli. The city of Kocaeli has 8 Natural Parks spreading on a total area of 34.419,6 decares, namely Ballıkayalar, Beskayalar, Eriklitepe, Kuzuyayla, Suadiye, Uzuntarla, Gazilerdağı and Uzunkum [16].

Within the scope of this study, the natural parks of "Ballıkayalar" and "Beskayalar" considered to have important values in terms of flora or botanic tourism were evaluated in terms of woody taxon included among the key and permanent elements of landscape.

MATERIALS AND METHODS

Research material and study area. The material of the study was composed of the natural parks of "Ballıkayalar" with an area of 16.029,73 decares and "Beşkayalar" with an area of 10.998,30 decares, which are located within the city borders of Kocaeli.

The city of Kocaeli, the third city of the Marmara region in terms of population, is located between the east longitudes of 29° 22'-30° 21' and the north latitudes of 40° 31'-41° 13' to the west of the Marmara Region. There is the Black Sea in the north; there are the cities of Istanbul and Yalova and the Sea of Marmara in the west; there are the cities of Bursa and Bilecik in the south; there is the city of Sakarya in the east.

While the Gulf coast and the Black Sea coast enjoy a temperate climate, the mountainous parts enjoy a harsh climate. It can be stated that the climate of Kocaeli forms a transition between the Mediterranean climate and the Black Sea climate. In the city center, summers are hot with a little rain and winters are rainy and from time to time snowy and cold [17]. According to the average of the data of 65 years, the annual rainfall is 809,3 kg/m^2 in the city. The average number of warm rainy days is 136,1; the annual average temperature is 14,9°C; the average number of snowy days is 12 [18].

The Ballıkayalar Natural Park. The Ballıkayalar Natural Park, which lies within the borders of the Gebze county of Kocaeli, is located between the north latitudes of 40° 49' 30", 40° 54' 00" and the east longitudes of 29° 30' 00", 29° 33' 30". The Ballıkayalar Natural Park is 6,5 km to the north of the Izmit Gulf. The highest points in the Natural Park are Topluca tepe with an altitude of 280 m in the north and Düzmese Tepe with an altitude of 224 m. Within the Ballıkayalar natural park, there are five continental ecosystems, namely Maquis/ Pseudomaquis ecosystem, Deciduous oak ecosystem, Anthropogenic meadow/pasture ecosystem, Wet forest ecosystem and Agricultural areas and Stream ecosystem [19] and an aquatic ecosystem (Figure 1).

The Beskayalar Natural Park. The Beskayalar Natural Park, which lies within the borders of the Izmit county of Kocaeli, is located between the north latitudes of 40° 35' 00", 40° 37' 30" and the east longitudes of 29° 52' 00", 29° 56' 30". The Beskayalar Natural Park is 12 km to the south of the Izmit Gulf. In the Natural park, the highest points are Bayrak tepe with an altitude of 1073 m in the central part of the park and Damla cape with an altitude of 1068 m in the southwest border. Moreover, the altitude of Kirazlıdere, which is in the northwest border, is 280 m. Within the Beskayalar natural park, there are two continental ecosystems, namely Deciduous forest ecosystem and Anthropogenic meadow/pasture ecosystem and Stream ecosystem [20] and an aquatic ecosystem (Figure 2).

Method. The method of the study was designed in two stages. In the first stage, interviews were held with the institutions responsible for the region and the natural parks and information about the study areas was collected through literature review. In the second stage, with the aim of determining the woody plants existing in both natural parks, terrain studies were carried out in different periods and the obtained data was compared with those of the previous studies [19-29] and evaluations were made in relation to the woody taxon existing in the natural parks.

FIGURE 1
The Borders of the Ballıkayalar natural park

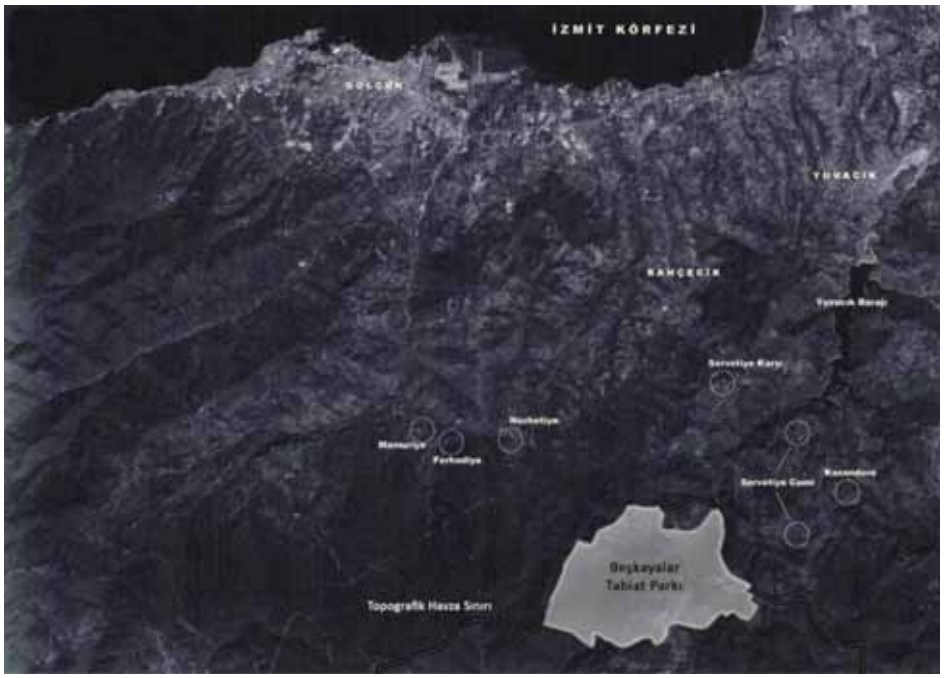

FIGURE 1
The Borders of the Beskayalar natural park

TABLE 1
Distribution of the woody plant groups in the natural parks

Natural parks	Taxonomic group	Number of taxon	
		Number	%
Ballıkayalar	Gymnospermae	5	3,58
	Angiospermae	59	42,14
Beşkayalar	Gymnospermae	3	2,14
	Angiospermae	73	52,14

RESULTS

The evaluations indicated that the Beskayalar natural park is richer than the Ballıkayalar natural park in terms of woody taxon. As a result of the evaluations, it was determined that there were 76 woody plant taxon in the Beskayalar natural park and there were 64 woody plant taxon in the Ballıkayalar natural park. It was observed that 94% of the woody plant taxon included in both natural parks fell in the category of Angiospermae (Table 1).

When the distribution of the woody taxon existing in both natural parks according to the phyto-geographical regions was examined, it was found that 46 of the determined 108 taxons fell into the category of Europe-Siberia, 18 fell into the category of Mediterranean and 44 fell into the category of Unknown. The biggest group was composed of the Europe-Siberia phyto-geographical region woody taxon (Table 2, Figure 3). It was determined that 26,57% of the woody taxon included within the borders of the Ballıkayalar natural park and 56,58% of the woody taxon included within the borders of the Beskayalar natural park were the elements of the Europe-Siberia phyto-geographical region (Figure 4).

It was observed that the woody taxon existing in both natural parks were included in 33 families, namely *Aceraceae, Anacardiaceae, Aquifoliaceae, Araliaceae, Betulaceae, Caprifoliaceae, Celastraceae, Cistaceae, Cornaceae, Corylaceae, Cupressaceae, Ephedraceae, Ericaceae, Fabaceae (Leguminosae), Fagaceae, Hypericaceae (Guttiferae), Juglandaceae, Lauraceae, Liliaceae, Moraceae, Oleaceae, Platanaceae, Pinaceae, Rhamnaceae, Rosaceae, Salicaceae, Santalaceae, Staphylleaceae, Styracaceae, Taxaceae, Tiliaceae, Ulmaceae, Vitaceae*. On the other hand, the woody taxons belonging to the families of *Aceraceae, Aquifoliaceae, Celastraceae, Hypericaceae (Guttiferae), Staphylleaceae, Taxaceae* and *Tiliaceae* were not encountered in the Ballıkayalar natural park and the woody taxons belonging to the families of *Cistaceae, Ephedraceae, Rhamnaceae, Santalaceae, Styracaceae,* and *Vitaceae* were not encountered in the Beskayalar natural park. It was determined that the woody taxons belonging to the family of *Rosaceae* existing within the borders of both parks placed the first in number (Figure 5).

When the distribution of the determined woody taxon according to species was examined, it was observed that there were 45 species of woody taxon in the Ballıkayalar natural park and there were 49 species of taxon in the Beskayalar natural park. Moreover, the number of common species was determined to be 24 (Table 3). When the taxons existing in both natural parks were examined, it was observed that some taxon were common in both natural parks; there were a total 108 taxon in the Ballıkayalar and Beşkayalar natural parks; the number of common taxon was 32 (Table 4).

TABLE 2
Numbers of the woody taxon according to the phyto-geographical regions

Phyto-geographical regions	Number of taxon
Euro-Siberian	46
Mediterranean	18
Non specific to particular phytogeographical region	44

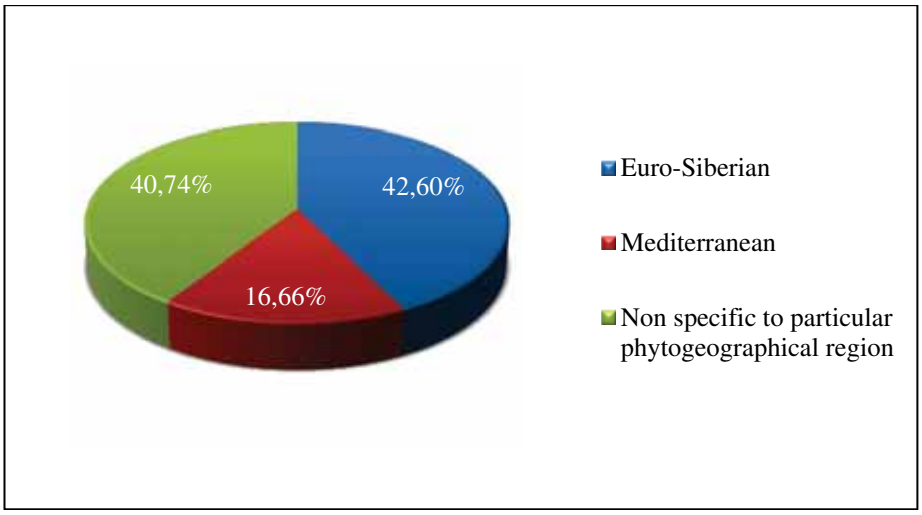

FIGURE 3
Distribution of the woody taxon according to the phyto-geographical regions (%)

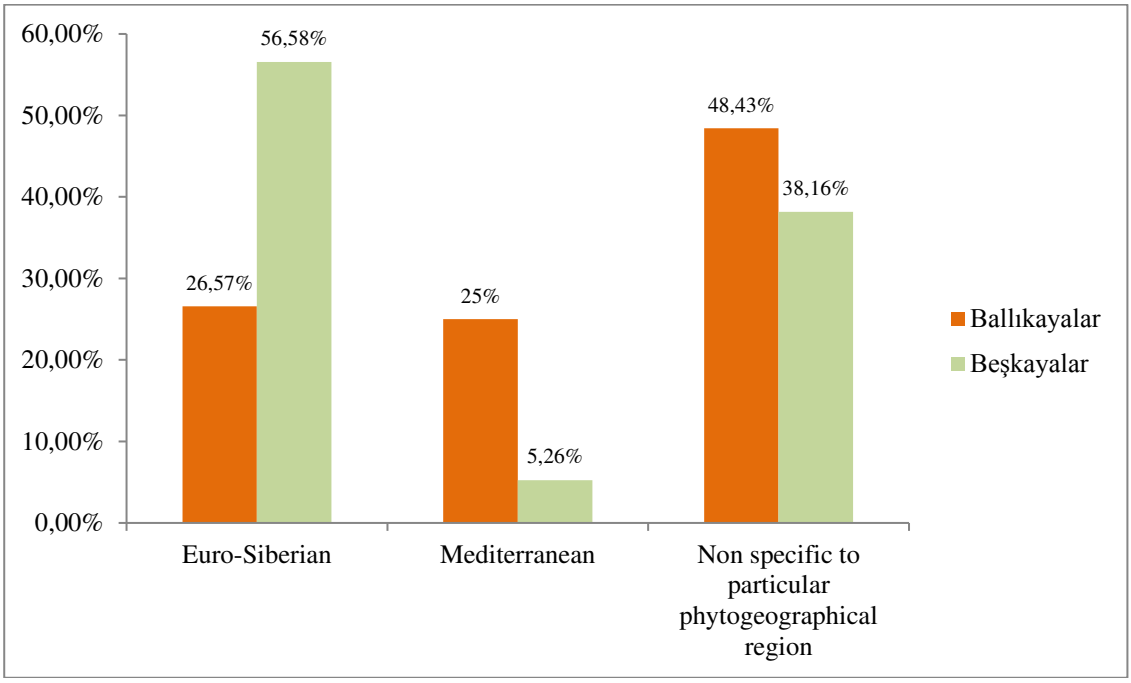

FIGURE 4
Distribution of the woody taxon into phyto-geographical regions according to the natural parks (%)

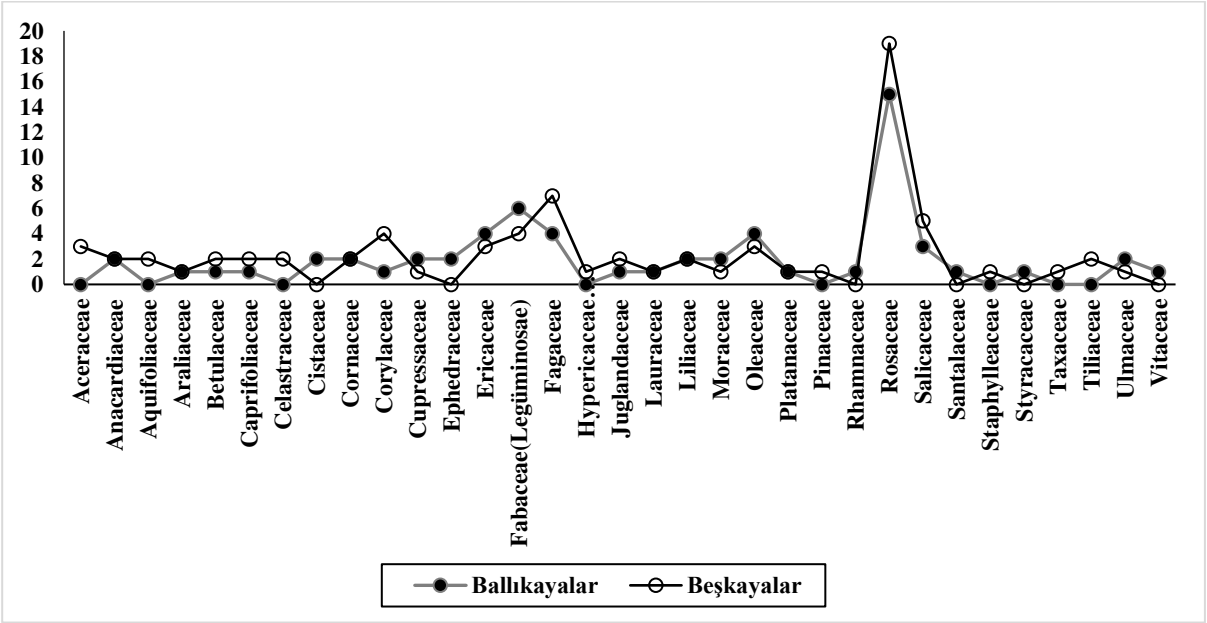

FIGURE 5
Distribution of the woody taxon according to the families

TABLE 3
Numbers of the woody taxon in the natural parks of Ballıkayalar and Beskayalar

Classification by Genus	Ballıkayalar	Beşkayalar
Genus number	45	48
Genus number (common)	24	24
Genus number (different)	21	25

TABLE 4
The woody taxon in the natural parks of Ballıkayalar and Beskayalar

Taxon	Ballıkayalar	Beşkayalar	Taxon	Ballıkayalar	Beşkayalar
Acer trautvetteri Medwed.		*	*Arbutus unedo* L.	*	
Acer campestre L. subsp. *campestre*		*	*Erica arborea* L.	*	*
Acer platanoides L.		*	*Erica manipuliflora* Salisb.	*	
Pistacia terebinthus L. subsp. *palaestina*	*		*Rhododendron ponticum* L. *subsp. ponticum*		*
Pistacia lentiscus L.	*		*Vaccinium arctostaphylos* L.		*
Cotinus coggyria Scop.		*	*Calicotome villosa* (Poiret) Link.	*	
Rhus coriaria L.		*	*Chamaecytisus hirsutus* (L.) Link.		*
Ilex aquifolium L.		*	*Chamaecytisus supinus* (L.) Link.	*	*
Ilex colchica Pojark.		*	*Genista carinalis* Gris.	*	
Hedera helix L.	*	*	*Genista lydia* Boiss. *var. Lydia* Griseb.	*	*
Alnus glutinosa (L.) Gaertn. *subsp. glutinosa*	*	*	*Genista tinctoria* L.	*	*
Betula litwinowii Doluch.		*	*Spartium junceum* L.	*	
Sambucus ebulus L.	*	*	*Fagus orientalis* Lipsky.		*
Sambucus nigra L.		*	*Castanea sativa Miller.*		*
Euonymus europaeus L.		*	*Quercus cerris* L. *var. cerris*		*
Euonymus latifolius (L.) Miller. subsp. latiolius		*	*Quercus coccifera* L.	*	
Cistus creticus L.	*		*Quercus frainetto* Ten.	*	*
Cistus salviifolius L.	*		*Quercus hartwissiana* Steven	*	*
Cornus mas L.	*	*	*Quercus infectoria* Olivier *subsp. infectoria*	*	
Cornus sanguinea L. *subsp. australis*	*	*	*Quercus petraea (Mattuschka) Liebl.subsp. petraea*		*
Carpinus betulus L.	*	*	*Quercus pubescens* Willd.		*
Corylus avellana L. *subsp. avellana*		*	*Hypericum calycinum* L.		*
Corylus maxima Mill.		*	*Juglans regia* L.	*	*
Corylus colurna L.		*	*Pterocarya fraxinifolia*		*
Cupressus sempervirens L.	*		*Laurus nobilis* L.	*	*
Juniperus oxycedrus L. subsp. *oxycedrus*	*	*	*Ruscus aculeatus* L. var. *aculeatus*	*	
Ephedra campylopoda C.A.Meyer	*		*Ruscus aculeatus* L. var. *angustifolius*	*	
Ephedra majör L.	*		*Ruscus aculeatus* L.		*
Arbutus andrachne L.	*		*Ruscus hypoglossum* L.		*

TABLE 4
The woody taxon in the natural parks of Ballıkayalar and Beskayalar

Taxon	Ballı-kayalar	Beş-kayalar	Taxon	Ballı-kayalar	Beş-kayalar
Ficus carica L.	*	*	*Rosa horrida* Fischer	*	*
Morus alba L.	*		*Rosa sempervirens* L.	*	*
Phillyrea latifolia L.	*		*Rubus sanctus* Schreber	*	*
Ligustrum vulgare L.	*	*	*Rubus canescens DC. var. glabratus*	*	*
Jasminum fruticans L.	*		*Rubus discolor* Weihe Et Nees.	*	*
Olea europaea L.	*		*Rubus hirtus* Waldst. Et Kit.		*
Fraxinus ornus L.		*	*Sarcopoterium spinosum* (L.) Spach.	*	
Fraxinus ornus L. *subsp. ornus*		*	*Sorbus aucuparia* L.		*
Platanus orientalis L.	*	*	*Sorbus torminalis* (L.) Crantz		*
Pinus maritima Poir	*		*Populus alba* L.	*	
Pinus sylvestris L.		*	*Populus tremula* L.		*
Paliurus spina-christi Miller	*		*Salix alba* L.	*	*
Crataegus microphylla C.Koch.	*	*	*Salix cinerea* L.	*	*
Crataegus monogyna Jacq. *subsp. monogyna*	*	*	*Salix elaeagnos* Scop.		*
Cydonia oblonga Miller	*	*	*Salix fragilis* L.		*
Laurocerasus oficinalis Roemer		*	*Osyris alba* L.	*	
Malus sylvestris Miller *subsp. orientalis*	*	*	*Staphylea pinnata* L.		*
Mespilus germanica L.		*	*Styrax officinalis* L.	*	
Prunus x domestica L.	*		*Taxus baccata L.*		*
Prunus spinosa L. *subsp. dasyphylla*		*	*Tilia argentea* Desf. Ex Dc.		*
Prunus divaricata Ledeb.		*	*Tilia cordata* Miller		*
Prunus laurocerasus L.		*	*Celtis australis* L.	*	
Pyracantha coccinea Roemer	*		*Ulmus glabra* Hudson	*	*
Pyrus amygdaliformis Vill.	*		*Vitis sylvestris* Gmelin	*	
Pyrus comminus L.	*	*			
Rosa canina L.	*	*			

DISCUSSION AND CONCLUSION

Various pressures having emerged in recent years in parallel to the phenomenon of industrialization and urbanization are creating negative effects on countries' floristic riches. In order for floristic riches to be sustainable and, at the same time, to be able to be used as a tourism resource, the protected areas are of great importance. At the same time, protected areas "clearly defined as geographical places established, certified and managed via laws and other effective means with the aim of protecting the nature in the long term together with ecosystem services and cultural values" [30, 31] appear as natural sites used for eco-tourism purposes in the world [32].

However, the impacts of tourism on rare flora including that in protected areas has not been generally recognized as a specific type of threat, even though there is evidence of negative environmental impacts from tourism on these taxa in protected areas [33]. For this reason, the areas which are rich in bio-diversity are evaluated under the protected area status with the aim of getting rid of these pressures. Budowski [34] mentioned that those protected areas where tourism is wholly or partially based on nature could provide an economic value for conservation of species and habitat [35].

Turkey having extremely rich plant diversity with more than 12000 taxons in terms of flora and botanic tourism, there are 203 natural parks with high taxon diversity and 8 of these natural parks are included within the borders of the city of Kocaeli. There are 416 taxon in the Ballıkayalar natural park [28] and 293 taxon in the Beskayalar natural park [27], which were evaluated within the scope of the study and are very important in terms of biological, physical and aesthetic resource values. When only the woody plant taxons are taken into consideration, it is observed that there are 108 woody taxons in

both natural parks. As it is known, natural and cultural resources are mentioned among the elements creating the tourism supply of countries and regions [36] and plants occupy an important place among these resources. Plants are alive landscape elements showing lively, dynamic, decorative, aesthetic and functional features and they are actively used both in urban and rural landscape applications [37]. In this context, the Ballıkayalar and the Beşkayalar natural parks, too, appear as important supply areas within the scope of flora or botanic tourism.

By considering the fact that not only the functions of the woody plants, which are the key and permanent elements of landscape [38], but also their such dendrological properties as sizes, shapes, textures and colours give shape to a landscape and make it acquire a character [6], trip routes should be created in the natural parks with the aim of evaluating these as a tourism resource. The trip routes should be created in a way to reflect all the diversity and the area or trip guides should be trained so as to be able to serve in the trip routes. On the other hand, units where the herbarium samples of the taxons belonging to the natural parks will be included and trainings will be given in relation to the environment and amenity spaces of which users and visitors can make use should be introduced to the area within the framework of long-term development plans.

In conclusion, these comprehensive activities to be carried out in the natural parks in relation to flora or botanic tourism activities might not only contribute to the sustainable uses of the areas and the protection of bio-diversity, but also they might promote the development of the local people via generating income.

REFERENCES

[1] Lenao, M., Basupi, B. (2016) Ecotourism development and female empowerment in Botswana: A review. Tourism Management Perspectives. 18(2016) 51–58

[2] Kaya, M. (2015) Ayancık ve Yakın Çevresinin Ekoturizm Potansiyeli. Ondokuz Mayıs University, Institute of Social Sciences. Geography Programs. Doctoral Thesis. 256p.

[3] Kamacı, S. (2015) Hakkari İlinde Ekoturizm Olanaklarının Araştırılması. Yüzüncü Yıl University, Institute of Social Sciences. Geography Departments. Graduate Thesis. 204p.

[4] Ceballos-Lascurain, H. (1996) Tourism, ecotourism and protected areas: the state of nature-based tourism around the world and guidelines for its development. IUCN. Protected Areas Programme, Gland. 301p.

[5] Scheyvens, R. (1999) Case study. Ecotourism and the empowerment of local communities. Tourism Management. 20(1999) 245-249.

[6] Irmak, M.A. (2008) Erzurum İli Yakın Çevresinin Flora Turizm Potansiyeli Açısından Değerlendirilmesi. Atatürk University, Institute of Natural Sciences, Landscape Architecture Programs. Doctoral Thesis. 248p.

[7] Yeşil Kapucu, G. (2010) Tabiat Parkı: Türkiye ve Almanya Karşılaştırması. Istanbul Technical University, Institute of Natural Sciences, Landscape Architecture Programs. Graduate Thesis. 127p.

[8] Özhatay, N. (2006) Important Plants Areas along the BTC Pipeline in Turkey. Publisher: BTC Co. Istanbul. 304p.

[9] Gungoroglu, C. (2017) Natura 2000: Its Status and Opportunities and Challenges for Forest Biodiversity in Turkey. Fresen. Environ. Bull. 26, 6217-6224.

[10] Anonymous (2017) National Park Law. No: 2873. www.milliparklar.gov.tr

[11] Anonymous (2012) Guide to Sustainable Tourism in Protected Areas. Baltic Sea Region Programme, 2007-2013, Europarc Federation, Hamburg, Germany. 149p.

[12] Anonymous (2003) European Charter for Sustainable Tourism. European Charter for Sustainable Tourism Booklet. 37-38.

[13] Pickering, C.M., Hill, W. (2007) Impacts of recreation and tourism on plant biodiversity and vegetation in protected areas in Australia. Journal of Environmental Management. 85(4), 791-800.

[14] Güleryüz, G. and Arslan, H. (2001) Doğal Alanların Korunmasında Vejetasyon Mozayiği ve Coğrafi Bilgi Sistemleri Tekniklerinin Önemi. Ekoloji, Çevre Dergisi. 10(38), 23-27.

[15] Spelleberg, J.F. (1995) Evaluation and Assessment of Conservation Biology. Series 4. Goldsmith, F.B. (Ed.) Chapmann and Hall, London.

[16] Anonymous (2017a) Türkiyenin Tabiat Parkları. T.C. Orman ve Su İşleri Bakanlığı, Doğa Koruma ve Milli Parklar Genel Müdürlüğü. www.milliparklar.gov.tr

[17] Özder, H., Algan, N., Çetin S., Açıkgöz, N., Adıgüzel, D. (2013) Kocaeli Doğa Turizmi Master Planı. (2013-2023). T.C. Kocaeli Valiliği, Orman ve Su İşleri I. Bölge Müdürlüğü, Kocaeli Şube Müd. 223p.

[18] Anonymous (2017b) Kocaeli İli Resmi İstatistikleri. T.C. Orman ve Su İşleri Bakanlığı, Meteroloji Genel Müdürlüğü. www.mgm.gov.tr

[19] Anonymous (2005) Ballıkayalar Tabiat Parkı, 1/25000 Ölçekli Uzun Devreli Gelişme Planı Çalışması, Analitik Etüt ve Sentez/ Değerlendirme Raporu. T.C. Çevre ve Orman Bakanlığı, Doğa Koruma ve Milli Parklar Genel Müdürlüğü, Milli Parklar Dairesi Başkanlığı. 279p.

[20] Anonymous (2005a) Beşkayalar Tabiat Parkı, 1/25000 Ölçekli Uzun Devreli Gelişme Planı Çalışması, Analitik Etüt ve Sentez/ Değerlendirme Raporu. T.C. Çevre ve Orman Bakanlığı, Doğa Koruma ve Milli Parklar Genel Müdürlüğü, Milli Parklar Dairesi Başkanlığı. 239p.
[21] Davis, P.H (1965-1985) Flora of Turkey and East Aegean Islands. Vol: I-IX. University Press. (Edinburg).
[22] Polunin, O. (1969) Flowers of Europe. Oxford University Press. London. 661p.
[23] Polunin, O., Huxley, A. (1981) Flowers of the Mediterranean. Chotto and Windus Ltd. London. 260p.
[24] Pamay, B. (1992) Plant Material I: Trees and Shrubs. Uycan Press, Istanbul.
[25] Yaltırık, F. (1993) Dendroloji II. Angiospermae. İstanbul Üniversitesi, Yayın No: 3767, Orman Fakültesi Yayın No: 420. İstanbul. 256p.
[26] Hillier, J. (1998) The Hillier Manual of Trees and Shrubs. Pocket Edition. A David and Charles Book. 928p.
[27] Akaydın, G., Çalışkan, G., Yılmaz, E.B. (2006) Beşkayalar Vadisi (Gölcük-Kocaeli)'nin Florası. Fırat Üniv. Fen ve Müh. Bil. Dergisi. 18(4), 459-469.
[28] Akaydın, G., Özmen, E., Özüdoğru, B. (2006a) Ballıkayalar Vadisi (Gebze-Kocaeli)'nin Florası. Fırat Üniv. Fen ve Müh. Bil. Dergisi. 18(3), 279-289.
[29] Yılancı, M.S., Sağıroğlu, M. (2013) Kocaeli-Karamürsel-Yalakdere beldesi ve çevresinin florası. SAÜ. Fen Bil. Der. 17(3), 407-42.
[30] Dudley, N. (2008) Guidelines for Applying Protected Area Management Categories. Gland, Switzerland, 978-2-8317-1086-0.
[31] Kuvan, Y. (2003) Turizm Alan ve Merkezlerinde Ormancılık ve Turizm Sektörler. In: Protected Natural Areas Symposium, Oral Paper Book. 8-10 September 2005. Isparta, 81-89.
[32] Şahin, G. (2014) Orman Kaynaklarının Ekoturizm Amaçlı Kullanımı. Istanbul University, Institute of Natural Sciences. Graduate Thesis. 140p.
[33] Keelly, C., Pickering, C.M., Buckley, R.C. (2003) Impacts of tourism on threatened plants taxa and communities in Australia. Ecological Restoration and Management. 4, 37-44.
[34] Budowski, G. (1976) Tourism and conservation: conflict, coexistence or symbiosis? Environmental Conservation. 3: 27-31.
[35] Lopez, R. (2002) Evaluating ecotourism in natural protected areas of La Paz Bay, Baja California Sur, México: ecotourism or nature-based tourism? Biodiversity & Conservation. 11(9), 1539-1550.
[36] Yılmaz, H. and Karahan, F. (2003) Eko-Turizm Yaklaşımlarında Flora Turizmi: Palandöken Dağlarının Potansiyeli. I. National Erciyes Symposium. Paper Book, 94-103.
[37] Seyidoglu Akdeniz, N., Ender, E., Zencirkiran M. (2017) Evaluation of Ecological Tolerance and Requirements of Exotic Conifers in the Urban Landscape of Bursa. Fresen. Environ. Bull. 26, 6064-6070.
[38] Var, M. (1992) Kuzeydoğu Karadeniz Bölgesindeki Odunsu Taksonların Peyzaj Mimarlığı Yönünden Değerlendirilmesi. Karadeniz Technical University, Institute of Natural Sciences, Landscape Architecture Programs. Doctoral Thesis. 342p.

Received: **11.12.2017**
Accepted: **21.02.2018**

CORRESPONDING AUTHOR

Murat Zencirkıran
Department of Landscape Architecture,
Faculty of Agriculture,
University of Uludag,
16 059 Gorukle, Bursa – Turkey

e-mail: mzencirkiran@uludag.edu.tr

© by PSP Volume 27 – No. 7/2018 pages 4822-4829 Fresenius Environmental Bulletin

VARIATIONS IN PLANTING DATES OF SWEET CORN AFFECT ITS AGRONOMIC TRAITS VIA ALTERING CROP MICRO-ENVIRONMENT

Zafar Hayat Khan[1], Shad Khan Khalil[2], Farman Ali[1], Badshah Islam[1], Amjad Iqbal[1], Ikram Ullah[3], Muhammad Ali[4], Farooq Shah[1,*]

[1]Department of Agriculture, Abdul Wali Khan University Mardan, Khyber Pakhtunkhwa Pakistan
[2]Department of Agronomy, University of Agriculture, Peshawar, Pakistan
[3]Department of Plant Breeding and Genetics, Bacha Khan University Charsadda, Khyber Pakhtunkhwa, Pakistan
[4]Department of Biotechnology, Bacha Khan University Charsadda, Khyber Pakhtunkhwa, Pakistan

ABSTRACT

Sweet corn landraces are grown for local markets in Khyber Pakhtunkhwa, Pakistan. The present study aimed to document agronomic characteristics of landraces under different microclimatic regimes. Four landraces {Mingora (MNG), Mansehra (MNS), Swabi (SWB) and Parachinar (PRC)} with cv. Azam (check) were planted on five dates at almost one month interval at New Developmental Farm University of Agriculture Peshawar, Pakistan. Randomized complete block (RCB) design with split plots was employed. Planting dates and landraces alone or in combination significantly affected all parameters studied. Sweet corn attained maximum internode length under early plantations (April/March) in 2007 and 2008. Whereas, maximum number of leaves plant^{-1}, ear length, kernels ear^{-1}and 1000-grain weight (TGW) were recorded from July plantations in both years. Landrace SWB produced maximum number of leaves plant^{-1}. However, higher ear length, kernels ear^{-1} and TGW were recorded for Azam (check) in both years. Landrace SWB is therefore recommended for planting late in July to obtain higher yield attributes.

KEYWORDS:
Sweet corn, maize, landraces, planting dates, ear length, grain weight

INTRODUCTION

Maize (*Zea mays* L.) is the third most important cereal crop in Pakistan. It is mainly grown worldwide for three distinct markets viz., fresh, canned, and frozen [1]. United Stated of America, Mexico, Nigeria, France and Hungary are the major producing countries [2]. Maize is grown in the widest range of environments. It is planted up to 58° N and 40° S in the Southern Hemisphere. It can grow below sea level in the Caspian plain and up to 4000 m above sea level in the Peruvian Andes [3]. Its production has not been able to keep pace with the demand, except in a very few countries [4]. Sweet corn (*Zea mays* L.var. *saccharata* Strut) is one of several types of maize, which also includes flint corn, dent corn, popcorn, flour corn, and pod-corn [5]. It is mainly produced for three distinct markets in the world-fresh, canning, and freezing. Sweet corn consumption, in the world, has increased over the past 30 years [6]. It is grown in different areas of Khyber Pakhtunkhwa including Swat, Mansehra and Swabi districts, for local markets [7]. There is great potential in sweet corn market and if its yield become at par with field corn the income of the farmers can be increased several fold. The main reason of low yield is due to very little systematic research been done on this crop, particularly in Khyber Pakhtunkhwa.

Early farmers selected seed from best-looking plants in their fields. In the course of selection, the farmer gave preference for certain traits, such as grain size, color, and taste [8]. This mechanism gave rise to the formation of landraces. It is important that landraces be collected and preserved throughout the world, particularly in areas where modern cultivars are replacing germplasm that have been used for crop production for a long time. Surveying both qualitative and quantitative traits of existing landraces may be useful in maintaining their genetic diversity and preserving them from genetic erosion [9]. Planting time, environment and variety selection are the key factors significantly affecting growth, yield and yield components [9-14]. Microclimate plays an important role in maximizing growth and yield of sweet corn. Microclimate can be altered in many ways among which planting date is the most important factor to be considered. To fully explore grain production potential of sweet corn, it is essential to know how plants interact morphologically and physiologically in a community and to realize management practices, which allow them to get the most out of growth resources in their environment [15].

Keeping in view the importance of indigenous landraces and role of planting date for achieving higher yields, this study was therefore initiated to document numerous qualitative and quantitative

traits of landraces and to find out optimum planting date.

MATERIALS AND METHODS

These experiments were carried out at New Developmental Farm (NDF), University of Agriculture Peshawar, Pakistan during 2007 and 2008. Experimental field is located at 34° N latitude, 71.3° E longitude and 350 m above sea level. The soil of the field was analyzed for organic matter [16], pH, EC [17], P and K [18]. Soil was low in organic matter (0.87 %), alkaline in reaction (pH 8.2), having EC (0.74 dSm^{-1}), total N (0.04 %), AB-DTPA extractable P (1.15 mg P_2O_5 kg^{-1}) and high in exchangeable K (506 mg K_2O kg-1). Temperature, humidity, and precipitation recorded during the period of experiment are given in Table 1.

The landraces were named and abbreviated against the names of the places from where they were collected. Landraces were Mingora (MNG), Mansehra (MNS), Swabi (SWB) and Parachinar (PRC). Variety Azam was included as check. Plating dates, during 2007, were 25th April, 25th May, 16th June, 26th July and 18th August, while in 2008, August sowing was omitted due to very poor crop stand and grain yield, instead sowing in March was added. Sowing dates during 2008 were 17th March, 30th April, 17th May, 21st June and 26th July. Landraces were planted in 4m × 3.6m plots having 6 rows, 4 m long. Treatments were replicated three times in randomized complete block design with split plot arrangements. Planting dates were allotted to main plots while landraces were maintained in sub-plots. Treatments were randomized in main and sub-plots. The crop was sown in 60 cm apart rows. A basal dose of 120:70 kg N:P_2O_5 ha^{-1} was used. Urea and single super phosphate were used as sources of N and P, respectively. The crop was irrigated at two weeks interval. Furadan (Carbofuran 3%) @ 19.76 kg ha^{-1} was applied in the early stages of growth to control attack of stem borers. Weeds were manually eradicated.

Data was recorded on number of leaves $plant^{-1}$, middle internode length, ear length, kernels ear^{-1}, and 1000-grain weight. The data on number of leaves $plant^{-1}$ was calculated by counting the number of leaves of 10 randomly selected plants in each subplot and were averaged. Middle internode length data was recorded with the help of measuring tape from 10 randomly selected plants in each subplot and averaged. Ear length was measured from 10 randomly selected ears in each subplot with measuring tape. Kernels ear^{-1} was calculated from 10 randomly selected ears in each subplot. Thousand grains were counted from each subplot and weighed by an electric balance to record data on 1000 grain weight. The data were statistically analyzed, using analysis of variance technique in MSTAT-C. Means were compared using least significant difference (LSD) test [19].

RESULTS AND DISCUSSION

Number of leaves $plant^{-1}$. Planting dates (P) and landraces (R), in both years, had significantly affected number of leaves $plant^{-1}$ (Fig. 1a). P×R interaction was also found significant. July planting resulted in maximum number of leaves $plant^{-1}$ during both years. However, in 2007, May and August planting produced lowest number of leaves $plant^{-1}$, while in 2008, May planting produced lowest number of leaves $plant^{-1}$. Final leaf number in maize depends upon the rate and duration of leaf initiation [20]. Significant effects of planting dates on leaf number in sweet corn are reported by Williams [21]. Shah and Ahmad [22] attributed more number of leaves to favorable climatic conditions particularly temperature which accelerated vigorous growth. Stevenson and Goodman [23] reported lowest leaf numbers in exotic races of maize under short day regime. They partially supported our results as lowest leaf numbers during 2007 were attained when grown under short days (August planting).

TABLE 1
Average air temperature and rainfall at NDF, Peshawar during the year 2007 and 2008.

Month	Average T (°c)	R. Humidity (%)	Total Rainfall (mm)
March	17.31 (21.18)	65.50 (47.81)	32.2 (0)
April	25.30 (22.92)	55.38 (52.03)	0.8 (16.8)
May	27.97 (29.29)	49.61 (41.97)	0.2 (0)
June	32.42 (32.55)	49.35 (62.73)	0 (16)
July	31.31 (32.56)	64.73 (72.45)	0 (27)
August	31.95 (31.29)	65.77 (75.61)	20.2 (150.9)
September	29.26 (28.98)	66.72 (69.90)	22 (16.7)
October	23.06 (24.46)	46.88 (65.07)	0 (0)
November	18.44 (18.68)	73.60 (56.37)	8 (0)
			83.4 (227.4)

Without parenthesis = for year 2007 With parenthesis = for year 2008

FIGURE 1a
Leaves plant^{-1} of sweet corn as affected by planting dates

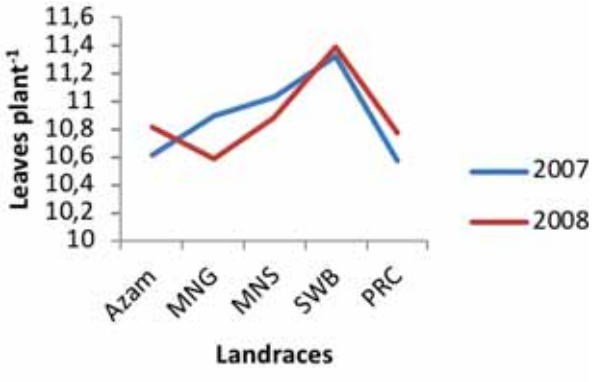

FIGURE 1b
Leaves plant^{-1} of sweet corn as affected by landraces

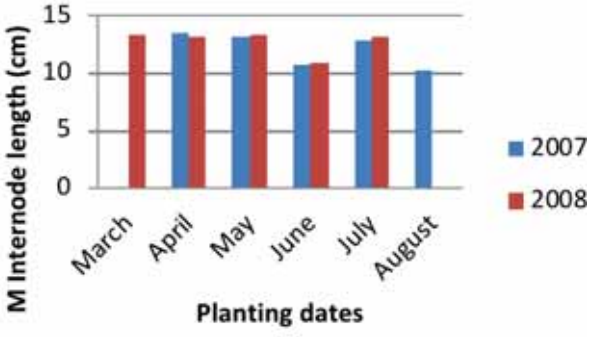

FIGURE 2a
Middle internode length of sweet corn as affected by planting dates

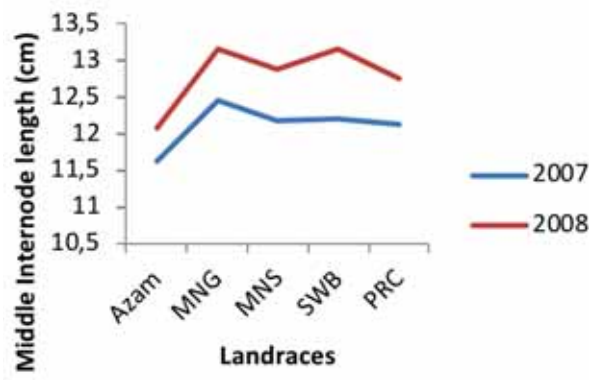

FIGURE 2b
Middle internode length of sweet corn as affected by landraces

During both years, landrace SWB produced significantly higher number of leaves (Fig. 1b). Lowest number of leaves was produced by PRC and Azam in 2007, while in 2008; PRC produced minimum number of leaves. Leaf number is an important trait for characterization of landraces in maize [24]. Different genotypes showed different number of leaves plant^{-1} when grown under a range of planting dates with varying temperature regimes. Presence of variability among different genotypes in response to temperature of leaf initiation and leaf appearance rate has been demonstrated by Padilla and Otegui [22]. Interaction SWB × July recorded maximum number of leaves during both years. Since different planting dates means different environments and when genotypes are compared over a range of environments their quantitative characters frequently vary with environments [25].

Middle internode length. The effects of planting date (P) and landraces (R) on internode length of sweet corn are depicted in Fig 2a & 2b. Analysis of the data revealed significant effects of treatments and their interaction. In year I, maximum internode length was recorded when crop was planted in April, while minimum internode length was observed in August sown crop. On the other hand, in year II, maximum internode length was noted in mid-March planting, while minimum internode length was observed in June planting. These results showed that early planted sweet corn resulted in lengthy internodes as compared to late plantings. This may be due to longer growth periods employed by early plantings. According to Birch et al. [26] growing environment may affect the pattern of internode extension. Salfer and Rawson [27] concluded in their study that photoperiod do have significant effect on reproductive phase of stem elongation. Internode elongation is a photomorphogenic process which requires very little light energy to get a growth-regulating response [28]. On the other hand, Berbecel and Eftimescu [29] and Novoa and Loomis [30] stated that moisture stress is mainly responsible for reduced internode length.

Landrace MNG recorded maximum internode length while, Azam noted minimum internode length during both years (Fig. 2b). Shorter internodes reduce evapo-transpiration and increase tissue water retention capacity during grain filling [31]. Internodes are active sinks during pollination and compete for assimilates during grain filling [32]. Hence, shorter internodes may be desirable as they compete

less for assimilates during grain filling. The differences in internode length may be due to stem elongation periods and differences among genotypes [27]. During both years P×R interaction was found significant. In 2007, P×R interaction showed that internode length of MNG was greater when planted in April, whereas, internode length of PRC was lowest when planted in May. In 2008, maximum internode length resulted from MNG × March planting. On the other hand lowest internode length was noted for PRC × June planting. These results evidenced that different genotypes interacted differently with different environments regarding internode elongation. These results are partially supported by Birch et al. [26] who evidenced the presence of genotype by environment interaction in relation to internode length.

Ear length (cm). Data on mean ear length of sweet corn as affected by planting dates (P) and landraces (R) are given (Fig 3a & 3b). Statistical analysis of the data showed that ear length of sweet corn was significantly affected by P and R during both years. P×R interaction was also found significant. Sweet corn planted in July recorded higher ear lengths during both years. May plantings recorded lowest ear lengths during both years. These results suggest that sweet corn planted late in July had more efficiently utilized the intercepted light with higher translocation of photo-assimilates to the ear. Rehman and Khalil [33] found higher ear length in mid-March planting as compared to other planting dates (March 3, 23, and April 2, 12 and 22). Their findings partially support our results as mid-March planting in 2008 produced longer ears compared to April planting. Significant effects of planting date on ear length of sweet corn were also reported by White [34] and Ming et al. [35].

In 2007, highest ear length was recorded by Azam followed by landrace SWB, while MNG and PRC recorded lowest ear lengths. On the other hand, Azam recorded highest ear length, while lowest ear length was noted for PRC in 2008. Azam is a composite cultivar possessing genetic potential for higher production [36] and because of genetic superiority Azam may have produced long ears. Similar results are reported by Rehman and Khalil [33]. They determine higher ear length in Azam when compared with other pop corn and sweet corn cultivars. Significant differences between varieties for ear length are reported earlier by other workers [35, 37, and 38] in corn. Landraces usually have smaller ears compared to improved varieties [39]. Data regarding P×R interaction showed that maximum ear length was noted when Azam was planted in July, while minimum ear length was recorded for PRC in May planting, during both years. The differences in ear length may be due to differences in genetic potential and adoptability to environmental conditions.

Number of kernels ear^{-1}. Grain yield, in maize, is mainly dependent upon the number of kernels plant^{-1} that reaches maturity [40, 41]. Kernels ear^{-1} (KPE) of sweet corn was significantly affected by planting dates (P) and landraces (R), during both years (Fig 4a & 4b). P×R interaction was also significant. In both years, maximum KPE were observed in July planting followed by April planting. Minimum KPE were observed in August planting during 2007, while in 2008, minimum KPE were recorded in May planting. Lower temperature and incident solar radiation during grain set and filling stage are important factors resulted in lowest KPE in August planting. Zaki et al. [42] also reported lowest KPE in mid-August planting. The number of kernels set is more critical and more affected by environmental conditions [43]. Otegui and Melon [44] stated that unfavorable conditions around silking can cause cessation of ear development and ear abortion. Therefore, reduction in the number of viable kernels ear^{-1} may occur [45, 46]. This may be the reason for mid-May planting which recorded lowest KPE. In 2007, Azam produced highest KPE followed by SWB, while PRC produced lowest KPE. In 2008, mean values for varieties suggested that Azam produced highest KPE followed by landrace SWB, while PRC produced lowest KPE. Different KPE among cultivars may be due to their different genetic makeup and adoptability to environmental conditions of Peshawar. As Azam is a synthetic cultivar hence it produced more KPE. Among landraces, SWB was superior in production of KPE and the possible reason may be that it was collected from an area (Swabi) whose environmental conditions are almost identical to Peshawar. These results advocate that late July may be an optimum time for sowing of sweet corn to gain maximum KPE. Tollenaar [47] attributed reductions in kernels plant^{-1} to unfavorable environmental conditions at flowering. Significant interaction of planting date and cultivar was also reported by Khan and Zada [48].

1000-grains weight (g). Data on mean 1000-grains weight (TGW) of sweet corn as affected by planting dates (P) and landraces (R) are given in fig. 5a & 5b. Statistical analysis of the data showed that TGW was significantly affected by P and R with significant P × R interaction, during both years. In 2007, TGW decreased from 178 in April and May planting to 176 in mid-June planting. In late July planting, however, TGW reached to maximum (185). Further delay in planting to mid-August realized minimum TGW value (156). In 2008, maximum TGW (189) was again obtained from late July planting, while minimum TGW (170) was observed in mid-May planting. Reduction in grain weight was found by delaying planting date from mid-September to mid-December [49]. Andrade et al. [50] stated that low temperature may have a negative effect on kernel weight

FIGURE 3a
Ear length of sweet corn as affected by planting dates

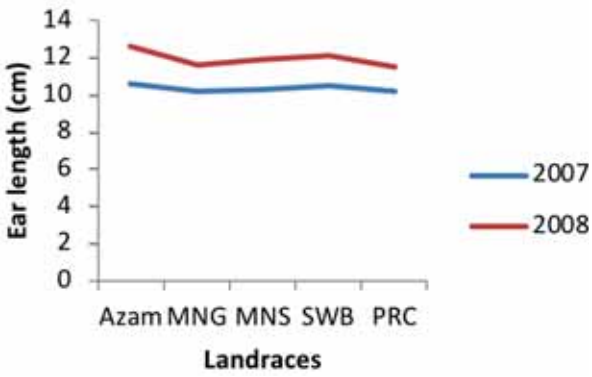

FIGURE 3b
Ear length of sweet corn as affected by landraces

FIGURE 4a
Kernels ear^{-1} of sweet corn as affected by planting dates

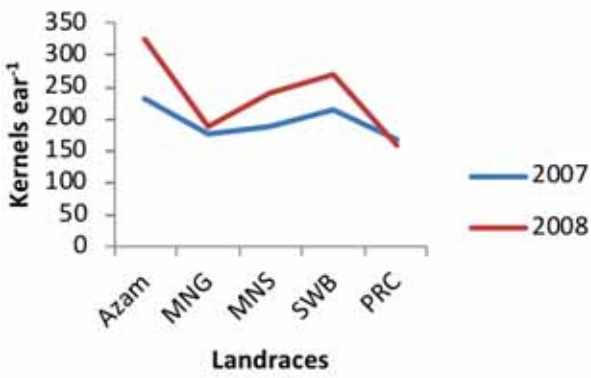

FIGURE 4b
Kernels ear^{-1} of sweet corn as affected by landraces

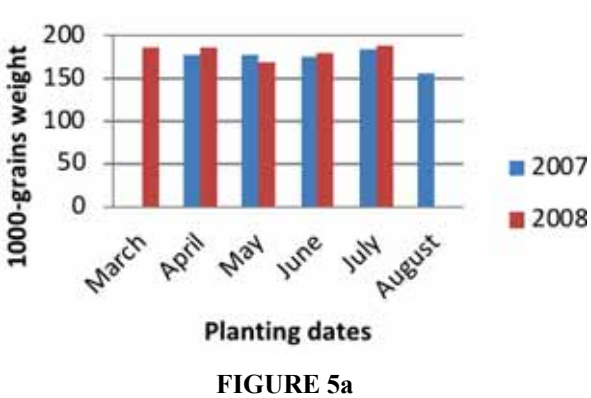

FIGURE 5a
1000-grains weight of sweet corn as affected by planting dates

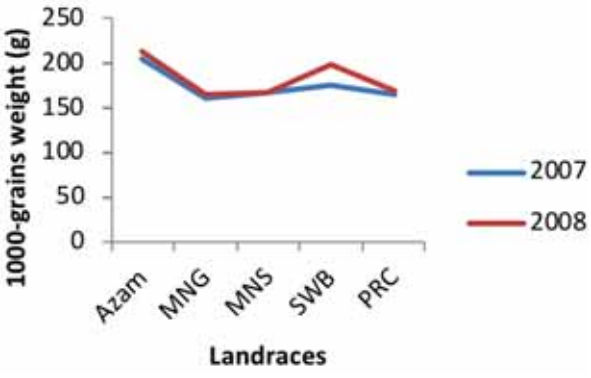

FIGURE 5b
1000-grains weight of sweet corn as affected by landraces

through biomass partitioning to the grains. This may be true in case of mid-August planting which produced grains of lowest weight. In August planting grain filling period coincided with low temperature (Table 1) which may have caused negative effect on grain weight.

During both years, Azam noted highest TGW followed by landrace SWB, whereas lowest TGW was recorded in MNG (Fig 5b). Since Azam is a synthetic variety which more efficiently translocated assimilates to the grains during grain set and filling period resulting in heavier grains. Among landraces SWB produced heavier grains compared to other races. Significant effect of cultivar on TGW was reported by others [51, 52]. In the first year, Azam recorded maximum TGW in July and April plantings, while minimum TGW was observed when PRC was planted in August. In the second year, interaction of

Azam × July recorded highest TGW, while minimum TGW was recorded from interaction of PRC × May. Grain set is a critical period which is mostly affected by temperature and genotype [53].

REFERENCES

[1] Khan, Z.H., Khalil, S.K., Iqbal, A., Ikramullah, Ali, M., Shah, T., Wu, W. and Shah, F. (2017) Nitrogen doses and plant density affect phenology and yield of sweet corn. Fresen. Environ. Bull. 26, 3809-3815.

[2] Khan, Z.H., Khalil, S.K., Shah, F., Iqbal, A., Ali, F., Islam, B., Ikramullah, and Ali, M. (2017) Plant density and nitrogen doses can affect growth of sweet corn. Fresen. Environ. Bull. 26, 3872-3879.

[3] FAO (1992) Maize in Human Nutrition. FAO, UN. Rome, Italy.

[4] Brewbaker, J.L. (2003) Corn production in the tropics- The Hawaii experience. College of Tropical Agric. and Human Resources. Uni. Hawaii, Manoa.

[5] Pomeranz, Y. (1987) Modern cereal science and technology. VCH Publishers, Weinheim.

[6] Oktem, A., Oktem, A.G. and Coskun, Y. (2004) Determination of sowing dates of sweet corn under Sanlurfa conditions. Turk. J. Agric. For. 28, 83–91.

[7] Khan, Z.H., Khalil, S.K., Farhatullah, Khan, M.Y., Israr, M. and Basir, A. (2011) Selecting optimum planting date for sweet corn in Peshawar. Sarhad J. Aric. 27(3), 341-347.

[8] Bennett, E. (1970) Adaptation in wild and cultivated plant populations. In: Frankel, O.H. and Bennett, E. (Eds.) Genetic resources in plants-their exploration and conservation. IBP Handbook No. 11. Blackwell, London, 115–129.

[9] Lucchin, M., Barcaccia, G. and Parrini, P. (2003) Characterization of flint maize (*Zea mays* L. convar. *mays*) Italian landrace: I. Morpho-phenological and agronomic traits. Genet. Resour. Crop Ev. 50(3), 315–327.

[10] Ramankutty, N., Foley, J.A., Norman, J. and McSweeney, K. (2002) The global distribution of cultivable lands: Current patterns and sensitivity to possible climate change. Global Ecol. Biogeogr. 11, 377–392.

[11] Khan, M. (2004) Maize varieties response to different sowing dates. In: Annual Research Progress Report, 2003-04. Cereal Crops Res. Inst. Pirsabak (Nowshera) Khyber Pakhtunkhwa, Pakistan, 90-92.

[12] Khan, Z.H., Shah, W.A., Bakht, J., Shafi, M. and Khan, M.A. (2004) Performance of maize varieties under different seed rates. Sarhad J. Agric. 20(2), 183–189.

[13] Khan, Z.H., Khalil, S.K., Nigar, S., Khalil, I.H., Haq, I., Ahmad, I., Ali, A. and Khan, M.Y. (2009) Phenology and yield of sweet corn landraces influenced by planting dates. Sarhad J. Aric. 27(3), 341-347.

[14] Rasheed, S.M., Rahman, H., Ikramullah, Khan, Z.H., Shah, S.S., Ali, M., Shah, T., Iqbal, A., Shah, W.A. and Ahmad, M. (2016) Stability of modified double cross maize hybrids for yield parameters across four environments. Fresen. Environ. Bull. 25, 3454-3460.

[15] Sangoi, L. (2001) Understanding plant density effects on maize growth and development: an important issue to maximize grain yield. Cienc. Rural [online]. 31(1), 159–168.

[16] Nelson, D.W. and Sommer, L.E. (1982) Total carbon, organic carbon and organic matter. p. 539–577. In: Page, A.L., Miller, R.H. and Keenay, D.R. (Eds.) Methods of soil analysis. Part II. 2nd ed. ASA, Inc. Wisconsin, USA.

[17] Ryan, J. (2000) Soil and plant analysis in the Mediterranean region: limitations and potential. Commun. Soil Sci. Plant Anal. Marcel Dekker Inc. Monticello, New York. 31(11/14), 2147-2154.

[18] Soltanpour, P.N. and Schawab, A.P. (1977) A new soil test for simultaneous extraction of macro & micronutrients inalkaline soil. Commun. Soil Sci. Pl. Anal. 8, 195-207.

[19] Steel, R.G.D. and Torrie, J.H. (1984) Principles and procedures of statistics. McGraw Hill Book Co., New York.

[20] Padilla, J.M. and Otegui, M.E. (2005) Co-ordination between leaf initiation and leaf appearance in field-grown maize: genotypic differences in response of rates to temperature. Ann. Bot. London. 96, 997–1007.

[21] Williams II, M.M. (2008) Sweet corn growth and yield responses to planting dates of the north central United States. Hort Science. 43(6), 1775–1779.

[22] Shah, M.A. and Ahmad, B. (1995) Effect of planting dates on varietal performance of maize during spring in Peshawar. M.Sc. (Hons) Thesis, Dept. Agron. Khyber Pakhtunkhwa Agric. Univ. Peshawar, Pakistan.

[23] Stevenson, J.C. and Goodman, M.M. (1972) Ecology of exotic races of maize. I. Leaf number and tillering of 16 races under four temperature and two photoperiods. Crop Sci. 12, 864–868.

[24] Ortiz, R., Crossa, J., Franco, J., Sevilla, R. and Burgueno, J. (2008) Classification of Peruvian highland maize races using plant traits. Genet. Resour. Crop Evol. 55, 151–162.

[25] Miura, H., Nakashima, H., Meno, A. and Tsuda, C. (1985) Genotype × environment interactions in single cross maize cultivar 'Pirika-sweet' and its parental inbred lines. J. Fac. Agr. Hokkaido Univ. 63(3), 211–221.

[26] Birch, C.J., Andrieu, B. and Fournier, C. (2002) Dynamics of internode and stem elongation in three cultivars of maize. Agronomie. 22, 511–524.
[27] Salfer, G.A. and Rawson, H.M. (1994) Sensitivity of wheat phasic development to major environmental factors: a re-examination of some assumptions made by physiologists and modelers. Aust. J. Plant Physiol. 21, 393–426.
[28] Decoteau, D.R. (1998) Plant physiology: Environmental factors and photosynthesis. Greenhouse glazing and solar radiation transmission workshop. Rutgers Uni.
[29] Berbecel, O. and Eftimescu, M. (1972) Effect of agrometerorological conditions on maize growth and development. Part I. Meteorolgy and hydrology No. 2. Inst. Meteorol. Hidrol. Bucuresti, Romania, 45-51.
[30] Novoa, R. and Loomis, R.S. (1981) Nitrogen and plant production. In: Monteith, J.L. and Webb, C. (Eds.) Soil water and nitrogen in Mediterranean-type environments. Kluwer Boston Inc., USA, 177–204.
[31] Singh, S.P. (2007) Drought resistance in the race Durango dry bean landraces and cultivars. Agron. J. 99, 1219–1225.
[32] Westgate, M.E. (2010) Physiology of high yielding corn and soybeans. International Plant Nutrition Institute. Georgia, U.S.A.
[33] Rehman, R.A. and Khalil, S.K. (1989) Response of pop and sweet corn cultivars to planting dates. M.Sc. (Hons) Thesis, Dept. Agron. Khyber Pakhtunkhwa Agric. Univ. Peshawar, Pakistan.
[34] White, J.M. (1984) Effect of plant spacing and planting date on sweet corn grown on muck soil in the spring. Proc. Flo. State Hort. Soc. 97, 162–163.
[35] Ming, L., Hong-bin, T., Pu, W. and Ya-jie, Z. (2009) Effects of sowing date on growth, yield formation and water utilization of spring maize. J. Maize Sci. 17(2), 108–111.
[36] Khalil, I.A. and Jan, A. (2002) Cropping technology. National Book Foundation, Islamabad.
[37] Sari, N., Dasgan, H.Y. and Abak, K. (2000) Effects of sowing times on yield and some agronomic characteristics of sweet corn in the GAP area of Turkey. ISHS Acta Hortic. 533: VIII International symposium on timing field production in vegetable crops. Bari, Italy.
[38] Arif, M., Ihsanullah, Khan, S., Ghani, F. and Yousafzai, H.K. (2001) Response of maize varieties to different planting methods. Sarhad J. Agric. 17, 159–163.
[39] Mabhaudhi, T. (2009) Response of maize (*Zea mays* L.) landraces to water stress compared with commercial hybrids. M. Sc (Agric) Thesis. Crop Sci. Dept. School Agric. Sci. Agribusiness, Univ. KwaZulu-Natal, South Africa.
[40] Cirilo, A.G. and Andrade, F.H. (1994) Sowing date and maize productivity: I. Crop growth and dry matter partitioning. Crop Sci. 34, 1039–1043.
[41] Otegui, M.E., Nicolini, M.G., Ruiz, R.A. and Dodds, P.A. (1995) Sowing date effects on grain yield components for different maize genotypes. Agron. J. 87, 29–33.
[42] Zaki, M.S., Shah, P. and Hayat, S. (1994) Effect of date of sowing on maize and non-flooded land rice. Sarhad J. Agric. 10, 191–199.
[43] Goldsworthy, P.R. (1984) Crop growth and development: The reproductive phase. In: Goldsworthy, P.R. and Fisher, N.M. (Eds.) The physiology of tropical field crops. New York: Wiley, 163-212.
[44] Otegui, M.E. and Melon, S. (1997) Kernel set and flower synchrony within the ear of maize: I. Sowing date effects. Crop Sci. 37, 441–47.
[45] Fischer, K.S. and Palmer, F.E. (1984), Tropical maize. In: Goldsworthy, P.R. and Fisher, N.M. (Eds.) The physiology of tropical field crops. New York: Wiley, 213-248.
[46] Kiniry, J.R. and Ritchie, J.T. (1985) Shade sensitive interval of kernel number of maize. Agron. J. 77, 711–715.
[47] Tollenaar, M. (1977) Sink-source relationships during reproductive development in maize. A review. Maydica. 22, 49–75.
[48] Khan, M.T. and Zada, K. (1990) Stability of harvest indices of maize varieties as affected by planting dates under different environments. M.Sc. (Hons) Thesis, Dept. Agron. Khyber Pakhtunkhwa Agric. Univ. Peshawar, Pakistan.
[49] Cirilo, A.G. and Andrade, F.H. (1996) Sowing date and kernel weight in maize. Crop Sci. 36(2), 325–331.
[50] Andrade, F.H., Uhart, S.A. and Cirilo, A. (1993) Temperature affects radiation use efficiency in maize. Field Crops Res. 32, 17–25.
[51] Rahman, A.M.A., Magboul, E.L. and Nour, A.E. (2001) Effect of sowing date and cultivar on the yield and yield components of maize in northern Sudan. 7th Eastern and Southern Africa Regional Maize Conference 11th–15th February, 2001. 295–298.
[52] Kandil, A.A. and Sharif, A.E. (2009) Morphological and physical-chemical characteristics identification of some summer oil crops genotypes. J. App. Sci. Res. 5(10), 1313–1319.
[53] Andrade, F.H., Cirilo, A.G. and Echarte, L. (2000) Factors affecting kernel number in maize. In: Otegui, M.E. and Slafer, G.A. (Eds.) Physiological bases for maize improvement. The Haworth Press Inc. USA, 59-74.

Received: **12.12.2017**
Accepted: **18.04.2018**

CORRESPONDING AUTHOR

Farooq Shah
Department of Agriculture,
Abdul Wali Khan University Mardan,
Khyber Pakhtunkhwa– Pakistan

E-mail: farooqshah@awkum.edu.pk

© by PSP Volume 27 – No. 7/2018 pages 4830-4837 Fresenius Environmental Bulletin

ASSESSMENT OF THE GRAIN QUALITY OF WHEAT GENOTYPES GROWN UNDER MULTIPLE ENVIRONMENTS USING GGE BIPLOT ANALYSIS

Mehmet Yildirim[1], Celaleddin Barutcular[2,*], Mujde Koc[2], Halef Dizlek[3], Akbar Hossain[4], Mohammad Sohidul Islam[5], Irem Toptas[2], Fatma Basdemir[1], Onder Albayrak[1], Cuma Akinci[1], Ayman El Sabagh[6]

[1]Department of Field Crops, Faculty of Agriculture, University of Dicle, Diyarbakir, Turkey
[2]Department of Field Crops, Faculty of Agriculture, University of Çukurova, Adana, Turkey
[3]Department of Food Engineering, Faculty of Engineering, University of Osmaniye Korkut Ata, Osmaniye, Turkey
[4]Wheat Research Center, Bangladesh Agricultural Research Institute, Nashipur, Dinajpur-5200, Bangladesh
[5]Department of Agronomy, Hajee Mohammad Danesh Science and Technology University, Bangladesh
[6]Department of Agronomy, Faculty of Agriculture, University of Kafrelsheikh, Kafrelsheikh, Egypt

ABSTRACT

The field experiment was conducted in agricultural research field under the department of field crops, faculty of agriculture, University of Dicle, Turkey (37°53' N, 40°16' E) during spring wheat growing season of 2011-12 for assessing the grain yield and quality of sixteen spring wheat genotypes grown under late sown rainfed condition (high temperature combined with drought stress) as compared with early sowing in irrigated condition (favourable environment). The experiment was laid out in a split-split plot design with three replications. Two sowing times: early sowing (cool environment) and late sowing (warm environment) were allocated in main plots, sub-plots were in two irrigation conditions (rainfed and irrigation) and finally sub-sub plots were arranged with sixteen spring wheat genotypes. Data on grain weight (GW), grain protein content (GPC), grain starch content (GSC), test weight (TW), Zeleny sedimentation volume (ZT), dry gluten content (DGC), gluten index (GI) and grain flour content (GFC) were determined to know the adverse effect of high temperature in combined with drought stress. The results of the present study indicates that high temperature combined with drought (late sown heat stress condition) significantly influenced the grain yield and quality parameters of all tested wheat genotypes. Grain protein content showed a positive correlations with DGC and ZT, while negative correlation with GW under normal and heat stress conditions. Moreover, a significant negative association was found between GSC and GPC content due to the adverse effect of high temperature in combined with drought stress. These results support that the performance of genotypes 'Inqilab-91', 'Cham-6', 'Adana-99' and 'Meta-2002' were better in respect of the most important traits of grain quality under adverse environment. Therefore, the genotypes may be considered as prospective good candidates for new wheat varieties for cultivation under heat (late sowing) and drought stress (rainfed) conditions of Turkey.

KEYWORDS:
GGE-biplot analysis, correlations, drought, heat, genotype, wheat, stress.

INTRODUCTION

Wheat (*Triticum aestivum* L.) is one of the widely adapted cereals, grown in warm and humid to dry and cold environments [1, 2]. Among the cereals, it is stands first in terms of production and acreage, while due to the frequent food shortages for increasing population its importance has been risen day by day [3, 4]. The global requirements of wheat by 2020 about 950 million tons to achieve food needs imposed by the increase of population and further, this could be reached, if global wheat productivity is improved by 2.5% per annum [5, 6].

The grains of wheat usually use as a number of edible product like chapatti, bread, biscuit, noodles and pasta [7]. Flour quality of wheat mainly depend on proteins, energy, amino acids, carbohydrates, lipids, minerals and vitamins. Based upon the solubility, grain proteins of wheat is classified as albumins, globulins and gliadins (monomeric) and glutenins (polymeric) [8]. The rheological properties like viscosity and elasticity of flour depends on the balance of these two proteins determines [9], for example, gliadins determine the viscosity, while glutenins is generally associated with elasticity of dough. However, starch is the major constituent of flour and plays a significant role in food product quality. During yeast fermentation, it is helpful in setting of bread loaf and retro-gradation during storage through providing carbon [10]. The large granules increase the resistance to extension of dough, while small starch granules increase the extensibility [11].

Although wheat has a wide range of climatic

adaptability, however, many biotic factors such as diseases, insect pests, and weeds and abiotic factors such as drought, high temperature, salinity, flooding, freezing, high irradiation, and nutrient deficiency or toxicities limit its yield [3, 4, 12]. Among the abiotic factors, high temperature and drought are the most important environmental factors that limiting the grain quality and net productivity of wheat in all over the world, especially in Mediterranean environment [13, 14], where high temperature combine with drought effect on the phenology, growth and productivity of rainfed crops than individual stress [3, 4].

According to Jiang et al. [15], anthesis and grain-filling period are the most critical growth stages of wheat under adverse environmental conditions that leads to negatively influence the grain quality of wheat. Under late sown condition, high temperature in combination with drought deteriorate the grain quality of wheat through late flowering, thereby forcing the grain filling period [1]. Similarly, Labuschagne et al. [9] reported that during grain filling period increased temperature, increase the severity of drought through reducing soil moisture as well as air humidity resulting to the force maturity through shortened the duration of glutenins synthesis. While, Wardlaw and Moncur [16], noticed that the late sown wheat face heat stress during flowering resulting to reduce grain size; but grain protein accumulation is increased than starch under heat stress condition.

Therefore, development of new drought and heat stress tolerant wheat genotypes with good grain quality are crucial to meet the food demand of increasing population in the world, under future changing climate such as heat and drought stress condition [14]. Currently various strategies are being applied to increase heat stress-tolerance in wheat through understanding the impact of climate variability (rise in temperature and drought stress) under rainfed conditions during grain-filling period of wheat [17]. But, little works have been done to study effect of high temperature and drought stress on protein and starch accumulation of wheat. In the context, the present study was undertaken to evaluate the effect of sowing time (especially early and late sown heat stress) in combine with drought on grain quality of wheat under rainfed and irrigated conditions.

MATERIALS AND METHODS

Experimental site and design. The field experiment was conducted in agricultural research field under the department of field crops, faculty of agriculture, University of Dicle, Turkey (37°53'N, 40°16'E) during spring wheat growing season (in the year 2011-12). The experiment was arranged in a split-split plot design with three replications. Two sowing times i.e., early sowing (cool environment) and late sowing (warm environment) were allocated in main plots and sub plots were arranged with two irrigation conditions (rainfed and irrigation) and finally sub-sub plots were arranged with sixteen spring wheat genotypes. Plot size was 8.4 m^2 (six rows, 20 cm apart)

Plant material and growing conditions. The sixteen spring bread wheat genotypes consist of commercial cultivars were used as plant material. The experimental methodologies have been followed as described previously by [18, 19]. Mean and maximum temperature (°C) during the early sowing (cool environment) and late sowing (warm environment) conditions are presented in (Fig.1).

Seed rate, fertilizers and irrigation. The seed rate was 450 seeds m^{-2}. Fertilizer, phosphorus (40 kg ha^{-1} P_2O_5) was added before sowing as triple super phosphate form. Whereas, nitrogen was applied as ammonium nitrate in three split 40, 80 and 40 kg N ha^{-1} at Zadok's growth stages (ZGS) 00, 20 and

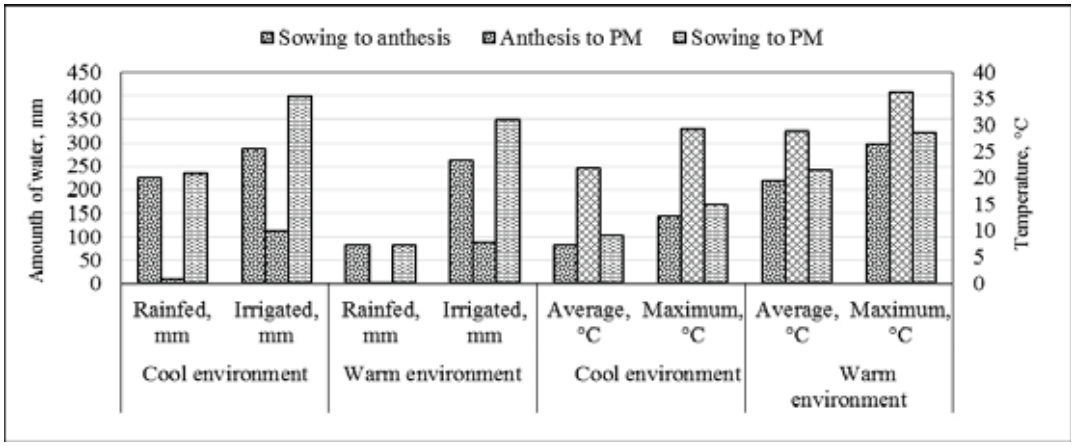

FIGURE 1
Climatic data in the cool and warm environments during the growing periods. [PM; physiological maturity].

30, respectively. The experiment were established as a first and second sowing time, December and April, respectively. While the first sowing time represented the conventional sowing date, the second sowing time with growing period was rather drought and high temperature than the previous sowing time.

The factor of irrigation was determined as rainfed (drought) and irrigated conditions. Rainfed conditions did not take supplementary irrigation, except only for emergence. Irrigated conditions were adjusted to keep plants to field capacity. Amount of water (mm) in the environment during the growing period were presented in (Fig. 1).

Determination of grain quality traits. Data on quality parameters, including grain weight (GW), as thousand grain weight (g), grain protein content (GPC) (%), grain starch content (GSC) (%), test weight (TW) (kg hl^{-1}), Zeleny sedimentation volume (ZT) were determined. The dry gluten content (DGC) were determined from grain samples with a near infrared transmittance spectrophotometer (Infratec 1241-grain analyzer, Foss Tecator AB, Sweden). Grain flour content (GFC, %), test weight (kg/hl), gluten index (GI) were measured according to Approved Method 38-12 [20].

Statistical analysis. GGE biplot analysis is a useful tool for data analysis, with visual displays, from trials conducted in multiple environments, as well as useful for plant breeders and geneticists to study complex genotype and environment interactions [21]. Specifically, in the GGE biplot analysis, two-way data from multi-location trials are displayed visually as the G main effect and the GE interaction effect. The data were statistically analyzed by using (Stat Soft, Inc., 2005, data analysis software system, version 7.1. www.statsoft.com.).

RESULTS

Results obtained from the present study revealed that mean square values of genotypes were significant for all studied traits due heat stress and irrigation regimes (Fig. 2 and Fig. 3). The highest value of major grain quality in this experiment was obtained from the genotypes 'Inqilab-91', followed by 'Cham-6', and 'Adana-99' under well-irrigated condition and the lowest values were in stress condition (late sown heat and drought (rainfed) condition). These genotypes, therefore be considered to cultivate under late sown drought (rainfed) condition.

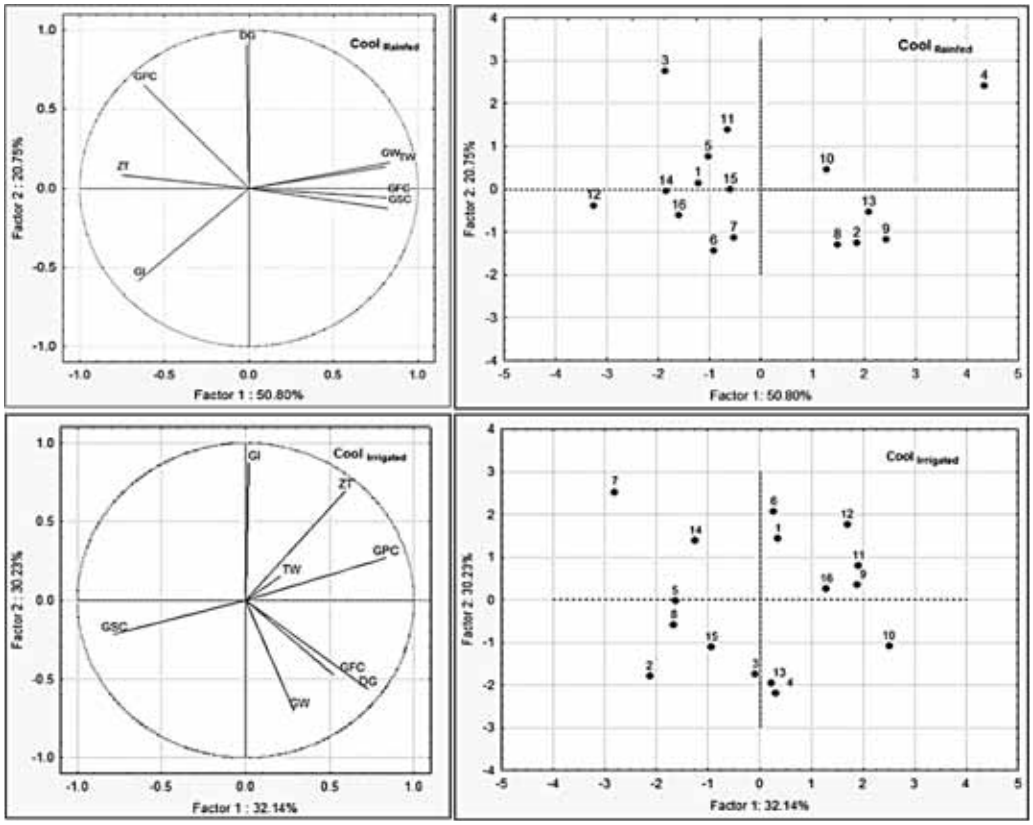

FIGURE 2

Biplot based on principal component analysis for grain quality traits in 16 wheat genotypes: Principal component analyses (PCA) score plots of PC1 versus PC2. Eigenvalues are presented as vectors for the following grain quality traits and genotypes in cool environments.GW, grain weight; GPC, grain protein content; GSC, grain starch content; TW, test weight; ZT, Zeleny sedimentation volume; DGC, dry gluten content; GI, gluten index and GFC, grain flour content.

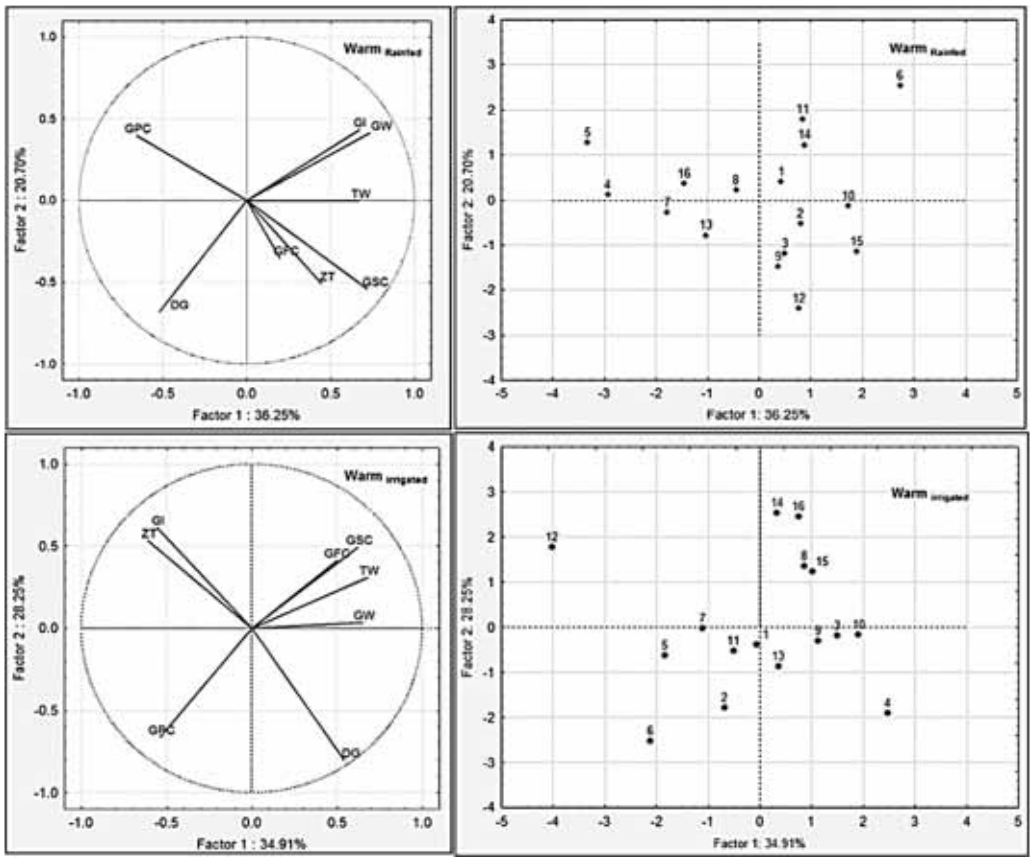

FIGURE 3

Biplot based on principal component analysis for grain quality traits in 16 wheat genotypes: Principal component analyses (PCA) score plots of PC1 versus PC2. Eigenvalues are presented as vectors for the following grain quality traits and genotypes in warm environments.GW, grain weight; GPC, grain protein content; GSC, grain starch content; TW, test weight; ZT, Zeleny sedimentation volume; DGC, dry gluten content; GI, gluten index and GFC, grain flour content.

The GGE-biplot analysis is a suitable method to analysis the interaction between wheat quality properties and wheat genotypes growing under different environments. In this research, quality traits of genotypes were explained by the Principal Component Analysis (PCA) to construct the zone with regard to quality trait expression. Hence, explanation was varied to environment (Fig. 2 and Fig. 3). The examined genotypes might be arranged into four groups based on their performance under stress and non-stress conditions.

Cool rainfed environment (Cool $_{Rainfed}$). Principal Component Analysis PC1 and PC2 explained up to 50.80% and 20.75% of total variance, respectively and total of 71.15% (Fig. 2). The results of grain weight (GW), test weight (TW), grain flour content (GFC) and grain starch content (GSC) are very important traits in discriminating the genotypes (Fig. 2). It was observed and grain weight and test weight were a group and they were positively and significantly correlated. In this concern, grain flour content and grain starch content was similarly a group and they have significantly and positively correlated with each other. In respect to differences among genotypes, 'Cham-6', 'Inqlab-91', 'Meta-2002', 'Genc-99', 'Balattila' and 'Galil' are situated in the positive sense of the grain weight (GW), test weight (TW), grain flour content (GFC) and grain starch content (GSC) vectors, indicating that they performed particularly well for these quality traits (Fig. 2). Furthermore, genotype 'Cham-6' (4) produced a higher grain weight (GW), test weight (TW) than other genotypes, as well as, it is also achieved high value in grain flour content (GFC) and grain starch content (GSC) (Fig. 2).

Cool irrigated environment (Cool $_{Irrigated}$). Regarding the cool irrigated environment Principal Component Analysis PC1 and PC2 explained up to 32.14% and 30.23% of total variance and total of 62.37% (Fig 2). Results indicated that Zeleny sedimentation volume (ZT), grain protein content (GPC), grain flour content (GFC), dry glutenins (DG) and grain weight (GW) are very important traits in discriminating the genotypes (Fig. 2). Under cool irrigated environment (Cool $_{Irrigated}$), genotypes, 'Cumakalesi', 'Mane Nick', 'Adana-99', 'Karacadağ-99', 'V-3210', 'Genç-99', 'Inqlab-91', 'Meta-2002' and 'Cham-6' are situated in the positive sense of the Zeleny sedimentation volume (ZT), grain protein content (GPC), grain flour content (GFC), dry

glutein (DG) and grain weight GW vectors, indicating that they performed particularly well at these quality traits (Fig. 2).

Concerning warm rainfed environment (Warm $_{rainfed}$). Under warm rainfed environment Principal Component Analysis PC1 and PC2 enlightened up to 36.25% and 20.70% of the total variance, and the total 56.95% (Fig. 3). Majority of quality parameters were positively correlated except test weight (TW) and grain starch content (GSC) were negatively correlated with each other. Glutenin index (GI), grain weight (GW) and grain starch content (GSC) are very important traits in discriminating the genotypes (Fig. 3). Genotypes 'Cumakalesi' is situated in the positive sense of the glutenin index and grain weight vectors indicating that they performed particularly well at these quality traits (Fig. 3). While, genotype 'Colfiorito' is only situated in the positive sense of the grain protein content vector (Fig. 3).

For warm irrigated environment (Warm $_{irrigated}$). For warm irrigated environment Principal Component Analysis (PC1) explained up to 34.91% of total variance and PC2 explained 28.25%, and total of 63.16% (Fig. 3). Similar to previous environmental condition, results of biplot analysis also indicated that grain starch content (GSC), grain flour content (GFC), test weight (TW) and grain weight (GW) are very important traits in discriminating the genotypes (Fig. 3). Furthermore, the environment in cool irrigated is most suitable followed by that of cool rainfed. The potentiality of genotypes 'Inqilab-91', 'Cham-6', 'Adana-99' and 'Meta-2002' were superior as good and stable genotypes for end-use quality parameters under stress environment.

DISCUSSION

Development of new drought and heat tolerant wheat genotypes with good grain quality are crucial for researcher to meet the food demand of increasing population in around world [13]. In the present study quality traits *viz.,* grain weight (GW), grain protein content (GPC), grain starch content (GSC), test weight (TW), Zeleny sedimentation volume (ZT), dry gluten content (DGC), gluten index (GI) and grain flour content (GFC)) of sixteen wheat genotypes were studied under favourable and adverse conditions (high temperature in combine with drought stress) for assessing the genotypes which are suitable to grow under adverse condition. Results obtained from the present study revealed that mean square values of all genotypes for all studied quality traits were significant due heat stress and irrigation regimes (Fig. 2, 3). The findings of the present study also similar with earlier study as reported by [9], who noticed that increased temperature and drought stress during grain filling period resulted to early maturity and shortened duration of glutenin synthesis, which in turn reduced dough strength. While, Jiang et al. [15], noticed that the late sown wheat face heat stress during flowering that lead to decrease the productivity as well as grain quality of wheat. Similarly, anthesis and grain-filling period are most important critical growth stages of wheat, but under stress conditions, the time duration of two stages are shorten that leads to negative effect on grain quality of wheat [16]. The results of the present study also confirm by earlier study, who noticed that under late sown condition, grain quality of wheat genotypes affects through flowering late, or forcing the grain filling period through the coincide of high temperature stress [1]. Furthermore, water stress/drought might lead to the significant effect on seed quality traits of different crops [22-31]. Wheat traits could be associated in a positive or a negative way to each other, and the association performance is independent of the breeding aims and could change from surroundings conditions to another [32].

Considering on the GGE-biplot analysis (Fig. 2 and Fig. 3), the results of the present study also confirmed by previous studies as reported by [33, 34], who noticed that the examined wheat genotypes were divided into some groups by GGE-biplot analysis. The genotypes which performed good under 30% of field capacity, were most suitable for regions with very short water availability [35]. Genotypes which were superior under 70% of field capacity, these have appropriate for the area of about normal water availability [35].

These results are in agreement with the findings of [36], [37]. Considering the biplot genotypes with scores gave high (stable genotypes), and genotypes with scores had low (unstable genotypes). These results appear some variations from that of the relationship analysis among pairs of properties as the biplot describes the inter-relationships among all traits concurrently on the basis of the overall data that offering [38].

Furthermore, the GGE-biplot could designate the interrelation among the genotypes, additionally their stability and contribution toward an individual character [39]. Genotypes grouping in the biplot designated that the genotypes of the quality traits groups appeared similar performance to quality attributes [34]. The protein contents, gluten quality and contents have significantly and negatively correlated with grain weights under normal and stress conditions [40]. Genotype-by-environment interactions and the negative correlation between grain yield and grain gluten content of wheat had been established in different studies [41].

CONCLUSION

From the results and discussion of the present study, it can be concluded that grain weight (GW), grain protein (GPC), grain starch (GSC), test weight (TW), Zeleny sedimentation volume (ZT), dry gluten (DGC), gluten index (GI) and grain flour content (GFC) of sixteen wheat genotypes significantly influenced by the adverse effect of high temperature in combine with drought stress. Among the quality parameter, grain protein showed the positive correlations with DGC and ZT, while GW showed the negative correlation under normal and stress conditions. Similarly, a significant negative association was found between GSC and GPC content due to the adverse effect of high temperature in combine with drought stress. Considering on genotypes, 'Inqilab-91', 'Cham-6', 'Adana-99' and 'Meta-2002' were found better in respect of the most important traits of grain quality under adverse environment. Therefore, the genotypes are prospective good candidate advance lines for new wheat varieties cultivation under heat (late sowing) and drought stress (rainfed) in Mediterranean Environment of Turkey.

ACKNOWLEDGEMENTS

This research was supported by the Scientific and Technological Research Council of Turkey (TUBITAK) Project no. 110O345

The authors declare no conflicts of interest.

REFERENCES

[1] Hakim, M.A., Hossain, A., Teixeira da Silva, J.A., Zvolinsky, V.P., Khan, M.M. (2012) Protein and Starch Content of 20 Wheat (*Triticum aestivum* L.) Genotypes Exposed to High Temperature Under Late Sowing Conditions. Journal of Scientific Research. 4(2), 477–489.

[2] FAO (Food and Agricultural Organization). (2016) FAO Production Yearbook for the year 2016. Rome, Italy.

[3] Hossain, A., Teixeira da Silva, J.A., Lozovskaya, M.V., Zvolinsky, V.P. (2012a) High temperature combined with drought affect rainfed spring wheat and barley in South-Eastern Russia: I. Phenology and growth. Saudi Journal of Biological Sciences. 19(4), 473–487.

[4] Hossain, A., Teixeira da Silva, J.A., Lozovskaya, M.V., Zvolinsky, V.P., Mukhortov, V.I. (2012b) High temperature combined with drought affect rainfed spring wheat and barley in south-eastern Russia: Yield, relative performance and heat susceptibility index. J. Plant Breeding Crop Science. 4(11), 184–196.

[5] Singh, K., Sharma, S.N., Sharma, Y. (2011) Effect of high temperature on yield attributing traits in bread wheat. Bangladesh Journal of Agricultural Research. 36(3), 415–426.

[6] Barutçular, C., El Sabagh, A., Koç, M., Ratnasekera, D. (2017) Relationships between Grain Yield and Physiological Traits of Durum Wheat Varieties under Drought and High Temperature Stress in Mediterranean Conditions. Fresen. Environ. Bull. 26, 4282–4291.

[7] Shewryi, P.R. (2009) Wheat. Journal of Experimental Botany. 60, 1537–1553.

[8] Hurkman, W.J., Vensel, W.H., Tanaka, C.K., Whitehand, L., Altenbach, S.B. (2009) Effect of high temperature on albumin and globulin accumulation in the endosperm proteome of the developing wheat grain. Journal of Cereal Science. 49, 12–23.

[9] Labuschagne, M.T., Elago, O., Koen, E. (2009) Influence of Extreme Temperatures during Grain Filling on Protein Fractions, and Its Relationship to Some Quality Characteristics in Bread, Biscuit, and Durum Wheat. Cereal Chemistry Journal. 86, 61–66.

[10] Erbs, M., Manderscheid, R., Jansen, G., Seddig, S., Pacholski, A., Weigel, H.J. (2010) Effects of free-air CO2 enrichment and nitrogen supply on grain quality parameters and elemental composition of wheat and barley grown in a crop rotation. Agriculture, Ecosystems and Environment. 136, 59–68.

[11] Larsson, H., Eliasson, A.C. (1997) Influence of the starch granule surface on the rheological behaviour of wheat flour dough. Journal of Texture Studies. 28, 487–501.

[12] Ahmed, M., Fayyaz-ul, H. (2015) Response of Spring Wheat (*Triticum aestivum* L.) Quality Traits and Yield to Sowing Date. PLoS ONE. 10(4), e0126097.

[13] Hossain, A., Sarker, M.A.Z., Saifuzzaman, M., Teixeira da Silva, J.A., Lozovskaya, M.V., Akhter, M.M. (2013) Evaluation of growth, yield, relative performance and heat susceptibility of eight wheat (*Triticum aestivum* L.) genotypes grown under heat stress. International Journal of Plant Production. 7(3), 615–636.

[14] Hossain, A., Teixeira da Silva, J.A. (2013) Wheat production in Bangladesh: its future in the light of global warming. AoB PLANTS. 5(1), pls042

[15] Jiang, D., Yue, H., Wollenweber, B., Tan, W., Mu, H., Bo, Y., Dai, T., Jing, Q. and Cao, W. (2009) Effects of Post-Anthesis Drought and Waterlogging on Accumulation of High-Molecular-Weight Glutenin Subunits and Glutenin Macropolymers Content in Wheat Grain. Journal of Agronomy and Crop Science. 195, 89–97.

[16] Wardlaw, I., Moncur, L. (1995) The Response of wheat to high temperature following anthesis. I. The rate and duration of kernel filling. Functional Plant Biology. 22, 391–397.
[17] Wardlaw, I.F., Blumenthal, C., Larroque, O., Wrigley, C.W. (2002) Contrasting effects of chronic heat stress and heat shock on kernel weight and 1270 flour quality in wheat. Functional Plant Biology. 29, 25–34.
[18] Barutçular, C., Yıldırım, M., Koç, M., Akıncı, C., Toptaş, I., Albayrak, O., Tanrıkulu, A., El Sabagh, A. (2016a) Evaluation of SPAD chlorophyll in spring wheat genotypes under different environments. Fresen. Environ. Bull. 25, 1258–1266.
[19] Barutçular, C., Yıldırım, M., Koç, M., Akıncı, C., Tanrıkulu, A., El Sabagh, A., Saneoka, H., Ueda, A., Islam, MS., Toptas, I., Albayrak, O., Tanrikulu, A. (2016b) Quality traits performance of bread wheat genotypes under drought and heat stress conditions. Fresen. Environ. Bull. 25, 6159–6165.
[20] AACC. (2000) Approved methods of the American Association of Cereal Chemists, 10th ed. American Association of Cereal Chemists, St. Paul, MN, USA.
[21] Frutos, E., Galindo, M.P., Leiva, V. (2014) An interactive biplot implementation in R for modeling genotype-by-environment interaction. Stochastic Environmental Research and Risk Assessment. 28(7), 1629–1641.
[22] Barutcular, C., Dizlek, H., El Sabagh, A., Sahin, T., El Sabagh, M., Islam, M.S. (2016c) Nutritional quality of maize in response to drought stress during grain-filling stages in Mediterranean climate condition. Journal of Experimental Biology and Agricultural Sciences. 4, 644–652.
[23] Barutcular, C., El Sabagh, A., Konuskan, O., Saneoka, H. (2016d) evaluation of maize hybrids to terminal drought stress tolerance by defining drought indices. Journal of Experimental Biology and Agricultural Sciences. 4, 610–616.
[24] El Sabagh, A., Barutçular, C., Islam, M.S. (2017a) Relationships between stomatal conductance and yield under deficit irrigation in maize (*Zea mays* L.). Journal of Experimental Biology and Agricultural Sciences. 5, 15–21.
[25] El Sabagh, A., Abdelaal, Kh.A.A, Barutcular, C. (2017b) Impact of antioxidants supplementation on growth, yield and quality traits of canola plants (*Brassica napus* L.) under irrigation intervals in North Nile Delta of Egypt. Journal of Experimental Biology and Agricultural Science. 5(2), 163–172.
[26] El Sabagh, A., Barutçular, C., Saneoka, H. (2015a) Assessment of Drought Tolerance Maize Hybrids at Grain Growth Stage in Mediterranean Area. World Academy of Science, Engineering and Technology: International Journal of Agricultural and Biosystems Engineering. 9(9), 1010-1013.
[27] El Sabagh, A.E., Sorour, S., Omar, A.E., Islam, M.S., Ueda, A., Saneoka, H. and Barutçular, C. (2015b) Soybean (*Glycine Max* L.) Growth Enhancement under Water Stress Conditions. International Conference on Chemical, Agricultural and Biological Sciences. Istanbul, Turkey. 144–148.
[28] El-Shawy, E.E., El Sabagh, A., Mansour, M., Barutcular, C. (2017) A comparative study for drought tolerance and yield stability in different genotypes of barley (*Hordeum vulgare* L.). Journal of Experimental Biology and Agricultural Sciences. 5(2), 151–162.
[29] Abd El-Wahed, M.H., El Sabagh, A., Zayed, A., Sanussi, A., Saneoka, H., Barutçular, C. (2015) Improving yield and water productivity of maize grown under deficit-irrigated in dry area conditions. Azarian Journal of Agriculture. 2(5), 123–132.
[30] Abdelaal, A.A.Kh., Hafez, Y.M., El Sabagh, A. (2017) Ameliorative effects of abscisic acid and yeast on morpho-physiological and yield characters of maize (*Zea mays* L.) plants under water deficit conditions. Fresen. Environ. Bull. 26, 7372–7383.
[31] Rashwan, E., Mousa, A., El-Sabagh, A., Barutçular, C. (2016) Yield and Quality Traits of Some Flax Cultivars as Influenced by Different Irrigation Intervals. Journal of Agricultural Science. 8, 226–240.
[32] Majid, M.A., Saiful, M.S., El Sabagh, A., Hasan, M.K., Barutcular, C., Ratnasekera, D., Islam, M.S. (2017) Evaluation of growth and yield traits in corn under irrigation regimes in subtropical climate. Journal of Experimental Biology and Agricultural Sciences. 5(2), 134–150.
[33] Kaya, Y. and Akcura, M. (2014) Effects of genotype and environment on grain yield and quality traits in bread wheat (*Triticum aestivum* L.). Food Science and Technology Campinas. 34, 386–393.
[34] Saint Pierre, C.S., Crossa, J.L., Bonnett, D., Yamaguchi-Shinozaki, K., Reynolds, M.P. (2012) Phenotyping transgenic wheat for drought resistance. Journal of Experimental Botany. 63, 1799–1808.
[35] Aslam, M., Ahmad, K., Maqbool, M.A., Bano, S., Zaman, Q.U., Talha, G.M. (2014) Assessment of adaptability in genetically diverse chickpea genotypes (*Cicer arietinum* L.) based on different physio morphological standards under ascochyta blight inoculation. International Journal of Advance Research. 2, (2)245–255.

[36] Farshadfar, E., Sutka, J. (2002) Multivariate analysis of drought tolerance in wheat substitution lines. Cereal Research Communication. 31, 33–39.
[37] Golabadi, M.A., Arzani, S.A., Maibody, M. (2006) Assessment of drought tolerance in segregating populations in durum wheat. African Journal of Agricultural Research. 1(5), 62–171.
[38] Yan, W., Fregeau-Reid, J.A. (2008) Breeding line selection based on multiple traits. Crop Science. 48, 417–423.
[39] Morris, C.F., Campbell, K.G., King, G.E. (2004) Characterization of the end-use quality of soft wheat cultivars from the eastern and western US germplasm pools. Plant Genetic Resources. 2, 59–69.
[40] Oury, F.X., Godlin C. (2007) Yield and grain protein concentration in bread wheat: how to use the negative relationship between the two characters to identify favourable genotypes? Euphytica. 157, 45–57.
[41] Tayyar, S. (2010) Variation in grain yield and quality of Romanian bread wheat varieties compared to local varieties in northwestern Turkey. Romanian Biotechnology Letters. 15(2), 5189–5196.

Received: **20.12.2017**
Accepted: **10.02.2018**

CORRESPONDING AUTHOR

Celaleddin Barutcular
Department of Field Crops,
Faculty of Agriculture,
University of Çukurova,
Adana – Turkey

e- mail: cebar@cu.edu.tr

© by PSP Volume 27 – No. 7/2018 pages 4838-4843 Fresenius Environmental Bulletin

EVALUATION OF SOME AGRONOMIC CHARACTERISTICS OF BROOMCORN GENOTYPES GROWN IN THE ADAPAZARI REGION

Serap Kizil-Aydemir[1,*], Farzad Nofouzi[2]

[1]Department of Field Crop, Faculty of Agriculture and Science, Bilecik Seyh Edebali University, 11230, Bilecik, Turkey
[2]Department of AnimalScience, Faculty of Agriculture, Ondokuz Mayıs University, 55139, Samsun, Turkey

ABSTRACT

This study was conducted to identify promising genotypes and provide materials for further breeding studies by evaluating the agronomic characteristics of broomcorn genotypes traditionally grown in Adapazarı and its vicinity. Six village genotypes grown at different locations were used as material and the study was conducted in 2015 and 2016. The results showed that plant heights of the genotypes were in the range of 182.10-154.50 cm. The tallest plant was Genotype-6. Leaf length was in the range of 7.42 to 6.13 mm. The longest leaf length was obtained at 7.42 mm in Genotype-2. The maximum leaf width of 8.12 mm was obtained in Genotype-1. The longest panicle length was in Genotype-1 and the heaviest panicle weight was obtained in Genotype-5. Panicle length and panicle weight are important morphological constructs. Genotype-1 and Genotype-5 were found to be promising genotypes for broomcorn production. The highest panicle seed weight and weight of 1000 seeds were obtained in Genotype-1. The results showed that there were positive and significant correlations among panicle weight, leaf width and leaf length, panicle length and panicle seed weight. On the other hand, leaf width, panicle seed weight and panicle weight had positive relationships, whereas panicle seed weight, weight of 1000 seeds and leaf width also had a significant relationship.

KEYWORDS:
Broomcorn, genotypes, agronomic characteristics

INTRODUCTION

Sorghum (*Sorghum bicolor* (L.) Moench) 2n=20 belongs to the Andropogoneae tribe of the Poaceae family [8]. It is a self-pollinated crop [16]. Sorghum and its varieties are used in many areas such as grains, silage, green and dry feed, brooms, sausages, wall coverings. *Sorghum bicolor* (L.) Mohench. vartechnicum (Körn.) is a type of sorghum with long fiber, flexible and sturdy panicule and it is used in broomcorn construction [3].

Broomcorn (*Sorghum vulgare*) is not actually corn but instead it is related to the sorghums used for grain and syrup (*Sorghum bicolor*). Broomcorn has a coarse and fibrous seed head that has been used to make various types of brooms and brushes for several centuries. While there are still craftspeople creating these natural brooms today, this crop is now more commonly used to make decorative items such as wreaths, swags, floral arrangements, baskets and autumn displays. It takes about 60 sprays (heads) to make a broom, but wreaths and dried arrangements require only a few plants [13]. This plant of Central African origin is mostly grown in Mediterranean countries. The long panicular varieties of broomcornwere first used in broomstones in Italy in the late 1500's [6, 19]. The U.S. demand for broomcorn has declined with the rise in sales of synthetic brooms. About half of the current national need for broomcorn is being met by imports from Mexico, another key factor contributing to the decline in domestic acreages. It may not be possible for Kentucky growers to compete with broomcorn wholesalers; however, there are still a number of artisans and craftspeople who pride themselves in making high-quality brooms by hand. These entrepreneurs, many of whom use imported broomcorn, may be interested in a readily available local supply. As with any specialty product, it is best to identify a market before planting the crop [13].

Broomcorn has been grown in Turkey for many years in the procinces of Sakarya and Edirne, as well as their districts. In recent years, with the widespread use of electric vacuum cleaners at homes and offices and the spread of brooms made of nylon (plastic) fibers, the craftsmanship of using natural fibers as a raw material has declined, leading to a decrease in the planting area of the broomcorn. The broomcorn, which is produced in small quantities, is sold to broom producers.

From very ancient times until recently, sweeping was one of the most common acts of houseworkseen throughout Turkey. Like other handcrafts, producing brooms for sweeping was quickly withdrawn from our daily lives, unable to keep pace with the innovations of modern life. For this reason, while organic sweeps used in cleaning houses are disappearing, a cultural accumulation formed over the

broom for centuries is also under the threat of extinction.

As a matter of fact, the United Nations Educational, Scientific and Cultural Organization [20] frequently points out that the socio-cultural characteristics of a country and distressing events lead to migration from rural areas to urban areas and emptying of rural areas. This is a tragedy of humanity, and it is emphasized that the cult created during hundreds of years is an unbearable loss. Today, if organic products are preferred, the use of hand-made sweeping tools is expected to become widespread. The broomcornused to make brooms from flower buds is seen as a result of work done especially in poultry feed, medicine and cosmetics industry, while stalks and leaves can be used in paper industry [10, 11]. In a survey, it was revealed that staple stalks of broomcorn had a low value as feed, but immature grains were close to the feed value of the oat [6]. U.S. broom is used in silage production and dairy fattening [15].

Studies were conducted to determine more closely the degree of dominance of the Dwa gene of sorghum [Sorghum bicolor (L.) Moench] and investigate further the relationships between height and other agronomic traits. Isogenic lines of 'Martin,' 'Plainsman', 'Redlan,' and 'Tx403,' homozygous for the dominant and recessive allele of Dws were compared to heterozygous lines produced from crosses of each short line to its tall counterpart.

The data were collected and analyzed for culm height, grain yield, test weight, kernel weight, panicles/plant, peduncle length and node number. Height genotype influenced total yield, test weight, panicles/plant and kernel weight, as well as culm height. Cultivar × height interactions were observed for height, test weight, and kernel weight. Height appeared to be partially dominant. The degrees of dominance recorded for Martin, Plainsman and Redlan were 0.70, 0.70 and 0.82, respectively. Yields of the heterozygous lines were not significantly different from those of the corresponding homozygous tall lines. In general, heterozygous lines had test weights and kernel weights equal to those of the tall homozygous fines and higher than those of the short parents. Heterozygous lines tended to have more panicles/plant than did either the tall or short lines [5].

According to Sakarya Commodity Exchange records, between 2010 and 2017, the amount of broomcorn cuts traded on the stock exchange ranged from 372 to 1000 tons. The prices of kilograms of broomcorn cuts harvested just below the panikiler ranged from 0.85 to 1.600 YTL in recent years. The price decreases annually when production is excessive, and it increases when production is low. The subject of this study was the broomcorn, which has an important place in the Sakarya region and has not been examined in Turkey in an agricultural perspective almost at all. The purpose of this study was to determine some agricultural characteristics of the broomcorn genotypes grown in Sakarya, the most important region where broomcorn is bred in Turkey, and determine the genotypes suitable for the regional conditions.

MATERIALS AND METHODS

This study was carried out in 2015 and 2016 in Adapazarı, which is located at 29º 57'-30º 53'E and 40º 17'- 41º 13'N in the northeastern part of the Marmara region where broomcorn is widely grown. The aim of this study was to identify promising genotypes and provide material for further breeding studies by evaluating the agronomic characteristics of the genetics of broomcorn that is traditionally grown in Adapazarı. For this reason, data were collected from

TABLE 1
Some climate values for the trial years.

		Climate Data				
Month		**Minimum Temperature**	**Maximum Temperature**	**Average Temperature**	**Average Rainfall**	**Humidity Average**
	2015	6.79	18.76	12.76	7.35	66.67
April	2016	10.54	24.78	18.59	5.95	58.80
	Long-term	8.60	19.30	13.30	63.70	62.73
	2015	13.80	25.40	19.11	5.63	72.53
May	2016	13.47	24.00	19.58	5.76	69.17
	Long-term	12.70	24.40	17.80	54.40	71.20
	2015	17.27	26.34	21.73	15.24	78.15
June	2016	18.32	30.28	25.29	13.95	65.75
	Long-term	16.60	28.10	22.10	80.80	70.90
	2015	19.07	29.91	26.03	9.80	68.04
July	2016	19.18	30.61	25.77	0.72	70.23
	Long-term	19.00	30.20	24.30	46.00	69.90
	2015	20.51	31.45	27.49	5.72	66.87
August	2016	21.09	31.55	25.73	9.17	78.00
	Long-term	19.20	30.30	24.20	47.10	71.90
	2015	19.07	29.51	25.00	14.73	73.23
September	2016	15.56	28.07	22.74	4.96	68.64
	Long-term	15.30	26.90	20.30	58.70	73.60

different places where broomcorn was grown. In the study, 6 village genotypes were used as the material. The data obtained from the study were analyzed for variance by combining yearsin a completely randomized design with three replications. The statistical significance of the differences between the means was determined by Duncan's analysis. Relationships between plant characteristics were determined by correlation analysis. All analyses were performed in the MSTATC package program.

The average temperature values for the first year of the study in April and June of 2015 were 12.76 and 21.73 °C respectively which is lower than the long-term average temperatures. In May, July, August and September, these values were 19.11, 26.03, 27.49, 25 °C respectively and they were found to be higher than the long-term average. In 2016, the second year of the study, the average temperatures were 18.59, 19.58, 25.29, 25.77, 25.73 and 22.74 °C in April, May, June, July, August and September respectively, which were higher than the long-term average. The average rainfall in 2015 and 2016 in months when broomcorn was grown well below the long-term average, but humidity was high (Table 1).

RESULTS AND DISCUSSION

The mean values of thecharacteristics for 6 broomcorn genotypes, Plant length, Leaf length, Leaf width, Panicle length, Panicle weight, Panicle seed weight and 1000 seeds weight are presented in Tables 2, 3 and respectively, and the relationships between characteristics are given in Table 4.

Plant height. According to the result ofthevariance analysis ontheplant height values of the broomcorn genotypes in the study, the genotype and year × genotype interaction was statistically significant at the level of 0.01. Total rainfall during the broomcorn growth season in the year 2015 was more than 1.6 times the total rainfall in 2016, and this caused significant differences in plant height. The mean plant height changed in the range of 182.10-154.50 cm among the genotypes (Table 2). Arslangiray [2] compared height and yield values for eight different plant species, including corn, sorghum, sudangrass, sorghum-sudangrass hybrids and broomcorn, among the second crop conditions in the Cukurova region. The researcher reported that sudangrass was the tallest (277 cm) plant in comparison tobroomcorn (261 cm). Geren and Kavut [9], between the years 2006 and 2007, used corn, sorghum, sudangrass, sorghum-sudangrass hybrid and broomcorn as their material and reported that plant height of these broomcorn varieties was in the range of 257.1-258.0 in. These results were differrent from thouse in our study. The highest plant height was obtained from Genotype-6 in both years of the experiment. The shortest plant height was detected in Genotype-2 in the second year of the experiment. Genotype-6 had the tallest plant in both years. Annual climate change did not affect this genotype. Therefore, the genotype is regarded as a stable genotype in terms of plant height.

Leaf length. According to the variance analysis results, the leaf length year × genotype interaction was significantat the level of0.01 level. Leaf length ranged from 7.42 to 6.13 mm based on genotype (Table2). The longest leaf length was obtained at 7.42 mm in Genotype-2 in both years. The shortest leaf length was 6.13 mm in 2015 in Genotype-3. Leaf length is a characteristic that varies based on genetics [4]. Leaf length is also affected by environmental conditions and it particularly decreases plant density [14].

Leaf width. As a result of the leaf width variance analysis, there was no statistically significant difference between the years, but there was a significant difference at the level of 0.01 among the genotypes. Genotype-1 had the maximum leaf width of 8.12 mm and Genotype-5 had the minimum leaf width of 5.57 mm. The plant has a broad leaf structure, so much that it has a direct impact on yield. Larger-leaved genotypes are do more photosynthesis than other genotypes and this causes higher performance. Therefore, leaf width has an important role in the genotypes preferred for yield.

TABLE 2
Duncan analysis in local genotypes for plant height, leaf length, leaf width and panicle length.

Genotypes	Plant Height (cm)			Leaf Length (mm)			Leaf Width (mm)			Panicle Length (cm)		
	2015	2016	Average	2015	2016	Average	2015	2016	Average	2015	2016	Average
Genotyp-1	175.40 b	178.40 ab	176.90 B	7.24 ab	7.10 ab	7.17 A	7.97	8.28	8.12 A	76.61 ab	77.25 a	76.93 A
Genotyp-2	158.70 de	154.50 e	156.60 F	7.42 a	7.42 a	7.42 A	7.62	7.25	7.43 B	74.42 bcd	74.19 bcd	74.31 B
Genotyp-3	160.40 d	161.10 d	160.70 E	6.13 e	6.67 cd	6.40 B	6.02	6.44	6.23 CD	72.64 cd	73.81 cd	73.22 B
Genotyp-4	175.80 b	170.30 c	173.00 C	6.39 de	6.64 cd	6.51 B	6.36	6.67	6.52 C	73.08 cd	75.25 abc	74.17 B
Genotyp-5	168.50 c	170.30 c	169.40 D	6.31 de	6.51 cde	6.41 B	5.57	5.57	5.57 D	74.31 bcd	74.53 bcd	74.42 B
Genotyp-6	182.10 a	181.20 a	181.60 A	6.27 de	6.89 bc	6.58 B	5.70	5.66	5.68 D	72.06 d	68.55 e	70.31 C
Mean	170.12	169.30		6.62	6.87		6.54	6.65		73.85	73.93	
LSD (1%)	4.532		3.205	0.3887		0.2749			0.6632	2.469		1.746

TABLE 3
Duncan analysis in local genotypes for panicle weight, panicle seed weight and 1000 seeds weight.

Genotypes	Panicle Weight (gr)			Panicle Seed Weight (gr)			1000 Seeds Weight		
	2015	2016	Average	2015	2016	Average	2015	2016	Average
Genotyp-1	72.97 abc	74.08 abc	73.53 B	34.91	35.92	35.42 A	20.55	20.11	20.33 A
Genotyp-2	76.67 ab	77.28 a	76.97 A	34.33	36.11	35.22 A	17.27	19.08	18.18 B
Genotyp-3	66.56 efg	72.36 bcd	69.46 C	33.27	34.81	34.04 AB	16.39	16.83	16.61 C
Genotyp-4	70.67 cde	72.17 bcd	71.42 BC	32.92	33.36	33.14 B	15.72	16.55	16.14 C
Genotyp-5	62.56 g	64.67 fg	63.61 D	32.14	33.44	32.79 BC	16.41	17.16	16.79 C
Genotyp-6	68.14 def	63.67 fg	65.90 D	31.64	30.83	31.24 C	16.64	16.72	16.68 C
Mean	69.59	70.70		33.20	34.07		17.16	17.74	
LSD (1%)	4.316		3.052			1.785			1.268

TABLE 4
Correlation coefficients among the characteristics of the broomcorn genotypes.

	Plant Height	Leaf Length	Panicle Length	Panicle Weight	Leaf Width	Panicle Seed Weight
Leaf Length	-0.255	1				
Panicle Length	-0.189	0.460	1			
Panicle Weight	-0.439	0.828*	0.487	1		
Leaf Width	-0.156	0.845*	0.736	0.874*	1	
Panicle Seed Weight	-0.547	0.719	0.812*	0.812*	0.878*	1
1000 Seeds Weight	0.073	0.780	0.694	0.551	0.862*	0.725

*(P≤0.05)

Panicle length. There are significant differences among punicule species of sorghum [1, 18]. The length of the panicle is a particularly important morphological factor for broomcorn. This is because, for a good broomcorn speciment, there should be a high number of branches of the panicle, uniform distribution, flexibility and the dimensions should be about 50.8 cm [6, 10]. In the study, significant differences in panicle length were found at the level of 0.01 in terms of genotype and year × genotype interactions. The longest panicle length was 77.25 cm and the shortest was 68.55 cm, which were obtained from Genotype-1 and Genotype-6 respectively in 2016 (Table 2). In the study by Deepakkumar Shinde [7], panicle length had a direct and positive (0.009) effect on grain yield on the genotypic level, while it had a direct and negative (-0.002) effect on the phenotypic level at Dharwad. In parallel to these results, Patel [17] reported a positive indirect effect on grain yield and and Ivanar [12] reported a positive direct effect on grain yield.

Panicle weight. Variance analysis of panicle weight revealed significant differences at the level of 0.01 in the genotypes and year × genotype interaction. Panicle weights in the year × genotype interaction changed between 62.56 and 77.28 g (Table 3). The highest panicle weight was found in Genotype-2 in 2016 and the lowest was found in Genotype-5 in 2015. The difference among the genotypes between the years may be explained by more rainfall in 2016 than in 2015.

Panicle seed weight. In the variance analysis of panicula grain weight and theyear × genotype interaction, statistically significant differences were found at the level of 0.01 level. Panicle grain weight varied in the range of 31.24-35.42 g in the year × genotype interaction (Table 3). The highest paniclegrain weight was found in Genotype-1 and the lowest was in Genotype-6.

1000 seeds weight. In the analysis of variance for 1000 seeds weights, statistically significant differences were found at the level of 0.01 in the year × genotype interaction.1000 seeds weight in the year × genotype interaction changed between 16.14 and 20.33 g (Table 3). The highest 1000 seeds weight was found in Genotype-1 and the lowest was in Genotype-4.

The correlation between characteristics. It is important to know the correlation between plant characteristics and characteristics of genotypes on the basis of breeding studies. For this purpose, a correlation analysis was performed for some characteristics. The results may be summarized as follows: Correlation coefficients between leaf length and panicle weight (r = 0.828*) and between leaf length and leaf width (r = 0.845*) were significant and positive (Table 4). Panicle length and panicle seed weight (r = 0.812*), panicle weight and leaf width (r = 0.874*) andpanicle weight and panicle seed weight (r = 0.812*) had positive and significant correlations. Leaf width and panicle seed weight (r = 0.878*), and leaf witdth and 1000 seeds weight (r = 0.862*) had positive and significant correlations. Zheng [21], in their their study in 2005, used the millet varieties of Xiagu 2, Hongtuigu, Jiugenqi, Shuanglugu, Datong 14, Huangruangu, Jingu 20, Jingu 21, Jingu 22, Jingu 27, Jingu 32, Jingu 33, Jingu 35, Yugu 9, Daligu to study the correlations between the main agronomic

characteristics of millet. Their results showed that the period of vegetative growth of millet, the seed weight of a spike, the area of the third leaf near the spike, the weight of a spike, the area of the second leaf near the spike had highly significant postive correlations with growth season. Spike weight, spike degree of thickness, the area of the second leaf and the area of the third leaf near the ear had highly significant positive correlations with the seed weight of a spike. The degree of spike thickness, the area of the second leaf near the spike, growth season, the period of vegetative growth of millet, the area of the third leaf near the spike hadhighly significant positive correlations with the weight of a spike. On the other hand, spike length had a significant negative correlation with the weight of a spike. All biological characteristics except plant height had a positive correlation with the others. For millet breeding, varities with a larger area of the second leaf near the spike, longer growth season, bigger seed weight of a spike, shorter and thicker spike should be used. The results are consistent with those in our study.

This study was conducted to identify promising genotypes and provide materials for further breeding studies by evaluating the agronomic characteristics of broomcorn genotypes traditionally grown in Adapazarı and its vicinity. Six village genotypes grown at different locations were used as material and the study was conducted in 2015 and 2016. In the study, plant height of the genotypes ranged from 182.10 to 154.50 cm. The tallest plant height was found in Genotype-6. The longest panicle length was in Genotype-1, while the highest panicle weight was in Genotype-5. Panicle length and panicle weight are important morphological characteristics, especially for broomcorn production. Therefore, Genotype-1 and Genotype-5 were found to be promising genotypes for broomcorn production.

CONCLUSIONS

As a result of the study, the highest panicle seed weight and 1000 seeds weight were obtain in Genotype-1. Panicle seed weight and 1000 seeds weight are important characteristics for grain production. This is the reason why Genotype-1 is a promising genotype for usage as feed.

REFERENCES

[1] Açıkgöz, E. (1991) Yembitkileri. Uludağ Universitesi, Ziraat FakültesiYayınları, 1, Bursa, 633p.

[2] Arslangiray, C., Tansı, V. ve Sağlamtimur, T. (1991) Çukurova Koşullarında II. Urün Olarak Yetiştirilen Mısır (*Zea mays* L.) ve Sorgum (*Sorghum sp*.) Tür ve Çeşitlerinin Gelişme Dönemlerine Göre Biyolojik Uretimlerinin Saptanması Uzerinde Bir Araştırma. Türkiye 2. Çayır Mera ve Yembitkileri Kongresi. 28-31 May 1991, İzmir. 369-378.

[3] Balkan, A. and Gençtan, T. (2008) Trakya Bölgesi'nde Yetiştirilen Süpürge Darısı (*Sorghumbicolor* (L.) Moench var. technicum (Körn.) Genotiplerinin Bazı Agronomik Özellikler Yönünden Değerlendirilmesi. Ankara Üniversitesi Ziraat Fakültesi Tarım Bilimleri Dergisi. 14(2), Ankara. 163-168.

[4] Burnside, O.C., Franster, C.R. and Wicks, G.A. (1964) Influence of Tillage, Row Spacing and Atracine on Yield Components of Dryland Sorghum in Nebraska. Agr. Jou. 56, 397-400.

[5] Campbell, I.G., Casady, A.J. and Crook, W.J. (1974) Effects of a Single Height Gene (DW3 of Sorghum on Certain Agronomic Characters. Crop Science Society of America. 15(4), 595-597.

[6] Carter, P.R., Hicks, D.R., Kaminski, A.R., Doll, J.D., Kelling, K.A. and Worf, G.L. (1990) Extension. Alternative Field Crops Manual.

[7] Deepakkumar Shinde, G., Biradar, B.D., Deshpande, S.K., Salimath, P.M., Kamatar, M.Y., Gayatree, G., Hiremath, P. (2011) Character association and path coefficient analysis among the derived lines of B × B, B × R and R × R crosses for productivity traits in rabi sorghum (*Sorghumbicolor* (L.) Moench). Electronic Journal of Plant Breeding. ISSN 0975-928X. 2(2), 209- 217.

[8] FAO (1995) Sorghum and Millets in Human Nutrition. FAO Food and Nutrition Series. No. 27, ISBN 92-5-103381-1.

[9] Geren, H. and Kavut, T. (2009) İkinci Ürün Koşullarında Yetiştirilen Bazı Sorgum (*Sorghumsp*.) Türlerinin Mısır (*Zea mays* L.) ile Verim ve Silaj Kalitesi Yönünden Karşılaştırılması Üzerine Bir Araştırma. Ege Üniv. Ziraat Fak. Derg. ISSN 1018 – 8851. 46(1), 9-16.

[10] Gürtanın, N. (1977) Süpürge Darısından (*Sorghum technicus*) Yararlanma Olanakları, Edirne'de Süpürge Sanatı ve Bu Sanatın Ekonomik Onemi. Türk Halk Bilim Araştırmaları Yıllığı, Kültür Bakanlığı, Yay. No:28, Ankara,103-117.

[11] Imik, H., Şeker, E. (1999) Farklı Tanen Kaynaklarının Tiftik Keçilerinde Yem Tüketimi, Canlı Ağırlık Artışı, Tiftik Verimi ve Kalitesi Uzerine Etkisi. Lalahan Hayvancılık Araştırma Enstitüsü Dergisi. 39(1), 85-100.
[12] Ivanar, K., Aapalan, A. and Ramasamy, P. (2001) Correlation and path analysis in sorghum. Annals of Agril. Res. 22, 495-497.
[13] Kaiser, C. and Ernst, M. (2013) Broomcorn. Cooperative Extension Service University of Kentucky College of Agriculture, Food and Environment. Center for Crop Diversification Crop Profile.
[14] Kün, E. (1985) Sıcak Iklim Tahılları. Ders Notları, Ankara Uni. Z.F. Yayın. 953- 276.
[15] Nevens, W.B. and Harshbarger, K.E. (1940) Broomcorn silage for dairly cattle. Illinois Agricultural Experiment Station, Urbana, Illinois, 1023-1029.
[16] Osman, E.I and Mohamed, M.A. (1992) Improved Sorghum Genotypes Suitable for Irrigation and Rain Fed Lands of Sudan. Proceedings of Sudan National Variety Release Committee. ARC, Wad Medani, Sudan.
[17] Patel, R.H., Desai, K.B., Raj, K.R.V. and Parikh, R.K. (1980) Estimates of heritability and genetic advance and other genetic parameters in an F2 populations of sorghum. Sorghum Newslr. 23, 22-23.
[18] Sağlamtimur, T., Tansı, V., Baytekin H. (1990) Yembitkileri Yetiştirme. Ç.Ü. Zir. Fak. Adana, 74.
[19] Swanson, A.F. and Laude, H.H. (1934) Varieties of Sorghum in Kansas. Agricultural Experiment Station, Kansas State College of Agriculture and Applied Science.
[20] UNESCO. (1983) Kırsal Kesim, UNESCO'dan GÖRÜŞ, Arkın Yayınları, 6, İstanbul.
[21] Zheng, X.Y. and Jin-Yun, W.U. (2005) Analysis for Correlation between Main Traits of Millet. Gansu Agricultural Science and Technology. 515.

Received: **20.12.2017**
Accepted: **04.04.2018**

CORRESPONDING AUTHOR

Serap Kizil-Aydemir
Department of Field Crop,
Faculty of Agriculture and Science,
Bilecik ŞeyhEdebali University,
Bilecik – Turkey

e-mail: serap.kizil@bilecik.edu.tr

© by PSP Volume 27 – No. 7/2018 pages 4844-4856 Fresenius Environmental Bulletin

IMMOBILIZATION OF POLYPHENOL OXIDASE ENZYME ON NEW MATRIX ANTIMONY DOPED TIN OXIDE (SnO_2:Sb) THIN FILM

Ayse Turkhan[1,2,*], Ozlem Faiz[1], Elif Duygu Kaya[3], Adem Kocyigit[4]

[1]Recep Tayyip Erdogan University, Department of Chemistry, 53100, Rize, Turkey
[2]Igdir University, Research Laboratory Application and Research Center, 76000, Igdir, Turkey
[3]Igdir University, Engineering Faculty, Food Engineering, 76000, Igdir, Turkey
[4]Igdir University, Engineering Faculty, Electrical Electronic Engineering, 76000, Igdir, Turkey

ABSTRACT

Polyphenol oxidase enzymes (PPOs) obtained from Agseftali (*Prunus persica* L.), which was native peach genotypes under Igdir province ecological condition in Turkey, was purified by affinity chromatography and then, PPOs immobilized on new matrix antimony doped tin oxide (SnO_2:Sb) thin films by adsorption method for the first time. In here, the films were synthesized by spray pyrolysis technique in laboratory condition, easily. The immobilization of PPOs onto SnO_2:Sb thin films was confirmed by scanning electron microscopy (SEM) and fourier transform infrared spectroscopy (FTIR). Obtained free and immobilized PPOs onto thin film were compared according to some enzyme optimization points such as optimum pH and temperature. The optimum pH of the free and immobilized PPOs was found as 6.0. The optimum temperature of PPOs increased from 20°C to 30°C with immobilization on the thin film. *K*m values of the free and immobilized enzymes were obtained as 2 mM and 1.4 mM, respectively. L-Tyrosine oxidation of the enzymes enhanced with immobilization of PPOs onto SnO_2:Sb thin films. The immobilization on SnO_2:Sb thin films aslo provided to increase the satibilty and life time of the PPOs because they could be used 3 times and retained approximately 50% of activity following 18 repeated usage in a 15 days. The PPOs can be thougt as an activist towards 4-methylcatechol substrate and, the usability of the enzymes can be significantly increased via immobilization onto SnO_2:Sb thin films.

KEYWORDS:
Polyphenol oxidase, purification, SnO_2:Sb thin film, immobilization

INTRODUCTION

Enzymes are biocatalysts with high specificity, high catalytic efficiency and bio-degradability and, hence they can be used major application in industrial applications and medical sciences since they increase the rate of chemical reaction by lowering of the activation energy [1]. When the enzymes are immobilized by some processes, they have many advantages as commercial [2]. Immobilzed enyzmes have high stability than free enzymes and, they can be easily separated from the reaction mixture, used repeatedly and continuously and so, the enzyme consumption is considerably reduced [3-4].

The enzyme immobilization materials are important for industrial processes and, the industry needs to alternative immobilization materials. Conductive metal oxides including TiO_2 [5-6], SnO_2 [7-9], ZnO [10-11] and tin doped indium oxide (ITO) [9, 12-16] have growing interest for enzyme immobilization [17-19]. In contrast to metallic or carbonaceous electrode materials, the high amount of oxygen functionalities on the metal oxide surface provides a protein-friendly environment [9]. Among the available conductive metal oxides, tin doped indium oxide (ITO) is the most widely used for the enzyme immobilizations [20], but indium is expensive and has limited availability in the nature [9]. Thus, beside the attempt to decrease the In/Sn molar ratio in novel types of ITOs [21], SnO_2-based conductive oxides have presented as promising alternatives [22-23]. Since the SnO_2 is a n-type semiconductor with a wide band gap energy (3.6 eV at 300 K), it can be used for various applications such as solar cells, electrochemistry sensors and biosensor [24]. In particular, antimony-doped tin oxide (ATO) is a very promising alternative due to high surface area, nontoxicity, good biocompatibility, catalytic activity and chemical stability [24]. To preparation of tin oxide thin films, some techniques such as spray pyrolysis [25], spin coating [26], chemical vapor deposistion [27] etc. have been performed by researchers. Among them, spray pyrolysis is a simple and inexpensive method for

doped or undoped tin oxide thin film deposition [28].

Polyphenol oxidase enzymes (PPOs; tyrosinase, catechol oxidase), (E.C. 1.14.18.1) are a copper containing metalloenzyme and, they are notably found in plants, fungi and some bacterial strains [29-30]. PPOs execute two different activites: first one is to serve for the hydroxylation reaction which transforms monophenols to o-diphenols (monophenolase activity) and, second activity is the oxidation reaction which transforms o-diphenols to o-quinones (diphenolase activity). At the end of the second activity, reaction products are polymerized to brown, red, or black pigments [31]. Because of these properties, PPOs can find extensive application in the field of biosensors [32], waste water treatment for removal of toxic compounds [33] and production of L-DOPA [34].

For immobilization of PPOs, various materials such as ZnO Nanorods [35], conducting polymer reduced with graphene oxide–metal oxide [36], graphite electrodes [37] were used. However, ATO has been only rarely employed in combination with biomolecules [38-39] and only a few reports exist for proteins [9, 40-41]. As far as we know, the immobilization of Agseftali PPOs on SnO_2:Sb thin film has not been reported in the literature. The main aims of this study are to purificate of polyphenol oxidase from Agseftali (Igdir province in Turkey ecological condition), to prepare a new matrix for the immobilization and to compare its optimum conditions before and after immobilization for the industrial treatments.

EXPERIMENTAL SECTION

Materials. Agseftali were picked from a native garden in the city of Igdir in Turkey and stored frozen at -20°C for experiments. All chemicals used in the study were purchased from Sigma Chemical Co. (St. Louis, MO) and Merck Millipore (Darmstadt, FRG). CNBr activated-Sepharose-4B was selected as a column matrix. *L*-tyrosine and *p*-amino benzoic acid were used as a spacer arm and ligand, respectively. An affinity gel used in this study was synthesized according to the method Arslan et al. 2004 [42].

Enzyme purification. A 25 g frozen Agseftali was grounded and homogenised in 50 mM of sodium acetate (pH 5.0) buffer solution which was containing 1% (w/v) polyethylene glycol (PEG) in a porcelain mortar [43]. It was filtered through muslin cloth (folded 4 times) and centrifuged for 30 minutes at 10000 rpm at 4°C. Supernatant of Agseftali was used as a crude enzyme extract. Cold acetone, which was equal to the volume of the supernatant acquired, was added to the crude enzyme extract and kept in an ice bath overnight at 4°C. The supernatant was also centrifuged at 10000 rpm for 30 minutes at 4°C. The precipitate of the extract was redissolved in a convenient volume of 50 mM acetate buffer (pH 5.0) solution [44]. Purified with the affinity column (Sepharose 4B-*L*-tyrosine-*p*-amino benzoic acid) was synthesized by Arslan et al [42] and concentrated via ultrafiltration (Ultracell Membrane 10,000 MWCO Millipore, Amicon, USA).

The protein concentration was determined according to Bradford's method using bovine serum albumin as a standard [45]. Polyacrylamide gel electrophoresis (PAGE) of the enzyme was performed according to the method of Laemmli (1970) (Bio-Rad Laboratories, Inc.) [46].

Determination of PPOs activity, substrate specificity and enzyme kinetics. PPOs activity was monitored spectrophotometrically at 494 nm for 4-methylcatechol and catechol, at 500 nm *L*-tyrosine and for the other substrates [47]. The assay was performed with substrate solution (stock 100 mM catechol, 100 µl). Equal volume of 3-methyl-2-benzothiazolinone hydrazone hydrochloride hydrate (stock 10 mM, 100 µl) and 20 µl dimethylformamide (original bottle) were diluted to 900 µl with 50 mM acetat buffer at pH 5.0 and then, 100 µl enzyme solution was added to the buffer. The reference cuvette was included all the reactantas outside enzyme (Spectrophotometer agilent cary 60 was used). One unit of PPO activity was defined as the amount of enzyme causing 0.001 increase of absorbance per minute in 1 mL of reaction mixture. Specific activity of PPO was calculated by enzyme activity per milligram of protein [48].

As to the activity of immobilized PPOs, it was calculated according to the surface area of support. The active units per surface area of support (A) is defined as:

$A(U/cm^2) = Uact/Acm^2$

where Uact is the activity of immobilized enzyme, Acm^2 is the surface area of support (cm^2).

One unit of immobilized PPOs activity was defined as the enzyme amount of per centimeter causing 0.001 increase of absorbance per minute in 1 mL of reaction mixture.

PPOs substrate specificity was assayed by three substrates; 4-methylcatechol, catechol and *L*-tyrosine. Activity of the enzymes were calculeted as a percent relative activity with respect to maximum activity (100%) [48].

The kinetic parameters of PPOs were obtained by measuring the rate of at various substrate concentrations ranging from 0.5 to 10 mM in the standard reaction mixture (at optimum conditions). The Michaelis–Menten constant (*K*m) and maximum velocity (*V*max) parameters were determined from Lineweaver–Burk plots [49].

SnO_2:Sb thin films preparation. To prepare

the thin film gel, 8.370 g $SnCl_2.2H_2O$ and 0.278 g $SbCl_3$ were added to 120 mL and 20 mL absolute ethanol in different vessels, respectively. These vessels were stirred separately on a magnetic stirrer for an hour at 80°C. Afterwards, the two solutions were mixed in one vessel and stirred for an hour again at 80°C. Finally, the clear homogenous gel was obtained [50].

Microscopic glasses (10 mm × 10 mm × 1 mm) were used as substrates. The substrates were cleaned an ultrasonic cleaner and then dried. The obtained gel solution was sprayed onto 270°C pre-heated substre using a perfume atomizer [51]. The substrate-nozzle distances were kept at 60 cm during all experiments. Finally, all films were annealed in a furnace for an hour at 500°C.

Immobilization of PPO onto SnO_2:Sb thin films by adsorption method. Immobilization of Agseftali PPOs onto SnO_2:Sb thin films was achieved by exposing the thin layers to the enzyme solutions. After overnight exposure of the thin films to the enzyme solution at 4°C, the samples were rinsed 3 times with pH 5.0 acetate buffer (50 mM) to remove any unbound proteins. The efficiency of immobilization was evaluated in terms of immobilization yield as shown below:

Immobilization yield (%) = (A - B) / A × 100

where A is the activity of PPOs added to the initial immobilization solution and, B is the total activity of the residual PPOs in the immobilization and washing solution after the immobilization procedure [52].

Characterization of enzyme immobilization on thin film surface. The surface morphology of the thin films before and after PPOs immobilization were analysed using scanning electron microscopy (SEM) (ZEISS, EVO LS10) and Fourier transform infrared (FT-IR) spectra, which is (Perkin Elmer) in the range of 650–4000 cm^{-1} at room temperature.

Optimum pH and pH stability of enzymes. The effect of pH on free and immobilized PPOs activity were examined using 50 mM glycine-HCI (pH 2.0 and pH 3.0), 50 mM sodium acetate (pH 4.0 and pH 5.0), 50 mM phosphate (pH 6.0 and pH 7.0) and 50 mM Tris-HCI (pH 8.0 and pH 9.0) buffers (under optimum conditions). The maximum activity was accepted as 100%, and the relative activities were calculated by comparing with it [48]. The pH stability of the free and immobilized PPOs activity were determined by incubating the protein in the above-mentioned buffers at 4°C for 24 hours. The percentage residual enzyme activities were calculated through comparison with non-incubated enzyme [48].

Optimum temperature and thermal stability of enzymes. The optimum temperatures were determined various temperatures in the range of 0–70°C, in the presence of suitable substrate. The results were expressed as the percentage of relative activity [48]. The thermal stabilities were measured by incubating the free and immobilized PPOs at various temperatures between 20°C and 70°C in a water bath for 15, 30, 45 and 60 minutes, then samples were rapidly cooled to the room temperature. The percentage residual enzyme activities were calculated through comparison with non-incubated enzymes [42].

Storage stability and reusability of immobilized PPOs. The storage stability at 4°C of the immobilized PPOs was investigated over a period of 15 days [53]. Immobilized PPOs based on repeated use were investigated by measuring the enzyme activity after each successive run. After each reaction with the substrate, the immobilized PPOs were washed with a phosphate buffer (50 mM, pH 6.0) and put into fresh substrate to restart the reaction [54].

RESULTS AND DISCUSSION

Enzyme purification. PPOs from the Agseftali were successfully purified 85.15-fold (Table 1) by the Sepharose 4B-L-tyrosine-p-amino benzoic acid affinity column. The amount of proteins was determined spectrophotometrically at 280 nm and, PPOs activity was analyzed for all fractions (Fig. 1). The peak with the highest protein content and maximum PPOs activity were separated and collected for further studies. Using the same affinity column, PPOs have previously been purified from *Morus alba* L. [42], *Boletus erythropus* [55], *Lactarius piperatus* L. [56], *Ocimum basilicum* L. [57] and *Pyrus elaegrifolia* [58] with purification of between 11.5-fold and 74-fold.

Polyacry-lamide gel (8%) was prepared for native and sodium dodecylsulphate gel electrophoresis. The purity of the PPOs after purification was analysed by native PAGE (Fig. 2A) and SDS–PAGE (Fig. 2B). As shown in Fig. 2A, one prominent band could be observed when one side of the native gel was stained with Coomassie Brilliant Blue R-250. When the other side of the native gel was stained with L-DOPA (24 mM L-3,4-dihydroxyphenylalanine; L-DOPA), the activity was observed within the same protein band, verifying that the purified protein was the one with PPOs activity.

The electrophoretic pattern of the protein from SDS–PAGE revealed that the purified PPOs contained two dominant bands with molecular weights of 41.11 and 48.16 kDa. These results have suggested that the protein has at least two subunits of different molecular weights (Fig. 2B). The graph of Rf vs. log Mw is shown in Fig. 2C. Similar native

gel and SDS gel profiles have previously been reported for the *Malpighia glabara* L. PPO [59]. The molecular weight of PPOs obtained from SDS PAGE has been reported to be 32.5 kDa for chestnut PPOs [60] and 40.0 kDa for *Lactarius piperatus* PPOs [56].

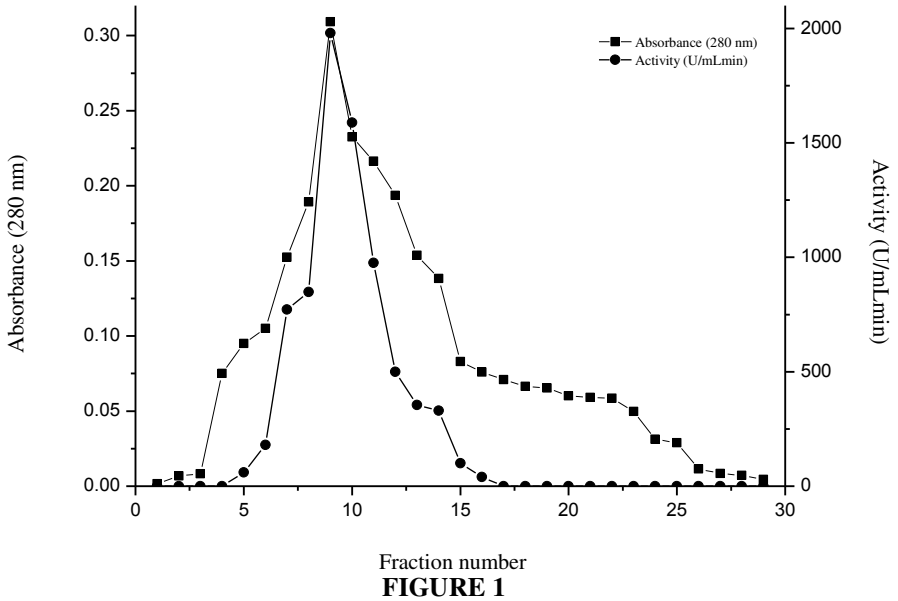

FIGURE 1
Purification of Agseftali (*Prunus persica* L.) PPO by affinity chromatography using 4B-L-tyrosine-p-amino benzoic acid.

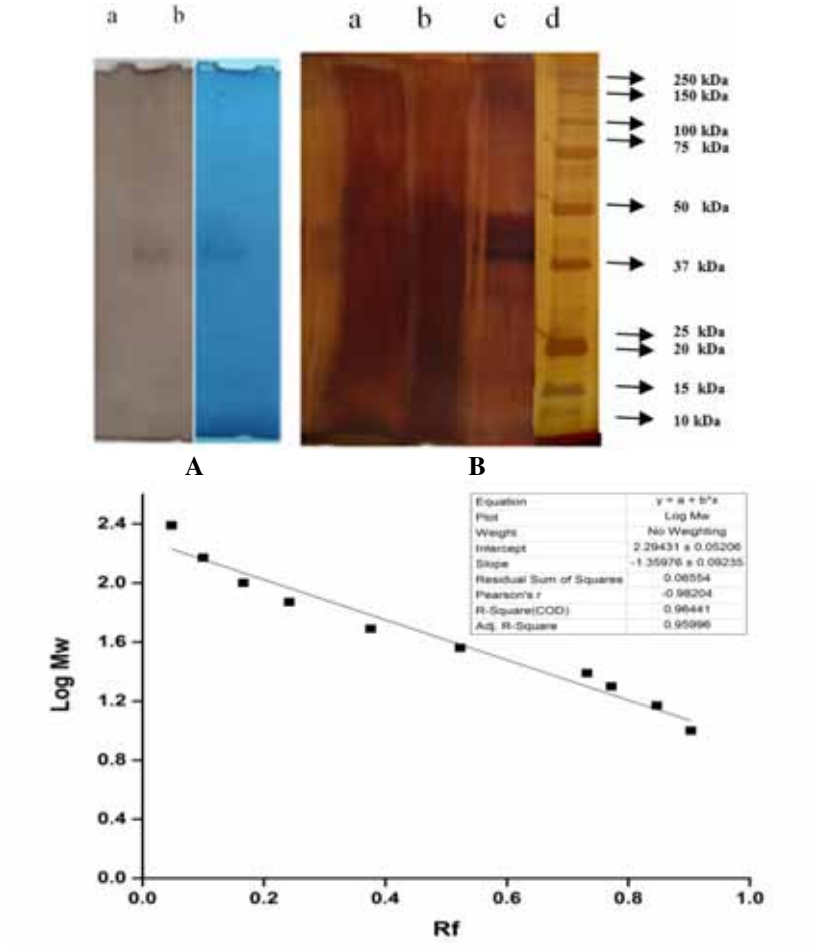

FIGURE 2
Native and SDS-gel electrophoresis of PPO from Agseftali (*Prunus persica* L.). A) Native electrophoresis of purified Agseftali (*Prunus persica* L.) PPO. a) Gel stained with 24 mM L-DOPA, b) Gel stained with

Coomassie Brillant Blue R-250. B) SDS-PAGE of purified Agseftali (*Prunus persica* L.) PPO. Gel was stained with silver. a) Crude extract, b) Acetone precitation, c) Prufied PPO, d) Molecular weight marker. 2C) Standart R_f vs. log Mw graph of PPO using the SDS-PAGE result

TABLE 1

Summary of purification of the polyphenol oxidase from Agseftali (*Prunus persica* L.)

Purification steps	Total activity	Protein (mg/mL)	Total protein (mg)	Specific activity (U/mg protein)	Yield (%)	Purification fold
Crude Extract	224000	3.74	187	1197.86	100.00	1
Acetone Precipitation	97200	0.49	4.9	19836.73	43.39	16.56
Affinity chromatography	8160	0.02	0.08	102000.00	3.64	85.15

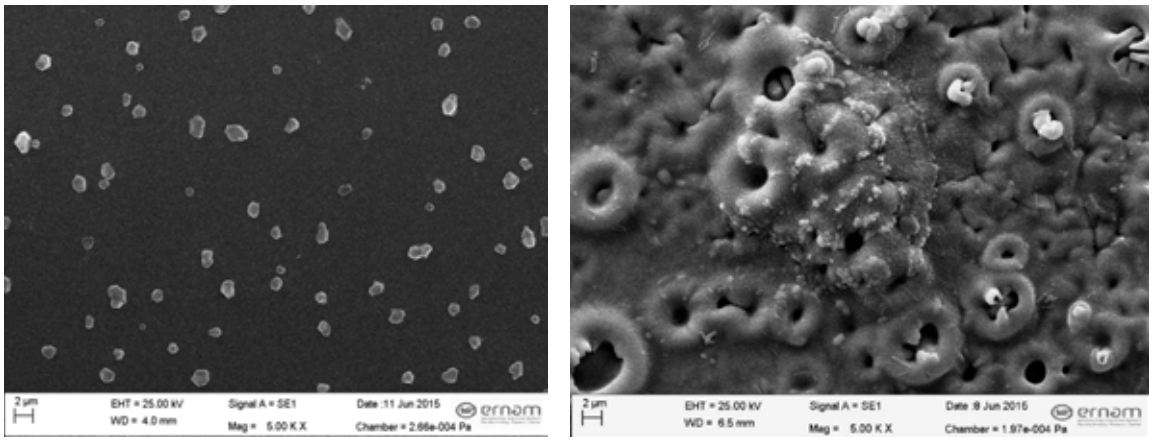

A **B**

FIGURE 3

SEM images of A) SnO_2: Sb thin film surface B) PPO immobilized SnO_2: Sb thin film

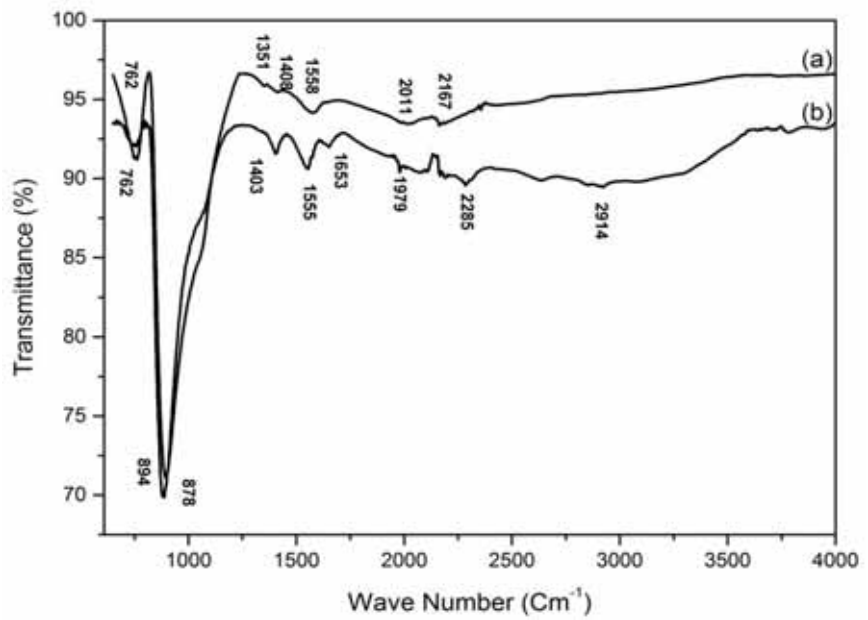

FIGURE 4

FTIR spectra of a) SnO_2:Sb thin film and b) PPO immobilized SnO_2:Sb thin film

Immobilization of polyphenol oxidase enzyme. Agseftali PPOs were immobilized on SnO_2:Sb thin films as 23.75% immobilization yield (As described in section 2.5). The surface structure of the thin films before and after immobilization were examined using a scanning electron microscope (SEM) with a magnification of 5000x. The surface morphologies of the thin films are completely different than after immobilization ones. The images have revelaed that the thin films is granular structure (Fig. 3A), and after immobilization, the granular structure of the thin films have disappeared and formed as spherical-like structure (Fig. 3B).

The FTIR spectras of the samples have been measured in the range of 650–4000 cm^{-1} and, they

are shown in Figs. 4a and 4b. The peaks at 762, 878 and ≈1408 cm^{-1} in Figs. 4a and 4b are assigned to the Sn-O-Sn, Sn-OH and SnO_2 lattice stretching vibrations, respectively [61]. In addition, the variable peaks between the 1558 and 2167 cm^{-1} wavenumbers correspond to the -OH groups of residual water and alcohol [62]. When Fig. 4a is compared with Fig. 4b, the broad band at 1558 cm^{-1} has disappeared and, sharp bands has appeared at 1555 and 1653 cm^{-1}. In Fig. 4b, the peaks at 1653 and 1555 cm^{-1} are assigned to the amide I band, which is associated with the C=O stretching vibration due to addition of protein molecules, and the amide II band resulted from N-H and C-N stretching of the protein backbone, respectively [63]. The broad peak at 2914 cm^{-1} can be attributed to the C-H stretching vibrations [1].

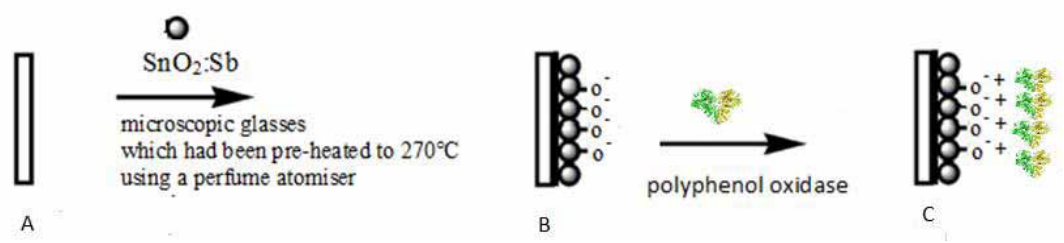

FIGURE 5
Schematic representation A) Microscopic glasses B) SnO_2:Sb thin film C) PPO immobilized SnO_2:Sb thin film

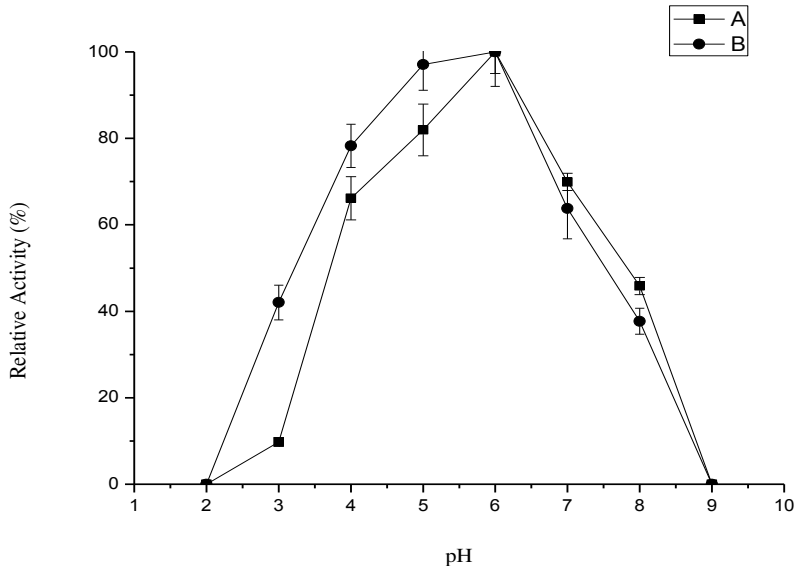

A

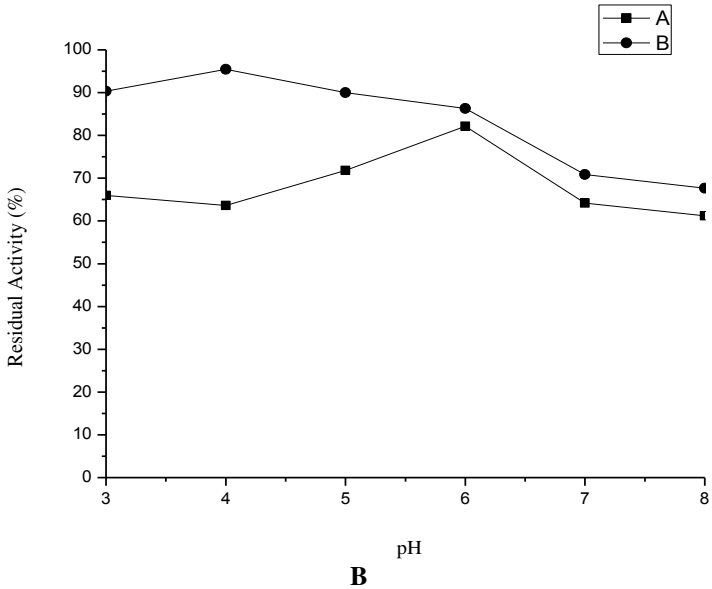

B

FIGURE 6
A) Effects of pH on the activity A) free and B) immobilized PPO B) The pH stability of A) free and B) immobilized PPO.

The peak broadening and shifting of the spectrum of SnO_2:Sb thin film with PPOs indicate that the internal environment is changed by the adsorption between PPOs and SnO_2:Sb thin films. Electrostatic, hydrophobic/hydrophilic and van der Waals forces interactions may be included in the attachment of protein to surfaces [64]. A schematic of the immobilization of PPOs is shown in Fig. 5.

Substrate specificity and enzyme kinetics. The free and immobilized PPOs were tested on different phenolic substrates such as 4-methylcatechol, catechol, *L*-tyrosine. The analyses were performed at pH 6.0 and 20°C for free enzyme, and at pH 6.0 and 30°C for immobilized enzyme.The highest activities were observed in the presence of 4-methylcatechol for free and immobilized enzymes (Table 2). The naturally occurring amino acid, 1-3,4-dihydroxy phenylalanine (L-DOPA) are a precursor of dopamine, which is a preferred drug for the remedyt of Parkinson's disease. L-DOPA can be produced from *L*-tyrosine using tyrosinase [65]. Therefore, the analysis of the tyrosinase activity of PPOs is important. In this study, we found that the relative *L*-tyrosine oxidation was enhanced by the immobilization procedure.

TABLE 2
Substrate specificities of the free and immobilized PPO of Agseftali (*Prunus persica* L.)

Substrate	Free PPO Relative activity (%)	Immobilized PPO Relative activity (%)
4-Methylcatechol	100.00	100.00
Catechol	75.70	79.72
L-Tyrosine	26.16	56.42

The substrate saturation curve for 4-methylcatechol suggests that the free and immobilized PPOs follow the simple Michaelis–Menten kinetics. *K*m and *V*max values for each activity of PPO were determined from the linear regression analysis of 1/V versus 1/[S]. The *K*m values of the free and immobilized enzymes are 2 mM and 1.4 mM, respectively. When the *V*max value the free enzymes is 100,000 U/mg protein, for immobilized enzymes, the *V*max values are 27.78 U/cm^2 and 14285.71 U/mg protein when calculated per square centimetre protein.

Effects of pH and temperature on PPOs activity and stability. The effect of pH on the free and immobilized PPOs activities were examined at different pH values between 2.0 and 9.0 with 4-methylcatechol as a substrate, using the 50 mM buffer system as described above. The PPOs activity of both the free and immobilized PPOs has been found to be the highest at pH 6.0 (Fig. 6A). The immobilized PPOs are retain greater activity at an acidic pH when compared to the soluble enzymes. This result is matched with the result of a study which investigated the immobilization of Solanum tuberosum PPOs on Celite 545 [66].

In addition, as shown in Fig. 6B, the behaviour of the immobilized enzymes were different from that of the free enzyme after incubation at various pH values between 3.0 and 8.0 for 24 hours. Despite there is no change in optimum pH values, when the enzymes have immobilized on the thin film, they have exhibited a much higher pH resistance than the free enzymes, especially in acidic conditions.

We investigated the effect of temperature on the activity of the free and immobilized PPOs within the 0–70°C temperature ranges. The optimum temperatures for the free and immobilized PPOs were found as 20°C and 30°C, respectively (Fig. 7A). A dramatic decrease in relative activity suggests that the free PPOs were sensitive above 20°C temperatures. However, the immobilized enzymes have showed broadening in temperature-activity profile when compared to the unimmobilized enzymes (Fig. 7A). Unlike the soluble enzymes, the immobilized enzymes retain significantly higher enzyme activity at higher temperatures. The immobilized PPOs have relatively more tolerance to temperatures between 30–70°C (Fig. 7A). These results have indicated that the usability of the PPOs at temperatures above 20°C can be improved by the immobilization. The binding of the enzymes to a matrix can make it more resistant to the denaturing effect of heat.

The activities of the free and immobilized PPOs were retained after a 60 minutes incubation between 20 and 40°C (data does not shown here). The thermal stability of the immobilized PPOs is more superior than the free PPOs between 50 and 70°C (Fig. 7B). At 70°C, the free PPOs have completely lost its initial activity, whereas the immobilized PPOs have retained approximately 20%, 19% and 16% of its initial activity after 30, 45 and 60 minute incubations, respectively. The higher thermal stability of immobilized PPOs can be attributed to the stabilisation of the enzymes via the prevention of conformational denaturation at high temperatures. These results are good aggrement with Forde et al. [67] and Xu et al. [68], who reported that the immobilization process induced a 10–15% greater activity within the tested temperature range. It has been reported that immobilized enzymes may have a higher thermal stability, which is connected

to the reduction of its conformational flexibility [69].

Storage stability and reusability of the immobilized PPO. Storage stability is one of the most important parameters for enzyme immobilization. The activity of the immobilized PPOs was determined following storage in a phosphate buffer (50 mM, pH 6.0) at 4°C every day for a period of 15 days (Fig. 8A). The results have showed that the immobilized PPOs have retained 59.13% of its initial activity after being stored for 15 days. The redisponibility of an enzymes are especially critical for industrial applications. The reusability of the immobilized enzymes have been displayed in Fig. 8B. We observed that the enzyme maintained 80.56% of its initial activity after each subsequent use, and had lost approximately 50% of its activity after being used 18 times. This results have implied that reusility in this study is higher than results reported for the potato PPOs immobilization on the tentacle carrier. The activity of the immobilized potato PPOs on the tentacle carrier reduced to 55% after six repeated tests [70].

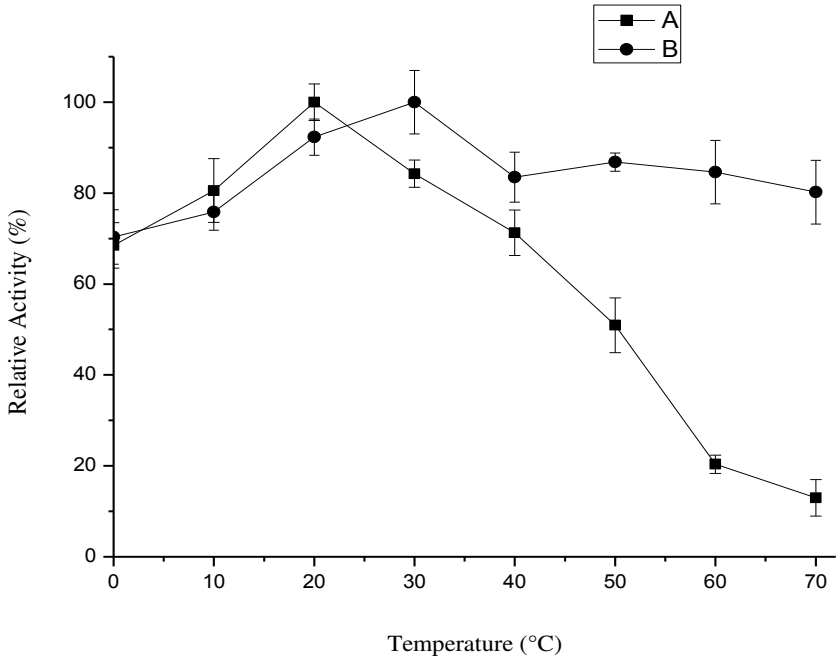

A

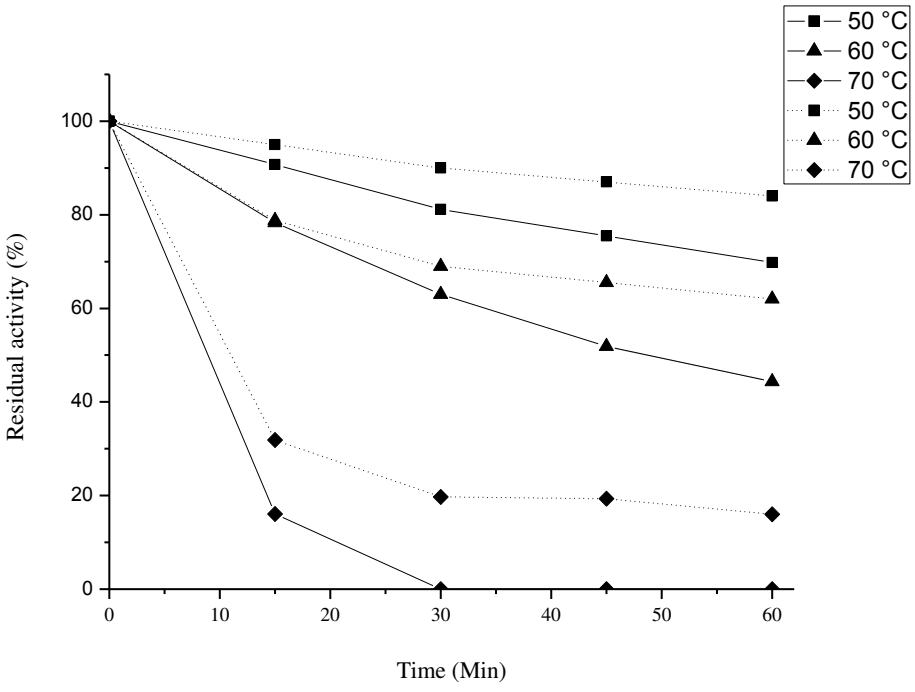

B

FIGURE 7

A) Effects of temparature on the activity A) of free and B) immobilized PPO. B) Thermal stability of free (straight line) and immobilized PPO (dotted line).

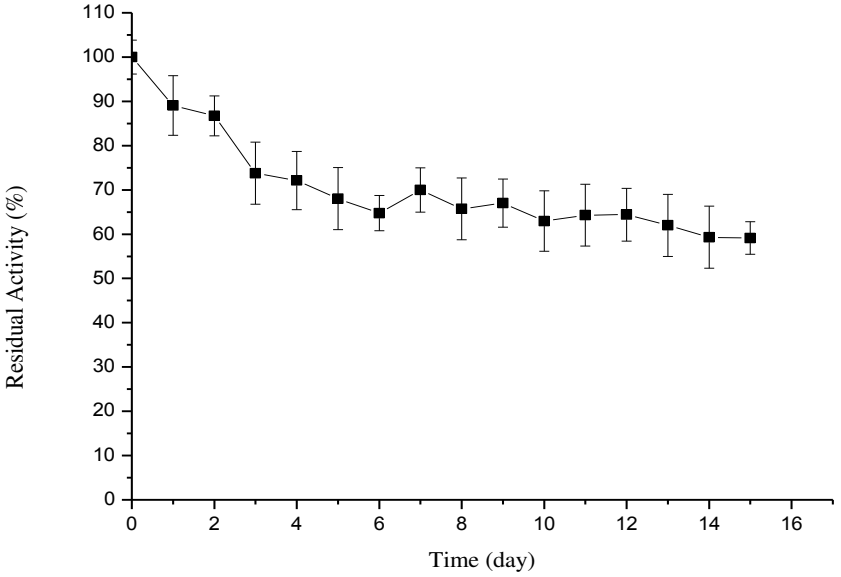

A

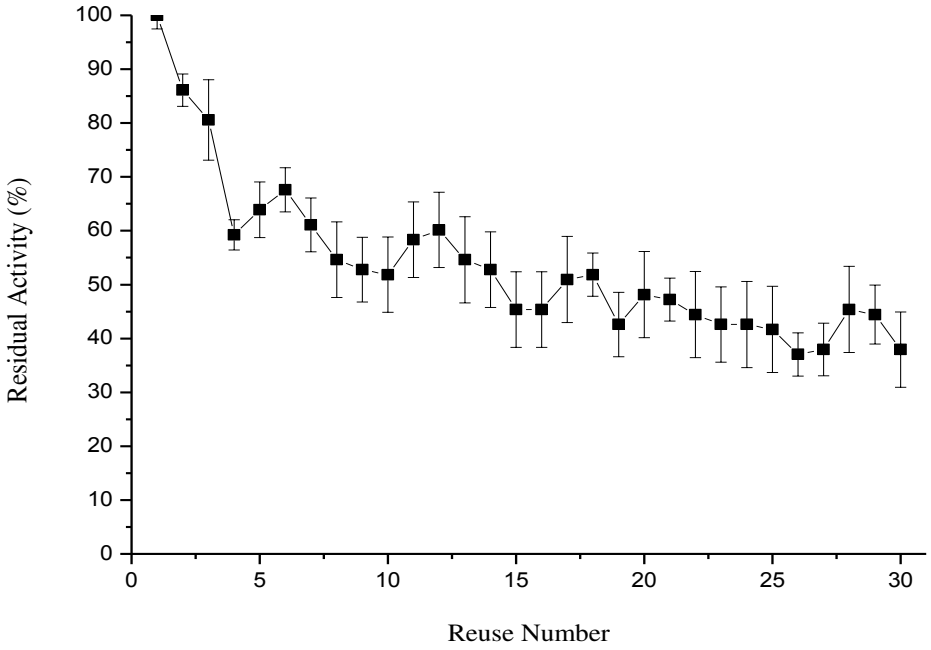

B

FIGURE 8
A) The storage stability profile of immobilized PPO B) Reusability of immobilized PPO

CONCLUSIONS

In this study, Agseftali (*Prunus persica* L.) PPOs were purified and immobilized onto new matrix SnO_2:Sb thin film, and both the free and immobilized enzymes were characterized for industrial applications. This study mainly aimed to prepare a new matrix for the immobilization of PPOs. Agseftali PPOs were successfully immobilized onto SnO_2:Sb thin film formed by the spray pyrolysis and, these results have been confirmed by SEM and FTIR analyzes. The immobilization process significantly was enhanced the thermal stability and pH stability at an acidic pH. We were able to successfully reuse the immobilized PPO 18 times, and 59.13% of its initial activity was retained over a period of 15 days. The relative L-DOPA formation via *L*-tyrosine oxidation was also increased by the immobilization procedure. According to the results the SnO_2:Sb thin films can be used as immobilization matrix for PPO in the production of L-Dopa. In addition, biosensor applications have become important nowadays. We predict that PPOs biosensors can be used in applications because they are

SnO_2:Sb thin film semiconductors [9]. The results from this kind SnO_2:Sb thin films demonstrate that the immobilized enzyme may be a good candidate for industrial and biotechnological applications for PPOs.

REFERENCES

[1] Kennedy, J.L., Selvi, P.K., Padmanabhan, A., Hema, K.N., Sekaran, G. (2007) Immobilization of polyphenol oxidase onto mesoporous activated carbons – isotherm and kinetic studies. Chemosphere. 69, 262–270.

[2] Ahmad, R., Sardar, M. (2015) Enzyme Immobilization: An Overview on Nanoparticles as Immobilization Matrix. Biochem Anal. Biochem. 4, 178.

[3] Tischer, W., Kasche, V. (1999) Immobilized Enzymes: Crystals or Carriers? Trends in Biotechnology. 17, 326–335.

[4] Sirin, Y., Yildirim-Akatin, M., Colak, A., Saglam-Ertunga, N. (2017) Dephytinization of food stuffs by phytase of Geobacillus sp. TF16 immobilized in chitosan and calcium-alginate. Int. J. Food Prop. 20(12), 2911-2922.

[5] Li, Q., Luo, G., Feng, J. (2001) Direct electron transfer for heme proteins assembled on nanocrystalline TiO_2 film. Electroanalysis. 13, 359-363.

[6] Sarauli, D., Riedel, M., Wettstein, C., Hahn, R., Stiba, C., Leimkühler, S., Schmuki, P., Wollenberger, U., Lisdat, F. (2012) Semimetallic TiO_2 nanotubes: new interfaces for bioelectrochemical enzymatic catalysis. J. Mater. Chem. 22, 4615-4618.

[7] Kemp, G.L., Marritt, S.J., Xiaoe, L., Durrant, J.R., Cheesman, M.R., Butt, J.N. (2009) Opportu-nities for mesoporous nanocrystalline SnO_2 electrodes in kinetic and catalytic analyses of redox proteins. Biochem. Soc. Trans. 37, 368-372.

[8] Ansari, S.G., Ansari, Z.A., Seo, H.K., Kim, G.S., Kim, Y.S., Khang, G., Shin, H.S. (2008) Ureasensor based on tin oxide thin films prepared by modified plasma enhanced CVD. Sens. Actuators B. 132, 265-271.

[9] Frasca, S., Milan, A.M., Guiet, A., Goebel, C., Pérez-Caballero, F., Stiba, K., Leimkühler, S., Fischer, A., Wollenberger, U. (2013) Bioelectrocatalysis at mesoporous antimony doped tin oxideelectrodes—Electrochemical characterization and direct enzyme communication. Electrochim. Acta. 110, 172– 180.

[10] Gupta, V. (2010) ZnO based third generation biosensor. Thin Solid Films. 519, 1141- 1144.

[11] Topoglidis, E., Cass, A.E.G., O'Regan, B., Durrant, J.R. (2001) Immobilisation and bioelectrochemistry of proteins on nanoporous TiO_2 and ZnO films. J. Electroanal. Chem. 517, 20-27.

[12] Cherry, R.J., Bjornsen, A.J., Zapien, D.C. (1998) Direct electron transfer of ferritin adsorbed at tin- doped indium oxide electrodes. Langmuir. 14 1971–1973.

[13] Fang, A., Ng, H.T., Li, S.F.Y. (2003) A high-performance glucose biosensor based on monomolecular layer of glucose oxidase covalently immobilised on indium-tinoxide surface. Biosens. Bioelectron. 19, 43-49.

[14] El Kasmi, A., Leopold, M.C., Galligan, R., Robertson, R.T., Saavedra, S.S., El Kacemi, K., Bowden, E.F. (2002) Adsorptive immobiliza-tion of cytochrome c on indium/tin oxide (ITO): electrochemical evidence for electron transfer-induced conformational changes. Electrochem. Commun. 4, 177-181.

[15] Frasca, S., Von-Graberg, T., Feng, J.J., Thomas, A., Smarsly, B.M., Weidinger, I.M., Scheller, F.W., Hildebrandt, P., Wollenberger, U. (2010) Mesoporous indium tin oxide as a novel platform for bioelectronics. ChemCatChem. 2, 839-845.

[16] Frasca, S., Richter, C., Von-Graberg, T., Smarsly, B.M., Wollenberger, U. (2011) Electro-chemical switchable protein-based optical device. Eng. Life Sci. 11, 554-558.

[17] Topoglidis, E., Campbell, C.J., Cass, A.E.G., Durrant, J.R. (2001) Factors that affect pro-tein adsorption on nanostructured titania films. A novel spectroelectro chemical application to sensing. Langmuir. 17, 7899-7906.

[18] Marritt, S.J., Kemp, G.L., Xiaoe, L., Durrant, J.R., Cheesman, M.R., Butt, J.N. (2008) Spectro-electrochemical characterization of a pentaheme cytochrome in solution and as electrocatalytically active films on nanocrystalline metal-oxide electrodes. J. Am. Chem. Soc. 130, 8588-8589.

[19] Astuti, Y., Topoglidis, E., Cass, A.G., Durrant, J.R. (2009) Direct spectroelectrochemistryof peroxidases immobilised on mesoporous metal oxide electrodes: towards reagentless hydrogen peroxide sensing. Anal. Chim. Acta. 648, 2-6.

[20] Granqvist, C.G., Hultåker, A. (2002) Transparent and conducting ITO films: new developments and applications. Thin Solid Films. 411, 1-5.

[21] Aksu, Y., Driess, M. (2009) A low-temperature molecular approach to highly conductivetin-rich indium tin oxide thin films with durable electro-optical performance. Angew. Chem. Int. Ed. 48, 7778-7782.

[22] Wang, Y., Brezesinski, T., Antonietti, M., Smarsly, B. (2009) Ordered mesoporous Sb-, Nb-, and Ta-doped SnO_2thin films with adjustable doping levels and high electrical conductivity. ACS Nano. 3, 1373-1378.

[23] Batzill, M., Diebold, U. (2005) The surface and materials science of tin oxide. Prog. Surf. Sci.

79, 47-154.

[24] Kafi, A.K.M., Wali, Q., Jose, R., Kumar-Biswas, T., Yusoff, M.M. (2017) A glassy carbon electrode modified with SnO2 nanofibers, polyaniline and hemoglobin for improved amperometric sensing of hydrogen peroxide. Microchim Acta. 184, 4443–4450.

[25] Battal, A., Tatar, D., Kocyigit, A., Duzgun, B. (2015) Effect of Substrate Temperature on Some Properties Doubly Doped Tin Oxide Thin Films Deposited by Using Spray Pyrolysis. Materials focus. 4, 445-456.

[26] Zhang, D., Deng, Z., Zhang, J., Chen, L. (2006) Microstructure and electrical properties of antimony- doped tin oxide thin film deposited. Mater. Chem. Phys. 98, 353-357.

[27] Outemzabet, R., Bouras, N., Kesri, N. (2007) Microstructure and physical properties of nanofaceted antimony doped tin oxide thin films deposited by chemical vapor deposition on different substrates. Thin Solid Films. 515, 6518–6520.

[28] Kim, H., Auyeung, R.C.Y., Piqué, A. (2008) Transparent conducting F-doped SnO_2 thin films grown by pulsed laser deposition. Thin Solid Films. 516, 5052–5056.

[29] Kumar, V.B.A., Mohan, T.C.K., Murugan, K. (2008) Purification and kinetic characterization of polyphenol oxidase from Barbados cherry (Malpighia glabra L.). Food Chem. 110, 328–33.

[30] Özen, A., Colak, A., Dincer, B., Güner, S. (2004) A diphenolase from persimmon fruits (Diospyros kaki L., Ebenaceae). Food Chem. 85, 431–437.

[31] Özel, A., Colak, A., Arslan, O., Yildirim, M. (2010) Purification and characterisation of a polyphenol oxidase from Boletus erythropus and investigation of its catalytic efficiency in selected organic solvents. Food Chem. 119, 1044–1049.

[32] Forzani, E.S., Solis, V.M. (2000) Electrochemical behaviour of polyphenoloxidase immobilized in self-assembled structures layer by layer with cationic polyallylamine. Anal. Chem. 72, 5300–5307.

[33] Wada, S., Ichikawa, H., Tatsumi, K. (1993) Removal of phenols from wastewater by soluble and immobilized tyrosinase. Biotechnol. Bioeng. 42, 854–858.

[34] Gayatri, S., Bradley, A.S. (2002) L-Dopa production from tyrosinase immobilized on zeolite. Enzyme Microb. Technol. 31, 747–753.

[35] Gu, B.X., Xu, C.X., Zhu, G.P., Liu, S.Q., Chen, L.Y., Li, X.S. (2009) Tyrosinase Immobilization on ZnO Nanorods for Phenol Detection. J. Phys. Chem. B. 113, 377–381.

[36] Sethuraman, V., Muthuraja, P., Anandha-Raj, J., Manisankar, P. (2016) A highly sensitive electrochemical biosensor for catechol using conducting polymer reduced graphene oxide–metal oxide enzyme, modified electrode. Biosens. Bioelectron. 84, 112–119.

[37] Yaropolov, A.I., Kharybin, A.N., Emneus, J., Marko-Varga, G., Gorton, L. (1995) Flow-injection analysis of phenols at a graphite electrode modified with co-immobilized laccase and tyrosinase. Anal. Chim. Acta. 308, 137–144.

[38] Stambouli, V., Labeau, M., Matko, I., Chenevier, B., Renault, O., Guiducci, C., Chaudouet, P., Roussel, H., Nibkin, D., Dupuis, E. (2006) Development and functionalisation of Sb doped SnO_2 thin films for DNA biochipapplications. Sens. Actuators B. 113, 1025-1033.

[39] Stambouli, V., Zebda, A., Appert, E., Guiducci, C., Labeau, M., Diard, J.P., Le-Gorrec, B., Brack, N., Pigram, P.J. (2006) Semi-conductor oxide based electrodes for the label-free electrical detection of DNAhybridization: comparison between Sb doped SnO_2 and $CdIn_2O_4$. Electrochim. Acta. 51, 5206-5214.

[40] Kwan, P., Schmitt, D., Volosin, A.M., McIntosh, C.L., Seo, D.K., Jones, A.K. (2011) Spectroelectrochemistry of cytochrome c and azurin immobilized innanoporous antimony-doped tin oxide. Chem. Commun. 47, 12367-12369.

[41] Reipa, V., Mayhew, M.P., Vilker, V.L. (1997) A direct electrode-driven P450 cycle forbiocatalysis. Proceedings of the National Academy of Sciences of the United States of America. 94, 13554–13558.

[42] Arslan, O., Erzengin, M., Sinan, S., Ozensoy, O. (2004) Purification of mulberry (Morus alba L.) polyphenol oxidase by affinity chromatography and investigation of its kinetic and electrophoretic properties. Food Chem. 88, 479–484.

[43] Aydemir, T. (2004) Partial purification and characterization of polyphenol oxidase from artichoke (Cynara scolymus L.) heads. Food Chem. 87, 59–67.

[44] Özen, A., Colak, A., Dincer, B., Güner, S.A. (2004) Diphenolase from persimmon fruits (Diospyros kaki L., Ebenaceae). Food Chem. 85, 431–437.

[45] Bradford, M.M. (1976) A rapid and sensitive method for the quantitation of microgram quantities of protein utilizing the principle of protein-dye binding. Anal. Biochem. 72, 248–254.

[46] Laemmli, U.K. (1970) Cleavage of Structural Proteins during the Assembly of the Head of Bacteriophage T4. Nature. 227, 680–685.
[47] Espin, J.C., Morales, M., Varon, R., Tudela, J., Garciacanovas, F. (1995) A Continuous Spectrophotometric Method for Determining the Monophenolase and Diphenolase Activities of Apple Polyphenol Oxidase. Anal. Biochem. 231, 237–246.
[48] Kolcuoğlu, Y. (2012) Purification and comparative characterization of monophenolase and diphenolase activities from a wild edible mushroom (Macrolepiota gracilenta). Process. Biochem. 47, 2449–2454.
[49] Lineweaver, H., Burk, D. (1934) The Determination of Enzyme Dissociation Constants. J. Am. Chem. Soc. 56, 658–666.
[50] Terrier, C., Chatelon, J.P., Roger, J.A. (1997) Electrical and optical properties of Sb:SnO_2 thin films obtained by the sol-gel method. Thin Solid Films. 295, 95–100.
[51] Ravichandran, K., Muruganantham, G., Sakthivel, B. (2009) Highly conducting and crystalline doubly doped tin oxide films fabricated using a low-cost and simplified spray technique. Phys. B Condens. Matter. 404, 4299–4302.
[52] Hou, C., Wang, Y., Zhu, H., Wei, H. (2015) Construction of Enzyme Immobilization System through Metal-Polyphenol Assisted Fe_3O_4/Chitosan Hybrid Microcapsules. Chem. Eng. J. 283, 397–403.
[53] Arıca, M.Y., Bayramoğlu, G., Bıçak, N. (2004) Characterisation of tyrosinase immobilised onto spacer-arm attached glycidyl methacrylate-based reactive microbeads. Process Biochem. 39, 2007–2017.
[54] Milani, M.M., Lofti, A.S., Mohsenifar, A., Mikaili, P., Kamelipour, N., Dehghan, J. (2015) Enhancing organophosphorus hydrolase stability by immobilization on chitosan beads containing glutaraldehyde. Res. J. Environ. Toxicol. 9, 34–44.
[55] Özel, A., Colak, A., Arslan, O., Yildirim, M. (2010) Purification and characterisation of a polyphenol oxidase from Boletus erythropus and investigation of its catalytic efficiency in selected organic solvents. Food Chem. 119, 1044–1049.
[56] Öz, F., Colak, A., Özel, A., Ertunga, N.S., Sesli, E. (2013) Purification and characterization of a mushroom polyphenol oxidase and its activity in organic solvents. J. Food Biochem. 37, 36–44.
[57] Dogan, S., Turan, P., Dogan, M., Arslan, O., Alkan, M. (2005) Purification and characterization of Ocimum basilicum L. polyphenol oxidase. J. Agric. Food Chem. 53, 10224–10230.
[58] Yerliturk, F.U., Arslan, O., Sinan, S., Gencer, N., Güler, Ö.Ö. (2008) Characterization of polyphenoloxidase from wild pear (Pyrus elaegrifolia). J. Food Biochem. 32, 368–383.
[59] Kumar, V.B.A., Mohan, T.C.K., Murugan, K. (2008) Purification and kinetic characterization of polyphenol oxidase from Barbados cherry (Malpighia glabra L.). Food Chem. 110, 328–33.
[60] Gong, Z., Li, D., Liu, C., Cheng, A., Wang, W. (2015) Partial purification and characterization of polyphenol oxidase and peroxidase from chestnut kernel. LWT - Food Sci. Technol. 60, 1095–1099.
[61] Zhang, B., Tian, Y., Zhang, J.X., Cai, W. (2010) Structural, optical, electrical properties and FTIR studies of fluorine doped SnO_2 films deposited by spray pyrolysis. J. Mater. Sci. 46, 1884–1889.
[62] Van-Tran, T., Turrell, S., Eddafi, M., Capoen, B., Bouazaoui, M., Roussel, P., Berneschi, S.,ighini, G., Ferrarie, M., Bhaktha, S.N.B., Cristini, O., Kinowski, C. (2010) Investigations of the effects of the growth of SnO_2 nanoparticles on the structural properties of glass–ceramic planar waveguides using Raman and FTIR spectroscopies. J. Mol. Struct. 976, 314–319.
[63] Gu, B.X., Xu, C.X., Zhu, G.P., Liu, S.Q., Chen, L.Y., Li, X.S. (2009) Tyrosinase immobilization on ZnO nanorods for phenol detection. J. Phys. Chem. B. 113, 377–81.
[64] Elagli, A., Belhacene, K., Vivien, C., Dhulster, P., Froidevaux, R., Supiot, P. (2014) Facile immobilization of enzyme by entrapment using a plasma-deposited organosilicon thin film. J. Mol. Catal. B Enzym. 110, 77–86.
[65] Yildiz, H.B., Caliskan, S., Kamaci, M., Caliskan, A., Yilmaz, H. (2013) L-Dopa synthesis catalyzed by tyrosinase immobilized in poly(ethyleneoxide) conducting polymers. Int. J. Biol. Macromol. 56, 34–40.
[66] Khan, A.A., Akhtar, S., Husain, Q. (2006) Direct immobilization of polyphenol oxidases on Celite 545 from ammonium sulphate fractionated proteins of potato (Solanum tuberosum). J. Mol. Catal. B Enzym. 40, 58–63.
[67] Forde, J., Tully, E., Vakurov, A., Gibson, T.D., Millner, P., Ó'Fágáin, C. (2010) Chemical modification and immobilisation of laccase from Trametes hirsuta and from Myceliophthora thermophile. Enzyme Microb. Technol. 46, 430–437.
[68] Xu, R., Zhou, Q., Li, F., Zhang, B. (2013) Laccase immobilization on chitosan/poly(vinyl alcohol) composite nanofibrous membranes for 2,4-dichlorophenol removal. Chem. Eng. J. 222, 321–329.
[69] Guzik, U., Hupert-Kocurek, K., Wojcieszyńska, D. (2014) Immobilization as a strategy for improving enzyme properties-

application to oxidoreductases. Molecules. 19, 8995–9018.

[70] Loncar, N., Vujcic, Z. (2011) Tentacle carrier for immobilization of potato phenoloxidase and its application for halogenophenols removal from aqueous solutions. J. Hazard. Mater. 196, 73–78.

Received: **24.12.2017**
Accepted: **15.04.2018**

CORRESPONDING AUTHOR

Ayse Turkhan
Igdir University,
Suveren Campus,
76000, Igdir – Turkey

e-mail: ayse.turkhan@igdir.edu.tr

© by PSP Volume 27 – No. 7/2018 pages 4857-4866 Fresenius Environmental Bulletin

GENETIC ANALYSIS OF SOME YIELD ASSOCIATED TRAITS OF F_3 SEGREGATING POPULATION OF BREAD WHEAT

Huseyin Gungor[1,*], Huseyin Basal[2], Iker Yuce[3], Ozgur Kekilli[3], Merve Akcadag[3], Ziya Dumlupinar[3]

[1]Duzce University, Agriculture and Natural Sciences Faculty, Field Crops Department, Duzce, Turkey
[2]Adnan Menderes University, Faculty of Agriculture, Department of Field Crops, Aydin, Turkey
[3]Kahramanmaras Sutcu Imam University, Agricultural Faculty, Agricultural Biotechnology Department, Kahramanmaras, Turkey

ABSTRACT

Diallel analysis are curial to determine the most suitable parents and crosses, and to select appropriate method in breeding programs. This study was conducted to investigate the genetic parameters, general and specific combining abilities for some yield component in an 8 × 8 half diallel bread wheat cross populations including 28 F_3 populations and their eight parental lines. The experiment was conducted in randomized complete block design with four replications at Lüleburgaz/ Kırklareli under farmer conditions in 2016-2017 cropping year. According to variance analysis, genotypes were found significantly different for all investigated traits. Based on results of the genetic parameters, all investigated traits were controlled by dominance gene effects. In addition, over dominance effects were found in all investigated traits. Due to low narrow sense heritability, selection in later generations might be much more useful. The general and specific combining abilities (GCA and SCA) were also found as significant for all investigated traits in this study. When general combining ability values were evaluated, Krasunia odes'ka and Lucilla were suitable genotypes for increased yield and yield components. According to specific combining ability values, Masaccio × Lucilla, Krasunia odes'ka × Lucilla, Krasunia odes'ka × Masaccio, Gl-14 × Masaccio, Esperia × Lucilla, Esperia × Masaccio, Esperia × Gl-14, As-14 × Krasunia odes'ka, Midas × Krasunia odes'ka and Midas × Gl-14 crosses were promising for all traits examined.

KEYWORDS:
Bread wheat, diallel analysis, combining ability, inheritance

INTRODUCTION

Wheat (*Triticum aestivum* L.) is the most used and widely grown crop plant [1] due to its rich nutrient content [2] and being the main ingredient of bread which is the most widely consumed fiber carrying food in Turkey and the world [3, 4]. Bread wheat is in the first place with 7.6 m ha production area and 20.6 m tons production in Turkey [5], however, mostly grown under rain-fed (77.1%) conditions [1]. Yield can be increased with some agricultural practices [6], grain yield is determined by environmental and genetic factors [7] and plant breeding is the most valid method to develop high yielding genotypes. However, increasing grain yield is a difficult task for both breeders and growers [8].

The grain yield is a complex trait affected by genotype and environment. The yield components such as grain number/weight per spike are also quantitative traits controlled by genotype and environment. The diallel analysis is the most used approach to understand the heritability of complex traits. It is a powerful tool to select parents and crossing the most combined genotypes for the desired traits. Predictions of genetic parameters are crucial for plant breeders to select the most suitable selection method [9, 10].

In breeding of self-pollinated crops such as wheat, it is very important to know gene effects to start selection in segregation populations. If the gene effect of the desired trait is additive gene effect, the selection starts in F_2 generation according to pedigree method, if the trait was controlled by non-additive gene effect, therefore, the selection would start in later generations according to the bulk method [11, 12].

The diallel analysis is a method to determine heritability of yield and yield components and suitable parents to use in breeding programs and it is usually applied in F_1 generation of the segregation populations. However, it might be used to obtain genetic information in F_2 and F_3 stages where heterozygosity is high. Once the genetic structure of the segregation populations is well known, the success of achieving the goal of breeding may be high [13].

The aim of the study were i; to determine heritability of wheat grain yield components ii; to select promising genotypes and parents to improve those yield components, and iii; contribute to current breeding programs.

MATERIALS AND METHODS

This study was carried out in Luleburgaz-Kırklareli location in 2016-2017 cropping season. The eight bread wheat (*Triticum aestivum* L.) genotypes such as Midas, As-14, Rumeli, Esperia, Gl-14, Krasunia odes'ka, Masaccio and Lucilla from different origins were used as plant materials. Those genotypes were crossed between each other as 8 × 8 non-reciprocal cross combinations in 2013-2014 cropping season and the F_1 plants were planted in 2014-2015 and the F_2 plants were planted in 2015-2016 growing season and F_3 plants were obtained. The plant materials (F_3 populations and the parents) were planted in a 3 meter 2 row plots with 20 cm apart and 10 cm inter-rows. The experiment was arranged in a randomized complete block design with four replications. The fertilizers were applied as 90 kg/ha N and 100 kg/ha P_2O_5 at planting and 90 kg/ha N as top dressing at tillering stage. Twenty plants were selected from each plot and spikes were collected. Spike length (SL), spikelet number per spike (SNS), grain number per spike (GNS), grain weight per spike (GWS), and grain yield per plant (GYP) were investigated.

The data obtained from the experiment was subjected to pre-variance analysis and the diallel tables were created for the statistically significant traits and diallel analysis were performed [14, 15]. The variance analysis of the diallel tables were done according to [16] and [17] by MS Excel software as described by [18]. The estimation of genetic parameters with diallel analysis were done as suggested by [16, 19, 20, 21, 22 and 23], the analysis of combining abilities were done in method 2 and model 1 which are developed by [24]. The diallel analysis was done using TARPOPGEN statistical software developed by [25].

TABLE 1
Mean values of some yield associated traits from parents and F_3 crosses in bread wheat

Genotype	Spike length (cm)	Spikelets number per spike (number)	Grain number per spike (number)	Grain weight per spike (g)	Grain yield per plant (g)
Genotypes					
Midas (1)	8.5 no	**19.5 e-j**	**48.2 g-m**	2.11 l-q	10.39 m-r
As-14 (2)	8.0 o	18.0 jkl	41.2 l-p	1.84 o-s	9.25 p-t
Rumeli (3)	8.9 mn	19.0 g-l	48.0 h-m	2.25 j-o	11.30 k-p
Esperia (4)	8.5 no	18.5 h-l	40.0 m-p	1.73 p-s	8.66 q-t
Gl-14 (5)	8.0 o	17.5 l	43.7 k-o	2.14 k-p	10.67 l-q
Krasunia odes'ka (6)	**9.4 lm**	18.5 h-l	44.0 k-o	**2.34 j-o**	**11.68 j-o**
Masaccio (7)	***7.2 p***	***15.2 m***	***34.5 p***	1.63 qrs	8.16 rst
Lucilla (8)	8.5 no	18.0 jkl	44.2 k-o	***1.49 s***	***7.54 t***
Crosses					
1X2	10.8 c-ı	22.0 abc	73.5 ab	3.62 bc	18.11 bc
1X3	11.1 b-f	20.0 d-h	51.7 f-k	2.63 f-k	13.19 f-k
1X4	10.5 f-j	18.0 jkl	55.5 d-h	2.68 f-j	13.37 f-k
1X5	11.2 a-e	21.2 bcd	61.7 cd	3.22 cde	16.15 cde
1X6	11.0 b-f	20.0 d-h	61.2 cde	3.06 d-g	15.29 d-g
1X7	10.2 ıjk	***17.7 kl***	41.2 l-p	2.00 n-r	9.98 n-s
1X8	10.2 ıjk	19.7 d-ı	58.0 def	**4.49 a**	**22.38 a**
2X3	10.3 g-k	20.7 c-f	53.2 d-j	2.73 e-j	13.72 f-k
2X4	10.1 jkl	19.7 d-ı	42.7 l-p	2.60 g-l	13.06 g-l
2X5	**11.9 a**	18.2 ı-l	38.5 nop	2.09 m-q	10.50 m-r
2X6	11.1 b-f	22.7 ab	54.2 d-ı	3.33 bcd	16.64 cd
2X7	***8.4 no***	17.7 kl	39.7 m-p	***1.53 rs***	***7.72 st***
2X8	10.2 h-k	18.2 ı-l	49.7 f-l	2.26 j-o	11.31 k-p
3X4	11.5 ab	**23.5 a**	45.0 j-o	2.54 h-m	12.75 h-m
3X5	10.6 e-j	18.0 jkl	57.0 def	3.02 d-h	15.15 d-h
3X6	9.7 kl	18.0 jkl	53.0 e-j	2.25 j-o	11.38 k-p
3X7	11.1 b-f	20.0 d-h	51.5 f-k	2.45 ı-n	12.30 ı-n
3X8	10.9 b-h	20.0 d-h	58.2 def	3.81 b	19.16 b
4X5	10.4 f-j	19.5 e-j	53.2 d-j	2.64 f-k	13.30 f-k
4X6	10.7 d-j	18.0 jkl	***36.7 op***	1.94 o-s	9.80 o-t
4X7	11.4 a-d	21.0 cde	51.5 f-k	3.11 def	15.50 def
4X8	11.4 abc	19.7 d-ı	55.5 d-h	2.90 d-ı	13.98 e-j
5X6	10.7 d-j	20.2 d-g	61.0 cde	2.86 d-ı	14.28 d-ı
5X7	11.0 b-g	19.2 f-k	46.2 ı-n	2.48 ı-n	12.57 ı-m
5X8	10.8 b-ı	20.0 d-h	44.2 k-o	2.54 h-m	12.80 h-m
6X7	**11.9 a**	20.5 c-g	67.2 bc	3.26 cd	16.29 cde
6X8	**11.9 a**	22.7 ab	56.7 d-g	3.23 cde	16.19 cde
7X8	11.1 b-f	20.7 c-f	**79.7 a**	3.30 cd	16.66 cd
F_3 mean values	10.8	19.9	53.5	2.81	14.05
Parental mean values	8.4	18.0	43.0	1.94	9.71
General mean values	10.0	19.0	49.7	2.55	12.77
C.V. %	4.86	6.00	11.94	13.63	13.17
LSD (0.05)	0.70-**	1.64-**	8.57**	0.50**	2.41**

*p≤0.05; ** p≤0.01

RESULTS AND DISCUSSION

The investigated traits, the genetic parameters for each trait, and general and specific combining ability have been shown in Table 1, Table 2, and Table 3, respectively. All investigated traits were found significantly different ($p \leq 0.01$) in this research.

Krasunia odes'ka had the highest spike length as 9.4 cm among the parents, while the F_3 plants from the As-14 x Gl-14, Krasunia odes'ka x Masaccio and Krasunia odes'ka x Lucilla crosses had the highest spike lengths as 11.9 cm among the crosses (Table 1). According to the half diallel variance analysis the dominance variance (b) and components (b_1 and b_3) were found significantly different (Table 2). The genetic parameters were found different and the difference between additive gene variance and dominance variance ($D-H_1$) was found negative (-5.094*), suggesting that the genetic effect for the spikelet length was concluded as dominance gene effect. The average value of dominance degree $(H_1/D)^{1/2}$ was found as 3.150 and exhibited over dominance. The dominant and recessive allele frequencies ($H_2/4H_1$) was found as 0.240 that meant inequality of dominant and recessive allele frequencies at dominant loci in parents. The dominant and recessive allele ratio (KD/KR) was found as 1.431 and this value indicated the majority of the dominance alleles. The effective gene number was determined as three because the value was found as 3.288 ($K= h^2/ H_2$) for the gene number.

The relationship between theoretical dominance and the actual value of parents was negatively correlated, indicated that parents with higher spike length had dominant genes. The narrow sense heritability was found as 0.098. The GCA and SCA were found significant as 0.515** and 1.807**, respectively and the ratio of GCA/SCA was found as 0.28. These data indicated the importance of SCA which also meant dominance gene effect on spike length. The GCA of the parents was identified positive and significant for Krasunia odes'ka as 0.348**, while negative and significant values were found as -0.352** and -0.287** for As-14 and Masaccio, respectively. In terms of specific combining ability of the crosses, As-14 x Gl-14 cross showed the highest value SCA value as 1.974** (Table 3). It was concluded that the spike length trait was controlled by dominance gene variance which was also indicated by previous studies [26, 27, 28]. However, Yıldırım [29] determined additive gene effect and Soylu [30] and Kutlu et al. [8] found both additive gene effect and non-additive gene effect.

The Wr-Vr graphic for variance (Vr_x) and covariance (Wr_y) values for spike length of the half diallel F_3 population was shown using eight genotypes in Figure 1.

In terms of Wr-Vr graphic for spike length, the regression line crossed the Y axis at negative direction (a:-0.768), which was evaluated as the heritability of the spike length by over dominance. It was supported by the average dominance degree $(H_1/D)^{1/2}$ determined as 3.150 (Table 2). The genotypes numbered as 1, 3, 4, 5, 6 and 8 were close to the origin evaluated as having mostly dominance genes and the genotypes numbered as 2 and 7 were far to the origin evaluated as having mostly recessive genes (Figure 1). In a previous work, Şener [31] reported over dominance for the spike length.

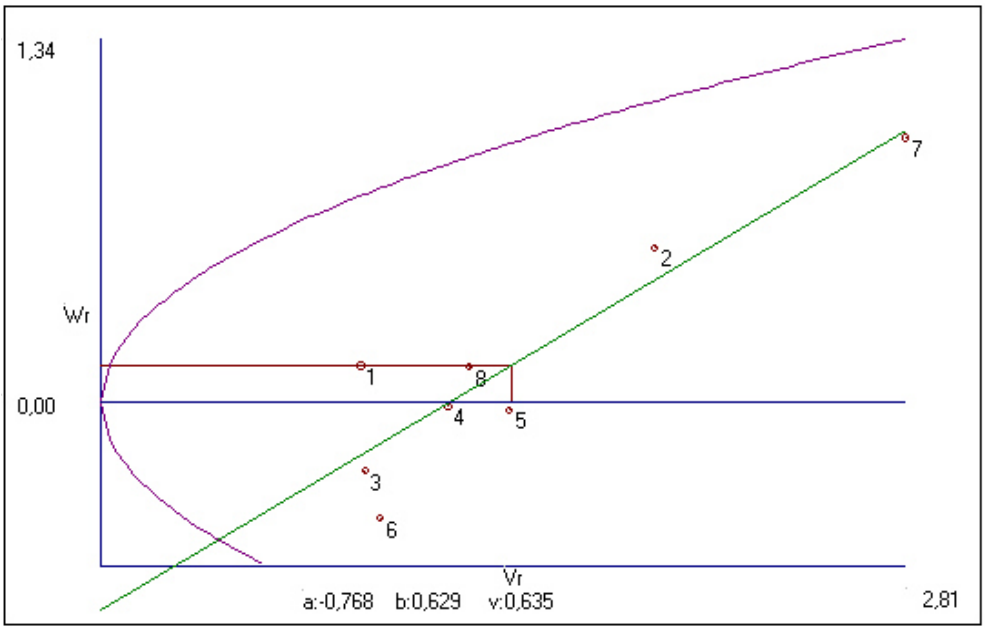

FIGURE 1
Wr/Vr Graphic for spike length
1-Midas, 2-As-14, 3-Rumeli, 4-Esperia, 5-Gl-14, 6-Krasunia odes'ka, 7-Masaccio, 8-Lucilla

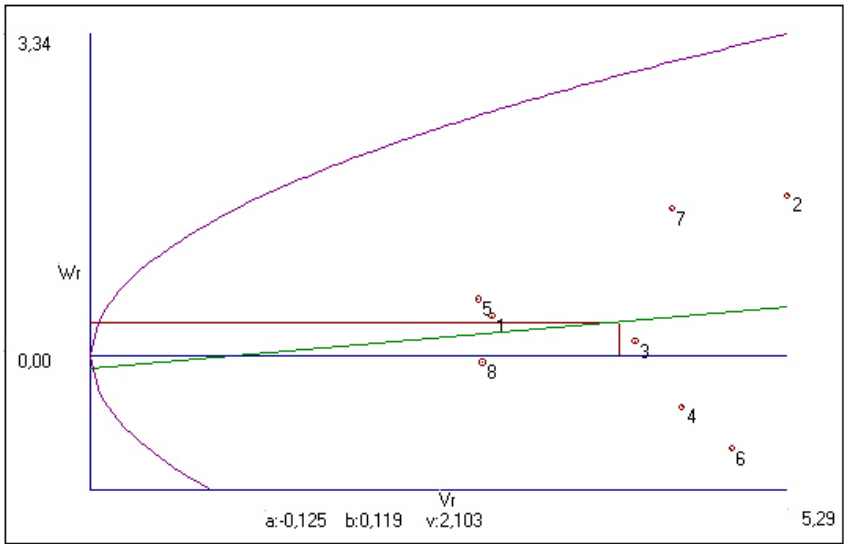

FIGURE 2
Wr/Vr Graphic for spikelet number per spike
1-Midas, 2-As-14, 3-Rumeli, 4-Esperia, 5-Gl-14, 6-Krasunia odes'ka, 7-Masaccio, 8-Lucilla

In terms of spikelet number per spike (SNS), Midas cultivar had the highest spikelet number (19.5) among parents, while Rumeli x Esperia cross had the highest spikelet number (23.5) among crosses (Table 1). According to half diallel variance analysis, dominance variance (b), and components (b_1 and b_3) were found significantly variable (Table 2). The genetic parameters were not found different and the difference between additive gene variance and dominance variance (D-H_1) was found as negative (-14.099) and the genetic effect for the spikelet number per spike was concluded as dominance gene effect. The average dominance degree $(H_1/D)^{1/2}$ was found as 2.995 that indicated the over dominance for the SNS. Dominant and recessive allele frequencies ($H_2/4H_1$) were found as 0.231 and also pointed inequality of dominant and recessive allele frequencies for SNS. The ratio of dominant and recessive alleles (KD/KR) was 1.553 and showed majority of the dominant alleles. The gene number ($K= h^2/ H_2$) was found as 0.729, therefore the effective gene number could not be calculated. The correlation between theoretical dominance and actual value of parents was found as negative and this concluded as genotypes with higher spikelet numbers had dominant genes. The specific combining ability of the SNS was found as 0.106. The SCA and GCA were found significant and the ratio of GCA/SCA was 0.48 which indicated that SNS was controlled by SCA and also dominance gene variance was important (Table 2). According to the GCA of the parents, Krasunia odes'ka was positive and, Gl-14 and Masaccio were negative and significant (-0.394* and -0.794**, respectively). According to the SCA of hybrid combinations, Rumeli x Esperia cross had the highest SCA value with 3.619* (Table 3). After comparing the three methods, it is proposed that dominance gene variance was effective for SNS. Previous literature reported dominance gene effect [27, 32], additive gene effect [29, 33] and both additive and non-additive gene effects [8] for spikelet number per spike.

According to Wr-Vr graphic for spikelet number per spike, the regression line crossed the Y axis under origin at negative direction (a:-0.125), which indicated over dominance was important for SNS. This evaluation was supported by the average dominance degree $(H_1/D)^{1/2}$ 3.150 (Table 2). The genotypes numbered as 1, 3, 5 and 8 were close to the origin and mostly had dominance genes. The genotypes numbered as 2 and 7 were far to the origin and had mostly recessive genes. In addition, the genotypes numbered as 4 and 6 were far to the regression line and it is concluded as the epistatic gene effect might be important for SNS (Figure 2). Incomplete dominance for spikelet number per spike was reported by [29].

According to grain number per spike (GNS), Midas cultivar had the highest grain number (48.2) among parents, while Masaccio x Lucilla cross had the highest number (79.7) among crosses (Table 1). The dominance variance (b) and the components (b_1 and b_3) were found significantly different as a result of half diallel variance analysis (Table 2). The genetic parameters were found insignificant and the differences between additive gene variance and dominance variance (D-H_1) was found as negative (-473.094) and indicated dominance gene variance effect on grain number per spike. The average dominance variance $(H_1/D)^{1/2}$ was found as 4.414 and showed over dominance on GNS. The dominance and recessive allele frequencies were found as 0.242 which indicated the imbalanced frequencies of dominance and recessive alleles in dominant loci. In addition, the ratio of dominance and recessive alleles was found as 1.153 which also exhibited the majority of the dominant alleles. The value for the gene number ($K= h^2/ H_2$) was found as

0.693, therefore the number of gene could not be calculated. The correlation between theoretical dominance and actual values of the parents was negative and exhibited that the parents with the higher GNS had dominant genes. The narrow sense heritability of the investigated traits was found as 0.007. The SCA and GCA were found significantly different (P≤0.01) and the ratio of GCA/SCA was found as 0.72 which indicated that dominance gene variance effective on GNS (Table 2). General combining ability of the parents was positive on Midas and Lucilla and negative on As-14 and Esperia. In terms of specific combining ability of the crosses, the highest values were obtained from Masaccio x Lucilla and Midas x As-14 crosses and the other positive SCA values might be considered to increase GNS (Table 3). When compared three methods used in the study to evaluated gene effects, it is stated that dominance gene variance was effective on grain number per spike. In previous studies, Akgün [11] and Aydoğan and Yağdı [27] reported non-additive gene effect while Şener et al. [33] determined additive gene effect on GNS. However, Kutlu et al. [8] indicated both additive and non-additive gene effect on GNS.

According to Wr/Vr graphic of GNS, the regression line crossed the Y axis at the positive direction (a: 3.164) which exhibited partial dominance on the heritability of the trait. In contrast to the Wr/Vr graphic, it was evaluated as superior dominance at the average dominance degree (4.414). The genotypes numbered as 1, 3, 4, 5 and 6 were close to the origin evaluated as having mostly dominance genes and the genotypes numbered as 2 and 7 were far to the origin had mostly recessive genes. The genotype 8 was took place far from the regression line evaluated that epistatic gene effect might be important on GNS (Figure 3). Yıldırım [29] reported a partial dominance on GNS in his work.

Krasunia odes'ka had the highest grain weight per spike (2.34 g) among parents while Midas x Lucilla was the highest among crosses (4.49 g) (Table 1). Additive variance (a), dominance variance (b), and components (b_1 and b_3) varied for GWS (Table 1). The dominance effect of heterozygote locus (h_2) was significantly different (P≤0.05) according to the half diallel cross analysis. The D-H_1 value was found as -2.043 and evaluated that dominance gene effect was effective on GWS. The average dominance degree $(H_1/D)^{1/2}$ was found as 4.590 and exhibited over dominance on GWS. The dominance and recessive alleles frequency ($H_2/4H_1$) was 0.232 and indicated imbalanced dominance and recessive allele ratio in dominance loci. The positive F value (0.162) indicated the majority of the dominance alleles for GWS. The ratio of dominance and recessive alleles (KD/KR) was 1.418 and supported the majority of dominance alleles. The value for gene number ($K= h^2/ H_2$) was 1.141, therefore the effective gene number was determined as 1 (Table 2). The theoretical dominance and actual value of the parents was negatively correlated which indicated the parents with higher GWS had dominance genes. The narrow sense heritability of the investigated traits was 0.046 (Table 2). Both GCA and SCA varied for GWS (P≤0.01) and the ratio of GCA/SCA was 0.63, indicated that dominance gene effect effective on GWS (Table 2). The GCA of the Midas, Krasunia odes'ka and Lucilla parents were positive and significant (Table 3). Of the three methods used in the study to determine gene effects showed different results, but this method was recommended by [15], it is proposed that GWS was controlled by dominance gene effect. Our findings were supported by [34], [35] and [36] that reported dominance gene effect on grain weight per spike.

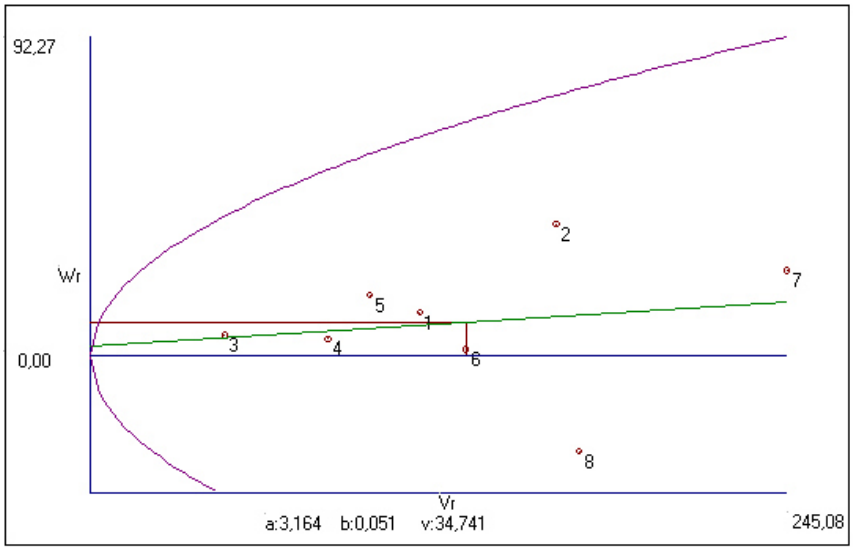

FIGURE 3
Wr/Vr Graphic for grain number per spike
1-Midas, 2-As-14, 3-Rumeli, 4-Esperia, 5-Gl-14, 6-Krasunia odes'ka, 7-Masaccio, 8-Lucilla

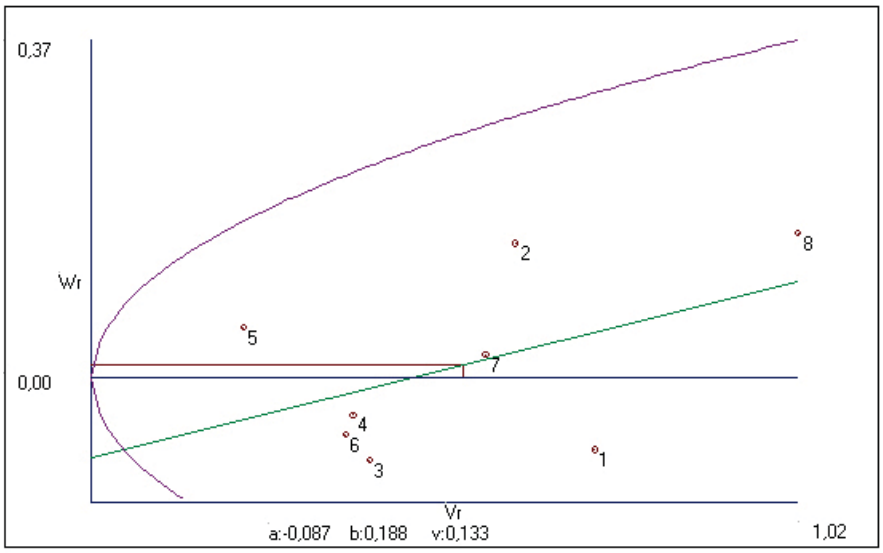

FIGURE 4
Wr/Vr Graphic for grain weight per spike
1-Midas, 2-As-14, 3-Rumeli, 4-Esperia, 5-Gl-14, 6-Krasunia odes'ka, 7-Masaccio, 8-Lucilla

TABLE 2
Genetic parameters for investigated traits

Genetic parameters	Spike length	Spikelet number per spike	Grain number per spike	Grain weight per spike	Grain yield per plant
a	0.499	1.626	77.161	0.304*	7.401*
b	1.798**	3.228**	107.848**	0.487**	12.134**
b_1	36,267**	21.542**	686.466**	4.653**	117.653**
b_2	0.232	0.712	30.882	0.252	6.061
b_3	0.623**	3.192**	105.855**	0.361**	8.984**
E	0.064	0.334	9.145	0.031	0.729
D	0.571	1.769	25.596	0.102	7.691
F	0.638	2.296	16.090	0.162	0.819
H_1	5.665*	15.867	498.690	2.144	41.111
H_2	5.434*	14.635	482.150	1.991	44.043
D-H1	-5.094*	-14.099	-473.094	-2.043	-33.421
$(H1/D)^{1/2}$	3.150	2.995	4.414	4.590	2.312
$H_2/4H_1$	0.240	0.231	0.242	0.232	0.268
KD/KR	1.431	1.553	1.153	1.418	1.047
h^2	17.869**	10.672	334.214	2.271*	8.908
$K= h^2/ H_2$	3.288	0.729	0.693	1.141	0.202
Hg	0.562	0.514	0.587	0.601	0.730
Hd	0.098	0.106	0.047	0.046	0.151
ryr, (Wr+Vr)	-0.921	-0.469	-0.746	-0.706	0.838
GCA	0.515**	1.582**	77.312**	0.305**	23.168**
SCA	1.807**	3.245**	107.814**	0.486**	8.195**
GCA/SCA	0.28	0.48	0.72	0.63	2.83

* $p \leq 0.05$; ** $p \leq 0.01$; "D"-"a"-"GCA": Measures additive effect, "H1"-"H2"-"(b-b_1-b_2-b_3)"-"SCA": Measures dominance effect, F: Determines frequencies of dominant to recessive alleles in parents, E: Shows environment effect, H2/4H1: Determines proportion of genes with positive and negative effects in the parents, √(H1/D):Measures average degree of dominance, (KD/KR): Ratio of the total number of dominant against recessive alleles.

The Wr-Vr graphic for grain weight per spike, and regression line crossed the Y axis under the origin on negative direction (a:-0.087). This situation was due to over dominance effect on the GWS. It was also supported by average dominance degree (4.590) of the GWS. The genotypes numbered as 3, 4, 5, 6 and 7 were close to origin had mostly dominance genes, while the genotypes numbered 2 and 8 were far to the origin concluded as having mostly recessive genes. The genotype with number 1 was far to the regression line and it considered that epistatic gene effect may be effective (Figure 4). Ljubicic et al. [36] stated over dominance effect on grain weight per spike.

In terms of plant grain yield (GYP), Krasunia odes'ka had the highest value (11.68 g) among the parents, while Midas x Lucilla cross had the highest grain yield per plant (GYP) (22.38 g) among F_3 crosses. According to half diallel variance analysis, additive variance (a), dominance variance (b) and

components (b_1 and b_3) were found significantly different (Table 2). The genetic parameters were calculated according to the half diallel variance analysis and they were not significant. The difference between additive gene variance and dominance variance (D-H_1) was -33.421, which showed dominance gene variance for GYP. The average dominance degree $(H_1/D)^{1/2}$ was found as 2.312 and it indicated a dominance gene variance effect on GYP. The dominance and recessive allele frequencies ($H_2/4H_1$) were determined as 0.268 that indicated an imbalanced dominance and recessive allele frequencies (Table 2). The ratio of dominance and recessive alleles (KD/KR) was determined as 1.047 that showed the majority of dominance alleles. The gene number ($K= h^2/ H_2$) was determined as 0.202, therefore the gene number could not be determined. The theoretical dominance and actual value of parent were positively correlated which exhibited that the genotypes with higher grain yield were affected by recessive genes. The narrow sense heritability of the GYP was 0.151. The GCA and SCA values were found statistically different for grain yield per plant and the ratio of GCA/SCA was 2.83 which meant GCA was important for GYP and also affected by additive gene variance (Table 2). In terms of GCA of the parents, As-14 and Lucilla were positive and significant (1.804** and 1.889**, respectively) and Midas and Rumeli were negative and significant (-2.977** and -0.663**, respectively). In addition, the highest SCA value was obtained from As-14 x Lucilla cross (5.597**) (Table 3). The used methods to determine gene effects showed different results in the study. Based on the analysis made according to [15], it was concluded that GYP was controlled by dominance gene effect. In previous studies, El-Hosary et al. [35], Ljubicic et al. [36], Topal and Soylu [37], Altınbaş and Tosun [38] and Yao et al. [39] also reported dominance gene effect. On the other hand, both additive and non-additive gene effects was reported by [40] on GYP.

According to the Wr-Vr graphic for grain yield per plant, regression line crossed the Y axis under the origin on negative direction (a:-1.490). This situation was concluded as over dominance effect on the GYP (Figure 5). It was also supported by average dominance degree (2.312) of the GYP. The genotypes numbered as 1, 3, 4, 5, 6 and 7 were close to origin and mostly had dominance genes, while the genotypes numbered 2 and 8 were far to the origin and determined as having mostly recessive genes. Our findings were in agreement with Kutlu et al. [8] and Ljubicic et al. [36] who reported over dominance effect on grain weight per spike.

CONCLUSIONS

Based on genetic parameters, the non-additive gene effects (b and components, H_1, H_2 and SCA) were found as significant, thus the selections in earlier stages would decrease the selection success. Single plant selections could be made in latter stages and the bulk selection method might be suitable for the traits affected by non-additive gene effects in this study.

Krasunia odes'ka and Lucilla cultivars were the most suitable parents according to the GCA values, while Masaccio x Lucilla, Krasunia odes'ka x Lucilla, Krasunia odes'ka x Masaccio, Gl-14 x Masaccio, Esperia x Lucilla, Esperia x Masaccio, Esperia x Gl-14, As-14 x Krasunia odes'ka, Midas x Krasunia odes'ka and Midas x Gl-14 crosses had the highest SCA values and were concluded as promising crosses.

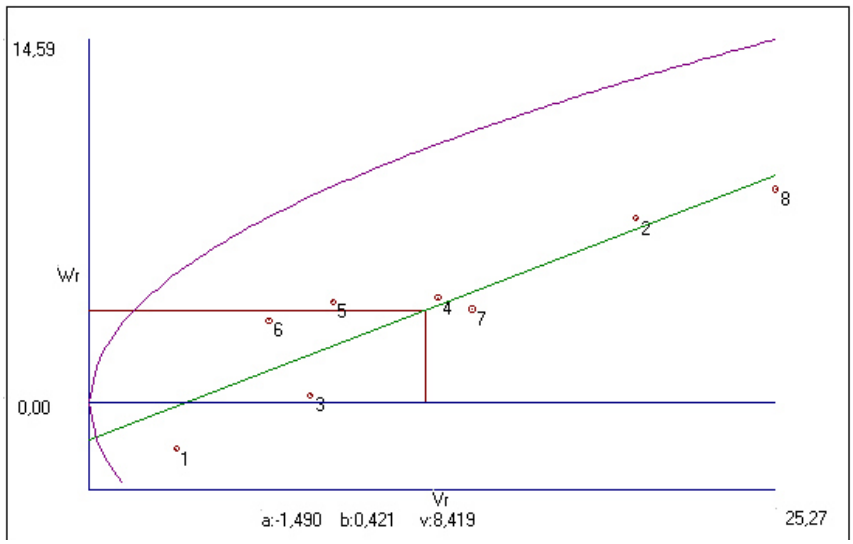

FIGURE 5
Wr/Vr Graphic for grain yield per plant
1-Midas, 2-As-14, 3-Rumeli, 4-Esperia, 5-Gl-14, 6-Krasunia odes'ka, 7-Masaccio, 8-Lucilla

TABLE 3
General and specific ability effects for investigated traits

Genotypes	Spike length	Spikelets per spike	Grains per spike	Grain weight per spike	Grain yield per plant
Midas (1)	-0.047	0.231	3.894**	0.241**	-2.977**
As-14 (2)	-0.352**	0.006	-2.631**	-0.167**	1.804**
Rumeli (3)	0.073	0.281	0.519	0.041	-0.663**
Esperia (4)	0.091	0.106	-4.031**	-0.166**	0.078
Gl-14 (5)	0.051	-0.394*	-1.106	-0.039	0.054
Krasunia odes'ka (6)	0.348**	0.381*	1.769	0.107*	0.093
Masaccio (7)	-0.287**	-0.794**	-1.431	-0.214**	-0.278
Lucilla (8)	0.123	0.181	3.019**	0.198**	1.889**
1x2	0.947**	2.269**	21.064**	0.932**	-2.664**
1x3	0.772**	-0.006	-3.836	-0.261	1.855**
1x4	0.179	-1.831**	4.464	-0.006	-1.534*
1x5	0.969**	1.919**	7.789**	0.406**	0.500
1x6	0.472*	-0.106	4.414	0.100	1.479*
1x7	0.257	-1.181**	-12.386**	-0.643**	-1.675*
1x8	-0.178	-0.156	-0.086	1.437**	-4.465**
2x3	0.327	0.969*	4.189	0.242	-1.038
2x4	0.084	0.144	-1.761	0.322	-1.604*
2x5	1.974**	-0.856	-8.936**	-0.313*	1.200
2x6	0.852**	2.869**	3.939	0.773**	0.301
2x7	-1.213**	-0.956*	-7.361**	-0.703**	-4.630**
2x8	0.177	-1.431**	-1.811	-0.380**	5.597**
3x4	1.134**	3.619**	-2.661	0.051	0.553
3x5	0.149	-1.381**	6.414**	0.404**	-1.981**
3x6	-0.973**	-2.156**	-0.461	-0.507**	4.123**
3x7	1.087**	1.019*	1.239	0.009	-4.423**
3x8	0.452*	0.044	3.539	0.957**	-3.001**
4x5	0.132	0.294	7.214**	0.228	1.930**
4x6	-0.016	-1.981**	-12.161**	-0.618**	-1.883**
4x7	1.319**	2.194**	5.789*	0.874**	-0.589
4x8	0.984**	-0.031	5.339*	0.251	4.108**
5x6	0.049	0.769*	9.164**	0.175	-3.432**
5x7	0.959**	0.944*	-2.386	0.116	2.632**
5x8	0.424*	0.719	-8.836**	-0.234	-1.053
6x7	1.587**	1.419**	15.739**	0.753**	-0.329
6x8	1.127**	2.694**	0.789	0.307*	-2.269**
7x8	1.012**	1.869**	26.989**	0.699**	1.489*

* $p \leq 0.05$; ** $p \leq 0.01$

REFERENCES

[1] Barutcular, C., Yildirim, M., Koc, M., Dizlek, H., Akinci, C., El Sabagh, A., Saneoka, H., Ueda, A., Islam, M.S., Toptas, I., Albayrak., O. and Tanrikulu, A. (2016) Quality traits performance of bread wheat genotypes under drought and heat stress conditions. Fresen. Environ. Bull. 25, 6159-6165.

[2] Gul, H., Hayit, F., Bicakci, S. and Acun, S. (2018) Effect of heat stabilized wheat germ on some properties of cookies. Fresen. Environ. Bull. 27, 1145-1151.

[3] Dorani, F., Ghavidel, R.A., Davood, M.G. and Ghavidel, R.A. (2016) Effect of soybean meal and basil seed gum on physical and sensory quality of wheat bread. Advances in Food Sciences. 38(1), 14-21.

[4] Hosseini, A. and Milani, J.M. (2016) Effect of coated bran on the physical properties of barbari bread. Advances in Food Sciences. 38(2), 70-75.

[5] TÜİK (2017) Turkish Statistical Institute. http://www.tuik.gov.tr. Access date: 15 September 2017.

[6] Erdem, H. and Torun, M.B. (2017) Assessment of sulphur efficiency of durum and bread wheat genotypes. Fresen. Environ. Bull. 26, 5891-5899.

[7] Barutçular, C., Yıldırım, M., Koç, M., Akıncı, C., Toptaş, I., Albayrak, O., Tanrıkulu, A. and El Sabagh, A. (2016) Evaluation of SPAD chlorophyll in spring wheat genotypes under different environments. Fresen. Environ. Bull. 25, 1258-1266.

[8] Kutlu, İ., Balkan, A. and Bilgin, O. (2015) Analysis of population differences and inheritance of some spike characteristics in bread wheat. KSU Journal of Natural Sciences. 18 (4), 40-47.

[9] Güngör, H. (2014) Inheritance of agronomical and fiber properties at half diallel crosses of some cotton (*Gossypium hirsutum* L. ve *Gossypium barbadense* L.) genotypes. University of Kahramanmaras Sutcu Imam, Graduate school of Natural and Applied Sciences, Department of field crops. Ph.D. Thesis. Kahramanmaraş. 211p.

[10] Verhalen, L.M. and Murray, J.C. (1967) A Diallel analysis of several fiber properties in upland cotton (G*ossypium hirsutum* L.). Crop Sci. 7, 501-505.

[11] Akgün, N. (2001) Inheritance of some agronomic characters in diallel crosses of durum wheat (*Triticum durum* Desf.). Selcuk University, Graduate school of Natural and Applied Sciences. Msc Thesis. Konya. 73p.

[12] Kanbertay, M. and Demir, İ. (1985) Studies on the Inheritance of periods and some other traits in four durum wheat hybrids. Journal of Agriculture Faculty of Ege University. 22, 91-111.

[13] Yıldırım, M.B., Öztürk, A., İkiz, F. and Püskülcü, H. (1979) Statistics in plant breeding-genetic methods. Directorate of Plant Protection Research Institute No:20, İzmir, 174p.

[14] Aksel, R., Johnson L.P.V. (1963) Analysis of diallel cross. A worked example. Advancing Frontiers of Plant Sci. 2, 37-53.

[15] Hayman, B.I. (1954a) The Analysis of variance of diallel tables. Biometrics. 10, 234-244.

[16] Jinks, J.L. and Hayman, B.I. (1953) The Analysis of diallel crosses. Maize Genet. Coop. News Letter. 27, 48-54.

[17] Jones, R.M. (1965) Analysis of variance of the half diallel table. Heredity. 20, 117-121.

[18] Yıldırım, M.B. and Şengonca, H. (1980) Diallel analysis. 4. Half diallel table variance analysis. Journal of Electronic accounting Sciences of Ege University. 3, 53-61.

[19] Hayman, B.I. (1954b) The Theory and analysis of diallel crosses. Genetics. 39, 789-809.

[20] Hayman, B.I. (1958) The Theory and analysis of diallel crosses. II. Genetics. 43, 63-85.

[21] Hayman, B.I. (1960) The Theory and analysis of diallel crosses. III. Genetics. 45, 155-172.

[22] Jinks, J.L. (1954) The Analysis of continous variation in a diallel cross of Nicotina Rustica varieties. Genetics. 39, 767-788.

[23] Jinks, J.L. (1956) The F_2 and backcross generation from a set of diallel crosses. Heredity. 10, 1-30.

[24] Griffing, B. (1956) Concept of general and specific combining ability in relation to diallel crossing systems. Aust.J.Biol. Sci. 9, 463-493.

[25] Özcan, K. (1999) A statistical packet program for population genetics. University of Ege, Graduate School of Natural and Applied Sciences, Department of field crops. Ph.D. Thesis. İzmir, 116 p.

[26] Aydogan, E. (2003) Determination of inheritance of some agricultural traits in common wheat by diallel analysis. Uludag Üniversity, Graduate School of Natural and Applied Sciences. Msc Thesis. Bursa. 58p.

[27] Aydoğan Çifci, E. and Yağdı, K. (2007) Determination of some agronomic traits by diallel hybrid analysis in common wheat (*Triticum aestivum* L.). Journal of Agricultural Sciences. 13(4), 354-364.

[28] Yağdı, K. and Ekingen, H.R. (1995) Inheritance for some agronomic traits in diallel crosses of five bread wheat. The Journal of Agricultural Faculty of Uludag University. 11, 81-93.

[29] Yıldırım, M. (2005) A study on heredity of some agronomical, physiological and quality characteristics in diallel F_1 offspring selected six bread wheat (*Triticum aestivum* L.) cultivars. University of Cukurova, Graduate school of Natural and Applied Sciences, Department of field crops. Ph.D. Thesis. Adana. 290p.

[30] Soylu, S. (1998) The Determination of suitable parents and crosses in durum wheat breeding for central Anatolian conditions through linextester method. University of Selcuk, Graduate School of Natural and Applied Sciences, Department of field crops. Ph.D. Thesis. Konya. 206p.

[31] Şener, O. (1997) Studies on the determination of inheritance of some agronomical characteristics by using the method of analysis of diallel crosses in common wheat. University of Cukurova, Graduate school of Natural and Applied Sciences, Department of field crops. Ph.D. Thesis. Adana. 155p.

[32] Chowdry, M.A., Arshad, M.T., Subhani, G.M. and Ihsan, K. (1997) Inheritance of some polygenic traits in Hexaploid Spring Wheat. Dep. of Plant Breeding and Genetics, Univ. of Agri. Faisalabad.

[33] Şener, O., Kılınç M. and Yağbasanlar, T. (2000) Estimation of inheritance of some agronomical characters in common wheat by diallel cross analysis. Turkish Journal of Agriculture and Forestry. 24(1), 121-127.

[34] Petrović, S., Dimitrijević, M., Ljubičić, N. and Banjac, B. (2012) Diallel analysis of quantitative traits in wheat crosses. In: Proceedings of the 47th Croatian and 7th International Symposium on Agriculture, Publisher University of Zagreb Faculty of Agriculture, Croatia, 313-317.

[35] El-Hosary, A.A., Gehan, A. and El-Deen, N. (2015) Genetic analysis in the F_1 and F_2 wheat generations of dilllel crosses. Egypt. J. Plant Breed. 19, 355 –373.

[36] Ljubicic, N., Petrovic, S., Kostic, M., Dimitrijevic, M., Hristov, N., Spika-Kondic, A. and Jevtic, R. (2017) Diallel analysis of some important grain yield traits bread wheat crosses. Turkish Journal of Field Crops. 22(1), 1-7.
[37] Topal, A. and Soylu, S. (1998) Studies on the determination of inheritance and heterosis of some agronomical characters in durum wheat (*Triticum durum* Desf.) diallel populations. The Journal of Agricultural Faculty of Selcuk University. 12, 1-6.
[38] Altınbaş M. and Tosun, M. (2002) Some agronomic and quality traits and interrelationships in the crosses between durum wheat (*Triticum durum* Desf.) and wild tetraploid wheat (*Triticum dicoccoides* Korn.). Anadolu J. of AARI. 12(1), 51-64.
[39] Yao, J., Ma, H., Yang, X., Yao, G. and Zhou, M. (2014) Inheritance of grain yield and its correlation with yield components in bread wheat (*Triticum aestivum* L.). Afr. J. Agric. Res. 13(12), 1379-1385.
[40] Tulukçu, E. and Sade, B. (2009) Identification of parents and hybrids with inheritance of some yield components of bread wheat using diallel methods in middle Anadolia conditions. Selcuk Journal of Agriculture and Food Sciences. 23(47), 18-26.

Received: **28.12.2017**
Accepted: **29.04.2018**

CORRESPONDING AUTHOR

Huseyin Gungor
Duzce University,
Faculty of Agriculture and Natural Sciences,
Department of Field Crops,
81620, Duzce – Turkey

e-mail: hgungor78@hotmail.com

© by PSP Volume 27 – No. 7/2018 pages 4867-4873 Fresenius Environmental Bulletin

BAROTRAUMA TREATMENT EFFECTS ON SURVIVAL RATES FOR SOME DISCARDED FISH BY TRAWL FISHERY

Emrah Simsek*, Aydin Demirci

Iskenderun Technical University Marine Sciences and Technology Faculty, Department of Marine Technologies, 31200, Iskenderun, Hatay, Turkey

ABSTRACT

The discard and its losses is an important issue with the principles of sustainable and responsible fishery for researchers and the fishing technology. In this study, discard fate, which is caught and released into the sea by discarding in the Iskenderun Bay trawl fishery, was investigated. Small individuals of *Nemipterus randalli* (N: 340), *Sparus aurata* (N: 236) and *Pagellus erythrinus* (N: 148) with low economic value were evaluated as discard fish in the commercial trawl fishery. In order to estimate survival rates, the three fish species individuals were taken to observation tanks on the fishing vessels and waited for 30 minutes after trawl was hauled. In addition to, barotrauma treatment experiments were carried out with a formed pressure tank which produces the pressure gradient at the depth where the species is caught. Barotrauma treatment has been providing a significant contribution to increase the discard survival rate. In particular, it was observed that barotrauma treatment significantly contributed to the survival rate of the *N. randalli* individuals. The discard survival rates of *N. randalli*, *S. aurata* and *P. erythrinus* were calculated 53.4%, 65%, 68.1% with barotrauma treatment and 12.9%, 41.8%, 59% with 1 atm respectively.

KEYWORDS:
Survival rate, discarded fish, Barotrauma treatment tank (BTT), Trawl Fishery

INTRODUCTION

Concept of fisheries has been changing day by day in accordance with the ecosystem approach. Nowadays, in global fisheries, ecosystem and protection are at the forefront instead of to catch more items [1, 2]. Sustainability, selectivity, charismatic fish species, protected species and discard concept in fisheries are essential issues in the fisheries research [2, 3].

Discard term in fisheries add up to the part of the catch giving back to the sea [4]. The annual amount of global discards was cited by Alverson et al. [5] in 1994, as 27 million tons while Kelleher [6] estimated it at 7.3 million tons in 2005. Studies have indicated that this value is approximately 10 million tons, in the last five years [2, 3]. This value ranges from 30% to 70% in the total catch for Iskenderun Bay trawl fishery [7]. The recent reform of the Common Fisheries Policy creates a landing obligation for species which are focus on catching limits and for species which are focus on the Minimum Conservation Reference Size as defined in Annex III of the 1967/2006 Regulation (EC) in the Mediterranean [8].

Fishing technology researches have been conducting very comprehensive studies sustainable ecosystem frame in different regions of the world to discard mitigation. [9-16]. These studies include modifications to increase species and length selectivity in trawl fishing gear [17-27]. Although there are positive results of these studies, discard and related mortality are still not well known in the trawl fishery. Estimation of discard mortality in fishery is basically carries out by using 2 methods. A method that can be defined as direct estimation. In this method, the survival rate is determined by observing in the tank the discarded individuals after the fishing operations [28, 29]. The other method can be called indirect methods. This method is evaluated by determining the differences in physiological parameters and behavioral impairment of discarded fish [30-35].

The main factor that affects survival rate when fish are discarded is the pressure differences and the resulting barotrauma effect [36-42]. These effects restrict swimming ability and behavior of fish by swelling the gases in body cavities especially in air-bladder [43]. This is an important problem especially in bony fish with swimming bladder [44-48]. In this study, exchanges of survival rates of discarded fish were investigated by turning depth pressure corresponding to the depth of the fish are caught with barotrauma treatment tank (BTT) after trawl operation.

MATERIALS AND METHODS

This study was conducted with commercial trawl fishing vessel in the Iskenderun Bay (Fig. 1). This region is preferred because of the depth and availability of the species used in the research.

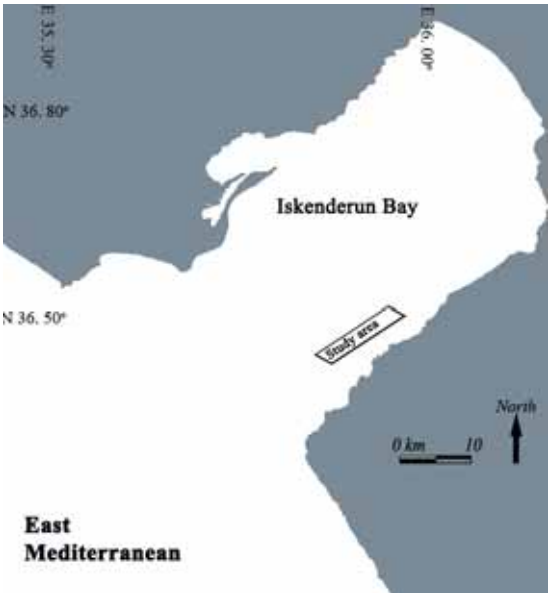

FIGURE 1
Study area (Iskenderun Bay-East Mediterranean)

TABLE 1
The information about the species used in the study.

Species	Barotrauma Treatment		Direct observation
	(N)	Mean length (cm)	Mean length (cm)
N. randalli	170	11.3±0.7	11.6±1.3
S. aurata	118	18.4±2.3	18.1±3.3
P. erythrinus	74	14.3±3.6	15.4±3.2

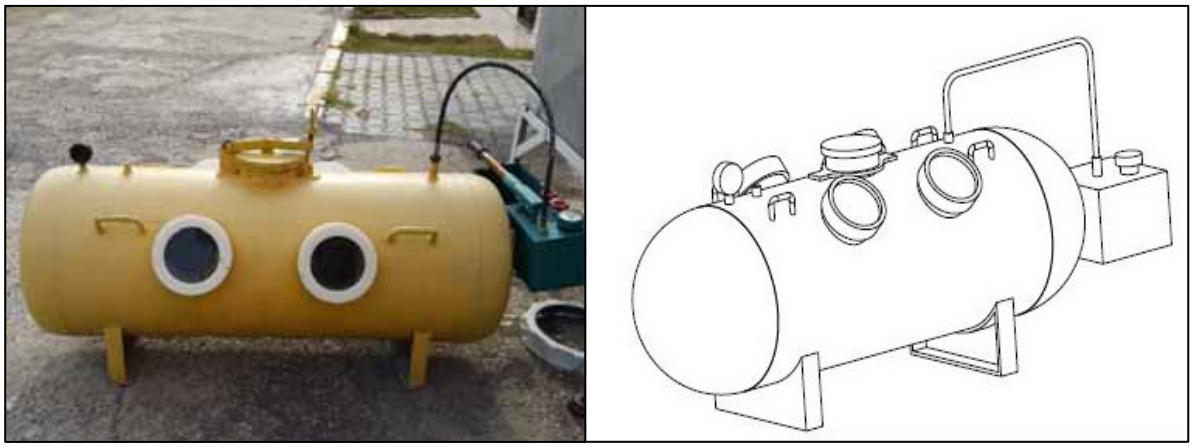

FIGURE 2
Barotrauma Treatment Tank (BTT)

10 trawl hauling operation were made for this study. All trawl hauling time is 120 minutes as standard for this study. The information about the species used in the study are given in Table 1.

Except for physically injuries or death, the fish exposed to barotrauma after trawling operation were observed in normal tank and barotrauma treatment tank (BTT). The tank is given Fig. 2 shows both real appearance and technical drawing. BTT is made of steel material and pressure to 16 bar test pressure. It has a capacity of 300 liters, transparent glass and water inlet. In this tank (BTT), the pressure is provided by simple hand pump. Immediately after fish have been put in this tank, the pressure is increased to 3 bar. Likewise, in the other group, the fish was taken to polyamide fish tanks size (Normal Tank) approximately the same.

The survival rates of discard were determined as percentages in the 30-minute observation results. The obtained results were compared with each other species separately by using ANOVA analysis in

SPSS package program. In addition, MANOVA test was used to demonstrate the overall effect of barotrauma treatment.

RESULTS AND DISCUSSION

In this study all individuals were treated with the assumption that they could be discarded after trawling operation. Because a significant proportion of the captured *P. erythrinus* and *S. aurata* individuals was below the minimum landing size (MLS) in this study. There was no minimum landing size (MLS) for *N. randalli*. At the same time mean length at first sexual maturity (Lm) for *N. randalli* in Iskenderun Bay is 11.02 cm [49]. At the end of this study it was observed that there were larger and smaller individuals in the *N. randalli*. In these experiments, the majority of *N. randalli* individuals affected by barotrauma indicated high survival rate with barotrauma treatment. This case was identified as a remarkable result for discarded N. randalli fate. were It was observed that When *N. randalli* individuals were observed in normal tanks without barotrauma treatment, it was recorded that the mortality occurred in a very short time. *N. randalli* individuals, which could not exhibit normal swimming behavior 15-20 minutes due to barotrauma in the normal fish observation tank, were showed rapid improvement and natural swimming behavior with 3 bar in barotrauma treatment tank (BTT). Because these barotrauma treatment experiments were limited to 30 minutes on the commercial fishing vessel, dead and survival individuals of *N. randalli* were determined rapidly (Table 2).

Survival rates of *N. randalli* individuals were showed that the barotrauma treatment gave successful results for survival rate after fishing operations. When SPSS ANOVA analysis was applied, it was observed that there were significant differences in survival rate. The survival rate data of *N. randalli* is the first data given after fishing operations.

TABLE 2
Survival rates for *N. randalli* after commercial trawl hauling operations with 30-minute observation in barotrauma treatment tank (BTT) and normal tank.

Hauling number	BTT (3 bar)			Normal Tank (1atm)		
	(N)	Survive	Survival rate (%)	(N)	Survive	Survival rate (%)
1	16	11	69	16	3	19
2	18	10	56	18	1	6
3	15	9	60	15	2	13
4	12	6	50	12	1	8
5	20	13	65	20	5	25
6	17	10	59	17	1	6
7	23	9	39	23	5	22
8	17	6	35	17	2	12
9	18	8	44	18	2	11
10	14	8	57	14	1	7
Mean			53.4±3.53			12.9±2.17

TABLE 3
Survival rates for *S. aurata* after commercial trawl hauling operations with 30-minute observation in barotrauma treatment tank (BTT) and normal tank

Hauling number	BTT (3 bar)			Normal Tank (1atm)		
	(N)	Survive	Survival rate (%)	(N)	Survive	Survival rate (%)
1	10	7	70	10	6	60
2	12	10	83	12	8	67
3	15	14	93	15	12	80
4	8	5	63	8	3	38
5	14	9	64	14	7	50
6	10	6	60	10	3	30
7	11	7	64	11	2	18
8	18	10	56	18	4	22
9	6	2	33	6	1	17
10	14	9	64	14	5	36
Mean			65±5.02			41.8±6.87

TABLE 4
Survival rates for *P. erythrinus* after commercial trawl hauling operations with 30-minute observation in barotrauma treatment tank (BTT) and normal tank

Hauling number	BTT (3 bar)			Normal Tank (1atm)		
	(N)	Survive	Survival rate (%)	(N)	Survive	Survival rate (%)
1	6	4	67	6	3	50
2	5	4	80	5	5	100
3	6	5	83	6	4	67
4	8	6	75	8	5	63
5	4	3	75	4	3	75
6	5	3	60	5	3	60
7	11	6	55	11	4	36
8	9	6	67	9	5	56
9	7	4	57	7	2	29
10	13	8	62	13	7	54
Mean			68.1±3.09			59±6.29

Survival rates for *S. aurata*, which is an important concentration in Iskenderun Bay trawl fisheries, were observed after trawl operation. Minimum landing size (MLS) for *S. aurata* 20 cm in the area. Nevertheless, lengths of captured *S. aurata* individuals in the area are below minimum landing size (MLS). It was observed that *S. aurata* had a very high survival rate after trawl operation. Although we were not observed barotrauma effects on *S. aurata* individuals after trawl hauling operation, we performed barotrauma treatment with barotrauma treatment tank (BTT). According to the results, barotrauma treatment gave positive result for survival rate of *S. aurata* not as much as *N. randalli* (Table 3). In statistical comparisons, barotrauma treatment was found to be beneficial by SPSS ANOVA analysis.

Survival rates of *P. erythrinus* were high after trawling fishery operations. This species has been evaluated as "Least Concern" according to the IUCN Red List of Threatened Species since 2014 [50]. However, there is no minimum landing size (MLS) for this species in our country commercial fishery regulations. At the same time mean length at first sexual maturity (Lm) of 14.2 cm for *P. erythrinus* in the Eastern Mediterranean [51]. Barotrauma treatment also gave positive results for this species according to observations of survival rate after the trawl hauling operation. The difference between the survival rates of barotrauma treatment and normal tanks was found to be significant by the ANOVA analysis of the SPSS package program.

Information of discard ratio was presented (as discards/total species catch) in EU Mediterranean (for Croatia, Greece, Italy and Spain) bottom trawl fisheries for selected bony fish, elasmobranch and decapod species [16]. According to Tsakagaris et al. (2017) [16], *P. erythrinus* showed different discard ratios depending on the regions. However, we could not find any literature about discard survival rates for *N. randalli*, *S. aurata* and *P. erythrinus* after trawl fishery operations. Therefore, discard survival rate data of these species could not be evaluated comparatively in this study.

CONCLUSIONS

As a result of this study, it was understood that pressure factor played an important role during the released for discard survival rates of *N. randalli*, *S. aurata* and *P. erythrinus* into the sea again. This study has showed that discards can survive after fishing operations if they release to sea under suitable conditions. The relevant literature on this issue also supports this idea.

ACKNOWLEDGEMENTS

This article is part of the first author's doctoral dissertation. The doctoral dissertation was supported by MKU-BAP and TUBITAK. Authors thanks to BAP Foundation of Mustafa Kemal University (Project No: 13484) and TUBITAK (Project No: 115O439) for their financial support. The authors would like to thank Dr. Yavuz MAZLUM from the Faculty of Marine Science and Technology Faculty Iskenderun Technical University for critical review of the manuscript.

REFERENCES

[1] Damalas, D. (2015) Mission impossible: Discard management plans for the EU Mediterranean fisheries under the reformed Common Fisheries Policy. Fisheries Research. 165, 96-99.

[2] Pauly, D. and Zeller, D. (2016) Catch reconstructions reveal that global marine fisheries catches are higher than reported and declining. Nature Communications. 7, 10244.

[3] Zeller, D., Cashion, T., Palomares, M. and Pauly, D. (2018) Global marine fisheries discards: A synthesis of reconstructed data. Fish and Fisheries. 19(1), 30-39.
[4] Catchpole, T.L., Feekings, J.P., Madsen, N., Palialexis, A., Vassilopoulou, V., Valeiras, J., Garcia, T., Nikolic, N. and Rochet, M-J. (2014) Using inferred drivers of discarding behaviour to evaluate discard mitigation measures. ICES Journal of Marine Science. 71(5), 1277-1285.
[5] Alverson, D.L., Freeberg, M.H., Murawski, S.A. and Pope, J.G. (1994) A global assessment of fisheries bycatch and discards. Fisheries Technical Paper. 339.
[6] Kelleher, K. (2005) Discards in the world's marine fisheries. FAO Fisheries Technical Paper. 470, 131.
[7] Demirci, A. (2003) Non-Target species and biomass of the Iskenderun Bay. Hatay: M. K. University, Institute of Science and Technology. Graduate Thesis.
[8] E.C. Council Regulation No. 1967/2006 of 21 December (2006) Concerning management measures for the sustainable exploitation of fishery resources in the Mediterranean Sea, amending Regulation (EEC) No. 2847/93 and repealing Regulation (EC) No. 1626/94. Official Journal of the European Union L, 409.
[9] Zeller, D. and Pauly, D. (2005) Good news, bad news: global fisheries discards are declining, but so are total catches. Fish and Fisheries. 6(2), 156-159.
[10] Catchpole, T.L. and Gray, T.S. (2010) Reducing discards of fish at sea: a review of European pilot projects. Journal of Environmental Management. 91, 717-723.
[11] Bellido, J.M., Santos, M.B., Pennino, M.G., Valeiras, X. and Pierce, G.J. (2011) Fishery discards and bycatch: solutions for an ecosystem approach to fisheries management? Hydrobiologia. 670(1), 317.
[12] Bellido, J.M., Carbonell, A., Garcia, M., Garcia, T. and González, M. (2014) The obligation to land all catches–consequences for the Mediterranean. European Parliament, Directorate-General for Internal Policies Policy Department B: Structural and Cohesion Policies. 52.
[13] Rochet, M.-J., Catchpole, T. and Cadrin, S. (2014) Bycatch and discards: from improved knowledge to mitigation programmes. ICES Journal of Marine Science. 71, 1216-1218.
[14] Sigurðardóttir, S., Stefánsdóttir, E.K., Condie, H., Margeirsson, S., Catchpole, T.L., Bellido, J.M., Eliasen, S.Q., Goñi, R., Madsen, N., Palialexis, A., Uhlmann S.S., Vassilopoulou, V., Feekings, J. and Rochet, M-J. (2015) How can discards in European fisheries be mitigated? Strengths, weaknesses, opportunities and threats of potential mitigation methods. Marine Policy. 51, 366-374.
[15] Paradinas, I., Marín, M., Grazia Pennino, M., López-Quílez, A., Conesa, D., Barreda, D., Gonzalez, M. and Bellido, J.M. (2016) Identifying the best fishing-suitable areas under the new European discard ban. ICES Journal of Marine Science. 73(10), 2479-2487.
[16] Tsagarakis, K., Carbonell, A., Brcic, J., Bellido, J.M., Carbonara, P., Casciaro, L., Edridge, A., García, T., González, M., Šifner, S.K., Machias, A., Notti E., Papantoniou, G., Sala, A., Škeljo, F., Vitale, S. and Vassilopoulou, V. (2017) Old Info for a New Fisheries Policy: Discard Ratios and Lengths at Discarding in EU Mediterranean Bottom Trawl Fisheries. Frontiers in Marine Science. 4, 99.
[17] Can, M.F., Demirci, A. and Demirci, S. (2006) Fisheries in Iskenderun Bay. Report of the ICES-FAO Working Group on Fishing Technology and Fish Behaviour (WGFTFB). 50.
[18] Macher, C., Guyader, O., Talidec, C. and Bertignac, M. (2008) A cost-benefit analysis of improving trawl selectivity in the case of discards: the *Nephrops norvegicus* fishery in the Bay of Biscay. Fisheries Research. 92(1), 76-89.
[19] Demirci, S. (2009) Size selectivity of square and diamond mesh trawl codend for fish with different body shapes. Ph.D. Thesis. Mustafa Kemal University, Hatay. 101p. (In Turkish).
[20] Feekings, J., Bartolino, V., Madsen, N. and Catchpole, T. (2012) Fishery discards: factors affecting their variability within a demersal trawl fishery. PloS one. 7(4), e36409.
[21] Sala, A., Lucchetti, A., Perdichizzi, A., Herrmann, B. and Rinelli, P. (2015) Is square-mesh better selective than larger mesh? A perspective on the management for Mediterranean trawl fisheries. Fisheries Research. 161, 182-190.
[22] Fauconnet, L. and Rochet, M.J. (2016) Fishing selectivity as an instrument to reach management objectives in an ecosystem approach to fisheries. Marine Policy. 64, 46-54.
[23] Sala, A., Herrmann, B., De Carlo, F., Lucchetti, A. and Brcic, J. (2016) Effect of codend circumference on the size selection of square-mesh codends in trawl fisheries. PLoS one. 11, e0160354.
[24] Demirci, S. and Akyurt, İ. (2017) Size selectivity of square and diamond mesh trawl codend for fish with different body shapes. Indian Journal of Geo-Marine Sciences. 46(4), 774-779.
[25] Demirci, S., Doğru, Z. and Şimşek, E. (2017) Effect of shortening the length of codend on brushtooth lizardfish caught in square mesh codend of otter trawl in Eastern Mediterranean. Indian Journal of Fisheries. 64(3), 29-34.

[26] McHugh, M.J., Broadhurst, M.K. and Sterling, D.J. (2017) Choosing anterior-gear modifications to reduce the global environmental impacts of penaeid trawls. Reviews in Fish Biology and Fisheries. 27(1), 111-134.
[27] Ulaş, F., Demirci, S. and Şimşek, E. (2017) The Importance of Visual on Trawl Codend Selectivity. International Advanced Researches & Engineering Congress Proceeding Book. 2228.
[28] Saygu, I. (2011) Determination of by-catch rays and their survival rates caught by demersal trawl fishery in the Antalya bay. Akdeniz University. M. Sc. Thesis 92p. (In Turkish)
[29] Saygu, İ. and Deval, M.C. (2014) The post-release survival of two skate species discarded by bottom trawl fisheries in Antalya Bay, Eastern Mediterranean. Turkish Journal of Fisheries and Aquatic Sciences. 14(4), 947-953.
[30] Davis, M.W. (2002) Key principles for understanding fish bycatch discard mortality. Canadian Journal of Fisheries and Aquatic Sciences. 59, 1834-1843.
[31] Davis, M.W. and Parker, S.J. (2004) Fish size and exposure to air: potential effects on behavioral impairment and mortality rates in discarded sablefish. North American Journal of Fisheries Management. 24, 518-524.
[32] Davis, M.W. (2005) Behaviour impairment in captured and released sablefish: ecological consequences and possible substitute measures for delayed discard mortality. Journal of Fish Biology. 66, 254-265.
[33] Davis, M.W. and Ottomar, M.L. (2006) Wounding and reflex impairment may be predictors for mortality in discarded or escaped fish. Fisheries Research. 82, 1-6.
[34] Davis, M.W. (2009) Fish stress and mortality can be predicted using reflex impairment. Fish and Fisheries. 11, 1-11.
[35] Brownscombe, J.W., Griffin, L.P., Gagne, T., Haak, C.R., Cooke, S.J. and Danylchuk, A.J. (2015) Physiological stress and reflex impairment of recreationally angled bonefish in Puerto Rico. Environmental Biology of Fishes. 98(11), 2287-2295.
[36] Jarvis, E.T. and Lowe, C.G. (2008) The effects of barotrauma on the catch-and-release survival of southern California nearshore and shelf rockfish (Scorpaenidae, Sebastes spp.). Canadian Journal of Fisheries and Aquatic Sciences. 65(7), 1286-1296.
[37] Brown, I., Sumpton, W., McLennan, M., Mayer, D., Campbell, M., Kirkwood, J., Butcher, A., Halliday, I., Mapleston, A., Welch D., Begg, G. A. and Sawynok, B. (2010) An improved technique for estimating short-term survival of released line-caught fish, and an application comparing barotrauma-relief methods in red emperor (*Lutjanus sebae* Cuvier 1816). Journal of Experimental Marine Biology and Ecology. 385(1), 1-7.
[38] Sumpton, W.D., Brown, I.W., Mayer, D.G., McLennan, M.F., Mapleston, A., Butcher, A.R., Welch, D.J., Kirkwood J. M., Sawynok, B. and Begg, G.A. (2010) Assessing the effects of line capture and barotrauma relief procedures on post-release survival of key tropical reef fish species in Australia using recreational tagging clubs. Fisheries Management and Ecology. 17(1), 77-88.
[39] Butcher, P.A., Broadhurst, M.K., Hall, K.C., Cullis, B.R. and Raidal, S.R. (2012) Assessing barotrauma among angled snapper (Pagrus auratus) and the utility of release methods. Fisheries Research. 127, 49-55.
[40] Carlson, T.J. (2012) Barotrauma in fish and barotrauma metrics. In: Popper, A.N., Hawkins, A. (eds.) The Effects of Noise on Aquatic Life. Springer New York, 229-233.
[41] Brown, R.S., Colotelo, A.H., Pflugrath, B.D., Boys, C.A., Baumgartner, L.J., Deng, Z.D., Silva, L.G.M., Brauner, C.J., Mallen-Cooper, M., Phonekhampeng, O., Thorncraft, G. and Singhanouvong, D. (2014) Understanding barotrauma in fish passing hydro structures: a global strategy for sustainable development of water resources. Fisheries. 39(3), 108-122.
[42] Hannah, R.W., Rankin, P.S. and Blume, M.T. (2014) The divergent effect of capture depth and associated barotrauma on post-recompression survival of canary (*Sebastes pinniger*) and yelloweye rockfish (*S. ruberrimus*). Fisheries Research. 157, 106-112.
[43] Rankin, P.S., Hannah, R.W., Blume, M.T., Miller-Morgan, T.J. and Heidel, J.R. (2017) Delayed effects of capture-induced barotrauma on physical condition and behavioral competency of recompressed yelloweye rockfish, *Sebastes ruberrimus*. Fisheries Research. 186, 258-268.
[44] Demirci, A., Demirci, S. and Şimşek, E. (2012) The Rate of Survival for Discards in Trawl Fishery. Fisheries and Aquatic Science Symposium Abstract Book. 61. (In Turkish).
[45] Şimşek, E. (2012) The Rate of Survival for Discards in Trawl Fishery. Mustafa Kemal University. M. Sc. Thesis. 28p. (In Turkish)
[46] Demirci A., Şimşek E. and Uluç S. (2013) Barotrauma in Fishery. Underwater Science and Technology Meeting Proceedings Book. 21-26. (In Turkish).

[47] Uluç, S. (2014) Barotrauma in fishing trials. Mustafa Kemal University. M. Sc. Thesis. 35p. (In Turkish)
[48] Şimşek E. and Demirci A. (2016) Analysis of Factors Affecting Life Fate of Groupers after Fishing Operations. Natural and Engineering Sciences. 1(3), 40.
[49] Demirci, S., Demirci, A. and Şimşek, E. (2018) Spawning Season and Size at Maturity of a Migrated Fish, Randall's Threadfın Bream (Nemipterus randalli) in Iskenderun Bay, Northeastern Mediterranean, Turkey. Fresen. Environ. Bull. 27, 503-507.
[50] IUCN, (2014) The IUCN Red List of Threatened Species-*Pagellus erythrinus* (Becker, Common Pandora, King of the Breams, Pandora, Spanish Sea Bream) http://www.iucnredlist.org/details/170224/0.
[51] Somarakis, S. and Machias, A. (2002) Age, growth and bathymetric distribution of red pandora (*Pagellus erythrinus*) on the Cretan shelf (eastern Mediterranean). Journal of the Marine Biological Association of the United Kingdom. 82(1), 149-160.

Received: **29.12.2017**
Accepted: **12.03.2018**

CORRESPONDING AUTHOR

Emrah Simsek
Iskenderun Technical University,
Marine Sciences and Technology Faculty,
Department of Marine Technologies,
31200, Iskenderun, Hatay – Turkey

e-mail: emrah.simsek@iste.edu.tr

© by PSP Volume 27 – No. 7/2018 pages 4874-4882 Fresenius Environmental Bulletin

COMPARISON OF MICROBIAL ACTIVITIES OF WETLANDS AREAS TO SOME SOIL CHARACTERISTICS

Ahu Alev Abaci-Bayar[1,*], Kadir Yilmaz[2]

[1]Soil Science and Plant Nutrition Department, Kirsehir Ahi Evran University, Agricultural Faculty, Kirsehir, 40200, Turkey
[2]Soil Science and Plant Nutrition Department, Kahramanmaras Sutcu Imam University, Agricultural Faculty, Kahramanmaras, 46100, Turkey,

ABSTRACT

The Eastern Mediterranean Region is described as the richest region in terms of wetlands and in this study aimed to examined the microbiological characteristics of the wetland lands of Amik, Gavur and Golbasi Lakes in Eastern Mediterranean Region. The relationships between total microorganism counts and some soil characteristics of 3 different wetland lands in the Eastern Mediterranean region have been determined. As a result of the biological analyzes carried out on three different wetland soils; the highest number of total actinomycetes were found from microorganisms in the field soils, this is followed by the moment of total algae, total bacteria and the total fungi. It was first observed that microbial activity in the soil of Amik Lake, where the most degradation was caused by drying, decreased. In the same area, the total amount of fungi, bacteria, algae and actinomycetes was found to be the lowest in this study. It has been found that the total amount of fungi, bacteria and actinomycetes in the soil of Gavur Lake, which has been degraded to moderate level, is the highest value. It has been observed that the total amount of algae is the highest in the Golbasi Lakes, which is still partially preserving its wetland characteristics. As a result, it has been determined that all microorganism groups in the Gavur and Golbasi Lake areas are considerably higher than Amik Lake soil, which has undergone decaying, based on the lands in the lake. There were statistical relations between total fungi with the soil organic matter (r= 0.432**), percent saturation (r= 0.555***), soil reaction (r= -0.526***), plastic limit (r= 0.413**) and liquid limit (r= 0.414**) values. There was a positive relationship between total algae with organic matter (r= 0.541***), and negative relations with soil reaction (r= -0.484***). It was determined that there was a positive correlation between the total actinomycet and the plastic limit and the liquid limit (r= 0.437**, r= 0.362*), which is negative between bulk weight and hydraulic conductivity (r= -0.360*, r= -0.381**).

KEYWORDS:
Wetland, Soil, Microorganism, Degradation, Drought

INTRODUCTION

Wetlands can be distinguished by three main criteria: hydrology, physico-chemical environment and biodiversity. They are natural areas, where biological diversity is the richest, with the functions and values that cannot be compared with any other ecosystem on earth. Soil, in addition to its physical and chemical functions, has a complex biological structure [1]. Microorganisms that provide biological activity in the soil provide soil fertility in various forms [2]. It is known that the major groups of microorganisms are bacteria, algae, fungus and actinomycetes [3]. The plant and organic layer on the soil are both a source of nutrients and shelter for fungi. All soil microorganisms are critically important in the preservation of soil functions, with their roles in key ecosystem processes such as decomposition of organic material; removal of toxic substances; carbon, nitrogen, phosphorus and sulfur cycles and formation of soil structure in natural soils and tillages [4]. The wetland ecosystem is characterized by hydric soils that support hydrophilic vegetation. Hydrology is known as a dominant factor that controls microbial processes in wetlands [5-6-7]. High water level increases the rate of the anaerobic functions such as denitrification, methane genesis and, amount of sulphate reducing [8]. And the aerobic function such as nitrification decreases this rate [9].

In a study in Amik, Gavur and Golbasi Lakes, the chemical properties of the field soils were investigated; and the higher level of degradation and mineral decomposition in Amik Lake soils is explained by the higher pH value of the plain soil and the relative increase in the amount of calcium carbonate in the soil [10]. The soil reaction is important for plant growth; and it has been noted that, pH has a great effect on the plant's uptake of nutrients, the solubility of toxic ions in water and the activity of microorganisms [11]. Many studies have indicated that; microbial activity should naturally increase as the level of organic material increases; and the microorganism activity and especially the number of fungi raise in environments where soil pH is low [12-15]. The decomposition of soil organic matter is proportional to the functions of all microorganisms in the soil.

The purpose of this study is; determine the total microorganism population in wetland soils of Gavur,

Amik and Golbasi Lakes, which are located in the Eastern Mediterranean Region. The statistics of the total numbers of microorganisms among the three areas were examined by making comparisons.

MATERIALS AND METHODS

Working area. Amik, Gavur and Golbasi Lakes, located in Eastern Mediterranean Region, are considered as important wetlands of Turkey (Figure 1). Amik Lake, which is the first research area, is located within the boundaries of the Hatay province of the Mediterranean Region. Gavur Lake, which is chosen as the second research area, is located in the Antakya-Kahramanmaras graben and with an average altitude of 478 m above sea level. The third research area was Golbasi Lakes in Adiyaman province. The Golbasi Lakes (Inekli, Azapli and Golbasi Lake), which form the most important wetland between the Mediterranean Region and the Southeastern Anatolia Region, are located in the Golbasi Depression within the Eastern Anatolian Fault Zone. Soil specimens were taken from the soil profiles opened with a cross section from the lake open-water zone of Amik, Gavur and Golbasi Lakes, according to the horizon basis. For microbiological analysis, 48 soil samples were used as material in this study.

Methods. The total number of microorganisms in the soil samples taken was determined in accordance with the principles reported by Jackson [16], Potato Dextrose Agar (PDA) medium for determining the total number of fungi; Plate Count Agar (PCA) medium for determining the total number of bacteria; algae medium for determining the total number of algae, and starch-casein medium for determining the total actinomycetes were created according to methods reported by Kiziloglu and Bilen [17]. Percentage of saturation with water was analyzed according to Demiralay (1993) [18], soil reaction analysis by Thomas [19], electrical conductivity by Tüzüner [20], organic matter analysis by Nelson and Sommers [21], available phoshorus analysis by Olsen et al. [22] reported by Kuo [23], bulk density analysis reported by Demiralay (1993) [18], aggregate stability analysis by Kemper and Koch [24], plastic limit and liguid limit analysis by Sayin [25]. Variance analysis was performed by using SPSS program (IBM SPSS Advanced Statistics version 19.0.0) with the data obtained from the biological analyses on all 48 soil samples taken from Amik, Gavur and Golbasi Lakes wetlands. As a result of the variance analysis performed on both the field soils and the soil contained in the lake open-water zone, the differences between the groups that were found to be significant were examined by Duncan's multiple comparison tests. In addition, a logarithmic transformation has been applied to the data to provide the assumptions of the variance analysis.

RESULTS AND DISCUSSION

The results of the biological analysis performed on three different areas are given in Table 1. When Table 1 was examined, the maximum average number of fungi was found in Gavur Lake soil with $3.97*10^5$ cfu g^{-1}, followed by Golbasi Lakes and Amik Lake respectively. The total number of bacteria was found to be the highest in Gavur Lake and the lowest in Amik Lake. The total number of algae was highest in Golbasi Lakes and the lowest in Amik Lake, and the total number of actinomycetes was found to be highest in the Gavur Lake and the least at Amik Lake. It was observed that the lowest total fungi, bacteria, algae and actinomycetes were found in the soil of Amik Lake, while the highest number of total fungi, bacteria and actinomycetes were found in Gavur Lake and the highest number of algae was found in Golbasi Lakes.

FIGURE 1
Satellite view of work areas

TABLE 1
Total number of soil microorganisms

Horizon	Fungi	Bacteria	Algae	Actinomycete
	cfu g^{-1}	cfu g^{-1}	cfu g^{-1}	cfu g^{-1}
		Amik Lake		
Minimum	$1.10*10^3$	$7.30*10^4$	$1.30*10^3$	$5.00*10^3$
Maximum	$6.00*10^5$	$1.09*10^6$	$2.40*10^5$	$4.05*10^6$
Average	$9.47*10^4$	$2.76*10^5$	$7.18*10^4$	$1.05*10^6$
		Gavur Lake		
Minimum	$4.00*10^3$	$2.90*10^4$	$2.00*10^3$	$4.20*10^4$
Maximum	$1.20*10^6$	$8.42*10^6$	$7.04*10^6$	$2.17*10^7$
Average	$3.97*10^5$	$1.34*10^6$	$1.19*10^6$	$3.26*10^6$
		Golbasi Lakes		
Minimum	$1.30*10^3$	$9.30*10^3$	$1.25*10^4$	$2.63*10^4$
Maximum	$2.50*10^6$	$8.40*10^6$	$1.39*10^7$	$1.53*10^7$
Average	$3.60*10^5$	$1.20*10^6$	$1.80*10^6$	$3.03*10^6$

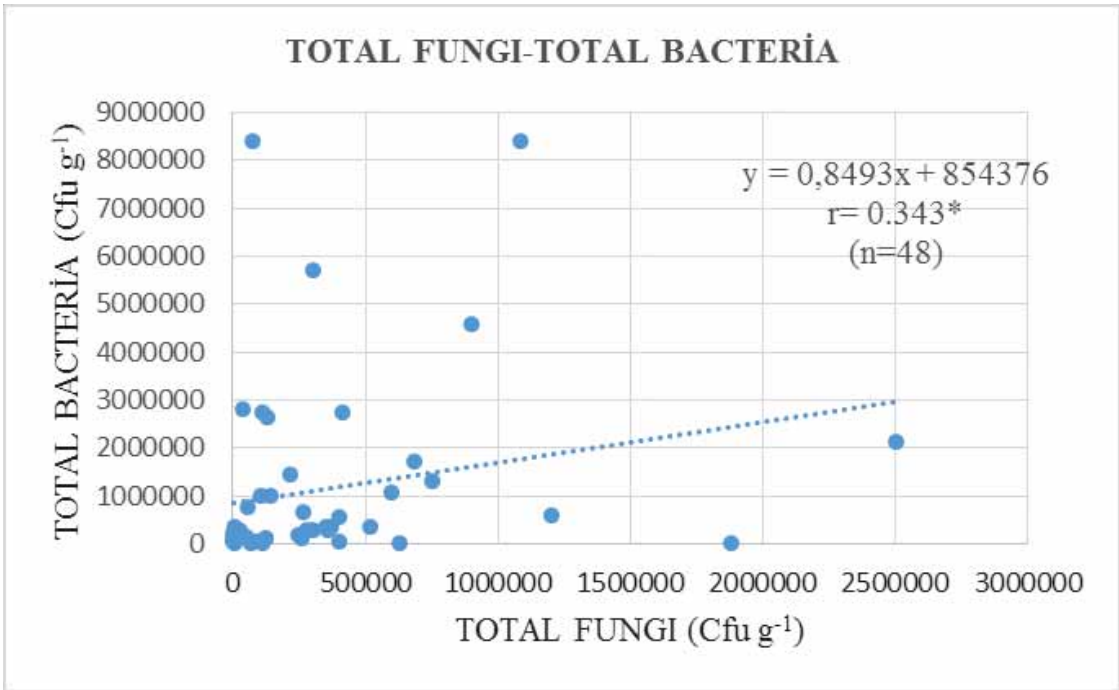

FIGURE 2
Relationship between total fungi and total bacteria

As a result of the correlation analysis, it was determined that there is a significant positive correlation ($p<0.5$) between the total number of fungi in the soil and the total number of bacteria (Figure 2). Similar findings have been reported by He et al. [26], where researchers have studied the soil under different vegetation. They reported that there was a strong positive correlation between total bacteria and total fungus counts by performing Pearson correlation analysis. The most important role of bacteria and fungi in the soil is to provide soil ventilation. It was determined that there was a significant positive correlation ($p<0.01$, $p<0.01$) between the total number of fungi and the total number of algae and the total number of actinomycetes. These findings support that the optimal living conditions for fungi and actinomycetes are similar. Huang et al. [27], have identified 3 wetlands in China's Chongqing city as pilot; and they have studied soil microorganisms and enzyme activities. They pointed out that there was a positive correlation between the total number of fungi in the soil and total actinomycete at the $p<0.01$ significance level. Egambardiyeva [28] investigated the microbial population activity in the soil of the Chatkal biosphere reserve. For this, 5 different soils (typical sierozem soil, dark sierozem soil, brown carbonated soil, typical brown soil, decomposed brown soil) were identified; and it was concluded that the least microbial activity was in sierozem soil and the most activity was in brown carbonated soil. İt has been reported that there is a similar increase in total actinomycetes and fungus amounts, especially in brown carbonated soil.

As a result of the correlation analysis between the total number of fungi in the soil and the saturation percentage value, soil organic matter and available phosphorus value; it is found that there is a significant positive ($p<0.01$, $p<0.1$, $p<0.5$) relationship. Since soil organisms play an important role in the decomposition of organic residues that fall on the soil, the diminution or disappearance of these creatures causes the organic waste falling to the soil to remain and accumulate for a long time without decomposing. Decreasing or stopping of the decomposition also slows down the supply of mineral nutrients required for plants [29]. As reported by Abaci Bayar [10], the amount of organic matter (1.23%) of Amik Lake soils, which are dried and subjected to the most soil degradation, is much lower than the amount of organic matter (11.42%) of Gavur Lake soils. In this case, it can be stated that the total microbial activity in Gavur Lake is higher than the microbial activity in the soil of Amik Lake. It was found by the same researcher that the value of the saturation percentage of Gavur Lake soils is different and higher than the values of Amik Lake and Golbasi Lakes.

It was determined that there is a significant negative ($p<0.01$) relationship between the total number of fungi and soil reaction. Many studies have indicated that there is a negative relationship between the amount of fungi in the soil and the soil reaction, regarding the numbers of microorganisms in both arid and rainy seasons. Because; it is found that the total number of fungi in the soil is the highest when the soil's pH is low and the soil is acidic; and many species of fungi can develop in these soils and they form the dominant flora [30]. Rousk et al. [31] in the research conducted in North and South America on arable lands; indicated that soil pH is associated with soil microorganisms and fungus concentration increases at low pH. They have indicated that fungal populations exhibit optimal growth and development at the maximum level at 4.5 pH value, and are less affected by pH and have a weaker relationship with it. This finding was supported by Aciego-Pietri and Brookes [32]. Vineela et al. [14], in a study conducted in semi-arid regions of India; have reported that, the microbial activity and especially the number of fungi have increased in environments where soil pH is low. Deslippe et al. [33], reported a negative correlation between the total amount of microorganisms and the soil reaction in their research, indicating that microbiological activity decreased at high pH.

It is stated that there is a significant negative ($p<0.1$) relationship between the total number of fungi and the volume weight of soil. Similar findings were reported by Li et al. [34]; in the experimental farm of Henan Agricultural University in China; that there is a negative correlation between volume weight and number of fungi in corn-cultivated soils; and the increase in volume weight negatively affects microorganism numbers and microbial activity. It was determined that there is a significantly positive ($p<0.5$, $p<0.1$, $p<0.1$) relationship between the total number of fungi and the wet aggregate stability, and between plastic limit and liquid limit values. Soil microorganisms show better growth in the soil with a good aggregate structure. In the research conducted by Kadioglu [35] on the lands of Tuzcu and Tepe villages, it was determined that from the topographic positions of peak point to the foothill, aggregate stability and total number of the fungi have increased.

As a result of the correlation analysis, it was determined that there was a significant positive correlation ($p<0.01$) between the total number of bacteria and the total number of total algae and total actinomycetes. Balasooriya et al. [9]; at the study on the wetland in the northern part of Bourgoyen-Ossemeersen in Belgium; have stated that, the amount of bacteria and the amount of actinomycetes increases, as the depth increases. It was stated that there was a significant positive correlation ($p<0.5$, $p<0.1$) between total bacterial count, and soil saturation percentage value and amount of organic matter. Soil organic matter is the source of nutrients for microorganisms in the soil. In particular, the soil organic matter consists of all the vegetative and animal carcass materials and their transformed products in and on the mineral soil. Naturally, as the level of organic matter increases, microbial activity will naturally increase. Morrissey et al. [36], in their search near Chesapeake Bay (Virginia); have stated that soil organic matter and active microbial activity in the soil are proportional to each other and there is a very strong positive correlation between them. Jeanneau et al. [37] and Kadioglu [35] found that there is a positive correlation between soil organic matter and microorganism amount. They stated that there is a high number of bacteria in the soil where the soil organic matter content is high and there is a positive relation between them.

It was found that there is a significant positive correlation ($p<0.01$) between the total number of algae and the total number of actinomycetes. Anand et al. [38], in their study at Canada in the Ontario region on the soil of industrial air pollution near Sudbury; Reported a positive correlation between total blue green algae and total actinomycetes numbers at $p<0.05$ significance level. It was found that there was a significant negative correlation ($p<0.01$) between the total number of algae and the soil reaction, and a significant positive correlation ($p<0.01$) between the total number of algae and the soil organic matter value (Figure 3). Lombard et al. [39] reported that microorganism structure in the soil and soil function are related to some physical and chemical properties such as soil pH and organic matter content.

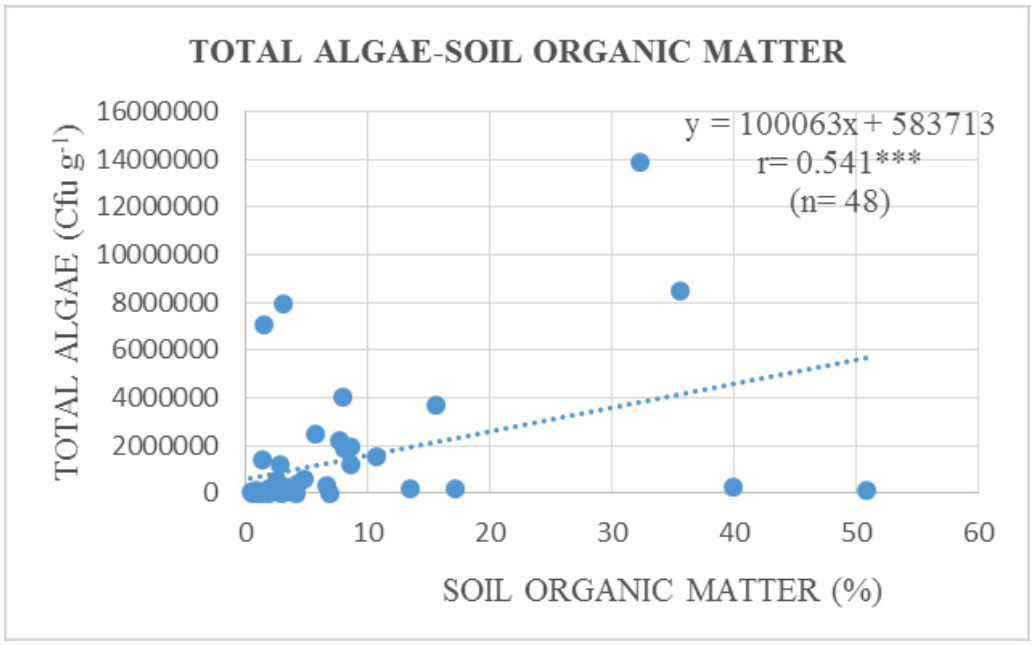

FIGURE 3
Relationship between total algae and soil organic matter

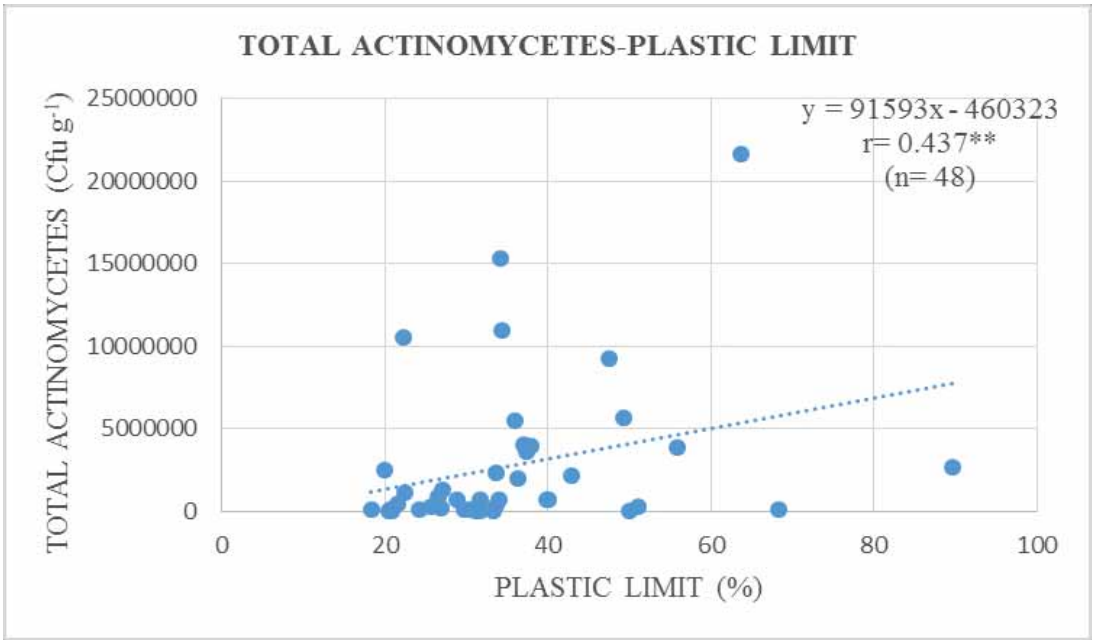

FIGURE 4
Relationship between total actinomycetes and plastic limit

Organic matter has a great effect on microorganisms by being basic nutrients in the soil, and serving nutrients to plants. Rousk et al. [15] reported that soil pH is associated with soil microorganisms, and it has been found that some microorganisms and algae are abundant in mild acid and slightly alkaline soil.

As a result of the correlation analysis made in the soil; ($p<0.5$, $p<0.01$) between the total number of actinomycetes in the soil and the percentage of saturations and organic matter values. In Gokcan's work [40] in Amasya Suluova, it has been observed that there is a linear increase in microbial activity due to the increase of organic matter in the soil. However, as the profile is followed to the lower layers; It has also been reported that there is a decrease in the microorganism population depending on organic matter and nutrient reduction. A significant negative ($p<0.5$, $p<0.1$) relationship was found between the total actinomycete number and the volume weight of the soil and the hydraulic conductivity value. In Li et al.'s study [34] conducted in China, similar findings indicated that there was a negative correlation between volume and actinomycete numbers in cultivated land and that the increase in volume was negatively affecting the number of microorganisms and

microbial activity. A significant positive correlation ($p<0.5$) was found between the total number of actinomycetes and the plastic limit and the liquid limit as the result of the correlation analysis (Figure 4).

One way analysis of variance was performed on the distributions of microorganisms in the first two horizons of Amik Lake, Gavur Lake and Golbasi Lakes soils, and the logarithmic transformation is applied to give the assumptions of the variance analysis. The difference between total fungus and total algae counts of Gavur and Golbasi Lakes soils was not statistically significant. The total number of fungi and total algae of Amik Lake soils were found to be different and lower than the values of the other two lake area soils. The difference between the total number of fungi and algae in the soil of Amik Lake and the soil of these two lake areas was statistically significant ($p<0.05$). It is stated that the difference in statistics between total bacteria and total actinomycet numbers of the Amik, Gavur and Golbasi Lakes soils is not significant. Organisms respond very quickly to soil and environmental changes. Udotong et al. [30] reported that the number of microorganisms in soil samples taken during the rainy season is higher than the population of microorganisms in the dry area, in the study of microbiological and physico-chemical field on the wetland soil in the Eketan city of Nigeria. Especially the high level of groundwater level of the Amik Lowland soils from the research area can be shown as the reason for the microorganism population to be lower than the other lake areas. Microorganisms that provide soil biologic activity provide soil fertility in a variety of forms. It is known that some rocks, especially serpentine, release the toxic elements (nickel, cadmium) that prevent plant life and at the same time inhibit microbial life [1]. By Abaci Bayar [10], it is stated that, limestone rich in calcium and serpentine rich in magnesium are widely found in the research areas of Amik, Gavur and Golbasi Lakes. It is thought that the alterable magnesium contents of Amik Lake is different and higher than the content of magnesium of Gavur and Golbasi Lakes, because of the more widespread serpentin-derived rocks in this area. It is known that in the regions of Islahiye, Hassa and Kirikhan, where lowland is fed with surface waters, serpentine rocks are widespread and many mining operations, where chromium mine is excavated, are found. Along with these findings; the fact that the presence of serpentine is dominant in the soil of Amik Lake, reveals that the population of microorganisms is lower. This data shows how wetland lands, which are intended to be included in agricultural production and use, are transformed into low-productivity soils.

When the research area in the open-water zone soils of the lakes are considered; all the microorganism groups in Gavur and Golbasi Lake area were found to be quite higher than the soils of Amik Lake; and the difference between the significant groups was examined by Duncan multiple comparison test and given in Table 2. Although the difference between the total number of algae of the Gavur and Golbasi Lakes is not statistically significant, the difference between the total number of algae of the Amik Lake and the other two lakes is statistically significant ($p<0.05$). It is known that, at the top of the main nutrition sources of microorganisms are the organic matter found in the soil. As stated by Abaci Bayar [10], the organic matter levels of the soils of Golbasi and Gavur Lakes (5.44%, 11.42%) are higher than the organic matter value of the soil of Amik (1.23%), which makes it possible to find higher microorganism populations in this soil. The productivity of soils is closely related to the level of keeping soil organisms. Along with the transformation of nutrients into the form that they can be used by the plants, the soil fertility ensures that many physical and chemical conditions are at suitable levels for plant breeding. The low level of organic matter in the soil affects the microbial activity, which causes the productivity of the soil to decrease or disappear. From this point of view, the productivity of Amik lowland soils is less than that of Golbasi and Gavur Lake lands. The fertility of the Amik lowland's soils, which began degradation many years ago, was observed at lower levels than the Gavur Lake and Golbasi soils that underwent less degradation. In addition the correlation table of some microbiological, physical and chemical analyzes made in the study area is shown in Table 3.

TABLE 2
Multiple comparison test of the microbiological properties of the soil in the lake open-water zone (Duncan Test) results

Area	Number	Fungi cfu g^{-1}	Bacteria cfu g^{-1}	Algae cfu g^{-1}	Actinomycete cfu g^{-1}
Amik Lake	6	4.6746±0.817	5.4240±0.341	4.6030^{b}±0.908	6.0038±0.579
Gavur Lake	8	5.2576±0.784	5.4782±0.553	5.1375^{a}±1.044	6.1308±0.846
Golbasi Lakes	16	5.2781±0.605	5.6476±0.916	5.8241^{a}±0.992	6.2055±0.896
Sig.		p<0.197	p<0.778	p<0.039	p<0.879

The average values shown in the same column with different symbols according to Duncan test was statistically significant at $p\leq0.05$.

TABLE 3
Correlation chart of microbiological, physical and chemical analyses made in soil

	TF	TB	TA	Tac	SP	OM	AP	pH	Db	WAS	Ks	PL	LL
TF	-												
TB	0.343*	-											
TA	0.487***	0.593***	-										
Tac	0.525***	0.592***	0.753***	-									
SP	0.555***	0.285*		0.366*	-								
OM	0.432**	0.390**	0.541***	0.506***	-	-							
AP	0.306*	-	-	-	-	-	-						
pH	-0.526***	-	-0.484***	-	-	-	-	-					
Db	-0.427**	-	-	-0.360*	-	-	-	-	-				
WAS	0.329*	-	-	-	-	-	-	-	-	-			
Ks	-	-	-	-0.381**	-	-	-	-	-	-	-		
PL	0.413**	-	-	0.437**	-	-	-	-	-	-	-	-	
LL	0.414**	-	-	0.362*	-	-	-	-	-	-	-	-	-

TF=Total fungus; TB=Total bacteria; TA=Total algae; Tac=Total actinomycete; SP=Saturation percentage; OM=Organic matter; AP=Available phosohorus; pH=Soil reaction; Db= Volume weight; WAS= Wet aggregate stability; Ks= Hydraulic conductivity; PL=Plastic limit; LL= Liquid limit

CONCLUSIONS

Wetlands are one of the most important ecosystem types of the earth with their natural functions and economic values, balancing the water regime of the environment, regulating the climate, realizing the highest of the world's carbon retaining function after the tropical forest and oceans, hosting many living creatures, and having extremely high biological productivity.

In this study, attempts were made to determine the changes occurring as the result of the applications on the three wetlands extending in the Eastern Mediterranean Region. These three wetlands are listed as Amik Lake in the south, Gavur Lake in the north, and Golbasi Lakes in the north. The elevation of the region increases from south to north, reaching 478 m in Gavur Lake basin and 885 m in Golbasi basin, while the height of the Amik basin is 83 m from the sea. The biological characteristics of a total of 48 soil samples in both the lake area and the lake open-water area of the research areas were examined, and the findings were evaluated, and the sizes of soil degradation in each field were compared in terms of microbial values. Although the difference between total fungus and total algae numbers of Gavur and Golbasi Lakes area is not statistically significant, the difference between total fungus and total algae counts of Amik Lake and two other lake areas is statistically significant. Firstly, it was observed that microbial activity decreased in Amik Lake soil, where the most degradation was occurred by drying, and total amount of fungi, bacteria, algae and actinomycetes were found to be at their lowest values. Microbial life is prevented because of the reasons such as the high level of groundwater level of the Amik Lake area soil, the widespread availability of serpentine, which is rich in magnesia, in the area. It is known that serpentine rocks are common in Islahiye, Hassa and Kirikhan regions, where lowland is fed with surface runoff waters, and many mining operations, from which chromium mine is extracted, are found. The amount of total algae was found to be the highest in the Golbasi Lakes, which partially retained their wetland characteristics. The Gavur Lake, which is moderately degraded, has the highest levels of total fungi, bacteria and actinomycetes in the soil. When the microorganism values of the soils of the lake open-water zone are examined statistically; although the difference between the total number of algae of the Gavur and Golbasi Lakes lands is not statistically significant; the difference between the total number of algae of the Lake Amik and the other two lakes is statistically significant. As the organic matter level of the Golbasi and Gavur Lake lands is higher than the organic matter level of the Amik Lake soils; populations of microorganisms in the soil were also found at higher levels. The extremely low microbial activity of the Amik Lake soils, which is one of our most important wetlands that have been dried and cultivated, has been assessed as a sign that the productivity of these soils are at low levels.

Amik Lake; depending on the beginning of the drying of its soils before the other lake areas; has lost its wetland characteristics due to the high level of mineralization and degradation in the soil. Despite there is a spatial increase in the agricultural land in this area, which is opened to agriculture by drying; it is concluded that, today, the fertility of the soil is in low levels regarding the crop production considering the many negative features present in the soil, and there also will be problems in the future. The area that is started to be dried in the second place was the wetland of Lake Gavur. Because of the inadequacy of the drainage channels in the ground, it is observed that; the soils were under the water during a significant part of the year, the progress that had been expected from the agricultural production couldn't be achieved, and after all, it lacked the economical and natural contributions of the lowlands as it had lost its lowland characteristics. The result was that the Golbasi Lakes soils, which had the least soil degradation, maintained their wetland characteristics at a better level than the other lake areas.

REFERENCES

[1] Schulz, S., Brankatschk, R., Dumig, A., Kogel-Knabner, I., Schloter, M., Zeyer, J. (2013) The role of microorganisms at different stages of ecosystem development for soil formation. Biogeosciences, 10, 3983-3996.

[2] Unver, İ., Cokusal, B., Anac, D., Kilic, C.C., Eryuce, N., Gurbuz Kilic, O., Colak Esetlili, B. (2011) Soil Knowledge and Plant Nutrition. Anadolu University Publication No: 2302 Academic Teaching Faculty Publication No: 1299.

[3] Revenga, C., Kura, Y. (2003) Status and Trends of Biodiversity of Inland Water Ecosystems. Secretariat of the Convention on Biological Diversity, Montreal, Technical Series No. 11.

[4] Garbeva, P., Van Veen, J.A., Van Elsas, J.D. (2004) Microbial Diversity in Soil: Selection of Microbial Populations by Plant and Soil Type and Implications for Disease Suppressiveness. Annu. Rev. Phytopathol. 42, 243-70.

[5] Bardgett, R.D., Shine, A. (1999) Linkages between plant litter diversity, soil microbial biomass and ecosystem function in temperate grasslands. Soil Biol. Biochem. 31, 317-321.

[6] Gutknecht, J.L.M., Goodman, R.M., Balser, T.C. (2006) Linking soil processes and microbial ecology in freshwater wetland ecosystems. Plant Soil. 289, 17-34.

[7] Mentzer, J.L., Goodman, R., Balser, T.C. (2006) Microbial seasonal response to hydrologic and fertilization treatments in a simulated wet prairie. Plant Soil. 284, 85-100.

[8] Coles, J.R.P., Yavitt, J.B. (2004) Linking below ground carbon allocation to anaerobic CH_4 and CO_2 production in a forested peat land, New York State. Geomicrobiol. 21, 445-455.

[9] Balasooriya, W.K., Denef, K., Peters, J., Verhoest, N.E.C., Boeckx, P. (2008) Vegetation composition and soil microbial community structural changes along a wetland hydrological gradient. Hydrology and Earth System Sciences. 12, 277-291.

[10] Abaci Bayar, A.A. (2016) Soil characteristics, efficiency levels and problems of wetlands in the eastern Mediterranean region. Kahraman maraş Sutcu Imam University, Institute of Science. Department of Soil Science and Plant Nutrition. Doctoral Thesis. 120-123p.

[11] Yaras K., Dasgan, H.Y. (2012) The Effect of Micronize-Bentonite-Sulfur and Organic Matter Applied to Soil in Greenhouse Conditions on Soil pH, Tomato Plant Growth, Yield and Fruit Quality. Agricultural Science Research Journal. 5(1), 175-180.

[12] Lewis, L., Clark, L., Krapf, R., Manning, M., Staats, J., Subirge, T., Townsend, L., Ypsilantis, B. (2003) Riparian Area Management Riparian-Wetland Soils. Technical Reference 1737-19. BLM National Business Center Printed Materials Distribution Service, BC-652.

[13] Altunbas, S. (2005) Investigation of the Degradation Dimensions of Some Wetlands in Goats by Substrate Level. Doctoral Thesis. Institute of Natural and Applied Sciences, Akdeniz University. Antalya.

[14] Vineela, C., Wani, S.P., Srinivasarao, C., Padmaja, B., Vittal, K.P.R. (2008) Microbial properties of soils as affected by cropping and nutrient management practices in several long-term manurial experiments in the semi-arid tropics of India. Applied soil ecology science direct. 40, 165-173.

[15] Rousk, J., Brookes, P.C., Baath, E. (2010a) The microbial PLFA composition as affected by pH in an arable soil. Soil Biol Biochem. 42, 516-520.

[16] Jackson, M.L. (1962) Soil Chemical Analysis. Prentice-Hall Inc., 183.

[17] Kiziloglu, T., Bilen, S. (1997) Soil Microbiology Laboratory Practice Book, Atatürk University Faculty of Agriculture Course publications No: 198. Erzurum.

[18] Demiralay, I. (1993) Soil Physical Analysis. Ataturk University Agricultural Faculty Publications. No:143, pp: 131, Erzurum.

[19] Thomas, G.W. (1996) Soil pH and Acidity. In: Sparks, D.L. (ed.) Method of Soil Analysis: Chemical Methods. Part 3. SSSA, Madison, WI. 475-491.

[20] Tüzüner, A. (1990) Soil and Water Analysis Laboratories Handbook. T.C. Ministry of Agriculture, Forestry and Rural Affairs General Directorate of Village Services. 21-27.

[21] Nelson, D.W., Sommers, L.E. (1996) Total Carbon, Organic Carbon, and Organic Matter. In: D.L. Sparks (ed.) Method of Soil Analysis: Chemical Methods. Part 3. SSSA, Madison, WI. 9611011.

[22] Olsen, S.R., Cole, V., Watanabe, F.S., Dean, L.A. (1954) Estimation of Available Phosphorus in Soils by Extraction with Sodium Bicarbonate. Washington D.C. U.S. Department of Agriculture.

[23] Kuo, S. (1996) Phosphorus. In: Sparks, D.L. (Ed.) Methods of Soil Analysis. Part 3, Chemical Methods, SSSA Book Series Number 5, SSSA., Madison, WI. 869-921.

[24] Kemper, W.D., Koch, E.J. (1966) Aggregate Stability of Soils from Western United States and Canada. U.S. Dept. Agriculture Tech. Bull. No. 1355.

[25] Sayın, M. (1981) Soil Mechanics Lecture Notes. Cukurova Univ. Faculty of Agriculture Soil Department. Adana.

[26] He, X.Y., Wang, K.L., Zhang, W., Chen, Z.H., Zhu, Y.G., Chen, H.S. (2008) Positive correlation between soil bacterial metabolic and plant species diversity and bacterial and fungal diversity in a vegetation succession on Karst. Plant Soil. 307, 123-134.
[27] Huang, L, Gao, X., Liu, M., Du, G., Guo, J., Ntakirutimana, T. (2012) Correlation among soil microorganisms, soil enzyme activities, and removal rates of pollutants in three constructed wetlands purifying micro-polluted river water. Ecological Engineering. 46, 98-106.
[28] Egamberdiyeva, D. (2006) Comparative analysis of the dynamics and functions of rhizosphere soil microbial community in two ecosystems of the Chatkal Biosphere Reserve. United Nations educational, Scientific and Cultural Organization, Final Report Tashkent State University of Agriculture, Uzbekistan.
[29] Kantarci, M. D. (2000) Soil Science. Istanbul University, Department of Earth Science and Ecology, Istanbul University Publication No. 4261, Faculty of Forestry Publication No. 462, Istanbul, 420p.
[30] Udotong, I.R., John, O.U.M., Udotong, I.R.J. (2008) Microbiological and Physicochemical Studies of Wetland Soils in Eket, Nigeria. World Academy of Science, Engineering and Technology International Journal of Biological, Biomolecular, Agricultural, Food and Biotechnological Engineering. 2(8), 176-181.
[31] Rousk, J., Baath, E., Brookes, P.C., Lauber, C.L., Lozupone, C., Caporaso, J.G., Knight, R., Fierer, N. (2010b) Soil bacterial and fungal communities across a pH gradient in an arable soil. 2010 International Society for Microbial Ecology. The ISME Journal. 4, 1340-1351.
[32] Aciego Pietri, J.C., Brookes, P.C. (2009) Substrate inputs and pH as factors controlling microbial biomass, activity and community structure in an arable soil. Soil Biol Biochem. 41, 1396-1405.
[33] Deslippe, J.R., Hartmann, M., Simard, S.W., Mohn, W.W. (2012) Long-term warming alters the composition of Arctic soil microbial communities. FEMS Microbiol Ecol. 82, 303-315.
[34] Li, C.H., Ma, B.L., Zhang, T.Q. (2002) Soil Bulk Density Effects on Soil Microbial Populations and Enzyme Activities During the Growth of Maize (*Zea Mays* L.) Planted in Large Pots Under Field Exposure. Can. J. Soil. Sci. 82(2), 147-154.
[35] Kadioglu, B. (2007) The Change of Some Soil Quality Index Parameters in Different Types of Topographical Positions in Embroidered Agriculture and Pasture Areas. Master Thesis. Ataturk University, Institute of Science, Department of Soil Science.
[36] Morrissey, E.M., Gillespie, J.L., Morina, J.C., Franklin, R.B. (2014) Salinity Affects Microbial Activity and Soil Organic Matter Content in Tidal Wetlands. Global Change Biology. 20, 1351-1362.
[37] Jeanneau, L., Jaffrezic, A., Pierson-Wickmann, A.C., Gruau, G., Lambert, T., Petitjean, P. (2014) Constraints on the Sources and Production Mechanisms of Dissolved Organic Matter in Soils from Molecular Biomarkers. Vadose zone Journal. 13(7).
[38] Anand, M., Ma, K.M., Okonski, A., Levin, S., McCreath, D. (2003) Characterising biocomplexity and soil microbial dynamics along a smelter-damaged landscape gradient. The Science of the Total Environment. 311, 247-259.
[39] Lombard, N., Prestat, E., Van Elsas, J.D., Simonet, P. (2011) Soil specific limitations for access and analysis of soil microbial communities by metagenomics. FEMS Microbiol. Ecol. 78, 31-49.
[40] Gokcan, E. (2012) Effects of Animal Compost and Biogas Wastes on Some Physical, Chemical and Microbiological Characteristics of Soils. Graduate Thesis. Department of Soil Science and Plant Nutrition, Gaziosmanpasa University Institute of Science.

Received: **05.01.2018**
Accepted: **16.05.2018**

CORRESPONDING AUTHOR

Ahu Alev Abaci-Bayar
Soil Science and Plant Nutrition Department,
Kirsehir Ahi Evran University,
Agricultural Faculty,
Kirsehir, 40200 – Turkey

e-mail: ahuabaci@gmail.com

© by PSP Volume 27 – No. 7/2018 pages 4883-4888 Fresenius Environmental Bulletin

ENVIRONMENTAL ASSESSMENT OF MANGANESE SULFATE RESIDUES DERIVED FROM PYROLUSITE PROCESS

Yongqiong Yang[1], Hannian Gu[2,*], Tengfei Guo[2,3], Yang Dai[2,3], Ning Wang[2]

[1]School of Geographic and Environmental Sciences, Guizhou Normal University, Guiyang 550001, China
[2]Key Laboratory of High-temperature and High-pressure Study of the Earth's Interior, Institute of Geochemistry, Chinese Academy of Sciences, Guiyang, 550081, China
[3]University of Chinese Academy of Sciences, Beijing 100049, China

ABSTRACT

Manganese sulfate residues would be generated when pyrolusite ore is used for manganese sulfate production. Two kinds of residues derived from different pyrolusite processes were characterized using XRF, ICP-MS, XRD and SEM, including manganese sulfate residue from pyrolusite and pyrite method (MSR-PP) and manganese sulfate residue from flue-gas desulfurization method (MSR-FD). The concentrations of water-soluble metals from MSR-PP and MSR-FD were investigated. It shows that water-soluble manganese concentrations in MSR-PP and MSR-FD were as high as 1850 and 2170 mg/L, respectively, which might be a manganese contaminant source. Extraction procedure for leaching toxicity experiments shows that MSR-PP should be identified as hazardous waste for its extraction metal of nickel achieved 5.79 mg/L.

KEYWORDS:
Manganese sulfate residue, characterization, toxicity assessment,pyrolusite, nickel

INTRODUCTION

Manganese has been widely used in industry. Pyrolusite (MnO_2) and rhodochrosite ($MnCO_3$) are the two most common mineral forms of manganese ores in China. For low valance manganese ores ($MnCO_3$), hydrometallurgical process can be used directly to obtain manganese through acid leaching and separation. For high valance manganese as main mineral (MnO_2), ores have to be treated through reduction roasting followed by acid leaching;alternatively, directly reductive leaching in acid medium in presence of different reductants [1]. The common reducing agents reported in literatures for manganese dioxide hydrometallurgical reduction and extraction include ferrous iron, H_2O_2 [2], sulfur dioxide/flue-gas [3, 4], sulfides, ig. sphalerite [5], CaS [6], pyrite [7, 8], organics matters, like methanol [9], oxalic acid [10], glucose [11], and waste/by-product of plant, such as sawdust [12], cane molasses [13], corncob [14], waste tea [15], etc.

In reality, most of the above reductants were based on laboratory scale study for reason of cost or efficiency. However, SO_2 flue-gas and pyrite have well been extended and applied as reductive leaching for low grade manganese oxide ores in industrial production for Chinese manufacturing enterprises. Correspondingly, two types of manganese sulfate residues would be generated from the two process.

Manganese sulfate residue from pyrolusite and pyrite (MSR-PP), is generated in the process of extraction of manganese sulfate production using pyrite as reductant. The pyrolusite and pyrite method, also called two-ores method, is a conventional method for manganese sulfate production and suitable for ores with 18-30% Mn, by which process about 50% manganese sulfate was produced in China. To produce 1 ton of manganese sulfate, 2-3 tons of MSR-PP would be produced (based on manganese ore with 20% Mn), and the situation is getting worse as the grade of manganese ores decreases with the depletion of rich ore resources.

Manganese sulfate residue from flue-gas desulfurization (MSR-FD), discharged from manganese mineral powder leaching process in presence of flue-gas desulfurization is another manganese sulfate residue. The flue-gas desulfurization method is newly developed for treatment of lower manganese ores (of 15-20 wt % Mn) and also solve the problem of flue-gas. What's more, under the same yield of manganese sulfate, the amount of MSR-FD is less than MSR-PP, ca. 2 tons for per ton manganese sulfate.

The aim of the present work was to characterize the two manganese sulfate residues and assess the environmental impacts of water soluble heavy elements. The corrosivity and toxicity test was also employed in this study to identify the category of manganese sulfate residues.

EXPERIMENT

Samples and analysis methods. Two kinds of manganese sulfate residues (MSR-FD and MSR-PP) were collected from a manganese sulfate plant in Guizhou, southwest of China. Representative samples were crushed and thoroughly homogenized for characterization and toxicity leaching test.

The main chemical compositions of the collected samples were determined using XRF (PANalytical PW2424), and the XRF analysis was determined in conjunction with a loss-on-ignition (LOI) at 1000°C. The resulting data from both determinations are combined to produce a "total". ICP-MS (Perkin Elmer Elan 9000) was used to analyze trace elements concentration in the samples. Residue samples were also characterized by powder X-ray diffraction (XRD) and scanning electron microscopy (SEM). Powder X-ray diffraction measurements were performed using a PANalytical Empyrean diffractometer with Cu Kα radiation. Samples were prepared by compaction into a silicon sample holder, and a 2θ range between 5° and 70° was scanned. Samples for SEM observation were viewed in an FEI Scios scanning electron microscope with an Oxford Instruments Energy 250 energy dispersive spectrometer system (EDS).

Water leaching and extraction toxicity experiments. Regarding to water leaching experiments, residue samples were leached using distilled water to investigate the water-soluble form of metal ion concentration**.** Specifically, 10.0 grams of each residue sample was weighted and placed in a 250 mL conical flask with 100 mL distilled water. After 8 h shaking and 16 h standing, the solution was centrifuged and filtered. The leached solution was then stored for water-soluble metal determination (ICP-MS or ICP-AES).

The corrosivity and toxicity of manganese sulfate residues were tested according to the standards for hazardous properties for hazardous wastes, i.e., the identification standard for hazardous wastes - Identification for corrosivity (Chinese national standard GB5085.1-2007) and Identification standard for hazardous wastes - Identification for extraction toxicity (Chinese national standard GB5085.3-2007), respectively. Specifically, 150 grams of each residue sample was weighted and placed in a conical flask with 1500 mL extraction solution, which was made up of guaranteed reagents (2:1 V/V of H_2SO_4: HNO_3) with a pH 3.2. After 18 h shaking, the acids extraction solution was centrifuged and filtered. The leached solution was then collected for extraction toxicity determination (ICP-MS or ICP-AES).

RESULTS AND DISCUSSION

Chemical composition. The results of major chemical composition of the samples obtained using XRF are listed in Table 1. It shows that SiO_2, Fe_2O_3, MnO, SO_3 and Al_2O_3 occurred as major constituents in both MSR-PP and MSR-FD. High SiO_2 and low MnO content of MSR-FD indicated a better efficiency of manganese extraction for flue-gas desulfurization method in comparison to two-ores method. The content of Fe_2O_3 in the two residues was close, of ca. 18-19%. Especially, CaO in MSR-PP was as high as 6.54%, while MSR-FD only contained 0.29% CaO. This difference can be attributed to pyrite accompanying with high calcium, and also addition of lime for neutralization in process of two-ore method. K_2O, Na_2O, MgO and TiO_2 were present in the both residues, but in less quantities, with contents of less than 1%.

Generally, trace metals can transfer and enrich in industrial by-product wastes in comparison to raw ores for extraction or separation of the valuable components. As an example of bauxite residue, gallium, scandium, yttrium and lanthanides were widely reported as secondary resources [16], whilst As, Cr and radioactive elements were regarded as hazardous to environment for the high concentrations [17-19]. In the study, from aspects of resource and environment, trace elemental analysis of the manganese sulfate residues was performed. Table 2 gives the minor and trace elements concentrations in MSR-FD and MSR-PP determined by ICP-MS. Ba presented in both MSR-FD and MSR-PP as the minor component,

TABLE 1
Main chemical composition of manganese sulfate residues (wt %)

Sample	SiO_2	Fe_2O_3	MnO	SO_3	Al_2O_3	CaO	K_2O	MgO	Na_2O	NiO	P_2O_5	TiO_2	LOI
MSR-PP	33.09	18.42	7.29	22.2	3.94	6.54	0.44	0.50	0.03	0.18	0.38	0.08	22.95
MSR-FD	54.06	19.74	4.81	6.18	5.23	0.29	0.45	0.08	0.58	0.04	0.60	0.12	11.79

TABLE 2
Concentrations of trace elements in MSR-FD and MSR-PP (μg/g)

	Ba	Ce	Cr	Cs	Dy	Er	Eu	Ga	Gd	Hf	Ho	La	Lu	Nb	Nd
MSR-PP	9640	144.5	280	3.33	11.50	6.34	2.43	15.0	12.65	1.5	2.34	70.2	0.79	5.5	53.0
MSR-FD	5700	135.5	370	2.74	11.70	6.72	2.50	13.1	12.35	1.9	2.40	70.3	0.91	6.8	53.5
	Pr	Rb	Sm	Sn	Sr	Ta	Tb	Th	Tm	U	V	W	Y	Yb	Zr
MSR-PP	13.15	22.1	11.30	29	720	1.0	1.93	4.25	0.85	5.79	461	6	83.0	5.11	58
MSR-FD	13.35	25.8	11.35	3	395	0.4	1.91	5.99	0.93	7.10	613	5	74.4	5.85	72

with a concentration of 5700 and 9640 μg/g, respectively. Rare elements including gallium, niobium, yttrium and lanthanides were lower than those in bauxite residue, and it had no economic value in current conditions.

Mineral composition. Powder X-ray diffraction was performed (Fig. 1) to identify the mineral phase composition of the two manganese sulfate residues since they are from different processes and possess different chemical compositions.

Quartz can be matched in XRD curves of MSR-FD and MSR-PP, and it was the dominant mineral phase accordingly to the chemical composition. Silicon oxide came from manganese ore without chemical reaction during the both hydrometallurgical leaching process. Iron, naturally present with manganese minerals, was mostly found in the form of iron alumosilicates and in small amounts in the manganese oxides [20]. Along with the dissolution of manganese oxides, iron oxides also entered into the solution, and then would be precipitated in the residue when manganese sulfate was separated. As observed from Fig.1, goethite and iron sulfite were suggested as iron-phase in MSR-FD, while hematite was obviously indentified in the pattern of MSR-PP. Besides, MSR-PP contained calcium sulfate, including gypsum ($CaSO_4 \cdot 2H_2O$) and calcium sulfate hydrate ($CaSO_4 \cdot 0.5H_2O$).

SEM analysis. The SEM micrographs of the samples are presented in Fig. 2. As seen from the images, MSR-PP was composed of (i) Columnar or large blocked idiomorphic structure, identified for gypsum by EDS, (ii) large particles, and (iii) very fine particles. The surfaces of large particles aggravated with small particles with complex compositions. SEM micrographs of MSR-FD also present different size of particles. The surface of silicon oxides was smooth with a clear crystal face (Fig. 2 B, point a), whilst the particles of manganese oxides had a porous surface with irregular shapes (Fig. 2 B, point b). The particle sizes of both residues generally were less than 10 microns.

Environmental properties: water-soluble metals. Water-soluble metals from the two kinds of manganese sulfate residues were determined and the

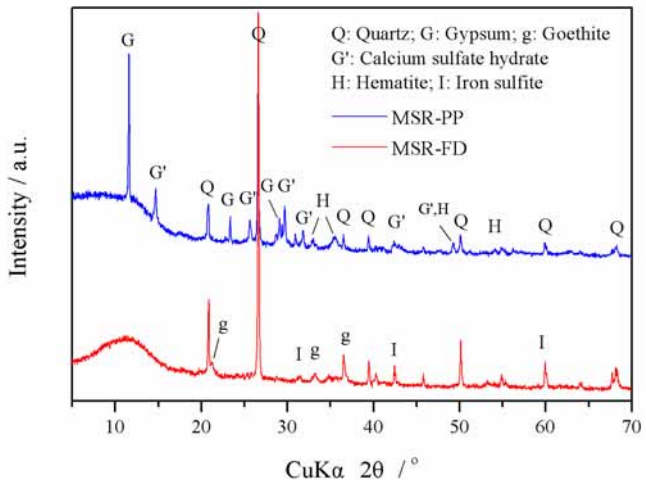

FIGURE 1
XRD patterns of MSR-PP and MSR-FD

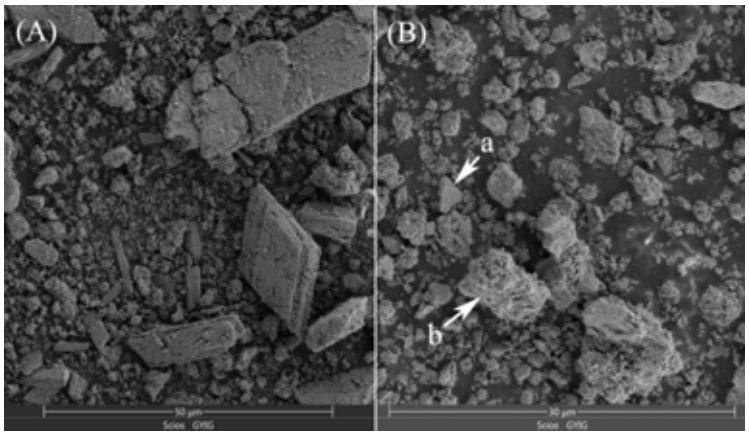

FIGURE 2
SEM images of manganese sulfate residues, (A) MSR-PP and (B) MSR-FD

data are presented in Table 3. It shows that the concentrations of silver, arsenic, beryllium, chromium, mercury and lead were under the concentration limits value stipulated in *Integrated Wastewater Discharge Standard (GB8978-1996).* However, the water-soluble cadmium and nickel in the leachate of both MSR-PP and MSR-FD exceeded the limit value, especially in MSR-PP the concentrations were as high as 0.771 and 5.11 mg/L, respectively. Table 3 also gives the concentrations of some metals which were not stipulated in the *Integrated Wastewater Discharge Standard.* The water-soluble manganese from MSR-PP and MSR-FD reached 1850 and 2170 mg/L, respectively. Although manganese is an essential metal, in excess, it is neurotoxic [21, 22]. According to the World Health Organization, concentration of manganese <0.1 mg/L in tap water is acceptable for users, but it is recommended that the concentration does not exceed 0.05 mg/L [23]. Manganese plays an important role inmetabolism and is essential for humans. However, it can also produce toxic effects, provided that their intake surpasses the suggested upper limits [24]. Since the water-soluble manganese concentrations of leachate from both MSR-PP and MSR-FD reached ca. 2000 mg/L, the residue could be a contaminated source when the rain water occurred on them.

Environmental properties: Identification for extraction toxicity. "Hazardous waste" is a category designated by the Basel Convention on the Control of Trans boundary Movements of Hazardous Wastes and Their Disposal for substances which present one or more hazardous properties, i.e. corrosivity and toxicity. In this study, the corrosivity and toxicity test from the MRS samples were conducted (Table 4). The results show that the pH values of samples do not exceed the corrosivity limit. However, nickel concentration of extracting solution from MSR-PP slightly exceed the limit value stipulated in *Identification standard for hazardous wastes-Identification for extraction toxicity* (GB5085.1-7, 2007). Therefore, MSR-PP should be categorized as a hazardous material, while MSR-FD is general industrial waste.

From this perspective, MSR-PP cannot be discharged directly for hazardous waste should be managed in a special way. MSR-PP is generated by the pyrolusite and pyrite method for manganese sulfate production, and nickel might come form pyrolusite or pyrite. It indicates that using flue-gas desulfurization to produce manganese sulfate is a clean industrial method, which discharge the residue with less contaminant than the pyrolusite and pyrite method.

TABLE 3
Testing results for water-soluble metals from manganese sulfate residues

	Unit	MSR-PP	MSR-FD	Limits [a]
Ag	mg/L	<0.001	<0.001	0.5
As	mg/L	0.01	<0.001	0.5
Be	mg/L	<0.001	<0.001	0.005
Cd	mg/L	0.771	0.253	0.1
Total Cr	mg/L	<0.001	<0.001	1.5
Hg	mg/L	0.001	0.002	0.05
Ni	mg/L	5.11	1.455	1.0
Pb	mg/L	0.001	0.001	1.0
Al	mg/L	0.71	0.72	
Cu	mg/L	0.001	0.002	
Fe	mg/L	0.04	0.11	
Mn	mg/L	1850	2170	
Se	mg/L	0.01	0.01	
Zn	mg/L	0.78	1.00	
pH		6.9	6.6	6-9

[a]The limits of water-soluble metals are reference to Integrated Wastewater Discharge Standard (GB 8978-1996).

TABLE 4
Testing results for corrosivity and extraction toxicity of manganese sulfate residues

	Unit	MSR-PP	MSR-FD	Limits [a]
Ag	mg/L	<0.001	<0.001	5
As	mg/L	0.01	<0.001	5
Ba	mg/L	0.151	0.113	100
Be	mg/L	<0.001	<0.001	0.02
Cd	mg/L	0.800	0.270	1
Cr	mg/L	<0.001	0.001	15
Cu	mg/L	0.001	0.001	100
Hg	mg/L	<0.001	0.005	0.1
Ni	mg/L	5.79	1.530	5
Pb	mg/L	0.001	0.002	5
Se	mg/L	0.01	0.01	1
Zn	mg/L	0.46	0.63	100
CN^-	mg/L	<0.005	<0.005	5
F^-	mg/L	0.99	0.53	100
pH		6.8	6.6	2.0-12.5

[a]The limits of hazardous properties are reference to Identification standard for hazardous wastes (GB5085.1-7, 2007).

CONCLUSIONS

The characteristics of manganese sulfate residues depend on ore sources and refining processes. Overall, two kinds of manganese sulfate residues (MSR-PP and MSR-FD) had a similar major components with a different content. MSR-PP had a high content of manganese (7.29% MnO) and sulphate (ca. 22 % SO_3) and low content of silicon (ca. 33% SiO_2), while MSR-FD contained high silicon (ca. 54% SiO_2) and low manganese (4.81% MnO) and sulphate (ca. 6% SO_3). In additional, MSR-PP contained 6.54% CaO, which was in the form of gypsum and calcium sulfate hydrate from the XRD analysis. Quartz was the dominant phase in the both residues.

Water-soluble manganese concentrations in MSR-PP and MSR-FD were as high as 1850 and 2170 mg/L, respectively. The high concentration of manganese was thought to be a contaminant source for environment pollution. Extraction procedure for leaching toxicity experiments showed that MSR-PP was identified as hazardous waste for its extraction metal of nickel achieved 5.79 mg/L while MSR-FD was a general waste according to Chinese Standard.

ACKNOWLEDGEMENTS

The work was financially supported by National Natural Science Foundation of China (Grant No. 41402039), Guizhou Provincial Science and Technology Foundation ([2014] 2130; [2016] 1155; LH[2017]7344) and Guizhou Science and Technology Major Program (No. [2016] 3015). The authors are grateful to Dr Y. Meng for the analytical test and examination.

REFERENCES

[1] Wang, Y., Jin, S., Lv, Y., Zhang, Y. and Su, H. (2017) Hydrometallurgical process and kinetics of leaching manganese from semi-oxidized manganese ores with sucrose. Minerals. 7(27), 1-13.

[2] Nayl, A.A., Ismail, I.M. and Aly, H.F. (2011) Recovery of pure $MnSO_4 \cdot H_2O$ by reductive leaching of manganese from pyrolusite ore by sulfuric acid and hydrogen peroxide. International Journal of Mineral Processing. 100, 116-123.

[3] Sun, W., Su, S., Wang, Q. and Ding, S. (2013) Lab-scale circulation process of electrolytic manganese production with low-grade pyrolusite leaching by SO_2. Hydrometallurgy. 133, 118-125.

[4] Ye, W., Li, Y., Kong, L., Ren, M. and Han, Q. (2013) Feasibility of flue-gas desulfurization by manganese oxides. Transactions of Nonferrous Metals Society of China. 23, 3089-3094.

[5] Yaozhong, L. (2004) Laboratory study: Simultaneous leaching silver-bearing low-grade manganese ore and sphalerite concentrate. Minerals Engineering. 17, 1053-1056.

[6] Li, C., Zhong, H., Wang, S., Xue J., Wu, F. and Zhang, Z. (2015) Manganese extraction by reduction−acid leaching from low-grade manganese oxide ores using CaS as reductant. Transactions of Nonferrous Metals Society of China. 25, 1677-1684.

[7] Dan, Z., Zhang, Y., Cai, J., Li, X., Duan, N. and Xin, B. (2016) Reductive leaching of manganese from manganese dioxide ores by bacterial-catalyzed two-ores method. International Journal of Mineral Processing. 150, 24-31.

[8] Nayak, B.B., Mishra, K.G. and Paramguru, R.K. (1999) Kinetics and mechanism of MnO_2 dissolution in H_2SO_4 in the presence of pyrite. Journal of Applied Electrochemistry. 29, 191-200.

[9] Momade, F.W.Y. and Momade, Z.G. (1999) Reductive leaching of manganese oxide ore in aqueous methanol–sulphuric acid medium. Hydrometallurgy. 51(1), 103-113.

[10] Sahoo, R.N., Naik, P.K., Das, S.C. (2001) Leaching of manganese from low-grade manganese ore using oxalic acid as reductant in sulphuric acid solution. Hydrometallurgy. 62, 157-163.

[11] Pagnanelli, F., Furlani, G., Valentini, P., Vegliò, F. and Toro, L. (2004) Leaching of low-grade manganese ores by using nitric acid and glucose: Optimization of the operating conditions. Hydrometallurgy. 75, 157-167.

[12] Hariprasad, D., Dash, B., Ghosh, M.K. and Anand, S. (2007) Leaching of manganese ores using sawdust as a reductant. Minerals Engineering. 20, 1293-1295.

[13] Su, H., Wen, Y., Wang, F., Sun, Y. and Tong, Z. (2008) Reductive leaching of manganese from low-grade manganese ore in H_2SO_4 using cane molasses as reductant. Hydrometallurgy. 93, 136-139.

[14] Tian, X., Wen, X., Yang, C., Liang, Y., Pi, Z. and Wang, Y. (2010) Reductive leaching of manganese from low-grade manganese dioxide ores using corncob as reductant in sulfuric acid solution. Hydrometallurgy. 100, 157-160.

[15] Tang, Q., Zhong, H., Wang, S., Li, J.Z. and Liu, G.Y. (2014) Reductive leaching of manganese oxide ores using waste tea as reductant in sulfuric acid solution. Transactions of Nonferrous Metals Society of China. 24, 861-867.

[16] Liu, Y., Naidu, R. (2014) Hidden values in bauxite residue (red mud): recovery of metals. Waste Management. 34, 2662-2673.

[17] Mayes, W.M., Jarvis, A.P., Burke, I.T., Walton, M., Feigl, V., Klebercz, O. and Gruiz, K. (2011) Dispersal and attenuation of trace contaminants downstream of the Ajka bauxite residue (red mud) depository failure, Hungary. Environment Science and Technology. 45, 5147-5155.
[18] Gu, H., Wang, N., Liu, S. (2012) Radiological restrictions of using red mud as building material additive. Waste Management and Research. 30(9), 961-965.
[19] Gu, H. and Wang, N. (2013) Leaching of uranium and thorium from red mud using sequential extraction methods. Fresen. Environ. Bull. 22, 2763-2769.
[20] Kononov, R., Ostrovski, O. and Ganguly, S. (2009) Carbothermal solid state reduction of manganese ores: 1. manganese ore characterisation. ISIJ International. 49(8), 1099-1106.
[21] Arndt, A., Borella, M.I. and Espósito, B.P. (2014) Toxicity of manganese metallodrugs toward Danio rerio. Chemosphere. 96, 46-50.
[22] Bjøklunda, G., Chartrandb, M.S. and Aaseth, J. (2017) Manganese exposure and neurotoxic effects in children. Environmental Research. 155, 380-384.
[23] Grygo-Szymanko, E., Tobiasz, A. and Walas, S. (2016) Speciation analysis and fractionation of manganese: A review. Trends in Analytical Chemistry. 80, 112-124.
[24] Jusufi, K., Stafilov, T., Vasjari, M., Korca, B., Halili, J. and Berisha, A. (2017) Measuring the presence of heavy metals and their bioavailability in potato crops around Kosovo's power plants. Fresen. Environ. Bull. 26, 1682-1686.

Received: **04.01.2018**
Accepted: **30.04.2018**

CORRESPONDING AUTHOR

Hannian Gu
Key Laboratory of High-temperature and
High-pressure Study of the Earth's Interior,
Institute of Geochemistry,
Chinese Academy of Sciences,
Guiyang, 550081 – China

e-mail:guhannian@vip.gyig.ac.cn

© by PSP Volume 27 – No. 7/2018 pages 4889-4899 Fresenius Environmental Bulletin

DETERMINATION OF THE VISUAL PREFERENCES OF DIFFERENT HABITAT TYPES

Engin Eroglu[1], Sertac Kaya[1], Tuba Gul Dogan[1], Alperen Meral[2,*], Sena Demirci[1], Nermin Basaran[1], Omer Lutfu Corbaci[3]

[1]Department of Landscape Architecture, Faculty of Forestry, Duzce University, Duzce, 81620, Turkey
[2]Department of Landscape Architecture, Faculty of Agriculture, Bingol University, Bingol, 12000, Turkey
[3]Department of Landscape Architecture, Faculty Fine Arts Design and Architecture, Recep Tayyip Erdogan University, Rize, 53100, Turkey

ABSTRACT

The unique qualities of areas with natural landscape features help provide sustainability. Moreover, their different vegetation covers and ecosystems contribute to the preservation of their visual attraction. In recent years, the demand for natural areas has not only been seen at a recreational level, but has also become associated with the conservation and sustainability of those areas. Although the concept of sustainability is expressed from an ecological point of view, studies indicate that the visual aspect is also an important component. Thus, in this study, a visual quality assessment was carried out which considered both objective and subjective evaluations of different habitat types. Efteni lake-wetland and Melen Ağzı dunes (Düzce), Anzer, Ayder, and Çat Düzü highlands (Rize), and Sultanmurat and Taşli highlands (Trabzon) were selected as the study areas. A visual quality analysis was conducted with a total of 43 participants (23 students, 16 local inhabitants and four lecturers) in order establish their preferences in areas with different landscape characteristics. For the determination of the visual qualifications of these areas, a total of 24 photographs showing typical images representing each habitat type (three photographs for each) were employed. Taking perceptual parameters into consideration, assessment of visual quality was made according to the points given to each photo by the participants. Consequently, differences in visual quality were found to be influenced by the demographic status of the participants, differences in habitat types, recreational trends and the conservation status of the habitats.

KEYWORDS:
Habitat, landscape, visual, differences, characteristics.

INTRODUCTION

Green and natural areas are an important part of the ecosystem as well as being important for their positive effects on the human psyche [1]. Today, considering the destruction and economic exploitation of these areas, their ecological importance is not always being taken into account. However, plants are an important source of that most basic of life requirements– oxygen, and thus, are very important indeed for the existence of future generations. In order to establish this perception, people must be made to understand through their own experience by spending time in natural surroundings that they need these areas. They must become aware that life is not possible without natural areas and therefore, these green areas must be maintained and their sustainability must be ensured for the future of human wellbeing. Today, the construction projects resulting from increasing human demands create pressure on urban green spaces, are not in harmony with existing historical buildings and disrupt the traditional texture of the city. This negative situation weakens the relationship between Man and the environment and contributes to the deterioration of the environmental perceptibility. For these reasons, environmental issues are often disregarded and rejected [2].

With the decline of open green spaces, awareness of the importance of nature and the value of the management of natural resources is rapidly increasing [3]. In order to preserve the diversity of natural landscapes, the importance of visual landscape quality as well as natural resource value must be considered [4]. Visual landscape quality is a term which emerged as a result of landscape evaluations made from the perceptual and emotional perspectives of the viewers [5]. Visual landscape has an important place in the human life experience [6]. The visual components of the landscape reveal not only aesthetic values, but also the cultural, economic and biological interrelationships of these values [7, 8, 9]. Today, visual quality assessment has become more important for data collection in planning studies. The purpose of visual quality assessment is to determine whether a landscape is aesthetically appropriate and to define some of the factors that affect the preferences for certain areas and physical landscape components [10].

In recent years, natural beauty has become one of the most important criteria for evaluating landscape. One reason for this is thought to be that people's visual perception is more developed than other types of perception [11]. Therefore, visual quality

can be seen as an important part of the human-environment interaction [12]. As well as the mental, physical and socio-economic differences among people, there are also differences in their evaluation of visual preferences for landscape [13].

Visual preferences are generally evaluated by research methods such as surveys. Researchers ask participants to select or score their favorite photographs to determine the variety of landscape preferences [13-19]. There are many visual quality evaluation studies on various habitat types, including those on rural landscapes [20, 21], wetlands, rivers, lake-wetlands [22-24], forests [25], agricultural landscapes [26, 27], roadside and road corridors [28-30], rocky habitats [31, 32], coastal landscape areas [33, 34] and mountainous areas [35, 36]. Most of these studies have attempted to assess the different settings found in a single habitat or to determine their seasonal changes. In the present study, habitats with different characteristics were selected and an attempt was made to determine the visual statuses among them.

The aim of this study was to assess the visual value of those areas that stand out with their natural landscape features and to determine the conservation status of the different habitat types in order to ensure their visual and ecological sustainability. Accordingly, visual landscape quality was assessed by photographing different types of visibly unique habitats which attract attention and can be seen along forest roads, in riparian areas, in forests, in rocky areas, in highlands, around waterfalls, in lake-wetlands and in aquatic-dune areas. The relationship between the parameters and preferences were evaluated according to the fractal dimension and visual quality of the photographs.

MATERIALS AND METHODS

Study area. The study areas selected were Anzer, Ayder, Sultanmurat, Çat Düzü and Taşlı (highlands), Efteni (lake-wetlands) and Melen Ağzı (sand dunes) in the provinces of Düzce, Rize and Trabzon, located on the northern Black Sea coast of Turkey (Figure 1). The main reasons for choosing these areas were that they have unique natural beauty, they accommodate different habitat types, and they are locations with special vegetative status in Turkey.

Material. The natural materials of the study were the habitat types, and the visual materials were the photographs taken in these areas (Figure 2), which included forests, riparian areas, rocky habitats, roadside venues, waterfalls and highland vegetation located in Rize and Trabzon, and dunes and lake-wetlands located in Düzce.

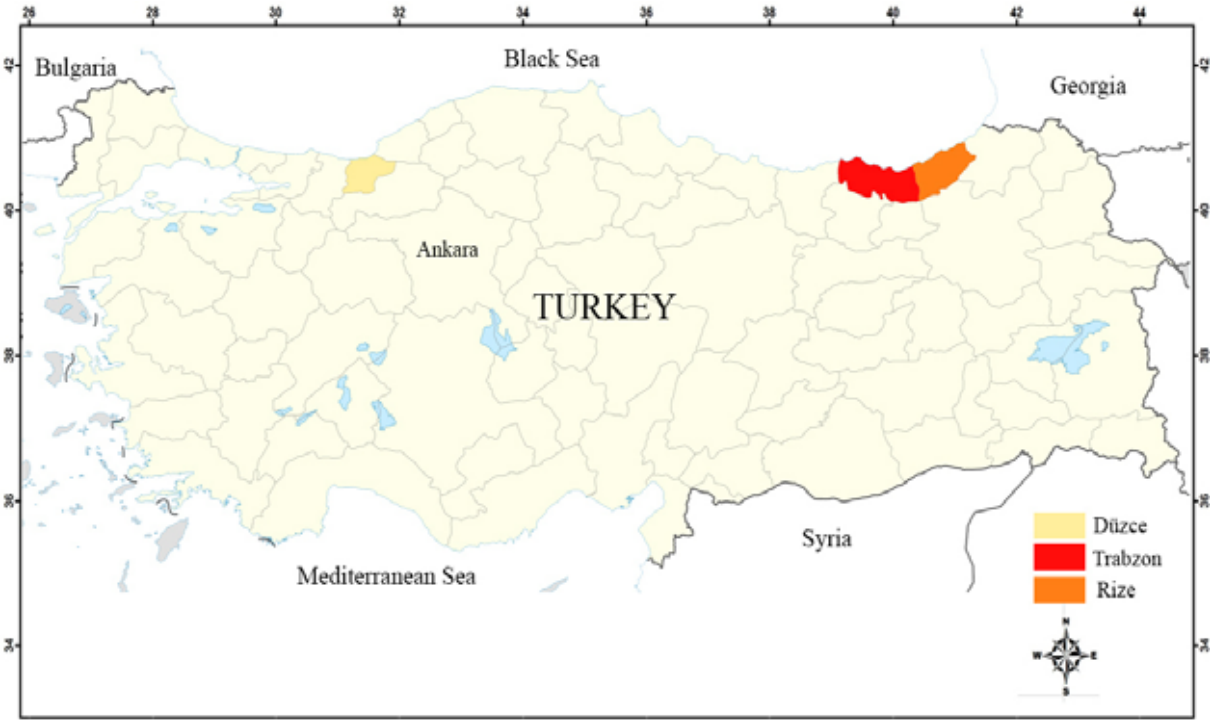

FIGURE 1
Map of Turkey showing study areas

a

b

c

d

e

f

g

h

i

j

k

l

m

n

o

p

FIGURE 2
Images of different habitat types used in the survey study
(a: Riparian Area Vegetation; b: Roadside Vegetation; c: Rocky Area Vegetation; d: Highland Vegetation; e: Waterfall Vegetation; f: Forest Vegetation; g: Lake-Wetland Vegetation; h: Dune Area Vegetation; i: Riparian Area Vegetation; j: Roadside Vegetation; k: Rocky Area Vegetation; l: Highland Vegetation; m: Waterfall Vegetation, n: Forest Vegetation, o: Lake-Wetland Vegetation; p: Lake-Wetland Vegetation; q: Riparian Area Vegetation; r: Roadside Vegetation; s: Rocky Area Vegetation; t: Highland Vegetation; u: Waterfall Vegetation; v: Forest Vegetation; w: Lake-Wetland Vegetation; x: Dune Area Vegetation)

Method. The analysis of the visual quality, as the primary stage of the research method, was based on the Scenic Beauty Estimation Method developed by Daniel [37] for visual quality estimation. This method is regarded as an effective means of revealing the reaction of viewers to groups of photographs [8, 11, 38] by enabling them to respond correctly and appropriately about the quality and visual evaluation of the landscape [36, 39]. In this study, which is discussed within this context, the purpose was to determine visual preference statuses of different habitat types by using visual evaluations. This method has been used in many previous studies [14, 20, 22, 29, 30, 31, 35, 40-44].

Typical images representing areas based on eight different habitat types were selected in order to determine visual landscape quality. Areas selected for the study were photographed in June and July 2015 in order to capture the most ideal vegetation period and to represent a remote overview of the habitats. In total, 941 photographs were taken in order to allow the assessment of the areas from all angles. The images were evaluated subjectively according to their picture quality, artificial elements in the picture such as cars, houses, infrastructural materials etc. and their ability to represent the habitat. Three examples from each habitat made up the 24 images used in the questionnaire.

Questionnaire study. With the help of the selected photographs, a questionnaire form was created for use in the visual landscape quality analysis. The questionnaire form prepared in the study framework was applied to 43 individuals representing three different groups (23 students, 16 local inhabitants and four lecturers).

The first part of the questionnaire concerned

participant demographic characteristics such as gender, age, and educational and occupational status. In the second part, the participants were asked to evaluate visual preference situations such as naturalness, diversity, impressiveness, clarity, compatibility, interestingness, excitement and attractiveness by assigning between 1 (lowest) and 7 (highest) points to each photo. In the third part, they were asked to score conceptual parameters such as the conservation status of the area and activities recommended for that area.

Statistical evaluations. According to the results of the questionnaires, the data belonging to the different habitat types were subjected to statistical evaluations. The obtained variables were converted into a Microsoft Excel file as raw data. The SPSS 22 program was then used to determine the relationships between these data. The following materials were used in the research process:

- Descriptive statistics to determine the demographic status of participants and the visual values of different habitat types and photo groups
- Correlation analysis in determining the reciprocal relationships between visual parameters and different habitat types and groups of photographs
- Regression analysis in the identification of the parameters that were the most important factors in determining the visual preferences of different habitat types and groups of photographs

The significance level was determined as $p < 0.05$ or $p < 0.01$. In the study, weighted means were assigned to the scores given for the visual qualities of the photographs by the individual study participants. These mean values were used to determine whether or not the preferences of the participants differed according to their profession, sex, age, or educational status [4, 13, 35, 45].

RESEARCH FINDINGS

Habitat properties. The eight different habitat types visually evaluated in the study and their general landscape characteristics are summarized in Table 1.

Demographic characteristics of participants. According to data obtained from the questionnaires, Table 2 shows that there are 43 participants, 60% male and 40% female. The highest participation rate in the age group category (68%) was of those ranging from 20-30 years old. In terms of education, illiterate individuals and primary–high school students had the highest participation rate (44%), whereas the ones who were studying at university had the lowest participation rate (12%). Regarding professional status, the highest participation rate was that of students (54%), with 37% allotted to other professions and the lowest participation rate belonging to teaching staff (9%).

TABLE 1
Habitat types and general landscape features

Habitat types	General features
Rocky Vegetation	Rocky surfaces create a barrier for the surrounding vegetation due to the combination of factors such as low water retention capacity, shortage of nutrients, seed holding and germination difficulties, and greater wind and sun exposure. Many Alpine plants are currently being used in landscaping and botanical design due to popular demand. It is generally possible to find succulent ground cover as well as *Juniperus communis* var. *alpina*, *Vaccinium myritillus*, *Rubus* spp. and occasionally woody species such as *Picea orientalis* in rocky vegetation habitats.
Riparian Vegetation	This includes true riparian vegetation and the wider vegetation band which affects the stream, covering only a narrow area and characterized by changes in water level and high soil moisture. Riparian habitats consist of streams, pebbles, stones, rocks, and water-tolerant plants that love humid soil. In addition to important herbaceous species and ground cover such as moss and fern, *Alnus glutinosa* species are also found in these places.
Waterfall Vegetation	This consists of cold-resistant plants which have high moisture and low heat demands, the most common types being fern, moss species, *Fagus orientalis*, *Carpinus betulus, Ilex colchicum* and *Rhododendron ponticum*. Plants found in these areas are similar to those of riparian habitats.
Highland Vegetation	This type consists of herbaceous ground cover plants of changeable nature found in the Eastern Black Sea highlands and also includes dwarf grass species.
Roadside Vegetation	The trees, shrubs and ground cover types in this habitat must be hardy because of their constant exposure to passing vehicles. *Picea orientalis*, *Alnus glutinosa, Fagus orientalis* species, as well as campanula, fern and some invasive ground cover species are included among roadside vegetation.
Dune Vegetation	The concepts of "sand" and "dune" cannot be considered separately. Sand is a soil component which is resistant to decomposition and rich in minerals. In order to for a dune to form in a place, a sand source must be present. However, dunes do not form in every sandy area, but must be supported by other factors. Dune vegetation includes shrubs and ground cover, with the most important plant species of this vegetation type being *Pancratium maritimum* and *Centaurea kilea*.
Forest Vegetation	This basically consists of trees. Forest trees include *Picea orientalis, Fagus orientalis, Carpinus betulus* and *Alnus glutinosa*. Also included are shrubs, ground cover and undergrowth such as *Vaccinium arctostophyllos, Rhododenron ponticum, Rhododendron luteum* and ferns.
Lake-wetland Vegetation	This comprises plants that love stagnant water and have a high demand for humidity, mainly ground cover or shrubs including wetland plants such as *Typha* spp., *Nymphaea* sp., *Nuphar* sp. Stones and rock fragments are typically found around lake-wetland areas.

TABLE 2
Demographic characteristics of participants

Participant Features		Number	Percentage (%)
Gender	Female	18	60
	Male	25	40
Age	20-30	29	68
	30-40	8	19
	40<	6	13
Education	None	19	44
	High school	19	44
	College and above	5	12
Occupation	Student	23	54
	Educational staff (lecturers)	4	9
	Other	16	37

TABLE 3
Visual quality values of the photographs (arithmetic means)

	Arithmetic means							
Photo Number	Naturalness	Diversity	Impressiveness	Clarity	Compatibility	Interestingness	Excitement	Attractiveness
1	6.30	4.42	5.23	5.16	5.88	3.98	5.07	4.21
2	5.07	4.51	4.72	5.12	4.74	4.09	4.63	4.98
3	6.30	5.49	5.86	5.79	5.65	5.77	5.79	5.72
4	5.79	4.28	4.53	4.74	4.98	4.23	4.33	4.51
5	6.40	5.70	6.14	5.79	5.91	5.67	6.12	6.23
6	6.23	4.93	4.72	4.98	5.51	4.37	4.37	4.63
7	6.30	5.09	5.70	6.07	5.74	5.26	5.51	5.67
8	4.93	3.35	3.44	4.05	3.42	3.12	3.14	3.60
9	6.40	6.09	6.19	6.07	6.05	5.77	5.93	6.12
10	5.91	5.21	5.05	5.07	5.19	4.72	4.84	5.05
11	6.26	5.28	5.47	5.40	5.56	5.47	5.33	5.33
12	6.51	6.19	6.19	6.23	6.30	5.98	6.00	6.19
13	6.42	6.07	6.02	6.02	6.14	6.09	6.07	6.05
14	6.14	5.86	5.67	5.86	5.84	5.49	5.60	5.74
15	6.51	5.28	5.81	6.05	5.86	6.09	5.74	5.91
16	5.88	5.05	4.56	4.63	5.16	4.67	4.47	4.51
17	6.56	6.23	6.33	6.19	6.26	5.60	5.91	6.19
18	5.58	5.21	5.07	5.33	4.98	4.74	4.84	5.07
19	6.49	5.21	5.81	5.56	5.79	5.98	5.84	5.58
20	6.30	5.81	5.51	5.60	5.58	5.26	5.44	5.40
21	6.77	6.33	6.49	6.42	6.47	6.40	6.42	6.40
22	6.30	5.72	5.26	5.51	5.72	4.74	4.72	5.00
23	6.30	5.72	5.26	5.51	5.72	4.74	4.72	5.00
24	5.02	3.70	3.30	3.58	3.53	3.42	3.19	3.21
Total	6.12	5.23	5.33	5.42	5.48	5.08	5.17	5.25

Visual characteristics of habitats. According to the arithmetic means of the photographs (referred to by their numbers) used in the questionnaire (Table 3), the most natural one was 21 and the most unnatural one was 8, the most diverse was 21 and the least diverse 8, the most impressive was 21 and the least impressive 24, the clearest was 21 and the least clear 24, the most compatible was 21 and the least compatible 8, the most interesting was 21 and the least interesting 8, the most exciting was 21 and the least exciting 8, the most attractive was 21 and the least attractive 24.

The visual quality values of the habitat types are given in Table 4. Among the eight habitats in the survey, the most natural one was the waterfall habitat and the least natural one the dune habitat, the most diverse was the waterfall habitat and the least diverse the dune habitat, the most impressive was the waterfall habitat and the least impressive the dune habitat, the clearest was the waterfall habitat and the least clear the dune habitat, the most compatible was the waterfall habitat and the least compatible the dune habitat, the most interesting was the waterfall habitat and the least interesting the dune habitat, the most exciting was the waterfall habitat and the least exciting the dune habitat, the most attractive was the waterfall habitat and the least attractive the dune habitat.

When the correlation analysis in Table 5 is examined, the scores for the survey photographs according to gender status show that the naturalness, diversity, impressiveness, clarity, compatibility, excitement, and attractiveness gradually decreased from males to females. Namely, the men found the photographs more natural or more interesting than the women did. As the ages of the participants increased, the perception of naturalness also increased. Although the older participants found the photographs more natural, the younger ones saw them as less natural. As educational status increased, the perception of naturalness, diversity, and clarity also increased in direct proportion. The university graduates found the photographs more natural, diverse and clear than the illiterate participants, while the high school students found the photos less natural than the university students. According to occupational status, the perception of naturalness was higher for other occupations than for the students, whereas the sense of interestingness, excitement, and attractiveness of the lecturers was higher than for the students and other occupations. Thus, although the students found the photos less natural, the lecturers found them more natural, and the lecturers and students saw the photos as more interesting, exciting and attractive, while those in other professions found them to be less interesting, exciting and attractive.

Regression analysis was performed in order to examine the prominent parameters in determining the visual quality values of the different habitat types. Accordingly, the main determinants in the visual quality assessment of different habitat types were responses to conservation issues as well as to excitement, interestingness, and attractiveness (Table 6).

Opinions on the preservation of different habitats. In the study, the participants were asked whether the presented habitat type should be preserved. According to their answers, the habitats illustrated in the numbered photographic images that should absolutely be protected were numbers a, c, e, i, l, m, n, o, q, s and u. The areas that should be partially protected were numbers b, d, f, g, j, k, p, r, t, v and w while the habitat in number 8 was selected as being less in need of protection and number 24 was selected as being in need of intervention. Regarding the assessment of habitat level, responses indicated that the riparian (a, i & q) and waterfall (e, m & 21) habitats should absolutely be protected, whereas the roadside (b, j & r), the rocky (c, k & s), the highland (d, l & t), the forest (f, n & v) and the lake-wetland (g, o & w) habitats were in need of partial protection. The dune area habitat (h, p & x) was considered as needing less protection.

TABLE 4
Visual quality values of habitat types (arithmetic means)

Arithmetic means								
Habitat Types	Naturalness	Diversity	Impressiveness	Clarity	Compatibility	Interestingness	Excitement	Attractiveness
Riparian	6.42	5.58	5.91	5.81	6.06	5.12	5.64	5.50
Roadside	5.52	4.98	4.95	5.17	4.97	4.52	4.77	5.03
Rocky	6.35	5.33	5.71	5.58	5.67	5.74	5.65	5.54
Highland	6.20	5.43	5.41	5.53	5.62	5.16	5.26	5.36
Waterfall	6.53	6.03	6.22	6.08	6.17	6.05	6.20	6.22
Forest	6.22	5.50	5.22	5.45	5.69	4.87	4.90	5.12
Lake-Wetland	6.43	5.00	5.47	5.69	5.60	5.48	5.35	5.46
Dune	5.28	4.03	3.77	4.09	4.04	3.74	3.60	3.78
Total	6.11	5.23	5.33	5.42	5.47	5.08	5.16	5.25

TABLE 5
Relationship between demographic status and conceptual parameters (correlation analysis)

Correlation									
		Naturalness	Diversity	Impressiveness	Clarity	Compatibility	Interestingness	Excitement	Attractiveness
Gender	P.C.	-.143**	-.165**	-.117**	-.090**	-.076*	-.126**	-.117**	-.038
	Sig.	.000	.000	.000	.004	.015	.000	.000	.219
Age	P.C.	.123**	-.018	-.039	.033	.036	-.043	-.059	-.058
	Sig.	.000	.567	.208	.282	.254	.165	.057	.063
Education	P.C.	.119**	.128**	.028	.080*	.059	.024	-.009	-.013
	Sig.	.000	.000	.367	.010	.057	.448	.764	.683
Occupation	P.C.	.151**	-.011	-.051	.035	.045	-.104**	-.137**	-.109**
	Sig.	.000	.720	.099	.256	.152	.001	.000	.000

TABLE 6
Basic components determining visual quality values of habitat types (regression analysis)

Coefficients						
	Model	Unstandardized Coefficients		Standardized Coefficients	t	Sig.
		B	Std. Error	Beta		
1	(Constant)	3.796	.122		31.062	.000
	Conservation	.386	.055	.214	7.015	.000
2	(Constant)	4.618	.319		14.484	.000
	Conservation	.287	.065	.159	4.405	.000
	Attractiveness	-.121	.043	-.101	-2.790	.005
3	(Constant)	4.390	.322		13.641	.000
	Conservation	.314	.065	.173	4.815	.000
	Attractiveness	-.306	.064	-.256	-4.810	.000
	Interestingness	.230	.058	.202	3.946	.000
4	(Constant)	4.509	.325		13.892	.000
	Conservation	.288	.066	.159	4.379	.000
	Attractiveness	-.214	.074	-.179	-2.913	.004
	Interestingness	.324	.069	.284	4.673	.000
	Excitement	-.201	.081	-.176	-2.489	.013

Recreational potential of different habitats. Participants who viewed the different habitat types were asked what kind of activities they wanted to conduct in that area. Hiking/trekking, with 112 responses, was the most recommended activity, and was suggested for photos b, j and v. In other words, this activity was recommended for the roadside and forest habitats. The second most selected activity was photography, with 73 responses, mainly for photos c, e, k, s and u, which were the rocky and waterfall habitats. The third most suggested activity was picnicking, with 53 responses, mostly for photos a and q, which were riparian habitats. Other preferred activities included camping (33 responses) in riparian and highland habitats, climbing (28 responses) in rocky habitats, bicycling (21 responses) in roadside and forest habitats, relaxing (21 responses) in rocky and lake-wetland habitats, fishing (19 responses) in dune and lake-wetland habitats, enjoying the scenery (16 responses) in lake-wetland habitats, motoring (13 responses) in roadside habitats, swimming (13 responses) in dune habitats, holidaying (9 responses) in highland habitats, swimming (7 responses) in riparian habitats, rafting (7 responses) in riparian habitats and animal husbandry (6 responses) in highland habitats. When the suggested activities were evaluated in terms of the habitats, the most preferred activities were picnicking in the riparian habitat, hiking in the roadside habitat, photography in the rocky habitat, hiking in the highland habitat, photography in the waterfall habitat, hiking in the forest habitat, camping in the lake-wetland habitat and swimming in the dune habitat.

RESULTS AND DISCUSSION

Visual evaluations of habitat types. In the study, all the results obtained in the determination of the visual values of the habitat types were related to the demographic status of the participants, which was quite similar to findings of previous studies [14, 23, 31, 35, 44]. The most prominent demographic feature was gender. Kaplan and Kaplan [11] stated that there was an important relationship between gender and perception of natural formations and explained that male and female participants have different visual tendencies. The reduction of green zones in urban areas in particular has made the residents' views on natural areas even more diverse. The visual desire and tendency toward natural areas has generally been attributed to the decline of green areas under the pressure of urbanization. At the same time, the increasing trend towards biodiversity (i.e., increased vegetation cover) has also revealed a rising interest in these fields [1]. According to the overall evaluations made by the participants, the general tendency in the visual preferences of habitats selected from natural areas was positive and the results obtained showed that an increase in diversity also affected the levels of appreciation and interest positively. There are differences between the visual preferences for changes in different landscape patterns and in perceptual tendencies towards natural and unnatural patterns, whether urban or rural; in particular, the size, variety and space-mass ratio of the pattern have different perceptual values [46].

One of the most important findings of this study was that the visual preference levels for different habitat areas based on water such as waterfalls and lake-wetlands were higher than for other landscape areas. Likewise, Kalın et al. [36] pointed out that of the different landscape characters, the most favored ones are the landscape habitats close to water such as riparian and lake-wetlands. The lowest visual conservation value in the present study belonged to the dune type that had the least vegetation cover. From this viewpoint, areas where biodiversity was high due to the increase in water and vegetation cover were found to be more deserving of preservation.

The presence of tree groups in a plant composition has been shown to be more favorable and preferable [43, 47] and this study determined that preferability levels and appreciation were quite high for forest vegetation with intense tree coverage.

The most effective visual evaluation parameters regarding different plant compositions and different landscape characters were determined to be naturalness, continuity, interestingness and excitement. As a result of this study, the most effective visual evaluation parameters in determining the visual preferences of different habitat types were impressiveness, interestingness, and excitement.

Recreational and conservation assessments of habitat types. Soliva and Hunziker [48] stated that areas which are protected and have protection status are more preferable than cultural landscape areas. At the same time, they emphasized that some highly appreciated areas have been determined as protected areas. This study indicated that areas with available protection status, such as wetlands and waterfalls, were more deserving of protection and had a higher visual preference. However, even when the vegetation status was low, the visual preference and protection status of the highland habitat was high. The main reason for this was the effect of the green color of the vegetation. In his study, Eroglu [43] revealed that color is the most important element among perceptual factors and that the presence of green color in a composition affects the visual appreciation positively.

It is recognized that the kind of recreational pursuits preferred in different habitats is an important factor, especially in determining the need for natural areas. The demands for outdoor recreational activities are increasing day by day, and people want to perform such activities largely in natural areas [17]. The different natural attractions of these areas play an important role in the diversity of such activities. Akbar et al. [28, 45] and Kent and Elliott [49] have indicated that this situation is not only related to the visual values that these areas possess, but also to their biodiversity and landscape characteristics. Moreover, in this study, it was shown that different activity preferences such as hiking, photography, picnicking and camping were also related to the visual appreciation of these diverse habitat types. One of the most important findings of this study was that the most preferred recreational tendency for all habitat types, regardless of their diversity, was hiking.

CONCLUSION AND RECOMMENDATIONS

In this study, it was determined that the most important factor in the appreciation of the natural areas was water (and habitat types associated with water). The more desirable images and habitats usually included a water element. Other images and habitats that did not include a water element were less preferred. It was concluded that those who viewed the different habitat types predominantly recommended hiking, photography, picnicking and camping in those habitats, respectively.

According to the results of the questionnaire, the most appreciated habitat type was the waterfall, while the sand dune habitat was the least appreciated. The habitats definitely determined to be in need of preservation were those of the riparian and waterfall, whereas the sand dunes were determined to require intervention.

In this, as in many such studies, the assessment and evaluation of the visual quality of a landscape were based on participant visual quality scores which depended on their appreciation of photographs. However, in determining the landscape character and visual quality of a natural landscape image through photographs, objective as well as subjective evaluations are useful. Different ecologically specific habitats contain vegetation types which offer an important visuality in terms of landscape. The sustainability of landscape aesthetics requires the preservation of the ecosystems that offer this visuality. Therefore, visual evaluation and analysis of different natural landscape components such as vegetation should be included in landscape planning and management studies.

REFERENCES

[1] Khew, J.Y.T., Yokohari, M., Tanaka, T. (2014) Public Perceptions of Nature and Landscape Preference in Singapore. Human Ecology. 42, 979–988.

[2] Özkan, D.G., Alpak, M.E., Özbilen, A. (2015) Kent Görünümlerinde Görsel Tercih: Trabzon Şehrindeki Değişimin Algılanması Ve Değerlendirilmesi. Proceedings of INTCESS15- 2nd International Conference on Education and Social Sciences. 948-957.

[3] Erdönmez, M.Ö., Kaptanoğlu, Y.Ç. (2008) Peyza Estetiği ve Görsel Kalite Değerlendirmesi. İstanbul Üniversitesi Ormancılık Dergisi. 58(1), 39-51.

[4] Sarı, D., Karaşah, B. (2015) Hatila Vadisi Milli Parkı'nda (Artvin) yer alan farklı vejetasyon tiplerinin görsel değerlendirmesi üzerine bir çalışması. Türkiye Ormancılık Dergisi. 16(1), 65-74.

[5] Kıroğlu, E. (2007) Erzurum Kenti ve Yakın Çevresindeki Bazı Rekreasyon Alanlarının Görsel Peyzaj Kalitesi Yönünden Değerlendirilmesi. Master's thesis. Atatürk Üniversitesi Fen Bilimleri Enstitüsü. Erzurum, Turkey.

[6] Lambe, R.A. (1986) Commercial highway landscape reclamation: A participatory approach. Landscape and Planning. 24(4), 353–385.

[7] Daniel, T.C., Vining, J. (1983) Methodological issues in the assessment of landscape quality. In: Altman, I., Wohwill, J.F. (Eds.) Behaviour and the Natural Environment. Plenum: New York, 39–83.
[8] Amir, S., Gidalizon, E. (1990) Expert-based method for the evaluation of visual absorption capacity of the landscape. Journal of Environmental Management. 30, 251–263.
[9] Angileri, V., Toccolini, A. (1993) The assessment of visual quality as a tool for the conservation of rural landscape diversity. Landscape and Urban Planning. 24(1–4), 105–112.
[10] Kane, P.S. (1981) Assessing landscape attractiveness: A comparative test of two new methods. Applied Geography. 1, 77–96.
[11] Kaplan, R., Kaplan, S. (1989) The experience of nature: A psychological perspective. Cambridge University Press: New York, ISBN 0-521-34139-6, 13-39.
[12] Parsons, R., Daniel, T.C. (2000) Good looking: In defense of scenic landscape aesthetics. Landscape and Urban Planning. 60(1), 43-56.
[13] Sevenant, M., Antrop, M. (2010) The use of latent classes to identify individual differences in the importance of landscape dimensions for aesthetic preference. Land Use Policy. 27(3), 827-842.
[14] Bulut, Z., Yilmaz, H. (2008) Determination of Landscape beauties through visual quality assessment method: A case study for Kemaliye (Erzincan/Turkey). Environmental Monitoring and Assessment. 141, 121–129.
[15] Canas, I., Ayuga, E., Ayuga, F. (2009) A contribution to the assessment of scenic quality of landscapes based on preferences expressed by the public. Land Use Policy. 26, 1173–1181.
[16] Tveit, M. (2009) Indicators of visual scale as predictors of landscape preference: A comparison between groups. Journal of Environmental Management. 90, 2882–2888.
[17] Kurdoglu, O., Kurdoglu, B. (2010) Determining recreational, scenic. and historical–cultural potentials of landscape features along a segment of the ancient Silk Road using factor analyzing. Environmental Monitoring and Assessment. 170, 99–116.
[18] Howley, P. (2011) Landscape aesthetics: Assessing the general public's preferences towards rural landscapes. Ecological Economics. 72, 161–169.
[19] Özkan, U.Y. (2014) Assessment of visual landscape quality using IKONOS imagery. Environmental Monitoring and Assessment. 186, 4067–4080.
[20] Arriaza, M., Ortega, J.F.C., Medueno, J.A.C., Aviles, P.R. (2004) Assessing the visual quality of rural landscapes. Landscape and Urban Planning. 69(1), 115 – 125.
[21] Rogge, E., Nevens, F., Gulinck, H (2007) Perception of Rural Landscapes in Flanders: Looking Beyond Aesthetics. Landscape and Urban Planning. 82(4), 159-174.
[22] Meitner, M.J. (2004) Scenic beauty of river views in the Grand Canyon: Relating perceptual judgments to locations. Landscape and Urban Planning. 68, 3-13.
[23] Bulut, Z., Yılmaz, H. (2009) Determination of waterscape beauties through visual quality assessment method. Environmental Monitoring and Assessment. 154, 459-468.
[24] Zhao, J., Luo, P., Wang, R., Cai, Y. (2013) Correlations between aesthetic preferences of river and landscape characters. Journal of Environmental Engineering and Landscpae Management. 21(2), 123-132.
[25] Eroğlu, E., Acar, C. (2011) Visual landscape character of oriental spruce (*Picea orientalis* (L.) LINK.) mountain forests in Turkey. Journal of Environmental Engineering and Landscape Management. 19(3), 189-197.
[26] Matthies, P.L., Briegel, R., Schüpbach, B., Junge, X. (2010) Aesthetic perefence for a Swiss alpine landscape: The impact of different agricultural land-use with different biodiversity. Landscape and Urban Planning. 98, 99-109.
[27] Acar, C., Eroğlu, E. (2010) Visual preferences for poplar plantations on roadside landscape in Turkey. Fifth International Poplar Symposium. Poplars and willows: From research models to multipurpose trees for a biobased society. 20-25 September 2010, Orvieto, Italy.
[28] Akbar, K.F., Hale, W.H.G., Headley, A.D. (2003) Assessment of scenic beauty of the roadside vegetation in northern England. Landscape and Urban Planning. 63, 139-144.
[29] Clay, G.R., Smidt, R.K. (2004) Assessing the validity and reliability of descriptor variables used in scenic highway analysis. Landscape and Urban Planning. 66, 239–255.
[30] Eroğlu, E., Demir, Z. (2016) Phenological and Visual Evoluations of some Roadside Deciduous Trees in Urban Area. Biological Diversity and Conversation. 9(1), 143-153.
[31] Acar, H., Eroglu, E., Acar, C. (2013) Landscape values of rocky habitats in urban and semi-urban context of Turkey: A study of Tokat city. Journal of Food Agriculture and Environment. 11(2), 1200-1211.
[32] Acar, C., Sakıcı. Ç. (2008) Assessing Landscape Perception of Urban Rocky Habitats. Building and Environment. 43, 1153-1170.
[33] Kalın, A. (2004) Çevre Tercih ve Değerlendirmesinde Görsel Kalitenin Belirlenmesi ve Geliştirilmesi: Trabzon Sahil Bandı Örneği. Unpublished Ph.D. thesis. K.T.Ü. Fen Bilimleri Enstitüsü, Trabzon, Turkey.

[34] Ak, M.K. (2010) Akçakoca Kıyı Bandı Örneğinde Görsel Kalitenin Belirlenmesi ve Değerlendirilmesi Üzerine Bir Araştırma. Ph.D. thesis. A.Ü. Fen Bilimleri Enstitüsü Peyzaj Mimarlığı ABD, Ankara, Turkey.
[35] Eroğlu, E. (2012) Defining of Native Plant Compositions Determined Landscape Character in Mountainous Area Roadside Corridors: A Case Study of Ataköy-Sultanmurat-Uzungöl-sulak alan Roadside Corridor. Karadeniz Technical University, The Graduate School of Natural and Applied Sciences Landscape Architecture Graduate Program.
[36] Kalın, A., Eroğlu, E., Acar, C., Çakır ,G., Güneroğlu, N., Kahveci, H., Gel, A. (2014) Visual quality in landscape character: Example of mountain-road corridor in Turkey. Journal of Balkan Ecology. 17(2), 161-180.
[37] Daniel, T.C. (1976) Measuring Public Arsthetis Preference. In: Thames, J. (Ed.) Disturbed Land Reclamation and Use in the Southwest. University of Arizona Press, Tucson.
[38] Cherry, G. (1975) Rural Planning Problems. Leonard Hill, London.
[39] Misgav, A. (2000) Visual Preference of the Public for Vegetation Groups in Israel. Landscape and Urban Planning. 48(3-4), 143-159.
[40] Clay, G.R., Daniel, T.C. (2000) Scenic Landscape Assessment: The Effects of Land Management Jurisdiction on Public Perception of Scenic Beauty. Landscape and Urban Planning. 49(1-2), 1-13.
[41] Fuente de Val, G.D.L., Atauri, J.A., Lucio, J.V.D. (2006) Relationship Between Landscape Visual Attributes and Spatial Patten Indices: A test Study in Mediterranean-Climate Landscapes. Landscape and Urban Planning. 77(4), 393-407.
[42] Acar, C., Kurdoğlu, B.Ç. (2005) Visual quality evaluation in Kaçkar Mointains. Sum on protected natural areas. Isparta, Turkey: Süleyman Demirel University. September 8–10, 2005.
[43] Eroğlu, E. (2004) Examining the Seasonal Variation of Some Plants and Plants Groups in Düzce City Open and Green Areas on Planting Design Perception. Master's Thesis. Abant Izzet Baysal University, The Graduate School of Natural and Applied Sciences Landscape Architecture Graduate Program, Bolu, Turkey.
[44] Müderrisoğlu, H., Ak, K., Aydın, Ş.Ö., Eroğlu, E. (2006) Visitor Satisfaction in the Example of Abant Nature Park. Journal of Balkan Ecology. 9(1), 55-62.
[45] Akbar, K.F., Hale, W.H.G., Headley, A.D. (2002) Assessment of scenic beauty of the roadside. Landscape and Urban Planning. 959, 1–6.
[46] Chen, Z., Xu, B., Devereux, B. (2015) Assessing public aesthetic preferences towards some urban landscape patterns: The case study of two different geographic groups. Environmental Monitoring Assessement. 188(4), 1-17.
[47] Zhao, J. (2013) Woody Plant Richness and Landscape Preference. Master's thesis. Graduate School of Landscape Architecture, University of Illinois at Urbana-Champaign, Illinois, USA.
[48] Soliva, R., Hunziker, M. (2009) How do biodiversity and conservation values relate to landscape preferences? A case study from the Swiss Alps. Biodiversity and Conservation. 18, 2483–2507.
[49] Kent, R.L., Elliott, C.L. (1995) Scenic routes linking and protecting natural and cultural landscape features: A greenway skeleton. Landscape and Urban Planning. 33 (1–3), 341–357.

Received: **06.01.2018**
Accepted: **04.05.2018**

CORRESPONDING AUTHOR

Alperen Meral
Department of Landscape Architecture
Bingöl University
Bingöl, 12000 – Turkey

e-mail: alperenmeral@bingol.edu.tr

© by PSP Volume 27 – No. 7/2018 pages 4900-4903 Fresenius Environmental Bulletin

DEVELOPMENT OF A DYNAMIC MODEL FOR THE DEGRADATION OF FATS, OILS AND GREASES DURING CO-COMPOSTING OF OLIVE MILL SOLID AND LIQUID WASTES

Christina Tsiodra, Efthymios Stathakis, Anestis Vlysidis, Apostolos Vlyssides*

School of Chemical Engineering, National Technical University of Athens, Iroon Polytechneiou 9, Zografou 157 80, Athens, Greece

ABSTRACT

Olive pomace or Olive Mill Solid Residue (OMSR) is the solid residue derived from the olive oil extraction process and it can be used as raw material in a composting process from which a high nutritional soil conditioner could be produced. Lipids are difficult to be biodegraded by aerobic microorganisms during the thermophilic composting period, and hence, a prolonged lag phase is observed with a very slow temperature increase when Fats, Oils and Grease (FOGs) are present. The objective of this study is the development of a dynamic model that can predict the biodegradation of a III-phase OMSR FOGs content during a composting period using industrial scale data of Water Holding Capacity (WHC), pH and Oxygen Uptake Rate (OUR). The created dynamic model was based on the theory of time series analysis and the theory of statistical analysis of residuals. The model was validated in a batch OMSR co-composting system with OMWW (Olive Mill Waste Water) and gave a prediction efficiency of 91%.

KEYWORDS:
Composting of OMSW, residual analysis, dynamic prediction model, FOG degradation.

INTRODUCTION

Composting consists, mainly, of three phases: (a) the thermophilic phase or stabilization phase of the biodegradable organic carbon, (b) the mesophilic phase or maturation phase, and finally (c) the psychrophilic phase or humification phase [1]. The most critical phase of composting is the thermophilic stabilisation phase. Its outcome affects the other two phases that follow. Therefore, adequate control of this phase is key to the success of the whole process of composting [2].

The co-composting of Olive Mill Solid Residues (OMSR) with Olive Mill Wastewater (OMWW) is a promising treatment method for Olive Mill Wastes (OMW) [3]. However, the high lipids content of OMSR (4-6%) is a strong inhibition factor for the development of the thermophilic stage [4]. The lag time for the increasing of temperature up to the thermophilic region is proportional with the remaining concentration of lipids (FOGs) inside the OMSR. Therefore, the FOGs reduction monitoring during the OMW composting process, is necessary for controling the "lag period of hydrophilication". On the other hand, there is not any accurate analysis on-line measurement of FOGs during composting, especially in a windrow system. Moreover, in order to have an effective control tool for the FOGs biodegradation in the OMSW composting system it is necessary to create a mathematical non-deterministic model that will be based on easy measurement parameters, such as pH, oxygen uptake rate (OUR) and water holding capacity (WHC) of the substrate, predicting the present FOGs concentrations from experimental data obtained from the previous composting days.

MATERIALS AND METHODS

Experimental procedure. The experimental results from a batch lab scale system of OMSR co-composting with OMWW, previously described by Tsiodra et al. [5], were used to create a dynamic model that correlates measurements of previous data of three of the most important variables (OUR, pH and WHC) with the present measurements of the FOGs. The cross-correlation procedure is based on residual theory created by [6]. According to this theory, a multi-function correlation is created between a dependent variable (e.g. FOGs) and multiple independent variables (e.g. OUR, pH and WHC), in a multi-parametric system, using a step by step procedure where in a following step the statistical effect of the previous examined parameters (residuals) are substitute from the total effect. In each step, using each of the possible linear equations, the best correlated parameter is taken and the effect of this equation is substituted from the correspondence value of the main examined parameter. The final model could be dynamic if measurements from previous dates of the independent variables are taken into account for

the estimation of the present value of the dependent variable. The dynamic model was validated twice in a batch industrial-scale open pile windrow composting system of OMSR which is described below.

TABLE 1
The composition of OMWW used in the experimental procedure

Characteristic	Amount
pH	4.2
BOD_5 (mg/L)	25850
COD (mg/L)	80250
Total Suspended Solids (TSS) (mg/L)	4580
Volatile Suspended Solids (mg/L)	4024
Total Phosphorous (mg/L)	870
Total Kjeldahl Nitrogen (mg/L)	1150
Total Phenolic Compounds (TPC) (mg/L)	14250

TABLE 2
The composition of OMSR used in the experimental procedure

Characteristic	Amount
Moisture, %	55.50
Fats and oils, % of TS (total Solids)	4.85
Nitrogen content substances, % of TS	7.39
Total sugars, % of TS	2.13
Cellulose, % of TS	37.39
Hemicellulose, % of TS	17.04
Ash, % of TS	3.66
Ether extraction substances, % of TS	8.61
Lignin, %of TS	21.97
Kjendahl Nitrogen content, % of TS	1.093
Phosphorous content as P_2O_5, % of TS	0.113
Potassium content as K_2O, % of TS	0.83
Calcium content as CaO, % of TS	0.95
Total Carbon content, % of TS	56.13
C/N ratio	51.34

The experimental procedure took place in the industrial area of a compost producing company (ORGANOHUMIKI THRAKIS IKE), where ten windrow lines of 100 tons of OMWR each were proceeded. The initial raw material consists with 90% of OMWR, 1-2% of olive leafs and 8-10% of maturated compost. The latter was added so as to provide the necessary microorganisms for an easy initiation of the process. Moreover, 27 kg of urea per ton of raw material was supplied in order to reduce the C/N ratio up to about 20/1. Every day, 50 kg of pretreated OMWW per ton of raw material were added to the composting pile. The OMWW was chemical pretreated with Fenton's reagents as described by Vlyssides et al. [7]. Both the OMWW and the OMSR were received from a typical centrifugal III-phase olive mill plant operating in the district of Alexandroupolis city. The windrow was agitated once per day by using a windrow turner. The temperature in the compost was initially decreased right after an agitation. However, the provided oxygen results in strengthening the microbial activity which recovers the drop in temperature 2-3 hours after the agitation occurs. The duration of the experimental procedure and sampling analysis were continued for 4 months. The initial composition of OMWW and OMSR used in the experiments are presented in Tables 1 and 2, respectively.

Analytical procedure. The temperature is monitored throughout the entire composting process. During three months of composting, every day three samples were taken for analysis from three different points of each pile. One from the middle of each windrow and two from the edges. For each sampling, the sample was taken from the internal of the windrow (at least 15 cm from the surface). The samples were analyzed for FOGs content (g/kg), pH, WHC (% of Total Solids) and Oxygen Uptake Rate g/kg/d (OUR) according to Standard test compost Methods of Analysis [8].

Model development. The obtained experimental data which were used to develop the dynamic regression model for FOG concentration prediction order to predict the FOG concentrations was based on other key variables such as the oxygen uptake rate (OUR), the pH and the WHC.

The dynamic model used in this study was developed from measurements recorded at equally spaced time intervals of one day. If the response of FOGs conc. at time t is denoted by Y_t, the model will contain terms of the form:

$Y_{t-1}, Y_{t-2}, \ldots, Y_{t-n}$

Where: Y_{t-n} = response n sampling periods in the past

Additionally, for variables, X_j, which act as inputs, terms of the following type will appear in the model:

$X_{j,t}, X_{j,t-1}, X_{j,t-2}, \ldots, X_{j,t-m}$

Where $X_{j,t-n}$ = current measurement of variable j at n sampling periods in the past

The model form, which is linear in the coefficients, is:

$Y_t = k_o + A_1Y_{t-1} + A_2Y_{t-2} + \ldots + A_nY_n + k_{10}X_{1,t} + \ldots + k_{1m}X_{1,t-m} + k_{20}X_{2,t} + \ldots + k_{2n}X_{2,t-n} + \ldots$.

This model is called a lagged regression model because the variables that are the "independent variables" are current values or values at previous times or "lags" [9].

The step by step building of the regression model using the residual analysis method consists of the following steps:

Step 1: Choose the variable best correlated with the Y-variable, transform it as necessary to produce a straight line, and perform a least-squares regression with the dependent variable (Y-variable to be predicted with a correlation coefficient R_0). The result will be an equation of the form:

$$\hat{Y} = b_0 + b_1 f(X_1)$$

Where: $\hat{Y}$ is the predicted value of Y-variable, b_0 and b_1 are constants and X_1 is a variable

Step 2: Calculate "residuals" as follows:

$Z_i = Y_i – [b_0 + b_1 f(X_{1,i})]$

Where: Z_i = residuals, Y_i = data for variable to be predicted and $X_{1,i}$ = data for variable X_1.

Step 3: Choose the best-correlated X-variable. Transform the X-variable, if necessary, to yield a linear plot.

Step 4: Add the new, transformed variable to the regression model, and perform a least-squares fit, resulting in:

$\hat{Y} = b_0 + b_1 f(X_1) + b_2 g(X_2)$

Step 5: Calculate residuals and repeat the process until all variables have been added. Each time the correlation coefficient R of the model is:

$R = R_0 + R_1 (1-R_0) + \ldots$

Each term of the equation expresses the participation of each variable in the final correlation coefficient.

Step 6: Check the goodness-of-fit of the model. Moderate deviations from a straight line may not be serious [6]. The adequacy of a theoretical model implies the difference between the observed and the expected results.

RESULTS AND DISCUSSION

During the composting process, the temperature was increased from 36ºC to 60ºC. However, the first 40 days (hydrophilication period) it did not exceed above 45ºC. The moisture of the composting material was maintained in the first weeks to 50-60% by adding pretreated OMWW while during the final stages of the composting process the moisture was dropped to 43%.

The Water Holding capacity (WHC) was reduced from 282% to 144%. The pH range was between 5.5 to 8.7 while the electrical conductivity was reduced from 3800 mS/cm to 1700 mS/cm. Moreover, the phytotoxicity values showed that the composting material at the end of the process has been bioconverted to a phytonutrient soil conditioner. The FOGs content was reduced from 5 %, which was the initial value, to 0.6 % during the first 40 days of composting. All the results are presented in Table 3.

According to obtained composting data from previous studies performed in our group [5] and the methodology described previously, the following equation was developed where R^2 is 91% in order to predict the concentration of FOGs:

$FOG_t = -1.953\ln(OUR)_t - 6 + 0.014*(WHC)_{t-5} - 0.170*pH_{t-2} + 2.291$

Where t is the present day measurement of corresponding parameter where as the (t-n) is the lag time measurement of corresponding parameter before n days.

TABLE 3
Experimental results of the industrial scale co-composting process of OMSR with OMWW

Time days	pH	WHC %	OUR (mg/g/d)	FOG %
1	5.55	279	0.00	5.0
2	5.75	259	0.79	4.0
3	5.95	247	0.64	3.7
4	5.84	253	0.31	3.2
5	5.35	272	1.59	3.0
6	5.79	282	1.27	3.9
7	5.55	284	1.11	3.3
8	5.55	280	1.43	3.7
9	5.53	243	1.75	3.7
10	6.00	243	1.59	2.8
11	5.90	243	1.60	3.0
12	6.10	220	2.10	2.5
13	5.99	265	3.10	2.4
14	6.20	237	2.10	2.7
15	6.50	260	2.06	2.5
16	5.92	260	2.31	2.7
17	6.46	223	2.48	3.0
18	6.50	231	2.90	2.4
19	5.82	223	3.30	2.4
20	5.87	247	3.00	1.8
21	5.77	233	3.30	1.9
22	6.13	263	3.00	1.8
23	5.60	234	3.50	1.3
24	5.68	230	3.80	1.3
25	5.55	237	3.30	1.2
26	6.28	222	3.81	1.5
27	6.63	214	3.50	1.1
28	6.02	232	4.05	1.5
29	6.04	202	4.29	1.3
30	6.48	223	4.76	1.2
31	6.92	237	5.10	1.4
32	6.35	247	5.46	0.0
33	6.31	255	5.79	1.2
34	5.67	255	6.28	0.9
35	5.87	219	6.61	0.1
36	6.05	248	6.40	0.0
37	6.40	222	6.94	0.4
38	6.93	256	8.81	0.8
39	6.69	242	7.71	0.6
40	6.07	259	8.50	0.6
41	6.80	240	9.10	0.6

According to this relationship, the present value of FOG in an OMSW-OMWW co-composting pile can be predicted by using the OUR value received before six days, the WHC value received before five days, and finally, the pH value received before two days. The above model was validated twice in a batch open pile windrow composting system. The results are presented in Table 3 as well as the predictions of FOGs are presented in Figure 1 together with the corresponding measurements. As it is observed, experimental data are adequately predicted by model simulations.

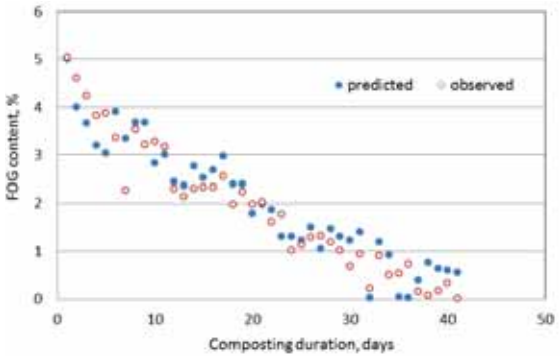

FIGURE 1
Experimental data and model predictions of FOGs during the first 40 days of composting

CONCLUSIONS

The experimental results demonstrate that the FOGs are completely degradated in about 35 days of composting. During that period, the temperature of the piles was not risen above 45ºC which proves that the assimilation of FOGs is not performed by thermophilic bacteria. The methodology of regression analysis by residuals for the construction of a dynamic model to predict the amount of FOGs present in the compost proved to be in agreement with the experimental findings.

ACKNOWLEDGEMENTS

This work was supported by ORGANO-HUMIKI THRAKIS IKE.

REFERENCES

[1] Muktadirul Bari Chowdhury, A.K.Md., Akratos, C.S., Vayenas, D.V. and Pavlou, S. (2013) Olive mill waste composting: A review. International Biodeterioration and Biodegradation. 85, 108-119.
[2] Vlyssides, G.A., Mai, S. and Barampouti, E.M., (2009) An integrated mathematical model for co-composting of agricultural solid wastes with industrial wastewater. Bioresource Technology. 100(20), 4797-480.
[3] Vlyssides, G.A., Loukakis, H., Karlis, P., Barampouti, E.M. and Mai, S. (2004) Olive mill wastewater detoxification by applying pH Related Fenton Oxidation Process. Fresen. Environ. Bull. 13, 501-504.
[4] Mangkoedihardjo, S. (2006) Revaluation of Maturity and Stability Indices for Compost. J. Appl. Sci. Environ. Mgt. September. 10(3), 83-85.
[5] Tsiodra, C., Lambrou, G., Seintis, G. and Vlyssides, A.G. (2016) A novel respirometer for the determination of compost stability. In: 4th International Conference on Sustainable Solid Waste Management. Limassol.
[6] Ingels, R.M. (1980) How to use the computer to analyze test data. Chem. Eng. Nov. 145–156.
[7] Vlyssides, G.A., Loisides, M. and Karlis, K.M. (2004) Integrated strategic approach for reusing olive oil extraction by-products. J. of Cleaner Production. 12, 603-611.
[8] Thompson, H.W. (2001) Test Methods for examination of composting and compost. US Composting Council.
[9] Hansen, L.J., Fiok, E.A. and Hovious, C.J. (1980) Dynamic modeling of industrial wastewater treatment plant. J. WPCF. 52, 1966-1975.

Received: **19.01.2018**
Accepted: **25.04.2018**

CORRESPONDING AUTHOR

Apostolos Vlyssides
School of Chemical Engineering,
National Technical University of Athens,
Iroon Polytechneiou 9, Zografou 157 80,
Athens – Greece

e-mail: avlys@tee.gr

© by PSP Volume 27 – No. 7/2018 pages 4904-4909 Fresenius Environmental Bulletin

EXPERIMENTAL INVESTIGATION OF UREA INJECTION DELAY STRATEGIES ON EMISSION CHARACTERISTICS OF HEAVY DUTY DIESEL ENGINE UNDER TRANSIENT TEST CYCLE

Shuzhan Bai*, Jianlei Han, Sun Qiang, Guihua Wang, Guoxiang Li

School of Energy and Power Eng., Shandong University, Jinan 250061, China

ABSTRACT

The influences of urea injection delay strategies on emission performance and NH3 slip in the transient test cycle conditions are studied with air-assisted urea injection system for a heavy duty diesel engine. The laws of the edge delay strategies are experimental studied about NOx conversion efficiency, NH_3slip and urea consumption. The experimental results indicate that NOx emission increases with the rising edge delay time increasing, and declines with the falling edge delay time increasing. The NH_3 slip has a inflection point along with the increasing of the rising edge delay time and the falling edge delay time. For this study, when both emission performance and urea consumption could achieve the best results when the rising edge delay time is 500ms and falling edge delay time is 100ms.

KEYWORDS:
Diesel engine, Selective catalytic reduction (SCR), Urea injection, Emission characteristics, NH3 slip

INTRODUCTION

With the deterioration of the environment and the consequent more stringent emission standards, a series of after-treatment system are proposed for the diesel engine applications. Among these after-treatment systems, the selective catalytic reduction (SCR) system is utilized to convert NOx emission to nitrogen, the diesel oxidation catalyst (DOC) is used to o oxidize the hydrocarbon and carbon monoxide, and the diesel particulate filter (DPF) is used to capture the particle matters [1, 2]. To meet future emissions legislation standards, high NOx conversion efficiency in the after treatment system is required in the SCR approach [3-5].

The urea solution is injected into the exhaust and decomposes to $NH_3$with heating by exhaust. Conversion efficiency of NOx is depending on the appropriate temperature, urea injection time and injection amount closely. However the temperature of cordierite carrier has a certain lag with the change of the diesel engine's working condition due to the specific heat capacity of the cordierite carrier [5]. The escape of ammonia will be very large when the working condition changes from low exhaust temperature to high exhaust temperature if this feature is not considered, which would be produced secondary pollution. On the other hand, it would lead to the lower NOx conversion efficiency if the urea injection is insufficient. So it is necessary to establish a reasonable urea injection strategy to obtain the required higher NOx conversion efficiency and lowerNH_3slip. Yujun Liao experimental studied the heat transfer characteristics of spray/Wall interaction in diesel SCR system under exhaust flow conditions [6]. Lucio Postrioti described a new methodology for inspecting the behaviour of urea-water sprays in realistic conditions based on a hot-air flow tunnel enabling optical inspection of the spray through phase-Doppler anemometry and back-light imaging [7]. JakovBaleta simulated the physical processes of all relevant phenomena occurring during the SCR process including chemical reactions taking part in the catalyst [8]. Jungmo Oh analyzed the spray characteristics of a urea injector and to determine the distribution of urea solution droplets in a transparent manifold using laser diagnostics and a high speed camera [9]. Jiang Lei researched the influence of injection precision of urea solution on the catalytic performance for diesel SCR system, and the load step ratio was introduced to modify the NOx emission during transient working conditions [10].

These studies have carried out detailed analysis of the effects of injection uniformity of urea solution, exhaust temperature on the catalytic efficiency. However, the temperature of the catalyst carrier is lagging behind the change of the exhaust temperature during the transient working condition. The influence of urea injection delay on the emission performance of SCR system during transient conditions is experimental studied using gas assisted urea injection system in this paper, the effects of different urea injection delay control strategy and delay time on the NOx conversion efficiency and the NH_3 slip is analyzed in this study.

EXPERIMENT SETUP AND METHODS

Experiment setup. The engine used in these experiments was equipped with common rail system of BOSCH. Table 1 and Fig.1 show the relating specifications and detailed information about the test bench, respectively. The urea injection used for SCR is air-assisted urea injection system; the detailed specification of SCR is shown in Table 2. The experiments were carried out by using Electric dynamometer, Exhaust gas analyzer and NH_3 slip analyzer to focus on torque and speed, concentration of NOx and O_2, and NH_3 slip, respectively, the details of these equipments were shown in Table 2.

Urea delay injection control strategy. The calibration of urea injection quantity is decided by the mass ratio of the ammonia and nitrogen oxides, which is based on exhaust flow (to reflect catalyst space velocity) and catalyst temperature (estimated by the exhaust temperature before and after the catalyst) under steady working condition, and the calibration process of urea injection quantity MAP in engine control is based on rotational speed and fuel quantity, which should weight and consider balance of the NOx conversion efficiency and NH_3 slip under calibration working conditions.

Catalyst temperature cannot be reflected truly by the exhaust temperature due to the thermal inertia of ceramic substrates when engine is ran intransient test cycle conditions, the changes of catalyst temperature lag behind which of the exhaust temperature when the load is changed. The actual amount of NH_3neededfor catalyst theoretically does not match to the decomposed NH3 by urea injection when load increased. So the no reacting NH3 will overflow and escape into atmosphere, which would lead to secondary pollution; on the other hand, the demanded NH_3 for catalytic reaction is insufficient when load declined, which is detrimental to the catalytic efficiency. In view of the characteristics of the SCR urea injection system, the characteristics of the rising edge delay and the falling edge delay were defined, and the first order system is introduced to amendment urea injection quantity. The differential equation of the rising edge delay and the falling edge delay were shown in equation (1) and (2).

$$C(s)=\frac{1}{s_1}-\frac{T}{Ts_1+1} \quad (1)$$

$$C(s)=\frac{1}{Ts_2+1} \quad (2)$$

TABLE 1
Test engine specifications

Project	Specification
Engine Type	6 cylinders in-line/Turbocharger /Inter-cooling
Fuel supply system	high pressure common rail
Bore×Stroke /mm×mm	126 ×155
Swept volume/L	11.6
Compress Ratio	17 : 1
Rated power / kW	338
Rated speed / r/min	1900
Maximum torque / N·m	2110
Idle Speed /r/min	650
EGR type	Electronic control EGR
After treatment	SCR
Emission standard	EURO IV

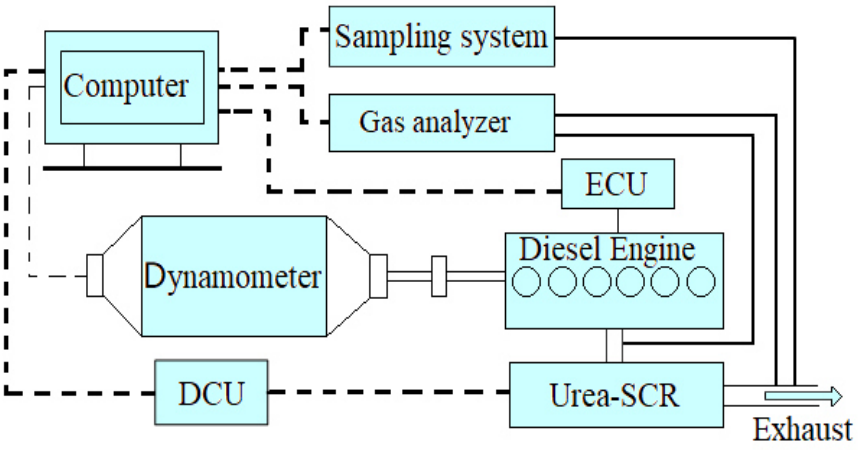

FIGURE 1
Schematic of experimental setup
TABLE 2

Specifications of SCR

Parameter/Unit	SCR
PGM/g/L	1.06
Material	Cordierite
Pore/(cell/cm^2)	62
Wall thick/mm	0.10
Diameter/mm	267
Length/mm	407
Volume/L	22

TABLE 3
Experimental setup

Equipment	Model	Manufacturer	Measuring principle	Accuracy of measurement
Electric dynamometer	INDYS66JD	AVL	- -	Speed: ±1r/min Torque: ±0.1%FS
Exhaust gas analyser	MEXA-7100D	HORIBA	NOx: GLD O_2:MPD	1ppmvol 0.01%vol
NH_3 slip analyser	LDS6	SIMENZ	In-situ optical measurement	1ppmvol

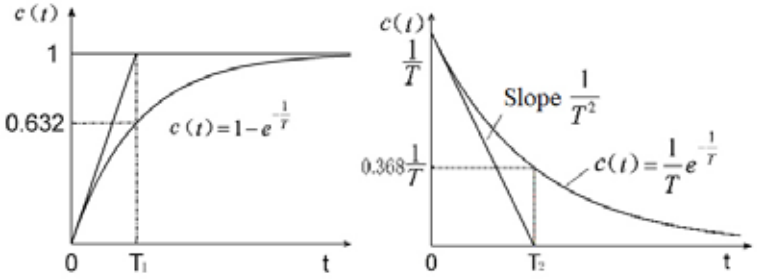

(a) The curve of unit step response (b)The curve of unit impulse response

FIGURE 2
First-order system response curve

In which s_1 is the plural variable of the rising edge delay, s_2 is the plural variable of the falling edge delay, T is the time constant of first-order system.

The unit step response of the rising edge delay and the unit impulse response with falling delay could be obtained by the Lagrangian inverse transformation for the equation (1) and (2), respectively.

$$c(t_1) = 1 - e^{-\frac{t_1}{T}} (t_1 \geq 0) \quad (3)$$

$$c(t_2) = \frac{1}{T} e^{-\frac{t_2}{T}} (t_2 \geq 0) \quad (4)$$

In which t_1 is the time of the rising edge delay, t_2 is the time of the falling edge delay, T is the time constant of first order system.

The unit impulse response curve of rising edge delay and falling edge delay were shown in Fig. 2. The transient output value at T_1 moment is 63.2% of steady state output valve during the process of the rising edge delay; and which is 36.8% of steady state output valve during the process of the falling edge delay. The urea injection adopts the rising delay strategy when the diesel engine changes from the low temperature to high temperature working condition, the actual injection increase with time gradually according the unit impulse response curve of rising edge delay, so the peak of NH3 slip due to the lag of temperature rising should be control. Conversely, the falling delay strategy when the diesel engine changes from the high temperature to low temperature working condition.

In order to achieve the purpose of taking into account the performance of emission and the economy of urea consumption, the delay strategies of rising edge and falling edge for correction of urea injection must be considered at the same time.

RESULTS AND DISCUSSION

The influence of rising edge delay strategy on the emission performance. The influences of the rising edge delay time on NOx conversion efficiency, NH3 slip and urea consumption under the ETC cycle is shown in Fig. 3.The urea consumption was gradually reduced with the increase of the delay time from 0 to 1000ms, which reduced 10.3%;the NOx conversion efficiency also decreased 12.2% at the same time,, when the delay time is set within 400 ms to 800 ms, the declining trend of the NOx conversion efficiency is slight; Amount of NH3 slip decreases first and then increases with the increase of the delay time, the inflection point appears at 600 ms. So the urea consumption and NH_3slip could be reduced effectively by using the rising edge delay strategy.

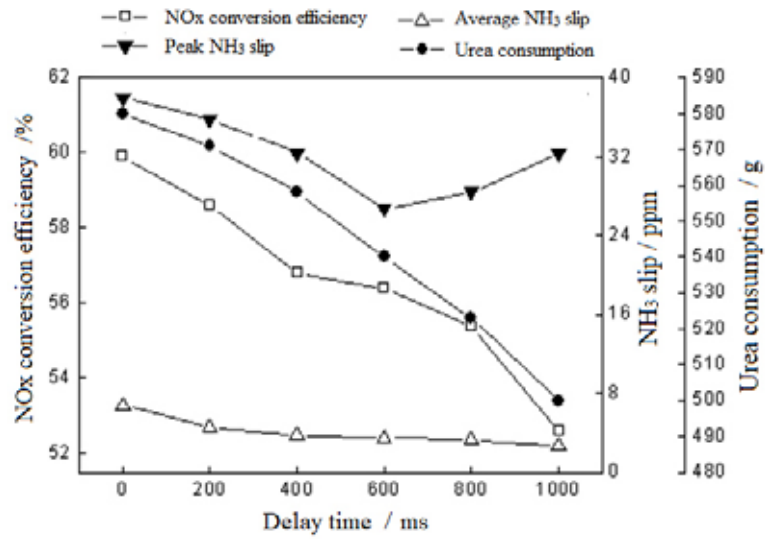

FIGURE 3
The influences of rising edge delay on the performance of emissions

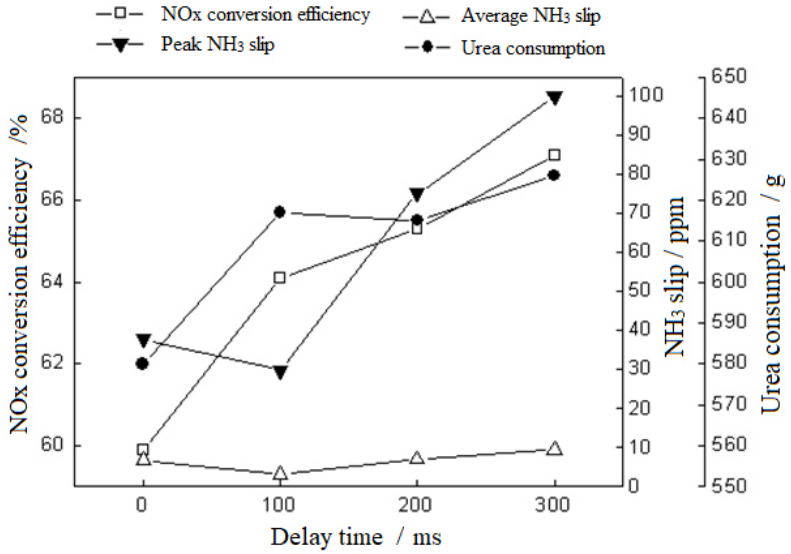

FIGURE 4
The influences of falling edge delay on the performance of emissions

The influence of falling edge delay strategy on the emission performance. The influences of the falling edge delay time on NOx conversion efficiency, NH3 slip and urea consumption under the ETC cycle is shown in Fig. 4. The urea consumption gradually increased with the increase of the delay time, and the NOx conversion efficiency increased at the same time. The urea consumption increased 7.9% and the NOx conversion efficiency increased 12.0%when the delay time increase from 0 ~ 300ms, however, it is important to note that the peak value of NH3 slop increased 164%. The peak concentrations of NH_3slip decreases first and then increases with the increase of the delay time, the inflection point appears at 100ms. Therefore, 100 ms was selected as falling edge delay time by weight and consider balance of between the emission performance and urea efficiency.

The influence of mixing delay strategies on the emission performance. The influence of falling edge delay time (set as 100 ms) and the rising edge delay time (set as 0, 200ms, 400ms, 600ms, 800ms) on NOx conversion efficiency and the NH3 slip were shown in Figure 5. It can be seen that the overall distribution is similar to the trend when the rise edge delay is only considered, namely he urea consumption and NOx conversion efficiency are declining along with the increase of the rising edge delay time, t, the decline trend of NH_3slip quantity is steady. When the rising edge delay time increased from 0 to 800 ms, urea consumption dropped 19.4% and NOx conversion efficiency decreased 12.9%. Comprehensive consideration, the better emission performance and efficiency of urea could be achieved when the falling edge delay time is 100ms and rising edge time is set within the range of 400ms to 600ms.

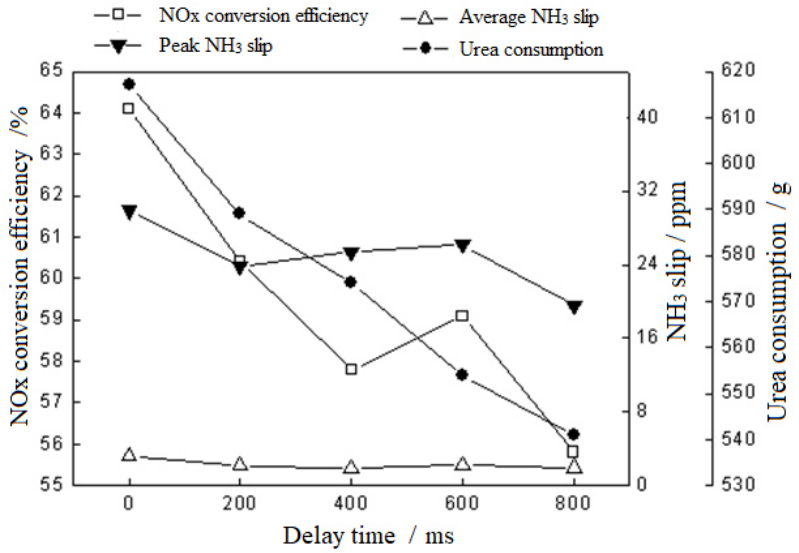

FIGURE 5
The influence of mixing delay strategies on the emission properties

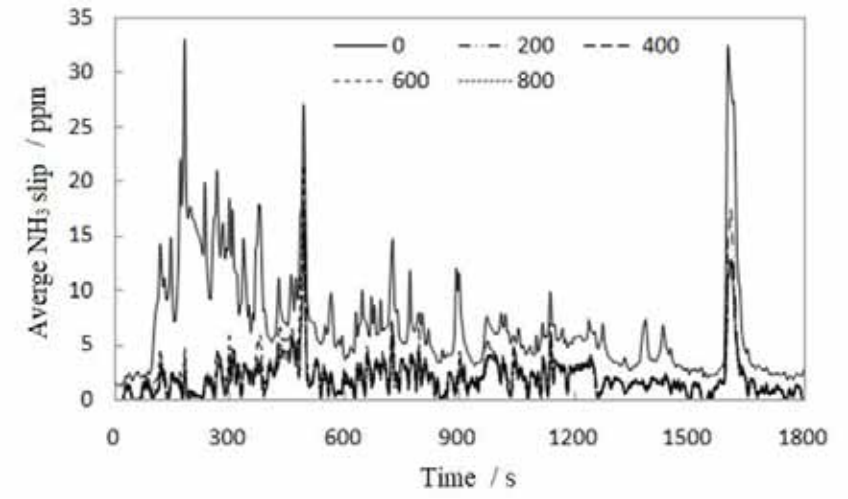

FIGURE 6
The influence of mixed delay strategies on the ammonia escape at ETC

The influence of the injection delay strategy on the transient NH_3 slip. The influence of injection delay strategy on the transient NH_3 slip during ETC cycle was shown in Figure 6. The transient NH_3 slip has a distinct decline trend within the first 450s of the test cycle and 1600s with the increase of the rising edge delay time. Diesel engine running in urban working conditions during the first 450s of ETC cycle, in which the working conditions changes frequently, most of the time in the speed and low load region, the exhaust temperature is low, so the NOx conversion efficiency is low, excessive urea injection could easily lead to an obvious increase in the peak NH_3 slip.

Near the 1600s of ETC cycle, the diesel engine is in the high speed condition, the speed is more stable at this period. The diesel engine load is low in the period of 35s before 1598s, so the exhaust temperature is low, so large amounts of NH_3 were stored inside the catalyst, which will be released when the exhaust temperature increased due to the engine load increase suddenly after 1598s, the reaction couldn't consume these NH_3, so leading to the emergence of the peak NH_3 slip. The injection delay strategy improved the responsiveness of urea injection to the change of exhaust temperature, which could reduce the NH3 slip obviously.

CONCLUSIONS

The influence of urea injection delay strategies on NOx conversion efficiency, NH3 slip in the transient test cycle conditions for urea SCR system is studied in this paper. A reasonable rising edge delay strategy not only can reduce the peak NH3 slip effectively, but also can reduce the urea consumption; and reasonable falling edge delay strategy is condu-

cive to make full use of the NOx conversion efficiency. Therefore, delay strategies can be used for weight and balance the NOx conversion efficiency, urea consumption and NH3 slip during the development and calibration of the urea injection strategies, furthermore, the emission performance and the economy of urea could be optimized.

ACKNOWLEDGEMENTS

This study was supported by the National key research and development program [Grant number 2017YFC0211305, 2016YFD0700705], Innovation plan of agricultural machinery equipment research and development in Shandong [Grant number 2016YF003], the national Engineering Laboratory for Mobile Source Emission Control Technology [Grant number NELMS2017A09] and Natural Science Foundation of Shandong Province [Grant number ZR2015EM051]. The authors would like to thank the reviewers whose constructive and detailed critique contributed to the quality of this paper.

REFERENCES

[1] Guan, B., Zhan, R., Lin, H., Huang, Z. (2015) Review of the state-of-the-art of exhaust particulate filter technology in internal combustion engines. Journal of Environmental Management. 154, 225-258.
[2] Durmaz, M., Kalender, S.S., Ergin, S. (2017) Experimental study on the effects of ultra-low sulfur diesel fuel to the exhaust emissions of a ferry. Fresen. Environ. Bull. 26, 5833-5840.
[3] Aksay, E.K., Akar, A. (2017) The filtration of black smoke from diesel engine exhaust using pumice ore. Fresen. Environ. Bull. 26, 2293-2301.
[4] Bai, S., Wang, G., Liu, Y., Sun. L. and Li, G. (2017) Experimental study on emission characteristics of non-electronic control diesel engine with DOC/POC/SCR combined system. Fresen. Environ. Bull. 26, 1359-1364.
[5] Stein, H.J. (2006) Diesel oxidation catalysts for commercial vehicle engines: strategies on their application for controlling particulate emissions. Applied Catalysis B: Environmental. 10(1-3), 69-82.
[6] Liao, Y., Roman, F., Panayotis, D.E., Konstantinos, B. (2017) Experimental investigation of the heat transfer characteristics of spray/wall interaction in diesel selective catalytic reduction systems. Fuel. 190, 163-173.
[7] Postrioti, L., Brizi, G., Ungaro, C., Mosser, M., Bianconi, F. (2015) A methodology to investigate the behavior of urea-water sprays in high temperature air flow for SCR de-NOx applications. Fuel. 150, 548–557.
[8] Baleta, J., Martinjak, M., Vujanovic, M., Pachler, K., Wang, J., Duic, N. (2017) Numerical analysis of ammonia homogenization for selective catalytic reduction application. Journal of Environmental Management. 203, 1047-1061.
[9] Oh, J., Lee, K. (2014) Spray characteristics of a urea solution injector and optimal mixer location to improve droplet uniformity and NOx conversion efficiency for selective catalytic reduction. Fuel. 119, 90-97.
[10] Jiang, L., Ge, Y., Ding, Y.. (2010) Study on Steady and Transient Characteristics of Urea-SCR System for Diesel Engine. Chinese Internal Combustion Engine Engineering, 31(6), 38-42.

Received: **21.01.2018**
Accepted: **15.04.2018**

CORRESPONDING AUTHOR

Shuzhan Bai
School of Energy and Power engineering,
Shandong University,
Jinan 250061 – China

e-mail: baishuzhan@sdu.edu.cn

© by PSP Volume 27 – No. 7/2018 pages 4910-4920 Fresenius Environmental Bulletin

CHANGES OF THE TIDAL SAND RIDGES IN THE SOUTHERN YELLOW SEA

Zhaojun Song[1,2,*], Hongbo Yan[1], Jue Huang[3] , Haijun Huang [4,5], Xingyu Yuan[1]

[1]Shandong Provincial Key Laboratory of Depositional Mineralization and Sedimentary Minerals, College of Earth Science and Engineering, Shandong University of Science and Technology, Qingdao, Shandong 266590, P.R. China
[2]Laboratory for Marine Mineral Resources, Qingdao National Laboratory for Marine Science and Technology, Qingdao, Shandong 266071, P.R China
[3]College of Geomatics, Shandong University of Science and Technology, Qingdao, Shandong 266590, P.R. China
[4]Key Laboratory of Marine Geology and Environment, Institute of Oceanology, Chinese Academy of Sciences, Qingdao, Shandong 266071, P.R China
[5]University of Chinese Academy of Sciences, Beijing 100049, P.R China

ABSTRACT

The large-scale fan-shaped tidal sand ridges in the south Yellow Sea along the Jiangsu Coast is characterized by a special geomorphology system in landform feature and in hydrodynamic conditions. This paper deals mainly with the changes of beach profile, tidal troughs in the sand ridges and present movement of the total tidal sand ridges using satellite images, bathymetric maps and field survey data. The results show that the tidal sand ridges are in a stage of separation with the number of sand ridges increasing and the average area of each ridge decreasing. The movement of tidal sand ridges in this area is affected by tidal currents and submarine topography. Tidal sand ridges formed rapidly and the tidal troughs were developed greatly in the condition of tidal current; the migration of main tidal troughs are the main drive of the whole sand ridges' changes and directly affect the shift direction of big sand ridges. Sand ridges tend to be accumulated in center area and outer area eroded.

KEYWORDS:
Tidal sand ridges, southern Yellow Sea, satellite images and GIS, change

INTRODUCTION

There are large-scale fan-shaped tidal sand ridges in the south Yellow Sea along the Jiangsu Coast (China), between the modern Changjiang River delta in the south and the abandoned Huanghe River delta in the north (Fig. 1). It extends about 200 km in length and 140 km in width, containing 10 large scale linear sand ridges (including submarine sand ridges), the largest sand ridges in China. It is a special geomorphology system in landform feature and in hydrodynamic conditions. The sand ridges extend in the direction of north, NE, east and south with a top point at Qianggang Town and look like a fan shaped. The tidal sand ridges consist of more than 70 individual tidal sand ridges.

The tidal sand ridges are an important kind of geomorphic unit on many continental shelves and coastal regions, and they are widely distributed in estuaries, coastal bays and at the ends of straits [1, 2]. Scientists have studied them since 1963. Since then, many studies have been made in tidal sand ridges. For instance, the internal structure and sedimentology of tidal sand ridges have been described [3, 4]; the formation and evolution of tidal sand ridges have been studied [5]; the depositional patterns and the classification of tidal sand ridges have been discussed [6, 7].

The radial tidal sand ridges in the southwestern Yellow Sea off the Jiangsu coast were discovered in the 1950s, first reported in literatures in the 1970s, and studied in detail in the 1980s [8, 9]. Previous studies basically focused on morphology, surface-sediment distribution, tidal current pattern, and partly concerned the formation and evolution of the marine radial tidal sand ridges [8, 10-15]. More recently, the tidal sand ridges' formation mechanism, dynamic environment and evolution have been analyzed [16, 17, 18] and its environment of formation and the sediment supplier were discussed recently [4, 19, 20].

Although there are many scientists have concerned the formation and change of the tidal sand ridges, the modern stability and its evolution have not paid attention yet. The paper deals mainly with the changes of beach profile, tidal troughs in the sand ridges and present movement of the total tidal sand ridges using satellite images, bathymetric maps and field survey data.

Experiment. Geological and oceanographic background. Sediments in the research area are mainly fine sand, silty sand and clayey silt. The coarser sediments are located near the coastline and the edge sand ridges, the finer seaward and the trough bottom between sand ridges. The tidal ridges are mainly composed of fine sand, while silty sand, silt and clayey silt are usually distributed in the

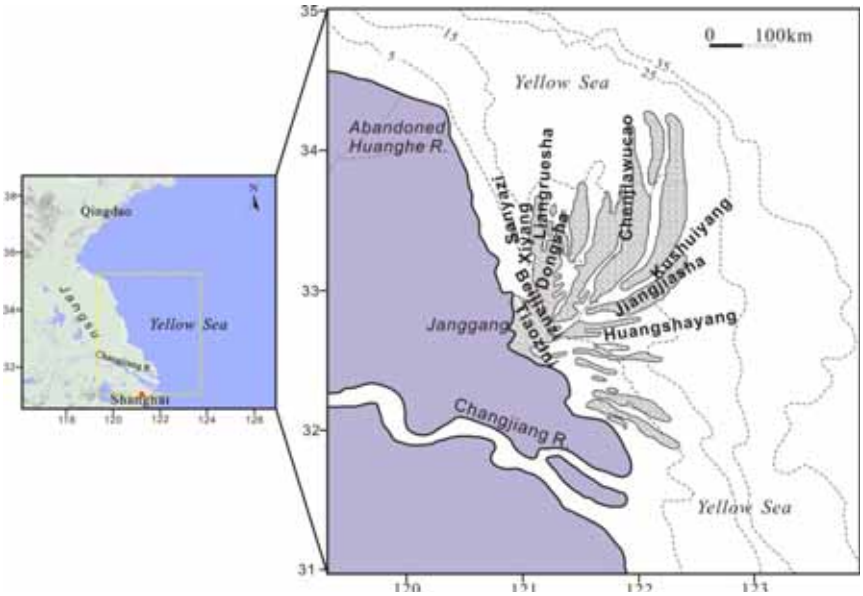

FIGURE 1
Location of the study area [21]

troughs. In some deeply eroded parts of the tidal channels, however, coarse calcic-cemented-sand-grain nodules can be found, comprising up to 29% of the sediments [22].

The facies is made up of sand, silt-sand and mud of gray color, with 40–85% sand, 15–40% silt, and 5–15% clay. Flaser bedding, bi-directional cross-bedding and graded bedding are well developed. Small cross-bedding, flaser and wavy bedding are present in the lower part of the unit and horizontal bedding and symmetric ripple marks occur in the upper part of the unit. Shell debris and foraminifers are common. The graded bedding is 10-20 cm thick and usually occurs in vertically superimposed sets to form rhythmite. The foraminifer assemblage indicates that the facies was deposited in a shallow marine environment [15].

There are many sediment suppliers in research area, including two important parts: erosion from the abandoned Huanghe River delta in the north and flow from the present Changjiang River in the south. The content of suspended sediment in satellite images was high at both places [23]. The strong erosion at the abandoned Huanghe River delta and its submarine bottom in the north provided the study area about 40 billion m^3 sediment [24], most of which entered the center of sand ridge areas and caused parts of the sand ridges to accrue rapidly up to 100 m/a in the north [25]. Comparison of different images showed that sand ridges in the north area moved frequently; and that the positional change rate of some small ones was up to 350 m/a [12], resulting in lots of sediment re-suspended.

Tidal currents are radial with flood tidal currents converging to the center of the research area and ebb currents diverging to the sea, and the tidal currents are forward and backward [26]. The convergent–divergent tidal current field in the study area is a result of propagation and reflection of the tidal waves in the East China Sea and the Yellow Sea. The progressive tidal wave from the Pacific Ocean, through the East China Sea, propagates in the Yellow Sea, which meets the Shangdong Peninsula and is reflected, forming an anti-clockwise rotary tidal wave system. The wave system meets the progressive tidal wave system from the East China Sea and form the special tidal current pattern in the tidal sand ridges area, off Qianggang area in southwestern Yellow Sea [19, 26, 27].

The tidal range is 6–7 m on an average at the research apical area. The maximum tidal range of 9.28 m appears at Huangshayang, and the tidal range decreases gradually toward south and north [15].

The surface velocity of spring tidal currents is more than 1.5 m/s with the maximum up to 4.4 m/s in the northern part of the research area [28] and 1.0 m/s, with the maximum of 2.5 m/s in the southern part [29]. The average velocity of the spring flood-ebb tidal currents is strong enough to erode loose sediments on the sea floor, which make them re-suspended. The re-suspended sediments are one of the sediment sources for the formation of the sand ridges which is similar to that in the North Sea [30, 31]. However there is something which are different from the North Sea. The sand ridges are located at near coast and parts of them are above the sea level and the waves are important factors which make the submarine sediments re-suspended.

Data source and processing. Satellite images including Landsat thematic mapper (TM), NOAA, Synthetic aperture radar (SAR) images acquired from 1987 to 2000 were used to monitor the movements of submarine main tidal troughs and sediments distribution and diffusion. Two bathymetric maps (1966 and 1979) were used to compare the

sand ridges' change in vertical and other bathymetric maps for additional comparison. Field survey (limited beach profiles) were made for testing.

Satellite images were processed in a special software-ENVI 5.0. Many methods of image processing, such as image enhancement, band stretching, multi-band false colour composite, histogram modification, supervised and unsupervised classification etc. were tested to see if they could improve images interpretation [32, 33]. Nine training samples for typical tidal sand ridges and seawater areas were chosen to analyze their optical features for supervised classification.

The nautical charts from 1966 to 1977 and SAR images in 1995 and 2000 were interpreted and analyzed to obtain the positions of main tidal trough talwegs. After the process of radiate reference, geo-rectify and speckle noise removal et al. in ENVI 5.0, SAR images were analyzed to extract the positions of main tidal trough in software-ArcGIS 10.2. Although the boundary standards of the trough's talwegs during different periods are different, there is a little difference in bordering the main trough's talwegs.

Bathymetric maps and aerial photos were digitized and analyzed in a GIS software-Mapinfo.12. Suitable number control points must be selected in order to compare shoreline changes in different maps or satellite images. Usually more or less permanent natural morphological features such as a corner of bluff edge, top point of escarpment on beach, the turn of beach scarp, branch of small river; permanent human made structures, such as human made channel on land, permanent building on beach, dam or big house, bridges et al., and the most seaward edge of permanent vegetation, such as big trees.

The beach profiles were measured between 1999 and 2000 using an GTS-310 metric apparatus with an accuracy of 0.01 m in order to analyze the beach profile changes and tidal troughs shift.

RESULTS AND DISCUSSION

Changes in beach profile of Tiaozini sand ridge. 4 E-W profiles from north to south and 2 or 3 times surveyed between January 16, 1999 and September 10, 2000 are used to monitor the seasonal changes of beach elevation. The results are shown in Figs. 2-5.

The profile 1 is located at north of Tiaozini sand ridge, which was surveyed between January 16, 1999 and June 3, 2000. The beach accumulated in winter and eroded in summer which covered almost all beach. The amount of erosion was changed from 0 (balance in erosion/accumulation) to 30 cm with the positional distance increasing seaward, and the general thickness of erosion was 20 cm with the maximum up to 50 cm. The small troughs' movements were more rapidly than that of tidal flat, especially for those troughs at 400 m and 2, 800 m from baseline, where the troughs are widened a lot with the maximum of 150 m (Fig. 2).

Profile 2 is located at south of profile 1, which was surveyed in January, May and September 2000. The result showed that the beach changes are small (only several centimeters) between September and January, but much large (up to 60-70 cm) between May. The beach altitudes at 2600 m from baseline are 3.19 m, 2.65 m and 3.14 m respectively surveyed in January, May and September, and the same value are 1.81 m, 1.24 m and 1.87 m at 4500 m, which showed erosion in May and deposition in January and in September. The types of troughs' changes are horizontal shift and vertical erosion for large ones and shift rapidly and merged for small ones (Fig. 3).

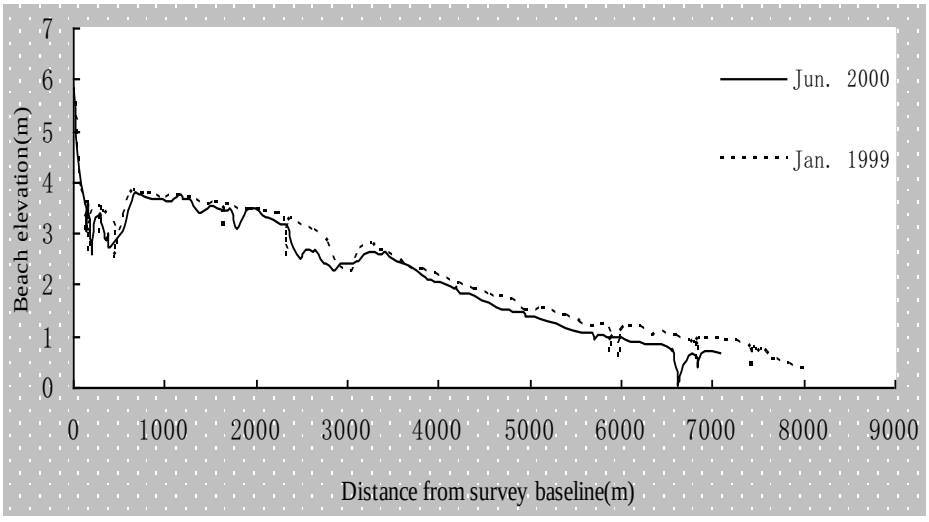

FIGURE 2
Beach changes at profile 1 (From 32^0 58' 59" N, 120^0 54' 11" E to East)

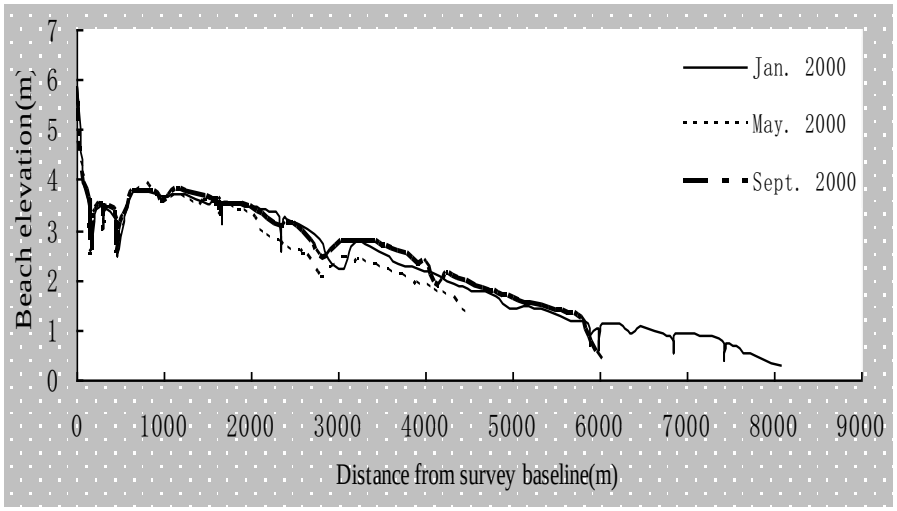

FIGURE 3
Beach changes at profile 2 (From 32^0 49' 58" N, 120^0 53' 39" E to East)

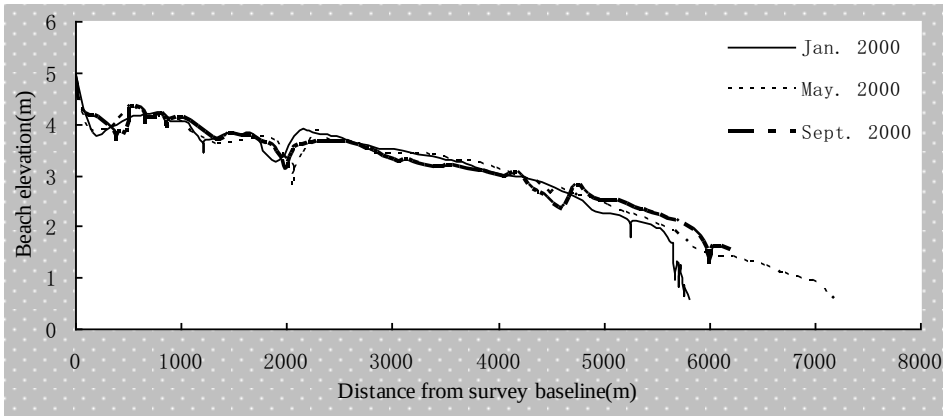

FIGURE 4
Beach changes at profile 3 (From 32^0 48' 11" N, 120^0 53' 29" E to East)

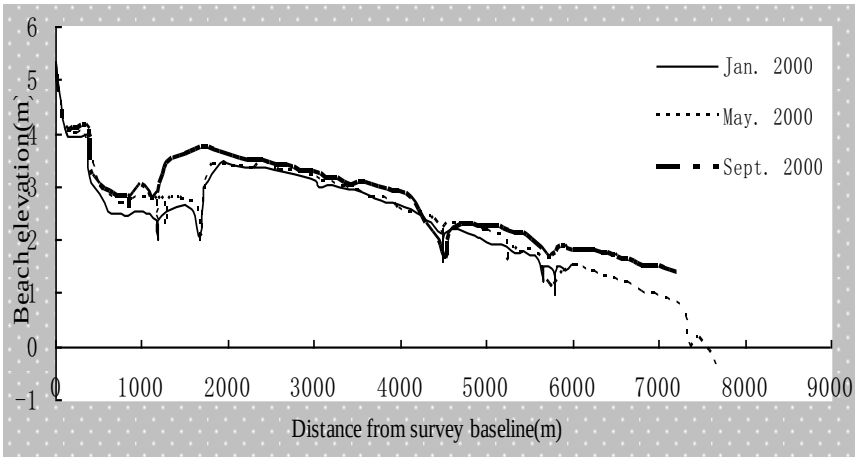

FIGURE 5
Beach changes at profile 4 (From 32^0 46' 36" N, 120^0 53' 01" E to East)

Profile 3 is located in the middle of the Tiaozini sand ridges with different beach change feature. There is erosion and deposition on beach and no change trend in the three surveys, especially the erosion in May is no obvious. The trough is shifting in side direction. A trough located at 200 m from baseline in May is moved 60 m seaward in

September. Some troughs are shifted forward and backward. There is a trough which crossed the profile at 1, 926 m from baseline in January and at 2,073 m in May and at 1, 988 m in September. There are less small troughs' mergence or disappearance (Fig. 4).

Profile 4 is located at south of Tiaozini sand ridge. Almost all the profile is deposition from January through May to September. The beach altitude at 250 m from baseline is 3.96 m in January, 3.99 m in May and 4.09 m in September and 13 cm sediments deposited. The same value at 3, 000 m from baseline is 3.12 m, 3.14 m and 3.26 m respectively and the difference is 14 cm. While the beach altitude at 7, 000 m from baseline is 0.89 m in May and 1.48 m in September and the difference is up to 59 cm. The depositional volume is increasing from upper to lower beach. The trough's changes are more obvious than that of tidal flat. The big trough is moved greatly in horizontal and in vertical. The east side of a trough crossed the profile at 1, 600 m from baseline moved 500 m westward from the position in May to that in September and the altitude of the trough bottom is 2.57 m in January, 2.62 m in May and 3.71 m in September. The thickness of sediment deposition is about 1m from May to September (Fig. 5).

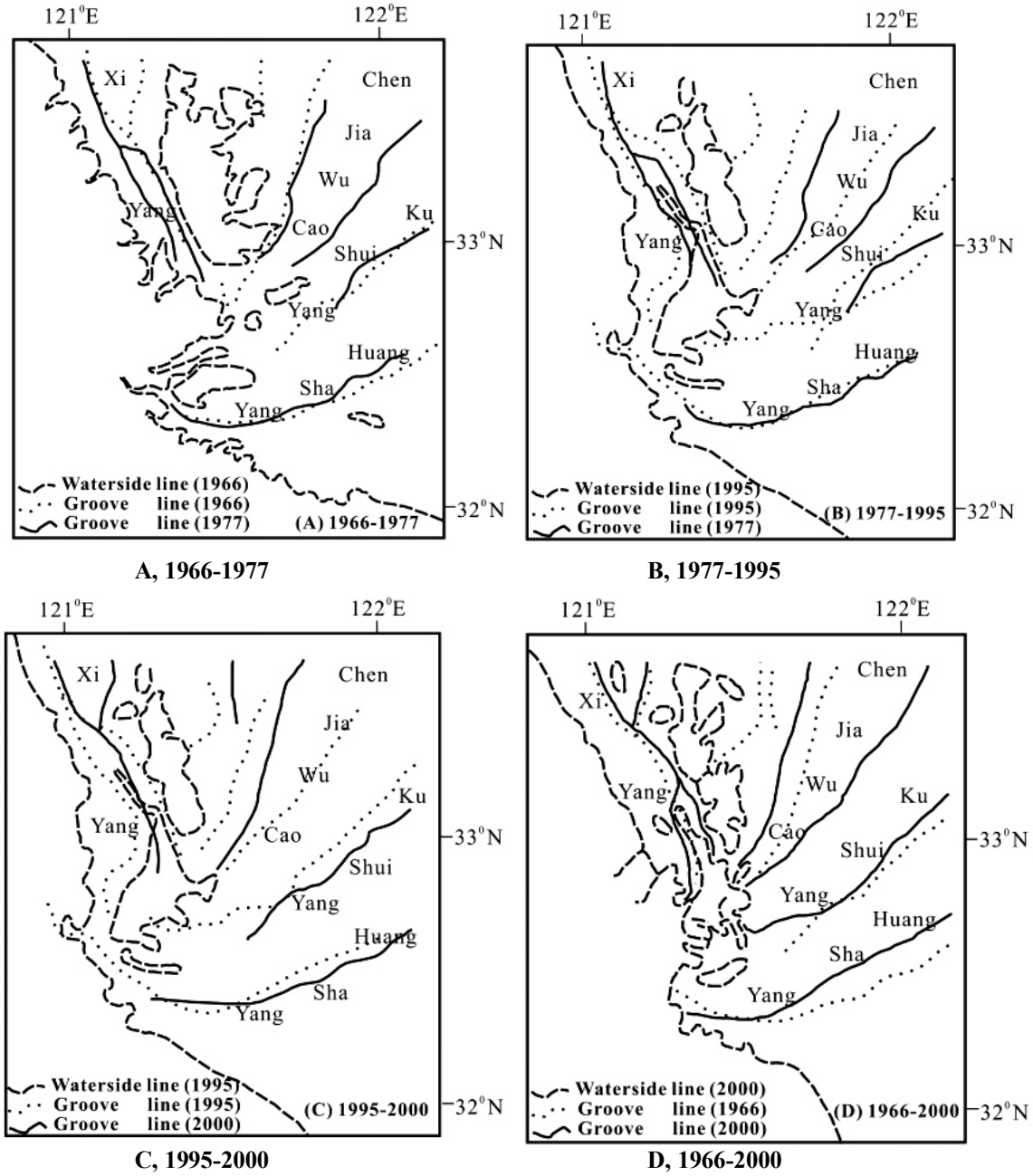

A, 1966-1977 **B, 1977-1995**

C, 1995-2000 **D, 1966-2000**

FIGURE 6
The changes of the main tidal troughs in northern of Jiangsu province beach tidal sand ridges

The main tidal troughs' movement. 2 bathymetric maps (1966 and 1977) and 2 SAR images (1995 and 2000) were used to analyze the velocity and the trend of trough's movements in a relative long period (more than 5 years).

Fig. 6A was the trough change map between 1966 and 1977. The south of the Xiyang trough in 1977 was divided into two parts by northward extended ridge—Beijianzi ridge and the main trough--east branch was located at the position similar to the single trough in 1966 (Fig. 6A). The pattern of northern Xiyang had no much changes except the position of the talweg's division point, which was moved about 2.5 km northward (Fig. 6A).

The Chenjiawu trough's talweg shifted southeastward with the maximum movement of 1.1 km at the outer of the tidal sand ridges, while the southwest part of the trough shifted slowly at the inner of the tidal sand ridges (Fig. 6A). The Kushuiyang trough moved westward or eastward with a range of 310 m-770 m at the outer of the tidal sand ridges during this period and moved southward at the inner of the tidal sand ridges obviously (Fig. 6A). The east part of the Huangshayang trough shifted northward, with the maximum movement of 1.1 km, while the west part shifted 400 m southward. The head of the trough was extended 1.1 km northwestward between 1966 and 1977 (Fig. 6A).

The two branches pattern of the Xiyang trough did not changed between 1995 and 1977, but the division point of trough moved 4.3 km northward. The division point of talweg moved westward slowly and the shift increased with the trough going north with the maximum movement of about 830 m (Fig. 6B). Chenjiawu trough moved 1.5-2.4 km westward and the shoreline of the Dongsha sand bank retreated too, parts of troughs extended inland of Dongsha sand bank with head water erosion (Fig. 6B). Kushuiyang trough moved north westward too with the maximum distance of movement about 2.1 km. Huangshayang trough moved north westward slightly (about 110 m) at the outer of the sand ridges and it had no change trend at the inner of the sand ridges (Fig. 6B).

The west branch moved 2.5 km (maximum) eastward and the east branch 100-200 m westward between the Chuandonggang harbor and the Dongtaihe River between 1995 and 2000 (Fig. 6C). Chenjiawu trough has little shift in 5 years, the north of which has small shift range of 200 m with no obvious trend, while the south of which moved eastward with an average distance of 300 m (Fig. 6C). Kushuiyang trough moved 0.4 to 1.1 km south eastward at the outer of the sand ridges and it has no shift trend at the inner of the sand ridges (Fig. 6C). Huangshayang trough has shifted 1 km (outer of the sand ridges) to 0.5 km (inner of the sand ridges) north westward and north in 5 years (Fig. 6C).

Xiyang has moved eastward totally after 34 years and the shift range was increased southward from the Sanyazi sand bank with its maximum of 1.5 km. The area of Xiyang's width was enlarged for the west side - the beach was moved westward, especially for the south part which mean the talweg's movement westward (Fig. 6D). Chenjiawucao trough was moved westward about 1.4 – 1.9 km (Fig. 6D). The movement of Kushuiyang trough was decreased from the outer (1.2 km) to inner (almost stable) of the sand ridges, then it was increased up to 2.4 km (Fig. 6D). Huangshayang trough was moved NWW about 2.8 to 1.2 km from outer to inner of the sand ridges and it was near stable at the upper reach of the trough (Fig. 6D).

GIS comparison of bathymetric maps. After digitized the Bathymetric maps in 1966 and 1979, the number of sand ridges, the area of each ridges and the total area of tidal sand ridges in the two period were compared in Mapinfor 7.0.

The results showed that there are 17 small sand ridges with area less than 10 km^2 (the area was counted above 0 m in bathymetric map, it is the same followed) and the average area of each one was 6.4 km^2 in 1966, while there were 21 sand ridges with the average area of about 5.8 km^2 in 1979. Some small sand ridges have decreased and even disappeared, for example, the area of Liangyuesha in the northern of the tidal sand ridges was decreased from 60.04 km^2 in 1966 to 43.92 km^2 in 1979. Other sand ridges were increased during this period; for example, the area of Sanyazi Island in the Xiyang trough was increased from 6.4 km^2 to 15.93 km^2 (1966-1979).

The elevation the tidal sand ridges were calculated too. The elevation of sand ridges is varied from –32 m to 5.8 m with the average elevation of –7.5 m in 1966, while it varied from –34 m to 7.8 m with the average elevation of –5.6 m in 1979. It shows that the sand ridges are accumulated of 1.9 m averagely after 13 years.

The center of tidal sand ridges with 60 km in E-W and N-S direction separately was calculated. The elevation of sand ridges is varied from -31.5 m to 5.8 m with the average elevation of –0.97 m in 1966, including sand ridges area of 2, 242 km^2 above sea level with the average elevation of 1.7 m and 1, 358 km^2 below sea level with the average elevation of –5.3 m. While it varied from –33.6 m to 7.8 m with the average elevation of 0.49 m in 1979, including sand ridges area of 2, 293 km^2 above sea level with the average elevation of 3.9 m and 1, 307 km^2 below sea level with the average elevation of –5.4 m. It shows that the sand ridges are accumulated of 1.46 m in all area and 2.2 m averagely in those sand ridges above sea level, while it eroded in trough after 13 years (Fig.7).

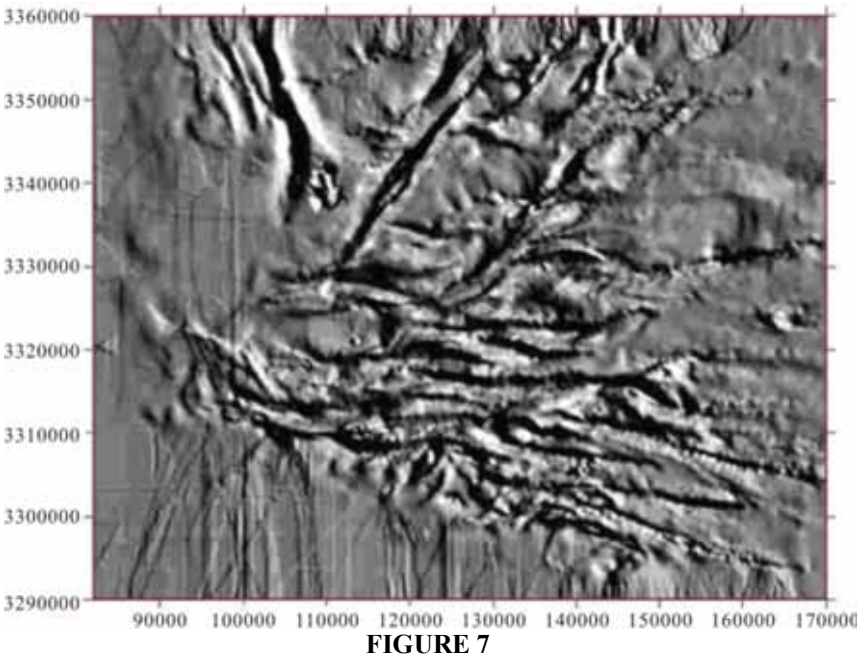

FIGURE 7
Space diagram of the central area of tidal sand ridges between 1960' and 1970'

Characteristic of changes in beach profile of Tiaozini sand ridges. The changes of beach profile is a long-tern result of interaction between beach and hydrodynamics [34]. Tidal currents, waves and tide are the main controls on the profile changes of erosion and accretion on beaches [35,36]. The seasonal characteristic of beach profile located at the Tiaozini sand ridges is accumulation in winter and erosion in summer (Figs. 2-5). However, it is different from other beach profile. For example, the beach accumulated in summer and eroded in summer at middle part of Huanghe River delta from 1985 to 1986 [35]. The reason caused the seasonal accumulation- erosion of beach is the seasonal change of wind-induced waves, whereas there is different mode wind-induced waves act on Tiaozini sand ridges and Huanghe River delta. The prevailing wind is southeast and weak in summer, and it is northeast and strong in winter at both Tiaozini sand ridges and Huanghe River delta. The strong waves caused by big wind in winter strongly act on tidal-flat in Huanghe River delta and result in erosion of beach profile in winter [35, 37]. Owing to Tiaozini sand ridges are surrounded by land at west, Dongsha sand ridge at northeast, Zhugesha sand ridge at east and Jiangjiasha sand ridge at southeast, and there is little influence of the wind-induced waves on Tiaozini sand ridges. However, strong wind-induced waves in winter erode submarine sediments and made higher sediment concentration in winter than sediment concentration in summer nearby sea area of Tiaozini sand ridges [38]. The water of high sediment concentration move toward beach of Tiaozini sand ridges [11]. The rotary tidal wave system of Southern Yellow Sea meets the progressive tidal wave system from the East China Sea in the Tiaozini sand ridges-Jiangjiasha sand ridge area and result in seawater jam and large numbers of sediment deposition around Tiaozini sand ridges, which caused Tiaozini sand ridges accumulate rapidly [11]. Consequently the seasonal erosion-accumulation changes of beach profile located at Tiaozini sand ridges mainly result from seasonal difference of high sediment concentration.

Relationship between the shift of the main tidal trough and the changes of sand ridges. Subei sand ridges were consisted of more than 70 sand ridges with many big tidal tronghs between them, including Xiyang trough, Chenjiawu trough, Kushuiyang trough, Huangshayang trough et al. (Fig. 1), which are the main channels for sand and water transportation in the radial tidal sand ridges. Their movements have close relationship with the change of sand ridges, although their shifts are backward and forward slowly. The movements of big tidal troughs directly affect the siltation-erosion changes and shifts direction of big sand ridges.

The comparison of two bathymetric maps showed that the changes of the central area in radial tidal sand ridge (Tiaozini and its surrounding beach) were mainly focused on the around tidal trough. The area with the maximum shift extended outward with an apex at radial tidal sand ridge and looked like a ray shape, which is similar to the distribution and the extend of the main tidal troughs (Figs. 1, 7) and it demonstrated the shifts of tidal troughs have very important influence on the changes of sand ridges.

The trough talweg was shifted eastward obviously with the maximum shift of 1.1 km at south of the Xiyang trough's East Branch and located near the west side of the Dongsha ridge in 1977, which eroded the southwest side of the Dongsha ridge a lot during 11 years. The head of the trough was extended southward and connected with some troughs,

separating the Dongsha ridge from the Tiaozini ridge completely (Fig. 6A).

The area of Dongsha sand ridge decreased obviously, especially at the east and south of the ridge due to the effect of trough's shifts at the east and west edge of the ridge during 1966-2000. Because the south branch of Xiyang trough shifted southeastward, the south of Dongsha sand ridge was incised and the area decreased. From 1966-1977, the tidal trough's talwegs of Huangshayang and Kushuiyang leaned southeastward and caused the Jiangjiasha sand ridge and some small ones shifted southeastward, the talweg of which located very near small sand ridges (Fig. 6A).

The distance between two branches' talweg of Xiyang trough increased from 1.4 km in 1977 to 2.7 km in 1995 in the south of division point, which resulted in the retreat of the west coast of the Dongsha sand ridge with the range of about 1.3 km (Fig. 6B). As a result of Xiyang trough's talweg movement, the beach of the Dongsha sand bank' south retreated about 2-3 km eastward during 1977-1995 (Fig. 6B).

The west branch of Xiyang trough was wide and extended south westward, which separated the Tiaozini sand bank from beach totally in flood tide in 1995. It moved eastward since then and the maximum movement was 3.4 km, the head of which have retreated about 2 km since 1995 (Fig. 6C).

Chenjiawucao trough was moved westward and caused the east beach of the Dongsha sand bank to retreat with the maximum range of 2.3 km. Some new small sand banks were formed in the east of the talweg (Fig. 6D).

Change of the tidal sand ridges. The formation of the modern tidal sand ridges in the northern part of the Changjing River Delta began about 150 years ago when the Huanghe River's channel turned northward. Before that, lots of sediments transported shoreward had already formed the large delta in the north of the research area. The evolution of the tidal sand ridges can be divided into three stages since then. In the first stage, ocean dynamics replaced river dynamics in the abandoned estuary. The sediment supply was sharply decreased by decreased river flow, but was increased by erosion sediments from the abandoned delta, submarine bottom, etc.; so the beach retreated rapidly. Lots of sediments were deposited and many small sand islands formed nearshore. Part of the sediments went southward with tidal current and was deposited in the research area. The Changjiang River estuary was then located north of its present position. River flow was an important sediment supply for the tidal sand ridges area. Historical records showed the Huanghe River channel burst into the Bohai Sea. This stage spanned about 10-30 years.

After that, the retreat of the abandoned delta beach slowed down but the erosion of the submarine bottom and small sand islands was still going on in the second stage. In the northern part of the sand ridges area, most of the small sand islands moved southward with the tidal current and alongshore current; while the Changjiang River estuary shifted southward gradually so that the supply of sediment for the southern part of the sand ridges area was decreased, which made the sand ridges change fast in the northern part and slowly in the southern part. Because of the limited sediment supply and domination by tidal current, the tidal channel formed rapidly and the tidal sand ridges were developed greatly at this stage.

When balance between the topography of sand ridges area and ocean dynamics was reached, the evolution of tidal sand ridges entered its third stage. It began at the beginning of the 20th century in the southern part of the sand ridges area and in the 1950s in the northern part. The main sand ridges (especially those in the north area) changed slowly, while the small sand ridges were still moving toward the center. Observational results together with contour maps and comparison between TM images in different time showed that the small sand ridges outside were moving toward the center at about 0.35-0.8 km/a, except for the NE areas' sand ridges, which extended outside recently. Typhoons and strong storms were the main disturbing factors in sand ridges evolution. A hydrodynamic survey showed that the sand ridges area had recovered recently from the erosion caused by the 1974 typhoon.

Although the changes of the sand ridges were undulate, it is in a stage of separation with the number of sand ridges increasing and the average area of each ridge decreasing. The range of the tidal sand ridges was drawn back from the beginning of the last century to 1970's. The north and the east edges have withdrawn about 20 km during this period. At the same time, the trunk tidal trough—Xiyang was widen and the main current line movement eastward, the head of tidal trough extension southward; the area of main sand ridge—Dongsha island decrease: backward in east, west and north sides and only forward in south side; the periphery of Tiaoziji ridge and other sand ridges run to bits and pieces and the area reduced evidently due to the head of trough extended.

From the comparison of two bathymetric maps, we can obtain that the total area and the average of sand ridges both decreased obviously despite the increase of total number of sand ridges, especially the number of outer small sand ridges with area less than 10 km^2. For example, the numbers of small sand ridges with area less than 10 km^2 (the area was counted above 0m in bathymetric map, it is the same followed) increased from 17 in 1966 to 21 in 1979; the total number of small sand ridges varied from 41 in 1966 to 61 in 1979, while the total area of sand ridges and annual average of area of sand ridges above sea level decreased 352 km^2 and 27 km^2, respectively. The sand volume in central area of sand

ridges was increased of $5.23*10^9$ m^3 and 71.2% of sand ridges area accumulated and 28.8% eroded. It is evident that the matter moved toward the center of tidal sand ridges (Fig.7).

CONCLUSIONS

This study discusses the movement or migration of tidal sand ridges in the south Yellow Sea along the Jiangsu Coast, using satellite images taken on different dates, bathymetric maps and field survey data. The results suggest that the changes of tidal sand ridges are governed by the southern Yellow Sea tidal wave system and topography of sand ridges area. The changes of tidal sand ridges can be described as: (1) big tidal sand ridges are separating and the total area of the sand ridges is decreasing in the condition of tidal current; (2) the rapid swing of main tidal troughs are the main drive of the whole sand ridges' siltation-erosion changes and directly affect the shift direction of big sand ridges; (3)the whole tidal sand ridge is generally prone to division and retreat, whereas peripheral sand ridges move obviously to the center of the tidal sand ridge and the center area of sand ridges is accumulated and outer area eroded. The migration modes of the tidal troughs play an important role in the changes of sand ridge and their interrelationships should be considered in future extensions of this study.

ACKNOWLEDGEMENTS

This work was financially supported by the National Natural Science Foundation of China (NSFC) (41472155, 41106036), Scientific and Technological Innovation Project Financially Supported by Qingdao National Laboratory for Marine Science and Technology (No. 2016ASKJ13).

REFERENCES

[1] Off, T. (1963) Rhythmic liner sand bodies caused by tidal currents. AAPG Bulletin. 47(2), 324-341.

[2] Liu, Z.X., Xia, D.X., Berne, S., Wang, K.Y., Marsset, T., Tang, Y.X. and Bourillet, J.F. (1998) Tidal depositional systems of China's continental shelf, with special refernce to the eastern Bohai Sea. Marine Geology. 145(3-4), 225-253.

[3] Berne, S., Vagner, P., Guichard, F., Lericolais, G., Liu, Z.X., Trentesaux, A., Yin, P. and Yi, H.I. (2002) Pleistocene forced regressions and tidal and ridges in the East China Sea. Marine Geology. 188, 293-315.

[4] Li, L., Su, J.B., Rao, W.B. and Wang, Y.G. (2017) Using geochemistry of rare earth elements to indicate sediment provenance of sand ridges in Southwestern Yellow Sea. Chinese Geographical Science. 27(1), 63-77.

[5] Snedden, J.W., Tillman, R.W., Kreisa, R.D., Schweller, W.J., Culver, S.J. and Winn, R.D. (1994) Stratigraphy and Genesis of a Morden Shoreface-attached Sand Ridge, Peahala Ridge, New Jersey. Journal of Sedimentary Research. 64(4), 560-581.

[6] Swift, D.J.P. (1975) Tidal sand ridges and shoal-retreat massifs. Marine Geology. 18(3), 105-134.

[7] Dyer, K.R. and Huntley, D.A. (1999) The origin, classification and modeling of sand banks and ridges. Continental Shelf Research. 19(10), 1285-1330.

[8] Li, C.Z. and Li, B.C. (1981) Studies on the formation of Subei sand cays. Oceanologia et Limnologia Sinica. 12(4), 321-331.

[9] Ren, M. (1986) Comprehensive Investigation of Coastal Zone and Tidal Flat Resources, Jiangsu Province, China. Beijing: Ocean Press.

[10] Yang, C.S. (1985) Discussion on genesis of Qianggang radial sand ridges. Marine Geology and Quaternary Geology. 5(3), 35-44.

[11] Zhang, R.S. and Chen, C.J. (1992) Evolution of Jiangsu offshore banks (radial offshore tide sands) and probability of Tiaozini sands merged into mainland. Beijing: China Ocean Press.

[12] Huang, H.J. and Li, C.Z. (1998) A Study on the evolution of Submarine Sand Ridges in the South Yellow Sea Using Remote Sensing Images. Oceanologia et Limnologia Sinica. 29(6), 640-645.

[13] Wang, J., Sha, R., Wang, Y.J., Xiao, J., Zhou, C.L., Hu, X.X. and Huang, X.C. (1997) Coastal development and environmental evolution in cental part of Jiangsu Province derived from a long drilling section. Acta Sedimentologica Sinica. 15, 51-56.

[14] Zhu, X.D., Ren, M.E. and Zhu, D.K. (1999) Changes in depositional environments in the area near the center of the north Jiangsu radial banks since the late Pleistocene. Oceanologia et Limnologia. 30(4), 428-434.

[15] Li, C.X., Zhang, J.Q., Fan, D.D. and Bing, D. (2001) Holocene regression and the tidal radial sand ridge system formation in the Jiangsu coastal zone, east China. Marine Geology. 173(1), 97-120.

[16] Huang, H.J., Du, T.Q. and Gao, A. (2009) Modern changes of tidal troughs among the radial sand ridges in northern Jiangsu coastal zone. Chinese Journal of Oceanology and Limnology. 27(3), 658-666, 2009.

[17] Xu, F., Tao, J.F., Zhou, Z., Coco, G. and Zhang, C.K. (2016) Mechanisms underlying the regional morphological differences between the northern and southern radial sand ridges along the Jiangsu Coast, China. Marine Geology. 371, 1-17.
[18] Zhang, K., Yang, F.L., Zhao, C.X. and Feng, C.K. (2016) Using robust correlation matching to estimate sand-wave migration in Monterey Submarine Canyon, California. Marine Geology. 376, 102-108.
[19] Xing, F., Wang, Y.P. and Wang, H.V. (2012) Tidal hydrodynamics and fine-grained sediment transport on the radial sand ridge system in the Southern Yellow Sea. Marine Geology. 291-294(4), 192-210.
[20] Song, Z.J., Li, J.P., Meng, F.X., Tang, W.J. and Yuan, X.Y. (2018) Seasonal Distribution of Suspended Particulate Matter near Radial Sand Ridges Area off China' Subei Coast. Polish Journal of Environmental Studies. 27(2), 1-8.
[21] Fan, D.D., Zhang, J.Q. and Li, C.X. (1999) Magmetic Fabric Characteristics and Sedimentary Environment of Subaerial Tidal Sand Body in Subei Area. Acta Sedimentologica Sinica. 17(4), 601-607.
[22] Wang, Y., Zhu, D.K., You, K.Y., Pan, S.M., Zhu, X.D., Zou, X.Q. and Zhang, Y.Z. (1998) Evolution of radiate sand ridge field of the South Yellow Sea and its sedimentary characteristics. Science in China (Series D). 28(5), 385-393.
[23] Huang, H.J. and He, Y.J. (2001) Monitoring the diffusion of suspended sediments and stability of tidal radial sand ridges area using multi-satellite remote sensing data in the northern part of the Changjiang River delta, the southern Yellow Sea. Chinese Journal of Oceanology and Limnology. 19(4), 361-367.
[24] Yu, Z.Y., Chen, D.C. and Jin, L. (1986) The formation and erosive structure of old Yellow Sea subaqueous delta in northern of Jiangsu province. Acta Oceanologica Sinica. 8(2), 197-206.
[25] Gong, X.S., Wan, Y.S. and Li, S.W. (1983) Primary Research on the Evolution of Subei Beach and the Model of Sand Ridge Changes in Subei Beach. Acta Oceanologica Sinica. 5(1), 62-70.
[26] Huang, Y.C. and Wang, W.Q. (1987) Discussion on dynamic mechanism of radial sand ridges in Jiangsu coast. Acta Oceanologica Sinica. 9(2), 209-215.
[27] Zhang, J.Q. (1997) Source and sedimentation of the tidal sand bodies in the northern Jiangsu and the Yellow Sea. PhD Thesis. Department of Marine Geology and Geophysics, Tongji University.
[28] Ye, H.S., Wang, W.Q. and Fang, X.Y. (1981) Preliminary analyses of tide character in the northern part of the coastal zone off Jiangsu Province. Ocean Research. 3, 1-9.
[29] Fang, X.Y., Ye, H.S. and Wang, W.Q. (1982) Analyses of tide-character in the southern part of the coastal zone off Jiangsu Province. Ocean Research. 2, 13-22.
[30] Stride, A.H. (1982) Offshore Tidal Sands: Process and Deposits. London: Chapman and Hall.
[31] Wang, Y., Zhang, Y.Z., Zou, X.Q., Zhu, D.K. and Piper, D. (2012) The sand ridge field of the south yellow sea: origin by river-sea interaction. Marine Geology. 291, 132-146.
[32] Chen, C.F., Liu, F.Y., Li, Y.Y., Yan, C.Q. and Liu, G.L. (2016) A robust interpolation method for constructing digital elevation models from remote sensing data. Geomorphology. 268, 275-287.
[33] Sun, L., Mi, X.T., Wei, J., Wang, J., Tian, X.P., Yu, H.Y. and Gan, P. (2017) A cloud detection algorithm-generating method for remote sensing data at visible to short-wave infrared wavelengths. Isprs Journal of Photogrammetry and Remote Sensing. 124, 70-88.
[34] Zhang, Z.L., Zhang, R.S., Li, J.L., Wang, Y.H. and Yan, S.Y. (2004) Temporal and spatial heterogeneous characteristic of profile configuration of Tiaozini alongshore tidal flats in Jiangsu. Marine Sciences. 28(6), 51-54.
[35] Li, P.Y., Wu, S.Y., Zang, Q.Y., Xu, X.S. and Zang, Q.N. (1992) Tidal-flat geomorphology and erosion-deposion changes in Huanghe seaport area. Acta Oceanologica Sinica. 14(6), 74-84.
[36] Larson, M., Capobianco, M. and Hanson, H. (2000) Relationship between beach profiles and waves at Duck, North Carolina, determined by canonical correlation analysis. Marine Geology. 163(1), 275-288.
[37] Wu, S.Y. (1991) The primary study of erosion-deposition changes at No. 5 sea area in Huanghe River delta. Ocean and Coastal Exploitation. 10(4), 67-69.
[38] Qin, Y.S., Li, F. and Xu, S.M. (1989) Suspended Matter in the Southern Yellow Sea. Oceanologia et Limnologia Sinica. 20(2), 101-112.

Received: **21.01.2017**
Accepted: **15.03.2018**

CORRESPONDING AUTHOR

Zhaojun Song
Shandong Provincial Key Laboratory of
Depositional Mineralization and
Sedimentary Minerals,
College of Earth Science and Engineering,
Shandong University of Science and Technology,
Qingdao, Shandong 266590 – P.R. China

e-mail: songzhaojun76@163.com

© by PSP Volume 27 – No. 7/2018 pages 4921-4929 Fresenius Environmental Bulletin

LABORATORY INVESTIGATION OF FLOW RESISTANCE IN COMPOSITE ROUGHENED RECTANGULAR OPEN CHANNELS

Sajjad Javid[1], Mirali Mohammadi[2], Mohsen Najarchi[1,*], Mohammad Mahdi Najafi Zadeh[3]

[1]Department of Civil Engineering, Islamic Azad University, Arak Branch, Arak, Iran
[2]Department of Civil Engineering, Faculty of Engineering, Urmia University, Urmia, Iran
[3]Department of Mechanical Engineering, Islamic Azad University, Arak Branch, Arak, Iran

ABSTRACT

In this research, a series of unique experiments were carried out in both smooth and composite roughened rectangular open channels using three types of river sediments over a wide range of flow characteristics. Five different boundary roughness combinations were considered on the walls and bed to have a comprehensive data in the case of symmetric and asymmetric boundary roughness distribution. At first, different estimation methods of Manning's coefficient for composite channels were evaluated. In this regard, Strickler's empirical formula was revised and the results showed that the Colebatch's method, using the proposed formula, provides better results compared to the other methods with an average relative error of 3.95%. Regarding Darcy-Weisbach friction factor, some empirically derived equations are presented which give the value of Nikuradse equivalent roughness size, k_s, as a function of the d_{50} value of roughness particle size. To overcome the implicit determination of the friction factor, f, a new formula is presented by using the gene expression programming for uniformly roughened rectangular channels with an average relative error and corresponding correlation coefficient of 6.7% and 98.8%, respectively. Another empirical equation is then presented to approximate the Manning's n with an average error less than 2.9%.

KEYWORDS:
Composite Channel, Flow Resistance, Friction Factor, Manning Roughness, Rectangular

INTRODUCTION

Flow in open channel engineering applications is always subjected to the resistance due to the flow, and dissipation of energy. In turbulent flow, unwanted developments of secondary currents and the effect of corners on the 3D behavior of flow showed the need for more refined analysis and detailed measurements [1]. Flow resistance in open channels cannot be easily determined as it depends upon the details of the cross-section shape [2, 3], the longitudinal variation in planform geometry [4], the boundary roughness distribution [5, 6, 7] and the structure of secondary flows [8, 9, 10].

After Chezy, Manning and Darcy-Weisbach, a large number of papers have been published on pipes and open channel flow with smooth and rough surfaces [11, 12, 13, 14, 15, 16]. It has long been acknowledged that the Karman-Prandtl and Colebrook-White pipe flow equations are inaccurate in open channels resistance studies. It is so, due to the effect of channel cross-sectional shape. In this regard, considerable experimental research efforts were carried out focusing on smooth channels with different cross sections [17, 18]. In nature, however, most rivers are complicated by the irregularities in their cross-sectional shape and the non-uniform distribution of resistance around the wetted perimeter. Some channels, for example, are made up of different materials for the walls and the bed or have a grassy vegetated banks. Some other researchers have focused on differentially roughened channels, using artificial uniform roughening materials on the boundary, (e.g. Tzelepis et al. [19]) or using natural gravels on the bed (e.g. Javid [20] and Zeng et al. [21]). However, there are few studies focusing on the flow resistance in composite or uniformly roughened rectangular channels with non-mobile boundaries.

Because of the importance of such channels from the viewpoint of designing, examination of flow resistance by evaluating the effect of roughness particle size and various combinations of lateral boundary roughness distribution under laboratory conditions becomes vital. To this extend, this study experimentally investigates the flow resistance in composite roughened rectangular channel using three types of sediments and five different roughness combinations. In addition, several methods are evaluated to determine the Manning's roughness coefficient. As it is necessary to obviate the determination of flow resistance in practical applications, this study, presents some empirically derived equations to predict the friction factor and the Manning's roughness coefficient for uniformly roughened and smooth rectangular open channels.

MATERIALS AND METHODS

Methodological considerations. In open channel flow analysis, the conventional approaches to calculate the resistance coefficients have been provided by the Manning, Darcy-Weisbach or Chezy form as follows:

$$n = \frac{K_n}{U} R^{2/3} S^{1/2} \quad (1)$$

$$f = \frac{8g}{U^2} RS \quad (2)$$

$$C = \frac{U}{\sqrt{RS}} \quad (3)$$

where K_n is a dimensional parameter which depends upon the selected units and is equal to 1 $m^{1/2}/s$ in SI units and equal to 1.486 $ft^{1/2}/s$ in *FPS* system; *U* is the cross-sectional mean velocity; *R* is hydraulic radius; *S* is the slope; and *g* is gravitational acceleration. By deriving *U* from the above three equations and setting equal the relationship between *n*, *f*, and *C* is then provided as

$$\sqrt{\frac{8}{f}} = \frac{C}{\sqrt{g}} = \frac{K_n}{\sqrt{g}} \frac{R^{1/6}}{n} \quad (4)$$

For either composite wall roughness or a mobile alluvial bed, Manning's roughness coefficient *n* has to be empirically derived for each channel reach or cross-section.

Manning Roughness coefficient *n*. In composite channels, wall roughness changes along the wetted perimeter and the local point wall shear and resistance also vary along the wetted perimeter. Therefore, the value of the resistance coefficient for the cross-section changes with the flow depth. A summary of composite roughness formulas is listed in Table 1.

It can be found from Table 1 that Equations (5)-(9) deals with the assumptions on how we can divide subareas to compute A_i and R_i. One of the common methods for dividing the subareas is the use of bisectors at the break points of the roughness or boundary of the channel cross-section. Some other division methods for open channels are comprehensively discussed by Javid [17] and Han et al. [30]. The simple linear division line is usually preferred in order to give more compatible values for different depths [1].

No laboratory and field data have been collected regarding rectangular channels for a comprehensive comparison of the formulas listed in Table 1. In addition, the precise determination of local roughness, n_i, in Equations (5)-(14) adds to the difficulty of estimating total roughness across the channel in flow resistance surveys. One of the most known methods to determine the n_i has been provided by the Strickler's empirical formula [31], as follows

$$n_i = C_n' d_m^{1/6} \quad (15)$$

where d_m is the characteristic particle size of the sediment, so that *m%* of the particles in the total grain size distribution are smaller than d_m; and C'_n is constant. Table 2 shows some suggested values of C'_n.

Friction Factor *f*. Colebrook-White [32] proposed the friction equation as

$$\frac{1}{\sqrt{f}} = -c_1 \, log\left(\frac{k_s}{c_2 \, R} + \frac{c_3}{R_e\sqrt{f}}\right) \quad (16)$$

in which k_s is the relative roughness and is termed the Nikuradse equivalent sand roughness [16], R_e is Reynolds number and c_1, c_2 and c_3 are constants which from Nikuradse's work are 2, 14.8 and 2.51, respectively [33]. Some other suggested values of these coefficients for smooth and rough channels were well reviewed by Javid [20]. Literature on sediment transport shows that the k_s can be related to d_m by the equation as follows:

$$k_s = \alpha . d_m \quad (17)$$

in the above formula α is the coefficient of proportionality. Such criteria for different values of *m* have been used by different investigators. Some proposed values of the coefficient α are listed in Table 3.

TABLE 1
Formulas for Composite Channel Resistance Coefficient

Eq. No.	n_c	Reference	Eq. No.	n_c	Reference
(5)	$= \frac{PR^{5/3}}{\sum P_i R_i^{5/3}/n_i}$	[22]	(10)	$= \left[\frac{1}{P}\sum\left(n_i^2 P_i\right)\right]^{1/2}$	[25]
(6)	$= \frac{\sum n_i P_i R_i^{1/3}}{PR^{1/3}}$	[16]	(11)	$= \left[\frac{1}{P}\sum\left(n_i^{3/2} P_i\right)\right]^{2/3}$	[26] & [27]
(7)	$= \frac{\sum (n_i P_i / R_i^{1/6})}{P/R^{1/6}}$	[16]	(12)	$= P/\sum\left(\frac{P_i}{n_i}\right)$	[28]
(8)	$= \frac{\sum\left(n_i A_i\right)}{A}$	US Army Corps of Engineering [23]	(13)	$= \frac{\sum\left(n_i P_i\right)}{P}$	[16]
(9)	$= \left[\frac{\sum\left(n_i^{3/2} A_i\right)}{A}\right]^{2/3}$	[24]	(14)	$= \exp\left[\frac{\sum P_i h_i^{3/2} . \ln n_i}{\sum P_i h_i^{3/2}}\right]$	[29]

TABLE 2
Proposed sediment size by different investigators in $C_n' = n/d_m^{1/6}$ (after Javid [20])

Investigator(s)	Measure of k_s	C_n'	$1/C_n'$
Strickler (1923)	d_{50}	0.0474	21.1
Meyer-Peter & Muller (1948)	d_{90}	0.0385	26
Keulegan (1938)	d_{50}	0.0395	25.3
Irmay (1949)	d_{65}	0.0416	24
Lane & Carlson (1953)	d_{75}	0.0473	21.14
Henderson (1966)	d_{50}	0.041	24.39
Hager (1999)	d_{50}	0.048	20.83
Sturm (2010)	d_{50}	0.039	25.64

TABLE 3
Some suggested values of coefficient of sand equivalent roughness size and sediment size for open channels. (after Javid [20])

Investigator(s)	Measure of Sediment Size, d_x	$\alpha=k_s/d_x$
Strickler (1923)	d_{50}	3.3
Keulegan (1938)	d_{50}	1
Meyer-Peter & Muller (1948)	d_{50}	1
Irmay (1949)	d_{65}	1.5
Einstein & Barbarossa (1952)	d_{65}	1
Lane & Carlson (1953)	d_{75}	3.3
Leopold et al. (1964)	d_{84}	3.9
Simons & Richardson (1966)	d_{85}	1
Engelund & Hansen (1967)	d_{65}	2.0
Limerinos (1970)	d_{84}	2.8
Mahmood (1971)	d_{84}	5.1
Ackers & White (1973)	d_{35}	1.23
Kamphius (1974)	d_{90}	2.0
Thompson & Campbell (1979)	d_{50}	2.0
Hey (1979), Bray (1979)	d_{84}	3.5
Gladki (1979)	d_{80}	2.5
Van Rijn (1982)	d_{90}	3.0
Ikeda (1983)	d_{84}	1.5
Hammond et al. (1984)	d_{50}	6.6
Colosimo et al (1986)	d_{84}	3.6
Ikeda et al (1987)	d_{90}	1.5
Whiting & Dietrich (1990)	d_{84}	2.95
Lopez and Barragan (2008)	d_{84}	2.8

Experimental Apparatus and Procedure. To meet the aims of this study, experiments were conducted at the University of Urmia under uniform flow conditions in a 15.4 m long glass-walled rigid tilting flume with a cross section of 302.7 mm wide × 450 mm deep. The flume was supported by two hydraulic jacks and rotated around a hinge joint beneath the beginning of the channel and the maximum obtainable slope was S_0=2%. We measured flow rates with a calibrated electromagnetic flowmeter with standard deviation about 0.9%. We also measured water temperature using a digital thermometer with an accuracy of 0.1^{oC}. To form the channel roughness, three types of river sediments materials were used which had been previously sifted using ASTM standard sieves. Figure 1(a) shows the curves of particle size distribution from sieve analysis for each type of materials used in this research. We densely glued these materials on 1m × 0.302m glass plates with 4 to 6 mm thickness using a waterproof glue and then placed consecutively inside the channel. Figure 1 (b) & (c) shows sample of three prepared roughened plates and some types of different composite channels, respectively.

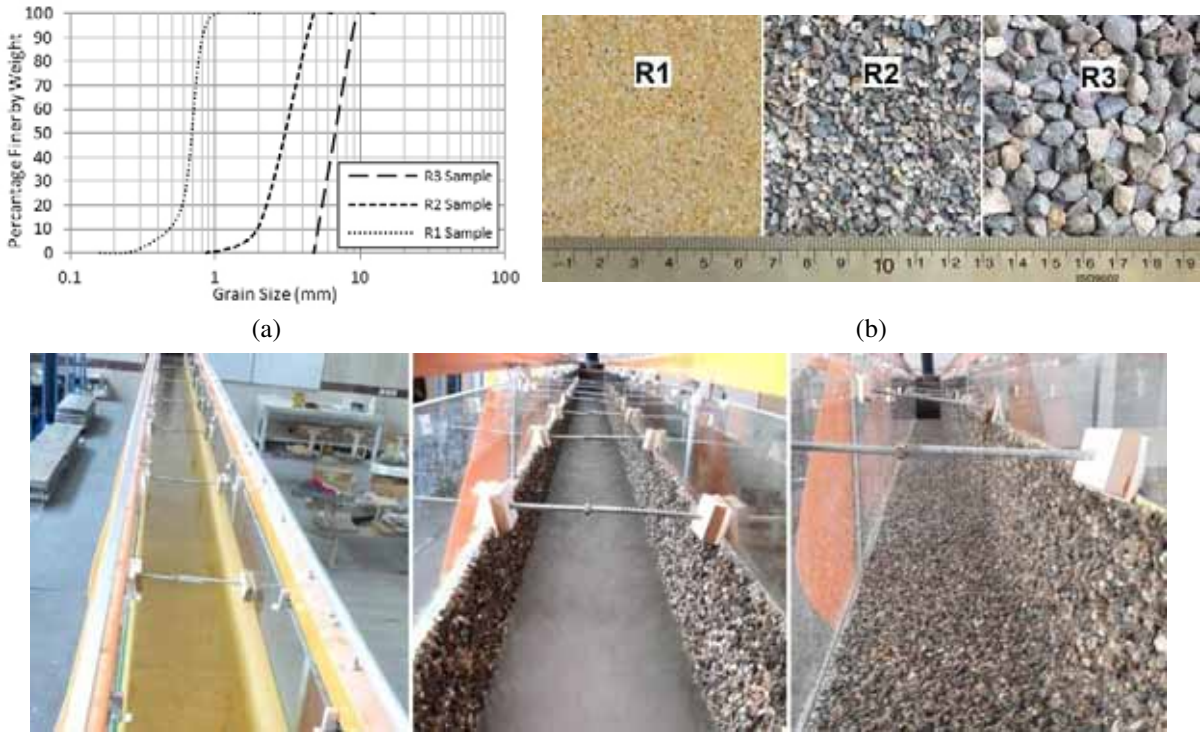

(a) (b)

(c)

FIGURE 1
(a) Particle Size Distribution; (b) Sample of roughened plates; (c) Some different types of roughened composite channels

TABLE 4
Series of experiments with different combination of R_2 roughness

Test Number	Left Wall Roughness	Right Wall Roughness	Bed Roughness
126 to 150	Smooth	Smooth	R_2
151 to 175	R_2	R_2	Smooth
176 to 200	R_2	R_2	R_2
201 to 225	Smooth	R_2	Smooth
226 to 250	Smooth	R_2	R_2

The d_{50} values of the roughness particle size of these materials were R_1 =0.697, R_2 =3.2 and R_3 =6.71 mm. We used the overall geometric mean line as the boundary of the channel cross section rather than irregular one to compute the hydraulic radius, area and wetted perimeter. Totally, we completed 393 tests for a wide range of flow condition with various roughened boundaries combinations, consisting of 97 tests on the uniformly roughened channel, including the simple smooth channel measurements, and 296 tests on the composite roughened channel. Some series of experiments with different combination of R_2 roughness on the channel boundary are listed in Table 4. We considered the flow discharges as 10, 15, 25, 30 and 45 *L/s*, and the channel slopes were 0.001, 0.002, 0.004, 0.009 and 0.016. In these experiments, in addition to the uniform flow depth measurements, velocity profiles and boundary shear stresses were also measured in most cases. The breadth of the flume, B, varied between 288.07 and 302.7 mm, and the depth of flow, H, varied between 25.7 and 300 mm. From the experimental measurements, R_e varied between 20378 and 102604, and the Froude number varied between 0.20 and 2.68.

RESULTS AND DISCUSSION

Regarding Equations (1)-(2), estimating the Manning's roughness coefficient, n, and the friction factor, f, in composite open channels is closely related to several parameters like flow characteristic, channel shape and boundary roughness. In order to evaluate the effects of these parameters on the flow resistance, the characteristics of flow were initially observed through the measurements of 393 different tests from different roughened boundary combinations with 4 types of roughness including the smooth boundary.

Manning Roughness Coefficient. To find the most compatible method which is listed in Table 1, first a comparison was made between the Manning's roughness coefficients estimated from the flow measurements and the prediction made using Equations (5)-(14). In this respect, a numerical investigation was conducted using Strickler's empirical formula [31]. Therefore, Equation (15) may be generally given as follows:

$$n_i = b_1 . d_{50}^{1/b_2} \quad (18)$$

in which b_1 and b_2 are constants. The analysis using SPSS software [34] pointed out that Strickler's formula [31] using the d_{50} value of the roughness particle size, has a better agreement with experimental measurements. The most precise results were achieved by choosing b_1=0.0474 and b_2=5.8. Then, another evaluation was made regarding dividing subareas to compute A_i and R_i, by altering the angle of linear division line at the break of the boundary of the channel cross-section. The analysis showed that using the bisector line (θ=45°) can yield the most acceptable results. It is necessary to mention that Manning's roughness coefficient for glass was considered as 0.00935 which was derived by averaging the experimental measurements for the smooth channel.

If one defines the relative error as

$$Relative\ Error\ (RE) = \left|\frac{Calculated - Measured}{Measured}\right| \quad (19)$$

then the average relative errors between the formulas in Table 1 and the experimental data can be summarized in Table 5. In Table 5, for example the SR_iR_j is related to the channel boundary condition with smooth glass on the left wall, R_i roughness on the bed and R_j roughness on the right wall.

One can see from Table 5, Equations (5)-(9) in which the computation of A_i or R_i play an important role, yields more suitable results in average compared with Equations (10)-(14). In this group of methods, Colebatch [24] method by using Equation (9), yields more precise results compared the others with an average error of 3.95%, although the scatter is significant. For Colebatch's formula, an average error about 4.62% was observed while using Strickler's formula [31], Equation (18), with the reference coefficient b_2=6 in Equation (18). Figure 2(a) illustrates the comparison between the n calculated from the flow measurements and the prediction made using Equation (9).

To summarize the calculation process it could be said that Equation (11) is more favorable and yields acceptable result that is independent of computing the A_i or R_i. As shown in Table 5 and Figure 2(a), Colebatch's formula, similar to the other methods in Manning's coefficient determination, yields a constant value for uniformly roughened channels. These errors are denoted by the dashed elliptical lines in Figure 2(a). To avoid these errors, another approach to Manning's n determination is discussed in the following section.

TABLE 5
Comparison of Manning's roughness coefficient calculated using Eqs. (7)-(16) and the experimental data

Roughness Combinations	Method name and Equation number									
	Lotter [22]	Yen [16]	Yen [16]	US Army [23]	Colebatch [24]	Pavlovskii [25]	Horton [26] & Einstein [27]	Felkel [28]	Yen [16]	Krishnamurthy & Christensen [29]
	Eq. 5	Eq. 6	Eq. 7	Eq. 8	Eq. 9	Eq. 10	Eq. 11	Eq. 12	Eq. 13	E1. 14
$R_3R_3R_3$	3.48	3.48	3.48	3.48	3.48	3.48	3.48	3.48	3.48	3.48
R_3SR_3	16.43	5.02	5.04	5.46	3.41	6.37	4.82	14.57	5.25	9.57
SR_3S	14.07	6.85	6.71	7.58	6.86	5.93	5.60	15.65	6.59	10.69
SR_3R_3	10.86	3.05	3.28	3.00	2.38	6.50	4.29	8.75	3.60	5.81
SSR_3	10.45	2.74	2.77	2.38	2.48	3.58	2.96	10.93	2.79	5.94
$R_2R_2R_2$	2.78	2.78	2.78	2.78	2.78	2.78	2.78	2.78	2.78	2.78
R_2SR_2	11.31	5.18	5.55	4.43	3.88	8.08	6.70	9.83	6.04	7.05
SR_2S	10.18	5.09	5.14	4.77	4.02	3.38	3.82	12.63	5.15	8.62
SR_2R_2	9.95	5.25	5.50	4.97	4.28	6.90	6.20	8.69	5.89	6.88
SSR_2	8.34	3.33	3.32	3.09	2.62	2.40	2.70	8.80	3.26	5.45
$R_1R_1R_1$	2.99	2.99	2.99	2.99	2.99	2.99	2.99	2.99	2.99	2.99
R_1SR_1	6.01	4.29	4.67	3.78	3.59	5.65	5.39	5.20	5.16	4.92
SR_1S	4.32	3.27	3.05	4.50	4.67	3.20	3.02	3.56	2.88	3.02
SR_1R_1	5.90	5.84	6.05	5.55	5.47	6.62	6.48	6.47	6.36	6.27
SSR_1	4.01	2.96	2.90	3.51	3.48	2.80	2.80	3.64	2.86	3.11
Smooth	6.79	6.79	6.79	6.79	6.79	6.79	6.79	6.79	6.79	6.79
Max Abs. Average *(%)*	16.43	6.85	6.71	7.58	6.86	8.08	6.79	15.65	6.79	10.69
Average *(%)*	7.98	4.30	4.37	4.32	3.95	4.84	4.43	7.80	4.49	5.84
Correlation Coefficient	0.861	0.892	0.896	0.895	0.900	0.897	0.901	0.902	0.902	0.902

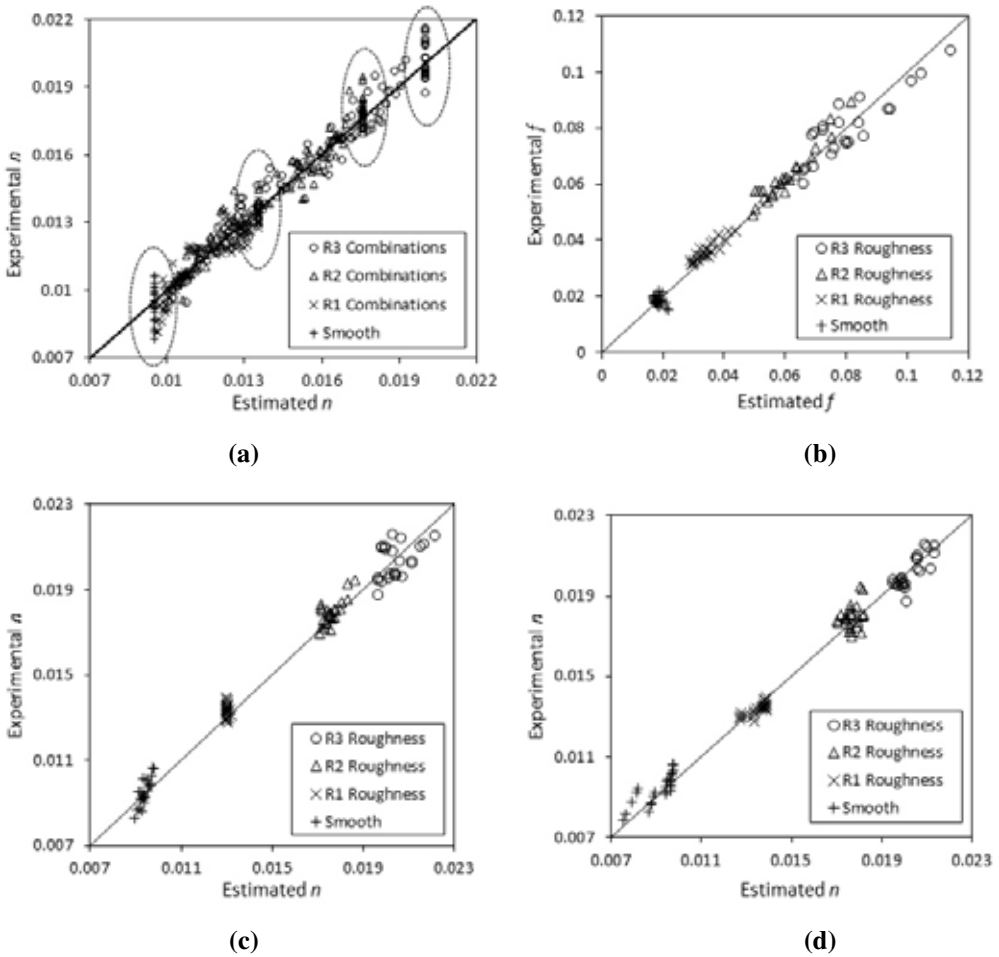

FIGURE 2
Comparison of the experimental measurements with (a) those estimated using Equation (9); (b) those predicted using Equation (22); (c) those calculated using Equation (23); (d) those calculated using Eqs. (22) & (4)

Friction Factor. According to Equation (16), estimation of the friction factor depends on the relative roughness (k_s) determination. Many investigators have tried to connect this theoretical concept to the physical characteristics of the surface roughness [35]. In Equation (16), Depending on the used particle size such as d_{50} or d_{84}, the values of c_1, c_2 and c_3 will differ for a set of data. In this case, for the channels with uniform boundary roughness distribution, k_s is calculated by substituting f, R_e and R from the flow measurements and the Nikuradse's constants in Equation (16). Under this Assumption, the average values of k_s for uniformly roughened channels with R_3, R_2, R_1 materials and the smooth channel were found to be equal to 16.59, 9.42, 2.17 and 0.16 mm with an average relative error of 0.09%, 0.08%, 0.09% and 1.15%, respectively.

In general, Equation (20) estimates the value of k_s with the average relative error and corresponding correlation coefficient of 2.8% and 99.9%, respectively.

$$k_s = 34.7(1 - e^{-0.095 d_{50}}) + 0.16 \qquad (20)$$

in which d_{50} and k_s are in millimetre.

Another numerical investigation points out that the α coefficient is not constant and depends on the d_{50} value of the roughness particle size. Equation (21) shows the relation between the α and the d_{50} value with an average relative error about 0.08% and a correlation coefficient of 99.9%.

$$\alpha = 3.13\, e^{-\frac{(d_{50}+0.514)^2}{220.5}} \qquad (21)$$

It can be found from Equation (21) that while d_{50} increases, α decreases.

Friction factors could be determined by using the Equation (16) together with Nikuradse's constants and the calculated values of k_s with an average relative error of 11.2%. But Equation (16) is implicit in f. To overcome this drawback, gene expression programming (GEP) method [36] is used to present Equation (22) [20]. This equation estimates the f with an average relative error and a corresponding correlation coefficient of 6.7% and 98.8%, respectively. The maximum relative average error about 9.9% was observed while using Equation (22) to determine the

friction factor in the channel with smooth boundaries.

$$f = 0.577\left[-Log\left(\frac{k_s}{25R}\right) + \frac{5}{(2R_e)^2}\right]^{-3} + 0.0086 \quad (22)$$

Figure 2(b) illustrates the friction factor *f* calculated from the flow measurements and the prediction made using Equation (22).

As mentioned in the previous part, using the traditional methods by means of Equations (5)-(14) to determine the *n* for uniformly roughened channels, yields a constant value. To avoid these incompatibilities and achieve an appropriate function, several attempts have been made using the above mentioned GEP method. Equation (23) agrees with the experimental measurements with an average relative error and a corresponding correlation coefficient of 2.88% and 99.3%, respectively.

$$n = \left(k_s{}^3 \frac{1}{2.2F^{0.75}}\right)^{R^{0.25}} + 10.4\left(\frac{1}{6.4 - Log(k_s) + 0.1F^{2.4}}\right)^3 \quad (23)$$

Figure 2(c) illustrates the *n* calculated from flow measurements and the prediction made using Equation (23). However, theoretically, to summarize the calculation process, *n* could be determined by using the Equation (22) and substituting the *f* in Equation (4). Figure 2(d) shows the results of the comparison between the calculated *n* from the flow measurements and the prediction made using Equation (22) and (4). Comparison between the Figures 2(c) and 2(d) shows that the predictions made using Equations (22) and (23), with a little negligence are similar. Although Equation (22) slightly underestimates the measurements for the channel with smooth boundary, but yields the most precise results in *n* determination for the rough channel with R_1 on the boundaries.

The authors believe that the presented Equations from (20)-(22), may be valid for uniformly roughened rectangular channels with d_{50} greater than 6.71 mm, although additional laboratory studies are needed. However, for uniformly roughened channels with d_{50} less than or equal to 6.71 mm many numerical studies have been conducted which all prove the validation of the presented relations in the range of experimental condition.

CONCLUSION

In this study, the new series of experimental data for composite roughened rectangular channels has been used to validate the most prominent methods for determination of Manning's roughness coefficient. In this regard, Strickler's empirical formula [31], has been revised to provide more accurate results. Numerical analysis pointed out that, Colebatch [24] method yields the most precise results with an average relative error and correlation coefficient of 3.95% and 90%, respectively.

Equations (20) and (21) were presented to formulate the relation between the relative roughness k_s and α coefficient with d_{50} value roughness particle size by an average relative error and correlation coefficient of less than 2.8% and 99.9%, respectively. Moreover, Equation (22) which generally agrees with the measurements by an acceptable average relative error less than 6.7% and correlation coefficient about 98.8% was offered in explicit form to predict the friction factor. Finally, Equation (23) was presented to determine the *n* with an average relative error and correlation coefficient about 2.88% and 99.3%, respectively.

The results verified that the proposed formulas are applicable for flows with Reynolds number ranging from 20378 and 102604, Froude number from 0.20 and 2.68, and the aspect ratio (*B/H*) from 0.95 to 11.78.

ACKNOWLEDGEMENTS

The present paper is based on PhD dissertation of Sajjad Javid, PhD student of Islamic Azad University and Arak branch. In addition, the contributions of this university are warmly appreciated.

REFERENCES

[1] Mohammadi, M. (1998) Resistance to Flow and The Influence of Boundary Shear Stress on Sediment Transport in Smooth Rigid Boundary Channels. PhD Thesis. University of Birmingham, Birmingham, England.

[2] Pillai, N.N. (1997) Effect of Shape on Uniform Flow through Smooth Rectangular Open Channels. Journal of Hydraulic Eng. 123(7), 656-658.

[3] Mohammadi, M. (2001) Shape effects and definition of hydraulic radius in Manning's equation in open channel flow. International Journal of Engineering. 10(3), 127.

[4] Dupuis, V., Proust, S., Berni, C. and Paquier, A. (2017) Compound channel flow with a longitudinal transition in hydraulic roughness over the floodplains. Environmental Fluid Mechanics. 17(5), 1-26.

[5] Knight, D.W., Alhamid, A.A.I., Yuen K.W.H. (1992) Boundary shear in differentially roughened trapezoidal channels. In: Falconer, R.A., Shiono, K., Matthew, R.G.S. (eds.) Hydraulic and Environmental Modelling: Estuarine and River Waters. Ashgate, Aldershot. 3–14.

[6] Yang, S.-Q. (2010) Depth-averaged shear stress and velocity in open channel flows. Journal of Hydraulic Engineering. 136(11), 952–958.

[7] Mohammadi, M., Javid, S. (2011) Evaluation of boundary shear stress in rectangular channels. The Sixth National Congress on civil engineering, Semnan, Iran. (In Farsi).
[8] Tominaga, A., Nezu, I., Ezaki, K., Nakagawa, H. (1989) Three dimensional turbulent structure in straight open channel flows. Journal of Hydraulic Research. 27(11), 149–173.
[9] Knight, D.W., Omran, M., Tang, X. (2007) Modeling depth averaged velocity and boundary shear in trapezoidal channels with secondary flows. Journal of Hydraulic Engineering. 133(1), 39–47.
[10] Javid, S., Mohammadi, M. (2012) Boundary shear stress in a trapezoidal channel. International Journal of Engineering, Trans. A. 25(4), 323-332.
[11] Nikuradse, J. (1933) Stromungsgesetze in rauhen Rohre (Low of flow in rough pipes). Forschungsheft No. 361, Verein Deutscher Inginieure, Berlin. (Translated into English as NACA TM 1292, Nov. 1950).
[12] Keulegan, G.H. (1938) Laws of Turbulent Flow in Open Channels. Journal of Research of the National Bureau of Standards. Research Paper 1151, 21, 707-741.
[13] ASCE Task Force Committee of the Hydraulic Division. (1963) Friction Factors in Open Channels, Progress Report of the Task Force on Friction factors in Open Channels of the Committee of the Hydraulic Division. J. of Hydr. Div. 89(HY2).
[14] Pillai, N.N. (1970) On uniform flow through smooth rectangular open channels. Journal of Hydraulic Research. 8(4), 403-418.
[15] Kazemipour, A.K., Apelt, C.J. (1980) Resistance to Flow in irregular Channels Dept. of Civil Eng., Research Report Series No. CE7, University of Queensland, Australia.
[16] Yen, B.C. (ed.) (1992) Channel flow resistance: centennial of Manning's formula. Water Resources Publication, Colorado, USA, 1-136.
[17] Javid, S. (2011) On the effect of cross sectional shape on shear stress distribution in open channel flow. MSc Thesis. Islamic Azad University, Mahabad Branch, Mahabad, Iran. (In Farsi).
[18] Cheng, N.S. (2017) Simple Modification of Manning-Strickler Formula for Large-Scale Roughness. Journal of Hydraulic Engineering. 143(9), 04017031.
[19] Tzelepis, V., Moutsopoulos, K.N., Papaspyros, J.N. and Tsihrintzis, V.A. (2015) Experimental investigation of flow behavior in smooth and rough artificial fractures. Journal of Hydrology. 521, 108-118.
[20] Javid, S. (2017) Resistance to Flow and Boundary Shear Stress Distribution in Rigid Composite Channels. PhD Thesis. Islamic Azad University, Arak Branch, Arak, Iran. (In Farsi).
[21] Zeng, C., Li, C., Tang, H., Wang, L. and Mao, J. (2015) Experimental study of depth-limited open-channel flows over a gravel bed. International Journal of Sediment Research. 30(2), 160-166.
[22] Lotter, G.K. (1933) Soobrazheniia k Gidravlicheskomu Raschetu Rusel s Razlichnoi Sherokhovatostiiu Stenok (Considerations on hydraulic design of channels with different roughness of walls). Trans. All-Union Sci. Res. Inst. Hydraulic Eng. Leningrad. 9, 238–241.
[23] Cox, R.G. (1973) Effective Hydraulic Roughness for Channels Having Bed Roughness Different from Bank Roughness: A State of the Art Report (No. AEWES-Misc-Paper-H-73-2). Army Engineer Waterways Experiment Station, Vicksburg, Miss.
[24] Colebatch, G.T. (1941) Model tests on the Lawrence Canal roughness coefficients. Journal Inst. Civil Eng. (Australia). 13(2), 27–32.
[25] Pavlovskii, N.N. (1931) On a design formula for uniform flow in channels with nonhomogeneous walls. Trans. All-Union Sci. Res. Inst. Hydraulic Eng., Leningrad. 3, 157–164. (In German).
[26] Horton, R.E. (1933) Separate roughness coefficients for channel bottoms and sides. Eng. News-Rec. 111(22), 652–653.
[27] Einstein, H.A. (1934) Der Hydraulische oder Profil-Radius (The hydraulic or profile radius). Schweizerische Bauzeitung, Zurich. 103(8), 89–91.
[28] Felkel, K. (1960) Gemessene Abflusse in Gerinnen mit Weidenbewuchs (Abflusse measured in flumes with willow vegetation) Mitteilungen der BAW, Heft 15, Karlsruhe, Germany.
[29] Krishnamurthy, M., Christensen, B.A. (1972) Equivalent roughness for shallow channels. J. Hydraul. Div. 98(12), 2257–2263.
[30] Han, Y., Yang, S.Q., Dharmasiri N., Sivakumar M. (2014) Experimental study of smooth channel flow division based on velocity distribution. Journal of Hydraulic Engineering. 141(4), 06014025.
[31] Strickler (1923) Beitrage zur frage der geschwindigkeitsformel und der rauhigkeitszahlen fuer stroeme kanaele und geschlossene leitungen (Contributions to the question of speed formula and the roughness pay for current channels and closed lines). Messages of the world Office for water management, Bern, Switzerland. N. 16 (in German).
[32] Colebrook, C.F., White, C.M. (1937) Experiments with fluid friction in roughened pipes. Proceedings of the Royal Society of London Series A. 161, 367-381.

[33] Gemici, Z., Koca, A., Kaya, K. (2017) Predicting the Numerical and Experimental Open-Channel Flow Resistance of Corrugated Steep Circular Drainage Pipes. Journal of Pipeline Systems Engineering and Practice. 8(3), 04017004.
[34] SPSS Statistics (2009) Version 18. https:// www.ibm.com/ products/ spss-statistics.
[35] Smart, G.M., Duncan, M.J., Walsh, J.M. (2002) Relatively Rough Flow Resistance Equations. Journal of Hydraulic Eng. 128(6), 568-578.
[36] Azamathulla, H. Md., Ahmad, Z., Ghani, A. Ab. (2013) An expert system for predicting Manning's roughness coefficient in open channels by gene expression programming. Journal of Neural Comput. and Applic. 50(5), 1343–1349.

Received: **22.01.2018**
Accepted: **18.04.2018**

CORRESPONDING AUTHOR

Mohsen Najarchi
Department of Civil Engineering,
Islamic Azad University,
Arak Branch,
P.O. Box 38135-567
Arak – Iran

e-mail: drmohsennajarchi@yahoo.com

© by PSP Volume 27 – No. 7/2018 pages 4930-4935 Fresenius Environmental Bulletin

STUDY ON THE TRANSFORMATION OF GINSENOSIDE COMPOUND K BY THE MICROBIAL FLORA

Haiming Sun, Keyu Chen, Yimin Yan, Yu Hou, Baoyan Liu, Guiyun Zhao*

Chemical and Biological College, Beihua University, Traditional Chinese Medicine Biotechnology Innovation Center in Jilin Province, Jilin 132013, China

ABSTRACT

It is a major method to produce ginsenoside compound K using microbial transformation. Therefore the selection of efficient strains is the prime requirement. Based on the synergetic relationship, the microbial flora R2A48 was obtained from the soil of planting ginseng, which had a strong capability to transform ginsenoside compound K by the method of TLC and HPLC, the content of ginsenoside compound K was 36.96mg/g. High-throughput sequencing results showed that the dominant flora of Bacterium were Bacillus (47.25%), Ochrobactrum (25.58%), Enterococcus(9.36%), Rhizobium (4.2), Exiguobacterium (2.06%), Buttiauxella (2.01%), Serratia (1.95%), Allobacillus (1.87%), and Stenotrophomonas (1.66%). The dominant flora of Fungus were unclassified (77.18%), Penidiella (4.37%), Penicillium (4.01%), Trichaptum (2.22%), Remersonia (1.78%), Pyrenophora (1.21%), Malassezia (1.07%). The transformation pathway was Rd→F2→compound K. Compared with single strain, this study provides a new method and mentality for the microbial transformation on ginsenoside compound K, and had the significance in the production of ginsenoside.

KEYWORDS:
Ginsenoside compound K, Micro flora R2A48, Dominant flora, Transform mechanism

INTRODUCTION

Ginsenoside is the main active components of Panax ginseng. At present, more than 50 kinds of ginsenosides have been isolated and identified [1]. Among them, ginsenoside compound K belongs to protopanaxadiol ginsenoside. It does not exist in Panax ginseng, and is a degradation product of other protopanaxadiol ginsenosides in the human intestinal tract. Ginsenoside compound K is an important active component to play a medicinal role, and a potential Anticancer drugs. It has effective inhibition on the growth and metastasis of cancer cells [2, 3], and a certain effect on anti-aging [4, 5], anti-inflammatory [6, 7] and so on. It is a key point that how to obtain a large amount of ginsenoside compound K in modern pharmaceutical research. The main methods for modifying glycosyl chains are chemistry, enzyme, and microbial transformation. Microbial transformation has been widely used because of low cost and less by-products compared with other methods. The transform mechanism of microbial transformation is that the glycosyl chains of ginsenosides is modified by microbial enzymes, and a new product is obtained through the change of the structure. Factors are affect the effect of microbial transformation such as strain, substrate, temperature and pH value [8-10].

The screening of effective transformation strains is the key to microbial transformation of ginsenoside compound K. Therefore, it is research focus that looking for the strain with high specificity and conversion rate at present. Many scholars once researched the transformation of ginsenoside by intestinal flora. For example, 4 strains belonging to Bifidobacterium, Eubacterium, and Bacteroides were obtained in the intestinal tract by Bae. et al. [11], and produced compound K from ginsenoside Rc. However, most of the intestinal flora in test were Anaerobicbacteria, and with high cost, low yield. scholars were constantly looking for some new strains for transformation of ginsenosides compound K, and focused on fungi. Fermentum A8 enriched and separated from the earth growing Gingsen by Han et al. [12], and could transform the Leaves Saponins of Panax Notoginseng to make the ginsenoside compound K production more specially and efficiently. The Fusarium spp. m14 was screened and isolated from the soil in the botanic garden planted for P. ginseng by Cui et al. [13], and found to transform the SFPG efficiently to ginsenoside compound K, the content of C-K was 24.99 mg/g. Paecilomyces Bainier sp.229 isolated from the soli of ginseng plantation localities by Li. et al. [14], shows strong glycisidase activity that can transform ginsenoside Rb1 to compound K efficiently. The optimum culture conditions required for the efficient production of ginsenoside compound K by P. bainier sp. 229 via biotransformation of ginseng saponin substrate have been determined, and resulted in an 82.6% yield of ginsenoside

compound K [15]. Penicillium oxalicum sp. 68 was screened from soil by Gao et al. [16], and found to be able to transform protopanaxadiol-type ginsenosides to produce a series of bioactive metabolites. The sole product is Compound K and the maximum yield reached 87.7 % (molar ratio) using the partially purified glycosidase. These research achievements provides an important basis for the industrialization of compound K. However, these studies mainly focused on the microbial transformation by single strain, and most were still in the initial stage.

There is a complex synergetic relationship between microorganism in nature. A composite microbial system MC1 with highly efficient cellulose degradation was obtained according to synergetic relationship by Cui et al. [17], and the efficiency was higher than that of pure culture, which greatly promoted the development and utilization of cellulose resources. However, the research has not been applied to the microbial transformation of ginsenoside. In this study, the microbial flora R2A48 was obtained from the soil of planting ginseng based on the synergetic relationship, which had a strong capability to transform ginsenoside compound K. This study provides a new method and mentality for the microbial transformation on ginsenoside compound K, and had the significance in the production of ginsenoside.

MATERIALS AND METHODS

Sampling. Experiments were conducted in the ginseng cultivation, Fusong Country, Jilin Province, PR China. Four 10m×10m sites were randomly selected at different growing years level (15 years, 20 years, 25 years, and 30years). We selected 1m×1m plot by five point sampling at each site and then proceeded to take the soil samples. The soil samples were taken using 13mm diameter core at a 10 cm depth. All samples were kept at 4°C.

Enrichment culture. 0.1ml were inoculated in conical flask with 50ml medium after serial dilution (100-fold) of 1g dry soil suspension, and kept 7 days at 30°C. R2A, MRS, PDA, and LB were selected for culture medium. Ginsenoside was used as substrate, the concentration was 0.1%.

Fermentation. The inoculum concentration of Enrichment culture was 0.5%, the substrate concentration was 3%, and shaking culture for 14 days with 110 r/min and 35°C.

Thin Layer Chromatography (TLC). The reaction mixture was extracted with n-butyl alcohol saturated with H_2O, and 5μl was used in silica gel G to isolate ginsenoside compound K. The eluent was $CHCl_3$/MeOH/H_2O (65:35:10, by vol., lower phase). Colored at 105°C with an alcoholic solution of sulfuric acid (10%) after removed eluent by volatilization. The compound K was collected via TLC analysis.

Estimation of compound K. HPLC was performed using Agilent 1260 (Agilent Technologies Inc.). The detection wavelength was 203 nm. The column used was a ODS, and the mobile phase utilized gradient conditions with CH_3CN (solvent A) and distilled H_2O (solvent B). The program of HPLC Gradient Elution were as follows: 0-35min, 19%A; 35-55min, 19%-29%A; 55-70min, 29%A; 70-100min, 29%-40%A. The column temperature was 30°C, flow rate was 1.0 ml/min, and sample size was 20μl.

DNA extraction, PCR amplification, and High-throughput sequencing. DNA was extracted from 4ml sample using E.Z.N.ATM Mag-Bind Soil DNA Kit (OMEGA) according to the instructions of the manufacturer. PCR amplification of bacterial communities 16S rDNA fragments was carried out using the primers 341F (CCCTACACGACGCT CTTCCGATCTGCCTACGGGNGGCWGCAG) and 805R (GACTGGAGTTCCTTGGCACCCG AGAATTCCAGACTACHVGGGTATCTAATCC). PCR amplification of fungal communities 18S rDNA fragments was carried out using the primers NS1 (CCTACACGACGCTCTTCCGATCTNGTA GTCATATGCTTGTCTC) and Fung (GACTGGA GTTCCTTGGCACCCGAGAATTCCAATTCCCC GTTACCCGTTG). The reaction mixture (30μL) consisted of 10-20ng Genomic DNA, 15μL of 2×Taq master Mix, 1μL of Bar-PCR primer F(10uM), and 1μL of Primer R (10uM). The first round PCR reaction conditions was 3min of denaturation at 94 °C, 5 cycles of 30s at 94 °C, 20s at 45°C and 20s at 65°C, and 20 cycles of 20s at 94 °C, 20s at 55°C, and 30s at 72°C, followed by an extension step at 72°C for 5 min. The second round PCR reaction conditions was 3min of denaturation at 95 °C, 5 cycles of 20s at 94 °C, 20s at 55°C, and 30s at 72°C, followed by an extension step at 72°C for 5 min.

The accurate quantification of PCR products was detected by Qubit3.0 DNA Kit, and mixed equally for high-throughput sequencing. High-throughput sequencing of PCR product was carried out by Sangon Biotech (Shanghai) Co., Ltd.

RESULTS

Screening of the microbial flora. The series of microbial flora that were initially isolated from the collected soil samples were incubated in the medium for the biotransformation tests. According to TLC analysis (Figure 1), the R2A48 was selected as the fermentation microbial flora which gave the

most effective biotransformation of ginsenoside compound K. HPLC analysis showed that the content of compound K was 36.96mg/g under the following conditions: substrate concentration was 3%, conversion temperature was 35°C, shaking rate was 140r/min, and conversion time was 14d.

Transformation pathway. In order to investigate the transformation pathway of ginsenoside compound K, the products were detected by TLC at different times. As shown in Figure 2, a portion of ginsenoside Rd was converted into F2 on the third day, the content of ginsenoside F2 decreased on the fifth day, and ginsenoside compound K was formed. This suggested that ginsenoside compound K was converted by the microbial flora R2A48 in the following sequence: Rd→F2→compound K.

Composition of the microbial flora. For revealing the composition of the microbial flora R2A48, DNA was extracted and selected for High-throughput sequencing. The diversity indices were analyzed and indicated in Table 1. The Seq num, Coverage, and Simpson index of Bacterium were lower than Fungus, the OUT num, Shannon index, ACE index, and Chao1 index were higher than Fungus. These suggested that the diversity of Bacterium was higher than Fungus in the microbial flora R2A48.

The composition of the microbial flora R2A48 were analyzed based on 16S rDNA fragments and18S rDNA fragments by High-throughput sequencing, and indicated in Figure 3 and Figure 4. The dominant flora of Bacterium were Bacillus (47.25%), Ochrobactrum (25.58%), Enterococcus (9.36%), Rhizobium (4.2), Exiguobacterium (2.06%), Buttiauxella (2.01%), Serratia (1.95%), Allobacillus (1.87%), and Stenotrophomonas (1.66%) (Figure 3). The dominant flora of Fungus were unclassified (77.18%), Penidiella (4.37%), Penicillium (4.01%), Trichaptum (2.22%), Remersonia (1.78%), Pyrenophora (1.21%), Malassezia (1.07%) (Figure 4). The community function was predicted and analyzed by PICRUSt. The results suggested that there were Membrane Transport, Carbohydrate Metabolism, Amino Acid Metabolism, Replication and Repair, Energy Metabolism, Cellular Processes and Signaling, Metabolism of Cofactors and Vitamins, Xenobiotics Biodegradation and Metabolism, et al.

DISCUSSION AND CONCLUSIONS

Many studies mainly focused on the microbial transformation ginsenoside compound K by single strain. However, the transformation of organic matter was usually carried out by synergetic relationship between microorganism in nature. Therefore, it is valuable to transform ginsenoside compound K base on synergetic relationship between microorganism.

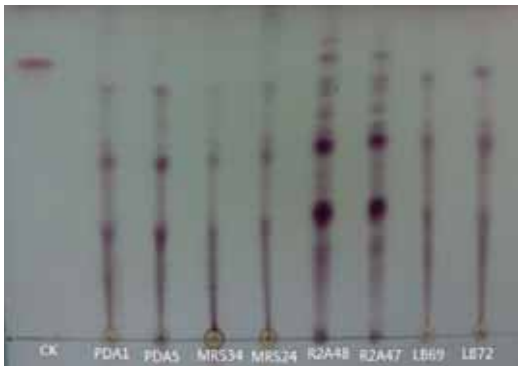

FIGURE 1
TLC mapping of the transformation of compound K in different microbial flora

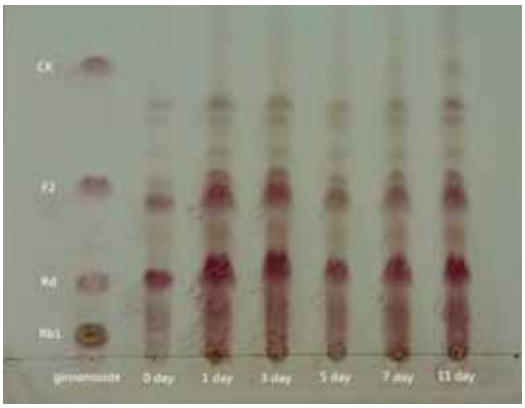

FIGURE 2
Time-course TLC analysis of metabolites by the microbial flora R2A48

TABLE 1
Diversity indices of the microbial flora R2A48 based on High-throughput sequencing

Microbial flora	Seq num	OUT num	Shannon index	ACE index	Chao1 index	Coverage	Simpson
Bacterium	38524	1942	2.82	113170.11	36467.55	0.95	0.13
Fungus	47064	770	1.51	18005.34	6278.72	0.99	0.55

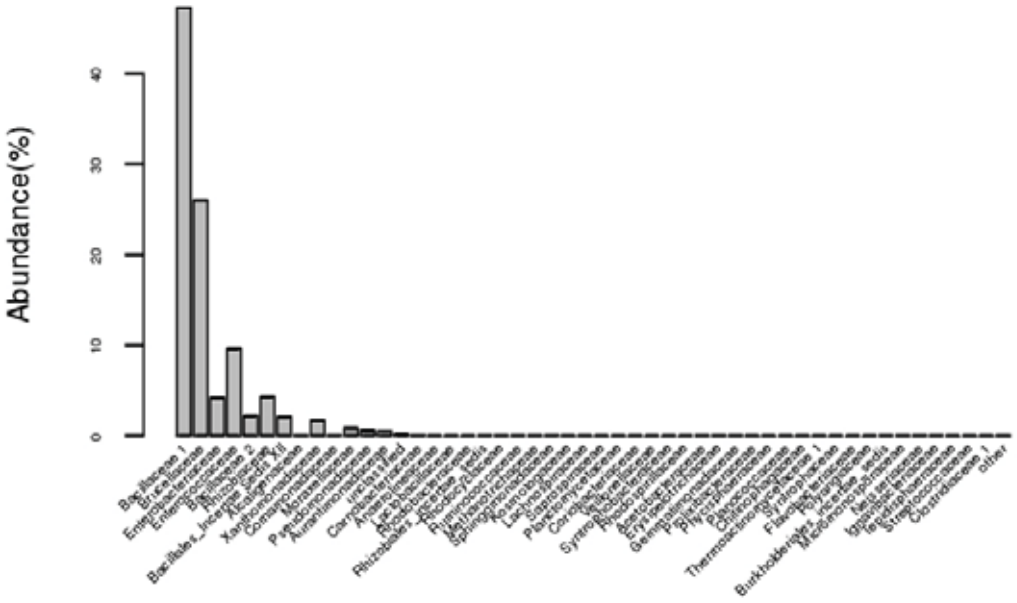

FIGURE 3
The composition of Bacterium based on based on 16S rDNA fragments

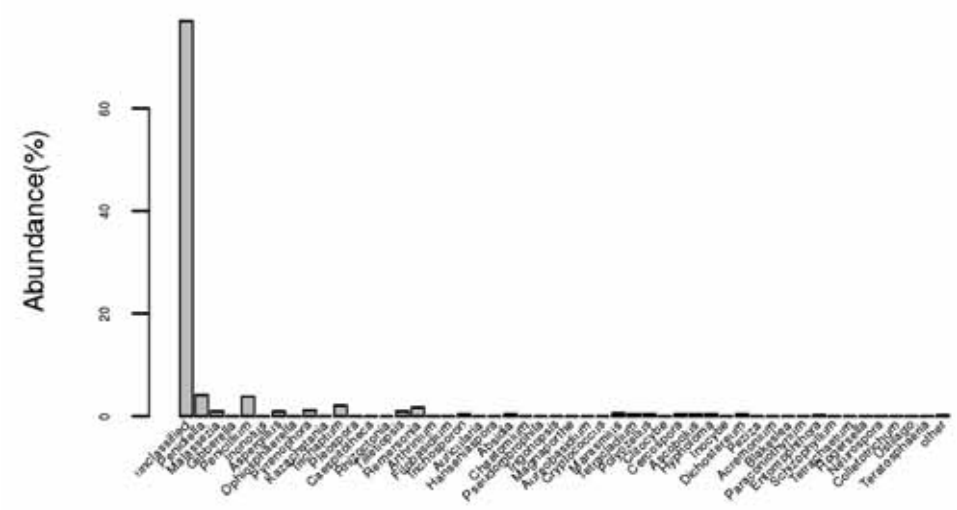

FIGURE 4
The composition of Fungus based on based on 18S rDNA fragments

In our study, the microbial flora R2A48 was obtained from the soil of planting ginseng, which had a strong capability to transform ginsenoside compound K. The transformation pathway was Rd→F2→compound K. The content of ginsenoside compound K was 36.96mg/g with ginsenoside as substrate, and higher than the content (24.99mg/g) reported by Cui et al. [13] This study provides a new method and mentality for the microbial transformation on ginsenoside compound K.

The dominant flora of Bacterium were Bacillus, Ochrobactrum, Enterococcus, Rhizobium, Exiguobacterium, Buttiauxella, Serratia, Allobacillus, and Stenotrophomonas in the microbial flora R2A48. However, it does not exist Bifidobacterium, Eubacterium, and Bacteroides reported by Bae et al. [11], Bifidobacterium, Lactobacillus delbrueckii reported by Chi et al. [18] It is possible to exist undetected Bacterium which could transform ginsenoside compound K. The dominant flora of Fungus were unclassified, Penidiella, Penicillium, Trichaptum, Remersonia, Pyrenophora, Malassezia in the microbial flora R2A48. Penidiella and Penicillium were extensive used in transformation of ginsenoside compound K [14-16]. The reason might be that they had strong ability to produce glucosidase [19-22]. No research on Trichaptum, Remersonia, and Pyrenophora in transformation of ginsenoside compound K. It is noteworthy that there was a large amount of unclassified (77.18%), Whether they could be used to transform ginsenoside compound K should have a future investigation.

Ginsenoside compound K is a promising natural product that could be used for the treatment of numerous human pathologies. Our study suggested that the microbial flora R2A48 may have potential applications in the microbial transformation of ginsenoside compound K. The transformation efficiency will be raised by optimization of strain and condition in the future, and provides the basis for industrialization.

ACKNOWLEDGEMENTS

This work was supported by the Scientific and Technological Research Projects of Jilin Provincial Education Department (No. JJKH20170041KJ), Jilin provincial science and technology development project (20180101259JC), Traditional Chinese Medicine Biotechnology Innovation Center in Jilin Province (No. 20170623064TC), and Scientific Research Foundation for the Doctor of Beihua University.

REFERENCES

[1] Cui, X.M., Jiang, Z.Y., Zeng, J., Zhou J.M., Chen, J.J., Zhang, X.M., Xu, L.S., Wang, Q. (2008) Two new dammarane triterpene glycosides from the rhizomes of Panax notoginseng. Journal of Asian natural products research. 10(9), 845-849.

[2] Hu, C., Song, G., Zhang, B., Liu, Z., Chen, R., Zhang, H., Hu, T. (2012) Intestinal metabolite compound K of panaxoside inhibits the growth of gastric carcinoma by augmenting apoptosis via Bid-mediated mitochondrial pathway. Journal of Cellular and Molecular Medicine. 16(1), 96-106.

[3] Wang, C.Z., Guang-Jian, D.U., Zhang, Z., Wen, X.D., Calway, T., Zhen, Z., Musch, M.M., Bissonnette, M., Chang, E.B., Yuan, C.S. (2012) Ginsenoside compound K, not Rb1, possesses potential chemopreventive activities in human colorectal cancer. International Journal of Oncology. 40(6), 1970-1976.

[4] Lei, X.J., Fen, K., Sun, L.W., Jiang, R., Li, C. Y., Wang, Y. P. (2010) Progress in Studying Anti-Aging Mechanism of Ginsenoside. Amino Acids and Biotic Resources. 32(1), 44-47.

[5] He, D., Sun, J., Zhu, X., Nian, S., Liu, J. (2011) Compound K increases type I procollagen level and decreases matrix metalloproteinase-1 activity and level in ultraviolet-A-irradiated fibroblasts. Journal of the Formosan Medical Association. 110(3), 153-160.

[6] Liu, W., Miao, J. (2013) Research of anti-inflammatory and neuroprotective effects of ginsenoside CK. China Medical Herald. 10(21), 13-16.

[7] Park, J.S., Shin, J.A., Jung, J.S., Hyun, J.W., Van, L.T.K., Kim, D.H., Park, E.M., Kim, H.S. (2012) Anti-inflammatory mechanism of compound K in activated microglia and its neuroprotective effect on experimental stroke in mice. Journal of Pharmacology and Experimental Therapeutics. 341(1), 59-67.

[8] Wang, S.Y., Chen, J.W., Zhang, W.X., Jiang, Y.P. (2009) Effect of Bidirectional Fermentation Technology on Content of Paeoniflorin and HPLC Fingerprint. Research and Practice of Chinese Medicines. 23(2), 6-9.

[9] Xu, J.H., Lu, W.Y., Lin, G.Q. (2006) Enzymatic transformation of ginsenoside Rg3 to Rh2 using newly isolated Fusarium proliferatum ECU2042. Journal of Molecular Catalysis B: Enzymatic. 38(2), 113-118.

[10] Cheng, L.Q., Na, J.R., Bang, M.H., Kim, M.K., Yang, D.C. (2008) Conversion of major ginsenoside Rb1 to 20(S)-ginsenoside Rg3 by Microbacterium sp.GS514. Phytochemistry. 69(1), 218-224.

[11] Bae, E.A., Choo, M.K., Park, E.K., Park, S.Y., Shin, H.Y., Kim, D.H. (2002) Metabolism of ginsenoside R (c) by human intestinal bacteria and its related antiallergic activity. Biological and pharmaceutical bulletin. 25(6), 743-747.

[12] Han, Y., Zhao, Y.Q., Jiang, B.H., Hu, X.M. (2005) Seletion of the microbe for preparing the anticancer constituent C-K by the transformation of microbe. Research and Information on Traditional Chinese Medicine. 7(2), 17-19.

[13] Cui, Y., Jiang, B.H., Han, Y., Zhao, Y.Q. (2007) Microbial transformation on ginsenoside compound K from total saponins in fruit of Panax ginseng. Chinese Traditional and Herbal Drugs. 38(2), 189-193.

[14] Li, X.W. (2008) Biotransformation of ginsenoside Rg3 and purification and characterization of metabolites from Paecilomyces Bainier sp. 229. Shanghai: Fudan University.

[15] Zhou, W., Yan, Q., Li, J.Y., Zhang, X.C., Zhou, P. (2008) Biotransformation of Panax notoginseng, saponins into ginsenoside compound K production by Paecilomyces bainier, sp. 229. Journal of Applied Microbiology. 104(3), 699-706.

[16] Gao, J., Xu, W., Fang, Q., Liang, F., Jin,R.T., Wu, D., Tai, G.H., Zhou, Y.F. (2013) Efficient biotransformation for preparation of pharmaceutically active ginsenoside Compound K by Penicillium oxalicum sp. 68. Annals of Microbiology. 63(1), 139-149.

[17] Cui, Z.J., Li, M.D., Piao, Z., Huang, Z.Y., Masaharu, I., Yasuo, I. (2002) Selection of A Composite Microbial System MC1 with Efficient and Stability Cellulose Degradation Bacteria and Its Function. Chinese Journal of Environmental Science. 23(3), 36-39.
[18] Chi, H., Kim, D.H., Ji, G.E. (2005) Transformation of ginsenosides Rb2 and Rc from Panax ginseng by food microorganisms. Biol Pharm Bull. 28(11), 2102-2105.
[19] He, Y.W., Jiang, L., Wang, J.F., Rao, J., Mao, H.L. (2011) Separation and Purification of β-Glucosidase from Penidiella sp. HEY-1 and Its Properties. Chemistry and Industry of Forest Products. 31(3), 110-114.
[20] Krogh, K.B., Harris, P.V., Olsen, C.L., Johansen, K.S., Hojer-Pedersen, J., Borjesson, J., Olsson, L. (2010) Characterization and kinetic analysis of a thermostable GH3 β-glucosidase from Penicillium brasilianum. Applied Microbiology and Biotechnology. 86(1), 143-154.
[21] Son, S., Ko, S.K., Kim, J.W., Lee, J.K., Jang, M., Ryoo, I.J., Hwang, G.J., Kwon, M.C., Shin, K.S., Futamura, Y., Hong, Y.S., Oh, H., Kim, B.Y., Ueki, M., Takahashi, S., Osada, H., Jang, J.H., Ahn, J.S. (2015) Structures and biological activities of azaphilones produced by Penicillium sp. KCB11A109 from a ginseng field. Phytochemistry. 122, 154-164.
[22] Fu, Y., Yin, Z., Wu, L., Yin, C. (2014) Fermentation of ginseng extracts by Penicillium simplicissimum GS33 and anti-ovarian cancer activity of fermented products. World Journal of Microbiology and Biotechnology. 30(3), 1019-1025.

Received: **29.01.2018**
Accepted: **11.04.2018**

CORRESPONDING AUTHOR

Guiyun Zhao
Chemical and Biological College,
Beihua University,
Traditional Chinese Medicine Biotechnology
Innovation Center in Jilin Province,
Jilin 132013 – China

e-mail: zhaoguiyun2014@163.com

© by PSP Volume 27 – No. 7/2018 pages 4936-4941 Fresenius Environmental Bulletin

DEEP TREATMENT OF COAL CHEMICAL WASTEWATER VIA SLUDGE ACTIVATED CARBON

Xu Chen*

Sichuan College of Architectural Technology, No. 139 Anshan Road, Jingyang district, Deyang, Sichuan, 618000, China

ABSTRACT

Sludge activated carbon is prepared by using waste water as main raw material and sulfuric acid as activator. The physicochemical properties of sludge activated carbon were characterized by specific surface area measurement and scanning electron microscopy. The bottle-point static adsorption experiments and dynamic column adsorption experiments were carried out to study the removal efficiencies of COD and colorimetric in activated sludge from coal-based chemical wastewater. The bottle-point method static test showed that the COD removal rate and colorimetric removal rate of activated sludge decreased with the increase of pH, and increased with the increase of dosage. The experimental sludge prepared activated carbon maximum adsorption capacity of single layer at 323K was 108.3 mg / g. The dynamic tests showed that the adsorption rate of 12 BV / h and the sludge adsorbent have a good effect on the removal of COD and chroma, which can reach the first grade of the national integrated wastewater discharge standard.

KEYWORDS:
Sludge Activated Carbon, Advanced Treatment, Coal Chemical Industry Wastewater

INTRODUCTION

Coal chemical wastewater is a complex industrial wastewater generated from coal treatment, including high temperature carbonation, coal gas purification and byproduct recovery processes. Currently, the treatment processes used for coal chemical wastewater generally include pretreatment and biological treatment [1]. Biological treatment process is the main treatment technology for coal chemical wastewater due to the low cost, simple operation and maintenance and maximal mineralization of contaminants [2]. Many contaminants in coal chemical wastewater are toxic, mutagene and carcinogenic, including phenols, mono- and poly-cyclic nitrogen-containing aromatics, oxygen- and sulfur-containing heterocyclic compounds and polynuclear aromatic hydrocarbons (PAHs) [3, 4], which makes coal chemical wastewater much recalcitrant for biodegradation. Thus, the secondary effluent from biological treatment process, namely bio-treated coal chemical wastewater (BCCW), contains certain amount of the above substances and cannot meet corresponding discharge standards. Hence, further removal of remaining refractory organic pollutants in BCCW remains of fundamental importance to the environment.

At present, the common method of coal chemical industry wastewater treatment is mainly flocculation method, adsorption method and activated sludge method. Flocculation method uses water treatment chemicals for coagulation and sedimentation of sewage treatment facilities, covers an area of large, contaminated material only transferred from the water to the sludge, not harmless degradation, and follow-up sludge disposal problems. Adsorption method using activated carbon and other adsorbent material, with high removal efficiency [5-8], but the expensive, short life, high operating costs. Preparation of inexpensive carbonaceous adsorbent can avoid the current lack of adsorption method, domestic and foreign sludge activated carbon has done a lot of basic research. Activated carbon is a kind of adsorbent which is widely used in environmental pollution control. The cost of existing commercial activated carbon is high, and the use of activated carbon is limited to a certain extent. It is always a hot topic to study the production of activated carbon from various types of carbonaceous materials with low cost. Sludge contains a large amount of organic matter, under high-temperature carbonization activation conditions, has the potential to convert to activated carbon [9-12].

Activated sludge treatment of sewage (waste water) in the process of generating a large number of excess sludge, the remaining sludge in addition to containing large amounts of water, but also contains refractory organic matter, heavy metals and salts and a small amount of pathogenic microorganisms and parasite eggs And so on, is a difficult to deal with solid waste. Since sewage sludge is rich in organic carbon, it can be converted into sludge activated carbon under suitable conditions [13-16]. This not only provides a new way for resource utilization of final sludge disposal, but also can Produces a lower cost adsorbent than commercial activated carbon. At pre-

sent, little research has been done on the deep treatment of wastewater from the production of coal chemical wastewater by sludge activated carbon. In this paper, the activated sludge from wastewater treatment plant was used as raw material to prepare sludge activated carbon by chemical activation method. The effects of activated sludge on COD of biochemical degradation of coal chemical industry wastewater and color removal are studied. In this paper, the physical and chemical properties of sludge adsorbent were characterized by specific surface area measurement and infrared analysis. The static and dynamic adsorption behavior of COD on activated sludge and chrominance was studied.

EXPERIMENTAL

Instruments, reagents and analytical methods. Instruments. Microwave oven NN-GT556W (Shanghai Matsushita Microwave Co., Ltd.), digital scanning electron microscope KYKY2800B (Chinese Academy of Sciences Instrument Factory), ASAP -2010 surface area aperture tester ((Micromeritics Instrument Co., Ltd.), 722 spectrophotometer (Shanghai Meida Instrument Co., Ltd.), TG328A electro-optical analytical balance (Shanghai Balance Analytical Instrument Factory), ZD-85 temperature oscillator (Jiangsu Jintan Medical Instrument Factory), diameter 12 mm glass adsorption column, DHL-B computer constant current pump (Shanghai Qingpu Huxi Instrument Co., Ltd.).

Reagents. Sodium hydroxide, hydrochloric acid, anhydrous ethanol, concentrated sulfuric acid, ferrous ammonium sulfate, potassium dichromate (analytical grade, Sinopharm Chemical Reagent Company); dehydrated sludge (water content 80.8%) (a sewage treatment plant in Shaanxi Province); Coal chemical waste water from a coal chemical plant in Yulin City sewage treatment station, the wastewater COD concentration of 134.6mg / L, 100 times the color.

Analysis method. In this experiment, the COD of waste water was determined by potassium dichromate method, and the colorimetric of waste water was determined by dilution factor method.

Test method. Preparation of sludge activated carbon. The sludge drying, the water content decreased to about 10%, with 25% sulfuric acid solution soaking, stirring, drained after 48h. Into the crucible with lid, and then into the microwave carbonization activation, microwave power 500W, to maintain 240s. Remove after cooling, fully immersed in hot water above 70 ° C, while sulfuric acid can be recovered. The activated carbon is then washed thoroughly with hot water to a pH greater than 5. After drying into the dryer cooling, grinding 100 mesh sieve to obtain sludge activated carbon, spare.

Different dosage on the adsorption. Weigh 0.2,0.4,0.6,0.8,1 g experimental preparation of activated carbon sludge placed 250mL conical flask, followed by adding 100mL coal chemical wastewater, placed at a temperature of 323 K water bath oscillator to 120 r / min speed oscillation 12 h, the adsorption to achieve equilibrium; Determination of equilibrium solution COD and color removal rate.

Different pH on the adsorption. Weigh the quality of 0.6g experimental preparation of 6 parts of activated sludge activated carbon, respectively, placed in 250mL conical flask, followed by adding 100mL coal chemical wastewater treatment, with NaOH to pH were adjusted to 2,4,6,8, 10,12, into a temperature of 323K water bath thermostatic oscillator, 120r / min speed oscillation 12h, to achieve equilibrium adsorption, the determination of equilibrium solution COD and color removal rate.

Sludge activated carbon static adsorption kinetics. Weigh the quality of 0.6g experimental preparation of sludge activated carbon 11, were placed 250mL conical flask, adding 100mL coal chemical wastewater, placed in 323 K water bath thermostatic oscillator to 120 r / min speed oscillation. Samples were taken every 10, 20, 30, 40, 50, 60, 80, 120, 180, 240 and 360 min to analyze the relationship between adsorption time and adsorption capacity.

Sludge activated carbon dynamic adsorption. 5 mL of the experimental sludge activated carbon was added to the adsorption column by a wet packing method. The coal chemical industry wastewater was collected at a flow rate of 12 BV / h (controlled by a constant current pump) through a glass adsorption column and collected and measured Adsorption of effluent COD and color values for its breakthrough curve.

RESULTS AND DISCUSSION

Activated carbon physical properties. Characterization The specific surface area (SBET), the Smicro, the total pore volume (Vt), the micropore volume (Vmicro) of activated carbon from sludge were determined by nitrogen adsorption at 77 K using an ASAP 2010 surface area analyzer, Transition pore volume (Vmeso) and average pore size (DP), the data in Table 1. As can be seen from Table 1, the sludge activated carbon prepared from mud activated carbon contains a certain amount of transition pores, and the average pore size lies in the transition pore region (2 to 50 nm is the transition pore region).

TABLE 1
Pore structure parameter of sludge based activated carbon

Adsorbent	$S_{BET}/m^2 \cdot g^{-1}$	$Smicro/m^2 \cdot g^{-1}$	$V_t/mL \cdot g^{-1}$	$V_{micro}/mL \cdot g^{-1}$	$V_{meso}/mL \cdot g^{-1}$	D_n/nm
Experimental preparation of sludge activated carbon	262.1	170.4	0.225	0.091	0.102	3.42

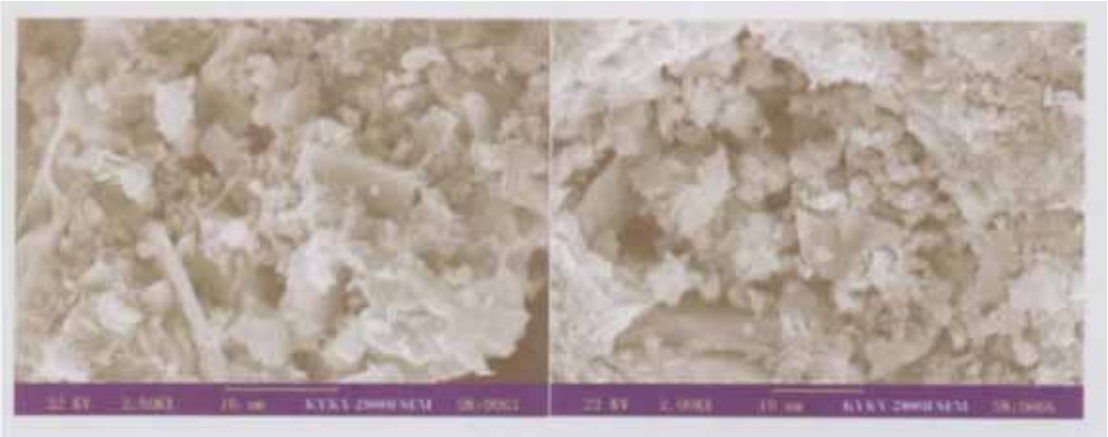

FIGURE 1
Sludge activated carbon scanning electron microscopy

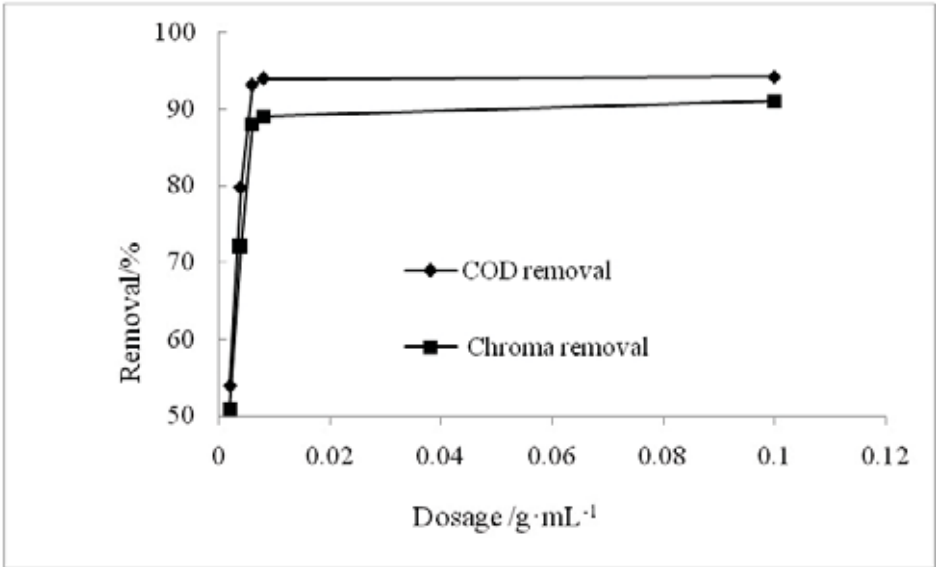

FIGURE 2
Effect of different dosages on COD and color removal efficiency

Sludge activated carbon by scanning electron microscopy. Surface morphology using the Chinese Academy of Sciences KYKY2800B scanning electron microscope (Figure 1). As is clear from Fig. 1, the surface of the sludge activated carbon basically exhibits an irregular porous structure. And the surface has obvious large aperture phenomenon, there are more large holes in the transition hole to the internal extension. In addition, there are particles of impurities inside the pores, which impede the further extension of the pores.

Effect of Different Dosage on Adsorption. Different sludge activated carbon dosage of coal chemical wastewater COD and color removal rate, the results shown in Figure 2. As can be seen from Fig. 2, when the dosage increases from 0.2g to 1g (based on 100mL wastewater), the removal rate of COD from coal-based chemical biochemical waste water increased from 53.9% to 94.2% 51% rate increased to 91%. When the dosage is 0.02 ~ 0.06g / mL, the removal rate increases rapidly. When the dosage is more than 0.06 g / mL, the removal rate

increases slowly. Therefore, in the subsequent adsorption experiments, sludge adsorbent dosage were selected 0.06 g / mL wastewater.

Effect of Different pH on COD and Color Removal Efficiency. The effect of different pH on the removal of COD and chroma in biochemical treatment of coal chemical wastewater by sludge activated carbon is shown in Fig.3. As can be seen from Figure 3, pH has a greater impact on activated sludge biofuel treatment of coal chemical industry. Sludge activated carbon COD and color removal rate increases with the increase of pH decreases. When the pH was increased from 2 to 12, the removal rate of COD from activated sludge was reduced from 93.1% to 80.2% and the color removal rate was reduced from 80% to 60%. The reason is that: experimental preparation of sludge activated carbon surface contains some polar functional groups, the surface functional groups under alkaline conditions negatively charged, while coal chemical industry wastewater mainly contains a variety of organic compounds, these organic compounds also have a negative charge in alkaline conditions, both Electrostatic repulsion between the two may result in a decrease in COD and color removal.

Adsorption isotherm. Experimental preparation of sludge activated carbon biochemical waste water coal chemical and COD adsorption isotherms shown in Figure 4 and Figure 5.

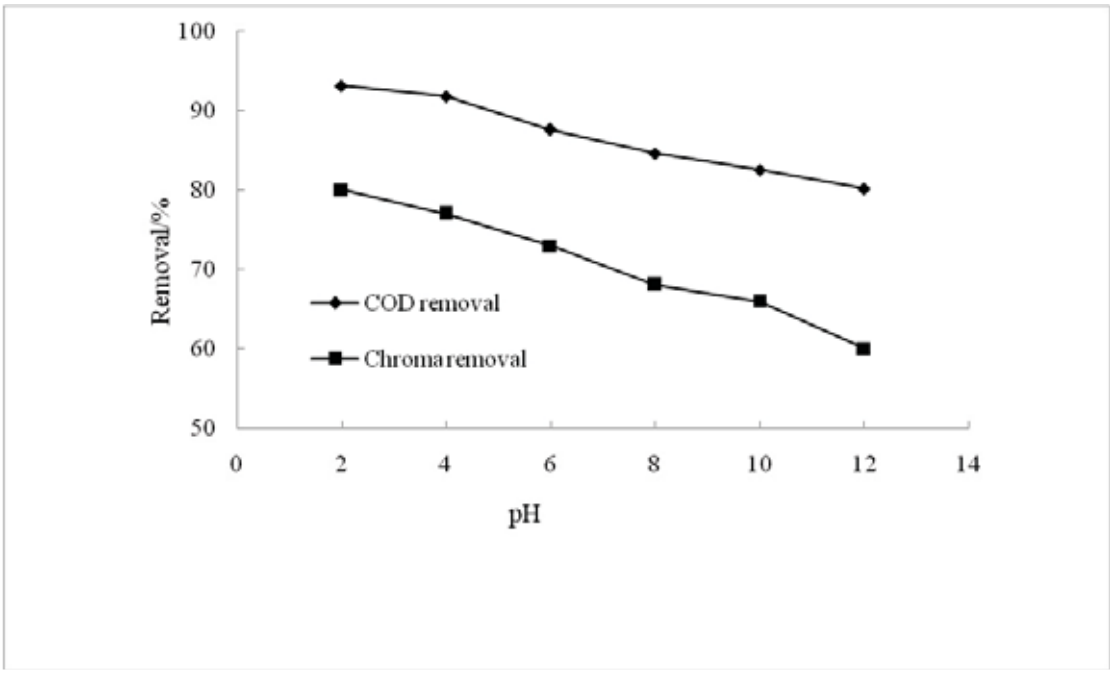

FIGURE 3
Effect of different pH on COD and color removal efficiency

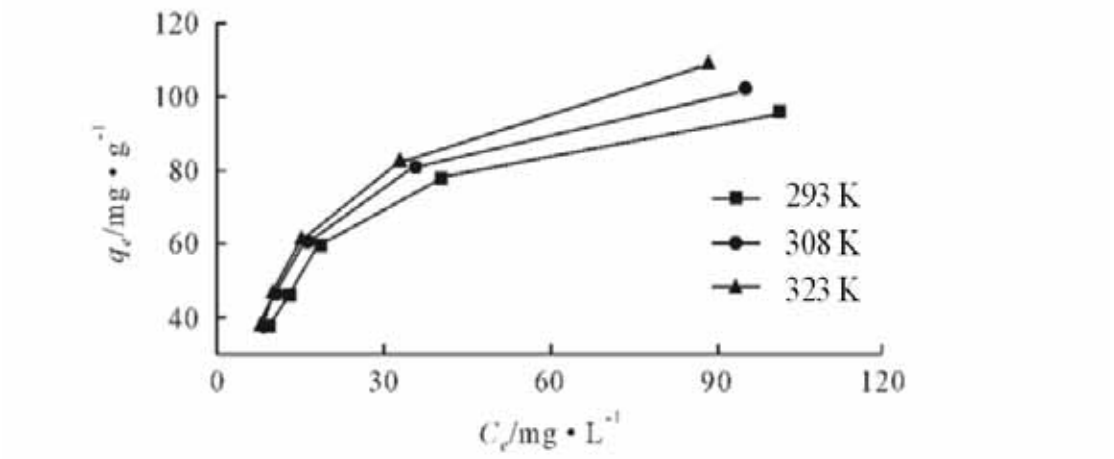

FIGURE 4
Laboratory preparation of sludge activated carbon COD adsorption isotherm

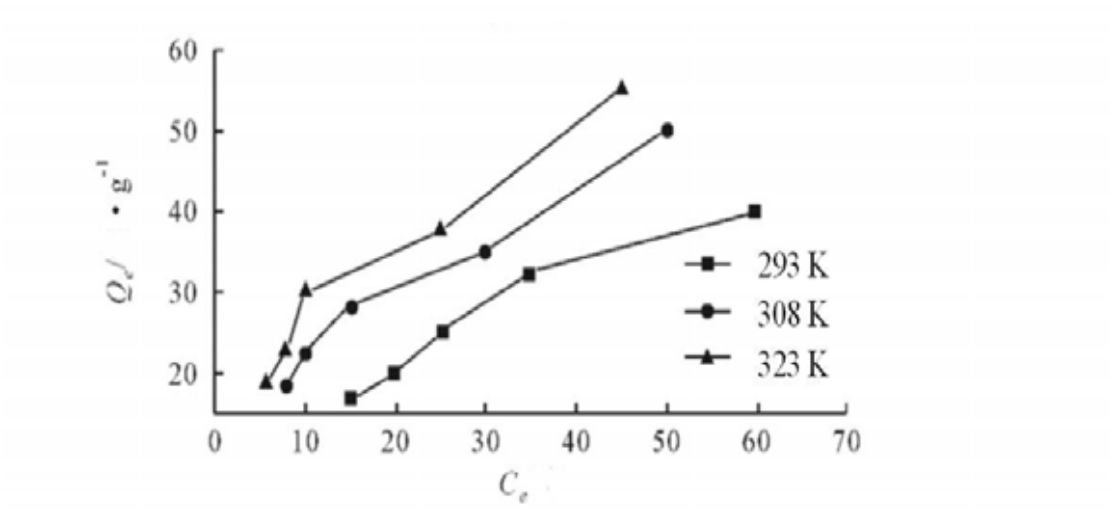

FIGURE 5
Laboratory preparation of sludge activated carbon color adsorption isotherm

With the increase of temperature, the amount of COD adsorbed by the two adsorbents increased, indicating that the adsorption process is an endothermic process. Appropriate temperature increase is favorable for adsorption. 323K. Under this experimental operating condition, the maximum COD and chromatic adsorption capacity of activated sludge prepared by the experiment was 108.3 mg / g and 50 times / g, respectively.

CONCLUSIONS

(1) The removal rate of COD and chroma of sludge activated carbon prepared from sulfuric acid and activated sludge decreases with the increase of pH, and increases with the increase of dosage.

(2) The activated sludge with sludge as raw material and sulfuric acid as activator has the specific surface area of 261.1m2 / g and the pore size is dominated by transition pore.

(3) Sludge Activated Carbon In the process of COD and colorimetric adsorption in biochemical waste water from coal chemical industry, the pH value and activated carbon dosage have a great influence. The adsorption of COD and chroma at activated sludge of activated sludge at 293, 308 and 323 K is endothermic.

(4) The sludge activated carbon prepared by laboratory has good dynamic adsorption capacity for COD and colorimetric in coal chemical industry wastewater, and can reach the national first-class discharge standard. In addition, the sludge activated carbon prepared by sludge and sulfuric acid microwave also has a good removal effect on ammonia nitrogen in the coal chemical industry biological wastewater, and the effluent can meet the national first-class discharge standard. The sludge activated carbon has very good performance in the process of coal chemical industry biological wastewater treatment Good research and development and application prospects.

REFERENCES

[1] Liu, J., Ou, H.S., Wei, C.H., Wu, H.Z., He, J.Z., Lu, D.H. (2016) Novel multistep physical/chemical and biological integrated system for coking wastewater treatment: Technical and economic feasibility. J. Water Process Eng. 10, 98-103.

[2] Yu, X.B., Wei, C.H., Wu, H.Z., Jiang, Z.M., Xu, R.H. (2015) Improvement of biodegradability for coking wastewater by selective adsorption of hydrophobic organic pollutants. Sep. Purif. Technol. 151, 23-30.

[3] Wang, R.K., Ye, X.M., Zhao, Z.H. (2018) Simultaneous disposal and utilization of coal chemical wastewater in coal and petroleum coke slurry preparation: Slurrying performance and mechanism. Fuel. 215, 312-319.

[4] Huang, Y., Hou, X.L., Liu, S.T., Ni, J.R. (2016) Correspondence analysis of bio-refractory compounds degradation and microbiological community distribution in anaerobic filter for coking wastewater treatment. Chem. Eng. J. 304, 864-872.

[5] Rozada, F., Otero, M., Morán, A. (2008) Adsorption of heavy metals onto sewage sludge-derived materials. Bioresource Technology. 99, 6332-6338.

[6] Wei, P., Liu, Z.R., Zeng, K. (2006) Adsorption and desorption characteristics of nickel to peat. Coal Science and Technology. 34, 46-49.

[7] Shi, X.N., Wang, S.Y., Sun, H.W., Peng, Y.Z. (2009) Research and Application Status of Landfill Leachate Treatment by Using SBR Process. Technology of Water Treatment. 35, 19-24.
[8] Zhang, W., Liu, W., Lv, Y., Li, B.J., Ying, W.C. (2010) Enhanced carbon adsorption treatment for removing cyanide from coking plant effluent. Journal of Hazardous Materials. 184, 135-140.
[9] Xiong, R.H., Wei, C. (2017) Current status and technology trends of zero liquid discharge at coal chemical industry in China. Journal of Water Process Engineering. 19, 346-351.
[10] Ren, Y., Wei, C., Wu, C., Li, G. (2007) Environmental and biological characteristics of coking wastewater. Acta Scientiae Circumstantiae. 27, 1094-1100.
[11] Zhang, N.Y., Tang, X.H., Zhou, P., Jia, Z.Y. (2005) Characteristics and Treatment Methods of Coal Coking Wastewater. Water Purification Technology. 24, 43-48.
[12] Zhang, Z.H., Li, L.G., Gao, Y.L. (2010) Coal Chemical Industrial Wastewater Pretreatment Process Improvement. Value Engineering. 22, 114-119.
[13] Liu, L.J., Wang, L.S., Fei, X.Y. and Yang, T. (2007) Research on the pretreatment method of coal-oil wastewater. Tianjin Chemical Industry. 21, 56-59.
[14] Xiang, W.D. (2002) The Application of A~2/O Biological Process in Coke Plant Wastewater Treatment. Shanghai Chemical Industry. 1, 10-13.
[15] Cui, P.Z., Mai, Z.H., Yang, S.Y., Qian, Y. (2017) Integrated treatment processes for coal-gasification wastewater with high concentration of phenol and ammonia. Journal of Cleaner Production. 142, 2218-2226.
[16] Fan, X., Zhang, X. (2008) Adsorption properties of activated carbon from sewage sludge to alkaline-black. Materials Letters. 62, 1704-1706.

Received: **29.01.2018**
Accepted: **18.03.2018**

CORRESPONDING AUTHOR

Xu Chen
Sichuan College of Architectural Technology
No. 139 Anshan Road, Jingyang district,
Deyang, Sichuan, 618000 – China

e-mail: 2871824841@qq.com

© by PSP Volume 27 – No. 7/2018 pages 4942-4951 Fresenius Environmental Bulletin

BIODEGRADATION OF *N*-HEXADECANE BY ENTERIC BACTERIA ISOLATED FROM AN OIL-FIELD WASTEWATER TREATMENT PLANT

Chunfang Zhang[1,2], Lian-hua Xu[1], Hanghai Zhou[1], Zihang Tan[2], Qinglin Xie[2], Yongjiu Xu[3,*]

[1]Institute of Marine Biology, Ocean College, Zhejiang University, Zhoushan 316021, China
[2]College of Environmental Science and Engineering, Guilin University of Technology, Guilin 541006, China
[3]School of Fishery, Zhejiang Ocean University, Zhoushan 316022, Zhejiang, China

ABSTRACT

Four biosurfactant-producing bacteria strains with high *n*-hexadecane degradation efficiency were isolated from activated sludge in a sequential batch reactor (SBR) in Weizhou terminal oilfield wastewater treatment plant, designated SBR14, SBR27, SBR28, and SBR45. Strains SBR14 and SBR45 were identified as *Leclercia adecarboxylata*, while strains SBR27 and SBR28 were identified as *Enterobacter* sp, based on 16S rDNA sequence analysis. The strains maintained growth activity under the following conditions: *n*-hexadecane concentration of 0.05–1% (v/v), salinity of 5–100 g/L, and pH of 5.0–9.0. Under optimal conditions: salinity of 15–25 g/L, pH of 6.0–7.0, inoculation amount of 5%, and a temperature and shaking speed of 37 °C and 160 rpm, respectively, the hexadecane (0.3%, v/v) degradation rate of each strain reached 93.74%, 65.66%, 73.27%, and 87.79% respectively, after 16 days of incubation. The crude products of these four strains were extracted, and the purified products were analyzed by thin layer chromatography and Fourier transform infrared spectroscopy. The products were identified as phospholipids biosurfactant, with yields of 0.564, 0.605, 0.435, and 0.657 g/L, for strains SBR14, SBR27, SBR28, and SBR45 respectively. The growth of strains agrees with the Logistic model, exhibiting specific growth rates of 0.1375, 0.254, 0.145, and 0.066 d^{-1}, respectively. Meanwhile, hexadecane utilization followed the first order reaction kinetics model, with half value periods of 5.874, 10.046, 7.967, and 6.729 days, respectively.

KEYWORDS:
n-hexadecane, *Leclercia adecarboxylata*, *Enterobacter* sp., metabolic dynamic kinetics, phospholipid biosurfactant

INTRODUCTION

Oil spill accidents occur during oil production, transport, and smelting processes, resulting in large amounts of crude oil flowing into the water and soil, which leads to serious environmental pollution and poses a serious threat to the ecological environment and human health [1, 2]. The major components of oil are alkanes, polycyclic aromatic hydrocarbons (PAHs), and cycloalkanes. As the most common petroleum contaminants, alkanes account for more than 50% of oil pollutants [3]. In the natural environment, short-chain alkanes (<C4) are easy to volatilize, while long-chain alkanes (>C17) have characteristics of a solid state and low pollution. However, medium chain alkanes (C5–C16) are liquid, chemically stable, non-volatile, and have high hydrophobicity. Therefore, they are not easily naturally degraded, and can cause persistent environmental pollution [4, 5]. *n*-hexadecane (hereafter C16) is an important medium chain alkane in paraffin-based crude oil, which is often used as the standard material for determining diesel combustion quality [6]. Needless to say, C16 poses tremendous harm to the human body and the environment.

Microbial remediation is currently one of the most important methods of decontaminating oil pollutants in the environment, but the hydrophobicity of C16 limits the use of microorganism substrates [7, 8]. As products of microbial metabolism, biosurfactants have stable chemical properties, good emulsification activity, low-toxicity, and are environmentally friendly [9, 10]; therefore, these can improve degradation of C16 by microorganisms.

Weizhou crude oil is obtained from the western South China Sea oil field, whose main ingredients are C13-C16 *n*-alkanes. Long-chain alkane degrading bacteria discovered in China and abroad are mostly found in petroleum contaminated soils [11-13]; however, highly salt resistant *n*-hexadecane degrading bacteria isolated from oil-field wastewater treatment plants are rarely reported, despite their improved remediation ability in hypersaline environments. The total salinity of wastewater sludge in the sequential batch reactor (SBR) of Weizhou terminal wastewater treatment plant is 27.4–31.8 g/L, and the concentration of oil is 30–52 mg/L, which makes this sludge an ideal source for the isolation of C16-degrading bacteria.

In this study, four biosurfactant-producing bacteria strains with high C16 degradation ability were

isolated from hypersaline sludge. This research represents the first analysis of C16 degradation and biosurfactant-production by *Leclercia adecarboxylata*, and will provide a theoretical basis and technical support for future use of bacteria in oil pollution remediation.

MATERIALS AND METHODS

Culture medium. The enrichment medium contained (per liter): 3.0 g beef extract, 10.0 g peptone, and 15.0 g NaCl. The mineral salt medium (MSM, per liter) consisted of 0.5 g NH_4Cl, 0.5 g KH_2PO_4, 1 g K_2HPO_4, 0.5 g $MgSO_4$, 0.01 g KCl, 15.0 g NaCl, and 1% trace element solution. The alkanes medium was prepared by adding a certain volume of *n*-hexadecane to the MSM. The composition of the trace element solution (per liter) was: 0.01 g $CaCl_2$, 0.5 g $FeCl_3$, 0.38 g $CuSO_4$, 1.15 g $ZnSO_4$, and 1.69 g $MnSO_4$.

Isolation and characterization of bacterial strains. One milliliter of activated sludge was added to a test tube containing 10 mL of sterile distilled water, and the tube was vortexed for 2 min. The microbes isolated from samples were enriched by cultivation in the MSM with 0.01% (v/v) C16 as the sole carbon source at 37 ℃ in a rotary shaker at 160 rpm for 7 d. After 7 d of incubation, 1 mL of the supernatant broth was transferred into another MSM with 0.01% (v/v) C16. Enrichment cultivation was carried out under the same conditions, and the same steps were repeated five times. The concentration of C16 gradually increased from 0.01% to 0.05% during cultivation. One ml of broth of each culture of the fifth inoculation was gradient diluted and spread on enrichment medium plates. After incubation at 37 ℃ for 2 d, single colonies were separated and inoculated in an alkane medium.

Identification of bacterial strains. 16S rDNA gene analysis of strains was conducted using the selected bacterial genomic DNA as a template under standard reaction conditions with the universal primers 27F (5'–AGAGTTTGATCCTGGCTCAG–3') and 1492R (5'–GGTTACCTTGTTACGACTT–3') to distinguish the genus of species. The 20 μL amplification system consisted of 4 μL 5×Fastpfu Buffer, 250 μmol/L dNTPs, 0.8 μL of primer, 0.4 μL of FastPfu DNA polymerase, 10 ng DNA template, and double distilled water. The PCR parameters were as follows: 2 min of pre-denaturation at 94°C, 30 cycles of denaturation at 95°C for 30 s, annealing at 55°C for 30 s, extension at 72°C for 45 s, and a final extension of 10 min at 72°C. PCR products were separated by electrophoresis in 1% (w/v) agarose gels for purification. The sequence similarity comparison was conducted using the BLAST database (https://blast.ncbi.nlm.nih.gov/) of the National Center for Biotechnology Information (NCBI). After multiple sequence alignments, the phylogenetic tree was constructed using the Neighbor-Joining method (Fig. 1).

Degradation of n-hexadecane. The enrichment culture broth (OD_{600} = 0.6) was inoculated with 5% (v/v) to 30 mL MSM, which contained different concentrations of C16 (0.05%, 0.1%, 0.3%, 0.6%, 1%, v/v), by shaking (160 rpm) at 37 °C for 7 d. Growth of microbes was determined by OD_{600} and C16 concentrations at regular intervals to study the tolerance of the substrate. Similarly, the effects of salinity and pH on C16 degradation were tested using different salinities (5, 15, 25, 35, 45, 75, 100 g/L) and pH (5.0, 6.0, 7.0, 8.0, 9.0) with a C16 concentration of 0.3% (v/v).

Analytical methods. Measurement of n-hexadecane. The degradation rate of *n*-hexadecane isolates was evaluated using a GC-2010 plus gas chromatograph (Shimadzu Co., Ltd., Japan). The concentration of C16 was determined by extracting the whole fermentation bottle at a certain time, and adding a certain volume of C16 to the fermentation broth, then thoroughly shaking. The supernatant broth was collected, and the residue was extracted repeatedly. Two supernatant broths were combined and dehydrated, followed by gas chromatograph analysis. Gas chromatography parameters were as follows: the temperature of interface was 280 °C, and the carrier gas was high purity N_2 with a flow rate of 3 mL/min. The sample size and the split ratio were 1 μL and 25/1, respectively. The initial column temperature was 120 °C, retention time was 1 min, and the temperature was raised to 280 °C at a speed of 15 °C /min. The flow rate of H_2 and air were 40 mL/min and 400 mL/min, respectively. The detector temperature was 280 °C [5].

Extraction and characterization of biosurfactant. The biosurfactant was extracted as described by Zhou et al. [14] with slight modification. The fermentation broth was centrifuged (4000 rpm at 4 ℃for 30 min) to remove bacteria. The supernatant broth was adjusted to pH 2.0 by adding 6 N HCl. The floccules were collected by centrifugation for 5 min at 4000 rpm after standing for 12 h at 4 ℃. Then, the faint yellow crude surfactant was obtained with a serial acid-alkaline wash. The crude product was extracted with ethyl acetate, and freeze-dried. Finally, the purified surfactant was obtained, and the eluted fractions were characterized by thin layer chromatography (TLC). A certain amount of purified surfactant was dissolved in methanol, and then spotted on a silica gel plate with a solvent system of chloroform : methanol : water (65:15:4, v/v) [15]. The chemical composition of purified biosurfactant samples was identified by Fourier transform infrared (FT-IR)

spectroscopy (Nicolet 5700).

RESULTS AND DISCUSSION

Sequence analysis of 16S Rdna. The segment lengths of DNA after PCR amplification were 1401 bp, 1380 bp, 1406 bp, and 1395 bp for strains SBR14, SBR27, SBR28, and SBR45, respectively. Fig. 1 illustrates that strains SBR14 and SBR45 were closely related to *Leclercia adecarboxylata*, and strains SBR14 and SBR45 had high sequence similarity with *Enterobacter* sp.. *Enterobacter* is a common oil-degrading bacteria. Khorasani et al. [16] found that *Enterobacter* sp. cloacae can degrade 78.9% of heavy oil under optimal conditions, and produce biosurfactant during the metabolic process. Hua et al. [17] found that the *Enterobacter cloacae* strain TU can efficiently degrade C16, and produce extracellular polysaccharides during metabolism, which facilitates the biological utilization of substrates. Pankajkumar et al. [18] discovered that an *Enterobacter* sp. strain could efficiently degrade alkanes and PAHs, and the alkane degradation rate was up to 98% within 30d. Previous research on the degradation of environmental pollution by *Leclercia adecarboxylata* is very limited; currently, there are only three studies involving the degradation of petroleum pollutants [19-21]. For example, Sarma et al. [20] reported that *Leclercia adecarboxylata* PS4040 isolated from oil sludge could degrade pyrene by up to 61.5% within 20d. This study is the first to report that *Leclercia adecarboxylata* is capable of degrading C16 and producing biosurfactant.

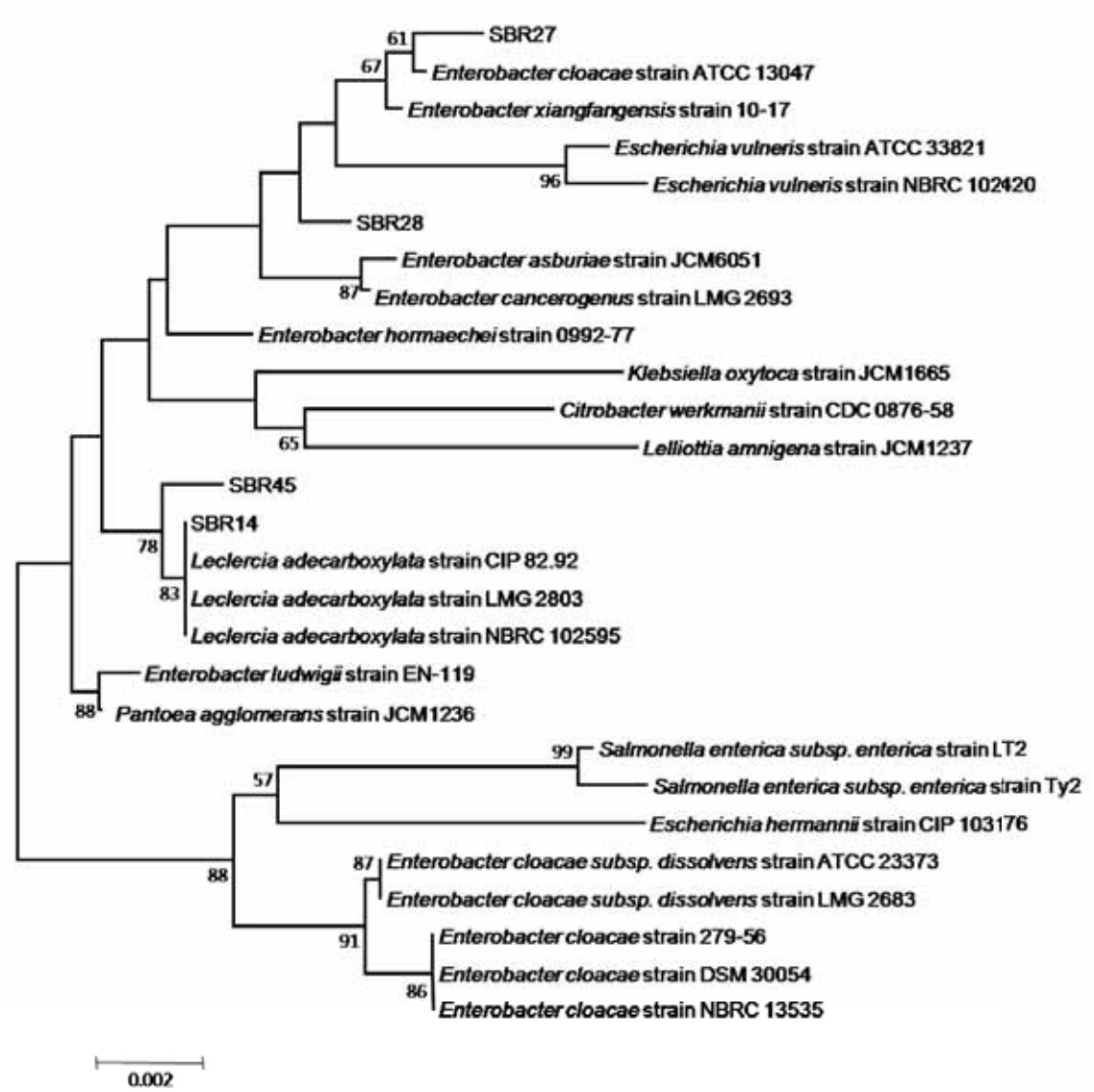

FIGURE 1
Phylogenetic tree based on the 16S rDNA gene sequence

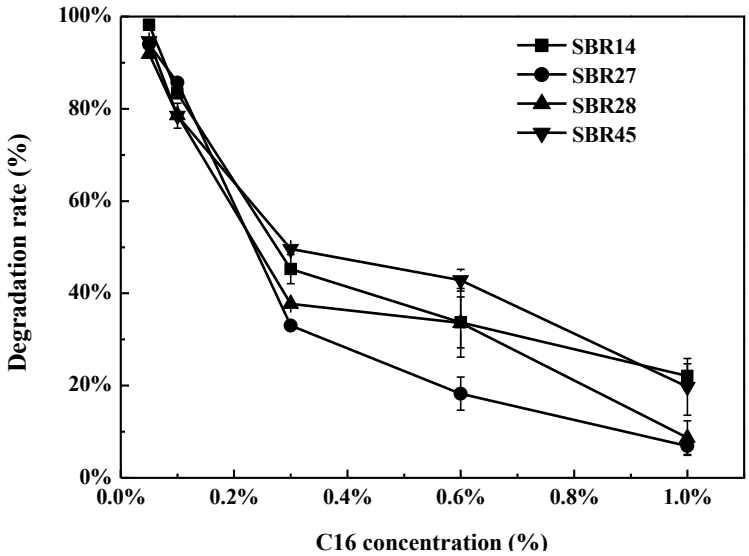

FIGURE 2
Influence of initial hexadecane concentration on degradation efficiency

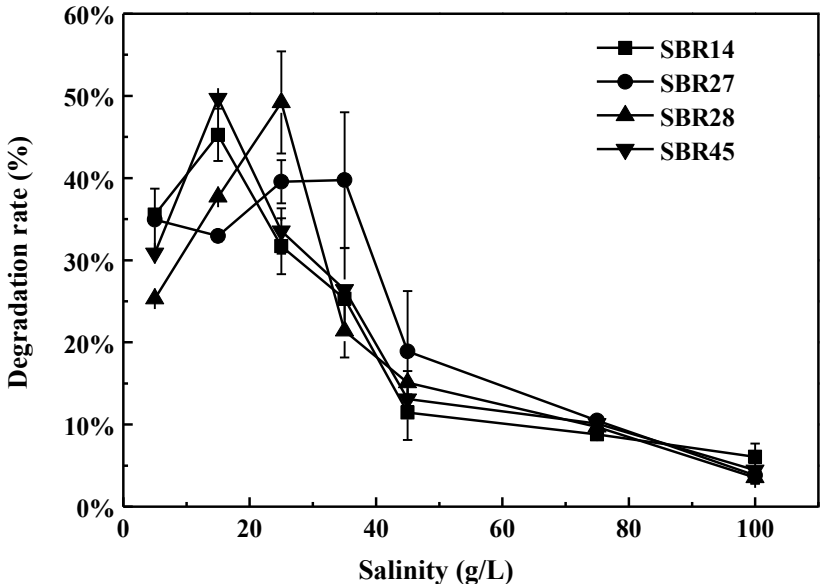

FIGURE 3
Influence of salinity on the degradation efficiency of hexadecane

C16 degradation under different conditions. Effect of initial concentration on degradation efficiency. As shown in Fig.2, the initial C16 concentration was in the range of 0.05%–1%, and all four strains showed the best performance when C16 concentration was set at 0.05%, with a degradation efficiency of over 90% within 7 d. With an increase of the initial C16 concentration, the degradation rate decreased accordingly. When the concentration increased to 0.1%, degradation efficiencies of all four strains were above 78.5%. However, as the concentration increased to 0.3%, the strains showed varied adaptability, and degradation efficiencies were 45.25%, 33.0%, 37.7%, and 49.65%, respectively, for strains SBR14, SBR27, SBR28, and SBR45. When the concentration reached 1%, the degradation rate of strains SBR14 and SBR45 decreased to 22.1% and 19.77%, respectively, while that of SBR27 and SBR28 was only 8.7% and 6.91%, respectively. This result is probably caused by the thick oil film covering on the liquid surface formed by a high concentration of C16, which limits the transmission of oxygen and inhibits microbial metabolic activity. In addition, *Leclercia adecarboxylata* showed better performance than *Enterobacter* sp. for C16 degradation at high initial concentrations.

Effect of salinity on degradation efficiency. As shown in Fig. 3, the strains tolerated a wide range of salinity, and maintained degradation efficiency over 20% for salinity values of 5–35 g/L. For strains SBR14 and SBR45, the degradation efficiency was positively correlated with salinity in the range of 5–15 g/L, with maximum degradation rates of 45.25%

and 49.65% within 7 d, respectively. With an increase of salinity, the degradation efficiency decreased markedly. For strain SBR28, the degradation efficiency increased with salinity within the range 5–25 g/L, with the highest degradation rate at 49.2%. Further increases in salinity caused a decrease in the degradation rate. Strain SBR27 showed a wider salinity tolerance range of 5–35 g/L, and degradation rates were between 32.95% and 39.75%. With salinity values between 35 g/L and 100 g/L, the C16 degradation rate became negatively correlated with salinity. This may be attributable to the salting-out effect in a hypersaline environment, which reduces the activities of dehydrogenase and oxidase in microorganisms. In addition, the increase of osmotic pressure may result in the dehydration of cells, which further leads to separation of the protoplasm, and affects cell metabolism. All four strains have strong salinity tolerance, and *Leclercia adecarboxylata* is superior to *Enterobacter* sp..This result is comparable to the result of Manoj et al. [22], which showed a maximum salinity tolerance of 100 g/L.

Effect of pH on degradation efficiency. As shown in Fig.4, all strains could tolerate a wide range of pH values in the range of 5.0–9.0, while strains SBR14, SBR28, and SBR45 were more adaptable to different pH environments. All strains showed better degradation efficiency at pH 6.0–7.0 than at pH 8.0–9.0. Strains SBR14 and SBR28 showed a maximum degradation rate of 52.47% and 53.97% at pH 7.0, respectively, while strains SBR27 and SBR45 reached a maximum degradation rate of 51.4% and 47% at pH 6.0, respectively. At pH 5.0, the degradation rate of SBR27 was much higher than that of the other three strains, suggesting that *Enterobacter* sp. has better acid tolerance than *Leclercia adecarboxylata*. The degradation rates of all four strains are similar to that of Ramasamy et al. [23] (54.20% on day 14).

Extraction and characterization of biosurfactants. The yield of the biosurfactant extracted from the fermentation broth of the four strains SBR14, SBR27, SBR28, and SBR45, was 0.564, 0.605, 0.435, and 0.657 g/L, respectively. TLC results showed that the spot color was light blue with R_f values of 0.52, 0.63, 0.54, and 0.33, respectively, when using phosphomolybdic acid-ethanol as the reagent for the color reaction. Thus, the surfactant produced by the four strains may contain phospholipid components. To our knowledge, only a few types of yeast and bacteria, such as *Bacillus* [24], *Pseudomonas* [25], and *K. pneumoniae* [26], can produce phospholipids; therefore, this result suggests the discovery of a new phospholipid-biosurfactant producer.

Fourier transform infrared spectra of biosurfactants extracted from the four strains are shown in Fig. 5. The peak at 3289 cm^{-1} was strong and wide with no splitting indicating a -OH bond. The absorption peaks at 2965 and 2931 cm^{-1} were caused by C-H stretching vibrations of $-CH_3$ and $-CH_2-$, showing saturated aliphatic chains in the products. The absorption peaks at 1680–1620 cm^{-1} corresponded to C=C bonds. Bimodal peaks at 1537 and 1405 cm^{-1} were formed by vibrational coupling of C=O absorption bands. A C-O stretching vibration appeared at 1320–1210 cm^{-1}. Some studies have found characteristic peaks of the phospholipid (P-O-C) at approximately 1090–1040 cm^{-1} [27, 28]. Combined with the TLC results, this suggests that the surfactant produced by the strains was a phospholipid.

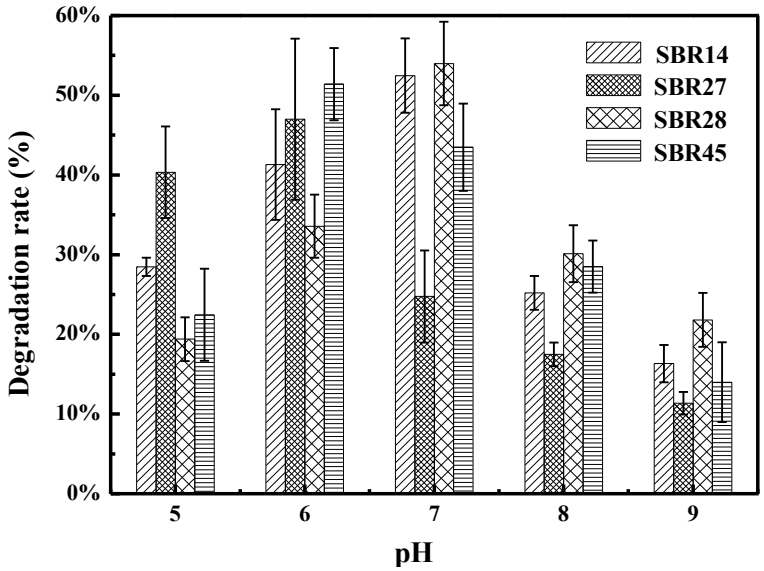

FIGUREE 4
Influence of pH on the degradation efficiency of hexadecane

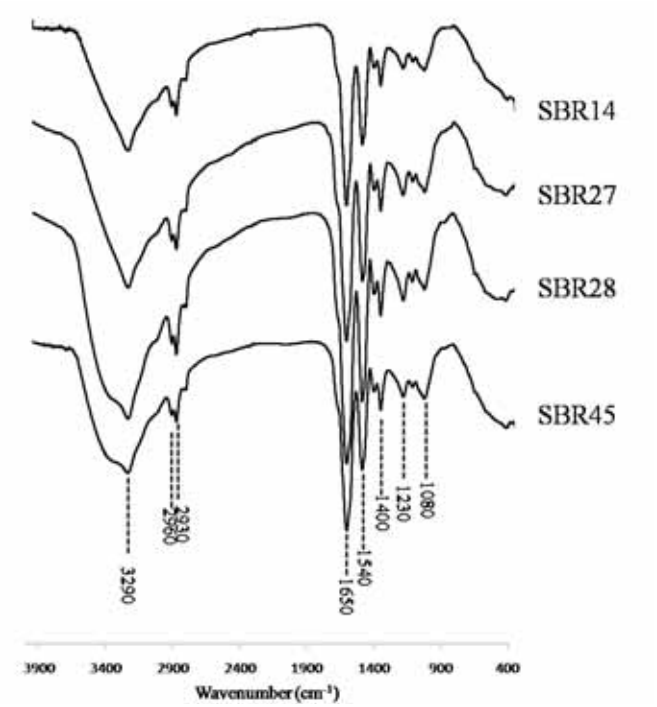

FIGURE 5
Fourier transform infrared spectra of biosurfactants extracted from the four strains

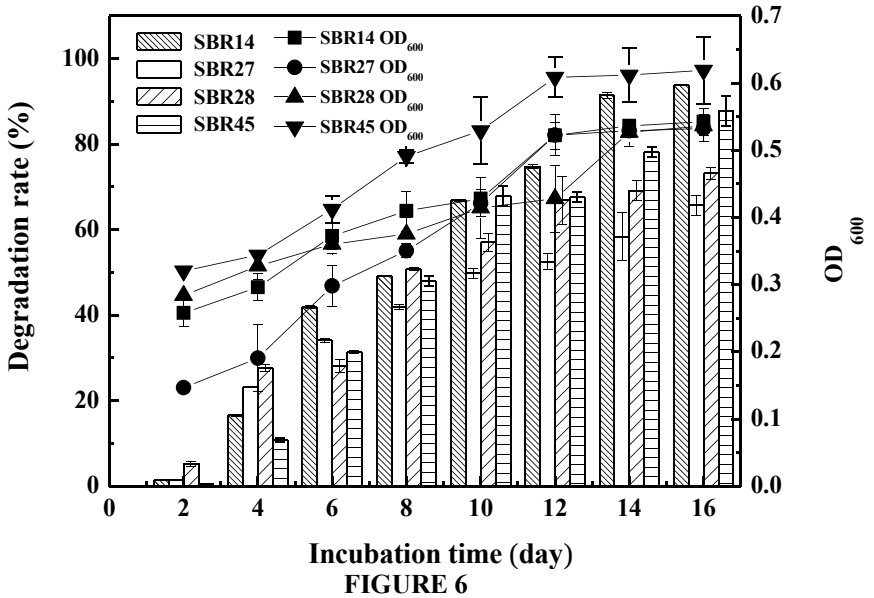

FIGURE 6
Utilization of hexadecane by bacterial strains over the 16days

Metabolic kinetics of the bacteria strains. Metabolism of the strains. The metabolic profiles of strains in MSM with *n*-hexadecane (volume concentration of 0.3%, mass concentration of 2.32 g/L) as the sole carbon source are shown in Fig. 6. The initial 0–3 d were the cell growth period, with slow cell growth and hydrophobicity limiting utilization of C16. The following 3–13 d constituted the logarithm growth period of bacteria. As the nutrient of beef extract and peptone in the enrichment medium was depleted by bacteria, C16 was utilized as a carbon source, and the bacteria started to secrete phospholipid surfactants to regulate the growth environment, increasing the contact area between cells and substrate, as well as utilization of the substrate. The OD_{600} of measured cells showed an obvious increase with time. Between day 13 and 16, the OD_{600} was the highest and most stable, and increased biomass and surfactant accumulation further promoted degradation of C16. The degradation rate of each strain increased with time, which was in accordance with the increase of OD_{600}. The C16 degradation rates of strains SBR14, SBR27, SBR28, and SBR45 were 93.74%, 65.66%, 73.27%, and 87.79%, respectively, at the end of 16 d.

TABLE 1
Equations of growth dynamics for bacterial strains

Strain	Linearfitting equation	R-squared value (R^2)	Growth dynamics equation
SBR14	y=-1.689+0.1375x	0.75006	$X_t = \frac{1.85}{1+5.414e^{-0.1375t}}$
SBR27	y=-2.248+0.254x	0.98899	$X_t = \frac{1.42}{1+9.469e^{-0.254t}}$
SBR28	y=-1.388+0.145x	0.84345	$X_t = \frac{1.4}{1+4.007e^{-0.145t}}$
SBR45	y=-1.05+0.066x	0.85246	$X_t = \frac{2.04}{1+2.858e^{-0.066t}}$

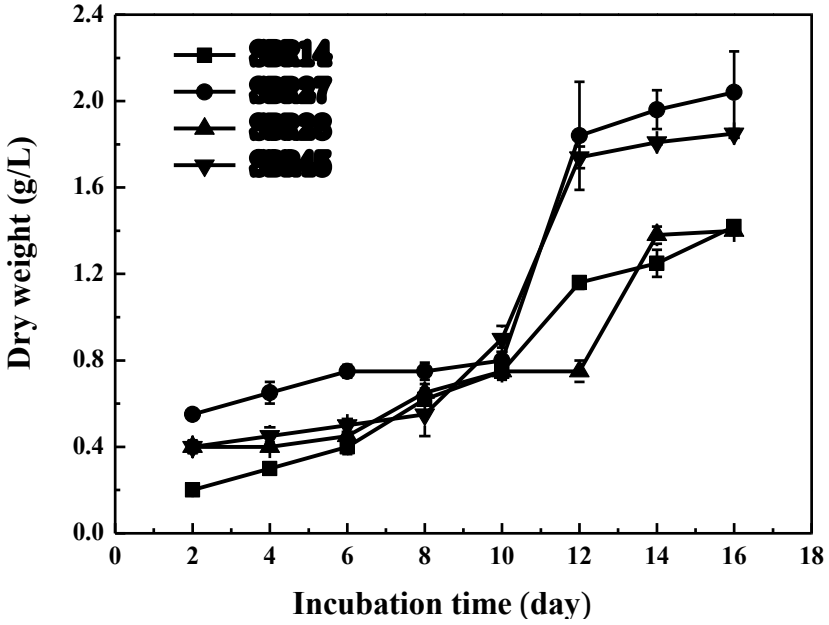

FIGURE 7
Relationship between biomass and incubation time

Growth kinetics of the strains. The dry weight of cells was determined by the constant weight method [29], and measured as X_t (Fig. 7). The logistic model is a function of biomass, initial biomass, growth rate, fermentation time, and maximum biomass, which analyzes the growth state of microorganisms grown in conditionally restricted environments, and it more accurately reflects the growth of bacteria. The equation is as follows:

$$X_t = X_0 e^{\mu_m t}\left[1-\frac{X_0\left(1-e^{\mu_m t}\right)}{X_{\max}}\right] \quad (1)$$

Where X_t is the microbial biomass at time t, g/L; X_0 is the initial biomass, g/L; μ_m is the growth rate constant, d^{-1}; and X_{max} is the maximum biomass of microorganisms, g/L.

$$In\frac{X_t}{X_{\max}-X_t} = \mu_m t - In(\frac{X_{\max}}{X_0}-1) \quad (2)$$

Equation (2) is obtained by taking the logarithm on both sides of equation (1). X_{max} and X_t can be measured during the experiment, making $In\frac{X_t}{X_{\max}-X_t}$ a straight-line equation for t, and the slope of the straight line is the rate constant of the cell growth. The biomass X_0 in the initial medium was calculated from the intercept as 0.288 g/L, 0.136 g/L, 0.279 g/L, and 0.529 g/L for strains SBR14, SBR27, SBR28, and SBR45, respectively. By substituting parameters X_{max}, X_0, and μ_m into Equation (1), the kinetic equation for cell growth during C16 degradation was determined. Compared with the growth rate constant, strain SBR27 showed the fastest growth rate, while SBR45exhibited the slowest growth. However, Fig. 6 shows that both the OD_{600} and C16 degradation rate of strain SBR45 were higher than those of SBR27 during the entire incubation process. The growth rate of strain SBR45 was the lowest, but it made full use of the substrate metabolism, so the degradation rate was relatively high. By fitting the equation R^2 values, it is clear that the model showed a good fit with the dry weight of the biomass.

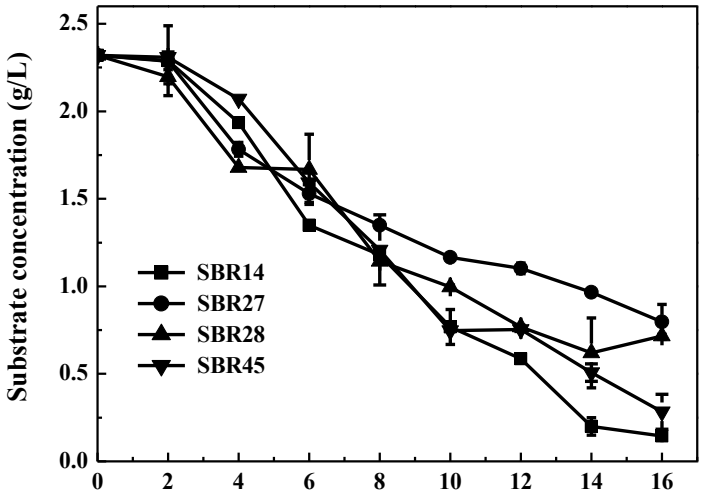

FIGURE 8
Change in hexadecane concentration over time

TABLE 2
Equations of the degradation dynamics of bacterial strains

Strain	First order reaction kinetics equation	R-squared value (R^2)	Second order reaction kinetics equation	R-squared vale (R^2)
SBR14	C_t=2.633e$^{-0.118t}$	0.91625	1/C_t-1/C_0=0.354t-1.277	0.6465
SBR27	C_t =2.403e$^{-0.069t}$	0.9732	1/C_t-1/C_0=0.049t-0.065	0.966
SBR28	C_t =2.443e$^{-0.087t}$	0.95742	1/C_t-1/C_0=0.076t-0.122	0.90316
SBR45	C_t =2.635e$^{-0.103t}$	0.91673	1/C_t-1/C_0=0.161t-0.506	0.730

Dynamic characteristics of substrate utilization. As shown in Fig. 8, the C16 degradation efficiency of the four strains was optimal within 16d.Through a regression analysis of the experimental data, C16 degradation can fit either primary or secondary reaction kinetics. The curves of $In(C_t/C_0)$-t and$(1/C_t\text{-}1/C_0)$-t were obtained according to the first order reaction kinetics equation (Equation 3) and the second order reaction kinetics equation (Equation 4), and the curve equation is shown in Table 2.

$$C_t = C_0 e^{-Kt} \quad (3)$$

$$1/C_t - 1/C_0 = Kt + A \quad (4)$$

C_t is the substrate concentration at time t, g/L; C_0 is the initial substrate concentration, g/L; K is the degradation rate constant, d^{-1}; and the half-life is $t_{1/2}$=(In2)/K,d.

As shown in Table 2, C16 degradation showed a higher fitting degree with the first-order reaction kinetic model according to the correlation coefficient R^2.The$K$ value suggests that SBR14 had the fastest degradation rate, i.e., $t_{1/2}$=5.874 d, while SBR27 was the slowest, i.e., $t_{1/2}$=10.046 d. Combined with the results of growth kinetics, it is apparent that, in a hypersaline environment (NaCl concentration of 15-25 g/L), the metabolic capacity of C16 of *Leclercia adecarboxylata,* SBR14 and SBR45, was superior to that of *Enterobacter* sp., SBR28 and SBR27. Thus, *Leclercia adecarboxylata* exhibited greater potential for bioremediation of oil pollutants in a high salinity environment.

CONCLUSIONS

(1) Four bacteria strains capable of *n*-hexadecane degradation coupled with biosurfactant production were isolated from the activated sludge of an SBR in Weizhou terminal oilfield wastewater treatment plant. Two strains were identified as *Leclercia adecarboxylata*; thus, this study is the first report on the C16 degradation capability of this strain. The other two strains were identified as *Enterobacter* sp.. The biosurfactant produced by the four strains was identified as a phospholipid.

(2) The strains utilized *n*-hexadecane under the following conditions: C16 concentration of 0.05–1% (v/v), salinity of 5–100 g/L, and a pH of 5.0–9.0, showing strong environmental adaptability. Under the optimum conditions: temperature of 37 °C, salinity of 15–25 g/L, pH 6.0–7.0, inoculation rate of 5% (v/v), and shaking speed of 160 rpm, the degradation rate of C16 (0.3%, v/v) for SBR14, SBR27, SBR28, and SBR45 was 93.74%, 65.66%, 73.27%, and 87.79%, respectively, after incubation for 16 days.

(3) The C16 degradation rate of *Leclercia adecarboxylata* was higher than that of *Enterobacter* sp.,

whereas the growth rate showed the opposite trend. Both genus of C16-degrading bacteria showed good potential for the remediation of oil pollutants, especially long-chain alkanes.

ACKNOWLEDGEMENTS

This study was supported by the National Natural Science Foundation of China (No.31400096), by the China Association of Marine Affairs (No. 2016AB033), and by the Open Foundation from Fishery Sciences in the First-Class Subjects of Zhejiang (No. 20160006).

The authors declare that there is no conflict of interest.

REFERENCES

[1] Ulrich, A.C., Guigard, S.E., Foght, J.M., Semple, K.M., Pooley, K., Armstrong, J.E., Biggar, K.W. (2009) Effect of salt on aerobic biodegradation of petroleum hydrocarbons in contaminated groundwater. Biodegradation. 20(1), 27-38.

[2] Hassanshahian, M. (2013) Hexadecane- degradation by *Teskumurella* and *Stenotro- phomonas* strains isolated from hydrocarbon contaminated soils. Jundishapur Journal of Microbiology. 6(7), 573-579.

[3] Xia, W., Du, Z., Cui, Q., Dong, H., Wang, F., He, P., Tang, Y. (2014) Biosurfactant produced by novel *Pseudomonas* sp. WJ6 with biodegradation of n-alkanes and polycyclic aromatic hydrocarbons. Journal of Hazardous Materials. 276(5), 489-498.

[4] Bouchez-Naïtali, M., Vandecasteele, J.P. (2008) Biosurfactants, an help in the biodegradation of hexadecane? The case of *Rhodococcus* and *Pseudomonas* strains. World Journal of Microbiology and Biotechnology. 24(9), 1901-1907.

[5] Shiri, Z., Kermanshahi, R.K., Soudi, M.R., Farajzadeh, D. (2015) Isolation and characterization of an *n*-hexadecane degrading *Acinetobacter baumannii* KSS1060 from a petrochemical wastewater treatment plant. International Journal of Environmental Science and Technology. 12(2), 455-464.

[6] Tao, L., Wang, F.H., Guo, L.P., Li, X.L., Yang, X.J., Ai, J.L. (2012) Biodegradation of *n*-hexadecane by bacterial strains B1 and B2 isolated from petroleum-contaminated soil. Science China Chemistry. 55(9), 1968-1975.

[7] Shavandi, M., Mohebali, G., Haddadi, A., Shakarami, H., Nuhi, A. (2011) Emulsification potential of a newly isolated biosurfactant- producing bacterium, *Rhodococcus* sp. strain TA6. Colloids and Surfaces B Biointerfaces. 82(2), 477-482.

[8] Nie, H., Nie, M., Xiao, T., Yan, W., Tian, X. (2016) Hexadecane degradation of *Pseudo- monas aeruginosa* NY3 promoted by glutaric acid. Science of the Total Environment. 575, 1423–1428.

[9] Rodrigues, L., Teixeira, J., Oliveira, R., Mei, H. C.V.D. (2006) Response surface optimization of the medium components for the production of biosurfactants by probiotic bacteria. Process Biochemistry. 41(1), 1-10.

[10] Gargouri, B., Contreras, M.d.M., Ammar, S., Segura-Carretero, A., Bouaziz, M. (2017) Biosurfactant production by the crude oil degrading *Stenotrophomonas* sp. B-2: chemical characterization, biological activities and environmental applications. Environmental Science and Pollution Research. 24(4), 3769-3779.

[11] Acer, Ö., Güven, K., Bekler, F.M., Gülgüven, R. (2016) Isolation and characterization of long-chain alkane–degrading sp. BT1A from oil-contaminated soil in Diyarbakır, in the Southeast of Turkey. Bioremediation Journal. 20(1), 80-87.

[12] Jing, S., Tang, Y. (2017) A Study on The Degradation Characteristics of a Strain of Degrading Medium-long Chain Alkane. Journal of China West Normal University. 38, 141–145

[13] Lu, M., Zhang, Z., Wei, X., Sun, S. (2011) Isolation and characterization of long-chain n-Alkane-degrading *Bacillus coagulans* from contaminated soil. Petroleum Science and Technology. 29(18), 1895-1905.

[14] Zhou, H., Chen, J., Yang, Z., Qin, B., Li, Y., Kong, X. (2015) Biosurfactant production and characterization of *Bacillus* sp. ZG0427 isolated from oil-contaminated soil. Annals of Microbiology. 65(4), 2255-2264.

[15] Dynska-Kukulska, K., Ciesielski, W., Zakrzewski, R. (2013) The use of a new, modified Dittmer-Lester spray reagent for phospholipid determination by the TLC image analysis technique. Biomedical Chromatography. 27(4), 458-465.

[16] Khorasani, A.C., Mashreghi, M., Yaghmaei, S. (2014) Optimization of biomass and biokinetic constant in Mazut biodegradation by indigenous bacteria BBRC10061. Journal of Environ- mental Health Science and Engineering. 12(1), 98-104.

[17] Hua, X., Wu, Z., Zhang, H., Lu, D., Wang, M., Liu, Y., Liu, Z. (2010) Degradation of hexadecane by *Enterobacter cloacae* strain TU that secretes an exopolysaccharide as a bioemulsifier. Chemosphere. 80(8), 951-956.

[18] Pankajkumar, J., Vijaik, G., Hardik, P., Madan, L., Jaroli, D.P. (2010) Characterization of 2T engine oil degrading indigenous bacteria, isolated from high altitude (Mussoorie), India. World Journal of Microbiology and Bio-technology. 26(8), 1419-1426.

[19] Sarma, P.M., Bhattacharya, D., Krishnan, S., Lal, B. (2004) Degradation of polycyclic aromatic hydrocarbons by a newly discovered enteric bacterium, *Leclercia adecarboxylata*. Applied and Environmental Microbiology. 70(5), 3163-3166.
[20] Sarma, P. M., Duraja, P., Deshpande, S., Lal, B. (2010) Degradation of pyrene by an enteric bacterium, *Leclercia adecarboxylata* PS4040. Biodegradation. 21(1), 59-69.
[21] Adetitun, D., Olayemi, A., Kolawole, O. (2014) Hydrocarbon-degrading Capability of Bacteria isolated from a Maize-Planted, Kerosene- contaminated Ilorin Alfisol. Biokemistri. 26(1), 13–18.
[22] Manoj, K., Vladimir, L., Angela, D.S.M., Olafa, I. (2007) A halotolerant and thermotolerant *Bacillus* sp. degrades hydrocarbons and produces tensio-active emulsifying agent. World Journal of Microbiology and Biotechnology. 23(2), 211-220.
[23] Ramasamy, S., Arumugam, A., Chandran, P. (2017) Optimization of *Enterobacter cloacae* (KU923381) for diesel oil degradation using response surface methodology (RSM). Journal of Microbiology. 55(2), 104-111.
[24] Adamu, A., Ijah, U.J.J., Riskuwa, M L., Ismail, H.Y., Ibrahim, U.B. (2015) Study on biosurfactant production by two *Bacillus* species. International Journals of Scientific Research. 3(1), 13-20.
[25] Janek, T., Łukaszewicz, M., Krasowska, A. (2013) Identification and characterization of biosurfactants produced by the Arctic bacterium *Pseudomonas putida* BD2. Colloids and Surfaces B Biointerfaces. 110(10), 379-386.
[26] Nwaguma, I.V., Chikere, C.B., Okpokwasili, G.C. (2016) Isolation, characterization, and application of biosurfactant by *Klebsiella pneumoniae* strain IVN51 isolated from hydrocarbon-polluted soil in Ogoniland, Nigeria. Bioresources and Bioprocessing. 3(1), 40-42.
[27] Garg, P., Pardasani, D., Mazumder, A., Purohit, A., Dubey, D.K. (2011) Dispersive solid-phase extraction for in-sorbent Fourier-transform infrared detection and identification of nerve agent simulants in analysis for verification of chemical weapon convention. Analytical and Bioanalytical Chemistry. 399(2), 955-963.
[28] Kycia, A. H., Vezvaie, M., Zamlynny, V., Lipkowskia, J. (2012) Non-contact detection of chemical warfare simulant triethyl phosphate using PM-IRRAS. Analytica Chimica Acta. 737(15), 45.
[29] Javers, J., Gibbons, W., Karunanithy, C. (2012) Optimizing a nitrogen-supplemented, condensed corn soluble medium for growth of the Polyhydroxyalkanoate producer *Pseudomonas putida* KT217. International Journal of Agricultural and Biological Engineering. 5(4), 62-67.

Received: **30.04.2018**
Accepted: **04.05.2018**

CORRESPONDING AUTHOR

Yongjiu Xu
School of Fishery,
Zhejiang Ocean University,
Zhoushan 316022, Zhejiang – China

e-mail: xuyongjiu@zjou.edu.cn

© by PSP Volume 27 – No. 7/2018 pages 4952-4964 Fresenius Environmental Bulletin

SPATIAL ECONOMETRIC ANALYSIS OF LIVING-ENERGY CARBON EMISSIONS IN CHINA AND ITS DRIVING FACTORS

Dong Tao, Shuang Li*, Yanyan Tang, Qing Xia

School of Management, China University of Mining and Technology, Xuzhou 221116, China

ABSTRACT

This study examined urbanization rate, resident consumption level, energy structure and energy intensity of per capital carbon emissions of residents' living energy (CERLE) with STIRPAT model incorporating ridge regression. Then, we measured per capital CERLE of China's 30 provinces from 2007 to 2012 and analyzed its distribution by using quartile maps, and finally used Moran's I index to conduct spatial correlation diagnoses. Empirical results indicate that energy structure can lead to a decrease in per capital CERLE while urbanization rate, resident consumption level and energy intensity are opposite. The estimated elastic coefficients suggest that energy structure is the most important driving factor of per capital CERLE. Additionally, the coefficients increase after the spatial correlation factors in the regions are introduced, which indicated that it will underestimate the effect of the driving factors on per capital CERLE if the spatial factors are not taken into account.

KEYWORDS:
Carbon emissions of residents' living energy (CERLE), STIRPAT, Moran' I index, spatial dependence, China

INTRODUCTION

The Intergovernmental Panel on Climate Change (2001) has pointed out that a feasible measure to address climate change—adjusting the pattern of household consumption. Some of the OECD countries have begun to implement the relevant emissions reduction policies to ease the pressure on CERLE [1]. China is at a stage of rapid industrialization and urbanization, with a large population, and the living standards of the residents have been rising steadily. This will inevitably lead to an increase in residents' living energy consumption and the scale of the production sector, which will eventually lead to a corresponding increase in carbon emissions [2]. Fig.1 indicates that the total amount of China's CERLE is rising rapidly and CERLE will face serious difficulties owing of residents' living energy will be further improved. People are accustomed to blaming the carbon emissions for the production department, observing carbon emissions from the perspective of the physical and technical economic perspectives(PTEP) associated with production, and doing a lot of researches [3, 4, 5, 6, 7], thereby ignoring the area of CERLE. However, with the increase of China's population, residents' income level and the change of consumption pattern, the promotion effect of residents' consumption will be more and more enhanced. Therefore, the contradiction between expansion of consumption and low-carbon energy conservation will intensify.

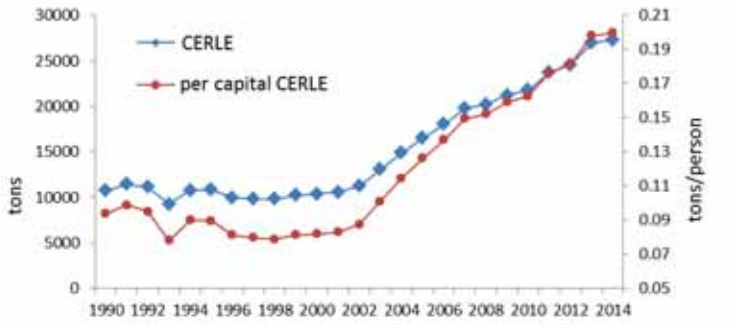

FIGURE 1
Trend of CERL

Carbon emissions reduction should be realized depending on the action taken and emissions reduction which is achieved at the provincial level. It is well known that because of its vast territory there is remarkable regional disparity among economic development and carbon emissions in China. The issue of spatial dependence cannot be ignored in making policy. The spatial effect indicates that policies of CERLE adopted in one province may cause spillover effects onto neighboring provinces, so provinces need take joint action to balance climate change mitigation and economic policy goals. The main focus of this study is the spatial dependence in regional CERLE. To identify the spatial dependence, we use provincial panel data in 2007 and 2012 to examine the spatial distribution of China's CERLE. In addition, we analyze this spatial dependence as well as the dominating factors by specifying spatial panel data models. We hope that this study can provide a scientific suggestion for policy makers to implement a regional carbon-reduction strategy of CERLE.

Many studies in China have shown that the proportion of CERLE in total carbon emissions is increasing year by year, and CERLE should not be ignored. Fan Ying et al. sort out the consumption of urban and rural residents from 1998 to 2002 and uses input-output method to calculate the carbon emissions generated by the energy consumption of residents' terminal energy [8]; Ding et al. calculated that China's energy consumption caused by household consumption was 29141.97 PJ in 2012, which accounts for 24.7% of the total energy consumption [9]; A study by Tian Xin et al. showed that Chinese residents' carbon dioxide emissions accounted for up to 35% of the total carbon dioxide emissions in 2007. At the same time, the trend of increasing household consumption carbon emissions was increasing seriously [10]; In addition, some scholars have also calculated the CERLE in various regions in other countries. Carbon emissions from consumption by French residents were already 90% of industrial carbon emissions by 2013 [11]; Common and Salma has been studying Australian household energy consumption since 1992 [12]; Shonali Pachauri has studied the changes in carbon emissions generated by the growth of electricity consumption in India [13]; Weber and Perrels calculated and compared CO_2 emissions from household consumption in France, Germany and the Netherlands [14]. Analyzing the influencing factors of carbon emissions is necessary to make polices and conduct scenario analysis for carbon emission reduction. Cellura et al. conducted SDA to analyze the relationship between indirect energy consumption, carbon emission and Italian household consumption [15]; Ala-Mantila et al. researched the relationship between urbanization, direct greenhouse gas emissions and consumption[16]; Sohag et al. measured the dynamic influence of household consumption on CO_2 emission from living energy consumption in Malaysia from 1971 to 2010 [17]; Ahmad et al. analyzed the impact of direct energy consumption on carbon emissions in Indian [18]; Lin et al. utilized STIRPAT to analyze how China's urbanization affects transportation energy consumption under different incomes [19]; Li et al. applied STIRPAT model to analyze the impact of urbanization and industrialization on energy consumption and carbon emissions [20]. Based on the STIRPAT, Fan et al. [21] and Li et al. [22] found that China's CO_2 emissions are determined by economic growth, the industrial structure, the population, and the urbanization rate and technical levels. A possible disadvantage of the above researches is that all ignore the significant spatial interaction influences. However, Anselin [23] and LeSage [24] found that a region would more or less affected by neighboring regions. It is necessary to consider the spatial effects when we study issues of carbon emissions. Based on this reason, this study tends to discuss the per capital CERLE from the spatial perspective.

The rest of this paper is organized as follows: Section 2 reviews many related literatures. Section 3 describes the methodologies used and data description. Section 4 gives empirical analyses and results. Section 5 summarize the conclusions and implications.

MATERIALS AND METHODS

Estimation of carbon emissions. CERLE are calculated through the carbon emission coefficient method provided by the IPCC [25], being that carbon emissions are the sum of the products of various types of energy consumption and their coefficients. This paper divides residents' living energy into five categories [26]: coal, oil, natural gas, heat and electricity. The corresponding formula for calculating CERLE is as Eq. (1):

$$C_l = \sum_{i=1}^{5} E_i \times f_i \quad (1)$$

Where, C_l stands for the sum of five types of CERLE; i is a natural number from 1 to 5, which represents coal, oil, natural gas, electricity and heat; E_i represents the consumption of i-th energy in residents' living energy use; f_i represents the carbon emission coefficient of i-th energy, the carbon emission coefficient of this paper has been deducted from oxygen.

STIRPAT model construction. Ehrlich and Holden established the IPAT(Impact=Population x Affluence x Technology) identity in the early 1970s [27]. The IPAT has been treated as an easily understandable, widely used framework for measuring the

driving factors of environmental pressure.

Later the IPAT was extended to STIRPAT model [28], which can statistically model non-proportionate impacts of variables on the environment. The model was described as follows:

$$\mathrm{I} = \mathrm{a} \times P^b \times A^c \times T^d \times e \quad (2)$$

Where, I denotes the environmental pressure indicator; P represents the population; A is the affluence; T is the technology; a is the model coefficient; b, c and d are coefficients of P, A and T; e denotes the random error. To analysis driving effect on growth factors of per capital CERLE, we select the urbanization rate as demographic factors; the resident consumption level as the rich degree of factors; the energy structure and energy intensity as the technical factors. By taking natural logarithm on both sides, the STIRPAT model was expanded as follows:

$$Ln\mathrm{I} = Ln\mathrm{a} + \mathrm{b}Ln\mathrm{P} + \mathrm{c}Ln\mathrm{C} + d_1 LnES + d_2 LnEI + Lne \quad (3)$$

Data sources. Based on the existing literatures on carbon emissions of living energy, as well as the availability of the data, we collected data of residents' living energy in China from 1990-2014 which are derived from *Energy Balance Sheet (standard amount)* in *China Energy Statistical Yearbook*. Data of urbanization rate, resident consumption level, energy structure and energy intensity are derived from *China Statistical Yearbook*. In order to eliminate the impact of price changes, data of resident consumption level and energy intensity are according to the calculation of the fixed value of 1990. Due to facilitate researches of indirect residents' carbon emissions and compare with CERLE, data of 2007 and 2012 are selected to be analyzed. The total amount of residents' direct energy consumption is derived from *Energy Balance Table* which is in the statistical yearbook of each province; The total population of each province comes from the *Total Population and Composition by Region of China Statistical Yearbook*. This study calculates per capital CERLE in 30 provinces. The results are shown in Table 2.

Spatial autocorrelation. The index of Moran's I is divided into Global Moran's I and Local Moran's I according to space. Global Moran's I was first proposed by Moran 1948, it analyzes the overall spatial relationship of all objects to determine whether there are discrete state, cluster state, or random state in space or not. However, it cannot distinguish the degree of spatial autocorrelation variation. In order to further analyze the degree and distribution of spatial autocorrelation, Local Moran's I is usually introduced to measure the spatial autocorrelation value of a unit area [29]. The Global Moran's I index is expressed as Eq. (4):

$$I = \frac{n\sum_{i=1}^{n}\sum_{j=1}^{n} w_{ij}(x_i-\bar{x})(x_j-\bar{x})}{(\sum_{i=1}^{n}\sum_{j=1}^{n} w_{ij})\sum_{i=1}^{n}(x_i-\bar{x})^2} \quad (4)$$

TABLE 1
Description of the variables used in the paper.

Variable	Definition	Unit	Symbol
per capital CERLE	per capital carbon emissions of residents' living energy	t/person	I
urbanization rate	proportion of urban population in the total population	%	P
resident consumption level	Money spent by residents.	yuan	C
energy structure	proportion of consumption of coal in living energy.	%	ES
energy intensity	per unit GDP of Energy consumption.	t/yuan	EI

TABLE 2
Per capital CERLE in provinces (unit: tons/person)

Number	Province	2007	2012	Number	Province	2007	2012
1	Beijing	0.41	0.44	16	Henan	0.11	0.19
2	Tianjin	0.34	0.43	17	Hubei	0.13	0.18
3	Hebei	0.16	0.25	18	Hunan	0.11	0.16
4	Shanxi	0.19	0.30	19	Guangdong	0.17	0.23
5	Neimenggu	0.29	0.65	20	Guangxi	0.07	0.13
6	Liaoning	0.30	0.35	21	Hainan	0.05	0.12
7	Jilin	0.19	0.24	22	Chongqing	0.11	0.19
8	Heilongjiang	0.21	0.39	23	Sichuan	0.04	0.17
9	Shanghai	0.29	0.31	24	Guizhou	0.18	0.25
10	Jiangsu	0.11	0.19	25	Yunnan	0.09	0.14
11	Zhejiang	0.16	0.24	26	Shanxi	0.12	0.23
12	Anhui	0.09	0.13	27	Gansu	0.14	0.20
13	Fujian	0.15	0.22	28	Qinghai	0.20	0.25
14	Jiangxi	0.08	0.11	29	Ningxia	0.18	0.22
15	Shandong	0.15	0.22	30	Xinjiang	0.19	0.34

Where, $\bar{x} = \frac{1}{n}\sum_{i=1}^{n} x_i$, n is the number of regions, x_i stands for observations of the i-th region, w_{ij} represents the spatial weight matrix. The value of w_{ij} is 1 when the region i is adjacent to the region j, the value of w_{ij} is 0 when the region i is not adjacent to the region j. The Local Moran's I index is expressed as Eq. (5):

$$I_i = \sum w_{ij} z_i z_j \quad (5)$$

Where w_{ij} represents the spatial weight matrix which accomplishes line standardization; z_i, z_j represent the value of Z after being normalized. I_i is the product of the value of the i-th area and the weighted average of its adjacent areas' value.

Space econometric model. There are two main types of spatial econometric models. The two models are corresponded with different setting modes of spatial interaction. The first one, namely the spatial lag model (SLM). It contains endogenous interaction effects among dependent variables. This model is applied to the situation where the economic activity of a region is affected by the economic activities of adjacent regions. The second one, namely the spatial error model (SEM). It contains interaction effects among the error terms. This model is applied to a situation where regional interaction effects are caused by the omitted variables that affect both the local and adjacent regions. [30-31]

The two models are specified as Eqs. (6)-(7):

SLM:

$$Y = \rho W_y + X\beta + \varepsilon \quad (6)$$

SEM:

$$\begin{cases} Y = X\beta + \mu \\ \mu = \lambda W_\mu + \varepsilon \end{cases} \quad (7)$$

Where, Y represents the dependent variable; X denotes an n×k matrix of exogenous explanatory variables; β reflects the influence of the explanatory variables on the dependent variable; W is spatial weight matrix of n×n order which usually being contiguity matrix; W_y is dependent variable of spatial lag which reflects the endogenous interaction effects among the dependent variable; μ and W_μ denote a vector of random error terms and the interaction effects among the random error terms; ε is a vector of random error terms that are normally distributed; ρ is the spatial autoregressive coefficient that reflects the spatial dependence of sample observation values; and λ is the spatial autocorrelation coefficient of the error terms. The ρ can be indicated that spatial spillover effects of the dependent variable are obvious if it is significant statistically. The λ implies that there are some factors different from the explanatory variables making contributions to the autocorrelation of the error terms if it is significant statistically.

RESULTS AND DISCUSSION

Analysis of STIRPAT. Due to per capital CERLE, urbanization rate, resident consumption level, energy structure, energy intensity and other variables all belong to time series, when the sequence is not stable, the traditional regression method is easy to obtain pseudo-regression results. Therefore, before regression, the sequence need to be tested for stationarity.

Stationarity test. Unit root tests on five sets of data were conducted one by one, the results of each variable are shown in Table 3. LnES and LnEI are stationary series while the other three variables are not. So further cointegration test is required.

Cointegration test. LnI, LnP and LnC were measured by OLS, then the unit root test of the residual series was conducted. The result is shown in Table 4. It can be concluded that there is a co-integration relationship among LnI, LnP and LnC. So the five series of STIRPAT model all pass the test and the next OLS can be conducted.

OLS regression. The OLS was used for multiple linear regression to determine whether there is multicollinearity between independent variables. It can be seen from Table 5 that R-squared of the regression equation was 0.988, F test was significant. However, VIF of the four independent variables are very big, so we can diagnose there is multicollinearity among the four variables.

TABLE 3
Each variable unit root test results.

Variable	Different order	t-value	Significance level	Critical value	Conclusion
LnI	1	-2.076	5%	-1.956	I(1)
LnP	2	-5.05	1%	-2.674	I(2)
LnC	1	-3.638	10%	-3.249	I(1)
LnES	0	-7.725	1%	-2.665	I(0)
LnEI	0	-3.755	5%	-3.622	I(0)

TABLE 4
Unit root test of residual series among LnI, LnP and LnC

Augmented Dickey-Fuller test statistic	t-Statistic	Prob.*
Test critical values	-2.903417	0.0057
1% level	-2.669359	
5% level	-1.956406	
10% level	-1.608495	

TABLE 5
Results of significance test

Variable	t-value	Sig	VIF
constant	-3.540	0.002	
LnP	-3.090	0.006	55.389
LnC	5.537	0.000	173.945
LnES	-2.324	0.031	121.385
LnEI	18.083	0.000	5.794

Note: R-squared=0.988, F=420.251, Sig=0.000

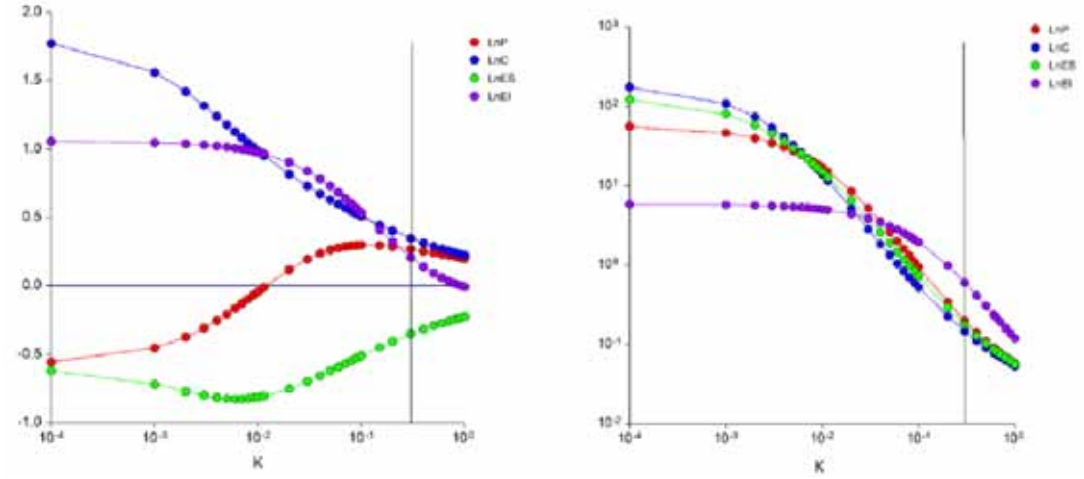

FIGURE 2
Ridge trace chart and VIF for LnI

Ridge regression. When multicollinearity occurs, its generation of large standard errors among related independent variables will happen; these errors have large variances in the regression model, and make the regression model unstable. These standard errors can be significantly eliminated by using a certain method so that the negative consequences of these errors can be effectively reduced. In order to reduce multicollinearity, this study adopted ridge regression, which can acquire acceptably biased estimates with smaller mean square errors in independent variables through bias–variance tradeoffs. In order to find the driving factors of energy-related CO_2 emissions in Guangdong, Wang et al. [32] employed ridge regression to his extended STIRPAT model.

Using NCSS to analyze ridge regression estimation based on Eq. (3), the relationship between VIF and k was shown in Fig.2. When k=0.64, standardized Betas are almost stable and VIF is low enough. Thus, k=0.64 was chosen to perform ridge regression based on our data. The results are shown in Table 6.

As indicated in Table 6, R square is 0.630 and the overall fit is basically good. T-value proved there is a significant relationship between the independent variables and the dependent variable. Additionally, the F statistic value is significant at the level of 0.01. Therefore, the fitted ridge regression equation is as Eq. (8):

$$Ln\mathrm{I} = 0.226Ln\mathrm{P} + 0.264Ln\mathrm{C} - 0.267LnES + 0.049LnEI \quad (8)$$

From a relative perspective, it is known by standard regression coefficients of individual variables that the importance of these driving factors can be described by the absolute values of their standardized coefficients in decreasing order from big to small as: energy structure, resident consumption level, urbanization rate, energy intensity. Energy structure has a biggest negative influence on per capital CERLE which indicate that the proportion of coal using in China's living energy has decreased, and the proportion of other energy sources (oil, gas, electricity, heat, etc.) has increased in the past two decades. In addition, it can be seen from the standardized coefficients of various influencing factors

that the impact of residents' consumption level and urbanization rate on per capital CERLE can be far greater than the impact of energy intensity on per capital CERLE.

Spatial difference in CERLE. GeoDa is used to map the spatial distribution of carbon emissions based on the quartile so we can analyze the differences in the spatial distribution of carbon emissions in 30 provinces of China [33, 34, 35]. Fig.3 and Fig.4 show the quartile graphs of per capital CERLE in 2007 and 2012 vividly.

It can be seen from the two graphs intuitively that the per capital CERLE is decreasing from north to south which means a large amount of per capital CERLE is mainly concentrated in the northern regions. Except Neimenggu, Jilin, Heilongjiang and other heavy industry provinces, Beijing, Tianjin and Shanghai which are economically developed municipalities also have relative higher per capital CERLE. In addition, by comparing the quartile of the two pictures, the inter-quartile ranges have increased from 0.083 tons per person to 0.128 tons per person which indicates the degree of dispersion and variation of per capital carbon emissions in 30 provinces in China between 2007 and 2012 has increased.

TABLE 6
Ridge regression results.

Ridge Regression Coefficient Section for k = 0.640				
Variable	**Coefficient**	**Standard Error**	**Standardized Coefficient**	**VIF**
LnP	0.300	0.053	0.226	0.085
LnC	0.149	0.021	0.264	0.074
LnES	-0.201	0.029	-0.267	0.082
LnEI	0.068	0.088	0.049	0.217
Constant	-3.701	0.000	0.000	0.000

Note: R-squared=0.630, F=8.513, Sig=0.000

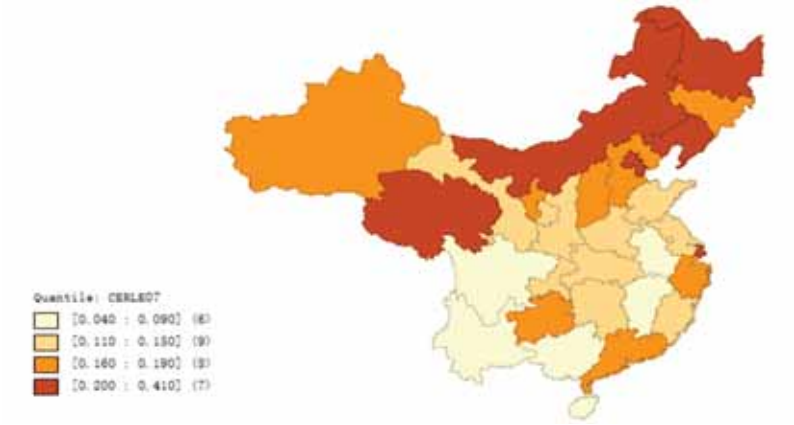

FIGURE 3
The map of distribution of per capital CERLE in 2007

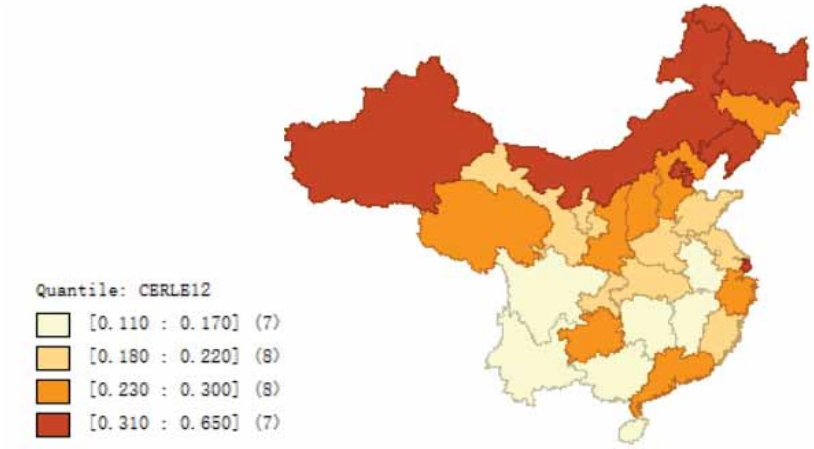

FIGURE 4
The map of distribution of per capital CERLE in 2012

TABLE 7
Results of the spatial diagnosis of CERLE

Year	Moran's I	SD	Z-value	P-value
2007	0.3523**	0.1118	3.6340	0.01
2012	0.3406**	0.1099	3.4055	0.01

Note: *, **, and *** indicate the significance level at 10%, 5%, and 1%, respectively.

In order to describe the distribution of CERLE in various regions specifically, this study analyzes the distribution change of carbon emissions detailedly according to the partition of four major economic areas (eastern, northeastern, central and western regions) in China [36].

(1) Northeastern region. The level of per capital CERLE is the highest in the northeastern region. From 2007 to 2012, the distribution of carbon emissions in the four northeastern provinces (including Heilongjiang, Jilin, Liaoning and Neimenggu) basically doesn't change significantly. Among them, Heilongjiang, Liaoning and Neimenggu have high carbon emissions while Jilin is slightly lower, but still in the middle and high level. The reason for this phenomenon is that Northeastern region is an important oilfield and coal base in China. Residents in the area are relatively more accessible to energy and have lower energy costs, especially energy has a steady development in Neimenggu in recent years. Therefore, the issue of CERLE should be pay attention to when energy resources are developped in Northeastern region.

(2) Central region. Among the six provinces of Shanxi, Henan, Hubei, Hunan, Jiangxi and Anhui, only Hunan province has ranged from the middle-low carbon emission zone to the low carbon emission zone in the five years, and the other provinces have remained unchanged. Overall, CERLE in the central region are not much, with Shanxi leading carbon emissions of this area.

(3) Eastern region. Beijing, Tianjin, Shanghai are in the high carbon emission levels; Hebei, Zhejiang, Guangdong are in the middle-high carbon emission levels; Shandong, Jiangsu, Fujian are in the middle-low carbon emission levels; only Hainan is in the low carbon emission level. The distribution of carbon emission in the eastern provinces has not changed from 2007 to 2012. Overall, there are significant differences in the level of carbon emissions of living energy in the eastern region, mainly because of the different economic development levels in the eastern provinces.

(4) Western region. Qinghai Province drops from the high level of carbon emissions in 2007 to the middle-high level of carbon emissions in 2012 while Xinjiang is the opposite. Ningxia drops from the middle-high level of carbon emissions to the middle-low level of carbon emissions while Chongqing and Shanxi from the low and middle-low level of carbon emissions to the middle-low and middle-high level of carbon emissions respectively. However, Gansu, Sichuan, Yunnan, Guizhou and Guangxi remain basically unchanged. Overall, there are also significant differences in the level of residents per capital carbon emissions in the western region, and per capital CERLE of provinces which make few carbon emissions maintains a relatively good level.

Diagnoses of correlation of CERLE. Global Moran's I index and GeoDa are selected to diagnose the spatial correlation of CERLE in the 30 provinces of China. Results of the diagnosis are shown in Table 7. The value of P is 0.01 (both less than 0.05) which indicates that there is a significant spatial dependence on Chinese per capital CERLE. The value of Moran's I is positive, which indicate that there is a positive spatial autocorrelation in Chinese per capital CERLE. That is, the adjacent provinces and cities in our country have mutual influence and similar property values.

In order to analyze the relationship between local provinces and neighboring provinces, this paper draws Fig. 5 and Fig. 6 which report the Moran's I scatter plots in 2007 and 2012. The two figures divide per capital CERLE by four quadrants into four spatial correlation patterns. The positive spatial autocorrelation exists in the provinces which are in the first and third quadrants while the negative spatial autocorrelation exists in the provinces which are in the second and fourth quadrants. Thereinto, the first quadrant represents that regions with high level of carbon emissions of per capita are surrounded by regions with high level of carbon emissions of per capita too; the second quadrant represents that regions with low level of carbon emissions of per capita are surrounded by regions with high level of carbon emissions of per capita; the third quadrant represents that regions with low level of carbon emissions of per capita are surrounded by regions with low level of carbon emissions of per capita; the fourth quadrant represents that regions with high level of carbon emissions of per capita are surrounded by regions with low level of carbon emissions of per capita [37].

As Fig.5 shows, Nengmenggu, Shanxi, Xinjiang, Heilongjiang, Jilin, Liaoning, Beijing, Tianjin and Ningxia are in the first quadrant which means these provinces is positive correlation between high per capital carbon emission and high spatial lag (H-H); Gansu, Hebei, Jiangsu are in the second quadrant which means these provinces is negative correlation

between low per capital carbon emission and high spatial lag (L-H); Shanxi, Shandong, Henan, Anhui, Sichuan, Hubei, Chongqing, Hunan, Jiangxi, Zhejiang, Fujian, Guangxi and Yunnan are in the third quadrant which means these provinces is positive correlation between low per capital carbon emission and low spatial lag (L-L); Qinghai, Shanghai and Guizhou are in the fourth quadrant which means these provinces is negative correlation between high per capital carbon emission and low spatial lag (H-L). Hainan stretches across the second and third quadrants and Guangdong stretches across the third and fourth quadrants. That is to say, most of the provinces are concentrated in the first and third quadrants, with sample size of 30% and 47% respectively, accounting for 77% of the total sample. It is indicated that positive correlations exist in per capital CERLE of China's most provinces and spatial clustering effects exist in provinces which have similar per capital carbon emissions levels.

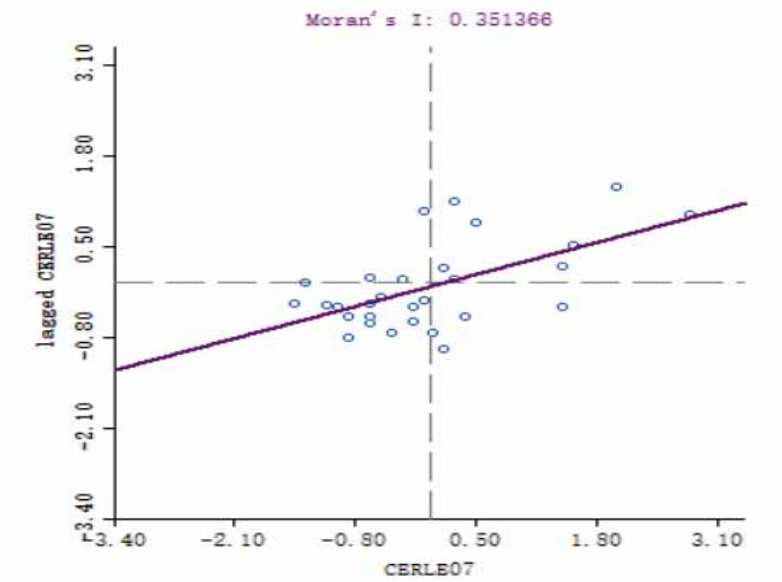

FIGURE 5

The Moran's I scatter plot of direct carbon emissions in 2007

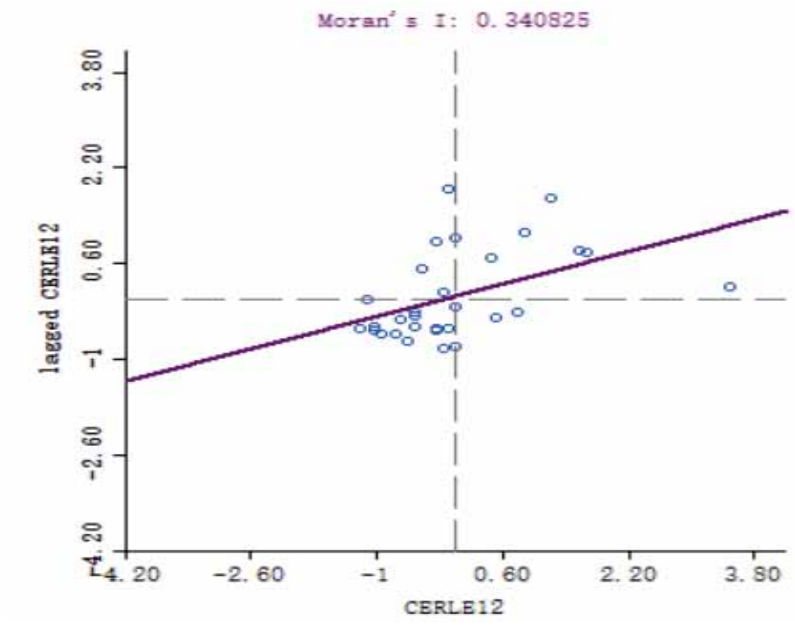

FIGURE 6

The Moran's I scatter plot of direct carbon emissions in 2012

As Fig.6 shows, Heilongjiang, Liaoning, Beijing, Tianjin, Neimenggu, Shanxi are in the first quadrant; Jilin, Shanxi, Ningxia, Gansu are in the second quadrant; Hebei stretches across the first and second quadrants; Shandong, Henan, Jiangsu, Zhejiang, Fujian, Jiangxi, Anhui, Hunan, Hubei, Chongqing, Sichuan, Yunnan, Guangxi, Guangdong are in the third quadrant; Hainan stretches across the second and third quadrants which is the same as 2007; there are Shanghai and Xinjiang in the fourth quadrant; Qinghai and Guizhou stretch across the third and fourth quadrants. Most of the provinces are concentrated in the first and third quadrants, with sample size of 23% and 47% respectively, accounting for 70% of the total sample which is 7% fewer. The results indicate that there is also a positive correlation of per capital CERLE in most provinces of China. However, there is a certain decrease in the clustering effect during the five years.

In addition, we can find that the spatial correlation between provinces and cities is generally similar except Xinjiang, Jilin, Ningxia and Jiangsu by comparing the distribution of Moran'I scatter plots in 2007 and 2012 (Table 8). Among these four provinces, Ningxia and Jilin transform the quadrants mainly because of changes in their own internal levels of carbon emissions while Xinjiang and Jiangsu have no changes in per capital carbon emissions with their H-H, L-H correlations turning into H-L, L-L correlations. In conclusion, this part proves that the spatial correlation of the 30 provinces and cities in China is significant [38].

Spatial econometric analysis of CERLE. In order to verify the spatial correlation and the degree of various factors furtherly, the spatial lag model and the spatial error model were both applied in the regression analysis. Table 9 exhibits the estimation results of influencing factors of per capital CERLE in 2007 and 2012 under different specifications. Columns 2 to 3 shows the results of the SLM model, and columns 4 to 5 shows the results of the SEM model.

TABLE 8
Categories of Moran's I in different provinces

Year	Quadrants	Number	Provinces
2007	H-H	9	Nengmenggu, Shanxi, Xinjiang, Heilongjiang, Jilin, Liaoning, Beijing, Tianjin, Ningxia
	L-H	3	Gansu, Hebei, Jiangsu
	L-L	13	Shanxi, Shandong, Henan, Anhui, Sichuan, Hubei, Chongqing, Hunan, Jiangxi, Zhejiang, Fujian, Guangxi, Yunnan
	H-L	3	Qinghai, Shanghai, Guizhou
	Others	2	Hainan with low per capital carbon emission; Guangdong with low spatial lag
2012	H-H	6	Beijing, Tianjin, Heilongjiang, Liaoning, Neimenggu, Shanxi
	L-H	4	Jilin, Shanxi, Ningxia, Gansu
	L-L	14	Shandong, Henan, Jiangsu, Zhejiang, Fujian, Jiangxi, Anhui, Hunan, Hubei, Chongqing, Sichuan, Yunnan, Guangxi, Guangdong
	H-L	2	Shanghai, Xinjiang
	Others	4	Hebei with high spatial lag; Hainan with low per capital carbon emission; Qinghai and Guizhou with low spatial lag

TABLE 9
Estimation results of influencing factors of per capital CERLE

Variables	SLM		SEM	
	2007	2012	2007	2012
LnP	0.562***(0.000)	0.818(0.207)	0.494***(0.000)	2.055***(0.000)
LnC	0.846***(0.000)	0.623(0.133)	0.793***(0.000)	-0.015(0.963)
LnES	0.141*(0.064)	0.144***(0.007)	0.119*(0.052)	0.118**(0.015)
LnEI	0.719***(0.000)	0.518***(0.000)	0.554***(0.000)	0.684***(0.000)
ρ/λ	0.043(0.683)	0.189(0.158)	0.551**(0.002)	-0.465*(0.090)
Adj-R^2	0.799	0.709	0.833	0.707
$Sigma^2$	0.056	0.048	0.047	0.049
Log-likelihood	0.538	2.801	2.078	2.137

Note: The numbers in parentheses represent p-values. *, **, and *** indicate the significance level at 10%, 5%, and 1%, respectively.

In 2007, as shown in column 2 and column 4, the coefficients of four factors were significantly positive, demonstrating that increases in factors improve per capital CERLE to a certain extent. Specifically, when other variables are constant, a 1% increase in urbanization rate will be accompanied by a 56.2% increase in per capital CERLE in the SLM model and a 49.4% increase in the SEM model; a 1% increase of resident consumption level was found to be associated with a 84.6% increase in per capital CERLE in the SLM model, and a 79.3% increase in the SEM model; line 5 and line 6 show that a 1% increase in energy structure and energy intensity will be along with a 14.1% and 71.9% increase in per capital CERLE in the SLM model and a 11.8% and 68.4% increase in the SEM model respectively when other variables are constant.

In 2012, the results showed that the P-value of LnP and LnC don't pass the significance test in the SLM model while only LnC doesn't pass the significance test in the SEM model. The fitted value of the space error model reaches 70.7%, which indicates that the spatial error model is in line with the actual situation. Among the three influencing factors which pass tests of P-value in the SEM model, the elastic coefficient of LnP is 2.055, the elastic coefficient of LnES is 0.118, and the elastic coefficient of LnEI is 0.684. These results indicated that the urbanization rate is the main influencing factor of per capital CERLE and the higher the proportion of urban population in China is, the higher per capital CERLE is; Energy intensity is also one of the factors which affect per capital CERLE in the provinces which indicates that the technological level of these technologically advanced provinces are not high enough to reduce per capital CERLE. LnP and LnEI also prove that our country is at the left end of the "inverted u-shaped" curve of the environmental Kuznets [39,40]; The energy structure also has a certain effect on per capital CERLE. It explains the provinces with high pollution energy also have high amount of per capital CERLE. All these empirical results are consistent with the literature [41] basically.

Comparing the results of Table 9 with Table 6, we can find that the degree of the influences of urbanization rate, energy structure and energy intensity on per capital CERLE have increased after the spatial correlation factors are introduced. That is to say, the increase of the urbanization rate, energy structure, energy intensity of a region can produce spillover effects and drive the development of neighboring regions. So, it will underestimate the effect of the three factors on per capital CERLE if the spatial factor is not taken into account.

CONCLUSIONS AND IMPLICATIONS

It is becoming increasingly difficult to ignore the spatial dependence in energy and environmental researches. However, past literatures hardly considered the spatial spillover effects on carbon dioxide emissions. In order to fill this gap, we firstly applied carbon emission coefficient method calculate CERLE and then examined the impact factors of per capital CERLE with STIRPAT model incorporating ridge regression, and finally analyzed the spatial situation of CERLE at the provincial level.

The Moran's I index was applied to make spatial correlation diagnosis for CERLE and the spatial econometric model was used to make a quantitative analysis of the significance of other factors after the introduction of spatial factors to CERLE. After the introduction of space elements, the urbanization rate, energy structure and energy intensity have a relative reduction in the impact of CERLE and the urbanization rate is the main influencing factor of per capital CERLE in Chinese 30 provinces and cities; The impact of residents' consumption level on CERLE is not significant, which indicates that the spatial element is one of the important factors in the study of CERLE in China. On the basis of the above conclusions, this research puts forward some feasible implications as follows:

(1) The research shows that the urbanization rate is the main factor which affect per capital CERLE in China. But in the next two decades, China is still at the stage of rapid urbanization which will bring heavy pressure on CERLE. We can't expect to reduce carbon emissions by controlling the rate of urbanization, so it is necessary to promote urbanization in low- carbon, high-quality and orderly. Cities' pattern should be designed scientifically, raising the residents' energy-saving awareness should be treated as an important goal of humanistic cultivation of urbanization and the development of urbanization should be in a new direction of intensive, green and low-carbon.

(2) According to past scholars' results, it showed that carbon emissions of fossil fuels still account for a large proportion of CERLE [42]. So, it is necessary to optimize and adjust the structure of residents' living energy, and actively promote China's low-carbon power generation industry and reduce the power supply of coal-fired power by increasing the development of clean energy.

(3) The energy intensity table proves China's industrial problem and its influence cannot be ignored under the spatial effect. The suggestions given by this study unfold in three aspects which are improving industrial process, upgrading industrial structure, optimizing industrial space layout and so on: firstly, the improvement of manufacturing pro-

cess needs to be taken seriously. In pursuit of quantity, we should pay more attention to quality; secondly, in order to upgrade the industrial structure, we need not only to speed up the upgrading of existing industrial products, but also to create a modern industrial corridor of green and low-carbon industries such as high-tech industries and services, so as to transform Chinese economy from extensive to intensive; finally, in terms of optimizing industrial space layout, the government needs to guide the scientific and efficient distribution and migration of industrial structure, and create regional industrial clusters with competitive advantages and green low carbon so that the government will have a leading role in the low-economic and high-emission provinces and cities.

ACKNOWLEDGEMENTS

This study was supported by the National Natural Science Foundation of China (Grant Nos. 71573256), and the National Key Research and Development Plan of China (Grant No. 2017YFC08 04408)

REFERENCES

[1] Zacarias-Farah, A., Geyer-Allély, E. (2003) Household consumption patterns in OECD countries: trends and figures. Journal of Cleaner Production. 11(8), 819-827.

[2] Fan, J.L., Zhang, Y.J., Wang, B. (2017) The impact of urbanization on residential energy consumption in China: an aggregated and disaggregated analysis. Renewable and Sustainable Energy Reviews. 75, 220-233.

[3] Ren, S., Yuan, B., Ma, X., Chen, X. (2014) The impact of international trade on China's industrial carbon emissions since its entry into WTO. Energy Policy. 69(3), 624-634.

[4] Sefeedpari, P., Shokoohi, Z., Behzadifar, Y. (2014) Energy use and carbon dioxide emission analysis in sugarcane farms- a survey on Haft-Tappeh sugarcane Agro- industrial company in Iran. Journal of Cleaner Production. 83(2), 212-219.

[5] Wang, K., Wei, Y.M. (2014) China's regional industrial energy efficiency and carbon emissions abatement costs. Applied Energy. 130(C), 617-631.

[6] Tian, X., Chang, M., Shi, F., Tanikawa, H. (2014) How does industrial structure change impact carbon dioxide emissions? a comparative analysis focusing on nine provincial regions in China. Environmental Science and Policy. 37(3), 243-254.

[7] Ouyang, X., Lin, B. (2015) An analysis of the driving forces of energy-related carbon dioxide emissions in China's industrial sector. Renewable and Sustainable Energy Reviews. 45, 838-849.

[8] Fan, Y., Liang, Q.M., Wei, Y.M., Okada, N. (2007) A model for China's energy requirements and CO_2, emissions analysis. Environmental Modelling and Software. 22(3), 378-393.

[9] Ding, Q., Cai, W., Wang, C., Sanwal, M. (2017) The relationships between household consumption activities and energy consumption in China— an input-output analysis from the lifestyle perspective. Applied Energy. 207, 520-532.

[10] Tian, X., Chang, M., Lin, C., Tanikawa, H. (2014) China's carbon footprint: a regional perspective on the effect of transitions in consumption and production patterns. Applied Energy. 123(1), 19-28.

[11] Erik Dietzenbacher, Bart Los, Robert Stehrer, Marcel Timmer, Gaaitzen de Vries. (2013) The construction of world input–output tables in the WIOD project. Economic Systems Research. 25(1), 71-98.

[12] Common, M.S., Salma, U. (1992) Accounting for changes in Australian carbon dioxide emissions. Energy Economics. 14(3), 217-225.

[13] Pachauri, S. (2014) Household electricity access a trivial contributor to CO_2 emissions growth in India. Nature Climate Change. 4(12), 1073-1076.

[14] Weber, C., Perrels, A. (2000) Modelling lifestyle effects on energy demand and related emissions. Energy Policy. 28(8),549-566.

[15] Cellura, M., Longo, S., Mistretta, M. (2012) Application of the structural decomposition analysis to assess the indirect energy consumption and air emission changes related to Italian households consumption. Renewable and Sustainable Energy Reviews. 16(2), 1135-1145.

[16] Ala-Mantila, S., Heinonen, J., Junnila, S. (2014) Relationship between urbanization, direct and indirect greenhouse gas emissions, and expenditures: a multivariate analysis. Ecological Economics. 104(3), 129-139.

[17] Sohag, K., Begum, R.A., Abdullah, S.M.S. (2015) Dynamic impact of household consumption on its co 2, emissions in Malaysia. Environment Development and Sustainability. 17(5), 1031-1043.

[18] Ahmad, S., Baiocchi, G., Creutzig, F. (2015) CO_2 emissions from direct energy use of urban households in India. Environmental Science and Technology. 49(19), 11312-11320.

[19] Lin, B., Du, Z. (2015) How China's urbanization impacts transport energy consumption in the face of income disparity. Renewable and Sustainable Energy Reviews. 52,1693-1701.

[20] Li, K., Lin, B. (2015) Impacts of urbanization and industrialization on energy consumption/CO_2, emissions: does the level of development matter? Renewable and Sustainable Energy Reviews. 52, 1107-1122.
[21] Fan, Y., Liu, L.C., Wu, G., Wei, Y.M. (2006) Analyzing impact factors of CO_2, emissions using the STIRPAT model. Environmental Impact Assessment Review. 26(4), 377-395.
[22] Li, H., Mu, H., Zhang, M., Li, N. (2011) Analysis on influence factors of China's CO emissions based on path–STIRPAT model. Energy Policy. 39(11), 6906-6911.
[23] Anselin, L. (1990) Spatial econometric: methods and models. Journal of the American Statistical Association. 85(411), 160.
[24] Lesage, J.P. (2010) An introduction to spatial econometrics. Revue d'économie industrielle. 123, 513–514.
[25] Lubetsky, J., Steiner, B.A., Lanza, R. (2006) 2006 IPCC Guidelines for National Greenhouse Gas Inventories.
[26] Zhu, Q., Peng, X.Z., Lu, Z.M., Juan, Yu. (2010) Calculation and analysis on carbon emissions from household energy consumption in China during 1980-2007. Journal of Safety and Environment. 02,72-76.
[27] Ehrlich, P.R., Holdren, J.P. (1991) Impact of population growth. Science. 171(3977), 1212-1217.
[28] York, R., Rosa, E.A., Dietz, T. (2003) STIRPAT, IPAT and ImPACT: analytic tools for unpacking the driving forces of environmental impacts. Ecological Economic. 46(3), 351-365.
[29] Yuan, Y., Cave, M., Zhang, C. (2018) Using local Moran's I to identify contamination hotspots of rare earth elements in urban soils of London. Applied Geochemistry. 88, 167-178.
[30] Liu, Q., Wang, S., Zhang, W., Zhan, D., Li, J. (2018) Does foreign direct investment affect environmental pollution in China's cities? a spatial econometric perspective. Science of the Total Environment. 613–614, 521-529.
[31] Long, R., Shao, T., Chen, H. (2016) Spatial econometric analysis of China's province-level industrial carbon productivity and its influencing factors. Applied Energy. 166, 210-219.
[32] Wang, P., Wu, W., Zhu, B., Wei, Y. (2013) Examining the impact factors of energy-related CO_2, emissions using the STIRPAT model in Guangdong province, China. Applied Energy. 106(11), 65-71.
[33] Jiang, J. (2016). China's urban residential carbon emission and energy efficiency policy. Energy. 109, 866-875.
[34] Mcclintock, N., Mahmoudi, D., Simpson, M., Santos, J.P. (2016) Socio-spatial differentiation in the sustainable city: a mixed-methods assessment of residential gardens in metropolitan Portland, Oregon, USA. Landscape and Urban Planning. 148,1-16.
[35] Huang, G., Ouyang, X., Yao, X. (2015) Dynamics of china's regional carbon emissions under gradient economic development mode. Ecological Indicators. 51, 197-204.
[36] Bao, H. (2010) Analysis on the Economic Differences of China's Four Major Economic Regions: Decomposition Analysis Based on Theil Index. Journal of Shijiazhuang University of Economics. 33(4),77-80.
[37] Anselin, L. (2005) Exploring spatial data with GeoDa: a workbook Spatial Analysis Laboratory, Department of Geography, University of Illinois, Urbana-Champaign.
[38] Bo, L.I. (2013) District technological innovation capacity and carbon emission per capita of China - an empirical analysis based on spatial econometric model of provincial panel data. Soft Science. 27(1), 26-30.
[39] Li, T., Wang, Y., Zhao, D. (2016) Environmental Kuznets curve in China: new evidence from dynamic panel analysis. Energy Policy. 91(2), 138-147.
[40] Wang, Y., Han, R., Kubota, J. (2016) Is there an Environmental Kuznets curve for SO2, emissions? a semi-parametric panel data analysis for China. Renewable and Sustainable Energy Reviews. 54, 1182-1188.
[41] Zhang, Y.J., Bian, X.J., Tan, W., Song, J. (2015) The indirect energy consumption and CO_2, emission caused by household consumption in china: an analysis based on the input–output method. Journal of Cleaner Production. 163, 69-83.
[42] Kunnas, J., Mclaughlin, E., Hanley, N., Greasley, D., Oxley, L., Warde, P. (2014) Counting carbon: historic emissions from fossil fuels, long-run measures of sustainable development and carbon debt. Scandinavian Economic History Review. 62(3), 243-265.

Received: **05.02.2018**
Accepted: **30.04.2018**

CORRESPONDING AUTHOR

Shuang Li
School of Management,
China University of Mining and Technology,
Xuzhou 221116 – China

e-mail: lishuang_cumt@126.com

© by PSP Volume 27 – No. 7/2018 pages 4965-4972 Fresenius Environmental Bulletin

EFFICACY OF THREE *BACILLUS* SPP. ON DEVELOPMENT OF TOBACCO WHITEFLY *BEMISIA TABACI* (GENNADIUS) (HOMOPTERA: ALEYRODIDAE)

Osama W Al Arabiat, Salah-Edden A Araj, Kholoud M Alananbeh, Tawfiq M Al-Antary*

School of Agriculture, Department of Plant Protection, University of Jordan, Amman 11942, Jordan

ABSTRACT

Tobacco whitefly (WF), *Bemisia tabaci* (Gennadius) (Hemiptera: Aleyrodiae) has been considered as an economic pest on many host plants worldwide. Three *Bacillus* spp.: *B. subtilis* (Bs), *B. amyloliquefaciens* (Ba) and *B. thuringiensis* var. *kurstaki* (Bt) has been tested againt the whitefly. Effect of bacterial strains on one whitefly generation revealed that numbers of adults and fourth nymphal instars were more in the control treatment compared to those of the three bacterial strains. Biological control of *B. tabaci* using *Bacillus* pathogens is vital and an evolving approach that needs to be investigated carefully and its ecological safety made it necessary for scientists and farmers to be interested of its importance.

KEYWORDS:
B. subtilis (Bs), *B. amyloliquefaciens* (Ba) and *B. thuringiensis* var. *kurstaki* (Bt), Tween20, Whitefly

INTRODUCTION

Cauliflower is considered one of several vegetables in the species *Brassica oleracea* in the genus *Brassica*, which is in the family *Brassicaceae.* It is an annual plant which reproduces by seeds. Only the head the cauliflower is eaten by human consumers [1,53]. Cauliflower is relatively difficult to grow compared to cabbage, with common problems such as an underdeveloped head and poor curd quality [2, 53, 54]. The plant grows best in cool daytime temperatures (21–29 °C), with plentiful sun, and moist soil conditions high in organic matter and sandy soils [3]. Pests affecting cauliflower are aphids, root maggots, cutworms, whitefly, moths, and flea beetles [2]. Tobacco whitefly (WF), *Bemisia tabaci* (Gennadius) (Homoptera: Aleyrodiae) has been considered as a major pest on more than 500 host plants worldwide [4, 53, 54], including vegetables, wild crops, ornamental plants [5, 53] and greenhouse crops [6, 53]. In Jordan, WF is a key pest of vegetables [7, 53, 54]. The crop damage could be directly by excessive sap removal, or indirectly by promoting the growth of sooty mold, inducing systemic disorders through feeding, or by transmitting viruses [8, 9, 53, 54] such as tomato yellow leaf curl virus (TYLCV) and cucumber vein yellowing virus (CVYV). These viruses are major trouble to tomato and cucurbits crops, which could cause yield reductions ranging from 50 to 100% [10, 53, 54].

The use of insecticides led to serious economic, social and environmental problems. Economically and there is high development and production costs of insecticides in addition to reduced pesticides effectiveness due to insects' resistance. As a result chemical pesticide industry continues to develop new more expensive compounds and led to increase pesticides prices. Socially and ecologically, they have caused human death and diseases and environment pollution. Target insect needs short time to be suppressed by an insecticide. However, more than 99.9% of the sprayed pesticide enters the environment through soil, water and food cycles [11, 53, 54]. Therefore, it is essential to search for other control methods to achieve integrated pest-management (IPM) programs for controlling this pest [12, 53, 54].

Alternative methods for insect control could provide acceptable levels of pest control with lower hazards. One of these alternatives is the use of bio insecticides that contain microorganisms or their biproducts. Bio insecticides have valued importance because their toxicity to animals and human is very low. Compared to insecticides, they are safe for both, farmers and consumers. Although chemical insecticides are more commonly used in the world, some bio control agents can replace them [13, 53, 54].

A number of biological control agents such as bacteria, fungi, viruses, pheromones, and plant extracts have been used for the control of insect pests that attack many agricultural crops [14, 53, 54]. The most widely used in the world are preparations of *Bacillus thuringiensis* (Bt) [15, 53]. The insecticidal activity of (Bt) is due to containing parasporal inclusions produced during sporulation. Bioinsecticides based on the proteinaceous-endotoxin of (Bt) constitute part of a more ecologically rational pest control strategy [16, 53]. Bt strains have been isolated worldwide from different habitats, including soil, insects, stored-product dust, and deciduous and coniferous leaves [17, 53, 54]. *B. thuringiensis* infects

many insects belonging to different orders including Lepidoptera, Diptera, Coleoptera, Hymenoptera, Hemiptera, Phthiraptera, Orthoptera, and Mallophaga [15, 53].

Plant growth-promoting rhizobacteria (PGPR) are defined as beneficial bacteria that live freely in the soil, rhizosphere, rhizoplane, and phylosphere [18, 53]. PGPR promotes plant growth either by affecting plant metabolism directly through supplying the plants with substances that are usually in short supply such as nitrogen, phosphorus and iron. Additionally, they enhance producing hormones and improve stresses tolerance in the plants. Moreover, a biocontrol-PGPB, promote plant growth indirectly by preventing harmful effects of some phytopathogenic bacteria, fungi, nematodes and viruses [19, 53, 54].

In the absence of major pathogens, many soil and especially rhizosphere bacteria can stimulate growth of crops by directly affecting plant metabolism and have been used in environmental applications [20, 53, 54].

The *Bacillus* species; *B. subtilis* and *B. amyloliquefaciens* are abundant in rhizospheres. They have proved to be effective in plant growth promoters that mean plant biomass increase, early reproductive maturity, and biotic and abiotic stress tolerance [17, 53]. *B. subtilis* is one of the widely soil studied bacteria for plant growth promotion [21, 53]. Its success is due to rapid surface colonization of plant through biofilm formation [22, 53] and offers many advantages to crops including increase in yield [20] and offers a role of systemic resistance against a variety of fungal and bacterial pathogens, and few phloem feeders [23, 53]. *B. amyloliquefaciens* is also one of the most persistent and abundant bacteria in rhizospheres [24, 53, 54] with anti-pathogen activities [25, 53]. It helps plant to take essential nutrients and therefore reduces the rates of fertilizer application [26, 53]. It was found to improve yield in lettuce and other vegetables [27, 53].

The beneficial effects of PGPR are believed to occur, to a certain extent, as a direct consequence of a resistance response known as 'induced systemic resistance' (ISR) [28, 29, 53]. The ISR is a plant defense state that is associated with an enhanced resistance to broad range of pathogens [30, 53]. However, the ISR produced by PGPR does not require substantial reprogramming of the transcriptome, since changes in gene expression are usually weak or undetectable [31, 53]. In contrast, ISR is characterized by the establishment of a primed state for defense in which defense-related responses are induced more rapidly upon pathogen or insect attack, thereby leading to an augmented and metabolically less costly state of resistance [30, 32, 53]

The genus *Bacillus* includes several beneficial PGPR species and related strains e.g. *B. pumilus, B. pasteurii, B. amyloliquefaciens* and *B. subtilis* which are often utilized as a bio-control agent [17, 53]. These bacteria can promote growth and provide plant protection by antibiosis and/or ISR elicitation in many crops. For example reduced insect herbivores in cucumber [33, 53, 54]; however ISR caused reduction of *P. syringae pv. tabaci* in the field and greenhouse [34, 53] and *Peronospora tabacina* [35, 53]. Another example for the ISR response was in the field and greenhouse against the cucumber mosaic virus [36, 53] and tomato mottle virus [37, 53], respectively. Recently, inoculation of *B. subtilis* to soilless tomato crops grown under greenhouse conditions provided the resistance of tomato to the whitefly *B. tabaci* [38, 53, 54]. However, it is the aim of this study to evaluate three *Bacillus* strains against the tobacco whitefly to the effective one with the other agricultural practices to decrease the pest population to less than the economic threshold.

MATERIALS AND METHODS

Bacterial Strains. Three *Bacillus* spp. were used in this study: *Bacillus amyloliquefaciens; Bacillus subtilis,* and *B. thuringiensis.* Information regarding the three *Bacillus* spp. are presented in Table (1) as previously mentioned by the same workers [53].

Enrichment of Bacterial Strains. A bacterial mass from each of the *Bacillus* strains were inoculated separately into nutrient broth (16g in one liter distilled water sterilized by autoclaving at 121 °C for 15 minutes) amended with 0.10 % Tween 20. The inoculated tubes were placed overnight on orbital shaker at 37 ºC± 2 ºC at 150 rpm.

TABLE 1
Information about bacterial strains used in this study.

Bacillus sp.	Host	Location	Year	Source
B. amyloliquefaciens	Mint	Madinah, KSA	2014	Taibah University
B. subtilis	Olive	Amman, Jordan	2016	Jordan University
B. thuringiensis subspecies *kurstaki* (*Btk*)	Formulated as powder		2013	NCARTT

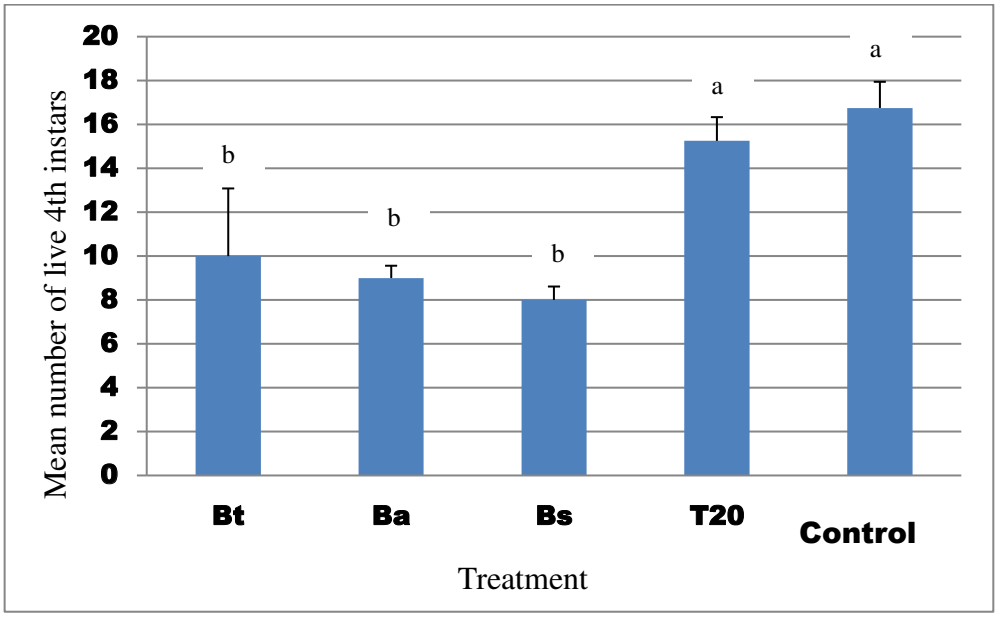

FIGURE 1

Effect of *Bacillus* strains, T20 and control on the mean number of WF 4th instars. Bacteria's suspensions (10^7–10^8 cells/ml) with a rate of 30 ml/kg soil were added to the pots at weekly intervals under green house condition. Bt: *B. thuringenesis*, Ba: *B. amyloliquifaciens*, Bs: *B. subtilis*, T20: Tween20, Control: Water.

***Bemisia tabaci* Culture.** A three weeks-old cauliflower (Solid Snow) transplants at the primary leaf stage were individually transplanted into a plastic pot (15 cm diameter) filled with (1: 1/soil: sand). Plants were kept in cages under greenhouse conditions and irrigated as needed. Whiteflies were reared under greenhouse conditions and identified according to Carver and Reid [39]. A whitefly culture was established and maintained at the greenhouses at the Department of Plant Protection, Faculty of Agriculture, and University of Jordan. WF colonies were kept in (1×1×1m) cages covered with fine mesh on all sides. A continuous supply of new cauliflower plants were provided as needed for the colony replenishment.

***B. tabaci* Development Bioassay .**The procedure used in bioassay was performed using Valenzuela-Soto [23] method. Cauliflower plants were sprayed with the following: *B. subtilis* ($1x10^8$ CFU/ml) - 24 hrs old + whitefly (WF); *B. subtilis* ($1x10^8$ CFU/ml)- 24 hrs old alone; *B. amyloliquefaciens* ($1x10^8$ CFU/ml)- 24 hrs old + whitefly (WF); *B. amyloliquefaciens* ($1x10^8$ CFU/ml)- 24 hrs old alone; *B. thuringiensis* var. *kurstaki* ($1x10^8$ CFU/ml)- 24 hrs old + whitefly (WF); *B. thuringiensis* var. *kurstaki* ($1x10^8$ CFU/ml)-24 hrs. old alone; WF alone, plants with distilled water or Tween 20 with whitefly as controls. Five plants per treatment were used. The experiments were performed using 7-days-old *B. tabaci* adults. Ten WF males and ten female adults were collected from *B. tabaci*-infested plant leaves by aspirator into glass vials and were released after being placed at the base of each pot individually covered with 10 cm diameter plastic jars. The jars were constructed to have three opening that were covered with muslin for ventilation.

The infested plants were confined inside Perspex cages (1×1×1m). After two days, *B. tabaci* adults were removed from the plants by gentle aspiration. Infested leaves were collected after 28 days in order to evaluate the development from egg to adult by counting the number of pupae and adults (or empty pupal casings left behind by the emerged adult at the end of the life cycle of *B. tabaci*) on plants.

Statistical Analysis . Data for the effect of bacterial strains on one WF generation was done using a two-way ANOVA, where treatment and WF stage were used as independent variables.

RESULTS

Effect of Bacterial Strains on One Whitefly Generation. Mean number of fourth instars. There was a significant difference in number of life-4th instars in (Ba, Bs and Bt) compared to (T20 and control) treatments ($F\ (8.45) = 8.36,\ P < 0.0001$) (Table 2). Bs, Ba and Bt had a negative effect on the 4th instars of WF (Figure 1).

Mean number of cast skins. Maximum mean number of cast skins was in control, followed by T20 treatment (Figure 2). Bt and Ba treatments had no significant difference in cast skins number, but less

than that in the control and T20 treatments. The lowest number of cast skins was in Bs treatment which was significantly less than all other treatments except with Ba treatment ($F(8.45) = 8.36$, $P < 0.0001$) (Table 2).

Mean number of adults. Maximum mean number of Adults was in control, followed by T20 treatment (Figure 3). Bt and Ba treatments have no significanct difference in adults number, but less than that in the control and T20 treatments. The lowest number of adult was in Bs treatment which was significantly less than all other treatments except Ba treatment ($F(8.45) = 8.36$, $P < 0.0001$) (Table 2).

Mean number of all stages. Control treatment had the maximum number of all WF stages (Figure 4), while Bs treatment has the lowest. There was a significance difference in number of all WF stages ($F(4.45)=89$, $P < 0.0001$) (Table 2). Bt, Ba and Bs treatments had significantly less number of all WF stages.

DISCUSSION

The current study aimed to test the effect of different *Bacillus* spp. as PGBR on cauliflower plant and on whitefly *B. tabaci* different stages mortality in vitro and under greenhouse conditions. *B. tabaci* is a globally devastating and harmful sucking insect that feeds directly as nymphs and adults on the plants, transfer many plant viruses mainly *Gemini* viruses [40, 41, 53, 54] and excrete honeydew that helps the development of sooty

TABLE 2
Effect of the *Bacillus* strains, T20 and control on the number of the different WF stages.

Treatment	Mean number of ±SE			
	Adult	Cast skin	Fourth instar	All stages
Ba	5.75±0.739cd	5.75±0.739cd	9.00±0.559b	6.8cd
Bs	2.00±0.790d	2.00±0.790d	8.00±0.612b	4.00d
Bt	9.25 ±2.814c	9.00±2.692c	10.00±3.082b	9.42c
T20	20.75±0.960b	20.50±0.829b	15.25±1.082a	18.83b
Control	32.75±1.243a	34.00±1.802a	16.75±1.192a	27.83a
LSD	2.96	2.96	2.96	2.3

*Means followed by different letters within each column are significantly different ($p < 0.05$) using LSD. Bt: *B. thuringenesis*, Ba: *B. amyloliquifaciens*, Bs: *B. subtilis*, T20: Tween20, Control: Water.

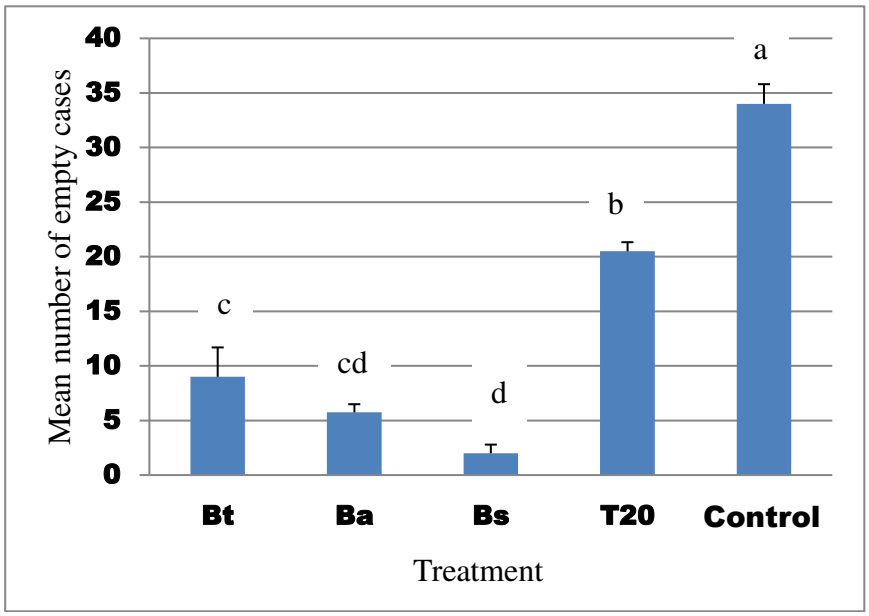

FIGURE 2
Effect of *Bacillus* strains, T20 and control on the mean number of WF cast skins. Bacteria's suspensions (10^7–10^8 cells/ml) with a rate of 30 ml/kg soil were added to the pots at weekly intervals under green house condition (20±5 ºC; 50-70 RH). Bt: *B. thuringenesis*, Ba: *B. amyloliquifaciens*, Bs: *B. subtilis*, T20: Tween20, Control: Water. Means followed by different letters within each row are significantly different ($p < 0.05$).

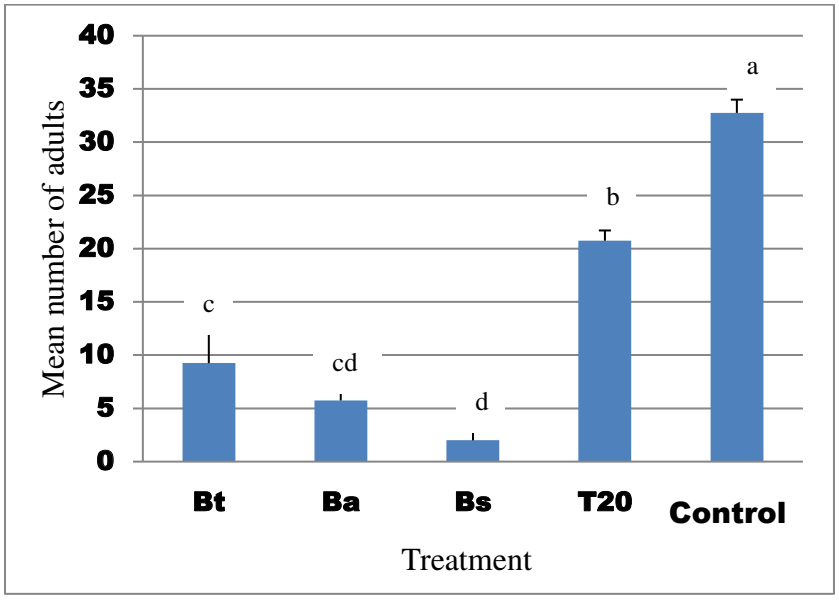

FIGURE 3

Effect of *Bacillus* strains, T20 and control on the mean number of WF adult. Bacteria's suspensions (10^7–10^8 cells/ml) with a rate of 30 ml/kg soil were added to the pots at weekly intervals under green house condition (20±5 ºC; 50-70 RH). Bt: *B. thuringenesis*, Ba: *B. amyloliquifaciens*, Bs: *B. subtilis*, T20: Tween20, Control: Water. Means followed by different letters within each row are significantly different ($p < 0.05$).

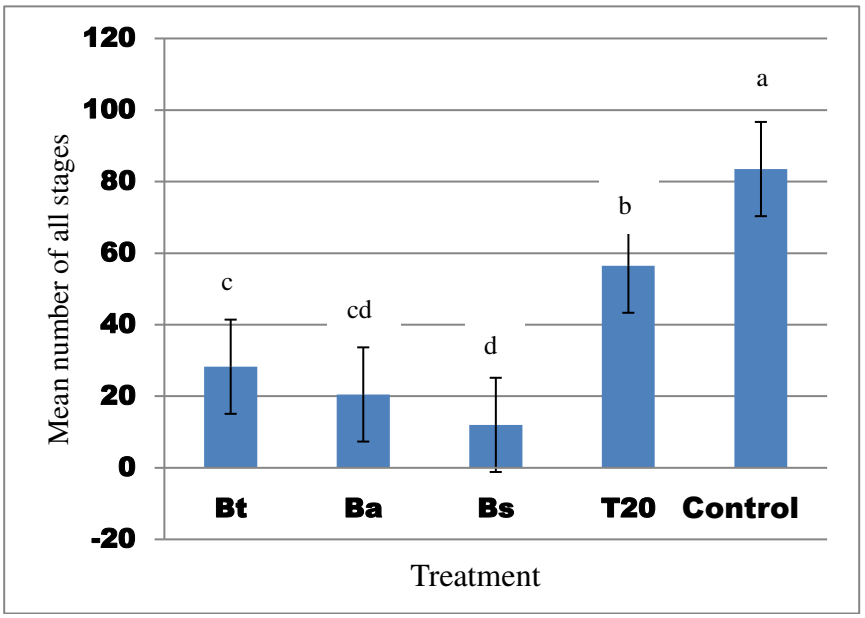

FIGURE 4

Effect of *Bacillus* strains, T20 and control on the mean number of all WF stages. Bacteria's suspensions (10^7–10^8 cells/ml) with a rate of 30 ml/kg soil were added to the pots at weekly intervals under green house condition. Bt: *B. thuringenesis*, Ba: *B. amyloliquifaciens*, Bs: *B. subtilis*, T20: Tween20, Control: Water.

mold and indirectly affect the photosynthesis [42, 53, 54]. It is difficult to control this pest conventionally due to its high reproductive rate and preference to habitat on the undersurface of leaves [43, 53, 54]. Biological control is one of the good alternative solutions to pesticides for fighting this pest, because it is environmentally friendly and effective against pathogens that are difficult to control by conventional means [44, 53, 54].

In this study, the bacterial strains were chosen because of their ability to control different plant diseases and insect pests on different plants. The plant-beneficial *Bacillus* spp. form resistant spores against many stresses such as chemicals, mechanical dam-

age, high temperature and pH [45, 53] and it can improve the plant health under adverse stress conditions [46, 53].

Results from our study indicated that the tested *Bacillus* strains-treated plants significantly increased the mortality of the different whitefly stages. Bs and Ba which promoted the plant growth had also the highest negative effect on survival of nymph and adult development of whitefly. Induced systemic resistance and growth promoting could be one explanation for this result. ISR is a latent defense that is activated only after the plant is under pathogen or pest attack [47, 53, 54]. Our outcome was in agreement with many earlier studies. For example, Hanafi [38] found that inoculation of tomato plants with a PGPR Bs strain led to a significantly lower survival of *B. tabaci's* nymphs and pupae. Valenzuela-Soto [23] found that *B. subtilis* inoculation on tomato plants retarded the development of *B. tabaci*. The results were not obvious until the 28th day of the experiment where the numbers of 4th instar nymphs, pupae, empty pupal cases, and emerged adults were reduced. That study demonstrated growth promoting and ISR establishment due to PR protein genes in response to *B. tabaci* infestation. Moreover, Murphy [37] found that certain strains *Bacillus* sp., i.e *B. amyloliquefaciens, B. subtilis*, and *B. pumilus* reduced the number of the silver whitefly WF (*Bremisia argentifolii*) significantly. Crystal inclusions could be another explanation for increasing mortality of the different stages of whitefly. In two studies conducted by Obeidat, *B. thuringenesis* isolates collected from different habitats in Jordan exhibited toxicity against larvae and adults of *Drosophila melanogaster* due to the different inclusions [48, 53] and due to the endo- and exotoxins they produce [49, 53]. Crystal proteins have been reported in *B. subtilis* [50]. On the other hand, a biosurfactant has been isolated from *B. amyloliquefaciens* and has a pesticidal effect on mosquito [51, 53] and *Spodoptera littoralis* [52, 53].

ACKNOWLEDGEMENTS

We would like to thank the Deanship of Academic Research of the University of Jordan, for their support this project. Special thanks for Faculty of Agriculture, Plant Protection Department.

REFERENCES

[1] Weise, C.H. (1841) Caii Plinii Secundi Historiae Naturalis. Edition Stereotypa: Tauchnitii, Lipsiae. 249p.

[2] Crozier, A.A. (1891) The Cauliflower. Register publishing company. Ann Arbor, Michigan, 12.

[3] Kaushal, M., Kaushal, R., Thakur, B.S. and Spehia, R.S. (2011) Effect of plant growth-promoting rhizobacteria at varying levels of N and P fertilizers on growth and yield of cauliflower in mid hills of Himachal Pradesh. Journal of Farm Sciences. 1(1), 19-26.

[4] Costa, H.S., Brown, J.K. and Byrne, D. (1991) Host plant selection by the whitefly, *Bemisia tabaci* (Gennadius), (Hom., Aleyrodidae) under greenhouse conditions. Journal of Applied Entomology. 112(105), 146-152.

[5] Gerling, D., Alomar, Ò. and Arnò, J. (2001) Biological control of *Bemisia tabaci* using predators and parasitoids. Crop Protection. 20(9), 779-799.

[6] Wagner, T.L. (1995) Temperature-dependent development, mortality, and adult size of sweet potato whitefly biotype B (Hemiptera: Aleyrodidae) on cotton. Environmental Entomology. 24(5), 1179-1188.

[7] Al Musa, A., Nazer, I. and Sharaf, N. (1987) Effect of certain combined agricultural treatments on whitefly population and incidence of tomato yellow leaf curl virus. Agricultural Sciences. 14(11), 127 – 134.

[8] Gerling, D. (1990) Whiteflies: their bionomics, pest status and management. Intercept Press. Andover, United Kingdom, 348p.

[9] Gerling, D. (1996) Bemisia: Taxonomy, Biology, Damage, Control and Management. New York. 752p.

[10] Al-Musa, A. (1982) Incidence, economic importance, and control of tomato yellow leaf curl in Jordan. Plant Disease. 66(7), 561-563.

[11] Metcalf, R. (1986) The Ecology of Insecticides and the Chemical Control of Insects. Wiley Sons, New York. 297p.

[12] Ateyyat, M.A., Shatnawi, M. and Al-Mazra'awi, M.S. (2009) Culturable whitefly associated bacteria and their potential as biological control agents. Jordan J Biol Sci. 2, 139-144.

[13] McDonald, B.A. and Linde, C. (2002) Pathogen population genetics, evolutionary potential, and durable resistance. Annual Review of Phytopathology. 40(1), 349-379.

[14] Yun, C., Yang, Y., Kim, C., Kim, S. and Kim, H. (2013) Identification of surfactin as an aphicidal metabolite produced by *Bacillus amyloliquefaciens* G1. Journal of the Korean Society for Applied Biological Chemistry. 56(6), 751-753.

[15] Federici, B.A. (1999) *Bacillus thuringiensis* in biological control. Handbook of Biological Control. Academic Press, San Diego, 575-593.

[16] Mehrabi, M. R., ZoghImofrad, L., Mazinani, M., Akbarzadeh, A. and Rahimi, A. (2015) A study of the effect of *Bacillus thuringiensis* serotype H14 (subspecies *israelensis*) delta endotoxin on *Musca* larva. Turkish Journal of Medical Sciences. 45, 794-799.

[17] Kloepper, W., Ryu, M. and Zhang, S. (2004) Induced systemic resistance and promotion of plant growth by *Bacillus* spp. Phytopathology. 94(11), 1259-1266.
[18] Bashan, Y. and De Bashan, L. (2005) Plant growth-promoting. Encyclopedia of Soils in the Environment. 1, 103-115.
[19] Bashan, Y. and Holguin, G. (1998) Proposal for the division of plant growth-promoting rhizobacteria into two classifications: biocontrol-PGPB (plant growth-promoting bacteria) and PGPB. Soil Biology and Biochemistry. 30(8), 1225-1228.
[20] Sharaf-Eldin, M., Elkholy, S., Fernández, A., Junge, H., Cheetham, R., Guardiola, J. and Weathers, P. (2008) *Bacillus subtilis* FZB24® affects flower quantity and quality of saffron (*Crocus sativus*). Planta Medica. 74(10), 1316.
[21] Lugtenberg, B. and Kamilova, F. (2009) Plant-growth-promoting rhizobacteria. Annual Review of Microbiology. 63, 541-556.
[22] Beauregard, B., Chai, Y., Vlamakis, H., Losick, R. and Kolter, R. (2013) *Bacillus subtilis* biofilm induction by plant polysaccharides. Proceedings of the National Academy of Sciences. 110(17), 1621-1630.
[23] Valenzuela-Soto, H., Estrada-Hernández, G., Ibarra-Laclette, E. and Délano-Frier, J.P. (2010) Inoculation of tomato plants (*Solanum lycopersicum*) with growth-promoting *Bacillus subtilis* retards whitefly *Bemisia tabaci* development. Planta. 231(2), 397-410.
[24] Kröber, M., Wibberg, D., Grosch, R., Eikmeyer, F., Verwaaijen, B., Chowdhury, P. and Schlüter, A. (2014) Effect of the strain *Bacillus amyloliquefaciens* FZB42 on the microbial community in the rhizosphere of lettuce under field conditions analyzed by whole metagenome sequencing. Frontiers in Microbiology. 5(252).
[25] Yu, G., Sinclair, J., Hartman, G. and Bertagnolli, B. (2002) Production of iturin A by *Bacillus amyloliquefaciens* suppressing *Rhizoctonia solani*. Soil Biology and Biochemistry. 34(7), 955-963.
[26] Adesemoye, O. and Kloepper, W. (2009) Plant–microbes interactions in enhanced fertilizer-use efficiency. Applied Microbiology and Biotechnology. 85(1), 1-12.
[27] Idriss, E., Makarewicz, O., Farouk, A., Rosner, K., Greiner, R., Bochow, H. and Borriss, R. (2002) Extracellular phytase activity of *Bacillus amyloliquefaciens* FZB45 contributes to its plant-growth-promoting effect. Microbiology. 148(7), 2097-2109.
[28] Kloepper, J.W., Tuzun, S. and Kuć, J.A. (1992) Proposed definitions related to induced disease resistance. Biocontrol Science and Technology. 2(4), 349-351.
[29] Pieterse, C.M., van Wees, S.C., van Pelt, J.A., Knoester, M., Laan, R., Gerrits, H. and van Loon, L.C. (1998) A novel signaling pathway controlling induced systemic resistance in *Arabidopsis*. The Plant Cell. 10(9), 1571-1580.
[30] Conrath, U., Pieterse, C.M. and Mauch-Mani, B. (2002) Priming in plant–pathogen interactions. Trends in plant science. 7(5), 210-216.
[31] Verhagen, B.W., Glazebrook, J., Zhu, T., Chang, H.S., van Loon, L.C. and Pieterse, C.M. (2004) The transcriptome of rhizobacteria-induced systemic resistance in *Arabidopsis*. Molecular Plant-Microbe Interactions. 17(8), 895-908.
[32] van Hulten, M., Pelser, M., van Loon, L.C., Pieterse, C.M. and Ton, J. (2006) Costs and benefits of priming for defense in *Arabidopsis*. Proceedings of the National Academy of Sciences. 103(14), 5602-5607.
[33] Zehnder, G., Kloepper, J., Tuzun, S., Yao, C., Wei, G., Chambliss, O. and Shelby, R. (1997) Insect feeding on cucumber mediated by rhizobacteria-induced plant resistance. Entomologia Experimentalis et Applicata. 83(1), 81-85.
[34] Park, K.S. and Kloepper, J.W. (2000) Activation of PR-1a promoter by rhizobacteria that induce systemic resistance in tobacco against *Pseudomonas syringae pv. tabaci.* Biological Control. 18(1), 2-9.
[35] Zhang, S., Reddy, M. and Kloepper, J.W. (2002) Development of assays for assessing induced systemic resistance by plant growth-promoting rhizobacteria against blue mold of tobacco. Biological Control. 23(1), 79-86.
[36] Zehnder, G.W., Yao, C., Murphy, J.F., Sikora, E.R. and Kloepper, J.W. (2000) Induction of resistance in tomato against *cucumber mosaic cucumovirus* by plant growth-promoting rhizobacteria. Biocontrol. 45(1), 127-137.
[37] Murphy, J.F., Zehnder, G.W., Schuster, D.J., Sikora, E.J., Polston, J.E. and Kloepper, J.W. (2000) Plant growth-promoting rhizobacterial mediated protection in tomato against Tomato mottle virus. Plant Disease. 84(7), 779-784.
[38] Hanafi, A., Traoré, M., Schnitzler, W.H. and Woitke, M. (2006) Induced resistance of tomato to whiteflies and Pythium with the pgpr *Bacillus subtilis* in a soilless crop grown under greenhouse conditions. Advances in soil and soilless cultivation under greenhouse conditions. International Society for Horticultural Science. 747, 315-323.
[39] Carver, M. and Reid, L.A. (1996) Aleyrodidae (Hemiptera: Sternorrhyncha) of Australia Systematic catalogue, host plant spectra, distribution natural enemies and biological control. CSIRO Entomology, Australia. 37, 37-55.

[40] Brown, J.K. (1991) An update on the whitefly-transmitted geminiviruses in the Americas and the Caribbean Basin. FAO Plant Protection Bulletin. 39(1), 5-23.
[41] Jones, D.R. (2003) Plant viruses transmitted by whiteflies. European Journal of Plant Pathology. 109(3), 195-219.
[42] Byrne, D.N. and Bellows, T.S. (1991) Whitefly biology. Annual Review of Entomology. 36(1), 431-457.
[43] Cahill, M., Denholm, I., Ross, G., Gorman, K. and Johnston, D. (1996) Relationship between bioassay data and the simulated field performance of insecticides against susceptible and resistant adult *Bemisia tabaci* (Homoptera: Aleyrodidae). Bulletin of Entomological Research. 86(2), 109-116.
[44] Danielsson J., Reva, O. and Meijer, J. (2008) Protection of oilseed rape (Brassica napus) toward fungal pathogens by strains of plant-associated Bacillus amyloliquefaciens. Microbial Ecolology. 54(40), 134-140.
[45] Schuster, D.J. (2004) Squash as a trap crop to protect tomato from whitefly-vectored tomato yellow leaf curl. International Journal of Pest Management. 50(4), 281-284.
[46] Zarate, S.I., Kempema, L.A. and Walling, L.L. (2007) Silverleaf whitefly induces salicylic acid defenses and suppresses effectual jasmonic acid defenses. Plant Physiology. 143(2), 866-875.
[47] Conrath, U., Beckers, G.J., Flors, V., García-Agustín, P., Jakab, G., Mauch, F., Newman, M., Pieterse, C., Poinssot, B. and Pozo, M. (2006) Priming: getting ready for battle. Molecular Plant-Microbe Interactions. 19(10), 1062-1071.
[48] Obeidat, M.M., Ahmad, F., Hamouri, N.A., Massadeh, A.M. and Athamneh, F.S. (2008) Assessment of nitrate contamination of karst springs, Bani Kanana, northern Jordan. Revista Mexicana de Ciencias Geológicas. 25(3), 426-437.
[49] Obeidat, M., Khyami-Horani, H. and Al-Momani, F. (2012) Toxicity of *Bacillus thuringiensis* β-exotoxins and δ-endotoxins to *Drosophila melanogaster*, *Ephestia kuhniella* and human erythrocytes. African Journal of Biotechnology. 11(46), 10504-10512.
[50] Rubikas, J., Androsiuniene, D., Chestukhina, G., Smirnova, T., Kapitonova, O. and Stepanov, V. (1987) Crystal protein formed by *Bacillus subtilis* cells. Journal of Bacteriology. 169(11), 5258-5262.
[51] Geetha, I., Aruna, R., and Manonmani, A. M. (2014) Mosquitocidal *Bacillus amyloliquefaciens*: Dynamics of growth and production of novel pupicidal biosurfactant. The Indian journal of medical research. 140(3), 427.
[52] Khedher, S.B., Boukedi, H., Dammak, M., Kilani-Feki, O., Sellami-Boudawara, T., Abdelkefi-Mesrati, L. and Tounsi, S. (2017) Combinatorial effect of *Bacillus amyloliquefaciens* AG1 biosurfactant and *Bacillus thuringiensis* Vip3Aa16 toxin on *Spodoptera littoralis* larvae. Journal of Invertebrate Pathology. 144, 11-17.
[53] Al Arabiat, O.W., Araj, S.A., Alananbeh, K.M. and Al-Antary, T.M. (2018) Effect of three *Bacillus* spp. on tobacco whitefly *Bemisia tabaci* (Gennadius) (Homoptera: Aleyrodidae). Fresen. Environ. Bull. 27, 3706-3712.
[54] Al-Momany, A. and Al-Antary, T.M. (2008) Pests of Garden and Home. Second edition. Publications of University of Jordan, Amman. 518p.

Received: **05.02.2018**
Accepted: **15.04.2018**

CORRESPONDING AUTHOR

Tawfiq M Al-Antary
School of Agriculture,
Department of Plant Protection,
University of Jordan,
Amman 11942 – Jordan

e-mail: tawfiqalantary@yahoo.com

© by PSP Volume 27 – No. 7/2018 pages 4973-4979 Fresenius Environmental Bulletin

TOXICOLOGICAL EFFECT OF POLYETHYLENE MICROSPHERE ON *BRACHIONUS PLICATILIS* AND *DAPHNIA MAGNA*

Ahmet Ali Berber[1,*], Meral Yurtsever[2]

[1]Canakkale Onsekiz Mart University, Vocational School of Health Services, 17100 Canakkale, Turkey
[2]Sakarya University, Engineering Faculty, Department of Environmental Engineering, 54187 Sakarya, Turkey

ABSTRACT

Pollution of the aquatic environment by microplastic could be having a massive impact on marine life. As far as the dimensions of the microplastics decrease, the negative effects are also increasing. In this study, the effects of 10-22 µm diameter fluorescent polyethylene microplastics (PEMs) on *Brachionus plicatilis* and *Daphnia magna* were investigated. The acute toxicity and population growth test were conducted on *Brachionus plicatilis*. According to the tests LC_{50} value was calculated as 0.764 mg/mL (0.4-1.458, 95% confidence limits). Statistically significant differences were found in the 90-hour population growth test compared to the control. According to genotoxic evaluation on *Daphnia magna* with single cell gel electrophoresis (Comet), tail length, tail intensity and tail moment were increased by PEMs compared to the control. In conclusion, PEMs (10-22 µm) have negative effects on both aquatic organisms *Brachionus plicatilis* and *Daphnia magna*.

KEYWORDS:
Acut toxicity, *Brachionus plicatilis*, *Daphnia magna*, microplastic, genotixicity, polyethylene

INTRODUCTION

Plastics are polymeric materials that are found in almost every aspect of our daily life because of their ease of handling and their many advantages. When the use of plastics began to become popular in the 1950's, the annual production amount was 1-1.5 million tons, but today it reached 330 million tons and it is estimated that this amount of consumption will reach about 540 million tons in 2020 [1]. Today, more than 20 different types of plastics have indirectly beneficial effects on public health as a result of their medical applications and their use. On the other hand, the toxic effects of organic compounds such as phthalates and their derivatives, bisphenol A (BPA) and di- (2-ethylhexyl) phthalate (DEHP) used in making plastics have been shown in many studies [2-7]. Unfortunately, it is a very unlikely situation to see microplastic particles starting from a few micrometers to 500 micrometers in aquatic ecosystems. Studies on this subject in previous years have shown that microplastics are found extensively throughout the world [8], even in Antarctica [9]. The 5 Gyres Institute estimates that a total of 15-51 trillion microparticles are present in the oceans, weighing between 93 and 236 tonnes [10]. Microplastics occur primarily as a result of personal care and cosmetic products, and secondly as a result of the disintegration of larger plastic wastes and they cause pollution by affecting the aquatic ecosystem [11]. Because of their size, microplastics that are thought to be food sources are ingested by many aquatic organisms as if it were part of the food chain. This ingestion has been shown on many living organisms such as Crustaceans (Copepod, Krill, Amphipoda), Molluscs (mussel, oyster) [12-15], fishes [16] and whale [17]. Digestion of the microplastics was determined in the laboratory studies on many organisms, such as algae [18], plankton [19], Cnidarians [20], Echinoderms [21, 22] and Polychaeta [23].

Microplastics, which are a common concern for potential toxic effects, have become important contaminants today. Therefore, studies on microplastics used by aquatic biota need to be increased.

MATERIALS AND METHODS

Test organisms. *Daphnia magna* was reared in ASTM (American Society for Testing and Materials) medium at 20 °C ± 1 under a constant light–dark cycle (14 h light–10 h dark). The culture medium was refreshed three times a week and they were fed three times per week with the Spirulina sp. and *Saccharomyces cerevisia*. Neonates used for toxicity tests were from the third to the fifth brood, and the sixth brood was used to start a new culture.

The acute toxicity of the microplastics on *Brachionus plicatilis* was evaluated with the use of the biotest, Rotoxkit M (MicroBioTests Inc., Belgium).

Fluorescent Polyethylene Microsphere (PEM). Polyethylene microspheres which are used

as application material in our work have been supplied by Cospheric Innovation in Microtechnology. PEMs have a density of 1.20 g/cc and diameters in the range of 10-22 µm (Cas no: 9002-88-4).

Acute toxicity and population growth. *Brachionus plicatilis* was obtained by placing rotifer cysts and incubated at 25°C in continuous light (3000-4000 lux for 24-26 h). Then, the newborn rotifers were separated into petri dish. All determinations for the acute toxicity were performed strictly according to producer protocols, compatible with ASTM E1440-91 [24].

For the population growth test, 500 rotifers were placed in 500mL beakers and observed for 5 days. The water salinity was adjusted to about 20 ppt, the temperature was 27-28 °C and the pH was around 7-8, and it was cultured under constant light. Based on LC_{50} values, the population growth studies were subjected to various concentrations of PEM such as, 0.05, 0.1, 0.2, and 0.4 µg/mL. The culture medium was renewed everyday with appropriate concentrations of PEM. The experiments were terminated after 5 days.

Comet Assay. Daphnia, less than 24 h old, is placed in 100 mL petri plates and exposed to PEMs at concentrations of 0.2, 0.1, 0.05 mg/mL for 24 hours. At the end of the period, hemolenf was obtained by homogenization of whole organism. 1 ml PBS, 20 mM EDTA and 10% DMSO solution were used as the buffer. Following homogenization, 150 µL of the sample is mixed with equal amounts of low melting agar (0.65%) and spread on the slides previously coated with agar (0.65%) and and immediately covered with a cover slip. The slides were placed on ice for 10–15 min. After solidification, the coverslip was gently removed and immersed in a cold lysing solution (2.5 M NaCl, 100 mM EDTA, 10 mM Tris pH=10, in which 10% DMSO and 1% Triton X-100 were added) at 4 ^{0}C for at least 1 h. After lysis, the slides are placed in buffer (300 mM NaOH, 1 mM EDTA, pH = 13) in the electrophoresis tank and allowed to stand for 20 min. The DNA was electrophoresed (1 V/cm, 300 mA) for 20 min, then the slides were rinsed with neutralization buffer (0.4 M Tris, pH=7.5). Each slide was stained with 50 mL of 20 µg/mL ethidium bromide. The slides were examined using a fluorescent microscope (BAB research microscope) equipped with an excitation filter of 546 nm and a barrier filter of 590 nm at 400X magnification. The tail length, tail moment and tail intensity (%) of 100 comets on each concentration were determined, using specialized Image Analysis System (BS 200 ProP; BAB Imaging System, Ankara, Turkey).

Evaluation of Results and Statistics. For the acute toxicity test, rotifers are examined under a stereomicroscope. For each concentration, 5 wells are examined separately, and live and dead rotifers are recorded. During the observation, rotifers that did not move for 5 seconds were evaluated as dead. The mortality rate for each concentration is calculated in percentage (%).

For reproductive and population growth test, 5 concentrations were calculated for each concentration and the average number of rotifers per mL. In addition, the body measurements of these individuals for development were evaluated in two different parameters, width and height under the BX51 Olympus stereo microscope.

Reproductive test results were analyzed by z-test, comet assay results by t-test, and LC_{50} values by probit analysis (IBM SPSS 22 package program) during the statistical analysis of the obtained data.

RESULTS

Acute toxicity. Concentrations of 0.5, 1, 5, 10 and 100 mg / mL were tried in preliminary studies on *Brachionus plicalitis* and at the concentrations of 5, 10 and 100 mg / mL all of them died and 9 and 14 individuals died at concentrations of 0.5 and 1 mg / mL, respectively. The data obtained with the determined concentrations are presented in Table 1 and probit analysis and regression graph are shown in Graphic 1.

TABLE 1
Acute concentration-related mortality rates with PEMs on *Brachionus plicatilis*

Test Substances	C mg/mL	NLO	NDO	M (%)
Control	-	29	1	3,3
PEMs (10-20 µm)	6,4	-	30	100
	3,2	8	22	73,3
	1,6	15	15	50
	0,8	14	16	53,3
	0,4	19	11	36,6
	0,2	23	7	23,3
	0,1	25	5	16,6
	0,05	30	0	-

C: concentrations, NLO: number of living organisms, NDO: number of dead organisms, M: mortality

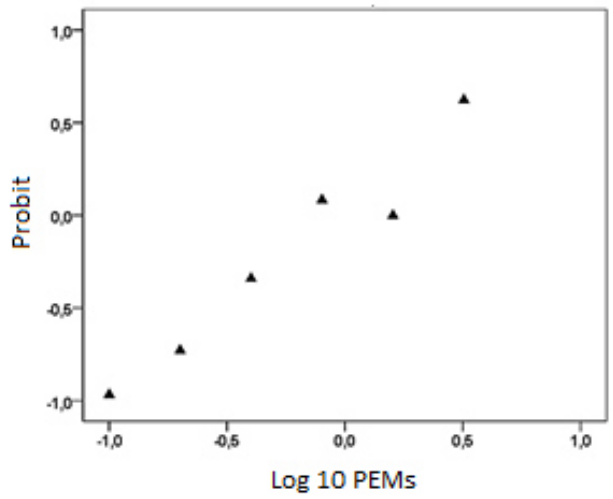

GRAPHIC 1
Probit values and regression graph for PEM in *Brachionus plicatilis*

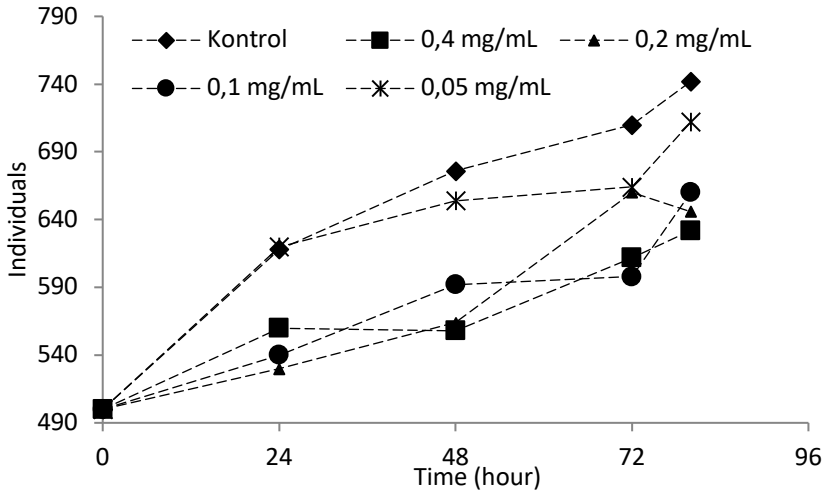

GRAPHIC 2
Changes in the intensity of reproduction according to the application dose depending on the time

TABLE 2
The effects of PEMs on the population growth of *Brachionus plicatilis* depending on time

TSs	0 h		24 h		48 h		72 h		96 h	
mg/mL	n/mL	n/500mL	n/mL	n/500mL	n/mL	n/500mL	n/mL	n/500mL	n/mL	n/500mL
Control	1	500		618		676		710		742
0,4	1	500		560*		558*		612*		632*
0,2	1	500		530*		564*		660**		646*
0,1	1	500		540*		592*		598*		660*
0,05	1	500		620		654		664**		712

* p<0,001, ** p<0,05, TS: Test substances, n: number of individuals

According to these results, probit analysis was performed to calculate the LC_{50} value and it was calculated as 0.764 mg/mL (0.4-1.458, 95% confidence limits).

Population growth. Brachionus plicatilis showed an increase in the number of starting individuals at all concentrations at the end of the 90-hour reproductive test (Graphic 2). This increase was 48% in control, 42.4% in 0.05, 32% in 0.1, 29.2% in 0,2 mg / mL and 26.4% in 0,4 mg/mL.

At the end of 24, 48, 72 and 96 h of application, all concentrations (except 0,05 mg/mL) decreased the number of individuals in the culture in a statistically significant manner compared to the control. (p<0,001) (Table 2).

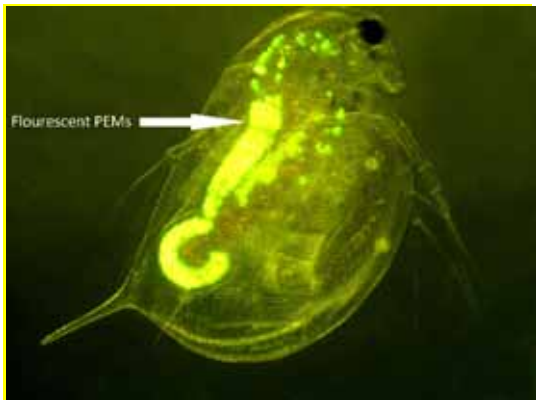

FIGURE 1
Fluorescent polyethylene microspheres taken into the body by *Daphnia magna*

The concentration of 0.05 mg / mL showed more proliferation than the control at the end of the 24 hour culture period. At the end of the following administration periods, the number of individuals in the control group was higher than the number of individuals in the application concentration of 0.05 mg/mL. This difference was found to be statistically significant only after 72 hours ($p < 0,05$). It is obvious that PEMs applied on this basis has negative effects on the reproduction of *Brachionus plicatilis*.

In the same test, 20 individuals were taken from each culture for each application concentration, and the growth rates were evaluated for each application time, both height and width. According to the results obtained no statistically significant difference was found between control and application concentrations.

Comet assay. It was determined that *Daphnia* individuals regarded miroplastics as nutrient source and ingested them when polyethylene microspheres were applied to *Daphnia magna* medium (Figure 1).

In this test, the genotoxic effect of polyethylene microspheres (10-22 μm) on *Daphnia magna* was determined by single cell gel electrophoresis. 100 cells were examined for each concentration, and the tail length, tail moment and tail density parameters were evaluated (Table 3).

According to the obtained data, tail length increased with PEM application in all concentrations compared to control. This increase was significant in all treatment concentrations except 0.05 mg/mL. When the increases in tail length were assessed according to the concentrations, it was determined that these increases were dose dependent ($r=0,82$) (Graphic 3-a).

Comet tail moment similarly increased in all concentrations compared to the negative control and 0.1 and 0.2 mg/mL, which provided these increases, were found to be statistically significant and they are dose depended ($r=0,73$) (Graphic 3-b).

In addition to the above comet parameters, it was found that all application concentrations significantly increased the tail intensity compared to the control. This increase also has a strong correlation ($r = 0.80$) (Chart 3-c).

TABLE 3
Genetic damage frequencies occurring in *Daphnia magna* with PEMs exposure

Test Substances	Period (h)	Concentrations	Tail Length	Tail Moment	Tail Intensity
Control	24	0	10,832±1,27	8,689±1,25	225,761±0,52
PEM	24	0,05	13,272±1,64	10,698±1,58	222,964±0,63[a]
		0,1	17,167±1,97[b]	14,507±1,89[b]	231,271±0,69[a]
		0,2	19,955±2,17[a]	16,903±2,12[a]	231,259±0,73[a]
		0,4	19,520±2,11[a]	15,420±1,93[a]	233,827±0,76[a]

a = $p < 0.001$, b = $p < 0.01$ (statistically different from negative control). PEM: Polyethylene microsphere

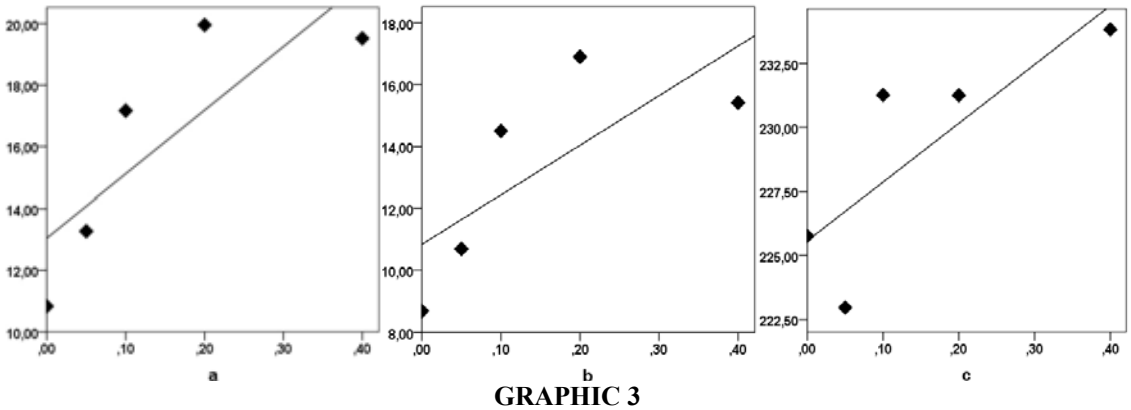

GRAPHIC 3
Dose related regression graphs (a) tail length, (b) tail mass, (c) tail density

RESULTS AND DISCUSSION

According to terrifying predictions made about plastics, about 10% of the plastics produced are entering our oceans [25, 26]. For this reason, unfortunately, it is not a surprise that plastics are the common pollutants of aquatic ecosystems. According to Enomia's [27] report, about 12.2 million tons of plastic are entering the ocean every year and 0.95 million tons of these are microplastics.

Microplastics can enter the sea in the form of polyethylene particles from materials such as shopping bags and polyester fibrils from textiles. Also, they can directly reach the aquatic ecosystem from cosmetics. Microplastics can passively float in the oceans as well as reach sediments. According to the report, microplastics which comes from marine paint (16 thousand tons), cosmetics (35 thousand tons), road paint (80 thousand tons), building paints (130 thousand tons), textiles (190 thousand tons), pellet spills (230 thousand tons), vehicle tyre dust (270 thousand tons) sink to the seabed.

The harmful effects of microplastics in the aquatic environment have recently started to be discussed and researched. In the literature, it is seen that the studies conducted in this subject have been started mostly within the last few years and the number of these studies needs to be increased.

Besseling et al. [18] evaluated reproduction and chlorophyll density of *Scenedesmus obliquus* exposed to polystyrene (~70 nm) at the concentrations of 0.22-103 mg / L for 5 days and the researchers found that there were decrease in terms of reproduction and chlorophyll density. Later, when these algae were used as nutrients in *Daphnia magna* culture, malformations in body shapes of Daphnia, decrease in body size and reproduction were detected. Au et al. [28] conducted a study on *Hyalella azteca*, an amphibian crust. In this study, polyethylene microspheres 10-27 µm in diameter to 0-100.000 particles/mL were applied and consequently, researchers found that they had an effect on growth and reproduction of *Hyalella azteca* and this effect was statistically significant. In our study, as in the studies mentioned above, when fluorescent polyethylene microplastics were given to *Brachionus plicatilis* culture media, they were perceived as nutrients and digested by these rotifers. The reproduction rate of *Brachionus plicatilis* was affected by PEMs at almost all application concentrations depending on time and in the 24-hour acute toxicity test, PEMs were found to cause mortality or immobilization.

Although the survival rates of *Tripneustes gratilla* did not show a significant decrease compared to the control in the application of polyethylene microplastics of 10-45 µm size for 5 days, there was a decrease in body mass [22]. Similarly, Ugolini et al. [29] stated that *Talitrus saltator* took PEM into the body within 24 hours, and microplastic presence was detected after 7 days in almost all individuals in their study of polyethylene microspheres 10-45 µm in diameter. They noted that the microplastics administered over a 7-day period had no effect on survival. In our study, it was also found that both *Brachionus plicatilis* and *Daphnia magna* took PEMs into the body within the first 24 hours. Unlike these studies, when we look at the data of *Brachionus plicatilis* at the end of 24 hours in our experiment, the applications of 0.1, 0.2, 0.4, 0.8 mg/mL are resulted in death or inactivity of 16.6%, 23.3%, 36.6% and 53.3%, respectively. The differences in results may be due to the microparticles we used were fluorescent and the particle sizes were smaller than used microparticle by the researchers.

The intake of microplastics by aquatic vertebrates and invertebrates has important effects on their physiological functions such as respiration, nutrition, growth and reproduction [23]. In addition to these effects, microplastics tend to adsorb persistent organic pollutants (POPs). In studies on this subject, the desorption of POPs has been shown in vivo and in vitro in various organisms (fish, mussel, lugworm). According to these studies, contaminated microplastics are first taken up by the organisms as nutrients. Then, POPs that are absorptive to these microplastics are also transferred to these organisms. The effects of both microplastic and POP + microplastic combination on neurotransmission, energy production and oxidative metabolism have been demonstrated [30-33]. In a study conducted on this subject, Avio et al. [32] showed that pyrene (PR) contamination of polyethylene (PE) and polystyrene (PS) microparticles increased with dose and time. Also, the researchers performed toxicological assessment of the separate effects of both contaminating (PE + PR, PS + PR) and pure microplastic (PE, PS) on *Mytilus galloprovincialis*. According to the results of the researchers, *Mytilus galloprovincialis* observed PR accumulation in different tissues of the body except microplastics. Single-cell gel electrophoresis (comet) and micronucleus test were performed from the mussel hemolymph by applying PE, PE+PR, PS and PS+PR at a size less than 100 µm. In the comet test, PE and PS caused statistically significant damage to mussel DNA. Unlike the comet test, in the micronucleus test in which the nuclear abnormality was evaluated, only statistically significant differences were found in PE + PR and PS + PR applications compared to the control. As a result, it is clear that polyethylene or polystyrene microplastics are causing damage to DNA. In our comet experiment, all application concentrations of the PEM of 10-22 µm in size significantly increased the DNA tail length, tail moment and tail intensity compared to the control. If we look at the microplastic dimensions used in our work and in the study of Avio et al. [32], it is unlikely that a material of this size (10-100 µm) will reach the DNA through the cell membrane and cause such genotoxic damage. The hypothesis

that should be considered here is that microplastics may increase the production of reactive oxygen species (ROS) and the increased amount of ROS may cause breakage of DNA strands. Intracellular ROS levels were evaluated by Jeong et al. [34] in *Brachionus koreanus* exposed to PS microplastics of sizes 0.05, 0.5 and 6 µm for 24 hours. According to the obtained results, the level of ROS increased in inverse proportion to the particle sizes. This result shows that the increase of microplastic and reactive oxygen species may lead to the eventual DNA damage.

The harmful effects of microplastics on living organisms are evident when the above mentioned studies and the results of our work are evaluated. In addition, as a result of the production trends of plastics, their mode of use and varying demographic data, the increasing frequency of microplastics in aquatic environments [35] undoubtedly leads to great concern.

CONCLUSION

In conclusion, more effort is needed to increase the studies about effect of microplastic on living systems and to make people aware of plastic/microplastic.

ACKNOWLEDGEMENTS

This study was funded by The Scientific and Technological Research Council of Turkey (TUBITAK) (Project Number: 115Y112).

REFERENCES

[1] Pardos (2005) World plastics consumption long term, 1960-2020. http://www.pardos-marketing.com/hot04.htm. Accessed 05.01.2018.

[2] Bility, M.T., Thompson, J.T., McKee, R.H., David, R.M., Butala, J.H., Vanden Heuvel, J.P., Peters, J.M. (2004) Activation of mouse and human peroxisome proliferator-activated receptors (PPARs) by phthalate monoesters. Toxicological Sciences. 82, 170-82.

[3] Ge, R.S., Chen, G.R., Tanrikut, C., Hardy, M.P. (2007) Phthalate ester toxicity in Leydig cells: developmental timing and dosage considerations. Reproductive Toxicology. 23, 366-73.

[4] Richter, C.A., Birnbaum, L.S., Farabollini, F., Newbold, R.R., Rubin, B.S., Talsness, C.E., Vandenbergh, J.G., Walser-Kuntz, D.R., vom Saal, F.S. (2007) *In vivo* effects of bisphenol A in laboratory rodent studies. Reproductive Toxicology. 24, 199-224.

[5] Lawson, C., Gieske, M., Murdoch, Ye, P., Li, Y., Hassold, T., Hunt, P.A. (2011) Gene expression in the fetal mouse ovary is altered by exposure to low doses of bisphenol A. Biology of Reproduction. 84,79-86.

[6] Zhang, H.Q., Zhang, X.F., Zhang, L.J., Chao, H.H., Pan, B., Feng, Y.M., Li, L., Sun, X.F., Shen, W. (2012) Fetal exposure to bisphenol A affects the primordial follicle formation by inhibiting the meiotic progression of oocytes. Molecular Biology Reports. 39, 5651-5657.

[7] Erlich, S., Williams, P.L., Hauser, R., Missmer, S.A., Peretz, J., Calafat, A.M., Flaws, J.A. (2013) Urinary bisphenol A concentrations and cytochrome P450 19 A1 (*Cyp19*) gene expression in ovarian granulosa cells: an *in vivo* human study. Reproductive Toxicology. 42, 18-23.

[8] Barnes, D.K.A., Galgani, F., Thompson, R.C., Barlaz, M. (2009) Accumulation and fragmentation of plastic debris in global environments. Philosophical Transactions of the Royal Society B. 364, 1985-1998.

[9] Zarfl, C., Matthies, M. (2010) Are marine plastic particles transport vectors for organic pollutants to the Arctic? Marine Pollution Bulletin. 60, 1810-1814.

[10] 5 Gyres Institute (2016) EIM0017. Available at http://data.parliament.uk/writtenevidence/committeeevidence.svc/evidencedocument/environmental-audit-committee/environmental-impact-of-microplastics/written/31804.pdf. Accessed 09.01.2018.

[11] Sivan, A. (2011) New perspectives in plastic biodegradation. Current Opinion in Biotechnology. 22, 422-426.

[12] Desforges, J.P.W., Galbraith, M., Ross, P.S. (2015) Ingestion of Microplastics by Zooplankton in the Northeast Pacific Ocean. Archives of Environmental Contamination and Toxicology. 69, 320-330.

[13] Leslie, H.A., Van Velzen, M.J.M., Vethaak, A.D. (2013) Microplastic Survey of the Dutch Environment: Novel Data Set of Microplastics in North Sea Sediments, Treated Wastewater Effluents and Marine Biota. IVM Institute for Environmental Studies. Final Report R-13/11. 30p.

[14] Mathalon, A., Hill, P. (2014) Microplastic fibers in the intertidal ecosystem surrounding Halifax Harbor, Nova Scotia. Marine Pollution Bulletin. 81, 69-79.

[15] Van Cauwenberghe, L., Janssen, C.R. (2014) Janssen. Microplastics in bivalves cultured for human consumption. Environmental Pollution. 193, 65-70.

[16] Phillips, M.B. (2014) The Occurrence and Amount of Microplastics Ingested by Fishes in the Watersheds of the Gulf of Mexico. M.Sc. Thesis. Texas State University.

[17] Fossi, M.C., Panti, C., Guerranti, C., Coppola, D., Giannetti, M., Marsili, L., Minutoli, R. (2012) Are baleen whales exposed to the threat of microplastics? A case study of the Mediterranean Fin whale (Balaenoptera physalus). Marine Pollution Bulletin. 64, 2374-2379.
[18] Besseling, E., Wang, B., Lürling, M., Koelmans, A.A. (2014) Nanoplastic Affects Growth of S. Obliquus and Reproduction of D. Magna. Environmental Science and Technology. 48, 12336-12343.
[19] Cole, M., Lindeque, P., Fileman, E., Halsband, C., Goodhead, R., Moger, J., Galloway, T.S. (2013) Microplastic ingestion by zooplankton. Environmental science and technology. 47, 6646-6655.
[20] Hall, N.M., Berry, K.L.E., Rintoul, L., Hoogenboom, M.O. (2015) Microplastic ingestion by scleractinian corals. Marine Biology. 162, 725-732.
[21] Graham, E.R., Thompson, J.T. (2009) Deposit- and suspension-feeding sea cucumbers (Echinodermata) ingest plastic fragments. Journal of Experimental Marine Biology and Ecology. 368, 22-29.
[22] Kaposi, K.L., Mos, B., Kelaher, B.P., Dworjanyn, S.A. (2014) Ingestion of microplastic has limited impact on a marine larva. Environmental science and technology. 48, 1638-1645.
[23] Wright, S.L., Thompson, R.C., Galloway, T.S. (2013) The physical impacts of microplastics on marine organisms: a review. Environmental Pollution. 178, 483-492.
[24] American Society for the Testing of Materials International (ASTM). (2004) Standard guide for acute toxicity test with the rotifer Brachionus. E 1440-91. Annual book of ASTM standards, vol 11.05. West Conshohocken, PA, 830-837.
[25] Cole, M., Lindeque, P., Halsband, C., Galloway, T.S. (2011) Microplastics as contaminants in the marine environment: a review. Marine Pollution Bulletin. 62, 2588-2597.
[26] Thompson, R.C. (2006) Plastic debris in the marine environment: Consequences and solutions. Marine Nature Conservation in Europe. 193, 107-115.
[27] Eunomia. (2016) Plastics in the Marine Environment, from http://www.eunomia.co.uk/reports-tools/plastics-in-the-marine-environment/
[28] Au, S.Y., Bruce, T.F., Bridges, W.C., Klaine, S.J. (2015) Responses of Hyalella azteca to acute and chronic microplastic exposures. Environmental toxicology and chemistry. 34, 2564-2572.
[29] Ugolini, A., Ungherese, G., Ciofini, M., Lapucci, A., Camaiti, M. (2013) Microplastic debris in sandhoppers. Estuarine, Coastal and Shelf Science. 129, 19-22.
[30] Oliveira, M., Ribeiro, A., Hylland, K., Guilhermino, L. (2013) Single and combined effects of microplastics and pyrene on juveniles (0+ group) of the common goby Pomatoschistus microps (Teleostei, Gobiidae). Ecological Indicators. 34, 641-647.
[31] Rochman, C.M., Hoh, E., Kurobe, T., Teh, S.J. (2013) Ingested plastic transfers hazardous chemicals to fish and induces hepatic stress. Scientific Reports. 3, 3263.
[32] Avio, C.G., Gorbi, S., Milan, M., Benedetti, M., Fattorini, D., d'Errico, G., Regoli, F. (2015) Pollutants bioavailability and toxicological risk from microplastics to marine mussels. Environmental Pollution. 198, 211-222.
[33] Besseling, E., Wegner, A., Foekema, E.M., Van Den Heuvel-Greve, M.J., Koelmans, A.A. (2012) Effects of microplastic on fitness and PCB bioaccumulation by the lugworm Arenicola marina (L.). Environmental science and Technology. 47, 593-600.
[34] Jeong, C.B., Won, E.J., Kang, H.M., Lee, M.C., Hwang, D.S., Hwang, U.K., Lee, J.S. (2016) Microplastic size-dependent toxicity, oxidative stress induction, and p-JNK and p-P38 activation in the monogonont rotifer (Brachionus koreanus). Environmental Science and Technology. 50, 8849-8857.
[35] Anthony, L. (2011) Microplastics in the marine environment. Marine Pollution Bulletin. 62, 1596-1605.

Received: **07.02.2018**
Accepted: **04.04.2018**

CORRESPONDING AUTHOR

Ahmet Ali Berber
Canakkale Onsekiz Mart University,
Vocational School of Health Services,
17100 Canakkale – Turkey

e-mail: aberber@comu.edu.tr

© by PSP Volume 27 – No. 7/2018 pages 4980-4985 Fresenius Environmental Bulletin

EFFECT OF LAND USE ON BUTTERFLY (LEPIDOPTERA, RHOPALOCERA) DIVERSITY IN THE REPUBLIC OF MOLDOVA

Turgay Serik[1], Haci Huseyin Cebeci[2,*], Valeriu Derjanschi[3]

[1]Institute of Graduate Studies in Science and Engineering, Istanbul University, Istanbul, Turkey
[2]Department of Forest Entomology and Protection, Istanbul University, Istanbul, Turkey
[3]Institute of Zoology of Academy of Sciences of Moldova, Republic of Moldova

ABSTRACT

A total of 3072 individuals with 99 species belonging to 6 families were identified in 43 sampling sites from the Republic of Moldova. The rates of individuals of three families (Pieridae, Hesperidae and Papilionidae) differed in the others when all habitat types: forest, meadow, moor and urban. The dominant group included *Colias hyale, Issoria lathonia, Maniola jurtina, Melitaea aurelia, Plebejus argus, Pieris napi, P. rapae, Pontia edusa* and *Pyrgus malvae*. The relative number of these species is more than 1.70 % and the totally 22.56 %. The forest habitats had the higher species richness than others. At the same time, they are more common in the areas within the Eurasian and Palearctic zones. Since the southern moors of Moldova were actually located on the western extension of the Eurasian's. The fauna in the Scythian zone was represented by only three species. The species, *Polyommatus thersites* from the family Lycaenidae was first identified for the Moldova with this study.

KEYWORDS:
Rhopalocera, habitat types, diversity indices, zoogeographical distribution, rare species.

INTRODUCTION

The ecological-faunistic complex situation of butterflies is important for biodiversity. Anthropogenic changes or interventions result in a reduction in the number of species at fauna [1]. The first study on butterflies of the Bessarabia region was made in 1906 and identified 59 species, 44 of them as Rhopalocera [2]. The places where the captured species are located (Şaba village, Şabolat, Hotin and Akerman) are now located within the borders of Belgorod-Dnestrovsk cities of Ukraine nowadays. Miller and Zubowsky [3, 4] formed the list of Lepidoptera from 103 species in Moldavia. A complete summary of the Lepidoptera including 1200 species was prepared and mentioned as Rhopalocera 96 of them, 4 in Papilionidae, 14 in Pieridae, 40 in Lycaenidae, 38 in Nymphalidae [5]. The bioecological characteristics of butterflies and informations of the 6 species (*Iphiclides podalirius* L., *Parnassius mnemosyne* L., *Polyommatus daphnis* Den. and Schiff., *Pontia daplidice* L., *Tomares nogelii* H.-S., *Zerynthia polyxena* Den. and Schiff.) were mentioned in the book, namely Rare and Endangered Species in Moldova [6]. The Law No. 439-XIII about living things including in 34 rare species of Lepidoptera fauna came into force on April 27, 1995 in the Republic of Moldova. These 6 species recorded in the law. Andreev and Derjanschi [7] collected 26 butterflies and 3 moths from the edges of forests, in the countryside and steppe plants around Kopanka, Talmaza and Reskeiets villages. Svechkarev and Tischenkov [8] determined 35 butterflies and 31 moths between 1989 and 1994 in the nature conservation area of Novo-Andriyaşevka at Slobodzeya province of Transdniyester region and was firstly found *Lasiommata megera* (L.) belonging to Nymphalidae family. In the nature reserve area of Yagorlik at the same region, Tischenkov [9] studied 52 species of Rhopalocera on the calcareous slopes of Goyan village covering vegetations and shrubs of step from 1997 to 2002 and added three new species – *Boloria selene* (Den. and Schiff., 1775), *Carcharodus orientalis* (Reverdin, 1913), *Lycaena hippothoe* (L., 1758) in Moldova fauna. Three years later, the same author took inventory of 39 butterflies and 46 moths in this area [10]. Danila [11] was to do the preliminary list of Lepidoptera fauna consisting of 55 species with 42 butterflies in the nature conservation areas of "Padurea Domneasca" and "Plaiul Fagului". One of the most important fauna reports for Rhopalocera is the list consisting of 103 species belong to 7 families in Rebuplic of Moldova. The diversity of species was evaluated 52 lepidopters with 25 butterflies belong to 5 families in areas which the nature conservation laws thought nothing of them [12]. Four species, *Everes decoloratus* (Staud., 1886), *Hipparchia fagi* (Scop., 1763), *Melitaea aurelia* (Nickerl, 1850) and *Pyrgus armoricanus* (Obert., 1910) were expressed for fauna newly. The catalog of the USSR butterflies stated one species of Pieridae family, *Colias myrmidone*

(Esper, 1781) previously unrecorded for the Republic of Moldova [13]. There were mentioned biologies, ecologies and distributions of 63 species belonging to 7 families in ecology encyslopaedia [14, 15]. Also, three species of Lycaenidae, *Lycaena dispar* Haw., *Plebejus idas* L. and *P. argyrognomon* Bergstr. were observed as ecological and biological [16]. G. Buşmachiu et al. [17] found 171 species of Collembola and Coleoptera as well as 21 species of butterflies in the course of the biodiversity researches of invertebrates on the slopes at river basins of Moldova.

After 1950, the studies on the biological properties of species focused on the effective control methods against lepidopter species damaging forests and agricultural cultures. In recent years, studies on fauna have been carried out by Danila [11] and research on the protection of rare species by Andreev and Derjanschi [7]. However, all of these studies are of narrow frame nature and not fully reflect the butterfly diversity and fauna of Moldova.

This study gives weight to the current situation and zoo-geographical analysis of Rhopalocera in natural ecosystems and agricultural areas of Republic of Moldova.

MATERIALS AND METHODS

A survey was conducted with species collecting from 43 sampling sites in Moldova (Figure 1). These sites noted altitudes and geographical coordinates display different land characteristics (Table 1). The lands were categorized as forest, meadow, moor and urban. Distribution of sampling localities was set as 43 settlements and around 23 provinces of Moldova, 9 in the north of the country, 8 in the center, and 6 in the south. All of the butterflies were collected with sweep net along transects using Pollard walk method [18]. Chi-square independence test was done to compare diversity among different land use patterns. Also, the collected data were analyzed using the Shannon-Weaver Diversity Index (H) [19]. The quantitative determination on species composition in Rhopalocera was categorized as dominant, multiple, moderate, small and rare abundance (D= abundance of a species in site (n) / total abundances in site (N)). The species was calculated as $D > 1.7$ %, $1.2\ \% < D < 1.70$ %, $0.7\ \% < D < 1.19$ %, $0.2\ \% < D < 0.69$ % and $D < 0.2$ % respectively [20].

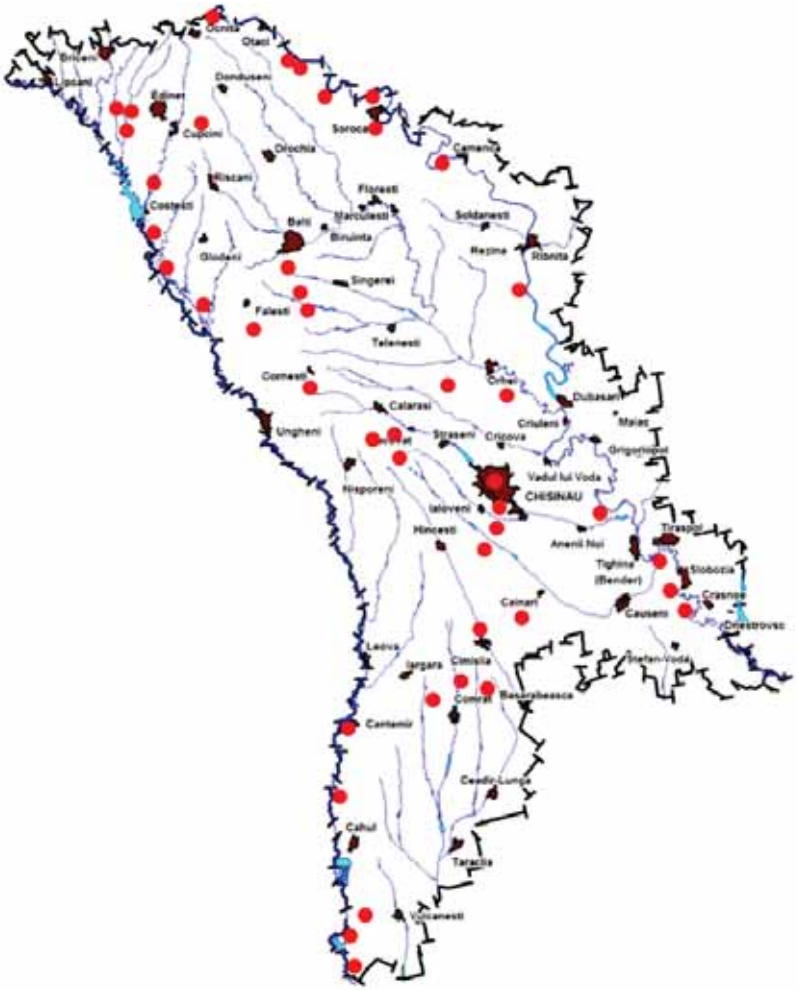

FIGURE 1
Sites of Rhopalocera collecting in the Republic of Moldova.

TABLE 1
Geographical positions and altitudes of sampling sites

No.	Sites	Geographical positions			Provinces		
		(N)	(E)	Altitude(m)	North	Centre	South
1.	Năslavcea	48°28'34"	27°33'47"	186	Ocnița		
2.	Brînzeni	48°05'20"	27°12'12"	253	Edineț		
3.	Fetești	48°10'32"	27°08'13"	265	Edineț		
4.	Gordinești	48°09'21"	27°08'23"	247	Edineț		
5.	Fîntîna Albă	48°09'27"	27°28'08"	223	Edineț		
6.	Druța-Horodiște	47°57'35"	27°16'33"	169	Rișcani		
7.	Balatina (“Suta de Movile”)	47°46'32"	27°16'52"	98	Glodeni		
8.	Lipovanca	47°40'35"	27°58'04"	132	Sîngerei		
9.	Chișcăreni	47°31'30"	28°04'18"	113	Sîngerei		
10.	Glinjeni	47°37'29"	27°51'41"	161	Sîngerei		
11.	Sărata Veche	47°29'59"	27°46'08"	65	Fălești		
12.	Balatina (“Pădurea Domnească”)	47°36'24"	27°23'34"	57	Glodeni		
13.	Arionești	48°22'88"	27°51'21"	181	Dondușeni		
14.	Rudi	48°20'02"	27°52'57"	221	Soroca		
15.	Grigorăuca	48°13'18"	28°05'55"	203	Soroca		
16.	Cosăuți	48°12'07"	28°14'55"	78	Soroca		
17	Soroca	48°08'13"	28°18'16"	108	Soroca		
18.	Napadova	48°01'11"	28°37'43"	86	Florești		
19.	Pruteni	47°31'43"	27°32'50"	49		Ungheni	
20.	Lopatna	47°30'48"	29°01'26"	158		Orhei	
21.	Ivancea	47°16'44"	28°52'44"	154		Orhei	
22.	Vatici	47°19'50"	28°35'32"	136		Orhei	
23.	Lozova (Codrii)	47°06'22"	28°21'42"	139		Strășeni	
24.	Cîprieana	47°05'55"	28°29'34"	346		Strășeni	
25.	Copanca	46°41'15"	29°34'51"	14		Căușeni	
26.	Rădenii Vechi (Plaiul Fagului)	47°17'46"	28°01'54"	199		Călărași	
27.	Sadova	47°12'37"	28°19'12"	249		Călărași	
28.	Chișinău	47°01'41"	28°50'23"	86		Chișinau	
29.	Codru	46°58'30"	28°49'39"	111		Chișinău	
30.	Calfa	46°53'31"	29°22'59"	125		Anenii Noi	
31.	Răzeni	46°43'49"	28°52'38"	183		Ialoveni	
32.	Purcari	46°30'54"	29°53'01"	55			Ștefan Vodă
33.	Cimișlia	46°33'13"	28°45'49"	82			Cimișlia
34.	Bugeac (“Bugeac”)	46°23'17"	28°40'38"	66			Comrat
35.	Vișnevca	46°19'55"	28°27'35"	144			Comrat
36.	Cucoara	46°03'27"	28°07'54"	6			Cantemir
37.	Cantemir	46°16'63"	28°10'78"	13			Cantemir
38.	Vadul lui Isac	45°44'34"	28°16'25"	120			Cahul
39.	Cioc-Maidan	46°20'10"	28°52'19"	104			Ceadîr-Lunga
40.	Răscăieți	46°35'03"	29°45'41"	83			Ștefan Vodă
41.	Giurgiulești	45°29'43"	28°10'52"	61			Cahul
42.	Troițcoie	46°31'24"	29°02'32"	165			Cimișlia
43.	Colibaș	45°43'28"	28°10'19"	5			Cahul

RESULTS AND DISCUSSION

A total of 3072 individuals with 99 species belonging to 6 families were identified in four land using types in Moldova. Nymphalidae family was dominant, whereas Riodinidae had the least number of individuals (Table 2). There was a significant difference in the species diversity among habitat types by Shannon’s diversity index. The highest index was found for the forest. There were no observed differences between the meadow and moor in the diversity indices, although the number of species and specimens are different. The lowest diversity was calculated for the urban, although the number of species and specimen is higher than the meadow (Table 3). The individuals were collected in habitat types to them of all families except Riodinidae. The rates of individuals of three families (Pieridae, Hesperidae and Papilionidae) differed from the others when all habitat types were taken into consideration. Regarding the dependency rate between family and land use, the chi-square independence test was applied data (Table 4). As a result of the chi-square independence test, there is a statistically dependence between the family and the land use at the significance level of $p = 0.001$. According to the obtained data and their presences in site, the dominant group included *Colias hyale, Issoria lathonia, Maniola jurtina, Melitaea aurelia, Plebejus argus, Pieris napi, P. rapae, Pontia edusa*

and *Pyrgus malvae*. The relative number of these species is more than 1.70 % and the totally 22.56 %. The multiple groups was represented with 19 species into the relative number varying between 1.20 % and 1.70 % in site and totally 26.37 %. There were 31 species from 0.70 % to 1.19 % in the moderate group. The total relative number of species in this group was 29.37 %. The small group with a relative number ranging between 0.20 % and 0.69 % covered 30 species and totally 11.53 %. There were 10 species in the rare group with a relative number not exceeding 0.20 % and totally 0.91 %. In this study, the indicator complex of Rhopalocera species consisted of 60 species. This complex represented by dominant, multiple and moderate groups covered a total relative number of 84.55 %.

These species underlying of fauna on the study area were *Aglais io, A. urticae, Gonepteryx rhamni, Nymphalis polychloros* and *Polygonia c-album* in April, *Anthocharis cardamines* and *Zerynthia polyxena* in May, *Aphantopus hyperantus, Issoria lathonia, Melitaea athalia, Neptis sappho* and *Pararge aegeria* from family Nymphalidae and *Colias hyale, Leptidea morsei* and *Pieris napi* from family Pieridae in June, species from families Hesperiidae, Pieridae, Nymphalidae and Lycaenidae in July. The highest species diversity of Rhopalocera was observed in June and July. Towards the end of the season, while number of the specimens were gradually decreasing, there was only a slight increase in population of them from families Nymphalidae and Lycaenidae at the end of August. The end of the season was seen *Vanessa atalanta* emerging in the fall and the species overwintering in September and October.

TABLE 2
The number of species and specimen of butterflies collected from habitat types in 2015

Family	Forest		Meadow		Moor		Urban	
	spp	spec	spp	spec	spp	spec	spp	spec
Hesperidae (11)	8	50	6	6	5	12	5	10
Papilionidae (4)	4	21	2	2	3	19	1	2
Pieridae (14)	14	463	9	46	10	145	8	35
Nymphalidae (38)	36	871	7	18	16	180	12	48
Riodinidae (1)	1	49	1	3	0	0	0	0
Lycaenidae (31)	30	468	6	56	14	291	15	277
Total	93	1922	31	131	48	647	41	372

TABLE 3
The Shannon-Weaver (H') and diversity indices (d) according to species and specimens for each habitat types in 2005

Habitat types	No. of spp.	No. of spec.	Shannon-Weaver	d
Forest	93	1922	1.518027	0.334913
Meadow	31	131	1.126075	0.327921
Moor	48	647	1.276932	0.329854
Urban	41	372	0.941668	0.253575

TABLE 4
Tests of family and land use as forest, meadow (with together moor) and urban

Family and Land Use				
Family	Land use			Total
	Forest	Meadow	Urban	
Hesperiidae	50	18	10	78
Papilionidae	21	21	2	44
Pieridae	463	191	35	689
Nymphalidae	871	198	48	1117
Riodinidae	49	3	0	52
Lycaenidae	468	347	277	1092
	1922	778	372	3072
Chi-Square Tests				
	Value	df	Asymp.Sig.(2-sided)	
Pearson Chi-Square	435,481[a]	10	,000	
Likelihood Ratio	438,549	10	,000	
Linear-by-Linear Association	220,776	1	,000	
N of Valid Cases	3072			

[a]0 cells (0,0%) have expected count less than 5. the minimum expected count is 5,33.

TABLE 5
The zoogeographical distribution of Rhopalocera in this study

Region	Habitat			
	Forest	Meadow	Moor	Urban
Cosmopolit	1	1	1	-
Holarctic	5	6	3	5
Palearctic	13	4	5	4
Western-Palearctic	16	4	10	7
Eurasian	44	10	22	17
European	9	2	3	5
Ponto-mediterranean	3	3	2	2
Mediterranean-Caucasian	2	1	1	1
Scythian	-	-	1	-
Total	93	31	48	41
%	93,93	23,23	48,48	41,41

Ten species of butterflies (*Cupido osiris, Glaucopsyche alexis, Phengaris alcon, Polyommatus thersites* and *Thecla betulae*) from family Lycaenidae, *Apatura iris, Argynnis pandora* and *Limenitis populi* from family Nymphalidae and, *Colias erate* and *Euchloe ausonia* from family Pieridae were rare. The majority of these species were found in the pristine environment on the urban areas. In the forest areas, there were *Apatura iris, Argynnis pandora, Cupido osiris, Glaucopsyche alexis, Limenitis populi, Polyommatus thersites* and *Thecla betulae*, while the species *Colias erate* was found in the meadow areas. The moor habitats included an species, *Euchloe ausonia* and *Phengaris alcon*. Protection of habitats is necessary to ensure the continuity of these species mentioned.

The zoogeographical distribution of the obtained butterflies was determined in this study (Table 5). They are more common in the areas within the Eurasian and Palearctic zones. Since the southern moors of the Republic of Moldova were actually located on the western extension of the Eurasian's. The fauna in the Scythian zone was represented by only three species. One of these species, *Melitaea trivia*, has been clarified with this study.

The forest habitats had the higher species richness than others. These findings are similar to other studies [21, 22]. According to Sagwe et al. [22] the land cover characteristics and diversity of host plants can affect butterfly richness and density.

CONCLUSION

This study is important to know the butterfly species richness for different habitats and zoogeographical distribution in the Republic of Moldova.

The species, *Polyommatus thersites* from the family Lycaenidae was first identified for the Republic of Moldova with this study.

The obtained data have been added to the new edition of the Red Book of the Republic of Moldova on rare and perennial species as one species, *Leptidea morsei* in the CR category, seven species in the EN category, six species in the VU category, six species in the LC category and one species in the DD category. Also, two species (*Glaucopsyche alexis* and *Lycaena dispar*) from family Lycaenidae have been recommended to be included in the National Operations List.

ACKNOWLEDGEMENTS

Authors thank the supports of Istanbul University and Academy of Sciences of Moldova for PhD thesis research.

REFERENCES

[1] Andreev, A., Josan, L., Şabanova, G., Ghendov, V., Munteanu, A., Postolachi, V., Jurminschi, S., Romanciuc, A., Sîrodoev, G. H., Şubernetkii, I., Ţurcanu, V., Derjanschi, V., Bondarenco, A. and Talmaci, I. (2009) Diversitatea biologică naturală şi reţeaua ecologică a Moldovei în context internaţional. Societatea ecoloică "BIOTICA", Tipografia "Elena V.I.", Chişinău, 37p.

[2] Krulikovskyi, L. (1906) K svedeniyam o cheshuekrylykh Bessarabii. Russkoe entomologicheskoe obozrenie. 6(3-4), 184-187.

[3] Miller, E. and Zubowsky, N. (1908) Materialy po entomologicheskoi faune Bessarabii. Cheshuekrylye (Macrolepidoptera). Trudy Bessarabskogo obshchestva estestvoispytatelei i lyubitelei estestvoznaniya. 1(3), 410-425.

[4] Miller, E. and Zubowsky, N. (1912) Materialy po entomologicheskoi faune Bessarabii. Cheshuekrylye (Macrolepidoptera). Dopolnenie I, Trudy Bessarabskogo obshchestva estestvoispytatelei i lyubitelei estestvoznaniya. 2(2), 93-96.

[5] Plugaru, S.G. (1983) Otryad Cheshuekrylye, ili Babochki – Lepidoptera, Zhivotnyi mir Moldavii, Nasekomye. Izdatelistvo Shtiintsa, Kishinev, 375p.

[6] Neculiseanu, Z.Z., Stratan, V.S., Veresciaghin, B.V. and Ostaficiuc, V.G. (1993) Insectele rare şi pe cale de dispariţie din Moldova. Editura Ştiinţa, Chişinău, 120p.
[7] Andreev, A.V. and Derjanschi, V.V. (1999) K faune cheshuekrylykh (Lepidoptera) Nizhnego Dnestra. Conservarea biodiversităţii bazinului Nistrului, Mater. Conf. Internaţ., Chişinău, 58-59.
[8] Svechkarev, E.I. and Tischenkov, A.A. (2001) Materialy k faune cheshuekrylykh zakaznika "Novo-Andriyashevka", Academician Leo Berg – 125 years. Collection of scientific articles, Bender, 131-133.
[9] Tischenkov, A.A. (2003) Fauna bulavousykh cheshuekrylykh zapovednika "Yagorlyk", Rol' prirodno-zapovidnykh teritoriy u pidtrimanni bioriznomanittya. Materialy naukovoi konferentsii, prisvyachenoi 80-richchyu Kanivs'kogo prirodnogo zapovidnika, Kaniv, 292-293.
[10] Tischenkov, A.A. (2006) Kratkie itogi inventarizatsii cheshuekrylykh (Lepidoptera) zapovednika "Yagorlyk", Zapovednik "Yagorlyk", Mezhdunarodnaya ecologicheskaya assotsiatsiya khranitelei reki "Eco-Tiras". Tiraspoli, 154-156.
[11] Danilă, A. (2003) Date preliminare privind fauna de macrolepidoptere (Insecta, Lepidoptera) din rezervaţiile ştiinţifice "Pădurea Domnească" şi "Plaiul Fagului", Pădurea Domnească – 10 ani, Rezumatele simpozionului, Glodeni, 61-64.
[12] Andreev, A.V. and Derjanschi, V.V. (2004) Materialy po otsenke vidovogo raznoobraziya i redkim vidam dnevnykh babochek (Lepidoptera, Rhopalocera), Managementul integral al resurselor naturale din bazinul transfrontalier al fluviului Nistru, Materialele conferinţei internaţionale, Chişinău, 31-33.
[13] Korb, S.K. (2005) A catalogue of butterflies of the ex-USSR, with remarks on systematics and nomenclature. Nizhny Novgorod. 156p.
[14] Cozari, T. (2008) Fluturii. Mică enciclopedie, Editura Arc, Chişinău, 160p.
[15] Cozari, T. (2008) Fluturii, Enciclopedie ecologică ilustrată, Editura Litera International. Chişinău, 200p.
[16] Timuş, A. and Derjanschi, V. (2011) Contribuţii la studiul unor specii de albăstriţe (Lepidoptera, Lycaenidae) din Republica Moldova. Revista Agrobuletin, Editat de Societatea de Inginerii agricole Timiş, an. III. 1(8), 25-34.
[17] Buşmachiu, G., Bacal, S. and Calestru, L. (2011) Diversitatea specifică a nevertebratelor (Collembola, Coleoptera, Lepidoptera) din ecosistemele riverane ale Republicii Moldova. Academician Leo Berg – 135, Collection of Scientific Articles, Eco-TIRAS, Bendery, 118-123.
[18] Pollard, E. and Yates, T.J. (1993) Monitoring butterflies for ecology and conservation. London: Chapman and Hall. 292p.
[19] Shannon, C.E. and Weaver, W. (1949) A Mathematical Model of Communication. Urbana, IL: University of Illinois Press, 125p.
[20] Lakin, G.F. (1990) Biometriya, Vysshaya Shkola, Moskva, 352p.
[21] Akbulut, S., Yüksel, B. and Keten, A. (2006) Investigation of Lepidoptera Richness at Different Time Periods and in Different Habitats in Duzce-Turkey. Forest Science. 4(27), 81-92.
[22] Sagwe, R.N., Muya, S.M. and Maranga, R. (2015) Effects of land use patterns on the diversity and conservation status of butterflies in Kisii highlands, Kenya. Journal of insect conservation. 19(6), 1119-1127.

Received: **09.02.2018**
Accepted: **15.04.2018**

CORRESPONDING AUTHOR

Haci Huseyin Cebeci
Department of Forest Entomology and Protection,
Istanbul University,
Istanbul – Turkey

e-mail: hcebeci@istanbul.edu.tr

© by PSP Volume 27 – No. 7/2018 pages 4986-4994 Fresenius Environmental Bulletin

EVALUATION AND CLASSIFICATION OF SIXTEEN NEW YELLOW MAIZE INBRED LINES USING LINE×TESTER ANALYSIS IN DIFFERENT LOCATIONS UNDER EGYPTIAN ENVIRONMENT

Mohamed Saad Abd El-Aty[1], Abd El-Wahed Abd El-Hameed El-Sayed[1], Esam Abd El-Fatah Amer[2], Mosa Sayed Rizk[2,*]

[1]Agronomy Department, Faculty of Agriculture, Kafrelsheikh University, Kafrelsheikh, Egypt
[2]Maize Research Department, Field Crops Research Institute, Agricultural Research Center, Kafrelsheikh, Egypt

ABSTRACT

The Identify of heterotic groups among inbreeds is key to the progress of a maize hybrid breeding program. So, the objectives of this study were aimed to determine combining ability and classify sixteen new yellow maize inbred lines which were crossed with three types of testers. The F1 resulting topcrosses plus two check hybrids were evaluated at two locations in a randomized complete blocks design with four replications. Analysis of variance indicated that the mean squares due to locations (Loc), crosses (C) and C x Loc interaction were highly significant for the major studied traits under investigation. Mean squares due to lines, testers and line×tester interaction were significant for all studied traits. The additive gene effects were most responsible for controlling the inheritance of all traits except for grain yield. The best inbred line which showed desirable GCA effects for grain yield was L10. Tester SC162(T2) was the best combiner for the major traits. The 16 inbred lines were classified into three different heterotic groups using HSGCA method. These groups could be used in breeding program for selecting the best parents in making crosses.

KEYWORDS:
Line×tester, combining ability, heterotic group, *Zea mays.*

INTRODUCTION

Maize is one of the most important staple food crop for more than 1.2 billion people in the world, specially at Africa and Latin America. Maize (*Zea mays* L.) is one of the main important cereal crops in global world [1]. It is using as food, fodder, and fuel. Furthermore, oil of maize is suitable for the consumption of human due to the presence of unsaturated fatty acids [2]. Further, it its high productivity of grain and forage yield [3]. In developed countries, maize is widely used as raw materials for pharmaceutical, livestock and many agro-allied industries [4].

In Egypt maize is the third most essential staple food crop both in terms of area and production [5]. The main goal of the Egyptian national maize program is to develop new single and three way crosses with high yielding especially yellow hybrids. The performance of hybrid is related to the general combining ability (GCA) and specific combining ability (SCA) of the inbred lines involved in the hybrid [6].

In any breeding program the choice of the correct parents is the secret of the success. Hence, estimation of combining ability (GCA and SCA) is important in breeding program for hybridization [7, 8]. The analysis of general combining ability (GCA) and specific combining ability (SCA) are important to screen the best inbred lines for hybrid improvement and hybrid combinations with good specific combining ability [9, 10]. Meanwhile, the inbred line can be used as [11, 12], further, the single cross can be used as a tester [13].

Heterotic group was defined as a group of related or unrelated genotypes from the same or different populations, which display similar combining ability and heterotic response when crossed with genotypes from other genetically distinct germplasm groups [14, 15]. Heterotic groups specific and general combining ability (HSGCA) method is a practical and easy to follow procedure to classify maize inbred lines into known heterotic groups, the new method was more reliable and efficient than traditional maize heterotic group classification methods that use SCA-GY and molecular markers [16, 17].

The objectives of this study were to determine general and specific combining ability effects, nature of inheritance for grain yield and other studied traits, identify the superior single and three way crosses in grain yield and classifying the inbred lines into heterotic groups using specific and general combining abilities (HSGCA method) derived from line x tester analysis.

TABLE 1
Combined analysis of variance for the studied traits across two locations.

S.O.V.	d.f	Days to 50% silking	Plant height	Ear height	Number of rows/ear	Number of kernels/ row	100kernels Weight	Grain yield
Locations(Loc)	1	1474.56**	372893.42**	108669.12**	11.63	568.82**	7213.97**	129.47**
Rep/Loc	6	46.60	3082.18	1192.48	3.97	21.73	32.75	9.11
Genotypes (G)	49	30.57**	1613.70**	1156.64**	6.94**	41.24**	61.99**	7.53**
Crosses (C)	47	29.45**	1498.73**	1119.26**	7.01**	37.28**	61.05**	7.69**
Checks (Ch)	1	20.25**	1207.56**	784.00**	6.76**	57.76**	76.12**	2.01
C. vs. Ch	1	93.53**	7423.43**	3286.14**	3.83*	210.84**	92.04**	5.13*
G ×Loc	49	3.35**	210.83	200.27**	1.29*	18.77**	22.37**	2.41**
C×Loc	47	3.09**	183.65	172.87**	1.30*	18.03**	19.12**	2.25**
Ch×Loc	1	4.00	22.56	650.25*	0.09	56.25**	111.83**	9.25**
C. vs. Ch×Loc	1	14.92**	1676.56**	1038.09**	2.02	16.07	85.66**	3.21
Error	294	1.61	177.75	104.83	0.84	6.31	6.23	0.87

*and** Significant at 0.05 and 0.01 levels of probability, respectively.

MATERIALS AND METHODS

The present investigation was conducted at two locations (Sakha and Sids Agricultural Research Stations), Agriculture Research Center Egypt, during the two growing summer seasons 2015 and 2016.

Genetic materials. The genetic materials used in this study were three types of testers as male parents namely; inbred line Cim/z (T1), single cross (SC)162 (T2) and population(Pop) Sk9 (T3) as well as sixteen new yellow inbred lines as female parents namely; Sk2 (L1), Sk3 (L2), SkD-4 (L3), Sk10 (L4), Sk11 (L5), Gz639 (L6), Gz658 (L7), Gz666 (L8), Gm1004 (L9), Gm1021 (L10), Hp704-10 (L11), Sk5003/20 (L12), Sk5010/6 (L13), Sk5011/2 (L14), Sk5007/32 (L15) and Sk8008/1 (L16) .

In 2015 season the three male testers and the sixteen female parents were crossed according to line x tester design to produce 48 F_1 top crosses as out lined by [18]. In 2016 season, two field experiments were conducted at two locations; Sakha and Sids Agricultural Research Stations.

The experimental design was Randomized Complete Blocks Design with four replications. Each replicate contained 48 $F_1$and two commercial check hybrids, single cross162 (SC162) and three-way cross 360 (TWC360). Each entry was grown in a single row 6 meter long, 0.80m and 25 cm between hills and one plant were left per hill. The agronomic processing and farming practices were done according to each experimental site.

Recorded Data. Days to 50% silking (was recorded as the number of days from planting to 50% silking), Plant height (cm) was measured from each plot from soil surface to upper most node as an average of 5 guarded plants, Ear height (cm) was measured from the soil surface to the upper most ear bearing node for 5 guarded plants from each plot, Number of rows / ear, Number of kernels / row. (Random sample of 10 ears was taken from each plot to measure traits, 4 and 5 as an average), 100 kernels weight (g) taken at random from the shelled grains of each plot and weight and Grain yield (shelled grain weight per plot adjusted to 15.5% grain moisture and transformed to ton per hectare).

Statistical analysis. Statistical analysis was performed for each location. Combined analysis between the two locations was done whenever homogeneity of error mean squares was detected for the studied characters according to [19]. The combining ability analysis was done using line×tester procedure as suggested by [18]. Heterotic groups specific and general combining ability (HSGCA) were made according to [16] as follows: HSGCA= cross mean ($\overline{LT}$)– tester mean ($\overline{T}$) = GCA + SCA

Where;

$\overline{LT}$ = the mean yield of the cross between the L^{th} line and T^{th} tester

$\overline{T}$= the mean yield of the T^{th} tester across the L^{th} lines.

RESULTS AND DISCUSSION

Analysis of variance. The combined analysis of variance for the studied traits across two locations is presented in Table 1. Mean squares of locations were highly significant for all studied traits except for number of rows/ear. This result indicated that the environmental conditions at the two locations were different for growing maize. These results are in agreement with [20, 21, 22, 23, 11, 12].

The mean squares due to Genotypes and their partitions; crosses(C), checks (Ch) and C vs. Ch were significant or highly significant for all studied

traits except for checks of grain yield. Similar results were obtained by [7, 23].

The interaction between the genotypes (G) and their partitions (C, Ch and C vs. Ch) with locations (Loc) were significant or highly significant for all studied traits except for G×Loc and C×Loc of plant height, for Ch×Loc of days to 50% silking, plant height and number of rows/ear and for C vs. Ch×Loc of number of rows/ear, number of kernels/row and grain yield. These results are in agreement with those obtained by [7] of crosses(C) for days to 50% silking, plant height and grain yield, indicating that these crosses differed in their order from location to another for these traits.

Mean performance. Mean performance of the F_1 top crosses and two check hybrids for nine traits across two locations are presented in Table 2. Number of days to 50% silking ranged from 59.63 days for L14xT3 to 69.25 days for L6xT2. Plant height ranged from 204.38cm for L14xT1 to 275.25cm for L10xT2. Ear height ranged from 99.75 cm for L14xT1 to 162.00 cm for L10xT2.

TABLE 2
Mean performance of F_1 top crosses and two checks for nine traits across two locations.

Genotype	Days to 50% silking	Plant height (cm)	Ear height (cm)	Number of rows/ear	Number of kernels/row	100 kernel Weight(g)	Grain yield (t/ha)
L1×T1	67.63	235.75	121.00	15.15	39.38	39.39	8.82
×T2	65.75	241.88	132.38	14.55	42.95	41.38	10.39
×T3	63.63	222.88	119.50	15.58	42.60	37.31	9.48
L2×T1	66.00	230.50	116.75	15.40	40.40	36.58	9.04
×T2	65.38	245.88	139.25	14.10	41.45	37.85	10.17
×T3	64.13	239.25	132.00	17.10	44.20	33.98	9.64
L3×T1	67.63	234.63	126.38	15.00	43.08	38.75	9.86
×T2	66.50	260.13	136.00	14.50	41.05	37.40	10.59
×T3	63.75	249.75	137.25	15.60	42.50	35.11	8.29
L4×T1	63.75	228.63	105.75	15.25	38.50	38.51	8.97
×T2	63.75	247.38	128.63	15.05	42.48	37.08	10.27
×T3	62.38	225.88	115.25	15.90	40.65	33.88	9.32
L5×T1	64.88	240.75	125.13	14.25	40.15	38.03	9.32
×T2	64.88	260.88	146.25	14.00	43.80	35.74	8.75
×T3	63.13	239.75	128.63	14.80	41.83	32.49	9.26
L6×T1	68.13	233.13	121.13	15.00	42.33	33.69	8.31
×T2	69.25	253.38	139.25	14.58	39.85	32.23	6.50
×T3	63.75	245.63	136.88	15.05	42.50	36.48	9.24
L7×T1	68.75	221.25	127.25	15.65	40.48	38.13	9.10
×T2	66.00	243.75	139.75	14.60	44.23	35.73	10.72
×T3	65.00	232.38	136.50	16.38	41.70	33.68	9.44
L8×T1	65.50	244.75	116.50	15.20	41.75	36.69	8.42
×T2	65.38	250.63	134.88	13.80	45.48	37.49	9.69
×T3	62.13	230.38	123.25	15.20	42.53	33.31	9.36
L9×T1	67.00	215.38	112.13	17.25	37.10	30.14	7.98
×T2	65.88	242.63	133.63	15.60	43.60	32.75	8.81
×T3	64.50	236.63	136.38	17.45	42.10	27.85	8.97
L10×T1	64.88	243.63	130.38	14.75	39.55	40.61	10.64
×T2	64.75	275.25	162.00	14.35	42.33	39.54	12.33
×T3	64.38	236.63	130.38	15.80	38.43	37.13	8.40
L11×T1	63.63	225.13	119.63	14.80	37.78	34.30	8.43
×T2	63.25	251.38	143.50	13.95	40.03	32.73	9.09
×T3	61.63	228.50	124.50	14.50	37.58	34.03	9.02
L12×T1	65.88	240.88	121.75	14.20	36.48	35.51	7.84
×T2	64.75	262.63	144.63	14.50	42.48	37.25	10.56
×T3	63.25	250.88	134.38	15.35	37.80	37.79	9.48
L13×T1	66.63	234.00	113.00	16.30	40.60	32.25	8.27
×T2	63.75	256.38	129.25	15.60	43.33	36.24	9.87
×T3	62.88	226.75	114.50	16.00	43.20	34.03	9.82
L14×T1	61.75	204.38	99.75	16.33	40.65	32.36	9.14
×T2	63.38	233.00	122.38	15.65	44.03	32.83	9.28
×T3	59.63	211.63	106.50	17.08	42.00	32.03	8.61
L15×T1	67.38	230.63	117.25	16.45	42.63	36.31	8.28
×T2	65.13	246.50	134.38	15.75	44.70	37.84	9.45
×T3	64.63	230.13	123.75	16.78	41.38	36.61	8.77
L16×T1	65.63	227.75	123.00	14.85	37.45	38.18	7.50
×T2	64.75	251.38	143.25	13.73	40.83	35.56	8.19
×T3	63.00	230.63	132.13	15.05	40.45	36.89	8.22
Check SC162	68.38	269.25	149.50	14.15	46.90	35.95	10.08
Check TWC360	66.13	251.88	135.50	15.45	43.10	40.31	9.37
LSD 0.05	1.24	13.06	10.03	0.90	2.46	2.44	0.91
LSD 0.01	1.63	17.20	13.21	1.18	3.24	3.22	1.20

TABLE 3
Line×tester analysis of F_1 top crosses for nine traits across two locations.

S.O.V	d.f	Days to 50% silking	Plant Height	Ear height	Number of rows/ear	Number of kernels/row	100 kernels Weight	Grain yield
Lines (L)	15	47.22**	1922.41**	1484.74**	13.74**	47.83**	125.76**	9.63**
Testess(T)	2	247.69**	16145.18**	12292.5**	45.97**	252.27**	128.35**	27.78**
L×T	30	6.01**	310.45**	191.63*	1.53*	17.92**	23.09**	5.39**
L×Loc	15	5.35**	229.05	317.66**	1.91*	33.36**	26.59**	2.26**
T×Loc	2	3.46	471.69	516.02*	4.95**	34.11*	35.66*	1.88
L×T×Loc	30	1.93	171.74	76.70	0.78	9.32	14.22*	2.25**
Error	282	1.79	176.32	113.44	0.98	7.73	8.14	0.87

*and** Significant at 0.05 and 0.01 levels of probability, respectively.

TABLE 4
Estimates of K^2_{GCA}, K^2_{SCA} and their interaction with locations for nine traits across two locations.

Genetic component	Days to 50% silking	Plant height	Ear height	Number of rows/ear	Number of kernels/row	100 kernel weight	Grain yield
K^2_{GCA}	1.83	114.44	85.15	0.35	1.52	1.26	0.22
K^2_{SCA}	0.52	17.33	14.36	0.09	1.07	1.11	0.35
$\sigma^2_{GCA\times Loc}$	0.06	4.57	7.98	0.064	0.68	0.61	0.03
$\sigma^2_{SCA\times Loc}$	0.03	000	000	000	0.39	1.52	0.34

Number of rows/ ear ranged from 13.73 for L16xT2 to 17.45 for L9xT3. Number of kernels /row ranged from 36.48 for L12xT1 to 46.9 for SC 162, 100 kernel weight ranged from 27.85 for L9xT3 to 41.38 for L1xT2. Grain yield ranged from 6.50t/ha for L6 x T2 to 12.33t/ha for L10xT2.

The results for grain yield exhibited that five three way crosses; L1×T2 (10.39t/ha), L3×T2 (10.59t/ha), L7×T2 (10.72t/ha), L10×T2(12.33t/ha) and L12×T2(10.56t/ha) increased significantly compared with commercial hybrid TWC360 (9.37t/ha). These hybrids will be test in yield trails for further evaluation and it could be used in breeding program to improve grain yield.

Line×tester analysis. The mean squares for lines (L), testers (T), lines×testers (L×T) and their interaction with locations (Loc) for all studied traits across two locations are presented in Table 3. The results showed that the mean squares for L, T and L×T were significant for all studied traits, indicating that the inbred lines behaved differently in their respective top crosses and that greater diversity exists between testers, while significant L×T interaction, meaning that the inbred lines performed differently their respective top crosses depending on the type of testers used for these traits. Similar results were obtained by [24, 12] for grain yield.

The interaction between L×Loc and T×Loc were significant or highly significant for all studied traits except for LxLoc of plant height and for T×Loc of days to 50% silking, plant height and grain yield. While, L×T×Loc were significant for 100 kernels weight and grain yield, only. These results are in agreement with those of [25, 26, 10].

Genetic components of both GCA and SCA. Estimates of genetic components of both GCA (additive gene effects) and SCA (non-additive gene effects) and their interaction with locations for the studied traits are presented in Table 4. Data showed that K^2_{GCA} was higher than K^2_{SCA} for all traits except for grain yield, indicating that the additive gene effects were the most responsible for controlling the inheritance of these traits. While, the non-additive gene effects were of greater importance in the inheritance of grain yield. These results were similar to those obtained by [24, 12] for grain yield.

$\sigma^2_{GCAxLoc}$ and $\sigma^2_{SCAxLoc}$ exhibited that the additive gene effects were more interacted by locations than non-additive gene effects for days to 50% silking, plant and ear heights, number of rows/ear and number of kernels/row while the reverse was true for 100kernel weight and grain yield. These results support the findings of [13, 12, 27] for 100 kernel weight and grain yield.

General combining ability effects. The general combining ability effects of 16 inbred lines and three testers for nine traits across two locations are presented in Table 5. Negative GCA effects are desirable when selecting for earliness, short plant and ear height, while positive GCA effects are desirable for improvement of grain yield and yield component traits.

The favorable GCA effects for earliness were shown in the inbred lines, L4, L11 and L14. The inbreed lines L7, L9 and L14 had significant negative values for short plants. For short ear height, the inbreed lines L4, L13 and L14 were the best combiner.

TABLE 5
General combining ability effects of 16 inbred lines and 3 testers for nine traits across two locations.

Inbred line and tester	Days to 50% silking	Plant height	Ear height	Number of rows/ear	Number of kernels/row	100kernels Weight	Grain yield
Inbred line L1	0.89**	-5.08	-3.58	-0.10	0.45	3.64**	0.39*
L2	0.39	-0.04	1.46	0.19	0.70	0.51	0.49**
L3	1.18**	9.59**	5.34*	-0.31	0.91	1.43*	0.41*
L4	-1.48**	-4.62	-11.33**	0.11	-0.80	0.85	0.38*
L5	-0.48	8.55**	5.46*	-0.93**	0.62	-0.20	-0.05
L6	2.27**	5.46*	4.54*	-0.43*	0.24	-1.57**	-1.15**
L7	1.81**	-6.12*	6.63**	0.32	0.74	0.14	0.58**
L8	-0.44	3.34	-3.00	-0.60**	1.99**	0.10	-0.01
L9	1.02**	-7.04**	-0.50	1.53**	-0.42	-5.28**	-0.58**
L10	-0.11	13.26**	13.04**	-0.35	-1.17*	3.39**	1.29**
L11	-1.94**	-3.58	1.34	-0.81**	-2.88**	-1.90**	-0.32
L12	-0.15	12.88**	5.71**	-0.68**	-2.34**	1.18*	0.13
L13	-0.36	0.46	-8.96**	0.69**	1.03	-1.45*	0.15
L14	-3.19**	-22.24**	-18.33**	1.11**	1.03	-3.24**	-0.15
L15	0.93**	-2.83	-2.75	1.03**	1.58**	1.22*	-0.33
L16	-0.32	-1.99	4.92*	-0.77**	-1.67**	1.18*	-1.19**
Tester T1	1.16	-7.88**	-9.33**	0.09	-1.44**	0.57*	-0.42**
T2	0.38**	12.86**	10.21**	-0.64**	1.36**	0.59*	0.50**
T3	-1.54**	-4.98**	-0.89	0.55**	0.08	-1.16**	-0.08
Lines L.S.D gi 0.05	0.53	5.31	4.26	0.39	1.11	1.14	0.37
L.S.D gi 0.01	0.70	6.99	5.61	0.52	1.46	1.50	0.49
L.S.D gi - gj0.05	0.75	7.51	6.03	0.56	1.57	1.61	0.53
L.S.D gi-gj 0.01	0.99	9.88	7.93	0.74	2.07	2.12	0.69
Testers L.S.D gi 0.05	0.23	2.30	1.84	0.17	0.48	0.49	0.16
L.S.D gi 0.01	0.30	3.03	2.43	0.22	0.63	0.65	0.21
L.S.D gi - gj0.05	0.32	3.25	2.61	0.24	0.68	0.69	0.22
L.S.D gi-gj 0.01	0.43	4.28	3.43	0.32	0.89	0.92	0.30

*and** Significant at 0.05 and 0.01 levels of probability, respectively.

Also, the results revealed that L9, L13, L14 and L15 had significant GCA effects for number of rows/ear, while L8 and L15 for number of kernels/row. For 100 kernel weight, L1, L3, L10, L12, L15 and L16 were the best combiner. The results exhibited that the inbred lines L1, L2, L3, L4, L7 and L10 had significant and desirable values for grain yield. These inbred lines could be used in maize breeding programs to improve grain yield.

On the other side in Table 5, the results showed that the inbred line, Cim/z(T1) as a tester was the best combiner for short plant and short ear height. While, tester SC162(T2) had the best and significant values of general combining ability for number of kernels/row, 100 kernel weight and grain yield. The population Sk9(T3) as a tester was the best combiner for earliness and number of rows/ear. Significant GCA effect for grain yield and other traits in maize was also reported by several researchers such as [24, 25].

Specific combining ability effects. The estimates of SCA effects of F_1 top crosses for the studied traits across two locations are presented in Table 6. The results exhibited that the desirable SCA effects were obtained for the topcrosses L6xT3, L7xT2, L10xT1, L13xT2, L14xT1 and L15xT2 for earliness, L10xT3 for short plant, L3xT2 and L10×T3 for ear height.

The results showed that L2xT3 had significant desirable SCA effects value for number of rows/ear. For number of kernels/row, the best SCA effects values were for L2xT3, L3xT1, L6xT1 and L12xT2. Four topcrosses (L5xT1, L6xT3, L9xT2 and L12xT3) had significant desirable values of SCA effects for100 kernel weight. While five topcrosses (L3×T1, L6xT1, L6xT3, L10xT2 and L12xT2) had the best significant desirable values of SCA effects for grain yield.

These top crosses could be useful in the maize hybrid program. Analysis of specific combining ability (SCA) is important to screen the better inbred lines for hybrid improvement [9].

TABLE 6
Specific combining ability effects of F_1 top crosses for nine traits across two locations.

Top cross	Days to 50% silking	Plant height	Ear height	Number of rows/ear	Number of ker-nels/row	100ker-nels Weight	Grain yield
L1×T1	0.80	10.13*	6.03	-0.01	-0.93	-0.53	-0.32
×T2	-0.30	-4.48	-2.13	0.22	0.01	1.33	0.32
×T3	-0.50	-5.65	-3.90	-0.21	0.92	-0.80	000
L2×T1	-0.33	-0.16	-3.26	-0.18	-0.18	-0.15	-0.16
×T2	-0.17	-5.53	-0.30	-0.94**	-1.99*	1.08	0.05
×T3	0.50	5.68	3.55	1.12**	2.17*	-0.93	0.11
L3×T1	0.51	-5.66	2.49	0.07	2.23*	1.18	0.69*
×T2	0.16	-0.90	-7.42*	0.06	-2.57**	-0.21	0.51
×T3	-0.67	6.56	4.93	-0.13	0.34	-0.97	-1.21**
L4×T1	-0.70	2.55	-1.47	-0.22	-0.68	1.51	-0.13
×T2	0.08	0.56	1.87	0.27	0.64	0.00	0.25
×T3	0.63	-3.11	-0.40	-0.05	0.05	-1.51	-0.12
L5×T1	-0.58	1.51	1.12	-0.18	-0.23	2.18*	0.63
×T2	0.20	0.89	2.70	0.43	0.34	-0.21	-0.86**
×T3	0.38	-2.40	-3.82	-0.26	-0.12	-1.97*	0.23
L6×T1	-0.08	-3.03	-1.97	-0.05	2.15*	-1.07	0.72*
×T2	1.83**	-3.53	-3.38	0.43	-3.03**	-2.46*	-2.01**
×T3	-1.75**	6.56	5.35	-0.38	0.88	3.53**	1.30**
L7×T1	1.01*	-3.33	2.08	0.07	-0.23	1.72	-0.23
×T2	-0.96*	-1.57	-4.96	-0.32	0.72	-0.67	0.46
×T3	-0.04	4.89	2.89	0.24	-0.49	-1.05	-0.23
L8×T1	0.01	10.72*	0.95	0.24	-0.10	0.39	-.031
×T2	0.66	-4.15	-0.21	-0.28	0.97	1.00	0.03
×T3	-0.67	-6.57	-0.74	0.04	-0.87	-1.39	0.28
L9×T1	0.05	-8.28	-5.92	0.36	-2.43*	-0.74	-0.18
×T2	-0.30	-1.78	-3.96	-0.53	1.39	2.00*	-0.28
×T3	0.25	10.06*	9.89**	0.16	1.05	-1.26	0.13
L10×T1	-0.95*	-0.33	-1.22	-0.39	0.82	0.97	0.60
×T2	-0.30	10.56*	10.87**	0.10	0.76	-0.17	1.37**
×T3	1.25**	-10.23*	-9.65*	0.29	-1.58	-0.80	-1.97**
L11×T1	-0.37	-1.99	-0.26	0.45	0.65	0.14	0.003
×T2	0.04	3.52	4.08	0.18	0.09	-1.50	-0.26
×T3	0.33	-1.52	-3.82	-0.63	-0.74	1.36	0.25
L12×T1	0.09	-2.70	-2.51	-0.55	-0.89	-1.95	-1.03**
×T2	-0.26	-1.69	0.83	0.43	2.18*	-0.09	0.76*
×T3	0.17	4.39	1.68	0.12	-1.28	2.03*	0.26
L13×T1	1.05*	2.84	3.41	0.45	-0.39	-2.57*	-0.63
×T2	-1.05*	4.47	0.12	0.06	-0.32	1.54	0.05
×T3	0.00	-7.32	-3.53	-0.51	0.72	1.03	0.58
L14×T1	-0.99*	-4.08	-0.47	-0.09	-0.14	-0.65	0.55
×T2	1.41**	3.81	2.62	0.02	0.43	-0.04	-0.23
×T3	-0.42	0.27	-2.15	0.08	-0.28	0.70	-0.32
L15×T1	0.51	2.76	1.45	-0.14	1.07	-1.24	-0.13
×T2	-0.96*	-2.11	-0.96	0.10	0.51	0.37	0.11
×T3	0.46	-0.65	-0.49	0.04	-1.58	0.86	0.02
L16×T1	0.01	-0.95	-0.47	0.16	-0.68	0.80	-0.05
×T2	-0.09	1.93	0.24	-0.23	-0.11	-1.96	-0.28
×T3	0.08	-0.98	0.22	0.08	0.80	1.16	0.33
L.S.Dsij 0.05	0.92	9.20	7.38	0.69	1.93	1.97	0.64
L.S.Dsij 0.01	1.22	12.11	9.71	0.90	2.54	2.60	0.85
L.S.Dsij –skl 0.05	1.31	13.01	10.44	0.97	2.72	2.79	0.91
L.S.Dsij –skl 0.01	1.72	17.13	13.74	1.28	3.58	3.68	1.20

*and** Significant at 0.05 and 0.01 levels of probability, respectively.

TABLE 7
Estimates of heterotic groups using specific and general combining ability (HSGCA method) for grain yield across two locations.

Inbred line	T1 (Cim/z)	T2 (SC162)	T3 (Pop Sk9)
L1	0.07	0.71	0.39
L2	0.33	0.54	0.60
L3	1.10	0.92	-0.80#
L4	0.25	0.63	0.26
L5	0.58	-0.91#	0.18
L6	-0.43	-3.16#	0.15
L7	0.35	1.04	0.35
L8	-0.32#	0.02	0.27
L9	-0.76	-0.86#	-0.07
L10	1.89	2.67	-0.68#
L11	-0.31	-0.57#	-0.07
L12	-0.91#	0.89	0.39
L13	-0.47#	0.20	0.73
L14	0.39	-0.38	-0.47#
L15	-0.43#	-0.22	-0.31
L16	-1.24	-1.46#	-0.86

means that this inbred line belongs to tester group.

Heterotic groups. Estimates heterotic groups specific and general combining ability effects (HSGCA) for grain yield are presented in Table 7. According to [16], the heterotic group specific and general combining ability (HSGCA) method was used to classify the inbred lines into groups according to the following; Step1, place all inbred lines (the 16 inbred lines) in the same heterotic group as their tester. Step 2, kept the inbred line with the heterotic group, where its HSGCA effects had the smallest value (or largest negative value) and it removed from other heterotic groups. Step 3, if the inbred line had positive HSGCA effect with all representative testers, it will be cautious to assign that line to any heterotic group because the line might belong to a heterotic group different from the testers used in the investigation.

For grain yield, there were three groups as follows. Group 1 (tester Cim/z): which contained four inbred lines (Gz666, Sk5003, k5010 and Sk5007), Group 2 (tester SC162): which contained five inbreed lines (Sk11, Gz639, Gm1004, Hp704 and Sk8008) , Group 3 (tester Pop Sk9): which contained three inbreed lines (SkD4, Gm1021 and Sk5011) and The method was not able to classify four inbred lines (Sk2, Sk3, Sk10 and Gz658).

The above results could be used in breeding program in selecting the best parents for making crosses. A heterotic group is a collection of closely related inbred lines which tend to result in vigorous hybrids when crossed with lines from a different heterotic group, but not when crossed to other lines of the same heterotic group [28]. GCA and SCA are essential under different conditions because under each conditions specific combiners were significant [8]. In selection followed by hybridization, GCA and SCA are essential; because GCA impacts are due to preponderance of genes with additive effects and SCA indicates predominance of genes with no additive effects [29, 8]. Although, both of GCA and SCA impacts are dependent on germplasm set assessment and the specific conditions sampling, so it mightn't be generalized application [30, 8].

CONCLUSION

From the mentioned results it could be reported that the additive gene effects were most responsible for controlling the inheritance of all traits except for grain yield. The tester SC162 behaved as an excellent combiner for most studied traits. Five three way crosses (L1xT2, L3xT2, L7xT2, L10xT2 and L12xT2) were significantly superior than the check TWC360. The inbred L10 exhibited good general combiner for grain yield. The TWC L10× T2 exhibited the highest SCA effects and suitable combination for grain yield. The resulting three heterotic groups could be used in breeding program for selecting the best parents in making crosses.

REFERENCES

[1] Majid, M.A., Saiful Islam, M., EL Sabagh, A., Hasan, M.K., Barutcular, B., Ratnasekera, D. and Islam, M.S. (2017a) Evaluation of growth and yield traits in corn under irrigation regimes in sub-tropical climate. Journal of Experimental Biology and Agricultural Sciences. 5(2), 143-150.

[2] Majid, M.A., Saiful Islam, M., EL Sabagh, A., Hasan, M.K., Saddam, M.O., Barutcular, C., Ratnasekera, D., Abdelaal, Kh.A.A. and Islam, M.S. (2017b) Influence of varying nitrogen levels on growth, yield and nitrogen use efficiency of hybrid maize (*Zea mays* L.). Journal of Experimental Biology and Agricultural Sciences. 5(2), 134-142.

[3] El Sabagh, A., Barutçular, C., Islam, M.S. (2017) Relationships between stomatal conductance and yield under deficit irrigation in maize (*Zea mays* L.). Journal of Experimental Biology and Agricultural Sciences. 5(1), 15-21.

[4] Bello, O.B., Abdulmaliq, S.Y., Afolabi, M.S. and Lag, S.A. (2010) Correlation and path coefficient analysis of yield and agronomic characters among open pollinated maize varieties and their F_1 hybrids in a diallel cross. African Journal of Biotechnology. 9, 2633-2639.

[5] Abdelaal, Kh.A.A, Hafez, Y.M., El Sabagh, A., Saneoka, H. (2017) Ameliorative effects of abscisic acid and yeast on morpho-physiological and yield characters of maize (*Zea mays* L.) plants under water deficit conditions. Fresen. Environ. Bull. 26, 7372-7383.

[6] Sprague, G.F. and Tatum, L.A. (1942) General vs specific combining ability in single crosses of corn. Journal of American Society of Agronomy. 34, 923-932.

[7] Aly, R.S.H. (2013) Relationship between combining ability of grain yield and yield components for some newly yellow maize inbred lines via Line × Tester analysis. Alexandria J. Agricultural Research Egypt. 58, 115-124.

[8] Majid, S., Rajab, C., Eslam, M. and Farokh, D. (2010) Estimation of combining ability and gene action in maize using Line × Tester method under three irrigation regimes. Journal of Research and Applied Science. 6, 19-28.

[9] Abrha, S.W., Zeleke, H.Z. and Gissa, D.W. (2013) Line×tester analysis of maize inbred lines for grain yield and yield related traits. Asian J. Plant Sci. Res. 3(5), 12-19.

[10] Noëlle, M.A.H., Richard, K., Vernon, G., Martin, Y.A., Laouali, M.N., Liliane, T.N. and Godswill, N.N. (2017) Combining ability and gene Action of tropical Maize (Zea mays L.) inbred lines under low and high nitrogen conditions. Journal of Agricultural Science. 9, 222-235.

[11] Hassan, M.A., El-Shenawy, A.A., Abo El-Haress, S.M. and Khalil, M.A.G. (2016) Combining ability of new yellow maize inbred lines for earliness and grain yield. Egyptian Journal of Plant Breeding. 20, 353- 362.

[12] Mosa, H.E., Abo El-Hares, S.M. and Hassan, M.A.A. (2017) Evaluation and classification of maize inbred lines by Line x Tester analysis for grain yield, late wilt and downy mildew resistance. Journal of Plant Production, Mansoura University, Egypt. 8, 97-102.

[13] Mosa, H.E. (2010) Estimation of combining ability of maize inbred lines using top cross mating design. Journal of Agricultural Research. Kafrelsheikh University, Egypt. 36, 1-16.

[14] Melchinger, A.E. and Gumber, R.K. (1998) Overview of heterotic groups in agronomic crops. In: Lamkey, K.R. and Staub, J.E. (Eds.) concepts and breeding of heterosis in crop plants. CSSA, Madison, W.I., USA. 29-44.

[15] Meena, A.K., Gurjar, D., Patil, S.S. and Kumhar, B.L. (2017) Concept of Heterotic Group and its Exploitation in Hybrid Breeding. International Journal of Current Microbiology and Applied Sciences. 6(6), 61-73.

[16] Fan, X.M., Zhang, Y.M., Yao, W.H., Chen, H.M., Tan, T., Xu, C.X., Han, X.L., Luo, L.M. and Kang, M.S. (2009) Classifying maize inbred lines into heterotic group using a factorial mating design. Agronomy Journal. 101, 106-112.

[17] Akinwale, R.O., Badu-Apraku, B., Fakorede, M.A.B. and Vroh-Bi, I. (2014) Heterotic grouping of tropical early-maturing maize inbred lines based on combining ability in Striga-infested and Striga-free environments and the use of SSR markers for genotyping. Field Crops Res. 156, 48-62.

[18] Kempthorne, O. (1957) An Introduction to Genetic Statistics. John Wiley & Sons Inc., New York, U.S.A.

[19] Snedecor, G.W. and Cochran, W.G. (1967) Statistical methods. 6th ed. Iowa State University press, Ames., Iowa, USA.

[20] Amer, E.A., El-Shenawy, A.A. and Motawei, A.A. (2003) Combining ability of new maize inbred lines *via* line x tester analysis. Egyptian Journal of Plant Breeding. 7, 229-239.

[21] Motawei, A.A. (2011) Combining ability of some prolific and non-prolific maize inbred lines for grain yield and other related traits. Journal of Agricultural Research, Kafrelsheikh University, Egypt. 37, 26-42.

[22] Abo El-Haress, S.M. (2015) Evaluation of new single and three way crosses for earliness and grain yield over three locations. Annals of Agricultural Science, moshtohor, Egypt. 53, 17-24.

[23] Abo El-Haress, S.M., El-Shenawy, A.A. and Hassan, M.A.A. (2016) Yellow maize inbred lines evaluation through line x tester analysis. Egyptian Journal of Plant Breeding. 20, 317-325.

[24] Amin, M.N., Amiruzzaman, M., Ahmed, A., and Ali, M.R. (2014) Evaluation of inbreed lines of maize (Zea mays L.) through Line × Tester method. Bangladesh J. Agril. Res. 39(4), 675-683

[25] El-Hosary, A.A.A. (2014) Relative values of three different testers in evaluating combining ability of new maize inbred lines. International Journal of Plant Breeding and Genetics. 8, 57-65.

[26] Motawei, A.A., Khalil, M.A.G., Hassan, M.A.A. and Amer, E.A. (2016) Superiority over check variety and combining ability based on line×tester analysis in maize. Egyptian Journal of Plant Breeding. 20, 341-352.
[27] Silva, J.C. and Hallauer, A.R. (1975) Estimation of epistatic variance in Iowa stiff stalk synthetic maize. Journal of Heredity. 66, 290-296.
[28] Lee, M. (1995) DNA markers and plant breeding programs. Advanced Agronomy. 35, 265-344.
[29] Kenga, R., Alabi, S.O. and Gupta, S.C. (2004) Combining ability studies in tropical sorghum (sorghum bicolor L. Moench). Field Crop Research. 88, 251-260.
[30] Falconer, D.S., Mackay, T.F.C. (1996) Introduction to quantitative Genetics. 4th Ed. Longman Group Ltd. Harlow, England.

Received: **10.02.2018**
Accepted: **05.04.2018**

CORRESPONDING AUTHOR

Mosa Sayed Rizk
Maize Research Department,
Field Crops Research Institute,
Agricultural Research Center,
Kafrelsheikh – Egypt

e-mail: mosasayed88@yahoo.com

© by PSP Volume 27 – No. 7/2018 pages 4995-5000 Fresenius Environmental Bulletin

CHEMICALLY INDUCED OXIDATIVE STRESS DECREASES HOMOLOGOUS RECOMBINATION RATE AND *REC12* GENE EXPRESSION IN THE FISSION YEAST

Deniz Yilmaz[1], Merve Yilmazer[2], Tayfun Tumkaya[3,4], Semian Karaer-Uzuner[2,*]

[1]Program of Molecular Biology and Genetics, Institute of Graduate Studies in Science and Engineering, Istanbul University, Istanbul, Turkey
[2] Department of Molecular Biology and Genetics, Faculty of Science, Istanbul University, Istanbul, Turkey
[3]Institute for Molecular and Cell Biology, A*STAR, 138673, Singapore
[4] Department of Physiology, National University of Singapore, 138673, Singapore

ABSTRACT

Homologous recombination plays an important role in maintaining the genome stability of prokaryotic and eukaryotic organisms. In this study, *rec12* gene expression and alterations in homologous recombination frequency were investigated under H_2O_2 and $CuSO_4$ induced oxidative stress in the unicellular, eukaryotic model organism, *Schizosaccharomyces pombe*.

In order to increase the recombination frequency, *Schizosaccharomyces pombe* mutant strains that possess distant located genes on the same chromosome were chosen and crossbred. The zygotes were treated with oxidative stress inducing $CuSO_4$ and H_2O_2. After the stress treatments, alterations in homologous recombination were investigated by using random spore analysis. Moreover, *Schizosaccharomyces pombe rec12* gene expression was analyzed with real-time PCR. We observed that the H_2O_2 and $CuSO_4$ stress treatments decrease both *rec12* gene expression and homologous recombination frequency in the fission yeast.

KEYWORDS:
Fission yeast, homologous recombination, *rec12*, H_2O_2 stress, $CuSO_4$ stress, oxidative stress, chemical stress

INTRODUCTION

Gene expression regulation is one of the crucial mechanisms by which organisms respond to alterations in pH, osmolarity, temperature, and harmful toxins in their environment. This regulation leads to an increase in the stress protein levels and decrease in non-essential cellular activities. The reduction in the non-essential cellular activity permits cellular resources to be conserved for adapting to the stress conditions, as well as repairing the damaged macromolecules [1].

Transition metals are important in facilitating many biological processes due to their ability to donate and accept electrons, iron, copper, and manganese. For example, transitions metals those are prosthetic groups of proteins can catalyze redox reactions. Nevertheless, excessive amounts of these metal ions can be toxic to cells [2]. A transitive metal, copper (Cu^{2+}), which serves as a cofactor to several enzymes, has been reported to cause extensive damage in microorganisms in high concenterations. Copper (Cu^{2+}) can react with superoxide anion (O_2^-) and hydrogen peroxide (H_2O_2); this reaction results in hydroxyl free radical (OH^-) release. Hydroxyl free radical (OH^-) is one of the reactive oxygen species (ROS), and can cause damage to various cellular macromolecules either directly – by oxidizing carbohydrates, amino acids, phospholipids, and nucleic acids – or indirectly [3, 4].

Reactive oxygen species (O_2^-, OH^-, H_2O_2) are produced during the aerobic growth mostly as a consequence of electron transfer in the mitochondrial membrane. A set of cellular defense mechanisms scavenge O_2^- and H_2O_2, so that a balance between production and detoxification is accomplished, and a non-toxic, steady-state is reached [5].

Homologous recombination is necessary for the recovery of the cells from oxidative stress [6]. Homologous recombination refers to the interaction of DNA sequences with homology and plays an essential role in the maintenance of genome stability in prokaryotic and eukaryotic organisms by (1) repairing double-strand breaks (DSBs), (2) repairing single-strand gaps that are caused by replication fork collapse or DNA-damaging agents. Homologous recombination is also vital in meiosis for establishing a physical connection between homologous chromosomes [7].

In *Schizosaccharomyces pombe* (*S. pombe*), both meiotic recombination and DNA breakage are regulated by rec6, rec7, rec12, rec14, and rec15 proteins; thus, breakage and recombination are biologically linked [8, 9]. The fission yeast rec12 protein catalyzes double-strand DNA (dsDNA) breaks that initiate recombination [10, 11]. Rec12 protein and its active site tyrosine are important for crossover recombination. In meiosis, catalytically-active rec12 is required for normal chiasmatic segregation, while catalytically-inactive rec12 protein facilitates achiasmatic segregation. Moreover, rec12 and its active

site tyrosine are necessary for proper equational chromosome segregation during Meiosis II [10].

S. pombe is an eukaryotic uni-cellular organism and ascomycete yeast that is often known as "fission yeast". The defining characteristic of this phylum is that sexual spores are formed inside a saclike structure called "ascus" [12]. Only after nutritional depletion, especially of a nitrogen source, zygotes are formed if partners are present of the opposite mating type [13]. *S. pombe* has been an important model organism in cell cycle regulation, sexual differentiation, chromosome dynamics, and polarized cell growth studies [14]. Furthermore, the fission yeast has also been used to understand the transition between the vegetative and sexual life cycles [15].

In this study, we investigated how H_2O_2 and $CuSO_4$ induced oxidative stress affects the *rec12* gene expression and homologous recombination rate in *S. pombe*. The gene expression was analyzed by using real-time PCR, while random spore analysis was performed to determine the differences in recombination frequencies. To spot any morphological changes on the asci, we utilized fluorescence microscopy techniques. Here, we report that chemically-induced oxidative stress reduces both *rec12* expression level and homologous recombination frequency in the fission yeast.

MATERIALS AND METHODS

Strains and growth conditions. *S. pombe* *972h*$^-$ and *975h*$^+$ wild-type strains; and *ura4h*$^-$, *ura3h*$^-$, *ade2h*$^+$, and *ade5h*$^+$ mutant strains were grown in standard rich media (YEA), minimal media (MMA), and sporulation media (SPA) as recommended by Gutz et al. [16] and Leopold et al. [17].

Stress conditions and crossbreeding. Stress conditions have been described in Table 1, and crossing scheme has been shown in Table 2.

Sporulation media was used for crossbreeding. After crossing, cultures were kept in a 25˚C incubator for 2 days for RNA isolation, and 21 days for random spore analysis.

Random spore analysis and fluorescent microscopy. Crossed strains (Table 2) were incubated for 21 days at 25°C. Samples were collected with distilled water. Then, 1 ml of the cell culture was mixed with 3 ml of absolute ethanol and 6 ml of distilled water and kept at 18°C for 20 minutes to kill the vegetative cells. Later, mixtures were diluted enough to be counted on a spread plate, both YEA (dilution factor 1:1000) and MMA (dilution factor 1:100), and were incubated at 30°C for 5 days.

TABLE 1
Stress conditions and duration of exposures.

Stress Condition	Duration of Exposure
Control Sample	-
0.5 M $CuSO_4$	60 minutes
1 mM H_2O_2	15 minutes

TABLE 2
Crossing scheme.

Crossing of strains
972 h$^-$ x *975 h*$^+$
ura4h$^-$ x *ade5h*$^+$
ura3h$^-$ x *ade2h*$^+$

As for the flourescent microscopy, stressed and crossbred strains were collected and fixed by using alcohol, following Forsburg and Rhind [18] method. DAPI (4',6-diamidino-2-phenylindole, Roche) stain was used, and ascus/zygote pictures were taken with an Olympus BX53F flourescent microscope.

RNA isolation and cDNA synthesis. Total RNA isolation was performed using Roche High Pure RNA Isolation Kit, according to manufacturer's instructions. Before using the kit, the cells were mechanically homogenized by shaking rigorously together with glass beads and Phosphate-Buffered Saline (PBS). Subsequently, isolated RNAs were converted to cDNA by Roche Transcriptor First Strand cDNA Synthesis Kit, according to manufacturer's instructions.

TABLE 3
***Rec12* primers.**

		Primers	G+C Ratio %	T_M ˚C	Product length (bp)
rec12	Forward	5'-CAAACCGTAGTCGATGAG -3'	50	57	155
	Reverse	5'- GGACCCAAATACCAATCC -3'	50	57	

TABLE 4
***Act1* primers [19].**

		Primers	G+C Ratio %	T_M ˚C	Product length (bp)
act1	Forward	5'- AGATTCTCATGGAGCGTGGT-3'	50	56,1	100
	Reverse	5' - TCAAAGTCCAAAGCGACGTA -3'	45	54,2	

Primer designs for *rec12* gene and gene expression analysis with Real-Time PCR. The sequence of *rec12* gene was obtained from NCBI database, and primers were selected based on the suggestions of PrimerQuest Tool software (Table 3). Primers were synthesized by Invitrogen.

The changes in mRNA levels of gene after the stress treatments were investigated by using Real-Time PCR, in which *S. pombe* actin primers used as the housekeeping genes (Table 4) and SYBR Green I used as the fluorescent marker. The reaction was performed in the Light Cycler 480 (Roche) instrument. The cDNAs from samples and the primers were added LightCycler 480 SYBR Green I Master (Roche), according to manufacturer's instructions.

RESULTS

$CuSO_4$ and H_2O_2 treatments decrease homologous recombination frequency. To investigate the effects of the chemically-induced oxidative stress on recombination, we tested two different crossbred strains' (*ura4h⁻ x ade5h⁺ and ura3h⁻ x ade2h⁺*) homologous recombination frequencies by using random spore analysis. Our results show that 0.5 M $CuSO_4$ treatment decreases the recombination rates by 34% in the *ura4h⁻ x ade5h⁺* strain, and 45% in the *ura3h⁻ x ade2h⁺* strain, compared to the respective controls (Table 5). The other stress treatment, 1 mM H_2O_2, reduces the recombination frequency by 13% in the *ura4h⁻ x ade5h⁺* strain, and 47% in the *ura3h⁻ x ade2h⁺* strain (Table 5).

***rec12* gene expression diminished upon stress treatments.** Given that the Rec12 protein is known to initiate homologous recombination by deploying double strand DNA breaks (dsDSBs), we probed the *rec12* gene expression levels by using real-rime PCR, which compares relative *rec12* mRNA levels to *actin* mRNA levels. Our analysis showed that 0.5 M $CuSO_4$ treatment decreased the *rec12* expression dramatically: ~50% in *ura4h⁻ x ade5h⁺*, and ~35% in the *ura3h⁻ x ade2h⁺* crossing (sample A and C, respectively, Figure 1). As for the 1mM H_2O_2 treatment, the *rec12* expression was reduced by ~35% in both of the strains (sample B and D, respectively, Figure 1).

TABLE 5
$CuSO_4$ and H_2O_2 treatments reduce homologous recombination frequency in both *ura4h⁻ x ade5h⁺* and *ura3h⁻ x ade2h⁺* strains.

Crossbreds	Stress treatment	Homologous recombination frequency (%)	Relative recombination frequency change
ura4h⁻ x ade5h⁺	control	38	-
ura4h⁻ x ade5h⁺	0.5 M $CuSO_4$	25	-34%
ura4h⁻ x ade5h⁺	1 mM H_2O_2	33	-13%
ura3h⁻ x ade2h⁺	control	36	-
ura3h⁻ x ade2h⁺	0.5 M $CuSO_4$	20	-44%
ura3h⁻ x ade2h⁺	1 mM H_2O_2	19	-47%

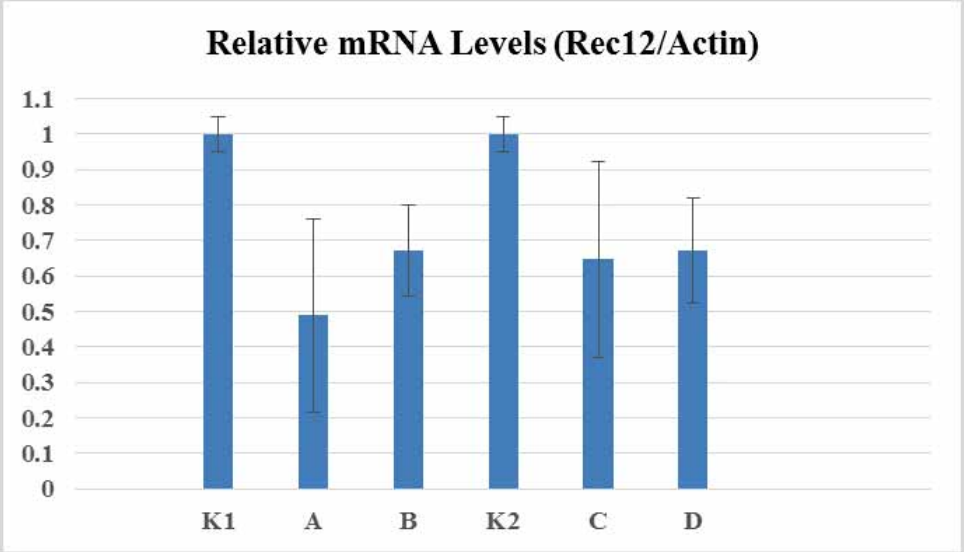

FIGURE 1
***Rec12* gene relative mRNA levels are reduced by stress treatment. (K1: *ura4h⁻ x ade5h⁺* control, A: *ura4h⁻ x ade5h⁺* 0.5 M $CuSO_4$ treatment, B: *ura4h⁻ x ade5h⁺* 1 mM H_2O_2 treatment, K2: *ura3h⁻ x ade2h⁺* control, C: *ura3h⁻ x ade2h⁺* 0.5 M $CuSO_4$ treatment, D: *ura3h⁻ x ade2h⁺* 1 mM H_2O_2 treatment.)**

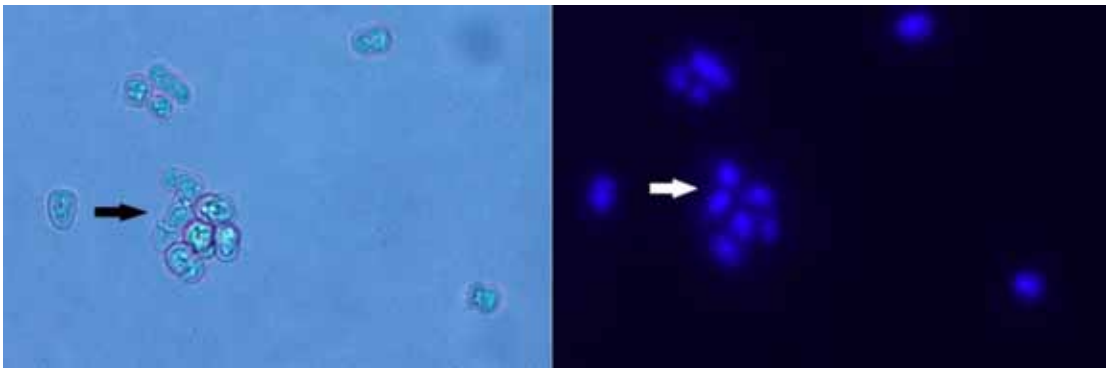

FIGURE 2
The morphological analysis of *ura4h⁻ x ade5h⁺* crossing treated with 0.5 M $CuSO_4$ to detect changes in ascus shape under visible and fluorescent lights.

***ura4h⁻ x ade5h⁺* strain developed morphological anomalies.** We observed morphological anomalies in *ura4h⁻ x ade5h⁺* crossing asci (1%) that were exposed to 0.5 M $CuSO_4$ (Figure 2). Other crossings and treatment conditions did not exhibit any kind of irregularities.

As mentioned before, tyrosine residue in the active site of the rec12 protein is important for crossover recombination. In order to examine its importance, we crossbred the cells in two different media: one including 50 mg/L tyrosine SPA, the other is the regular SPA. SPA with tyrosine had 11/200 ascus/vegetative cell ratio comparing to 3/200 of the regular SPA media (data not shown).

DISCUSSION

Developmental defects such as abnormal spore placement, decreased number of spores, and abnormal spore formation are frequently observed in *rec12* mutants. It has been reported that such phenotypes occur due to a disruption in Meiosis II. Spore formation of *S. pombe* is controlled by spindle pole body in Meiosis II [10]. *Rec12* is directly related to nucleosomes, and histone modifications are thought to alter chromatin-Spo11 / Rec12 interactions [20]. Mallela et al. [21] showed that *rec12* mutants have reduction in the survival rate of their spores. To date, studies on wild-type *S. pombe* showed that the cells are more resistant to hydrogen peroxides (Menadion, 1-chloro-2,4-dinitrobenzene etc.) than any other stress factors, due to the fact that hydrogen peroxide molecules can be efficiently decomposed by the catalase enzyme [22].

Chen et al. [23] investigated the effects of H_2O_2 treatment in three concentrations (low: 0.07 mM, medium: 0.5 mM, and high: 6 mM) on the fission yeast, and they found that the gene expression profile is readjusted as a response. It was reported that the expression of more than 3000 genes has changed in at least one dose of hydrogen peroxide; approximately 150 genes were induced at all the three doses. The gene expression responses in medium and high H_2O_2 cells remained almost identical; however, changes in transcript levels were peaked at the medium concentration. They reasoned that it was because cellular regulatory mechanisms were damaged due to the overexposure. Mortality rates of the cells were 67% in the high dose and 22% in the medium dose. An increase in the formation of superoxide radicals was identified in H_2O_2-treated cells, and it was suggested that the damage initiated by H_2O_2 causes further damage with the formation of superoxide radical [24].

Almost all living cells need copper (Cu^{+2}) for some biological processes, such as iron transportation, oxidative stress protection, hormone production, blood coagulation, and cell growth [25].

Copper (Cu^{+2}) metal is an integral part of enzymes that are vital and play a role in many biological processes. Copper, normally bound to proteins, can also be in free form to catalyze hydroxyl radicals. *In vivo* and *in vitro* studies show that copper causes oxidative damage and affects important cellular events. When copper is applied at high concentrations, it causes oxidative damage to lipids, proteins, and DNA, leading to neurodegenerative diseases [26].

Copper metabolism of *S. pombe* is less studied than *S. cerevisiae*. The fission yeast responds much quicker to copper stress in lower concentrations compared to *S. cerevisiae* [27]. Copper uptake in *S. pombe* is necessary for copper and copper-dependent proteins to function. Thus, in case of copper deficiency, the alterations in meiosis and the gene expression profile of copper transporters are examined [28].

In this study, *S. pombe* cells were exposed to stress conditions of H_2O_2 and $CuSO_4$, and the recombination frequencies were analyzed by using random spore analysis method. It was observed that the cells exposed to 0.5 M $CuSO_4$ stress had the most dramatic reduction in the recombination frequency. In a study conducted by Chen et al. in 2008 [23], it was determined that the cells exposed to 1 mM H_2O_2 stress, which is considered medium-low, had a higher recombination frequency than 0.5 M $CuSO_4$

stress.

Physiological differences in some of the *ura4h*$^-$ x *ade5h*$^+$ *S. pombe* strains treated with 0.5 M $CuSO_4$ stress (1%) were observed under fluorescence microscope as well. In studies conducted by Sharif et al. in 2002 [10], developmental defects were frequently observed in the *rec12* mutants.

Environmental conditions which require adaptation, such as stress, have always been important research subject to understand how these conditions affect the organisms, and how they respond to these conditions. Whether organisms respond to the alterations in their natural habitats in a cellular level has always been a curious question. The stress factors we have chosen have been studied in different groups of organisms, including yeast; and in this study we aimed to illuminate the cellular response to these conditions. When mutations occur in some *S. pombe* genes related to recombination (*rec13* and *rec17-rec21*), a decrease in the meiotic recombination frequency has been observed [29]. As our real-time PCR analysis show the expression of the *rec12* gene decreased, as well as the recombination frequency. As a result, gene expression and homologous recombination of the *rec12* gene are both reduced and affected by chemically-induced oxidative stress.

Taking PubMed as a reference, there are not enough publications on $CuSO_4$ stress condition in yeast -162 articles, of which only 3 are in *S. pombe*. Our study contributes to the research on $CuSO_4$ stress in the fission yeast, and gives insight into how copper-related stress influences homologous recombination. We hope that our study helps in understanding oxidative stress responses in the eukaryotic cells.

ACKNOWLEDGEMENTS

This research was funded by the Scientific Research Project Coordination Unit of Istanbul University, Project No: 48846.

REFERENCES

[1] Reiter, W., Watt, S., Dawson, K., Lawrence, C.L., Bahler, J., Jones, N. and Wilkinson, C.R.M. (2008) Fission yeast MAP Kinase Sty1 is recruited to stress-induced genes. J Biol Chem. 283(15), 9945–9956.

[2] De Freitas, J., Wintz, H., Kim, J.H., Poynton, H., Fox, T. and Vulp, C. (2003) Yeast, a model organism for iron and copper metabolism studies. BioMetals. 16(1), 185–197.

[3] Halliwell, B. and Gutteridge, J.M.C. (1989) Free Radicals in Biology and Medicine. 2nd Edition, Oxford Science Publications, Clarendon.

[4] Ikner, A. and Shiozaki, K. (2005) Yeast signaling pathways in the oxidative stress response. Mutat Res-Fund Mol M. 569(1), 13-27.

[5] Paulo, E., García-Santamarina, S., Calvo, I.A., Carmona, M., Boronat, S., Domènech, A., Ayté, J. and Hidalgo, E. (2014) A genetic approach to study H2O2 scavenging in fission yeast – distinct roles of peroxiredoxin and catalase. Mol Microbiol. 92(2), 246–257.

[6] Hayashi, M., and Umezu, K. (2017) Homologous recombination is required for recovery from oxidative DNA damage. Genes and genetic systems. 92(2), 73-80.

[7] Krogh, B.O. and Symington, L.S. (2004) Recombination proteins in yeast. Annu Rev Genet. 38(2004), 233-271.

[8] Davis, L. and Smith, G.R. (2001) Meiotic recombination and chromosome segregation in *Schizosaccharomyces pombe*. P Natl Acad Sci Usa. 98(15), 8395–8402.

[9] 9. Young, J.A., Schreckhise, R.W., Steiner, W.W. and Smith, G.R. (2002) Meiotic recombination remote from prominent DNA break sites in *S. pombe*. Mol Cell. 9(2), 253-263.

[10] Sharif, W.D., Glick, G.G., Davidson, M.K. and Wahls, W.P. (2002) Distinct functions of S. pombe Rec12 (Spo11) protein and Rec12-dependent crossover recombination (chiasmata) in meiosis I; and a requirement for Rec12 in meiosis II. Cell & Chromosome. 1(1), 1.

[11] DeWall, K.M., Davidson, M.K., Sharif, W.D., Wiley, C.A. and Wahls, W.P. (2005) A DNA binding motif of meiotic recombinase Rec12 (Spo11) defined by essential glycine-202, and persistence of Rec12 protein after completion of recombination. Gene. 356(2005), 77-84.

[12] Hoffman, C.S., Wood, V. and Fantes, P.A. (2015) An ancient yeast for young geneticists: A primer on the Schizosaccharomyces pombe model system. Genetics. 201(2), 403-423.

[13] Egel, R. (2004) The molecular biology of Schizosaccharomyces pombe: Genetics, genomics and beyond. Springer Science and Business Media. 1st ed. Springer-Verlag Berlin Heidelberg.

[14] Lundblad, V. and Struhl, K. (2008) Yeast. In: Ausubel, F.M., Brent, R., Kingston, R.E., Moore, D.D., Seidman, J.G., Smith, J.A., Struhl, K. (eds.) Current Protocols in Molecular Biology. John Wiley and Sons, Chapter 13.

[15] Hayles, J. and Nurse, P. (2016) Introduction to fission yeast as a model system. Cold Spring Harbor Protocols. Cold Spring Harbor Protoc. Chapter 1. 2016(8).

[16] Gutz, H., Heslot, H., Leupold, U. and Loprieno, N. (1974) *Schizosaccharomyces pombe*. In Bacteria, Bacteriophages, and Fungi. Springer, Boston, MA, 395-446.

[17] Leupold, U. (1970) Genetical methods for Schizosaccharomyces pombe. In: Prescott DM, editor. Methods in Cell Physiology. Volume 4, NY, USA: Academic Press, 169-177.
[18] Forsburg, S.L. and Rhind, N. (2006) Basic methods for fission yeast. Yeast. 23(3), 173-183.
[19] Palabiyik, B., Kig, C., Pekmez, M., Dalyan, L., Arda, N. and Temizkan, G. (2012) Investigation of the relationship between oxidative stress and glucose signaling in Schizosaccharomyces pombe. Biochemical genetics. 50(5-6), 336-349.
[20] Acquaviva, L., Székvölgyi, L., Dichtl, B., Dichtl, B.S., Saint André, C.D.L.R., Nicolas, A., and Géli, V. (2013) The COMPASS subunit Spp1 links histone methylation to initiation of meiotic recombination. Science. 339(6116), 215-218.
[21] Mallela, S., Latypov, V. and Kohli, J. (2011) Rec10-and Rec12-independent recombination in meiosis of Schizosaccharomyces pombe. Yeast. 28(5), 405-421.
[22] Mutoh, N., Kawabata, M. and Kitajima, S. (2005) Effects of four oxidants, menadione, 1-chloro-2, 4-dinitrobenzene, hydrogen peroxide and cumene hydroperoxide, on fission yeast *Schizosaccharomyces pombe*. J Biochem. 138(6), 797- 804.
[23] Chen, D., Wilkinson, C.R., Watt, S., Penkett, C.J., Toone, W.M., Jones, N. and Bähler, J. (2008) Multiple pathways differentially regulate global oxidative stress responses in fission yeast. Mol Biol Cell. 19(1), 308-317.
[24] Perrone, G.G., Tan, S. and Dawes, I.W. (2008) Reactive oxygen species and yeast apoptosis. Biochim Biophys Acta. 1783(7), 1354–1368.
[25] Puig, S. and Thiele, D.J. (2002) Molecular mechanisms of copper uptake and distribution. Curr Opin Chem Biol. 6(2), 171-180.
[26] Gaetke, L.M. and Chow, C.K. (2003) Copper toxicity, oxidative stress, and antioxidant nutrients. Toxicology. 189(1-2), 147-163.
[27] Rustici, G., van Bakel, H., Lackner, D.H., Holstege, F.C., Wijmenga, C., Bahler, J. and Brazma, A. (2007) Global transcriptional responses of fission and budding yeast to changes in copper and iron levels: a comparative study. Genome Biol. 8(5), R73.
[28] Beaudoin, J., Ekici, S., Daldal, F., Ait-Mohand, S., Guérin, B. and Labbé, S. (2013) Copper transport and regulation in Schizosaccharomyces pombe. Biochem Soc T. 41, 1679–1686.
[29] DeVeaux, L.C., Hoagland, N.A. and Smith, G.R. (1992) Seventeen complementation groups of mutations decreasing meiotic recombination in Schizosaccharomyces pombe. Genetics. 130(2), 251–262.

Received: **12.02.2018**
Accepted: **29.04.2018**

CORRESPONDING AUTHOR

Semian Karaer-Uzuner
Department of Molecular Biology and Genetics, Faculty of Science,
Istanbul University,
Istanbul – Turkey

e-mail: semka@istanbul.edu.tr

© by PSP Volume 27 – No. 7/2018 pages 5001-5007 Fresenius Environmental Bulletin

FULL FACTORIAL EXPERIMENTAL DESIGN ANALYSIS OF REACTIVE DYE REMOVAL BY HETEROGENEOUS FENTON'S PROCESS

Yeliz Asci*, Merve Cam

Eskisehir Osmangazi University, Faculty of Engineering and Architecture, Department of Chemical Engineering, Eskisehir, Turkey

ABSTRACT

In the present paper, Reactive Yellow 15 removal from aqueous solution by heterogeneous fenton oxidation was investigated using 2^3 full factorial design. Fenton oxidation was conducted using a Fe/CuO catalyst in the presence of hydrogen peroxide (H_2O_2) in a batch process. The effects of pH of the reaction, catalyst concentration and reaction time were examined under the following conditions: 30° C of temperature, 50 ppm initial dye concentration, 8% Fe and 50 mM H_2O_2 concentration. The factors used in experiments and their levels have been determined as follows: initial pH: (2.0 and 8.0) Catalyst amount: (0.025g/25 ml and 0.1g/25 ml) and reaction time (10 and 60 minutes). The significance of effects has been statistically identified through ANOVA (variance analysis) within the confidence interval of 95% (statistical software, Minitab-18). When the effects of main factor are analysed, ANOVA results have indicated that time has the highest critical effect. While pH has had a negative effect, catalyst amount has had a positive effect. When the dual interactions are analysed, it has been observed that time-pH interaction has had the highest effect. A maximum colour removal was achieved as 97.6% at a low initial pH (2), high catalyst amount (0.1g), and high time (60 min) in a significance level of 5%.

KEYWORDS:
Experimental Design Method, Dye removal, Fenton's process, Fe/CuO catalyst, Wastewater

INTRODUCTION

Since synthetic dyes are extensively used in textile industries, textile wastewater is an important problem for conventional treatment plants in the entire World [1, 2]. Among these dyes, the most used type is the reactive azo dye. Additionally, these dyes are the most problematic pollutants of textile wastewaters [1]. Approximately 10–15% of overall production is released into the environment, mainly via wastewater. This is very dangerous since these dyes are non-biodegradable under aerobic conditions, and therefore the discharge of reactive azo dyes-containing wastewaters can cause several problems to the aquatic life [3, 4].

Traditionally, coagulation/flocculation [5], membrane cut-off [6] and adsorption processes (active carbon) [7] are applied in refinement of solutions containing dye. All these methods are costly and ineffective or create toxic waste-products. Therefore, alternative methods named advanced oxidation processes have started to draw attention in recent years [3, 8]. Advanced oxidation processes (H_202/UV, TiO_2/UV,O_3/UV, Fe^{+2}/H_2O_2) are based on the formation of quite reactive species such as OH radicals which have the ability of oxidising substantial amount of organic pollutants found in industrial waste water. Advanced oxidation processes could indiscriminately transform toxic and permanent organic substances into harmless end products [9-11].

Among advanced oxidation processes, Fenton's process has not only transformed chemically polluting agents, but present very attractive advantages such as the complete mineralization of some compounds, their oxidation at very low concentrations, the generation of environmentally friendly by-products, the applicability within wide temperature ranges, and the low consumption of energy in comparison with other wastewater treatment methods [9, 12]. The Fenton's process is based on the reaction between Fe^{+2} and H_2O_2 to produce hydroxyl radicals [13] and the efficiency of this process is dependent on Fe^{+2} and H_2O_2 concentration and the reaction pH. According to studies carried out, pH value should be between 3 and 5 [14]. Although the Fenton's process could be applied as homogenous and heterogeneous systems, homogenous systems are generally not sufficient since these systems contains ferric ion mud and this causes high levels of metal concentration in the solution. Besides, these systems allow working within a narrow pH range (2-3) and there is a possibility for ferric ions to be deactivated because of complex substances [15]. Due to these disadvantages, fenton like heterogeneous catalysts have started to be used recently where ferric ions are immobilized on a solid support [16]. It is easy for these catalysts to leave the liquid phase and they could be used over and over [17]. In this study,

we have used the Fe-supported CuO catalyst for decolourization of Reactive Yellow 15 (RY15).

The technique known as statistical design of experiments is a powerful technique for process characterisation, optimisation and modelling [18]. The Design of experiments is used with minimal effort for the evaluation of the statistical significance of individual experiment parameters as well as the interaction between factors that are not possible in a classical experiment. Thus, much information can be extracted with a minimal number of experimental trials [19].

In recent years, the most commonly used designs have been two level full/fractional factorial designs. Full factorial design is considered to be the most suitable design when the study is directed towards gaining knowledge of the effect of the variables on the process [20]. This study is an application of the full factorial design of experiment to determine the effects of operational parameters on the heterogeneous Fenton-type oxidation of the RY15. In order to find out the optimum Fenton oxidation conditions, a two-level factorial design (2^3) has been used. To the best of our knowledge, a statistical design of colour removal of RY15 using Fe/CuO as a catalyst has not been reported previously.

MATERIALS AND METHODS

Materials. All chemicals were used without further treatment. The Reactive Yellow 15 (RY15) azo dye used in this study was supplied from the Burboya Co. (Bursa, Turkey). The molecular formula and molecular weight of RY15 is $C_{20}H_{20}N_4Na_2O_{11}S_3$ and 634.57 g/mol, respectively. The chemical structure of RY15 is shown in Figure 1. Hydrogen peroxide (30% w/w) and $Fe(NO_3)_3{\cdot}9H_2O$ were obtained by Sigma-Aldrich Co. (Germany). CuO (Acros organics) (97%) was purchased from Thermo Fisher Scientific (Belgium). Moreover, all of the solutions were prepared using distilled water.

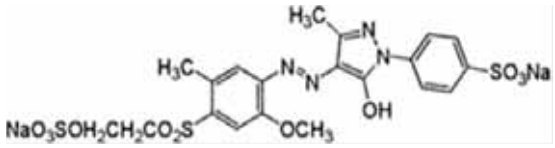

FIGURE 1
Structure of RY15

Catalyst. The 8.0 wt.%. Fe/CuO catalyst was prepared with co-precipitation. For this purpose, solutions containing the metal salt and salt of a compound that would be converted into the support were contacted by stirring with a base solution in order to precipitate as hydroxide form. After washing, it is converted into oxides by being heated.

The surface morphology of catalyst was determined by scanning electron microscopy (Model SEM-JEOL JSM 5600LV). The specific surface area (SSA) of the catalyst was also calculated by the BET (Brunauer, Emmett and Teller) theory using a Quantochrome Autosorb 1-C device. Both of preparation and characterization of the catalyst was detailed in our previous study [21].

Experiments. The Fenton tests were conducted at 30°C temperature in 100 mL flasks kept in thermostatic water-bath. The required amounts of catalyst and H_2O_2 were added simultaneously into the dye solution with adjusted pH and the solution was placed in the water bath. Thereafter, samples were withdrawn periodically and centrifuged to remove suspended particles for 5 min at 4000 rpm. After it was centrifuged, the absorbance value of the solution was read at a wavelength of 413 nm at the upper phase in the UV-spectrophotometer (Shimadzu, model UV-120-01). Finally, the decolorization efficiency was found by determining the concentration difference before and after the reaction.

RESULTS AND DISCUSSION

Statistical analysis. Initially, preliminary experiments were conducted to decide the most influential operating parameters such as pH, catalyst concentration, contact time and their levels. The results of preliminary experiments were given in our previous study [21]. After the preliminary experiments, the effect of the experimental parameters chosen as independent variables, initial pH of the reaction (A), catalyst amount (B) and contact time (C), was investigated using a 2^3 full factorial design under the following conditions: 30°C of temperature, 50 ppm initial dye concentration, 8% Fe and 50 mM H_2O_2 concentration.

The factors and levels used in the experiments were shown in Table 1. Experiments were performed according to the full factorial design matrix (with two repetitions) given in Table 2. The results were analyzed with the Minitab 18 software to obtain the effects, coefficients, and other statistical plots (Pareto, main effects, interactions).

TABLE 1
Variable levels of the factors

Factors	Low level (-1)	High level (+1)
pH (A)	2	8
Catalyst amount (B) g/25 ml	0.025	0.1
Time (C) min	10	60

The significance of the effects was checked by the ANOVA (Table 3) with a confidence level of 95%. T-test is used for determining the significance of regression coefficients of factors. As seen in the variance table, the corrected R^2 value is 97.33% and the estimated R^2 value is 94.31%. The fact that R^2

values are high indicates that the change in the colour removal could be explained by the relevant factors. The F values indicates the significance of interaction between variables. Higher values of T and F shows the most effective factor. The fact that the probability values are lower than 0.05 ($p<0.05$) means factors have an interaction between each other; however, if the values are higher than 0.05, it means the relevant factors do not have a significant effect or even it may be ignored. To sum up, as seen in the Table 3, it has been concluded that time is the most important factor and catalyst amount comes after it while the least effective factor is pH.

Normal probability diagram is used to identify the real effects (Figure 2). As seen in the Figure 2, the catalyst amount, time and pH-time all have a critical effect. In the normal probability diagram, those on left side of the curve has a negative effect (AC) while those on the right side of the curve (B, C) has a positive effect. C (time) that is farthest to the curve has the biggest effect.

TABLE 2
Design Table

				Color Removal %	
Run	A	B	C	Actual	Predicted
1	-1	-1	-1	9.00	8.00
2	+1	-1	-1	23.0	26.5
3	-1	+1	-1	34.0	30.4
4	+1	+1	-1	50.2	44.1
5	–1	-1	+1	83.0	80.9
6	+1	-1	+1	66.2	62.2
7	-1	+1	+1	97.6	97.1
8	+1	+1	+1	79.7	76.2
9	-1	-1	-1	7.00	8.00
10	+1	-1	-1	30.0	26.5
11	-1	+1	-1	26.8	30.4
12	+1	+1	-1	38.0	44.1
13	-1	-1	+1	79.0	80.9
14	+1	-1	+1	58.2	62.2
15	-1	+1	+1	96.6	97.1
16	+1	+1	+1	72.6	76.2

TABLE 3
ANOVA results for color removal Analysis of Variance

Source	DF	Adj SS	Adj MS	F-Value	P-Value
Model	7	13332.7	1904.7	79.14	0.000
Linear	3	11999.9	4000.0	166.19	0.000
pH	1	14.3	14.3	0.59	0.464
Catalyst amount	1	1226.8	1226.8	50.97	0.000
Time (min)	1	10758.9	10758.9	447.02	0.000
2-Way Interactions	3	1331.0	443.7	18.43	0.001
pH*Catalyst amount	1	12.1	12.1	0.50	0.499
pH*Time (min)	1	1294.2	1294.2	53.77	0.000
Catalyst amount*Time (min)	1	24.8	24.8	1.03	0.340
3-Way Interactions	1	1.8	1.8	0.07	0.794
pH*Catalyst amount*Time (min)	1	1.8	1.8	0.07	0.794
Error	8	192.5	24.1		
Total	15	13525.2			

*Significant effects at 95% confidence level ($p < 0.05$)

Model Summary

S	R-sq	R-sq(adj)	R-sq(pred)
4.90593	98.58 %	97.33%	94.31%

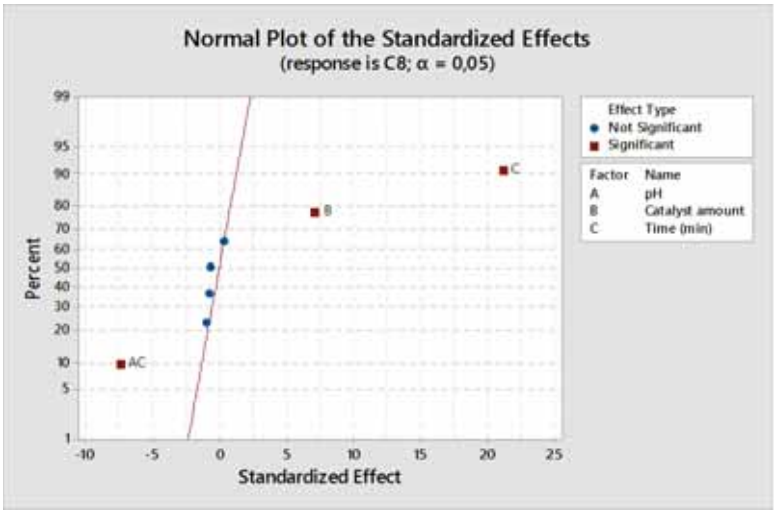

FIGURE 2
Normal plot of the standardized effects

The effects of the main factor and the interaction between the factors have been respectively analysed in order to determine the level of those having a critical effect in Figure 3 and 4. In the effects of main factor diagram, it could be seen that how the three factors (catalyst amount, pH, and time) affect dye removal process. As seen in the Figure 3, better results have been obtained when the time and catalyst amount is at their higher level and pH is at its lower level. In other words, pH has created a negative effect while catalyst amount and time have had a positive effect. Since the curve of time diagram is higher, time factor creates the highest critical effect.

The diagram in the Figure 4 indicates the interaction between a factor and other factors. Since the lines of time and pH intercept here, the interaction of pH-time creates a substantial effect.

The interactions on the right side of the line of the pareto chart is significant (Figure 5). According to this chart, the amount of catalyst, time and pH-time dual interaction are the most important parameters affecting dye removal. With regard to the results, the effect of time (C) is more significant than the amount of catalyst (B) and pH value (A). In other words, the effect of time is much more than that of other factors. The effect of time-pH interaction is more than that of catalyst amount.

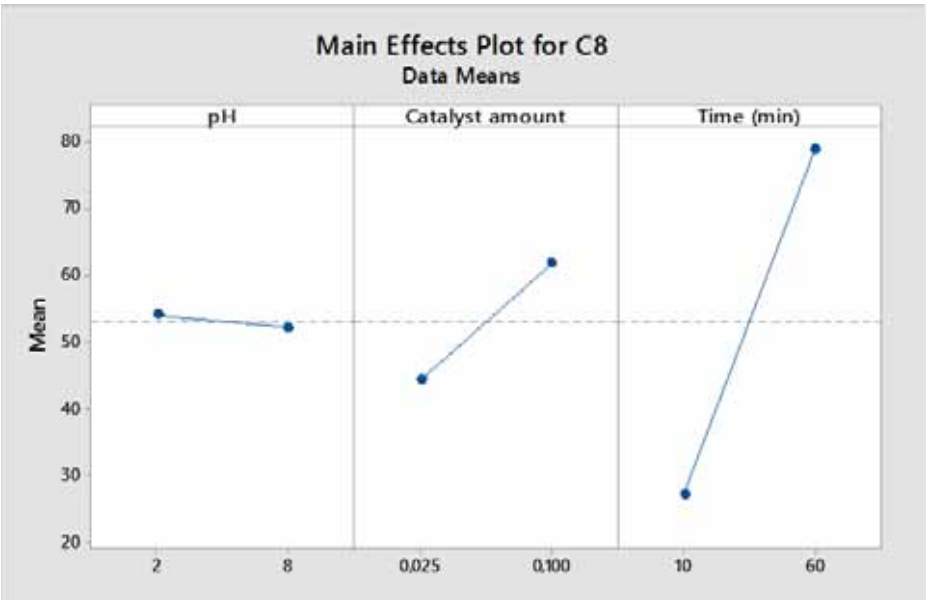

FIGURE 3
The main effect plots for colour removal

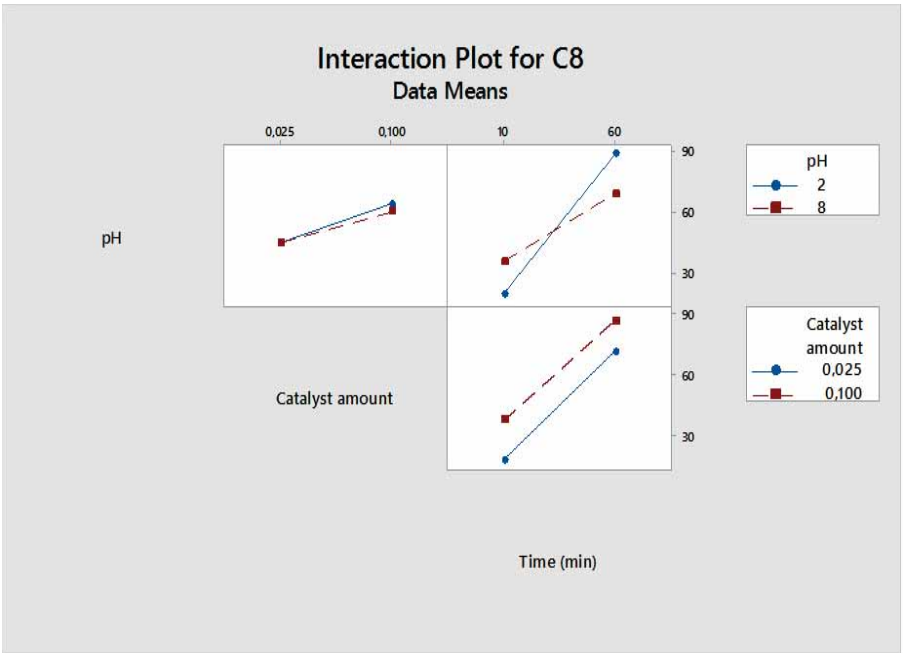

FIGURE 4
The main effect plots for colour removal

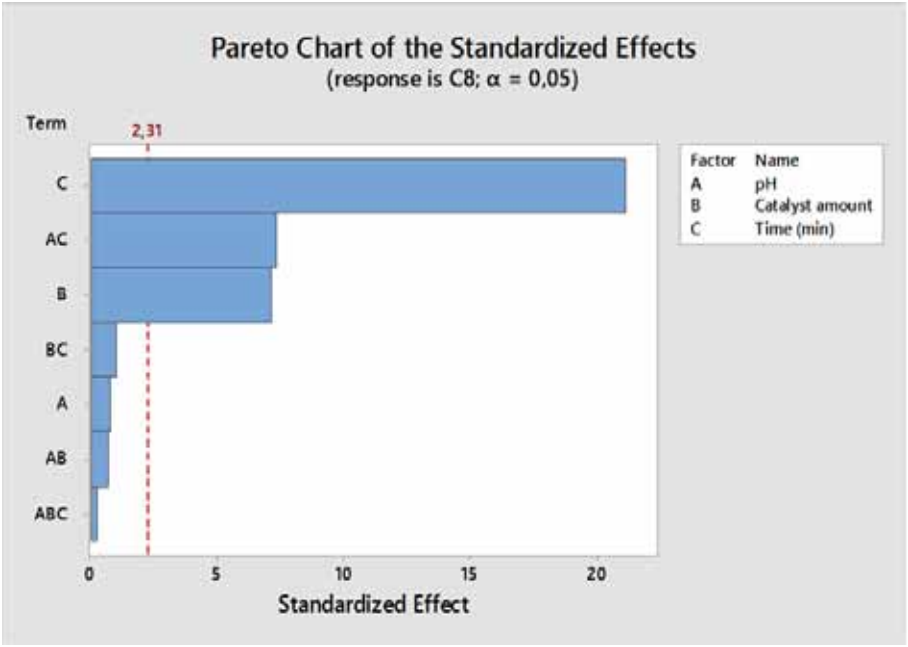

FIGURE 5
Pareto chart of the standardized effects

TABLE 4
Coded Coefficients

Term	Effect	Coef	SE Coef	T-Value	P-Value	VIF
Constant		53.18	1.23	43.36	0.000	
pH	-1.89	-0.94	1.23	-0.77	0.464	1.00
Catalyst amount	17.51	8.76	1.23	7.14	0.000	1.00
Time (min)	51.86	25.93	1.23	21.14	0.000	1.00
pH*Catalyst amount	-1.74	-0.87	1.23	-0.71	0.499	1.00
pH*Time (min)	-17.99	-8.99	1.23	-7.33	0.000	1.00
Catalyst amount*Time (min)	-2.49	-1.24	1.23	-1.01	0.340	1.00
pH*Catalyst amount*Time (min)	0.66	0.33	1.23	0.27	0.794	1.00

The estimated coefficients are obtained in terms of coded variables as seen in Table 4. Similarly, the regression equation created for dye removal is as seen Equation 1. Since A and C (pH-time) have a critical effect together, A (pH) is left within the model. The estimated percentage values gave been obtained for dye removal by using regression model and these have been given in the last column of Table 2.

$$\text{Colour\%}=53.18-0.94\,A+8.76\,B+25.93\,C-0.87\,AB-8.99\,AC-1.24\,BC+0.33\,ABC \quad (1)$$

The obtained maximum percentage for dye removal is 97.10 as seen in Table 2. Namely, dye removal could be realised in maximum levels when pH level is lower and time and the amount of catalyst is at their higher levels. In addition to this, time is the most important factor of all. As a result of the validity test carried out with the best values obtained, the similar result have been achieved with 97.6% and the first is result is confirmed. Consequently, it is thought that the model used in studies is valid.

CONCLUSION

In this work, the decolourization of Reactive Yellow 15 (RY15) was conducted using Fe(III)-sepiolite catalyst in the presence of hydrogen peroxide (H_2O_2) in a batch process. In order to determine the effects of various operational parameters, a full factorial design was performed. According to the statistical procedure, the time was found to have the most significant effect upon the colour removal. Moreover, the interactions between factors AC also significantly influence the removal. The value of the predicted determination coefficient (R^2(pred) = 94.31%) is in reasonable agreement with the value of the adjusted determination coefficient (R^2(adj) = 97.33 %). Under the optimum conditions (the initial pH = 2, catalyst concentration = 0.1 g/25 mL, and contact time = 60 min), colour removal is predicted as 97.10% and the corresponding confirmatory trial value is 97.6. This value fits well to the dataset of predicted values by considering 95% prediction interval.

ACKNOWLEDGEMENTS

The authors wish to thank Eskisehir Osmangazi University Scientific Research Projects Commission for partially supporting this study financially (Project No.201415F10).

REFERENCES

[1] Lucas, M.S. and Peres, J.A. (2006) Decolorization of the azo dye Reactive Black 5 by Fenton and photo-Fenton oxidation. Dyes and Pigments. 71, 236-244.
[2] Hameed, B.H. and Lee, T.W. (2009) Degradation of malachite green in aqueous solution by Fenton process. Journal of Hazardous Materials. 164, 468-472.
[3] Rodriguesa, C.S.D., Madeirab, L.M. and Boaventuraa, R.A.R. (2009) Optimization of the azo dye Procion Red H-EXL degradation by Fenton's reagent using experimental design. Journal of Hazardous Materials. 164, 987–994.
[4] Işık, M. and Sponza, D.T. (2004) A batch kinetic study on decolorization and inhibition of Reactive Black 5 and Direct Brown 2 in an anaerobic mixed culture. Chemosphere. 55, 119-128.
[5] Moghaddam, S.S., Moghaddam, M.R.A. and Arami, M. (2010) Coagulation/flocculation process for dye removal using sludge from water treatment plant: Optimization through response surface methodology. Journal of Hazardous Materials. 175, 651-657.
[6] Kavak, D. (2017) Treatment of dye solutions by DL nanofiltration membrane. Desalination and Water Treatment. 689, 116–122.
[7] Daoud, M., Benturki, O., Kecira, Z., Girods, P. and Donnot, A. (2017) Removal of reactive dye (BEZAKTIV Red S-MAX) from aqueous solution by adsorption onto activated carbons prepared from date palm rachis and jujube stones. Journal of Molecular Liquids. 243, 799-809
[8] Valiente, M., Idel, R., Yaacoubi, A., Tanouti, B. and López, M. (2011) Rapid decolourization and mineralization of the azo dye C.I. Acid Red 14 by heterogeneous Fenton reaction. Journal of Hazardous Materials. 186, 745-750.
[9] Hanay, Ö. and Hasar, H. (2007) Decolorizing of textile Industry wastewater with Fenton oxidation process. Science and Engineering Journal of Fırat Üniversity. 19, 505-509.
[10] Kocakaplan, N., Ertugay, N. and Malkoç, E. (2014) Removal of Acid Yellow 36 Dyestuff with Fenton and Fenton-Like advanced oxidation methods. Journal of The Institute of Science and Technology. 4, 41-49.
[11] Güneş, E. and Cihan, M.T (2015) COD and color removal from wastewaters: Optimization of Fenton Process. Pamukkale University Journal of Engineering Sciences. 21, 239-247.
[12] Ayodele, O.B., Lim, J.K. and Hameed, B.H. (2012) Pillared montmorillonite supported ferric oxalate as heterogeneous photo-Fenton catalyst for degradation of amoxicillin. Applied Catalysis A: General. 413– 414, 301– 309.
[13] Sun, J., Shi, S., Lee, Y. and Sun, S. (2009) Fenton oxidative decolorization of the azo dye Direct Blue 15 in aqueous solution. Chemical Engineering Journal. 155, 680–683.
[14] Hameed, B.H. and Lee, T.W. (2009) Degradation of malachite green in aqueous solution by Fenton process. Journal of Hazardous Materials. 164, 468-472.
[15] Duarte, F. and Madeira, L. (2009) Azo-dye Orange II degradation by Fenton‟s reaction using Fe/ZSM-5 zeolite as catalyst. EAAOP2, Portugal.
[16] Hassan, H. and Hameed, B.H. (2011) Decolorization of Acid Red 1 by heterogeneous Fenton-like reaction using Fe-ball clay catalyst. International Conference on Environment Science and Engineering, Singapore.
[17] Soon, A.N. and Hameed, B.H. (2011) Heterogeneous catalytic treatment of synthetic dyes in aqueous media using Fenton and photo-assisted Fenton process. Desalination. 269, 1-16.
[18] Öztürk, N. and Kavak, D. (2008) Boron removal from aqueous solutions by batch adsorption onto cerium oxide using full factorial design. Desalination. 223, 2008, 106-112.
[19] Bingöl, D., Saraydin, D. and Özbay, D.S. (2015) Full Factorial Design Approach to Hg(II) Adsorption onto Hydrogels. Arabian Journal Science Engineering. 40, 109–116.
[20] Aşçı, Y., Demirtaş, E.A., İşçen, C.F. and Anagün, A.S. (2015) A Statistical Experimental Design to Determine the Azo Dye Decolorization and Degradation by The Heterogeneous Fenton Process. Fresen. Environ. Bull. 24, 3717–3726.
[21] Aşçı, Y. and Çam, M. (2017) Treatment of synthetic dye wastewater by using Fe/CuO particles prepared by co-precipitation: Parametric and kinetic studies. Desalination and Water Treatment. 73, 281–288.

Received: **12.02.2018**
Accepted: **29.04.2018**

CORRESPONDING AUTHOR

Yeliz Asci
Eskisehir Osmangazi University,
Faculty of Engineering and Architecture,
Department of Chemical Engineering,
Eskişehir - Turkey

e-mail: yelizbal@ogu.edu.tr

© by PSP Volume 27 – No. 7/2018 pages 5008-5021 Fresenius Environmental Bulletin

THE ROOTSTOCK EFFECTS ON AGRONOMIC AND BIOCHEMICAL QUALITY PROPERTIES OF MELON UNDER WATER STRESS

Saliha Dinc[1,2], Meryem Kara[2,3], M Zeki Karipcin[4,*], Nebahat Sari[5], Zehra Can[6], Hacer Cicekci[2], Mehmet Akkus[2]

[1]Selcuk University, Cumra Applied Sciences High School, Konya, Turkey
[2]Selcuk University, Advanced Technology Research and Application Center, Konya, Turkey
[3]Selcuk University, Cumra Vocational High School, Konya, Turkey
[4]Siirt University, Faculty of Agriculture, Siirt, Turkey
[5]Cukurova University, Faculty of Agriculture, Adana, Turkey
[6]Giresun University, Sebinkarahisar Vocational High School, Giresun, Turkey

ABSTRACT

In this study Edali F1 and Balhan F1 melons (*Cucumis melo* L.) grafted onto different rootstocks (TZ 148 and Jumbo) under water stress conditions (W1-100%, W2-50%, W3-25%). FRAP (Ferric reducing antioxidant power) values increased with the use of TZ 148 and Jumbo rootstocks. At water stress, grafting generally increased ascorbic acid values. Maximum β-carotene amount was stated for Balhan F1 with W3 level and the β-carotene values of Balhan/TZ148 melons increased with water stress. *p*-hydroxybenzoic acid was the compound with the highest quantity among the tested phenolic compounds. Citric, maleic, fumaric and formic acid quantities increased with enhancement of water deficiency whereas tartaric, succinic and acetic acid decreased. Fructose and saccharose quantity decreased as the amount of water given to plant decreased but glucose level was not affected. Consequently, grafting of melons onto favorable rootstocks seems to enhance the amount of health related compounds under water stress conditions.

KEYWORDS:
Agronomic properties, bioactive compounds, grafting, melon, rootstock, water stress.

INTRODUCTION

Drought, which is one of these environmental stresses affects the functions of almost all plants, and reduces the efficiency of a product. For instance, water stress causes serious reduction both in growth and in quantity and quality of many plants. Until now, it has been attempted to increase the product resistance against water stress or drought through the traditional breeding programs. Hence, new approaches such as efficient use of water, selection of drought-tolerant species and rootstocks are used to alleviate the effects of water stress. Of these approaches, a method of grafting high-yield genotypes onto selected rootstocks as an alternative to traditional breeding methods is a promising approach to increase the tolerance of vegetables to biotic and abiotic stresses [1]. Herein, grafting is a method for improving water use efficiency in arid conditions, and reducing product loss and water stress [2]. Grafting is also used for enhancing the tolerance of plants to adverse soil conditions (low soil and weather temperatures, salinity and excessive moisture etc.), better uptake of water and nutrients and their efficient usage, earliness and providing increased yields [3]. Considering the effects of global warming, the production of grafted seedling will become popular in the future. Grafting is generally applied to the crops belong to *Solanaceae* (tomatoes, potatoes and peppers) and *Cucurbitaceae* (watermelon, melon and cucumber) families in Japan, Korea, China, Israel, Turkey, Spain, Italy, Greece, France, Netherlands, Germany and USA [4]. The production and consumption of melon (*Cucumis melo*), a member of *Cucurbitaceae* family, is quite common both in the world and Turkey. In Turkey, melon is the most commonly grown vegetable in terms of quantity after the watermelon. RS 841, TZ 148, Strongtosa, Maximus, Macis, Nun 9075 and Sguash No:3, Jumbo are the most widely used rootstocks recently. The agricultural and physiological processes that affect the fruit quality of grafted plants have been more studied particularly for watermelon, melon, cucumber and tomatoes. Additionally, studies conducted on the effects of grafting have generally focused on official quality parameters such as size, shape, color, form and freshness etc. Nevertheless, the quality attributes such as bioactive compounds, organic acids, sugars and flavor are not much considered or pay very little attention. Furthermore, the biochemical and molecular mechanisms in the grafting process still have not been fully understood [5]. Understanding the effects of agricultural and technological factors and their interactions is an important issue for the production of foods rich in bioactive compounds [6].

Therefore, new and deep studies are required for understanding biochemical and molecular mechanisms of grafted plants on flavor and health related compounds [5]. For example; some of following findings were observed in the studies focused on effects of different rootstocks: Increase in the level of β-carotene of melon grafted onto P360 rootstock [7]; lycopene increment in grafted watermelon [8] and increase in ascorbic acid content of grafted cucumber [9]. Amongst phenolic compounds; rutin and quercetin were found to be higher in grafted melons compared with standard and hybrid types [10]. However, researches on the effects of grafting on health related compounds including phenolic components, vitamins and organic acids under water stress are limited. Therefore, the selection of the appropriate rootstock/scion combinations with favorable effects on fruit quality particularly the bioactive compounds is an essential necessity [5]. Considering the consumer demand for vegetables rich in health related compounds, we have investigated the effects of different rootstocks/scion combinations on bioactive compounds (ascorbic acid, beta-carotene, phenolic compounds and organic acids), sugar components and antioxidant activity as well as agronomic properties (morphological, physiological, stomatal screening, pomological, quantitative and qualitative features) under water stress. The idea focused in this study is whether the utilization of different rootstocks (TZ148 and Jumbo) in grafting of different melon cultivars (Edali F1 and Balhan F1) is able to increase the bioactive compounds under different water stress conditions. To our knowledge, the effects of grafting of melon cultivar on above mentioned attributes of melons under water stress have not yet been investigated in detail. For this purpose, Edali F1 winter-melon (*Cucumis melo* var. *inodorus*) genotype from Altinbas group and summer-melon Balhan F1 from cantaloupe group were grafted onto the most commonly used rootstocks TZ 148 and Jumbo derived from crosses of *Cucurbita maxima* x *C. moschata.* Grafted seedlings were grown under water stress treatments consisting of W1-control (100 %) W2-50 % and W3-25 % water application levels. Agronomic and biochemical properties of melons were examined.

MATERIALS AND METHODS

Chemicals. Standards of phenolic compounds (purity > 99%) gallic acid, catechin, *p*-hydroxybenzoic acid, vanillic acid, caffeic acid, chlorogenic acid, rutin, *trans-p*-coumaric acid, *trans*-ferulic acid, myricetin, *trans*-resveratrol, *trans*-cinnamic acid, naringenin, kaempferol, isorhamnetin were from Ehrenstorfer GmbH, syringic acid and quercetin were from Alfa Aesar, protocateuchuic acid was from HWI Analytik. Methanol, metaphosphoric acid, acetic acid, hexane, acetone, ethanol and acetonitrile were from Merck (Darmstadt, Germany). Ascorbic acid, sugars, lycopene, beta-carotene and 2,2-diphenyl-1-picrylhydrazyl (DPPH) were from Sigma-Aldrich (St. Louis, MO). Trolox (6-hydroxy-2,5,7,8-tetramethyl chroman-2-carboxylic acid) and Folin-Ciocalteu's phenol reagent were from Fluka Chemie GmbH (Switzerland).

Grafting and Growth Conditions of Melons. Two melon cultivars Edali F1 winter-melon (*Cucumis melo var. inodorus*) genotype from Altinbas group and summer-melon Balhan F1 from cantaloupe group were used in this research. These melon cultivars were grafted onto the most commonly used rootstocks TZ 148 and Jumbo derived from crosses of *Cucurbita maxima* x *C. moschata* in Turkey in 2013. Grafting was carried out in Antalya seedling facilities. Slant-cut grafting method was used. Ungrafted seedlings were used as controls. Grafted melon seedlings were planted on open-field area by locating the graft union to be remained above the soil line considering recent rainfall statistics in the GAP Agricultural Research Institute (GAPTAEM) in Sanliurfa region in Turkey in May 2013 at an altitude of 410 meters at a latitude and longitude of 36º42' and 38º58', respectively. The experiment field was characterized as clay textured soil. Field capacity of the soil was about 32.21 % and 21.61 % at wilting point. The average dry bulk density at a 90 cm soil depth was 1.41 g/cm^3 with pH of 7.6. Electrical conductivity and pH of the irrigation water were 0.52 dS/m and 7.3, respectively. The weather during the experiment at the field was dry and hot with air temperatures up to 46°C and relative humidity averaging about 34 %. Annual average rainfall was about 380 mm. The seedlings were planted with 2 m and 0.6 m spacing between and within rows with 10 plants per plot. The trial was based on completely randomized split block design by laying irrigation application in main plots and cultivars in subplot and rootstocks in sub-subplots. Randomized split block design was established according to 3 different rootstocks (TZ 148, Jumbo and ungrafted control), 2 cultivars (Edali F1 and Balhan F1) and 3 different irrigation levels (100 %, 50 % and 25 %) with three replications each, in the total (3x2x3x3) 54 plots. Preplant soil samples from three different soil depth (0-30, 30-60 and 60-90 cm) were taken from the field and analyzed. According to results of soil analysis fertilization practice was applied using 10:15:20 kg/ha N:P_2O_5:K_2O one month before planting. The whole part of phosphorus fertilizer was applied before deep pre-plowing through fertilizer sprinkler machine whereas nitrogen and potassium fertilizers through drip irrigation system in 4 and 2 portions, respectively. Required maintenances were conducted in the plots. Weed control was carried out with mechanical and chemical means and finally, disease and pest control were performed using chemical methods through

continuous monitoring. The first and last plants of each plot were reserved for the buffers and three plants after planting with one-month interval for biomass and other morphologic measurements. Yield and yield components were analyzed in the rest of plants. Melons were harvested at a full ripe stage starting from July 2013 considering the harvesting criteria and transferred to cold storage (relative humidity about 50-60%, temperature 18 °C) keeping in separated compartments.

Irrigation Treatments. Three irrigation levels were established. The amount of water applied to each plot was determined by considering the field capacity. The control plots received 100 % (W1-control) field capacity irrigation. To impose water deficit stress, the moisture level equivalent to 50 % (W2) and 25 % (W3) of field capacity irrigation was maintained. Drip irrigation was used. Irrigation was started in all plots when 50 % of the water holding capacity at the 90 cm soil depth is removed and continued to apply irrigation until existing field moisture level attained. Profile probe was used for the determination of soil moisture content.

Agronomic Properties of Melon Plants. The method by Smart and Bingham [11] was used to evaluate leaf relative water content (LRWC) of melons. LRWC of melon plants was determined on leaves which completed their development at fifteen days interval between 13:00 to15:00 hours. These measurements, taken at intervals of fifteen days, were assessed. The leaf samples were soaked for 4 hr to achieve turgidity following measurement of fresh weight and then oven-dried at 85ºC for 24 hours. LRWC was calculated using the following formula:

LRWC (%) = [(FW-DW) / (TW-DW)] x 100 where FW: Fresh weight DW: Dry weight TW: Turgor weight

The plant dry matter ratio was determined to be used for the calculation of water use efficiency. Plants were cut 2 cm above the root collar and dried at room temperature for a while. Then, plants were dried in an oven at 65 ° C until constant weight. Results were presented as percentage.

Water usage efficiency for each irrigation level and cultivars was determined according to Alizadeh et al. [12]. Water usage efficiency for each irrigation level and cultivars was determined in units of kg/m^3 using the soil moisture change during the vegetation.

Stoma experiments were determined according to the method supplied by Sari et al. [13]. From each plot 3 leaves were analyzed for the stomatal characteristics during the cultivation period for once in July using microscope. 3 stomata width and length per leaf and stoma number in unit area were determined.

Total yield, early yield and marketable yield (kg/da) were evaluated in harvested melons. Furthermore, fruit weight (kg)of melons were measured in three samples in each plot. Brix (soluble solid) values with hand refractometer (Atago, JAPAN). Panel test (0-5 scale) was conducted with 10 panel members where 0 indicated the very bad and 5 very good.

Biochemical Properties of Melons. Ferric reducing antioxidant power (FRAP) assay, DPPH radical scavenging method and total phenolic content (TPC) were used for the determination of antioxidant activity of melon samples. The method by Benzie and Strain [14] was used for FRAP assay. The FRAP reagent was prepared by mixing 25 mL of 0.3 mol/L acetate buffer at pH 3.6 with 2.5 mL of 10 mmol/L 2,4,6-tripyridyl-striazine (TPTZ) solution in 40 mmol/L HCl, and 2.5 mL of 20 mmol/L $FeCl_3.6H_2O$ solution. One hundred microliters of the melon juice was mixed with 3 mL of freshly prepared FRAP reagent and incubated for 4 min. Absorbance was measured at 593 nm. The method by Molyneux [15] was used for DPPH radical scavenging activity of melons. Trolox (25-1000 µM) was used as a positive control for the calibration curve. 2,2-diphenyl-1-picrylhydrazyl (DPPH) radical scavenging activity of melon samples was tested. The change of absorbance of purple coloured DPPH radical was monitored in the presence of antioxidants at 517 nm wavelength. Trolox (0,001-0,02 mg/mL) was used as a positive control. The values are expressed as SC_{50} (mg sample/mL) required to scavenge 50% of the initial DPPH. Lower DPPH values indicate higher antioxidant activity. Folin-Ciocalteau procedure was used for the determination of TPCs of melon samples the results were calculated as a mg of gallic acid equivalents (GAE) per mL melon juice [16]. Folin-Ciocalteau procedure was used for the determination of TPCs of melon samples the results were calculated as a mg of gallic acid equivalents (GAE) per mL melon juice.

After the washing under the tap water, melons were peeled and seeded. To prepare the samples for the chemical and biochemical analyses, about 700 g edible mesocarp tissue of melons was combined and homogenized with Waring blender. The homogenized portion was filtered through Whatman No.1 filter paper and the filtrate was centrifuged 9000g for 10 min at +4 ºC. Then the supernatant was kept at -80 ºC until the analyses of phenolic compounds, organic acids and sugars. For the ascorbic acid and β-carotene analyses , 5 gr of homogenized portion of melon samples were kept at -18 ºC under nitrogen atmosphere until analyses performed in a short time.

Ascorbic acid content of melon samples was determined using the method developed by Sawant et al. [17]. Ascorbic acid content of melon samples was determined using a HPLC system (Shimadzu, Japan) (Model SPD-20A/20AV) equipped with a

UV-Vis detector. Separation was carried out on a 4.6 mm x 250 mm ODS 4 RP-C18 column with a particle diameter of 5 µm at wavelength a of 278 nm. The oven temperature and flow rate were 30 ° C, and 0.9 mL/min, respectively. Mobile phase A was prepared from 1% (v/v) acetic acid in ultra-pure water, while B was methanol (A: 95%, B: 5%). Quantification was performed using standard curve plotted with standard solutions of ascorbic acid (1-75 mg/L).

β-carotene was determined according to method of Mu-Lin et al. [18]. β-carotene was determined with HPLC system (Shimadzu, Japan) (Model SPD-20A/20AV) equipped with a UV-Vis detector. A C18 column (250 x 4.6 I.D., 5 µm particles, Inertsil ODS 2) was used for the separation at 450 nm wavelength. Mobile phases were A (acetonitrile-H_2O 9:1) and B (ethyl acetate). Flow rate and column temperature were maintained at 1.0 mL/min and 30 ºC, respectively. Quantification was performed with different concentrations of β-carotene standards (1-75 mg/L).

Separation of phenolic compounds was performed with the method developed by Wen et al. [19] with the some modifications. Separation of phenolic compounds was performed on a HPLC system (Shimadzu, Japan) (Model SPD-20A/20AV) equipped with a UV-Vis detector. A 0.05 % glacial acetic acid in water (A) and an acetonitrile (B) mixture were used with the following gradient : 0-2 min 8-10 % B; 2-27 min 10-30 % B; 27-37 min 30-56 % B; 37 min 8 % B, before it returned to the initial conditions. was used. Separation wavelength, column, flow rate and temperature values were as follow: 280 nm wavelength, ODS3 column (250 mm × 4.6 mm id, 5 µm particle; Inertsil),1.2 mL/min and 30 ºC, respectively. Quantification was done with different concentrations of phenolic compounds standards (1-50 mg/L). Before injection, the pH of supernatant of melon samples was adjusted to 1.0 and it was subjected to solid phase extraction tubes (Finisterre SPE C18). The elution of phenolic compounds was performed with methanol-acetic acid (70:30).

Determination of organic acids (citric, tartaric, succinic, maleic, formic, acetic and fumaric acids) was performed on a HPLC system (Shimadzu, Japan) (Model SPD-20A/20AV) equipped with a UV-Vis detector. MetaCarb 87H Column (300*7.8 mm, Agilent Technologies) and guard column MetaCarb 87H (50*4.6 mm, Agilent Technologies) were used for the separation. Oven temperature, flow rate and wavelength were 35 ° C, 0.6 mL/min and 210 nm, respectively. 0.1 N H_2SO_4 was used as a mobile phase. Quantification was performed with different concentrations of organic acid standards (3-150 mg/L). The sugar content (glucose, fructose, sacsharose, ribose, arabinose, galactose, maltose, trehalose, mellebiose, melezitoz of melon samples was conducted using HPLC (Elite LaChrom, Hitachi, Japan) system equipped with refractive index detector. Reverse phase-amide column (200/4.6 Nucleosil 100-5 NH_2) was used for the separation of sugars. Oven temperature and flow rate values were 45 ºC and 1.5 mL/min, respectively. Mobile phase and injection volume were (79: 21, v/v) and 25 µL, respectively.

Statistical Analysis. The data were analyzed with JMP statistical software. The treatments were established according to randomized split block design with three replicates. The acquired data were subjected to variance analysis (ANOVA) and the means were compared with least significant differences (LSD) test.

RESULTS AND DISCUSSIONS

Agronomic Performance of Melons. Leaf-water relationship is one of the most important parameters used for determination of resistance of plants against drought or their level of tolerance. There is a relationship between water stress and leaf relative water capacity [20]. When LRWC is 50% or lower, stomas close and this causes a decrease in the assimilation of CO_2. This leads to decrease in photosynthesis, unsustainable plant development and occurrence of oxidation damages [21]. For plants which are resistant or adapted to drought, the rates of LRWC are higher [22]. LRWC values are significantly affected from water stress (Figure 1a). When the effects of water levels on leaf water capacity are considered, the highest LRWC rate was obtained in all measurement periods with W1 (whole water) application and the lowest LRWC rate was obtained from W2 water application. LRWC values of all Edali melons were higher than those of all Balhan melons. LRWC values of TZ 148 rootstock were higher than those of Jumbo rootstock.

In the case of drought, variation occurs in dry matter accumulation of different stages of plant vegetation [23]. In this study, the highest rate of dry matter was generally determined with W3 water application and the lowest value was determined in W2 water parcels (Figure 1b). Dry matter values belonging to Balhan F1 were found to be higher than those of Edalı F1.

When water usage efficiency, one of most important of samples to which water reduction or drought were applied were investigated, maximum water usage efficiency values (4.54 kg/m^3) were obtained for ungrafted Edali F1 plants with W3 water application (Figure 1c). Minimum water usage efficiency values, on the other hand, were determined for Balhan F1 grafted onto Jumbo

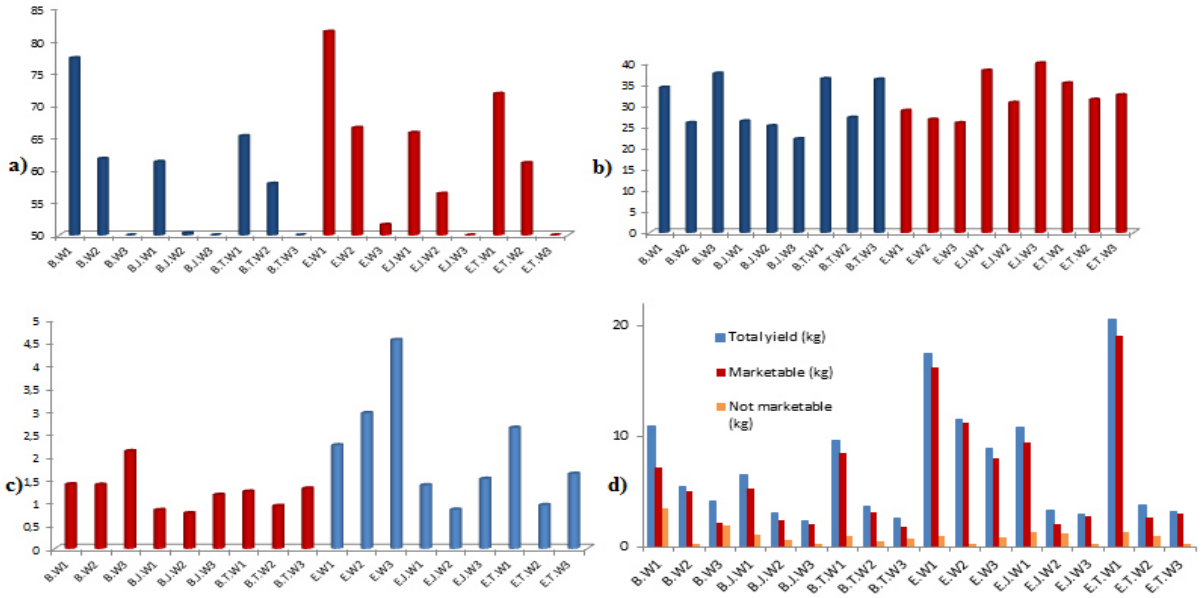

FIGURE 1
Relationship between water stress and a) leaf relative water content (%) b) plant dry mater of melons (%) c) water usage efficiency (kg/m^3) d) total, marketable, not marketable yield (kg) B.W1: Balhan F1. Control, B.W2: Balhan F1. 50 % Water, B.W3: Balhan F1. 25 % Water, B.J.W1: Balhan. Jumbo. Control, B.J.W2: Balhan. Jumbo. 50 % Water, B.J.W3: Balhan. Jumbo. 25 % Water, B.T.W1: Balhan. TZ148. Control, B.T.W2: Balhan. TZ148. 50 % Water, B.T.W3: Balhan. TZ148. 25 % Water, E.W1: Edalı F1. Control, E.W2: Edalı F1. 50 % Water, E.W3: Edalı F1. 25 % Water, E.J.W1: Edalı. Jumbo. Control, E.J.W2: Edalı. Jumbo. 50 % Water, E.J.W3: Edalı. Jumbo. 25 % Water, E.T.W1: Edalı. TZ148. Control, E.T.W2: Edalı. TZ148. 50 % Water, E.T.W3: Edalı. TZ148. 25 % Water.

TABLE 1
The effect of water stress on fruit weight, brix and sensory properties of melons

	Fruit Weight (Kg)	Brix (%)	Panel Test
BALHAN F1-W1	1.49^{B-D}	13.33^{a}	**5^{a}**
BALHAN F1-W2	1.10^{E-G}	11.31^{bc}	**5^{abc}**
BALHAN F1-W3	1.13^{d-f}	8.14^{e-h}	**5^{a}**
BALHAN/ JUMBO-W1	0.88^{F-I}	9.00^{d-g}	**3^{efg}**
BALHAN /JUMBO –W2	0.90^{F-I}	11.50^{bc}	**3^{fgh}**
BALHAN/JUMBO-W3	0.55^{J}	7.60$^{g-ı}$	**3^{h}**
BALHAN /TZ148-W1	1.40^{C-E}	9.83^{c-f}	**4^{efg}**
BALHAN/TZ148 –W2	0.88^{F-I}	11.50^{bc}	**4^{bcd}**
BALHAN/TZ148-W3	0.85^{G-J}	8.20^{f-h}	**3^{fgh}**
EDALI F1-W1	1.98^{A}	12.50^{ab}	**5^{ab}**
EDALI F1-W2	1.41^{CD}	7.17^{hı}	**4^{def}**
EDALI F1-W3	1.43^{CD}	10.50^{c-e}	**5^{abc}**
EDALI /JUMBO-W1	1.69^{A-C}	7.00^{hı}	**4^{def}**
EDALI/ JUMBO – W2	0.66^{H-J}	9.00^{d-g}	**3^{gh}**
EDALI/ JUMBO-W3	0.60^{IJ}	6.33^{ij}	**3^{gh}**
EDALI/ TZ148-W1	1.78^{AB}	10.67^{cd}	**4^{def}**
EDALI/ TZ148-W2	1.01^{FG}	9.17^{d-g}	**4^{cde}**
EDALI/ TZ148-W3	0.96^{F-H}	5.17^{j}	**5^{ab}**

* Means followed by the same letter are not significantly different, Small letters indicate significant differences at p<0,01, capital letters at p<0.05, Bolded values mean statistically not significant.

rootstock plants in parcels with W2 water application. Drought endamages stomatal regulation. This, at the same time, means that no loss of water for plants in the case of water loss periods [24]. The plants that are tolerable to abiotic conditions such as water stress and drought are the ones which can arrange their stomatal mechanisms. The variations in the width, length and number of stoma are important in terms of understanding the cellular reactions of plants under stress conditions. When the width measurements of stoma were investigated, water levels

did not affect the width of stoma (Table 1). Balhan F1 grafted onto Jumbo had the highest stoma lenght value at W2 water level. Stoma number were increased with water stress (Table 1). Balhan F1 had the highest stoma number at W3 water level.

When the data were taken into consideration in terms of total, marketable and unmarketable yield, it was determined that as water reduction increased, total, marketable and unmarketable yield also decreased (Figure 1.d). Edalı F1 grafted on to TZ 148 had maximum yield (total and marketable) but with water stress yield values decreased too much.

Average fruit weight values of all Edali melons was found higher than that of all Balhan melons (Table 1). For rootstock groups, on the other hand, fruit weights of ungrafted applications were found higher than TZ 148 and Jumbo rootstocks. The lowest fruit weight was found for the cultivars grafted onto Jumbo rootstock. Edelstein et al. [25] stated that grafted plants had more improved values in terms of fruit weights. There are also studies in literature that are inconsistent with each other about the effect of using grafting on the quality of fruits. It should be regarded that these differences might be due to differences in environmental conditions [26]. In this study, as the water reduction increased, the weights of fruits decreased. This result was in accordance with the studies of Karipcin et al. [27] carried out for watermelon.

Brix degree is one of the most important parameters identifying the quality of fruits. As seen in Table 1 among these cultivars, brix degree of Balhan F1was found to be higher. The maximum brix degree among rootstocks was determined for ungrafted (control) plants. Brix degree values of TZ 148 and Jumbo rootstocks were statistically in the same group. It can be stated that the brix degree values of grafted melons decreased. It was determined by Soteriou et al. [28] that water-soluble dry matter values were not affected by grafting. In addition to water reduction, brix degree values decreased. Long et al. [29] stated in their study that water stress affected the brix degree negatively before and during harvest. Water stress that might occur in the critical period of sugar accumulation slows down the rate of photosynthesis and decreases sugar accumulation. Yildirim et al. [30] stated that 75% irrigation level during maturation period increased water-soluble dry matter content.

Irrigation levels and cultivars did not indicate a statistical difference in terms of panel test. When the rootstocks were investigated, maximum panel score was determined for ungrafted (control) group and the second maximum score was indicated for TZ 148 group (Table 1).

Antioxidant Capacity of Melons. Antioxidant capacity of melons was measured via total polyphenolic matter procedure, FRAP (Fe(III) Reduction Antioxidant Capacity) and DPPH (2,2- diphenil-1-picrylhydrazil) radical scavenging methods. When Table 2 was investigated, it was observed that different water regimes, rootstocks and scions affected FRAP, DPPH and total phenolic contents significantly.

When total polyphenol values were investigated, grafting increased total polyphenol content of melons. Highest values were determined for Balhan F1 grafted onto Jumbo and Edalı F1 grafted onto TZ148. As water reduction increased, total polyphenol values decreased (Table 2). Similarly, it was recorded by Mehrjerdi et al. [31] that total phenol values of chickpea types to which water stress was applied decreased. Total polyphenol values recorded for control group were found higher than total polyphenol values of Edali F1 grafted onto *Cucurbita moschata* rootstock under normal irrigation conditions in a study performed by Kolayli et al. [10]. Although total polyphenol content is an important parameter in terms of antioxidant activity, differences were observed with their radical scavenging values. The reason for these differences might be due to the radical scavenging capacity effects of antioxidant enzymes or other components having antioxidant properties which were not determined during this study [32]. Undergoing a functional change for different phenolic compounds under different environmental conditions might be another reason for these differences [4].

When DPPH values were investigated in terms of cultivars (Table 2), DPPH radical scavenging effect of Edali F1 was found higher than that of Balhan F1. Radical scavenging effects of TZ 148 rootstock and control (ungrafted) rootstock were found lower than that of Jumbo rootstock. When the effect of water reduction was considered, it was determined that as water reduction increased, DPPH radical scavenging effect decreased.

A statistical difference was not observed between FRAP values of cultivars. When the rootstocks were investigated, the FRAP values of TZ 148 and Jumbo rootstocks were in the same group and were found higher than the values of ungrafted (control) group. As water reduction increased, a decrease in FRAP values was observed. The highest FRAP value was determined at W1 level for Edali F1 grafted onto TZ 148 rootstock whereas the lowest FRAP value was obtained at W2 irrigation level for Balhan F1 grafted onto Jumbo rootstock (Table 2). FRAP values of control group were found higher than the FRAP values of Edali F1 grafted onto *Cucurbita moschata* rootstock under normal irrigation conditions in the study of [10].

Ascorbic acid, β –carotene and phenolic compounds of melons. Stress changes the morphological, physiological and biochemical responses of plants. In order to decrease negative effects of reactive oxygen components formed under stress condi-

tions, the plants produce antioxidants such as ascorbic acid, glutation,

TABLE 2
The effect of water stress on antioxidant activity

	Total Phenolic Content mg GAE / mL melon juice	DPPH-SC_{50} g/mL melon juice	FRAP µmol/mL melon juice
BALHAN F1-W1	0.10^{cd} ±0.07	0.12^{de} ±0.01	0.33^{e-g}±0.05
BALHAN F1-W2	0.07^{cd} ±0.02	0.64^{a}±0.21	0.22^{hi}±0.03
BALHAN F1-W3	0.01^{d}±0.00	0.23^{cd}±0.02	0.27^{f-i}±0.03
BALHAN/ JUMBO-W1	1.17^{a}±0.20	0.09^{e}±0.01	0.31^{f-h}±0.05
BALHAN /JUMBO –W2	0.24^{c}±0.00	0.16^{de}±0.02	0.17^{i}±0.01
BALHAN/JUMBO-W3	0.07^{cd} ±0.00	0.12^{de} ±0.03	0.35^{d-g}±0.04
BALHAN /TZ148-W1	0.24^{c}±0.04	0.13^{de}±0.02	0.52^{b}±0.07
BALHAN/TZ148 –W2	0.12^{cd}±0.06	0.41^{b}±0.18	0.31^{f-h}±0.06
BALHAN/TZ148-W3	0.15^{cd} ±0.01	0.29^{bc}±0.01	0.35^{d-g}±0.07
EDALI F1-W1	0.64^{b}±0.21	0.17^{e-e}±0.04	0.27^{g-i}±0.01
EDALI F1-W2	0.59^{b}±0.12	0.09^{de} ±0.01	0.42^{b-e} ±0.01
EDALI F1-W3	0.52^{b}±0.05	0.07^{e} ±0.01	0.22^{hi}±0.03
EDALI /JUMBO-W1	1.09^{a}±0.18	0.08^{e} ±0.02	0.48^{bc}±0.05
EDALI/ JUMBO – W2	0.17^{cd}±0.05	0.19^{c-e}±0.05	0.40^{c-f}±0.03
EDALI/ JUMBO-W3	0.01^{d} ±0.00	0.06^{e} ±0.00	0.45^{b-d}±0.02
EDALI/ TZ148-W1	1.14^{a}±0.21	0.07^{e} ±0.02	0.64^{a}±0.02
EDALI/ TZ148-W2	0.15^{cd} ±0.05	0.12^{de} ±0.01	0.29^{f-h}±0.03
EDALI/ TZ148-W3	0.02^{d}±0.00	0.41^{b}±0.10	0.31^{f-h}±0.04
TROLOX (mg/mL)		0.013±0.00	

*Means followed by the same letter are not significantly different at p<0.01.

TABLE 3
The effect of water stress on ascorbic acid and β-carotene values of melons

	Ascorbic acid mg/100 g melon	β-carotene mg/100 g melon
BALHAN F1-W1	48.32^{a}±5.18	0.76^{b}±0.08
BALHAN F1-W2	22.58^{c-e}±4.13	0.54^{c}±0.03
BALHAN F1-W3	36.82^{b}±10.84	0.97^{a}±0.02
BALHAN/JUMBO-W1	17.18^{e-g}±0.77	0.18^{f-h}±0.05
BALHAN/JUMBO –W2	22.39^{c-e}±0.47	0.01^{h}±0.00
BALHAN/JUMBO-W3	16.52^{f-h}±0.78	0.50±0.29
BALHAN/TZ148-W1	18.40^{d-g}±2.17	0.37^{c-e}±0.03
BALHAN/TZ148–W2	23.76^{cd}±3.04	0.48^{cd}±0.09
BALHAN/TZ148-W3	27.51^{bc}±5.19	0.89^{ab}±0.07
EDALI F1-W1	14.58^{gh}±2.31	0.25^{e-g}±0.03
EDALI F1-W2	15.15^{gh}±2.14	0.31^{d-f}±0.29
EDALI F1-W3	15.21^{gh}±1.96	0.20^{e-g}±0.04
EDALI/JUMBO-W1	17.02^{e-g}±2.00	0.31^{d-f}±0.11
EDALI /JUMBO – W2	11.04^{h}±3.38	0.16^{f-h}±0.03
EDALI /JUMBO-W3	21.32^{d-f}±2.86	0.12^{gh}±0.01
EDALI/ TZ148-W1	15.06^{gh}±1.56	0.19^{e-h}±0.02
EDALI/ TZ148-W2	15.30^{gh}±1.03	0.19^{e-h}±0.05
EDALI /TZ148-W3	16.54^{f-h}±3.39	0.19^{e-h}±0.04

*Means followed by the same letter are not significantly different at p<0.01.

carotenoid as well as enzymes having antioxidant properties [33].

In our study maximum ascorbic acid value was determined for Balhan F1 (Table 3). When rootstock effect was considered, grafting adversely affected ascorbic acid values of Balhan however grafting increased slightly ascorbic acid value of Edalı melons. When the effect of water on ascorbic acid was investigated, a significant rate of decrease in ascorbic acid level of Balhan F1 was recorded at W2 irrigation level compared to control level however, with W3 irrigation level, an increase was obtained again (Table 3). At W2 level ascorbic acid levels of Balhan were increased with grafting. The ascorbic acid value of Edalı/Jumbo at W3 was determined as maximum within all Edalı melons . From this point of view, grafting generally caused an increase of ascorbic acid values at water stress. Ascorbic acid amount of Balhan F1 in control group was found quite higher than ascorbic acid values of melons which were grafted but not applied a water reduction in a study carried out by Kolayli et al. [10]. Ascorbic acid amounts of Balhan/TZ148, Balhan/Jumbo and Edali/Jumbo under water reduction conditions were found higher than the values recorded by Kolayli et al. [10].

β-carotene rates of melons varied between 0.01-0.97 mg/100 gr melon (Table 3). Maximum β-carotene amount was stated for Balhan F1 with W3 level. Among Balhan melons amount of β-carotene increased with water stress. The values of Balhan melons were higher than those of Edalı melons. Grafting decreased β-carotene amount. However, the β-carotene values of Balhan/TZ148 melons increased with water stress. Among Balhan/Jumbo melons, maximum level was stated with W3 level. However, those of Edalı /TZ148 melons were not af-

fected with water stress. The effect of water deficiency on carotenoids was reported as negative, positive or as insignificant by different researchers [34]. Condurso et al. [7] determined 56% increase in β-carotene and α-carotene amounts in melon sample for which P360 rootstock was grafted however water reduction was not applied. On the contrary, a decrease was indicated in carotenoid content for cherry tomatoes under water stress conditions [35]. It is necessary to identify the reason for the differences in these results and it is due to genetic and seasonal factors or it is related with the period and intensity of the application used [34].

One of the main secondary metabolites, phenolic compounds has an important physiological and morphological importance in plants. The protective effect of phenolic compounds in plants is arisen from antioxidant effect and radical scavenging properties. Furthermore, they have significant role as a protective in stress [36]. We evaluated 18 phenolic compounds in melons (Table 4). The reduction occurred in the total amount of phenolic compounds with increase in water deficiency in ungrafted Edali F1 and Balhan F1 cultivars. By contrast, the total amount of phenolic compounds increased in Edali /Jumbo, Balhan /TZ148 and Balhan /Jumbo pairs with the water effect of water stress (Table 4). The decrease was recorded in total phenolic compounds of Edali /TZ148 at W2 irrigation level compared to control group whereas an increase at W3 irrigation level. In our study, grafting is said to positively influence the amount of phenolic compounds of melon cultivars together with water deficiency. To our knowledge, no published report is available concerning the change of phenolic compounds with water deficiency in melons. However, plants have ability to accumulate many antioxidants including phenolic compounds under water stress. Sánchez-Rodríguez et al. [37] found that the amount of phenolic compounds increased in grafted cherry tomatoes under water stress. This result was attributed to high activity of synthesis enzyme and the decrease in phenol-degrading enzymes. On the other hand, Krol et al. [38] found decrease in phenolic compounds and antioxidants of grapevine leaves exposed to long term and continuous drought stress. Researchers attributed this result to minimum energy consumption of plant until the stress factor is removed. The cultivar with the highest amount of phenolic compounds among each irrigation level was ungrafted Balhan F1 while the cultivar with the lowest quantity was Edali / Jumbo rootstock at W1 irrigation (control) level. The cultivars with the highest number of phenolic compounds were Edali F1 and Balhan /Jumbo at W1 irrigation level and Edali /Jumbo and ungrafted Balhan F1 at W3 irrigation level. Of the tested phenolic acids, *p*-hydroxybenzoic was found to be highest in quantity. Gallic acid, protocatechuic acid, *p*-hydroxybenzoic acid, caffeic acid, chlorogenic acid, *trans*-ferulic acid, myricetin, quercetin and isorhamnetin were the phenolic compounds detected in all melons at each three irrigation level. The highest amount of *p*-hydroxybenzoic acid was detected at W1 level. When analyzed at rootstock basis, the highest quantity was detected in ungrafted (control) group. This value is higher than that is found by Kolayli et al. [10] who investigated standard, hybrid and grafted melons.

Organic Acids of Melons. Seven organic acids (citric acid, tartaric acid, maleic acid, succinic acid, formic acid, acetic acid and fumaric acids) were investigated in melons (Table 5). The amount of organic acids showed differences according to cultivars, rootstocks and irrigation levels. The cultivar with the highest organic acid quantity was Edali / TZ148 at W3 irrigation level. The accumulation of organic

TABLE 4
The effect of water stress on phenolic compounds (mg/100 mL melon juice)

	W1- control					
Parameter	**EDALI F1**	**EDALI /TZ 148**	**EDALI/JUMBO**	**BALHAN F1**	**BALHAN/ TZ 148**	**BALHAN /JUMBO**
Gallic acid	$0.07^{a}\pm0.00$	$0.02^{g}\pm0.00$	$0.02^{g}\pm0.00$	$0.04^{c-e}\pm0.00$	$0.05^{b-e}\pm0.00$	$0.03^{fg}\pm0.01$
Protocatechuic acid	$0.09^{a}\pm0.01$	$0.04^{e-h}\pm0.01$	$0.03^{g-j}\pm0.00$	$0.06^{c-e}\pm0.01$	$0.02^{ij}\pm0.00$	$0.01^{j}\pm0.00$
Catechin	$0.14^{b-d}\pm0.05$	$0.18^{b}\pm0.01$	$0.10^{d-g}\pm0.01$	$0.07^{gh}\pm0.01$	$0.06^{h}\pm0.00$	$0.10^{d-g}\pm0.01$
p-hydroxybenzoic acid	$0.11^{f-h}\pm0.02$	$0.02^{j}\pm0.00$	$0.01^{j}\pm0.00$	$1.07^{a}\pm0.00$	$0.07^{hi}\pm0.00$	$0.12^{fg}\pm0.01$
Vanillic acid	$0.03^{d}\pm0.01$	$0.00^{e}\pm0.00$	$0.00^{e}\pm0.00$	$0.00^{e}\pm0.00$	$0.00^{e}\pm0.00$	$0.04^{b}\pm0.01$
Caffeic acid	$0.05^{e}\pm0.00$	$0.05^{ef}\pm0.00$	$0.05^{ef}\pm0.00$	$0.07^{c}\pm0.00$	$0.09^{b}\pm0.00$	$0.06^{cd}\pm0.00$
Syringic acid	$0.01^{e-f}\pm0.00$	$0.02^{ab}\pm0.00$	$0.01^{ef}\pm0.00$	$0.02^{f}\pm0.00$	$0.01^{a}\pm0.00$	$0.01^{d-f}\pm0.00$
Chlorogenic acid	$0.03^{d-g}\pm0.00$	$0.03^{f-h}\pm0.00$	$0.01^{j}\pm0.00$	$0.03^{e-h}\pm0.01$	$0.02^{ij}\pm0.00$	$0.03^{c-f}\pm0.01$
Rutin	$0.00^{b}\pm0.00$	$0.00^{b}\pm0.00$	$0.00^{b}\pm0.00$	$0.00^{b}\pm0.00$	$0.00^{b}\pm0.00$	$0.00^{b}\pm0.00$
trans-p-coumaric acid	$0.00^{e}\pm0.00$	$0.01^{d}\pm0.00$	$0.00^{e}\pm0.00$	$0.01^{cd}\pm0.00$	$0.01^{d}\pm0.00$	$0.01^{bc}\pm0.00$
trans-ferulic acid	$0.01^{DE}\pm0.00$	$0.01^{DE}\pm0.00$	$0.01^{DE}\pm0.00$	$0.03^{A}\pm0.00$	$0.02^{BC}\pm0.01$	$0.01^{CD}\pm0.00$
Myricetin	$0.05^{c-e}\pm0.01$	$0.06^{c}\pm0.01$	$0.04^{d-g}\pm0.01$	$0.04^{f-j}\pm0.00$	$0.03^{j-l}\pm0.00$	$0.04^{f-j}\pm0.01$
trans- resveratrol	$0.01^{h}\pm0.00$	$0.04^{a}\pm0.00$	$0.01^{gh}\pm0.00$	$0.00^{l}\pm0.00$	$0.02^{c}\pm0.00$	$0.01^{gh}\pm0.00$
Quercetin	$0.05^{ab}\pm0.00$	$0.05^{ab}\pm0.01$	$0.02^{cd}\pm0.00$	$0.03^{c}\pm0.01$	$0.05^{b}\pm0.01$	$0.01^{d}\pm0.00$
trans-cinnamic acid	$0.03^{b}\pm0.00$	$0.01^{fg}\pm0.00$	$0.00^{gh}\pm0.00$	$0.02^{d}\pm0.00$	$0.01^{f}\pm0.00$	$0.01^{f}\pm0.00$
Naringenin	$0.01^{b}\pm0.00$	$0.00^{cd}\pm0.00$	$0.00^{d}\pm0.00$	$0.00^{cd}\pm0.00$	$0.00^{d}\pm0.00$	$0.00^{d}\pm0.00$
Kaempferol	**$0.00^{a}\pm0.00$**	**$0.00^{a}\pm0.00$**	**$0.00^{a}\pm0.00$**	**$0.00^{a}\pm0.00$**	**$0.00^{a}\pm0.00$**	**$0.00^{a}\pm0.00$**

Isorhamnetin	**0.17^{a-d}±0.00**	**0.16^{a-d}±0.01**	**0.16^{a-d}±0.02**	**0.18^{ab}±0.03**	**0.18^{a-c}±0.01**	**0.13^{d}±0.04**
Total	0.87±0.11	0.67±0.06	0.48±0.05	1.66±0.10	0.62±0.04	0.62±0.10

* Means followed by the same letter are not significantly different. Small letters indicate significant differences at p<0.01, capital letters at p<005. Bolded values mean statistically not significant

acids is a physiological response of plants when exposed to stress [39]. The dominant organic acid was tartaric acid and the other acid was citric acid. Formic acid was detected only in Balhan / Jumbo at W2 irrigation level and in Edali F1 and Balhan F1 pairs at W3 irrigation level. Kolayli et al. [10] didn't found citric acid in melons grafted but not exposed to water stress. When the effect of irrigation on the acids was considered, citric acid, maleic acid, fumaric acid and formic acid quantities increased with enhancemnet of water deficiency whereas tartaric acid, succinic acid and acetic acid decreased. In accordance with our results; oxalic acid, malic acid and citric acid levels of *Isatis indigotica* cultivated under water stress increased with severity of water stress [40]. When the influence of rootstocks was considered, the highest amount of citric, tartaric and maleic acids values were attained in cultivars grafted onto TZ148 rootstock. On the other hand, the highest succinic, formic and fumaric acid values were obtained in cultivars grafted onto Jumbo rootstock. On the other hand, the highest citric acid quantity was detected in Edali / TZ148. The information on the influence of different rootstocks on organic acid levels of melons cultivated under water stress is limited. In one of the study, where germination and growth parameters of wheat cultivated under water stress were examined, the decrease in organic acids was observed. On the contrary, it was reported that formic acid showed an opposite effect. The change in the organic acid levels was attributed to adaptive mechanism of wheat seedlings to maintain their osmotic balance under water stress [39].

Sugar Contents of Melons. Sweetness is an important parameter in determining the fruit quality. Glucose, fructose, saccharose, ribose, arabinose, galactose, maltose, trehalose, mellebiose and mellesitose were investigated in melon samples but only glucose, fructose and saccharose were found in

TABLE 5
The effect of water stress on organic acids (mg/100 mL melon juice)

	Citric acid	Tartaric acid	Maleic acid	Succinic acid	Formic acid	Acetic acid	Fumaric acid	Total
BALHAN F1-W1	47.07^{n}±0.48	107.57^{o}±0.60	0.93^{d}±0.00	14.44^{l}±0.06	0.00^{d}±0.00	160.91^{a}±1.05	3.45^{e}±0.10	334.36±2.29
BALHAN F1-W2	133.70^{h}±2.14	149.56^{n}±1.56	0.91^{de}±0.00	12.47^{l}±0.03	0.00^{d}±0.00	151.57^{b}±2.59	0.00^{q}±0.00	448.20±6.31
BALHAN F1-W3	45.55^{n}±2.40	45.63^{q}±1.23	1.13^{c}±0.03	7.78^{m}±0.13	4.59^{b}±0.12	39.73^{i}±1.51	2.00^{ij}±0.03	146.41±5.45
BALHAN/ JUMBO-W1	13.78^{o}±0.42	158.50^{m}±0.54	1.05^{c}±0.01	103.17^{b}±1.31	0.00^{d}±0.00	107.26^{c}±1.16	2.45^{g}±0.03	386.20±3.47
BALHAN /JUMBO – W2	0.00^{p}±0.00	69.48^{p}±0.27	0.50^{jk}±0.15	139.15^{a}±0.76	17.00^{a}±0.77	65.32^{f}±0.59	6.32^{b}±0.02	297.79±2.56
BALHAN/J UMBO-W3	52.10^{m}±8.60	222.76^{k}±1.11	0.80^{fg}±0.01	29.92^{h}±2.36	0.00^{d}±0.00	71.88^{e}±4.30	3.59^{d}±0.10	381.05±16.47
BALHAN /TZ148-W1	154.36^{f}±0.07	378.11^{a}±0.32	1.07^{c}±0.00	27.52^{hi}±0.05	0.00^{d}±0.00	106.38^{c}±0.17	2.06^{hi}±0.01	669.50±0.61
BALHAN/T Z148 –W2	113.22^{k}±1.46	169.77^{l}±0.55	0.00^{l}±0.00	19.84^{k}±0.63	0.00^{d}±0.00	53.49^{h}±1.90	7.34^{a}±0.05	363.67±4.58
BALHAN/T Z148-W3	242.76^{b}±2.01	307.29^{h}±3.24	10.18^{a}±0.07	29.20^{h}±0.90	0.00^{d}±0.00	80.50^{d}±3.72	3.15^{f}±0.06	673.08±9.99
EDALI F1-W1	123.41^{j}±0.38	323.33^{g}±0.50	0.79^{fg}±0.00	34.23^{g}±0.16	0.00^{d}±0.00	56.07^{gh}±0.18	1.85^{mn}±0.00	539.67±1.22
EDALI F1-W2	166.40^{e}±0.25	352.09^{e}±0.19	1.39^{b}±0.00	24.71^{ij}±0.07	0.00^{d}±0.00	60.32^{g}±0.11	1.90^{lm}±0.00	606.81±0.62
EDALI F1-W3	178.37^{c}±0.79	358.08^{d}±2.62	0.48^{k}±0.18	37.83^{f}±0.00	2.53^{c}±0.13	11.75^{k}±0.05	4.58^{c}±0.00	593.62±3.78
EDALI /JUMBO-W1	139.87^{g}±1.23	342.20^{f}±0.86	0.84^{d-f}±0.00	44.83^{e}±7.31	0.00^{d}±0.00	21.88^{j}±0.25	1.92^{kl}±0.00	551.54±9.66
EDALI/ JUMBO – W2	95.10^{l}±0.60	257.14^{i}±1.13	0.58^{ij}±0.01	30.36^{h}±0.68	0.00^{d}±0.00	40.66^{i}±0.39	1.77^{op}±0.00	425.61±2.81
EDALI/ JUMBO-W3	249.67^{a}±1.74	376.39^{a}±0.79	0.71^{gh}±0.00	62.33^{d}±1.34	0.00^{d}±0.00	13.64^{k}±0.53	1.71^{p}±0.01	704.45±4.40
EDALI/ TZ148-W1	131.41^{hi}±0.14	364.20^{b}±0.50	0.67^{hi}±0.00	42.59^{e}±0.04	0.00^{d}±0.00	39.97^{i}±0.40	1.79^{no}±0.00	580.63±1.09
EDALI/ TZ148-W2	127.92^{i}±0.70	362.15^{c}±0.37	0.82^{ef}±0.00	21.74^{jk}±0.37	0.00^{d}±0.00	57.53^{gh}±10.43	2.11^{h}±0.02	572.26±11.90
EDALI/ TZ148-W3	174.35^{d}±1.19	251.39^{j}±0.54	0.71^{gh}±0.00	77.08^{c}±0.34	0.00^{d}±0.00	5.94^{l}±0.04	1.97^{jk}±0.00	511.44±2.11

*Means followed by the same letter are not significantly different at p<0.01.

the melons (Figure 2a). Grafting onto TZ148 and Jumbo rootstocks affected the sugar levels in a different ways under different water deficit stresses. The decrease was noted in fructose and saccharose quantity as the amount of water given to plant decreased but glucose level was not affected. Considering the effect of rootstocks; the highest fuctose ratios were determined in Jumbo and TZ148 rootstocks where the highest glucose and saccharose ratios in ungrafted (control) plants. Glucose and fructose were detected in all rootstock/scion combinations. On the other hand, saccharose is found in all groups except in Edali/TZ148 and Balhan/Jumbo cultivated at W3 irrigation level. The cultivar and rootstock/scion combinations with the highest sweetness were Edali F1, Edali/TZ148, Edali/Jumbo cultivated at well-watered condition (control) and Edali F1 cultivated at W2 water stress. Reduction occured in the sweetness level of Edali F1, Edali/TZ148 and Edali/Jumbo combinations as water deficiency increased. The reduction in the sweetness level may be attributed to carbon deficiency [34]. An increase was detected in the sweetness level of Balhan / TZ148 with the water deficiency. Mirabad et al. [41] also found an increase in the sweetness of cantaloupe melon with the water stress. Glucose level of Edali F1 increased with the water stress. In the case of Edali/ TZ148, glucose level increased at the W2 irrigation level whereas it decreased at W3 irrigation level. The amount of glucose decreased in Edali / Jumbo as the water deficiency increased. In Balhan/TZ148 and Balhan/Jumbo, glucose level increased as the water deficiency increased. Zeinali et al. [42] found the raise in saccharose and glucose level of *Cucumis melo var. reticulatus cv.* Samsoury at severe water stress. The highest fructose ratio was detected in non-grafted Edali F1 melon cultivar at full irrigation regime. The amount of saccharose in Edali F1, Edali / TZ148 ve Edali / Jumbo decreased with the increase of water stress. While the glucose quantity of Edali / Jumbo decreased as the water deficiency increased, that of Balhan / TZ148 and Jumbo rootstocks increased. Fructose/glucose ratio is an important indicator for most of the fruit juices [10] and the ratio among different sugars affect the fruit taste [43]. The highest fructose/glucose ratio was detected in Balhan / TZ148 rootstock at full irrigtion regime (Figure 2b). The fructose/glucose ratio of rootstock/scion combinations decreased with the severity of water stress except Balhan F1.

Correlations of Irrigation Levels and Rootstocks with Some Biochemical Parameters of Melons. Correlation coefficients of irrigation levels and rootstocks with some biochemical parameters of melon cultivars (Edali F1 and Balhan F1) are presented in Table 6. Although statistically not significant, total polyphenol was positively and high correlated with the utilization of rootstocks at W1 and W2 irrigation levels. The correlation between the rootstocks and FRAP values of melons were the highest (r^2= 0.99) at W3 irrigation level. In other words, FRAP values were positively effected from the utilization

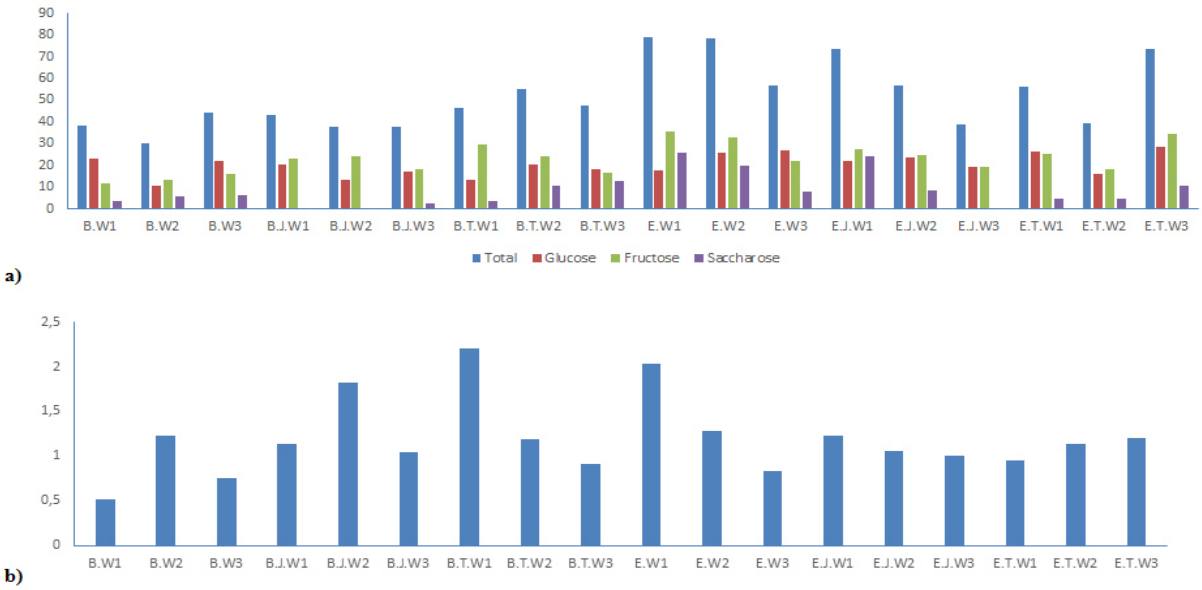

FIGURE 2
Relationship between water stress and a) sugar content (mg) b) ratio of fructose to glucose B.W1: Balhan F1. Control, B.W2: Balhan F1. 50 % Water, B.W3: Balhan F1. 25 % Water, B.J.W1: Balhan. Jumbo. Control, B.J.W2: Balhan. Jumbo. 50 % Water, B.J.W3: Balhan. Jumbo. 25 % Water,

B.T.W1: Balhan. TZ148. Control, B.T.W2: Balhan. TZ148. 50 % Water, B.T.W3: Balhan. TZ148. 25 % Water, E.W1: Edalı F1. Control, E.W2: Edalı F1. 50 % Water, E.W3: Edalı F1. 25 % Water, E.J.W1: Edalı. Jumbo. Control, E.J.W2: Edalı. Jumbo. 50 % Water, E.J.W3: Edalı. Jumbo. 25 % Water, E.T.W1: Edalı. TZ148. Control, E.T.W2: Edalı. TZ148. 50 % Water, E.T.W3: Edalı. TZ148. 25 % Water.

TABLE 6
Correlation values among irrigation levels/rootstocks (TZ 148/Jumbo) and some biochemical parameters of melons

Irrigation Levels	Rootstocks (Control/ TZ148/Jumbo)	Beta-Carotene	Ascorbic acid	*p*-hydroxy benzoic acid	Catechin	Tartaric acid
W1	Edalı	0.51*	0.94*	-0.87*	-0.54*	1.00**
	Balhan	-0.98*	-0.88*	-0.85*	0.73*	0.18*
W2	Edalı	-0.95*	-0.85*	-0.98*	-0.94*	0.87*
	Balhan	-0.92*	-0.13*	-1.00**	0.99**	-0.75*
W3	Edalı	-0.91*	0.95*	-0.94*	0.96*	-0.79*
	Balhan	-0.94*	-1.00***	-0.07*	-0.91*	0.66*
		Citric acid	**Glucose**	**Fructose**	**Saccharose**	
W1	Edalı	0.49*	0.99*	-0.14***	-0.90*	
	Balhan	-0.23*	-0.87*	0.68*	-0.84*	
W2	Edalı	-0.54*	0.24*	-0.85*	-0.95*	
	Balhan	-0.93*	0.67*	0.43*	-0.42*	
W3	Edalı	-0.05*	-0.97*	-0.96*	-0.42*	
	Balhan	0.03*	-0.46*	0.88*	-0.47*	

Statistical significance: *= Not significant, **=p<0.01, *** =p<0.05

of rootstocks. Negative correlation between rootstocks and DPPH for Balhan F1 at W2 irrigation level means good radical scavenging activities. The amount of ascorbic acid in Balhan F1 correlated negatively with rootstocks at W3 irrigation level. Correlation values of β-carotene, citric acid, glucose and saccharose with rootstocks were statistically insignificant. However, correlation values between among rootstocks and β-carotene and glucose were high for Edali F1 at W1 irrigation level. Catechin value of Balhan F1 at W2 irrigation level strongly correlated with utilization of rootstocks. On the other hand, *p*-hydroxy benzoic acid negatively correlated with the usage of rootstocks. Among the tested sugars, only corellation between fructose and rootstocks for Edali F1 at W1 irrigation level was statistically important and it was negatively correlated.

CONCLUSIONS

Our study indicated that the grafting of hybrid melon cultivars (Edali F1 and Balhan F1) onto TZ 148 and Jumbo rootstocks highly affected the biochemical and growth-yield parameters of the melons exposed to water stress conditions. The grafting of hybrid melon cultivars onto TZ 148 and Jumbo rootstocks enhanced the health-promoting compounds of melon cultivars (Edali F1 and Balhan F1) under water stress conditions. Elucidation of genetic and environmental factors and their interactions on the agronomic and biochemical properties especially bioactive compounds of the melon cultivars is required if the breeders aim to produce crops with health-promoting effects. Furthermore, these findings are physiologically and biochemically important to assess the metabolic changes of the tested compounds under water deficit stress conditions. On the other hand, the utilization of TZ 148 and Jumbo rootstocks under water stress didn't improve some yield and growth parameters which depend not only on the rootstock but also the interaction between rootstock/scion combinations, environmental factors, cultivars and growth conditions. Although grafting didn't improve growth and yield parameters, its positive effect on health-promoting compounds is remarkable. Because, recently consumers'demand is towards to health benefits of fruits and vegetables. So, the adverse affects of grafting under water stress on growth and yield parameters may be ignored in this respect. However, future researches may focus on screening of different rootstock/scion combinations compatible for particularly in arid and semiarid regions to get melons with both high biochemical and agronomic quality.

ACKNOWLEDGEMENTS

The authors would like to thank Selcuk University Scientific Research Projects (Project number: 14401036) Council. We would also like to thank to GAP Agricultural Research Institute for melon cultivation and Selcuk University Advanced Technology Research and Application Centre for their research infrastructure.

Compliance with Ethical Standards. This study was funded by Selcuk University Scientific

Research Projects Council (Project number: 14401036). The authors declare that they have no conflict of interest.

REFERENCES

[1] Bolat, I., Dikilitas. M., Ercisli, S., Ikinci, A., Tonkaz, T. (2014) The effect of water stress on some morphological, physiological and biochemical characteristics and bud success on apple and quince rootstocks. Scientific World Journal. 2014, 8p.

[2] Schwarz, D., Rouphael, Y., Colla, G., Venema, J.H. (2010) Grafting as a tool to improve tolerance of vegetables to abiotic stresses: Thermal stress, water stress and organic pollutants. Scientia Horticulturae. 127, 162–171.

[3] Savvas, D., Colla, G., Rouphael, Y., Schwarz, D. (2010) Amelioration of heavy metal and nutrient stress in fruit vegetables by grafting. Scientia Horticulturae. 127, 156–161.

[4] Gharibi, S., Tabatabaei, B.E.S., Saeidi, G., Goli, S.A.H. (2016) Effect of drought stress on total phenolic, lipid peroxidation, and antioxidant activity of achillea species. Applied Biochemistry and Biotechnoly. 178, 796–809.

[5] Rouphael, Y., Schwarz, D., Krumbein, A., Colla, G. (2010) Impact of grafting on product quality of fruit vegetables. Scientia Horticulturae. 127, 172–179.

[6] Sánchez-Rodríguez, E., Ruiz, J.M., Ferreres, F., Moreno, D.A. (2012) Phenolic profiles of cherry tomatoes as influenced by hydric stres and rootstock technique. Food Chemistry. 134, 775–782.

[7] Condurso, C., Verzera, A., Dima, G., Tripodi, G., Crinò, P., Paratore, A., Romano, D. (2012) Effects of different rootstocks on aroma volatile compounds and carotenoid content of melon fruits. Scientia Horticulturae. 148, 9-16.

[8] Proietti, S., Rouphael, Y., Colla, G., Cardarelli, M., De Agazio, M., Zacchini, M., Rea, E., Moscatello, S., Battistelli, A. (2008) Fruit quality of mini-watermelon as affected by grafting and irrigation regimes. J.Sci Food Agric. 88, 1107–1114.

[9] Goreta Ban, S., Žanić, K., Dumičić, G., Raspudić, E., Selak, G.V., Ban, D. (2014) Growth and yield of grafted cucumbers in soil infested with root-knot nematodes. Chilean J. Agric. Res. 74(1), 29-34.

[10] Kolayli, S., Kara, M., Tezcan, F., Erim, F.B., Sahin, H., Ulusoy, E., Yazicioglu, R. (2010) Comparative Study of Chemical and Biochemical Properties of Different Melon Cultivars: Standard, Hybrid, and Grafted Melons. J. Agric. Food Chem. 58, 9764–9769.

[11] Smart, R.E., and Bingham, G.E. (1974) Rapid estimates of relative water content. Plant Physiol. 53, 258-60.

[12] Alizadeh, A., Khazai, M., Baghani, J., Haghnia, G.H. (1999) Effect of deficit irrigation by drip and furow systems on the yield and quality of melon at Mashad. Iran. Irrigation Under Conditions Of Water scarcity. Vol. 1C. 17th ICID International Congress On Irrigation And Drainage. 13-17 September 1999. Granada, Spain. 263-269.

[13] Sari, N., Abak, K., Pitrat, M. (1999) Comparison of ploidy level screening methods in watermelon (Citrullus lanatus (Thunb.) Matsum and Nakai). Scientia Horticulturae. 82 (3-4), 265-277.

[14] Benzie, I.F.F. and Strain, J.J. (1996) The ferric reducing ability of plasma (FRAP) as a measure of ‘‘antioxidant power”: The FRAP assay. Analytical Biochemistry. 239, 70–76.

[15] Molyneux, P. (2004) The use of the stable free radical diphenylpicryl- hydrazyl (DPPH) for estimating antioxidant activity. SJST. 26, 211-219.

[16] Singleton, V.L. and Rossi, J.L. (1965) Colorimetry of total phenolics with phosphomolybdic phosphotungstic acid reagents. Am J EnolVitic. 16,144-158.

[17] Sawant, L., Prabhakar, B., Pandita, N. (2010) Quantitative HPLC Analysis of Ascorbic Acid and Gallic Acid in Phyllanthus Emblica. Journal of Analytical and Bioanalytical Techniques. 1(111).

[18] Mu-Lin, L., Bo-Di, H., Ke-Nuo. P. (2007) Quantitative Analysis of Lycopene from Tomato and Its Processed Products by C18-HPLC-PDA. Food Science. 28, 453-456.

[19] Wen, D., Li, C., Di, H., Liao, Y., Liu, H. (2005) A universal HPLC method for the determination of phenolic acids in compound herbal medicines. Journal of Agricultural and Food Chemistry. 53, 6624-6631.

[20] Sinclair, T.R., and Ludlow, M.M. (1985) The unfulfilled potential of plant water potential. Australian Journal of Plant Physiology. 12, 213-217.

[21] Tang, A.C., Kawamitsa, Y., Kanechi, M., Boyer, J.S. (2002) Photosynthesis at low water potential in leaf discs lacking epidermis. Annals of Botany. 89, 861-870.

[22] Stewart, B.A., and Howell, T.A. (2003) Drought evidence and drought adaptation. Encyclopedia of Water Science. New York. Marcel Dekker. 1076p.

[23] Mullet, J.E. and Whitsitt, M.S. (1996) Plant cellular responses to water deficit. Plant Growth

Regulation. 20 (2), 119-124.
[24] Cowan, I.R. (1982) Regulation of water use in relation to carbon gain in higher plants, O.L. Lange and J.D. Bewley. Encyclopedia of Plant Physiology. Vol: 12B. Springer-Verlag, Berlin. 535-562.

[25] Edelstein, M., Burger, Y., Horev, C., Porat, A., Meir, A., Cohen, R. (2014) Assessing the effect of genetic and anatomic variation of Cucurbita rootstocks on vigour, survival and yield of grafted melons. The Journal of Horticultural Science and Biotechnology. 79(3), 370-374.
[26] Singh, P.K. and Rao, K.M. (2014) Role of grafting in cucurbitaceous crops A review. Agricultural Reviews. 35(1), 24-33.
[27] Karipcin, M.Z. (2009) The determination of drought tolerance of domestic and wild watermelon genotypes. PhD Thesis. Cukurova University, Agriculture Faculty, Adana, Turkey.
[28] Soteriou, G.A,, Kyriacou, M.C., Siomos, A.S., Gerasopoulos, D. (2014) Evolution of watermelon fruit physicochemical and phytochemical composition during ripening as affected by grafting. Food chemistry. 165, 282-289.
[29] Long, R.L., Walsh, K.B., Midmore, D.J. (2006) Irrigation scheduling to increase muskmelon fruit biomass and soluble solids concentration. Hortscience. 41(2), 367-369.
[30] Yildirim, E., Dursun, A. (2009) Effect of Foliar Salicylic Acid Applications on Plant Growth and Yield of Tomato under Greenhouse Conditions. Acta Horticulturae. 807(1), 395-400.
[31] Mehrjerdi, M.Z., Bagheri, A., Bahrami, A.R., Nabati, J., Massomi, A. (2013) Effect of drought stress on photosynthetic characteristics, phenolic compounds and radical scavenging activities in different chickpea (Cicer arietinum L.) genotypes in hydroponic conditions. Journal of Science and Technol. Greenhouse Culture. 3(12), 59-77.
[32] Salandanan, K., Bunning, M., Stonaker, F., Külen, O., Kendall, P., Stushnoff, C. (2009) Comparative Analysis of Antioxidant Properties and Fruit Quality Attributes of Organically and Conventionally Grown Melons (Cucumis melo L.). Hortscience. 44(7), 1825–1832.
[33] Kusvuran, S., Kiran, S., Ellialtioglu, S.S. (2016) Antioxidant Enzyme Activities and Abiotic Stress Tolerance Relationship in Vegetable Crops. Abiotic and Biotic Stress in Plants. Intech.
[34] Ripoll, J., Urban, L., Staudt, M., Lopez-Lauri, F., Luc, P.R., Bertin, B.N. (2014) Water shortage and quality of fleshy fruits—making the most of the unavoidable. Journal of Experimental Botany. 65, 3-21.
[35] De, P., Martino, A., Raimondi, G., Maggio, A. (2007) Comparative analysis of water and salt stressinduced modifications of quality parameters in cherry tomatoes. Journal of Horticultural Science and Biotechnology. 82 (2), 283–289.

[36] Nadernejad, N., Ahmadimoghadam, A., Hossyinifard, J., Poorseyedi, S. (2013) Evaluation of PAL activity, Phenolic and Flavonoid Contents in Three Pistachio (Pistacia vera L.) Cultivars Grafted onto Three Different Rootstocks. Journal of Stress Physiology and Biochemistry. 9(3), 84-97.
[37] Sánchez-Rodríguez, E., Ruiz, J.M., Ferreres, F., Moreno, D.A. (2011) Phenolic metabolism in grafted versus nongrafted cherry tomatoes under the influence of water stress. Journal of Agriculture and Food Chemistry. 59(16), 8839-46.
[38] Krol, A., Amarowicz, R., Weidner, S. (2014). Changes in the composition of phenolic compounds and antioxidant properties of grapevine roots and leaves (Vitis vinifera L.) under continuous of long-term drought stress. Acta Physiologiae Plantarum. 36, 1491–1499.
[39] Guo, R., Hao, W.P., Gong, D.Z., Zhong, X.L., Gu, F.X. (2013) Effects of water stress on germination and growth of wheat, photosynthetic efficiency and accumulation of metabolites. Chapter 13. In: Hernandez Soriano, M.C. (ed.) Soil processes and current trends in quality assesment. Intech open. 367-380.
[40] Chen, X., Zhou, J., Tang, X., Wang, K. (2009) Effect of water stress on content of four organic acids in different cultivated populations of Isatis indigotica. Zhongguo Zhong Yao Za Zhi. 34(24), 3195-3198.
[41] Mirabad, A.A, Lotfi, M., Roozban, M.R. (2013) Impact of Water-Deficit Stress on Growth, Yield and Sugar Content of Cantaloupe (Cucumis melo L.). International Journal of Agriculture and Crop Sciences. International Journal of Agriculture and Crop Science. 5(22), 2778-2782.
[42] Zeinali, N., Haghbeen, S.K., Delshad, M. (2016) Water deficit effects on some physiological characteristics, sugars and proline as osmolytes in Cucumis melo var. reticulates cv. Samsoury. Journal of plant process and function. 5(16), 105-116.
[43] Desnoues, E., Gibon, Y., Baldazzi, V., Signoret, V., Genard, M., Quilot-Turion, B. (2014) Profiling sugar metabolism during fruit development in a peach progeny with different fructose-to-glucose ratios. BMC Plant Biology. 14, 336-349.

Received: **13.02.2018**
Accepted: **30.04.2018**

CORRESPONDING AUTHOR

Muhemet Zeki Karipcin
Siirt University
Agricultural Faculty
Department of Horticulture
Siirt – Turkey

e-mail: zkaripcin@siirt.edu.tr

© by PSP Volume 27 – No. 7/2018 pages 5022-5026 Fresenius Environmental Bulletin

EFFECT OF NANO-ZINC FOLIAR APPLICATION WHEAT UNDER DROUGHT STRESS

Azizollah Ghassemi[1,*], Farhad Farahvash[2]

[1]Member of Scientific Association of Agronomy and Plant Breeding, Tabriz Branch, Islamic Azad University, Tabriz, Iran
[2]Department of Agronomy and Plant Breeding, Tabriz Branch, Islamic Azad University, Tabriz, Iran

ABSTRACT

Drought stress is an abiotic stresses that can decreased absorption nutrition from soil by plants and causes decreased yield of plants. In order to evaluation effect of Nano-zinc foliar application in wheat cultivar (chamran) under drought stress at the Research Station of the Islamic Azad University, Tabriz Branch, Tabriz, Iran. The trial was carried out in a split-plot factorial experiment based on randomized complete block design with four replications. The main plots were two levels of drought stress (one with commonly available irrigation water referred to as control and the other interrupted irrigation during flowering stage), and five levels of Nano-zinc foliar application (control, before stem elongation stage (2 g/L), before stem elongation stage (4 g/L), flowering stage (2 g/L) and flowering stage (4 g/L)) were assigned as sub-plots. The results showed that drought stress was significantly decreased grain yield and its components, plant height, relative water content (RWC) and chlorophyll content, but Nano-zinc foliar application had positive effect on them. The result is shown that 2 g/L in flowering stage of wheat was best condition to grain yield and its components, plant height, relative water content (RWC) and chlorophyll content. Correlation between in studied traits of wheat showed that yield grain had significantly positive with number of grains spike, and significantly correlations were observed between spike height with RWC, chlorophyll content and harvest index. Results showed that Nano-zinc could be used for improving wheat growth under drought stress.

KEYWORDS:
Drought stress, Grain yield, Nano-zinc, Wheat

INTRODUCTION

Grain crops strongly suffer from insufficient water supply, showing various morphological, physiological, biochemical, and molecular responses to drought. Drought stress can cause negative reversible and irreversible physiological changes of plant state in the vegetative and reproductive periods of plant development [1]. Wheat (*Triticum aestivum* L.) is one of the most important crops in the world. The growth of wheat has been seriously influenced by drought in many regions. Under drought stress, photosynthesis and grain yield decreases due to stomata limitation when light energy absorption exceeds its capacity for utilization [2]. Zinc (Zn) is essential plant micronutrient which is involved in many physiological functions, protein and carbohydrate synthesis [3]. The application of Zn under drought conditions would influence crop yield and quality. It plays a significant role in regulating stomata and ionic balance in crops to reducing the detrimental effects of drought [4].

Nano fertilizers with emerging nutrient management tools in agriculture have potential to increase crop yield, nutrient use efficiency and farmer income with reduced environment pollution resulted from application of overdose of fertilizers in crop production [5]. Nano fertilizers have high surface area, water solubility and penetrability which help to increase availability of nutrient to the crop plant from applied surface. Hence, it is visualized as a rapidly evolving field in nutrient management which has potential to revolutionize agriculture and food systems and improve the conditions of the poor [3, 4]. The influence of nanoparticles on physiological state of plants at the different levels of their organization, beginning from molecular, has been studied at various plants. It is known that nanoparticles in different concentrations can impact both positive and negative biological effects [5]. Several studies have been shown that a small amount of nutrients, particularly Zn applied by foliar spraying can significantly increase the yield of crops [3, 6]. Also, foliar nutrition is an option when nutrient deficiencies cannot be corrected by applications of nutrients to the soil [6]. It is likely therefore, in open-field conditions, where the factors that influence the uptake of the nutrients are very variable, foliar fertilization is a privilege [7]. Among the micronutrients, Zn nutrition can affect the susceptibility of plants to drought stress. Zn plays an important role in the production of biomass [6, 7]. Furthermore, Zn may be required for chlorophyll production, pollen function, fertilization and germination [5]. Therefore, the present study aimed to determine the effect of foliar application of zinc on growth and grain yield of wheat under drought stress.

MATERIALS AND METHODS

Plant materials and field experiments. A field experiment was carried out during 2016-2017 growing season at the Research Station of the Islamic Azad University, Tabriz Branch, Tabriz, Iran. The soil at the experimental site was sandy-loam (pH= 7.7 and organic matter 1.3%). The trial was carried out in a split-plot factorial experiment based on randomized complete block design with four replications. The main plots were two levels of drought stress (one with commonly available irrigation water referred to as control and the other interrupted irrigation during flowering stage), and five levels of Nano-zinc foliar application (control, before stem elongation stage (2 g/L), before stem elongation stage (4 g/L), flowering stage (2 g/L) and flowering stage (4 g/L)) were assigned as sub-plots.

Traits measurement. Grain yield, yield components, and plant height of wheat were evaluated. The leaf water content (RWC) was estimated following the gravimetric method as described by [8]. The chlorophyll content of the second and third leaf was measured with a SPAD-502 Chlorophyll Meter (Minolta Corporations, Ramsey, NJ, USA). Leaf area was measured with a portable leaf area meter LI-3000C, (LICOR Inc., Lincoln, NE, USA).

Statistical analysis. Data of the three repeats years were combined and the combined data were subjected to normal distribution tests and analysis of variance and least significant difference (LSD) for comparison of means were performed using statistical analysis system (SAS 9.1).

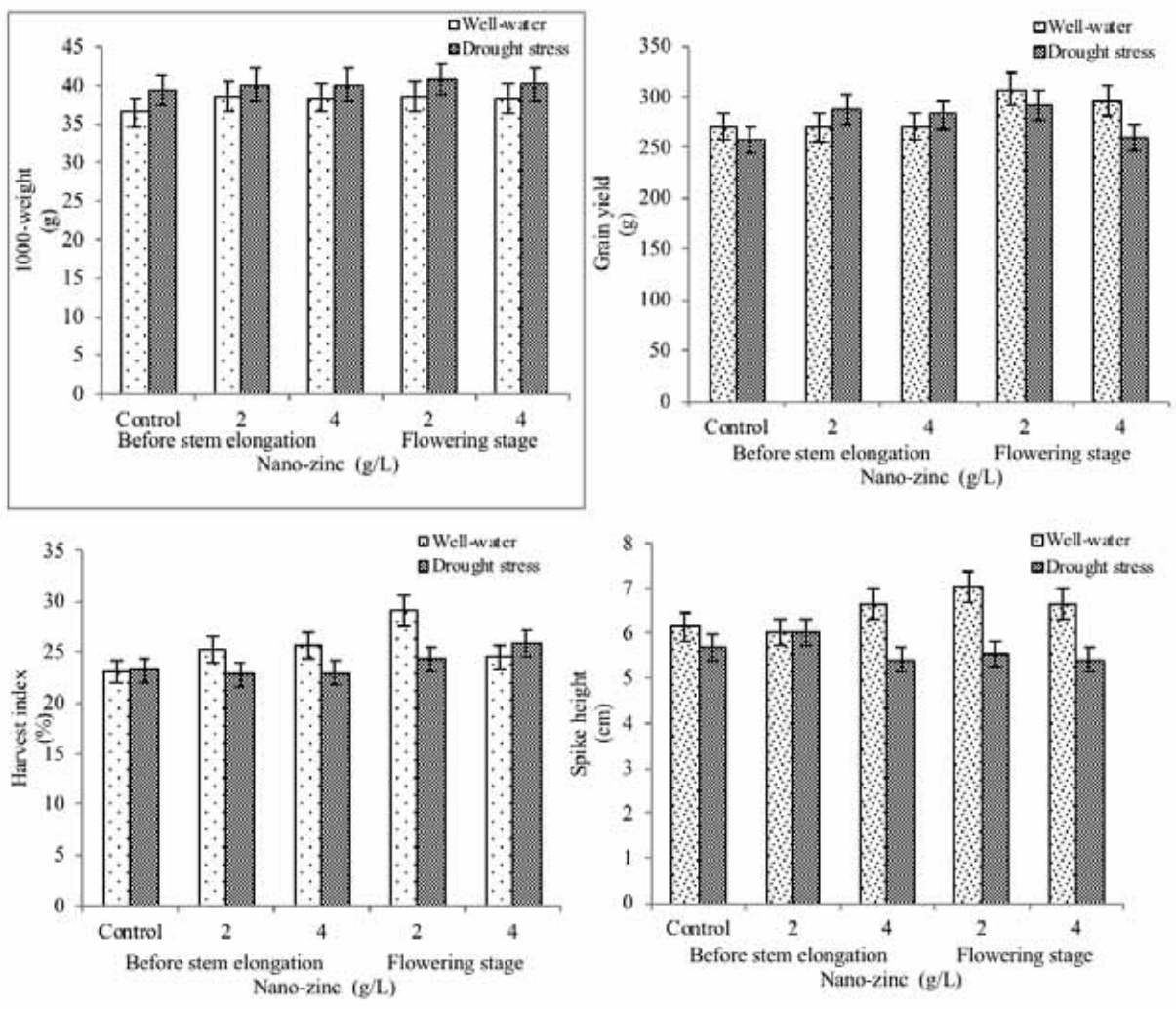

FIGURE 1
Effect of Nano-zinc foliar application on grain yield, spike height, 1000-grain weight and harvest index under drought stress in wheat.

RESULTS AND DISCUSSION

Agronomy traits. The analysis of variance of data to assess the effect of Nano-zinc foliar application on wheat under drought stress showed a highly significant difference for agronomy traits (variance analysis not shown). There were significant differences drought stresses for grain yield, 1000-seed weight, number of grain in spike, spike height, harvest index and plant height ($P < 0.001$). The effect of Nano-zinc foliar applications were significant for grain yield, 1000-seed weight, number of grain in spike, harvest index and plant height ($P < 0.001$). Drought × Nano-zinc foliar application interactions for grain yield, 1000-seed weight, spike height and harvest index were significant ($P< 0.001$).

Agronomy attributes of wheat cultivar was reduced significantly by drought stress. Our results indicated that the grain yield and plant height of majority of wheat cultivar were significantly decreased, probably by diminished cell expansion and cell division under water deficit stress [11]. The grain yield, 1000-seed weight, spike height and harvest index were drastically impaired under drought stress in wheat cultivar. However, this impairment was lower in 4 g/L Nano-zinc foliar application under drought stress as compared to 2 g/L Nano-zinc in flowering stage, while maximum grain yield, 1000-seed weight, spike height and harvest index were recorded in wheat cultivar raised under well-watered with 2 g/L Nano-zinc in flowering stage conditions (Fig. 1). The result showed that Nano-zinc foliar application was extremely enhancement effect on yield and its components under drought stress on wheat cultivar. Reduction in grain yield and its components in the wheat cultivar caused by drought stress could be attributable to some key physio-biochemical processes regulating plant growth [1]. Yavas and Unay [4] found 35% yield reduction in wheat when drought was imposed at the silk emergence stage. In another study Taran et al. [13] reported a marked decrease in grain yield and plant height in wheat when it was subjected to short-term drought. Movahhedy-Dehnavy et al. [6] reported the foliar application of zinc can increase the production of yield and its components. A similar protective effect of zinc sulfate was also observed by Malek-Mohammadi et al. [12].

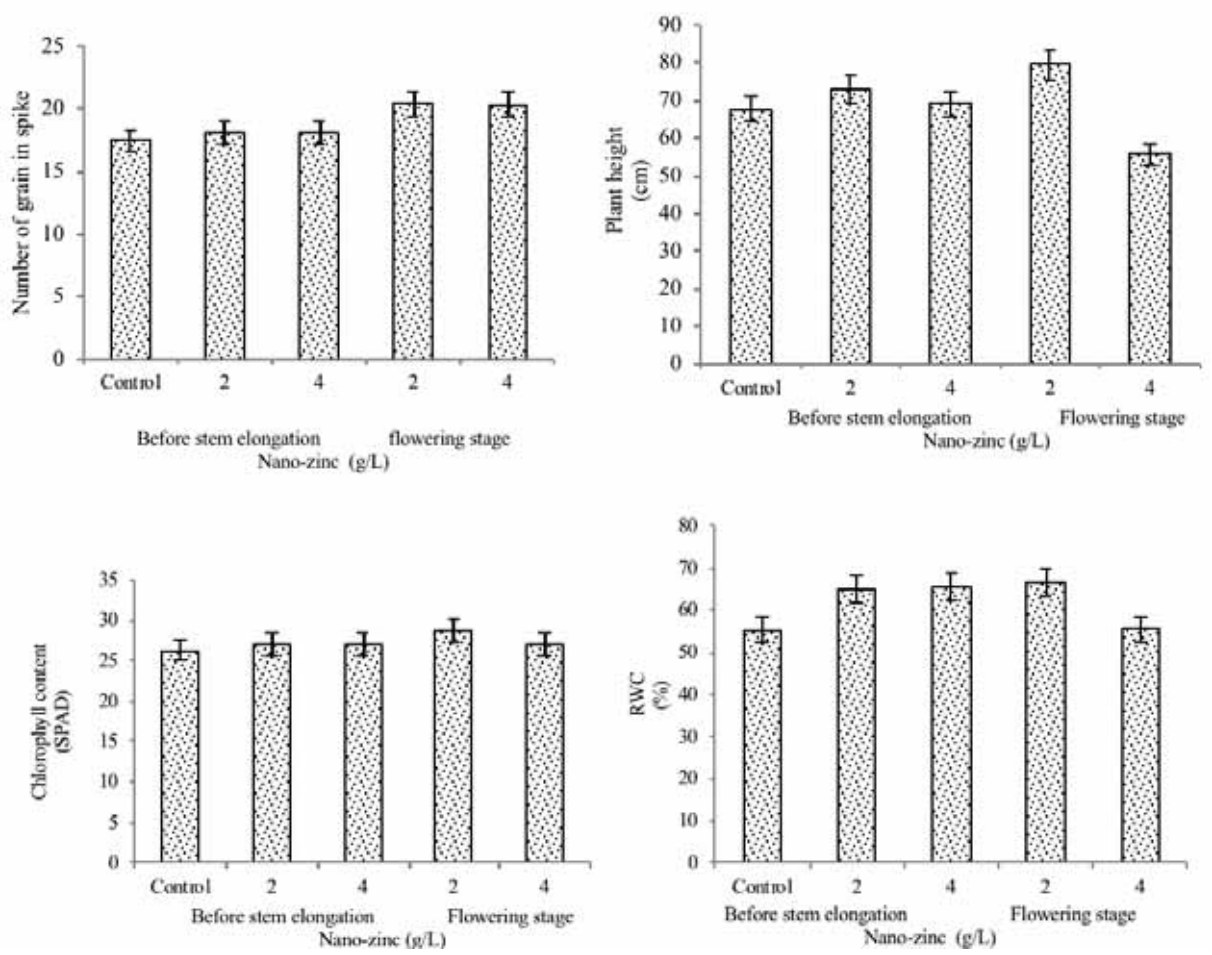

FIGURE 2
Effect of Nano-zinc foliar application on plant height, number of grain in spike, RWC and chlorophyll content in wheat.

TABLE 1
Correlation between studied traits of wheat.

	Height spike	Plant height	Number of grain in spike	Yield grain	Harvest index	RWC	Chlorophyll Content	1000-seed weight
Height spike	1							
Plant height	0.26	1						
Number of grain in spike	0.52**	-0.03	1					
Yield grain	0.29	0.31	0.43*	1				
Harvest index	-0.76**	0.45*	0.38	0.08	1			
RWC	0.58**	-0.11	0.64**	0.32	0.34	1		
Chlorophyll Content	0.82**	0.63**	0.13	0.16	0.44*	0.68**	1	
1000-seed weight	-0.28	-0.41	-0.10	-0.01	-0.16	-0.20	-0.04	1

*, **: significant differences at 5 and 1% probability, respectively

The mean comparisons of number of grain in spike and plant height, for which Nano-zinc foliar applications were significant, are shown in Fig. 2. It seems that 2 g/L Nano-zinc in flowering stage had a stable to both characteristics. It is shown that Nano-zinc foliar applications had good effect on number of grain in spike and plant height in wheat. These results are in agreement with those obtained by Yavas and Unay [4] and Yadavi et al. [3], they reported that drought stress reduced wheat plant height. The positive effects of foliar spray of zinc on grain in spike and plant height of wheat under drought stress were in accord with the results observed by some investigators [9]. In one study it was found that drought stress on wheat reduced the plant height, but with zinc application significantly increased the plant height [10].

Physiological traits. Analysis of variances for chlorophyll content and RWC showed that the drought stress and Nano-zinc foliar application have a significant effect on both attributes in wheat cultivar ($P< 0.001$). Drought stress × Nano-zinc foliar application interactions were not significant for chlorophyll content and RWC (variance analysis not shown).

For chlorophyll content and RWC a significant decrement was obtained in drought stress condition, and it caused a significant decrease in grain yield of majority of wheat cultivar relative to them under control condition. RWC may accurately define the demand and supply of water. Plants, for their survival under water deficit conditions, tend to retain reasonable amount of water so as to ensure the control functioning of all cellular metabolic processes. It is generally believed that RWC decreases in most plants in response to drought stress [11]. Chlorophyll concentration is known to be one of the major factors affecting photosynthetic capacity [8,10]. There are many conflicting opinions in the literature about the change in chlorophyll content of leaves under drought stress. Some studies carried out to investigate chlorophyll content under drought stress have reported reductions in wheat [8]. A similar protective effect of zinc was also observed in this study (Fig. 2). The results of this study are in good agreement with the findings of Malek-Mohammadi et al. [12] and Yavas and Unay [4] who observed zinc application induced enhancement of RWC and chlorophyll content.

Correlation. Significant and positive correlations were observed between grain yield and number of grain in spike. Significant and positive correlations were observed between spike height with RWC, chlorophyll content and harvest index (Tables 1). Of various correlations between grain yield and yield components were reported in wheat [12, 13]. The positive and significant correlation was observed between grain yield and plant height and test weight (hectoliter) under supplemental irrigation condition [14]. The grain yield, a major selection criterion *versus* drought stress, is a complex trait that determined by several physiological, biochemical and metabolic plant processes and its genetics and associations are greatly ambiguous [15].

ACKNOWLEDGEMENTS

The author would like to thanks Tabriz Branch, Islamic Azad University for the financial support of this research, which is based on research project contact.

REFERENCES

[1] Ashraf, M. (2010) Inducing drought tolerance in plants: some recent advances. Biotechnology Advance. 28, 169-183.

[2] Ghafari, H. and Razmjoo, J. (2015) Response of durum wheat to foliar application of varied sources and rates of iron fertilizers. Journal of Agricultural Science and Technology. 17, 321-331.

[3] Yadavi, A., Aboueshaghi, R.S. Dehnavi, M.M. and Balouchi, H. (2014) Effect of micronutrıents foliar application on grain qualitative characteristics and some physiological traits of bean (*Phaseolus vulgaris* L.) under drought stress. Indian journal of fundamental and applied life sciences. 4, 124-131.

[4] Yavas, I. and Unay, A. (2016) Effects of zinc and salicylic acid on wheat under drought stress. The Journal of Animal and Plant Sciences. 26, 1012-1018.

[5] Kisan, B., Shruthi, H., Sharanagouda, H., Revanappa, S.B. and Pramod, N.K. (2015) Effect of Nano-zinc oxide on the leaf physical and nutritional quality of spinach. Agrotechnology. 5, 1-3.

[6] Movahhedy-Dehnavy, M., Modarres-Sanavy, S.A.M. and Mokhtassi-Bidgoli, A. (2009) Foliar application of zinc and manganese improves seed yield and quality of safflower (*Carthamus tinctorius* L.) grown under water deficit stress. Industrial Crops and Products. 30, 82–92.

[7] Cakmak, I. (2008) Enrichment of cereal grains with zinc: agronomic or genetic bio-fortification? Plant Soil. 302, 1–17.

[8] Tambussi, E.A., Nogues, S. and Araus, J.L. (2005) Ear of durum wheat under water stress: water relations and photosynthetic metabolism. Planta. 221, 446-458.

[9] Maqbool, M.M., Ali, A., Haq, T., Majeed, M.N. and Lee, D.J. (2015) Response of spring wheat (*Triticum aestivum* L.) to induced water stress at critical growth stages. Sarhad Journal of Agricultural. 31, 53-58.

[10] Monjezi, F., Vazini, F. and Hassanzadehdelouei, M. (2013) Effects of iron and zinc spray on yield and yield components of wheat (*Triticum aestivum* L.) in drought stress. Cercetări Agronomice în Moldova. 46, 23-32.

[11] Farajzadeh, E., Valizadeh, M., Shakiba, M., Ghaffari, M. and Moharramnejad, S. (2017) Relationship between antioxidant enzyme activities and agro-physiological traits in sunflower lines under field water deficit stress. Fresen. Environ. Bull. 26, 2974-2982.

[12] Malek-Mohammadi, M., Maleki, A., Siaddat, S.A. and Beigzade, M. (2013) The effect of zinc and potassium on the quality yield of wheat under drought stress conditions. International Journal of Agriculture and Crop Sciences. 6, 1164- 1170.

[13] Taran, N., Storozhenko, V., Svietlova, N., Batsmanova, L., Shvartau, V. and Kovalenko, M. (2017) Effect of zinc and copper nanoparticles on drought resistance of wheat seedlings. Nanoscale Research Letters. 12, 1-6.

[14] Mohammadi, M., Sharifi, B., Karimizadeh, R. and Shefazadeh, M.K. (2012) Relationships between grain yield and yield components in bread wheat under different water availability (dryland and supplemental irrigation conditions). Notulae Botanicae Horti Agrobotanici Cluj-Napoca. 40, 195-200.

[15] Ali, M.A., Abbas, A., Awan, S.I., Jabran, K. and Gardezi, S.D.A. (2011) Correlated response of various morpho-physiological characters with grain yield in sorghum landraces at different growth phases. Journal of Animal and Plant Science. 21, 671-679.

Received: **14.02.2018**
Accepted: **09.04.2018**

CORRESPONDING AUTHOR

Azizollah Ghasemi
Member of Scientific Association of Agronomy and Plant Breeding,
Tabriz Branch,
Islamic Azad University,
Tabriz – Iran

e-mail: azizollahghassemi@gmail.com

© by PSP Volume 27 – No. 7/2018 pages 5027-5032 Fresenius Environmental Bulletin

INFLUENCE OF CHLORANTRANILIPROLE TOXICITY ON IONIC REGULATION OF GILL AND MUSCLE ATPASE ACTIVITY OF NILE FISH (*OREOCHROMIS NILOTICUS*)

Ozge Temiz[1,*], Hikmet Yeter Cogun[2], Ferit Kargin[1]

[1]Department of Biology, Faculty of Science and Letters, Cukurova University, 01330 Adana, Turkey
[2]Faculty of Ceyhan Veterinary Medicine, Cukurova University, 01920 Adana, Turkey

ABSTRACT

The objective of this study is to determine the effects of chlorantraniliprole (CHL) pesticide on ATPases (Na^+/K^+ ATPase, Ca^{2+} ATPase and Mg^{2+} ATPase) of gill and muscle in *O. niloticus.* Fish were exposed to acute and chronic chlorantraniliprole (CHL) exposure (0.5, 1.5 and 3.0 mg/L). UV-vis spectrophotometric methods were used to determining enzymes activity. When compared to control fish, the most inhibitions determined to Ca^{2+} ATPase > Na^+/K^+ ATPase > Mg^{2+} ATPase on gill and muscle tissues. This work showed that Ca^{2+} ATPase is more sensitive biomarker chlorantraniliprole (CHL) pesticide than other ATPase enzymes. In our study, *O. niloticus* could be a suitable biomarker for chlorantraniliprole (CHL) and ATPases are very important early warning ecotoxicologic parameters.

KEYWORDS:
Chlorantraniliprole (CHL), ATPase, *Oreochromis niloticus,* toxicology

INTRODUCTION

Pesticides have a important potentialy hazard for environment. As a result of excessive use of pesticides, it is groundwater mixes with rainwater and effect to organisms [1-3]. Among the pesticide varieties, Chlorantraniliprole, which is widely used in our region, is an important agricultural activity and it is called to IUPAC name is 3-bromo-4'-chloro-1-(3-chloro-2-pyridyl)-2'-methyl-6'-(methylcarbamoyl) pyrazole-5-carboxanilide. The chlorantraniliprole (CHL) is an anthranilic diamide class which is lead to disrupt calcium storage and causes irregular muscle contractions in organisms [4]. Recently, fish are very important indicators for the aquatic environmental toxicity. In fish, *Oreochromis niloticus* has been reported by many researchers to be an important organism [5-7].

ATPases are conserved membrane enzymes which occurs active and passive ion exchange in gill and muscle and also, accompanied by perturbation of hydromineral balance on membrane potantial [8-10]. ATPases for these tissues give early warning signal of pollutants such as pesticides and occurs damage to the osmoregulation systems [11]. Although there are many studies on fish related to ATPase for heavy metals [12-14], there are little study for pesticides [15-16]. But there are not study about the chlorantraniliprole (CHL) pesticide on *O. niloticus*. The membrane enzymes, Ca^{2+} ATPase and Mg^{2+} ATPase, are involved in oxidative phosphorylation in the cell mitochondrion as well as ion regulation in the cell membrane.

The aim of this study was to determine the effects of Chlorantraniliprole exposures on ATPases (Na^+/K^+ ATPase, Ca^{2+} ATPase and Mg^{2+} ATPase) from the gill and muscle of *O. niloticus* for 24 hours, 96 hours and 28 days.

MATERIALS AND METHODS

Chemicals. Commercial formulation of Chlorantraniliprole is Coragen 20SC DuPont was purchased from Turkey distribitor. The chemicals used were obtained from Sigma Aldrich and Merck.

Fish maintenance. *O. niloticus* were obtained from pools and kept to acclimatize in the laboratory for two month at 25±1°C. After this period, the mean length and weight of the animals were 13.8±1.92 cm and 40.5±3.11 gr., respectively. Water quality characteristics in tanks are as follow; pH: 8.1±0.9, Temperature: 25±1°C, Dissolved Oxygen: 7.8±0.8 mg/L, Total Hardness: 196.5±7.42 $CaCO_3$ mg/L, Total Alkalinity: 318.2±8.1 $CaCO_3$ mg/L.

Exposure to Chlorantraniliprole. The sublethal concentrations of chlorantraniliprole (CHL) were filled with 120 L of 4 glass aquarium tanks in the size of 40 cm x 100 cm x 40 cm for the control group together with 0.5 mg / L, 1.5 mg / L and 3.0 mg / L. Randomly selected fishes are placed in 9 fish for each period (3 times x 3 fish) per aquarium. The pesticides were mixed in fresh water aquariums freshly prepared for CHL concentrations so that the ratio of pesticide in the water was not changed and the toxicity test was completed by transferring the

fish. The control fishes were kept in the same laboratory conditions. The gills and muscle tissues of the fish were removed by decapitation method after 24 hours and 96 hours of acute periods and 28 days after chronic periods. The fishes were quickly cleaned with 0.59% NaCl on ice plate and weighed to -85 °C until biochemical analysis the samples have been stored.

Preparation of Gill and Muscle Tissue Homogenates for Enzyme Activity and Protein Quantity Measurements. Tissues (1:10, w/v) were homogenized for 5 min in each tissue sample with a steel homogenizer (UltraTurrax T-18) with buffer (PBS, 136 mmol/L NaCl, 1.5 mmol/L KH_2PO_4, 0.9 mmol/L $CaCl_2$, 8.1 mmol/L Na_2HPO_4, 2.7 mmol/L KCl, and 0.24 mmol/L $MgCl_2$, 7.4 pH) containing 2.5 mM ATP in ice cold. The homogenates were centrifuged at 16,000 x g for 20 min. at 4°C. were used for spectrophotometric determination of protein and ATPase enzymes obtained with supernatants.

Measurement of protein quantities in tissues by Bradford method. Protein quantities were determined using the Bradford method [17] using bovine serum albumin as standard in mg / mL at 595 nm in a microplate reader.

ATPase activity assay. The activity of ATPase was measured by determination of the inorganic phosphate (Pi) liberated from the hydrolysis of the substrate adenosine triphosphate (ATP) at 37 °C. For the measurement of Na^+/K^+ ATPase activity of gill and muscle were 40 mM Tris–HCl, 120 mM NaCl, 20 mM KCl, 3 mM $MgCl_2$, 7.7 pH, and 1 mM ouabain. In addition, incubation media (pH 7.7) containing 40 mM Tris–HCl, 4 mM $MgCl_2$, 1 mM $CaCl_2$ and 1 mM EGTA was used for Ca^{2+} ATPase activity. Homogenates were centrifuged at 1000 g to remove the debris for 15 minutes. ATPase activity was carried out with supernatant immediately on the resulting supernatant. Ca^{2+} ATPase activity was calculated by subtracting Mg^{2+} ATPase (containing ouabain) activity from total-ATPase (ouabain-free) activity. Enzyme activities was given μmol Pi / mg protein/h. Similarly, this method to given in detailly described by Atkinson et al. [18].

Statistical analyses. Data are presented as mean ± standard error. For the statistical analysis, a One-Way Analysis of Variance (ANOVA) was used, followed by Duncan and LSD test, using SPSS 22.0 statistical software (SPSS Inc., Chicago, IL). Differences were considered significant if $P < 0.05$.

RESULTS AND DISCUSSION

Throughout the experiments, no mortality was recorded at concentrations of the chlorantraniliprole (CHL). The statistical analysis which was done with "Duncan and LSD" differences among groups were measured to be significant at $P<0.05$. Figure 1-6 show of ATPase (Na^+/K^+ ATPase, Ca^{2+} ATPase and Mg^{2+} ATPase) parameters of chlorantraniliprole (CHL) exposed to *O. niloticus* over 24 hours 96 hours and 28 days period, respectively. The concentrations of gill and muscle Na^+/K^+ ATPase, Ca^{2+} ATPase and Mg^{2+} ATPase activity declines were observed at all exposure periods (fig 1-6).

Our study, Na^+/K^+ ATPase in gill a significant inhibition of Na^+/K^+ ATPase activity was observed with CHL concentrations (0.5 ppm CHL, 1.5 ppm CHL and 3 ppm CHL) to compared with controls (Fig. 1A) for 24 h, 96 h and 28 h.The 0.5 ppm CHL, 1.5 ppm CHL and 3.0 ppm CHL concentrations were decreased (11%, 30% and 36%) for 24h, (48%, 54% and 69%) for 96h and (65%, 76% and 90%) for 28d, respectively. The Na^+/K^+ ATPase activity in the gill, depending on time (fig. 1B), was reduced to 0.5 ppm CHL concentration 42% and 60%, 1.5 ppm CHL concentration 35% and 65% and 3.0 ppm CHL concentration 51% and 84% for 24h compared to 96h and 28d ($P<0.05$).

Ca^{2+} ATPase activity was observed with CHL concentrations (0.5 ppm CHL, 1.5 ppm CHL and 3 ppm CHL) to compared with controls (fig. 2A) for 24 h, 96 h and 28 h. The 0.5 ppm CHL, 1.5 ppm CHL and 3.0 ppm CHL concentrations were decreased (19%, 28% and 40%) for 24h, (66%, 73% and 82%) for 96h and (87%, 94% and 90%) for 28d, respectively. The Ca^{2+} ATPase activity in the gill, depending on time (fig. 2B), was reduced to 0.5 ppm CHL concentration 52% and 81%, 1.5 ppm CHL concentration 57% and 90% and 3.0 ppm CHL concentration 65% and 81% for 24h compared to 96h and 28d ($P<0.05$).

In gill Mg^{2+} ATPase activity was observed with CHL concentrations (0.5 ppm CHL, 1.5 ppm CHL and 3 ppm CHL) to compared with controls (Fig. 3A) for 24 h, 96 h and 28 h. The 0.5 ppm CHL, 1.5 ppm CHL and 3.0 ppm CHL concentrations were decreased (9%, 13% and 12%) for 24h, (14%, 20% and 25%) for 96h and (44%, 59% and 72%) for 28d, respectively. The Mg^{2+} ATPase activity in the gill, depending on time (fig. 3B), was reduced to 0.5 ppm CHL concentration 4% and 35%, 1.5 ppm CHL concentration 5% and 51% and 3.0 ppm CHL concentration 13% and 67% for 24h compared to 96h and 28d ($P<0.05$).

In muscle, a significant inhibition of Na^+/K^+ ATPase activity was observed with CHL concentrations (0.5 ppm CHL, 1.5 ppm CHL and 3 ppm CHL) compared to controls (fig. 4A) for 24 h, 96 h and 28 d. The 0.5 ppm CHL, 1.5 ppm CHL and 3.0 ppm CHL concentrations were decreased (25%, 26% and

42%) for 96h and (70%, 74% and 89%) for 28d, respectively. Although 1.5 ppm CHL and 3.0 ppm CHL concentrations were decreased, there was no statistical change in the effect of 0.5 ppm CHL at 24 h ($P > 0.05$). The Na^+/K^+ ATPase activity in muscle, depending on time (fig. 4B), was reduced to 0.5 ppm CHL concentration 5% and 64%, 1.5 ppm CHL concentration 24% and 80% and 3.0 ppm CHL concentration 64% and 80% for 24h compared to 96h and 28d ($P<0.05$).

Ca^{2+} ATPase activity was observed with CHL concentrations (0.5 ppm CHL, 1.5 ppm CHL and 3 ppm CHL) to compared with controls (fig. 5A) for 24 h, 96 h and 28 d. The 0.5 ppm CHL, 1.5 ppm CHL and 3.0 ppm CHL concentrations were decreased (64%, 67% and 67%) for 24h, (74%, 80% and 87%) for 96h and (89%, 95% and 97%) for 28d, respectively. The Ca^{2+} ATPase activity in the gill, depending on time (fig. 5B), was reduced to 0.5 ppm CHL concentration 29% and 55%, 1.5 ppm CHL concentration 40% and 74% and 3.0 ppm CHL concentration 61% and 79% for 24h compared to 96h and 28d ($P<0.05$).

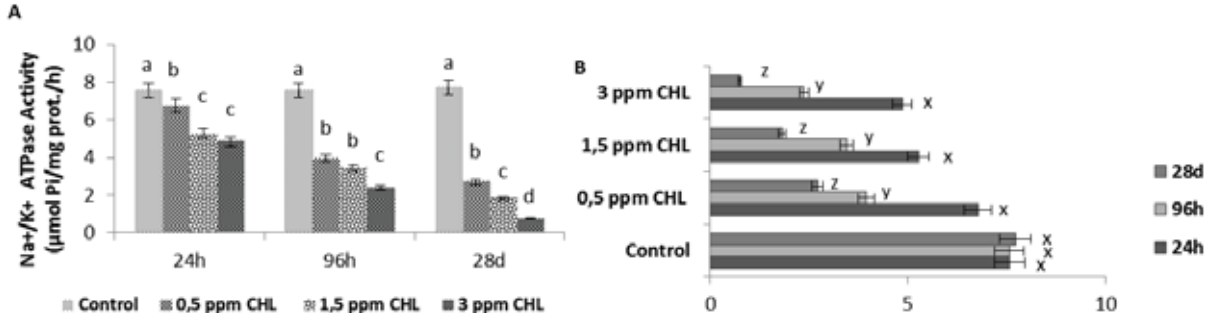

FIGURE 1

The effects of CHL on Na^+/K^+ ATPase activity in gill tissues of *O. niloticus*. A- The letters of a, b, c and d show significant differences between CHL exposure groups at the same duration, B- The letters of x, y and z show significant differences between CHL exposures groups different duration ($P < 0.05$)

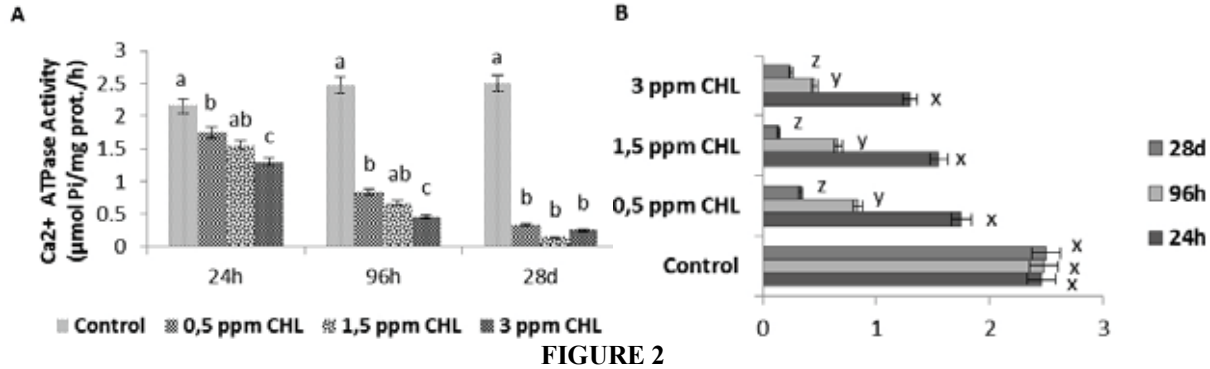

FIGURE 2

The effects of CHL on Ca^{2+} ATPase activity in gill tissues of *O. niloticus*. A- The letters of a, b, c and d show significant differences between CHL exposure groups at the same duration, B- The letters of x, y and z show significant differences between CHL exposures groups different duration ($P < 0.05$)

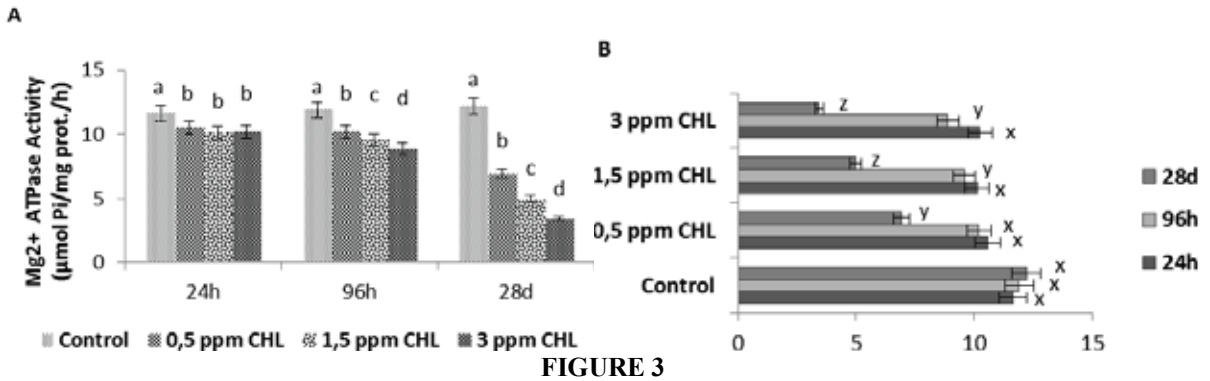

FIGURE 3

The effects of CHL on Mg^{2+} ATPase activity in gill tissues of *O. niloticus*. A- The letters of a, b, c and d show significant differences between CHL exposure groups at the same duration, B- The letters of x, y and z show significant differences between CHL exposures groups different duration ($P < 0.05$)

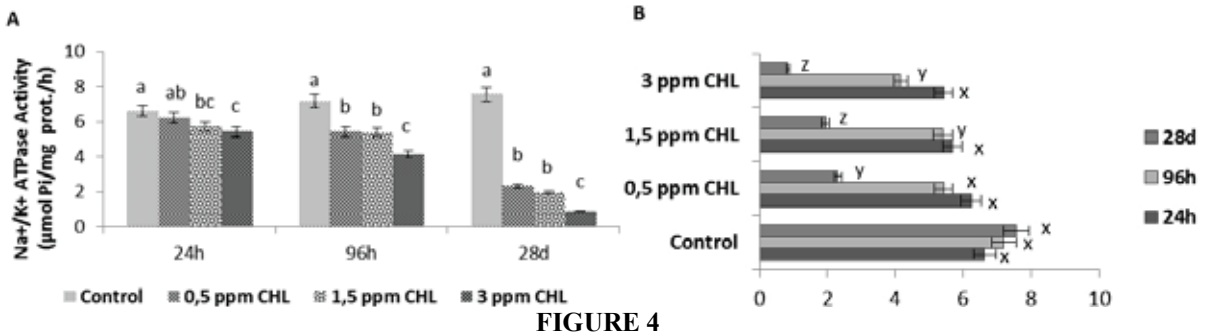

FIGURE 4

The effects of CHL on Na^+/K^+ ATPase activity in muscle tissues of *O. niloticus*. A- The letters of a, b, c and d show significant differences between CHL exposure groups at the same duration, B- The letters of x, y and z show significant differences between CHL exposures groups different duration ($P < 0.05$)

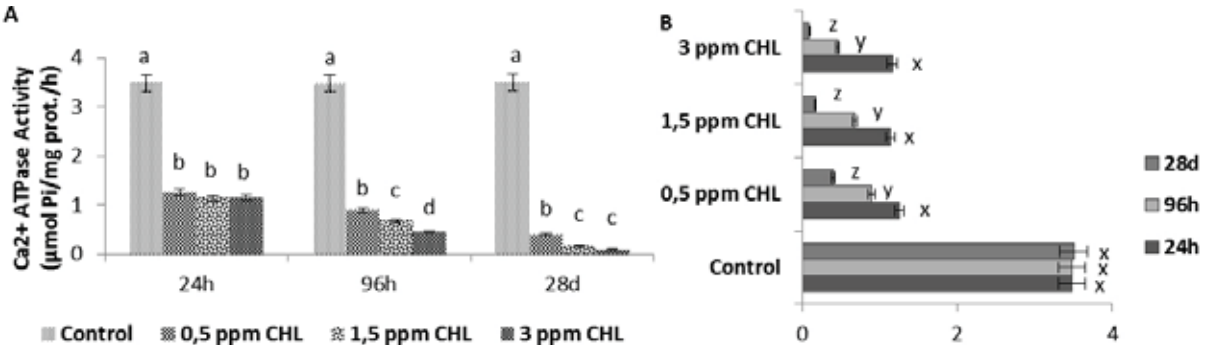

FIGURE 5

The effects of CHL on Ca^{2+} ATPase activity in muscle tissues of *O. niloticus*. A- The letters of a, b, c and d show significant differences between CHL exposure groups at the same duration, B- The letters of x, y and z show significant differences between CHL exposures groups different duration ($P < 0.05$)

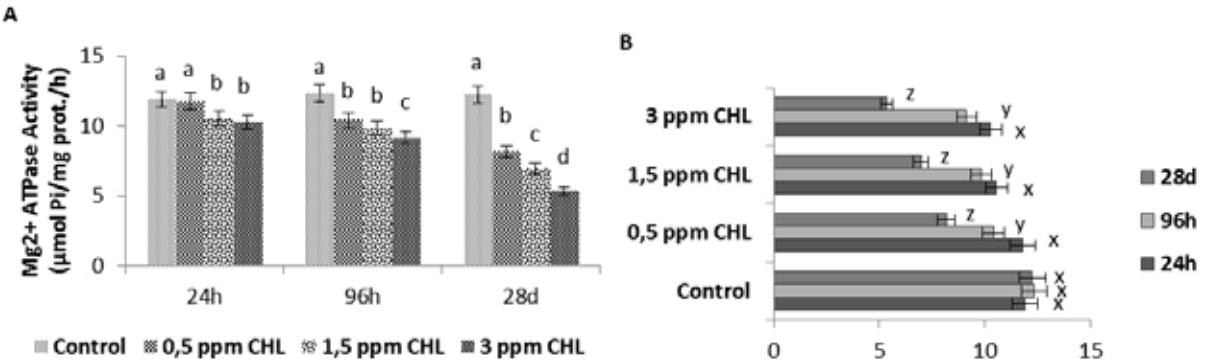

FIGURE 6

The effects of CHL on Mg^{2+} ATPase activity in muscle tissues of *O. niloticus*. A- The letters of a, b, c and d show significant differences between CHL exposure groups at the same duration, B- The letters of x, y and z show significant differences between CHL exposures groups different duration ($P < 0.05$)

In muscle Mg^{2+} ATPase activity was observed with CHL concentrations (0.5 ppm CHL, 1.5 ppm CHL and 3 ppm CHL) to compared with controls (Fig. 6A) for 24 h, 96 h and 28 d. However, 1.5 ppm CHL and 3.0 ppm CHL concentrations were decreased, there was no statistical change in the effect of 0.5 ppm CHL at 24 h ($P > 0.05$). The 0.5 ppm CHL, 1.5 ppm CHL and 3.0 ppm CHL concentrations were decreased (16%, 20% and 26%) for 96h and (33%, 43% and 56%) for 28d, respectively. The Mg^{2+} ATPase activity in muscle, depending on time (fig. 6B), was reduced to 0.5 ppm CHL concentration 12% and 21%, 1.5 ppm CHL concentration 7% and 29% and 3.0 ppm CHL concentration 11% and 42% for 24h compared to 96h and 28d ($P<0.05$).

Gills and muscle of freshwater fish plays important role of active transport systems, osmotic and ionic balance. Adenosine triphosphatase (ATPase) is a highly conserved membrane enzyme essential for ion homeostasis, plays to regulate cellular functions, and to be a sensitive indicator of environmental toxicity [19-20] and also especially Na^+/K^+ ATPase

is found in the basolateral membrane of gill epithelial cells [21]. They are exceedingly in the tubular system of chloride cells [22-23]. Dang et al. [24] has been found that fish gills play a very important role in ion transport for ATPases. Decrease in Na^+/K^+ ATPase enzymes of gill and muscle tissue is shown in fig1 and fig4. Similar results are there Na^+/K^+ ATPase enzyme activity decreased in gills [25]. Another study, this enzymes was also observed to decrease in *Cyprinus carpio* [26]. The decreased of this enzymes may be in gill, first contact with water to pesticides, is occur breaks the ion balance and permeability of the gill region.

Ca^{2+} and Mg^{2+} ATPase activity play an important role in the regulation of Ca and Mg ions in fish tissues [21]. In fish, Ca^{2+} and Mg^{2+} ATPase are serve as membrane enzymes involve adenosine triphosphate (ATP) as a substrate for their functioning [27]. Thaker et al. [28]. show that inhibition of Ca^{2+} ATPase activity in tissues of *Periophthalmus dipes.* Ca^{2+} and Mg^{2+} ATPase activity were served as oxidative phosphorylation of mitochondria [29]. In this study, Ca^{2+} and Mg^{2+} ATPase activity were decreased with CHL exposure in time and concentrations of *O. niloticus*. Similar results, Marigoudar [30] reported that this inhibitions indicates of cellular ionic regulation in gill and muscle of the fish. The pesticide inhibits this enzymes may result from the breakdown of the active ion transport systems and oxidative phosphorylation of mitochondria.

CONCLUSION

The present study reveals that sublethal exposure of the Fish, *O. niloticus*, to the chlorantraniliprole (CHL) results in significant effects on ATPases (Na^+/K^+ ATPase, Ca^{2+} ATPase and Mg^{2+} ATPase) from the gill and muscle of *O. niloticus* for 24 hours, 96 hours and 28 days. Na^+/K^+ ATPase, Ca^{2+} ATPase and Mg^{2+} ATPase activity were observed decreased during at all exposure periods. Based on these data, it can be stated that O. niloticus could be a suitable biomarker for pesticides and ATPases are very important early warning ecotoxicologic parameters.

REFERENCES

[1] Nur, G., Yılmaz, M., Karapehlivan, M., Kaya, I., Nur, O. and Deveci, A. (2017) The effect of tebuconazole on serum paraoxonase and aminotransferase activities in *Cyprinus carpio* (L. 1758). Fresen. Environ. Bull. 26, 6212-6216.

[2] Papa, S., Bartoli, G., Alvarez-Romero, M., Barbato, G., Vitale, A., Ferrante, C., Fioretto, A. (2017) Trace metals accumulatıon and their translocation in *Phragmites australis* (cav.) Collected along the sarno river. Fresen. Environ. Bull. 26, 467-474.

[3] Taher, M., Javani, M., Beyaz, R., Yildiz, M. (2017) A new environmental friendly production method in sunflower for high seed and crude oil yields. Fresen. Environ.Bull. 26, 4004-4010.

[4] Rathnamma, V.V. and Nagaraju, B. (2013) Median lethal concentrations (LC_{50}) of Chlorantraniliprole and its effects on behavioral changes in Freshwater Fish *Labeo Rohita*. International Journal of Public Health Science. 4, 137-142.

[5] Almeida, J.A., Diniz, Y.S., Marques, S.F.G., Faine, L.A., Ribas, B.O., Burneiko, R.C., and Novelli, E.L.B. (2002) The use of the oxidative stres responses as biomarkers in Nile Tilapia (*Oreochromis niloticus*) exposed to in vivo cadmium contamination. Environment International. 27, 673-679.

[6] Tan, K.W. and Sze, K.Z. (2017) Determination of heavy metal concentration in fish species in kampar mining lake, Perak State of Malaysia. Fresen. Environ. Bull. 26, 4202-4207.

[7] Cogun, H.Y., Firidin, G.G., Aytekin, T., Firat, O., Firat, O., Temiz, O., Varkal, H.S. and Kargin, F. (2017) Acute toxicity of nitrite on some biochemical, hematological and antioxidant parameters in Nile Tilapia (*Oreochromis niloticus* L, 1758). Fresen. Environ. Bull. 26, 1712-1719.

[8] Canlı, M., and Stagg, R.M. (1996) The effects of in vivo exposure to cadmium, copper, and zinc on the activities of gill ATPases in the Norway Lobster *Nephrops norvegicus*. Archive of Environmental Contamination and Toxicology. 31, 491–501.

[9] Kundu, R., Lakshmi R., Mansuri, A.P. (1992) The entry of mercury through the membrane: an enzymological study using a tolerant fish Boleophthalmus dentatus. Proc. Acad. Environ. Biol. 1, 1–6.

[10] Alam, M., Frankel, T. (2006) Gill ATPase of silver perch, *Bidyanus bidyanus*, and golden perch, *Macquaria ambigua*: effects of environmental salt and ammonia. Aquaculture. 251, 118–133.

[11] Stagg, R.M., Goksoyr A., Rodger, G. (1992) Changes in branchial Na^+/K^+-ATPase, c metallothionein and P450 1A1 in dab *Limanda limanda* in the German Bight: cindicators of sediment contamination? Marine Ecology Prog Ser. 91, 105-115.

[12] Watson, C.F., Benson, W.H. (1987) Comparative activity of gill ATPase in three freshwater teleosts exposed to cadmium. Ecotoxicol Environ Safe. 14, 252–259.

[13] Grosell, M., Wood, C.M., Walsh, P.J. (2003) Copper homeostasis and toxicity in the elasmobranch Raja erinacea and the teleost *Myoxocephalus octodecemspinosus* during exposure to elevated water-borne copper. Comp Biochem Physiol. 135C, 179–190.

[14] Ay, O., Kalay, M., Tamer, L., Canli, M. (1999) Copper and lead accumulation in tissues of a freshwater fish *Tilapia zillii* and its effects on the branchial Na, K-ATPase activity. Bull Environ Toxicol. 62, 160–168.
[15] Balaji, G., Nachiyappan, M. and Venugopal, R. (2015) Sub-Lethal Effect of Cypermethrin on Ca^{+}, Mg^{+} and Na^{+}/K^{+}-ATPase Activity in Fresh Water Teleost, *Cyprinus carpio*. World Journal of Zoology. 10(3), 168-174.
[16] Vesna, V., Tatjana, M., Marijana P., Danijela, K. (2008) Na^{+}/K^{+}-ATPase as the target enzyme for organicand inorganic compounds. Sensors. 8, 8321-8360.
[17] Bradford, M.M. (1976) A rapid and sensitive method for the quantitation of microgram quantities of protein utilizing the principle of protein-dye binding. Anal. Biochem. 72, 248–254.
[18] Atkinson, A., Gatemby, A.O., Lowe, A.G. (1973) The determination of inorganic orthophosphate in biological systems. Biochim Biophys Acta. 320, 195–204.
[19] Reddy, P.M., Philip, G.H. (1994) In vivo inhibition of AChE and ATPase activities in the tissues of freshwater fish, *Cyprinus carpio* exposed to technical grade cypermethrin. Bull. Environ. Contam. Toxicol. 52, 619–626.
[20] Koksoy, A.A. (2002) Na^{+}/K^{+} ATPase: a review. J. Ankara Med. Sch. 24, 73–82.
[21] Begum, G. (2011) Organ-specific ATPase and phosphorylase enzyme activities in a food fish exposed to a carbamate insecticide and recovery response. Fish Physiol. Biochem. 37(1), 61-69.
[22] Metz, J.R., Van den Burg, E.H., Wendelaar Bonga, S.E., Flik, G. (2003) Regulation of branchial Na^{+}/K^{+}-ATPase in common carp *Cyprinus carpio* L. acclimated to different temperatures. J. Exp. Biol. 206, 2273–2380.
[23] Grosell, M., McDonald, M.D., Walsh, P.J., Wood, C.M. (2004) Effects of copper exposure in the marine gulf toadfish *Opsanus beta*. II. Copper accumulation, drinking rate and Na^{+}/K^{+}-ATPase activity in osmoregulatory tissues. Aquat. Toxicol. 68, 263–275.
[24] Dang, Z., Lock, R.A.C., Flik, G., Wendelaar Bonga, S. (2000) Na^{+}/K^{+}-ATPase immuno-reactivity in branchial chloride of *Oreochromis mossambicus* exposed to copper. J. Exp. Biol. 20, 370–387.
[25] Narra, M.R., Rajender, K., Reddy, R.R., Murty, U.S., Begum, G. (2011) Insecticides induced stress response and recuperation in fish: Biomarkers in blood and tissues related to oxidative damage. Chemosphere. 168, 350-357.
[26] Oruç, E.O., Usta, D. (2007) Evaluation of oxidative stress responses and neurotoxicity potential of diazinon in different tissues of *Cyprinus carpio*. Environ. Toxicol. Pharmacol. 23, 48-55.
[27] David, M., Sangeetha, J., Harish, E.R., Shrinivas, J., Naik, V.R. (2014) Deltamethrin induced alteration in Na^{+}-K^{+}, Mg^{2+}, Ca^{2+} associated ATPases activity in the freshwater fish *Cırrhınus mrıgala*. International Journal of Pure and Applied Zoology. 2, 175-181.
[28] Thaker, J., Chhaya, J., Nuzhat, S., Mittal, R. (1996) Effects of chromium (VI) on some ion-dependent ATPases in gills, kidney and intestine of a coastal teleost Periophthalmus dipes. Toxicology. 112, 237–244.
[29] Tiwari, B.S., Belenghi, B. and Levine, A. (2002) Oxidative stress increased respiration and generation of reactive oxygen species, resulting in ATP depletion, opening of mitochondrial permeability transition, and programmed cell death. Plant physiology. 128(4), 1271-1281.
[30] Marigoudar, S.R., Ahmed, R.N. and David, M. (2009) Cypermethrin induced respiratory and behavioural responses of the freshwater teleost, *Labeo rohita* (Hamilton). Veterinarski Archives. 79(6), 583-590.

Received: **15.02.2018**
Accepted: **29.04.2018**

CORRESPONDING AUTHOR

Ozge Temiz
Cukurova University
Faculty of Science and Letters
Department of Biology
Adana – Turkey

e-mail: temizozge@gmail.com

© by PSP Volume 27 – No. 7/2018 pages 5033-5036 Fresenius Environmental Bulletin

PRESENCE OF AFLATOXIN M1 IN KAYMAK PRODUCED IN AFYONKARAHISAR PROVINCE

Recep Kara[1,*], Sinan Ince[2]

[1]Afyon Kocatepe University, Faculty of Veterinary Medicine, Department of Food Hygiene and Technology, Afyonkarahisar, Turkey
[2]Afyon Kocatepe University, Faculty of Veterinary Medicine, Department of Pharmacology and Toxicology, Afyonkarahisar, Turkey

ABSTRACT

Aflatoxins are highly cancerogenic compounds produced by *Aspergillus* genus. The form of aflatoxin in milk is the aflatoxin M1 (AFM1) form. When dairy animals consume feed containing aflatoxin, it can be transformed to the AFM1 in the organism and excreted with milk. AFM1 is comparatively stable during milk pasteurization, storage, and production of various milk products. Contamination of milk and milk products (Kaymak, butter, cheese, and yogurt etc.) with AFM1 is a certain hygienic risks for public health. In this study, 90 Afyon Kaymak samples were obtained randomly during the August and December 2014 in Afyonkarahisar province. Samples were tested for AFM1 contamination by Enzyme Linked Immuno Sorbent Assay (ELISA) method. Twenty three (25.55 %) samples were found to be contaminated with AFM1, only 4 (4.44 %) samples (26.08, 26.41, 33.59, and 34,01 ng/l) could pose a risk to public health. In contrast, AFM1 levels in all samples were not found high levels in terms of the maximum residue limit (50 ng/l) according to Turkish Food Codex and Codex Alimentarius. In conclusion, it is necessary to carry out periodic analysis of AFM1 residues of milk and its products in terms of public health.

KEYWORDS:
Aflatoxin M1, Kaymak, Buffalo milk, milk product

INTRODUCTION

Kaymak is a traditional dairy product in Turkey due to its unique flavor and aroma [1]. Traditional Afyon kaymak is produced by bolting buffalo milk which is heated at 90 °C for at least 2 min and after to cooled according to the technical procedure. Especially, it is produced by family business at province of Afyon, Edirne, Kocaeli, İstanbul, Bursa, and Ankara. Also, kaymak is produced in different parts of the world which are Balkans, Middle East, Asia, Iran, Afghanistan, and India. At these country, kaymak is the same pronunciation as ''kajmak, kaimak, gemagh or geymar'' [2]. According to the Turkish Food Codex Cream and Cream notification, kaymak must be contained at least 60 % milk fat by weight [3].

Mycotoxins, especially aflatoxins, are known carcinogens [4]. AFM1 can cause DNA damages, gene mutation, and chromosomal anomalies in mammalian cells [5]. Mainly substances of aflatoxin are B1, B2, G1, G2 and M1 [6] and B1 contaminated feed excrete M1 in milk [7, 8]. In addition, these toxins are resistant to high temperature process including pasteurization and sterilization [4, 9]. In Turkey and other countries, many studies were found different levels of AFM1 in milk and milk products such as cow milk [9, 10, 11, 12, 13], buffalo milk [14, 15], cheese [16, 17, 18], butter [10] and ice cream [19]. There was no found any study on the presence of AFM1 in Afyon kaymak. Therefore, presence of the AFM1 residue levels in Afyon Kaymak was investigated with Enzyme Linked Immuno Sorbent Assay method (ELISA) in this study.

MATERIALS AND METHODS

Totally 90 Afyon Kaymak samples were obtained from Afyonkarahisar province during the August and December 2014. Collected samples were quickly transported to the laboratory inside a portable refrigerator and tested for presence of AFM1.

Method for analysis of AFM1. The quantitative analysis of AFM1 in Afyon kaymak samples was studied by Enzyme Linked Immuno Sorbent Assay (ELISA). AFM1 ELISA kit was purchased from HELICA Biosystema Inc., USA (CAT. NO. 961AFLMO1M).

Preparation of milk samples. Preparation of kaymak samples was performed with regard to the instructions of kit. For this purpose, Afyon Kaymak samples were centrifuged at 3500 rpm for 10 min, then the 200 µl lower phases of supernatant was handled per well in the test.

ELISA test procedure. ELISA test procedure was performed with regard to the instructions of kit. 200 µl of standard solutions (0, 5, 10, 25, 50, and 100 ng/l) and specimen were joined into microplate

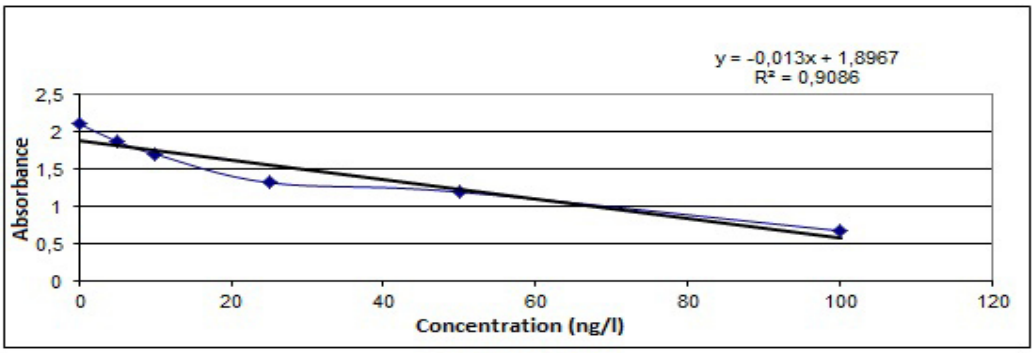

FIGURE 1
AFM1 levels with standard-concentration curve

TABLE 1
Minimum, maximum, and average values of AFM1 in Afyon Kaymak samples.

	≤0.5 ng/l	0.5-25 ng/l	25-50 ng/l	50 ng/l ≥
Positive samples	67 (74.44%)	19 (21.11%)	4 (4.44%)	0
Minimum	-	0.659	26.077	-
Maximum	-	23.740	34.007	-
Average	-	7.467	30.021	-

wells and incubated for 2 hrs at 19–25 °C in the dark. Afterwards, wells were cleaned at three times with PBS Tween 20®. Later 100 µl of the conjugate was added into the wells and baked for 15 min at 19-25 °C in the dusky conditions. Then the wells were washed at three times with PBS Tween 20®. Following, 100 µl of enzyme substrate was added and incubated for 15-20 min. As a result, 100 µl of the stop reagent was joined into the wells and the absorbance was determined at 450 nm in ELISA plate reader (RAYTO Microplate Reader, Hamburg, Germany). According to AFM1 kit guidelines, the minimum identification level of AFM1 is 5 ng/l.

RESULTS

AFM1 levels were calculated with standard-concentration curve (Figure 1). After the analyses, 23 samples (25.55%) were found to be contaminated with AFM1. In contrast, only 4 (4.44%) samples (26.08, 26.41, 33.59, and 34,01 ng/l) could pose a risk to public health (Table 1). However, AFM1 levels in all samples were not found to be over the maximum residue limit (50 ng/l) according to Turkish Food Codex and European Union criteria.

DISCUSSION

Some studies were found different levels of AFM1 in milk and milk products in Turkey. Kara and Ince [14] investigated AFM1 levels by high-performance liquid chromatography with tandem mass spectrometry in 126 buffalo and 124 cattle milk samples from Afyonkarahisar city. AFM1 was not identified in cattle milk, but AFM1 was found above the limit of detection in 27% (34 out of 126) of the buffalo milk and they suggested that the significance of continual observation of consumed dairy product for AFM1 contamination in Turkey. Similarly, Oruc et al. [20] concluded AFM1 levels in 115 raw cattle milk obtained from during March and April 2003 in Bursa city. The samples were analysed by ELISA method and the mean concentration of AFM1 was determined as 78.06 ± 6.34 ng/kg (0-212.40 ng/kg) in milk of plain villages and 71.72 ± 5.52 ng/kg (12.30-164.10 ng/kg) in those of mountain villages. In their study, AFM1 levels in milk samples were determined sinificantly high (99.13 %) with about 60 % of the samples surpassing the European Union and Turkish tolerance limit of 50 ng/kg.

In the other studies which are investigated AFM1 in milk products; Atasever et al. [10] determined the levels of AFM1 by ELISA method in 80 butter samples taken from shops in Erzurum province. In their study, it was determined in 66 (82.5%) samples at levels, from 10 to121 ng/kg. As a result, they suggested that the levels of AFM1 in 13 (16.3%) specimen were higher than the normal limit accepted by Codex Alimentarious Commission but none of the contaminated butter sample surpassed the normal level ruled out by Turkish Food Codex for AFM1. AFM1 residue levels were also determined using thin layer chromatography in cheeses obtained by ewe's milk in Urfa, Turkey and AFM1 was found in concentrations between 20-2000 ng/kg in 14 of 50 samples (28%). Also, they reported that five cheese products (10%) were at high levels that surpass the routine limits of 250

ng/kg stated by the Turkish Food Codex [15]. Similar to these researches, in this study AFM1 residues were found in Afyon kaymak samples but it was not found to be high level according to the Turkish Food Codex and European Union criteria (the maximum residue limit of AFM1 in milk and its product is 50 ng/L).

In conclusion, aflatoxin formation in feed should be avoided or farm animals must be fed with feed that does not contain aflatoxin and it is necessary to carry out periodic analysis of AFM1 residues of milk and its products in terms of public health.

ACKNOWLEDGEMENTS

This study was presented as a summary at the 8th Asian Buffalo Congress.

REFERENCES

[1] Baytok, M.Y. (1999) Afyon kaymağı ve kaymaklı şeker üretimi. Afyon Kocatepe Üniversitesi, Fen Bilim Derg. 1, 35-40.

[2] Cakmakcı, S., Hayaloglu, A.A. (2011) Evaluation of the chemical, microbiological and volatile aroma characteristics of Ispir Kaymak, a traditional Turkish dairy product. International Journal of Dairy Technology. 64, 444-450.

[3] Türk Gıda Kodeksi Yönetmeliği, Krema ve Kaymak Tebliği, R.G. Tarihi: 27.09.2003 R.G. Sayısı: 25242.

[4] Awasthi, V., Bahman. S., Thakur, L.K., Singh, S.K., Dua, A., Sanjeev, G. (2012) Contaminants in milk and impact of heating: an assessment study. Indian J Public Health. 56, 95–99.

[5] Caloni, F., Stammati, A., Friggè, G., De Angelis, I. (2006) Aflatoxin M_1 absorption and cytotoxicity on human intestinal in vitro model. Toxicon. 47, 409–415.

[6] Decastelli, L., Lai, J., Gramaglia, M., Monaco, A., Nachtmann, C., Oldano, F., Ru, Y.M., Sezian, A., Bandirola, C. (2007) Aflatoxins occurrence in milk and feed in Northern Italy during 2004- 2005. Food Contr. 18, 1263–1266.

[7] Chopra, R.C., Chhabra, A., Prasad, K.S.N., Dudhe, A., Murthy, T.N., Prasad, T. (1999) Carry-over of aflatoxin M1 in milk of cows fed aflatoxin B1 contaminated ration. Ind J Anim Nutr. 16, 103–106.

[8] Kuilman, M.E., Maas, R.F., Fink-Gremmels, J. (2000) Cytochrome P450-mediated metabolism and cytotoxicity of aflatoxin B1 in bovine hepatocytes. Toxicol In Vitro. 14, 321–327.

[9] Çelik, T.H., Sarımehmetoğlu, B., Küplülü, Ö. (2005) Aflatoxin M1 contamination in pasteurised milk. Veterinarski Arhiv. 75(1), 57-65.

[10] Atasever, M.A., Atasever, M., Özturan, K. Urçar, S. (2010) Determination of Aflatoxin M1 Level in Butter Samples Consumed in Erzurum, Turkey. Kafkas Univ Vet Fak Derg. 16(Suppl-A), 159-162.

[11] Buldu, H.M., Koc, A.N., Uraz, G. (2011) Aflatoxin M1 contamination in cow's milk in Kayseri (central Turkey). Turk. J. Vet. Anim. Sci. 35(2), 87-91.

[12] Duraković, L., Mrkonjić-Fuka, M., Skelin, A, Duraković, S., Redžepović, S. (2012) Assessment of aflatoxin M1 levels in ewe's raw milk used for the production of Istrian cheese. Mljekarstvo. 62(1), 14-23.

[13] Zheng, N., Wang, J.Q., Han, R.W., Zhen, Y.P., Xu, X.M., Sun, P. (2013). Survey of aflatoxin M1 in raw milk in the five provinces of China. Food Additives and Contaminants: Part B. 6(2), 110–115.

[14] Kara, R. and Ince, S. (2014) Aflatoxin M1 in buffalo and cow milk in Afyonkarahisar, Turkey. Food Additives and Contaminants: Part B: Surveillance. 7(1), 7-10.

[15] Kamkar, A., Yazdankhah, S., Nafchi, A.M., Nejad, A.S.M. (2014) Aflatoxin M1 in raw cow and buffalo milk in Shush city of Iran. Food Additives and Contaminants: Part B: Surveillance. 7(1), 21-24.

[16] Filazi, A., Ince, S., Temamogulları, F. (2010) Survey of the occurrence of aflatoxin M1 in cheeses produced by dairy ewe's milk in Urfa city, Turkey. Ankara Üniv Vet Fak Derg. 57, 197-199.

[17] Oliveira, C.A.F., Franco, R.C., Rosim, R.E., Fernandes, A.M. (2011) Survey of aflatoxin M1 in cheese from the North-east region of Sa˜ o Paulo, Brazil. Food Additives and Contaminants: Part B. 4(1), 57–60.

[18] Rahimi, E., Anari, M.M., Alimoradi, M., Rezaei, P., Arab, M., Goudarzi, M.A., Esfahani, M.T., Torki, Z. (2012) Aflatoxin M1 in Pasteurized Milk and White Cheese in Ahvaz, Iran. Global Veterinaria. 9(4), 384-387.

[19] Çadırcı, Ö, Gucukoglu, A, Ozpinar, N, Terzi, G, Alisarlı, M. (2011) Aflatoxin M1 Contamination of Ice Cream in Samsun, Turkey. Journal of Animal and Advances. 10(15), 2047-2050.

[20] Oruc, H.H., Kalkanli, O., Cengiz, M. and Sonal, S. (2005) Aflatoxin M1 in raw milks collected from plain and elevated mountain villages in Bursa. Milchwissenschaft. 60(1), 71-72.

Received: **18.02.2018**
Accepted: **03.05.2018**

CORRESPONDING AUTHOR

Recep Kara
Afyon Kocatepe University,
Faculty of Veterinary Medicine,
Department of Food Hygiene and Technology,
Afyonkarahisar – Turkey

e-mail: recepkara@aku.edu.tr

© by PSP Volume 27 – No. 7/2018 pages 5037-5044 Fresenius Environmental Bulletin

DETERMINATION OF INDICATOR SPECIES IN COASTAL SUCCESSIONS IN TENTSMUIR NATIONAL NATURE RESERVES (NNR), SCOTLAND

Gokhan Aydin*

Suleyman Demirel University, Atabey Vocational School, 32670 Atabey, Isparta, Turkey

ABSTRACT

In this study we have tested whether carabid beetles can be used as indicator for both habitat description and disturbed-undisturbed dune successions. For this purpose carabid beetles were sampled in natural and disturbed matched pairs of sites in five coastal successions; fore dune, dune slack, yellow dune, grey dune, and woodland. 23 species and 3404 individuals of carabid beetles were recorded along this gradient. Most frequent among carabid beetles was *Calathus erratus* (Sahlberg, 1827) which occurred mostly in undisturbed grey dune with 1998 individuals. Nine indicator species of carabid beetles were identified for habitat description and seven indicator species of carabid beetles for habitat destruction. The highest indicator value was provided by *Bembidion pallidipenne* (Illeger, 1802) (IndVal: 100%; P= 0.001), a species found only found in dune slack. Overall, this study reveals the interaction between succession and human activities on biodiversity, in this fragile coastal dune system.

KEYWORDS:
Carabidae, Indicator Species Analyse, Pitfall trap, population density

INTRODUCTION

Bioindicator is a species or species group whose population, present/absent situation (status), and/or function, can reveal the qualitative status of the ecosystems [1-4].

The indicator value of a species in relation to environmental factors can be measured in numerous ways. Some species positively or negatively react because of environmental effect in their habitat [5-7]. This reaction can be explained by presence/absence situation or variable of population dynamic of the environmental, ecologic or biologic indicator species [1, 8]. Long term measurement of species present/absent situation and their population dynamic can provide monitor the health of an environment or ecosystem [9, 10]. After all an indicator species defines a feature or characteristic of the environment and can be a sign of an environmental condition. [10].

Measurement of biodiversity is commonly used to evaluate and monitor the health of ecosystems and as a tool for conservation planning [11]. Species richness is often used for these purposes, wherein standardized methods are used to sample and catalog species-level diversity within a designated area [11].

Many authors consider that carabidae family members are sensitive and accurate indicators of the condition of the environment [12-15]. Since carabidae family members are a good model group to reveal hierarchical interactions and structures at different spatial scales, they have been widely studied [16].

Tentsmuir National Nature Reserves (NNR) consists of three sites; Tentsmuir Point, Tayport Heath and Morton Lochs. Tentsmuir Point where present study has been maintained became a NNR in 1954. Scottish Natural Heritage (SNH) merged the sites together to become Tentsmuir NNR in 2003. One of the most important threats for European heathlands are considered as Land use changes [17].

Purpose of the present study is to determine indicator species to understand whether carabid beetles can be used as indicator for determination, destruction and/or sustainability of the habitats.

MATERIALS AND METHODS

Study sites. Tentsmuir Point (became NNR in 1954), Tayport Heath (became NNR, 1988) and Morton Lochs (became a NNR in 1952) are three sites of Tentsmuir NNR. Scottish Natural Heritage (SNH) merged mentioned sites to become Tentsmuir NNR in 2003.

Fore dune, Duneslack, Yellowdune, greydune, and forest were chosen as five main stages of coastal succession for understanding response of carabid beetles for habitat description and fragmentation in Tentsmuir Forest.

The distance between natural and semi-natural (affected by tourism) area were chosen as 500 m. Dune succession habitats were determined in natural and semi-natural dune successions with 3 repli-

cations. Distance between each dune succession were determined as 50 m. (15 plots in total for each block; natural and disturbed dune succession with a minimum distance of 50 m to each other) hence totally 30 dune succession constituted study area in Tentsmuir Forest.

Samples were stored in 70% alcohol before determination to species level. According to Luff [18, 19], Carabid species were identified and confirmed to Martin L. Luff (School of Biology, University of Newcastle upon Tyne).

Data Analysis. Indicator species analyse combines a species-relative abundance with its relative frequency of occurrence in the various groups were generated using the IndVal procedure of Dufrêne and Legendre [16] for each of the five successional stages. Indicator values range from 0 to 100 and 0 shows no indication while 100 shows perfect indication. The statistical significance of the indicator values was tested using a Monte-Carlo procedure with 1000 permutations.

All species represented by <9 specimens were not taken into account in the analyse of indicator species. Therefore, the studied data set contains 3378 specimens belonging to 13 species. This data set is characterized by 464 zeroes, corresponding to 92.18% of the records.

PC-ORD software package (version 6) was used for the indicator species analysis [16] and evaluate statistical significance of IV_{max} by a Monte Carlo method [20, 21].

$$IndVal_{ij} = A_{ij} * B_{ij} * 100$$

A_{ij}: is specificity, i.e. the proportion of the individuals of species "i" that are in class "j"

B_{ij}: is fidelity, i.e. the proportion of sites in class "j" that contain species "i"

Ordination diagram was created by Canoco program (version 4.5) and the distance between habitat types in the diagram approximates the dissimilarity of their species composition, measured by their Euclidean distance [22, 23].

Sampling Method. Carabid beetles were sampled using pitfall traps along the successional gradient containing five stages that were replicated threefold thus obtaining a total number of 15 plots for each natural and disturbed block. In each plot three pitfall traps were set up with the soil surface, distance of 5 m to each other. The pitfall traps, 6 cm in diameter, 8 cm deep, were filled with a 70% Propylene Glycol - Ethanol solution and were protected with a 15 cm petri dishes roof against litter and precipitation. Totally 90 pitfall traps in the study area were sampled and emptied each 3 days.

RESULTS AND DISCUSSION

Capture statistics. Totally 23 species and 3404 individuals of carabid beetles were recorded along the successional gradient. Most frequent among carabid beetles were *Calathus erratus* (Sahlberg, 1827) with 1998 individuals (representing 58.69% of the total catch), *Pterostichus niger* (Schaller, 1783) with 533 individuals (15.66%), *Broscus cephalotes* (Linnaeus, 1758) with 330 individuals (9.69%), and *Calathus mollis* (Marsham, 1802) with 264 individuals (7.76%). Ten species of carabid beetles were found with very rare abundance, less than 9 individuals for each.

Highest species number was found in natural dune slack, and yellow dune with 16 species (250 individuals), 14 species (496 individuals), respectively (Fig1). Highest individual number of carabid beetle was found in natural grey dune with 1503 (Fig1).

Most frequent among carabid beetles (The most abundant species: *C. erratus, P. niger*, *B. cephalotes*, and *C. mollis,* respectively) in our study were also confirmed by many previous studies [19, 24-28].

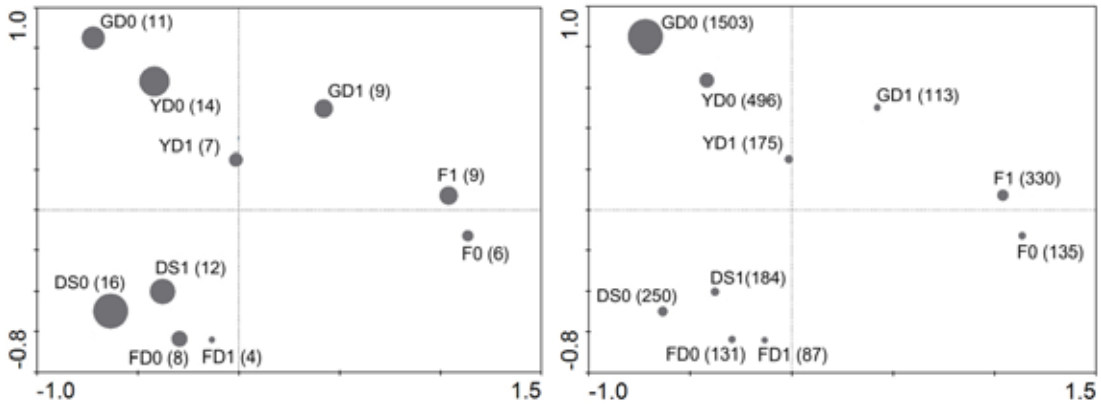

FIGURE 1

Ordination diagram of the carabid species (left) and their individual numbers (right) in natural (0) and unnatural (1) habitats (*). (Habitat points: the distance between the symbols in the diagram approximates the dissimilarity of their species composition, measured by their Euclidean distance)
(*) FD (Fore dune), DS (Dune slack), YD (Yellow dune), GD (Grey dune), F (Forest)

TABLE 1
Indicator value of carabid beetle for habitat description in five successional stages

Species	IndVal (%)	FD	DS	YD	GD	F
Agonum marginatum	.		O			
Amara aenea	**44.4**				**O***	
Amara familiaris	.		O			
Amara fulva	.	O				
Amara tibialis	.				O	
Bembidion pallidipenne	**100.0**		**O*****			
Broscus cephalotes	29.7		O			
Calathus erratus	**69.6**				**O****	
Calathus melanocephalus	**48.9**				**O***	
Calathus mollis	**50.4**		**O****			
Carabus problematicus	**57.9**					**O***
Cicindela campestris	.		O			
Curtonotus aulicus	.			O		
Cychrus caraboides	**38.5**					**O***
Dyschirius politus	31.6		O			
Leistus terminatus	30.8			O		
Loricera pilicornis	**58.3**		**O****			
Nebria brevicollis	18.5		O			
Notiophilus germinyi	.			O		
Paradromius linearis	.			O		
Pterostichus niger	**73.7**					**O*****
Syntomus foveatus	.				O	
Trechus quadristriatus	.	O				

Indicator values were applied sensu Dufrêne and Legendre (1997). (Significance of indicator values was estimated using Monte Carlo randomization set at 1000 permutations at P<0.05; Random number seed:632). Presence situation of the species were shown as a symbol of O. Species with <9 individuals were not evaluated and shown with point. Significant levels are indicated as *** P\0.001, ** P\0.01, * P\0.05 (Species and their indicator value were shown bold).

Indicator species for habitat description and destruction. We identified nine indicator species of carabid beetles for habitat description and seven indicator species of carabid beetles for habitat destruction (Table 1-2). Six carabid species *Bembidion pallidipenne* (Illeger, 1802), *Calathus erratus* (Sahlberg, 1827), *Calathus melanocephalus* agg. (L., 1758), *Calathus mollis* (Marsham, 1802), *Loricera pilicornis* (F., 1775), and *Pterostichus niger* (Schaller, 1783) were found indicator for both habitat description and habitat usage (Table 1-2). Three species of Carabidae family; *Amara aenea* (Degeer, 1774), *Carabus problematicus* Herbst, 1786, and *Cychrus caraboides* (Linnaeus, 1758) showed indicator value for only habitat description (Table 1), and one species *Leistus terminatus* (Hellwig, 1793) was observed that it was negatively affected by tourism activity in Yellow Dune (Table 2).

Amara aenea **(Degeer, 1774).** Indicator value of *A. aenea* was calculated with low rate, 44.4%, for habitat description however this proportion was found statistically significant according to indicator species analyse (P=0.0200) (Table 1).

The adults of genus Amara is generally considered granivorous, since many have been observed feeding on flower heads or plant-seeds. Recent study have showed that adults also eat animal food, the abundance of adults of several species is significantly higher in weedy than weedless habitats [29, 30]. Mostly seeds are the preferred food of adults of several Amara species and a potential food of their larvae [30]. *A. aenea* is very common eurytopic species of open habitats [31] and widely distributed in Scotland and Ireland [18]. The species inhabits in dry grassland, gardens, dunes and waste land [19]. Some studies showed that adults were also found at fruit orchards, such as apple, blackberry and raspberry [32]. However Morris et al. [33] declared that *A. aenea* is characteristic of sandy coastal areas in Scotland. Although the species is known widespread and abundant for the most of recent studies, 90% of population of the mentioned species was found in grey dune at Tentsmuir NNR.

Bembidion pallidipenne **(Illeger, 1802).** All specimens of *B. pallidipenne* were found in dune slack (100%) in both natural (61.54%) and disturbed (%38.46) parts. Indicator value of *B. pallidipenne* was calculated with %100 (P=0.001) for habitat description and %61.5 (P=0.003) for habitat usage (tourism activity/habitat destruction) (Table 1 and 2).

B. pallidipenne is often coastal and occurring on bare sand by freshwater springs or flushes [19]. It occurs from Spain north to southern Scandinavia [18]. The most typical carabid species for the dune slack is found *B. pallidipenne* with 94.5% indicator value (P=0.0020) by Desender et al. [34]. *B. pallidipenne* were found as indicator for habitat description (dune slack). The recent study declared the same results. In addition of this information we found out that the species was also indicator for habitat usage and its population was negatively affected by tourism activity in dune slack.

TABLE 2
Indicator value of carabid beetle for habitat usage (tourism activity) in five successional stages

Species	IndVal (%)	FD	DS	YD	GD	F
Agonum marginatum	.		-			
Amara aenea	44.4				-	
Amara familiaris	.		-			
Amara fulva	.	-				
Amara tibialis	.				-	
Bembidion pallidipenne	**61.5**		**-****			
Broscus cephalotes	29.7		+			
Calathus erratus	**67.4**				**-****	
Calathus melanocephalus	**39.1**				**-***	
Calathus mollis	**39.0**		**-***			
Carabus problematicus	47.4					+
Cicindela campestris	.		+			
Curtonotus aulicus	.			-		
Cychrus caraboides	30.8					-
Dyschirius politus	31.6		-			
Leistus terminatus	**38.5**			**-***		
Loricera pilicornis	**43.7**		**-***			
Nebria brevicollis	37.0		-			
Notiophilus germinyi	.			-		
Paradromius linearis	.			+		
Pterostichus niger	**50.8**					**+****
Syntomus foveatus	.				-	
Trechus quadristriatus	.	-				

Indicator values were applied sensu Dufrêne and Legendre (1997). (Significance of indicator values was estimated using Monte Carlo randomization set at 1000 permutations at P<0.05; Random number seed:3423). Species with <9 individuals were not evaluated and shown with point. A positive effect of a parameter on species abundance is indicated by ''+'' and negative by ''-''. Significant levels are indicated as ** P\0.01, * P\0.05 (Species and their indicator value were shown bold)

***Calathus erratus* (Sahlberg, 1827).** *C. erratus* was found indicator for both habitat description (IndVal=69.6%; P=0.005) and anthropogenic affect (IndVal=67.4; P=0.004) in grey dune. Its population decrease in unnatural grey dune showed statistically significant therefore the mentioned species could be said negatively affected by tourism activity in grey dune (Table 1 and 2).

C. erratus lives in dry sandy localities and coastal dunes [19]. This species is widespread throughout Britain and found throughout Europe except the extreme south [18]. *C. erratus* abundance in habitat which is dominated plant species *Corynephorus* mostly present in grey dune [35]. In addition, habitat type of mentioned species is signed as heathland and moorland [36]. *C. erratus* is also evaluated as indicator species and find out that the species is indicator of the unburnt plots [26].

C. erratus was found indicator for both habitat description and anthropogenic affect in grey dune in our study. The population of the species was found less in unnatural grey dune than natural ones. This result showed statistically significant therefore the mentioned species could be said negatively affected by tourism activity in grey dune.

***Calathus melanocephalus agg.* (Linnaeus, 1758).** *C. melanocephalus* was the one of the indicator species for habitat description and destruction in our study. Its indicator value for both habitat description (grey dune) and anthropogenic affect are 48.9% (P=0.013) and 39.1% (P=0.044), respectively (Table 1 and 2).

C. melanocephalus is a widely distributed species in Britain and Ireland. The species is found in open habitats ranging from coastal dunes and low land heaths to upland grass land and moors. Upland specimens the var. *nubigena* Haliday is all black, with all or most of the legs also darkened [18, 19, 37]. Schirmel and Bucholz [28] affirmed that population and presence/absence situation of *C. melanocephalus* is negatively affected by *Calluna vulgaris* while one of the lowest cover in grey dunes (IndVal=87.2%; P<0.001). Brouwers and Newton [36] declared in their study that the species mostly find in heathland and moorland according to reference of Baars, 1979. *C. melanocephalus* was found indicator species for habitat description and destruction in our study.

***Calathus mollis* (Marsham, 1802).** The present study showed that *C. mollis* indicator for dune slack in Tentsmuir (Indicator Value: 50.4%; P=0.008) and its population was negatively affected by tourism activity in mentioned dune transect (Indicator value: 39.0%; P= 0.013) (Table 1 and 2).

The species *C. mollis* is almost exclusively coastal, being found commonly in sand dunes around the whole of Britain and Ireland. Its range extends throughout Western Europe and around the Mediterranean [18, 33]. *C. mollis* is found typical and abundant species of Marram dunes which is almost exclusively on the first line of coastal sand dunes [38]. *C. mollis* is found indicator species for dune slack with 90.3% indicator value (P=0.001) by Desender et al. [34]. We agree with the authors that

the mentioned species could be used as indicator for dune slack. Besides its population was negatively affected by tourism activity in mentioned dune transect.

***Carabus problematicus* (Herbst, 1786).** Statistical parameters of *C. problematicus* was found significant and it was found indicator for forest habitat (IndVal=57.9%; P=0.013) (Table 1).

C. problematicus is one of the commonest *Carabus* species, and one of the best known British carabids. The species occurs especially frequent in long grassland, woodland, moorland and on heaths [18, 19]. Brouwers and Newton [36] also declared the species occurs mostly in woodland. Morris et al. [33] announced that species characterized in dry open heathland. *C. problematicus* shows a variable habitat preference. It prefers old forests habitats [39]. *C. problematicus* was found indicator for forest habitat in present study. Previous study showed that mentioned species occurs in many but similar type of habitats, such as grassland, woodland, moorland etc. The Tentsmuir Forest present study sustained was originally moorland before acquisition by the Forestry Commission in the 1920s. The moorland has largely disappeared now and has been replaced by conifer forest. Our study showed similar result with previous studies.

***Cychrus caraboides* (Linnaeus, 1758).** *C. caraboides* was found statistically significant for habitat description although with lowest ratio of indicator value (38.5%) in all carabid indicator species. The mentioned species were not found indicator for habitat destruction (Table 1).

C. caraboides is found mainly in woodland, damp moorland and grassland at higher altitudes [18], in woods and on peaty moors [19]. It is usually found singly, and is a specialist mollusc-feeder [18]. Determined habitat types for *C. caraboides* are very similar with *C. problematicus*. *C. caraboides* was also found statistically significant for habitat description although with lowest ratio of indicator value (38.5%) in all carabid indicator species. Both species were not found indicator for habitat destruction. We thought that the reason of these two species occur in woodland is feeding behaviour. Although snails have become adapted to almost every kind of habitat, in Tentsmuir, we observed them with highly abundance in forest part.

***Loricera pilicornis* (Fabricius, 1775).** Indicator value of mentioned carabid species was calculated 58.3% (P=0.004) and sampled 14 sampling sites in dune slack and 6 sampling sites in forest with 58.33% and 41.67%, respectively. The mentioned species is negatively affected by tourism activity in dune slack with one of the lowest indicator value (43.7%; P=0.05) (Table 1 and 2).

L. pilicornis is an extremely common and wide spread species throughout both Britain and Ireland. It is found especially near water and in damp grasslands [18, 31] and usually associated with moist soil [33]. The diurnal larvae have specialised mouth parts that act as a sticky trap to catch Collembola and similar prey. The species occurs throughout continental Europe, and in North America [18]. Kočárek [40] declared that *L. pilicornis* (F., 1775) preferred meadow habitat and Desender et al. [34] provided him with similar result that the species mostly occurred in new salt marsh habitat however indicator value of the species was found 39.6% and not statistically significant. In our study *L. pilicornis* was found indicator species for dune slack. Besides the mentioned species was found indicator for habitat destruction.

***Pterostichus niger* (Schaller, 1783).** *P. niger* was sampled all successional dune ecosystems even with rare individuals it was found with one of the highest indicator value for habitat description (73.7%; P=0.001), forest in Tentsmuir. Population dynamic and presence/absence situation of mentioned carabid species was also found statistically significant for positively affected by tourism activity in forest (woodland) (IndVal: 50.8; P=0.002) (Table 1 and 2).

P. niger is common throughout Britain and Ireland. It is an autumn breeder, whose range extends over most of Europe. [18]. Mentioned species is found in woodland and damp grassland, and on upland moors [18], frequent in hills [31] mostly woodland associated [36], almost totally restricted to the oldest stages of succession [27]. Müller-Motzfeld [41] declared that the species is known to be typical European forest species. *P. niger* was found indicator for habitat description. Besides the study result showed that population of the mentioned species was positively affected by tourism activity in forest (woodland)

Leistus terminatus (Hellwig, 1793). The species could not be found indicator for habitat description, statistical result showed that population and presence/absence situation was negatively affected by tourism in yellow dunes with 38.5% indicator value, (P=0.027) (Table 2).

L. terminatus occurs in damp grasslands, woodland and gardens. Widespread in both Britain and Ireland and very abundant [19]. Abildsnes and Tømmerås [42] declared that the abundance of *L. terminates* is significantly negatively affected by habitat fragmentation. It shows that the species is highly sensitive for habitat changes. However the species could not be found indicator for habitat description in our study but statistical result showed that population and presence/absence situation was negatively affected by tourism in yellow dunes.

CONCLUSION

Coastal successional dunes have very characteristic carabid assemblages and many species are seriously affected by deterioration because of tourism activity (Impact of recreation pressure-including dogs, path roads, rubbish dumping, etc). Across Europe fixed dunes have been the most threatened part of the dune system [43]. Increasing some anthropogenic affects such as tourism, foot traffic, removal of plant species, etc. can cause habitat fragmentation hence invertebrate assemblages which provide natural stability will be changed (presence/absence and population dynamic). In long-term environmental follow-up, conservation, ecological management studies provide finding bio-indicator species for habitat types to preserve or rehabilitate.

Our study has showed habitat preferences and influenced degree of carabid beetles by human activities in Tentsmuir NNR. Sustainability of protected areas can be provided by using indicator species in different geographical zones [44]. Models that assess geographical variation in the trends of multiple species and their interactions with habitats are therefore urgently required to bridge gaps in our understanding of biodiversity declines [45].

ACKNOWLEDGEMENTS

This study is presented orally and published as summary at the Fifth Plant Protection Congress of Turkey. We would like to thank the scientific committee of the congress.

Many thanks to Prof. Dr. Anne Magurran (University of St Andrews, Scottish Oceans Institute, St Andrews, KY16 8LB, Scotland), Iain Matthews and Grant Brown (University of St Andrews, School of Biology, Fife KY16 9TS, Scotland) to guide me to complete present study.

REFERENCES

[1] Aydin, G. (2011) Insect Bio-diversity and Evaluation of Using Insect as Bio-indicator for Sustainability of Protected Areas. Protected Areas Planning-Management-Monitoring. 273-289.

[2] Duran, M., Tuzen, M. and Kayim, M. (2003) Exploration of Biological Richness and Water Quality of Stream Kelkit, Tokat-Turkey. Fresen. Environ. Bull. 12, 368-375.

[3] McGeoch, M.A. (2007) Insects and bioindication: theory and progress. In: Stewart, A.J.A., New, T.R. and Lewis, O.T. (eds.) Insect Conservation Biology: Proceedings of the Royal Entomological Society's. 23rd Symposium. CABI, Cambridge, MA. 144-174.

[4] Ozkoç, H.B. and Taylan, Z.S. (2010) Assessment of various parameters of metal biology in marine microalgae *Phaeodactylum tricornutum* and *Dunaliella tertiolecta*. Fresen Environ. Bull. 19, 2981-2986.

[5] Corduk, N., Hacioglu-Dogru, N., Gul, C. and Tosunoglu, M. (2018) Monitoring of Micronuclei Nuclear Abnormalities in Pelophylax Ridibundus Erythrocytes from the Biga Stream (Canakkale, Turkey). Fresen. Environ. Bull. 27, 147-153.

[6] Liu, Z., Ju, T., Xiao, H. and Zhang, Q. (2018) Investigation of Mountain Spring Water Quality of Fuling, Chongqing (China). Fresen. Environ. Bull. 27, 600-604.

[7] Xu, Q. and Xu, K. (2018) Evaluation of Ambient Air Quality Based on Synthetic Cloud Model. Fresen. Environ. Bull. 27, 141-146.

[8] McCune, B. (2011) Nonparametric Multiplicative Regression for Habitat Modelling. http://www.pcord.com/NPMRintro.pdf.

[9] Bertollo, P. (1998) Assessing Ecosystem Health in Governed Landscapes: A Framework for Developing Core Indicators. Ecosystem Health. 4(1), 33-51.

[10] Kurtz, J.C., Jackson, L.E. and Fisher, W.S. (2001) Strategies for evaluating indicators based on guidelines from the Environmental Protection Agency's Office of Research and Development. Ecological Indicators. 1(1), 49-60.

[11] Magurran, A.E. (1988) Ecological Diversity and Its Measurement. Princeton University Press, Princeton, NJ. 179p

[12] Desender, K. and Turin, H. (1989) Loss of Habitats and Changes in the Composition of the ground and tiger beetle Fauna in Four West-European Countries Since 1950 (Coleoptera: Carabidae, Cicindelidae) Biological Conservation. 48, 277-294.

[13] Turin, H., Alders, K., Den Boer, P.J., Van Essen, S., Heijerman, T.H., Laane, W. and Penterman, E. (1991) Ecological Characterisation of Carabid Species (Coleoptera: Carabidae) in the Netherlands from thirty years pf pitfall sampling. Tijdschrift voor Entomologie. 134, 279-304.

[14] Rainio, J., Niemelä, J. (2003) Ground beetles (Coleoptera: Carabidae) as bioindicators. – Biodiversity and Conservation. 12, 487–506.

[15] Gerisch, M., Schanowski, A., Figura, W., Gerken, B., Dziock, F. and Henle K. (2006) Carabid Beetles (Coleoptera, Carabidae) as Indicators of Hydrological Site Conditions in Floodplain Grasslands. Internat. Rev. Hydrobiol. 91, 326-340.

[16] Dufrêne, M. and Legendre, P. (1997) Species assemblages and indicator species: the need for a flexible asymmetrical approach. Ecological Monographs. 67, 345-366.

[17] Webb, N.R. (1998) The traditional management of European heathlands. J Appl Ecol. 35, 987–990.
[18] Luff, M. (1998) Provisional atlas of the ground beetles (Coleoptera, Carabidae) of Britain. Biological Records Centre Institute of Terrestrial Ecology, Huntingdon. 194p.
[19] Luff, M. (2007) The Carabidae (ground beetles) of Britain and Ireland (Handbooks for the Identification of British Insects). Royal Entomological Society, St Albans. 247p.
[20] McCune, B., Grace, J.B. and Urban, D. L. (2002) Indicator Species Analyses. In: Analysis of Ecological Communities. MjM Software Design Publishers, Oregon, 198-204.
[21] McCune, B. and Mefford, M.J. (2011) PC-ORD. Multivariate Analysis of Ecological Data. Version 6. MjM Software. Gleneden Beach, Oregon, U.S.A.
[22] ter Braak, C.J.F. and Šmilauer, P. (2002) CANOCO Reference Manual and CanoDraw for Windows User's Guide: Software for Canonical Community Ordination (version 4.5). Ithaca, NY, USA (www.canoco.com): Microcomputer Power.
[23] Lepš, J. and Šmilauer, P. (1999) Multivariate Analysis of Ecological Data. Faculty of Biological Sciences. University of South Bohemia, České Budějovice. 110p.
[24] Desender, K. (1996) Diversity and Dynamics of Coastal Dune Carabids. Ann. Zool. Fennici. 33, 65-76.
[25] Noordijk, J., Schaffers, A.P. and Sýkora, K.V. (2008) Diversity of ground beetles (Coleoptera: Carabidae) and spiders (Araneae) in roadside verges with grey hair-grass vegetation. Eur. J. Entomol. 105, 257–265.
[26] Samu, F., Kádár, F., Ónodi, G., Kertész, M., Szirányi, A., Szita, É., Fetykó, K., Neidert, D., Botos E. and Altbäcker, V. (2010) Differential ecological responses of two generalist arthropod groups, spiders and carabid beetles (Araneae, Carabidae), to the effects of wildfire. Community Ecology. 11(2), 129-139.
[27] Schirmel, J. (2010) Short-Term Effects of Modern Heathland Management Measures on Carabid Beetles (Coleoptera: Carabidae). Applied Ecology and Environmental Research. 8(3), 165-175.
[28] Schirmel, J. and Buchholz, S. (2011) Response of Carabid Beetles (Coleoptera: Carabidae) and Spiders (Araneae) to Coastal Heathland Succession. Biodiversity and Conservation. 20, 1469-1482.
[29] Honek, A., Martinkova, Z. and Jarosik, V. (2003) Ground beetles as seed predators. Eur. J. Entomol. 100, 531-544.
[30] Hurka, K. and Jarosik, V. (2003) Larval omnivory in Amara aenea (Coleoptera: Carabidae). Eur. J. Entomol. 100, 329-335.
[31] Šťastná, P. and Hula, V. (2012) Carabidae (Coleoptera) of Sinkholes in the Northern Part of Moravian Karst. Acta Universitatis Agriculturae et Silviculturae Mendelianae Brunensis. LX (26), 219-237.
[32] Cetin, G., Hantas, C. and Erenoglu, B. (2007) The Species of Beneficial Insects and Acari Determined in Some Small Fruits Orchards in Bursa and Yalova Provinces and Their Densities. 2nd Plant Protection Congress of Turkey. 27-29 August 2007, Isparta. 181.
[33] Morris, M.G., Duffey, E.A.G., Greatorex-Davies, J.N., Jones, P.E., Harding, P.T., Welch, R.C., Snazell, R.G., Skelton, M.J.L. and Moller, G.J. (1979) The invertebrate fauna of dune and machair sites in Scotland. Vol II Part (1) The Outer Hebrides site dossiers. Report to the Nature Conservancy Council. NERC/ Institute of Terrestrial Ecology, 189.
[34] Desender, K., Maelfait, J.P. and Baert, L. (2007) Ground Beetles as "Early Warning- Indicators" in Restored Salt Marshes and Dune Slacks. In: Isermann, M., Kiehl, K. (eds.) Restoration of Coastal Ecosystems Coastline Reports. 7, 25-39.
[35] Nijssen, M., Alders, K., Smissen, N. and Esselink, H. (2001) Effects of grass-encroachment and grazing management on carabid assemblages of dry dune grasslands. Proc. Exper. Appl. Entomol., Nev Amsterdam. 12, 113-120.
[36] Brouwers, N.C. and Newton, A.C. (2009) Movement rates of woodland invertebrates: a systematic review of empirical evidence. Insect Conservation and Diversity. 2(1), 10-22.
[37] Niedobová, J., Hula, J.V. and Šťastná, P. (2011) Ground Beetles (Carabidae) from slopes of Macošska Straň and Vilemovicka Straň (Protected Landscape Area of Moravsky Kras, Czech Republic). Acta Universitatis Agriculturae et Silviculturae Mendelianae Brunensis. LIX (3), 143-149.
[38] Desender, K., Baert, L. and Maelfait, J.P. (2006) Evaluation of recent nature development measures in the river IJzer estuary and long-term ground beetle and spider monitoring (Coleoptera, Carabidae; Araneida). Entomologie. 76, 103-122.
[39] Gaublomme, E., Dhuyvetter, H., Verdyck, P., Mondor-Genson, G., Rasplus, J. and Desender, K. (2003) Isolation and Characterization of Microsatellite loci in the Ground Betle Carabus problematicus (Coleoptera, Carabidae). Molecular Ecology Notes. 3, 341–343.
[40] Kočárek, P. (2002) Decomposition and Coleoptera succession on exposed carrion of small mammal in Opava, the Czech Republic. European Journal of Soil Biology. 39, 31–45.

[41] Müller-Motzfeld, G. (2001) Laufkäfer in Wäldern Deutschlands. Angew Carabidol Suppl. 2, 9-20.
[42] Abildsnes, J. and Tømmerås, B.Å. (2000) Impacts of experimental habitat fragmentation on ground beetles (Coleoptera, Carabidae) in a boreal spruce forest. Annales Zoologici Fennici. 37, 201-212.
[43] European Commission (DG ENV B2) (2008) Management of Natura 2000 habitats. Fixed coastal dunes with herbaceous vegetation ('grey dunes') 2130. Technical Report 2008 04/24, 30p.
[44] Aydin, G. and Kazak, C. (2010) Selecting Indicator Species Habitat Description and Sustainable Land Utilization: A Case Study in a Mediterranean Delta. International Journal of Agriculture and Biology. 12(6), 931-934.
[45] Magurran, A.E. and McGill, B.J. (2010) Biological Diversity: Frontiers in Measurement and Assessment. Oxford University Press, Oxford. 345p.

Received: **22.02.2018**
Accepted: **30.04.2018**

CORRESPONDING AUTHOR

Gokhan Aydin
Süleyman Demirel University,
Atabey Vocational School,
32670 Atabey, Isparta – Turkey

e-mail: gokhanaydin@sdu.edu.tr

© by PSP Volume 27 – No. 7/2018 pages 5045-5052 Fresenius Environmental Bulletin

ANTIMICROBIAL AND ANTIOXIDANT SCREENING, SYNERGY STUDIES OF *HELICHRYSUM CHIONOPHILUM* EXTRACTS AGAINST TO RESISTANT MICROBIAL STRAINS

Kadriye Ozcan[1,*], Tuba Acet[2]

[1]Department of Genetic and Bioengineering, Faculty of Engineering, Giresun University, Giresun, Turkey
[2]Department of Genetic and Bioengineering, Faculty of Engineering and Natural Sciences, Gumushane University, Gumushane, Turkey

ABSTRACT

In this study, the antimicrobial activities and antioxidant properties of five different extracts of *Helichrysum chionophilium* plants from Gumushane/Turkey were investigated. To determine the antimicrobial activity disc diffusion and microdilution methods were used against to fifteen microorganisms. The effect of plant extracts and antibiotic combinations against to vancomycin-resistant *Enterococcus faecium* and methicillin-resistant *Staphylococcus aureus* were investigated as well. Total phenolic and flavonoid contents were determined by spectrophotometric techniques. Antioxidant properties of plant extracts evaluated by free radical scavenging assays which ABTS and DPPH. The plant ethyl acetate extract showed the highest level of total phenolic (423.01±0.8 mg GAE/g extract) and flavonoid contents (100.18±1.4 mg QE/g extract). Similarly, ethyl acetate extract exhibited the highest level of DDPH (IC_{50}: 67.44±0.9 µg/ml). However, hexane extract exhibited the highest level activity of ABTS (IC_{50}: 55.20±1.3 µg/ml). The highest MIC value was determined as 8 µg/ml against to *Pseudomonas aeruginosa* on ethyl acetate extract. Besides, all of extracts exhibited antimicrobial activity on at least one test organism. Plant extracts with some antibiotic combinations generated synergies or partial synergic activity against to VREF and MRSA. These findings revealed that the plant has strong antimicrobial and antioxidant properties. Finally, using the plant extracts and antibiotic combinations might be a good tool in fighting with antibiotic resistance strains.

KEYWORDS:
ABTS, antimicrobial activity, DPPH, medicinal plant, MIC, MBC, synergy

INTRODUCTION

Helichrysum, belonging to the family Asteraceae, includes approximately 500 species, widespread around the world. This genus is represented in Turkish flora by 27 taxa, 15 of which are endemic and are widely found in Anatolia [1, 2, 3]. These species generally are known as “everlasting flower” around the world and “ölmez çiçek” or “altınotu” in Turkey [4, 5]. The *Helichrysum* species commonly used in folk medicine due to the anti-inflammatory [6], antioxidant [7, 8], insecticidal [9] and antimicrobial activity [10, 11] both in Turkey and some different places of the world. *Helichrysum chionophilum* is a one of the endemic plants which is belonging to the *Helichrysum* genus in Turkey. And this is using by people very commonly as a medicinal plant for some purposes such as a natural antimicrobial agent, tea and food.

Some bacterial mutations have caused the several kinds of antibiotic resistant bacterial strains that are now a threat to public health globally [12]. This problem has a crucial importance about peoples' health and it should be solved urgently. Today, the discovering to novel active compounds against to antibiotic resistant organisms or trying with different combinations of available ones has become the priority of fight to the resistant pathogens. In this case, medicinal plants have started to more popular. Already, these have been using by people for various purposes for a long time due to the having active phytochemicals.

Several researchers have documented that plants have exhibited antioxidant and antimicrobial properties [13, 14, 15, 16, 17, 18]. In particular, some of them exhibited an antibacterial activity of standard clinical strains [19]. On the other hand, [13] reported that some medicinal plants produced both bactericidal compounds and antibacterial resistance inhibitors. Although there are some different researches as mentioned, especially endemic plants which located in extreme conditions and high mountain area has not been tested pharmacologically yet. As already known that plants can accumulate hyper secondary metabolites for adapt to stress

conditions. Because of that, in this study activity was searched in the extracts of *H. chionophilum* plants that collected from Artabel National Park in Gumushane Province. This park is a region with a rare ecosystem extending up to a height of 3200 meters.

Although *H. chionophilum* plants have collected from different parts of our country, Turkey and searched antimicrobial [5] and antioxidant properties [8], there are not any scientific reports about plants that collected from Artabel area. So, antioxidant and antimicrobial properties of plant extracts (hexane, ethyl acetate, ethanol, methanol, water) were investigated in this study. The plant extracts and different kind of antibiotic combinations were also used and this is the first study of literature that MIC values and synergistic activities on pathogenic stains were reported.

MATERIALS AND METHODS

Plant materials. *Helichrysum chionophilum* plants were collected in August 2016 from Gumushane -Turkey. Voucher specimen of the plant was deposited in the Genetic and Bioengineering Department of Gumushane University, Turkey. The plant aerial parts were chopped, dried and powdered with using miller (Fritsch P- 15, Germany).

Sample preparation and extraction procedure. The plant aerial parts (20 g) were extracted using 400 ml each solvent (hexane, ethyl acetate, ethanol, methanol, and water) during 24 h at 37 °C 125 rpm. The extracts were filtered using Whatmann filter paper (No:1) and then concentrated under 40 °C using a rotary evaporator system. The extracts obtained were stored in a freezer at -20 °C until further tests.

Total phenolic content. Total phenolic content in extracts was determined according to Folin-Ciocalteu method with minor modifications [20]. Briefly, 31.25 µl of sample solution (1 mg ml^{-1}) were put into a test tube containing 125 µl of Folin-Ciocalteu's reagent and 93.75 µl of 7.5% Na_2CO_3. After 2 h incubation at room temperature, the absorbance was measured at 750 nm with microplate absorbance reader (iMark™ 1681135, Bio-Rad). The total phenolic content was calculated as Gallic acid equivalents (GAE) in milligram per gram of extract (mg GAE/g extract).

Total flavonoid content. The total flavonoid content of the extract was determined according $AlCl_3$ colorimetric method with some minor modification [21]. Shortly, 20 µl of sample solutions (1 mg ml^{-1}) was mixed with 172 µl methanol, 4 µl 10% $AlCl_3$, and 54 µl 1 M potassium acetate and waited 40 minutes. After incubation mixture was measured at 415 nm. The total flavonoid content was calculated in milligrams of rutin equivalents (RE) per gram of extract.

Antioxidant activity. DPPH and ABTS assays were used for determine antioxidant activities of plant extracts. The effect of the plant extracts on 1, 1-diphenyl-2-picrylhydrazyl (DPPH) radical was estimated according to [22] with minor modification. Briefly 125 µl of the plant extract was added to 125 µl 0.1 mM DPPH. The mixture was waited 45 minutes and measured at 490 nm. The antioxidant capacity of each extract was calculated as trolox equivalents (TE) (mg TE g^{-1} extract). The antioxidant capacity of each extract was calculated as trolox equivalents (TE) (mg TE g^{-1} extract). ABTS (The 2, 2-azinobis-3-ethylbenzothiazoline-6-sulfonic acid) free radical caption scavenging activity was determined using a colorimetric method according to [23] with minor modifications. Shortly, 80 µl sample and 160 µl ABTS solution mixed and waited at 6 minutes. The mixture was measured at 734-750 nm and the antioxidant capacity of each extract was calculated as trolox equivalents (TE) (mg TE g^{-1} extract).

Inhibition of free radical DPPH and ABTS in percent (I %) was calculated in the following way:

$$\% \text{ inhibition} = (A_{blank} - A_{sample})/A_{blank}) \times 100,$$

Where A_{blank} is the absorbance of the control reaction (containing all reagents except the test compound), and A_{sample} is the absorbance of the test compound. Extract concentration providing 50% inhibition (IC_{50}) was calculated from the graph of inhibition percentage against extract concentration. Tests were carried out in triplicate.

Test microorganisms. The extracts were tested against a total of twelve randomly selected bacterial strains, *Enterococcus faecalis* ATCC 29212, *Staphylococcus epidermidis* ATCC 12228, *Staphylococcus aureus* ATCC6538, *Enterococcus faecium* DSMZ 13590, MRSA ATCC 43300, *Enterococcus hirae* ATCC 10541, *Klebsiella pneumoniae* ATCC 13883, *Pseudomonas aeruginosa* ATCC 27853, *Escherichia coli* ATCC 29998, *Yersinia enterocolitica* ATCC 27729, *Vibrio parahaemolyticus* ATCC 17802, *Salmonella typhimurium* CCM 5445 and three yeasts, *Candida albicans* DSMZ 5817, *Candida albicans* ATCC 10231, *Candida tropicalis* NRRLL YB-366.

Antimicrobial assay. Disc diffusion method was used for determine antimicrobial activity. 10 mg/ml stock solution was prepared by each plant extract dissolved in DMSO. Firstly, petri dishes were prepared by Mueller-Hinton agar and then inoculated with test organisms (0.5 McFarland). Then 20 µL impregnated discs were put on the petri dishes were waited at 4 °C for diffusion of extracts

to the media. After this treatment petri dishes were incubated at 37 °C and 25 °C for bacteria and yeast, respectively. Afterwards 2 days incubation, inhibition zone around the discs was measured as millimeter [22]. As a positive control chloramphenicol was used equal concentration with samples.

Determination of minimum inhibitory and bactericidal concentrations. MIC (minimum inhibitory concentrations) and MBC (minimum bactericidal concentrations) values of the extracts were determined by 96-well microtiter plates using the broth dilution method [24]. Samples were dissolved in DMSO and serial dilution obtained concentration range from 0.512-0.001 mg ml^{-1} were used for determine antimicrobial activities. Suspensions of standard microorganisms (0.5 MacFarland turbidity) were inoculated to the microplates. After 48 h incubation at 37 °C the growth of the microorganisms was observed by using a microplate absorbance reader. The MIC values were described as the lowest concentrations of the plant extracts to inhibit the growth of microorganisms. In order to determine MBC, the broth was taken from each well and inoculated on Mueller Hinton agar for 24 h at 37 °C. The MBC values were defined as the lowest concentration of the extracts at which 99.9% of inoculated bacteria were killed.

Checkboard assay. Plant extracts and some antibiotic (novobiocin, chloromphenicol and nalidixic acid) combinations were tested against to two resistant clinical pathogens methicillin-resistant *Staphylococcus aureus* ATCC 43300 (MRSA) and Vancomycin-resistant *Enterococcus faecium* DSMZ 13590 (VREF) by checkboard assay [25]. The final concentration of samples and antibiotics used in the study was in the range of 4MIC to 1/64MIC. Overnight cultures of these pathogens were diluted to 0.5 MacFarland turbidity and 96 well-plates incubated for 24 h at 37 °C. The fractional inhibitory concentration (FIC) index was used to quantify the synergistic interactions between the plant extracts and antibiotics against both VREF and MRSA. FIC_{index} was calculated in the following way:

$FIC_{antibiotic}$ = MIC of antibiotic in combination / MIC of antibiotic alone

$FIC_{plant\ extract}$= MIC of plant extract in combination / MIC of plant extract alone

$FIC_{index} = FIC_{antibiotic} + FIC_{plant\ extract}$

FIC index values of less than 0.5 indicated synergy, 0.5–0.75 indicated partial synergy, 0.76–1 indicated an additive effect, and >2 indicated antagonism [26].

Statistical analysis. All the analyses were carried out in triplicate. The data was recorded as mean±standard deviation and analysed by SPSS (version 20.0 for Windows 2000, SPSS Inc.). One-way analysis of variance was performed by ANOVA procedures. Significant differences between means were determined by Duncan post hoc tests. $P<0.05$ was accepted as significant.

RESULTS AND DISCUSSION

Total phenolic and flavonoid content. The total phenolic content of the extracts, as determined ranged from 63.91±0.5 to 423.01±0.8 mg GAE/g extract (Table 1). The highest value was detected at ethyl acetate extract while hexane was the lowest. Besides, *H. chionophilum* extracts exhibited total flavonoid contents ranged from 15.22±0.5 to 100.18±1.4 at ethyl acetate and hexane extracts, respectively (Table 1). Total phenolic and flavonoid contents of the plants extract were found similar to literature. According to researches about *Helichrysum* species, the total phenolic content of the methanolic extract of *H. chionophilum* collected from Kayseri was 106.97±0.6 mg GAE/g extract, *H. arenarium* (L.) Moench subsp. *erzincanicum* was 125.57±1.0 mg GAE/g extract; *H. arenarium* (L.) Moench subsp. *rubicundum* was 71.81±1.0 mg GAE/g extract; *H. armenium* DC. subsp. *araxinum* was 86.01±0.6 mg GAE/g extract; *H. plicatum* DC. subsp. pseudoplicatum was 144.50±1.2 mg GAE/g extract [5, 27] and aqueous crude leaf extract of *H. pedunculatum*'s flavonoid content was 0.618 mg GAE /g extract [28]. The differences in the total and flavonoid contents of *Helichrysum* species may be due to differences in their collection area, collection time and chemical composition.

Antioxidant activity. Antioxidant activities were determined by two methods which are ABTS and DPPH. The ABTS assay is especially interesting in plant extracts because the wavelength absorption at 734 nm eliminates colour interference [29]. ABTS trolox equivalent values (TEAC) of plant extracts ranged from 118.67±1.3 (µg/ml) to 85.44±1.2 (µg/ml). The highest level of ABTS TEAC was found in hexane extract and the lowest was water. However, IC_{50} values of plant extracts were 55.20±1.3 in hexane and 62.57±0.1 in ethanol extracts (Table 1). This case might have been raised from by ethanolic extracts which had a different kind of antioxidant compounds except for trolox, so scavenged to reactive oxygen species with them. ABTS data could not be compared with other researches because of no references concerning the ABTS method in this plant. The DPPH trolox equivalent values of plant extracts ranged from 95.44±0.8 (µg/ml) to 15.52±0.2 (µg/ml). The highest level of DPPH TEAC was found in the ethyl acetate extract while the lowest was in water extract. As estimated, IC_{50} values of plant extracts were 67.44±0.9 (µg/ml) in ethyl acetate and 334.95±3.1 (µg/ml) in water extract. In other words, water extract was a weak scavenger of the stable

DPPH radical unlike ethyl acetate extract (Table 1).

IC_{50} values of some similar plants were reported in the past study. According to this, IC50 values of *H. chionophilum* collected from Sivas exhibited 40.5 (µg/ml) in methanolic extracts [8] while IC_{50} values of *H. chionophilum* collected from Kayseri, showed 53.10 (µg/ml) in methanolic extracts [27]. These DPPH scavenger activities were higher than our result that 67.44±0.9 (µg/ml) in ethyl acetate extract, but they collected plants from different parts of Turkey, it might be a reason for this variety.

Antimicrobial activity. At 200 µg concentrations of extracts that obtained from different kind of solvents such as water, methanol, ethanol, ethyl acetate and hexane antimicrobial activities by disc diffusion method were investigated against to 6 gram (+), 6 gram (-) bacteria and 3 yeasts (Table 2). The tested plant extracts showed various antimicrobial activities at least on five bacteria except for water extract. The inhibition zones were 8 to 28 mm for microorganism and if compared to their positive control (chloramphenicol), the most effective plant extract was ethyl acetate on *P. aeruginosa* with zone inhibition 28 mm in diameter.

It was reported that antimicrobial activity of the methanol extract of the plant collected from Kayseri by well diffusion method [27]. They applied 400 µg extract on wells and measured the inhibition zones for 15 microorganisms. They found that methanol extract in this concentration showed the low effect on all test organisms. According to their results methanolic extract of the plant showed low activity on *K. pneumoniae* (6 mm), *P. aeruginosa* (19 mm) and *S. aureus* (11 mm) than our study. In addition to this, they have not found any activity on *E. coli* but we detected activity on *E. coli* (10 mm). It is clear that even though we used half-concentration of plant extract against similar organisms, more effective inhibition results were obtained. Also no activity was found against the yeasts similar to our study. In a study of the antimicrobial activity of *H. italicum* (Roth) G. Don essential oil detected significant effect on *M. luteus* and *S. aureus* with 30 ± 0.2 mm and 27 ± 0.1 inhibition zone, respectively [30].

The MIC and MBC values of the plant extracts ranged from 128 to 8 (µg/ml) against tested organisms (Table 3). The greatest antibacterial activity was observed in both MIC and MBC values with 8 (µg/ml) on *P. aeruginosa* followed by hexane extract on *E. faecalis* with the 16 (µg/ml) MIC and MBC values. The extracts exhibited equal or lower MIC value than positive control chloramphenicol against to *P. aeruginosa, V. parahaemolyticus, Y. enterocolitica, E. faecium, E. faecalis, S. aureus,* MRSA, *E. hirae* and *S. epidermidis.* However, antibacterial activity of the methanolic extract of *Helichrysum arenarium* (L.) Moench subsp. *arenarium* against pathogens were investigated [31]. As a result significant activity on *S. aureus* and *S. pneumoniae* as MIC values were 0.62 and 1.25 mg/mL, respectively were detected.

On the other hand, antimicrobial activity of the plant extracts and antibiotic combinations were investigated to detect estimated plant extracts for potentials of synergy with antibiotics (Table 4). Results have shown that plant ethyl acetate and ethanol extracts with NV combinations had synergy on vancomycin resistant *E. faecium* while ethyl acetate extract with CH and methanol extract with NV combinations had partial synergy. In addition, plant hexane extracts with both NL and CH combinations had a synergistic effect on methicillin-resistant *S. aureus* which is major cause of clinical infections. However, ethanolic and methanolic extracts of plants and CH combinations did not show any synergistic effect on neither VREF nor MRSA. Chloramphenicol inhibits bacterial protein synthesis, which causes bacterial cells to prematurely die [32].

TABLE 1
Total phenolic content, total flavonoid content, antioxidant capacity and IC_{50} values of plant extracts.

Extracts*	Total phenolic content (mg GAE/g extract)	Total flavonoid mg QE/g extract))	ABTS TAEC value (µg/ml)	ABTS IC_{50} value (µg/ml)	DPPH TAEC value (µg/ml)	DPPH IC_{50} value (µg/ml)
H	63.91^{d}±0.5	15.22±0.5^{d}	**118.67^{a}±1.3**	**55.20^{d}±1.3**	85.44^{b}±0.8	74.45^{d}±0.7
EA	**423.01^{a}±0.8**	**100.18±1.4^{a}**	105.50^{b}±1.6	63.80^{c}±1.3	**95.44^{a}±0.8**	**67.44^{e}±0.9**
E	141.67^{b}±0.5	83.90±0.9^{b}	107.05^{b}±0.1	62.57^{c}±0.1	41.32^{d}±0.4	153.19^{b}±1.9
M	118.97^{c}±0.8	83.01±2.2^{b}	100.47^{c}±0.1	68.03^{b}±0.1	69.44^{c}±0.4	88.56^{c}±1.4
W	110.13^{c}±0.5	18.96±0.3^{c}	85.44^{d}±1.2	87.00^{a}±1.2	15.52^{e}±0.2	334.95^{a}±3.1

*Extracts H: hexane; EA: ethyl acetate, E: ethanol, M: methanol, W: water
Note: Different letters between cultivars denote significant differences (Duncan test, $p < 0.05$). Different letters between susceptible and resistant cultivars denote significant differences (LSD test, $p < 0.05$).

TABLE 2
Disc diffusion zones of plant extract (200 µg/ disc) (mm)

Test organisms	Disc diffusion zone diameter (200 µg/ disc) (mm)					
	W	M	E	EA	H	*
Gram (-) bacteria						
Escherichia coli ATCC 29998	-	10	10	10	-	16
Klebsiella pneumoniae ATCC 13883	-	-	9	11	9	12
Pseudomonas aeruginosa ATCC 27853	-	16	25	28	9	16
Salmonella typhimurium CCM 5445	-	9	10	12	11	15
Vibrio parahaemolyticus ATCC 17802	-	8	-	11	12	10
Yersinia enterocolitica ATCC 27729	-	-	-	10	12	12
Gram (+) bacteria						
Enterococcus faecium DSMZ 13590	-	14	15	17	18	10
Enterococcus faecalis ATCC 29212	-	-	-	-	18	15
Staphylococcus aureus ATCC 6538	-	9	-	10	12	10
MRSA ATCC 43300	-	18	-	23	28	15
Enterococcus hirae ATCC 10541	-	-	-	18	22	17
Staphylococcus epidermidis ATCC 12228	-	-	-	-	18	17

* Inhibition zone diameter of chloramphenicol as positive control

TABLE 3
MIC value/MBC values of the plant extract (µg/ml)

Test organisms	MIC value/MBC value (µg/ml)					
	*	W	M	E	EA	H
Gram (-) bacteria						
Escherichia coli ATCC 29998	16	-	64/64	64/64	-	64/128
Klebsiella pneumoniae ATCC 13883	32	-	64/128	64/64	64/64	64/64
Pseudomonas aeruginosa ATCC 27853	16	-	32/64	16/16	8/8	64/64
Salmonella typhimurium CCM 5445	16	-	64/128	64/128	64/64	64/ 128
Vibrio parahaemolyticus ATCC 17802	64	-	64/64	-	64/64	64/64
Yersinia enterocolitica ATCC 27729	32	-	-	-	32/64	32/32
Gram (+) bacteria						
Enterococcus faecium DSMZ 13590	32	-	64/64	64/128	64/128	64/64
Enterococcus faecalis ATCC 29212	16	-	-	-	-	16/ 16
Staphylococcus aureus ATCC 6538	128	-	64/128	-	64/64	64/64
MRSA ATCC 43300	32	-	64/64	64/128	64/64	64/64
Enterococcus hirae ATCC 10541	32	-	-	-	32/32	32/32
Staphylococcus epidermidis ATCC 12228	16	-	-	-	-	32/64

* MIC value of chloramphenicol as positive control

TABLE 4
Antimicrobial activity of the plant extracts and antibiotic combinations.

VRFE*		Extract / NV		Extract / CH	
Test samples	MIC value µg/ml	FIC *index*	Outcome	FIC *index*	Outcome
EA Extract	64	0.3125	synergy	0.75	partial synergy
E Extract	64	0.3125	synergy	1.5	no effect
M Extract	64	0.625	partial synergy	1.5	no effect
Novobiocin (NV)	1				
Chloramphenicol (CH)	2				
MRSA**		Extract / NL		Extract /CH	
Test samples	MIC value µg/ml	FIC *index*	Outcome	FIC *index*	Outcome
H Extract	64	0.3125	synergy	0.3125	synergy
Chloramphenicol(CH)	32				
Nalidixic acid (NL)	64				

*VREF: vancomycin resistant *E. faecium*, **MRSA: Methicillin-resistant *S. aureus*

Synergy between seven medicinal plants and some antibiotics were reported before [12]. In related work, they have reported that 3 out of 32 plant extracts and antibiotic combinations demonstrated synergy with FIC index values range from 0.38 to 0.5 against to methicillin-resistant *E. coli.* Antimicrobial impacts of *M. officinalis, V. officialis*, *D. genkwa* with antibiotic combination increased to activity against MRSA reported in another study [26]. *H.arenarium* (L.) Moench subsp. *arenarium* methanolic extract with ciprofloxacin combination's antimicrobial activity was investigated against to *S. pneumoniae* and *S. aureus* in a study [31]. Synergy against *S. pneumoniae* isolates (FIC *index* = 0.5) and partial synergy against *S. aureus* isolates (FIC *index* = 0.62) were determined at the end of the study. Similar to them *H. chionophilum* various extract were exhibited synergic or partial synergic activity on special clinic strains MRSA and VREF.

CONCLUSIONS

Consequently, the results of this study revealed that except for the water extract, different solvent of *H. chionophilium* plant has promising antimicrobial and antioxidant properties. The misuse and widespread use of antibiotics around the world has caused some mutations in pathogenic strains and this problem getting worst for public health in our era. Therefore, either people should discover new antibiotics or try new treatments. In this aspect, medicinal plants with antibiotic combinations might have a synergistic effect on resistance bacteria thought inspired to our study. According to our results, some of the *H. chionophilium* plant extracts had synergistic effects with different antibiotic combinations. Overall, this plant might be used as a natural antimicrobial and antioxidant agent for the solving some health or food problems consider to damages of synthetic ones. Even if this study gave important clues for synergistic effects of plant and antibiotic combinations, further studies should be carried out for the evaluation of the in vitro and in vivo potential uses of plants and antibiotic combinations to overcome the resistance strains.

ACKNOWLEDGEMENTS

This work was supported by the "Gumushane University, Scientific Research Project Unit [grant number 16.F5119.02.01].

REFERENCES

[1] Davis, P.H., Mill, R.R., Tan, K. (1988) Flora of Turkey and the East Aegean Islands. Edinburgh University Press. Edinburgh

[2] Guner, A., Ozhatay, N., Ekim, T. (2000) Flora of Turkey and the East Aegean Islands. Edinburgh University Press. Edinburgh.

[3] Sumbul, H., Gokturk, R.S., Dusen, O.D. (2003) A new endemic species of *Helichrysum Gaertn*. (Asteraceae-Inuleae) from south Anatolia. Bot J Linn Soc. 141, 251-254.

[4] Lesa, F., Vendittib, A., Másedasa, G., Frezzac, C., Guisob, M., Sciubbab, F., Serafinic, M., Biancob, A., Valerod, M.S., Lópeza, V. (2017) Everlasting flower (*Helichrysum stoechas* Moench) as a potential source of bioactive molecules with antiproliferative, antioxidant, antidiabetic and neuroprotective properties. Industrial Crops and Products. 108, 295-302.

[5] Albayrak, S., Aksoy, A., Sagdıç, O., Budak, U. (2010) Phenolic compounds and antioxidant and antimicrobial properties of *Helichrysum* species collected from eastern Anatolia, Turkey. Turk J Biol. 34, 463–473.

[6] Sala, A., Recio, M.C., Giner, R.M., Manez, S., Tournier, H., Schinella, G., Rios, J.L., (2002) Anti- inflammatory and antioxidant properties of *Helichrysum italicum*. J. Pharm. Pharmacol. 54, 365–371.

[7] Czinner, E., Hagymási, K., Blázovics, A., Kéry, Á., Szoke, É., Lemberkovics, É. (2001) The in vitro effect of *Helichrysi flos* on microsomal lipid peroxidation. J. of Ethnopharmacol. 77, 31–35.

[8] Tepe, B., Sokmen, M., Akpulat, H.A., Sokmen, A. (2005) In vitro antioxidant activities of the methanol extracts of four *Helichrysum* species from Turkey. Food Chem. 90, 685–689.

[9] Gokturk, T., Kordali, S., Calmasur, O., and Tozlu, G. (2011) Insecticidal Effects of Essential Plant Oils Against Larvae of Great Spruce Bark Beetle*, Dendroctonus Micans* (Kugelann) (Coleoptera: Curculionidae: Scolytinae). Fresen. Environ. Bull. 20, 2357-2364.

[10] Sagdic, O., Karahan, A.G., Ozcan, M., Ozkan, G. (2003) Effect of some spice extracts on bacterial inhibition. Food Sci. and Technol. Internat. 9, 353–356.

[11] Dimitroval, L., Zaharieva1, M.M., Popova, M., Kostadinova, N., Tsvetkova, I., Bankova, V., Najdenski, H. (2017) Antimicrobial and antioxidant potential of different solvent extracts of the medicinal plant Geum urbanum L. Chem. Centr. J. 11, 113.

[12] Vambe, M., Aremu, A.O., Chukwujekwu, J.C., Finnie, J.F., Staden, J.V. (2018) Antibacterial screening, synergy studies and phenolic content of seven South African medicinal plants against drug-sensitive and -resistant microbial strains. South Afric. J. of Bot. 114, 250–259.

[13] Stermitz, F.R., Lorenz, P., Tawara, J.N., Zenewicz, L.A. and Lewis, K. (2000) Synergy in a medicinal plant: Antimicrobial action of berberine potentiated by 5′-methoxyhyd-nocarpin, a multidrug pump inhibitor. Proceedings of the National Academy of Sciences of the United States of America. 97(4), 1433–1437.

[14] Al-Fatimi, M., Wurster, M., Schröder, G., Lindequist, U. (2007) Antioxidant, antimicrobial and cytotoxic activities of selected medicinal plants from Yemen. J. of Ethno-pharmacol. 111, 657–666.

[15] Kaynar, P. (2017) Antimicrobial Activity of Quercus Robur L. (Acorn). Fresen. Environ. Bull. 26, 6992-6995.

[16] Tang, X., Xu, C., Yagiz, Y., Simonne, A., Marshall, M.R. (2018) Phytochemical profiles, and antimicrobial and antioxidant activities of Greater Galangal [Alpinia galanga (Linn.) Swartz.] flowers. Food Chem.

[17] Yilar, M., Kadioglu, I., Telci, I. (2018) Chemical Composition and Antifungal Activity of *Salvia officinalis* (L.), *S. cryptantha* (Montbret Et Aucher Ex Benth.), *S. tomentosa* (Mill.) Plant Essential Oils and Extracts. Fresen. Environ. Bull. 27, 1695-1706.

[18] Sevindik, M., Akgul, H., Dogan, M., Akata, I., Selamoglu, Z. (2018) Determination of Antioxidant, Antimicrobial, DNA Protective Activity and Heavy Metals Content of Laetiporus sulphureus. Fresen. Environ. Bull. 27, 1946-1952.

[19] Pezeshkpour, V., Khosravani, S.A., Ghaedi, M., Dashtian, K., Zare, F., Sharifi, A., Jannesar, R., Zoladl, M. (2018) Ultrasound assisted extraction of phenolic acids from broccoli vegetable and using sonochemistry for preparation of MOF-5 nanocubes: Comparative study based on micro-dilution broth and plate count method for synergism antibacterial effect. Ultrason. Sonochemist. 40, 1031–1038.

[20] Slinkard, K., Singleton, V.L. (1977) Total phenol analyses: automation and comparison with manual methods. Am J Enol Viticult. 28, 49-55.

[21] Moreno, M.I., Isla, M.I., Sampietro, A.R., Vattuone, M.A. (2000) Comparison of the free radical-scavenging activity of propolis from several regions of Argentina. Journal of Ethnopharmacology. 71, 109-114.

[22] Bauer, A.W., Kirby ,W.M., Sherris, J.C., Turck, M. (1966) Antibiotic susceptibility testing by a standardized single disk method. Am J Clin Pathol. 45(4), 493-496.

[23] Re, R., Pellegrini, N., Proteggente, A., Pannala, A., Yang, M., Rice-Evans, C. (1999) Antioxidant activity applying an improved ABTS radical cation decolorization assay. Free Radical Biology and Medicine. 26, 1231-1237.

[24] CLSI (Clinical and Laboratory Standards) (2007) Performance standards for antimicrobial susceptibility testing. 17th Informational Supplement, M100-S17, 27:1.

[25] Rand, K., Houck, H., Brown, P., Bennett, D. (1993) Reproducibility of the microdilution checkerboard method for antibiotic synergy. Antimicrobial Agents and Chemotherapy. 37, 613-615.

[26] Kuok, C.-F., Hoi, S.-O., Hoi, C.-F., Chan, C.-H., Fong, I.-H., Ngok, C.-K., Fong, P. (2017) Synergistic antibacterial effects of herbal extracts and antibiotics on methicillin-resistant *Staphylococcus aureus*: A computational and experimental study. Experimental Biology and Medicine. 242(7), 731–743.

[27] Albayrak, S., Aksoy, A., Sagdıc, O., Hamzaoglu, E. (2010) Compositions, antioxidant and antimicrobial activities of *Helichrysum* (Asteraceae) species collected from Turkey. Food Chemistry. 119, 114-122.

[28] Aiyegoro, O.A. and Okoh, A.I. (2009) Phytochemical Screening and Polyphenolic Antioxidant Activity of Aqueous Crude Leaf Extract of Helichrysum pedunculatum. International Journal of Molecular Sciences. 10(11), 4990–5001.

[29] Li, H.B., Wong, C.C., Cheng, K.W., Chen, F., (2008) Antioxidant properties in vitro and total phenolic contents in methanol extracts from medicinal plants. LWT-Food Sci. and Technol. 41, 385–390.

[30] Djihane, B., Wafa, N., Elkhamssa, S., Pedro, D. H. J., Maria, A. E., Mohamed Mihoub, Z. (2017) Chemical constituents of Helichrysum italicum (Roth) G. Don essential oil and their antimicrobial activity against Gram-positive and Gram-negative bacteria, filamentous fungi and Candida albicans. Saudi Pharmaceutical Journal : SPJ. 25(5), 780–787.

[31] Gradinaru, A.C., Silion, M., Trifan, A., Miron, A., Aprotosoaie, A.C. (2014) *Helichrysum arenarium* subsp. *arenarium*: phenolic composition and antibacterial activity against lower respiratory tract pathogens. Nat Prod Res. 28(22), 2076-2080.

[32] Siibak, T., Peil, L., Xiong, L., Mankin, A., Remme, J., Tenson, T. (2009) Erythromycin- and chloramphenicol-induced ribosomal assembly defects are secondary effects of protein synthesis inhibition. Antimicrobial Agents and Chemotherapy. 53, 563–571.

Received: **23.02.2018**
Accepted: **04.05.2018**

CORRESPONDING AUTHOR

Kadriye Ozcan
Department of Genetic and Bioengineering,
Faculty of Engineering,
Giresun University,
28200, Giresun – Turkey

e-mail: kadriye.ozcan@giresun.edu.tr

© by PSP Volume 27 – No. 7/2018 pages 5053-5065 Fresenius Environmental Bulletin

IMPORTANCE OF SPATIAL SOIL VARIABILITY FOR LAND USE PLANNING OF A FARMLAND IN A SEMI-ARID REGION

Mesut Budak*

Siirt University, Faculty of Agriculture, Department of Soil Science and Plant Nutrition, Siirt, Turkey

ABSTRACT

Assessing the spatial variability of soil properties is vital in proper planning of agricultural farmlands. The aim of this study is to determine and map the spatial variability of important physical and chemical soil properties using geoistatistical models for land use planning of a farm located in Thrace region of Turkey. Two hundred fifty-four surface and subsurface soil samples were collected from at approximately the corners of 150m x 150m size grids cells. The land area of study area was 557 ha and used for what and sunflower production. Soil samples were analyzed for particle size distribution, soil reaction (pH), electrical conductivity (EC), organic matter (OM), lime content ($CaCO_3$), available phosphorus (P) and extractable potassium (K). Penetration resistance was also measured at each sampling point. Soil pH ranged from 4.46 to 8.20 in surface and 4.01 to 8.30 in subsurface soils. Sand content was the least variable (CV=11.5% and 13.9% for surface and subsurface) soil property, while the variability of P content (CV=105.9 and 119.8%) was higher than the rest of the soil properties. The lowest range value was obtained for P content (113 and 134 m) and the longest-range value was for available K content (5899 and 6099 m) of soils. Spatial distribution maps helped to identify and deliniate the zones need to be limed, deficient in available P and compacted zones within the study area. Sustainable management strategies in a farm can be planned and implemented using the information obtained from spatial structures and maps of major soil characterics.

KEYWORDS:
Land use planning, geoistatistics, spatial variability, farm land

INTRODUCTION

The best use options of a land require a comprehensive and accurate characterizations of soil, climate and other environmental factors influencing the sustainability of investment. The purpose of land use planning is to determine the best land use option that helps to protect and improve the functioning potential of soils. The best use option to be implemented needs information on spatial variability of soil properties within the farmland. The information on spatial distribution of soil properties is needed for various purposes such as ecological modellings, environmental predictions, precision agriculture, and natural resources management, as well as land-use planning requires [1].

The variability of soil properties across from a field to a larger landscapes and regions defined as the medium and large-scale variability is affected by inherent or soil forming factors [2]. The differences in management practices for various crops alter the inherent spatial structure of soil propertes [3, 4]. The variability of soil properties within agricultural fields is often described by classical statistical methods using meand along with standard error of mean [3] and coefficient of variation [5]. The mean value of an attribute for a single field is expected to be the value everywhere in the field, and the estimation error is considered as the variance within the field [3]. Interpreting the variability of soil properties in a farm using the coefficient of variation is not enough to identify and delineate the areas with their extreme values for their effective managements. In order to define the variation of soil properties within a farmland or even in a single field scale can be achived by using geostatistical tecniques which enable spatial relationship among values of sampling locations [3].

Assessment and mapping of spatial distribution on the physical and chemical properties of the soil are important drivers in the advancement of land use planning of a farm from the earliest days of agriculture [6]. Spatial distribution maps for a farmland helps to identify and delineate the problematic zones and may serve as effective tools in site specific nutrient management [7], reclamation of salinity and boron toxicity [8, 9]. The information on the spatial distribution of soil properties within a farm is a prerequsite for the best management decisions such as selection of the appropriate fertilizer dose, application methods and frequency, improvement of soil drainage [10, 11], and monitoring of soil quality changes in time [12]. The purposes of this study are to assess the status of some physical and chemical

soil properties which have great importance in agricultural production; (ii) to investigate the spatial variability of soil properties, and (iii) to define critical zones of nutrient deficiency, acidity and compaction for site specific management of remediation.

MATERIALS AND METHODS

Study area. The study area is located in Kırklareli province, Thrace Region of Turkey, between latitude 41°37' N and 41°39' N; longitude 27°11' E and 27°13' E. The area comprises about 557 ha land (Fig. 1) with an altitude ranging from 120 to 171 m. The area formed over Kircasalih geological formation (Thrace formation). The Quaternary materials deposited over Kırcasalih formation which composed of unconsolidated gravel, coarse grained conglomerate, sandstone claystone and sparse granular clay stone. The gravels generally consist of quartz, quartzite, rarely schist, metagranite and volcanic rocks. The geological unit in study area formed in stream environment [13]. Entisols, Inceptisols and Ultisols are the commonly encountered soil ordos in study area. Long-term total annual average rainfall of the area is 570.1 mm and mean soil temperature is 13.3°C.

Soil Sampling and Laboratory Analyses. The study area was divided into 150*150m grids, and soil samples at a depth of 0-20cm and 20-40 cm were collected from the nodes of 127 grids. Thus, a total of 254 soil samples were taken to investigate the spatial distribution of soil properties. Soil samples were air-dried and thoroughly mixed and ground to pass a 2.0 mm sieve. Physical and chemical soil properties of soil samples were measured using standard laboratory methods. Particle size distribution was determined by the hydrometer method in a sedimentation cylinder, using sodium hexamethaphosphate as the dispersing agent [14]. Penetration resistance was measured with a hand pushed penetrometer [15]. Electrical conductivity and pH of soils were measured at 1:2.5 soil water suspension [16]. Soil organic matter (OM) was determined using the technique described by Walkley and Black [17]. $CaCO_3$ was determined by using calcimeter method as mentioned by Allison and Moodie [18]. Avaliable P was extracted using 0.5 M $NaHCO_3$ and using the molybdenum-blue method [19]. Available potassium was determined by atomic absorption spectrophotometer after extraction using 1M ammonium acetate at pH 7.0 [20].

Statistical and Geostatistical Analysis. Descriptive statistics (minimum, maximum, mean, standard deviation and skewness) and correlation analyses were conducted using SPSS 22.0 statistical software (SPSS, Inc., Chicago, IL). Spatial variability of soil properties was determined using geostatistical techniques. Modeling of experimental semivariogram was performed with GS^+ (version 7) statistical software Gamma Design Software. The data

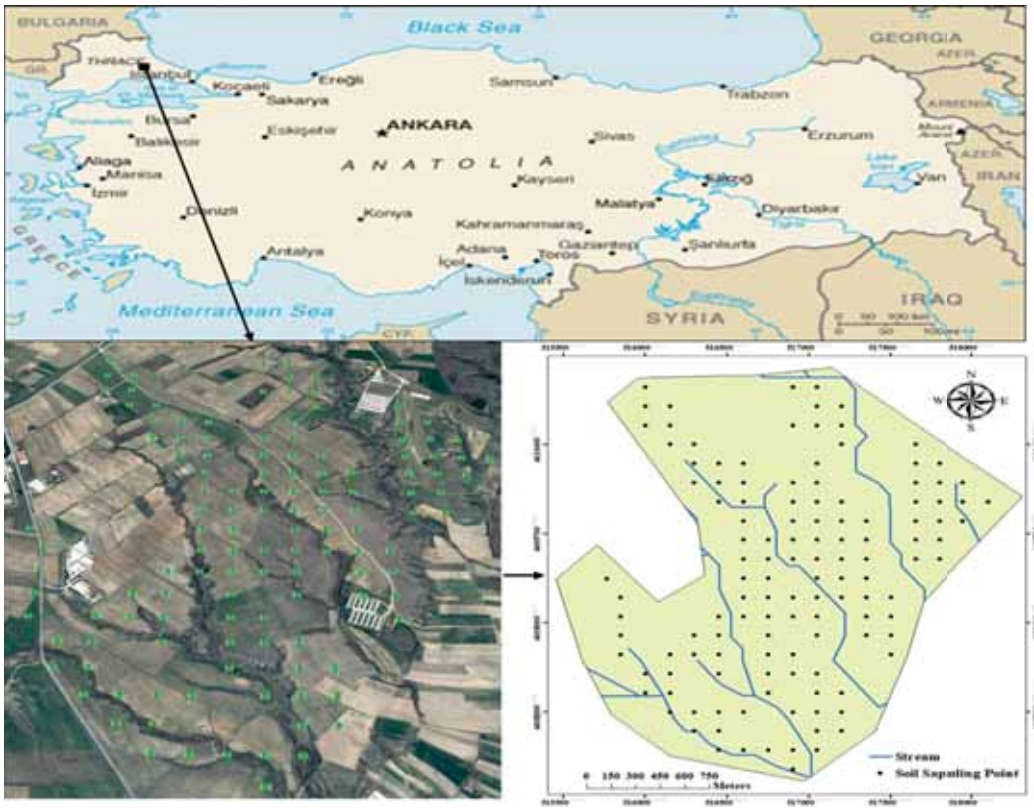

FIGURE 1
Location of the study area and sampling points in Kırklareli province, Turkey

with nonn-normal distribution (EC, $CaCO_3$, OM, P and K) were subjected to log transformation [21].

The semivariogram models were constructed using the Eq.1.

$$\gamma(h) = \frac{1}{2\,N(h)} + \sum_{i=1}^{N(h)} [z(x_i + h) - z(x_i)]^2 \quad \text{(Eq. 1)}$$

where; h is separation distance between x_i and x_i+h, N(h) is the numbr of pairs separated by h distance; $z(x_i)$ is the data measured at x point; $z(x_i + h)$ is data for a location separated by x+h distance [22].

The best fit model for each of soil properties was determined based on r^2 and RSS (Residual Sum of Squares) values of the semivariogram model. Models with r^2 values close to 1.0, and RSS values close to zero were selected as the best fitted model [23]. Cross validation process was also performed to determine the success of the created models. The accuracy of the estimates for the unsampled locations depends on the components of the semivariogram models (range, sill, nugget, lag number), the type of kriking method, and the number of nearest neighbor selected for the estimation. The reliability of estimates and spatial structure of soil properties were discussed using each of the specified factors.

The most appropriate parameters obtained by semi-variogram models and cross validation technique were used to obtain spatial distribution maps of each variable. The kriging maps of soil properties were created using the geostatistical extension of ArcGIS 10.2.1 [24].

RESULTS AND DISCUSSIONS

The parameters for descriptive statistics (minimum, maximum, mean, standard deviation (SD), coefficient of variation (CV), and skewness) of soil physical and chemical properties are presented in Table 1. The average sand contants of soils, formed over alluvial parent materials, were 54.4 and 53.7%, respectively (Table 1). Soil pH has a great influence on availability of plant nutrients and microbial activity responsible from oxidation of organic matter [25]. The pH value ranged from 4.46 to 8.20 in surface and from 4.01 to 8.30 in subsurface soils of the study area. Soil acidity is an important indicator of land degradation and has been shown to restrict fertility in agricultural land, resulting in reduced plant biomass and lower crop yields [25, 26]. In addition, the increased heavy metal mobility has been reported under acidic conditions for sandy soils [27]. The pH values indicate that the existence of very strongly acidic areas in the study area. Therefore, spatial distribution of pH values in a farmland should be taken into account for land use planning.

The average organic matter (OM) content (1.33%) of surface soils were low that was ranged from inadequate (0.46%) to high (6.82%) levels. Similar to the surface soils, the OM content of subsurface soils was between 0.31% to 4.95 with a mean value of 1.09%. The soils had adequate available P and K concentrations. The P concentration ranged from 3.19 to 331.20 mg kg^{-1} with a mean value of 47.06 mg kg^{-1} and the K concentration of soils ranged from 64.84 to 1603.65 mg kg^{-1} with a mean value of 141.13 mg kg^{-1} in surface soils (Table 1).

TABLE 1
Descriptive statistics of soil properties

Variable	Depth (cm)	Unit	Min.	Max.	Mean	Std. Dev.	CV*	Skewness
Sand	0-20	%	40.7	72.3	54.4	6.23	11.5	0.39
	20-40		33.9	71.4	53.7	7.44	13.9	0.00
Clay	0-20		15.2	42.7	24.2	4.91	20.3	0.70
	20-40		15.2	43.6	25.9	6.72	26.0	0.80
Silt	0-20		10.0	30.9	21.4	4.81	22.5	-0.27
	20-40		11.6	33.4	20.5	4.30	21.0	0.20
Penetration Resistance	0-20	MPa	0.26	1.76	0.74	0.28	38.3	0.96
	20-40		0.31	2.53	1.41	0.42	29.8	-0.36
pH	0-20		4.46	8.20	5.98	0.93	15.6	0.51
	20-40		4.01	8.30	5.89	0.87	14.7	0.53
Electrical Conductivity	0-20	dS m^{-1}	0.03	0.48	0.12	0.09	78.3	1.91
	20-40		0.03	0.53	0.13	0.10	81.5	1.88
CaCO3	0-20	%	1.47	6.46	1.98	0.57	28.7	5.41
	20-40		1.17	4.55	1.90	0.40	20.9	3.74
Organic Matter	0-20		0.46	6.82	1.33	0.69	52.0	4.33
	20-40		0.31	4.95	1.09	0.54	49.4	3.28
Available P	0-20	mg kg^{-1}	3.19	331.20	47.06	49.82	105.9	2.99
	20-40		2.39	223.30	29.98	35.93	119.8	2.83
Available K	0-20		64.84	1603.65	141.13	142.83	101.2	8.91
	20-40		41.28	1105.50	124.81	105.77	84.7	7.27

*Coefficient of variation (%)

The variability of attributes within study area was interpreted using the coefficient of variation (CV). The soil attribute was classified into the most (CV ≥ 35%), moderate (CV 15–35%) and least (CV ≤ 15%) variable classes according to the criteria proposed by Wilding [5]. The values of CV for soil properties ranged from 11.5 (sand) to 105.9% (P) in surface and 13.9 (sand) to 119.8% (P) in subsurface soil (Table 1). Although the study area is not very large, the EC, OM, available P and K contents in both soil depths and the PR in surface soils are classified as the most variable class. Recent application of manure in some fields of the study area resulted in high variability of OM, P and K contents. Clay, silt and $CaCO_3$ of soils in both soils depths had moderate variability. Similarly, Trangmar et al. [3] indicated that variabilities of soil properties readily affected by soil management (e.g., available P, EC, compaction) are higher compared to the morphological (e.g., color, A horizon thickness), physical (e.g., clay, sand and silt contents), and chemical (e.g., ction exchange capacity, pH) properties used to define taxonomic units. The results on variability of soil properties within a farmland are in line with data reported by Marques et al. [28] who indicated that the most variable soil attributes were available P and PR with CV values of 51.1% and 37.2%. Similar to this, Denton et al. [29] found that available P concentration of surface and subsurface soils had the highest variability with a CV value of 40.19 and 73.14%, respectively. High variability of dynamic soil properties i.e available P and PR can be attributed to the difference in management practices carried out in different fields of the study area.

Correlation Between Soil Attributes. The results of correlation test between soil attributes were given in Table 2. Sand content had significant negative correlations with OM contents of surface ($P<0.05$) and subsurface ($P<0.01$) soils, while significant positive correlations were obtained with sand and available P contents at boh soil depths (Table 2). Soil pH was significantly ($P<0.01$) correlated to EC value and $CaCO_3$ content of surface and subsurface soils. Similar to the relationship between pH and $CaCO_3$ obtained in this study, Suarez [30] found a significant positive relation between pH and $CaCO_3$ of soils. Essential plant nutrients, P and K had significant ($P<0.01$) positive correlations with soil OM content at both soil depths. Similarly, Srinivasan et al. [31] reported positive correlations between soil OM content and available P ($P <0.05$) ve K ($P<0.01$) contents of orchard soils.

Spatial Variability of Soil Properties. Parameters of semivariograms for each physical and chemical soil properties are presented to obtain the in Table 3. Analysis of the isotropic variogram indicated that the clay, OM, $CaCO_3$ and available P semivariograms were well described by exponential model in both soil depths. The spherical (surface soils) and exponential (subsurface soils) models were the best fit models for sand, silt and pH. The spatial distribution of PR was better described with exponential (surface) and spherical (subsurface), and gaussian model was the best model for available K in both soil depths (Table 3).

TABLE 2
Correlation coefficients between soil properties in 0-20 cm and 20-40 depth

0-20 cm	Sand	Clay	Silt	PR	pH	EC	$CaCO_3$	OM	P
Clay	-0.651**								
Silt	-0.631**	-0.178*							
PR	-0.162	0.015	0.194*						
pH	0.120	0.121	-0.279**	-0.152					
EC	-0.103	0.342**	-0.215*	0.011	0.515**				
$CaCO_3$	-0.025	0.198*	-0.171	-0.031	0.353**	0.382**			
OM	-0.206*	0.129	0.134	0.250**	0.072	0.223*	0.317**		
P	0.197*	-0.056	-0.198*	0.135	0.209*	0.422**	0.265**	0.414**	
K	0.014	0.107	-0.128	0.060	0.239**	0.386**	0.429**	0.748**	0.593**
20-40 cm	**Sand**	**Clay**	**Silt**	**PR**	**pH**	**EC**	**$CaCO_3$**	**OM**	**P**
Clay	-0.820**								
Silt	-0.448**	-0.144							
PR	0.024	0.035	-0.097						
pH	0.137	0.011	-0.253**	0.049					
EC	-0.094	0.206*	-0.159	-0.012	0.387**				
$CaCO_3$	0.094	0.009	-0.177*	0.117	0.262**	0.318**			
OM	-0.196*	0.118	0.153	-0.129	0.169	0.281**	0.245**		
P	0.323**	-0.229**	-0.201*	0.017	0.258**	0.295**	0.298**	0.366**	
K	0.063	0.049	-0.186*	0.058	0.315**	0.346**	0.464**	0.673**	0.591**

**. Correlation is significant at the 0.01 level *. Correlation is significant at the 0.05 level

TABLE 3
Semivariogram parameters of soil properties

Variable	Depth	Model	Nugget	Sill	% SD*	Range (m)	r^2	RSS**	CVr***
Sand	0-20	Spherical	20.8	48.68	42.73	1005	0.96	6.6	0.229
	20-40	Exponential	33.0	94.0	35.11	2235	0.92	26.1	0.270
Clay	0-20	Exponential	1.05	22.75	4.62	252	0.93	0.72	0.064
	20-40	Exponential	0.0029	0.055	5.27	250	0.68	1.16E-05	0.136
Silt	0-20	Spherical	12.59	36	34.97	3609	0.96	5.02	0.287
	20-40	Exponential	9.93	19.87	49.97	382	0.92	2.82	0.221
Penetration Resistance	0-20	Exponential	0.035	0.156	22.44	369	0.9	7.44E-05	0.054
	20-40	Spherical	0.126	0.218	57.80	706	0.96	1.67E-0.4	0.137
Organic Matter	0-20	Exponential	0.0004	0.2378	0.17	202	0.77	1.18E-04	0.030
	20-40	Exponential	0.0058	0.2626	2.21	204	0.81	1.53E-04	0.034
$CaCO_3$	0-20	Exponential	0.0023	0.0556	4.14	180	0.74	1.82E-06	0.015
	20-40	Exponential	0.0234	0.127	18.43	657	0.54	1.96E-04	0.006
Available P	0-20	Exponential	0.024	0.618	3.88	113	0.61	6.27E-03	0.063
	20-40	Exponential	0.446	0.893	49.94	134	0.91	5.32E-03	0.113
Available K	0-20	Gaussian	0.102	1.12	9.11	5899	0.93	4.59E-03	0.003
	20-40	Gaussian	0.131	0.866	15.13	6099	0.92	4.82E-03	0.007
pH	0-20	Spherical	0.447	0.965	46.32	1011	0.98	2.85E-03	0.344
	20-40	Exponential	0.417	0.851	49.00	485	0.9	1.46E-02	0.242
Electrical Conductivity	Pure Nugget								

*Spatial Dependence ** Residual Sum of Squares **Cross Validation r

Spatial dependence (SD) is commonly used to describe the spatial dependence of soil properties. The SD is defined as the raito between nugget variance and sill (Co/Co+C) that is expressed as a percentage [32]. The clay (4.6 and 5.3%), OM (0.2 and 2.2%), $CaCO_3$ (4.1 and 18.4%), and available K (9.1 and 15.1%) contents showed strong SD (<25%) in both surface and sub-surface and available P and PR had strong SD in surface soils. The SD of all other soil properties ranged from 35.0 to 57.8 indicating moderate SD (Table 3). The strong spatial dependency is considered a result of intrinsic (e.g., parent material, climate, topography), whereas weak and moderate spatial dependences indicates the contribution of management related factors (i.e, fertilizer or manure application, soil tillage, irrigation) [7].

Range value is an important component of semivariograms which implies the length of spatial dependence, and classical statistics do not consider the spatial range of soil properties. The differences in characteristics of soil properties within a given range are considered as a function of their spatial separation [3], and measurements are spatially correlated within the observed range values [33]. In the present study, we determined grid interval as 150 m and range values varied from 113 to 5899 m in surface and 134 m to 6099 in subsurface soils suggesting that the results of interpolation could be reliable under the Thrace region conditions.

The lowest range values in surface and subsurface soils were 113 and 134 m for available P, 202 and 204 m for OM and 252 and 250 m for clay content of soils. Similar to the results of this study, Liu et al. [34] found a short-range scale for organic carbon contents of soils and attributed this short range for organic carbon to the land use. Contradictrory to the reports on long range values for inherent charcteristcs [34, 35, 36, 37, 38], the range value for clay content was significantly lower than many of dynamic soil properties (Table 3). The highest range values for surface (5899 m) and subsurface (6099 m) soils were obtained for available K contents. The range value of soil properties that is useful criteria for the evaluation of sampling design and the mapping of soil properties [39]. The range values, however, obtained in this study (except for available P) are higher than the distance of grid interval that shows the inconsistence in the distribution of all the parameters within the study area [7]. Parent material [40, 41, 42], management practices [22, 41, 43] and the size of study area [7, 41] had great influence on the variation of range values. Vasu et al. [7] reported shorter range value for potassium (1054 m) in a 215 km^2 study area compared to the range found in this study, whereas range values for soil OM (1054 m), pH (1029 m) and available P (1027 m) were higher than what we have reported in this study. In a larger study area (4.949 km^2), Dey et al. [44] found higher range values for pH, soil OM and available K content (95.8 km), EC (92.7 km) and available P (24.8 km). The differences in management practices and parent materials in the study area resulted in varying range values of the soil properties.

Spatial distribution maps obtained using ordinary kriging were presented in Figures 2, 3 and 4. The spatial distribution maps helped to identify the extent and magnitude of soil properties within study area. Sand content in both soil depths was gradually increased from north east to west and south east side of the study area, and the percent sand ranged from 40.7 to 72.3% in surface and from 33.9 to 71.4% in subsurface layers (Fig. 2). In contrast to spatial structure of sand particles, clay content of soils exhibited an irregular distribution and ranged from 15.2 to

42.7%. Due to the significant impacts on many physical, chemical and biological properties [45, 46, 47], soil texture should be used as an important factor in land use planning, determining in tillage practices, crop rotation, irrigation tecqhnique and amount of water, type and amount of fertilizer, etc. Variation in clay content of soils within study area is ascribed by the fluctuations in sediment load of rivers in a year or among years. Similar to the assumption on irregularity in distribution for some of particle size components, Turgut and Öztaş [48] indicated irregular distribution of silt content in an alluvial plain, and irregularity was attributed to the differences in silt content of sediments brought by the river at different times.

Root growth, infiltration of water, aeration and many other vital process in soil are directly related to physical conditions of soil. Compaction is one of the most frequently encountered problems in agricultural fields, and severely restricts the plant growth leading to significant yield loss [49]. The wheel traffic and axle load, starting from seed bed preparation till the harvest of the crops are the main contributors to soil compaction that increased by the use of heaver farm machineries [50]. Penetration resistance (PR) is measured to identify the soil compaction in the study area. The critical limit of 2 MPa for root penetration in coarse textured soils has been widely used to characterize the soil physical quality [51]. In this study, the PR values measured in subsurface soils exceeded the critical limit of 2 MPa, and compatected zones can easily be defined in the spatial distribution maps. The PR values in study area were ranged from 0.26 to 1.76 MPa in surface, and increased by soil depth which was between 0.31 and 2.53 MPa in 20-40 cm depth (Fig. 3). Higher PR values in subsurface layers are indications of human-induced compaction, and are the consequences of repeated and/or untimely use of conventional tillage practices. Similar to the findings in this study, Celik et al. [52] reported increased PR values with depth under long term conventional tillage practices.

The surface and sub-surface distribution maps of pH showed that majority of soils in study area is acidic and extremely acidic (ranged from 4.5 to 7.0 and 4.0 to 7.0 in surface and subsurface) on the easth, north-easth and south-eastern of the study area. The pH values were alkaline (ranged from 7.0 to 8.2 and 7.0 to 8.3 in surface and subsurface) in the west, north-west and south-west of the farm (Figure 3). The coarse particle size distibution, leaching of basic cations due to the efficient rains and long-term flood irrigation, and the consumption of fertilizers with ammonium caused to the low pH of soils. The most common and effective practice to ameliorate constraints of soil acidity for optimal crop production is limings [53]. Spatial distribution maps of liming requirement for the study area will increase the efficiency of liming procedure. The owner of the farm has randomly applied lime to increase pH, and manure to increase soil OM content in some part of the study area that can easily be defined in the distribution maps of soil pH. The differences in management within the study area resulted in a variation of soil pH from 4.5 to 8.2 in surface and from 4.0 to 8.3 in subsurface soils (Table 1). The pH values lower than 5.6 may cause nutrient deficiencies and toxicities, decline in activities of beneficial microorganisms, and retard plant root growth which limits absorption of nutrients and water [54]. A soil pH below about 5.6 are considered low for most crops. The effects of soil-forming factors (parent material, time, relief or topography, climate, and organisms) are the major sources of natural soil pH. However, soil pH can be changed overtime by the land use and management. Decline in organic matter due to intensive conventional agriculture, depletion of soil minerals by crops, removal of surface soils by erosion, and continues use of ammonium and sulfur fertilizers cause to decline in soil pH [55]. Acidity of soil in an alluvial plain in was attributed to nature of sediments deposited by the river [56].

Calcium carbonate content of surface and subsurface soils is low in the entire study area. The owner of the farm has applied lime in some fields which have slightly higher calcium carbonate contents compared to the surrounding soils. Positive correlations between pH and calcium carbonate content in surface ($r=0.353$, $P<0.01$) and subsurface ($r=0.262$, $P<0.01$) soils show that pH will increase by application of lime. The similarity in spatial distribution maps of pH and calcium carbonate is accordance with the positive correlations between them. The soil pH is neutral or slightly alkaline in limed fields and acidic in the rest of the study area (Fig. 3). The distribution maps of calcium carbonate and pH may guide to the efficiency of liming in the farmland. Variability in pH and calcium carbonate in the farmland requires variable rates of lime application which will increase the efficiency of reclamation process, lower the cost and labor.

The spatial distribution maps of soil OM, available P and K were given in Figure 4. The soil OM content has direct or indirect effects on most of soil physical (aggregation, stability of aggregates, water retention and water holding capacity, aeration and soil temperature) and chemical (cation exchange capacity, buffering capacity, pH and nutrient retention) [57]. The OM contents of soils in north west and east side of the study area were higher than 1.2% ad reached to 6.82% in some fields (Fig. 4). The soils on the north and south side of the farmland are poor in OM. Long term conventional tillage practices, stubble burning and lack of application of organic amendents are the causes of low OM content. Relatively higher OM content in some fields of farmland is a result of recent application of manure. The results of Acar et al. [58] on low OM content under

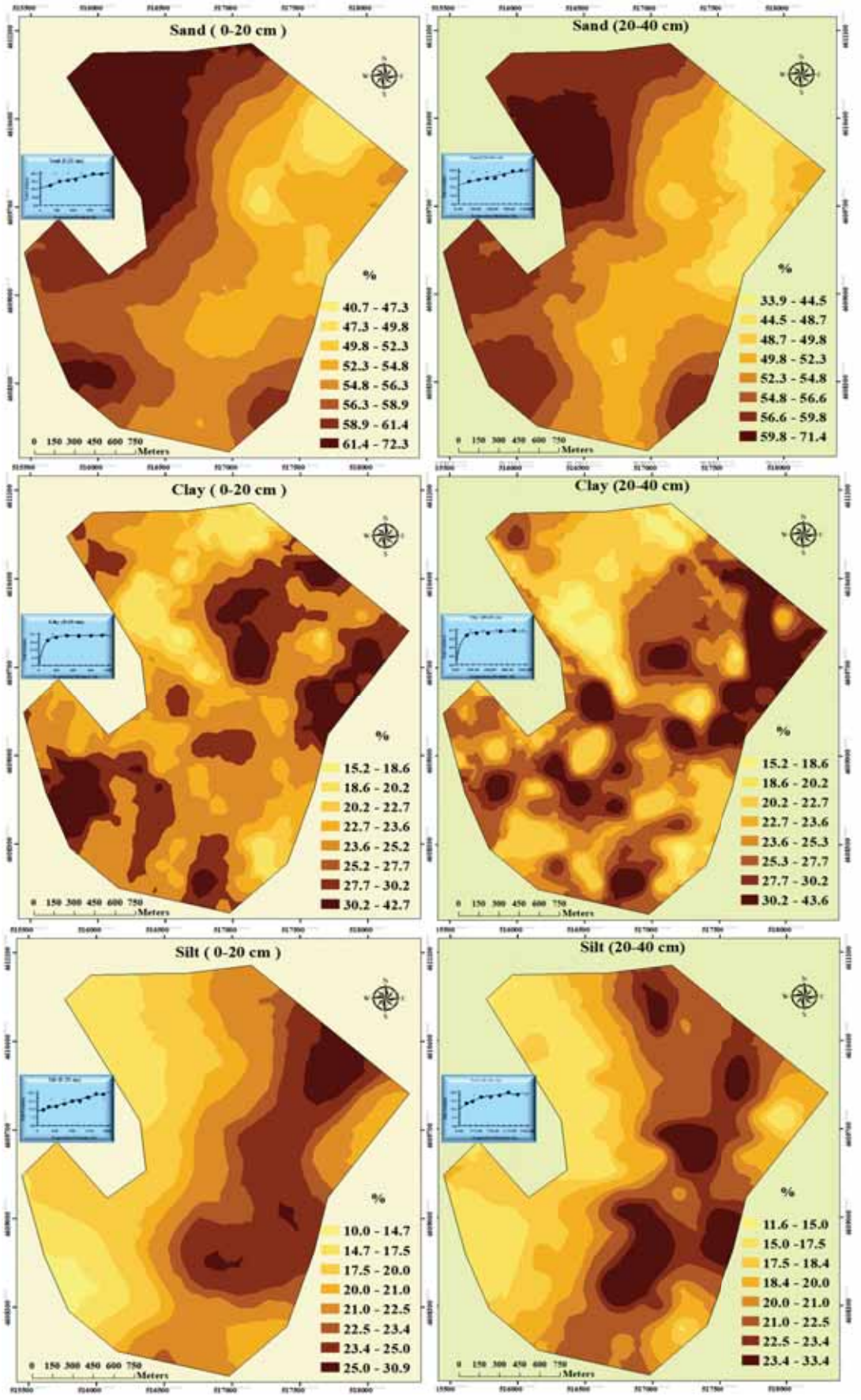

FIGURE 2
Spatial distribution of particle sand, clay and silt contents of soils

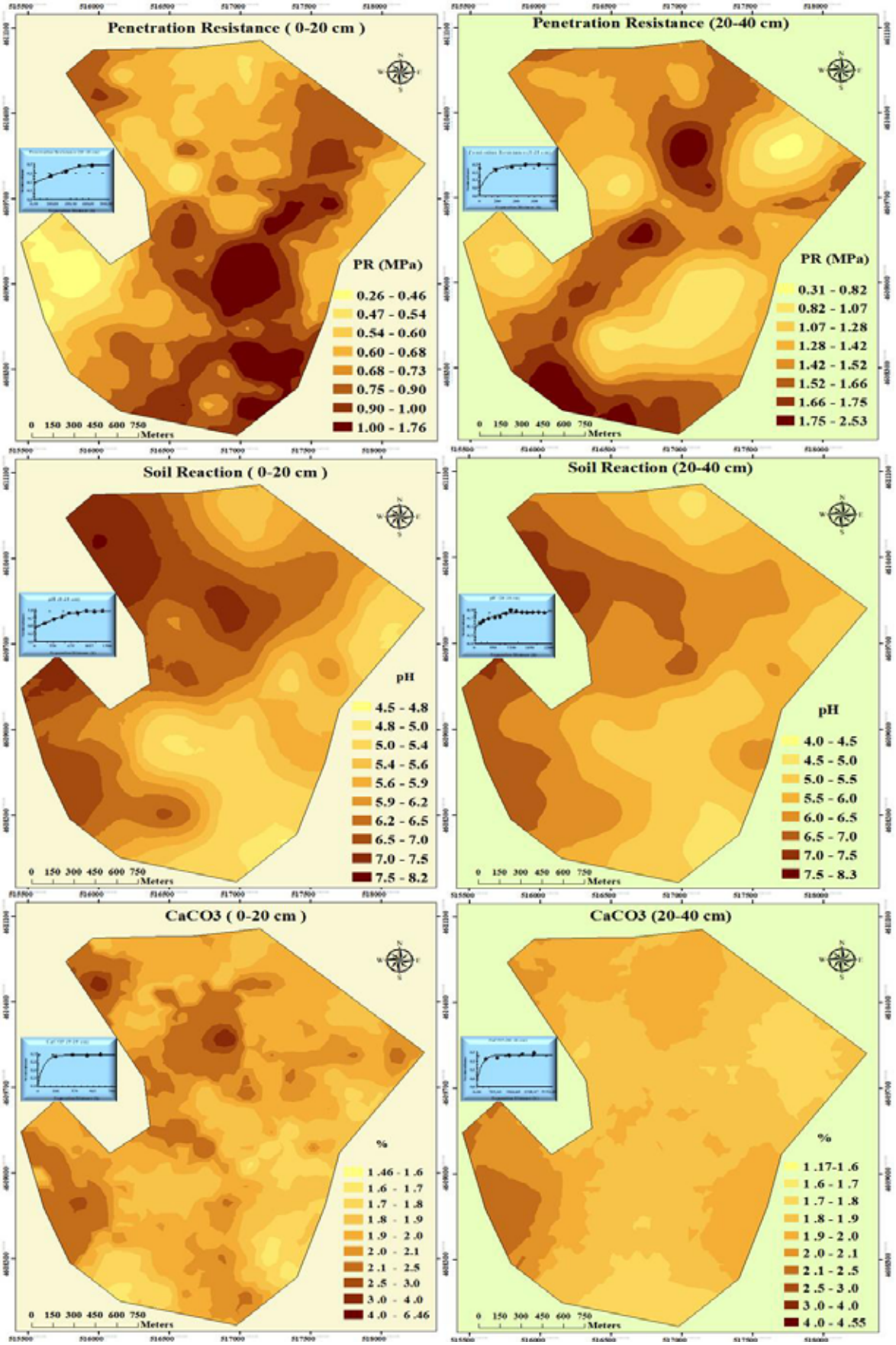

FIGURE 3
Spatial distribution of penetration resistance (PR), pH and calcium carbonate ($CaCO_3$)

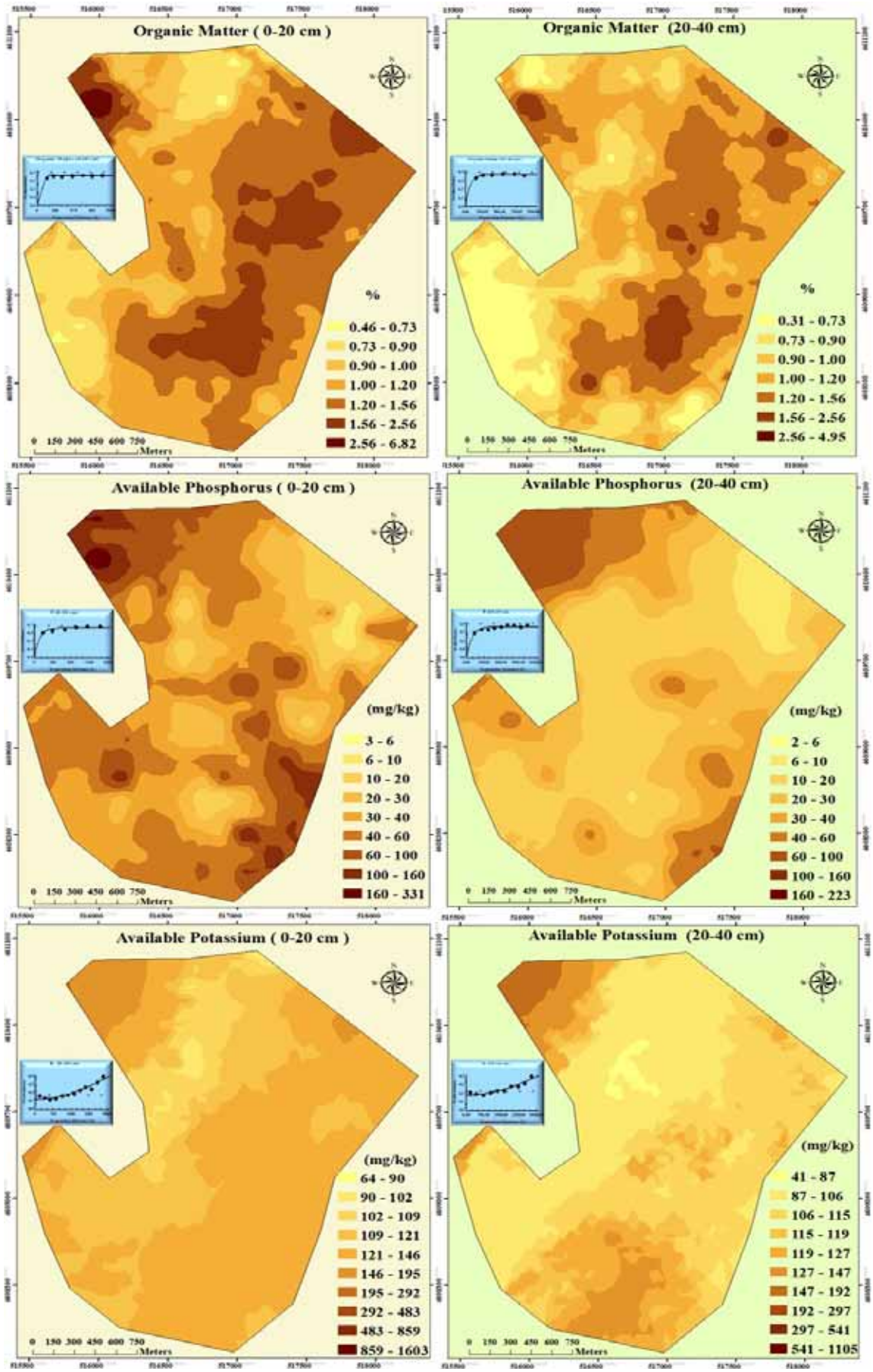

FIGURE 4
Spatial distribution of organic matter, available phosphorus and potassium

long-term conventional tillage practices are in line the finding in this study.

The phosphorus along with nitrogen, is the most limiting and most extensively used nutrient for crop production. Due to the active roles in a plant storing and transfering energy produced by photosynthesis for use in growth and reproductive processes, the P is considered as an essential plant nutrient [59]. The distribution maps for surface and subsurface layers indicates high variability in available P concentrations of soils. The available P content in majority of the farland soils is lower than the threshold value of 10 mg kg^{-1} for an healty crop growth based on criteria set by Horneck et al. [60]. The deficiency of P in the study area under neutral to strongly acidic conditions may be attributed to inherent low P status of parent materials and low organic matter conent of soils. Therefore, distribution map for available P is useful to reveal the P status of a farmland and to plan site specific P fertilization that will optimize the supply of available P over time and space to match the P requirements of crops. The P management based on spatial distribution maps of available P will prevent farmers from extra cost due to the over fertilizer in some areas, and yield reduction due to under fertilizer in some areas or improper balance of nutrients for soil and crop [61]. Irregular application of manure within farmland resulted in strong spatial heterogeneity of soil P content as well as soil OM content.

CONCLUSIONS

In this study, spatial distribution of soil properties was assessed and mapped for land use planning of a farm in Kırıklareli province of Turkey. The results revealed that agricultural practices (application of manure and lime) had significant influence on the spatial variation of soil properties within the study area, and soil organic matter and available phosphorus content in particular had very high spatial variation in short distance. The results also helped to identify and delineate critical zones of nutrient deficiency, acidity and compaction. The available P content of soils was lower than deficiency threshold valus and low concentration of P is attributed to the low organic matter and high sand contents of farmland. The soil pH in the eastern, southeastern and northeastern parts of the study area was acidic that was below the threshold value restricting crop production. Spatial distribution maps of farmland can be used in reclamation of soil compaction, phosphorus deficiency and acidity within the study area. Manure application to improve low organic matter content of soils can efficiently be planned using spatial distribution maps of soil organic matter. Consdering the increased cost of input management in agriculture, land use planning based on spatial distribution of soil properties will increase the efficiency of inputs, correct the problems, sustain the agricultural productivity and increase the profits of farms.

REFERENCES

[1] Tan, K.H., Dowling P.S. (1984) Effect of Organic Matter on CEC Due to Permanent and Variable Charges in Selected Temperate Region Soils Geoderma. 32(2), 89–101

[2] Cambardella, C.A., and Karlen, D.L. (1999) Spatial analysis of soil fertility parameters. Precision Agriculture. 1(1), 5-14.

[3] Trangmar, B.B., Yost, R.S., and Uehara, G. (1986) Application of geostatistics to spatial studies of soil properties. Advances in agronomy. 38, 45-94.

[4] Budak, M., Günal, H., Acir, N., Çelik, İ., Yıldız, H. (2016) Spatial analyses of plant available phosphorus concentration under different management practices. In: VII International Scientific Agriculture Symposium. Agrosym 2016. 6-9 October 2016, Jahorina, Bosnia and Herzegovina. Proceedings. University of East Sarajevo, Faculty of Agriculture. 2205-2210.

[5] Wilding, L.P. (1985) Spatial Variability: its documentation, accommodation, and implication to soil surveys. In: Nielsen, D.R., Bouma, J. (Eds.) Soil Spatial Variability. Pudoc, Wageningen, Netherlands.

[6] Brevik, E.C., Calzolari, C., Miller, B.A., Pereira, P., Kabala, C., Baumgarten, A. and Jordán, A. (2016) Soil mapping, classification, and pedologic modeling: History and future directions. Geoderma. 264, 256-274.

[7] Vasu, D., Singh, S.K., Sahu, N., Tiwary, P., Chandran, P., Duraisami, V.P., and Kalaiselvi, B. (2017) Assessment of spatial variability of soil properties using geospatial techniques for farm level nutrient management. Soil and Tillage Research. 169, 25-34.

[8] Sürücü, A., Günal, H. and Acir, N. (2013) Importance of spatial distribution in reclamation of boron toxic soils from Central Anatolia of Turkey. Fresen. Environ. Bull. 22, 3111-3122.

[9] Budak, M. and Günal, H. (2015) Geostatistical analysis and mapping spatial distribution of boron concentration in saline-alkaline soils. Journal of Ege University Faculty of Agriculture. 52(2), 191-200.

[10] Mali, S.S., Naik, S.K., and Bhatt, B.P. (2016) Spatial Variability in Soil Properties of Mango Orchards in Eastern Plateau and Hill Region of India. Vegetos-An International Journal of Plant Research Vegetos. 29, 3.

[11] Rosemary, F., Indraratne, S.P., Weerasooriya, R. and Mishra, U. (2017) Exploring the spatial variability of soil properties in an Alfisol soil catena. Catena. 150, 53-61.

[12] Paz-Ferreiro, J. and Fu, S. (2016) Biological indices for soil quality evaluation: perspectives and limitations. Land Degradation and Development. 27(1), 14-25.
[13] Perinçek, D., Nurdan, A., Karatut, Ş. and Erensoy, E. (2015) Trakya Havzasinda, Danişmen Formasyonu İçindeki Linyit Katmanlarinin Potansiyelini Kontrol Eden Jeolojik Faktörler. Maden Tetkik ve Arama Dergisi. 150, 79-110.
[14] Gee, G.W., Bauder, J.W. and Klute, A. (1986) Particle Size Analysis, Methods of Soil Analysis. Part 1. Physical and Mineralogical Methods, Soil Since Society of America. Inc., Madison, WIS, USA.
[15] Eijkelkamp (1990) Equipment for soil research. Giesbeek (The Netherlands): Eijkelkamp Corporation.
[16] Hendershot, W.H., Lalande, H. and Duquette, M. (1993) Soil Reaction and Exchangeable Acidity. In: Carter, M.R. (ed.) Soil Sampling and Methods of Analysis. Canadian Society of Soil Science, CRC Pres Inc. Boca Raton, Florida. USA.
[17] Nelson, D.W. and Sommer, L.E. (1982) Total carbon, organic carbon, and organic matter. In: Page, A.L. (ed.) Methods of Soil Analysis. 2nd Ed. ASA Monogr. 9(2). Amer. Soc. Agron. Madison, 539- 579.
[18] Allison, L.E., Bollen, W.B. and Moodie, C.D., (1965) Total Carbon. In: Black, C.A. (Ed.) Methods of Soil Analysis, 2. Am. Soc. of Agronomy, Madison, Wisc., 1346-1366.
[19] Olsen, S.R., Cole, C.V., Watanabe, F.S. and Dean, L.A. (1954) Estimation of available phosphorus in soil by extraction with sodium bicarbonate. USDA Circ., 939. U.S. Cov. Print Office, Washington D.C.
[20] Thomas, G.W. (1982) Exchangeable cations. In: Page, A.L., Miller, R.H., Keeney, D.R. (eds.) Methods of soil analysis. part 2. Chemical and microbiological properties. 2nd edn. ASASSSA No. 9: Madison, Wisconsin, USA; 159–165.
[21] Webster, R. (2001) Statistics to support soil research and their presentation. European Journal of Soil Science. 52, 331-340
[22] Emadi, M., Baghernejad M., Emadi, M., Maftoun M. (2008) Assessment of Some Soil Properties by Spatial Variability in Saline and Sodic Affected Soils in Arsanjan Plain, Fars Province, Southern Iran. Pakistan Journal of Biological Sciences. 11(2), 238-243
[23] Yang, F., Zhang, G., Yin, X. and Liu, Z. (2011) Field-scale spatial variation of saline-sodic soil and its relation with environmental factors in Western Songnen Plain of China. International journal of environmental research and public health. 8(2), 374-387.
[24] ESRI (2014) ArcGIS 10.2.1 https://community.esri.com/thread/87472.
[25] Behera, S.K., and Shukla, A.K. (2015) Spatial distribution of surface soil acidity, electrical conductivity, soil organic carbon content and exchangeable potassium, calcium and magnesium in some cropped acid soils of India. Land Degradation and Development. 26(1), 71-79.
[26] Andrew, J. and Gazey, C. (2010) A preliminary examination of the spatial distribution of acidic soil and required rates of ameliorant in the Avon River Basin, Western Australia. In: Proceedings 2010 World Congress Soil Science Symposium, Brisbane, Australia.
[27] Domínguez, M.T., Alegre, J.M., Madejón, P., Madejón, E., Burgos, P., Cabrera, F., T. Marañón, T. and Murillo, J.M. (2016) River banks and channels as hotspots of soil pollution after large-scale remediation of a river basin. Geoderma. 261, 133-140.
[28] Marques Jr., J., Siqueira, D.S., Camargo, L.A., Teixeira, D.D.B., Barrón, V. and Torrent, J. (2014) Magnetic susceptibility and diffuse reflectance spectroscopy to characterize the spatial variability of soil properties in a Brazilian Haplustalf. Geoderma. 219, 63-71.
[29] Denton, O.A., Aduramigba-Modupe, V.O., Ojo, A.O., Adeoyolanu, O.D., Are, K.S., Adelana, A.O. and Oke, A.O. (2017) Assessment of spatial variability and mapping of soil properties for sustainable agricultural production using geographic information system techniques (GIS). Cogent Food and Agriculture. 3(1), 1279366.
[30] Suarez, D.L. (1995) Carbonate Chemistry in Computer Programs and Application to Soil Chemistry. Soil Science Society of America, American Society of Agronomy. Special Publication, 42, 53-73.
[31] Srinivasan, R., Singh, S.K., Nayak, D.C. and Dharumarajan, S. (2017) Assessment of Soil Properties and Nutrients Status in three Horticultural Land Use System of Coastal Odisha, India. International Journal of Bio-Resource and Stress Management. 8(1), 033-040.
[32] Cambardella, C.A., Moorman, T.B., Parkin, T.B., Karlen, D.L., Novak, J.M., Turco, R.F. and Konopka, A.E. (1994) Field-scale variability of soil properties in central Iowa soils. Soil science society of America journal. 58(5), 1501-1511.
[33] Webster, R. and Oliver, M.A. (2001) Geostatistics for environmental scientists (Statistics in Practice).
[34] Liu, Y., Lv, J., Zhang, B. and Bi, J. (2013) Spatial multi-scale variability of soil nutrients in relation to environmental factors in a typical agricultural region, Eastern China. Science of the Total Environment. 450, 108-119.

[35] Liu, X.M., Xu, J.M., Zhang, M.K., Huang, J.H., Shi, J.C., and Yu, X.F. (2004) Application of geostatistics and GIS technique to characterize spatial variabilities of bioavailable micronutrients in paddy soils. Environmental geology. 46(2), 189-194.

[36] Zhao, Y., Xu, X., Darilek, J.L., Huang, B., Sun, W. and Shi, X. (2009) Spatial variability assessment of soil nutrients in an intense agricultural area, a case study of Rugao County in Yangtze River Delta Region, China. Environmental Geology. 57(5), 1089-1102.

[37] Lv, J., Liu, Y., Zhang, Z. and Dai, J. (2013) Factorial kriging and stepwise regression approach to identify environmental factors influencing spatial multi-scale variability of heavy metals in soils. Journal of hazardous materials. 261, 387-397.

[38] Du, C., Liu, E., Chen, N., Wang, W., Gui, Z. and He, X. (2017) Factorial kriging analysis and pollution evaluation of potentially toxic elements in soils in a phosphorus-rich area, South Central China. Journal of Geochemical Exploration. 175, 138-147.

[39] Zhang, Z., Yu, D., Shi, X., Wang, N. and Zhang, G. (2015) Priority selection rating of sampling density and interpolation method for detecting the spatial variability of soil organic carbon in China. Environmental Earth Sciences. 73(5), 2287-2297.

[40] Iqbal, J., Thomasson, J.A., Jenkins, J.N., Owens, P.R., Whisler, F. D. (2005) Spatial Variability Analysis of Soil Physical Properties of Alluvial. Soil Sci. Soc. Am. J. 69, 1338-1350.

[41] Roger, A., Libohova, Z., Rossier, N., Joost, S., Maltas, A., Frossard, E. and Sinaj, S. (2014) Spatial variability of soil phosphorus in the Fribourg canton, Switzerland. Geoderma. 217, 26-36.

[42] Kavianpoor, H., Ouri A.E., Jeloudar Z.J., Kavian, A. (2012) Spatial Variability of Some Chemical and Physical Soil Properties in Nesho Mountainous Rangelands American Journal of Environmental Engineering. 2(1), 34-44.

[43] O'Halloran, I.P., Kachanoski, R.G., and Stewart, J.W.B. (1985) Spatial variability of soil phosphorus as influenced by soil texture and management. Canadian journal of soil science. 65(3), 475-487.

[44] Dey, P., Karwariya, S. and Bhogal, N.S. (2017) Spatial Variability Analysis of Soil Properties Using Geospatial Technique in Katni District of Madhya Pradesh, India. International Journal of Plant and Soil Science. 17(3), 1-13.

[45] Dexter, A.R. (2004) Soil physical quality: Part I. Theory, effects of soil texture, density, and organic matter, and effects on root growth. Geoderma. 120(3-4), 201-214.

[46] Plante, A.F., Conant, R.T., Stewart, C.E., Paustian, K. and Six, J. (2006) Impact of soil texture on the distribution of soil organic matter in physical and chemical fractions. Soil Science Society of America Journal. 70(1), 287-296.

[47] Ali, S., Hayat, R., Begum, F., Bohannan, B. J. M., Inebert, L. and Meyer, K. (2017) Variation in Soil Physical, Chemical and Microbial Parameters under Different Land uses in Bagrot Valley, Gilgit, Pakistan. Journal of the Chemical Society of Pakistan. 39(1). 97-104

[48] Turgut, B. and Öztaş, T. (2012) Assessment of Spatial Distribution of Some Soil Properties with Geostatistics Method. Suleyman Demirel Üniversitesi Ziraat Faküttesi Dergisi. 7(2), 10-22.

[49] Korucu, T., Arslan, S., Günal, H. and Şahin, M. (2009) Spatial and temporal variation of soil moisture content and penetration resistance as affected by post harvest period and stubble burning of wheat. Fresen. Environ. Bull. 18, 1736-1747.

[50] Bayat, H., Sheklabadi, M., Moradhaseli, M. and Ebrahimi, E. (2017) Effects of slope aspect, grazing, and sampling position on the soil penetration resistance curve. Geoderma. 303, 150-164.

[51] de Lima, C.L.R., Miola, E.C.C., Timm, L.C., Pauletto, E.A. and da Silva, A.P. (2012) Soil compressibility and least limiting water range of a constructed soil under cover crops after coal mining in Southern Brazil. Soil and Tillage Research. 124, 190-195.

[52] Celik, I., Günal, H., Acar, M., Gök, M., Barut, Z.B. and Pamiralan, H. (2017) Long-term tillage and residue management effect on soil compaction and nitrate leaching in a Typic Haploxerert soil. International Journal of Plant Production. 11(1), 131-150.

[53] Fageria, N.K. and Baligar, V.C. (2008) Ameliorating soil acidity of tropical Oxisols by liming for sustainable crop production. Advances in agronomy. 99, 345-399.

[54] Fageria, N.K., Baligar, V.C. (2003) Fertility management of tropical acid soils for sustainable crop production. In: Rengel, Z. (Ed.) Handbook of soil acidity. Marcel Dekker, New York. 359–385.

[55] NRCS (2011) Soil Quality Indicators: soil pH. In: Soil Quality Indicator Sheets, Chemical Indicators. USDA Natural Resources Conservation Service. Washington, USA.

[56] Kumari A. (2014) Encyclopedia of Bihar. New Delhi: Prabhat Books Publisher.

[57] Tan, X., Guo, P.T., Wu, W., Li, M.F., and Liu, H.B. (2017) Prediction of soil properties by using geographically weighted regression at a regional scale. Soil Research. 55(4), 318-331.

[58] Acar, M., Celik, I. and Günal, H. (2018) Effects of long-term tillage systems on aggregate-associated organic carbon in the eastern Mediterranean region of Turkey. Eurasian Journal of Soil Science. 7(1), 51-58.
[59] NRCS (2014) Soil Phosphorus. Soil Health-Guides for Educators. USDA Natural Resources Conservation Service. Washington, USA.
[60] Horneck, D.A., Sullivan, D.M., Owen, J.S., and Hart, J.M. (2011) Soil test interpretation guide. Corvallis, Or.: Oregon State University, Extension Service.
[61] Richards, M.B., Butterbach-Bahl, K., Jat, M.L., Lipinski, B., Ortiz-Monasterio, I., Sapkota, T. (2015) Site-Specific Nutrient Management: Implementation guidance for policymakers and investors. Copenhagen, Denmark: CGIAR Research Program on Climate Change, Agriculture and Food Security (CCAFS).

Received: **23.02.2018**
Accepted: **15.04.2018**

CORRESPONDING AUTHOR

Mesut Budak
Siirt University
Faculty of Agriculture,
Department of Soil Science and Plant Nutrition,
Siirt – Turkey

e-mail: m.budak@siirt.edu.tr

© by PSP Volume 27 – No. 7/2018 pages 5066-5071 Fresenius Environmental Bulletin

JUNGLE RICE (*ECHINOCHLOA COLONUM* (L.) LINK) CONTROL WITH SOME BAND AND BROADCAST SPRAY APPLICATION METHODS

Ali Bolat[1,*], Ozcan Tetik[2], Ali Bayat[3], Ugur Sevilmis[1]

[1]Eastern Mediterranean Agricultural Research Institute, Adana, Turkey
[2]Biological Control Research Institute, Adana, Turkey
[3]Çukurova University, Dept. of Agricultural Machinery Adana, Turkey

ABSTRACT

Novel spray Jungle rice (*Echinochloa colonum* (L.) Link) is a common weed species in maize cultivation. High yield losses occur if fight with this weed is not achieved. In this research, sprayings with were conducted with two broadcast application types (Standard XR spraying nozzle, Air induction nozzles) and three band application types (Even Flat Fan nozzles, Under Leaf Banding Application and Row Application Kit method) in total five different methods. Comparisons were made under 3 different aplication volumes (200, 300 ve 400 l.ha^{-1}) with a post-emergence herbicide. During the maize growing season, Jungle rice counts were done during different stages of maize before and after sprayings. All methods and volumes resulted with reductions in Jungle rice numbers compared to control. This reduction was highest at 400 l.ha^{-1} application volume. The most appropirate method to control Jungle rice during early critical growth stage of maize was Row Application Kit method (band application) at 400 l.ha^{-1} application volume.

KEYWORDS:
Jungle rice (Echinochloa colonum *(L.) Link),* Band application, Broadcast application, Spraying nozzle

INTRODUCTION

Maize is the third cultivated cereal in the world with estimated total 875 million tons production [1]. In 2016, in Turkey, a total area of 0.68 million ha of maize acreaches cultivated and 6.4 million t/ha grain produced [2]. One of the most important factors which affect maize yields and product quality is the population of weeds in fields, which compete especially for space, light and other inputs with crop. Weeds hosts pests and diseases and cause damage to crops with their secretions [3]. In Cukurova plain in the Mediterranean Region of Turkey, 18 weed species is common in maize cultivation areas and Jungle rice *(Echinochloa colonum* (L.) Link) is one of the most harmful one [4]. According to [5], weeds constitute the most important harmful group for maize plants and can cause up to a 37% potential loss in yields. To overcome this problem, farmers prefer to use chemical control methods for their high success rates, easiness to implement, low labour costs and high profitability compared to other weed fight methods. Pre-sowing and pre-emergent herbicides are common to fight weeds but are needed if weed population is at economic damage levels [6]. Common post emergence herbicides to fight weeds in maize are nicosulfuron, rimsulfuron or foramsulfuron from group sulphonilure [7]. Foramsulfuron, is a systemic herbicide used to fight weeds in maize cultivation. Foramsulfuron is used in Jungle rice weed fight in maize at 2-6 leaf stage of weeds. Foramsulfuron usage in maize has increased in last years [8]. Foramsulfuron registered at an application rate of 35 g ai.ha^{-1} up to the eight-leaf stage of maize [9]. Herbicides should be applied at the right time, minimum dose and with an appropriate spraying technique for chemical fight of weeds [10]. [11] found that, 98% of the producers use domestic conic spray nozzles for herbicides applications in Turkey. However, the proportion of small droplets (<100 µm) produced by these nozzles is high and therefore preferred for insecticide applications [12]. According to [13], droplets smaller than 100 µm drift off the target, while droplets smaller than 50 µm totally evaporate without reaching the target. To reduce fuel costs by reducing transportation of water, spraying technology has evolved toward lower carrier volumes [14]. To reduce drift potential of these sprayers, many farmers use drift-reducing nozzles. Air induction (AI) nozzles produce larger droplets, which drift less compared to extended range (XR) nozzles [15]. According to [16], smaller droplets produced by XR nozzles were more effective than larger droplets for postemergence herbicide applications. [17] informed that, better control was obtained for velvetleaf (Abutilon theophrasti Medik.) and common lambsquarters (*Chenopodium album* L.) when application volume was increased at AI and XR nozzles. According to [18], different type of nozzles and carrier volumes result with varying levels of control for different weed species.

Air indution nozzles suck air and liquid in, mix each other and spray out droplets containing air bubbles out of the nozzle. Thus, by this method, larger diameter droplets are produced and drift off of droplets occur less frequently [19]. In band spraying method, one nozzle (Even Flat Nozzle-EFN) may be used for each band. Another method is to spray each band with multiple nozzles -Under Leaf Banding Application (UBN) and Row Application Kit (RAK). These methods distribute herbicides with better coverage rates on bands [20]. Application volume is another important factor affecting the success of sprayings. High application volume results with high herbicide usage and economic loss [21]. It is important to determine the performance of different application volumes with different methods.

The aim of this research is to determine the effect of some broadcast and band weed spraying methods to control Jungle rice at different application volumes (200, 300 and 400 $l.ha^{-1}$) in maize cultivation.

MATERIALS AND METHODS

Field trials of the research were conducted in 2013 and 2014 years in Eastern Mediterranean Agricultural Research Institute, Turkey. Five different herbicide spraying methods were tested. Tested methods were: (1) Standard XR spraying nozzle (XRN: XR11003), (2) Air induction nozzles (AIN: IDN120025), (3) Even Flat fan nozzles (EFN: TP4002E), (4) Air induction nozzles with under leaf banding application (UBN: AIUB8502) and (5) Row application kit (RAK: XR8002). Applications was carried out with modified boom sprayer with 800 litter tank capacity. Nozzles spacings in broadcast applications (XRN and AIN) were 50 cm, while in band applications (EFN, UBN and RAK) were 70 cm. In RAK method one of three nozzles was located on top to spray upper canopy of plants and other two located on right and left sides of plants with 45º angle. UBN contained 2 nozzles for one band and EFN contained one nozzle on one band. By this way all plant canopy has been sprayed. Spray parameters, application methodology and application conditions for the methods used in the investigation are given in Table 1. To make a sense of drift potential and droplet uniformity of sprayings, characteristic droplet diameters such as $Dv_{0.5}$ of nozzles were measured under laboratory conditions by using a laser measurement device (Malvern Spraytec -Open Spray). Droplet size distribution of all nozzle types were determined under same pressure (2 bar) during 60 second periods. Nozzle flow rates given in Table 1 was measured three times and liquid produced by each nozzle was determined in one minute time period. Tractor speed was calculated in relation with target liquid volumes. Spraying volumes were diversified to 200, 300 and 400 $l.ha^{-1}$ for each method.

The wind speed, temperature and relative humidity measurements were carried out with a digital anemometer (Lechler pocket wind IV) during sprayings (Table 2).

TABLE 1
The spraying methods and sprayer operating parameters

Methods	Application Volume ($l.ha^{-1}$)	Pressure (bar)	Application Methodology	Flow Rate ($l.min^{-1}$)	Nozzle Spacings (cm)	$Dv_{0.5}$ (µm)*
	200	2				
XRN	300	2	Broadcast	0.92	50	186.5
	400	2				
	200	2				
AIN	300	2	Broadcast	0.95	50	451.2
	400	2				
	200	2				
EFN	300	2	Band	0.76	70	149.4
	400	2				
	200	2				
UBN	300	2	Band	1.45	70	428.5
	400	2				
	200	2				
RAK	300	2	Band	1.57	70	188.6
	400	2				

*$Dv_{0.5}$: Volume median diameter (%50 of the volume)

TABLE 2
Meteorological conditions measured during applications

Methods	2013			2014		
	Temperature (°C)	Humidity	Wind Speed ($m.sn^{-1}$)	Temperature (°C)	Humidity	Wind Speed ($m.sn^{-1}$)
XRN	36.7	61.4	1.4	35.2	63.2	1.4
AIN	34.8	62.9	1.3	35.8	65.1	1.5
EFN	37.5	58.9	1.4	34.0	59.7	1.3
UBN	33.8	60.4	1.1	36.7	60.4	1.1
RAK	36.0	61.0	1.2	33.5	61.4	1.5

TABLE 3
Dates and periods of weed counts

Counts	Phenological Stage	Growth Stage (**BBCH scale)	Count Dates	
			2013	2014
0 DAT*	Before herbicide application	15	03.07.2013	15.07.2014
15 DAT	20-30 days after herbicide application	53	25.07.2013	07.08.2014

*DAT: Days after herbicide application
** BBCH scale is a system for a uniform coding of phenologically similar growth stages of all mono- and dicotyledonous plant species

TABLE 4
Herbicide control efficiency rates of each methods on Jungle rice

Methods	Control Efficiency (%)					
	200 $l.ha^{-1}$		300 $l.ha^{-1}$		400 $l.ha^{-1}$	
	2013	2014	2013	2014	2013	2014
XRN	47.7 b	48.9 a	62.2 ab	66.6 a	77.1 b	83.7 ab
AIN	41.3 b	46.7 ab	60.2 a-c	63.5 ab	63.8 c	72.0 bc
EFN	45.6 b	40.2 ab	53.1 bc	51.6 b	67.3 c	68.9 c
UBN	30.4 c	32.0 b	47.6 c	52.0 b	64.3 c	75.0 a-c
RAK	55.6 a	53.7 a	72.4 a	71.8 a	86.1 a	86.9 a
Lsd	7.2**	15.7 *	13.2*	13.8*	8.1**	14.4*

**: the values shown with the same letters on a vertical column are not significant in the level of $p<0.01$
* : the values shown with the same letters on a vertical column are not significant in the level of $p<0.05$

Average wind speed was in appropriate range for sprayings during field tests. The average air temperatures during second crop maize cropping season in Turkey is at high level and to overcome this problem, sprayings was done early in the morning.

Each parcel was 28 m^2 (10mx2.8m) and a block contained 6 parcels. Each application volume tested in 6 blocks and 24 parcels in total 12 blocks and 72 parcels. 5 meters spacings left between blocks and 3 meters spacings left between parcels to secure applications from superposition. Each block contained one control (no chemical containment) parcel.

To evaluate the performance of the spraying methods, weeds were counted in wooden frames located on 8 different points on middle 2 rows in each parcel and weed control efficiencies calculated. Each frame covered 0.15 m^2 (0.3mX 0.5m) and weed counted total surface area was 1.2 m^2. In the scope of the study, the reference count points were recorded by counting the number of Jungle rice which exists into the counting frames.

Jungle rice counts in the experiment area were carried out on 2 different phenological growth stages (BBCH Scale Number) of maize plant [22]. Dates and periods of weed counts for control efficiencies are given in Table 3.

A registered brand (Ekipp Super WG61) containing foramsulfuron was used to determine the weed control efficiency of each method used in the study. The indicated herbicide was used at the recommended dose (150 $g.ha^{-1}$ granule and 2000 $ml.ha^{-1}$ Mero). To determine percent efficiency, application parcels were compared with control parcels and calculations were made via "Abbott" formula (Equation 1).

$$E(\%)=(WNC-WNAP)/WNC*100 \quad (1)$$

Where; E: Efficiency (%), WNC: Weed number in control, WNAP: Weed number in application parcels.

Statistic program JUMP 5.0 has been used to

analyze results. Analysis was done based on randomized complete block design and averages of significant factors compared via LSD tests.

RESULTS AND DISCUSSION

The number of *E. colonum* was determined over economic damage threshold in the trial area during spraying periods. Different application methods and volumes resulted with different control efficiency rates on Jungle rice (Table 4).

Under 200 l.ha^{-1} application volume, control efficiencies ranged between 30.4-55.6% in year 2013 and 32.0-53.7% in year 2014. RAK method produced highest control efficiency rates in year 2013 whereas all methods except UBN were similar in 2014 trials for 200 l.ha^{-1} application volume. Under 300 l.ha^{-1} application volume, control efficiencies ranged between 47.6-72.4 % in year 2013 and 51.6-71.8 % in year 2014. XRN, AIN and RAK produced better results compared to EFN and UBN both in year 2013 and 2014 under 300 l.ha^{-1} . Under 400 l.ha^{-1} application volume control efficiencies ranged between 63.8-86.1% in year 2013 and 68.9-86.9% in year 2014. Highest control efficiency rate was obtained by RAK method in year 2013 and by XRN, UBN and RAK in 2014 trials under 400 l.ha^{-1}. Weed average counts were made under all application volumes. Weed average counts under 200 l.ha^{-1} application volume with different methods are given in Fig. 1.

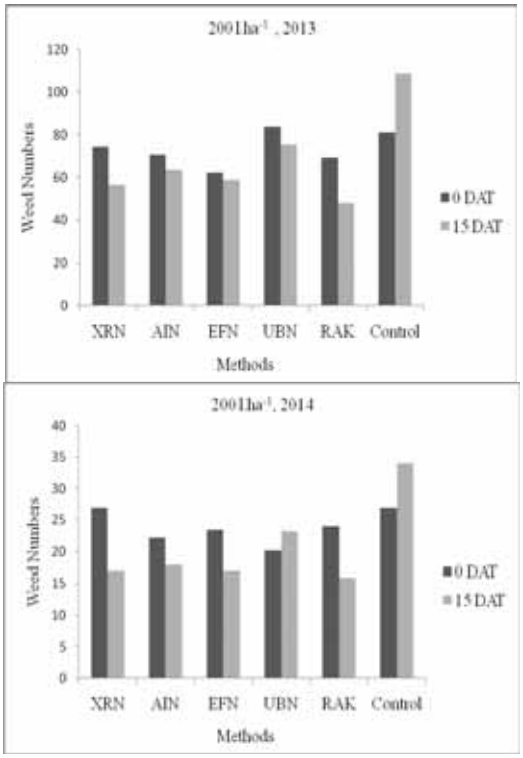

FIGURE 1
Jungle rice counts under 200 l.ha^{-1} application volume in 2013 and 2014

There is an increase in the number of weeds in control parcels in year 2013 whereas weed numbers reduced by applications where reduction is highest by RAK method (30.5%) and followed by XRN (standard) method (23.8%) during the period starting from 0 DAT to 15 DAT. In year 2014, number of weeds increased both in control and UBN application parcels. Highest weed number reduction occurred with XRN method (37.0%) and followed by RAK method (33.3%) in 2014. Weed average counts under 300 l.ha^{-1} application volume with different methods are given in Fig. 2.

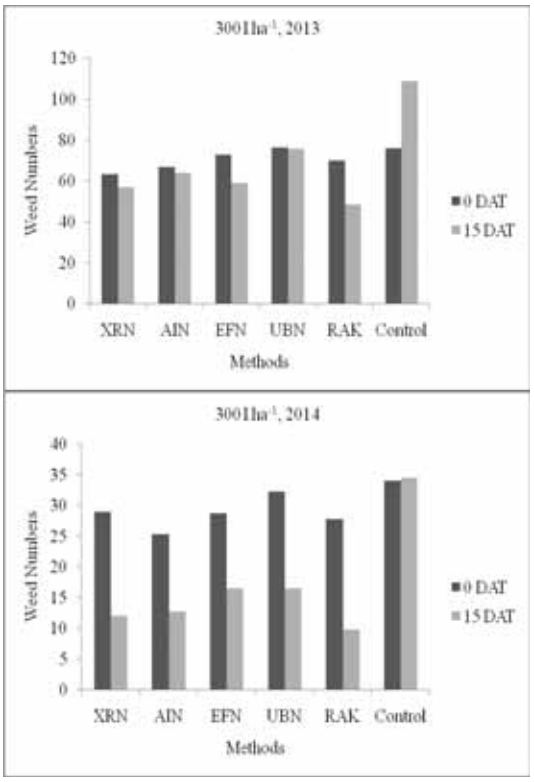

FIGURE 2
Jungle rice counts under 300 l.ha^{-1} application volume in 2013 and 2014

When 300 l.ha^{-1} applications analyzed, weed numbers reduced by all applications where reduction is highest at RAK method (31.1%) and lowest at UBN method (0.9%) in year 2013. In year 2014, highest weed number reduction occurred with RAK method (64.9%) which is followed by XRN method (58.6%).

After analysing 400 l.ha^{-1} application volume, there is an increase in the number of weeds in control parcels in both years (Fig. 3).

In 2013, weed numbers reduced by applications where reduction is highest at RAK method (52.4%) and followed by AIN method (47.3%) during the period starting from 0 DAT to 15 DAT. In year 2014 highest weed number reduction occurred with RAK method (85.1%) and followed by XRN method (84.4%) in 2014. RAK method which is containing 3 nozzles targeted to band surface has

advantages to XRN method despite both contains same types of nozzles. The source of this effect is high efficiency of this application method.

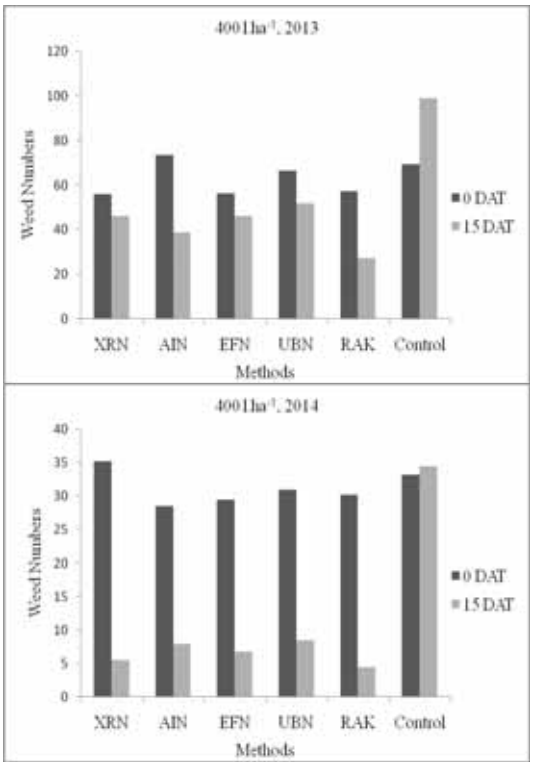

FIGURE 3
Jungle rice counts under 400 l l.ha^{-1} application volume in 2013 and 2014

CONCLUSION

Our results indicate that RAK and UBN multiple band application methods were superior to other methods including one band and two broadcast application methods. Similar to our study, [23] found that banding was as effective as broadcast application where different bandwidths with even flat fan nozzles gave similar weed control and maize yield.

According to [17], the control of Echinochloa crus-galli (barnyardgrass) was improved when herbicide was applied with flat fan nozzles compared with air induction nozzles. Also [18] indicated that flat fan nozzles, compared to air induction (AI) nozzles, provided better control of crus-galli E. with nicosulfuron. Similar results were obtained from our study.

[24] found that, post-emergence herbicides (2,4-D and Lactofen) application efficacy increased with higher application volumes. Increased application volume in our study was also more effective in the fight of Jungle rice in all methods. This reduction level was highest at 400 l.ha-1 application volume.

ACKNOWLEDGEMENTS

This research was funded by General Directorate of Agricultural Research and Policies (TAGEM) as TAGEM-BS-12/12-03/03-01 project number. The authors thank to TAGEM for their contribution to the project.

REFERENCES

[1] FAOSTAT Production Cited. (2014) http://faostat.fao.org/site/567/DesktopDefault.aspx?PageID=567#ancor.
[2] Turkish Statistical Database (2016) https://biruni.tuik.gov.tr/bitkiselapp/bitkisel.zul
[3] Freud-Williams, R.J. (2002) Weed Competition. In: Naylor, R.E.L. (ed.) Weed Management Handbook: 9th Editions. Blackwells. 16-38.
[4] Hancerli, L., Uygur, F.N. (2017) Weed Species Infesting Corn Growing Areas In Çukurova Region. Turkish Journal of Weed Science. 20(2), 55-60 (In Turkish).
[5] Oerke, E.C., Dehne, H.W. (2004) Safeguarding production—losses in major crops and the role of crop protection. Crop Prot. 23, 275–285.
[6] Hurle, K. (1996) Weed management impact on the abiotic environment in particular on water and air quality. In: Proceedings of the Second International Weed Control Congress. 1153-1158, Copenhagen.
[7] Hartzler, D.B. (2002) Post emergence options for grass control in corn. Department of Agronomy, Iowa State University.
[8] Kir, K., Dogan, M.N. (2010) Influence of Different Treatment Timing on the Efficacy of Foramsulfuron. Journal of Adnan Menderes University Agricultural Faculty. 7(2), 57-64.
[9] OMAF (2004) Guide to weed control, Publication 75. Toronto, ON. 109-147.
[10] Kudsk, P. and Streibig, J.C. (2003) Herbicides a two edged sword. Weed Res. 43(2), 90-102.
[11] Gungor, M., Uygur, F.N. (2005) The importance and possible problems of chemıcal control of weeds in Adana province corn fields. Master Thesis. Cukurova University, Adana, Turkey.
[12] Bayat, A (1998) Yeni Geliştirilmiş Bazı Memelerin Damla Spektrumu ve Drift Potansiyeli. Çukurova Üniversitesi Ziraat Fakültesi Tarım Makinaları Bölümü Semineri. Seminer No. 98/16.
[13] Zhu, H., Reichard, D.L., Fox, R.D., Brazee, R.D., Ozkan, H.E. (1994) Simulations of Drift of Discrete Size of Water Droplet from Field Sprayers. T. ASAE. 37(5), 1401-1407.

[14] Etheridge, R.E., Womac, A.R., Mueller, T.C. (1999) Characterization of the spray droplet spectra and patterns of four venturi-type drift reduction nozzles. Weed Technol. 13(4), 765-770.
[15] Ellis, M.B., Swan, T., Miller, P.C.H., Waddelow, S., Bradley, A., Tuck, C.R. (2002) PM—Power and Machinery: Design Factors Affecting Spray Characteristics and Drift Performance of Air Induction Nozzles. Biosyst. Eng. 82(3), 289-296.
[16] Knoche, M. (1994) Effect of droplet size and carrier volume on performance of foliage-applied herbicides. Crop Prot. 13(3), 163-178.
[17] Sikkema, P.H., Brown, L., Shropshire, C., Spieser, H., Soltani, N. (2008) Flat fan and air induction nozzles affect soybean herbicide efficacy. Weed Biol. Manag. 8(1), 31-38.
[18] Brown, L., Soltani, N., Shropshire, C., Spieser, H., Sikkema, P.H. (2007) Efficacy of Four Corn (Zea mays L.) Herbicides When Applied with Flat Fan and Air Induction Nozzles. Weed Biol. Manag. 7(1), 55-61.
[19] Bayat, A., Bolat, A., Soysal, A., Gullu, M., Sarihan, H. (2010) Efficiency of Different Spray Application Methods in Second Crop Maize. 23RD Annual Conference on Liquid Atomization and Spray Systems, Brno, Czech Republic, September 2010.
[20] Grisso, R., H.E. Ozkan, V. Hofman, A. Womac, R. Wolf, W.C. Hoffman, J. Williford, T. Walco. (2000). Pesticide application equipment. In: Conservation Tillage Systems and Management, 2nd Edition, Chapter 29, Mid-West Plan Service, Ames, IA, pp.235-249.".
[21] Guler, H., Urkan, E., Tozan, M., Tekin, B., Caner, O. (2010) Tarımsal Savaşım Mekanizasyonunda Teknolojik Gelişmeler. http://www.zmo.org.tr/resimler/ekler/3f445b0ff5a783e_ek.pdf.
[22] Anonymous (2001) Growth stages of mono- and dicotyledonous plants (BBCH Monograph). Edited by Uwe Meier. Federal Biological Research Centre for Agriculture and Forestry.
[23] Uremis, I., Bayat, A., Uludag, A., Bozdogan, N., Aksoy, E., Soysal, A., Gonen, O. (2004) Studies on different herbicide application methods in second-crop maize fields. Crop Protection. 23(11), 1137-1144.
[24] Creech, C.F., Henry, R.S., Werle, R., Sandell, L.D., Hewitt, A.J., Kruger, G.R. (2015) Performance of post-emergence herbicides applied at different carrier volume rates. Weed technology. 29(3), 611-624.

Received: **27.02.2018**
Accepted: **26.04.2018**

CORRESPONDING AUTHOR

Ali Bolat
Eastern Mediterranean Agricultural Research Institute,
Adana – Turkey

e-mail: bolat.ali@tarim.gov.tr

© by PSP Volume 27 – No. 7/2018 pages 5072-5077 Fresenius Environmental Bulletin

A POPULATION FLUCTUATION AND DAMAGE RATES OF *CERATITIS CAPITATA* (DIPTERA: TEPHRITIDAE) ON PERSIMMON FRUITS IN TURKEY

Gamze Kilic, Nihat Demirel*

Mustafa Kemal University, Faculty of Agriculture, Department of Plant Protection, 31034 Hatay, Turkey

ABSTRACT

The Mediterranean fruit fly (Medfly), *Ceratitis capitata* (Wiedemann) (Diptera: Tephritidae), is a serious pest on persimmon fruits in Turkey. The study was conducted in 2013-2014 to evaluate population fluctuation and damage rates of *C. capitata* on persimmon fruits in Hatay province of Turkey. The eostrap® invaginada traps baited with % 95 trimedlure impregnated in a polymeric plug-type dispenser were used. After two years of the study, the mean of catches, percentages of male and female and damage ratio of *C. capitata* varied in the sampling period and orchard. In 2013, the largest mean of catches per trap were recorded on 4 August in Belen and 25 August in Harbiye districts. The percentages of male per trap with 78.69 in Belen and 91.35 in Harbiye districts were higher than females with 21.31 in Belen and 8.65 in Harbiye districts. In 2014, the largest mean of catches per trap were recorded on 10 August in Belen and 17 August in Harbiye districts. The percentages of male per trap with 84.62 in Belen and 67.47 in Harbiye districts were higher than females with 15.38 in Belen and 32.53 in Harbiye districts. The percentages of damage ratio of *C. capitata* varied in each of the sampled orchard in both years. In 2013, the highest damage ratio of this pest was observed at the Belen IX orchard with 10.08 percent. In 2014, the highest damage ratio of *C. capitata* was observed at the Harbiye III orchard with 7.01 percent. In conclusion, the largest mean catches and percentages of male and female per trap were significantly high in August in both years and the percentages of damage ratio of this pest increased ripening and harvesting time of persimmon fruits in Hatay province of Turkey.

KEYWORDS:
Medfly, trimedlure, traps, persimmon, Turkey.

INTRODUCTION

Persimmon, *Diospyros* (Ebaneceae: Ebenales), is an important tropical and subtropical tree [1], widespread in Turkey where it comprise approximately 2.302 ha with a total produce of 34.650 tons of fruit per annum, and Hatay province's share is 207,4 ha and 3.249 tons [2]. The Mediterranean fruit fly (Medfly), *Ceratitis capitata* (Wiedemann) (Diptera: Tephritidae), is one of the most important fruit pests throughout the world [3, 4]. The Medfly is a polyphagous tropical fruit fly which attacks more than three hundred and fifty botanical species from sixty five different families [5, 6]. The females puncture the fruits and lay eggs below the skin of the host fruits, which are destroyed by larval feeding [3, 7, 8, 9]. This pest causes significant damages on persimmon fruits in Turkey [8]. Insecticidal protection from medfly is possible by using a cover spray or a bait spray [10]. Protein bait sprays mixed with organophosphates (phosmet, malathion) or low toxicity insecticides (spinosad, lambda-cyhalothrin) are successfully used as area-wide to control *C. capitata* populations [11, 12]. Traps baited with trimedlure and attractants are important tools for detection, monitoring and controlling of the Medfly [12, 13, 14, 15]. The purpose of the current study was to evaluate population fluctuation and damage rates of *C. capitata* on persimmon fruits in Hatay province of Turkey.

MATERIALS AND METHODS

The study was conducted in 2013-2014 at thirty one persimmon orchards in Belen and Harbiye (Defne) districts of Hatay province in Turkey. In the first year, the study was carried out seventeen persimmon orchards, in which eleven of them located in Belen district and six of them Harbiye district (Table 1). In the second year, the study was conducted fourteen persimmon orchards, in which nine of them located in Belen district and five of them Harbiye district. In both year, the study was carried out using the Eostrap® invaginada traps (Sanidad Agricola Econex, Santomera, Murcia, Spain) baited with % 95 Trimedlure, (formulated in a polymeric plug-type dispenser) (Sanidad Agricola Econex, Santomera, Murcia, Spain) and dichlorvos or 2.2- dichlorovinyl dimethyl phosphate (DDVP) tablet (Sanidad Agricola Econex, Santomera, Murcia, Spain). The traps

TABLE 1
The investigated districts, number of traps used, dates of installation of the traps, dates of changing the baits, and dates of removal the traps in 2013-2014.

District of Hatay province	Number of traps (sites)		Dates of installation of the traps		Dates of changing the baits		Dates of removal of the traps	
	2013	2014	2013	2014	2013	2014	2013	2014
Belen	11	9	29 June	03 August	29 September	No changing	10 November	09 November
Harbiye	6	5	29 June	03 August	29 September	No changing	10 November	09 November
Total	17	14						

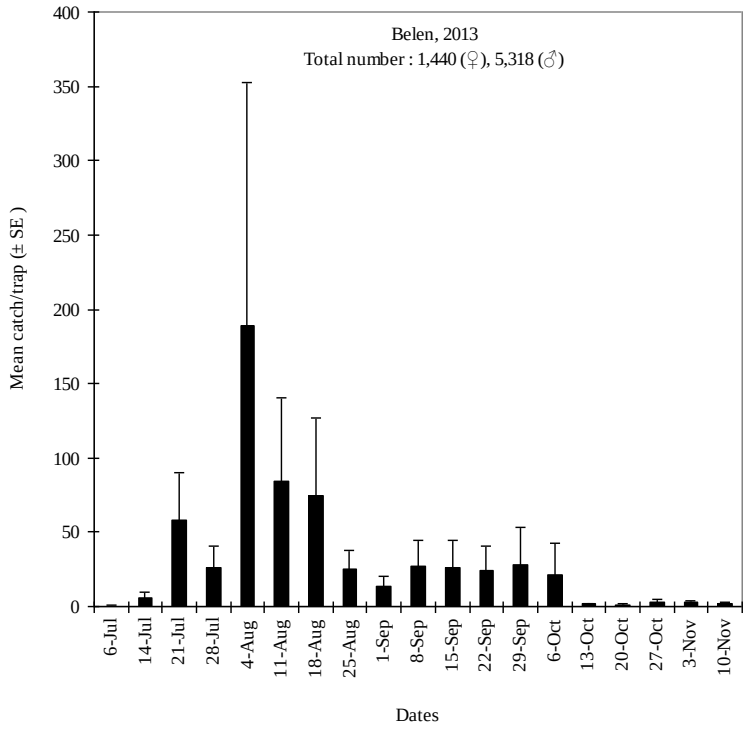

FIGURE 1
Mean (±SE) catches of medfly adults in traps baited with trimedlure (29 June–10 November, 2013) at persimmon orchards in Belen district.

were set up 29 June and removed on 10 November in 2013. In the following year, the traps were set up 3 August and removed from persimmon orchards on 9 November. The traps were placed 1.5 m above ground and checked weekly, trapped the *C.capitata* were counted and removed from the traps in both years. The trimedlure and DDVP taplet in traps were replaced with the new ones in every 90 days. All data were analyzed by analysis of variance (ANOVA) with using the SAS software [16].

Damages Rates in 2013-2014. The fruit damage assessment was measured by the percentage of *C.capitata* punctures in five times (22, 29 September, 6, 13, 20 October) in 2013 and seven times (14, 21, 28 September, 12, 19, 26 October, 2 November) in 2014. For this purpose, except from the trap baited with trimedlure hanging tree, a three-hundred fruits were chosen randomly from each of the orchards and checked for *C.capitata* punctures and infested fruits were counted. The percentage of fruit damage was calculated by dividing the number of infested fruits by the total number of sampled fruits in each orchards to evaluate the percentage of the damaged fruits in each of the orchard.

RESULTS AND DISCUSSION

The population fluctuation and damage rates of *C. capitata* on persimmon fruits varied in each of the sampling year and orchard. The pest was recorded all persimmon orchards, in which the studies were conducted in 2013-2014. In the first year, an eleven persimmon orchards in Belen district were sampled and a total of 6758 adults were caught by traps (Figure 1). The largest mean of catches *C. capitata* per trap was recorded on 4 August, followed by 11 August, 18 August, while the lowest mean of catches per trap was recorded from 13 October to 10 November. The percentage of catches male per trap with 78.69 was higher than female with 21.31 during the sampling period.

A six persimmon orchards in Harbiye district were sampled and a total of 1168 adults were caught by traps (Figure 2). The largest mean of catches *C. capitata* per trap was recorded on 25 August, followed by 11 August, 18 August, while the lowest mean of catches *C. capitata* per trap was recorded on 22 September. The percentage of catches male per trap with 91.35 was higher than female with 8.65 during the sampling period.

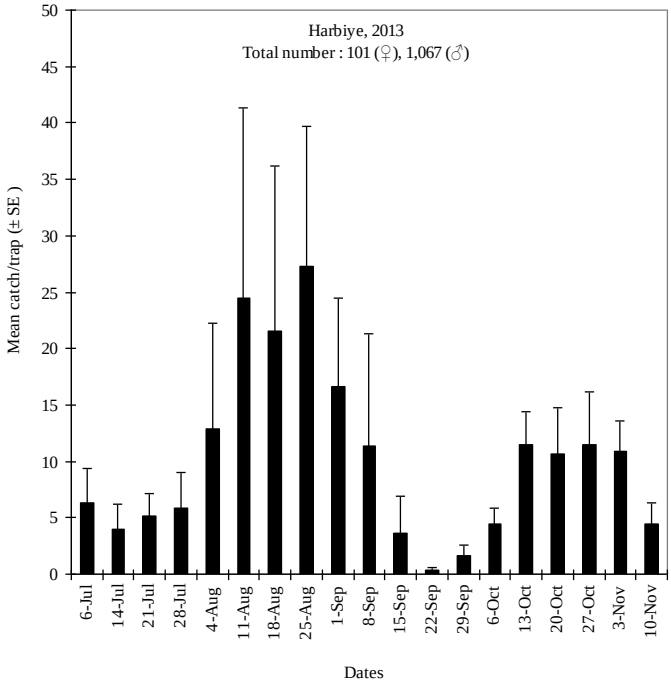

FIGURE 2
Mean (±SE) catches of medfly adults in traps baited with trimedlure (29 June–10 November, 2013) at persimmon orchards in Harbiye district.

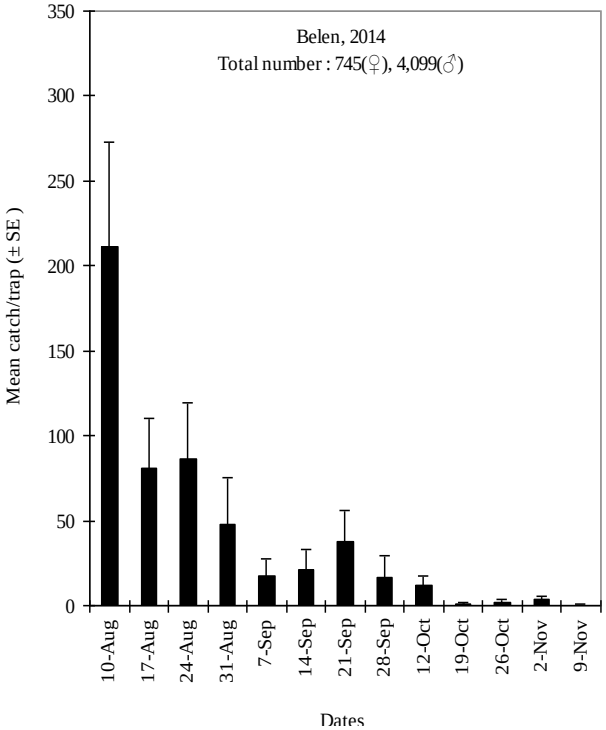

FIGURE 3
Mean (±SE) catches of medfly adults in traps baited with trimedlure (3 August–9 November, 2014) at persimmon orchards in Belen district.

In the second year, a nine persimmon orchards in Belen district were sampled and a total of 4844 adults were caught by traps (Figure 3). The largest mean of catches *C. capitata* per trap was recorded on 10 August, followed by 17-24 August, while the lowest mean of catches per trap was recorded from 19 October to 9 November. The percentage of catches male per trap with 84.62 was higher than female with 15.38 during the sampling period.

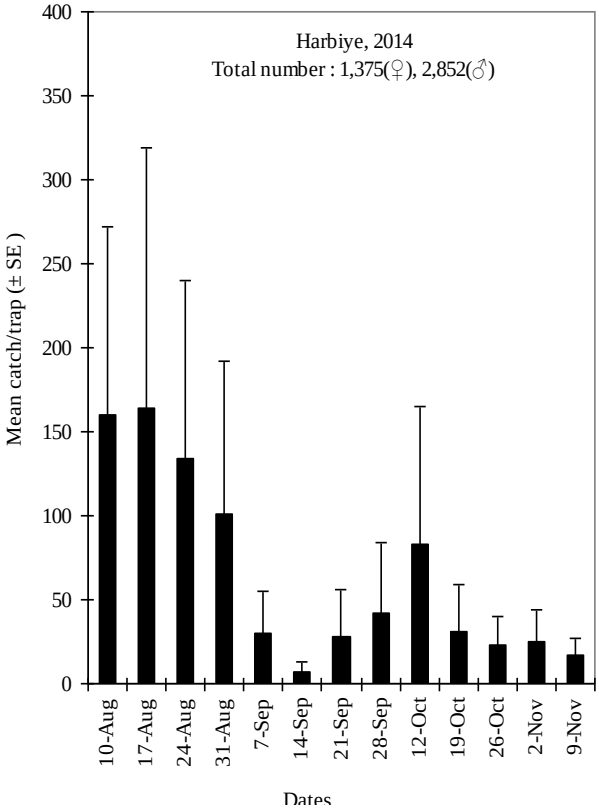

FIGURE 4
Mean (±SE) catches of medfly adults in traps baited with trimedlure (3 August–9 November, 2014) at persimmon orchards in Harbiye district.

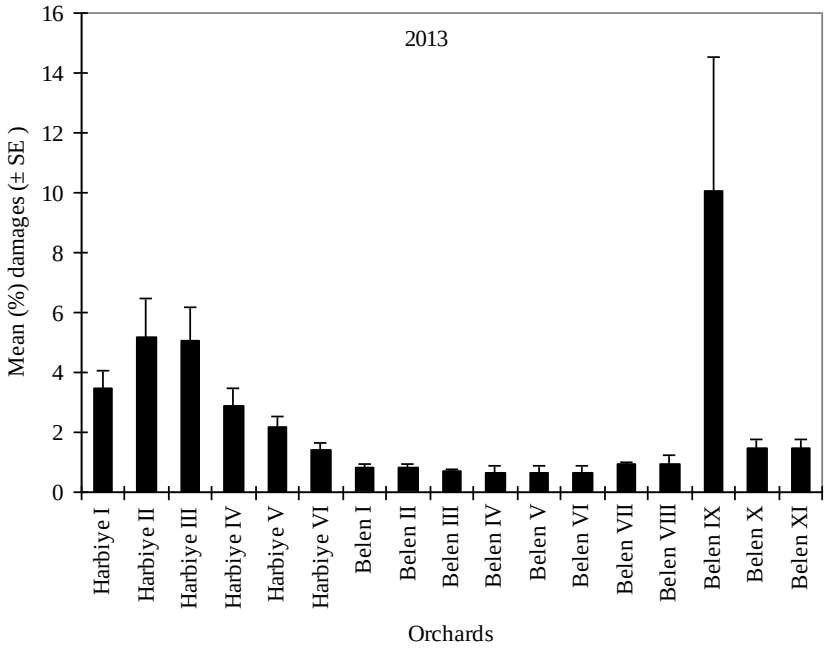

FIGURE 5
Percentage of the damaged fruits by medfly in persimmon orchards in Harbiye and Belen districts in 2013

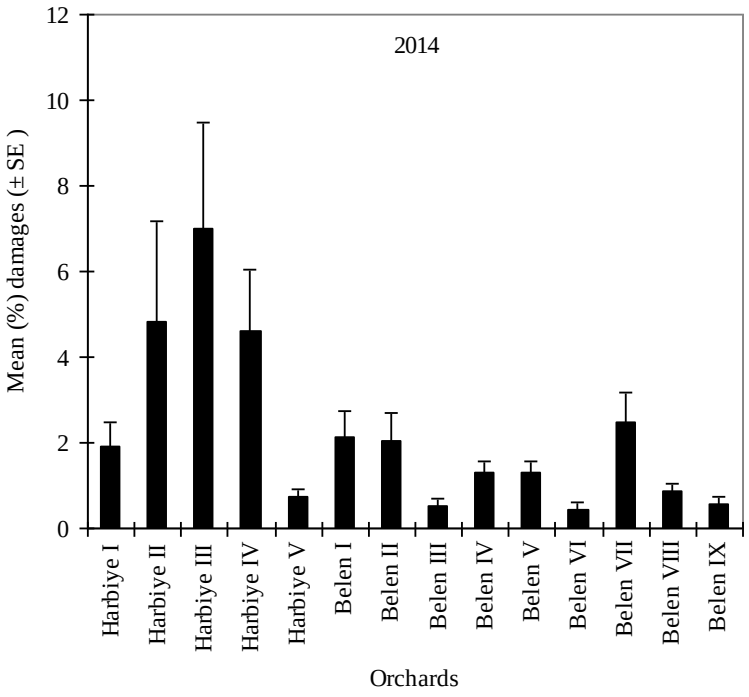

FIGURE 6
Percentage of the damaged fruits by medfly in persimmon orchards in Harbiye and Belen districts in 2014

A five persimmon orchards in Harbiye district were sampled and a total of 4227 adults were caught by traps (Figure 4). The largest mean of catches *C. capitata* per trap was recorded on 17 August, followed by 10 August, 24 August, while the lowest mean of catches per trap was recorded on 14 September. The percentage of catches male per trap with 67.47 was higher than female with 32.53 during the sampling period.

Detection and monitoring systems are critical components to control *C. capitata* in the world [12]. The trimedlure (tert-butyl 4(and 5) chloro-2-methylcyclohexane 1-carboxylate) contained in Jackson traps and McPhail traps baited with hydrolyzed protein were the primary detection and monitoring tools used for *C. capitata* [12, 13]. The percentage of catches male per trap with 85.47 was higher than female with 14.53 in Dörtyol district [8]. In addition, the percentage of catches male per trap with 83.11 was higher than female with 16.89 in Antakya district [8].

Damages Rates in 2013-2014. The percentages of damage rates of *C. capitata* were observed in each of the sampled orchard in both years. In 2013, the highest mean of damage ratios of *C. capitata* were observed at the Belen IX, followed by Harbiye II, III orchards, while the lowest mean of damage rates of *C. capitata* were observed on Belen I-VIII orchards (Figure 5). In 2014, the highest mean of damage ratios of *C. capitata* were observed at the Harbiye III, followed by Harbiye II, IV orchards, while the lowest mean of damage rates of *C. capitata* were observed on Harbiye V, Belen III, VI and Belen IX orchards (Figure 6). The Medfly causes significant damages on persimmon fruits in Hatay province of Turkey [8]. Kılıç [8] reported that the highest mean of the damage rates of *C. capitata* were observed in Dörtyol district with 64.62 percent, followed by Antkaya district with 63.0 percent in 2013. In addition, the highest mean of the damage rates of *C. capitata* were observed in Antkaya district with 74.64 percent, followed by Dörtyol district with 74.57 percent in 2014.

CONCLUSION

The present study was conducted by traps baited with trimedlure to evaluate population fluctuation and damage rates of *C. capitata* on persimmon fruits in Belen and Harbiye districts of Hatay province in Turkey. As a result of two-year investigations, this pest was recorded all thirty one sampled sites. The results also indicated that the largest mean and percentages of male and female *C. capitata* were significantly high in August in both years and the percentages of damage ratio of *C. capitata* increased ripening and harvesting time of persimmon fruits in both years.

ACKNOWLEDGEMENTS

This project was supported by University of Mustafa Kemal of Scientific Research Projects (BAP) (project number: 12162).

REFERENCES

[1] Yonemori, K., Sugiura, A. and Yamada, M. (2000) Persimmon genetics and breeding. Plant Breeding Reviews. 19(6), 191-225.

[2] Anonymous (2016) Turkiye istatiktik kurumu. https://biruni.tuik.gov.tr/bitkiselapp/bitkisel. zul. 15.02.2018.

[3] White, I.M. and Elson-Harris, M. (1992) Fruit flies of economic importance: their identification and bionomics. CAB international, Wallingford, U.K. 60p.

[4] Demirel, N. (2007) Behavior paradigms in the Mediterranean fruit fly, Ceratitis capitata (Weidemann). Journal of Entomology. 4(2), 129-135.

[5] Weems, H.V. Jr. (1981) Mediterranean fruit fly, *Ceratitis capitata* (Wiedemann) (Diptera: Tephritidae). Entomology Circular, Division of Plant Industry, Florida Department of Agriculture and Consumer Services. 12p.

[6] Liquido, N.J. Shinoda, L.A. and Cunningham, R.T. (1991) Host Plants of the Mediterranean Fruit Fly (Diptera Tephritidae): An Annotated World Review. Entomological Society of America. Miscellaneous Publications, No. 77.

[7] Christenson, L.D. and Foote, R.H. (1960) Biology of fruit flies. Annual Review of Entomology. 5, 171-192.

[8] Kılıç, G. (2015) Hatay İli Trabzon Hurması Bahçelerinde Akdeniz Meyve Sineği, *Ceratitis capitata* (Wiedemann) (Diptera: tephritidae)'nin Popülasyon Yoğunluğu ve Zarar Oranının Belirlenmesi. Mustafa Kemal Üniversitesi, Fen Bilimleri Enstitüsü, Master Thesis. Hatay, 142p.

[9] Demirel, N. (2016) Population density and damage ratios of Mediterranean fruit fly, *Ceratitis capitata* (Wiedemann) (Diptera: Tephritidae) on pomegranate orchards in Turkey. Entomology and Applied Science Letters. 3(5), 1-7.

[10] Roessler, Y. and Chen, C. (1994) The Mediterranean fruit fly, *Ceratitis capitata*, a major pest of citrus in Israel, its regulation and control. Bulletin OEPP/EPPO Bulletin. 24, 813-816.

[11] Urbaneja, A., Chueca, P., Monton, H., Pascual-Ruiz, S., Dembilio, O., Vanaclocha, P., Abad-Moyano, R., Pina, T. and Castanera, P. (2009) Chemical alternatives to malathion for controlling *Ceratitis capitata* (Diptera: Tephritidae), and their side effects on natural enemies in Spanish citrus orchards. J. Econ. Entomol. 102, 144-151.

[12] Shelly, T.E., Epsky, N., Jang, E.B., Reyes-Flores, J. and Vargas, R.I. (2014) Trapping and the Detection, Control, and Regulation of Tephritid Fruit Flies. Lures, Area-Wide Programs, and Trade Implications. 643p.

[13] IAEA (International Atomic Energy Agency) (2003) Trapping guidelines for area-wide fruit fly programmes. Insect Pest Control Section, International Atomic Energy Agency, Vienna, Austria.

[14] Navarro, V., Alfaro, F., Dominguez, J., Sanchis, J. and Primo, J. (2008) Evaluation of traps and lures for mass trapping of Mediterranean fruit fly in citrus groves. J. Econ. Entomol. 101, 126–131.

[15] Boulahia-Kheder, S., Loussaïef, F., Ben Hmidène, A., Trabelsi, I., Jrad, F., Akkari, Y. and Fezzani, M. (2012) Evaluation of two IPM programs based on mass-trapping against the Mediterranean fruit fly *Ceratitis capitata* on citrus orchards. Tunisian Journal of Plant Protection. 7, 53-66.

[16] SAS Institute (1998) User's Guide, version 6. SAS Institute, Cary, NC, USA.

Received: **28.02.2018**
Accepted: **29.04.2018**

CORRESPONDING AUTHOR

Nihat Demirel
Mustafa Kemal University,
Faculty of Agriculture,
Department of Plant Protection,
31034, Hatay – Turkey

e-mail: ndemirel@mku.edu.tr

© by PSP Volume 27 – No. 7/2018 pages 5078-5084 Fresenius Environmental Bulletin

DETERMINATION OF MORPHOLOGICAL, AGRICULTURAL AND QUALITY PARAMETERS AT DIFFERENT GROWTH STAGE OF *BITUMINARIA BITUMINOSA* GENOTYPES

Fatih Kumbasar[1], Zeki Acar[1], Erdem Gulumser[2,*], Mehmet Can[1], Ilknur Ayan[1]

[1]Department of Field Crops, Faculty of Agriculture, Ondokuz Mayıs University, 55100 Samsun, Turkey
[2]Department of Field Crops, Faculty of Agriculture and Natural Science, Bilecik Seyh Edebali University, 11230 Bilecik, Turkey

ABSTRACT

This study was conducted to determine some morphological, agricultural and quality traits at different growth stage (the beginning of growth, stem elongation, budding, flowering and seed set) of *Bituminaria bituminosa* (L.) C.H. Stirtion (*Bitbit*) genotypes collected from 25 different locations in Samsun, Sinop and Kastamonu, the Middle Black Sea Region of Turkey. The experiment was conducted in Samsun ecological conditions and was carried out for two years (2012-2013 and 2013-2014) and the observations were conducted in the second year. Plant height, number of branch, main stem diameter, leaflet width and length and leaf ratio, dry plant weight, crude protein, ADF and NDF ratios, K, P, Ca and Mg contents of *Bitbit* genotypes were investigated. The highest plant height and dry plant weight were determined at the budding stage (118.65 cm and 205.0 g), while the lowest were determined at the beginning of the growth stage (26.32 cm and 58.4 g). Crude protein, ADF and NDF ratios ranged between 7.28-23.41%, 19.80-47.14% and 27.37-56.38%, respectively.

According to the correlation and path analysis regarding the agricultural and quality traits at the flowering stage, plant height, main stem diameter, and number of branch had significant positive effects on yield increase, while ADF and NDF ratios had a negative effect on RFV. The highest crude protein yield was obtained at the flowering stage while it was lowest at the beginning of growth.

As a result of, Bitbit genotypes harvesting at flowering stage may be the most appropriate in terms of yield and quality traits in Black Sea region conditions.

KEYWORDS:
Bituminaria bituminosa, Genotype, Growing stage, Quality.

INTRODUCTION

Turkey has a highly variable climate and soil conditions and this variability enables the growth of many forage crops which is engaged in agriculture in many parts of the world. Turkey is also the genetic centre of the majority of these forage crops, however, they cultivated very low in the country. The cultivars brought from abroad are not always available to adapt to the climate and soil conditions of our regions and the desired yield is not achieved because of being highly affected by the diseases and harmful effects. For this reason, new varieties are needed to be developed by taking advantage of the natural, vegetative populations that adapt to the ecological conditions of our regions [1].

On the other hand, according to global climate change scenarios summer temperatures and drought increase are estimated in our country. In addition, according to the projection of global climate models of the Intergovernmental Panel on Climate Change (IPCC) a vast part of Turkey will experience the effect of a quite dry and hot climate in 2100. The temperature will increase 2 °C in the winter and 2-3 ° C in the summer and there will be 10% precipitation increase in the winter and 5-10% precipitation decrease in the summer and 15-25% decrease in total soil moisture in the summer is also estimated [2]. For this reason, regarding the future of our country the hot and drought-resistant plants such as *Bituminaria bituminosa* are expected to be very important in increasing the quality and the efficiency of pastures, in the evaluation of the marginal fields and the protection of biological diversity, the preservation of soil and water resources during the summer stages.

In this study, it is aimed to determine some agricultural and quality traits in different growth stage (the beginning of growth, the stem elongation, the budding, the flowering and the seed set) of *Bituminaria bituminosa* (L.) C.H. Stirtion genotypes collected from 25 different locations in the Middle Black Sea Region.

MATERIALS AND METHODS

In this study, agricultural and quality traits of *Bituminaria bituminosa* (L.) C.H. Stirtion (*Bitbit*) genotypes collected from 25 different locations in Samsun (15 locations), Kastamonu (5 locations) and Sinop (5 locations) in the Middle Black Sea Region of Turkey during 2012-2013 and 2013-2014 growing years were investigated. The experiment was conducted in Samsun ecological conditions. After cleaning the collected seeds, they were dried at 30ºC [3]. Each genotype was firstly sown into seed trays and then they were transplanted to experimental area with 70x70 cm spaces in autumn.

The properties of experimental area soil which were gathered from 0-15 cm deep were determined as a pH of 6.45, 7.90% CaCO3 and saltless (0.052 mmhos/cm). The average of long term annual precipitation of Samsun was about 679.7 mm and the average temperature was 13.79 ºC. The average rainfall of Samsun throughout a year in 2014 (604.1 mm) was higher than the precipitation average over long years stage of time.

Plants were harvested at different growing stages (beginning of growth, stem elongation, budding, flowering and seed set). Morphological traits were determined as plant height (cm), the number of branch, stem diameter (mm), leaflet width and length (mm) and leaf ratio (%). Harvested plant samples were dried at 65 ^{0}C until they have a constant weight and they were to determine dry plant weight. Crude protein ratio, acid detergent fiber (ADF), neutral detergent fiber (NDF), Potassium (K), Phosphorus (P), Calcium (Ca), Magnessium (Mg) contents of hay were determined by using Near Infrared Reflectance Spectroscopy (NIRS, 'Foss 6500') with software package program.

Relative feed value (RFV) was estimated according to the following equations adapted from [4] (Table 1).

Relative feed value (RFV) = (DDM% * DMI%) /1.29

DDM% (Dry matter digestibility) = 88.9 - (0.779 x ADF%);

DMI% of BW (Dry matter intake) = 120 / NDF%.

TABLE 1
Legumes, grass and legume-grass mixture relative feed value standarts (RFV)

Quality standarts	Protein % of dry matter	ADF% of dry matter	NDF% of dry matter	Relative feed value (RFV)
Beginning	>19	<31	<40	>151
1	17-19	31-40	40-46	151-125
2	14-16	36-40	47-53	124-103
3	11-13	41-42	54-60	102-87
4	8-10	43-45	61-65	86-75
5	<8	>45	>65	<75

In this study, relations between agricultural and quality traits with other traits were determined by means of correlation and path analysis methods by using TARIST software package program at the flowering stage.

RESULTS AND DISCUSSION

Morphological and Agricultural traits. The plant height, the number of branch, the stem diameter, the leaflet width and length, the leaf ratio and the dry plant yield of *Bitbit* genotypes in different growth stages were given in Table 2. The highest plant height was determined as 118.65 cm (budding stage), while the lowest plant height was determined as 26.32 cm.

There is an increase in the plant height as its growth stage progresses. The increase is related with the vegatation stage. The increase in the plant height is an expected situation for the plants which grow vertically when the harvest time is delayed [5] In previous studies, plant height was reported as 20 – 140 cm [6, 7].

The average number of branch in *Bitbit* genotypes ranged between 19.76 – 21.04 and the stem diameter ranged between 7.08 – 8.16 mm. The highest number of branch and main stem diameter was determined during the budding stage (Table 2).

The highest leaflet width was determined as 40.94 mm during stem elongation stage and the leaflet length was determined as 55.07 mm at the flowering stage. The lowest leaflet width and length were determined at the seed set stage (Table 2). There were differences in leaflet width and length between growing stages. Especially, the leaflet width was narrowed with the progress growing period. This may be due to the genetic structure of *Bitbit*. The leaflets measured during each growing stage were taken from the middle parts of the plant. This indicates that the measured leaflets are determined at the upper parts of the plants during the growing stage. Gulumser [8] reported that the leaflet length and width of *Bitbit* ranged between 1.9-2.1 and 3.5-4.5 mm of respectively.

The dry plant weight increased during the plant growth and it was determined as 205.0 g during the seed set stage while it was 58.4 g at the beginning of the growth. Dry plant weight increased with the progression of growth time. Temel and Tan, (2002) [9] reported that the hay yield increased since new tissues are formed with the progression of ripening. The dry plant weight of present study was similar to different research [10].

Leaf ratio ranged between 30.84 and 78.47%. Because the stem and branches did not form in the beginning of the growth, most of the parts of the plants above the soil consisted of leaves. Therefore, as the growth stage progressed, the dry matter accumulation increased with the stem and the branch while the leaf ratio decreased of *Bitbit* genotypes.

TABLE 2
Some morphological and agricultural traits of *Bitbit* genotypes during the plant growing stages

Morphological and Agricultural traits	Plant growing stages				
	Beginning of growth	Stem elongation	Budding	Flowering	Seed set
Plant height (cm)	26.32	36.49	79.15	116.41	118.65
Number of branch	-	19.76	21.04	19.80	19.80
Main stem diameter (mm)	-	7.86	8.16	7.08	7.39
Leaflet width (mm)	-	40.94	33.72	27.40	16.89
Leaflet length (mm)	-	46.78	52.07	55.07	42.65
Dry plant weight (g)	58.4	81.6	125.3	185.6	205.0
Leaf ratio (%)	-	78.47	48.00	30.84	-

TABLE 3
Some quality traits of *Bitbit* genotypes during plant growing stages

Quality traits	Plant growing stage				
	Beginning of growth	Stem elongation	Budding	Flowering	Seed set
RFV	249.7	229.53	154.84	151.46	86.0
Crude protein ratio (%)	23.41	22.55	17.70	15.29	7.28
ADF (%)	19.80	20.16	31.46	35.84	47.14
NDF (%)	27.37	29.90	41.05	44.90	56.38
K (%)	2.33	2.55	2.59	2.01	0.51
P (%)	0.39	0.40	0.39	0.33	0.18
Ca (%)	1.87	1.61	1.35	1.30	1.41
Mg (%)	0.40	0.39	0.37	0.35	0.37
Ca/P	4.78	4.15	3.42	3.74	7.98
K/(Ca+Mg)	1.03	1.27	1.58	1.30	0.29

Quality traits. Crude protein ratio, ADF, NDF, K, P, Ca, Mg content and Ca/P and K/(Ca+Mg) ratios related with the *Bitbit* genotypes gathered from different locations were given in Table 3. The crude protein ratio decreased because of the decrease of the leaf ratio and due to the increase of the structural carbohydrate accumulation which was bound up with the aging in the tissues during the progression of the growth stage. In many studies, it is reported that crude protein ratio in *Bitbit* ranged between 15.9 and 20.3% [11, 12, 10].

The greatest ratios of ADF and NDF (47.14-56.38%), were observed at the seed set stage and the lowest ratios of ADF and NDF (19.80-27.37% of respectively) were observed at the beginning of the growth (Table 3). ADF and NDF ratio usually increases with the progress of plant growth [13]. This may be due to the cellulose and lignin content increased with the leaf/stem ratio decrease when delayed harvest time. Therefore, the obtained ratios of ADF and NDF at the beginning of growth were less than the ratios at the seed set stage.

The ratio of Relative Feed Value (RFV) is a measurement which is the representation of the fodder quality in terms of numeral [14]. RFV values decreased with the progression of growing period and it ranged from 86.0 to 249.7. Lignin and cellulose contents continuously are increases depending on advancement in maturity. Therefore, ADF and NDF content increased with progression growth stage while RFV values decreased. In this study, the RFV values that determined had a good quality class of fodder except the obtained values at the seed set stage (Table 1).

Minerals have significant effects on both plant and animal metabolisms as reported by Egritas and Asci, (2015). Potassium (K) content ranged between 0.51 – 2.59%, phosphorus (P) content varied between 0.18 – 0.40%, Calcium (Ca) content ranged between 1.30 – 1.87% and Magnesium content varied between 0.35 – 0.40%. There needed to be at least more than 0.3% Ca in the feed of cows and the need for magnesium varied between 0.1 – 0.2% [15]. When these values were taken into consideration, calcium and magnesium contents in this study were sufficient. The highest ratio of K was determined as 2.59% at the budding stage and the lowest ratio of K was determined as 0.51% at the seed set stage. Ventura et al. (2004) [16] and Gulumser (2011) [8] reported that potassium and phosphorus contents of *Bitbit* were between 0.26-1.28% and 0.25-0.32% of respectively.

While the highest ratio of Ca/P was determined at the seed set stage (7.98), the lowest ratio was determined at the budding stage (3.42). The ratios of Ca/P needed to be between 1-2, however, if a sufficient amount of vitamin D was taken by animals, it is ratio could be tolerated up to 7/1 [17].

The highest K/(Ca+Mg) ratio was as 1.58 at the budding stage, and the lowest was determined as 0.29 at the seed set stage (Table 3). For this reason, the ratio of K/(Ca+Mg) was below the desired level (2.2) in terms of tetany risk in all growth stages in this study [18].

Crude protein yield per plant of *Bitbit* genotypes are given Figure 1. The highest crude protein yield was obtained at the flowering stage (28.37 g) and it was lowest at the beginning of growth (13.67 g). Crude protein yield at the flowering stege was more than at the beginning of growth (Figure 1). This is result from Bitbit genotypes hay yield continuously increases during growth stage.

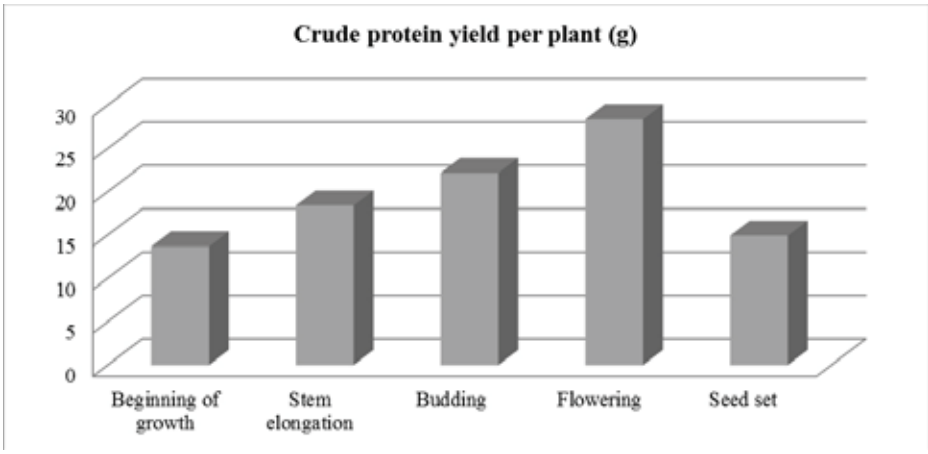

FIGURE 1
Crude protein yield per plant of *Bitbit* genotypes during the plant growing stage

TABLE 4
The correlation values between agricultural traits in *Bitbit* genotypes

Agricultural traits	PH	NB	MSD	LW	LL	LR
Dry plant weight	0.761**	0.436*	0.596**	0.321	0.50	-0.486**
Plant height (PH)		0.131	0.660**	0.346	0.382	-0.515**
Number of branch (NB)			-0.308	0.297	-0.052	0.026
Main stem diameter (MSD)				0.124	0.256	-0.361
Leaflet width (LW)					0.574**	0.225
Leaflet length (LL)						0.117

*: p< 0.05, **: p< 0.01; LR: Leaf ratio

TABLE 5
The correlation values between quality traits in *Bitbit* genotypes

Quality traits	CPR	ADF	NDF	K	P	Ca	Mg	Ca/P	K+/(Ca+Mg)
RFV	0.634**	-0.668**	-0.866**	0.011	-0.110	0.745**	0.517**	0.572**	-0.123
CPR		-0.466*	-0.633**	0.011	0.374	0.479**	0.576**	0.079	0.092
ADF			0.668**	0.020	0.252	-0.611**	-0.423*	-0.562**	0.178
NDF				-0.263	-0.144	-0.777**	-0.584**	-0.430*	-0.003
K					0.737**	-0.190	-0.049	-0.568**	0.882**
P						-0.190	0.124	-0.751**	0.561**
Ca							0.704**	0.783**	-0.414**
Mg								0.385	-0.256
Ca/P									-0.599**

*: p< 0.05, **: p< 0.01. RFV: Relative feed value; CPR: Crude protein ratio;

Correlation analysis. Correlations between the investigated agricultural and quality traits at the flowering stage are given in Table 4 and 5. As seen in Table 4, the strongest correlation was observed between dry plant weight and plant height (0.761), then it was followed by plant height and stem diameter (0.660). These correlations were significant and positive. It was also determined that there was a significant and negative correlation between leaf ratio and plant height. This indicated that there was an increase in the number of branches of *Bitbit* genotype; however, there was a decrease in the ratio of its leaves during the growing stage. A significant positive correlation (0.574, p<0.01) was observed between the leaflet width and length while an insignificant and positive correlation was determined between the leaflet width and other traits (Table 4).

When the quality traits of plant taken into consideration, a significant positive correlation (0.634, p<0.01) was observed between RFV and crude protein ratio and a significant negative correlation was determined between ADF (0.668, p<0.01) and NDF (0.866, p<0.01). According to this correlation, it can be said that as the ratios of ADF and NDF increase, the ratio of RFV decreases. The strongest positive correlation was determined between K and K/(Ca+Mg) ratio (0.882, p<0.01) (Table 5).

Path analysis. Correlation is the most appropriate method in determining the relationship between independent characters. However, the whole effects of the characters on each other are not direct; the relations between each other are formed indirect effects. Therefore, to determine the relationship between characters is not possible only with correlation, and it is necessary to exhibit indirect and direct effects [19]. Path coefficients and contribution rates which show direct and indirect effects on relative

feed value and on dry plant weight in *Bitbit* genotypes are given in Table 6 and 7.

As seen in Table 6, the number of branch (69.40%) and main stem diameter (57.88%) had a direct positive effect on dry plant weight. The direct negative effect was due to leaf ratio (36.78%) on dry plant weight. This situation indicate that dry plant weight increased with the number of branches increased in *Bitbit* genotypes but, the number of leaflet decreased. It was also observed a high correlation between plant yield and plant height. The direct effect of plant height was positive of this correlation coefficient (24.29%) (Table 6).

TABLE 6
Path coefficients, direct and indirect effects on dry plant weight in *Bitbit* genotypes

DE	IE	PATH	EFFECT (%)	DE	IE	PATH	EFFECT (%)
PH		0.200	24.29	**LW**		0.110	21.80
	NB	0.075	8.80		PH	0.069	13.60
	MSD	0.374	45.44		NB	0.164	32.25
	LW	0.038	4.65		MSD	0.070	13.85
	LL	-0.031	3.81		LL	-0.047	9.28
	LR	0.106	12.98		LR	-0.046	9.19
NB		0.552	69.40	**LL**		-0.082	19.56
	PH	0.026	3.29		PH	0.076	18.15
	MSD	-0.174	21.95		NB	-0.028	6.80
	LW	0.032	4.13		MSD	0.145	34.57
	LL	0.004	0.534		LW	0.063	15.12
	LR	-0.005	0.678		LR	-0.024	5.77
MSD		0.567	57.88	**LR**		-0.207	36.78
	PH	0.132	13.48		PH	-0.103	18.23
	NB	-0.170	17.39		NB	-0.014	2.54
	LW	0.013	1.40		MSD	-0.205	36.30
	LL	-0.021	2.15		LW	-0.024	4.47
	LR	0.075	7.67		LL	-0.009	1.70

DE: Direct effect; ID: Indirect effect; PH: Plant height; NB: Number of branch; MSD: Main stem diameter; LW: Leaflet width; LL: Leaflet length; LR: Leaf ratio

TABLE 7
Path coefficients and the direct and indirect effects on RFV in *Bitbit* genotypes

DE	IE	PATH	E (%)	DE	IE	PATH	E (%)	DE	IE	PATH	E (%)
CPR		0.342	25.42	**ADF**		0.043	3.61	**NDF**		-0.935	57.66
	ADF	-0.020	1.49		CPR	-0.159	13.43		CPR	-0.216	13.36
	NDF	0.592	43.94		NDF	-0.625	52.57		ADF	0.028	1.77
	Ca	-0.088	6.59		Ca	0.113	9.52		Ca	0.144	8.88
	K	-0.189	14.09		K	-0.012	1.02		K	0.158	9.78
	P	-0.019	1.42		P	-0.129	1.08		P	0.007	0.455
	Mg	-0.038	2.85		Mg	0.028	2.37		Mg	0.039	2.405
	Ca/P	0.016	1.23		Ca/P	-0.118	9.97		Ca/P	-0.090	5.595
	K/(Ca+Mg)	0.039	2.93		K/(Ca+Mg)	0.075	6.38		K/(Ca+Mg)	-0.001	0.073
DE	**IE**	**PATH**	**E (%)**	**DE**	**IE**	**PATH**	**E (%)**	**DE**	**IE**	**PATH**	**E (%)**
Ca		-0.185	11.47	**P**		-0.051	4.22	**Ca/P**		0.211	14.35
	CPR	0.164	10.15		CPR	0.128	10.54		CPR	0.027	1.83
	ADF	-0.026	1.62		ADF	0.010	0.89		ADF	-0.024	1.64
	NDF	0.726	44.93		NDF	0.134	11.09		NDF	0.402	27.34
	K	0.114	7.07		Ca	0.038	3.19		Ca	-0.145	9.87
	P	0.010	0.66		K	-0.443	36.56		K	0.342	23.27
	Mg	-0.047	2.90		Mg	-0.008	0.68		P	0.038	2.61
	Ca/P	0.165	10.22		Ca/P	-0.158	13.05		Mg	-0.023	1.62
	K/(Ca+Mg)	-0.177	10.98		K/(Ca+Mg)	0.239	19.74		K/(Ca+Mg)	-0.256	17.42
DE	**IE**	**PATH**	**E (%)**	**DE**	**IE**	**PATH**	**E (%)**	**DE**	**IE**	**PATH**	**E (%)**
K		-0.602	39.34	**Mg**		-0.066	5.65	**K/(Ca+Mg)**		0.427	34.20
	CPR	0.108	7.05		CPR	0.197	16.71		CPR	0.031	2.52
	ADF	0.009	0.05		ADF	-0.018	1.54		ADF	0.007	0.61
	NDF	0.246	16.09		NDF	0.546	46.32		NDF	0.002	0.20
	Ca	0.035	2.30		Ca	-0.130	11.06		Ca	0.076	6.15
	P	-0.037	2.46		K	0.029	2.47		K	-0.531	42.50
	Mg	0.003	0.21		P	-0.006	0.54		P	-0.028	2.30
	Ca/P	-0.120	7.85		Ca/P	0.075	6.40		Mg	0.017	1.36
	K/(Ca+Mg)	0.377	24.63		K/(Ca+Mg)	-0.109	9.26		Ca/P	-0.126	10.11

DE: Direct effect; IE: Indirect effect; E: Effect; CPR: Crude protein ratio; ADF: Acid detergent fiber; NDF: Neutral detergent fiber; Ca: Calcium; K: Potassium; P: Phosphorus; Mg: Magnesium.

RFV was regarded as a variable and the other traits observed during the study were regarded as relative variables in path analyses. K/(Ca+Mg) (34.20%) and crude protein ratio (25.42%) had direct positive effects on RFV. The strongest direct negative effects on RFV were exhibited by NDF (57.66%) (Table 7). Although ADF had a direct positive effect on RFV, there observed a negative correlation between them. Singh and Chaudhary (1997) [20] reported that indirect effects were the consequences of the correlation and indirect effects needed to be considered at the same time. Strong correlations were observed between RFV and with of Ca and Mg. Ca (11.47%) and Mg (5.65%) had negative and direct effects of these correlation coefficient (Table 7).

CONCLUSION

Bituminaria bituminosa (L.) C.H. Stirtion is one of the most studied plants because of its being extremely tolerant to the temperature and drought, its capability of elongation and protecting its greenery during the summer and its capability of growing without watering in sloping and stony marginal areas which lost its upper soil layer and have low depth soil. *Bitbit* may be considered as a fodder crop in terms of its vegetative parts with mineral content, ADF, NDF and Relative Feed Value.

1) In this study, it was observed that dry plant weight increased but its quality decreased during the progressed growth stage of *Bitbit.*

2) According to the correlation and path analysis done during the flowering stage; the plant height, the main stem diameter and the branch number had significant positive effects on yield increase. It was also observed that while crude protein ratio had a positive effect on RFV, ADF and NDF ratio had negative effects on RFV.

3) The highest crude protein yield was obtained at the flowering stage while it was lowest at the beginning of growth.

As a result of, Bitbit genotypes harvesting at flowering stage may be the most appropriate in terms of yield and quality traits in Black Sea region conditions. In addition, while interpreting the future studies about seed collection, agricultural characteristics and nutrient content, it should not be focused on developing a new varieties which provide a high yield and quality and which have tall leafy and have the content of high Ca and Mg.

ACKNOWLEDGEMENTS

This Project was supported by TUBITAK with the Project number TUBITAK 111 O 651. Also, a part of data given on the articles is taken from Fatih Kumbasar's master thesis.

REFERENCES

[1] Ayan, I., Acar, Z., Kutbay, G.H., Ascı, O.O., Mut, H., Basaran, U., Tongel, M.O. (2011) Investigation of the Possibility of Collection, Identification and Cultural of Some grasses in the Central Black Sea Region. TUBITAK Result Report Samsun.

[2] Anonymous (2011) http://www.antoloji.com/climate-change (13.07.2011).

[3] Walker, D.J., Bernal, M.P. and Correal. E. (2007) The influence of heavy metals and mineral nutrient supply on Bituminaria bituminosa. Water Air Soil Pollut. 184, 335-345.

[4] Rohweder, D.A., Barnes, R. and Jorgensen, N. (1978) Proposed Hay Grading Standard Based on Laboratory Analyses for Evaluating Quality. J Anim Sci. 47, 747-759.

[5] Anwar, A., Ansar, M., Nadeem, M., Ahmad, G., Khan, S. and Hussain, A. (2010) Performance of Non-Traditional Winter Legumes with Oats for Forage Yield Under Rainfed Conditions. Journal of Agric. Res. 48, 171-179.

[6] Davis, P.H. (1965) Flora of Turkey and the East Aegean Islands. Edinburg University Press. Edinburg, 1-9.

[7] Gulumser, E. and Acar, Z. (2012) Morphological and chemical characters of Bituminaria bituminosa (L) C.H. (Stirtion) grown naturally in the middle Black Sea region. Turkish Journal of Field Crops. 17, 101-104.

[8] Gulumser, E. (2011) Characterization and Determination of Agricultural Characterstics of *Bituminaria bituminosa* L. (Syn. L. *Psoralea bituminosa* L.) Genotypes Naturally Grown at the Central Black Sea Region. Master Thesis. Ondokuz Mayıs University, Faculty of Agriculturue Samsun, Turkey.

[9] Temel, S. and Tan, M. (2002) A Research on Determination of Seeding and Cutting Time in Common Vetch (Vicia *sativa* L.) under Erzurum Conditions. Journal of the Faculty of Agriculture. 33, 363-368.

[10] Gulumser, E., Basaran, U., Acar, Z., Ayan, I. and Mut, H. (2010) Determination of some agronomic traits of Bituminaria bituminosa accessions collected from Middle Black Sea Region. Options Mediterraneennes Congress. 7-10 April 2010. The contributions of grasslands to the conservation of Mediterranean biodiversity, 92, 105-108.

[11] Ventura, M.R., Flores, M.P. and Castanon, J.I.R. (1999) Nutritive value of forage shrubs: Bituminaria bituminosa. Acacia salicina and Medicago arborea. In: Cahiers Options Mediterraneennes Congress. 26-29 November 1999. Dynamic and sustainability of Mediterranean pastoral systems, 39, 171-173.

[12] Acar, Z., Ayan, I. and Gulser C. (2001) Some morphological and nutritional properties of legumes under natural conditions. Pakistan Journal of Biological Sciences. 4, 1312-1315.
[13] Acar, Z., Gulumser, E., Ascı, O.O., Basaran, U., Mut, H. and Ayan, I. (2017) Effects of sowing ratio and harvest periods on hay yields, quality and competitive characteristics of Hungarian vetch + cereal mixtures. Legume Research. 40, 677-683
[14] Yavuz, T., Sürmen, M. and Çankaya, N. (2011) Effect of row spacing and seeding rate on yield and yield components of common vetch *(Vicia sativa* L.). Journal of Food Agriculture and Environment. 9, 369-371.
[15] Kidambi, S.P., Matches, A.G. and Grigs, T.C. (1989) Variability for Ca. Mg. K. Cu. Zn and K/(Ca+Mg) ratio 3 wheat grasses and on the southern sainfoin high plains. J. Range Management. 42, 316-322.
[16] Ventura, M.R., Castanon, J.I.R., Pieltain, M.C. and Flores, M.P. (2004) Nutritive value of forage shrubs: Bituminaria bituminosa. Rumexlunaria. Acacia salicina. Cassia sturtii and Adenocarpus foliosus. Small Rumin. Res. 52, 13-18.
[17] Miller, D.A and Reetz-Jr, H.F. (1995) Forage fertilization. Iowa State Univ Press, Iowa, 79-91.
[18] Korkmaz, A., Gulser, C., Manga, I. and Sancak, C. (1993). The effects of sowing sys-tem and cutting time on mineral matter content and quality of hay in Samsun region. Doga Tr. J. Of Agriculture and Forestry. 17, 1069-1080.
[19] Karakurt, E. and Ekiz, H. (2000) Effect of Nitrogen Fertilizer Doses on Important Agronomic Characters in some Grasses. Journal of Institute of Sci. 9, 1-11.
[20] Singh, R.K. and Chaudhary, B.D. (1977) Biometrical Methods in Quantitative Genetics Analysis. Kalyani Publishers, New Delhi. 54-68.

Received: **01.03.2018**
Accepted: **28.04.2018**

CORRESPONDING AUTHOR

Erdem Gulumser
Department of Field Crops,
Faculty of Agriculture and Natural Science,
Bilecik Şeyh Edebali University,
Bilecik 11230 – Turkey

e-mail: erdem.gulumser@bilecik.edu.tr

© by PSP Volume 27 – No. 7/2018 pages 5085-5090 Fresenius Environmental Bulletin

PLASMA MACRO AND TRACE ELEMENT LEVELS OF MALE RATS VACCINATED WITH GNRH HORMONE

Leyla Mis[1,*], Funda Eski[2], Asli Cilingir-Yeltekin[3]

[1]Department of Physiology, Faculty of Veterinary Medicine, Yuzuncu Yil University, TR-65080 Van, Turkey
[2]Department of Obstetrics and Gynecology, Faculty of Ceyhan Veterinary Medicine, University of Cukurova, Balcali, Adana, Turkey
[3]Department of Chemistry, Faculty of Science, Yuzuncu Yil University, TR-65080 Van, Turkey

ABSTRACT

GnRH hormone is important in both male and female reproduction. Chemical agents are preferred to prevent fertility in some animals. Trace elements play an important role in reproduction. In this study, it was aimed to investigate the changes in macro- and trace element levels in blood plasmas of 6th and 12th months of GnRH vaccination (Repro-Bloc ™) male rats. 50 male Wistar Albino rats were used in the study. Each rat in the experimental group was administered a single 200 µl intramuscular dose of GnRH. The levels of Cu, Fe, Mn, Zn, Se, K, P, Ca, and Mg elements were determined by analyzing the collected plasma samples using inductively coupled plasma-optical emission spectroscopy (ICP-OES).

It was determined that zinc, manganese and selenium levels of the trace elements showed statistically significant changes in the first 6 months and Cu and Fe levels were statistically significant ($P<0.05$). In the twelfth month, it was observed that the levels of Fe, Mn, Se and Zn trace elements differ statistically. In the macro elements, K, P elements in the first 6 months period and Ca, Fe and Mg element levels in 16 months period gave statistically significant results ($P<0.05$). Conclusions: It was observed that levels of macro and micro elements were affected in male rats administered GnRH vaccine for immunocastration

KEYWORDS:
Trace element, Macro element, GnRH vaccine, Immunocasration, ICP-OES

INTRODUCTION

Hormones are vital chemical substances that affect many important events such as body weight, metabolism, appetite, growth, development and reproductive activities. The natural hormone, GnRH, is synthesized from the hypothalamus and stimulates synthesis and secretion of the gonadotropic hormones (FSH and LH) from adenohypophysis. Therefore, this hormone is important in both male and female reproduction [1].

Recently, there are unwanted increases in the number of domestic and wild animals. Therefore, the use of effective and safe contraceptive methods has become mandatory [2].

Many animal owners prefer chemical agents to chirurgical methods in terms of reliability, efficiency and cost to prevent unwanted mating. These methods prevent fertility from being recycled.

Hormonal applications involving progestogens, androgens, and the use of Gonadotropin Releasing Hormone (GnRH) analogues show the effect of discontinuing the direct hormonal-receptor relationship or indirectly controlling the reproduction through negative feedback [3].

It is stated that the vaccine developed against GnRH hormone showed its effect by reducing or preventing the secretion of gonadotropic hormones. Reduction or inhibition of secretion of gonadotrophic hormones causes atrophy of gonadal tissues, inhibition of gametogenesis, and therefore inhibition of reproductive behaviour. Vaccination of an individual after vaccination remained sterile for an average of 12 months, circulating immunoglobulin level decreased after the reproductive ability gained again was expressed. It has been claimed that immunocontraceptive vaccines, which allows return to the fertile period, having no systemic side effects, by providing success in one application and are relatively inexpensive compared to other methods [2].

Although high concentrations of heavy metals have negative effects on all living things, the effects of heavy metals and trace elements on reproductive capacity have not been fully explained [4]. Trace elements can cause beneficial and harmful effects on animal and human life due to their concentration. Trace elements, which are not possible to be synthesized by our bodies, must be taken from the outside from the basic food elements. Cell protection is important for healthy bone and skin structure. Trace elements also play an important role in blood pressure, heart rhythm, muscle function, maintaining fluid balance in the body, reproduction and many other functions. Scientific studies have shown that mineral loss and deficiency directly affect health. These elements are important because they act as antioxidants in the body, as they are cofactors of various enzymes and because they are involved in assimilation. In addition, metalloenzyme and metalloproteinase are involved as structural components and as stabilizers in

the membrane [5].

In this study, a GnRH vaccine (Repro-Bloc™) obtained in combination with cytosine phosphodiester guana oligodeoxynucleotide (CPG ODN) for the recombinant antigenic ovalbumin-GnRH fusion protein molecule in non-chirurgical control of reproduction in male rats was administered in the sixth year of the study and at 6th and 12th months, it is aimed to investigate the changes in the macro and trace elements.

MATERIALS AND METHODS

Animal material. Male rats, weighing about 3-4 months and 250-300 grams, were obtained from Van Yüzüncü Yıl University Experimental Animals Unit.50 male rats in the study were divided into 2 groups as 35 experimental groups and 15 control groups. For the study, permission was obtained from the Local Ethics Committee of Van Yüzüncü Yıl University in accordance with the decision numbered 03, dated 31.03.2011.

Application of the vaccine: at the beginning of each study of rats in the experimental group, from the GnRH Vaccine in the injectable form (Repro Bloc™), with a volume of 200 µl (Amplicon Vaccine, the single dose recommended by L.L.C.) was administered in a single dose intramuscularly. 15 rats in the control group were also injected into the muscle as sterile serum physiologic (ph: 7.2) as much as the volume of the vaccine.

Blood Collection. Intraperitoneal injection of ketamine (Ketalar, PFIZER) was applied before the blood was taken and general anaesthesia was applied. After anaesthesia, blood was taken from the heart of rats into the EDTA tubes. Blood samples were centrifuged for 20 minutes at 1600 rpm at 4 ° C in a refrigerated centrifuge to separate blood plasmids for analysis. Blood collection was carried out in 6th and 12 th months. The obtained plasma samples were stored at -20 ºC until the analysis of macro and trace elements was carried out.

Biochemical study. Papageorgiou et al.'s [6] method was used with some modifications. The plasma samples were taken into 1ml glass tubes and centrifuged in 2000-3000 rpm by adding 3 % HNO3 solution from 65 % HNO3 (Merck, Germany) and 1mlwas added. The remaining particles in the tubes were drained and then added 1ml 1 % Triton-X and the volume was completed to 10 ml with deionised pure water. The levels of Cu, Fe, Mn, Zn, Se, K, P, Ca, Mg elements were analyzed with ICP-OES (inductively-coupled plasma-optic emission spectroscopy) Thermoscientific ICAP 6000 series (0.005 ppm detectable limit) device.

Statistical analysis. descriptive statistics for continuous variables in our study were expressed as mean and standard deviation. Mann Whitney U test was used to compare the group mean of continuous variables. Statistical significance level in calculations was taken as 5 % and SPSS for calculations (IBM Corp. Released 2013). IBM SPSS statistics for Windows, Version 22.0. Armonk, NY: IBM Corp.) statistical package program was used.

RESULTS

Levels of Cu, Fe, Mn, Zn, Se, K, P, Ca and Mg were determined in plasma samples obtained from the blood taken at 6th and 12th. months for male rats and control groups applied GnRH vaccination.

In the sixth month, the levels of Cu and Fe trace elements in plasma samples showed statistically significant differences compared to the control group. P and K levels were determined to be statistically significant as macro elements (Table 1) (Figure 1-2).

In the twelfth month, it was observed that the levels of Fe, Mn, Se and Zn trace elements differ statistically. The levels of CA and Mg, among the macro elements, were determined to be statistically different (Table 2) (Figure 1-2).

TABLE 1
Macro and trace element levels at 6 months in male rats (µg/ml)

	Control	Experiment
Cu	1,100±0,670	0,697±0,129*
Fe	1,346±0,067	1,204±0,686*
K	141,338±86,039	108,410±30,694*
Mg	4,642±2,095	4,438±1,449
Mn	0,192±0,116	0,175±0,077
P	132,284±61,053	102,928±20,438*
Se	0,142±0,053	0,091±0,035
Zn	0,109±0,092	0,156±0,115

***p<0.05**

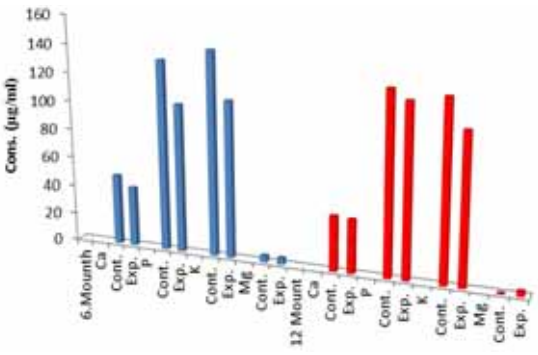

FIGURE 1
Change of macro elements at 6th and 12th months.

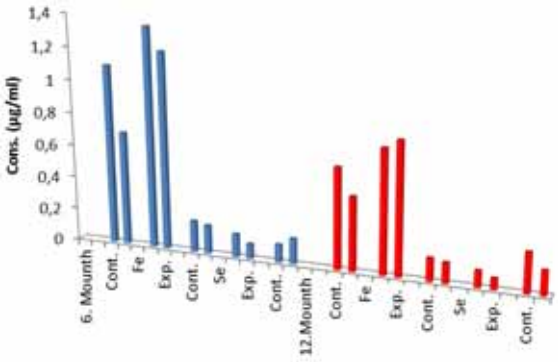

FIGURE 2
Change of trace elements during 6th and 12th months.

TABLE 2
Macro and trace element levels at 12 months in male rats (µg/ml)

	Control	Experiment
Cu	0,612±0,133	0,449±0,115
Fe	0,748±0,461	0,800±0,146*
K	122,454±17,891	102,480±36,235
Mg	0,158±0,336	3,434±1,926*
Mn	0,140±0,001	0,124±0,053*
P	124,924±18,206	118,000±32,271
Se	0,100±0,001	0,067±0,038*
Zn	0,242±0,367	0,148±0,063*

***p<0.05**

DISCUSSION

Trace elements are very important elements in the organism that are involved in many biochemical and metabolic reactions and are necessary for the immune system. The need for trace element in animals varies with such factors as age, production level, pregnancy and lactation period [7]. Macro and trace elements must be present in the organism for normal growth and continuity of life. The level of trace element in the metabolism is very important in the hormone system. There is an important relationship between hormones and trace elements. Both trace elements are involved in hormone metabolism, and disturbances in hormone function can alter the levels of trace elements in the blood and tissues [8].

In a study of plasma mineral (CA, P, mg, Zn, Cu, Co, Fe and Mn) levels investigated by applying Buserelin acetate to buffalos in pre-adolescence period it was found that only CU and Co levels were changed [9]. In a study in which intracytoplasmic sperm injection was performed with GnRH antagonist, serum and follicular fluid (Cd, Pb, Hg, As, Cu, Zn, Fe) levels were determined. It was determined that Pb's blood concentrations and Cu's follicular liquid concentrations may have significant effects on the reproductive cycle [10]. Maldonado et al. [11], in the study of reproductive and follicle development of cows, by injecting both trace element (Cu and Zn) and GnRH to Holstein cows, concluded that trace element injection may be a suitable way to increase the rate of pregnancy in cows in follicular and Corpus luteum development. Another study conducted in this area examined the changes in endocrine system by applying Zn, Cu, Mn and Co elements in different doses to the bulls in the prepubertal period. In the present study, it was found that the increase in testosterone concentration in each group and the LH ratio in pubertal bulls decreased compared to prepubertal bulls [12]. Zinc is one of the most important elements in this work involved in hormone metabolism [8]. Our work has resulted in such a way as to support this situation.

Copper is also the third major trace element found in the body after iron and zinc. Changes in the activity of some hormones are also known to affect copper metabolism [13]. A study of changes in trace element (Zn, Cu, Mn, Fe) levels of goats with follicular atresia in their ovaries was conducted. In this study, it is stated that trace elements provide basic data that can be used in the fertility improvement plan [14]. Phosphorus (P), after calcium, is the second largest element in the body. Phosphorus is a macro-nutrient that is responsible for the metabolism of carbohydrates, proteins and fats [15]. Testosterone can cause P and K to be retained. It can cause sodium and water retention depending on the pressure of testosterone and it can be expected to decrease by P and K level [16]. in our study, Cu, K and P levels decreased significantly in the 6 months after GnRH vaccination compared to the control group ($p<0.05$). This difference has been eliminated in the 12 months period, when the effect of the vaccine decreased. It was found that Plasma Fe level decreased in the 6 months period and increased in 12 months period.

This may well indicate that an important element such as Cu, which is particularly effective in the electron transport system, is suppressed under the influence of the GnRH vaccine.

At the end of the 12 month period, Zn, Se and Mn levels decreased significantly. This shows how effective Zn is on the metabolism of reproductive hormones in accordance with other literature. It is known that zinc is found in more than 2,000 proteins involved in gene expression by more than 300 enzymatic reactions [8].

In a study performed by Adedara et al. [17] through applying Mn and main elements to rats, pituitary-gonad suppression was tried to be done. In the study, it was found that there was a significant decrease in sperm quantity and quality in all rats. In a study to determine the link between concentrations of trace element (Zn, Cu, Mn, Fe, Co) and the release of testosterone in male rabbits, the protection of trace element levels was found to be important for both human and animal fertility and infertility problems [18]. In another study, it was concluded that trace elements (Cu, Co, Zn, Fe, Mn) should be taken in daily

nutrition in order to meet the need for trace elements for healthy growth and reproduction [19]. Manganese, glutamine synthetase, pyruvatedcarboxylase, as well as zinc as a cofactor are also found in the composition of enzymes such as superoxide dismutase. The superoxide dismutase containing Mn protects the cell against carcinogens caused by chemicals and radiation. Growth retardation, structural and chemical abnormalities in bones, infertility in females and disorders in lipid metabolism were observed in the lack of Mn in laboratory animals; [20]. In our study, it was observed that Mn levels in accordance with other literature showed significant changes at the end of 12 months.

Selenium, commonly found in nature, is one of the essential trace elements required for the normal development of human and animal organisms. In some studies, changes in hormone activity caused significant differences in selenium levels [21]. A study was conducted on the effects of selenium deficiency on testicular morphology and function in rats. In this study, it was determined that testicular morphology and function were influenced by selenium deficiency and that selenium element is necessary for testosterone biosynthesis, spermatozoa formation and normal development [22]. A study was conducted on how the application of pinealectomy and melatonin affects the elements in the blood and various tissues of rats. In this study, it was shown that pinealectomy significantly disrupts the metabolism of elements in the blood and various tissues of rats, and melatonin administration may have a regulatory effect on body element metabolism [23]. In our study, it was observed that the Se element value decreased during the 12 months period. This shows how effective hormone metabolism is on the Se element.

Magnesium is a macro element that participates in nerve conduction, muscle contracture and more than 300 enzymatic reactions [24]. Magnesium is the fourth in terms of quantity in the body, and the second most common cation after potassium intracellularly. Although it is found in all the cells, it has a higher concentration in the bones, muscles and soft tissues [24]. A study of the levels of trace elements in tissue in patients with myoma and uterine cancer shows that there was a significant increase in CA and Mg concentration in uterine cancer tissue compared to normal uterine tissue [25]. Chandra et al found that the addition of Mg increased the level of androgenic enzymes and testosterone [26]. In our study, Mg was significantly increased in 12 months.

Calcium is the most important element in the body and must be taken. It is also a cofactor of many enzymes. Testosterone increases the total amount of bone main substance (matrix), besides providing calcium accumulation. It is believed that the increase in the matrix is due to the anabolic effect of testosterone and the increase in Ca storage is due to the proliferation of bone matrix [16].

In the present study, it was observed that the level of Ca in the 12-month period was lower than the level of control and that it was influenced by GnRH hormone. In a study in which AI + GnRH (20μg) mixture was applied to cows for 3 months, the macro (Ca, P, Mg) and micro (Zn, Cu, Fe, Co, Mn) element levels were investigated and only Zn and Cu levels were changed [27]. The fact that the results of the studies we give in the light of this data are meaningful according to the results of the other studies may be due to the longer follow-up and the higher dose used.

CONCLUSIONS

As a result of the study, it was found that statistically significant changes were observed in trace elements for Cu, Fe levels at the 6th month after single dose GnRH and at Se, Zn Mn, Fe levels at 16th month. In addition, the macro elements K, P levels in the 6th month, and Ca, Mg levels in the 16th month produced statistically significant results. As a result, GnRH vaccine may be thought to have an effect on macro-element and trace element levels, and, depending on the dose and duration of use, interventions to the hormone system may cause long-term effects on metabolism.

REFERENCES

[1] Conforti, V.A., De Avila D.M., Cummings, N.S., Zanella, R., Wells, K.J., Ulker, H. (2008) CpG motif-based adjuvant as a replacement for Freund's complete adjuvant in a recombinant LHRH vaccine. Vaccine. 26, 907-913.

[2] Serin, G., Serin, İ. (2005) Immunocontrast methods 1. Zona Pellucida vaccines. IU School of Veterinary Journal. 31, 133-139.

[3] Kutzler, M., Wood, A. (2006) Non-surgical methods of contraception and sterilization. Theriogenology. 66, 514-525.

[4] Bloom, M.S., Kim, K., Kruger, P.C., Parsons, P.J., Arnason, J.G., Steuerwald, A.J. (2012) Associations between toxic metals in follicular fluid and in vitro fertilization (IVF) outcomes. Journal of Assisted Reproduction and Genetics. 29, 1369-1379.

[5] Ganjavi, M., Ezzatpanah, H., Givianrad, M.H., Shams, A. (2010) Effect of canned tuna fish processing steps on lead and cadmium contents of Iranian tuna fish. Food Chem. 118, 525-528.

[6] Papageorgiou, T., Zacharoulis, D., Xenos, D., Androulakis, G. (2002) Determination of trace elements (Cu, Zn, Mn, Pb) and magnesium by atomical absorption in patients receiving total parenteral nutrition. Nutrition. 18, 32-34.

[7] Hamzeh, M.A., Aftabi, A., Mirzaee, M. (2011) Assessing geochemical influence of traffic and other vehicle-related activities on heavy metal contamination in urban soils of Kerman city, using a GIS-based approach. Environ Geochem Health. 33, 577-594.
[8] Ravaglia, G., Forti, P., Maioli, F., Nesi, B., Pratelli, L., Savarino, L. (2000) Blood micronutrient and thyroid hormone concentrations in the oldest-old. J Clin Endocrinol Metab. 85, 2260-2265.
[9] Dhamsaniya, H.B., Parmar, S.C., Jadav, S.J., Bhatti, I.M., Patel, V.K. (2016) Plasma Minerals Profile in delayedpubertal Surti buffalo heifers treated with GnRH alone and with Phosphorus. Journal of Livestock Science (ISSN online 2277-6214). 7, 157-161.
[10] Tolunay, H.E., Şükür, Y.E., Ozkavukcu, S., Seval, M.M., Ateş, C., Türksoy, V.A. (2016) Heavy metal and trace element concentrations in blood and follicular fluid affect ART outcome. Eur J Obstet Gynecol Reprod Biol. 198, 73-77.
[11] Maldonado, J.G., Santos, R.R, Lara, R.R., Peña, O.G. (2017) Effect of injectable trace mineral complex supplementation on development of ovarian structures and serum copper and zinc concentrations in over-conditioned Holstein cows. Animal Reproduction Science. 181, 57-62.
[12] Geary, T.W., Kelly, W.L., Spickard, D.S., Larson, C.K., Grings, E.E., Ansotegui, R.P. (2016) Effect of supplemental trace mineral level and form on peripubertal bulls. Animal Reproduction Science. 168, 1-9.
[13] Zhang, F., Liu, N., Wang, X., Zhu, L., Chai, Z. (2004) Study of trace elements in blood of thyroid disorder subjects before and after 131I therapy. Biol Trace Elem Res. 97, 125-134.
[14] Bhardwaj, J.K., Sharma, R.K. (2011) Changes in trace elements during follicular atresia in goat (Capra hircus) ovary. Biol Trace Elem Res. 140, 291-298.
[15] Li, L., Liu, C., Lian, X. (2010) Gene expression profiles in rice roots under low phosphorus stress. Plant Mol Biol. 72, 423-432.
[16] Yılmaz, B. (1999) Hormones and Reproduction Physiology. Feryal Matbaacılık. ISBN 975-96982-0-X. 368-370.
[17] Adedara, I.A., Abolaji, A.O., Awogbindin, I.O., Farombi, E.O. (2017) Suppression of the brain-pituitary-testicular axis function following acute arsenic and manganese co-exposure and withdrawal in rats. J Trace Elem Med Biol. 39, 21-29.
[18] Qureshi, I.Z., Abbas, Q. (2013) Modulation of testicular and whole blood trace element concentrations in conjunction with testosterone release following kisspeptin administration in male rabbits (Oryctolagus cuniculus). Biol Trace Elem Res. 154, 210-216.
[19] Soni, D.K., Khasatiya, C.T., Rede, A.S., Chaudhary, S.S. (2015) Modulation of serum trace mineral profiles in post-partum acyclic surti buffaloes with GnRHalone and in combination with vitamin A, D3, E and toldimphos sodium preparation therapy. The Asian Journal of Anımal Science. 10, 124-131.
[20] Baysal, A. (2002) Nutrition. 9. Ed. Ankara: Hatiboğlu, 110-145.
[21] Liu, N., Liu, P., Xu, Q., Zhu, L., Zhao, Z., Wang, Z. (2001) Elements in erythrocytes of population with different thyroid hormone status. Biol Trace Elem Res. 84, 37-43.
[22] Behne, D., Weiler, H., Kyriakopoulos, A. (1996) Effects of selenium deficiency on testicular morphology and function in rats. J Reprod. Fertil. 106, 291-297.
[23] Köykun, Z. (2012) Effects of Pinealectomy and Melatonin on the Levels of Several Elements in Blood and Tissues in Rats. Master Thesis T.C. Selçuk University Health Sciences Institute. Konya.
[24] Ivy, J., Portman, R. (2004) The Future of Sports Nutrition: Nutrient Timing. anasci.org. Original Publisher's. 71-79.
[25] Nasiadek, M., Krawczyk, T., Sapota, A. (2005) Tissue levels of cadmium and trace elements in patients with myoma and uterine cancer. Hum Exp Toxicol. 24, 623-630.
[26] Chandra, A.K., Sengupta, P., Goswami, H., Sarkar, M. (2013) Effects of dietary magnesium on testicular histology, steroidogenesis, spermatogenesis and oxidative stress markers in adultrats. Indian Journal of Experimental Biology. 51(1), 37–47.
[27] Patel, K.R., Dhami, A.J., Savalia, K.K., Hadiya, K.K., Pande, A.M. (2014) Influence of Mid-Cycle Pg Treatment and Gnrh at AI on Plasma Minerals Profile in Conceiving and Non-Conceiving Repeat Breeding Crossbred Cows. The Indian Journal of Field Veterinarians. 10, 86.

Received: **05.03.2018**
Accepted: **29.04.2018**

CORRESPONDING AUTHOR

Leyla Mis
Department of Physiology,
Faculty of Veterinary Medicine,
Yuzuncu Yil University,
TR-65080 Van – Turkey

e-mail: leylaaslan23@hotmail.com

© by PSP Volume 27 – No. 7/2018 pages 5091-5095 Fresenius Environmental Bulletin

A NEW METHOD FOR THE SYNTHESIS OF PURINE AMINO THIOCARBAMYL PHOSPHATE

Qingling Liu*

Xinxiang University, Xinxiang, 453000, China

ABSTRACT

A new method for the synthesis of purine amino thiocarbamyl phosphate was developed. 6 -iodine -9 -benzyl purine was obtained from 6 -iodine -9 -benzyl purine and hydrogen iodate via substitution reaction. Then, toluene as solvent, the C6-I was substituted by commercially available silver thiocyanate at 110 ℃ for 12 h. Purine amino thiocarbamyl phosphate was first synthesized by C6-NCS purine and $HPO(OEt)_2$, which provides a new method for synthesizing.

KEYWORDS:
purine amino thiocarbamyl phosphate, synthesis, isothiocyanate, purine

INTRODUCTION

Isothiocyanates is ubiquitary structural functional class in many biological and pharmaceutical active compounds and it has been used as versatile important synthetic intermediates for the synthesis of many natural products and hetero cycles, such as thiohydantoins, thiopyrimidones, thioquinazolones, mercaptoimidizoles, thioamidazolones, pyridinethiones, pyrrolidine and benzothiazine [1]. Furthermore, isothiocyanates can be used as chemoselective electrophiles in bioconjugate chemistry [2].

Structurally diverse isothiocyanates including allyl isothiocyanate (AITC), phenethylisothiocyanate (PEITC), benzyl isothiocyanate (BITC) and sulforaphane (SF) are released from the corresponding glucosinolate precursors present in plants of the Brassicales order, including mustards, wasabi, broccoli, and garden cress [3]. The isothiocyanates display an impressive array of bioactivities including potentiation of insulin signaling [4], inhibition of cancer cell proliferation [5], antibacterial properties [6], TRP channel activation, the ability to induce neuritogenesis [7] and prevention of chemically-induced carcinogenesis [8,9]. In general, isothiocyanates are thiol-reactive chemicals that can modify critical cysteine residues on a variety of proteins [10–12]. In order to gain a better understanding of the molecular mechanisms underlying the myriad bioactivities of the isothiocyanates, it is important to explore potential protein targets of these compounds.

The synthesis of thiopurine has received much attention [13, 14], but the synthesis of purine amino thiocarbamyl phosphate has rarely been reported. In this paper, the first time the purine amino thiocarbamyl phosphate was synthesized by the reaction of purine iodine and silver thiocyanate. Purine amino thiocarbamyl phosphate was first synthesized by C6-NCS purine and $HPO(OEt)_2$. This method opens up a new path for the synthesis of thiopurine and also lays the foundation for the study of the activity of purine amino thiocarbamyl phosphate.

EXPERIMENTAL

Instruments and reagents. AC 400 magnetic resonance spectrometer ($CDCl_3$ solvent, TMS for the internal standard, the German company Bruker); Q-TOF MS / MS high-resolution mass spectrometry (Waters Corporation); XRC- 1-type micro melting point instrument (Sichuan University Scientific Instruments Plant.) 6-Chloro-9-benzylpurine was prepared beforehand and hydroiodic acid, silver thiocyanate, TiO_2, $HPO(OEt)_2$ were of commercial analytical grade and all other reagents used were used without further treatment.

Method of synthesis. In this paper, 6-chloro-9-benzylpurine and hydroiodic acid were used as raw materials to obtain 6-iodo-9- benzylpurine, then reacted with commercial silver thiocyanate directly at 110 ℃ for 12 h with toluene as solvent. 6-isothiocyanate purine was obtained. Purine amino thiocarbamyl phosphate was first synthesized by C6-NCS purine and $HPO(OEt)_2$.

Synthesis of 6-iodo-9-benzylpurine. Weigh 1 mmol of 6-chloro-9-benzyl purine into a 25 mL round bottomed flask and add 2.5 mmol of hydrogen iodide to it. Add 10 mL of distilled water to the solution and react at 0 ° C for 24 h h, after the reaction was completed to room temperature, suction filtration to give 6-iodo-9-benzyl purine.

TABLE 1
The effect of reaction solvent on the yield

Solvent	Ethanol	Acetonitrile	DMSO	Toluene	Dichloromethane	DMF
Yield (%)	0	0	48	89	0	76

Synthesis of 6-isothiocyanate purine. Weigh 1 mmol of 6-iodo-9-benzyl purine in a 25 mL round bottom flask, add 2 mmol of silver thiocyanate and 15 mL of toluene as solvent and reflux for 12 h until the reaction is complete, Cooled to room temperature and filtered to give 6-isothiocyanate-9-benzylpurine as a white solid.

Synthesis of prine amino thiocarbamyl phosphate. Purine amino thiocarbamyl phosphate was first synthesized by C6-NCS purine and $HPO(OEt)_2$.

Experiment method. Test Method Test The main study in Figure 1, the second step by the 6-iodine - 9-benzyl purine and silver thiocyanate reaction synthesis. The reaction conditions of 6-isothiocyanate-9-benzylnitrite, including the reaction time of the reaction solvent and the effect of the ratio of the raw materials on the yield.

Reaction solvent was set to 9 h reaction time, the ratio of raw materials 1: 2, were investigated ethanol, methylene chloride,

Effect of Acetonitrile, DMSO, Toluene and DMF on the Reaction Yield. Reaction time use the best reaction solvent, the ratio of raw materials 1: 2, 3, 6, 9, 12, 15 h on the yield were investigated reaction.

The best reaction time of the best reaction solvent was selected, Effect of 1: 2.5 on reaction yield

RESULTS AND DISCUSSION

Effect of the reaction solvent on the yield. The results of the study are shown in the Table 1.

As can be seen from Table 1: dichloromethane, ethanol, acetonitrile, these low-boiling point solvents can not reach the desired reaction temperature, the reaction can not be carried out; DMSO due to post-processing difficulties, the yield was only 48%; DMF yield can reach 76% Toluene solvent was more efficient, the yield reached 89%.

Effect of the reaction time on the yield. Using 1 mmol 6-iodo-9-benzyl purine as template and toluene as solvent, the reaction time was changed and the reaction time was investigated. The results are shown in Table 2.

As can be seen from Table 2, with the progress of the reaction, the yield gradually increased, the reaction was slow for the first 6 hours, the peak reached the peak from the 6th hour to the 12th hour, and the yield reached 87% 15 h, the yield began to decline.

TABLE 2
The effect of reaction time on the yield

Time (h)	3	6	9	12	15
Yield (%)	25	36	74	89	85

Effect of the raw material proportion on the yield. Raw material ratio to 1 mmol 6-iodo-9-benzyl-purine as a template to change the amount of silver thiocyanate to examine the effect of raw material ratio on the yield, the results in Table 3.

TABLE 3
The effect of raw material proportion on the yield

n(C6-I):n(Ag SCN)	1:1	1:1.5	1:2	1:2.5
Yield (%)	57	77	88	81

Table 3 shows that when the ratio is 1: 1, the yield is only 57%; the amount of silver thiocyanate is increased by 2 times and the yield is up to 88%; continuing to increase the amount of silver thiocyanate instead the yield was decreased. The optimum conditions for the experiment were as follows: toluene as solvent, the reaction for 12 h, the ratio of raw materials was 1: 2, the highest yield reached 88%.

Study on Box-Benhnken. Total yield (%) = 53.2 + 12.48 A - 0.51 B + 0.78 C + 20.0 A*A - 9.6 B*B- 6.5 C*C + 1.5 A*B + 12.4 A*C + 5.7 B*C

Three factors at three level central composite rotatable response surface design was used to investigate the influence of process variables on the yield. To understand the interaction between the independent variables and estimate the yield over independent variables, three-dimensional (3D) response surfaces were obtained by Design-Expert Fig.1.

Effect of factors on the yield. As seen from Fig. 2, the yield increased as proportion increased.

As seen from Fig. 3, the yield increased as proportion increased.

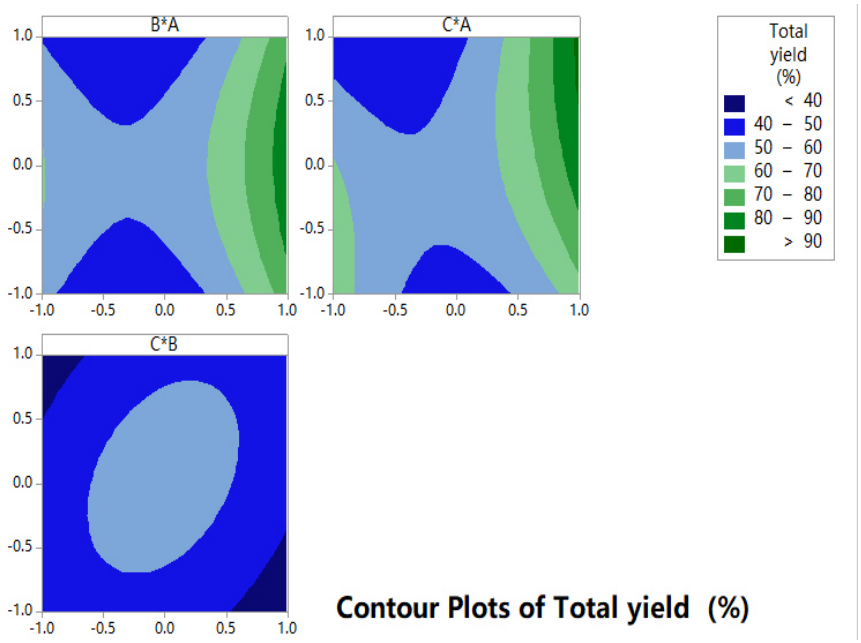

FIGURE 1
Contour plot

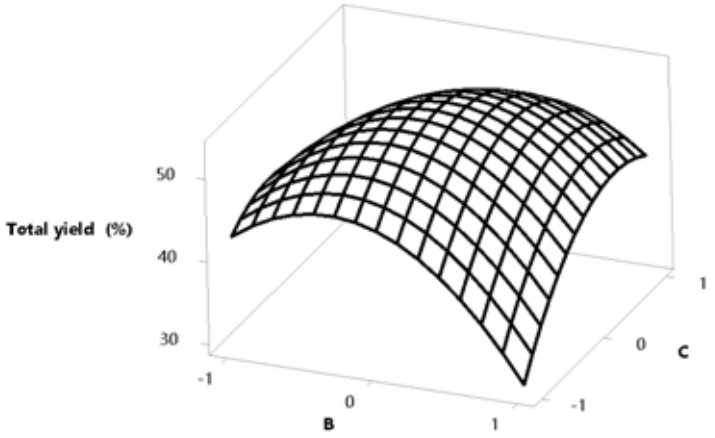

FIGURE 2
Effect of proportion and reaction time on the yield

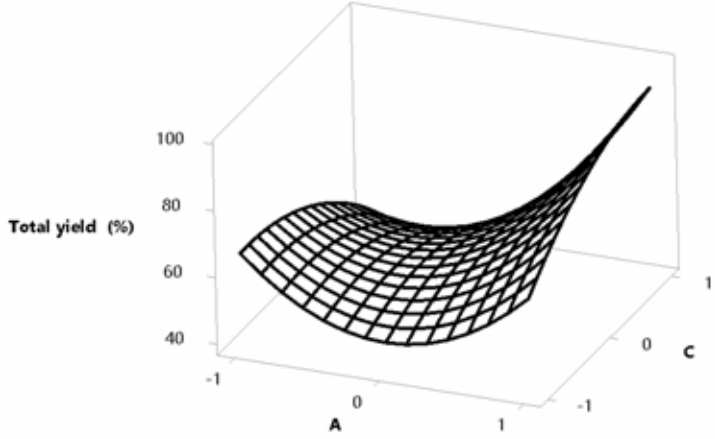

FIGURE 3
Effect of proportion and reaction solvent on the yield

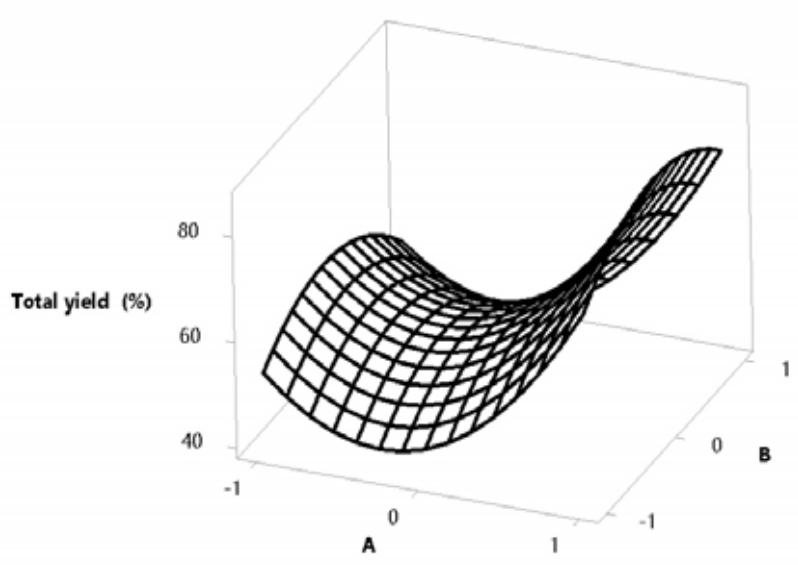

FIGURE 4
Effect of reaction solvent and reaction time on the yield

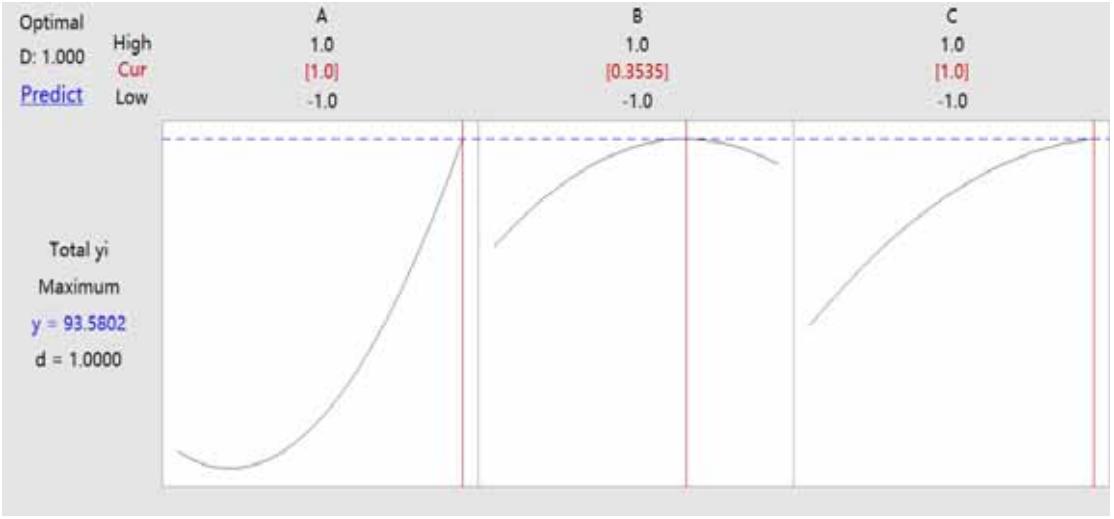

FIGURE 5
Optimization of the yield

As seen from Fig. 4, the yield increased as reaction solvent increased.

It is obtained from model optimization and calculation that: Toluene (15 mL), reaction time (7.05 h), proportion (1:2). The maximal yield is 93.58%.

CONCLUSION

In conclusion, 6-iodo-9-benzylpurine was obtained from 6-chloro-9-benzylpurine and hydroiodic acid, and then reacted with silver thiocyanate by using toluene as solvent to obtain 6-isothiocyanate Cyanuric acid purine. Purine amino thiocarbamyl phosphate was first synthesized by C6-NCS purine and $HPO(OEt)_2$. This method is the first synthesis of 6-isothiocyanate substituted purine, the reaction process to avoid the harsh conditions of the traditional iodide. The method is easy to get raw materials, easy to operate, isothiocyanate substitution. The synthesis of purines and their analogs provides a new approach.

In this study, BBD was proved to be useful for optimization the yield. The statistical analysis based on a BBD design showed that the optimum conditions were found to be oluene (15 mL), reaction time (7.05 h), proportion (1:2). The maximal yield is 93.58%.

ACKNOWLEDGEMENTS

This paper is supported by the first batch of scientific and technological innovation and development program in Xinxiang (No. CXGG16032).

REFERENCES

[1] Tang, P.X., Sun, G. (2018) Highly sensitive colorimetric paper sensor for methyl isothiocyanate (MITC): Using its toxicological reaction. Sensors and Actuators B: Chemical. 261, 178-187.

[2] Mandapati, U., Pinapati, S., Rudraraju, R. (2017) Copper promoted desulfurization towards the synthesis of isothiocyanates. Tetrahedron Letters. 58, 125-128.

[3] Steinmetz, K.A., Potter, J.D. (1996) Vegetables, fruit, and cancer prevention: a review. Journal of the American Dietetic Association. 96, 1027- 1039.

[4] Gao, L., Zhao, Z.Y., Zheng, X.H., Shi, G.L., Zhang, H.J. (2015) Cost-effectiveness analysis of capecitabine plus docetaxel versus epirubicin plus docetaxel for advanced or metastatic breast cancer. Chin J Mod Appl Pharm. 32, 493- 497.

[5] Dimopoulou, A., Mant, S., Parmenopoulou, V., Gkizis, P., Coutouli-Argyropoulou, E., Schols, D., Komiotis, D. (2015) Synthesis of novel thiopurine pyranonucleosides: evaluation of their bioactivity. Nucleosides Nucleotides and Nucleic Acids. 34, 289- 308.

[6] Elion, G.B. (1989) Nobel lecture in physiology or Medicine- 1988. The purine path to chemotherapy. Vitro Cellular and Developmental Biology Journal of the Tissue Culture Association. 25, 321- 330.

[7] Agerbirk, N., Nicola, G.R.D., Olsen, C.E., Müller, C., Iori, R. (2015) Derivatization of isothiocyanates and their reactive adducts for chromatographic analysis. Phytochemistry. 118, 109-115.

[8] Rytwo, G., Moshe, S.B. (2017) Evaporation of allyl isothiocyanate from clay minerals and organoclays. Applied Clay Science. 137, 30-32.

[9] Revelou, P.K., Kokotou, M.G., Pappas, C.S., Constantinou-Kokotou, V. (2017) Direct determination of total isothiocyanate content in broccoli using attenuated total reflectance infrared Fourier transform spectroscopy. Journal of Food Composition and Analysis. 61, 47-51.

[10] Cinar, M., Karabacak, M., Chand, S., Shukla, V.K. (2015) Conformational and spectroscopic behaviors of 2,4-xylyl isothiocyanate. Journal of Molecular Structure. 1087, 113-120.

[11] Fratoddi, I., Cartoni, A., Venditti, I. (2018) Gold nanoparticles functionalized by rhodamine B isothiocyanate: A new tool to control plasmonic effects. Journal of Colloid and Interface Science. 513, 10-19.

[12] Zhang, C., Ma, Z.Q., Zhang, X., Wu, H. (2017) Transcriptomic alterations in Sitophilus zeamais in response to allyl isothiocyanate fumigation. Pesticide Biochemistry and Physiology. 137, 62-70.

[13] Mautner, F.A., Berger, C., Fischer, R.C., Massoud, S.S., Vicente, R. (2018) Synthesis, structural characterization and magnetic properties of Mn(II) isothiocyanate complexes based on pyridine-N-oxide derivative co-ligands. Polyhedron. 141, 17-24.

[14] Upadhyaya, P., Zarth, A.T., Fujioka, N., Fritz, V.A., Hecht, S.S. (2018) Identification and analysis of a mercapturic acid conjugate of indole-3-methyl isothiocyanate in the urine of humans who consumed cruciferous vegetables. Journal of Chromatography B. 1072, 341-346.

Received: **05.03.2018**
Accepted: **29.04.2018**

CORRESPONDING AUTHOR

Qingling Liu
Xinxiang University,
Xinxiang, 453000 – China

e-mail: liuqingling888@outlook.com

© by PSP Volume 27 – No. 7/2018 pages 5096-5106 Fresenius Environmental Bulletin

CLIMATE CHANGE RECORD IN THE PRIMARY PRODUCTIVITY OF DALI-NOR LAKE SINCE 2100 CAL A BP

Zhilei Zhen [1,2], Wenbao Li [2,*], Changyou Li [2]

[1]College of Urban and Rural Construction, Shanxi Agricultural University, Taigu 030800, China.
[2]College of Water Resources and Civil Engineering, Inner Mongolia Agricultural University, Hohhot 010018, China

ABSTRACT

Lakes close to the limit of the East Asia summer monsoon (EASM) are sensitive to climate fluctuations, which records significant information about environmental changes. Here, one 200-cm sediment core was collected from Dali-Nor Lake on the northern margin of the EASM in China and high-resolution multi-proxies were analyzed. The constant rate of supply (CRS) model based on ^{137}Cs and ^{210}Pb contents, which combined calibrated ages (AMS^{14}C) with the 2σ error, provided a detailed history of the primary productivity and EASM changes over the past 2100 cal a BP. The primary productivity (P2) was calculated based on the proportion of $\delta^{13}C_{org}$ in authigenic and terrigenous organic carbon. Total organic carbon (TOC), total nitrogen (TN), total phosphorus (TP) and $\delta^{13}C_{org}$ in the sediment core suggested a decreasing EASM since 2100 cal a BP. Further, P2 showed a drastic fluctuation due to the temperature and nutrient variations caused by the EASM and we could also observe a decreasing trend based on P2. Compared to the EASM, precipitation from the winter monsoon (WM) had no significant impact on primary productivity variations. The higher values of P2 during the periods of 1700-1550 cal a BP, 1400-1250 cal a BP, 1100-850 cal a BP and 500-350 cal a BP indicated that the Dali-Nor Lake basin may have been greatly affected by ENSO events during these periods.

KEYWORDS:
Primary productivity, Sediment, East Asian summer monsoon, winter monsoon, Dali-Nor Lake

INTRODUCTION

Lakes located on the north margin of the East Asian summer monsoon (EASM) in China are sensitive to regional climate change. They are considered as ideal sites for reconstruction of process variations in the paleoclimate and paleoenvironment [1-3]. As a fact, the physical and chemical conditions in north of China leave a very short growing season (generally ice - covered half of the year) for aquatic organisms. Therefore, the role of climate is very important.

The nutrient concentrations will be limited by the inflowing water that primarily originates from runoff of melting ice, snow and springs. The runoff transports more silt, salt, organic and inorganic particles in summer, as well as atmospheric deposition of substances into the lake. Due to the fact that low nutrient availability in the shorter summer days, the relatively lower average temperatures will limit the species richness and a lower primary production will be present [4]. Furtherly, organic matter (OM) in lake deposits only record a fraction of the total biological productivity in surface waters of the lake. Export productivity is the part of the phytoplankton biomass that "escape" from the generally efficient recycling presenting in the surface water, and then delivered to the sediment–water interface following additional degradation [5]. However， it displays a correlation between the final burial flux and surface water productivity despite the complications redox conditions. It is relatively facile to illuminate that primary production can be affected by climate change depend on short duration instrumental records [6]. Similarly, many lakes sediments record major climate events at a longer time scales, for example, the termination of Pleistocene glacial conditions and onset of Holocene warming, or the shorter duration changes associated with the beginning and end of the Younger Dryas, by dramatic changes in trophic state and total productivity [7-9]. From the above, variations in productivity and source of OM to lake can provide clues as to how the lake responded to changes in palaeohydrology and palaeoclimatic events [10].

In present study, Dali-Nor Lake (Dali Lake hereafter) is selected as the research object, which close to the north margin of EASM. The lake productivity and natural linkages with climate has receive a little attention in Dali Lake basin over past 2100yr, although some palaeolimnology investigations and valuable information has been conducted on Dali lake level evolution [11-13] and environment variations [14]. Here, we determined high-resolution environment proxies and focus on variability on decadal time-scales in lacustrine sediments of Dali Lake. And, two computational methods coupled with geochemical proxies to illuminate levels of primary production during the Late Holocene. The overall objective of this paper was to develop an understanding of

the history of climate changes around the basin and the driving mechanism to provide a sound scientific basis for local environmental protection at present and prediction for future development of the climate in north China.

MATERIALS AND METHODS

Study area. Field surveys indicate that the landform in the western region of the lake comprises a lava terrace and basalt gravel. Parts of the area in the north and inner parts of the lake contain volcanic gravel and metamorphic rocks. The lake water is mainly recharged by four rivers (Figure 1). Virtually no discharge routes exist except for surface water evaporation. The area is also regarded as a karst-dammed lake. The climate is mainly influenced by westerly winds and the EASM. The average annual precipitation is approximately 300 mm [15], and the average annual evaporation is 1425.3 mm. Rainfall mainly occurs from June to August because of the EASM, which provides approximately 70% of the annual precipitation during this period. The maximum ice thickness is around 1.0 m, and an additional of 0.2 m snow layer may cover the ice, which will prevent light penetration. There are few vascular plant species distributing along the shores and are typically low in abundance.

Sampling and testing. A 238-cm-long sediment core (43°19′20″ N, 116°39′43″ E), DL-1, was collected with a gravity corer (ZL 2015 1 0161906.6) from the center of Dali Lake in February 2015 at an 8-m-deep site (Figure 1). The upper 200 cm of the sediment core was divided at intervals of 2-cm for laboratory analyses.

Environment proxies in lacustrine sediment were measured at the State Key Laboratory of the Nanjing Institute of Geography and Limnology at the Chinese Academy of Sciences. Total nitrogen (TN%), total phosphorus (TP%) and total organic carbon (TOC%) were measured by an EA3000 elemental analyzer (Euro Vector, Italy). Organic carbon stable isotopes ($\delta^{13}C_{org}$) were analyzed by a Delta V Plus Mass Spectrometer and a Thermo Flash EA Elemental Analyzer equipped with a ConFlo Ⅲ system. Isotopic values are relative to the Vienna Pee Dee Belemnite (V-PDB).

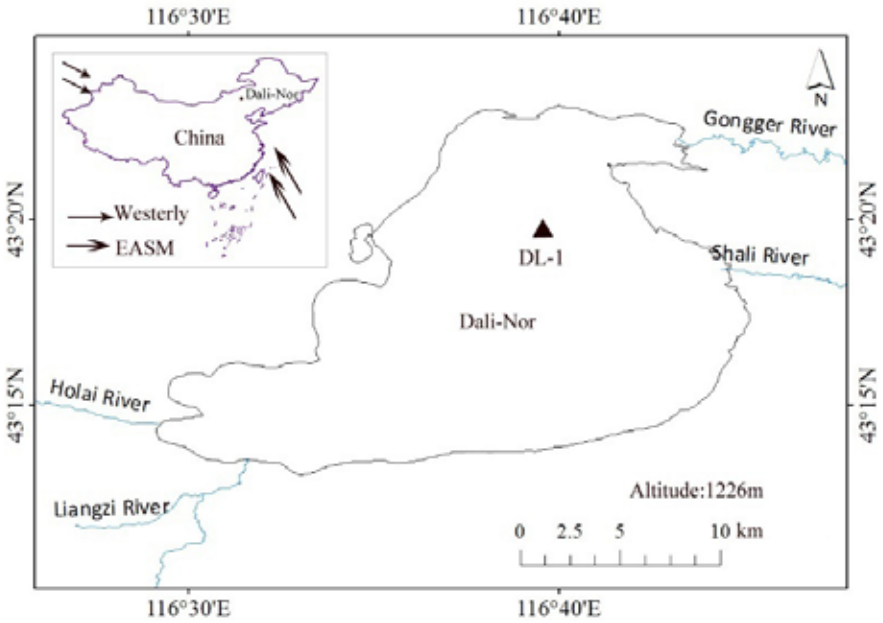

FIGURE 1
Dali Lake location and DL-1 sediment core

TABLE 1
Samples used for AMS radiocarbon age dating

Laboratory number	Depth interval (cm)	Dating material	AMS ^{14}C age (^{14}C a BP)	Calibrated ^{14}C age (2σ) (cal a BP)	$^{210}Pb_{ex}$ and ^{137}Cs dating results (cal a BP)
	0	Organic matter			-65*
	18	Organic matter			0*
BA150369	100-102	Organic matter	1415±25	1354-1290	
BA150370	150-152	Organic matter	1635±25	1606-1417	
BA150371	200-202	Organic matter	2090±30	2145-1991	

* The DL-1 core was obtained in 2015 AD. Therefore, the core surface was 2015 AD (-65 cal a BP) and the 18-cm-depth interval was inferred to be 1950 AD (0 cal a BP).

The $^{210}Pb_{ex}$ and ^{137}Cs values of the 30 samples under the DL-1 core surface were measured at the State Key Laboratory of the Nanjing Institute of Geography and Limnology by following the method described by Wu et al. [16] and Bai et al. [17]. Three radiocarbon samples were used for dating at the Accelerator Mass Spectrometry (AMS) facility at the Laboratory of Quaternary Dating, Peking University (Table 1). Organic carbon was extracted and dated from samples following the method described by Xiao et al. [11], and the OxCal3.1 radiocarbon age calibration program [18] with IntCal04 calibration dating [19] was applied to convert the conventional ages to calibrated ages. The ^{14}C ages of the sediment samples were measured with a half-life of 5,568 years.

Primary productivity. In this study, two methods were selected to calculate the authigenic carbon. 1) The first method is based on the method of Qian and Chen [20], Equations (Eq.):

$$\%TOC = \%C_a + \%C_t \quad (1)$$

$$\%TN = \%N_a + \%N_t \quad (2)$$

$$\%C_a / \%N_a = 8 \quad (3)$$

$$\%C_t / \%N_t = 25 \quad (4)$$

where $\%C_a$ is the authigenic organic carbon; $\%N_a$ is the authigenic organic nitrogen; $\%C_t$ is the terrigenous organic carbon; $\%N_t$ is the terrigenous organic nitrogen; and $\%TOC$ and $\%TN$ are the measured values. The end member C/N value in the organic matter (OM) from the aquatic environment is supposed to be 8 but is 22 due to terrigenous material [14, 21].

2) The second method for calculating the authigenic carbon is based on the method of Cai et al. [22], Eq.:

$$\delta^{13}C_S = f_a \cdot \delta^{13}C_a + f_t \cdot \delta^{13}C_t \quad (5)$$

$$f_a + f_t = 1 \quad (6)$$

$$C_a = f_a \cdot C_S \quad (7)$$

where $\delta^{13}C_s$ is the measured value of samples in core DL-1; f_a is authigenic organic carbon percentage (%); f_t is terrigenous organic carbon percentage (%); $\delta^{13}C_a$ is the end member value of authigenic organic carbon; $\delta^{13}C_t$ is the end member value of terrigenous organic carbon; C_a is the authigenic organic carbon content; and C_s is the total organic carbon content in samples. The end member $\delta^{13}C_{org}$ value is supposed to be -28‰ from terrigenous matter and -20% from authigenic matter [23].

Finally, the primary productivity (P: g C m^{-2} a^{-1}) is calculated following by Müller and Suess [24], Eq.:

$$P = (\%C_a \times D)/(0.0030 \times S^{0.3}) \quad (8)$$

where $\%C_a$ is the authigenic organic carbon content; D is the dry density (g·cm^{-3}); and S is the sedimentation rate (cm·ka^{-1}).

RESULTS

Core chronology. It shows the vertical distribution of the $^{210}Pb_{ex}$ and ^{137}Cs contents in the DL-1 sediment profile in Figure 2. The $^{210}Pb_{ex}$ activity at a depth of 2.5 cm reached the maximum 277.36 Bq kg^{-1}. It generally shows a decreasing trend between the depths of 7.5 cm and 27.5 cm, at which the minimum of 7.78 Bq kg^{-1} is reached. Moreover, the DL-1 sediment core has less interference, and it is preserved completely. Given that the outcome of the atmospheric testing of nuclear weapons occurs on a global scale, the presence of a subsurface peak in the concentration identifies 1963 AD in most cases. At sites where fallout from the Chernobyl accident exists, the presence of a second recent peak identifies 1986 AD [25]. The ^{137}Cs contents are within the scope of 42.5 Bq kg^{-1}. A typical concentration peak

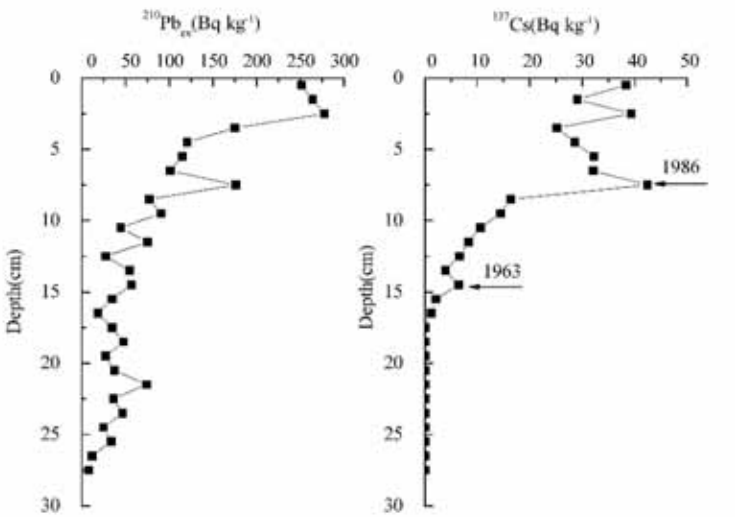

FIGURE 2
$^{210}Pb_{ex}$ and ^{137}Cs distribution in the DL-1 core

exists at a depth of 7.5 cm in the DL-1 profile, and it corresponds to the nuclear leak in the former Soviet Union in 1986 AD. The ^{137}Cs residue exists at a depth of 16.5 cm, and this finding
indicates the beginning of global nuclear testing in 1954 AD. Then, the first peak appears at 14.5 cm, which indicates the outbreak of global nuclear testing in 1963 AD.

The ^{137}Cs time mark and result of the constant rate of supply (CRS) model show a high degree of coincidence (Figure 3). Therefore, the CRS model would be selected in this study. According to the results of $^{210}Pb_{ex}$ and ^{137}Cs (Figure 2), the upper 18-cm of the core was 1950 AD, which could be regarded as 0 cal a BP according the AMS ^{14}C dating. And then the core surface could be defined as -65 cal a BP.

Calibrated ages with a 2σ error combined with the results of the CRS model were used to produce an age-depth model with a linear fit for the upper 200 cm of the DL-1 sediment core (Figure 4), which span the past 2100 years. An average sedimentation rate of approximately 95 $cm \cdot ka^{-1}$ in sediment core DL-1 indicates that a sampling interval of 1 cm provides a temporal resolution of approximately 11 year.

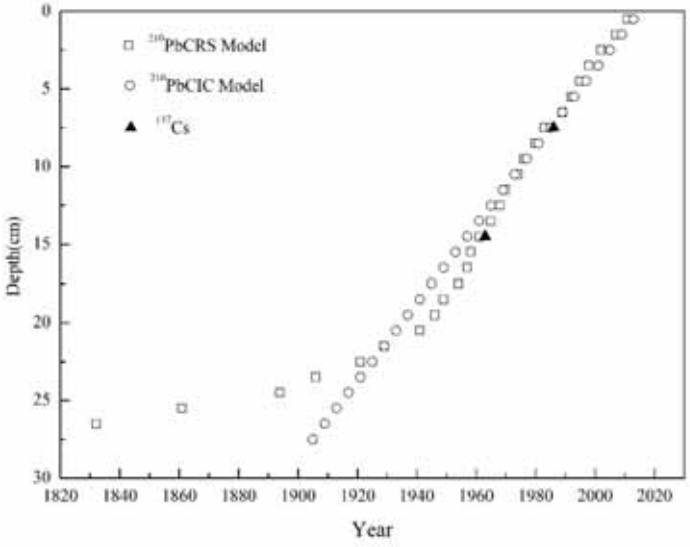

FIGURE 3
^{210}Pb CRS and ^{210}Pb CIC model

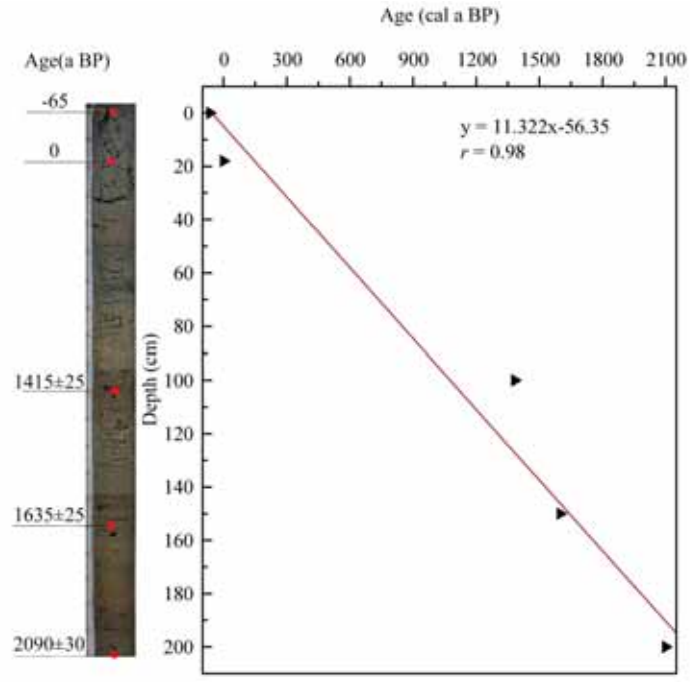

FIGURE 4
Age-depth model

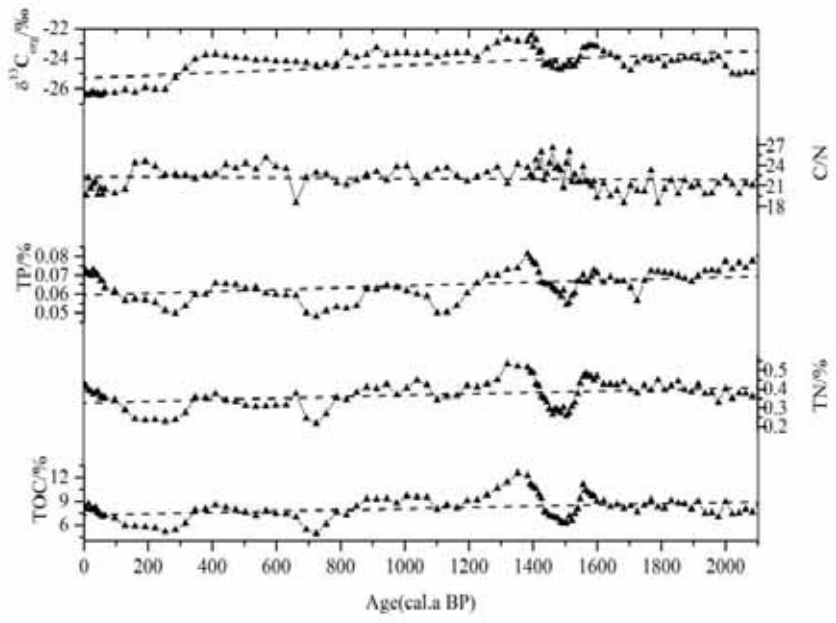

FIGURE 5
Distribution characteristics of environmental proxies in the DL-1 core from Dali Lake. Dashed line indicates the change trend over the past 2100 cal a BP

It is worth noting that the age-depth model in this study is different from those in Xiao et al. [11] and Fan et al. [14], in which the reservoir ages were 611 years and 472 years, respectively. Accurate AMS^{14}C ages may be difficult to obtain due to the scarcity of terrestrial macrofossils or plant debris in the core sediments. However, the study on the terminal Zhuyeze Lake in north China suggested that the reservoir effect did not exist [26]. In this study, the reasons why the reservoir effect was not discussed are as follows:

1) The average depth is 8 m at the sampling site. It can be inferred from the lake shoreline that the lake was much deeper in the past. There are no plants growing in the lake, and thus, the dating results would not be affected by plants.

2) Field investigations suggested that poor carbonate was spread over the Dali Lake basin. Therefore, the content of carbonate including recalcitrant carbon or dead carbon in the lake body was very low, and the ^{14}C radioactivity in the lake body would be similar to the ^{14}C radioactivity in the atmosphere during the same period.

3) The DL-1 core in this study was on a short time scale compared to those in Xiao et al. [11] and Fan et al. [14]. In addition, the AMS^{14}C age in the surface of the DL-1 core was replaced by accurate dating results of $^{210}Pb_{ex}$ and ^{137}Cs.

4) It is obvious that the Dark Ages Cold Period (DACP) was observed and the Little ice age period (LIA) could also be recorded in the DL-1 core [27, 28] (Figure 5).

Organic fraction. TOC (%) reflects the quantity of OM present in the sediment. The content of TOC in sediment core DL-1 change from 4.93% to 12.55%, with an average value of 8.15%; the content of TN range from 0.22% to 0.54%, with an average value of 0.37%; TP vary from 0.048% to 0.081%, with an average of 0.065%; and C/N range from 18.45 to 26.44, with an average of 22.05. TOC, TN and TP showed similar fluctuation variations of a decreasing trend (Figure 5).

The average depth of Dali Lake is 8.0 m, and there is no aquatic plant growing in the center. There are only a few aquatic plants distributed in the northeastern area of the lake. In addition, the influences of aquatic plants on the value of $\delta^{13}C_{org}$ are not considered in this study. As shown in Figure 5, the value of $\delta^{13}C_{org}$ vary from -22.49‰ to -26.47‰, with an average value of -24.33‰, which also show a decreasing trend since 2100 cal a BP.

DISCUSSION

The meaning of TOC, TN and δ^{13}Corg. The TOC content was typically used to reconstruct the primary productivity in lakes [29]. In general, an increase in primary productivity, terrestrial input and OM reserve may increase the content of TOC in sediments [30]. Research from Tyson [31] suggested that TOC content would not be affected by the sedimentation rate when the sedimentation rate was greater than 35 cm ka^{-1}, whether it was anaerobic or aerobic at the lake bottom. The result of 95 cm · ka^{-1} in this study indicates that TOC content had nothing to do with the sedimentation rate. The TOC was mainly affected by terrestrial input from the TOC/TN (Figure 5). In addition, the value of $C_{organic}/N_{total}$ was sometimes changed by inorganic nitrogen [32], which would lead to a misjudgment of the

material source. In this study, a linear regression between TN and TOC in the DL-1 sediment core indicated the inorganic nitrogen content in the DL-1 sediment core was too low (TOC = 0, TN = 0.02; Figure 6) and that it could be ignored [33].

The $\delta^{13}C_{org}$ and C/N values were generally affected by early diagenesis in the lake sediments. During the process of sediment storage, the value of $\delta^{13}C$ would be reduced because of diagenesis [34]. Meanwhile, nitrogen (N) was preferentially mineralized compared to carbon (C) under the effect of early diagenesis. As shown in Figure 5, the values of TOC/TN were higher in the lower part of the DL-1 core than in the upper part. In addition, the $\delta^{13}C_{org}$ values were more positive in the lower part of the DL-1 core. Therefore, the DL-1 core in this study was inferred to be rarely affected by early diagenesis. In addition, there was a good linear relation between $\delta^{13}C_{org}$ and C/N, which can indicate changes in lake productivity, lake area and lake nutritional status. The $\delta^{13}C_{org}$ values in sediments are much higher, and the climate is much warmer. The lower these values, the colder the climate [35]. Thus, the climate showed a trend of cooling in the Dali Lake basin since 2100 cal a BP.

Primary productivity based on two methods. The results of the primary productivity calculated by the two methods showed obvious differences. As shown in Figure 7, the authigenic carbon content from the first method ranged from 0 to 1.38% since 2100 cal a BP, with an average value of 0.54%, and the primary productivity (P1) calculated based on the value of authigenic carbon varied between 0 and 115 g C m^{-2} a^{-1}, with an average of 45.55 g C m^{-2} a^{-1}. Authigenic carbon calculated based on the second method ranged between 1.25% and 8.08%. The value of primary productivity (P2), with an average of 338.55 g C m^{-2} a^{-1}, is distinctly higher than P1.

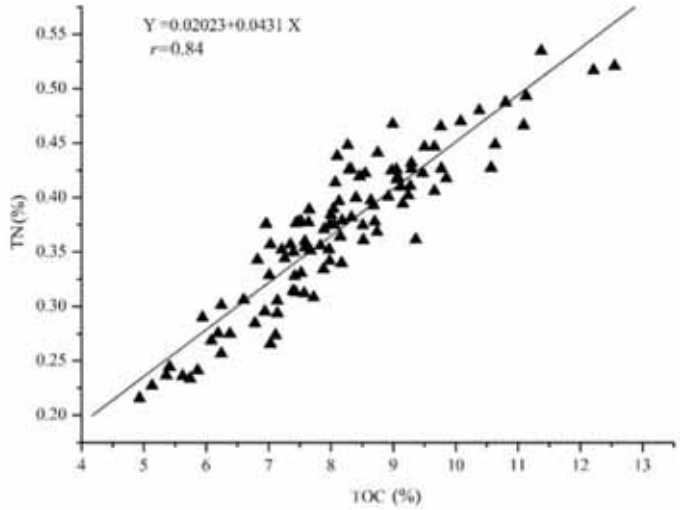

FIGURE 6
Linear regression between TOC and TN in the DL-1 core

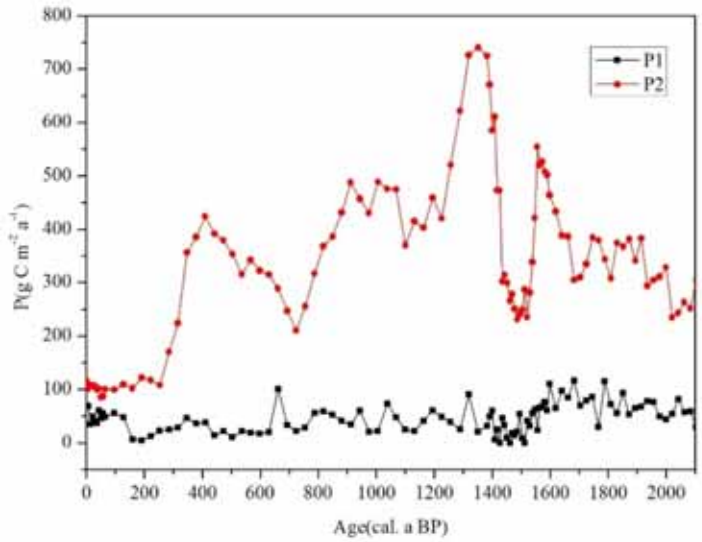

FIGURE 7
The distribution of primary productivity (P1 and P2) recorded in the DL-1 core

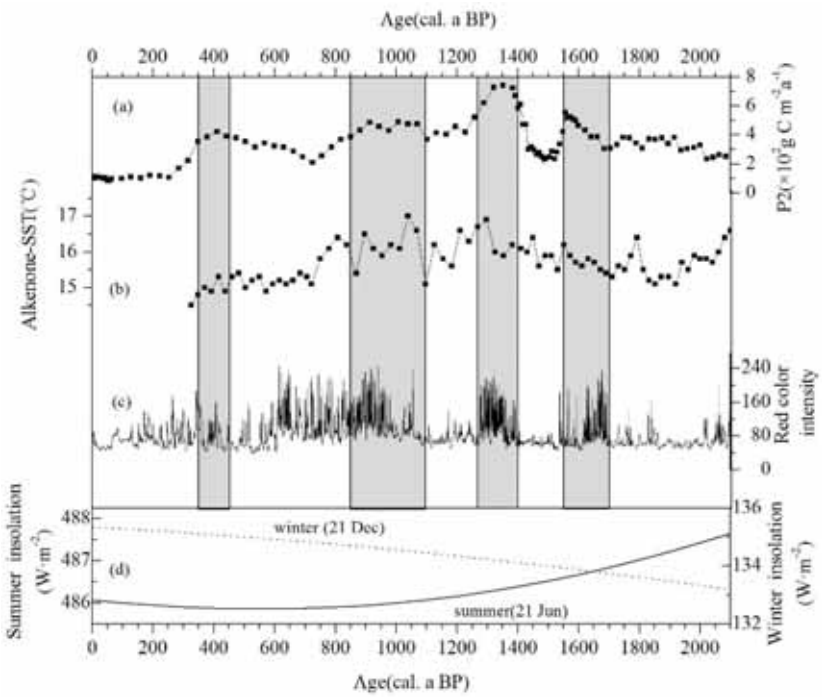

FIGURE 8

a. Primary productivity (P2) results in the DL-1 core for the past 2100 cal a BP; b. Alkenone SST record for core PC6; c. Most recent 2100 cal a BP for the time series of red-colored intensity; d. The summer (solid line) and winter (broken line) daily insolation at 43°N in the Northern Hemisphere for the last 2100 years. Gray band indicated the ENSO events

Dali Lake has been under the condition of eutrophication in recent years [36]. Meyers [37] suggested that the primary productivity ranged from 100 to 310 g C m^{-2} a^{-1} in the mesotrophic lake and from 370 to 640 g C m^{-2} a^{-1} in the eutrophic lake. Most of the reconstructed P1 values in the DL-1 sediment core were much lower than the boundary value of 100 g C m^{-2} a^{-1} (Figure 7). This indicated that there was a low mesotrophic level in Dali Lake, even with no history of eutrophication, which contradicted recent research. In addition, the fluctuation of P2 was basically consistent with the trends of the TN, TP and TOC. Therefore, the results of P2 would be applied for discussion in this study.

Factors impacting primary productivity. It was suitable for plankton to breed largely when the climate was warm and humid, and the primary productivity in the lake would increase. Specifically, factors that would impact the variations in the primary productivity included light, temperature, nutrients and hydrodynamic conditions. There was a close relationship between the temperature and chemical reaction in biological metabolism. Proper temperature in the lake could promote a biological enzymatic reaction and enhance the biological metabolic rate. When the water temperature increased by 10°C, the cell division rate became 1-3 times higher than usual [38]. Jiang et al. [39]suggested that the dry and cold climate would lead to a reduction in the temperature of the lake surface, which would contribute to the decrease in algae biomass and authigenic OM in the lake sediments. Therefore, the periods of higher primary productivity recorded in the Dali Lake sediments would indicate a warm climate. Compared to temperature, nutrients were the necessary energy and source of material synthesis during the process of phytoplankton growth [40]. The result of the C/N ratio (Figure 5) in this study indicated that nutrients mainly originated from terrestrial input, which was controlled by a varied, large-scale physioclimate, such as the EASM and westerly winds. An enhanced EASM leads the humidity to increase in the Dali Lake basin and leads to a warmer climate. Therefore, variation in the primary productivity can be used to indicate changes in the EASM. In addition, plants and animals are active before the ice has melted [41]. The enhanced influx of light in April means that sufficient light can penetrate the snow and ice layer for photosynthesis and a consequent phytoplankton biomass increase. It shows that light is the limiting factor for primary production prior to ice–out compared with water temperature. While the ice slowly melts, the phytoplankton growth increases, primarily because the high nutrient concentrations input by runoff. Above all, light was not a limiting factor for primary production compared with others. It can be also suggested by solar insolation variation at 43°N in the Northern Hemisphere [42], Dali Lake is located (Figure 8d), which could satisfy the aquatic organisms growth needs since 2100 cal a BP.

Driving mechanism of climate changes. Researchers have suggested that the climate during the Holocene became cold and dry [43, 44], which may relate to the summer solar insolation decrease over the past 11500 years [45]. In this study, the results (Figure 8d) indicated summer solar insolation at 43°N in the Northern Hemisphere has been decreasing since 2100 cal a BP. This demonstrated that the EASM, which was controlled by solar insolation in the Dali Lake basin, was gradually decreasing. However, winter insolation (Figure 8d) gradually increased at 43°N in the Northern Hemisphere since 2100 cal a BP. This indicates an enhanced winter monsoon (WM). The possibility of a cold wave break would increase with an enhanced WM. Subsequently, this could induce snow storm events in the winter and dust storm events in the spring [46]. However, the extreme snowfall in the most recent 30 years in central eastern Inner Mongolia was only 17.41 mm [47], which was much less than the average annual precipitation total of 300 mm. Therefore, compared to the EASM, the precipitation from WM had no significant impact on the primary productivity in Dali Lake.

It is well known that the interannual climate changes in East Asia are significantly related to ENSO circulation [48]. Research indicated ENSO during the first year had a negative relationship with precipitation in north China but had a positive relationship with precipitation in southern coastal China [49]. Therefore, it would be hysteretic in response to ENSO events in northern China, which may relate to the anomalous positive pressure cyclone replacement toward southwest moisture [50]. In fact, the EASM was influenced by ENSO mainly through regulating the monsoon trough in the western North Pacific and the location of the North Pacific subtropical high [51, 52]. Consequently, the oceanic conditions of the Pacific may play a decisive role in driving the EASM circulation. Palcacocha Lake, which is located in southern Ecuador, was strongly influenced by ENSO events, and the sediments recorded the ENSO event frequency (Figure 8c) [53]. The reconstructed results based on red-colored intensity units in the Palcacocha Lake sediments were collected. In addition, the sea surface temperature (SST) reconstructed by the PC6 core (Figure 8b) from the northwest North Pacific was also collected for discussion in this study [54]. The results are shown in Figure 8a and indicate four significant warm and humid periods, 1700-1550 cal a BP, 1400-1250 cal a BP, 1100-850 cal a BP and 450-350 cal a BP in this study, which corresponded to a higher SST in the northwest North Pacific and more frequent red-colored intensity units in Palcacocha Lake. [11] suggested that a high variability in the EASM since 7,600 cal a BP, which was marked by large fluctuations in the Dali Lake level, might have been directly associated with variations in the intensity and frequency of ENSO events. The latest research [55] suggested that hydrological and ecological changes in the EASM margin during the Holocene were closely related to the combined effects of regional precipitation and temperature, which were ultimately controlled by the Northern Hemisphere summer insolation, boundary conditions and physical environment of the ocean current. Therefore, we inferred that the primary productivity in Dali Lake during these periods would likely be affected by ENSO events. The warm, moist air was driven into inland China by the temperature gradient and subsequently brought forth significant rainfall events. This would lead to a mass of nutrients in the lake being carried away by runoff, which would induce an increase in primary productivity.

Many studies have been carried out on the margin of the EASM. These studies provide a great deal of information to evaluate climate changes since the Holocene. However, there are no unified conclusions that can specifically define the variations in the EASM. A high-resolution pollen record from Lake Zhuyeze [56] indicated an alternation of drying and wetting during the Late Holocene (3.8-0 cal ka BP). Contrary to our research, it was relatively humid between 1.2 cal ka BP and 0.5 cal ka BP based on the research in Lake Zhuyeze. Study on Daihai Lake by Peng et al. [2] suggested that the climate showed a trend of drying since 3.1 ka BP, which supported our results that the EASM had weakened in the Dali Lake basin since 2100 cal a BP. Ge et al. [57]suggested that there have been four warm periods over past 2000 years: Western Han dynasty and Eastern Han dynasty (2215 cal a BP-1835 cal a BP), Sui and Tang dynasties (1470 cal a BP-1205 cal a BP), Song and Yuan dynasties (1080 cal a BP-695 cal a BP) and the 20th century. Therefore, it was obvious that the climate was being driven by ENSO during 1400-1250 cal a BP and 1100-850 cal a BP.

CONCLUSION

This study focused on a comparative analysis of multi-proxy data from a high-resolution sediment core in Dali Lake along the north margin of the EASM and provides climate changes over the past 2100 cal a BP. In addition, the factors impacting the lake, as well as the driving mechanism of climate changes, were discussed. The increasing of primary productivity (P2) in the DL-1 sediment core indicated a warm and humid climate and vice versa. Since 2100 cal a BP, P2 in Dali Lake suffered a wide fluctuation due to the climate changes that were mostly caused by the EASM changes. The enhanced EASM not only provided suitable existing conditions for living activity but also brought a mass of nutrients through runoff. Therefore, the primary productivity would correspondingly increase. In this study, four significant warm and humid periods of 1700-1550 cal a BP, 1400-1250 cal a BP, 1100-850

cal a BP and 500-350 cal a BP corresponded to a higher SST in the North Pacific and more frequent red-colored intensity units in Palcacocha Lake, which indicated that the Dali Lake basin during these periods may likely have been affected by ENSO events.

ACKNOWLEDGEMENTS

The research reported in this manuscript is funded by the Natural Science Foundation of China (Grants No. 51709162, 51469025, 51509133, 51669021).

There are no conflicts to declare.

REFERENCES

[1] Liu, X., Vandenberghe, J., An, Z., Li, Y., Jin, Z., Dong, J., Sun, Y. (2016) Grain size of Lake Qinghai sediments: Implications for riverine input and Holocene monsoon variability. Palaeogeography Palaeoclimatology Palaeo ecology. 449, 41-51.

[2] Xu, Q.H., Xiao, J., Li, Y.C., Tian, F., Nakagawa, T. (2010) Pollen-based quantitative reconstruction of Holocene climate changes in the Daihai Lake area, Inner Mongolia, China. Journal of Climate. 23(11), 2856-2868.

[3] Peng, Y., Xiao, J., Nakamura, T., Liu, B., Inouchi, Y. (2005) Holocene East Asian monsoonal precipitation pattern revealed by grain-size distribution of core sediments of Daihai Lake in Inner Mongolia of north-central China. Earth and Planetary Science Letters. 233(3–4), 467-479.

[4] Christoffersen, K.S., Amsinck, S.L., Landkildehus, F., Lauridsen, T.L., Jeppesen, E. (2008) Lake Flora and Fauna in Relation to Ice-Melt, Water Temperature and Chemistry at Zackenberg. Advances in Ecological Research. 40, 371-389.

[5] Tribovillard, N., Algeo, T.J., Lyons, T., Riboulleau, A. (2006) Trace metals as paleoredox and paleoproductivity proxies: An update. Chemical Geology. 232(1–2), 12-32.

[6] Plisnier, P.D., Coenen, E.J. (2001) Pulsed and Dampened Annual Limnological Fluctuations in Lake Tanganyika. In: Munawar, M., Hecky, R.E. (eds.) The great lakes of the world: food-web, health and integrity. Backhuys, Leiden, Netherlands, 83-96.

[7] Birks, H.H., Battarbee, R.W., Birks, H.J.B. (2000) The development of the aquatic ecosystem at Kråkenes Lake, western Norway, during the late glacial and early Holocene - a synthesis. Journal of Paleolimnology. 23(1), 91-114.

[8] Johnson, T.C., Gasse, F. (2000) A High-Resolution Paleoclimate Record Spanning the past 25,000 Years in Southern East Africa. Science. 296(5565), 113-132.

[9] Cohen, A.S., Lezzar, K.E., Cole, J., Dettman, D., Ellis, G.S., Gonneea, M.E., Plisnier, P.D., Langenberg, V., Blaauw, M., Zilifi, D. (2006) Late Holocene linkages between decade–century scale climate variability and productivity at Lake Tanganyika, Africa. Journal of Paleolimnology. 36(2), 189-209.

[10] Hladyniuk, R., Longstaffe, F.J. (2015) Paleo productivity and organic matter sources in Late Quaternary Lake Ontario. Palaeogeography Palaeoclimatology Palaeoecology. 435, 13-23.

[11] Xiao, J., Si, B., Zhai, D., Itoh, S., Lomtatidze, Z. (2008) Hydrology of Dali Lake in central-eastern Inner Mongolia and Holocene East Asian monsoon variability. Journal of Paleolimnology. 40(1), 519-528.

[12] Xiao, J., Chang, Z., Si, B., Qin, X., Itoh, S., Lomtatidze, Z. (2009) Partitioning of the grain-size components of Dali Lake core sediments: evidence for lake-level changes during the Holocene. Journal of Paleolimnology. 42(2), 249-260.

[13] Lan, Y., Tian, M., Zhang, X., Wen, X., Kang, C. (2018) Evolution of a Late Pleistocene palaeolake in Dali Nor area of southeastern Inner Mongolia Plateau, China. Geoscience Frontiers 9(1), 223-237.

[14] Fan, J., Xiao, J., Wen, R., Zhang, S., Wang, X., Cui, L., Yamagata, H. (2017) Carbon and nitrogen signatures of sedimentary organic matter from Dali Lake in Inner Mongolia: Implications for Holocene hydrological and ecological variations in the East Asian summer monsoon margin. Quaternary International. 452, 65-78.

[15] Zhen, Z.L., Li, C.Y., Zhang, S., Li, W.B., Shi, X.H., Sun, B. (2015) Characteristics and indications of hydrogen and oxygen isotopes distribution in lake ice body. Water Science and Technology. 71(7), 1065-1072.

[16] Wu, J., Gagan, M.K., Jiang, X., Xia, W., Wang, S. (2004) Sedimentary geochemical evidence for recent eutrophication of Lake Chenghai, Yunnan, China. Journal of Paleolimnology. 32(1), 85-94.

[17] Bai, Z.G., Wan, E.Y., Wang, C.S., Huang, R.G. (2005) Coupling between $^{210}Pb_{ex}$ and organic matter in sediments of a nutrient-enriched lake: an example from Lake Chenhai, China. Chemical Geology. 224(4), 223-236.

[18] Ramsey, C.B. (2001) Development of the Radiocarbon Calibration Program. Radiocarbon. 43, 355-363.

[19] Baillie, M.G.L., Reimer, P.J. (2004) IntCal04 Terrestrial Radiocarbon Age Calibration, 0-26 cal kyr BP. Radiocarbon. 46(3), 1029-1058.

[20] Qian, J.L., Wang, S.M., Xue, B., Chen, R.S., Ke, S.Z. (1997) A method to quantitatively estimate allochthonous organic carbon in lake sediment. Chinese Science Bulluten. 42(15), 1655-1658 (in Chinese).
[21] Meyers, P.A. (2003) Applications of organic geochemistry to paleolimnological reconstructions: a summary of examples from the Laurentian Great Lakes. Organic Geochemistry. 34(2), 261-289.
[22] Cai, D., Tan, F.C., Edmond, J.M. (1988) Sources and transport of particulate organic carbon in the Amazon River and Estuary. Estuarine, Coastal and Shelf Science. 26(4), 1-14.
[23] Fan, J.W., Xiao, J.L., Wen, R.L., Zhai, D.Y., Wang, X., Cui, L.L., Shigeru, I. (2015) Holocene environment variations recorded by stable carbon and nitrogen isotopes of sedimentary organic matter from Dali Lake in Inner Mongolia. Quaternary Sciences. 35, 856-870. (in Chinese).
[24] Müller, P.J., Suess, E. (1980) Productivity, sedimentation rate, and sedimentary organic matter in the oceans—I. Organic carbon preservation. Deep Sea Research Part A Oceanographic Research Papers. 26(12), 1347-1362.
[25] Appleby, P.G. (2001) Chronostratigraphic techniques in recent sediments. In: Last, W.M., Smol, J.P. (eds.) Tracking environmental change using lake sediments volume 1: basin analysis, coring, and chronological techniques. Kluwer, Dordrecht, 171–203.
[26] Long, H., Lai, Z.P., Wang, N.A., Zhang, J.R. (2011) A combined luminescence and radiocarbon dating study of Holocene lacustrine sediments from arid northern China. Quaternary Geochronology. 6(1), 1-9.
[27] Zhang, P., Cheng, H., Edwards, R.L., Chen, F., Wang, Y., Yang, X., Liu, J., Tan, M., Wang, X., Liu, J. (2008) A test of climate, sun, and culture relationships from an 1810-year Chinese cave record. Science. 322(5903), 940-942.
[28] Helama, S., Jones, P.D., Briffa, K.R. (2017) Dark Ages Cold Period: A literature review and directions for future research. The Holocene. 27(10), 1600-1606.
[29] Choudhary, P., Routh, J., Chakrapani, G.J. (2009) An environmental record of changes in sedimentary organic matter from Lake Sattal in Kumaun Himalayas, India. Science of the Total Environment. 407(8), 2783-2795.
[30] Stein, P.D.R. (1991) Accumulation of Organic Carbon in Marine Sediments. Lecture Notes in Earth Sciences. Berlin Springer Verlag, 34.
[31] Tyson, R.V. (2001) Sedimentation rate, dilution, preservation and total organic carbon: some results of a modelling study. Organic Geochemistry. 32(2), 333-339.
[32] Talbot, M.R., Lærdal, T. (2000) The Late Pleistocene - Holocene palaeolimnology of Lake Victoria, East Africa, based upon elemental and isotopic analyses of sedimentary organic matter. Journal of Paleolimnology. 23(2), 141-164.
[33] Chen, R., Shen, J., Li, C., Zhang, E., Sun, W., Ji, M. (2014) Mid- to late-Holocene East Asian summer monsoon variability recorded in lacustrine sediments from Jingpo Lake, Northeastern China. Holocene. 146(3), 454-468.
[34] Spiker, E.C., Hatcher, P.G. (1984) Carbon isotope fractionation of sapropelic organic matter during early diagenesis. Organic Geochemistry. 5(4), 283-290.
[35] Stuiver, M., Braziunas, T.F. (1987) Tree cellulose 13C/12C isotope ratios and climatic change. Nature. 328(12), 58-60.
[36] Xu, Q., Jia, K.L., Li, W.B. Wang, L.M., Zhao, S.N., Yu, R.X., Yang, J.H. (2016) Characteristics of the Summer Phytoplankton Community Structure in Dalinor Lake. Journal of Hydroecology. 37(6), 14-22. (in Chinese).
[37] Meyers, P.A. (1997) Organic geochemical proxies of paleoceanographic, paleolimnologic, and paleoclimatic processes. Organic Geochemistry. 27(5–6), 213-250.
[38] Yang, D.F., Chen, S.T., Hu, J., Wu, J.P., Huang, H. (2007) Magnitude order of the effect of light,water temperature and nutrients on phytoplankton growth. Marine Environmental Science. 26(3), 201-207. (in Chinese).
[39] Jiang, S., Liu, X., Xu, L., Sun, L. (2011) Application of Biogenic Silica On Reconstruction Of Palaeo-Primary Productivity In East Antarctica Lakes. Chinese Journal of Polar Research. 23(1), 26-34. (in Chinese).
[40] Fu, M.Z., Wang, Z.L., Sun, P., Li, Y., Li, R.X. (2009) Spatial distribution characteristics and the environmental regulation mechanisms of phytoplankton chlorophyll a in Southern Yellow Sea during summer 2006. Acta Ecologica Sinica. 29(10), 5366-5375. (in Chinese).
[41] Hobbie, J.E., Bahr, M. and Rublee, P.A. (1999) Arch. Hydrobiol. Special Issues Adv. Limnol. 54, 61-76.
[42] Berger, A.L. (1978) Long-Term Variations of Daily Insolation and Quaternary Climatic Changes. Journal of the Atmospheric Sciences. 35(12), 2362-2367.
[43] Fleitmann, D., Burns, S.J., Mudelsee, M., Neff, U., Kramers, J., Mangini, A., Matter, A. (2003) Holocene forcing of the Indian monsoon recorded in a stalagmite from southern Oman. Science, 300(5626), 1737-1739.

[44] Fleitmann, D., Burns, S.J., Mangini, A., Mudelsee, M., Kramers, J., Villa, I., Neff, U., Al-Subbary, A.A., Buettner, A., Hippler, D. (2007) Holocene ITCZ and Indian monsoon dynamics recorded in stalagmites from Oman and Yemen (Socotra). Quaternary Science Reviews. 26(1), 170-188.
[45] Kutzbach, J.E., Street-Perrott, F.A. (1985) Milankovitch forcing of fluctuations in the level of tropical lakes from 18 to 0 kyr BP. Nature. 317(6033), 130-134.
[46] Min, W., Yang, S., Kumar, A., Zhang, P.Q. (2009) An analysis of the large-scale climate anomalies associated with the snowstorms affecting China in January 2008. Monthly Weather Review. 137(3), 1111-1131.
[47] Li, X.C., Wang, J., Yang, J. (2013) Charac teristics and Mechanism Analysis of Extreme Snow Change in Eastern Inner Mongolia Pasturing Area. Scientia Geographica Sinica. 33(7), 884-889. (in Chinese).
[48] Wang, C., Deser, C., Yu, J.Y., Dinezio, P., Clement, A. (2017) El Niño and Southern Oscillation (ENSO): A Review. In: Glynn, P., Manzello, D., Enochs, I. (eds.) Coral Reefs of the Eastern Tropical Pacific. Coral Reefs of the World. vol 8. Springer, Dordrecht.
[49] Tao, S., Zhang, Q. (1998) Response of the Asian Winter and Summer Monsoon to ENSO Events. Scientia Atmospherica Sinica. 22(4), 399-407. (in Chinese).
[50] Wu, R., Hu, Z.Z., Kirtman, B.P. (2003) Evolution of ENSO-related rainfall anomalies in east Asia. Journal of Climate. 16(22), 3742-3758.
[51] Bo, W., Zhou, T.J., Li, T. (2009) Contrast of rainfall-SST relationships in the Western North Pacific between the ENSO-developing and ENSO-decaying summers. Journal of Climate. 22(16), 4398-4405.
[52] Wang, B., Jian, L., Jing, Y., Zhou, T.J., Wu, Z.W. (2009) Distinct principal modes of early and late summer rainfall anomalies in East Asia. Journal of Climate. 22(13), 3864-3875.
[53] Moy, C.M., Seltzer, G.O., Rodbell, D.T., Anderson, D.M. (2002) Variability of El Niño/ Southern Oscillation activity at millennial timescales during the Holocene epoch. Nature. 420(6912), 162-165.
[54] Minoshima, K., Kawahata, H., Ikehara, K. (2007) Changes in biological production in the mixed water region (MWR) of the northwestern North Pacific during the last 27kyr. Palaeogeography Palaeoclimatology Palaeoecology. 254(3), 430-447.
[55] Chen, F.H., Cheng, B., Zhao, Y., Zhu, Y., Madsen, D.B. (2006) Holocene environmental change inferred from a high-resolution pollen record, Lake Zhuyeze, arid China. Holocene. 16(16), 675-684.
[56] Ge, Q.S., Zheng, J.Y., Hao, Z.X., Liu, H.L. (2013) General characteristics of climate changes during the past 2000 years in China. Science China Earth Sciences. 56(2), 321-329.

Received: **06.03.2018**
Accepted: **27.04.2018**

CORRESPONDING AUTHOR

Wenbao Li
College of Water Resources and Civil Engineering,
Inner Mongolia Agricultural University,
Hohhot 010018 – China

e-mail: zhencheng7666@163.com

© by PSP Volume 27 – No. 7/2018 pages 5107-5112 Fresenius Environmental Bulletin

APPLICATION OF ELECTRONIC TONGUE TECHNOLOGY AND MULTIVARIATE STATISTICAL ANALYSIS IN WATER ENVIRONMENT

Xu Liu*

School of Electronic and Electrical Engineering, Bengbu University, Bengbu 233030, China

ABSTRACT

With the advancement of science and technology, conventional method of heavy metal detection in water could not satisfy the higher requirement for fast, intelligent and non-invasive detection. Towards these, electronic tongue technology shipped born, it has the advantages of fast and simultaneous measurement, low-cost, low energy consumption and has been widely used in the field of environmental monitoring. In this paper, electronic tongue technology has been applied for detecting the concentrations of six kinds of heavy metals (Pb, Co, Cr, Mn, Ni and Cu) in water from a collapsing lake in a coalmine resource-based city, China, and higher coefficients of variation indicated these metals may be affected by multifactors. Based on multivariate statistical methods (hierarchical cluster analysis and principal component analysis), three main sources were present: Mn and Co were possibly related to waste discharge; Pb, Cu and Ni were mainly derived from the leaching of coal gangue; and Cr mainly originated from soil erosion and rock weathering. The method proposed in this paper can achieve rapid detection and comprehensive pollution source identification, it has the theoretical and practical significance in water environmental protection.

KEYWORDS:
Electronic tongue, environmental detection, multivariate statistical analysis, water environmental protection

INTRODUCTION

Due to the rapid development of the economy and society, human activities have made a profound negative impact on the environment [1-3]. Industrial water, sewage and other wastes are directly discharged into rivers and lakes, which has caused water pollution [4-5]. Heavy metal pollution is especially serious, which affects the water quality of industrial and agricultural production and daily life of human being, further threatens the ecological environment and sustainable development of the river basin [6-8]. Therefore, to study the real-time monitoring of heavy metals concentrations will be more helpful for the sustainable development of ecological environment.

Electronic tongue technology based on anodic stripping voltammetry can quickly and accurately detect heavy metal concentrations, it will not bring errors brought by fatigue [9]. Compared with the traditional detection methods and remote sensing detection, this method is not impacted by spatio-temporal environment factors, so it is widely used in the field of environmental monitoring [10-13]. In this study, a total of fifty-three water samples have been collected from a collapsing lake in a coalmine resource-based city, China, and the concentrations of six kind of metals (Pb, Co, Cr, Mn, Ni and Cu) have been detected by electronic tongue technology, then their possible sources have been identified by hierarchical cluster analysis (HCA) and principal component analysis (PCA), it can provide information for water environmental protection.

MATERIALS AND METHODS

Anodic stripping voltammetry. The anodic stripping voltammetry is an electrochemical measurement technology which combines the two processes of electrolysis enrichment and electrolysis dissolution [14-15]. Firstly, electrolytic ion is deposited on the electrode at a certain potential, and then the potential of the electrode is scanned back to make the deposited material electrolysis and record the voltammetric curve in the dissolution process. This curve is called the dissolution volt-ampere curve, and the peak current in the curve is proportional to the measured ion concentration under certain conditions. Electrolytic deposition process is equivalent to an enrichment process, the measured ions are deposited from large volume solutions to small volume electrodes, which will lead to a great increase in their concentration. The larger currents the dissolution process, the higher sensitivity the stripping voltammetry. The sensor for stripping voltammetry is usually a three electrode system, a working electrode, a reference electrode, and an auxiliary electrode, three electrode system can automatically compensate the ohmic potential drop in the solution, which can measure

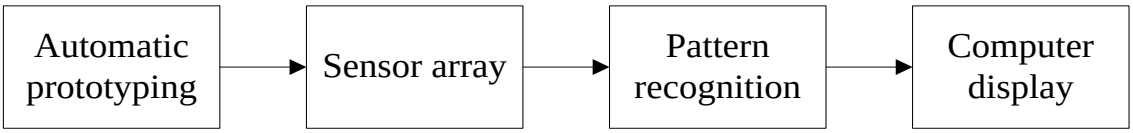

FIGURE 1
Block diagram of electronic tongue equipment

the resistance of the solution between the measured electrodes. Moreover, the three electrode system can keep the constant of the potential of the working electrode, which makes the precision of the experiment greatly improved. Normally, the mercury electrode is used as the working electrode, the Ag/AgCl electrode is used as the reference electrode, and the platinum is selected as the auxiliary electrode.

Water sampling and test analysis. A total of 53 water samples were collected from a collapsing lake in a coalmine resource-based city according to the technical guidance of water quality sampling, and each sample was collected for 2.0L. The exact location (longitudes and latitudes) of each sample point was collected by GPS, and water samples were collected 0.5 meter below the water. After sampling, the samples were filtered immediately by 0.45 um cellulose acetate filtration membrane, and the required volume of filtrate was collected. The electronic tongue equipment used in the experiment is mainly composed of four parts: automatic prototyping, sensor array, pattern recognition and computer display. The frame diagram is illustrated in figure 1.

Prior to use of instruments, it is necessary to check whether the electronic tongue automatic sampler and signal communication are normal, then initialize and calibrate it, so as to ensure the accuracy and stability of the detection. The test temperature is controlled at 25℃. In order to improve the efficiency of electrolytic enrichment, the electrode can be rotated or stirred to accelerate the rate of the transported substance to the electrode surface, while in the electrolytic dissolution process, the solution should remain stationary. Some specific test parameters are set as follows: the data acquisition time of each sample is set to 120 s, and the mean value of the last 20 s measurements is taken as the output value of the stable data; each water sample was repeated 9 times, and the response intensity of the sensor was stable after 2~3 times of the electronic tongue measurement, so the mean value of the last 6 measurements was collected in this study.

HCA and PCA. The cluster analysis is a statistical technique used to indentify sites group or variables group based on similarities. Being one of the cluster analyses, HCA is based on the core idea of objects being more related to nearby objects than to objects farther away, these algorithms connect "objects" to form "clusters" based on their distance. While PCA is a statistical procedure that is used to analyze the covariance matrix, so as to reduce the dimension of the data and keep the maximum contribution to the difference of the data set [16-18], the specific calculation process are as follows[19]:

(1) The first step is to calculate a matrix for standard data indicators (formula 1).

$$X = \begin{vmatrix} x_{11} & \cdots & x_{1n} \\ \cdots & \cdots & \cdots \\ x_{m1} & \cdots & x_{mn} \end{vmatrix} \quad (1)$$

Where n is the number of heavy metal, m is the number of sampling point, X_{ij} is the j value in the ith sampling point.

(2) The second step is to calculate the correlation matrix (formula 2).

$$r_{ij} = \frac{\sum_{k=1}^{n} \left|(x_{ki} - \overline{x_i})\right\|(x_{kj} - \overline{x_j})\right|}{\sqrt{\sum_{k=1}^{n}(x_{ki} - \overline{x_i})^2 \sum_{k=1}^{n}((x_{kj} - \overline{x_j})^2)}} \quad (2)$$

Where r_{ij} is the correlation coefficients between the index i and j.

(3) The third step is to obtain the eigenvalues and eigenvectors of the correlation coefficient matrix, as well as the variance contribution rate and the accumulative contribution rate. Principal components with eigenvalues higher than 1.0 were extracted, which can explained about 85% of the total variance. The contribution rate can be described as follows:

$$C = (c_1, c_2, ..., c_q) \quad (3)$$

(4) The fourth step is to extract q feature vectors and standardize them (formula 4).

$$A = [e_f - \min(e_f)]/[\max(e_f) - \min(e_f)] \quad (4)$$

Where e is feature vector, $f \in [1, q]$.

(5) The final step is to calculate the contribution rate of each index, and treat the data with normalization method (formula 5, formula 6).

$$p = C * A^Q / \sum_{i=1}^{q} C_i = (p_1, p_2, ..., p_n) \quad (5)$$

$$W = p_j / \sum_{1}^{n} p_j = (w_1, w_2, ..., w_n) \quad (6)$$

Where w_j is the weighting of the ith indicator.

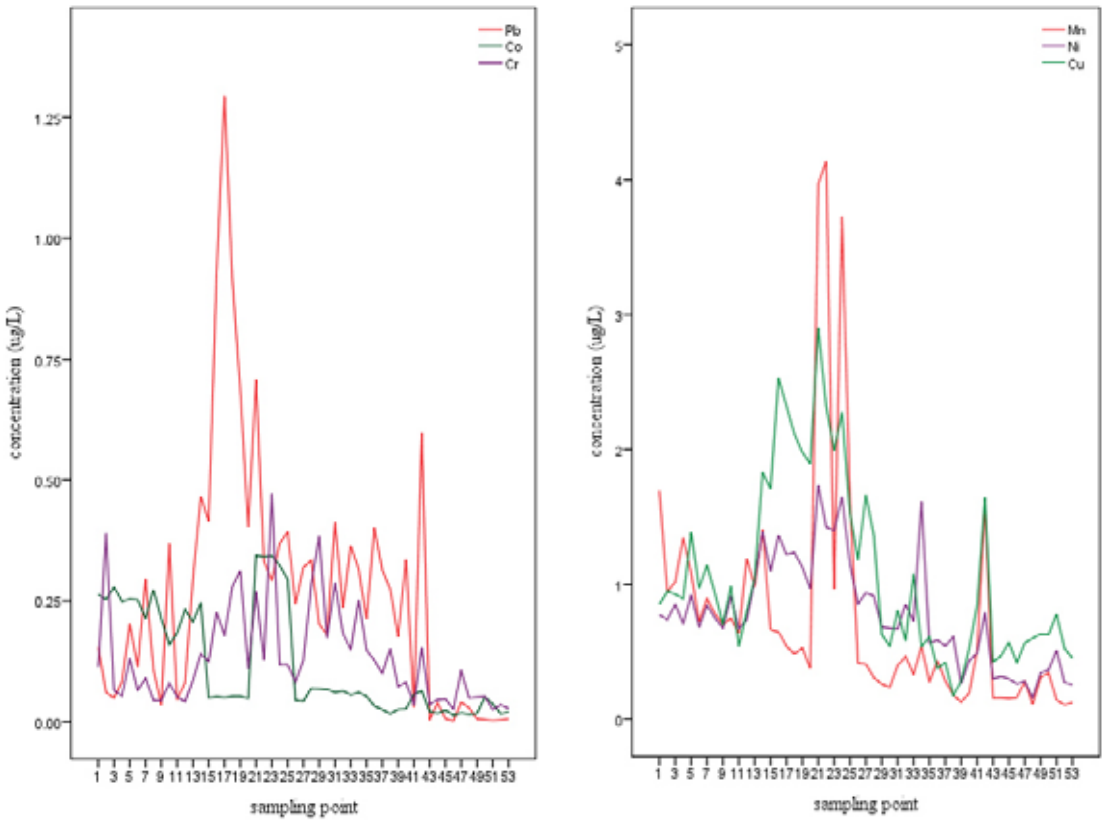

FIGURE 2
Line plot of heavy metal concentrations

TABLE 1
Descriptive statistics of heavy metal concentrations (ug/L)

	Pb	Co	Cr	Mn	Ni	Cu
Mean value	0.27	0.12	0.13	0.77	0.78	1.07
Median value	0.24	0.06	0.11	0.48	0.74	0.85
Std. Dev	0.27	0.11	0.10	0.89	0.39	0.67
Background value	0.2	0.05	0.50	-	0.3	0.57
CV	1.0	0.92	0.77	1.16	0.51	0.62
p-value	>0.05	<0.05	>0.05	<0.05	>0.05	>0.05

Std. Dev: Standard deviation

RESULTS AND DISCUSSION

Descriptive statistics. The line plot of heavy metal concentrations were shown in Figure 1. It was intuitively plausible that the contents of Mn, Ni and Cu were significantly higher than that of Pb, Co and Cr. Statistical summary of the metal contents were presented in Table 1. From the table and figure, the measured heavy metal contents varied greatly as follows: Pb, 0.002-1.3ug/L, with an average of 0.27ug/L; Co, 0.01-0.34ug/L, with an average of 0.12ug/L; Cr, 0.02-0.47ug/L, with an average of 0.13ug/L; Mn, 0.11-4.18ug/L, with an average of 0.77ug/L; Ni, 0.15-1.74ug/L, with an average of 0.78 ug/L; Cu, 0.17-2.90ug/L, with an average of 1.07ug/L. The mean contents of heavy metals were in the order: Cu > Ni >Mn > Pb > Cr > Co. According to the background values, the mean concentrations of the heavy metals (Pb, Co, Ni, Cu) were higher than their background values, whereas Cr concentration was lower than its background value. Comparing with the grade III standard of surface water environment quality level (Pb, 50ug/L; Co, 1000ug/L; Cr, 50ug/L; Mn, 100ug/L; Ni, 20ug/L; Cu, 1000ug/L), the heavy metal contents of the collapsing lake were significantly lower than the corresponding limits. Coefficients of variation (CV) is an indicator of variation degree, it is generally accepted that a high CV (>0.9) indicated a high degree of human influence. In this study, the contents of heavy metals varied distinctly among the sampling sites. This was particularly true for Mn, Pb and Co, with the CV of 1.16, 1.0 and 0.92, respectively. The One-Sample Kolomogorov-Semirnov test (K-S test) was conducted in the variables, the results showed that the data of Mn and

Co were not conform to normal distribution ($p<0.05$), so logarithm transition was applied for the following analysis [20]. After logarithm transition, they were both obey normal distribution.

HCA. Based on the data of heavy metal concentrations in different sampling points, HCA was performed to analyze the similarity for the variables with the method of between-groups linkage. Variables cluster (heavy metal cluster) was calculated by HCA, and the icicle plot and dendrogram were shown in Figure 3. As can be observed in Figure 3, six kind of heavy metals can be distinguished into three major groups, the metals (Mn and Co) belonged to cluster 1, the metals (Ni, Cu and Pb) belonged to cluster 2, while Cr belonged to cluster 3.

PCA and source profiles. To further discriminate the possible sources of heavy metals, PCA was conducted on the normalized data of heavy metal concentration from the collapsing lake in a coalmine resource-based city. KMO test value (0.756) showed that the heavy metal concentrations were suitable for PCA. Similarly, the P value for Bartlett's test was 0 ($p< 0.05$), indicating that there was significant correlation among the variables [21-22]. Therefore, PCA was effective to identify the sources of heavy metals in this study. As present in Table 2, a total of three principal components were extracted with eigenvalues higher than 1.0, the first principal component (PC1) is dominated by Mn and Co and followed by Ni, Cu, Cr and Pb. The second principal component (PC2) is dominated by Pb, Cu, Ni and followed by Mn, Cr and Co, whereas the third principal component (PC3) is dominated by Cr and followed by Ni, Pb, Cu, Co and Mn. The component plot in rotated space was shown in Figure 4, the heavy metals pairs (Mn-Co and Cu-Pb-Ni) were very close to each other, suggesting that these heavy metals may share the same source. However, Cr was far away from the other five metals, implying the different origin in the collapsing lake. The results of PCA were well consistent with the results of HCA.

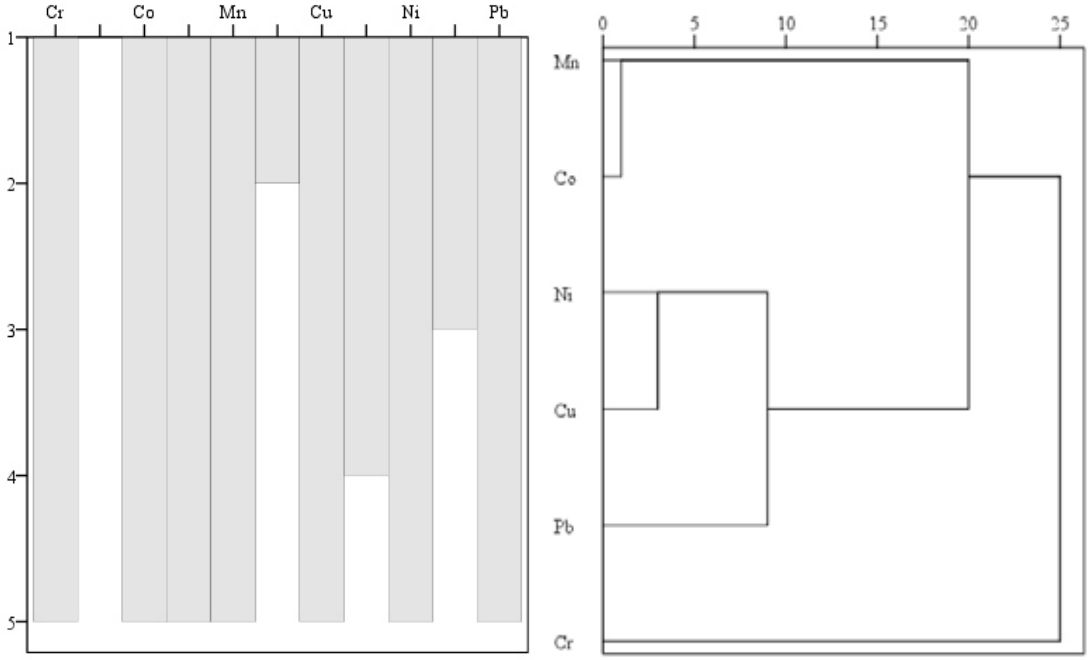

FIGURE 3
Icicle plot and dendrogram of the heavy metal concentrations

TABLE 2
Rotated principal component matrix

	Rotated principal components		
	PC1	PC2	PC3
Pb	0.006	0.928	0.245
Cr	0.114	0.270	0.954
Mn	0.912	0.333	0.034
Co	0.967	0.043	0.120
Ni	0.606	0.659	0.314
Cu	0.430	0.829	0.145
Eigenvalue	2.333	2.167	1.104
Variance contribution rate (%)	62.127	20.585	10.695
Cumulative contribution rate (%)	62.127	82.711	93.407

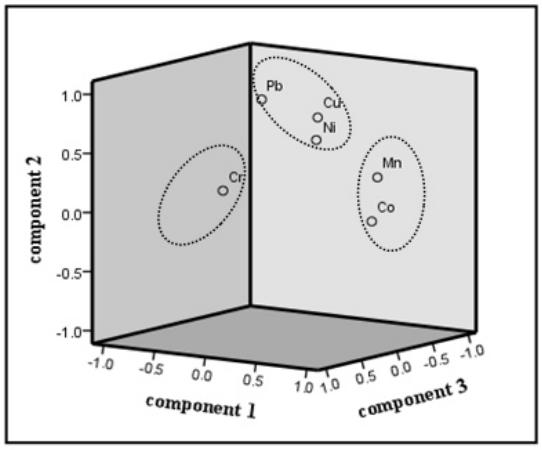

FIGURE 4
Component plot in rotated space

PC1, as revealed by the Table 2 and Figure 4, explained 62.127% of the total variance loaded heavily on Mn and Co (loading>0.90). Mn was considered to be main pollution related to waste discharge except for N, P and Fe [23]. According to the investigation, there were many garbage landfill around the sampling points, the long history of deposit refuse may result in Mn accumulation in this lake, so PC1 was considered to be the source related to waste discharge. PC2 accounting for 20.585% of the total variance connected with Pb, Cu and Ni (loading>0.60), mining activities can lead to accumulation of heavy metals such as Pb, Cu and Ni in coal mining area, and the coal gangue may be the important reason [24]. Leaching of coal gangue formed acidified water, and the heavy metals in coal gangue released to the environment in the form of solution, PC2 may be explained to be the source related to the leaching of coal gangue because the collapsing Lake was filled by coal gauge during the last decades. PC3 can be explained to be the source related to geological weathering or dissolution. That's because Cr was mainly contributed by this factor (loading>0.90), and Cr was the only metal that its mean concentration was lower than the background value (Table 1). Moreover, some studies also revealed that this metal was likely to be contributed by soil erosion and rock weathering [25-27].

CONCLUSIONS

Useful tools and methods, such as electronic tougue technology, multivariate statistical analyses (HCA and PCA) were employed to detect heavy metal concentration and indentify the possible sources of heavy metals from a collapsing lake in northern Anhui province, earthern China. The results showed that the mean concentrations in the water decrease as Cu > Ni > Mn > Pb > Cr > Co, and the CV were all higher than 0.5, which suggested that they may have different natural and anthropogenic conditions. Multivariate statistical analyses indicated that Mn and Co were mainly influenced by waste discharge; Pb, Cu and Ni were mainly influenced by the dumping of coal gauge; Cr was considered to be a natural source.

ACKNOWLEDGEMENTS

This research project was supported by the National Natural Science Foundation of China (No. 41773100, 41373095) and the Natural Science Foundation of Bengbu university (No. 2017ZR19).

REFERENCES

[1] Li, H., Chen, L., Yu, L. (2017) Pollution characteristics and risk assessment of human exposure to oral bioaccessibility of heavy metals via urban street dusts from different functional areas in Chengdu, China. Science of the Total Environment. 586, 1076-1084.

[2] Ma, L., Gui, H. (2017) Accumulation of heavy metals in surface soils of Bengbu higher education mega center, China. Fresen. Environ. Bull. 26, 4697-4703.

[3] Huang, D., Gui, H., Lin, M., Peng, W. (2017) Accumulation characteristics and health risk of heavy metals in soil and plant: a case study from Huaibei coalfield, China. Fresen. Environ. Bull. 26, 631-639.

[4] Yuan, Z., Liu, G., Lam, M. H., Liu, H., and Da, C. (2016) Occurrence and levels of polybrominated diphenyl ethers in surface sediments from the yellow river estuary, China. Environmental Pollution. 212, 147-154.

[5] Devic, G., Sakan, S., Đorđevic, D. (2016) Assessment of the environmental significance of nutrients and heavy metal pollution in the river network of Serbia. Environmental Science and Pollution Research. 23(1), 282-297.

[6] Gomez-Parra, A., Forja, J.M., Del Valls, T.A., Saenz, I. and Riba, I. (2000) Early contamination by heavy metals of the Guadalquiver estuary after the Aznalcollar mining spill (SW Spain). Marine Pollution Bulletin. 40(12), 1115-1123.

[7] Wang, R., Xu, Q., Zhang, X, Wei, Q., Yan, C. (2012) Health risk assessment of heavy metals in typical township water sources in Dongjiang River Basin. Environmental Science. 33(9), 3083-3088. (in Chinese).

[8] Wang, Z., Lu, Y., Liu, G., and Liu, W. (2014) Heavy metals in water, sediments and submerged macrophytes in ponds around the DianChi lake, China. Ecotoxicology and Environmental Safety. 107(9), 200-206.

[9] Huang, X., Zhang, H., Zhao, J. (2007) Research and application of electronic tongue technology in food industry. Food Science and Technology. 189(7), 20-24. (in Chinese).
[10] Gutés, A., Céspedes, F., Del Valle, M. (2007) Electronic tongues in flow analysis. Analytica Chimica Acta. 600(1-2), 90-96.
[11] Mimendia, A., Legin, A., Merkoçi, A. and Del Valle, M. (2010) Use of sequential injection analysis to construct a potentiometric electronic tongue: application to the multidetermination of heavy metals. Sensors and Actuators B Chemical. 146(2), 420-426.
[12] Rudnitskaya, A., Legin, A., Seleznev, B., Kirsanov, D., and Vlasov, Y. (2008) Detection of ultra-low activities of heavy metal ions by an array of potentiometric chemical sensors. Microchimica Acta. 163(1-2), 71-80.
[13] Krantz-Rülcker, C., Stenberg, M., Winquist, F., Lundström, I. (2001) Electronic tongues for environmental monitoring based on sensor arrays and pattern recognition: a review. Analytica Chimica Acta. 426(2), 217-226.
[14] Chen L. (2011) Fast determination of heavy metals in water by MetalSafe portble analyzer. Environmental Monitoring Management and Technology. 23(2), 51-53. (in Chinese).
[15] Denuault, G. (2009) Electrochemical techniques and sensors for ocean research. Ocean Science Discussions. 6(2), 1857-1893.
[16] Pearson, K. (1901) Principal components analysis. The London, Edinburgh, and Dublin Philosophical Magazine and Journal of Science. 6(2), 566.
[17] Loska, K., Wiechuła, D. (2003) Application of principal component analysis for the estimation of source of heavy metal contamination in surface sediments from the Rybnik Reservoir. Chemosphere. 51(8), 723-733.
[18] Ma, X., Zuo, H., Tian, M., Zhang, L., Meng, J., Zhou, X., Min, N., Chang, X., Liu, Y. (2015) Assessment of heavy metals contamination in sediments from three adjacent regions of the Yellow River using metal chemical fractions and multivariate analysis techniques. Chemosphere. 144(3), 264-272.
[19] Wang, Y., Wang, J., Yao, Y., Wang, J. (2014) Evaluation of drought vulnerability in Southern China based on principal component analysis. Ecology and Environmental Sciences. 23(12), 1897-1904. (in Chinese).
[20] Ma, L., Gui, H. (2017) Authropogenic impacts on heavy metal concentrations in surface soils from the typical polluted area of Bengbu, Anhui province, eastern China. Human and Ecological Risk Assessment. 23(7), 1763-1774.
[21] Kaiser, H. (1960) The application of electronic computers to factor analysis. Educational and Psychological Measurement. 20(1), 141-151.
[22] Hu, B., Li, J, Zhao J., Bai, F., Dou, Y. (2013) Heavy metal in surface sediments of the Liaodong Bay, Bohai Sea: distribution, contamination, and sources. Environmental Monitoring and Assessment. 185(6), 5071-5083.
[23] Yan, X. (2008) Shallow groundwater pollution near a landfill site and water environmental health risk assessment. Doctoral dissertation. Hefei: Hefei University of Technology.
[24] Li, R., Hao, H., Li, G., Jiang, Y., Zhang, H, Han, X. (2011) Characteristics and sources analysis of soil heavy metal pollution in Taian city, Shangdong, China. Journal of Agro-Environment Science. 30(10), 2012-2017. (in Chinese).
[25] Zhu, X., Tang, L, Ji, H., Li, X., Hao, R. (2010) Analysis of heavy metals in sediments of water system in the north of Beijing. Acta Scientiae Circumstantiae.30(12), 2553-2562. (in Chinese)
[26] Li, N., Tian, Y., Zhang, J., Zuo, W., Zhan, W., Zhang, J. (2017) Heavy metal contamination status and source apportionment in sediments of Songhua River Harbin region, Northeast China. Environmental Science and Pollution Research. 24(4), 1-12.
[27] Wang, Y., Wen, A., Jin, G, Shi, Z., Yan, D. (2017) Spatial distribution, sources and ecological risk assessment of heavy metals in Shenjia River watershed of the three gorges reservoir area. Journal of Mountain Science. 14(2), 325-335.

Received: **06.03.2018**
Accepted: **30.04.2018**

CORRESPONDING AUTHOR

Xu Liu
School of Electronic and Electrical Engineering
Bengbu University
Bengbu – P.R. China

e-mail: liuxu-100@163.com

© by PSP Volume 27 – No. 7/2018 pages 5113-5118 Fresenius Environmental Bulletin

COMPARISON OF ALLERGEN SENSITIZATION ACCORDING TO AGE AND SEX USING SKIN PRICK TEST IN PATIENTS WITH ALLERGIC RHINITIS

Ahmet Hamdi Kepekci[1,2,*], Mustafa Yavuz Koker[3,4]

[1]Division of Audiology, Istanbul Yeni Yuzyil University, Istanbul, Turkey
[2]Department of Otolaryngology, Meltem Hospital, Istanbul, Turkey
[3]Department of Immunology, Erciyes Medical School, Kayseri, Turkey
[4]Kok Biotek, Technocity of University of Erciyes, Kayseri, Turkey

ABSTRACT

The aim of the present study was to investigate inhalant allergen sensitivity in adult patients with allergic rhinitis (AR) and to compare allergen sensitization based on age and sex under ecological conditions of urban areas.

In this cross-sectional study, 2391 patients diagnosed with rhinitis symptoms in the Istanbul area were evaluated. Skin prick test (SPT) with standard extracts, including house dust mite, pollen, fungal allergen, and animal dander, was performed. Patients with sensitization were divided into four different age groups with 10-year intervals for evaluation.

Of the 2391 patients with rhinitis, 1586 (66.3%) had at least one allergen sensitization on SPT, whereas 805 (33.7%) had no allergen sensitization. The most common sensitization (57.1%) was observed for pollen allergens. Multiple allergen sensitizations were lowest (38.8%) in the animal dander-sensitive group. The percentage of allergen sensitization was highest in age group 2 and lowest in age group 4 for both the sexes.

The data obtained from this study are important for monitoring allergen sensitivity in patients with rhinitis under ecological conditions of a large city. Allergen sensitization decreased with increasing age in all the study groups, and the percentage of sensitization changed according to age and sex. Monitoring allergen sensitization according to age and sex is important for environmental regulation, design of living spaces, working conditions, and preventive health services.

KEYWORDS:
Skin prick test, allergic rhinitis, inhalant allergens

INTRODUCTION

Allergic rhinitis (AR), also known as hay fever, is an allergic disease which is mostly affected by environmental factors [1]. AR is a heterogeneous disorder with high prevalence and often remains undiagnosed for a long time. It is characterized by one or more symptoms of rhinitis, such as sneezing, itching, nasal congestion, and rhinorrhea [2]. Seasonal AR is relatively easy to identify because of the rapid onset and offset of symptoms due to pollen exposure, whereas perennial AR is more difficult to detect because of overlapping symptoms with sinusitis, respiratory infections, and vasomotor rhinitis [2]. According to the World Health Organization (WHO), hundreds of millions of people in the world are affected by allergic disease. AR affects the quality of life and is an important disease in terms of community health, affecting socio-economic well-being [1].

Allergic disease prevalence varies depending on environmental allergen variation and the level of exposure to or inhalation of allergens. In recent years, the prevalence of allergic diseases has increased in both developed and developing countries [1]. In industrialized countries, sensitivity to aeroallergens within the general population ranges from 25% to 50% [3, 4]. In the literature, the prevalence of AR in the community varies between 2.9% and 54.1%, depending on the race, age, and geographical region [5]. AR is a major health problem that concerns the general public.

Global climate change and air pollution increase the release and production of weed and tree pollen mix. Rising temperatures increase the growth of molds and fungi, which are important allergens for people with rhinitis [6].

Skin prick test (SPT) is used for the measurement of allergen reactivity. The recommended method for SPT includes the appropriate use of specific allergen extracts, maintenance of positive and negative controls, and interpretation of the test results 15–20 min after application [4, 5]. SPTs are minimally invasive, easy to apply, and produce a response to multiple allergens at once, which are important advantages of the test. The most useful allergens for testing inhalant allergies are house dust mites (HDMs), such as dermatophagoides, animal dander, and fungi (molds). Many causative agents have been associated with AR, including pollen, mold, dust mite, and animal dander.

The present study was conducted using the data from SPTs of 2391 patients who visited our ENT clinic due to rhinitis symptoms and 1586 of patients were found to be positive for AR and the results were evaluated in accordance with age and sex.

MATERIALS AND METHODS

The diagnosis of AR was made according to Allergic Rhinitis and its Impact on Asthma (ARIA) guidelines from the European Forum for Research and Education in Allergy and Airway Diseases [7]. Retrospective data were collected from patients with rhinitis who visited an ENT clinic in Istanbul between March 2008 and August 2015. A total of 2391 adult patients were diagnosed with rhinitis symptoms based on medical history and physical examination findings, such as sneezing, nasal congestion, frequent and transparent watery runny nose, nasal itching, and burning in the eyes. Those who had at least one allergen sensitization on SPT were included in this study. The ages of both male and female patients were in the range of 20–59 years, and patients were divided into four different age groups for analysis and comparison. Group 1 included patients aged 20–29 years, group 2 included those aged 30–39 years, group 3 included those aged 40–49years, and group 4 included those aged 50–59 years. Patients aged >60 years and older were not included in this study because of lack of homogeneity due to current secondary diseases and medication. SPT was administered to all the patients who had rhinitis symptoms. To avoid false-negative results, patients using antihistamine medications, immunosuppressive drugs, and antidepressants were not included in the study because these drugs may interfere with test results [2].

The recommended method of prick testing included the appropriate use of specific allergen extracts, maintenance of positive and negative controls, and interpretation of the test results 15–20 min after application. A positive result was defined as a wheal of ≥3 mm in diameter than the wheal diameter of the negative control [8].

SPT was used for allergens Allergo-pharma (Reinbek, Germany), which were investigated in terms of both individual responses and types (tree pollen mix, olive, poplar, red oak, grass pollen, grain pollen, weed pollen, *Alternaria alternata*, *Aspergillus fumigatus*, *Dermatophagoides farinae*, *D. pteronyssinus*, dog epithelium, and cat epithelium).

Statistical analysis was performed using the SPSS for Windows, version 21.0 (SPSS Inc., USA). The Kruskal–Wallis test was performed to determine the significance of differences in allergen sensitivity according to age and sex. Significant relationships between age groups and allergen sensitivities were compared using the Tukey's test, and $p < 0.05$ was considered significant.

RESULTS

Patients and allergen sensitization. In this study, the SPT data of 2391 adult patients with rhinitis were evaluated, and 1586 (66.3%) had at least one allergen-positive SPT response to allergens, such as pollen, house dust, fungi, or animal dander. Of those with positive test results due to allergen sensitization, 1023 (64.5%) were female and 563 (35.5%) were male. These patients were diagnosed with AR. The average age of females was 37.13 ± 9.96 years, while that of men was 36.99 ± 9.28 years. SPT results showed that 805 (33.7%) patients with rhinitis had no allergen sensitization. Of those with negative test results, 556 (69.1%) were female and 249 (30.9%) were male, and these patients without allergen sensitization were not included in the analysis and comparison.

The number of allergen sensitizations for each allergen type is provided in Figure 1. The results showed sensitization to pollen in 905 patients, house dust in 667, mold in 443, and animal dander in 298 (Figure 1). The detailed number of patients, allergen types, and multiple sensitization data are also provided in Figure 1. Sensitization to only one type of allergen is indicated by A^1 (1039 patients; 65.5%). Patients who showed positive response to only two allergens are indicated by A^2 (386; 24.3%), those who showed positive response to only three allergens are indicated by A^3 (142; 9.0%), and those who showed positive response to four allergens (pollen, HDM, mold, and animal dander) are indicated by A^4 (19; 1.2%).

The percentage of patients with multiple allergen sensitizations was lowest (38.8%) in the group of patients with positive response to animal dander and was highest in groups of patients with positive responses to pollen, HDM, and mold (68.2 %, 63.6 %, and 62.3 %), respectively (Figure 1).

Sensitization to allergen groups and types. More than half of the patients (57.1%) had sensitization to pollen (tree pollen mix, grass pollen, grain pollen, wild herb pollen, olive tree pollen, poplar pollen, and red oak pollen). Sensitization to house dust (D. farinae and D. pteronyssinus) was seen in 42.1% of the patients, whereas that to mold (A. alternata and A. fumigatus) was seen in 27.9%; furthermore, 18.8% of patients had sensitization to animal dander (cat and dog dander) (Figure 2).

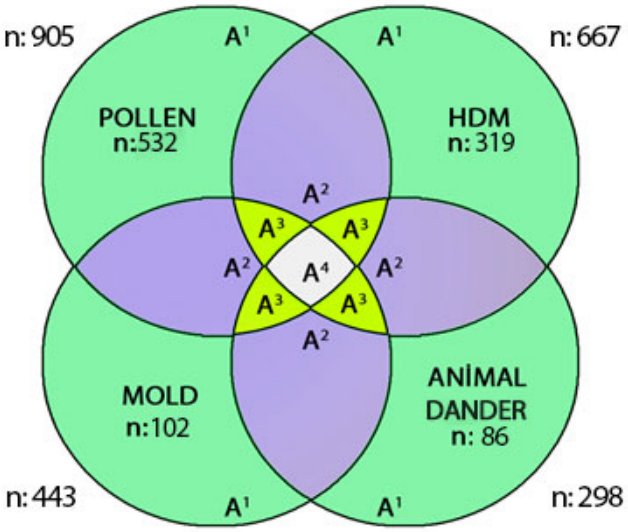

FIGURE 1
Allergen groups and number of patients with allergen sensitization
In total, 1586 of 2391 patients with rhinitis had positive results on SPT for allergen sensitization and were diagnosed with AR. A1: patients with one allergen sensitization, A2: patients with two allergen sensitizations, A3: patients with three allergen sensitizations, A4: patients with four allergen sensitizations.

FIGURE 2
Allergen types and number of patients with sensitization. The number of allergen reactivity include patients positive for multiple allergens in an ENT clinic in Istanbul.

The number of sensitive patients according to each allergen type is presented in Figure 2. The highest number of patients were sensitive to D. farinae and lowest to dog dander (Figure 2). Interestingly, the most prevalent allergen types in Istanbul were *Dermatophagoides* (*D. pteronyssinus* + *D. farinae*) and tree pollen mix (Figure 2).

TABLE 1
Percentage of sensitization according to age and sex for each allergen type

		Group 1 n (%)	Group 2 n (%)	Group 3 n (%)	Group 4 n (%)	p value
Pollen	**M**	53 (17.43%)	125 (41.12%)	89 (29.28%)	37 (12.17%)	0.00
	F	145 (24.13%)	209 (34.78%)	165 (27.45%)	82 (13.64%)	0.36
	All	198 (21.88%)	334 (36.91%)	254 (28.07%)	119 (13.15%)	0.05
HDM	**M**	71 (28.98%)	93 (37.96%)	51 (20.82%)	30 (12.24%)	0.02
	F	122 (28.91%)	128 (30.33%)	99 (23.46%)	73 (17.3%)	0.17
	All	193 (28.94%)	221 (33.13%)	150 (22.49%)	103 (15.44%)	0.12
Mold	**M**	39 (25.49%)	64 (41.83%)	36 (23.53%)	14 (9.15%)	0.08
	F	80(27.59%)	95(32.76%)	79(27.24%)	36(12.41%)	0.47
	All	119 (26.86%)	159 (35.89%)	115 (25.96%)	50 (11.29%)	0.06
Animal	**M**	32 (33.68%)	40 (42.11%)	16 (16.84%)	7 (7.37%)	0.00
dander	**F**	62 (30.54%)	76 (37.44%)	45 (22.17%)	20 (9.85%)	0.03
	All	94(31.54%)	116 (38.93%)	61 (20.47%)	27 (9.06%)	0.00
Total	**M**	130 (23.09%)	230 (40.85%)	139 (24.69%)	64(11.37%)	0.22
	F	264 (25.81%)	349 (34.12%)	268 (26.2%)	142 (13.88%)	0.25
	All	394 (24.84%)	579 (36,51%)	407 (25,66%)	206 (12,99%)	0,15

M: Male, F: Female, n: number of patients, p: Kruskal–Wallis test

Allergen sensitization according to age and sex. Patients were divided into four different age groups with 10-year intervals. Age groups 1, 2, 3, and 4 had 394, 579, 407, and 206 individuals, respectively. The highest sensitization to all allergen groups was observed in group 2 (36.5%) and the lowest was in group 4 (13.0%) (Table 1). The highest sensitization in male patients was observed in group 2 (40.9%) and lowest in group 4 (11.4%). Sensitization in female patients was also highest in group 2 (34.1%) and lowest in group 4 (13.9%) (Table 1). There was no significant difference in terms of allergen sensitization between males and females in the same age groups ($p > 0.05$) (Table 1). Additionally, allergen sensitization to pollen, HDM, mold, and animal dander was highest in group 2 and lowest in group 4 in both the sexes (Table 1).

DISCUSSION

Our results show that 66.3% of patients (total, 1586) with rhinitis symptoms had AR based on at least one sensitive response on SPT; i.e., two of three patients with rhinitis may have an atopic reaction. Therefore, SPT is one of the main tests for the diagnosis of patients with AR with an atopic reaction. These results were similar to the results on SPT and percentage of patients with sensitization reported in a study in a small city 150 km away from Istanbul [9, 10].

Most patients (65.5%) have sensitization to only one type of allergen (pollen, HDM, mold, or animal dander); multiple allergen sensitizations were lowest (38.8%) for animal dander and highest (68.2%) for pollen (Figure 1). Therefore, results of the current study showed that patients affected with indoor allergens have a lower number of multiple allergen sensitizations. This may be a result of repeated exposure to indoor allergens in living areas, affecting the patient's immune system and developing tolerance to the allergens. However, pollen exerts a stimulating effect on the immune system, and cross reactions to other allergens may develop.

Sensitivity to allergens is associated with many factors, such as climate, geography, lifestyle, and humidity. These factors affect allergen responses of the population to pollen, HDM, fungi, and animal dander. The results observed in the city of Bushehr in the southwestern part of Iran are consistent with the results of the current study on allergen sensitization [11]. In the study in Iran, pollen was the most common allergen in a rural region, but the percentage of indoor allergens, such as HDMs, was lower than that in the current study. Lifestyle and local climate, especially humidity, may have resulted in this difference [12, 13].

HDMs live on carpets, soft furnishings, and bedding. They thrive at approximately 25–30°C with relative humidity between 75% and 80% [14, 15]. Istanbul's temperature and humidity rates constitute a suitable environment for mites. Animal-borne allergens at home and workplace are of clinical importance. Hair, urine, and saliva of cats and dogs are sources of allergy, in addition to dander. In European and Western countries, there is a higher sensitivity to these allergens [2]. In European and North American countries, sensitivity to cat and dog dander is an important consideration for common aeroallergens [1, 16].

Indoor allergens, such as HDMs, are the most prevalent, affecting more than 56% of sensitive patients (e.g., Mexico City) [17]. Outdoor allergens, such as pollen, are the most prevalent in Istanbul re-

gion, affecting approximately 57.1% of sensitive patients, which may be explained by the characteristics of various flora; climatic factors, such as wind rate and high humidity; and regional geographical conditions.

The high rate of sensitivity to pollen allergens, pollen-bearing trees, grass, and flowers may be attributed to their heavy presence throughout the year in Istanbul. Indeed, airborne allergens, such as pollen and spores, have been suggested as the main cause of allergic respiratory problems in temperate countries [18]. Grass, weeds, and tree pollen mix are spread by the wind rather than by insects, and the clinical significance of pollen varies depending on the geographic location [19].

The least common sensitive allergens in Istanbul were animal dander (Table 1). The overall sensitization to cats and dogs in the European population is very similar, but regional differences are found. Cat dander sensitization was seen in an average of 26.3% (range, 16.8%– 49.3%) of patients. The rate of sensitization to dog allergens was 27.2% (range, 16.1%–56%) [20]. House-dwelling animals are not common in Istanbul compared with Europe. The current results showed that sensitization to animal dander was observed in 18.8% of patients, which was lower than the lowest ranges in European countries. This difference may be attributed to the lifestyles of individuals in Istanbul [20]. Living arrangements, mostly apartments, do not allow for coexistence of animals with humans in indoor settings in Istanbul.

Sensitivity to inhalant allergens and its clinical presentation are affected by age, and the number of studies including age and sensitivity has been increasing worldwide [21]. The symptoms of AR often begin in adolescence but may start at any age [22]. The allergen sensitization in our study was found to be highest (36.5%) in group 2 (age range, 30–39 years) and lowest (13%) in group 4 (age range, 50–59 years) ($p < 0.01$; Table 1). There are many parameters influencing decreased sensitization in older age. The most probable causes are lifestyle, senescence of immunity inducing tolerance, and long-term exposure to allergens that triggers a state of anergy to immunogens. In a recent study from Iran, there was a significant difference between different age groups with respect to the frequency of AR ($p = 0.006$) [11].

The main difference according to sex was increased sensitization to HDM and animal dander in males compared with females in group 2 (Table 1). This difference may have resulted due to occupational, lifestyle, and hormonal differences. Exposure to HDMs and animal dander occurs at home. In Istanbul, males aged 20–29 years generally spend lesser time at home than females, which may have resulted in the differences in results. Lifestyle changes in males in this age range, such as getting married and working, may result in increased exposure to indoor allergens (Table 1).

The cases in our study reflected age and sex characteristics of the population of our region. An additional prospective study is in progress to include comparisons of sensitization for variations in occupation, lifestyle, and climatic conditions.

In conclusion, this study was important for monitoring allergen sensitivity of patients with rhinitis in a large city. It also showed that sensitization decreases with increasing age for all types of allergens, and the percentage of sensitization may change according to the age and sex of the patient. Monitoring patients with allergen sensitization according to age groups and sex is important for environmental regulation, design of living spaces, working conditions, and physical and biological materials in the living space. These data will be useful for the evaluation of ecological effects of global climate change and environmental conditions on allergic diseases and regulation of preventive health services.

The authors declare no conflict of interest. The authors declare that this study received no financial support. Protocol of this study was approved by ethics committee.

REFERENCES

[1] Salo, P.M., Arbes, S.J., Jaramillo, R., Calatroni, A., Weir, C.H., Sever, M.L., Hoppin, J.A., Rose, K.M., Liu, A.H., Gergen, P.J. (2014) Prevalence of allergic sensitization in the United States: results from the National Health and Nutrition Examination Survey (NHANES) 2005-2006. Journal of Allergy and Clinical Immunology. 134, 350-359.

[2] Tran, N.P., Vickery, J., Blaiss, M.S. (2011) Mana-gement of rhinitis: allergic and non-allergic. Allergy, asthma and immunology research. 3, 148-156.

[3] Dottorini, M., Bruni, B., Peccini, F., Bottini, P., Pini, L., Donato, F., Casucci, G., Tantucci, C. (2007) Skin prick-test reactivity to aeroallergens and allergic symptoms in an urban population of central Italy: a longitudinal study. Clinical and Experi-mental Allergy. 37, 188-196.

[4] Katelaris, C., Lee, B., Potter, P., Maspero, J,. Cingi, C., Lopatin, A., Saffer, M., Xu, G., Walters, R. (2012) Prevalence and diversity of allergic rhinitis in regions of the world beyond Europe and North America. Clinical and Experimental Allergy. 42, 186-207.

[5] Olivieri, M., Verlato, G., Corsico, A., Lo Cascio, V., Bugiani, M., Marinoni, A., de Marco, R. (2002) Prevalence and features of allergic rhinitis in Italy. Allergy. 57, 600-606.

[6] Dorner, T., Lawrence, K., Rieder, A., Kunze, M. (2007) Epidemiology of allergies in Austria. Results of the first Austrian allergy report. Wiener Medizinische Wochenschrift. 157, 235-242.

[7] Bousquet, J., Khaltaev, N., Cruz, A., Denburg, J., Fokkens, W., Togias, A., Zuberbier, T., Baena-Cagnani, C., Canonica, G., Van Weel, C. (2009) Allergic Rhinitis and its Impact on Asthma (ARIA) 2008 update: In collaboration with the World Health Organization, GA (2) LEN and AllerGen [ARIA update 2008: Die allergische rhinitis und ihr einfluss auf das asthma].
[8] Duggan, E.M., Sturley, J., Fitzgerald, A.P., Perry, I.J., Hourihane, J.O.B. (2012) The 2002–2007 trends of prevalence of asthma, allergic rhinitis and eczema in Irish schoolchildren. Pediatric allergy and immunology 23: 464-471.
[9] Öztürk, Ö., Tokmak, A., Güçlü, E., Yıldızbaş, Ş., Gültekin, E. (2005) Düzce'de allerjik rinitli hastalarda prick testi sonuçları. Düzce Tıp Fakültesi Dergisi. 1, 11-14.
[10] Ceylan. E., Gencer, M., Şan, İ., Iyinen, İ. (2006) Allerjik Rinitli Olgularımızda Prick Testlerde Saptanan Aeroallerjen Dağılımı. Turkiye Klinikleri Journal of Medical Sciences. 26, 370-374.
[11] Farrokhi, S., Gheybi, M.K., Movahed, A., Tahmasebi, R., Iranpour, D., Fatemi, A., Etemadan, R., Gooya, M., Zandi, S., Ashourinejad, H. (2015) Common aeroallergens in patients with asthma and allergic rhinitis living in southwestern part of Iran: based on skin prick test reactivity. Iranian Journal of Allergy, Asthma and Immunology. 14, 133.
[12] Cingi, C., Topuz, B., Songu, M., Kara, C.O., Ural, A., Yaz, A., Yıldırım, M., Miman, M.C., Bal, C. (2010) Prevalence of allergic rhinitis among the adult population in Turkey. Acta Otolaryngol (Stockh). 130, 600-606.
[13] Yasan, H., Aynali, G., Akkuş, Ö., Doğru, H, Özkan, M., Şahin, M. (2006) Alerjik rinitten sorumlu alerjen profilinin değişimi ve semptomlarla korelasyonu. KBB-Forum. 5(4), 158-160.
[14] Høst, A., Halken, S. (2003) Practical aspects of allergy-testing. Paediatric respiratory reviews. 4, 312-318.
[15] Höst, A., Andrae, S., Charkin, S., Diaz-Vázquez, C., Dreborg, S., Eigenmann, P., Friedrichs, F., Grinsted, P., Lack, G., Meylan, G. (2003) Allergy testing in children: why, who, when and how? Allergy. 58, 559-569.
[16] Bousquet, P.J., Chinn, S., Janson, C., Kogevinas, M., Burney, P., Jarvis, D. (2007) Geographical variation in the prevalence of positive skin tests to environmental aeroallergens in the European Community Respiratory Health Survey I. Allergy. 62, 301-309.
[17] Larenas-Linnemann, D., Michels, A., Dinger, H., Shah-Hosseini, K., Mösges, R., Arias-Cruz, A., Ambriz-Moreno, M., Barajas, M.B., Javier, R.C., Moreno, M.A.C. (2014) Allergen sensitization linked to climate and age, not to intermittent-persistent rhinitis in a cross-sectional cohort study in the (sub) tropics. Clinical and translational allergy. 4, 1.
[18] Morris, A. (2009) Atopy, anamnesis and allergy testing. InnovAiT: The RCGP Journal for Associates in Training. 2, 158-165.
[19] Hawarden, D., Motala, C. (2009) Diagnostic testing in allergy. S Afr Med J. 99, 531-535.
[20] Zahradnik, E,. Raulf, M. (2014) Animal allergens and their presence in the environment. Frontiers in immunology. 5.
[21] Pawankar, R., Canonica, G., Holgate, S., Lockey, R. (2011) World Allergy Organization (WAO) white book on allergy. Wisconsin: World Allergy Organisation Available online at: http://www worldallergy org/UserFiles/file/ WAO-White-Book-on-Allergy web pdf.
[22] Singh, A.B., Kumar, P. (2003) Aeroallergens in clinical practice of allergy in India. An overview. Annals of Agricultural and Environmental Medicine. 10, 131-136.

Received: **07.03.2018**
Accepted: **22.04.2018**

CORRESPONDING AUTHOR

Ahmet Hamdi Kepekci
Division of Audiology,
İstanbul Yeni Yüzyıl University,
Bağcılar caddesi No: 52
Haznedar Güngören
Istanbul, 34160 - Turkey

e-mail: ahmethamdi.kepekci@yeniyuzyil.edu.tr

© by PSP Volume 27 – No. 7/2018 pages 5119-5124 Fresenius Environmental Bulletin

ENHANCED A^2/O PROCESS FOR TREATMENT OF HETEROCYCLIC AND POLYCYCLIC AROMATIC HYDROCARBONS IN COAL GASIFICATION WASTEWATER

Peng Xu[1,2,*], Hao Xu[1,2]

[1]College of Civil Engineering, Hunan University, Changsha, Hunan 410082, China
[2]Key Laboratory of Building Safety and Energy Efficiency, Ministry of Education, Changsha, Hunan 410082, China

ABSTRACT

Based on the comparison of A/O and A^2/O processes, the removal characteristics of heterocyclic and polycyclic aromatic hydrocarbons(PAHs) in A^2/O process were investigated. Additionally, the effects of anaerobic co-metabolism, multistage co-metabolism and step feeding on the removal rates were studied. The results showed that the kinds and concentrations of heterocyclic and PAHs in the effluent of A^2/O process were less than that of A/O process. The removal rates of pyridines, quinolines, biphenyls and naphthalenes at the optimum HRT of 52h were 64.2%, 58.1%, 61.7% and 67.4% respectively. When 200 mg/L glucose was anaerobically co-metabolized, the removal rates increased by 4.1%, 5.1%, 3.6% and 5%, respectively, but it has no obvious difference with the enhanced glucose concentrations. Effect of multistage co-metabolism could improve the COD, TOC removal efficiencies from 83.5%, 84.2% to 90.6%, 89.4% by improving the treatment effect of each section of the process; Step feeding can promote the removal of heterocyclic and PAHs, and the effect was more remarkable at the ratio of anaerobic:anoxic stage of 2:1.

KEYWORDS:
Coal Gasification Wastewater; polycyclic aromatic hydrocarbons, A^2/O, multistage co-metabolism, step feeding

INTRODUCTION

Due to the present increase in the consumption of natural gas, coal gasification technology is gaining more and more attention. However, wastewater generated during the coal gasification processes contains a large number of toxic and refractory compounds, such as phenolic compounds, cyanide, pyridine, and long-chain alkanes, posing a major challenge to environmental safety [1, 2]. Although the pretreatment processes of ammonia-stripping and solvent extraction are effective for the reduction of ammonia and phenolic compounds, the content of refractory organic compounds in the coal gasification wastewater (CGW) remains high [2, 3]. Biological treatment is by far the most widely applied and cost-effective process for wastewater treatment [4]. However, due to a certain number of refractory and inhibitory pollutants in CGW, COD and total phenols are poorly removed by the conventional activated sludge process.

Recently, much attention has been directed to anoxic-oxic (A-O) and anaerobic–anoxic–oxic (A^2/O) due to its capability to improve the biodegradability of CGW [5]. Rava and Chirwa [6] found that the biological enrichment-modified A/O process can achieve COD and TN removal rates of 99% and 80%, respectively. Liu et al. [7] found that A^2/O-MBR process can achieve COD and ammonia removal rates of 96.6% and 85.6%, respectively. However, the above-mentioned reports are limited to the removal of comprehensive index, e.g. COD or TN, few studies on heterocyclic or polycyclic aromatic hydrocarbons (PAHs) were reported. Actually, the heterocyclic and PAHs existed in CGW not only inhibits microbial activity and reduces the treatment efficiency, but also turns into a variety of intermediate products that can not be completely degraded [8, 9]. Thus, the effective removal of these pollutants is the key to improve the efficiency of CGW treatment and to enhance the quality of effluent [10].

In this study, the removal characteristics of heterocyclic and PAHs in A^2/O process were investigated. Additionally, the effects of anaerobic co-metabolism, multistage co-metabolism and step feeding on the removal rates were studied. The results can provide theoretical basis for enhancing the biological treatment process of CGW and controlling the discharge of heterocyclic and polycyclic aromatic hydrocarbons.

MATERIALS AND METHODS

Experimental set-up. The experiment adopts a self-made A^2/O system. The main body is composed of anaerobic tank (3L), anoxic pool (3L) and aerobic pool (9L). The system is operated in two phases: ① the raw water is directly flowed into the anoxic tank, making the system run as a A/O system, and the treatment effect of the A/O process is investigated. ② after the operation of A/O is stabilized, the anaerobic tank is accessed to examine the effect of the A^2/O.

Inoculum and wastewater. Seed sludge was collected from the full scale aerobic reactors treating real CGW at China Coal Longhua Harbin Coal Chemical Industry Co. Ltd. The reactors had been operating for 12 months, and the sludge was grey-black with good settlement characteristics; MLVSS/MLSS≈0.69. Real CGW used in this study was obtained from the same coal gasification plant mentioned above. The main characteristics of real CGW after phenol extraction with diisopropyl ether and ammonia stripping are COD 2021.3~2081.9 mg/L, BOD_5 696.5~731.3 mg/L, TOC 799.6~827.8 mg/L, total phenols 601.5~623.1 mg/L, NH_3-N 106.1~114.7 mg/L, pH 6.5~7.5.

Analytical methods. Heterocyclic and polycyclic aromatic hydrocarbons were determined by high performance liquid chromatograph (HPLC) (HP7950, Agilent). Culture samples for HPLC analysis were filtered through 0.25 μm membrane [11]. COD, BOD_5, toatl phenols, TOC, MLVSS, MLSS and ammonia were determined according to standard methods [12].

RESULTS AND DISCUSSION

Comparison of processing efficiency between A/O and A^2/O. As shown in Fig. 1, the removal efficiencies of COD, BOD_5, TOC, total phenolics and ammonia nitrogen in the A/O process were 66.3%, 86.1%, 65.5%, 69.5% and 85.4%, compared that of 81.5%, 89.6%, 79.2%, 78.5% and 90.6% respectively in A^2/O process. The reason that the BOD_5 and ammonia nitrogen removal rates are basically the same is that the former is formed mainly of easily degradable phenols and is rapidly oxidized and decomposed by the microorganisms; On the other hand, a sufficiently long aerobic time to be making ammonia nitrogen fully converted by the ammoxidation bacteria. On the contrary, the difference between CODCR and TOC removal rate is larger, for this reason, two kinds of process effluent were analyzed by GC/MS, and result showed that the types and concentrations of heterocyclic and polycyclic aromatic compounds in A^2/O process effluent were obviously lower than that of A/O process effluent.

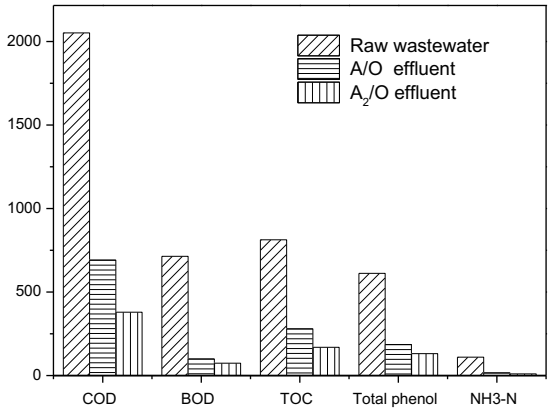

FIGURE 1
Comparison of A/O and A^2/O in treatment of coal gasification wastewater

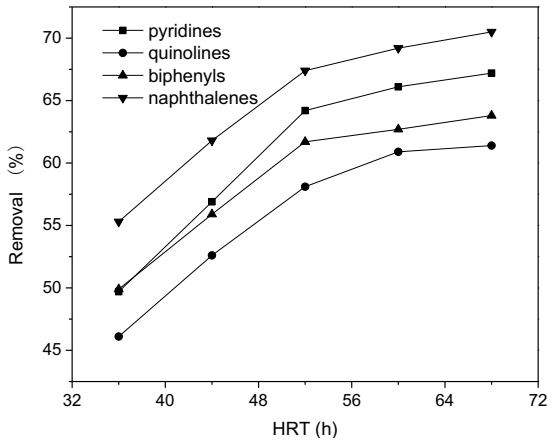

FIGURE 2
The removal of heterocyclic and PAHs at various HRT

Removal of heterocyclic and polycyclic aromatic hydrocarbons by A^2/O process. HRT is an important factor that determines the design and operation of biological treatment processes. Appropriate HRT can not only increase the contact oxidation time between microorganisms and organic matters, but also reduce the process footprint and investment costs [13]. As shown in Fig.2, the removal rates of pyridines, quinolines, biphenyls and naphthalenes with HRT of 36 h were 49.7%, 46.1%, 49.9% and 55.3%, and increased to 64.2%, 58.1%, 61.7% and 67.4% respectively with HRT of 52 h, indicating that the prolongation of HRT could promote the removal of heterocyclic and polycyclic aromatic hydrocarbons. However the removal rates have not changed significantly with a more largerer HRT. Therefore, the optimal HRT for the A^2/O process is 52 h.

As can be seen from Fig. 3, the heterocyclic

and PAHs are removed in all stages of the A^2/O process, but the removal rates are generally lower than 40% in each stage. The reason may be that the coexistence of multiple toxic substances causes a synergistic inhibitory effect, resulting in a significant reduction in the activity of degrading enzymes [14]. In addition, the removal rates of heterocyclic and polycyclic aromatic hydrocarbons in anaerobic and anoxic stages were significantly higher than those in aerobic stage. The removal of pyridine pollutants in anaerobic, anoxic and aerobic stage accounted for 40.1%, 42.5% and 17.4% of the total removal, and the quinolines were 34.5%, 56.2% and 9.3% and the biphenyls were 48.6%, 35.4% and 16%, and the naphthalenes were 46.4% and 36.2% and 17.4% respectively. That is, nitrogenous heterocyclic compounds such as pyridines and quinolines were most removed in the anoxic stage, while PAHs such as biphenyls and naphthalene were most removed in the anaerobic stage. Nevertheless, the A^2/O process effluent still contains a high concentration of organic pollutants. Therefore, for the removal of heterocyclic and PAHs, it is difficult to achieve the ideal effect only by prolonging HRT, which needs to change the microbial living and metabolic environment to weaken the toxicity and inhibition of pollutants.

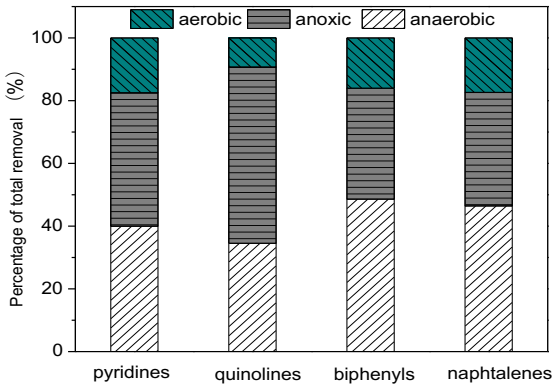

FIGURE 3

Ratio of pollutant removal in each stage of A^2/O process

Optimization of A^2/O process. Anaerobic co-metabolism alone. For refractory organic contaminants, adding appropriate amount of glucose as a carbon source and energy for microbial catabolism can improve the substrate removal ability [15]. Fig. 4 shows that 200 mg/L glucose can make the removal rates of pyridines, quinolines, biphenyls and naphthalenes from 64.2%, 58.1%, 61.7% and 67.4% to 68.3%, 63.2%, 65.3% and 72.4%, respectively, indicating that glucose could promote the removal of heterocycles and polycyclic aromatic hydrocarbons in A^2/O process, but the removal rates of all four compounds did not increase significantly with the increase of glucose concentration to 300 mg/l and 400 mg/l. This may be due to the high degradation of glucose itself, which results in the degradation of glucose in the anaerobic phase and failure to play a role in the subsequent treatment unit. Additionally, a high proportion of growth substrate or target pollutants is not conducive to co-metabolism. Thus, when the glucose concentration exceeds a certain value, the effect of co-metabolism is not obvious.

In order to confirm the above theory, the removal effect of four kinds of compounds in different stages at various glucose concentration was analyzed.

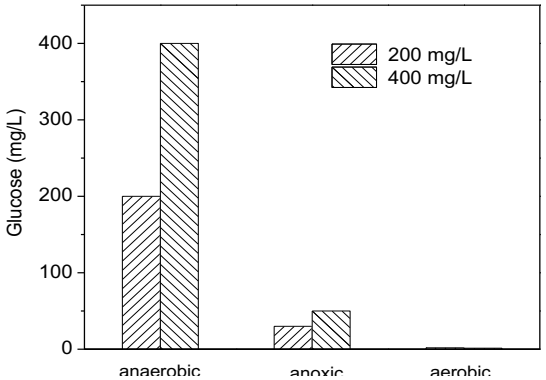

FIGURE 4

Glucose concentrations in each stage of A^2/O process

It can be seen from Table 1 that the removal rates of four kinds of compounds in anaerobic stage can be significantly increased by 200 mg/L glucose, but the removal rates were almost not changed at 400 mg/L, which indicated that excessive glucose does not promote the removal of heterocycles and PAHs in anaerobic stage. On the contrary, the removal rates in anoxic and aerobic sections were basically unaffected. As shown in Fig.4, regardless of the concentration of glucose in the anaerobic stage, in the anoxic stage, it is less than 50 mg/L, and disappeared in the aerobic stage, indicating that glucose has been fully degraded in anaerobic stage. Therefore, in order to give full play to the role of glucose co-metabolism, glucose could be added to anaerobic, anoxic and aerobic stages separately.

Multistage co-metabolism. In order to make full use of the effect of co-metabolism, 400mg/L glucose was put into each stage of the A^2/O process according to anaerobic 200 mg/L, anoxic 100 mg/L and aerobic 100 mg/L, and the removal of heterocyclic and PAHs in multistage co-metabolism was investigated.

TABLE 1
Effect of glucose concentration on pollutants removal in each stage

	anaerobic（%）			anoxic（%）			aerobic（%）		
Glucose（mg/L）	0	200	400	0	200	400	0	200	400
pyridines	24.8*	30.5	30.9	33.6	34.1	35.3	20.5	18.4	19.6
quinolines	21.7	29.4	30.2	36.4	35.8	37.4	17.3	16.9	17.2
biphenyls	28.4	37.2	38.1	25.7	26.9	29.5	12.8	13.5	11.8
naphthalenes	30.1	39.4	40.9	29.6	31.2	31.1	19.6	20.1	19.4

The result is the average of triple experiments.

TABLE 2
Effect of metabolic conditions on contaminants removal in each stage (%)

Compounds	Anaerobic co-metabolism			Multistage co-metabolism		
	anaerobic	anoxic	aerobic	anaerobic	anoxic	aerobic
pyridines	34.6	38.5	24.7	33.8	43.8	31.2
quinolines	29.6	42.2	12.8	28.3	46.5	18.1
biphenyls	37.2	34.1	19.8	35.5	39.7	26.1
naphthalenes	42.7	37.2	26.9	41.2	45.4	35.7

TABLE 3
The removal of heterocyclic and PAHs at various feeding patterns

Compounds	(anaerobic:anoxic)			
	anaerobic only	2:1	1:1	1:2
pyridines	64.2	68.3	64.3	58.9
quinolines	58.1	64.5	59.5	50.4
biphenyls	61.7	66.4	63.6	54.6
naphthalenes	67.4	73.3	70.2	60.8

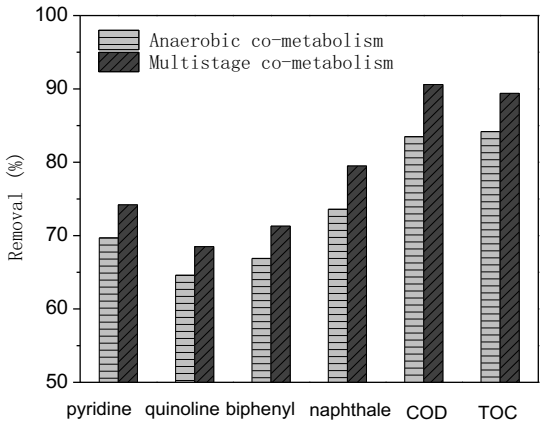

FIGURE 5
Effect of metabolic conditions on pollutant removal rates

It is shown from Table 2 that the removal rates of four compounds in anaerobic stage under two metabolic conditions was similar, the difference of the removal rates in the anoxic section and the aerobic stage was significantly, which indicated that the presence of glucose improved the transformation of heterocyclic and PAHs in the latter two stages. As shown in Fig.5, by increasing the removal rates of heterocyclic and PAHs, the removal rates of COD and TOC were increased from 83.5% and 84.2% to 90.6% and 89.4%，indicating that multistage co-metabolism could effectively improved the removal ability of A^2/O process.

Effect of step feeding. As a phenolic compound with large content in coal gasification wastewater, phenol can promote the transformation of heterocyclic and PAHs by the method of co-metabolism [16]. However, the study showed that too high concentration of phenol weakens the removal efficiency [17]. The removal of heterocyclic and PAHs was investigated when the inflow in anaerobic and anoxic stage at the ratio of 2:1, 1:1 and 1:2, respectively.

As shown in Table 3, the removal rates of pyridines, quinolines, biphenyls and naphthalenes increased from 64.2%, 58.1%, 61.7% and 67.4% to 68.3%, 64.5%, 66.4% and 73.3% respectively when the water ratio was 2: 1, indicating that the step feeding has a significant effect on the removal of heterocyclic and PAHs. However, gradually increasing the amount of wastewater in the anoxic section resulted in a sharp decrease in the removal rates, which was reduced to 58.9%, 50.4%, 54.6% and 60.8% at the ratio of 1: 2. Even the removal of heterocyclic and PAHs at 1:1 was similar to that of 1:2, the COD, BOD_5 and TOC removal rates were significantly lower. The reason may be that a large

number of wastewater directly into the anoxic section, which can only be removed from the latter two segments. This would results in many easily degradable substances flowing out of the system without thorough transformation. Therefore, the optimum influent ratio of anaerobic:anoxic stage of A^2/O process was 2: 1.

CONCLUSIONS

The results indicated that the kinds and concentrations of heterocyclic and polycyclic aromatic hydrocarbons (PAHs) in the effluent of A^2/O process were less than that of A/O process. The removal rates of pyridines, quinolines, biphenyls and naphthalenes in A^2/O process was 64.2%, 58.1%, 61.7% and 67.4% respectively, at the optimal HRT of 52 h. Multistage co-metabolism could make full use of the effect of co-metabolism and effectively improved the removal ability of A^2/O process. The optimum influent ratio of anaerobic:anoxic stage of A^2/O process was 2: 1. The results can provide theoretical basis for enhancing the biological treatment process of CGW and controlling the discharge of heterocyclic and PAHs.

ACKNOWLEDGEMENTS

This work was financially supported by the National Natural Science Foundation (51708196) and the Natural Science Foundation of Hunan Province, China (2018JJ3060).

REFERENCES

[1] Xu, P., Xu, H. and Shi, Z. (2018) A novel bio-electro-Fenton process with $FeVO_4$/CF cathode on advanced treatment of coal gasification wastewater. Sep Purif Technol. 194, 457-461.

[2] Wang, H., Quan, B., An, X., Yang, Y. and Tian, C. (2017) Advanced Decomposition of Coking Wastewater in Relation to Total Organic Carbon Using an Electrochemical System. Pol J Environ Stud. 26, 941-947.

[3] Xu, P., Ma, W., Hou, B. and Shi, Z. (2017) A novel integration of microwave catalytic oxidation and MBBR process and its application in advanced treatment of biologically pretreated Lurgi coal gasification wastewater. Sep Purif Technol. 177, 233-238.

[4] Hou, B., Li, Z., Deng, R. and Ren, B. (2017) Advanced treatment of coal chemical industry wastewater by expansive flow biological aerated filter. Fresen Environ Bull. 26, 4517-4521.

[5] Lu, H., Zhang, G., Lu, Y., Zhang, Y., Li, B. and Cao, W. (2016) Using co-metabolism to accelerate synthetic starch wastewater degradation and nutrient recovery in photosynthetic bacterial wastewater treatment technology. Environ Technol. 37, 775-784.

[6] Rava, E. and Chirwa, E. (2016) Effect of carrier fill ratio on biofilm properties and performance of a hybrid fixed-film bioreactor treating coal gasification wastewater for the removal of COD, phenols and ammonia-nitrogen. Water Sci Technol. 73, 2461-2467.

[7] Liu, J.X., Li, W.G., Wang, X.H., Liu, H.Y. and Wang, B.Z. (1998) Removal of nitrogen from coal gasification wastewater by nitrosofication and denitrosofication. Water Sci Technol. 38, 39-46.

[8] Zhao, Q., Han, H., Hou, B., Zhuang, H., Jia, S. and Fang, F. (2014) Nitrogen removal from coal gasification wastewater by activated carbon technologies combined with short-cut nitrogen removal process. J Environ Sci-China. 26, 2231-2239.

[9] Zhang, Q., Yu, C., Fang, J., Xu, H., Jiang, Q., Yang, S. and Wang, W. (2017) Using the Combined Fenton-MBR Process to Treat Cutting Fluid Wastewater. Pol J Environ Stud. 26, 1375-1383.

[10] Xu, P., Han, H., Hou, B., Zhuang, H., Jia, S., Wang, D., Li, K. and Zhao, Q. (2015) The feasibility of using combined TiO2 photocatalysis oxidation and MBBR process for advanced treatment of biologically pretreated coal gasification wastewater. Bioresource Technol. 189, 417-420.

[11] Dabrowska, J., Bawiec, A., Paweska, K., Kaminska, J. and Stodolaki, R. (2017) Assessing the Impact of Wastewater Effluent Diversion on Water Quality. Pol J Environ Stud. 26, 9-16.

[12] Xu, P., Ma, W., Han, H., Jia, S. and Hou, B. (2015) Isolation of a Naphthalene-Degrading Strain from Activated Sludge and Bioaugmentation with it in a MBR Treating Coal Gasification Wastewater. B Environ Contam Tox. 94, 358-364.

[13] Zhang, Y. and Li, H. (2017) Tolerance and recovery ability of moving bed biofilm reactor to phenol and cresol shock load under vary dissolved oxygen concentration. Fresen Environ Bull. 26, 4268-4276.

[14] Li, Y., Tabassum, S. and Zhang, Z. (2016) An advanced anaerobic biofilter with effluent recirculation for phenol removal and methane production in treatment of coal gasification wastewater. J Environ Sci-China. 47, 23-33.

[15] Wang, W., Han, H., Yuan, M. and Li, H. (2010) Enhanced anaerobic biodegradability of real coal gasification wastewater with methanol addition. J Environ Sci-China. 22, 1868-1874.
[16] Osuna-Ramirez, R., Arreola Lizarraga, J. A., Padilla-Arredondo, G., Arturo Mendoza-Salgado, R. and Celina Mendez-Rodriguez, L. (2017) Toxicity of wastewater from fish-meals production and their influence on coastal waters. Fresen Environ Bull. 26, 6408-6412.
[17] Zhang, H., He, Y., Jiang, T. and Yang, F. (2011) Research on characteristics of aerobic granules treating petrochemical wastewater by acclimation and co-metabolism methods. Desalination. 279, 69-74.

Received: **08.03.2018**
Accepted: **02.05.2018**

CORRESPONDING AUTHOR

Peng Xu
College of Civil Engineering,
Hunan University,
Changsha, Hunan 410082 - China

e-mail: xp12904@163.com

© by PSP Volume 27 – No. 7/2018 pages 5125-5130 Fresenius Environmental Bulletin

COMPARATIVE EVALUATION OF MAIZE HYBRIDS UNDER WATER STRESS AND RAIN-FED CONDITIONS

Sekip Erdal*

Bati Akdeniz Agricultural Research Institute, 07100, Antalya, Turkey

ABSTRACT

In this study, commercial and experimental maize hybrids were tested under managed water stress (WS), rain-fed (RF) (mild stress) and well-watered conditions at two sites to determine hybrid responses to different water stress conditions. According to the results, mean yield reduction due to the water stress and rain-fed conditions were determined 77% and 9% respectively. Anthesis date delayed, anthesis-silking interval increased, plant height shortened, number of ear per plant and yield sharply decreased under water stress when compared to rain-fed and well-watered conditions. ADA 351 was identified as the most water stress tolerant commercial hybrid in terms of stress tolerance index (STI), drought resistance index (DI) and yield reduction ratio (YRR). ANT KTH-3 experimental hybrid was identified as a water stress tolerant hybrid in terms of STI index. It was determined that KALUMET and ANT KTH-4 hybrids were sensitive to water stress. P31G98, ANT KTH-3 and DKC6589 hybrids were the best hybrids in terms of STI and DI indices in RF experiment. Interestingly ANT KTH-4, a sensitive hybrid, was also identified as mild water stress sensitive hybrid. This study identified tolerant and sensitive maize hybrids to severe and mild water stress and showed the importance of the germplasm for water stress.

KEYWORDS:
Maize, Drought stress, Tolerance, Yield, Stress indices

INTRODUCTION

Water is vital for the plants. Plants use water as a solvent, as a cooling agent, as a reagent and for maintaining plant structure. When the plants wilts, its turgor decreases, cells collapses, membranes and protein structures lose their functions [1]. Depending the duration of the water scarcity, plants can even be completely die.

Although many part of the world has suffered from the water stress during crop production, it is predicted that global warming is affecting the climate, and thus this situation will be worse in the future [2]. In order to cope with the water stress for a sustainable agricultural production the water must be delivered to the plant using modern irrigation systems and the varieties that tolerant to water deficit should be preferred.

Water stress or drought is probably the most important abiotic stress that limits maize production in the world [1, 3]. Drought stress currently has adversely affects Sub-Saharan Africa, South America and Asia maize production. With the effort by International Wheat and Maize Improvement Center (CIMMYT) targeting these tropical or sub-tropical environments positive results has achieved [4]. However, maize production in temperate regions gets little attention when compared with these mentioned areas [5]. Turkey produces maize during summer season and irrigation has to be applied for a profitable production especially in southern part of the country. Although rain is adequate for the maize production in northern Turkey, irrigation is done when needed. However, 90% of Turkey's maize production is being irrigated. Turkey is not a country that rich in freshwater resources and classified as water deficit country [6].

In order to mitigate water stress effects on maize, maize hybrids that tolerant to drought stress must be identified and used in the production. The objectives of this study were to: i) determine performances of commercial and experimental maize hybrids under managed water stress and rain-fed conditions in two different environments of a temperate region, ii) investigate yield reduction due to the water stress, iii) identify hybrid or hybrids that tolerant to drought based on investigated traits.

MATERIALS AND METHODS

Four high yielded commercial checks and four experimental maize hybrids that selected from drought tolerance maize breeding studies were used in the study. ADA 351, DKC6589, P31G98 and KALUMET were the commercial checks. ANT KTH-1 and ANT KTH-2 are maize hybrids that generated from tropical line x temperate line crosses. ANT KTH-3 is a temperate x temperate cross and parents of this hybrid (TK 72 and Ant 24702) reported as tolerant to drought stress [7]. ANT KTH-4 is another temperate x temperate cross and male parent of this hybrid (Ant-I-84) identified as a sensitive

line to drought [7].

The experimental hybrids were generated at Bati Akdeniz Agricultural Research Institute's (BATEM) Field Crops Department, Antalya (36052'N, 30045'E) in 2015. Experimental hybrids and commercial checks, total eight hybrids were tested in BATEM, Antalya (Southern of Turkey) and Maize Research Institute's field, Sakarya (Northern) (40°48'N 30°25'E) in 2016.

Water stress (stress) and well-watered (normal) experiments were conducted side by side in each location. Reproductive stage water stress targeted and therefore water withdrawn 2-3 weeks before flowering until harvest as suggested by [1] and [3].

Experiments were designed as Randomized Complete Blocks with three replications. Plots consisted of three rows, 5 meters long with row spacing of 0.7 meters. Fertilization and plant protection measures were undertaken according to local recommendations.

Mean precipitation, humidity and temperature data during the period of the study for Antalya (water stress location) and Sakarya (rain-fed location) was shown in Figure 1 and Figure 2 respectively. It can be seen from the figures that there is no or insignificant precipitation in Antalya location where is a severe water stress site during reproductive stage of maize to harvest, while precipitation was recorded in Sakarya that is considered as rain-fed environment. Also, Sakarya location's temperature data is more suitable for maize production when compared to Antalya.

The traits evaluated in the research were measured according to [1] and [8]. Anthesis-Silking Interval (ASI), plant height (PH), number of ears per plant (EPP), and yield traits which were reported to be the most important traits [4] in drought stress studies were used for the study.

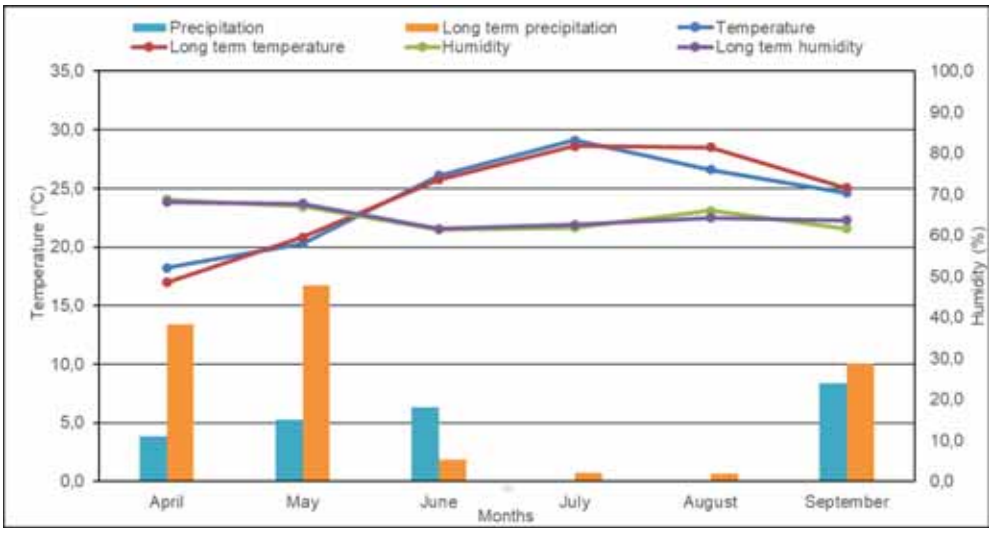

FIGURE 1
Precipitation, temperature and humidity data of Antalya (water stress) location

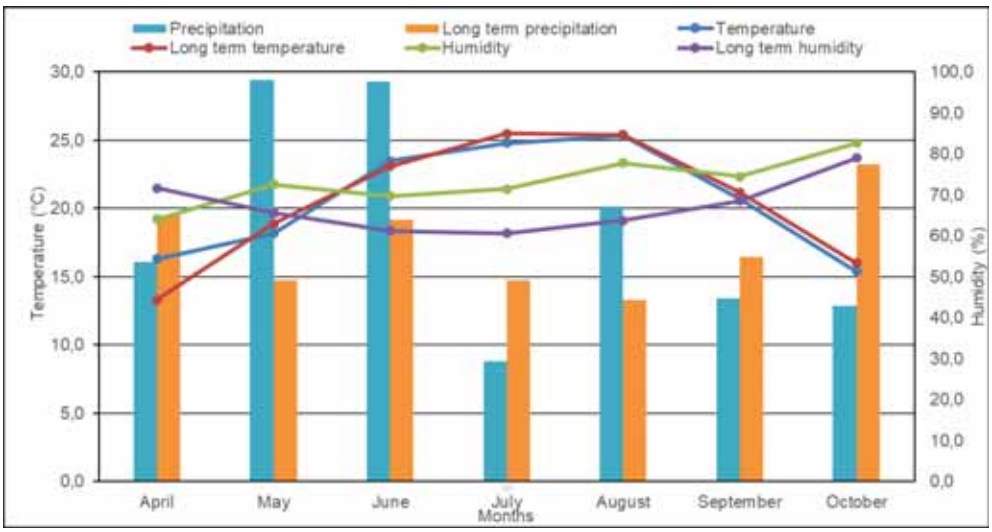

FIGURE 2
Precipitation, temperature and humidity data of Sakarya (rain-fed) location

Analysis of variance was performed on data in WW and WS experiments. Genotype x environment interactions were calculated and in the present of the interaction every location was evaluated separately. Drought Resistance Index (DI) [9], Stress Tolerance Index (STI) [10] and Yield Reduction Ratio (YRR) [11] indices were computed using Excel files.

$STI = (Ys \times Yp)/(\bar{Y}p^2)$
$DI = (Ys \times (Ys/Yp))/\bar{Y}s$
$YRR = 1 - (Ys/Yp)$

In the above formulas, Ys, Yp, $\bar{Y}$s and $\bar{Y}$p represent the trait under stress (WS), trait under well-watered (WW) for each genotype and experiment trait means in WS and WW conditions for all genotypes, respectively.

RESULTS AND DISCUSSION

Results of the analysis of variance for anthesis date (AD) and anthesis-silking interval (ASI) obtained from well-watered (WW), water stress (WS) and rain-fed (RF) experiments were shown in Table 1. According to the analysis, genotype (G) by environment (location, E) interaction was found to be significant for both traits. Highly significant differences ($P<0.01$) were determined amongst genotypes for AD except for Sakarya RF experiment. Studies have shown that anthesis or tasseling in maize can be partially delayed under severe water stress [12, 13, 14, 15]. Since Antalya WS experiment was carried out under severe water stress, it seems anthesis delayed for 1.2 days (72 days) when compared with the Antalya WW (70.8 days) conditions. However, mean anthesis date in other experiments including Sakarya RF is similar. When ASI values investigated, Antalya WS experiment showed that under severe water stress conditions ASI increased in between hybrids. Lowest ASI values were detected in DKC6589 (2.3) and P31G98 (2.7) hybrids, while highest values were obtained from ANT-KTH-2 and ANT-KTH-4 hybrids. Rain-fed conditions (Sakarya RF) did not affect ASI showed little or no water stress in that location. During flowering silk growth in maize is more susceptible to water stress or other several abiotic stresses [1]. Silk growth is delayed under water stress conditions and this situation causes an increase in ASI. Therefore, selection for lower ASI values were being suggested by previous studies [16, 17, 18].

Genotype x environment interaction was found to be statistically insignificant for plant height (Table 2). When mean plant height values evaluated, plant height of all hybrids decreased under water stress conditions compared to well-watered counterpart. This finding confirms previous studies [19, 20, 18]. Ear per plant values under Sakarya RF, Antalya WW and Sakarya WW conditions seems to be around one ear per plant. However, severe water stress affected negatively EPP in Antalya WS conditions. It is known that hybrids that have more ear per plant are tolerant to drought [1, 21]. According to the EPP results KALUMET seems to be more drought sensitive hybrid when compared other tested germplasm.

Mean grain yield (kg/ha) of the hybrids obtained from water stress (Antalya WS), rain-fed (Sakarya RF) and well-watered conditions (Antalya WW and Sakarya WW) was given in Table 3. According to the results, experiment mean of the Antalya WS was 2129.6 kg/ha while mean of the Antalya WW trial was 9340.4 kg/ha. Yield reduction because of the water stress in Antalya location was calculated as 77% showing occurrence of the severe water stress in that location. On the other hand, mean grain yield of the Sakarya RF experiment and Sakarya WW experiments were recorded as 11329.1 kg/ha and 12356.8 kg/ha respectively. Small amount of yield loses (9%) due to water stress was determined in the location.

TABLE 1
Anthesis date and anthesis-silking interval values obtained from the experiments

	Anthesis date (AD)				Anthesis-Silking Interval (ASI)			
Hybrids	Antalya WS	Sakarya RF	Antalya WW	Sakarya WW	Antalya WS	Sakarya RF	Antalya WW	Sakarya WW
ADA 351	69.0 c	69.7	68.3 d	69.3 cd	4.0 bc	1.0	2.0 ab	0.7 d
ANT KTH-1	77.7 a	70.7	74.7 a	74.0 a	4.3 sc	1.3	1.0 c	1.3 bc
ANT KTH-2	74.3 b	71.7	73.7 ab	74.0 a	6.0 a	1.0	2.3 a	2.0 a
ANT KTH-3	66.3 d	68.0	66.3 e	67.7 d	4.3 bc	1.0	2.0 ab	1.0 cd
ANT KTH-4	72.3 b	70.7	71.7 c	71.7 b	5.0 ab	1.0	2.0 ab	1.7 ab
DKC6589	69.7 c	70.3	68.0 de	69.3 cd	2.3 d	1.0	1.3 bc	1.0 cd
KALUMET	73.7 b	70.3	71.3 c	70.0 bc	3.3 cd	0.7	1.3 bc	1.0 cd
P31G98	73.3 b	71.3	72.7 bc	70.3 bc	2.7 d	1.0	1.7 ac	1.0 cd
Mean	72.0	70.3	70.8	70.8	4,0	1.0	1.7	1.2
CV	1.59	2.09	1.54	1.4	15	26.9	24	26.3
LSD	2.00**	2.58ns	1.91**	1.7**	1.06**	0.82ns	0.71*	0.56**
G x E	**		*		**		*	

Mean values in the same column followed by the same letter are not significantly different from each other.
* and ** indicate significance at 0.05 and 0.01, respectively; ns indicates not significant.

Three commercial checks (ADA 351, P31G98 and DKC6589) and a drought tolerant x drought tolerant (ANT KTH-3) hybrid showed good yield performance in the Antalya WS where was a controlled drought conditions. KALUMET and ANT KTH-4 (drought sensitive x drought tolerant) can be identified as the sensitive hybrids when compared other hybrids. ANT KTH-4 gave similar result that was obtained from Sakarya RF experiment. However, KALUMET check had good yield in Sakarya RF indicated that this hybrid can tolerate small amount of water stress.

In order to identify hybrids that tolerance to water stress (Antalya WS) or mild stress conditions (Sakarya RF), stress tolerance index (STI), drought resistance index (DI) and yield reduction ratio (YRR) was analyzed and the results were given in Table 4. According to the results, ADA 351 was identified as the most water stress tolerant hybrid in terms of three indices. ANT KTH-3 experimental hybrid was identified as a water stress tolerant hybrid in terms of STI index. It was determined that KALUMET and ANT KTH-4 hybrids were sensitive to water stress. When results of the mild stress (Sakarya RF) experiment evaluated P31G98, ANT KTH-3 and DKC6589 hybrids were the best hybrids in terms of STI and DI indices. Interestingly ANT KTH-4, a sensitive hybrid, was also identified as mild water stress sensitive hybrid. The yield reduction in this hybrid was 27% in mild water stress. Researches showed that stress tolerance increased in commercial modern maize hybrids due to the selection under high plant densities [22, 23, 24]. Commercial maize hybrids tested in this study except KALUMET showed good performance under severe water stress. This study's findings are in concordance with the mentioned studies above.

TABLE 2
Mean plant height and ear per plant characteristics of the hybrids from water stress, rain-fed and well-watered conditions

	Plant height (cm)				Ear per plant (EPP)			
Hybrids	Antalya WS	Sakarya RF	Antalya WW	Sakarya WW	Antalya WS	Sakarya WW	Antalya WW	Sakarya WW
ADA 351	205.0 ab	293.3	222.5	296.7	0.74 a	1.0	1.0 ab	1.0
ANT KTH-1	203.3 bc	293.3	245.0	296.7	0.73 a	1.0	1.0 ab	1.0
ANT KTH-2	205.0 ab	293.3	241.7	291.7	0.66 b	1.0	0.9 b	1.0
ANT KTH-3	193.3 c	293.3	218.3	290.0	0.70 a	1.0	1.0 ab	1.0
ANT KTH-4	207.5 ab	286.7	241.1	290.0	0.63 b	1.0	0.7 b	1.0
DKC6589	209.2 ab	300.0	233.3	283.3	0.72 a	1.0	1.0 ab	1.0
KALUMET	208.0 ab	293.3	240.8	300.0	0.47 c	1.1	1.0 ab	1.0
P31G98	214.4 a	293.3	230.0	296.7	0.68 a	1.0	1.1 a	1.0
Mean	205.7	293.3	234.1	293.1	0.7	1,0	1.0	1.0
CV	2.87	2.74	5.49	3.44	10.2	4,34	5.58	2.96
LSD	10.34 *	14.06ns	22.51ns	17.68ns	0.12**	0,08ns	0.09 *	0.05ns
G x E	ns		ns		**		**	

Mean values in the same column followed by the same letter are not significantly different from each other.
* and ** indicate significance at 0.05 and 0.01, respectively; ns indicates not significant.

TABLE 3
Mean grain yield (kg/ha) of the hybrids obtained from water stress, rain-fed and well-watered conditions

Hybrids	Antalya WS	Sakarya RF	Antalya WW	Sakarya WW
ADA 351	2850.7 a	9527.8 c	9524.0 b	10459.7 cd
ANT KTH-1	2195.6 bc	12003.5 ab	9208.6 b	12272.0 bc
ANT KTH-2	1932.1 cd	10248.4 bc	7882.0 c	11512.8 bcd
ANT KTH-3	2534.5 ab	12511.1 a	10625.2 a	13341.8 ab
ANT KTH-4	840.9 e	7160.6 d	6781.0 d	9641.9 d
DKC6589	2510.0 ab	12659.1 a	10104.3 ab	13518.1 ab
KALUMET	1513.3 d	12713.6 a	10624.1 a	12996.5 b
P31G98	2659.5 a	13810.0 a	9974.0 ab	15111.2 a
Mean	2129.6	11329.1	9340.4	12356.8
CV	11.78	10.71	5.70	9.60
LSD	439.45**	2126.2**	933.48**	2077.7**
Genotype x Environment	**		*	

Mean values in the same column followed by the same letter are not significantly different from each other.
* and ** indicate significance at 0.05 and 0.01, respectively.

TABLE 4
Stress tolerance index (STI), drought resistance index (DI) and yield reduction ratio (YRR) values of the hybrids

	Antalya						Sakarya					
Hybrids	STI		DI		YRR		STI		DI		YRR	
ADA 351	0.31	a	0.40	a	0.70	c	0.66	de	0.77	c	0.09	b
ANT KTH-1	0.23	b	0.25	b	0.76	bc	0.96	bc	1.04	ab	0.02	b
ANT KTH-2	0.17	c	0.23	b	0.75	bc	0.78	cd	0.82	bc	0.10	b
ANT KTH-3	0.31	a	0.29	ab	0.76	b	1.10	ab	1.04	abc	0.06	b
ANT KTH-4	0.07	d	0.05	c	0.88	a	0.47	e	0.48	d	0.27	a
DKC6589	0.29	a	0.29	ab	0.75	bc	1.12	ab	1.05	ab	0.06	b
KALUMET	0.18	bc	0.10	c	0.86	a	1.08	b	1.10	a	0.02	b
P31G98	0.30	a	0.34	ab	0.73	bc	1.37	a	1.12	a	0.08	b
Mean	0.23		0.24		0.77		0.94		0.93		0.09	
CV	12.76		16.87		4.37		16.7		16.8		8.3	
LSD	0.05**		0.11**		0.06**		0.28**		0.27**		0.14*	

Mean values in the same column followed by the same letter are not significantly different from each other.
* and ** indicate significance at 0.05 and 0.01, respectively.

CONCLUSIONS

In conclusion, maize hybrids were tested under water stress and rain-fed conditions in two different locations of Turkey and hybrids responses to either severe water stress or mild water stress were different. According to the results obtained from this study revealed that ADA 351 maize hybrid was the most water stress tolerant commercial genotype in terms of three stress tolerance indices. ANT KTH-3 experimental hybrid was identified as a water stress tolerant hybrid in terms of stress tolerance index. The study identified KALUMET and ANT KTH-4 as sensitive to water stress. P31G98, ANT KTH-3 and DKC6589 hybrids were the best hybrids in terms of stress tolerance index and drought resistance index. This study identified tolerant and sensitive maize hybrids to severe and mild water stress and showed the importance of the germplasm for water stress.

REFERENCES

[1] Banziger, M., Edmeades, G.O., Beck, D., Bellon, M. (2000) Breeding for drought and nitrogen stress tolerance in maize, from theory to practice. Mexico, D.F.: CIMMYT.

[2] Anonymus, (2015) Water scarcity and global warming. Time for change. http://timeforchange.org/water-scarcity-and-global-warming. Access date: 02.02.2018.

[3] Bruce, W.B., Edmeades, G.O., Barker, T.C. (2002) Molecular and physiological approaches to maize improvement for drought tolerance. Journal of Experimental Botany. 53, 13-25.

[4] Edmeades, G.O. (2013) Progress in achieving and delivering drought tolerance in maize - An Update. ISAAA, Ithaca, NY.

[5] Erdal, S. Pamukcu, M., Ozturk, A., Aydinsakir, K., Soylu, S. (2015) Combining abilities of grain yield and yield related traits in relation to drought tolerance in temperate maize breeding. Turk Journal of Field Crops. 20(2), 203-212.

[6] Oktem, A.U. and Aksoy, A. (2014) Report of the Turkey's water. http://www.wwf.org.tr/?4180. Access date: 02.03.2018.

[7] Erdal, S. (2014) Determination of drought tolerance level of maize (Zea mays L.) inbred lines and molecular characterization. Suleyman Demirel University, Graduate School of Applied and Natural Sciences, Department of Field Crops. Isparta.

[8] UPOV. (2009) International Union for The Protection of New Varieties of Plants. www.upov.int.

[9] Lan, J. (1998) Comparison of evaluating methods for agronomic drought resistance in crops. Acta Agriculturae Boreali-occidentalis Sinica. 7, 85–87.

[10] Fernandez, G.C.J. (1992) Effective selection criteria for assessing plant stress tolerance. Proceeding of The International Symposium on Adaptation of Vegetables and Other Food Crops in Temperature and Water Stress, Aug. 13–16, Shanhua, Taiwan, 257–270.

[11] Golestani, S.A., Assad, M.T. (1998) Evaluation of four screening techniques for drought resistance and their relationship to yield reduction ratio in wheat. Euphytica. 103, 293–299.

[12] Abrecht, D.G and Carberry, P.S. (1993) The influence of water deficit prior to tassel initiation on maize growth, development and yield. Field Crops Research. 31, 55-69.

[13] Oteigui, M.E., Andrade, F.H. and Suero, E.E. (1995) Growth, water use and kernel abortion of maize subjected to drought at silking. Field Crops Research. 40(2), 87-94.

[14] Oktem, A. (2008) Effects of deficit irrigation on some yield characteristics of sweet corn. Bangladesh J. Bot. 37(2), 127-131.
[15] Aslam, M., Zamir, M.S.I., Afzal, I., Yaseen, M. (2013) Morphological and physiological response of maize hybrids to potassium application under drought stress. Journal of Agriculture Research. 51(4), 443-454.
[16] Bolanos, J., Edmeades G.O. (1993) Eight cycle of selection for drought tolerance in lowland tropical maize. ii. responses in reproductive behaviour. Field Crops Research. 31, 269-289.
[17] Ribaut, J.M., Gonzalez-de-Leon, D., Jiang, C., Edmeades, G.O. and Hoisington, D.A. (1997) Identification and transfer of ASI quantitative trait loci (QTL): A strategy to improve drought tolerance in maize lines and populations. In: Edmeades, G.O.,
[18] Ziyomo, C., Bernardo, R. (2012) Drought tolerance in maize: indirect selection through secondary traits versus genome wide selection. Crop Science. 53,1269–1275.
[19] Witt, S., Galicia, L., Lisec, J., Cairns, J., Tiessen, A., Araus, J.L, Palacios-Rojas, N., Fernie, A.R. (2011) Metabolic and phenotypic responses of greenhouse grown maize hybrids to experimentally controlled drought stress. Molecular plant. 5(2), 401-417.
[20] Araus, J.L., Serret, M.D., Edmeades, G.O. (2012) Phenotyping maize for adaptation to drought. Frontiers Physiology. 3, 305.
[21] Bao-cheng, S., Cheng L., Yun-su, S., Yan-chun, S., Tian-yu, W., Yu, L. (2010) Relationships between ear number per plant and drought tolerance in maize Hybrids. Xinjiang Agricultural Sciences. 2007-05.
[22] Duvick, D.N. (1977) Genetic rates of gain in hybrid maize during the last 40 years. Maydica. 22, 187-196.
[23] Duvick, D.N. (1992) Genetic contributions to advances in yield of U.S maize. Maydica. 37, 69-87.
[24] Tollenar, M., Wu, J. (1999) Yield improvement in temperate maize is attributable to greater stress tolerance. Crop Science. 39, 1597-1604.

Received: **09.03.2018**
Accepted: **30.04.2018**

CORRESPONDING AUTHOR

Sekip Erdal
Bati Akdeniz Agricultural Research Institute,
07100, Antalya – Turkey

e-mail: sekip65@yahoo.com

© by PSP Volume 27 – No. 7/2018 pages 5131-5136 Fresenius Environmental Bulletin

BIOLOGICAL INHIBITION AND CO-METABOLISM OF HETEROCYCLIC AND POLYCYCLIC AROMATIC HYDROCARBONS

Peng Xu[1,2,*], Hao Xu[1,2]

[1]College of Civil Engineering, Hunan University, Changsha, Hunan 410082, China
[2]Key Laboratory of Building Safety and Energy Efficiency, Ministry of Education; Hunan University, Changsha, Hunan 410082, China

ABSTRACT

From the perspective of kinetics, the biodegradation of pyridine, quinoline, biphenyl and naphthalene in aerobic, anoxic and anaerobic conditions were investigated. The results showed that the addition of substrates did not change the degradation kinetic types, but inhibited the degradation of the original substrates. The inhibition strength was related to substance types of additive and original substrate as well as the degradation conditions; In aerobic condition, pyridine and quinoline to other substances is highly inhibition, diphenyl is moderately inhibition, naphthalene is low inhibition; In anoxic condition, the nonstructural analogs were low inhibition and the structural analogs were moderately inhibition; In anaerobic condition, the structural analogs were low inhibition and the nonstructural analogs were moderately inhibition. Glucose co-metabolism could promote the degradation of heterocyclic and polycyclic aromatic hydrocarbons, and it has a more significant effect on the substances with poorer degradation performance.

KEYWORDS:
Biodegradation, inhibition, co-metabolism, heterocyclic, polycyclic aromatic hydrocarbons

INTRODUCTION

Heterocyclic and polycyclic aromatic hydrocarbons (PAHs) are an important class of organic pollutants and widely exist in various types of wastewater such as coking, agriculture, medical treatment and chemical industry [1-3]. They are carcinogenic and mutagenic and seriously damage the environment and human health. Many treatment techniques such as activated carbon adsorption, chemical oxidation, and biodegradation have been developed to remove them from contaminated environment [4, 5]. Of these options, biological treatment has the advantages of low energy consumption and no secondary pollution, and gradually replace the physicochemical process as the preferred method to degradation of such pollutants [6].

At present, environmental workers have carried out studies on their biodegradation under various conditions. Shen et al. [7] found that glutaraldehyde is the main intermediate of pyridine anoxic degradation by GC/MS analysis. Thangaraj et al. [8] reported that the degradation rate constant decreased with the increase of the number of benzene rings in aerobic biodegradation of some aromatic hydrocarbons. Also many studies showed that a number of bacterial strains are able to utilize naphthalene and its derivatives under aerobic and anaerobic conditions [9-11].

Nevertheless, the above reports are mostly limited to the single substrate degradation by a single microflora, few studies on mixed pollutants was studied. However the actual wastewater is often in a difficult and easily degradable pollutants coexist state. Studies have shown that the addition of substrates may inhibit cell enzyme activity and weaken microbial degradation capacity, but also may increase the degradation of refractory substances through co-metabolism effect [12].

In this study, the biodegradation of four kinds of heterocycles and polycyclic aromatic hydrocarbons (PAHs) such as pyridine, quinoline, biphenyl and naphthalene were studied. The inhibitions of heterocycles and polycyclic aromatic hydrocarbons under different degradation conditions were determined. The effects of glucose as a co-metabolic substrate on the biodegradation of four compounds were also investigated. It provides the basis for controlling the discharge of pollutants and guiding the biological treatment of sewage.

MATERIALS AND METHODS

Inoculation sludge. The activated sludge was obtained from aerobic sludge reflux system of a coal chemical company, with the MLVSS/MLSS of 0.69. After 1 day of aeration, activated sludge was pretreated by centrifugation, distilled water washing, and was finally diluted with phosphate buffer solution to make an MLSS 20 g/L sludge concentrate. Mineral salt medium (MSM), described by Jeswani and Mukherji [10] was used in the acclimation and biodegradation experiments. The sludge was domesticated in mineral salt medium with heterocyclic or

polycyclic aromatic hydrocarbons as solo carbon source.

According to the pollutants and experimental conditions, 12 groups were acclimated in 3 L beaker (aerobic) or 2.5 L glass jar (anoxic, anaerobic) by sequential batch culture method. Regulation of MLSS 1 g/l, DO 3~5 mg/l (aerobic), 0.3~0.5 mg/l (anoxic), 0~0.2 mg/l (anaerobic), pH 6.5~7.5, temperature 25~30°C, respectively. In addition, $NaNO_3$ solution was added to make the COD/NO_3^--N 8.0 in anoxic conditions. Four cycles were acclimated at each concentration of 10 mg/l, 20 mg/l, 30 mg/l and 50 mg/l, respectively, with 24 h each cycle. Then it would be stored in 4 °C refrigerator.

Experimental method. Dual substrate inhibition experiments were performed in 500 ml Erlenmeyer flasks (aerobic) or stoppered bottles (anoxic, anaerobic). Taking pyridine as an example, the experiment was divided into four groups under each condition. A certain amount of domesticated sludge and culture medium with pyridine as substrate was added into each flask/bottle. Regulation of MLSS 1 g/l, DO 3~5 mg/l (aerobic), 0.3~0.5 mg/l (anoxic), 0~0.2 mg/l (anaerobic), pH 6.5~7.5. Each group contained pyridine 50 mg/L. Except for the control group, the other three groups contained quinoline 15mg/l, biphenyl 15mg/l or naphthalene 15mg/l, respectively. The flask was placed in a constant temperature shaking chamber (120 rpm) in aerobic or in a magnetic agitator during degradation. The remaining concentration of pyridine in each group was measured periodically and the average value of three times was recorded.

The glucose co metabolism experiment was divided into seven groups, except 50 mg/L pyridine in each bottle, also containing glucose 0, 25, 50, 100, 200, 300 or 400 mg/L, respectively. The conditions and operations were the same as that in the previous experiment.

Analysis method. Heterocyclic and polycyclic aromatic hydrocarbons were determined by high performance liquid chromatograph (HPLC) (HP7950, Agilent). Culture samples for HPLC analysis were filtered through 0.25 μm membrane, the determination of nitrate nitrogen using phenol method [7]. Other items were measured based on literature [11].

The biodegradation inhibition rate η of the additive to the test substance is calculated according to the formula $\eta = (k_1\text{-}k_2)/k_1 \times 100\%$. In the formula, k_1 is the test substance single substrate degradation rate constant; k_2 is the test substance degradation rate constant with additive.

The hibitory strength evaluation criteria: η<20%, low inhibition, 20%<η<40%, moderately inhibition, η>40%, highly inhibition.

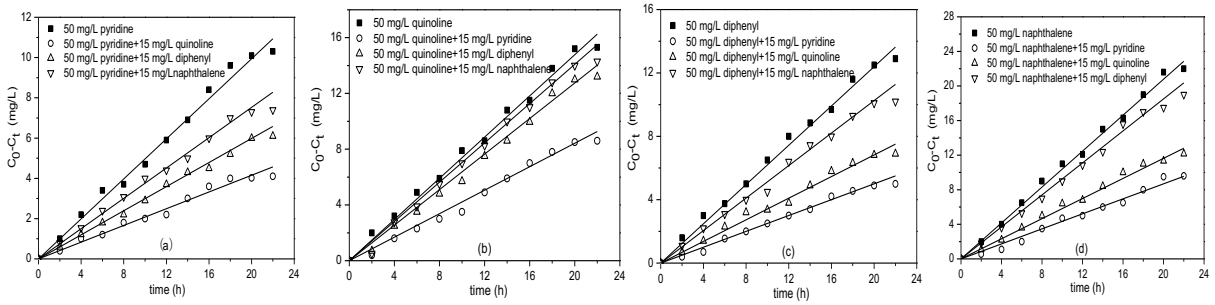

FIGURE 1
Aerobic degradation kinetics of heterocyclic and polycyclic aromatic hydrocarbons in dual substrates degradation, (a) pyridine; (b) quinoline; (c) diphenyl; (d) naphthalene

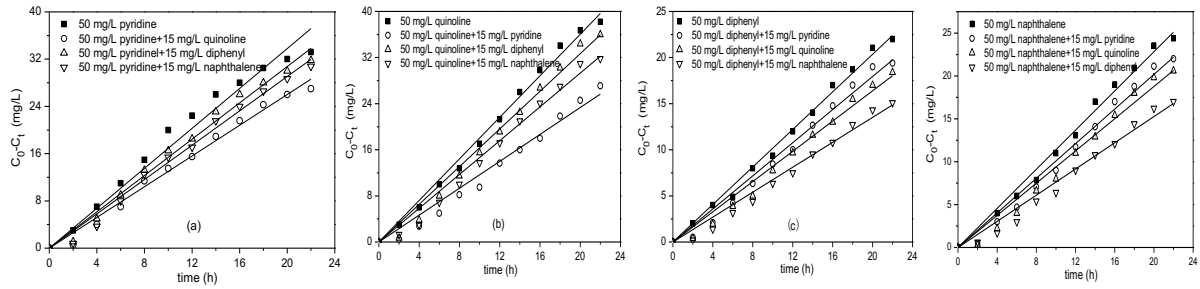

FIGURE 2
Anoxic degradation kinetics of heterocyclic and polycyclic aromatic hydrocarbons in dual substrates degradation, (a) pyridine; (b) quinoline; (c) diphenyl; (d) naphthalene

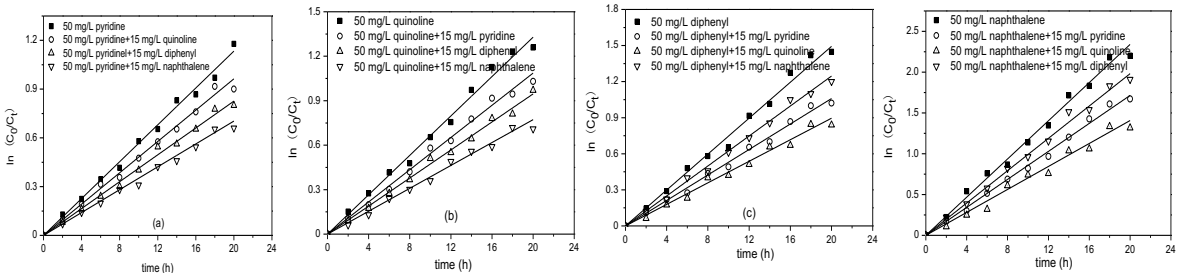

FIGURE 3
Anaerobic degradation kinetics of heterocyclic and polycyclic aromatic hydrocarbons in dual substrates degradation, (a) pyridine; (b) quinoline; (c) diphenyl; (d) naphthalene

TABLE 1
Degradation rate constant of original substrate in dual substrates

original substrate	Additive substrate	Degradation rate constant *k* (mg/(L·h)) Aerobic	Anoxic	Anaerobic
pyridine	-	0.463	1.869	0.0561
	quinoline	0.207	1.349	0.0475
	diphenyl	0.304	1.651	0.0402
	naphthalene	0.382	1.548	0.0351
quinoline	-	0.719	2.141	0.0632
	pyridine	0.425	1.366	0.0525
	diphenyl	0.568	1.918	0.0459
	naphthalene	0.689	1.727	0.0399
diphenyl	-	0.606	1.172	0.0724
	pyridine	0.263	1.055	0.0545
	quinoline	0.341	0.968	0.0469
	naphthalene	0.526	0.797	0.0612
naphthalene	-	1.007	1.308	0.1091
	pyridine	0.437	1.177	0.0859
	quinoline	0.567	1.104	0.0741
	diphenyl	0.805	0.906	0.0963

TABLE 2
Inhibition strength of four compounds in dual substrate under different conditions

Sub-strate	Aerobic				Anoxic				Anaerobic			
	pyr	qui	dip	nap	pyr	qui	dip	nap	pyr	qui	dip	nap
pyr	-	H*	M*	L*	-	M	L	L	-	L	M	M
qui	H	-	M	L	M	-	L	L	L	-	M	M
dip	H	H	-	L	L	L	-	M	M	M	-	L
nap	H	H	M	-	L	L	M	-	M	M	L	-

H, highly inhibition; M, moderately inhibition; L, low inhibition.

RESULTS AND DISCUSSION

Inhibition performance of heterocyclic and polycyclic aromatic hydrocarbons. Figs.1-3 were degradation kinetics of heterocyclic and polycyclic aromatic hydrocarbons in dual substrates degradation under aerobic, anoxic and anaerobic, respectively. It can be seen that adding substrate did not change the degradation kinetics of original substrate. The degradation process of four compounds was in accordance with the zero-order kinetics under aerobic and anoxic conditions, and was in accordance with the first-order kinetics under anaerobic condition. Nevertheless, as shown in Table 1, there is an identical characteristic that the degradation rate constant of original substrate in dual substrate (with additive) was significantly lower than that of in single substrate degradation, which indicated that the addition of substrates inhibited the degradation of the original substrates. A similar phenomenon was observed by others in the biodegradation systems for naphthalene removal, which could be attributed to the recalcitrance and the toxicity of quinoline [10].

Characteristics of inhibition strength. It can been seen based Section 3.1 and Table 1 that though the addition of substrates did not change the degradation kinetics type, but it inhibited the degradation of the original substrates. The inhibition strength was related to substance types of additive and original substrate as well as the degradation conditions. The inhibition strength of four compounds on other substrates under different conditions was investigated, as shown in Table 2.

Table 2 shows that under aerobic conditions, pyridine and quinoline were highly inhibition on the degradation of other substances, diphenyl was moderately inhibition, naphthalene was low inhibition,

which indicated that pyridine and quinoline were more toxic to aerobic degrading bacteria acclimated by other substrates. In contrast, the increase in naphthalene load has a weaker effect on the original substrate biodegradation. Thus in actual wastewater treatment, it is necessary to reduce the concentration of pyridine and quinoline in order to improve their self-degradation and to enhance the removal efficiency of polycyclic aromatic hydrocarbons (PAHs) such as diphenyl and naphthalene in aerobic biological treatment. Under anoxic conditions, structural analogs compounds were moderately inhibition, such as pyridine and quinoline, diphenyl and naphthalene; while nonstructural analogs compounds were low inhibition, such as pyridine and diphenyl, quinoline and naphthalene. This is due to the fact that the organism needs to be bound to the active site of the enzyme during its degradation. The selection of enzyme on substrate usually has specific structural requirements, which leads to the formation of competitive relationship between structural analogs compounds and a decrease in the catalytic effect [13]. The inhibition between nonstructural analogs compounds was caused by the additive inhibiting the activity of microbial cells, so the inhibition strength was relatively low. Under anaerobic conditions, structural analogs compounds were slightly inhibited each other, such as pyridine and quinoline, diphenyl and naphthalene, while nonstructural analogs compounds were moderately inhibition, such as pyridine and biphenyl, quinoline and naphthalene. The possible reason may be that anaerobic microbes have more abundant enzymes and have stronger tolerance to structurally similar pollutants after acclimation, and are susceptible to different structural pollutants [14].

Effect of glucose co-metabolism. One possible method of increasing the tolerance of the cells to substrate inhibition is to supplement the growth medium with conventional carbon sources, such as yeast extract or glucose [14]. The effect of glucose co-metabolism on the degradation of heterocyclic and polycyclic aromatic hydrocarbons was shown in Table 3.

It is shown from Table 3 that the degradation rate of four compounds increase with the increase of glucose concentration under different conditions, which indicated that glucose has a promote effect on the degradation of heterocyclic and polycyclic aromatic hydrocarbons. In the dual-substrate system, glucose is an excellent primary substrate since it not only easily induces the monooxygenase required for heterocyclic and polycyclic aromatic hydrocarbons transformation, but the glucose oxidation can also efficiently regenerates the consumed NADH, which is participating in the degradation pathway of the organic pollutant as electron donor [11]. Moreover, the addition of glucose greatly accelerated the degradation of heterocyclic and polycyclic aromatic hydrocarbons due to the increase of biomass production.

In spite of this, the increased amount of the degradation rate decrease with the increase of glucose concentration, which may be due to the lack of specificity of the catabolic enzyme, resulting in a competition between the growth substrate and the pollutants. The above relationship between the concentration of the co-substrate and the degradation rate can be expressed as follows [14]:

$E\text{-}E_0=\Delta E_{max}S/(K_b+S)$

Where E_0 is the degradation rate of the compound in single substrate, %; E is the degradation rate of the compound in glucose co-metabolism, ΔE_{max} is the possible maximum increase of the degradation rate, %; K_b is the half-saturation constant, mg/L; S is the glucose concentration, mg/L.

Taking $1/(E\text{-}E_0)$ as the ordinate Y, 1/s as the horizontal axis X, the linear regressions were fitted, and the results were shown in Table 4.

According to Table 3 and Table 4, not only the relationship between the degradation rates of four compounds and glucose concentrations can be obtained from E_{max}, K_b and E_0, but also the maximum degradation rate of each substance under different conditions can be obtained by E_0+E_{max}. In addition, the results of E_{max} under different conditions are

TABLE 3
Effect of glucose concentration on the degradation rate of four compounds (%)

Condition	Glucose (mg/L)	0	25	50	100	200	300	400
aerobic	Pyridine (50 mg/L)	22.0	29.2	33.8	39.4	44.7	47.4	48.9
	quinoline（50 mg/L）	33.8	39.3	42.6	46.4	49.8	51.4	52.3
	diphenyl (50 mg/L)	25.8	31.2	34.9	39.5	44.2	46.6	48.1
	naphthalene (50 mg/L)	41.2	43.9	46.1	48.9	52.3	54.2	55.6
anoxic	Pyridine (50 mg/L)	71.7	73.9	75.4	77.2	79.1	80.1	80.6
	Quinoline (50 mg/L)	77.2	79.2	80.6	82.3	84.8	86.1	86.7
	Diphenyl (50 mg/L)	42.2	47.3	50.9	55.8	61.1	63.8	65.5
	Naphthalene (50 mg/L)	47.1	50.6	53.4	57.3	62.1	65.2	66.9
anaerobic	Pyridine (50 mg/L)	67.4	71.2	73.5	77.0	81.2	82.3	83.2
	Quinoline (50 mg/L)	70.6	73.1	75.1	77.5	80.1	81.2	82.1
	Diphenyl (50 mg/L)	76.5	78.4	79.9	81.6	83.8	84.9	85.7
	Naphthalene (50 mg/L)	88.7	90.2	91.3	92.6	93.7	94.3	94.6

TABLE 4
Regression equations and parameters at glucose cometabolism

Condition	Substrate	Regression equations	R^2	$\triangle E_{max}$ (%)	K_b (mg/L)
aerobic	Pyridine	y=276.4x+2.96	0.9936	33.8	93.2
	quinoline	y=345.8x+4.36	0.9917	22.9	79.3
	diphenyl	y=381.4x+3.36	0.9883	29.7	113.5
	naphthalene	y=799.2x+4.73	0.9954	19.5	155.7
anoxic	Pyridine	y=917.7x+8.85	0.9715	12.6	103.7
	Quinoline	y=1043.7x+7.94	0.9872	11.3	131.5
	Diphenyl	y=405.2x+3.28	0.9736	30.5	123.6
	Naphthalene	y=614.8x+3.62	0.9924	27.6	169.8
anaerobic	Pyridine	y=533.5x+4.93	0.9904	20.3	108.3
	Quinoline	y=783.9x+6.71	0.9931	14.9	116.8
	Diphenyl	y=1049.6x+8.01	0.9927	12.5	131.2
	Naphthalene	y=1247.3x+13.51	0.9956	7.4	142.6

compared, results indicated that the effect of co-metabolism is related to the biodegradation performance of the compound itself. The more difficult to be degraded, the more obvious of the effect of co-metabolism. For example, the order of E_{max} in anoxic condition is diphenyl>naphthalene> pyridine>quinoline, which is just opposite to its single substrate degradability as shown in Table 3.

CONCLUSIONS

Results from this study demonstrated that the addition of substrates did not change the degradation kinetics type, but it would inhibit the degradation of the original substrates. Under aerobic conditions, pyridine and quinoline were highly inhibition on the degradation of other substances, diphenyl was moderately inhibition, naphthalene was low inhibition; Under anoxic conditions, structural analogs compounds were moderately inhibition, while nonstructural analogs compounds were low inhibition. Glucose co-metabolism can promote the degradation of heterocyclic and polycyclic aromatic hydrocarbons, and the relationship between the concentrations of the co-substrate and the degradation rates can be expressed as $E\text{-}E_0=\Delta E_{max}S/(K_b+S)$.

ACKNOWLEDGEMENTS

This work was financially supported by the National Natural Science Foundation (51708196) and the Natural Science Foundation of Hunan Province, China (2018JJ3060).

REFERENCES

[1] Haritash, A.K. and Kaushik, C.P. (2009) Biodegradation aspects of Polycyclic Aromatic Hydrocarbons (PAHs): A review. Journal of Hazardous Materials. 169, 1-15.

[2] Li, J., Luo, C., Song, M., Dai and Zhang, G. (2017) Biodegradation of Phenanthrene in Polycyclic Aromatic Hydrocarbon-Contaminated Wastewater Revealed by Coupling Cultivation-Dependent and-Independent Approaches. Environmental Science and Technology. 51, 3391-3401.

[3] Boruszko, D. (2017) Research on the influence of anaerobic stabilization of various dairy sewage sludge on biodegradation of polycyclic aromatic hydrocarbons PAHs with the use of effective microorganisms. Environmental Research. 155, 344-352.

[4] Kronenberg, M., Trably, E., Bernet, N. and Patureau, D. (2017) Biodegradation of polycyclic aromatic hydrocarbons: Using microbial bioelectrochemical systems to overcome an impasse. Environmental Pollution. 231, 509-523.

[5] Simeon, N., Mercier, G., Blais, J., Ouvrard, S. and Guedon, E. (2008) Decontamination of contaminated soils by polycyclic aromatic hydrocarbons in the presence of supplementary organic structures. Journal of Environmental Engineering and Science. 7, 467-479.

[6] Liu, Y., Han, H. and Fang, F. (2013) Application of bioaugmentation to improve the long-chain alkanes removal efficiency in coal gasification wastewater. Fresen. Environ. Bull. 22, 2448-2455.

[7] Shen, J., Zhang, X., Chen, D. and Wang, L. (2015) Characteristics of pyridine biodegradation by a novel bacterial strain, Rhizobium sp. NJUST18. Desalination and Water Treatment. 53, 2005-2013.

[8] Thangaraj, K., Kapley, A. and Purohit, H.J. (2008) Characterization of diverse Acinetobacter isolates for utilization of multiple aromatic compounds. Bioresource Technology. 99, 2488-2494.

[9] Li, Y., Zhou, J. and He, Q. (2017) Biodegradation of pyridine in sequencing batch biofilm reactor based on dissolved oxygen control. Fresen. Environ. Bull. 26, 1858-1864.

[10] Jeswani, H. and Mukherji, S. (2012) Degradation of phenolics and polynuclear aromatic hydrocarbons in a rotating biological contactor. Bioresource Technology. 111, 12-20.
[11] Kaisarevic, S., Luebcke-von Varel, U. and Pogrmic, K. (2009) Effect-directed analysis of contaminated sediment from the wastewater canal in Pancevo industrial area, Serbia. Chemosphere. 77, 907-913.
[12] Sun, Z., Li, J., Zhang, J., Wang, J.and Hu, X. (2017) Effect of glucose as co-metabolism substrate on the biodegradation of dichlorophenols. Fresen. Environ. Bull. 26, 6017-6027.
[13] Cascaval, D., Blaga, A.C. and Galaction, A. (2018) Diffusional effects on anaerobic biodegradation of pyridine in a stationary basket bioreactor with immobilized Bacillus sp. cells. Environmental Technology. 39, 240-252.
[14] Zhao, G., Chen, S. and Wei, C. (2014) Interaction and biodegradation evaluate of m-cresol and quinoline in co-exist system. International Biodeterioration and Biodegradation. 86, 252-257.

Received: **12.03.2018**
Accepted: **29.04.2018**

CORRESPONDING AUTHOR

Peng Xu
Key Laboratory of Building Safety and
Energy Efficiency,
Ministry of Education,
College of Civil Engineering,
Hunan University,
Changsha, Hunan 410082 – China

e-mail: xp12904@163.com

© by PSP Volume 27 – No. 7/2018 pages 5137-5141 Fresenius Environmental Bulletin

EVALUATION OF OZONATION TREATMENT EFFECT ON TOMATO FRUITS AND LETTUCE COLOUR

Asma M Shaderma[1], Maher B Al-Dabbas[2], Tawfiq M Al-Antary[3,*], Kholoud M Alananbeh[3]

[1]Ministry of Agriculture, Jordan.
[2]Department of Nutrition and Food Technology, School of Agriculture, University of Jordan, Amman, 11942, Jordan
[3]Department of Plant Protection, School of Agriculture, The University of Jordan, Amman, 11942, Jordan

ABSTRACT

This study was conducted to monitor the effect of ozonation treatment at different ozone concentrations for different periods of time on the red colour of tomato fruits and green colour of lettuce heads using Lovibond colourimeter. The results showed that ozonation is significantly affected all the colour values for both tomato fruits and lettuce heads, it was in a concentration- time dependent manner. The average Brightness for untreated tomato fruits and lettuce samples were 96.254 and 88.862, respectively, and after ozonation for 15 min at concentration of 5 ppm the average brightness were significantly increased (98.397 and 100.846), respectively. On the other hand, redness/ greenness and yellowness values of tomato fruits and lettuce were decreased significantly when compared with the untreated samples. The average redness/greenness values for untreated tomato fruits and lettuce samples were -0.815 and -14.629, and after ozonation for 15 min at concentration of 5 ppm the average redness /greenness were significantly decreased to -4.462 and -35.09, respectively, and yellowness values were decreased from 76.536 and 83.249 in untreated tomatoes and lettuce samples to 43.174 and 31.476, respectively. These results indicate that the red colour of tomato fruits and green colour of lettuce degraded significantly with ozone treatment, although this degradation in colour does not affect the marketable value of these products.

KEYWORDS:
Colour value, Lovibond, Tomato, Lettuce, Ozonation.

INTRODUCTION

Tomato and lettuce are among frequently consumed in several dishes in Jordan. In 2016, the produced amounts were 837344.4 and 70557.3 tons of tomatoes and lettuce, respectively [1]. The annual per capita consumption of vegetables is around 106.35 kg, and of tomato fruit is 33.7 kg [2].

Tomatoes and lettuce are among perishable products and can be attacked by different agricultural pests, as a result farmers have to use pesticides to improve their products quality and quantity. The intensive use of pesticides resulted in residuals remains in agricultural products after harvest, and in many cases these residues exceed the maximum residues limits (MRL) recommended by the Codex Alimntarous or EU MRL's, which may have the potential of adverse health impacts on human [3].

Ozonation treatment, ultraviolet radiation, washing vegetables with salts or vinegar or salt and vinegar mixture at different concentrations have been used in many agricultural products to reduce or eliminate pesticides residues and microbes [4, 5, 6]. Ozone, in particular, has been recognized as a strong oxidizing agent and could be used in gaseous or liquid state [4, 5, 6, 7].

In any treatment or processing of food, the most important factor to be considered is to maintain the food sensory properties, so several researches conducted to investigate the effect of ozonation treatment on colour, texture and flavor of fruits, vegetables and grains, in addition to demonstrate the relation between the state of ozone, its concentration and the length of the treatment period and its efficiency as a disinfection and toxin reduction in fruits and vegetables.

Strawberries surface colour was not affected by treatments with either gaseous or aqueous O_3[8]. In addition, the red colour of grapes after exposure to gaseous 8 ppm O_3 for 30 minutes was not significantly affected [9]. Koyuncu et al. [10] studied the effect of ozone treatment on sweet cherries colour and firmness. They stated that ozone treatment did not affect either the colour, firmness or the external appearance. On the other hand, the carrot colour intensity damaged when it was exposed to gaseous ozone in the range of (0.3 - 60) ppm [11].

The optimum concentration for washing iceberg lettuce was recommended by [12] to be 2.5 ppm for 2.5 min. This concentration enhanced the loss in colours, firmness together with appearance of browning; in addition it extended the shelf life of lettuce up to 9 days. The effect of ozone treatment on broccoli was studied by Zhuang et al [13]. They recommended that ozonation for (10 – 15) min at 1 ppm accelerated the discolouration and ascorbic acid loss. Tomato juice colour was not affected by gaseous ozone treatment as shown by Aguayo et al. [14].

Tzortzakis et al. [15] showed that 70% of the panelist preferred the subjected tomato to low concentration of ozone.

The objective of this study was to investigate the effect of continuous exposure to aqueous ozone at 0.5, 2 and 5 ppm for 5, 10 and 15 min on the colour of tomato fruits and lettuce heads. Which could be useful to minimize pesticides residues in some commodities such as tomato fruits and lettuce.

MATERIALS AND METHODS

This study was conducted at University of Jordan, School of Agriculture. Department of Nutrition and Food Technology, Jordan.

Chemicals and Reagents. Ethanol(C_2H_6O, HPLC-grade, assay of 99.8%) (LAB-SCAN analytical sciences, Ireland), ethyl acetate ($C_4H_8O_2$, assay 99%) (J. T. Baker, USA), acetone (C_3H_6O, GC-grade, assay 99.8%) (LabChem, USA), and water (H_2O, HPLC-grade of assay 99.9%) (AVONCHEM, UK).

Apparatus and Equipment. Teflon centrifuge tubes of 50 ml., Pipettes 10 ml for transferring the sample extract to the lovibond cell., containers: weighing boats, volumetric flasks, graduated cylinders, and other containers in which to contain samples, extracts, and solutions, balance (Mettler PM6400, USA) for weighing the samples, vortex mixer (Heidolph, Germany) used for shaking the samples with the extraction solution., centrifuge (Jouan, France) for holding 50 ml centrifuge tubes, with speed of 1500-3000 rpm, food chopper (Fimar, Italy) used for sample homogenization before taking the required weight for extraction, blender (Laboratory blender 8010D, USA) used for further homogenisation of subsamples, ozone generator (ZAET Fruit and Vegetable Washer by Ozone, China) model ZA-BF-L with properties: height 290 mm, length 378 mm and width 300 mm. It consists of Acrylonitrile Butadiene Styrene (ABS) plastic cleaning chamber with 9 L capacity, transparent cover, and at the bottom of the machine the ozone generator which generates ozone by Oxidation Reduction Potential electrode (ORP) to generate ozone at concentration of 0.4 ppm, also ozone diffuser is located at the bottom of the machine, power 35 W, 220 V. This machine applies the CE marketing in accordance with European Union rules, and A_2Z ozone generator, USA, can produce ozone in the range of (1- 9) ppm.

Monitoring of Tomato Fruits and Lettuce Colour after Ozonation Treatment at Different Concentrations for Different Periods of Time. Samplingof tomato fruits and lettuce. Ninety samples of tomato fruits and lettuce were collected randomly from the local market during the period of October –November, 2017. The size of each sample taken for analysis was around 250gm. All samples were kept in polyethylene plastic bags, then labelled and refrigerated at 5^{o}C until analysis. All the samples of tomato fruits have chosen of the same degree of maturity in order to get consistent colour for all the samples. In the other hand, the lettuce heads have chosen to contain all the layers of the leaves especially the outer green leaves.

Sample preparation and extraction of tomato fruits. The method for extraction of lycopene from tomato fruits has been optimized by [16] using different solvents to extract the maximum amount of lycopene. Ethanol and ethyl acetate mixture of (1:1) ratio recommended to be used to obtain maximum lycopene content in tomatoes samples homogenate. 5 ml of ethyl acetate and ethanol mixture was used for each 1g of tomato homogenate as follows:

Two hundred and fifty grams of the collected tomato fruits sample of the same maturity level was ozonated using ozone concentration in the range of 0.5, 2 and 5 ppm for different periods of time 5, 10 and 15 min for each concentration, except the control sample. The ozonated samples left to dry at room temperature. These samples were homogenised by blender into small pieces, then 50 g was taken for extraction of lycopene in 500 ml eliminar flask. For extraction of lycopene 250 ml of ethanol and ethyl acetate mixture were added onto 50 gm of tomatoes sample homogenate, then the sample left at 40 ^{o}C for 5 h to achieve maximumrecovery of lycopene from the tomato fruits samples. The obtained extract was characterised for its colour value using lovibond to get the readings of the colour values L* (brightness), a*(redness/greenness) and b*(yellowness) after taking proper amount of the extract in 10 ml cell. Before taking readings of L*, a*and b* the lovibond instrument baseline had been stabilized on empty cell by pressing zero.

Sample preparation and extraction of lettuce heads. Chlorophyll from lettuce samples extracted using method of Koka et al. [17]. Twenty millimetre of 90% acetone water mixture added to 3 gm of chopped lettuce sample and extracted as follows:

Two hundred and fifty grams of lettuce heads sample was ozonated using ozone concentration in the range of 0.5, 2 and 5 ppm for different periods of time 5, 10 and 15 min for each concentration, except the control sample. The ozonated samples left to dry at room temperature, then samples are homogenised by chopper into small pieces, 3 g was taken for extraction of lycopene in 50 ml eliminar flask. On the other hand, for extraction of chlorophyll 25 ml of 90% acetone was added onto 3 gm of lettuce sample homogenate, and then the sample sonicated for 5 min, after that the its left to steep in refrigerator for

24 hours. The extract clarified using centrifugation at 3000 rpm for 5 min, and characterised for its colour value using lovibond to get the readings of L*, a*and b* after taking proper amount of the extract in 10 ml cell. Before taking readings of L*, a*and b* the lovibond instrument baseline had been stabilized on empty cell by pressing zero.

Statistical analysis. The design of the experiment was factorial with ten replicates. Mean values and standard errors were calculated and analysed. The obtained data were subjected to statistical analysis using Minitab programme, version 18, were Tukey was used at 0.01 probability level. The obtained results were summarized in the results section.

RESULTS AND DISCUSSION

Effect of Ozonation Treatment at Different Concentrations and Exposure Times on Tomato and Lettuce Colour. Tomato fruits. The results of 10 analysed tomato fruits samples which had been collected randomly from the local market from October to November,2017, were each sample repeated for ten times showed that as the concentration of ozone and the time of exposure increased the values of a and b decreased significantly lower than the control sample as shown in Table (1). This means that the treated samples with ozone had become less redness/yellowness or colour bleached with ozone treatment. However, as the ozone concentration and the exposure time increased more colour bleached were the percentage of reduction in colour after 15 min of exposure to 5 ppm ozone for a and b 81.61% and 43.59%, respectively. On the contrary, brightness which indicated by L* value increased significantly more than the control sample by 2.23%. These findings indicated that ozone treatment at 0.5, 2 and 5 ppm for 5, 10 and 15 min had significant effect on tomato fruits colour, showing that the characteristic red colour could be bleached by ozone, because ozone is a strong oxidizing agent [18]. However, by visual inspection for the treated tomato fruits, it indicated that the treated tomatoes were of marketable value. These results agreed with Glowacz et al. [19]. They observed that bleaching effect of ozone concentration was at 0.45, 0.9 and 2 µmol/mol for the characteristics red colour of red pepper. Shaarawi et al. [20] found that the red colour of the plum reduced significantly after exposure to ozone for four weeks at concentration of 0.5 and 1 ppm, where L* value increased and hue angle increased to indicate the reduction of the colour intensity.

In another study carrot colour intensity decreased significantly after exposure to ozone gas at 0.3 to 60 ppm. This reduction was proportional with ozone concentration and exposure time [11].

Lettuce head. The results for the 10collected lettuce heads samples from the local market in October and November, 2017, after each sample repeated for 10 times showed that the chlorophyll which is responsible for the green colour could be degraded significantly by ozonation treatment where the increase percentage in lightness (L) of 5.18%, 8.09% and 13.49% after 15 min of exposure to ozone concentration of 0.5, 2 and 5 ppm as shown in Table (2). On the contrary, a and b values decreased significantly as the concentration of ozone increased and the exposure time increased which indicated the chlorophyll colour bleached with ozone treatment.

TABLE 1
The effect of ozone treatment on colour values of tomato fruits at different concentrations for different periods of time.

		Means of colour values ± SE		
Ozone conc. (ppm)	Exposure time (min)	L (Brightness/Lightness)	a (Redness/greenness)	b (Yellowness)
Blank	0	$96.25^{a*} \pm 0.27$	$-0.82^{a} \pm 0.06$	$76.54^{a} \pm 0.22$
	5	$97.09^{b} \pm 0.05$	$-1.64^{b} \pm 0.12$	$74.76^{b} \pm 0.19$
0.5	10	$97.16^{b} \pm 0.08$	$-1.75^{b} \pm 0.04$	$73.60^{c} \pm 0.08$
	15	$97.24^{b} \pm 0.23$	$-2.40^{c} \pm 0.02$	$71.54^{d} \pm 0.11$
	5	$97.38^{b} \pm 0.04$	$-2.71^{c} \pm 0.06$	$70.60^{d} \pm 0.14$
2	10	$97.42^{b} \pm 0.06$	$-3.29^{d} \pm 0.05$	$68.48^{e} \pm 0.06$
	15	$97.96^{c} \pm 0.11$	$-3.30^{d} \pm 0.05$	$62.97^{f} \pm 0.09$
	5	$98.01^{d} \pm 0.16$	$-3.52^{d} \pm 0.03$	$56.04^{g} \pm 0.08$
5	10	$98.19^{d} \pm 0.08$	$-3.96^{e} \pm 0.05$	$46.88^{h} \pm 0.35$
	15	$98.40^{d} \pm 0.19$	$-4.46^{f} \pm 0.04$	$43.17^{i} \pm 0.29$

*Colour values within the same column for L, a and b sharing the same letters in superscript are not significantly different using Tukey test at 0.01 probability level.

TABLE 2
The effect of ozone treatment on colour values of lettuce fruits for different periods of time.

Means of colour values ± SE				
Ozone conc. (ppm)	Exposure time (min)	L (Brightness/Lightness)	a (Redness/greenness)	b (Yellowness)
Blank	0	$88.86^{a*} \pm 0.10$	$-14.63^{a} \pm 0.03$	$83.25^{a} \pm 0.08$
	5	$91.46^{b} \pm 0.24$	$-22.90^{b} \pm 0.03$	$76.06^{b} \pm 0.08$
0.5	10	$93.23^{c} \pm 0.08$	$-25.49^{c} \pm 0.03$	$75.55^{b} \pm 0.08$
	15	$93.46^{c} \pm 0.06$	$-28.89^{d} \pm 0.04$	$74.14^{c} \pm 0.11$
	5	$93.74^{c} \pm 0.15$	$-29.37^{e} \pm 0.04$	$73.47^{d} \pm 0.23$
2	10	$94.73^{d} \pm 0.09$	$-30.59^{f} \pm 0.12$	$67.48^{e} \pm 0.07$
	15	$96.05^{e} \pm 0.11$	$-31.86^{g} \pm 0.04$	$65.57^{f} \pm 0.08$
	5	$97.50^{f} \pm 0.08$	$-32.74^{h} \pm 0.03$	$57.97^{g} \pm 0.11$
5	10	$98.11^{g} \pm 0.05$	$-33.22^{i} \pm 0.09$	$51.97^{h} \pm 0.07$
	15	$100.85^{h} \pm 0.07$	$-35.09^{j} \pm 0.04$	$31.48^{i} \pm 0.08$

* Colour values within the same column for L, a and b sharing the same letters in superscript are not significantly different using Tukey test at 0.01 probability level.

A value decreased from -14.63 for the control sample to -35.09 after 15 min exposure to 5 ppm ozone concentration, and b value decreased from 83.25 for the control sample to 31.48. These findings agreed with Klockow and Kneer [21] study results. They showed that the treated spinach leaves with gaseous ozone for 24 hours at gradual increase in ozone concentration from 1.6 to 4.3 ppm its colour degraded gradually. In addition, Singh et al. [22] showed discolouration of iceberg lettuce leaves during ozone treatment with 5.2 and 7.6 ppm O_3 concentration for 10 or 15 min. Glowacz and Rees [19] showed that the characteristic green colour of the green pepper skin bleached after ozone treatment at 0.45, 0.9 and 2 µmol/ mol. This could be explained due to accelerated chlorophyll degradation. The ability of ozonation in reduction of these pesticides amount is related to the ability of ozone to generate hydroxyl radicals in aqueous solution, which are highly effective to colour of tomato fruits and lettuce heads. As the time of exposure increased hydroxyl radicals continued to be generated throughout the treatment, and more colour bleached [23].

CONCLUSION

Ozone have many applications in food industry since it's used as a sanitizer and for reduction of many kinds of toxins in food especially pesticides residues, it is used at wide range of concentrations, but If it is improperly used, ozone can cause several deleterious effects on physiology and quality of products such as losses in sensory quality. For effective and safe use in food processing, optimum ozone concentration and contact should be defined. The finding of this study indicated that the use of ozone up to 5 ppm concentration for 15 min did not lead to loss of tomato fruits and lettuce leaves colour even it leads to increase in brightness and decrease in redness/greenness and yellowness for both cases but it does not lead to loss the marketable value, because both of the products still visually acceptable to be purchased.

ACKNOWLEDGEMENTS

The authors would like to thank the University of Jordan and Ministry of Agriculture/ Jordan for their support and help.

The authors have declared no conflict of interest.

REFERENCES

[1] Department of Statistics (2016) Annual Book. Amman, Jordan.
[2] Department of Statistics (2015) Annual Book. Amman, Jordan.
[3] Al-Antary, T. (1996) Pesticides and toxicity. Al-Quds Al-Maftoha University Publications: Amman.
[4] Al-Dabbas, M. Shaderma, A. and Al-Antary, T. (2014) Effect of ozonation on methomyl, oxamyl and carbosulfan residues in tomato juice. Life science journal. 11(2), 68-73.
[5] Al Antary, T.M., Al-Dabbas, M. and Shaderma, A.M. (2015). Effect of heat treatment on three carbamate pesticides residues in tomato juice. Fresenius Environmental Bulletin, 24, 2926-2930.
[6] Al-Antary, T., Al-Dabbas, M., and Shaderma, A. (2014) Effect of UV-radiation on methomyl, oxamyl, and carbosulfan residues in tomato juice. Fresen. Environ. Bull. 23, 924-928.
[7] Skog, L. and Chu, C. (2001) Effect of ozone on qualities of fruits and vegetables in cold storage. Can. J. Plant Sci. 81(4), 773-778.
[8] Nadas, A., Olmo, M. and Garcia, J. (2003) Growth of *botrytis cinerea* and strawberry quality in ozone-enriched atmosphere. J. Food Sci. 68, 1798-1802.
[9] Hernandez, F., Artez, F. and Tomaz-Barberan, F. (2003) Quality and enhancement of bioactive phenolics in Cv. Napoleon table grapes exposed to different postharvest gaseous treatment. J. Agr. Food Chem. 51, 5290-5295.

[10] Koyuncu, M., Seydim, A., Dilmacunal, T., Savran, H. and Tas, T. (2008) Effect of different precooling treatments with ozonated water on the quality of sweet cherry fruit. Acta Hortic. 795, 831 -836.
[11] Song, J., Fan, I., Forney, C., Hildebrand, P., Jordan, M., Rendors, W. and Rae, K. (2003) Ozone and 1-MCP treatments affect the quality and storage life of fresh carrots. Acta Hortic. 628, 295-301.
[12] Olmez, H. and Akbas, M. (2009) Optimization of ozone treatment of fresh cut green leaf lettuce. J. Food Eng. 90, 487-494.
[13] Zhuang, H., Lewis, L., Michelangeli, C., Hildebrand, D., Payne, F., Bastin, S. and Brath, M. (1996) Ozone water treatment for preserving quality of packaged, fresh cut broccoli under refrigeration. Sci. Tech. Froid. 6, 267-276.
[14] Aguayo, E., Escalona, V. and Artes, F. (2006) Effect of cyclic exposure to ozone gas on physiochemical, sensorial and microbial quality of whole and sliced tomatoes. Postharvest Biol. Technol. 39, 169-177.
[15] Tzortzakis, N., Broland, A., Singlton, I. and Barnes, J. (2007) Impact of atmospheric ozone-enrichment on quality related attributes of tomato fruits. Postharvest Biol. Technol. 45, 317-325.
[16] Pandya, D., Akbari, S., Bhatt, H. and Joshi, D. (2017) Standardization of solvent extraction process for lycopene extraction from tomato pomace. Journal of Applied Biotechnology and Bioengineering. 2(1), 19-23.
[17] Koka, N., Karadeniz, F. and Burdurlu, H. (2006) Effect of pH on chlorophyll degradation and colour loss in balanced green peas. Food Chemistry. 100, 609-615.
[18] Kim, J., Yousef, A., Khadre, M. (2003) Ozone and its Current and Future Application in the Food Industry. Advances in Food and Nutrition Research. 45, 167–218.
[19] Glowacz, M. and Rees, D. (2016) Exposure to ozone reduces postharvest quality loss in red and green chili peppers. Food Chemistry. 210, 305-310.
[20] Shaarawi, S., Mshraky, A. and El-Kady, A. (2017) Effect of postharvest safe treatments on quality attributes and storage life of "celebration' plum fruits. Middle East Journal of Agriculture. 6(01), 24-32.
[21] Klockow, P. and Keener, K. (2009) Safety and quality assessment of packaged spinach treated with a novel ozone-generation system. LWT - Food Science and Technology, 42: 1047-1053.
[22] Singh, N., Singh, R., Bhunia, A. and Stroshine R. (2002) Efficacy of chlorine dioxide, ozone and thyme essential oil or sequential washing in killing Escherichia coli O157: H7 on lettuce and baby carrots. LWT - Food Science and Technology, 35: 720-729.
[23] Chen, J., Lin, Y. and Kuo, W. (2013) Pesticide Removal from Vegetables by Ozonation. Journal of Food Engineering. 114(3), 404-411.

Received: **16.03.2018**
Accepted: **28.04.2018**

CORRESPONDING AUTHOR

Tawfiq M Al-Antary
Department of Plant Protection,
School of Agriculture,
University of Jordan,
Amman, 11942 – Jordan

e-mail: tawfiqm@yahoo.com

© by PSP Volume 27 – No. 7/2018 pages 5142-5146 Fresenius Environmental Bulletin

STUDY ON CHEMICAL OXIDATION TREATMENT OF OILFIELD SLUDGE

Tengfei Wang, Jiexiang Wang*, Xingbang Meng, Weipeng Yang, Chang Liu, Guoyu Chu

College of Petroleum Engineering, China University of Petroleum East China, Qingdao, 266580, China

ABSTRACT

Wet oxidation (WO) of oilfield sludge was performed in a batch reactor. Effect of reaction parameters such as residence time, reaction temperature, Fe^{2+} concentration and oxidant concentration were investigated. The experimental results showed that WO can effectively remove the organic compounds of the oilfield sludge, the residence time and reaction temperature are the main factors for total organic carbon (TOC) removal of oilfield sludge. The TOC removal is up to 98.6%. The cross-test range analysis shows that the effect of the experimental parameters on the TOC removal rate from large to small is: reaction temperature> Fe^{2+} concentration> oxidant concentration> residence time.

KEYWORDS:
WO, oilfield sludge, Fe^{2+}, TOC, cross-test range analysis

INTRODUCTION

The oil industry unavoidably generates large quantities of oily and viscous residue called oilfield sludge, which is formed during crude oil exploitation and development of various productions in oilfields, transportation, and refining processes. The oilfield sludge is a complex mixture of petroleum hydrocarbons and water with solid mineral admixtures, such as soil and sand, adversely affecting human health and posing environmental problems. The major sources of oil sludge include oilfield sludge, petrol storage tank sludge, and residue derived from the crude oil refining processes. In China, it is estimated that more than 3 million tones of oilfield sludge discharged by the petrochemical industry [1]. Most of them were disposed in landfills and drains from the treatment process of oil storage tank cleanup which may pollute the groundwater and cause health problems. Although oilfield sludge is listed in the China National Hazardous Waste List because of its toxicity and harmful compounds, only a minor amount of oilfield sludge was disposed in a safe manner. The conditional disposals of oilfield sludge involve aerobic biodegradation [2] and ultrasound oil recovery [3, 4]. Nevertheless, it has been found that such methods cause secondary pollution.

Advanced oxidation processes (AOPs) like ozonation, Fenton, and photo Fenton processes, Ozone/UV radiation are the potential alternatives for tertiary treatment of tannery effluent [5]. Among the existing AOPs, ozonation was an effective method to remove colour from wastewater, which cleave the unsaturated bonds in aromatic moieties found in humic substances, chromophores of dyes, and other pigmented compounds, thereby reducing the colour [6]. Researchers have also reported that pH and wastewater characteristics have a significant effect on ozonation and vice versa [7-11]. Oller et al. [12] in his review article has emphasized the importance on combining AOPs and biological process for treatment of synthetic and real industrial wastewater on recent studies and large-scale combination schemes reported for non-biodegradable wastewater treatment and reuse. Prashant et al. [13] evaluated the performance of chemical manufacturing and pharmaceutical industries CETP. They tried to reduce the chemical oxygen demand (COD) and biochemical oxygen demand (bod) using different chlorine, Hydrogen Peroxide (H_2O_2), Fe_2SO_4 doses, different pH values and contact time for identifying the optimum values. They have achieved COD and BOD reduction of 64.35% and 68.57% in optimized conditions. Dhinakaran et al. [14] conducted the feasibility studies on performance improvement for tannery effluent through chemical oxidation and biological treatment. They used solar Fenton process to enhance the biodegradability index (BDI) ratio. They achieved improved BDI ratio of 0.35–0.4. Rameshraja and Suresh [15] reviewed the treatment of tannery wastewater by various oxidation and combined processes. They reviewed the different combination of oxidation processes such as UV/H_2O_2/Hypochlorite's, Fenton and electro-oxidation, photo-chemical, photo-catalytic, electro-catalytic oxidation, wet air oxidation, ozonation, biological followed by ozone/ UV/H_2O_2, coagulation or electro-coagulation.

In this paper, effect of reaction parameters such as residence time, reaction temperature, oxidant concentration and Fe^{2+} concentration on TOC of oilfield sludge were investigated.

EXPERIMENTAL

The oil sludge used in the experiment was from Shengli Oilfield. After analysis, the sludge had w (oil) of 52.7%, w (water) of 45.5%, and w (silt) of 1.8%.

The experiments are carried out in an intermittent reacting system for WO. It includes a reactor, heater reactor, gas–liquid separator and other major equipment. Firstly water and oilfield sludge were put into the reactor, and then nitrogen flowed through the system and removed the air within the system; the valves around the reactor were closed when the air was removed entirely. The reactor was heated, and hydrogen peroxide was added into the hydrogen peroxide container; when reactor temperature reached the scheduled value, hydrogen peroxide was injected into the reactor by using a high pressure pump. When the reaction residence time was attained, the reaction fluid was put into the gas–liquid separator, and the gas and the liquid were separated; opening the reactor vessel, the sediment was removed directly. Reaction pressure and reaction temperature were measured by a thermocouple and a pressure transducer. The entire system does not need high-pressure pump following the turbocharging system, the different reaction pressure was controlled by reaction temperature and by means of putting water into the reactor, and the high-pressure pump was used only when hydrogen peroxide and Fe^{2+} was injected into the reactor. The reactor is made from 1Cr18Ni9Ti, and the reactor volume is 650 ml.

Total organic carbon of treated effluent samples was measured using TOC analyzer (Shimazdu, TOC-Vcph, Japan). The TOC was determined by subtraction of inorganic carbon from total carbon. The instrument was calibrated by using standard solution of potassium di hydrogen phthalate along with sodium carbonate for measurement of total carbon and inorganic carbon, respectively. High pure zero-air was used as a carrier gas. Pressure of the carrier gas was maintained at the recommended level of about 200 kPa and gas flow rate at 150 ml/min throughout the analysis.

RESULTS AND DISCUSSION

Research at home and abroad on the wet oxidation of oily wastewater or wastes proves that during the wet oxidation process, petroleum hydrocarbons can be rapidly oxidized and removed. Wet oxidation technology has proved to be an efficient oily wastewater or waste treatment method. This is wet oxidation. Technical treatment of oily sludge provides lessons and guidance. Therefore, this paper proposes the use of wet oxidation treatment of oily sludge, aiming to provide a environmentally friendly technology for the treatment of oily sludge.

Single factor experimental study. Effect of residence time on TOC removal. Residence time has a significant impact on the TOC removal, since the removal increases with the rise of residence time. Therefore, it is crucial to choose a suitable residence time. In this experiment, the residence time varies from 5 to 20 min.

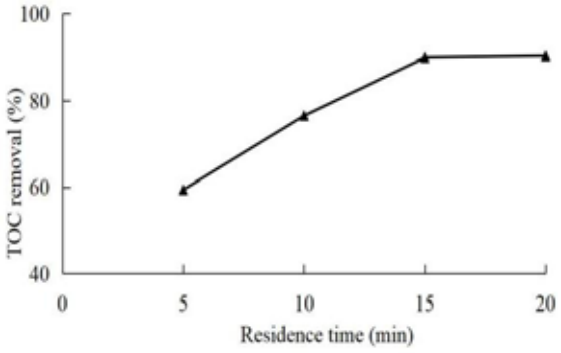

FIGURE 1
Effect of residence time on TOC removal

Fig.1 shows that the TOC removal of the oilfield sludge is affected by residence time. TOC removal of the oilfield sludge increases with the rise of residence time, which is shown in Fig. 1, when the residence time was up to 20 min, the COD removal of the oilfield sludge increased gently. So the appropriate residence time was 20 min. It shows that the organic matter in the oilfield sludge is easily oxidatively degraded under wet oxidation conditions. This is because, at the beginning, as the residence time of the reaction is extended, the substrate concentration decreases rapidly, the reaction rate is fast, and organic compounds are more easily oxidized and degraded.

Effect of reaction temperature on TOC removal. The highest design temperature of reactor was 450°C, which was based on the range of reaction temperatures [240°C, 330°C]. An experimental result shows that obvious changes in the removal of TOC occurred when the reaction temperature changed in an increment of 30 °C.

Fig. 2 shows that the TOC removal of the oilfield sludge is affected by reaction temperature. Fig. 2 indicates the TOC removal radiate upward trend with the rise of reaction temperature. TOC removal is low at low reaction temperature (240–270 °C),

but TOC removal rate increases quicker than that of under high reaction temperature (300–330 °C). When the residence time is 20 min and reaction temperature increases from 270 to 300 °C, TOC removal increases from 79.3% to 88.2%, while it increases from 88.2% to 90.26% when temperature increases from 300 to 330 °C.

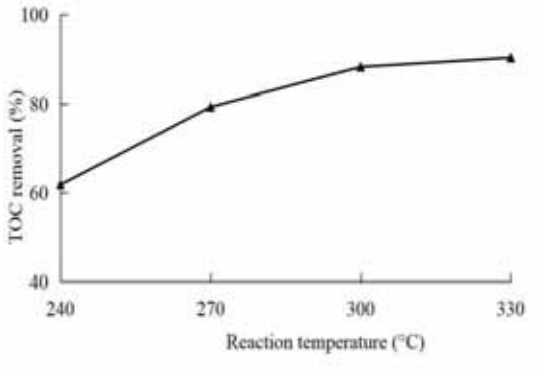

FIGURE 2
Effect of reaction temperature on TOC removal

This can be explained from two aspects: On the one hand, the oxidation of organics is an irreversible reaction. When the temperature rises, the reaction rate is accelerated, eventually leading to an increase in the oxidation rate of organics; on the other hand, under conditions of constant pressure, the temperature Elevation will reduce the density of water and decrease the concentration of the substrate. This will cause the reaction rate to slow down. However, increasing the temperature causes the rate constant to increase much more than the decrease in concentration, so the TOC removal increased temperature increases the phenomenon.

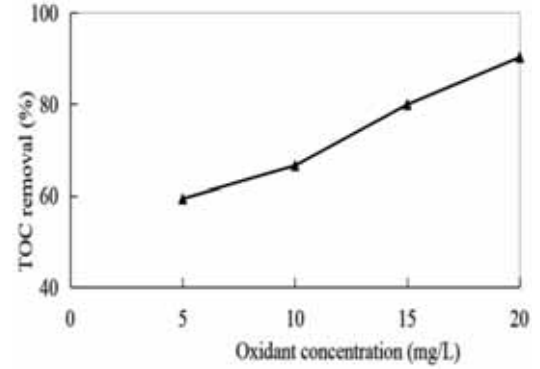

FIGURE 3
Effect of oxidant concentration on TOC removal

Effect of oxidant concentration on TOC removal. The experimental results showed that WO can effectively remove the organic compounds of the oilfield sludge, the residence time and reaction temperature are the main factors for TOC removal of oilfield sludge.

Fig. 3 shows that TOC removal is affected by oxidant concentration. The reaction temperature is 330 °C and the residence is 20 min. The TOC removal increases with the rise of oxidant concentration, which is shown in Fig. 3. The TOC removal increasing trend becomes gentle when oxidant concentration is over 20 mg/L.

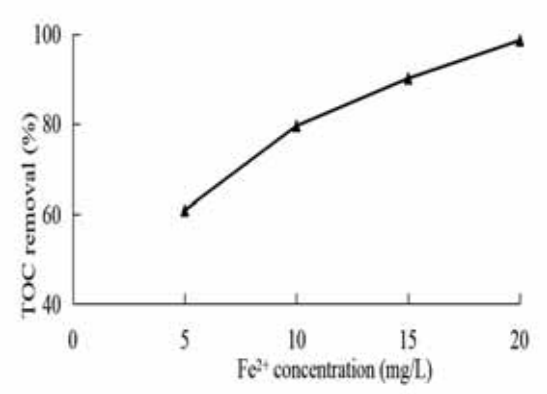

FIGURE 4
Effect of Fe^{2+} concentration on TOC removal

Effect of Fe^{2+} concentration on TOC removal. Fig. 4 shows that TOC removal is affected by Fe^{2+} concentration. The reaction temperature is 330 °C, oxidant concentration is 20 mg/L, and the residence time is 20 min. The TOC removal increases with increasing Fe^{2+} concentration, which is observed from Fig. 4. When Fe^{2+} concentration reaches 20 mg/L, the TOC removal can be up to 98.6%. When the Fe^{2+} concentration is 5–20 mg/L, the TOC removal changes gently, i.e., increasing from 60.8% to 98.6%.

Orthogonal experimental results. In the batch reactor, four factors were selected: reaction temperature (A), reaction residence time (B), Fe^{2+} concentration (C), and oxidant concentration (D). Three different levels were selected for each factor, ie, 270, 300, 330 °C, 10, 15, 20 min and 10, 15, 20 mg/L, 10, 15, 20 mg/L, according to L_9 (3^4) orthogonal table for testing, the results are shown in Table 1.

From Table 1, it can be seen that when the reaction temperature is 300°C, the reaction residence time is 20 min, the Fe^{2+} concentration is 10 mg/L, and the oxidant concentration is 15 mg/L, the TOC removal rate is 70%. $R_A > R_C > R_D > R_B$. The cross-test range analysis shows that the effect of the experimental parameters on the TOC removal rate from large to small is: reaction temperature> Fe^{2+} concentration> oxidant concentration> residence time. The reason for the analysis is as follows: In the WO process, the reaction rate is increased due to the temperature increase, and the reaction is accelerated, which is favorable for the oxidative

TABLE 1
Orthogonal experimental results

No.	A	B	C	D	TOC removal /%
1	1	1	1	1	40
2	1	2	2	2	42
3	1	3	3	3	44
4	2	1	2	3	54
5	2	2	3	1	60
6	2	3	1	2	70
7	3	1	3	2	56
8	3	2	1	3	58
9	3	3	2	1	50
K_1	126	150	168	150	
K_2	184	160	146	168	
K_3	164	164	160	156	
R	58	14	22	18	

decomposition of organic substances. With the increase of reaction residence time, the oilfield sludge rapidly decomposed into CO_2 and H_2O. The increase of the oxidant concentration will make the oxygen concentration relatively increase. From the perspective of reaction kinetics, it is favorable for the oxidation reaction. The higher the Fe^{2+} concentration, the better the oxidative decomposition. Using the WO process to treat oily sludge, organic matter can be completely oxidized to harmless CO_2 and water, and inorganic salts formed inorganic salts completely settle at the bottom of the reactor.

CONCLUSIONS

The decomposition of the oilfield sludge was studied under isothermal and isobaric conditions at 240, 270, 300, and 330 °C, and residence time from 5 up to 20 min, oxidant concentration from5 to 20 mg/L, Fe^{2+} concentration from 5 to 20 mg/L. The results showed that WO can effectively remove organic compounds of the oilfield sludge, the TOC removal is up to 98.6% when the conditions are not very harsh in the circumstances. Reaction temperature, residence time, Fe^{2+} concentration and oxidant concentration are the important factors that affect TOC removal, and the cross-test range analysis shows that the effect of the experimental parameters on the TOC removal rate from large to small is: reaction temperature> Fe^{2+} concentration> oxidant concentration> residence time.

REFERENCES

[1] Cheng, Y., Guo, Y.H. (2017) Oil-field wastewater treatment by SCWO with metal-organic framework. Fresen. Environ. Bull. 26, 6599-6602.

[2] Zhang, H.X., Li, Y., Li, Z.D., Ma, C.M., Zhang, S.X., Shi, H., Tian, M., Dai, H.T., Li, W. (2017) Catalytic Treatment of Oilfield Wastewater Based on Response Surface Method. Fresen. Environ. Bull. 26, 5999-6003.

[3] Baraj, E., Celo, V., Shehu, A., Totoni, R., Baraj, B. (2016) Study of the matrix effects on the determination of iron in oilfield brines in albania, using AAS technique. Fresen. Environ. Bull. 25, 3941-3947.

[4] Li, Y., Hu, Y., Du, X.Y., Wang, Y. (2012) Investigation on the dynamic environmental behaviour of petroleum-derived polycyclic aromatic hydrocarbons in an oilfield, China. Fresen. Environ. Bull. 21, 986-994.

[5] Dang, N.M., Lee, K. (2018) Decolorization of organic fertilizer using advanced oxidation process and its application for microalgae cultivation. Journal of Industrial and Engineering Chemistry. 59, 297-303.

[6] Lee, D.S. (1996) Heterogeneous Oxidation Kinetics of Acetic Acid in Supercritical Water. Environ. Sci. Technol. 30, 3487–3492.

[7] Tang, W.W., Zeng, X.P., Hu, Z.H. (2006) Study of Fenton's reagent and wet hydrogen peroxide oxidation for treatment of emulsified waste water. Acta Scientiae Circumstantiae. 26, 1265-1270.

[8] Nidheesh, P.V., Zhou, M.H., Oturan, M.A. (2018) An overview on the removal of synthetic dyes from water by electrochemical advanced oxidation processes. Chemosphere. 197, 210-227.

[9] Kishimoto, N., Katayama, Y., Kato, M., Otsu, H. (2018) Technical feasibility of UV/electrochlorine advanced oxidation process and pH response. Chemical Engineering Journal. 334, 2363-2372.

[10] Schrank, S.G., José, H.J., Moreira, R.F.P.M., Schroder, H.Fr. (2004) Elucidation of the behavior of tannery wastewater under advanced oxidation conditions. Chemosphere. 56, 411-423.
[11] Arslan-Alaton, I., Balcioglu, A. (2002) Biodegradability assessment of ozonated raw and biotreated pharmaceutical wastewater. Environ. Contam. Toxicol. 43, 425-431.
[12] Oller, I., Malato, S., Sanchez-Perez, J.A. (2011) Combination of Advanced Oxidation Processes and biological treatments for wastewater decontamination—a review. Sci. Total Environ. 409, 4141-4166.
[13] Lalwani, P.K., Devadasan, M.D. (2013) Reduction of COD and BOD by oxidation: a CETP case study. Int. J. Eng. Res. Appl. 3, 108-112.
[14] Dhinakaran, S., Navaneethagopalakrishnan, A. (2015) Feasibility studies on performance improvement for tannery effluent through chemical oxidation. J. Chem. Pharm. Sci. 2015, 439-442.
[15] Rameshraja, D., Suresh, S. (2011) Treatment of tannery wastewater by various oxidation and combined processes. Int. J. Environ. Res. 5, 349-360.

Received: **19.03.2018**
Accepted: **29.04.2018**

CORRESPONDING AUTHOR

Jiexiang Wang
College of Petroleum Engineering,
China University of Petroleum (East China),
Qingdao, 266580 - China

e-mail: jiexiangwang@upc.edu.cn

© by PSP Volume 27 – No. 7/2018 pages 5147-5152 Fresenius Environmental Bulletin

ESTIMATION OF GLOBAL WOOD PELLET PRODUCTION AS A RENEWABLE ENERGY SOURCE BY ARIMA METHOD

Rifat Kurt, Erol Imren, Yildiz Cabuk*, Selman Karayilmazlar

Bartin University, Faculty of Forestry, Department of Forest Industrial Engineering, 74100 Bartin, Turkey

ABSTRACT

Due to the adverse effects of fossil fuels on the environment and failing to meet increasing energy demand, the importance of renewable energy resources have increased even more. For this reason, starting from the fact that the need for energy will be even higher in the future, it is important that the current status and the possible future production of the renewable energy resources should be studied and considered carefully by the related parties. For this purpose, the current status of wood pellet production, which is one of the renewable energy resources in the world, was studied and a forecast was made in this study. World pellet production between the years of 2017 and 2026 was forecasted by ARIMA (Box-Jenkins) method. Although the forecast results, as expected, indicate that production will increase over time, it is predicted that these production quantities will not be adequate to meet the energy demand.

KEYWORDS:
Renewable Energy, World Pellet Production, Estimation, ARIMA Method

INTRODUCTION

The need for energy increases day by day depending on the increase in world population. The fact that the fossil fuel resources, which have a large share in energy use, are rapidly running out and the fact that they cause irrecoverable damages to the natural life and the environment, while they are running out threaten the lives of future generations. For this reason, studies for utilizing renewable energy resources have gain even more importance in recent years [1]. Rapid dissemination of renewable energy resources plays an important role in dealing with global warming and related environmental problems. Biomass has a great importance among renewable energy resource.

Biomass is stated as all organic matter composing of plants, various products and wastes that can be renewed in less than 100 years [2, 3, 4]. Biomass, which emerges as the fourth largest source of energy after coal, petroleum and natural gas, covers about two-thirds of all renewable energy resources and is absolutely the fastest-growing sector [5, 6].

The fuels, of which at least 80% of the total volume is obtained from the living organisms grown in the last decade, are called biofuels [7, 8]. The wood and wood energy products, which had low value at the beginning, are among the most important renewable resources for heat generation [9]. The sector involves a great variety of resources with different characteristics such as wood logs, bark, wood flour and pellets recently.

Wood pellet is a fuel product compressed from grinded wood. The use of wood pellets has increased even more in the 1990s in Sweden, Denmark and Austria and today in North America [10]. Pelleting is one of the most economical and energy-saving methods of transforming high energy density and consistent quality biomass into a fuel. Pellet is an ideal fuel for small scale heating systems in terms of convenient delivery and storage features due to its high energy content. Because of this, it has a fast-growing market world-wide in terms of biomass, mainly in Europe.

The general status of world wood pellet production. Considering the world wood pellet production in general, it is seen that the pellet production, which was 1.7 million tonnes in 2000, has gradually increased up to 29.1 million tonnes until 2016 (Figure 1). Especially, with the aggressive emissions policy of the European Union (EU), the production of wood pellets has increased even more in recent years.

The USA and Canada rank first in 2016 world wood pellet production (Figure 2). In the United States of America, wood pellet production has recently been focusing on the export market. Almost 80% of wood pellets are used domestically. One of the strongest reasons for Canada to have a vibrant wood pellet industry is because of its large amount of forest resources and manufactured forest products. The pellets predominantly imported from the USA and Canada are generally used for industrial purposes. In the EU countries, Germany is the country making the largest production.

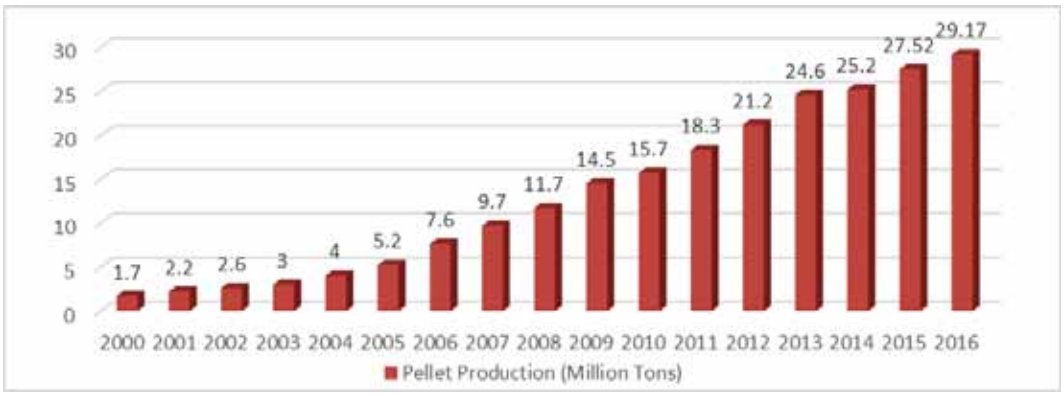

FIGURE 1
World pellet production values [11, 12]

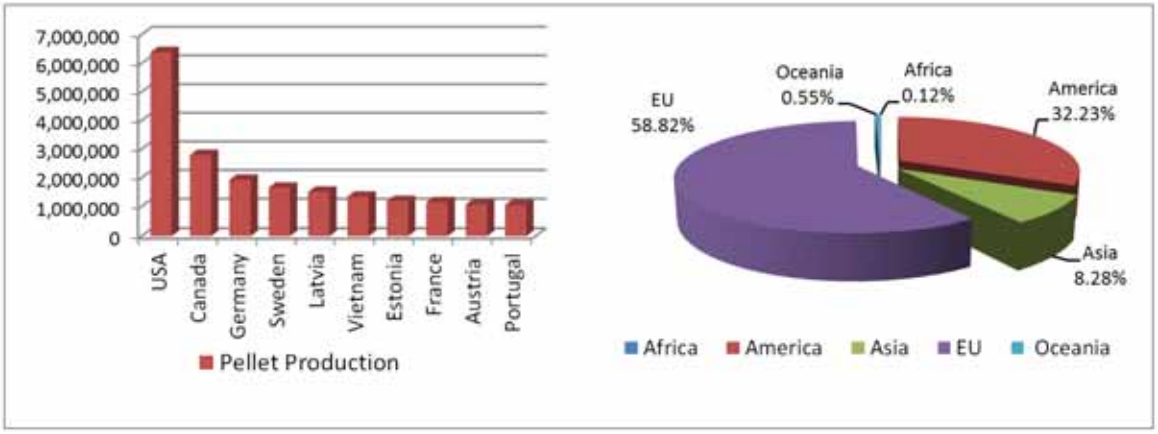

FIGURE 2
World wood pellet production quantities and regional distribution in 2016 [12]

When pellet production is examined on a regional basis, it is seen that almost all of the production is made in Europe (58.8%) and America (32.23%) (Figure 2). Even though Europe is the largest producer, it is also the main consumer of wood pellets and is in the position of the world's largest pellet importer. A high level of wood pellet trade is carried out between the Member States of the European Union.

It is a stubborn fact that the availability of wood and wood-based resources, growing timber industries and increasing energy demand in Asia and Latin America will provide significant increases in production, consumption and trade of wood pellets. In most of the countries in these regions, the wood pellet production is still in its infancy stage and reports on production facilities and capacities are extremely scarce and the information is not sufficient.

MATERIALS AND METHODS

Material. 16 years of wood pellet production quantities of the world between 2000 and 2016 constitutes the study material (Figure 1). Since the pellet production values in the years of 2012 and 2013 were stated differently by different statistical institutions, the values, which were considered to be the most suitable according to the annual increase and to have positive effect on the success of the model to be established, were defined as production values. Eviews was used in unit-root tests and the stationarity of data and MINITAB program was used for establishing the ARIMA models and for forecasting processes.

Method. In order to estimate the future global pellet production values in the study, the Autoregressive Integrated Moving Average, commonly known as ARIMA (Box-Jenkins) method, which is one of the time-series analysis techniques widely used in forecasting processes in literature, was used.

Before the ARIMA model was established and the forecasting stage began, one of the most important assumptions of the model, whether the world pellet production values met the stationarity condition or not was tested with the Augmented Dickey-Fuller (ADF) test, which is one of the unit root tests, and then the forecasting stage was proceeded to.

ARIMA (Box-Jenkins Method). The method, which was described by Box and Jenkins (1970) as a family of linear stochastic models in the time-series analysis books, is known as Box-Jenkins or ARIMA today and is applied to the series that are non-stationary but transformed into stationary by differencing [13].

The ARIMA (Box-Jenkins) method is a univariate process. In this method, the AR (p) component is obtained by correlating the current values of a data series with the past values in the same series. The current values of a random error term are correlated with past values and the MA (q) component is obtained. At the same time, it is assumed that the mean and variance values of current and past data have not changed over time. If necessary, in order to remove the change, an I (d) component is added by differencing. Thereby, the model is referred to as ARIMA (p, d, q).

$$Y_t = \phi_0 + \phi_1 Y_{t-1} + \phi_2 Y_{t-2} + ... + \phi_p Y_{t-p} + \varepsilon_t - \theta_1 \varepsilon_{t-1} - \theta_2 \varepsilon_{t-2} - ... - \theta_q \varepsilon_{t-q}$$

It is generally as ARIMA (p,d,q) model. Here, Y_t indicates the observational values differenced from the degree of d; ε_t indicates the error terms at the time of t; $\phi_i(i=1,2,3...p)$ and $\theta_j(j=1,2,3...q)$indicate the model parameters; and p and q indicate the autoregressive process (AR) and moving average (MA) respectively.

It is an important assumption for this series, in which this method quite successful in short-term forecasts is applied, to be a discrete and stationary series of observational values obtained at equal time intervals [14]. The concept of stationarity in time series is defined as the fact that the series does not have any trend effect, which means that no change occurs in mean and variance over time, and that it has a covariance related to the level of delay.

Today, different methods are used in determination of stationarity and the unit-root tests developed for this purpose are utilized. One of the most widely used tests is the Augmented Dickey-Fuller test (ADF). This test, which is discussed by Dickey and Fuller [15, 16], shows whether the time series variables can be expressed with autoregressive (AR) processes and if autocorrelation is found in the error term as a result of the test, it indicates that time series cannot be expressed with the first order autoregressive process [17]. The ADF test includes the following equation.

$$\Delta Y_{t=}\alpha + \beta t + \rho Y_{t-1} + \sum_{j=1}^{k} \gamma_j \Delta Y_{t-j+} \varepsilon_t$$

Here, t indicates the time trend and k indicates the delay length in dependent variable.

FINDINGS

ADF Unit Root Test. Considering the ADF test results of world pellet production values (Table 1), since the test statistic is larger than the critical values of 5.883035, it is seen that the series contains a unit-root. Moreover, the fact that the significance level is 1.0000> 0.05 indicates that the series is not stationary. For this reason, pellet production values have been made stationary by differencing before forecasting process.

In the ADF test carried out after the first-order differencing, the pellet production values were found to be non-stationary and they were made stationary by second-order differencing. Table 2 shows the ADF test results for world pellet production values which are made stationary.

Considering the ADF test results of the pellet production values after the second-order differencing in Chart 1, it is seen that the test statistic is smaller than the critical value of -6.752123. In a word, the serial unit does not contain a unit root. Again, the fact that the significance level is less than 0.000 <0.05 indicates that the series has become stationary and that the data has become suitable for forecasting by the ARIMA model.

TABLE 1
ADF results of pellet production values

		t-statistic	p-values
Augmented Dickey-Fuller test statistic		5.883035	1.0000
Test critical values	**%1**	-2.717511	
	%5	-1.964418	
	%10	-1.605603	

TABLE 2
ADF test results for pellet production values with the second-order differencing

		t-statistic	p-values
Augmented Dickey-Fuller test statistic		-6.752123	0.0000
Test critical values	**%1**	-2.740613	
	%5	-1.968430	
	%10	-1.604392	

TABLE 3
ARIMA (0,2,1) model results

Type	Coeficients	Standart Error	T	P
MA 1	1.2551	0.3108	4.04	0.001
Constant	0.07406	0.07725	0.96	0.355

Differencing	2	**Number of observations (Original series)**	17	**Number of observations (After differencing)**	15
DF (Degrees of Freedom)	13	**MSE (Mean Squared Error)**	0.56297	**SS (Sum Squares)**	7.31867

Box-pierce (Ljuing box) Chi-Square statistic				
Lag	12	24	36	48
Chi-Square	7.4	-	-	-
DF	10	-	-	-
P-Value	0.684	-	-	-

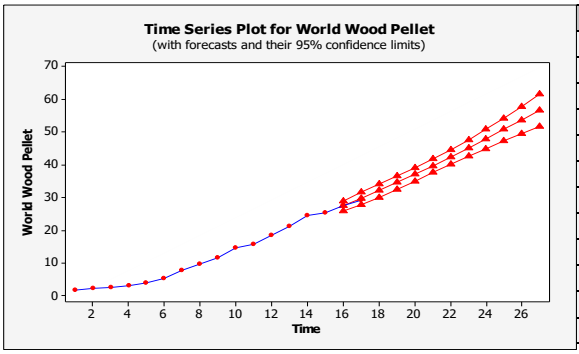

Period	Forecast	Lower	Upper	Actual	MSE	MAPE
2015	27.4199	25.949	28.8909	27.52	0.0100	0.3637
2016	29.7139	27.8798	31.5481	29.17	0.2958	1.8646
2017	32.082	30.1114	34.0527			
2018	34.5241	32.5235	36.5248	Average	0.03058	0.2228
2019	37.0403	35.0394	39.0412			
2020	39.6305	37.5891	41.672			
2021	42.2948	40.1094	44.4803			
2022	45.0332	42.5611	47.5053			
2023	47.8456	44.9381	50.7531			
2024	50.7321	47.2557	54.2085			
2025	53.6926	49.5347	57.8505			
2026	56.7272	51.7934	61.6611			

FIGURE 3
World Pellet production ARIMA (0,2,1) forecast results

Establishing the ARIMA (Box-Jenkins) Model and Forecast. After the data of world pellet production values were made stationary, the model establishment phase began. ARIMA (0,2,1) and ARIMA (1,2,1) models were determined as the most suitable ARIMA models as a result of different experiments. It was decided that the ARIMA (0,2,1) structure was the most suitable model among these models with its more meaningful values and better predictive performance. Table 3 shows the MINITAB program outputs where the statistical results of the ARIMA (0,2,1) model are included.

When Table 3 is examined, it is seen that the model is meaningful at the significance level of 0.05 ($p < 0.05$). The mean squared error (MSE) value was obtained as low as 0.56297. Again, considering the chi-square statistics of Ljuing box are examined, it is seen that the model is meaningful at the 5% ($p > 0.05$) significance level and adequate. It is to say that the model can be used for forecasting. Figure 3 indicates the forecast results of world pellet production values obtained from ARIMA (0,2,1) model between the years of 2017 and 2026.

When Figure 3 is examined, it is seen that world pellet production will continue to increase gradually, reaching approximately 56.7 million tons in 2026. In addition, when the ARIMA (0,2,1) model's prediction performance for the years 2015-2016 is considered, the low MSE (Mean Squared Error) and MAPE (Mean Absolute Percentage Error) values show that the model can make quite successful predictions.

CONCLUSION

Today, the need for energy is increasing day by day due to growing population, industrialization and urbanization. The fact that the fossil fuels meeting the majority of the world's energy demand, meaning the non-renewable energy resources, are shortening and are not economic, environmental pollution and global climate change have diverted the societies to alternative energy resources. Renewable energy resources are the most important ones among these resources. Biomass obtained from wood and wood based wastes and industrial and agricultural wastes occupies an important place among the renewable energy resources. The wood pellet, which is included in the scope of biomass, is becoming more and more important due to its provision of high energy and low cost.

In this study, world pellet production values were forecasted using the ARIMA (Box-jenkins) method. 17-years of pellet production values between the years of 2000 and 2016 were used for

forecasting. ARIMA (0,2,1) model was determined to be the most suitable ARIMA model and the pellet production values of the next 10 years were forecasted. Considering the obtained results in general, it was seen that the world pellet production, which was 29.17 million tonnes in 2016, will increase by 35.85% (1.358 times) up to 39.63 million tonnes in 2020 and by 94.5% (1.945 times) up to 56.727 million tonnes in 2026.In general, it is predicted that world pellet production will increase incrementally between the years of 2017 and 2026 as well. Although these results are indicative of an increasing trend towards renewable energy resources, it is seen that the worldwide production of pellets will be limited to major countries only. Yet, it is clear that pellet production, which is one of the renewable energy resources, is a sector that importance should be placed due to these superior characteristics mentioned above.

Especially the countries with large forest area and are foreign-dependent in terms of energy need have the potential of providing a significant portion of the world's energy need through pellet and similar renewable energy resources. Through this study, it is wished to make this potential noticeable and to contribute to both the country's economy and the efficient use of natural resources.

REFERENCES

[1] Karayılmazlar, S., Saraçoğlu, N., Çabuk, Y., Kurt, R. (2011) Biyokütlenin Türkiye'de Enerji Üretiminde Değerlendirilmesi. Bartın Orman Fakültesi Dergisi. 13(19), 63-75.

[2] Hatunoğlu, E.E. (2010) Biyoyakıt Politikalarının Tarım Sektörüne Etkileri. DPT Uzmanlık Tezleri. http://www.surdurulebilirkalkinma.gov.tr/ wpcontent/uploads/2016/ 06/Biyoyakit_Politikalarinin_Tarim_Sektorune _Etkileri.pdf. Accessed 18 jan 2018.

[3] Saraçoğlu, S. (2017) Yenilenebilir Enerji Kaynağı Olarak Biyokütle Üretiminin Dünyada ve Türkiye'de Durumu. Fiscaoeconomia. 1(3), 126-155.

[4] Sözen, E., Gündüz, G., Aydemir, D., Güngör, E. (2017) Evaluation of Biomass Use In terms of Energy, Environment, Health and Economy. Journal of Bartin Faculty of Forestry. 19, 148-160.

[5] EIA (2016) U.S. Energy Information Administration International Energy Outlook, U.S. Department of Energy, Washington, DC, USA.

[6] Adar, E., Ince, M.B. and Bilgili, M.S. (2017) Gasification of Municipal Sewage Sludge by Supercritical Water: A Review. Fresen. Environ. Bull. 26, 1503-1519.

[7] Taşyürek, M., Acaroğlu, M. (2007) Biyoyakıtlarda (Biyomotorinde) Emisyon Azatlımı ve Küresel Isınmaya Etkisi. Uluslararası Küresel İklim Değişikliği ve Çevresel Etkileri Konferansı, Konya.

[8] Sabancı, A., Ören, M.N., Yaşar, B., Öztürk, H.H., Atal, M. (2010) Türkiye'de Biyodizel ve Biyoetanol Üretiminin Tarım Sektörü Açısından Değerlendirilmesi. Ziraat Mühendisliği VII. Teknik Kongresi Bildiriler Kitabı. 11-15 January 2010, Ankara, 1-19.

[9] Eker, M. and Ozcelik, R. (2017) Estimating Recoverable Fuel Wood Biomass from Small Diameter Trees in Britain Pine (Pinus Brutia Ten.) Stands. Fresen. Environ. Bull. 26, 8286-8297.

[10] Saracoglu, N., Gunduz, G. (2009) Wood Pellets-Tomorrow's Fuel for Europe. Energy Sources, Part A: Recovery, Utilization, and Environmental Effects. 31(19), 1708-1718.

[11] Statista (2017) The statistical portal, https:// www.statista.com/statistics/509075/global-wood-pellet-production/. Accessed 16 jan 2018.

[12] FAO (2017) Food and Agriculture Organization of the United Nations, Website, http://www.fao.org/faostat/. Accessed 16 jan 2018.

[13] Box, G.E.P., Jenkins, G.M. (1970) Time Series Analysis: Forecasting and Control. Holden-Day Inc., San Francisco, Calif.

[14] Çelik, Ş. (2013) Sert Kabuklu Meyvelerin Üretim Miktarının Box-Jenkins Tekniği ile Modellenmesi. YYÜ Tarım Bilimleri Dergisi. 23(1), 18-30.

[15] Dickey, D.A., Fuller, W.A. (1979) Distribution of the estimators for autoregressive time series with a unit root. Journal of The American Statistical Association. 74, 727-431.

[16] Dickey, D.A., Fuller, W.A. (1981) Likelihood ratio statistics for autoregressive time series with a unit root. Econometrica. 49(4), 1057-1072.

[17] Göktaş, Ö. (2005) Teorik ve Uygulamalı Zaman Serileri Analizi. Beşir Kitabevi, İstanbul, 166p.

Received: **22.03.2018**
Accepted: **29.04.2018**

CORRESPONDING AUTHOR

Yildiz Cabuk
Bartin University,
Faculty of Forestry,
Department of Forest Industrial Engineering,
74100 Bartin – Turkey

e-mail: yildizcabuk@yahoo.com

© by PSP Volume 27 – No. 7/2018 pages 5153-5162 Fresenius Environmental Bulletin

IMPACTS OF HIGH VOLTAGE ELECTRIC FIELD (HVEF) APPLICATIONS ON GERMINATION AND SEEDLING GROWTH OF WHEAT SEED (*TRITICUM AESTIVUM* L.) WITH ANALYSIS BY FOURIER TRANSFORM INFRARED (FTIR) SPECTROSCOPY

Ozlem Ince-Yilmaz[1,*], Taskin Erol[1], Kamil Kara[2], Mustafa Dogan[3], Umit Erdem[3]

[1]Department of Plant and Animal Production, Kırıkkale VHS, Kirikkale University, 71450, Kirikkale, Turkey
[2]Department of Plant and Animal Production, Delice VHS, Kirikkale University, 71450, Kirikkale, Turkey
[3]The Scientific and Technological Researches Application and Research Center, Kirikkale University, 71450, Kirikkale, Turkey

ABSTRACT

Wheat is an important widely grown cereal that its grains used worldwide as a staple food. In this study, germination and seedling growth characteristics of grains of *Triticum aestivum*, the most widely grown species of the genus, in response to HVEF applications were studied. Three different intensities (50, 100 and 200 kV/m) were applied for 1, 5 and 10 min durations. Germination percentages were not affected by treatments, while germination speeds were inhibited by high intensities at long durations. Maximum enhancement in seedling growth measures which were given as root and shoot lengths and dry weights was determined for 5 min 50 kV/m treatment, where increases in average seedling lengths and dry weights were 34.2 % and 26.1 %, respectively. 1 min durations of treatments were also highly improved seedling growth, particularly at root measures. ATR technique was used to analyze the roots and first foliage leafs of treated seeds at FTIR spectroscopy. FTIR results supported that HVEF treatment could be a useful tool for enhancement of wheat seedling growth in early stages of development.

KEYWORDS:
Electric field, wheat, germination, seedling growth, FTIR.

INTRODUCTION

Seed germination and plant growth has long been known to be effected by natural or artificial electric and magnetic field [1, 2]. Studies have shown that both electric and magnetic field applications have potential to increase seed germination and sprout growth with proper treatments at certain intensities and durations [2–6]. Moreover, these applications are found to have positive impacts on some physiological metabolisms like enzyme activities of α-amylase, dehydrogenase and protease or antioxidant activities, and thus capable of increasing plant's resistance against different types of stressors [7–9].

Electric field, especially at high intensities has multiple applications like preserving, thawing or drying processes in food industry [10–12]. Electric field has also been found to be effective in increasing seed vigor, particularly for aged seeds and promote germination of infected seeds as an alternative method for chemical treatments [3, 6, 13].

Spectroscopic techniques like mid-infrared (MIR), near-infrared (NIR), Fourier transform infrared-(FT-IR) and Raman spectroscopy have been widely used to analyze analytical and chemical properties of plant materials for their fast, accurate, easy to use characteristics and very small amount of sample requirements [14–17]. FTIR spectroscopy technique enables analysis of molecular structures like proteins, lipids, cellulose and cell wall components of plant parts by quantifying range of functional groups [18–21]. The technique has successfully been used for components of plants and their products for identification, quality parameters and quantification purposes [17, 22–25], as well as the detection of structural changes and chemical responses of plants to different types of stressors [26, 27].

Wheat is a globally important cereal and indispensible food source providing a wide variety of products desirable in human diet. There are very few researches about effects of electric field applications on wheat seed germination, growth or yield parameters [28]. Besides, information about the impacts of this kind of applications to chemical and molecular structure of plants are still very limited [29, 30].

In this study, we aimed to find the impacts of HVEF applications on wheat seed germination and seedling growth characteristics, by determining seed germination rate and seedling growth by means of germination percentages, root and seedling lengths and dry weights. Additionally, we examined chemical structural responses of roots and leaves to applications by using FTIR spectroscopic analysis technique, which has shown to be an effective and informative technique to detect the changes at structural composition of plant parts [31].

MATERIALS AND METHODS

FTIR Analysis. FTIR spectra were used to assess the effect of HVEF treatment via functional groups in root and leaf samples of treated and untreated wheat seeds. FTIR spectrometer with ATR (diamond-crystal) attachment was used for spectral analysis (Alpha, Bruker Optics, Ettlingen, Germany). Spectrums were recorded in MIR range with a resolution of 4 cm^{-1} and 32 scans in the spectral wave number range of 4000 – 400cm^{-1}. The changes in FTIR peak absorbance patterns were analyzed for all applied electric field voltages and durations separately for composite samples of roots and leaves. The FTIR (MIR-ATR) absorbance spectrum was calculated from the attenuated beam and displayed as wave number (cm^{-1}) in spectrum graphics. Also spectra were compared for the similarity by cluster analyses (software OPUS-version 7.0, Bruker Optics, Ettlingen Germany). Therefore, spectra were normalized and offset-corrections were also done. Spectral intensities were compared by superpositioning and peak differences were also investigated in detail.

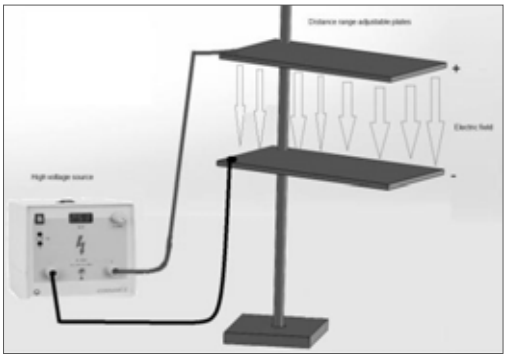

FIGURE 1
Experimental set up for HVEF application.

HVEF Treatment. Leybold high voltage source was used to create a stable electric field (Leybold Instruments, model number: 521 721). High voltage source load capacity was maximum 0.5 mA, and provided a stable voltage from zero to 25 kV. Discharge energy was maximum 200 mJ. Two square shaped parallel plates with an edge of 20 cm were used to obtain a stable electric field (Figure 1). Distance range adjustable parallel plates were fixed to 10 cm, and 5 kV, 10 kV and 20 kV high voltages applied between the plates. In this way, seeds were treated with 3 different electric fields of 5, 10 and 20 kV/m. Each electric field intensity was applied at three different time durations of 1, 5 and 10 minutes. During the treatments, seeds with the embryos facing upward were placed uniformly on a glass between the plates over the negative plate at the midpoint.

Plant Material. Wheat seed (*Triticum aestivum* L.) of Ayyıldız variety which was used in this study is bread wheat improved by East Anatolian Agricultural Research Institute. Experimental seeds were inspected for their physical appearance and weighted before the experiment to minimize the impact of seed abnormities and weight on germination and seedling growth parameters. Seeds having weight of 44 ± 6 mg was used in this study. Seeds were soaked into 20ºC distilled water and kept in an incubator for 2 hours at 20ºC prior to treatment to eliminate potential effects of humidity differences in seeds. Soaking time was accepted as the start of the experiment.

Germination and Seedling Growth. Seeds were treated with electric field following two hours of soaking process. Subsequently, seeds were placed on germination papers (Hahnemühle, 3644 Blotter blue) with the embryos facing upward. Germination papers were previously moistened with dH_2O at a ratio of about 2.5 times the weight of dry paper. Control and each treatment were prepared as 10 replicates; 4 replicates with 25 seeds and 6 replicates with 50 seeds, thus 400 seeds were used for each trial. Germination vessels were put into a seed germination chamber (Nüve, GC 400) at 20ºC and 60 % humidity with 8/16 hours of light/dark cycles for 7 days.

Methods of International Seed Testing Association [32] were used for determination of seed germination and normal and abnormal seeds. On the eighth day, the counts of normal, abnormal and ungerminated seeds were recorded for all replicates. Normal seedlings were well-developed seedlings with healthy essential structures of coleoptile and radicles. Seedlings having stunted radicles and defected, twisted or no coleoptiles, also seedlings infected by fungi or bacteria sourced from parent seed were counted as abnormal seedlings. Normal seedlings were used for determining seedling growth parameters and FTIR analysis. Germination percentage was also calculated by using the counts of normal seedlings.

Germinated seeds in all replicates were counted for calculating germination speed at 24, 30, 48 and 72 hours after the start of experiment. Germination speeds were calculated according to Maguire [33] using the following formula;

$$Germination\ speed = \sum (\frac{n}{t})$$

where n is the number of newly germinated seeds at time t in days following the start of experiment.

Randomly selected 10 seedlings from the replicates with 25 seeds were separated for growth parameters. Number of radicles and millimetric measurements of root and shoot lengths were recorded. Collected roots and shoots were put into an oven at 100 ºC for 24 hours for dry weight measurements. Similarly, another 10 seedlings from the same replicates were separated for roots and first foliage leafs

to be used in FTIR analysis. Roots and leaves were then dried at 60 ºC for 72 hours. Dry roots and leaves were powdered in an agate mortar and stored until FTIR analysis.

Statistical Analysis. The data obtained from all parameters as means ± SD were analyzed by one-way analysis of variance (ANOVA) followed by post hoc LSD multiple comparison test at significance level of $p < 0.05$, using SPSS 18 software.

RESULTS AND DISCUSSION

Effect of HVEF on Percentage and Speed of Germination. Electric field treatments are capable of increasing germination percentage and speed of seeds [4, 6, 34]. Seeds used in this study were selected, high quality seeds with similar weight and appearance. Thus, germination percentage of seeds was very high with 97.5 % of mean value and found to be 97.7 % for control (Table 1). Although 1 min applications of HVEF enhanced germination percentages to some degree, differences were not statistically significant between control and the treatments (Figure 2). 5 min 200 kV/m treatment was an exception that although still having high value of 95.0 %, its mean percentage was significantly lower than other treatments.

Enhancement of germination speed is often found associated with water uptake properties of seeds [35]. In the current study, when compared with control (41.5), germination speed increased at 1 and 5 min applications of 50 kV/m treatments with mean values of 42.4 and 42.7 respectively, and the highest value was found for the latter (Table 1). However, the differences were not statistically significant. Similarly, although non-significant, 1 min applications of 100 and 200 kV/m treatments were slightly higher than the control. As the durations and intensities increased, germination speeds were started to be affected negatively beginning from 10 min 50 kV/m treatment (Table 1, Figure 2). Especially at 5 and 10 min of 100 and 200 kV/m treatments, germination speeds were sharply decreased up to 31.3 % with high significance levels (mostly at $p<0.001$) when compared with control and other treatments. 2 hours of presoaking process, which aimed to eliminate humidity differences of seeds prior to experiment was probably an important factor determining the results obtained for germination speed. Since water imbibition rates for wheat are highest at first hours of incubation [36], presoaking process was likely to inhibit any enhancement on germination speeds due to water uptake. Contrarily, since absorbed water increased dielectric strength, seeds with high water content would be affected adversely by high intensities especially at long durations.

TABLE 1
Comparisons of germination and seedling growth parameters of wheat seed in response to HVEF treatments, given as means±standard deviation.

T	EF	TT	GP	%DC-GP	GS	%DC-GS	RL	%DC-RL
C	0	0	97.7±1.8	-	41.5±2.2	-	39.9±0.6	-
1	50	1	98.4±1.3	0,7	42.4±2.1	2,2	42.8±1.5	7,1
2	50	5	97.9±1.6	0,2	42.7±2.8	2,7	48.5±1.9	**21,5**
3	50	10	97.6±1.5	(-0,1)	40.2±4.2	(-3,1)	41.5±3.8	3,8
4	100	1	97.9±1.6	0,2	41.7±2.9	0,4	46.5±2.3	**16,5**
5	100	5	97.4±1.2	(-0,4)	37.5±2.9	**(-9,8)**	41.1±2.1	2,8
6	100	10	97.6±2.7	(-0,1)	35.2±2.2	**(-15,2)**	42.8±0.8	7,3
7	200	1	98.8±1.2	1,1	41.8±1.9	0,8	44.1±2.1	**10,5**
8	200	5	95.0±2.6	(-2,8)	28.5±4.1	**(-31,3)**	41.0±1.5	2,6
9	200	10	96.9±1.6	(-0,9)	34.0±2.6	**(-18,2)**	42.4±3.2	6,3
T	**EF**	**TT**	**SL**	**%DC-SL**	**RW**	**%DC-RW**	**SW**	**%DC-SW**
C	0	0	8.5±0.2	-	61.4±1.9	-	65.7±3.2	-
1	50	1	8.7±0.3	2,5	70.0±2.9	**14,0**	64.1±3.0	(-2,4)
2	50	5	9.6±0.7	**12,7**	73.1±2.5	**19,0**	70.4±4.9	7,1
3	50	10	8.3±0.8	(-1,8)	66.6±8.5	8,4	68.9±10.6	4,8
4	100	1	9.5±0.3	**12,3**	70.2±3.9	**14,3**	65.1±3.1	(-0,9)
5	100	5	8.2±0.2	(-2,8)	64.9±2.6	5,6	65.0±3.2	(-1,1)
6	100	10	8.6±0.6	1,2	67.2±3.9	9,4	64.6±4.2	(-1,8)
7	200	1	8.9±0.5	5,3	69.5±7.4	**13,1**	66.5±3.7	1,2
8	200	5	8.7±0.4	2,3	63.9±4.1	4,0	63.4±1.8	(-3,5)
9	200	10	8.4±0.2	(-1,3)	66.4±4.5	8,1	61.4±3.0	(-6,6)

T: Treatment; EF: Electric field (kV/m); TT: Treatment time (min); GP: Germination percentage; %DC: Percent difference from control (bold numbers indicate significant differences at $p<0.05$); GS: Germination speed; RW: Root dry weight (mg); SW: Shoot dry weight (mg); RL: Root length (cm); SL: Shoot length (cm). Normal + lowered treatment symbols: significant at $p<0.05$; bold + italic symbols: significant at $p<0.01$; bold + Italic + underlined symbols: significant at $p<0.001$; treatments with no symbols: non-significant at $p<0.05$.

Effect of HVEF on Length and Weight Measurements of Roots and Shoots. As an indicative seedling growth measures, root and shoot lengths were determined for experimental seeds. When we look at the results of both root and shoot lengths from Table 1, we see that the lowest means for roots and shoots were determined for control and 5 min 100 kV/m treatment with 39.9 and 8.2 cm, respectively. 5 min 50 kV/m treatment had the highest values with 48.5 cm root length and 9.6 cm shoot length and increased 34.2 % in total seedling length (21.5 % root + 12.7 % shoot length) when compared with control. This treatment was followed by 1 min 100 kV/m treatment with 46.5 and 9.5 cm values for root and shoot lengths respectively and total seedling length was 28.8 % higher than control (16.5 % root + 12.3 % shoot length). At 1 min 200 kV/m treatment mean root length was also increased 10.5 % (p<0.05). Seedling growth was distinctively better for especially 5 min 50 kV/m and 1 min 100 kV/m treatments by means of both root and shoot lengths approved by high statistical differences found with control and almost all other treatments for both measures (Table 1, Figure 2).

In accordance with the results of root and shoot lengths, dry weights of roots and shoots had also similar patterns. 5 min 50 kV/m treatment had the highest dry weights with 73.1 and 70.4 mg for roots and shoots, respectively and while shoot weight was also improved by 7.1 %, only root weight was significantly higher than control (Table 1, Figure 2) with 19.0 % difference (26.1 % increase in total seedling weight). The control had the lowest root weight among treatments with 61.4 mg, but shoot weight did not differ significantly. 1 min of 100 and 200 kV/m treatments had also higher root weights than control with 70.2 mg (14.3 %) and 69.5 mg (13.1 %) respectively (p<0.05). Despite of having relatively low root length of 42.8 cm, 1 min 50 kV/m treatment also had unexpectedly higher root weight than control (p<0.05) with 70.0 mg weight which corresponded to 14.0 % increase.

At the beginning of the experiment low germination speeds determined for treatments at high intensities and long durations. HVEF in these treatments may have induced some type of inhibitory factors related to mechanical or biochemical processes in seeds resulting with decreases in germination speeds. Among the possible mechanical effects of electrical field applications are electroporation or electrical breakdown of cell membrane [37] or perturbation of the membrane systems. These processes may breakdown cell membrane irreversibly with complete damage of cell membranes [38, 39] or may cause irregular absorption of water resulting with reorientation and disarrangement of the membrane components and unexpected swelling of stored macromolecules [40]. But since the length and weight measurements of these treatments resulted with similar or higher mean values for all treatments when compared with control, suppression of germination speed was probably not due to this kind of permanent negative effect or damage. It was more likely a temporary effect causing slowdown of germination processes and may have recovered in later growth stages.

Impact of electric field applications on germination and seedling growth has long been studied for different seeds and aspects [1], but since dielectric strengths, sizes and biochemical growth mechanisms changes for different plant species, seed specific applications are needed for improving growth characteristics. Standardized studies are still very limited in the field, thus agricultural implementations of this kind of alternative methods are not currently available. Electric field application on wheat seed in this study did not improve germination rate and speed significantly, probably due to the presoaking process, but remarkably enhanced seedling growth. Moon and Chung [4] studied with tomato seeds and found that electric field treatment accelerated percent germination rates by up to 2.8 percent. In the study, higher enhancements achieved at 400–1200 kV/m electric field treatments for 30–45 s. Exposure time longer than 60 s and intensities higher than 1200 kV/m inhibited germination. Costanzo [41] applied continuous electric field to soybean seeds at low intensities (3.6 and 1.8 kV/m) and extremely low frequency (50 Hz) and achieved up to 12 % increases in seedling lengths. Results of another experiment with onion seeds at 200–1400 kV/m intensities and 15–150 s durations revealed that germination percent and rate as well as the seedling length and dry weight increased at certain exposures [34].

Although the underlying impact mechanisms of electric field applications are not yet fully understood, it has been believed that they cause ion activations and dipole polarizations in living cells [4, 42] and by effecting biochemical processes related to free radicals, they increase protein and enzyme activities in cells [3, 6, 43]. Studies have also shown that electric field applications increase the antioxidant enzyme activity and glutathione content, thereby providing a self-healing ability of aged seeds to recover from dormancy and increasing the bioprotective capacity by alleviating the stress conditions [6, 44].

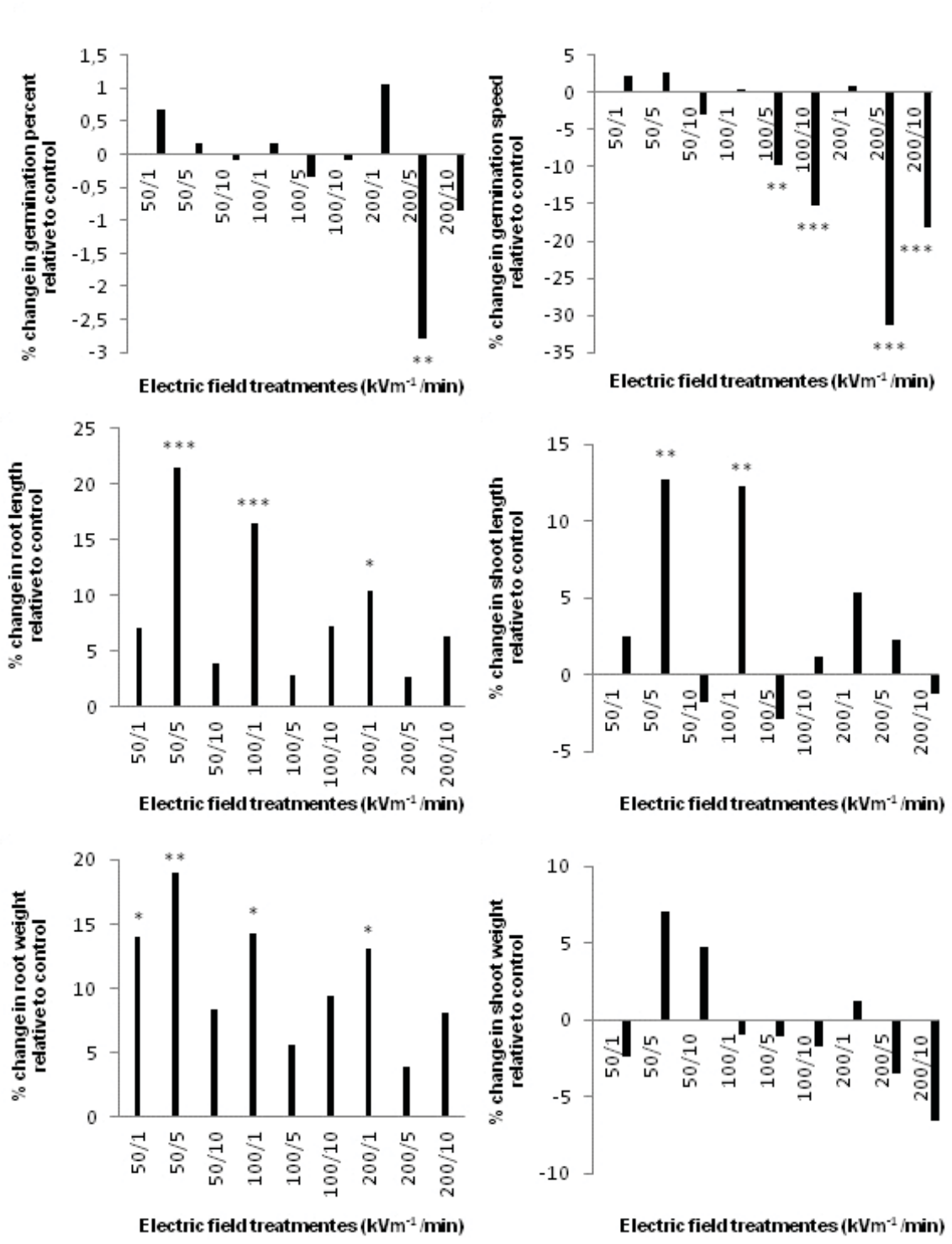

FIGURE 2
Percent changes in mean values of wheat germination and seedling growth parameters for electric field treatments relative to control. * significant at p<0.05; ** significant at p<0.01; * significant at p<0.001.**

FTIR Analysis. FTIR is a successfully used spectroscopic technique for demonstrating conformational changes in functional groups of plant parts in response to different types of treatments and environmental stressors [26, 27, 31, 45]. In this study ATR-FTIR technique was used to detect possible changes in main structure of roots and first foliage leafs of untreated and HVEF treated wheat seeds. Figure 3 and 4 shows the comparisons of root and leaf FTIR spectra, respectively. Each voltage applied was analyzed for roots and leaves separately by comparing with untreated control results. General patterns of spectra were similar for roots and leaves. Broad absorption bands between 3200 and 3600

cm^{-1} show O-H stretching vibrations, indicating the presence of alcohols and phenols in the structure [46]. Peaks in the region of 3000 to 2800 cm^{-1} represents C-H stretching vibrations of aliphatic hydrocarbons [46]. The absorption bands at ~1730 cm^{-1} and ~1640 cm^{-1} show the presence of the carbonyl groups (C= O) imply to carboxylic acids, aldehydes and ketones in both root and leaf samples. Aromatic rings are characteristic chemical groups for lignin, which is one of the components of wheat. The bands between 1500 and 1550 cm^{-1} are associated with aromatic C-O stretching of lignin in the guaiacyl ring structure and C-N stretching and N-H bending vibrations of amide II structure [46, 47].

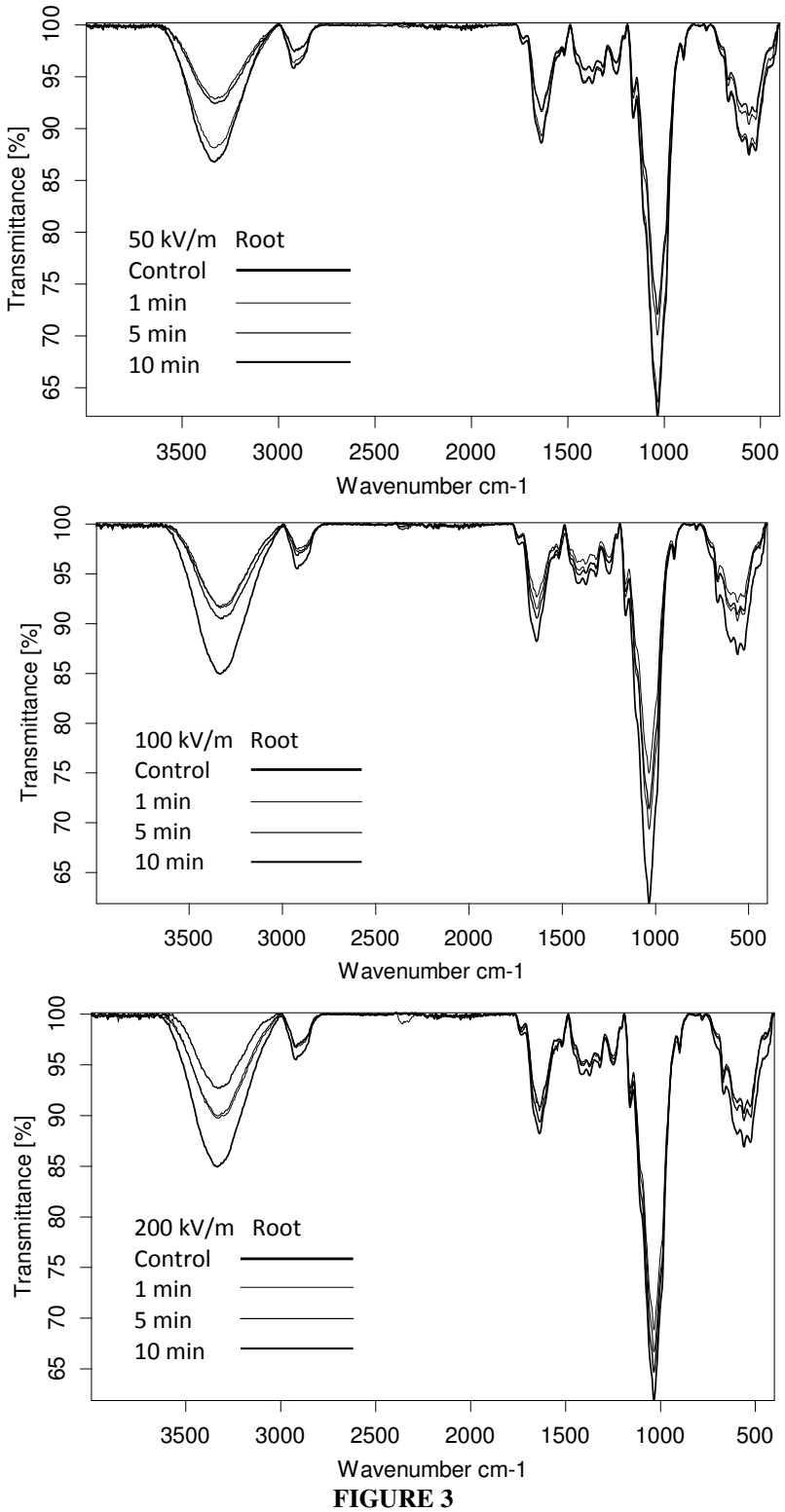

FIGURE 3
FTIR spectra of treated and untreated control seedling roots of wheat.

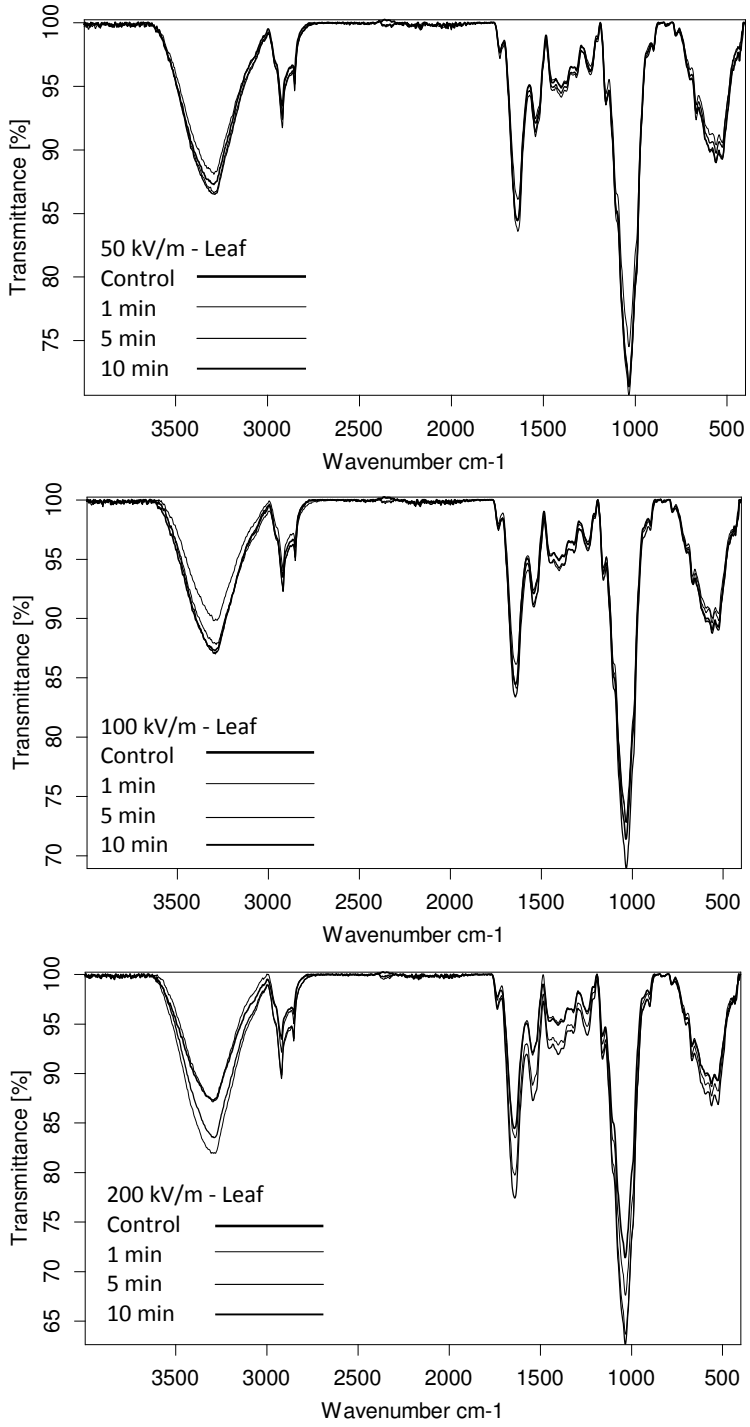

FIGURE 4
FTIR spectra of treated and untreated control seedling leaves of wheat

In fingerprint region absorption bands at 1370 cm^{-1} and 1320 cm^{-1} assigned aliphatic C–H stretching and guaiacyl rings, respectively [48, 49]. The bands near 1240 cm^{-1} in both root and leaf samples are due to C-O stretching vibrations of aryl group in lignin [50]. In fingerprint region, the most distinctive peaks detected at approximately 1030 cm^{-1}, which is the characteristic C-O stretching vibrations of alcohol both in cellulose and hemicelluloses structure [51, 52].

Seedling roots and leaves of HVEF treated wheat seeds were compared with untreated seedlings of control for any structural changes that could be distinguished from appearance, disappearance or shifting of characteristic bands in the spectrum. FTIR spectroscopic analysis revealed that, there was no distinctive variation in absorptions bands in spectra of untreated and HVEF treated samples. Instead, changes in the intensities were observed especially in root samples, where the samples having lower intensities were mostly belonged to the treatments of

well-developed roots that would explain possible decreases in concentrations for the seedlings grown under seed limited nutritional conditions.

CONCLUSION

In this study, HVEF were tested for possible enhancements on germination and seedling growth characteristics of wheat seeds. There was no significant increase on germination percent or speed at any treatments. Instead, the suppression of germination speeds at high intensities with long durations was observed, but this didn't reflect on seedling measurements which were similar to control at these treatments. When compared to control, the highest growth measures were achieved with 5 min 50 kV/m treatment with an increase of 34.2 % in mean seedling lengths and 26.1 % in mean seedling weights. This treatment was followed by treatments with 1 min durations of respectively 100, 200 and 50 kV/m intensities. These treatments were also highly enhanced seedling growth with lengths and weights up to 28.8 and 14.3 % respectively.

Overall view of the results revealed that HVEF treatment on wheat seeds with proper durations and intensities, as supported by the results of FTIR analysis, is a promising and powerful technique to enhance seedling growth in early stages of development. However, further studies are needed to understand the mechanisms behind this enhancement, in addition to the potential impacts of treatments on plants in later stages of growth for possible improvements on product quality or plant's resistance to different types of environmental stressors.

ACKNOWLEDGEMENTS

This research project was supported by Scientific Research Projects Coordination Unit, Kırıkkale University, Turkey (Project no. 2017/21).

REFERENCES

[1] Barman, P., Bhattacharya, R. (2016) Impact of Electric and Magnetic Field Exposure on Young Plants-A Review. International Journal of Current Research and Academic Review. 4, 182-192.

[2] Maffei, M.E. (2014) Magnetic field effects on plant growth, development, and evolution. Frontiers in Plant Science. 5, 1-15.

[3] Morar, R., Munteanu, R., Simion, E., Munteanu, I. and Dascalescu, L. (1999) Electrostatic treatment of bean seeds. IEEE Transactions on Industry Applications. 35, 208-212.

[4] Moon, J.D., Chung, H.S. (2000) Acceleration of germination of tomato seed by applying AC electric and magnetic fields. Journal of Electrostatics. 48, 103-114.

[5] Sedighi, N.T., Abedi, M. and Hosseini, S.E. (2013) Effect of electric field intensity and exposing time on some physiological properties of maize seed. European Journal of Experimental Biology. 3, 126-134.

[6] Wang, G., Huang, J., Gao, W., Lu, J., Li, J., Liao, R. and Jaleel, C.A. (2009) The effect of high-voltage electrostatic field (HVEF) on aged rice (*Oryza sativa* L.) seeds vigor and lipid peroxidation of seedlings. Journal of Electrostatics. 67, 759–764.

[7] Vashisth, A. and Nagarajan, S. (2010) Effect on germination and early growth characteristics in sunflower (*Helianthus annuus*) seeds exposed to static magnetic field. Journal of Plant Physiology. 167, 149-156.

[8] Cakmak, T., Cakmak, Z.E., Dumlupinar, R., Tekinay, T. (2012) Analysis of apoplastic and symplastic antioxidant system in shallot leaves: impacts of weak static electric and magnetic field. Journal of Plant Physiology. 169, 1066-1073.

[9] Chen, Y.P., Li, R., He, J.M. (2011) Magnetic field can alleviate toxicological effect induced by cadmium in mung bean seedlings. Ecotoxicology. 20, 760–769.

[10] Dalvi-Isfahan, M., Hamdami, N., Le-Bail, A. and Xanthakis, E. (2016) The principles of high voltage electric field and its application in food processing: A review. Food Research International. 89, 48-62.

[11] Mousakhani-Ganjeh, A., Hamdami, N., Soltanizadeh, N. (2015) Impact of high voltage electric field thawing on the quality of frozen tuna fish (*Thunnus albacares*). Journal of Food Engineering. 156, 39-44.

[12] Hsieh, C.W. and Ko, W.C. (2008) Effect of highvoltage electrostatic field on quality of carrot juice during refrigeration. Food Science and Technology. 41, 1752-1757.

[13] Ling, Y. and Hai-long, S. (2011) Effect of electrostatic field on seed germination and seedling growth of *Sorbus pohuashanesis.* Journal of Forestry Research. 22, 27−34.

[14] Schulz, H., Krähmer, A., Naumann, A., Gudi, G. (2014) in Infrared and Raman Spectroscopic Imaginged. Salzer, R., Siesler, H.W. Wiley-VCH Verlag GmbH&Co.KGaA, Weinheim. 225-293.

[15] Ferreira, D.S., Galão, O.F., Pallone, J.A.L. and Poppi, R.J. (2014) Comparison and application of near-infrared (NIR) and mid-infrared (MIR) spectroscopy for determination of quality parameters in soybean samples. Food Control. 35, 227-232.

[16] Ignat, I.V., Popa, I. and Valentin, I.A. (2001) A critical review of methods for characterisation of polyphenolic compounds in fruits and vegetables. Food Chemistry. 126, 1821-1835.
[17] Bunaciu, A.A., Aboul-Enein, H.Y. and Fleschin, S. (2012) FTIR spectrophotometric methods used for antioxidant activity assay in medicinal plants. Applied Spectroscopy Reviews. 47, 245-255.
[18] Liu, R., Yu, H. and Huang, Y. (2005) Structure and morphology of cellulose in wheat straw. Cellulose. 12, 25–34.
[19] Marcott, C., Reeder, R.C., Sweat, J.A., Panzer, D.D. and Wetzel, D.L. (1999)) FT-IR spectroscopic imaging microscopy of wheat kernels using a mercury–cadmium–telluride focal-plane array detector. Vibrational Spectroscopy. 19, 123-129.
[20] Barron, C., Parker, M.L., Mills, E.N., Rouau, X. and Wilson, R.H. (2005) FTIR imaging of wheat endosperm cell walls in situ reveals compositional and architectural heterogeneity related to grain hardness. Planta. 220, 667-677.
[21] Manley, M., McGoverin, C.M., Snyders, F., Muller, N., Botes, W.C., Fox, G.P. (2013) Prediction of Triticale Grain Quality Properties, Based on Both Chemical and Indirectly Measured Reference Methods, Using Near-Infrared Spectroscopy. Cereal Chemistry. 90, 540–545.
[22] Sujka, K., Koczoń, P., Ceglińska, A., Reder, M. and Ciemniewska-Żytkiewicz, H. (2017) The Application of FT-IR Spectroscopy for Quality Control of Flours Obtained from Polish Producers. Journal of Analytical Methods in Chemistry. 2017, 9p.
[23] Su, W.H. and Sun. D.W. (2018) Fourier Transform Infrared and Raman and Hyper-spectral Imaging Techniques for Quality Determinations of Powdery Foods: A Review. Comprehensive Reviews in Food Science and Food Safety. 17, 104-122.
[24] Zhao, L., Liu, X., Hu, Z., Li, L. and Li, B. (2017) Molecular Structure Evaluation of Wheat Gluten during Frozen Storage. Food Biophysics. 12, 60–68.
[25] Attaviroj, N., Kasemsumran, S., Noomhorm, (2011) Rapid variety identification of pure rough rice by fourier-transform near-infrared spectroscopy. Cereal Chemistry. 88, 490–496.
[26] Sharma, S. and Uttam, K.N. (2016) Investigation of the manganese stress on wheat plant by attenuated total reflectance Fourier transform infrared spectroscopy. Spectroscopy Letters. 49, 520-528.
[27] Rico, C.M., Peralta-Videa, J.R. and Gardea-Torresdey, J.L. (2015) Differential Effects of Cerium Oxide Nanoparticles on Rice, Wheat, and Barley Roots: A Fourier Transform Infrared (FT-IR) Microspectroscopy Study. Applied Spectroscopy. 69, 287 295.
[28] Ozel, B. (2003) High voltage electrical current on the yield and yield components of different bread wheat cultivars. M.Sc Thesis. Univ. of Kahramanmaras Sutcu Imam. Department of Field Crops, Turkey.
[29] Singh, A., Lahlali, R., Vanga, S.K., Karunakaran, C., Orsat, V. and Raghavan, V. (2016) Effect of High Electric Field on Secondary Structure of Wheat Gluten. International Journal of Food Properties. 19, 1217–1226.
[30] Hanaf, M.S., Mohamed, H.A. and Abd El-Hady, E.A. (2006) Effect of low frequency electric field on growth characteristics and protein molecular structure of wheat plant. Romanian Journal of Biophysics. 16, 253-271.
[31] Wei, Z., Jiao, D. and Xu, J. (2015) Using Fourier Transform Infrared Spectroscopy to Study Effects of Magnetic Field Treatment on Wheat (*Triticum aestivum* L.) Seedlings. Journal of Spectroscopy. 2015, 9p.
[32] The Germination Test in International Rules for Seed Testing. ISTA, Bassersdorf, Switzerland, 2017, 111-167.
[33] Maguire, J.D. (1962) Speed of germination-aid in selection and evaluation for seedling emergence and vigor. Crop Science. 2, 176-177.
[34] Molamofrad, F., Lotfi, M., Khazaei, J., Tavakkol-Afshari, R., Shaiegani-Akmal, A.A. (2013) The effect of electric field on seed germination and growth parameters of onion seeds (*Allium cepa*). Advanced Crop Science. 3, 291–298
[35] Shine, M.B., Guruprasad, K.N. and Anand, A. (2011) Enhancement of Germination,Growth, and Photosynthesis in Soybean by Pre-Treatment of Seeds With Magnetic Field. Bioelectromagnetics. 32, 474-484.
[36] Clarke, J.M. (1980) Measurement of relative water uptake rates of wheat seeds using agar media. Canadian Journal of Plant Science. 60, 1035-1038.
[37] Neumann, E. and Rosenheck, K. (1972) Permeability changes induced by electric impulses in vesicular membranes. Journal of Membrane Biology. 10, 279–290.
[38] Crowley, J.M. (1973) Electrical breakdown of bimolecular lipid membranes as an electromechanical instability. Biophysical Journal. 13, 711-724.
[39] Dimitrov, D.S. (1984) Electric field induced breakdown of lipid bilayers and cell membranes: a thin visco elastic film model. Journal of Membrane Biology. 78, 53-60.

[40] Isobe, S., Ishida, N., Koizumi, M., Kano, H. and Hazlewood, C.F. (1999) Effect of electric field on physical states of cell-associated water in germinating morning glory seeds observed by 1H-NMR. Biochimica et Biophysica Acta (BBA). 1426, 17-31.
[41] Costanzo, E. (2008) The influence of an electric field on the growth of soy seedlings. Journal of Electrostatics. 66, 417–420.
[42] Johnson, C.C. and Guy, A.W. (1972) Non-ionizing electrostatic wave effects in biological materials and systems. Proceedings of the IEEE. 60, 692-718.
[43] Kurinobu, S. and Okazaki, Y. (1995) Dielectric constant and conductivity of one seed in the germination process. Annual Conference Record of IEEE/IAS. 1329-1334.
[44] Leong, S.Y., Burritt, D.J. and Oey, I. (2016) Electropriming of wheatgrass seeds using pulsed electric fields enhances antioxidant metabolism and the bioprotective capacity of wheatgrass shoots. Scientific Reports. 6, 1-13.
[45] Agnieszka, N., Lamorska, J. (2013) Determination of food quality by using spectroscopic methods. In: Grundas, S. (ed.) Advances in Agrophysical Research. InTech. 356-359.
[46] Stuart, B.H. (2004) Infrared Spectroscopy: Fundamentals and Applications. John Wiley and Sons. 46-203
[47] Pandey, K.K. (1999) A study of chemical structure of soft- and hardwood and wood polymers by FTIR spectroscopy. Journal of Applied Polymer Science. 71, 1969-1975.
[48] Faix, O. (1991) Classification of lignins from different botanical origins by FT-IR spectroscopy. Holzforschung. 45, 21–27.
[49] Vazquez, G., Antorrena, G., Gonzalez, J. and Freire, S. (1997) FTIR, H-1 and C-13 NMR characterization of acetosolv-solubilized pine and eucalyptus lignins. Holzforschung. 51, 158–166.
[50] Le Troedec, M., Sedan, D., Peyratout, C., Bonnet, J.P., Smith, A., Guinebretiere, R., Gloaguen, V. and Krausz, P. (2008) Influence of various chemical treatments on the composition and structure of hemp fibres. Composites Part A. 39, 514-522.
[51] Sun, R.C., Tomkinson, J., Wang, Y.X. and Xiao, B. (2000) Physico-chemical and structural characterization of hemicelluloses from wheat straw by alkaline peroxide extraction. Polymer. 41, 2647–2656.
[52] Mascarenhas, M., Dighton, J. and Arbuckle, G.A. (2000) Characterization of plant carbohydrates and changes in leaf carbohydrate chemistry due to chemical and enzymatic degradation measured by microscopic ATR FT-IR spectroscopy. Applied Spectroscopy. 54, 681-686.

Received: **31.03.2018**
Accepted: **30.04.2018**

CORRESPONDING AUTHOR

Ozlem Ince-Yilmaz
Department of Plant and Animal Production,
Kırıkkale VHS,
Kırıkkale University,
71450, Kırıkkale – Turkey

e-mail: oince@kku.edu.tr

© by PSP Volume 27 – No. 7/2018 pages 5163-5172 Fresenius Environmental Bulletin

IN VITRO PROPAGATION OF *QUERCUS PUBESCENS* WILLD. (DOWNY OAK) VIA ORGANOGENESIS FROM INTERNODES

Mehmet Sezgin*

Science Faculty, Biology Department, Cankiri Karatekin University, Cankiri, Turkey

ABSTRACT

In this study, the *in vitro* propagation of Downy oak (*Quercus pubescens* Willd.) was carried out via micropropagation technique for the first time. The 6-benzylaminopurine (BA) [0, 0.5, 1 and 2 mg/L doses], 1-Phenyl-3-(1,2,3-thiadiazol-5-yl) (TDZ) [0, 0.1, 0.5 and 1 mg/L doses] and indole-3-acetic acid (IAA) [0, 0.1 and 0.5 mg/L doses] were added for the first time in triplicate combinations to the basal media of Murashige and Skoog (MS), Gresshoff and Doy (GD) and Woody Plant Medium (WPM). All media were supplemented with 500 mg/L L-glutamine and 3 mg/L polyvinylpyrolidone (PVP) to prevent phenolic substance secretion. When the cytokinin and auxin group Plant Growth Regulators (PGRs) were tested simultaneously, the explant response in WPM basal media supplemented with 1 mg/L BA, 1 mg/L TDZ and 0.5 mg/L IAA was obtained at the internodes up to 95% ratio without callus formation, after 8 weeks. Prior to the rooting step, the shoots were transferred to WPM containing 0.1 mg/L BA and 0.1 mg/L GA_3 for development and maturation. The explants reaching shoot size up to about 4 cm were cultured in WPM containing 0, 0.5, 1, 2 and 3 mg/L doses of indole-3-butyric acid (IBA), IAA and naphthalene acetic acid (NAA). The highest regeneration rate was 95% in the medium containing 1 mg/L IBA. The triple combinations of auxin and cytokinins gave successful results for shoot regeneration and growth without callus formation. The rooted plantlets were successfully acclimatized at the ratio of 55%.

KEYWORDS:
Internode culture, micropropagation, *Quercus pubescens* Willd., plant regeneration, triple PGR combination

INTRODUCTION

Forestry has a great importance worldwide for a majority of people to carry on their vital activities. Forest trees have a wide range of uses in human life, such as firewood and material [1]. In developing countries, about 90% of forest products are used as firewood [2]. Among the functions of the forests, those concerned with the preservation and continuation of life and natural balances should be in front of the function of wood production as an economic value because forests host environments for many living beings, provide natural balance chains with water and air, earth and air protection, national park areas for sports, entertainment, and resting [3]. Reproduction of forest trees is practically done with seeds. However, in forest trees, seedling production is limited due to the infrequent number of years with abundant seed, the problems of long-term storage of seeds and the difficulty in collecting seeds. For these reasons, vegetative propagation techniques also have to be used in reproduction. It is also necessary to use vegetative propagation techniques in order to reproduce the forest trees superior in nature (resistant to diseases and harmful, abundant seeds, smooth body structure etc.) without change in genetic structure [4].

Downy oak (*Quercus pubescens* Willd.) is an important species that can be used for arid area reforestation due to its drought-tolerance and terrestrial biocompatibility beside an advanced root system [5, 6]. Downy oak, which has a very important place among the oaks spreading in Turkey, is being used both as firewood and building material (in furniture, lumber, plastering, parquet, etc.) having contribution to economy.

In vitro culture of internodes is an important technique involved in plant biotechnology. With this technique, intense clonal propagation can be achieved in a short time. In addition, unlike shoot tip culture, the donor is affected to a minimum level when a small number of shoots are taken. There are many studies on the *in vitro* propagation of different species of oak [7], such as *Q. rubra* [8, 9, 10, 11], *Q. suber* [12, 13, 14], *Q. robur* [15, 16]. For *Q. pubescens* there is only one study performed by Bellarosa [17]. In the study, for the first time, auxin and cytokinin group Plant Growth Regulators (PGRs) were used in triplicate combination and tested in three different media aiming to develop a protocol for *in vitro* propagation of downy oak.

MATERIALS AND METHODS

The internodes of fresh shoots were taken from the young individuals (aged 5-7 years) from the mixed stands formed by *Q.pubescens* together with *Pinus nigra* and *Quercus cerris* in Çankırı-İndağı site.

Explants sterilization. The plants brought to the laboratory were sterilized before they were planted *in vitro*. For this purpose, firstly the shoots were washed 15 min with running tap water, then 4-5 drops of Tween 20 were added to a second wash. After this pre-wash, the shoots were shaken for 5 min in 0.05% (w/v) mercuric chloride solution and rinsed 3 times for 5 min each time with purified water to remove mercuric chloride. After this step, the shoots were separated into their internodes to buds having size of ca. 2 cm, and kept in 70% ethanol for 1 minute. Then, the explants were sterilized in a 20% commercial sodium hypochlorite solution containing a few drops of Tween 20 for 15 min. Afterwards, in order to remove sodium hypochlorite on the tissues, it was rinsed 3 times with sterile distilled water for 5 minutes.

In vitro shoot propagation. 1. Woody Plant Medium (WPM) [18] 2. Murashige and Skoog (MS) [19] and 3. Gresshoff and Doy (GD) [20] basal media were used in order to induce shoot formation from the internodes. Doses of 0, 0.5, 1 and 2 mg/L of BA, doses of 0, 0.1, 0.5 and 1 mg/L of TDZ and doses of 0, 0.1 and 0.5 mg/L of IAA were combined in triplicate. 500 mg/L L-glutamine, 30 g/L sucrose and 7 gr/L agar were added to each medium and the pH of the medium was adjusted to 5.7. In the initial stages, 3 mg/L polyvinylpyrolidone (PVP) was added to the medium to prevent the release of phenolic substances in *in vitro* propagations of plants belonging to the family Fagaceae (*Quercus* sp., *Fagus* sp. *Castanea* sp. etc.) [15, 16, 21, 22]. To avoid contamination, Plant Preservative Mixture ™ (PPM) was added to all media at 1 ml/L, and each explant was transferred to 20 ml volumes of media in glass tubes of 15x150 mm size (Figure 1a). Explants were incubated in 16 h light 8 h darkness at 25±2°C. For all basal media, PGR combinations were applied separately, and for each combination, 40 internodes were used. The explants were taken to fresh medium after 4 wk. After 8 wk, shoots of at least 1 cm in length were transferred in a WPM medium containing 0.1 mg/L BA and 0.1 mg/L GA_3 for the development and maturation of the shoots formed on the nodules. In this step, Magentha™ containers containing 50 mL of medium were used and the shoots were kept in this medium for 4 wk and then placed in the rooting medium.

Rooting of in vitro shoots. New shoots having a length of at least 2 cm were placed in round vessels with hermetic cover and breathing strips containing 50 mL media for rooting. 30 g/L sucrose, 7 g/L agar with doses of 0, 0.5, 1, 2 and 3 mg/L of IBA, IAA and NAA were added to the WPM medium and the pH of the medium was adjusted to 5.7. In order to induce root development, shoots were incubated at 25±2°C in 5d darkness. It was then incubated for 16 h at 4 wk in 8 h darkness at 25±2°C. For each plant growth regulator, 20 individuals were used.

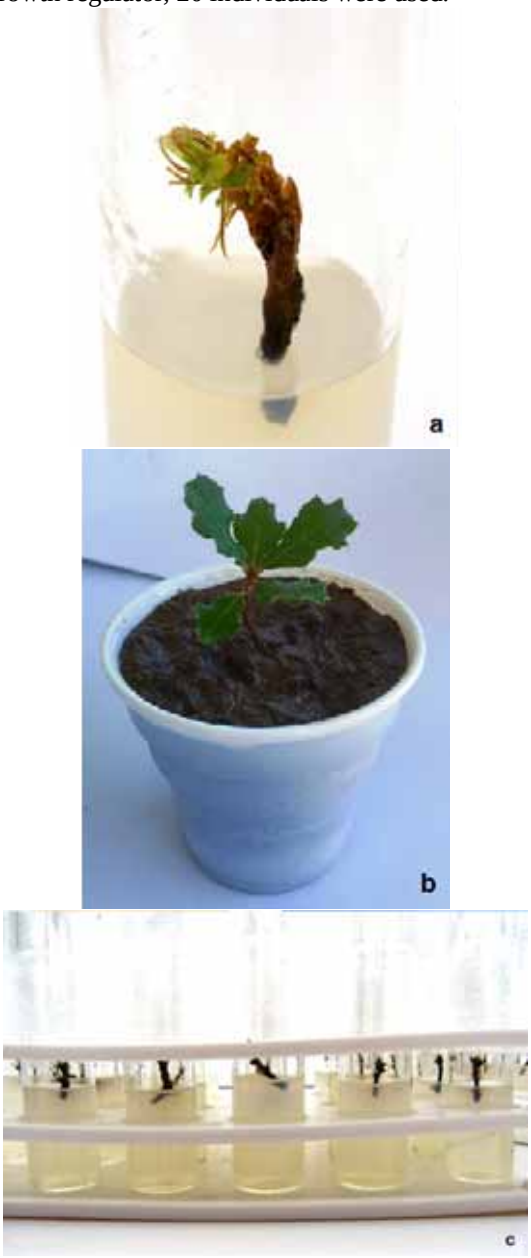

FIGURE 1
***In vitro* propagation of *Q.pubescens* Willd.**
a) Shoot induction from internode explant on WPM with 1 mg/L BA+1 mg/L TDZ+0.5 mg/L IAA. b) Acclimatized plantlet. c) Internode explants without callusing and phenolics.

In both shoot propagation and rooting stages, all experiments were repeated 3 times. All the media used in the experiments were 20 min autoclaved at 121 °C and 1.2 atm pressure.

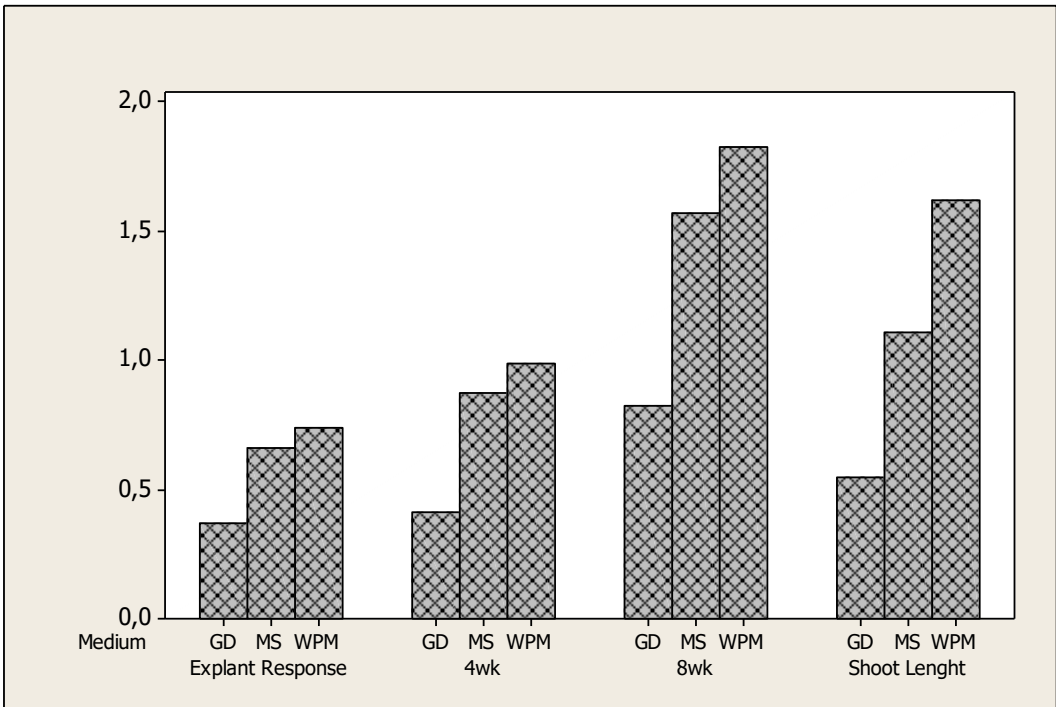

FIGURE 2
The mean values of explant response, number of shoots per explant after 4 and 8 wk and shoot lenght.

Acclimatization. Plantlets with good roots and shoot growth were thoroughly washed under running water until they were removed from the remaining medium and agar. These plants were then planted in 10x8 cm plastic pots containing autoclaved mixture of 1:3 garden soil, 1:3 sand and 1:3 perlite. The watered plants were covered with plastic bags and small air vents were opened to prevent moisture loss. These plants were incubated in a humidity controlled incubator at 25±2 °C in 16 h light conditions (35 µmol $m^{-2}.s^{-1}$). The plants were acclimatized between 4 and 6 wk, and the plastic bags on the pots were completely opened gradually.

Statistical analyses. All of the experiments in the study were established according to the "Coincidence Parcel Experimental Design". The effect of 2 different applications (3 basal media x 48 PGR combinations) in the shoot formation experiments was investigated and each experiment was set up as 40 explants (5760 internode). During the rooting, a basal medium with 5 doses of 3 PGRs were studied and 20 shoots were used in each trial. All the experiments were repeated for 2 years.

The data obtained from *in vitro* shoot propagation and rooting were tested as the mean of the replicates via variance analysis (ANOVA) and F-test ($P < 0.05$) using SPSS package program [23]. Significant differences were determined using the Tukey's multiple comparison test based on a 5% error limit, and the differences were indicated using letters.

RESULTS AND DISCUSSION

In the study initiated by the culture of the internodes of *Q.pubescens*, the formation of new shoots was observed within 4 wk. The rate of shoot formation reached up to 95% after 8 wk. However, this amount varied according to the concentrations of PGR combinations and the medium. While internodes explants showed their best development in the WPM medium, they exhibited less development in MS and GD media than WPM. In trials involving triple PGR combinations, shoot formation was better in combinations with BA, TDZ, and IAA compared to the control group.

Effect of BA, TDZ and IAA on shoot propagation and explants response. When four axillary buds developed from a single explant were used, and cytokinin and auxin group PGRs were combined, 95% explant response was obtained in WPM supplemented with 1 mg/L BA, 1 mg/L TDZ and 0.5 mg/L IAA without callus formation (Table 1). However, high shoot formation rates have also been reached in the triplicate combinations of BA, TDZ and IAA at different concentrations (Figure 1c) (Table 1, 2 and 3). In terms of explant response, the combinations containing 0.5 mg/L BA + 0.5 mg/L TDZ + 0.1 mg/L IAA, and 1 mg/L BA + 1 mg/L TDZ + 0.5 mg/L IAA showed 95% viability (Figure 1a). The highest statistically significant ($P<0.05$) rates of shoot formation in the same PGR combinations were reached at the end of 4 wk (1.57 ± 0.67) and 8 wk (2.97 ± 1.02) (Table 1, 2 and 3).

In the BA alone media, explant viability was 90% at 2 mg/L, with a shoot number of 2.37 ± 1.00 ($P<0.05$) after 8 wk (Figure 2). It was reported that BA produced better results in increasing the number of shoots compared to other PGRs in the cytokines group [11, 12, 24, 25, 26]. In the micropropagation studies with the utilization of shoot tip as an explant source, and with lower concentrations than 0.5 mg/L of BA, an increase in the shoot number was emphasized [27, 28, 29]. Here, both utilization of explant source and the BA were efficient in induction of axillary shoots because the explants taken from shoot tip are younger than the ones from shoot base, and their propagation rate is higher [30, 31]. High doses of BA (0.5 to 2 mg/L) were therefore used to promote the formation of shoots of internodes used in the study. This high concentration is neither related to vitrification and basal callogenesis [32] nor to hyperhydricity, malformation, and twisted leaves in *Q. robur* [33]. This might also be resulted from IAA found in PGR combinations. Manzanera and Pardos [12] emphasized that NAA in the auxin group increases the shoot propagation rate in *Q. suber*. In the medium with TDZ alone, the number of shoots was

TABLE 1
Effect of WPM medium with BA, TDZ and IAA on multiple shoot proliferation and regeneration from internode explants of downy oak

WPM	Plant Growth Reg.(mg/L)			Explant Response (%)		No of shoots per explant after 4wk		No of shoots per explant after 8wk		Shoot length (cm)	
	BAP	TDZ	IAA								
1	0	0	0	0.05±0.22	g*	0.0±0.0	g	0.05±0.22	g	0.25±0.11	g
2	0	0	0.1	0.05±0.22	g	0.0±0.0	g	0.05±0.22	g	0.02±0.11	g
3	0	0	0.5	0.05±0.22	g	0.0±0.0	g	0.05±0.22	g	0.02±0.12	g
4	0	0.1	0	0.32±0.47	fg	0.15±0.36	g	0.40±0.63	g	0.17±0.27	g
5	0	0.1	0.1	0.47±0.50	ef	0.30±0.46	g	0.60±0.70	g	0.26±0.30	g
6	0	0.1	0.5	0.52±0.50	def	0.35±0.48	g	0.55±0.55	g	0.30±0.33	g
7	0	0.5	0	0.62±0.49	abcdef	0.47±0.50	fg	0.72±0.64	fg	0.36±0.31	g
8	0	0.5	0.1	0.72±0.45	abcde	0.65±0.48	efg	1.05±0.81	fg	0.59±0.40	g
9	0	0.5	0.5	0.77±0.42	abcde	0.75±0.77	cdefg	1.32±1.04	defg	0.89±0.59	g
10	0	1	0	0.87±0.33	abc	1.00±0.87	abcdefg	2.12±1.11	abcde	1.18±0.55	g
11	0	1	0.1	0.85±0.36	abcd	**1.40±0.90**	**ab**	1.95±1.21	bcdef	1.59±0.80	efg
12	**0**	**1**	**0.5**	**0.92±0.26**	**ab**	1.17±0.63	abcde	2.15±1.09	abcde	2.34±0.81	abcde
13	0.5	0	0	0.55±0.50	cdef	0.37±0.49	g	0.62±0.62	g	0.28±0.29	g
14	0.5	0	0.1	0.60±0.49	bcdef	0.70±0.72	defg	1.02±1.09	fg	0.63±.0.57	g
15	0.5	0	0.5	0.65±0.48	abcdef	0.72±0.75	defg	1.15±1.12	efg	0.94±0.78	g
16	0.5	0.1	0	0.80±0.40	abcde	1.15±0.76	abcde	2.02±1.27	abcdef	1.11±0.64	g
17	**0.5**	**0.1**	**0.1**	**0.90±0.30**	**ab**	**1.47±0.75**	**ab**	2.72±1.30	abc	2.34±1.03	abcde
18	0.5	0.1	0.5	0.82±0.38	abcd	1.30±0.88	abcd	1.90±1.25	bcdef	1.60±0.90	efg
19	0.5	0.5	0	0.75±0.43	abcde	0.92±0.85	bcdefg	1.80±1.28	cdef	1.31±0.95	fg
20	**0.5**	**0.5**	**0.1**	**0.95±0.22**	**a**	**1.57±0.71**	**a**	**2.87±1.15**	**ab**	2.64±0.96	abc
21	0.5	0.5	0.5	0.70±0.46	abcde	0.95±0.84	abcdefg	1.82±1.41	cdef	0.95±0.73	g
22	0.5	1	0	0.80±0.40	abcde	0.97±0.83	abcdefg	1.87±1.20	bcdef	1.88±1.09	cdefg
23	0.5	1	0.1	0.82±0.38	abcd	1.00±0.81	abcdefg	2.07±1.22	abcde	2.22±1.20	abcde
24	**0.5**	**1**	**0.5**	**0.90±0.30**	**ab**	1.22±0.80	abcde	2.27±1.03	abcd	2.24±0.97	abcde
25	1	0	0	0.75±0.43	abcde	0.90±0.84	bcdefg	1.80±1.28	cdef	1.24±0.89	g
26	1	0	0.1	0.87±0.33	abc	1.17±0.78	abcde	1.17±0.78	bcdef	1.92±1.16	g
27	1	0	0.5	0.82±0.38	abcd	1.00±0.81	abcdefg	2.20±1.24	abcd	1.51±0.90	efg
28	1	0.1	0	0.72±0.45	abcde	0.90±0.84	bcdefg	1.72±1.24	cdefg	1.07±0.84	g
29	1	0.1	0.1	0.80±0.40	abcde	1.15±0.76	abcde	2.22±1.32	abcd	2.16±1.36	abcdef
30	**1**	**0.1**	**0.5**	**0.92±0.26**	**ab**	1.22±0.73	abcde	2.60±1.08	abc	2.38±1.12	abcde
31	1	0.5	0	0.82±0.38	abcd	1.10±0.81	abcdef	2.20±1.20	abcd	1.53±0.90	efg
32	1	0.5	0.1	0.82±0.38	abcd	1.25±0.77	abcde	2.37±1.33	abc	2.18±1.24	abcdef
33	1	0.5	0.5	0.87±0.33	abc	1.37±0.74	abc	2.55±1.17	abc	2.21±1.04	abcde
34	1	1	0	0.85±0.36	abcd	1.25±0.70	abcde	2.10±1.12	abcde	1.81±0.90	cdefg
35	1	1	0.1	0.82±0.38	abcd	1.32±0.79	abcd	2.35±1.25	abc	2.16±1.22	abcdef
36	**1**	**1**	**0.5**	**0.95±0.22**	**a**	**1.57±0.67**	**a**	**2.97±1.02**	**a**	2.55±0.82	abcd
37	**2**	**0**	**0**	**0.90±0.30**	**ab**	1.27±0.67	abcde	2.37±1.00	abc	2.29±1.01	abcde
38	2	0	0.1	0.70±0.46	abcde	1.00±0.78	abcdefg	1.77±1.34	cdef	1.75±1.33	defg
39	2	0	0.5	0.80±0.40	abcde	1.12±0.72	abcde	2.12±1.24	abcde	2.09±1.25	abcdef
40	2	0.1	0	0.72±0.45	abcde	1.12±0.82	abcde	2.00±1.37	abcdef	1.89±1.34	bcdefg
41	2	0.1	0.1	0.87±0.33	abc	1.27±0.67	abcde	2.57±1.21	abc	2.61±1.18	abcd
42	2	0.1	0.5	0.85±0.36	abcd	1.20±0.68	abcde	2.45±1.28	abc	**2.94±1.39**	**a**
43	2	0.5	0	0.82±0.38	abcd	**1.42±0.90**	**ab**	2.32±1.26	abcd	2.38±1.35	abcde
44	2	0.5	0.1	0.80±0.40	abcde	1.17±0.78	abcde	2.32±1.38	abcd	2.63±1.50	abc
45	2	0.5	0.5	0.80±0.40	abcde	1.12±0.72	abcde	2.40±1.33	abc	**2.76±1.53**	**ab**
46	2	1	0	0.75±0.43	abcde	1.12±0.82	abcde	1.90±1.31	bcdef	2.22±1.50	abcde
47	2	1	0.1	0.85±0.36	abcd	**1.40±0.74**	**ab**	2.45±1.17	abc	**2.93±1.38**	**a**
48	2	1	0.5	0.85±0.36	abcd	1.37±0.83	abc	2.45±1.25	abc	**2.89±1.39**	**a**

*Different lowercase letters indicate significant differences between treatments

2.12 ± 1.11 (P<0.05) after 8 wk, and the highest explant response was 87% at the 1 mg/L dose, whereas the explant response and the number of shoot were the lowest when only IAA was used (Table 1). In tissue cultures cytokinins are necessary for plant cell division [34, 35]. A large number of new shoots were emerged due to the presence of BA and TDZ in the medium. Moreover, unlike Vangadesan and Pijut [11], the presence of TDZ and BA in the same medium caused increase in both the number and the length of shoots. Additionally, *in vitro* propagation studies in *Acer* sp. and *Fraxinus* sp. using TDZ alone and in combination with other PGRs produced very successful results [36, 37, 38, 39, 40].

Positive effects were observed on the explant response as well as shoot number and length when BA and TDZ were used alone, in combination with IAA, or utilization of triplicate combinations (Figure 2). However, no statistically significant result was achieved in basal media (GD, MS and WPM) without PGR.

TABLE 2
Effect of MS medium with BA, TDZ and IAA on multiple shoot proliferation and regeneration from internode explants of downy oak

MS	Plant Growth Reg.(mg/L)			Explant Response (%)		No of shoots per explant after 4wk		No of shoots per explant after 8wk		Shoot length (cm)	
	BAP	TDZ	IAA								
1	0	0	0	0.02±0.15	g*	0.0±0.0	g	0.02±0.15	g	0.01±0.07	h
2	0	0	0.1	0.02±0.15	g	0.0±0.0	g	0.02±0.15	g	0.01±0.07	h
3	0	0	0.5	0.02±0.15	g	0.0±0.0	g	0.02±0.15	g	0.01±0.09	h
4	0	0.1	0	0.20±0.40	fg	0.15±0.36	g	0.25±0.54	g	0.08±0.18	h
5	0	0.1	0.1	0.30±0.46	efg	0.17±0.38	g	0.37±0.62	g	0.12±0.19	h
6	0	0.1	0.5	0.37±0.49	defg	0.15±0.36	g	0.37±0.49	g	0.14±0.19	h
7	0	0.5	0	0.45±0.50	cdef	0.20±0.40	fg	0.50±0.59	fg	0.21±0.25	h
8	0	0.5	0.1	0.52±0.50	bcdef	0.32±0.47	efg	0.70±0.79	efg	0.39±0.41	h
9	0	0.5	0.5	0.55±0.50	abcdef	0.50±0.75	defg	0.92±1.09	defg	0.55±0.55	h
10	0	1	0	0.70±0.46	abcd	0.75±0.89	cdefg	1.65±1.31	abcde	0.84±0.60	gh
11	0	1	0.1	0.70±0.46	abcd	1.12±0.96	abcd	1.50±1.28	bcdef	1.11±0.88	defgh
12	0	1	0.5	0.65±0.48	abcd	0.70±0.75	cdefg	1.35±1.21	cdefg	1.56±1.22	abcde
13	0.5	0	0	0.45±0.50	abcde	0.20±0.40	fg	0.50±0.59	fg	0.21±0.25	h
14	0.5	0	0.1	0.55±0.50	cdef	0.50±0.75	defg	0.92±1.09	defg	0.55±0.55	h
15	0.5	0	0.5	0.55±0.50	abcdef	0.50±0.75	defg	0.92±1.09	defg	0.55±0.55	h
16	0.5	0.1	0	0.70±0.46	abcdef	0.85±0.89	bcdef	1.77±1.38	abcd	0.84±0.60	gh
17	0.5	0.1	0.1	0.80±0.40	abc	1.32±0.85	abc	2.32±1.49	abc	1.94±1.17	abc
18	0.5	0.1	0.5	0.70±0.46	abcd	1.12±0.96	abcd	1.50±1.28	bcdef	1.11±0.88	defgh
19	0.5	0.5	0	0.70±0.46	abcd	0.75±0.89	cdefg	1.65±1.31	abcde	0.84±0.60	gh
20	0.5	0.5	0.1	0.80±0.40	abc	1.32±0.85	abc	2.32±1.49	abc	1.94±1.17	abc
21	0.5	0.5	0.5	0.70±0.46	abcd	0.85±0.89	bcdef	1.77±1.38	abcd	0.84±0.60	gh
22	0.5	1	0	0.70±0.46	abcd	0.75±0.89	cdefg	1.65±1.31	abcd	1.52±1.14	abcdefg
23	0.5	1	0.1	0.70±0.46	abcd	0.70±0.85	cdefg	1.52±1.15	bcdef	1.54±1.16	abcdef
24	0.5	1	0.5	0.77±0.42	abc	0.80±0.85	bcdefg	1.62±1.07	abcde	1.63±1.07	abcde
25	1	0	0	0.70±0.46	abcd	0.90±0.84	abcde	1.67±1.30	abcde	0.86±0.62	fgh
26	1	0	0.1	0.67±0.47	abcde	0.90±0.84	abcde	1.62±1.33	abcde	0.86±0.64	fgh
27	1	0	0.5	0.77±0.42	abc	1.00±0.81	abcd	1.90±1.23	abcd	1.20±0.80	defgh
28	1	0.1	0	0.70±0.46	abcd	0.90±0.84	abcde	1.67±1.30	abcde	0.86±0.62	fgh
29	1	0.1	0.1	0.65±0.48	abcde	0.92±0.82	abcde	1.65±1.36	abcde	1.13±0.92	defgh
30	1	0.1	0.5	0.77±0.42	abc	1.00±0.81	abcd	1.90±1.23	abcd	1.20±0.80	defgh
31	1	0.5	0	0.70±0.46	abcd	0.90±0.84	abcde	1.67±1.30	abcd	0.97±0.68	efgh
32	1	0.5	0.1	0.82±0.38	abc	1.20±0.75	abc	2.12±1.20	abc	1.52±0.86	abcdefg
33	**1**	**0.5**	**0.5**	**0.92±0.26**	**a**	**1.45±0.74**	**ab**	**2.50±1.08**	**ab**	**1.97±0.77**	**ab**
34	1	1	0	0.82±0.38	abc	1.25±0.77	abc	2.05±1.21	abc	1.62±0.90	abcde
35	**1**	**1**	**0.1**	**0.92±0.26**	**a**	**1.45±0.74**	**ab**	**2.50±1.08**	**ab**	**1.97±0.77**	**ab**
36	**1**	**1**	**0.5**	**0.92±0.26**	**a**	**1.55±0.74**	**a**	**2.65±1.14**	**a**	**2.09±0.79**	**a**
37	2	0	0	0.80±0.40	abc	1.20±0.82	abc	1.97±1.25	abc	1.33±0.84	bcdefg
38	2	0	0.1	0.75±0.43	abcd	1.10±0.81	abcd	1.90±1.33	abcd	1.26±0.88	cdefg
39	2	0	0.5	0.87±0.33	ab	1.27±0.71	abc	2.22±1.16	abc	1.54±0.77	abcdef
40	2	0.1	0	0.80±0.40	abc	1.25±0.83	abc	2.07±1.24	abc	1.48±0.88	abcdefg
41	2	0.1	0.1	0.87±0.33	ab	1.30±0.72	abc	2.37±1.14	abc	1.69±0.81	abcd
42	2	0.1	0.5	0.80±0.40	abc	1.15±0.76	abcd	2.02±1.27	abc	1.41±0.87	abcdefg
43	2	0.5	0	0.77±0.42	abc	1.20±0.85	abc	2.00±1.32	abc	1.44±0.97	abcdefg
44	2	0.5	0.1	0.80±0.40	abc	1.15±0.76	abcd	2.07±1.20	abc	1.54±0.88	abcdef
45	2	0.5	0.5	0.85±0.36	ab	1.25±0.74	abc	2.20±1.15	abc	1.16±0.87	abcd
46	2	1	0	0.82±0.38	abc	1.30±0.82	abc	2.15±1.25	abc	1.64±0.94	abcd
47	2	1	0.1	0.75±0.43	abcd	1.20±0.85	abc	2.00±1.33	abc	1.51±1.01	abcdefg
48	2	1	0.5	0.77±0.42	abc	1.20±0.85	abc	2.17±1.33	abc	1.49±0.98	abcdefg

*Different lowercase letters indicate significant differences between treatments

TABLE 3
Effect of GD medium with BA, TDZ and IAA on multiple shoot proliferation and regeneration from internode explants of downy oak

GD	Plant Growth Reg. (mg/L)			Explant Response (%)	No of shoots per explant after 4wk			No of shoots per explant after 8wk		Shoot length (cm)	
	BAP	TDZ	IAA								
1	0	0	0	0.0±0.0	f*	0.0±0.0	g	0.0±0.0	g	0.0±0.0	h
2	0	0	0.1	0.0±0.0	f	0.0±0.0	g	0.0±0.0	g	0.0±0.0	h
3	0	0	0.5	0.0±0.0	f	0.0±0.0	g	0.0±0.0	g	0.0±0.0	h
4	0	0.1	0	0.05±0.22	ef	0.02±0.16	fg	0.05±0.22	g	0.01 ±0.66	h
5	0	0.1	0.1	0.10±0.30	def	0.05±0.22	efg	0.12±0.40	g	0.04±0.13	h
6	0	0.1	0.5	0.10±0.30	def	0.05±0.22	efg	0.10±0.30	g	0.03±0.10	h
7	0	0.5	0	0.15±0.36	cdef	0.15±0.36	defg	0.20±0.51	fg	0.07±0.51	h
8	0	0.5	0.1	0.20±0.40	bcdef	0.20±0.40	cdefg	0.25±0.54	efg	0.11±0.24	h
9	0	0.5	0.5	0.17±0.38	bcdef	0.20±0.46	cdefg	0.30±0.72	efg	0.17±0.42	h
10	0	1	0	0.35±0.48	abcdef	0.27±0.55	bcdefg	0.67±0.99	abcdefg	0.35±0.49	defgh
11	0	1	0.1	0.25±0.43	bcdef	0.37±0.70	abcdefg	0.50±0.98	bcdefg	0.27±0.47	fgh
12	0	1	0.5	0.35±0.48	abcdef	0.47±0.71	abcdefg	0.70±1.04	abcdefg	0.52±0.75	abcdefgh
13	0.5	0	0	0.30±0.46	abcdef	0.20±040	cdefg	0.35±0.57	defg	0.15±0.25	h
14	0.5	0	0.1	0.25±0.43	bcdef	0.35±0.66	abcdefg	0.45±0.90	cdefg	0.25±0.48	gh
15	0.5	0	0.5	0.35±0.48	abcdef	0.30±0.60	bcdefg	0.52±0.84	bcdefg	0.34±0.50	efg
16	0.5	0.1	0	0.30±0.46	abcdef	0.42±0.71	abcdefg	0.77±1.25	abcdefg	0.37±0.59	cdefg
17	0.5	0.1	0.1	0.40±0.49	abcdef	0.57±0.78	abcdefg	1.05±1.41	abcdefg	0.73±0.95	abcdefgh
18	0.5	0.1	0.5	0.37±0.49	abcdef	0.60±0.87	abcdef	0.85±1.23	abcdefg	0.48±0.66	abcdefgh
19	0.5	0.5	0	0.40±0.49	abcdef	0.25±0.58	bcdefg	0.82±1.12	abcdefg	0.43±0.55	cdefgh
20	0.5	0.5	0.1	0.42±0.50	abcde	0.62±0.80	abcde	1.07±1.38	abcdefg	0.79±0.96	abcdefgh
21	0.5	0.5	0.5	0.42±0.50	abcde	0.37±0.66	abcdefg	0.97±1.27	abcdefg	0.46±0.55	bcdefgh
22	0.5	1	0	0.37±0.49	abcdef	0.20±0.51	cdefg	0.77±1.12	abcdefg	0.66±0.91	abcdefgh
23	0.5	1	0.1	0.45±0.50	abcde	0.27±0.55	bcdefg	0.85±1.00	abcdefg	0.85±1.01	abcdefg
24	0.5	1	0.5	0.42±0.50	abcde	0.25±0.54	bcdefg	0.75±0.95	abcdefg	0.73±0.91	abcdefgh
25	1	0	0	0.45±0.50	abcde	0.47±0.67	abcdefg	0.92±1.09	abcdefg	0.48±0.55	abcdefgh
26	1	0	0.1	0.40±0.49	abcdef	0.42±0.63	abcdefg	0.85±1.14	abcdefg	0.46±0.60	abcdefgh
27	1	0	0.5	0.42±0.50	abcde	0.40±0.59	abcdefg	0.95±1.19	abcdefg	0.57±0.75	abcdefgh
28	1	0.1	0	0.45±0.50	abcde	0.47±0.67	abcdefg	0.95±1.15	abcdefg	0.49±0.57	abcdefgh
29	1	0.1	0.1	0.30±0.46	abcdef	0.32±0.52	abcdefg	0.70±1.13	abcdefg	0.45±0.72	bcdefgh
30	1	0.1	0.5	0.50±0.50	abcd	0.52±0.67	abcdefg	1.07±1.14	abcdefg	0.69±0.77	abcdefgh
31	1	0.5	0	0.40±0.49	abcdef	0.60±0.84	abcdef	1.02±1.32	abcdefg	0.56±0.71	abcdefgh
32	**1**	**0.5**	**0.1**	**0.67±0.47**	**a**	**0.90±0.74**	**a**	**1.60±1.21**	**a**	**1.10±0.84**	**a**
33	1	0.5	0.5	0.52±0.50	abc	0.77±0.86	abc	1.40±1.42	abc	1.01±1.02	abc
34	1	1	0	0.52±0.50	abc	0.75±0.80	abc	1.30±1.30	abcd	0.86±0.89	abcdefg
35	1	1	0.1	0.50±0.50	abcd	0.47±0.64	abcdefg	1.20±1.30	abcde	0.89±0.94	abcdefg
36	**1**	**1**	**0.5**	**0.57±0.50**	**ab**	0.67±0.82	abcd	**1.45±1.33**	**ab**	**1.08±0.98**	**ab**
37	2	0	0	0.50±0.50	abcd	0.37±0.62	abcdefg	1.07±1.18	abcdefg	0.75±0.81	abcdefgh
38	2	0	0.1	0.42±0.50	abcde	0.37±0.62	abcdefg	0.95±1.21	abcdefg	0.62±0.76	abcdefgh
39	**2**	**0**	**0.5**	**0.57±0.50**	**ab**	**0.82±0.81**	**ab**	**1.45±1.37**	**ab**	0.88±0.80	abcdefgh
40	2	0.1	0	0.47±0.50	abcd	0.55±0.74	abcdefg	1.17±1.33	abcdefg	0.81±0.91	abcdefgh
41	2	0.1	0.1	0.52±0.50	abc	0.77±0.83	abc	1.47±1.48	ab	0.98±1.01	abcd
42	2	0.1	0.5	0.50±0.50	abcd	0.55±0.74	abcdefg	1.10±1.17	abcdefg	0.76±0.81	abcdefgh
43	2	0.5	0	0.47±0.50	abcd	0.55±0.84	abcdefg	1.17±1.39	abcdef	0.69±0.77	abcdefgh
44	2	0.5	0.1	0.47±0.50	abcd	0.57±0.67	abcdefg	1.12±1.26	abcdef	0.82±0.91	abcdefgh
45	2	0.5	0.5	0.50±0.50	abcd	0.62±0.70	abcde	1.17±1.25	abcdef	0.90±0.94	abcdef
46	2	1	0	0.52±0.50	abc	0.60±0.77	abcdef	1.17±1.27	abcdef	0.91±0.95	abcde
47	2	1	0.1	0.45±0.50	abcde	0.50±0.84	abcdefg	1.10±1.37	abcdefg	0.80±0.92	abcdefgh
48	2	1	0.5	0.42±0.50	abcde	0.55±0.78	abcdefg	1.10±1.35	abcdefg	0.80±0.98	abcdefgh

*Different lowercase letters indicate significant differences between treatments

Shoot elongation. At the end of 8 wk, the length of the shoots was measured. The longest shoot length was observed as 2.94±1.39 in WPM medium with 2 mg/L BA+0.1 mg/L TDZ+0.5 mg/L IAA, as 2.93±1.38 in 2 mg/L BA+1 mg/L TDZ+0.1 mg/L IAA containing medium, and 2.89±1.39 ($P<0.05$) in 2 mg/L BA+1 mg/L TDZ+0.5 mg/L IAA containing medium (Table 1, 2 and 3). Statistically, these three PGR combinations did not differ from each other. The average lengths of the shoots were about 4 cm. The shoot length was to be 2.55 ± 0.82 in the medium with 1 mg/L BA + 1 mg/L TDZ + 0.5 mg/L IAA which gives the best results statistically for the explant response and number of shoots. Although this result is statistically in the same group, its average is lower than the others. The use of BA and TDZ in PGR combinations with higher doses than IAA affected shoot formation and length positively. Indeed, the presence of IAA in combination provided cytokinins to form the plantlet directly without callus formation; a similar result was obtained by Vieitez et al. [8] testing different doses of IBA in *Q. rubra*. Prior to rooting stage, culturing of the shoots in the WPM medium containing 0.1 mg/L BA and 0.1 mg/L GA_3 for 4 wk also helped to increase the shoot length.

Similarly, GA_3 found in the medium has an effect of increasing shoot length in *Q. leucotrichophora* and *Q. glauca* [41].

Effect of subculture. The number of shoots was higher after 8 wk than the initial stage (Table 1, 2 and 3). The shoots taken in fresh medium with subcultures were beneficial both in terms of increase in number of axillaries shoots and increase in shoot length [30, 31]. The results obtained in this study are better than the other studies related to *Quercus* sp. micropropagation. San-Jose et al. [42] reported that the subculture in *Q. robur* physiologically halts the development of explants *in vitro* propagation, but increases *Q. petraea* exactly [27]. In *Castanea sativa* Mill.'s *in vitro* propagation, subculture on a monthly basis is absolutely necessary for shoot propagation and elongation [37, 43, 44]. In the study conducted in *Prosipsis cineraria*, it was found that transfer of plants to fresh medium was inhibiting the defoliation on shoots [45]. In addition to this important benefit of subculture in *in vitro* micropropagation studies, it was utilized in order to prevent inhibitory effect of phenolic substance secretion on growth, encountered in *in vitro* propagation of the plants in Fagaceae family (*Quercus* sp., *Fagus* sp., *Castanea* sp. etc.) [15, 16, 21, 46, 47, 48].

TABLE 4
Effect of IAA, NAA and IBA on rooting response of in vitro regenerated shoots from internode explants of downy oak

Plant Growth Reg.(mg/L)		Response (%)		No of roots/shoots		Shoot length (cm)	
	0	0.15±0.36	b*	0.12±0.31	b	0.08±0.21	c
	0.5	0.40±0.50	ab	0.63±0.83	ab	0.48±0.61	bc
IAA	1	**0.65±0.48**	**a**	**1.19±0.98**	**a**	**1.73±1.46**	**a**
	2	0.50±0.51	ab	**0.99±1.07**	**a**	1.41±1.52	ab
	3	0.45±0.51	ab	0.78±0.93	ab	1.06±1.23	abc
	0	0.05±0.22	b	0.025±0.11	b	0.25±0.11	c
	0.5	0.35±0.48	ab	0.69±1.10	ab	0.41±0.58	bc
NAA	1	**0.55±0.51**	**a**	**0.99±1.09**	**a**	0.90±0.88	ab
	2	**0.55±0.51**	**a**	**1.14±1.21**	**a**	**1.47±1.43**	**a**
	3	**0.55±0.51**	**a**	**0.89±0.89**	**a**	**1.31±1.31**	**a**
	0	0.10±0.30	c	0.07±0.24	c	0.05±0.15	d
	0.5	0.55±0.51	b	0.99±1.09	b	0.87±0.87	cd
IBA	1	**0.95±0.22**	**a**	**2.06±0.84**	**a**	**3.41±1.38**	**a**
	2	0.75±0.44	ab	1.41±0.94	ab	2.42±1.72	ab
	3	0.65±0.48	ab	1.08±0.88	b	1.80±1.47	bc

*Different lowercase letters indicate significant differences between treatments

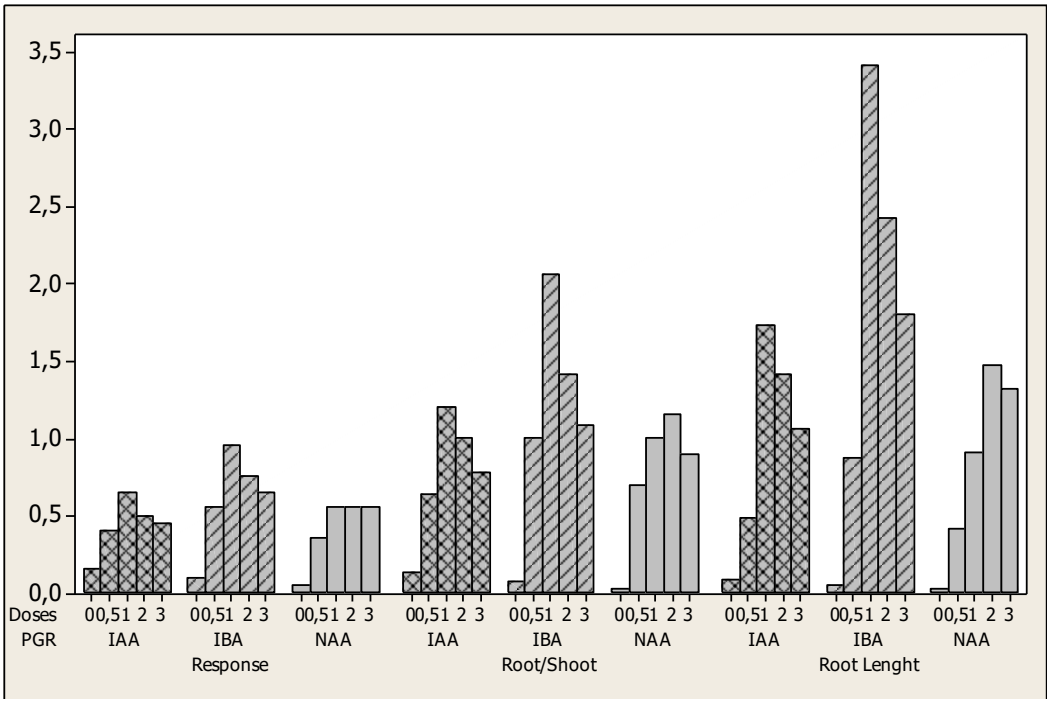

FIGURE 3
The mean values of explant response, number of root/shoots per explant and root length.

Effect of basal media. In this study of culturing internode explants, WPM, MS and GD media were used in combination with different dosages of BA, TDZ and IAA. Among these three media containing different salt formulations, WPM gave the best results (Table 1, 2 and 3). Although some data in the MS medium are close to that of the WPM medium, the WPM is statistically more significant. The GD medium is not as effective as WPM and MS for *Q. pubescens*. The half-strength use of macronutrients in WPM and MS media was successful in inducing shoot induction in some *Quercus* species [22]. Manzenera and Pardos [12] reported that Sommer's and Heller's media are suitable for growth and proliferation in *Q. suber* due to their high salt concentrations. They reported that MS medium gave the worst results in terms of explant response and shoot elongation. Vieitez et al. [24] and Vieitez et al. [49] reported that the GD medium provided better outcomes for *Q. robur* and *Q. petraea* than other media, since the GD medium was able to produce healthy shoots. On the other hand, it was reported that the WPM medium is inevitable for *Quercus* sp. in *in vitro* propagation studies [11, 22, 41, 50].

Rooting of in vitro shoots. After the initial stage, shoots with approximately 3 cm length were transferred to WPM containing 0.1 mg/L BA and 0.1 mg/L GA_3 for their development and maturation. Transfer of the explants from the medium containing high dose of cytokinin during 8 wk to lower dose helps the explants develop without callus formation. Due to the promoting feature of the gibberellins during the development stage, GA_3included in the medium ensures that young shoots form healthy stems and roots before the rooting stage [51, 52].

Shoots reaching at least 2 cm in length for rooting were cultured in WPM medium with doses of 0, 0.5, 1, 2 and 3 mg/L of IBA, IAA and NAA. In the shoots that were subcultured after 4 wk, at the end of subculture II, stem formation was 95% in the medium containing 1 mg/L IBA. Selection of the most suitable PGR in the auxin group and incubation at dark resulted in this high ratio as also reported by Sanchez et al. [10], Rugini et al. [53], George and Debergh [31], and Hutchinson et al. [54]. In this study, the shoot length was 3.41 ± 1.38 ($P<0.05$) while the root/shoot ratio was 2.06 ± 0.84 ($P<0.05$) (Table 4). Among the IBA IAA and NAA used in the rooting stage, it was clear that IBA gave the best result for *Q.pubescens* (Figure 3). Ostrolucka and Bezo [9] reported that in *Q. rubra*, low doses of IBA and NAA brought about rooting at 90% ratio.

Acclimatization. The rooted plants were planted in plastic pots containing a mixture of sterilized garden soil, sand and perlite for acclimatization purposes. 55% of these plants survived (Figure 1c).

This study is the first successful report of *in vitro* propagation of downy oak via internodes. It is an important protocol that can be used for breeding and reproduction purposes. In the initial stage, the triple combination of auxin and cytokinins gave very successful results in both shoot formation and growth as well as also in callus formation, by adding 2 mg/L BA + 0.1 mg/L TDZ + 0.5 mg/L IAA to the WPM medium. The different results obtained in the amount of shoot formation in *Quercus* species depending on the difference in PGR types [22, 28, 41, 50] and genotypes [24, 49]. During the rooting stage, the healthiest rooting of the shoots were observed in the WPM medium containing 1 mg/L IBA, and 55% of the plantlets were acclimatized. This revealed that the internode is a good explant source that can be used for *in vitro* propagation.

ACKNOWLEDGEMENTS

This study was supported by Ankara University Institute of Biotechnology (project number G-7). I would like to thank Dr.Haydar KOÇ (Çankırı Karatekin University, Science Faculty and Department of Statistics) for valuable assistance in the statistical analyzes.

There is no conflict of interest. All experiments were performed by MS. The manuscript was written by MS.

REFERENCES

[1] Campbell, M.M., Brunner, A.M., Cones, H.M. and Strauss, S.H. (2003) Forestry's fertile crescent: the application of biotechnology to forest trees. Plant Biotech. 1, 141-154.

[2] FAO (2017) State of the World's Forests 2017. www.fao.org/forestry/sfm/en/.

[3] Özyurt, B. (1998) Orman, çevre ve halk. In: Hızlı gelişen türlerde yapılan ağaçlandırma çalışmalarının değerlendirmesi ve yapılacak çalışmalar. Workshop 8-9 December 1998, Ankara, Turkey. 28-36.

[4] Şimşek, Y. (1993) Orman ağaçları ıslahına giriş. Ormancılık Araştırma Enstitüsü Yayınları, Ankara, Türkiye. Yayın No: 65.

[5] Anşin, R. and Özkan, C. (2006) Tohumlu Bitkiler (Spermatophyta) Odunsu Taksonlar. Trabzon, Türkiye. K.T.Ü Orman Fak.Yay. 167.

[6] Aydınözü, D., Çoban, A. and Tunç, H. (2017) Tüylü meşe'nin (Quercus pubescens) Türkiye'de yeni bir yayılış alanı: Elmalı Dağı (Kayseri). Doğu Coğ. Der. 22(37), 83-98.

[7] Sezgin, M. and Dumanoğlu, H. (2009) Fagaceae familyasinda in vitro tekniklerin kullanımı ve son gelişmeler. Süleyman Demirel Ün. Orman Fak. Derg. 1(2), 147-159.

[8] Vieitez, A.M., Ferro, E.M. and Ballester, A. (1993) Micropropagation of Fagus sylvatica L. In Vitro Cell. and Dev. Biol. 29,183-188.

[9] Ostrolucka, M.G. and Bezo, M. (1994) Utilization of meristem cultures in propagation of oak (Quercus sp.). Genet. Polonica. 353, 161–169.
[10] Sanchez, M.C., San-Jose, M.C., Ballester, A. and Vieitez, A.M. (1996) Requirements for in vitro rooting of Quercus robur and Q. rubra shoots derived from mature trees. Tree Physiol. 16, 673–680.
[11] Vangadesan, G. and Pijut, P.M. (2009) In vitro propagation of northern red oak (Quercus rubra L.). In Vitro Cell. Dev. Biol.-Plant. 45, 474–482.
[12] Manzanera, J.A. and Pardos, J.A. (1990) Micropropagation of juvenile and adult Quercus suber L. Plant Cell Tiss. Org. Cult. 21, 1–8.
[13] Bueno, M.A., Astorga, R. and Manzanera, J.A. (1992) Plant regeneration through somatic embryogenesis in *Quercus suber*. Physiologia Plantarum. 85, 30-34.
[14] Romano, A. and Louçao, M.A.M. (1999) In vitro cold storage of cork oak shoot cultures. Plant Cell Tissue and Organ Culture. 59, 155-157.
[15] Mala, J.K., Cvrckova, H., Cvikrova, M. and Eder, J. (2000) The effect of reduction of exuded phenolic substances level on rooting of oak microcuttings. Acta Hort. 530, 353-360.
[16] Racchi, M.L., Bagnoli, F., Balla, I. and Danti, S. (2001) Differential activity of catalase and superoxide dismutase in seedlings and in vitro micropropagated oak (Quercus robur L.). Plant Cell Rep. 20, 169-174.
[17] Bellarosa, R. (1988) In vitro propagation of oaks (Q.suber, Q.pubescens, Q.cerris). Acta Hortic. 227, 433-435.
[18] Lloyd, G. and McCown, B. (1981) Commercially feasible micropropagation of mountain laurel, Kalmia latifolia by use of shoot-tip culture. Proc. Int. Plant Prop. Soc. 30, 421–437.
[19] Murashige, T. and Skoog, F. (1962) A revised medium for rapid growth and bioassays with tobacco tissue cultures. Physiol. Plant. 15, 473–497.
[20] Gresshoff, P.M. and Doy, C.H. (1972) Development and differentiation of haploid Lycopersicon esculentum (Tomato). Planta. 107, 161–170.
[21] Meier, K. and Reuther, G. (1994) Factors controlling micropropagation of mature Fagus sylvatica. Plant Cell Tis. Org. Cult. 39, 231-238.
[22] Ostrolucka, M.G., Gajdosova, A. and Libiakova, G. (2007) Protocol for micropropagation of Quercus spp. In: Jain, M.S., Haggman, H. (eds.) Protocols for micropropagation of woody trees and fruits. Springer, Dordrecht, The Netherlands, 85-93.
[23] SPSS. (2017) IBM SPSS Statistics Package Programe 22.0.
[24] Vieitez, A.M., San-Jose, M.C. and Vieitez, E. (1985) In vitro plantlet regeneration from juvenile and mature Quercus robur L. J. Hort. Sci. 601, 99–106.
[25] Favre, J.M. and Juncker, B. (1987) In vitro growth of buds taken from seedlings and adult plant material in Quercus robur L.. Plant Cell Tiss. Org. Cult. 8, 49–60.
[26] Butova, G.P. and Skrobova, L.L. (1989) Morphogenesis and regeneration of pedunculate oak plants in culture in vitro. Fiziologia Rastenii. 35(5), 1023-1030.
[27] San-Jose, M.C., Vieitez, A.M. and Ballester, A. (1990) Clonal propagation of juvenile and adult trees of sessile oak by tissue culture techniques. Silvae Genet. 392, 50–55.
[28] Chalupa, V. (1993) Vegetative propagation of oak (Quercus robur and Q.petraea) by cutting and tissue culture. Ann. Sci. For. 501, 295–307.
[29] Meier-Dinkel, A., Becker, B. and Duckstein, D. (1993) Micropropagation and ex vitro rooting of several clones of late-flushing Quercus robur L.. Ann. Sci. For. 50(S1), 319–322.
[30] Mansuroğlu, S. and Gürel, E. (2002) Mikroçoğaltım. In: Babaoğlu, M., Gürel, E. and Özcan, S. (eds.) Bitki Biyoteknolojisi I. Selçuk Üniv. Vakfı Yayınları, Konya, Turkey, 262-281.
[31] George, E.F. and Debergh, P.C. (2008) Micropropagation: uses and methods. In: George, F.E., Hall, M.A. and Jan De Klerk, G. (eds.) Plant propagation by tissue culture 3rd edition. Springer, Dordrecht, The Netherlands, 29-65.
[32] Juncker, B. and Favre, J.M. (1994) Long-term effects of culture establishment from shoot-tip explants in micropropagating oak (Quercus robur L.). Ann. Sci. For. 51, 581–588.
[33] Puddephat, I.J., Alderson, P.G. and Wright, N.A. (1997) Influence of explant source, plant growth regulators and culture environment on culture initiation and establishment of Quercus robur L. in vitro. Journal of Experimental Botany. 48, 951–962.
[34] Van Staden, J., Zazimalova, E. and George, E.F. (2008) Plant growth regulators II: Cytokinins, their analogues and antagonists. In: George, F.E., Hall, M.A. and Jan De Klerk, G. (eds.) Plant propa-gation by tissue culture 3rd edition. Springer, Dordrecht, The Netherlands, 205-227.
[35] Singh, C.K., Raj, S.R., Jaiswal, P.S., Patil, V.R., Punwar, B.S., Chavda, J.C. and Subhash, N. (2016) Effect of plant growth regulators on in vitro plant regeneration of sandalwood (Santalum album L.) via organogenesis. Agroforest Syst. 90, 281–288.
[36] Kim, M.S., Schumann, C.M. and Klopfenstein, N.B. (1997) Effect of thidiazuron and benzyladenine on axillary shoot proliferation of three green ash (Fraxinus pennsylvanica Marsh.) clones. Plant Cell Tiss. Org. Cult. 48, 45–52.

[37] San-Jose, M.C., Ballester, A. and Vieitez, A.M. (2001) Effect of thidiazuron on multiple shoot induction and plant regeneration from cotyledonary nodes of chestnut. J. Hort. Sci. and Bio. 76(5), 588-595.
[38] Brassard, N., Richer, C., Tousignant, D. and Rioux, J.A. (2013) Multiplication vegetative de l'Acer saccharum. Can. J. For. Res. 33, 682–690.
[39] Cappelletti, R., Sabbadini, S. and Mezzetti, B. (2016) The use of TDZ for the efficient in vitro regeneration andorganogenesis of strawberry and blueberry cultivars. Scientia Horticulturae. 207, 117-124.
[40] Fei, Y., Xiao, B., Yang, M., Ding, Q. and Tang, W. (2016) MicroRNAs, polyamines, and the activities antioxidant enzymes are associated with in vitro rooting in white pine (*Pinus strobus* L.). SpringerPlus. 5(416), 2-11.
[41] Purohit, V.K., Tamta, S., Chandra, S., Vyas, P., Palni, L.M.S. and Nandi, S.K. (2002) In vitro multiplication of Quercus leucotrichophora and Q. glauca: important Himalayan oaks. Plant Cell Tiss. Org. Cult. 69, 121–133.
[42] San-Jose, M.C., Ballester, A. and Vieitez, A.M. (1988) Factors affecting in vitro propagation of Quercus robur L. Tree Physiol. 4, 281–290.
[43] Vieitez, A.M., Vieitez, M.L. and Vieitez, E. (1986) Chestnut (Castanea spp.). In: Bajaj, Y.P.S. (ed.) Biotechnology in agriculture and forestry. Vol. 1: Trees I. Springer-Verlag, Berlin, Heidelberg, 393-414.
[44] Sanchez, M.C., San-Jose, M.C., Ferro, E., Ballester, A. and Vieitez, A.M. (1997) Impro-ving micropropagation conditions for adult-phase shoots of chestnut. J. Hort. Sci. 72(3), 433-443.
[45] Shekhawat, N.S., Rathore, T.S., Singh, R.P., Deora, N.S. and Rao, S.R. (1993) Factors affecting in vitro clonal propagation of Prosopis cineraria. Plant Growth Reg. 12, 273–280.
[46] Barker, J.B., Pijut, P.M., Ostry, M.E. and Houston, D.R. (1997) Micropropagation of juvenile and mature american beech. Plant Cell, Tissue and Organ Culture. 51, 209-213.
[47] Ballester, A., San-Jose, M.C., Vidal, N., Fernandez-Lorenzo, J.L. and Vieitez, A.M. (1999) Anatomical and biochemical events during in vitro rooting of microcuttings from juvenile and mature phases of chestnut. Annals of Botany. 83, 619-629.
[48] Cuenca, B., Ballester, A. and Vieitez, A.M. (2000) In vitro adventitious bud regeneration from internode segments of beech. Plant Cell Tiss. Org. Cult. 60, 213-220.
[49] Vieitez, A.M., Sanchez, M.C., Amo-Marco, J.B. and Ballester, A. (1994) Forced flushing of branch segments as a method for obtaining reactive explants of mature Quercus robur trees for micropropagation. Plant Cell Tiss.Org. Cult. 37, 287–295.
[50] Chalupa, V. (1984) In vitro propagation of oak (Quercus robur L.) and linden (Tilia cordata Mill.). Biol. Plant. 265, 374–377.
[51] Moshkov, I.E., Novikova, G.V., Hall, M.A. and George, F.E. (2008) Plant growth regulators III: gibberellins, ethylene, absisic acid, their analogues and inhibitors; miscellaneous compounds. In: George, F.E., Hall, M.A. and Jan De Klerk, G. (eds.) Plant propagation by tissue culture 3rd edition. Springer, Dordrecht, The Netherlands, 227-283.
[52] Sezgin, M. and Dumanoğlu, H. (2016) In vitro propagation potential via somatic embryogenesis of the two maturing early cultivars of European chestnut (Castanea sativa Mill.). American J. Plant Sci. 7,1001-1012.
[53] Rugini, E., Bazzoffia, A. and Jacoboni, A. (1988) A simple in vitro method to avoid the initial dark period and to increase rooting in fruit trees. Act. Hort. 227, 438–440.
[54] Hutchinson, M.J., Onamu, R., Kipkosgei, L. and Obukosia, S.D. (2014) Effect of Thidiazuron, NAA and BAP on in vitro propagation of Alstroemeria aurantiaca cv. 'rosita' from shoot tip explants. J. of Agric. Sci. Tech. 16(2), 58-71.

Received: **02.04.2018**
Accepted: **28.04.2018**

CORRESPONDING AUTHOR

Mehmet Sezgin
Science Faculty,
Biology Department,
Çankırı Karatekin University,
Çankırı – Turkey

e-mail: sezgin@karatekin.edu.tr

© by PSP Volume 27 – No. 7/2018 pages 5173-5178 Fresenius Environmental Bulletin

DIET OF SAND SMELT, *ATHERINA BOYERI* (RISSO, 1810) DURING THE REPRODUCTIVE PERIOD IN KARACAOREN DAM LAKE (TURKEY)

Zehra Arzu Becer[1,*], Meral Apaydin-Yagci[2], Abdulkadir Yagci[2], Ahmet Alp[3]

[1]Akdeniz University, Fisheries Faculty, Dumlupinar Bulvari Campus/Antalya, Turkey
[2]Fisheries Research Institute, Republic of Turkey Ministry of Food, Agriculture and Livestock, 32500, Egirdir, Isparta, Turkey
[3]Department of Fisheries, Faculty of Agriculture, Kahramanmaras Sutcu Imam University, Kahramanmaras, Turkey

ABSTRACT

We studied a variation in food consumption and the composition of the stomach contents of sand smelt, *Atherina boyeri* during the reproductive period from December 2009 to April 2010 in Karacaoren Dam Lake in Turkey. In this study, differences in feeding related to size and sex were examined. The diet composition of *A. boyeri* in Karacaoren Dam Lake includes 20 types of prey items. 12806 individual preys were counted from 190 *A. boyeri* examined. The main prey taxa in the diet of females and males of *A. boyeri* were Cladocera, Rotifera, Copepoda, and Odonata respectively. The main prey taxa in the diet of *A. boyeri* were Rotifera (61.82 %) Cladocera (24.40 %), Copepoda (11.79 %) and Odonata (1.14 %) respectively. *Keratella cochlearis* (61.09 %) represented the largest proportion of the diet followed by *Bosmina longirostris* (11.96 %), *Cyclops* sp (10.50%) and *Ceriodaphnia quadrangula* (9.38 %). Males (54%) had higher feeding intensity than females (46%). In Karacaoren Dam Lake, *A. boyeri* fed as the frequency of occurrence mainly on *Bosmina longirostris* (47.89%), Cyclops sp. (41.57%) and *Keratella cochlearis* (38.42 %). The fact that the species diversity for diet showed a homogeneous distribution in 5.0- 5.4/ 5.5- 5.9 and 6.0- 6.4 length classes. Schoeners's Overlap index values, there was a high degree of consumed food between 5.0- 5.4/ 6.0- 6.4 (C_{xy}=0.86), 5.5- 5.9/ 5.5- 5.9 (C_{xy} =0.96), 5.5- 5.9/ 6.0- 6.4 (C_{xy} = 0,82).

KEYWORDS:
Sand smelt, *Atherina boyeri*, diet, feeding, Karacaoren Dam Lake, Turkey

INTRODUCTION

The sand smelt, *Atherina boyeri* (Risso 1810) is a small, short-lived, euryhaline species that is common in coastal lagoons and estuarine waters of the Mediterranean Basin and adjacent areas, and in the northeast Atlantic [1-3]. This euryhaline species is mainly coastal and estuarine ecosystems but it was introduced into freshwater lakes and shows dense populations in these habitats [3-5]. There have been many studies regarding the feeding habits *of A. boyeri* in marine and brackish [6-10], and freshwater ecosystems [2-3, 5, 9, 11].

A population of *A. boyeri* inhabits Lake Karacaoren Dam Lake (Turkey), having been naturally introduced into this ecosystem during past centuries. *A. boyeri* has been found to feed mainly upon planktonic or benthic invertebrates and it has been characterized as a generalistand opportunistic predator [9]. The natural distribution area of the fish in Turkey is Akyatan and Tuzla Lakes (Adana), Bafa Lake (Aydin), Koycegiz Lake (Mugla), Gediz Stream (Izmir), Buyukcekmece Reservoir and Kucukcekmece Lagoon (Istanbul), Peso Lake (Edirne), Sapanca Lake (Sakarya) and some estuaries in the East Black Sea Region such as Yesilirmak (Samsun), Karadere (Kastamonu) [12-13].

These studies are important for evaluation of the ecological role of the species as well as the understanding of its position in the food web structure in the lake.

MATERIALS AND METHODS

A. boyeri was collected starting from December 2009 to April 2010 in Karacaoren Dam Lake. *A. boyeri* samples were collected using electrofishing equipments. The specimens were transported to the laboratory where total (TL) length was measured to the nearest 0,1 mm using digital caliper and weight (W) to the nearest 0,001 g using a digital balance. All the captured fish specimens were immediately preserved in a plastic barrel containing 70 % ethyl alcohol solution for later analysis. For each fish, total weight (g), fork length (mm) and sex were recorded. The differences between length and weights of females and males were tested with the "*t*" test. In addition, the differences between prey types and genders were analyzed by two-way contingency table employed and the source of variations was identified with the χ^2 test [14-16].

The Fullness Index (FI) was calculated to investigate the variations in feeding intensity, using the

equation: FI = (Weight of stomach contents/Total weight of fish)*10000 [17].

Schoner's (1970) similarity index was calculated as:

Cxy = 1 - 0.5 ∑ |pxi-pyi|; where pxi and pyi are the proportions by number of prey type i in the diets of groups (length or sex (female-male)) x and y, respectively. Overlap index ranging from 0 (no overlap) to 1 (complete overlap). If the C value is bigger than 0.80, it means that the diet of the 2 groups is similar [3,18-19].

The Margalef species richness (d) and Shannon's Diversity (H`) were used to evaluate species composition within and between fish size groups. Margalef species richness was calculated as:

d= (*S*- 1)/(*Log N*) ; where S is the number of species and N is the number of specimens. Shannon's diversity was calculated as:

$$H`=-\sum_{i=1}^{i=S}(Pi * Log_e Pi)$$; where P is the ratio of species *i* [20].

The use of the Shannon-Wiener index provides an objective indication of niche breadth [21]. Low values indicate diets with few prey items (specialist predators) and high values indicate generalist diets.

RESULTS AND DISCUSSION

Sand smelt, *Atherina boyeri* (Risso, 1810) enters rivers, lakes, ponds, canals, and reservoirs by coincidence but become dominant in these habitats because of its biological features. It abundantly and unintentionally reproduces in natural environments and, as an invasive species, competes with native fish for food, dissolved oxygen, and space. [22].

Feeding Intensity. The total length of *A. boyeri* varied from 4.5 cm to 7.1 cm and W ranged from 0.633 g to 2.404 g. For females, TL and W varied between 4.5 cm and 7.1 cm (5.46± 0.45) and 0.73 g to 2.404 g (1.19±0.31) respectively, whereas for males it ranged from 4.9 cm to 6.4 cm (5.57± 0.35) and 0.633g to 1.747 g (1.14± 0.23) respectively. The lengths and weights of the females and males were not different, statistically (t= 1.835, df= 188; p= 0.068 for lengths and t= 1.456, df= 188; p= 0.147 for weights).

The stomach content of *A. boyeri* in Karacaoren Dam Lake includes 20 types of prey items. 12806 individual preys were counted from 190 *A. boyeri* examined. Only 14 specimens (8 females and 6 males) had empty stomachs (Fig. 1). *A. boyeri* between 4.5-4.9 cm and 6.0- 7.4 cm fed most intensively, while feeding intensity decline 5.0- 5.9 cm length groups.

Diet Composition. The main prey taxa in the diet of *A. boyeri* were Cladocera, Rotifera and Copepoda respectively (Table 1). *Keratella cochlearis* (N= 61.09 %) were important in the diet of females and males of *A. boyeri*, followed by *Bosmina longirostris* (N= 11.96 %), *Cyclops sp.* (N= 10.50 %) and *Ceriodaphnia quadrangularis* (N= 9,38 %).

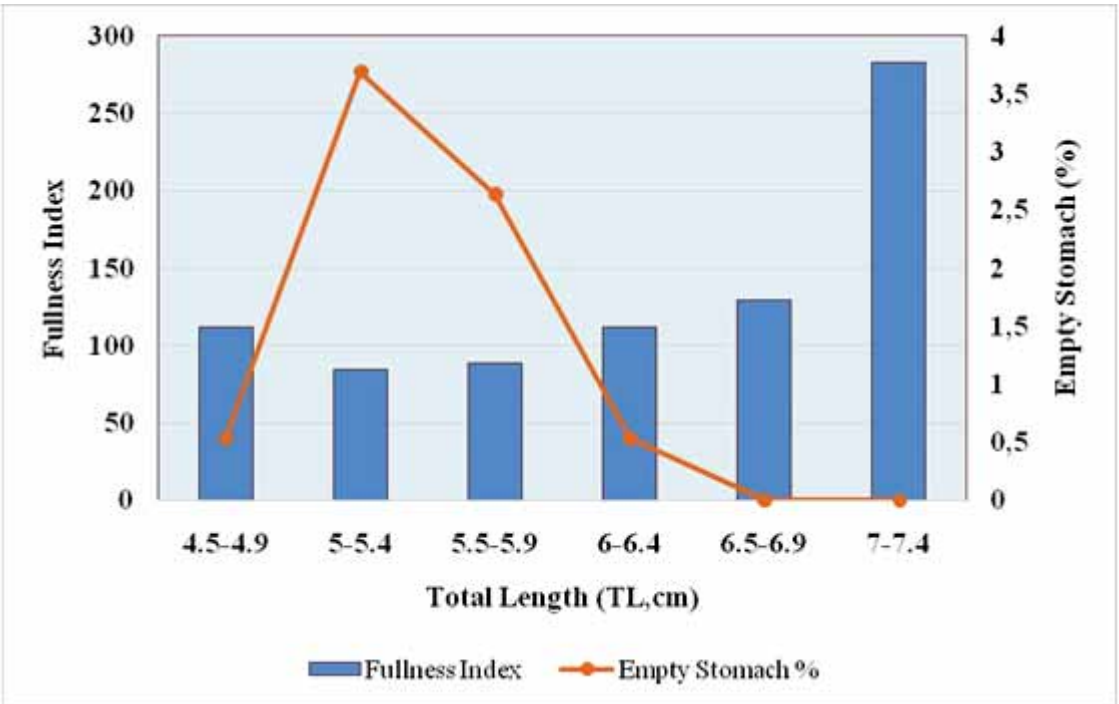

FIGURE 1
Fullness index and empty stomach of *A. boyeri* in different length classes

TABLE 1
***A. boyeri* diet in Karacaoren Dam Lake: prey number (N), frequency of occurrence (FO), female (F), male (M)**

ORGANISMS	F+M				F				M			
	FO	FO %	N	N %	FO	FO %	N	N %	FO	FO %	N	N %
ROTIFERA	**62**	**32.6316**	**7917**	**61.8226**	**34**	**17.8947**	**3929**	**30.6809**	**43**	**22.6316**	**3993**	**31.1807**
Keratella cochlearis	73	38.42105	7824	61.09636	30	15.78947	3870	30.22021	43	22.63158	3959	30.9152
Trichocerca similis	20	10.52632	51	0.398251	10	5.263158	33	0.257692	10	5.263158	18	0.140559
Lecane luna	3	1.578947	3	0.023427	2	1.052632	2	0.015618	1	0.526316	1	0.007809
Unidentified rotifera	12	6.315789	39	0.304545	4	2.105263	24	0.187412	8	4.210526	15	0.117133
CLADOCERA	**99**	**52.1053**	**3125**	**24.4026**	**48**	**25.2632**	**1124**	**8,77714**	**79**	**41,5789**	**2000**	**15,6177**
Daphnia longispina	38	20	109	0.851164	14	7.368421	29	0.226456	24	12.63158	80	0.624707
Bosmina longirostris	91	47.89474	1532	11.96314	39	20.52632	625	4.880525	52	27.36842	907	7.082618
Ceriodaphnia quadrangula	71	37.36842	1202	9.386225	23	12.10526	424	3.310948	48	25.26316	778	6.075277
Disparalona rostrata	17	8.947368	72	0.562236	7	3.684211	21	0.163986	10	5.263158	51	0.398251
Cydorus sphaericus	16	8.421053	23	0.179603	6	3.157895	11	0.085897	10	5.263158	12	0.093706
Alona quadrangularis	35	18.42105	170	1.327503			13	0.101515	27	14.21053	157	1.225988
Alona guttata	1	0.526316	1	0.007809	1	0.526316	1	0.007809				
Alona rectangula	1	0.526316	13	0.101515					1	0.526316	13	0.101515
Moina sp.	1	0.526316	2	0.015618					1	0.526316	2	0.015618
Leydigia leydigi	1	0.526316	1	0.007809	1	0.526316	1	0.007809				
COPEPODA	**82**	**43.1579**	**1511**	**11.7992**	**42**	**22.1053**	**653**	**5.09917**	**64**	**33.6842**	**858**	6.699984
Cyclops sp.	79	41.57895	1345	10.50289	30	15.78947	593	4.630642	49	25.78947	752	**5.87225**
Nitocra hibernica	64	33.68421	166	1.296267	26	13.68421	60	0.46853	38	20	106	0.827737
ODONATA	**38**	**20**	**146**	**1.14009**	**20**	**10.5263**	**110**	**0.85897**	**18**	**9.47368**	**36**	**0.28112**
DIPTERA	**25**	**13.1579**	**73**	**0.57005**	**13**	**6.84211**	**59**	**0.460722**	**12**	**6.315789**	**14**	**0.109324**
Chironomus larvae	25	13.15789	73	0.570045	13	6.842105	59	0.460722	12	6.315789	14	0.109324
TRICHOPTERA	**2**	**1.05263**	**5**	**0.03904**	**1**	**0.52632**	**1**	**0.00781**	**1**	**0.52632**	**4**	**0.03124**
FISH (egg. scale)	**13**	**6.84211**	**29**	**0.22646**	**4**	**2.10526**	**14**	**0.10932**	**9**	**4.73684**	**15**	**0.11713**
TOTAL			**12806**	**100**			**5891**	**46.0019**			**6915**	**53.9981**

Cladocerans were the most common prey (52.10 %) and of these *Bosmina longirostris* were the most common (FO= 47.89 %) followed by *Cyclops* sp. (FO= 41.57 %) *Keratella cochlearis* (FO= 38.42 %), *Ceriodaphnia quadrangula* (FO= 37.36 %) and *Nitocra hibernina* (FO= 33.68 %). Fish (egg, scale) represented FO= 6.84 %. The main prey taxa in the diet of *A. boyeri* were Rotifera (N= 61.82%) Cladocera (N= 24.40 %) and Copepoda (N= 11.79 %) respectively. These groups organisms; *Keratella cochlearis* (61.09 %) represented the largest proportion of the diet followed by *Bosmina longirostris* (11.96 %), *Cyclops* sp (10.50 %) and *Ceriodaphnia quadrangula* (9.38 %). The most frequency of occurrence prey in the stomach were *Bosmina longirostris* (47.89 %) *Keratella cochlearis* (38.42 %), *Cyclops* sp. (41.57 %), *Ceriodaphnia quadrangular* (37.36 %) and *Nitocra hibernica* (33.68 %), fish (eggs, scale) (6.84 %) represented (Table1). Sand smelt is known to consume fish eggs and larvae [2-3, 5]. In our study, fish (egg, scale) in the stomach was minimal in number which is the same that was found by the researches.

Feeding properties of *A. boyeri* have been studied in freshwater lakes. *A. boyeri* fed on a larger zooplankton, such as adult copepods and copepod in freshwater ecosystems [3, 11, 23]. [5] noted that *Dreissena polymorpha* and *Diaphanasoma brachyurum* were dominant prey items in Lake Trichonis. Besides, [5] reported that *Bosmina longirostris, Alona quadrangularis, Nitocra hibernica, Mesocyclops leuckarti* and *Corophium curvispinum* were dominant prey items included. In other study, [2] reported that *Atherina boyeri* consumed cladocerans, copepods and bivalvia larvae. Compared to other studies, sand smelt fed mainly on planktonic in our study.

The number of organism per stomach was higher in males (54 %) than in females (46 %) showing significant differences (χ^2= 40.94 > $\chi^2_{1,0.05}$= 3.841) (Table 2). Two-way contingency analysis indicated that prey organism consumed by females and males is significantly different. The main source of variation comes from *Alona quadrangularis, Ceriodaphnia quadrangula*, Odonata, *Keratella cochlearis*, *Chironomus larvae* and *Daphnialongispina*. *Cyclops* sp., *Chydorus sphaericus*, fish scale and Trichoptera didn't show differences between females and males.

Stomach contents in relation to fish size. *A. boyeri* total length ranged from 4.5-7.1 cm. (Table 3). Significantly higher numbers of *Bosmina longirostris* were found in the stomachs of the 4.5- 4.9 cm length groups. Odonata and Chrinomus larvae was dominant food item in the length groups of 6.0-6.9 cm. Fish eggs and scales were found in the stomach of fishes 5.0-6.4 cm in length groups.

TABLE 2
Contingency table analysis of the gender variations of 14 different prey items.

Organisms	Female	Male	Ni	χ^2
Keratella cochlearis	3870 (3603)	3954 (4221)	7824 (7824)	36.619*
Cyclops sp.	593 (619)	752 (726)	1345 (1345)	2.086
Nitocra hibernica	60 (76)	106 (90)	166 (166)	6.522*
Ceriodaphnia quadrangula	424 (554)	778 (648)	1202 (1202)	56.244*
Bosmina longirostris	625 (706)	907 (827)	1532 (1532)	17.025*
Alona quadrangularis	13 (78)	157 (92)	170 (170)	100.957*
Daphnia longispina	29 (50)	80 (59)	109 (109)	16.597*
Trichocerca similis	33 (24)	18 (28)	51 (51)	7.122*
Odonata	110 (67)	36 (79)	146 (146)	50.506*
Chironomus larvae	59 (34)	14 (39)	73 (73)	35.576*
Disparalona rostrata	21 (33)	51 (39)	72 (72)	8.319*
Chydorus sphaericus	11 (11)	12 (12)	23 (23)	0.028
Fish scale	14 (13)	15 (16)	29 (29)	0.050
Trichoptera	24 (18)	15 (21)	39 (39)	3.714
Ni	5886 (5886)	6895 (6895)	12781 (12781)	
χ^2	184.064*	157.305*		341.369*

$\chi^2_{(0.05)}$ (df:1)= 3.841; $\chi^2_{(0.05)}$ (df:13)= 22.362
(The bold values of χ^2 indicate highly significant ($p<0.05$))

TABLE 3
Prey number of stomach contents in *A. boyeri* Karacaoren Dam Lakes according to length classes (TL)

	4.5-4.9		5-5.4		5.5-5.9		6-6.4		6.5-6.9		7-7.4	
ORGANISMS	N	**N%**	N	**N%**	N	**N%**	N	**N%**	N	**N%**	N	**N%**
ROTIFERA												
Keratella cohclearis			2962(33)	**70.33**	3147(33)	**67.86**	1713(6)	**78.11**	2(1)	**7.14**		
Trichocerca similis			11(7)	**0.26**	31(10)	**0.67**	9(3)	**0.41**				
Lecane luna			3(3)	**0.07**								
Unidentified rotifera			22(4)	**0.52**	29(7)	**0.62**	3(1)	**0.14**				
CLADOCERA												
Daphnia longispina			21(11)	**0.49**	51(21)	**1.1**	37(6)	**1.55**				
Bosmina longirostris	132(5)	**95.65**					26(5)	**1.18**				
Ceriodaphnia quadrangular			527(26)	**12.51**	600(41)	**12.94**	75(4)	**3.42**				
Disparalona rostrata			28(7)	**0.66**	16(8)	**0.34**	28(2)	**1.27**				
Cydorus sphaericus			7(6)	**1.16**	11(7)	**0.24**	5(3)	**0.23**				
Alona quadrangularis	1(1)	**0.72**	17(13)	**0.4**			4(2)	**0.18**				
Alona guttata							1(1)	**0.04**				
Alona rectangula							13(1)	**0.59**				
Moina sp.							2(1)	**0.09**				
Leydigia leydigi			1(1)	**0.02**								
COPEPODA												
Cyclops sp.			557(35)	**13.23**	644(37)	**13.89**	144(7)	**6.56**				
Nitocra hibernica	5(3)	**3.62**	48(27)	**1.14**	86(26)	**1.85**	27(8)	**1.23**				
ODONATA							87(14)	**3.97**	24(3)	**85.71**	1(1)	**3.45**
DIPTERA												
Chironomus larvae							11(6)	**0.5**	2(2)	**7.14**	28(1)	**96.55**
TRICHOPTERA			4(1)				1(1)	**0.04**				
FISH (egg. scale)			3(3)		22(8)	0.47	7(2)	**0.32**				
TOTAL	**138**		**4211**		**4637**		**2193**		**28**		**29**	

TABLE 4
Number of species, diversity ane species richness of A. boyeri in different length classes from Karacaoren Dam Lake

Length classes	Number of species(S)	*Diversity (H')*	Species richness (d)
4.5-4.9	3	*0.198*	0.434
5-5.4	12	*1.009*	2.385
5.5-5.9	10	*1.049*	1.954
6-6.4	18	*0.987*	3.693
6.5-6.9	3	*0.509*	0.434
7-7.4	2	*0.150*	0.217

TABLE 5
Schoener overlap index of *A. boyeri* sampled in different length classes

C (N %)	4.5-4.9	5-5.4	5.5-5.9	6-6.4	6.5-6.9
4.5-4.9	0.01				
5-5.4	0.09	**0.96***			
5.5-5.9	0.03	**0.83***	**0.82***		
6-6.4	0.00	0.07	0.07	0.12	
7.0-7.4	0.00	0.00	0.00	0.04	0.11

[23] stated that the similarity of diet in large fish of 30 mm (TL) is important, and cannibalism is found in large-sized individuals. Simultaneously, the study conducted at Hirfanlı Dam Lake showed that 100.0-109.9 mm of *A. boyeri* were fed with *Bosmina sp* (99.88%) and 90.0-99.9 mm of *A. boyeri* were fed with Cyclopoid copepods (83.90%). In addition, [3] reported that individuals in the range of 7.0-8.4 and 8.8-9.9 cm (FL) were predominantly fed with arthropoda, cladocera, insect, copepod and fishes. In this study, 4.5- 4.9 / 6- 6.4 cm length range of individuals were fed with rotifera, cladocera, copepod and, Individuals between 6.5- 6.9 / 7.0-7.4 cm in length were found to be fed with odonata and trichoptera. In our study, it was found that the *A. boyeri* in the range of 5.5- 5.9 / 6.0- 6.4 cm length class contains fish egg, scale at very low level.

Shannon's diversity index values are shown in Table 4. The food niche breadth of *A. boyeri* was relatively wide; it ranged from 0.217 to 3.693 for all size groups. The maximum value of 1.049 for the Shannon's diversity index was found in 5.5- 5.9 cm length classes. The fact that the species diversity for diet showed a homogeneous distribution in 5.0- 5.4/ 5.5- 5.9 and 6.0- 6.4 length classes (Table 5). Schoener's overlap index was estimated for size groups and female-male to determine the diet similarity [18]. According to Schoener Overlap index, sand smelt for sex groups (female-male) (C=0.632) had not similar diet compositions because of low values (C<0.8). Sand smelt fed mainly on zooplankton and insecta such as *Bosmina longirostris, Ceriodaphnia quadrangula, Keratella cochlearis, Alona quadrangularis, Cyclops* sp, Odonata and *Chironomus* larvae, and index values indicated almost complete diet overlap (values >0.8).

CONCLUSION

This study shows that *A. boyeri* is fed on very dense zooplankton species (rotifera, cladocera and copepod) and the diet and feeding behavior changes related to sex and fish size. *A. boyeri* in the range of inland water sources as invasive in Turkey, showing the typical diet in Karacaoren Dam Lake, has chosen zooplankton organisms. As the zooplankton forming the food in the larval stage of other fish in the lake is preferred by the invasive species entering the lake, it is inevitable that there will be changes in the food chain of the dam. Such studies are important in terms of revealing the negative effects of invasive fish species on the ecosystems. This scientific data on the feeding ecology of sand smelt will contribute to similar studies to be done later.

REFERENCES

[1] Quignard, J.P. and Pras, A. (1986) Atherinidae. In: Whitehead, P.J.P., Bauchot, M.L., Hureau, J.C., Nielsen, J. and Tortonese, E. (Eds.) Fishes of the North-Eastern Atlantic and the Mediterranean. UNESCO, Paris, 1207–1210.

[2] Doulka, E., Kehayias, G., Chalkia, E. and Leonardos, D. (2013) Feeding strategies of *Atherina boyeri* (Risso 1810) in a freshwater ecosystem. J. Appl. Ichthyol. 29(1), 200-207.

[3] Apaydın Yağcı, M., Alp, A., Yağcı, A., Uysal, R. and Yeğen, V. (2018) Feeding ecology and prey selection of sand smelt, *Atherina boyeri* Risso, 1810 in Egirdir Lake (Southern Anatolia, Turkey). Journal of Applied Ichthyology. 10.1111/jai.13676 (online press).

[4] Innal, D. and Erk'akan, F. (2006) Effects of exotic and translocated fish species in the inland waters of Turkey. Rev. Fish. Biol. Fisher. 16, 39-50.

[5] Chrisafi, E., Kaspiris, P. and Katselis, G. (2007) Feeding habits of sand smelt (*Atherina boyeri,* Risso 1810) in Trichonis Lake (Western Greece). J. Appl. Ichthyol. 23, 209–214.

[6] Danilova, M.M. (1991) Diet of juvenile silversides, *Atherina boyeri*, from the Black Sea. J. Ichthyol. 31, 137–145.

[7] Trabelsi, M., Kartas, F. and Quignard, J.P. (1994) Comparison of diet between a marine and a lagoonal of *Atherina boyeri* from Tunisian coasts. Vie Milieu. 44, 117–123.

[8] Gisbert, E., Cardona, L. and Castello, F. (1996) Resource partitioning among planktivorous fish larvae and fry in a Mediterranean coastal lagoon. Estuar. Coast. Shelf S. 43, 723–735.

[9] Bartulovic, V., Lucic, D., Conides, A., Glamuzina, B., Dulcic, J., Hafner, D. and Batistic, M., (2004) Food of sand smelt, *Atherina boyeri* Risso, 1810 (Pisces: Atherinidae) in the estuary of the Mala Neretva River (middle–eastern Adriatic, Croatia). Sci. Mar. 68, 597-603.

[10] Vizzini, S. and Mazzola, A. (2005) Feeding ecology of the sand smelt *Atherina boyeri* (Risso 1810) (Osteichthyes, Atherinidae) in the western Mediterranean: evidence for spatial variability based on stable carbon and nitrogen isotopes. Environ. Biol. Fishes. 72, 259–266.
[11] Rosecchi, E. and Crivelli, A.J. (1992) Study of a sand smelt (*Atherina boyeri* Risso 1810) population reproducing in freshwater. Ecol.Freshw. Fish. 1, 77–85.
[12] Kuru, M., Balik, S., Ustaoglu, M.R., Unlu, E., Taskavak, E., Gul, A., Yilmaz, M., Sari, H. M., Kucuk, F., Kutrup, B., Hamalosmanoglu, M. (2001) Türkiye'de bulunan sulak alanların Ramsar Sözleşmesi balık kriterlerine göre değerlendirilmesi projesi. T.C. Çev. Bak. Çevre Kor. Gen. Müd. ve Gazi Üniv. Vakfı, Kesin Raporu. Ankara.
[13] Saç, G., Gaygusuz, O. and Tarkan, A.S. (2015) Reoccurrence of a commercial euryhaline fish species, *Atherina boyeri* Risso, 1810 (Atherinidae) in Büyükçekmece Reservoir (Istanbul, Turkey). Journal of Aquaculture Engineering and Fisheris Research. 1(4), 203-208.
[14] Cortes, E. (1997) A critical review of methods of studying fish feeding based on analysis of stomach contents: application to elasmobranch fishes. Can. J. Fish. Aquat. Sci. 54(3), 726-738.
[15] Oh, C.W., Hartnoll, R.G. and Nash, R.D. (2001) Feeding ecology of the common shrimp *crangon crango*n in Port Erin Bay, Isle of Man, Irish Sea. Marine ecology. Progress series. 214, 211-223.
[16] Alp, A. (2017) Diet shift and prey selection of the native European catfish, *Silurus glanis*, in a Turkish Reservoir. Journal of Limnology and Freshwater Fisheries Research. 3(1),15-23.
[17] Windell, J.T. (1971) Food analysis and rate of digestion. In: Ricker, W.E. (ed.) Methods for assessment of fish production in freshwaters 2nd ed. Blackwell, Oxford. 215-226.
[18] Schoener, T. (1970) Non synchronous spatial overlap of lizards in patchy habitats. Ecology. 51(3), 408-418.
[19] Yazıcıoğlu, O., Yılmaz, S., Yazıcı, R., Yılmaz, M. and Polat, N. (2017) Food Items and Feeding Habits of White Bream, *Blicca bjoerkna* (Linnaeus, 1758) Inhabiting Lake Ladik (Samsun, Turkey). Turkish Journal of Fisheries and Aquatic Sciences. 17, 371-378.
[20] Shannon, C.E. and Weaver, W. (1949) The mathematical theory of communication. Urbana: University of Illinois Press.
[21] Marshall, S. and Elliott, M. (1997) A comparison of univariate and multivariate numerical and graphical techniques for determining inter- and intraspecific feeding relationships in estuarine fish. Journal of Fish Biology. 51, 526–545.
[22] Kuçuk F., Gulle I., Guclu S.S., Gumus E. and Demir, O. (2006) Effect on fishing and lake ecosystem of sand smelt (*Atherine boyeri* Risso, 1810) as an invasive species. In: National Fishing and Rezervoir Management Symp. 7-9 February, Antalya, Turkey. 119-128. (in Turkish).
[23] Gencoglu, L., Kirankaya, S.G., Yogurtcuoglu, B. and Ekmekci, F.G. (2017) Feeding Properties of the Translocated Marine Fish Sand Smelt *Atherina boyeri* Risso, 1810 (Atherinidae) in a Freshwater Reservoir. Acta Zoologica Bulgaria. Suppl. 9, 131-138.

Received: **10.04.2018**
Accepted: **29.04.2018**

CORRESPONDING AUTHOR

Zehra Arzu Becer
Akdeniz University,
Fisheries Faculty,
Dumlupinar Bulvari Campus
Antalya – Turkey

e-mail: abecer@akdeniz.edu.tr

© by PSP Volume 27 – No. 7/2018 pages 5179-5187 Fresenius Environmental Bulletin

SELECTION THE BEST BARLEY GENOTYPES TO MULTI AND SPECIAL ENVIRONMENTS BY AMMI AND GGE BIPLOT MODELS

Erol Oral*, Enver Kendal, Yusuf Dogan

Mardin Artuklu University, Kiziltepe Vocational Training High School, Department of Plant and Animal Production, Mardin, Turkey

ABSTRACT

The stability of genotypes is significant to selection and improves new varieties. The effect of genotype x environment interaction is revealed by different analysis methods. Nowadays, majority of researchers have been used the AMMI (Additive main effects and multiplicative interaction) and GGE biplot analysis in multi-environment trials. Therefore, ten barley advanced line and cultivars were used in the study. The experiments were performed according to a complete randomized block design with four replications at six environments in 2010-2011 seasons. The stability and superiority of genotypes for yield was determined using AMMI and GGE biplot analysis. Factors (G, GE, and GEI) were found to be highly significant ($P < 0.01$) for grain yield. AMMI analysis indicated that the major contributions to treatment sum of squares were environments (89.77%), genotypes (7.25%) and GE (2.96%), respectively, suggesting that grain yield of genotypes were effected environmental conditions. The GGE biplot indicated that PCA 1 axes (Principal component) was significant as $P<0.01$ and supplied to 75.33% of complete GxE interaction. The AMMI indicated that G6 was stable, while G10 and G9 were high yielding for grain yield in multi-environment. Moreover, E1 and E4 were high yielding, while E2, E5 and E6 low yielding as forecast. On the other hand, GGE biplot indicated that three group were occurred among environments, first group (E1, E2 and E6), second group (E3, and E4), third group (only E5). Moreover: the study showed that G6 and G9 were the best genotypes for first group, G10 for second and G1 for third of environments, while other genotypes didn't show any relation with environments. The results of AMMI and GGE biplot models indicated that G6 was stable in all environments. Therefore this genotype can be recommend for release to all environments, while G9 for first group and G10 for second group.

KEYWORDS:
Barley, AMMI, GGE biplot, Grain yield, Stability.

INTRODUCTION

Considering of the Food and Agriculture Organization of the United Nations (FAO), the World harvested area of barley (*Hordeum vulgare* L.) was nearly 49.5 million hectares, and the yield of barley was 2923 kg/ha in 2014 [1], while, the Turkey harvested area of barley nearly was 6.5 million hectares, the yield of barley was 2840 kg/ha in 2015 [2]. The results of statistic showed that the yield per hectare of barley in Turkey seems to be under to the world average. For this reason, it is very important to develop new and efficient varieties to raise the average yield per hectare in barley.

Barley (*Hordeum vulgare* L.) is the second important cereal crop of Turkey and accounts for about 25% of the total cereal production (SAP 2010). In South-Eastern Anatolia, barley has been cultivated for many years and has a significant role. It is also grown mainly on rainfall conditions, but genotype × environment interaction (GEI) restricts the progress in yield improvement under rainfed and unpredictable climatic conditions. Therefore, experimental research needs to be carried out over multiple environment trials in order to identify and analyses the major factors that are responsible for genotype adaptation and final selection [15, 16].

The yield of each variety in any environment is a sum of environment (E) main effect, genotype (G) main effect and genotype by environment interaction (GE or GEI) [5]. Yield is a complex quantitative trait that is often controlled by several genes and influenced by environmental conditions. The importance of genotypes by environment interaction (GEI) in national cultivar evaluation and breeding programs has been demonstrated in almost all major crops [4, 11, 12]. Farmers need varieties that show high performance in terms of yield and other essential agronomic traits. Modern barley breeding is largely directed towards the development of genotypes characterized with increased yield potential, wide adaptation and high responses to agronomic inputs [21].

The stability of promising lines is important for testing to estimate of theirs performance under across environments [8]. Therefore, the AMMI (analysis additive main effects and multiplicative

interaction) is widely used for GEI investigation among the multivariate methods. This model combines ANOVA for the genotype and environment main effects with principal components analysis to analyze the residual multiplicative interaction between genotypes and environments to determine the sum of squares of the G × E interaction, with a minimum number of degrees of freedom [7]. This method enables better understanding of genotypes performance over several environments, and selection of stable and high yielding genotypes [17]. The degree of complexity of AMMI estimation model is more depend on range of environmental conditions [19, 11]. Therefore, it is most useful for breeders and identifies the best genotypes to release decisions, and also it is very important to identify genotypes for specific sub-region [13].

This study aimed to estimate the adaptability and yield stability of barley genotypes using AMMI and GGE analysis to identification and introduction of genotype that have both high performance and high stability to reach the exact potential under changeable and unstable conditions.

MATERIALS AND METHODS

Plant genetic materials. The experimental material comprising ten genotypes (Table 1) were evaluated in 2010-2011 growing season (Table 2).

TABLE 1
The information's about genotypes.

Genotype	Spike type	Growing type
G1	2 rows	Spring
G2	6 rows	Spring
G3	2 rows	Spring
G4	2 rows	Spring
G5	2 rows	Spring
G6	6 rows	Spring
G7	2 rows	Spring
G8	2 rows	Spring
G9	6 rows	Spring
G10	6 rows	Spring

The experiment was conducted in a randomized block design with four replications at 2010-11 growing seasons. The seeding rate was used 450 seeds m^{-2}. Plot size was 7.2 m^{-2} (1.2 × 6 m) consisting of 6 rows spaced 20 cm apart. Sowing was done by winter stagier drill. The fertilization rates for all plots were used 60 kg N ha^{-1} and 60 kg P ha^{-1} with sowing time and 60 kg N ha^{-1} was applied to plots at the early stem elongation. Harvest was done using Hege 140 harvester up on 6 m^2. The general information about locations is given in Table 2.

Statistical analysis. The data grain yields of ten (10) genotypes in 2010-11 growing seasons was evaluated by AMMI analysis [7]. The AMMI and GGE biplot were used to identify the mega- environments and superior genotypes for grain yield and other traits. All statistical analyses were performed using GenStat Release 14.1 (Copyright 2011, VSN Int. Ltd.) and GGE biplot software programs.

The data were graphically analyzed for interpreting GE interaction using the GGE biplot software [31]. GGE biplot methodology is composed of the biplot concept [6] and GGE concept [32]. The graphs generated based on (1) The AMMI 1 model showing genotype x environment means,(2) Mega environments "which-won-where" pattern to identify the best genotypes in each season, (3) GGE biplot showing the performance of each cultivar at each environment, (4)The biplot showing the group of environments and performance of each cultivar at each environments, (5) Ranking genotypes based on traits by mean and stability, (6) The GGE Ranking model shows the stable and high yield genotypes on six environment, The GGE Comparison model compare the desirable genotypes to ideal center.

RESULTS AND DISCUSION

Combined analysis variance of ten genotypes under six environment revealed significant ($p \leq 0.01$) effects of genotypes, environments and interaction (Table 3). The effect interaction of PCA (1, 2 and 3) was also significant, while PCA4 was not significant. The analysis showed that the effect of environment was very high (89.8%) than genotype effect (7.3%) and interaction effect (3.0).

TABLE 2
Years, sites, codes, coordinate status of environment long term of precipitation

Year	Sites	Code of Sites	Altitude(m)	Latitude	Longitude	Annual Rainfall(mm)
2010-2011	Diyarbakır	E1	611	37° 55' N	40°14' E	470
	Hani	E2	995	38° 24' N	40° 24' E	892
	Siverek	E3	800	37° 45' N	39° 19' E	670
	Mardin	E4	495	37° 25′ N	41° 01' E	350
	Kızıltepe	E5*	484	37° 19' N	400 58' E	230
	Adıyaman	E6	685	37° 46' N	400 56' E	592

*(E5) was irrigated in two times (for germination and before heading time (150 mm))

TABLE 3
The variance of AMMI analysis on grain yield of barley

Source	Df	SS	MS	F	Explained SS (%)
Total	239	559148185	2339532		
Treatments	59	465164813	7884149	15.95	
Genotypes	9	46877818	5208646	10.53**	7.3
Environments	5	322349980	64469996	83.58**	89.8
Block	18	13884109	771339	1.56	
Interactions	45	95937016	2131934	4.31**	3.0
IPCA1	13	64139135	4933780	9.98**	60.7
IPCA2	11	17820383	1620035	3.28**	19.9
IPCA3	9	9463204	1051467	2.13*	12.9
IPCA4	7	3658723	522675	1.06ns	6.4
Residuals	5	855571	171114	0.35	
Error	162	80099263	494440		

Df; degrees of freedom; ns: not significant, **: p<0.01; , **: p<0.05.

TABLE 4
The grain yield and IPCA scores of ten genotypes in six environment.

Gen. No	Grain yield (kg ha^{-1})						Mean	IPCAg [1]	IPCAg [2]	IPCAg [3]	IPCAg [4]	**IPCAg (1+2+3+4)***
	E1	E2	E3	E4	E5	E6						
1	5362	2110	3458	3792	3033	1194	**3795**	-38.2311	6.46936	-14.6425	-15.3862	**-61.7904**
2	6613	2093	4067	1971	3925	2135	**3968**	12.47478	17.37798	9.2118	-1.10725	**37.95731**
3	5655	2349	3538	3340	3504	2063	**3951**	-17.5591	1.61898	-2.74515	3.10002	**-15.5852**
4	5330	2377	3408	2356	3063	2183	**3695**	-11.2078	-11.74532	8.82528	-1.08189	**-15.2098**
5	5245	2403	3608	2188	3553	2192	**3773**	-9.00804	-0.29703	17.40825	6.07466	**14.17784**
6	7226	2829	4142	1835	4245	3238	**4661**	14.21454	2.39513	5.31835	4.1401	**26.06812**
7	6954	2238	2710	1748	2679	3200	**3895**	18.23325	-31.45165	-18.1128	3.03128	**-28.2999**
8	5622	2831	3721	2387	3473	2640	**4085**	-9.0951	-12.20352	12.90255	2.84533	**-5.55074**
9	8497	3003	4102	1333	4520	3263	**4793**	35.05002	7.02931	-0.06747	-18.6268	**23.38507**
10	7725	2105	4308	2850	4558	2988	**4964**	5.12849	20.80676	-18.0983	17.01072	**24.84763**
Mean	**6423**	**2434**	**3706**	**2380**	**3655**	**2510**						

*(IPCAg 1+2+3+4)>0 = stable and high yielding genotype, (IPCAg 1+2+3+4)<0 = unstable and low yielding genotype

The grain yield and IPCA scores ten genotypes in six environment showed in Table 4. The grain yield of genotype were ranged from 3695 kg/ha^{-1} (G4) to 4964 kg/ha^{-1}(G10). On the other hand, the grain yield of environment were ranged from 2510 kg/ha^{-1} (E6) to 6423 kg/ha^{-1}(E1). The grain yield of genotypes were changed depend on the genetic characteristics of the genotypes, while the yield of environments were changed depend on the climate, soil, altitude and other characteristics of the locations. The genotypes which have high positive IPCA (1+2+3+4) scores, it means that these genotypes are yielding, while low IPCA scores mean low yielding. Some environmental factors, such as soil type and management practices are predictable, i.e. they are not different from year to year. On the other hand, the year-dependent factors, such as precipitation, temperature and disease attack, cause a high year-to-year variability. These random factors are highly variable and have a strong influence on the G × E interaction.

The degree of complexity of AMMI estimation model was more depend on range of environmental conditions. The results of AMMI analysis was supported by results of [4] and [30], reported that the environment effect had the highest effect than other factors on barley and soybean grain yield respectively. The results of Environment, Genotype and G x E effects obtained from this study illustrated similar results of the studies described above and the effect of environment > genotypes > GEI. The existence interaction of grain yield displayed by GGE biplot, especially when the interaction portioned between two-interaction principal component axes (PCA) (Table 3).

This status of GGE biplot made it establish and the biplot calculate effects of genotype and environment. The results of mean square of the interaction axis PCA 1 was significant (p<0.01), while PCA 2 was not significant [14, 25]. Results of GGE biplot analysis also indicated that the PCA 1 axis accounted 50.87%, PCA2 accounted for 24.46% (Fig. 2). GGE biplot showed existence interactions of G x E, so it was portioned between first and second IPCA (Interaction Principal Component Axes). The barley grain yield variation is more depending on environment factors as shown Table 3 and Fig 2. [7], AMMI stability parameter

(ASV) is also one of parameters that are used to estimate genotypes stability. ASV in fact is distance of a special genotype from the origin coordinates of IPCA1 against IPCA2 two -dimensional scatter plot. Lower amount of ASV value shows greater stability of genotypes [22]. On the other hand, [13] suggested that the AMMI model is the most accurate a model because it can predict using the first two IPCAs.

The AMMI model showing genotype x environment means of grain yield. In the AMMI model, x-axis represents the genotypes and environment main effect and y axis represents the effects of interaction (Fig. 1). According to AMMI, G9, G10 and G6 showed good performance, because of they took place above on axis (mean yield). On the other hand, G4 and G5 and other genotypes demonstrated low performance, due to they located under on axis (mean yield). The environment E1, E4 located above mean axis. Moreover, E2, E5 and E6 had low yield potential environment. G9 and G10 lines had high yield potential, but unstable, while G6 was stable, and yield potential. E1 and E4 could be recommended to tested genotypes with high potential and IPCA values, while other environments are not to be recommended to tested genotypes because of low yield potential. Similar outputs were recorded by [18], in barley. According to [17], the genotypes have small IPCA1 values are more stable, [11], the AMMI analysis supply more useful information for acquiring certain results and the identity of mega-environments and wining genotypes are inevitable.

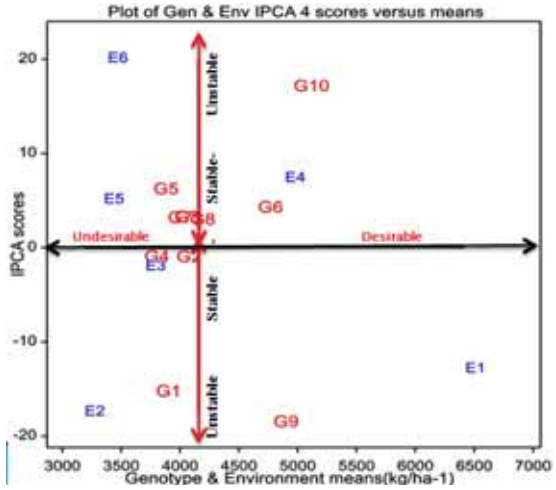

FIGURE 1

The AMMI 1 model showing grain yield (kg/ha-1) of genotypes(G) in 6 environments (E).

Mega environments "which-won-where" pattern to identify the best genotypes in each environment. Discriminating the target environment into meaningful mega-environments and deploying different cultivars for different mega-environments is the only way to utilize positive GE and avoid negative GE and the sole purpose for genotype by environment interaction analysis [31]. A mega-environment is defined as a group of environments that consistently share the same best cultivar(s) [30] This definition explain the following biplot based on the multi-environment trials (MET) data of barley yield illustrates two points: 1) A mega-environment may have more than one winning genotypes (sector 2), and 2) even if there exists a universal winner (G9, G10), it is still possible, and beneficial, to divide the target environments into meaningful mega-environments (Fig. 2 and Fig. 4).

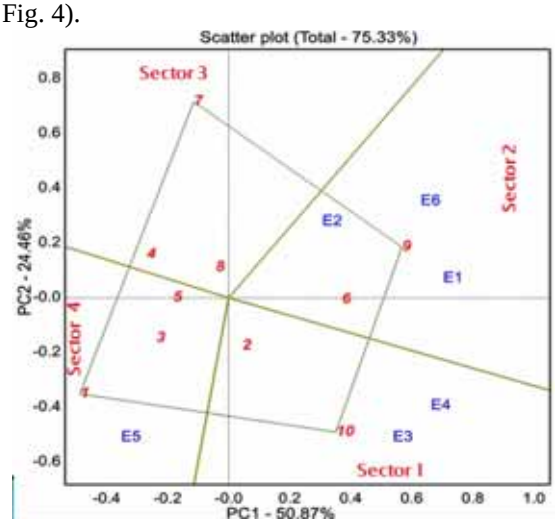

FIGURE 2

The which-won-where view of the GGE biplot.

Mainly, the four lines of biplot graph divide the biplot into four sectors (Fig. 2). The environments located in three separate sectors; this means that the environments had different ecological conditions. On the other hand, first sector consists of G10, and it was high yielding and represented of vertex the E3 and E4 with G2. The second sector consists of E1, E2 and E6 with G9 and G6 and the G9 took places of vertex of this sector. The third sector just consists of some genotypes (G7, G4 and G7), which are not related with study environments. The fourth sector was consisting of G1, G3 and G5 with E5 and the G1 represented of vertex of this sector. Consequently, G9 had high yielding for E1, E6 and E2, G10 for E3 and E4, G1 for only E5; while G4, G7 and G8 did not related with any environments. The result of this study showed that G9, G10 and G1 are suitable to recommend to high potential for special environments. [26], reported that there is a strong correlation between environments, which located in same sector. [23], the large variation due to environment indicated strong influence of environments and existence of mega-environment among trial conducting locations; this suggests the usefulness of GGE biplot technique for identifying mega- environments among barley

TABLE 5
The first four AMMI selections per environment

Environments	Mean	Score	1	2	3	4
E1	6423	33.42	G9	G10	G6	G7
E2	3189	-9.01	G9	G8	G6	G4
E3	3706	-6.79	G10	G6	G9	G2
E4	4893	7.23	G10	G9	G6	G2
E5	3352	-47.06	G1	G10	G3	G8
E6	3385	22.22	G7	G9	G6	G10

growing locations. [19], reported that the GGE biplot graphic analysis defining mega-environments and the cultivars that optimize performance in such mega-environments. Although the crop yield is a result of E, G and G × E interaction effects, only G and G × E are relevant for cultivar and mega-environment identification [29], GGE biplot is a data visualization tool that allows the visual interpretation of the G × E interaction, including environmental evaluation. According to [28], due to the discriminative ability and representativeness of GGE view, the biplot was an effective tool for environments evaluation.

The recommendation of environment: The average grain yield of six environments ranged from 3189 kg/ha to 6423 kg/ha of spring barley genotypes (Table 5). The AMMI analysis indicated that the E1 was the best yielding among test environments, followed E4, since the positive IPCA scores. On the other hand, E2 was the lowest yielding for among test environments, because of the very low IPCA scores. Therefore, the first four AMMI selection genotypes for per environment showed that firstly; G9, G10 and G6 should have been select for E1-E4, while G1 for E5, G7 for E6, because of recommendation of AMMI. [13], reported that it is important to select the genotypes for environment on first four AMMI recommendation.

The GGE Biplot Analysis of genotypes by environments. In this analysis, the results of genotype and environments interaction were examined by GGE Biplot analysis using figure. The biplot of the principal component analysis illustrates relationships between the studied barley genotypes at six environments (Figure 3). The GGE biplot graphically allows PC1 and PC2 to be readily displayed in a two-dimensional biplot so that each genotype × environment interaction is visualized [11]. The first two principal components (PC1 and PC2) were obtained by partitioning the G and G × E interaction trough the GGE biplot analysis. PC1 accounted to 50.87%, while PC2 amounted to 24.46 of the G and G × E interaction. Together, they accounted to 75.33% of the G and G × E interaction sum of squares.

According to Ding et al (2008), GGE biplot is an effective tool for: 1) analysis of mega-environments and specific genotypes can be recommended to specific mega-environments, 2) evaluation of genotype, and 3) evaluation of environment (the power to discriminate among genotypes in target environments). On a GGE biplot, both the genotypic and environmental vectors are shown in Figure 2, illustrating the specific interactions of each genotype with each environment (i.e., the performance of each genotype in each environments).

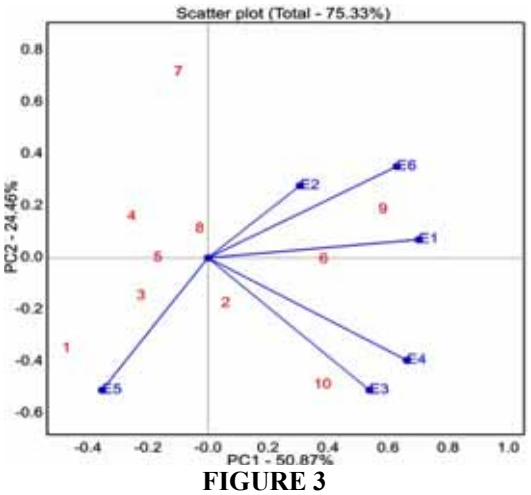

FIGURE 3
GGE biplot showing the performance of each cultivar at each environment

Figure 3 is useful for ranking the genotypes based on their performance in any environment and ranking environments in terms of the relative performance of any genotype. If the angle between environments and genotypes are obtuse, environments and genotypes are negatively correlated. If angle is acute, environments and genotypes are positively correlated, while environments and genotypes are not associated when the angle is 90º [13, 8]. Since, the angle of E5 with other environment is looking negative, while the angle is looking positive between E3 and E4, among E1, E2 and E6. So we can say that there were three groups among test environments (Fig. 4). Close associations between testing environments, suggest that same information about cultivar characteristics could be available from fewer testing environments, reducing the test cost [27]. The presence of an obtuse angle among environments is an indicator of a strong crossover of the G × E interaction [32]. According to [20] the variation in barley grain yield was mostly under control of the growing season and the genotype ×

year interaction. Similarly, [21] reported that in yield trials the effect of the environment affected 80-90% of the treatment variation, and the variation due the G × E interaction was higher than the genotypic variation. Mortazavian et al. [19] also reported that the environment constitutes the highest percent of the total yield variation, while the influence of the G and G × E interaction is usually smaller. On the other hand, there is a relation among genotypes and environment, depend on places of genotype on figure. The G10 with G2 were highly correlated with E3 and E4, the G9 and G6 correlated with E1, E2 and E6, the G1 and G3 correlated with E5, while other genotypes (G4, G5, G7 and G8) which are not related with study environments. The results showed that there is high variation among genotypes; because the genotype located different part of figure. Genotypes located near the center of the biplot contributed less to G and/or GE, whereas genotypes are far of the biplot showed the greatest contribution of G and/or GE [25]. Thus, G9 and G10, which is far from the center of biplot, contributed most to positive outcomes, whereas others, such as genotype G8, is near the center of biplot and contributed less. Thus, these genotypes aligned with specific environments. Although G made major contributions to grain yield, because some of these have opposite directions in the biplot, the genetic contributions may be very different [9].

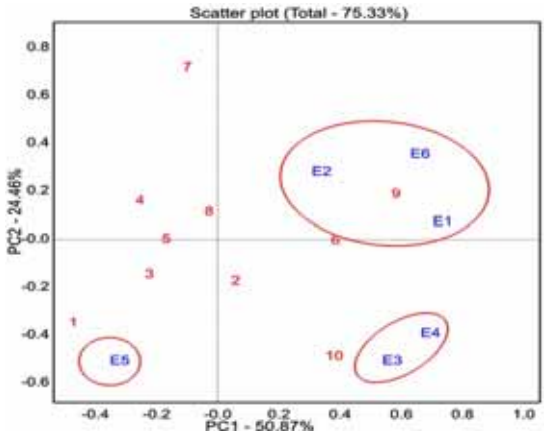

FIGURE 4
The biplot showing the group of environments and performance of each cultivar at each environment.

Ranking genotypes based on mean grain Yield and in stability: The genotype has both high traits mean and high stability is called a favorable genotype. It should have both high mean performance and high stability for all traits (Fig. 5). The center of the concentric circles (ideal) is a point on the AEA ("absolutely stable") in the positive direction and has a vector length equal to the longest vectors of the traits on the positive side of AEA ("highest mean performance"). Therefore, genotypes located closer to the stabile line and has high mean values of traits are meaning that it is more favorable than others [31, 5]. The G6 is located center of AEA ("absolutely stable"), but; G2, G9 and G10 took place of near center of AEA and high mean of grain yield. So, these genotypes are favorable than others. According to Fig.6, the G9, and G10 are low stable and more favorable, while G6 are "stable" and favorable, because this genotype has high mean grain yield in all environments. From this example, we can recommend G6 to study for more environments. On the other hand, some genotypes (G1, G3, G4, G5, G7, G8) were unfavorable, because these genotypes had low mean grain yield in study environments.

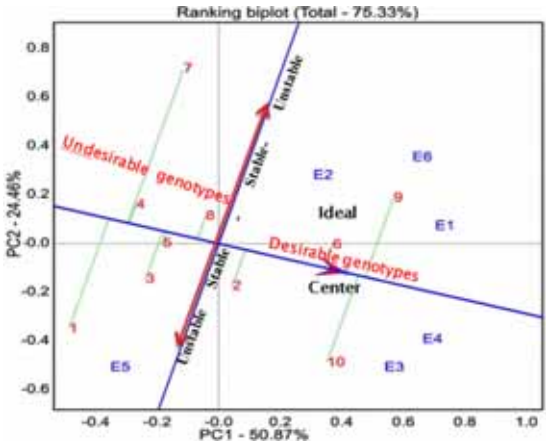

FIGURE 5
The GGE ranking model shows the stable and high yield genotypes on six environments

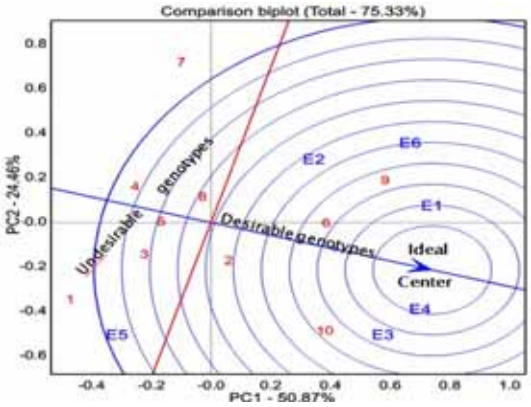

FIGURE 6
The GGE Comparison model compare the desirable genotypes to ideal center

Comparison of genotypes based on grain yield by ideal genotype: The genotype has both high grain yield and high stability is called an ideal genotype (Fig. 6). The center of the concentric circles is a point on the AEA ("absolutely ideal") in the positive direction and has a vector length equal to the longest vectors of the genotypes on the positive side of AEA ("highest mean performance"). So, genotypes located closer to the ideal circle

TABLE 6
The plant height and heading time of ten genotypes in six environment.

Gen. No	Plant Haigh (cm)						Mean	Heading time (date)						Mean
	E1	E2	E3	E4	E5	E6		E1	E2	E3	E4	E5	E6	
1	125	95	100	120	100	-	108	128	130	126	106	114	118	120
2	105	95	90	115	90	-	99	112	116	112	93	102	110	108
3	115	95	85	120	95	-	102	121	123	122	109	110	115	117
4	90	65	70	90	70	-	77	122	122	127	103	108	116	116
5	90	60	75	100	70	-	79	121	123	126	104	104	116	116
6	110	95	80	115	75	-	95	113	110	112	98	102	110	108
7	105	90	75	100	75	-	89	107	107	106	90	102	105	103
8	90	85	75	95	70	-	83	121	118	126	108	110	114	116
9	110	85	85	120	80	-	96	117	116	113	97	101	111	109
10	117	75	85	110	95	-	96	116	116	113	106	105	112	111
Mean	106	84	82	109	82			118	118	118	101	106	118	

are meaning that it is ideal genotype than others [31, 11]. In the study, any genotype was not located center of AEA ("absolutely stable"), but; G6, G9 and G10 took place of near center of AEA. So these genotypes are ideal than other genotypes. Consequently, G6, G9 and G10 are close to ideal and desirable genotype, so, these genotypes can be recommended for release in terms of grain yield. On the other hand, more genotypes located far from ideal genotype and, these (G1, G3, G4, G5, G7, G8) are undesirable genotypes to study and release. The researchers reported that the biplot show excellent discriminating to select genotypes for all traits and to recommendation for release [20, 24, 11].

The plant height of genotypes were changed from 77(G4) to 108(G1) cm, while the plant height of environment were changed from 82(E5) to 109(E1) cm (Table 6). On the other hand; the heading time of genotypes were ranged from 103 to 120 dates, while the heading time of environments were changed from 101 to 118 dates. The plant height and heading time of genotypes are depend on genetic variability and some environmental factors, such as soil type and management practices are predictable, i.e. they are not different from location to location. On the other hand, the location-dependent factors, such as precipitation, temperature and disease attack, cause a high location-to-location variability. These random factors are highly variable and have a strong influence on the G × E interaction [11], reported that the environmental factors and genetic variability is effect the genotypes and environment plant height and heading time.

CONCLUSION

The results of study indicated that yield performance of barley genotypes were highly influenced by environments. The AMMI indicated that G6 was stable, while G10 and G9 were high yielding for grain yield in multi-environment. Moreover, GGE biplot indicated that three group were occurred among environments, first group (E1, E2 and E6), second group (E3, and E4), and third group (only E5). E1 and E4 were high yielding, while E2, E5 and E6 low yielding as forecast. Moreover: the study showed that G6 and G9 were the best genotypes for first group, G10 for second and G1 for third of environments, while other genotypes didn't show any relation with environments. The results of AMMI and GGE biplot models indicated that G6 was stable in all environments. Therefore this genotype can be recommend for release to all environments, while G9 for first group and G10 for second group.

ACKNOWLEDGEMENTS

The abstract of this article was published in" SA2017" the 52nd Croatian & 12th International Symposium on Agriculture, February 12-17, Dubrovnik | Croatia, Webpage: http://sa.pfos.hr.

REFERENCES

[1] Anonymus1. (2015) https://www.google.com.tr/?gws_rd=ssl#q=faostat&.
[2] Anonymus2. (2015) Turkey Statistik Foundation. Tuik.
[3] Ding, M., Tier, B., Yan, W., Wu, H.X, Powell, M.B., McRae, T.A. (2008) Application of gge biplot analysis to evaluate genotype (g), environment (e), and g×e interaction on "Pinus radiata": A Case Study. New Zealand Journal of Forestry Science. 38(1), 132-142.
[4] Doğan, Y., Kendal, E., Oral, E. (2016) Identifying of relationship between traits and grain yield in spring Barley by GGE biplot analysis. The Journal Agriculture and Forestry. 62(4), 239-252.

[5] Farshadfar, E., Rashidi, M., Jowkar, M.M., Zali, H. (2013) GGE Biplot analysis of genotype × environment interaction in chick-pea genotypes. European Journal of Experimental Biology. 3(1), 417-423.
[6] Gabriel, K.R. (1971) The biplot graphic display of matrices with application to principal component analysis. Biometrika. 58, 453-467.
[7] Gauch, H.G. and Zobel, R.W (1997) Identifying mega-environments and targeting genotypes. Crop. 37, 311-326.
[8] Hagos, G.H., Abay, F. (2013) AMMI and GGE Biplot analysis of bread wheat genotypes in the northern part of Ethiopia. Journal Plant Breeding and Genetic. 1, 12-18.
[9] Jalata, Z. (2011) GGE-biplot Analysis of Multi-environment yield trials of barley (*Hordeum vulgare* L.) genotypes in Southeastern Ethiopia Highlands. International J. of P. Breeding and Gen. 5(1), 59-75.
[10] Kendal, E., Sayar, M.S. (2016) The stability of some spring triticale genotypes using biplot analysis. The Journal of Animal and Plant Sciences. 26(3), 754-765.
[11] Kendal, E., Sayar, M.S., Tekdal, S., Aktas, H., Karaman, M. (2016) Assessment of the impact of ecological factors on yield and quality parameters in triticale using GGE biplot and AMMI analysis. Pak. J. Bot. 48(5), 1903-1913.
[12] Kendal, E. (2016) GGE Biplot analysis of multi-environment yield trials in barley (Hordeum vulgare L) cultivars. Ekin J. of Crop Breeding and Genetics. 2-3, 90-99.
[13] Kendal, E., Dogan, Y. (2015) Stability of a Candidate and Cultivars (*Hordeum vulgare* L) by GGE Biplot analysis of Multi-environment Yield Trials in Spring Barley. Agriculture and Forestry. Podgorica. 61(4), 307-318.
[14] Kendal, E. (2016) GGE Biplot analysis of Multi-environment Yield Trials in Barley (*Hordeum vulgare* L) Cultivars. Ekin J. of Crop Breeding and Genetics. 2-3, 90-99.
[15] Kilic, H. (2014) Additive main effect and multiplicative interactions (AMMI) Analysis of grain yield in barley genotypes across environments. J. Agr. Sc. 20, 337-344.
[16] Kizilgeci, F., Yildirim, M., Albayrak, O., Akıncı, C. (2016) Investigation of yield and quality parameters of barley genotypes in Diyarbakır and Mardin conditions. Iğdır Univ. J. Inst. Sci. and Tech. 6(3), 161-169.
[17] Mirosavlievic, M., Przulj, N., Bocanski, N., Stanisavlievic, D., Mitrovic, B. (2014) The application of AMMI model for barley cultivars evaluation in multi-year trials. Genetika. 46(2), 445-454.
[18] Mohammadi, M., Karimizadeh, R., Noorinia, A.A., Ghojogh, H., Hosseinpour, T., Khalilzadeh, GR., Mehraban, A., Roustaii, M. Hasanpor Hosni, M. (2013) Analysis of yield stability in multi-environment trials of barley (*Hordeum vulgare* L.) genotypes using AMMI model. Current Opinion in Agriculture Curr. Opin. Agric. 2(1), 20-24.
[19] Mortazavian, S.M.M., Nikkhah, H.R., Hassani F.A., Sharif-al-Hosseini M., Taheri, M., Mahlooji, M. (2014) GGE Biplot and AMMI Analysis of yield performance of barley genotypes across different environments in Iran. J. Agr. Sci. Tech. 16, 609-622.
[20] Pržulj, N., Momčilović, V. (2012) Spring barley performances in the Pannonian zone. Genetika. 44, 499-512.
[21] Przulj, N., Momcilović, V., Simić, J., Mirosavljević, M. (2014) Effect of growing season and variety on quality of spring tworowed barley. Genetika. 46, 59-73.
[22] Purchase, J.L., Hatting, H. and Van Deventer, C.S. (2000) Genotype × environment interaction of winter wheat in south Africa: II. Stability analysis of yield performance. Afr. J. Plant Soil. 17, 101-107.
[23] Sarkar, B., Sharma, R.C.R, Verma, A., Sarkar, P.S., Sharma, I. (2014) Identifying superior feed barley genotypes using GGE biplot for diverse environments in India. Indian J. Genet. 74(1), 26-33.
[24] Sayar, M.S., Anlarsa, A.E., Basbag, M. (2013) Genotype–environment interactions and stability analysis for dry-matter yield and seed yield in Hungarian vetch (Viciapannonica CRANTZ.). Turkish J. of F. Crops. 18(2), 238-246.
[25] Sayar, M.S., Han, Y. (2015) Determination of seed yield and yield components of grasspea (*Lathyrussativus* L.) lines and evaluations using GGE Biplot analysis method. Tarim Bilimleri Dergisi - J. Agric. Sci. 21(1), 78-92.
[26] Solonechnyi, P., Vasko, N., Naumov, A., Solonechnaya, O., Vazhenına, O., Bondareva, O., Lovnivenko, Y. (2015) GGE biplot analysis of genotype by environment interaction of spring barley varieties. Zemdirbyste-Agri. 102, 431–436.
[27] Yan, W., Frégeau-Reid, J., Martin, R., Pageau, D., Mitchell-Fetch, J. (2015) How many test locations and replications are needed in crop variety trials for a target region. Euphytica 202(3), 361-372.
[28] Yan, W., Kang, M.S., Ma, B., Woods, S., Cornelius, P.L. (2007) GGE Biplot vs. AMMI analysis of genotype-by-environment data. Crop Science. 47, 643-655
[29] Yan, W., Holland, J.B. (2010a) A heritability adjusted GGE biplot for test environment evaluation. Euphytica. 171(3), 355−369.

[30] Yan, W., Rajcan, I. (2002) Biplot analysis of test sites and trait relations of soybean in Ontario. Crop Science. 42, 11-20.
[31] Yan, W., Tinker, N.A. (2006) Biplot analysis of multi-environment trial data; Principles and applications. Canadian Journal of Plant Science. 86, 623-645.
[32] Yan, W.L., Hunt, A., Sheng, Q., Szlavnics, Z. (2000) Cultivar evaluation and mega-environment investigation based on the GGE biplot. Crop Sci. 40, 597-605.

Received: **30.01.2018**
Accepted: **29.04.2018**

CORRESPONDING AUTHOR

Erol Oral
Mardin Artuklu University,
Kızıltepe Vocational Training High School,
Department of Plant and Animal Production,
Mardin – Turkey

e-mail: eroloral65@gmail.com

AUTHOR INDEX

SUBJECT INDEX

FEB – GUIDE FOR AUTHORS

General

FEB accepts original papers, review articles, short communications, research abstracts from the entire sphere of environmental-chemistry,-biology,-microbiology,- technology, -biotechnology and-management, furthermore, about residue analysis/ and ecotoxicology of contaminants.

Acceptance or no acceptance of a contribution will be decided, as in the case of other scientific journals, by a board of reviewers. Papers are processed with the understanding that they have not been published before (except in form of an abstract or as a part of a published lecture, review or thesis);that they are not under consideration for publication elsewhere; that their publication has been approved by all co-authors, if any, as well as-tacitly or explicitly- by the responsible authorities at the institute where the work has been carried out and that, if accepted, it will not be published elsewhere in the same form, in either the same or another language, without the consent of the copyright holders.

Language

Papers must be written in English. Spelling may either follow American (Webster) or British (Oxford) usage but must be consistent. Authors who are less familiar with the English language should seek assistance from proficient colleagues in order to produce manuscripts that are grammatically and linguistically correct.

Size of manuscript

Review articles should not exceed 30 typewritten pages. In addition up to 5 figures may be included.

Original papers must not exceed 14 typewritten pages. In addition up to 5 figures may be included.

Short-Communications should be limited to 4 typewritten pages plus not more than 1 illustration.

Short descriptions of the authors, presentation of their groups and their research activities (with photo) should together not exceed I typewritten page. Short research abstracts should report in a few brief sentences (one-fourth to one page) particularly significant findings. Short articles by relative newcomers to the chemical innovation arena highlight the key elements of their Master and PhD-works in about I page.

Book Reviews are normally written in-house, but suggestions for books to review are welcome.

Preparation of manuscript

Dear authors,

FEB is available both as printed journal and as online journal on the web. You can now e-mail your manuscripts with an attached file. Save both time and money. To avoid any problems handling your text please follow the instructions given below:

When preparing your manuscripts have the formula K/SS (Keep It Simple and Stupid) in mind. Most word processing programs such as MS-Word offer a lot of features. Some of them can do serious harm to our layout. So please do not insert hyperlinks and/or automatic cross-references, tables of contents, references, footnotes, etc.

1. Please use the standard format features of your word processor (such as standard.dot for MS Word).
2. Please do not insert automatisms or secret link-ups between your text and your figures or tables. These features will drive our graphic department sometimes mad.
3. Please only use two fonts for text or tables "Times New Roman" and for graphical presentations "Arial".
4. Stylesheets, text, tables and graphics in shade of grey
5. Turn on the automatic language detection in English (American or British)
6. Please - check your files for viruses before you send them to us!!

Manuscripts should send to:parlar@wzw.tum.de
or:parlar@prt-parlar.de

Thank you very much!

STRUCTURE OF THE MANUSCRIPT

Title page: The first page of the manuscript should contain the following items in the sequence given: A concise title of the paper (no abbreviations). The names of all authors with at least one first name spelled out for every author. The names of Universities with Faculty, City and Country of all authors.

Abstracts: The second page of the manuscript should start with an abstract that summarizes briefly the contents of the paper (except short communications). Its length should not exceed 150-200 words. The abstract should be as informative as possible. An extended repetition of the paper's title is not considered to be an abstract.

Keywords: Below the Summary up to 6 key words have to be provided which will assist indexers in cross-indexing your article.

Introduction: This should define the problem and, if possible, the frame of existing knowledge. Please ensure that people not working in that particular field will be able to understand the intention. The word length of the introduction should be 150 to 300 words.

Materials and methods:
Please be as precise as possible to enable other scientists to repeat the work.

Results: Only material pertinent to the subject must be included. Data must not be repeated in figures and tables.

Acknowledgements: Acknowledgements of financial support, advice or other kind of assistance should be given at the end of the text under the heading "Acknowledgements". The names of funding organisations should be written in full.

References: Responsibility for the accuracy of references rests with the authors. References are to be limited in number to those absolutely necessary. References should appear in numerical order in brackets and in order of their citation in the text. They should be grouped at the end of the paper in numerical order of appearance. Abbreviated titles of periodicals are to be used according to Chemical or Biological Abstracts, but names of lesser known journals should be typed in full. References should be styled and punctuated according to the following examples:

ORIGINALPAPERS:
l. Author, N.N. and Author, N.N. (Year) Full title of the article. Journal and Volume, first and last page.
BOOK OR PROCEEDING:
2. Author, N.N. and Author, N.N. (Year) Title of the contribution. In: Title of the book or proceeding. Volume (Edition of klitor-s, ed-s) Publisher, City, first and last page

DOCTORAL THESIS:
3. Author, N.N. (Year) Title of the thesis, University and Faculty, City

UNPUBLISHED WORK:
Papers that are unpublished but have been submitted to a journal may be cited with the journal's name followed by "in press". However, this practice is acceptable only if the author has at least received galley proofs of his paper. In all other cases reference must be made to “unpublished work" or "personal communication".

Discussion and Conclusion: This part should interpret the results in reference to the problem outlined in the introduction and of related observations by the author/s or others. Implications for further studies or application may be discussed. A conclusion should be added if results and discussion are combined.

Corresponding author: The name of the corresponding author with complete postal address

Precondition for publishing:
A minimum number of 25 reprints must be ordered and prepaid.
1 - 4 pp.: 200,- EURO + postage/handling
5 - 8 pp.: 250,- EURO + postage/ handling
More than 8pp: 1.50 EURO/page x number of reprints +postage/ handling.
The prices are based upon the number of pages in our journal layout (not on the page numbers of the submitted manuscript).
Postage/ Handling: The current freight rate is Germany 10 €, Europe 18,00 €, International 30 €.
VAT: In certain circumstances (if no VAT registration number exists) we may be obliged to charge 7% VAT on sales to other EU member countries.MESAEP and SECOTOX members get a further discountof 20% (postage/ handling full).